

1422/ST

**PROCEEDINGS
INTERNATIONAL
SOLVENT EXTRACTION
CONFERENCE
1974**

VOL. 2



S.C.I.

SOLVENT EXTRACTION

Proceedings
of the
International Solvent Extraction Conference

I.S.E.C. 74

Lyon; 8-14th September 1974

SOCIETY OF CHEMICAL INDUSTRY
LONDON
1974

SOCIETY OF CHEMICAL INDUSTRY

14 BELGRAVE SQUARE

LONDON S.W.1.

Editorial Committee

Prof. J. D. Thornton

Dr. A. Naylor

Dr. H. A. C. McKay

Prof. G. V. Jeffreys (Editor)

©1974 SOCIETY OF CHEMICAL INDUSTRY

In Four Volumes

ALL RIGHTS RESERVED

Printed in England

- 134 FIDELIS I - Warsaw Institute of Nuclear Research, Poland - Double-double effects in the free energy and enthalpy changes of the extraction of heavy lanthanides in the HDEHP-HNO₃ system.
- 141 ALSTAD J, AUGUSTSON, J H, DANIELSSEN T and FARBU L - Oslo University, Norway.- A comparative study of the rare earth elements in extraction by HDEHP/Shell Sol T from nitric and sulphuric acid solutions.
- 167 MYASOEDOV B F, CHMUTOVA M K, KOTCHETKOVA H E and PRIBYLOVA G A - Moscow Academy of Sciences, USSR - Extraction of trivalent transplutonium elements and europium by a mixture of di-2-ethylhexylorthophosphoric acid and phosphorus pentoxide from strongly acid media.
- 206 KORPUSOV G V, DANILOV N A, KRYLOV Yu S, KORPUKOVA R D, DRYGIN A I and SHVARTSMAN V Ya - Moscow Academy of Sciences, USSR - Investigation of rare-elements extraction with different carboxylic acids.
- 228 PUSHLENKOV M F, VODEN V G and OBUKHOVA M E - State Committee for the Utilization of Atomic Energy, USSR - The extraction of americium, thorium and europium with capryl-hydroxamic acid (CHA)

SESSION 11 EXTRACTION TECHNOLOGY (Common Metals)

- 2 HUGHES M A and LEAVER T M - Bradford University, UK - The solvent extraction of anions from chromium bearing liquors - binary equilibria.
- 124 LAKSHMANAN V I and LAWSON G J, Birmingham University, UK - The extraction of cadmium (II) and zinc (II) from sulphate and chloride solutions with Kelex 100 and Versatic 911 in kerosene.
- 152 CUER J P, STUCKENS W and TEXIER N - Produits Chimiques Ugine Kuhlmann, France - The technique of solvent extraction applied to the treatment of industrial effluents.
- 201 BOZEC C, DEMARTHE J M and GANDON L - Societe le Nickel, France - Recovery of nickel and cobalt from metallurgical waste by solvent extraction.
- 223 MERIGOLD C R and JENSEN W H - Minerals Industries, USA - The separation and recovery of nickel and copper from a laterite-ammonia leach solution by liquid ion exchange.
- 246 MIHALOP P, Charter Consolidated Ltd, Mrs C J BARTON, LOGSDAIL D H, McKAY H A C and SCARGILL D - AERE, Harwell, UK - Design of a process for the purification of cobalt by means of di-2-ethylhexyl phosphoric acid.
- 251 DEMARTHE J M, TATNERO M, MIQUEL P and GOUMONDY J P - CEA, France - Example of nitric acid recovery by solvent extraction.

SESSION 12 EQUIPMENT (Axial Mixing Phenomena)

- 77 INGHAM J, Bradford University, UK, BOURNE J R, Zurich Technisch Chemisches Laboratorium and MOGLI A Kuhni A.G, Switzerland - Backmixing in a Kuhni Liquid-liquid extraction column.
- 119 CHOUDHURY P R, AMBROSE P T, McNAB G S, FISH L W and CAVERS S D - University of British Columbia, Canada - Liquid-liquid spray columns: Correction of driving force for axial mixing.
- p. 1341 140 BORRELL A, MURATET G and ANGELINO H - Laboratoire Associe CNRS, France - Contribution of the dispersed phase to the longitudinal mixing in a rotating disc contactor.
- p. 1371 191 WATSON J S and McNEESE L E - Oak Ridge National Laboratory, USA - Hydrodynamic behaviour of packed liquid-liquid extraction columns with fluids of different densities.

WEDNESDAY, 11th September

SESSION 13 CHEMISTRY OF EXTRACTION (Thermodynamics)

- 41 IVANOV I M, GINDIN L M and CHICHAGOVA G N - The Siberian Branch of the Academy of Sciences, USSR - Thermodynamic characteristics of the extraction of anions.
- 59 O'BRIEN W G and BAUTISTA R G - Iowa State University, USSA - A thermodynamic activity model for a single lanthanide nitrate liquid-liquid extraction system.
- 74 KRASNOV K S, KASAS T S and KUZNETSOV V S - Ivanov Institute of Chemistry and Technology, USSR - Thermodynamics of extraction of salts with noble gas ions.
- 142 ALLARD B, JOHNSSON S and RYDBERG J - Chalmers University of Technology, Sweden - Thermodynamics and solvent influence in zinc and copper acetylacetonate extraction
- 177 TSIMERING L and KERTES A S - The Hebrew University, Israel - Correlation of excess enthalpies of mixing in tributylphosphate - N - alkane system.
- 178 GRAUER F and KERTES A S - The Hebrew University, Israel - Formation of trialkylammoniumchlorides in dry and wet benzene.

SESSION 14 EXTRACTION TECHNOLOGY (Nuclear Processes I)

- 14 DWORSCHAK H and HALL A - CNEN - Eurex Plant, Italy - Experiences of highly enriched uranium reprocessing in the Eurex pilot plant.
- 61 WARNER B F, NAYLOR A, DUNCAN A and WILSON P D - BNFL, UK - A review of the suitability of solvent extraction for the reprocessing of fast reactor fuels.
- 110 MILLS A L and LILLYMAN E - UKAEA, Dounreay, UK - Fast reactor fuel reprocessing at Dounreay.
- 150 TUNLEY T H, Johannesburg, National Institute for Metallurgy and NEL V W - Palabora Mining Co Ltd., South Africa - The recovery of uranium from uranathoria-nite at the Palabora Mining Co. Ltd.
- 153 LEWIS L C and ROHDE K L - Idaho Chemical Processing Plant, USA - Fission product behaviour in a two-solvent extraction system for enriched uranium.
- 253 BOUDRY J C, CENF and MIQUEL P - CEA, France - Adaptation of the purex process to the reprocessing of fast reactor fuel

SESSION 15 EQUIPMENT (Contactor Performance I)

- 1571 17 BAIRD M H I, McMaster University and RITCEY G M - Department of Energy, Canada - Air pulsing techniques for extraction columns.
- 1891 24 MUMFORD C J and ~~AL~~-HEMERI A A A - Birmingham University UK - The effect of wetting characteristics upon the performance of a rotating disc contactor.
- 25 ARNOLD D R, JEFFREYS G V and MUMFORD C J - Birmingham University, UK - Droplet size distribution and interfacial in agitated contactors.
- 55 OLDSHUE J Y, HODGKINSON F and AGOUTIN M - Mixing Equipment Co Inc, USA - Mixing effects in a multi-stage mixer column.
- 78 HAFEZ M M, NEMECEK M and PROCHAZKA J - Academy of Sciences, Czechoslovakia - Hold-up and flooding in reciprocating-plate extractors.
- p.1619
- p.1671

SESSION 16 CHEMISTRY OF EXTRACTION (Common Metals)

- 47 EINAGA H - National Institute for Researches in Inorganic Materials, Japan - Distribution characteristics of iron (III) as benzoic acid complex between benzene and 1.0 M (Na, H) C_{10}H_8 aqueous solution.
- 73 RAIS J, KYRS M and KADLECOVA L - Institute of Nuclear Research, Czechoslovakia - Extraction of some univalent and bivalent metals in the presence of macrocyclic polyether.
- 94 MUHL P, GINDIN L M, KHOLKIN A I, GLOE K and LUBOSHNIKOVA K S - Dresden Academy of Science and Siberian Branch of Academy of Science, USSR - Investigations on the mechanism of Fe (III) extraction by n-caprylic acid.
- 163 EGER I - Negev University, Israel - Salting out effect of some metal chlorides on FeCl_2 extraction from aqueous phase with methyl isobutyl-ketone.
- 205 BREZHNEVA N E, KORPUSOV G V, PROKHOROVA N P, PROKOPCHUK Yu Z, SVETLAKOV V I and TRUKHANOV S Ya - Moscow Academy of Sciences, USSR - Investigation of extraction and some processes of separation of alkali-earth elements.
- 213 DANESI P R, MEIDER-GORICAN H, CHIARIZIA R, CAPUANO V and SCIBONA G - CNEN, Italy - Alkali metals extraction by the cyclic polyether dibenzo-18-crown-6.
- 236 LASKARIN B N, YAKSHIN V V, UL'YANOV V S and MIROKHIN A M - Moscow Academy of Sciences, USSR - The effect of structure of 2 - hydroxyphenonoximes on the formation of their copper complexes.

SESSION 17 CHEMISTRY OF EXTRACTION (General and other Interactions)

- 34 FROLOV Yu G and SERGIEVSKY V V - Moscow Institute of Chemical Technology, USSR - The hydration of organic phase components and its influence on extraction equilibrium.
- 69 SEKINE T, KOKISO M and HASEGAWA Y - Tokyo University, Japan - Effect of inert salts on the solvent extraction of metal complexes.
- 117 ASHTON N, SOARES L de J and ELLIS S R M - Birmingham University, UK - Prediction of multicomponent liquid equilibria data.
- 218 MAKSIMOVIC Z B and Mrs MIOCINOVIC - Boris Kidric Institute, Yugoslavia - Solvent extraction of PETN and RDX from nitric acid solution.

- 227 KOMAROV E V and KOMAROV V N - Leningrad State University, USSR - Peculiarities of solvent extraction by deeply associated reagents.
- 229 SHMIDT V S, MEZHOV E A and SHESTERIKOV V N - State Committee for the Utilization of Atomic Energy, USSR - Prediction and analysis of extraction system properties with linear free energies relations (LFER)
- 242 BAGREEV V V, ZOLOTOV Yu A, TSERYUTA Yu S, YUDUSHKINA L M and KUTYREV I M - Moscow Academy of Sciences - FISCHER G and MUHL P - Dresden Academy of Sciences GDR - Mutual effects of elements in the extraction by long-chain amine salts.

THURSDAY, 12th September

SESSION 18 CHEMISTRY OF EXTRACTION (New and Unusual Extractants)

- 28 DZIAMKO V M, IVANOV O V, ANVILINA V N, IVASHCHENKO A V and KASAKOVA T S - All-Union Scientific Research Institute, USSR - Recent developments in the study of heterocyclic amine extraction chemistry. Application of the formation of intramolecular hydrogen bonding between ligand and co-ordinated anions in the salt extraction.
- 82 GORBANEV A I, MARGULIS V B, DZEVITSKII B E - Moscow Academy of Sciences and SHALYGIN V M - All-Union Research Institute of Petrochemical Processes, Leningrad, USSR - Principle of systematic activation and its application for synthesis of extractants with predicted selectivity.
- 83 ZOLOTOV Yu A, SERIAKOVA I V and VOROBYEVA G A - Moscow Academy of Sciences, USSR - New sulphur-containing extractants.
- 139 MAKSIMOVIC Z B, RUVARAC A Lj and HALASI R - Boris Kidric Institute of Nuclear Sciences, Yugoslavia - Solvent extraction of metal chloride complex by tri-n-laurylamine oxide.
- 154 LAURENCE G J, Mrs T L THAI, ENSCP France, BOURGUIGNON J R and MICHEL P - CENF, France - Metals extraction by and -monosubstituted tetrahydrofurans in chlorhydric medium
- 224 UHLEMANN E - Potsdam College of Education, E Germany - The extraction and photometric determination of metals by means of thiodibenzoylmethane.
- 264 PROSKURYAKOV V A and GAILE A A - Leningrad Institute of Technology, USSR - New extractive agents for aromatic hydrocarbons.

SESSION 9

Tuesday 10th September: 9.00 hrs

M A S S T R A N S F E R P H E N O M E N A

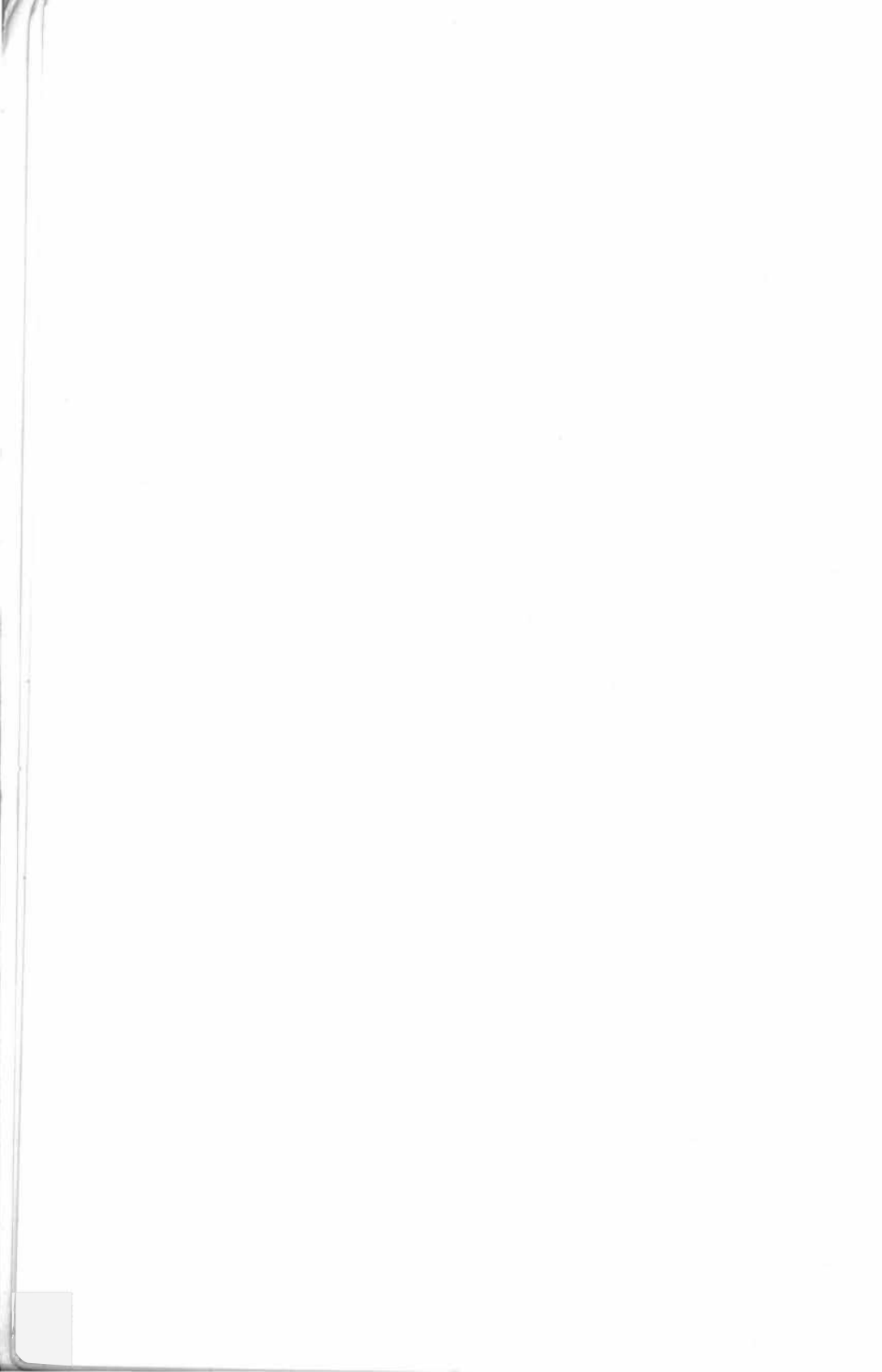
Chairman:

Dr. H. Sawistowski

Secretaries:

Dr. G. Stewart

Mr. J. Breysse



HEAT OR MASS TRANSFER IN LIQUID-LIQUID SPRAY
COLUMNS WAKE PHENOMENA AND ENTRAINMENT FLOW.

B. PAULES* and M. PERRUT**

ABSTRACT

A model describing heat or mass transfer in spray columns is presented. A reverse continuous phase flow, called "entrainment flow", induced by the droplets is considered. The wake model proposed by Letan and Kehat is discussed when no transfer with the dispersed phase occurs, it is shown to be a specific case of our model. Its three parameters are evaluated from experimental results obtained by several investigators.

* Centre de Cinétique Physique et Chimique du CNRS, Département
Génie Chimique 54042 NANCY (France)

**Centre de Recherches ELF, B.P. no.22, 69360 SAINT SYMPHORIEN
D'OZON (France)

INTRODUCTION

The effects of axial mixing in liquid-liquid spray columns - such as end effects, temperature or concentration jumps at the inlet of the continuous phase, - are well known for a long time.

The axial dispersion model is usually used ; it gives a correct interpretation of temperature or concentration profiles in both phases.

However, several authors have shown that drops or rigid spheres moving in a continuous phase carry along wakes of this phase. Yeheskel and Kehat (1) have presented an interesting bibliography of these works.

Taking into account the role of wakes in the mechanism of heat transfer in spray columns, Letan and Kehat (2) have proposed a two- parameters model for the interpretation of the temperature profiles obtained with dispersed (2) or dense (2,3) packings flows. Markowitz and Birglis (4) have also used this model. Transposing their model to the case of mass transfer. Kehat and Letan (3) have obtained a good agreement with results from heat transfer experiments.

Different papers concerning single drops and assemblages of drops are reviewed in the present work. The model of Letan and Kehat (2,3) is criticized and generalised and another three- parameters model is presented which seems to be nearer to reality.

The wake phenomenon:

Single drops

Photographical (8 - 11) and cinematographical observations (14) have led to a description of the formation, development and shedding of wakes.

Hendrix et al.(12) have correlated the wake volumes to the two-phase physical properties, for non-oscillating drops; using the same method for evaluating the wake volume V_s , Yeheskel and Kehat (1) have obtained a good agreement with the empirical relation:

$$(1) \quad M = \frac{V_s}{V_g} = 14.21 \frac{\Delta P}{\rho_c} - 0.42$$

$\frac{\rho_c}{1.00}$	$\frac{\Delta P}{0.10}$	$\frac{M}{1.00}$
*	0.20	2.42

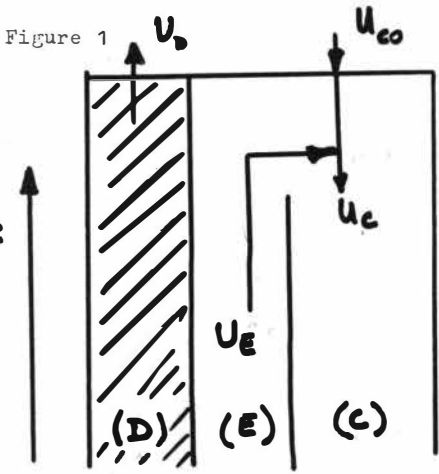
(V is the drop volume); for several liquid-liquid systems, the distance required to shed a volume equivalent to the wake volume is nearly constant with an average of 17.6 cm.

Assemblage of drops

As an intermediate step between single drops and packings of drops, vertical and horizontal assemblages of drops have been studied by Yeheskel and Kehat (15): They observed an entrainment flow different from the wake phenomenon, induced by the droplets on the neighbouring continuous phase: the velocity of this flow is about one third of the drop velocity. For vertical assemblages, the relative wake size M is decreased by two thirds as compared to a single drop wake. On the contrary, for horizontal assemblages,

M is roughly 50% larger than for a single drop and the enhancement of the wake shedding rate is approximately 2.

Heat or mass transfer models



The calculations proposed here concern heat transfer the results can be easily transposed to the mass transfer case.

The phase flows can be schematized as shown on Figure 1:

- the dispersed phase flow (D)
- a part of the continuous phase circulating in the deflection of the drops or "entrainment flow" (E)
- A counter-current continuous flow (C)

Their flowrates are noted respectively U_D , U_E and U'_C .

The inlet continuous phase flowrate being U_{CO} , it is evident that:

$$U_C = U_{CO} + U_E$$

The wake-model:

Letan and Kehat (2) have proposed a model considering the role of wakes. They have made some assumptions, the most original of which concerns the heat transfer mechanism, a continuous phase element contact the drop of temperature T_D , reaches this temperature T_D and then enters the wake while another element of same volume leaves the wake (of temperature T_E). This assumption of perfect heat transfer between the element and the drop seems very restrictive; therefore, a third parameter can be introduced: the contact efficacy

$$E = \frac{T'_C - T_C}{T_D - T_C}$$

where T'_C is the temperature of the element entering the wake.

(Letan and Kehat's model corresponds to the case $E = 1$).

The heat balance in the three flows can be written:

$$U_E \frac{dT_E}{dz} = q_E E (T_D - T_C) + q_E (T_C - T_E) \quad (2)$$

$$- U_C \frac{dT_C}{dz} = q_E (T_E - T_C) \quad (3)$$

$$U_D (\rho C_p)_D \frac{dT_D}{dz} = q_E E (T_C - T_D) (\rho C_p)_C \quad (4)$$

q_E is the total flowrate exchanged per unit of column height between the wakes and the continuous phase.

As Letan and Kehat, we introduce the two parameters

- relative wake volume $M = \frac{V_s}{V_g} \equiv \frac{U_E}{U_D} - (R)$

- shedding rate $S = \frac{1}{V_D} \frac{dV_s}{dz}$ which is the volume of wakes shed per volume of drop and unit length of column.

$$S = \frac{1}{V_D} \frac{dV_E}{dz} - ?$$

1000

Obviously $U_E = MU_D$ (5) and we obtain easily $q_E = SU_D$ (6)

Comparison with the axial dispersion model:

The equations of the model with axial dispersion in the continuous phase only are (5, 7, 16):

$$\frac{d^2 T_C}{dz^2} + \frac{P_C}{L} \cdot \frac{dT_C}{dz} - \frac{N_C P_C}{L^2} \cdot (T_C - T_D) = 0 \quad (7)$$

$$\frac{dT_D}{dz} - \frac{N_C r}{L} \cdot (T_C - T_D) = 0 \quad (8)$$

with $r = \frac{(P_{Cp})_C U_{co}}{(P_{Cp})_D U_D}$, N_C and P_C transfer unit and Peclet numbers.

Eliminating $N_C(T_C - T_D)$ between (7) and (8) we obtain:

$$\frac{d^2 T_C}{dz^2} + \frac{P_C}{L} \cdot \frac{dT_C}{dz} - \frac{P_C}{Lr} \frac{dT_D}{dz} = 0 \quad (9)$$

Eliminating also T_E between (2) and (3), then using (4) we obtain:

$$\frac{d^2 T_C}{dz^2} + \frac{U_C - U_E}{U_C U_E} q_E \frac{dT_C}{dz} - \frac{1}{r} \frac{U_C - U_E}{U_C U_E} q_E \frac{dT_D}{dz} = 0 \quad (10)$$

It is obvious that equations (9) and (10) are equivalent and that both models lead to the same result if:

$$P_C = \frac{U_{co}}{U_{co} + MU_D} \frac{S}{M} L \quad (11) \quad \text{and} \quad N_C = \frac{U_D}{U_{co}} SEL \quad (12)$$

Discussion

It can be easily seen that for value of E near 1, the temperature of wakes T_E is not between T_D and T_C although the entrainment flow is materially situated between the dispersed and the continuous phase. We think the cause of this rather surprising result is the assumption that the element of fluid entering the wake comes from the continuous phase before contacting the drop; we are going to present now another model which seems to describe the phenomenon more closely.

The entrainment-flow model?

The results obtained by Yeheskel and Kehat (15) that we have reported above suggest consideration of the existence of an entrainment flow instead of a wake flow. The heat is transferred between the entrainment flow and the continuous phase by exchange of fluid elements with a rate q_E (per unit length of column); heat transfer between the drops and the entrainment flow is characterized by a heat transfer coefficient h' and the specific contact area of the dispersion a_{DE} .

The heat balance in the three flows can be written:

$$U_E \frac{dT_E}{dz} = q_E (T_C - T_E) + q_E' (T_D - T_E) \quad (13)$$

$$- U_C \frac{dT_C}{dz} = q_E (T_E - T_C) \quad (14)$$

$$\frac{(PCp)_D}{(PCp)_C} U_D \frac{dT_D}{dz} = q_E' (T_E - T_D) \quad (15)$$

where $q_E' = h'_{DE} \frac{a_{DE}}{(PCp)_C}$ has the dimensions of a flowrate per unit length.

The three parameters of this model are U_E , q_E and q_E' .

Comparison with the axial dispersion model and the wake model

After some manipulating of these equations, it is possible to obtain again the equation (10) :

$$(10) \frac{d^2 T_C}{dz^2} + \frac{U_C - U_E}{U_C U_E} q_E \frac{dT_C}{dz} - \frac{1}{r} \frac{U_C - U_E}{U_C U_E} q_E \frac{dT_D}{dz} = 0$$

which leads to $P_C = \frac{U_C - U_E}{U_C U_E} q_E L$ (16)

Besides from (14) and (15) we can obtain:

$$(17) T_C - T_D = U_C \left[\frac{1}{q_E} \frac{dT_C}{dz} + \frac{1}{q_E'} \cdot \frac{1}{r} \cdot \frac{dT_D}{dz} \right]$$

Only when $v_c = v_{co}$, i.e. no axial dispersion (see text)

from which it is possible to derive a true transfer units number N_C corresponding to the case of no axial mixing, i.e.

$$* U_C = U_{Co} \text{ and } \frac{dT_C}{dz} = \frac{1}{r} \frac{dT_D}{dz} ;$$

equation (16) becomes: $U_C = ?$ (2nd axial mixing, i.e. $U_C = U_{CO}$)

$$(18) \quad T_C - T_D = \frac{U_{CO}}{r} \left[\frac{1}{q_E} + \frac{1}{q_E'} \right] \frac{dT_D}{dz} \quad (18)$$

which may be compared with (8) giving

$$N_C = \frac{q_E \ q_E'}{U_{CO} (q_E + q_E')} L \quad (19)$$

Therefore, our model appears as a generalization of the axial mixing model the parameters N_C , P_C of which can be obtained from U_E , q_E and q_E' , by equations (16) and (19).

As can be seen easily from the general equations, our model is also identical to the wake model if no transfer occurs with the dispersed phase ($E = 0$; $q_E' = 0$).

Temperature T_E of the entrainment flow:

In this model, $(T_E - T_C)$ and $(T_E - T_D)$ have always opposite signs (equations (14) and (15) and therefore T_E is between T_C and T_D , which is more satisfactory from the physical point of view than the results obtained with the wake model.

Interpretation of experimental results:

The parameters of our model have been calculated from experimental profiles obtained in heat transfer (5) and in mass transfer (6, 7). We have introduced M and S , relative entrainment flowrate and relative shedding rate by analogy with the wake model; we define also:

$$S' = \frac{q_E'}{U_D}$$

Variation of M:

M has been calculated from the temperature (or concentration jump) existing at the inlet of the continuous phase with the assumption that in this region the temperature of the entrainment flow T_E and of the drops T_D are very near (figure 2), assumption confirmed by a flat T_D profile in this region (5) $\left(\frac{dT_D}{dz} = 0\right)$

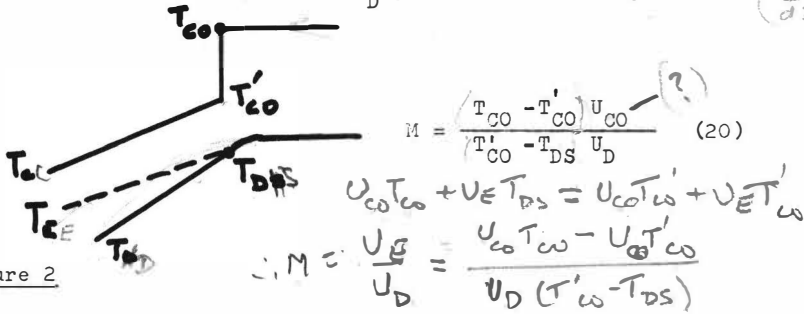


Figure 2

The variation of M with the dispersed phase holdup are reported on figure 3 (heat transfer (4, 17)) and 4 (mass transfer (17)); the results are in good agreement with those recently obtained by Letan and Kehat (19) using a tracer method, whereas the results of an earlier work of these authors (2) are in disagreement with them, M being evaluated in the dispersed packing part of the column where it is sensibly higher than in the dense packing part for high holdups.

The average curve (figure 3) extrapolates at zero holdup to the value $M = 2,15$ obtained with a single kerosene drop rising in water (1).

It can be also seen that M is about two times lower for mass transfer than for heat transfer; probably this difference results from interfacial modification due to mass transfer.

Variation of S:

The values of N_C and P_C (axial mixing model) have been calculated from the profiles (5,7) and S is evaluated from (11) and from the value of M:

$$S = \frac{U_{CO} + M U_D}{U_{CO}} \frac{M P_C}{L} \quad (21)$$

Known with a relatively low precision, S seems to be independent of the holdup and its average value \bar{S} for a given system of liquids can be correlated to the Margoulis number (related to the continuous phase)

$$M_{SC} = \frac{hc}{Vr} (PC)_c \text{ or } \frac{k_c}{Vr}, \text{ } h_c \text{ and } k_c \text{ being the transfer coefficient obtained from the true transfer unit number } N_C \text{ (5, 7)}$$

$$\bar{S} = 14 (M_{SC})^{0.8} \quad (28)$$

It can be noticed that the \bar{S} value for heat transfer between kerosene and water was found to be 0,023 to 0,030 cm^{-1} by Letan and Kehat (2), 0,05 cm^{-1} in this work from Loutaty et al's results (5) and 0,122 cm^{-1} for a single drop (1).

Evaluation of q'_E :

From (17) and the S value it is possible to evaluate:

$$q'_E = \frac{N_C S U_D}{LS \frac{U_D}{U_{CO}} - N_C} \quad (\text{subst (19) for } q'_E \text{ and put } q_E = S U_D) \quad (23)$$

which is proportional to h'_{DE} (or k'_{DE}) heat (or mass) transfer coefficient between the dispersed phase and the entrainment flow. It is interesting to compare h'_{DE} (or k'_{DE}) with the true overall transfer coefficient h (or k) evaluated from N_C .

The ratios $\frac{h'_{DE}}{h}$ and $\frac{k'_{DE}}{k}$ have been reported on figure 6 versus the holdup β .

The results are dispersed but it can be seen that these ratios range from 1,4 to 3 ; these low values show that the assumption of perfect heat transfer between the entrainment flow and the drops by Letan and Kehat is generally invalid.

CONCLUSION

The model for heat and mass transfer we have presented takes into account the existence of an entrainment flow between the continuous and the dispersed phase of a spray column. No particular assumption has been made concerning this flow; especially, its average velocity can be different from that of the dispersed phase.

The three parameters of this model are: the ratio of entrainment flow-rate to dispersed phase flow rate M , and S and S' characterizing the heat or mass exchanges between the different regions. A rough assumption concerning the continuous phase inlet region has been made to estimate M and then S and S' . A more direct method of determining M and S would be preferable, for example experiments with a tracer insoluble in the dispersed phase. In this case, our model applies with $S' = 0$.

Our model could also be used for other types of contactors, provided that the radial uniformity of concentrations can be assumed.

In conclusion, we will stress the fact that this model can be regarded as a physical interpretation of the axial ^{dispersion} model.

LITERATURE CITED

1. Yeheskel J., Kehat E., Chem.Eng.Sci., 26, 1223 (1971)
2. Letan R., Kehat E., A.I.Ch.E. J., 14, 398 (1968)
3. Kehat E., Letan R., A.I.Ch.E. J., 17, 984, (1974)
4. Markowitz A., Bergles A.E., 9th Nat.Heat Transfer Conf. AiChE - ASME, Minneapolis no.11 (1969)
5. Loutaty R., Vignes A., Le Goff P., Chem.Eng.Sci., 24, 1795 (1970)
6. Cavers S.D., Ewanchyna J.E., Can J Chem Ing, 35, 113 (1957)
7. Perrut, M., Loutaty R., Le Goff P., Chem.Eng.Sci., 28, 1541 (1973)
8. Magarvey R.M., Bishop R.L., Can.J.Phys., 39, 1418 (1961)
9. Magarvey R.M., Bishop R.L., The Phys. of Fluids, 4, 800 (1961)
10. Magarvey R.M., Blackford B.L., Can. J. Phys., 40, 1036 (1962)
11. Magarvey R.M., Maclatchy C.S., A.I.Ch.E. J., 14, 260 (1968)
12. Hendrix C.D., Dave S.B., Johnson M.F., A.I.Ch.E. J., 13, 1073 (1967)
13. Wilson M.P., Jeffreys G.V., Int. Sol. Extr. Conf. La Haye no. 24 (1971)
14. Edge R.M., Grant C.D., Int. Sol. Extr. Conf. La Haye no.71 (1971)
15. Yeheskel and Kehat, Chem. Eng.Sci. 26, 2037 (1971)
16. Miyauchi T., Vermeulen T., Land EC ~~Ind~~, no.2, 2, 113 (1963)
17. Perrut, M., These, Universite de Nancy 1 (1972)
18. Letan R., Kehat E., A.I.Ch.E. J., 16, 955 (1970)
19. ~~Letan R.~~ ^{Yeheskel J.}, Kehat E., A.I.Ch.E. J., 19, no.4, 720 (1973)
20. Letan R., Kehat E., A.I.Ch.E. J., 14, 831, (1968).

NOTATION

a	specific interfacial area (cm^2/cm^3)
C _p	heat capacity ($\text{cal}/\text{g}\cdot^{\circ}\text{C}$)
E	contact efficacy
h'	heat transfer coefficient ($\text{cal}/^{\circ}\text{C}\cdot\text{cm}^2\cdot\text{s}$)
k, k'	mass transfer coefficients (cm/s)
L	length of the column (cm)
M	ratio of wake to drop volumes
M _g	Margoullis number
N	number of transfer units
P _C	Peclet number
q, q'	exc angled flow rate per unit length of column (cm^2/s)
r	= $U_{CO} (\rho C_p)_C / U_D (\rho C_p)_D$ - 18
S	volume of wake elements shed per volume of drop and unit length of column (cm^{-1})
T	temperature ($^{\circ}\text{C}$)
U	flow rate (cm^3/s) $U_{CO} = \text{feed rate}$
V	volume (cm^3)
PPH	holdup of the dispersed phase
PPH	density (g/cm^3)
PPH	cross sectional area of the column (cm^2)

SUBSCRIPTS

C	continuous phase
D	dispersed phase
E	entrainment flow

FIGURE 3

Variation of M versus dispersed phase holdup β .
Heat transfer with kerosene-water

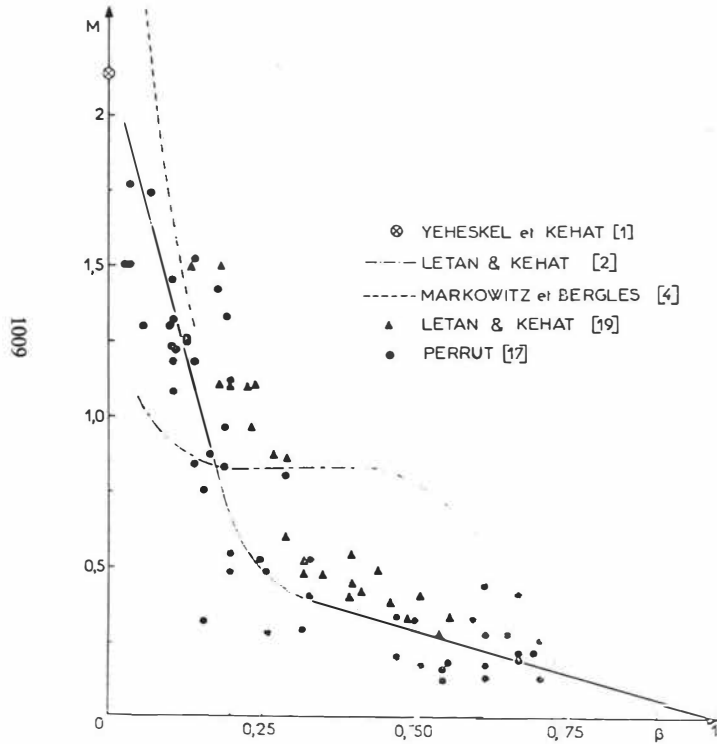
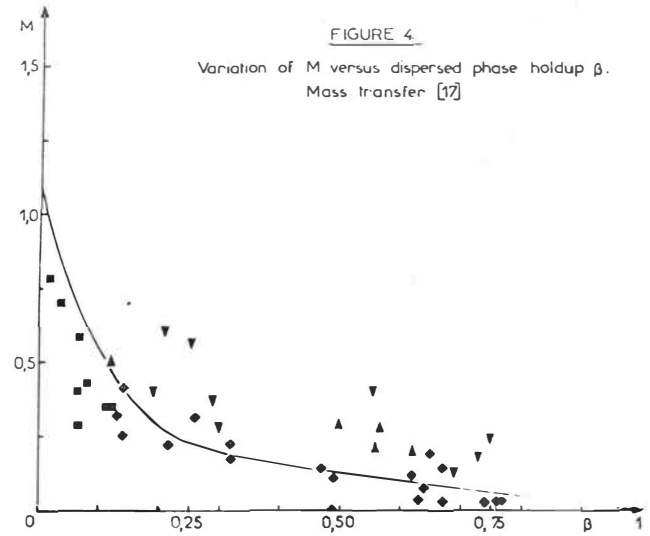


FIGURE 4

Variation of M versus dispersed phase holdup β .
Mass transfer [17]



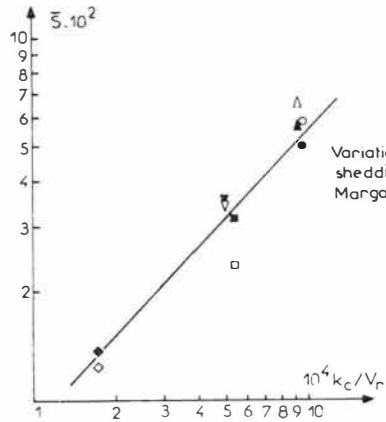


FIGURE 5

Variation of average relative shedding rate \bar{S} versus Margoules number [17]

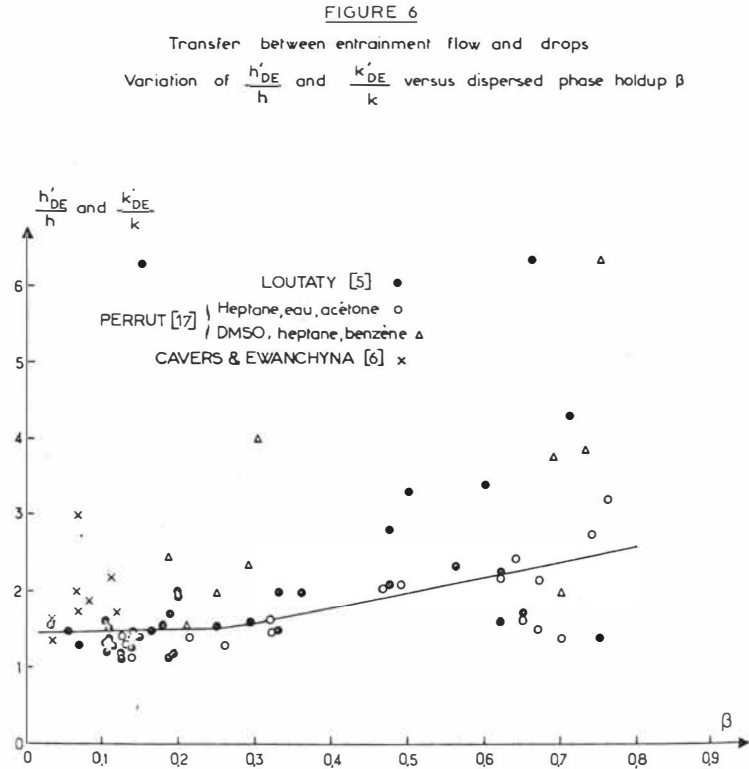


FIGURE 6

Transfer between entrainment flow and drops

Variation of $\frac{h'_{DE}}{h}$ and $\frac{k'_{DE}}{k}$ versus dispersed phase holdup β

ELECTRICALLY AUGMENTED LIQUID-LIQUID EXTRACTION IN A TWO-COMPONENT SYSTEM II - MULTIDROPLET STUDIES

P.J. Bailes[†] and J.D. Thornton^{*}

The behaviour of a population of electrically charged droplets has been studied in a d. c. field with particular reference to droplet size and velocity. A limited number of mass transfer measurements were also carried out. The liquid-liquid system used was furfural/n-heptane so that the results were directly comparable with those reported previously⁽¹⁾ for single droplet systems.

Whilst the droplet sizes were somewhat larger than those produced from an isolated nozzle, the velocities relative to the continuous phase were higher indicating the possibility of a redistribution of the space charge with a consequent enhancement of the average bulk field strength. Under conditions of low dispersed phase holdup, the average droplet velocity was found to be a unique function of the droplet size.

The extraction efficiency, as measured by the number of dispersed phase transfer units, was comparable with that observed in the case of single droplets and there appears to be an optimum electrode spacing at which the number of transfer units increases rapidly with applied voltage. This effect is significant from the point of view of extractor development and merits further investigation.

[†]Present Address: Schools of Chemical Engineering, University of Bradford, BD7 1DP. U.K.

^{*}Department of Chemical Engineering, The University, Merz Court, Newcastle upon Tyne, NE1 7RU. U.K.

INTRODUCTION

In Part I of the this study⁽¹⁾ charged droplets were produced at a single metallic nozzle forming part of a parallel plate electrode system submerged in an immiscible, insulating, liquid continuum. The application of a dc potential difference across the plates enabled the droplets to be not only charged during formation at the nozzle but subsequently upon detachment to be accelerated through the continuous phase. It was found that the droplet size could be controlled by the applied voltage gradient and furthermore that the droplets exhibited a high degree of electrically induced interfacial mobility and internal circulation. This turbulence was almost certainly the cause of the enhanced dispersed phase mass transfer coefficients which were recorded at higher potential gradients.

SCOPE OF THE PRESENT INVESTIGATION

The results which have been presented on the behaviour and performance of conducting droplets formed in an electric field in liquid-liquid systems were all obtained from experiments on droplets forming sequentially from a single charging nozzle. No attention has been paid to the way in which the presence of an ensemble of droplets might modify the electrical conditions between the electrodes. The present work was therefore undertaken with the two-fold object of firstly studying the effect of an applied potential difference on droplet size and velocity in a multi droplet situation (since a comparison of this data with single droplet results for the same system might indicate the extent to which the droplet population modified electrical environment). Secondly, it was thought desirable to obtain a quantitative measure of mass transfer into an ensemble of charged droplets.

The work was confined to the measurement of droplet size, holdup and mass transfer rates over a range of applied potential differences in a multi droplet countercurrent contactor. The experiments were conducted on one size of nozzle and for several contactor heights. As before⁽¹⁾ furfural droplets dispersed in n-heptane were selected as the test system and unidirectional mass transport into the droplets was studied using the Colburn and Welsh technique. Analysis of the exit dispersed phase was accomplished by vapour phase chromatography whilst droplet size and holdup were determined from the cine film which was taken during each run. It was considered desirable to operate at low holdups in order to minimise the "hindered settling" effects which always accompany finite populations of

droplets.

EXPERIMENTAL

Equipment

A modified version of the basic single droplet extraction cell was used and a diagram of this is shown in Fig. 1. In this equipment the upper electrode comprised a spray head incorporating a detachable nozzle plate and guard electrode. Distribution of liquid to the nozzles was achieved using a packing of glass beads positioned in the spray head by a disc of fine mesh stainless steel gauze, this allowed the production of a monodisperse system. The nozzle plate had 19 nozzles, made from stainless steel hypodermic tubing, located equidistant from one another on a 0.75 cm triangular pitch. To prevent wetting, the tips of the nozzles were bevelled at 45°. The lower electrode was unchanged in design, but a perforated brass plate was attached to it parallel to the upper guard electrode. In operation the interface was position immediately above this plate so that the potential difference was applied directly across the effective gap between the nozzles and the bulk interface.

The dispersed and continuous phases were pumped to the cell by tappings from two "pump around" systemsemploying flameproof positive displacement pumps. Flowrates were measured using $\frac{1}{4}$ inch Triflat precision bore flow-rators with constant density glass floats. The liquid and electrical circuits are detailed in Fig. 2. In order to avoid a short circuit from the 50 kV HV unit along the dispersed phase input line to earth it was found necessary to effect a break in the liquid circuit. This was done by using the double syphon arrangement shown in Fig. 3.

High speed cine pictures were taken at 250 or 400 frames per second using a Milliken DBM 5 camera, with sidelighting provided by two 500W "Photofloods".

Procedure

Steady state operation of the cell under no-voltage conditions was achieved as follows: Both pumps were switched on, the continuous phase was metered at a high rate directly to the cell, the dispersed phase at a low rate to the syphonic break. When the gap between the two electrodes was almost filled with continuous phase the flowrates of both phases were adjusted to the desired values. At this stage some adjustment of the control valve below

the double syphon was necessary to maintain a constant liquid level of dispersed phase in the glass capacity vessel. The interface level within the cell was controlled by a needle valve on the dispersed phase exit line to just cover the perforated brass base plate. A potential difference was then applied across the gap between the two electrodes.

To facilitate comparison with the single droplet results already available the experiments on the multidroplet cell were conducted with the same nozzle diameter, continuous phase throughput and flowrate of dispersed phase per nozzle as detailed in Part I. The droplet formation frequency and dispersed phase holdup were measured accurately from the slow motion film record, whilst mass transfer measurements were made by analysing samples of the bulk dispersed phase below the interface once a steady state had been reached.

Results

Droplet size and holdup measurements were made over contactor heights from 4 cm to 12 cm and applied voltages up to 9.6 kV. The material transferred was recorded for each of these experiments and also for a number of runs at voltages in excess of 9.6 kV.

The size of the droplets which detached from the multiple nozzles was consistently uniform although the actual magnitude of the droplets was altered by changes in voltage conditions. The droplets tended to oscillate between an oblate spheroidal and near spherical shape and so for convenience the droplet size has been expressed as the mean equivalent spherical droplet diameter (\bar{d}_e). These data are shown plotted against applied voltage for five different cell heights in Fig. 4.

In the case of a population of droplets in countercurrent flow, the velocity of each droplet is influenced by its neighbours and it is customary to use a mean droplet slip velocity (U_s^x) which is related to the fractional holdup of dispersed phase and the phase superficial velocities by means of the well known equation:

$$U_s^x = \frac{V_d}{x} + \frac{V_c}{1-x} \dots\dots\dots(1)$$

The slip velocities were calculated from equation (1) and are shown plotted against the applied voltage in Fig. 5.

Results for the transfer of n-heptane into the furfural are presented in Fig. 6 in terms of the number of dispersed phase film transfer units overall, in other words including the mass transferred during droplet formation, free fall, coalescence and across the bulk interface. In this connection it should be noted that the charged droplets coalesced almost instantaneously with the bulk interface.

DISCUSSION

An imperfect liquid dielectric may contain various ionic species and often polar molecules and dissolved gases. The effect of an electric field is to concentrate these charge carriers at the electrodes. For example, if a negative space charge is concentrated near the positive electrode a correspondingly higher positive charge accumulates on the electrode itself and the field strength in the immediate vicinity of the electrode will become very high and will gradually decrease away from the electrode. This process occurs at both electrodes and, since the total applied voltage difference must remain unchanged, it causes the overall potential profile between the electrodes to be non-linear although the field strength in the bulk of the liquid remains substantially linear (Fig. 7). Furthermore, the difference in mobility of the positive and negative charge carriers results in the electric field enhancement at the cathode being greater than at the anode. The existence of this non-linear field is demonstrated in Fig. 8b where droplet size data from Fig. 4 are plotted against cell height in each case with nominal field strength as parameter. If in these experiments the voltage profile between the electrodes was linear the actual field would equal the nominal field and the droplet sizes would be constant for a given field strength. It is apparent that this is not the case and so we may deduce that the field is non-linear. The practical implications of this are that at the present time it is impossible to predict droplet size, charge and velocity from the nominal field strength. The comparison of single charged droplet behaviour with that of multidroplets is also hampered for the same reason.

It is clear from the results that the general trends observed for multidroplets under electric field conditions are similar to those exhibited by single droplets. A closer examination, however, reveals certain discrepancies which warrant further attention. The first of these is that

up to a cell height of 10 cm the droplet size decreases with increasing nozzle voltage at a slower rate and to a lesser degree under multidroplet conditions. A possible explanation of this could be that the presence of a population of droplets between the electrodes tends to distribute space charge more uniformly and thus reduces the magnitude of the field enhancement at the electrodes. This hypothesis will be discussed later but certainly such a situation would cause a reduction in the electrostatic force on the charged droplet at the nozzle and in consequence cause an increase in the size of droplet detaching from the nozzle. The second point of note is that if the mean droplet size is plotted against column height for several different nominal field strengths a family of curves can be drawn with field strength as parameter (Fig 8b). Interestingly the minimum in each of these curves occurs at a cell height of about 10 cm which is also the height at which the mass transfer performance of the cell improved most rapidly with applied voltage. The single droplet data can in fact be plotted the same way and shown to have minima at a column height of 7 cm (Fig 8a). As yet, however, insufficient data are available to attach any significance to this finding.

Despite the use of the guard electrode which surrounded the nozzles the falling droplets still diverged visibly whilst passing through the cell. This was due to the charged droplets exerting a repulsive force on each other which depended upon the magnitude of the charge and the interdroplet distance. Strictly speaking, this force cannot be estimated from the simple Coulomb law for point charges, since for particles which are close together in relation to their diameter the force depends on the nature of the particle as well. Due to charge mobility, the charges on a conducting droplet may also migrate over the surface away from those of the same sign on a neighbouring droplet. In this way the charges tend to move further apart resulting in a lower repulsive force than that indicated by Coulomb's law, but nevertheless sufficient to account for the observed divergence of the droplet stream and the substantial absence of interdroplet coalescence over the low holdup range investigated in this study. The fact that the droplets do diverge and, in so doing, fill the column means that the droplets can be regarded as being uniformly distributed over the column cross-section and consequently the fractional holdup can be converted with negligible error into a mean droplet slip velocity using equation (1). This approximation

was valid for all the cell heights except the shortest where little divergence of the droplet stream occurred; dispersed phase holdup was also difficult to measure in this region.

It has already been shown that the nominal field strength bears little relation to the actual field strength experienced by a droplet during the various stages in its history. It might be advantageous therefore, to seek a correlation between droplet behaviour and droplet size since the observed droplet size reflects the way in which the actual field in the vicinity of the nozzle changes as the nominal field strength is increased. This alternative approach should make it possible to relate the behaviour of a population of droplets to that of a single droplet in a two electrode system.

If the voltage profile between the electrodes is of the general form shown in Fig. 7 then a single droplet forms at the charging nozzle under the influence of an average field strength E_I , and after detachment falls under the influence of an average field strength E_B . In a multidroplet situation the space between the two electrodes contains a population of charged droplets which modifies the space charge distribution and hence the voltage profile between the electrodes. If therefore in both single and multidroplet situations, the detached droplet size is the same for a particular liquid/liquid system, nozzle size and flowrate then it could be argued that the average effective field strength (E_I) is also the same in each case, although the nominal applied field strengths may differ. On the other hand, the field strengths in the bulk continuous phase (E_B) will almost certainly differ because of the dissimilar space charged distributions. These conditions are illustrated diagrammatically in figure 9.

In a single droplet situation, the observed droplet size detaching from the nozzle would be expected to be a function of the nozzle size, the phase flowrate, the magnitude of the droplet charge, the inducing field, the acceleration due to gravity and the physical properties of the system, thus:

$$d_e = f_I (D_N, L_d, Q, E_I, g, \rho) \dots\dots\dots(2)$$

This expression may be simplified by noting that the charge Q is a unique function of d_e for any one system and nozzle size⁽²⁾. Furthermore if the concentration of ionic impurities is small it is not unreasonable to suppose that the inducing field will depend upon the nominal field and the inter-

electrode distance so that:

$$E_I = f_2 (E_{Nom}, L) \dots\dots\dots(3)$$

On this basis, it will be apparent that:

$$d_e = f_3 (E_{Nom}, L) \dots\dots\dots(4)$$

for a given system, nozzle size and dispersed phase flowrate. This is borne out by the family of curves shown in Fig. 8a.

A similar line of reasoning is applicable to the present work where a multi-nozzle assembly was employed. It should be noted however that the inducing field will now also depend upon the geometrical arrangement of the nozzles so that the analogue of equation (4):

$$\bar{d}_e = f_4 (E_{Nom}, L) \dots\dots\dots(5)$$

will have the additional restriction that it is only applicable to a particular nozzle geometry. Again the form of dependence indicated by equation (5) is confirmed by the data shown in Fig. 8b. The somewhat larger droplets observed under multidroplet conditions has already been referred to above. In addition to the possibility of a reduced space charge effect, a secondary factor may be a reduction in the effective inducing field due to the fact each nozzle is surrounded by others charged to the same potential. Both these effects require further study before equations (2)-(5) can be written in a more explicit form.

The velocity of a single charged droplet relative to the continuous phase would be expected to depend upon the droplet size, the physical properties of the two phases, the droplet charge, the electric field in which the droplet is moving and the acceleration due to gravity, i. e.

$$U_s = f_5 (d_e, \vartheta, Q, E_B, g) \dots\dots\dots(6)$$

Noting the unique dependence of Q upon d_e for a given system and nozzle size, it will be seen that U_s should exhibit a functional dependence upon d_e and E_B .

In multidroplet situations, two additional factors arise which can influence the average droplet velocity. One is the hindered settling effect associated with a finite population of droplets. The other is the field effect due to the spatial distribution of the charged droplets. If it is assumed that the former is an analogous effect to that found in uncharged spray systems, the hindered settling effect will be well represented ⁽³⁾ by the holdup function (1 - x). The field effect is more difficult to quantify but would be expected to be related to the magnitude and distribution of the charges carried by the

droplets. This effect of bulk charge will be additional to space charge effects due to ionic impurities. A rigorous analysis of droplet velocities would call for a separate evaluation of these field effects. Since this has not been attempted, a theoretical analysis of the problem is not yet possible.

In the present work however, some simplification is possible since all the runs were carried out at low values of the dispersed phase holdup (less than 5.6%). Under these conditions, the hindered settling effect will be negligible and the way in which the bulk field is modified by the charged droplets should not fluctuate over wide limits. With this simplification in mind, it would again be expected that U_S^* would approximate to a function of \bar{d}_e and the bulk field strength. In practice however, the velocity was substantially independent of the bulk field and correlated well with droplet size (Figs. 10(a) and (b) for single and multidroplet systems respectively. The former data were taken from hitherto unpublished measurements by the present authors). This effect is not yet fully understood but may be due to partially compensating changes in the gravitational and electrostatic forces acting on the droplets. Figure 10 (b) shows the single droplet curve for comparison and it will be seen that the multidroplet velocities are higher than the single droplet values at corresponding droplet sizes. Since, under the present conditions, droplets of the same size carry the same charge it would appear that the effective bulk field strength is higher in the multidroplet situation.

These findings relate of course to the particular extraction system studied. At larger values of the dispersed phase holdup at least two further complications will arise. Firstly, the hindered settling term will become progressively more important and would be expected to counteract the increase in slip velocity caused by the enhanced electric field strength. Secondly the risk of an electrical short circuit between the electrodes will be increased. It has been shown⁽⁴⁾, however, that this restriction can be minimised by introducing a nitrogen filled gap between the nozzles and the bulk continuous phase.

Although the primary object of the present work was to compare the observed droplet sizes and velocities for single and multidroplet systems, the number of "overall" dispersed phase transfer units were also determined

for a range of nominal field strengths and cell heights. In the present context, the term "overall" is used to denote the combined mass transfer occurring at the nozzle, during free fall and after coalescence of the droplets at the bottom of the cell. The data are shown in graphical form in Fig.6. By comparison with the previous single droplet measurements⁽¹⁾ it will be seen that whilst the data are comparable the values of $(NTU)_{do}$ are up to 50% greater. Furthermore at an inter-electrode gap of 10 cm., the number of transfer units increases very rapidly with progressive increases in the nominal field strength. From a practical point of view, the latter finding is significant and indicates that considerable advantages may accrue from operating at a specific inter-electrode gap. A full interpretation of these measurements together with a discussion of the applicability of certain mass transfer models will be dealt with subsequently in Part III of the present paper.

CONCLUSIONS

The behaviour of a population of charged droplets has been studied in a d.c. field and has been found to follow the general trends already reported for single droplet systems. The use of a multinozzle dispersed phase distributor gives rise to somewhat larger droplets by comparison with those produced at a single nozzle under similar conditions. Furthermore it is probable that a redistribution of space charge also occurs in multi-droplet systems in such a way that the average bulk field strength is enhanced by comparison with that associated with single charged droplets of the same size. The net effect is to enhance the average droplet velocity relative to the continuous phase. Under conditions of low dispersed phase holdup, the average droplet velocity has been shown to be a unique function of the droplet size.

There also appears to be an optimum electrode spacing at which the number of dispersed phase transfer units increases very rapidly with applied voltage. This effect is important in connection with the development of commercial contactors and merits further attention.

ACKNOWLEDGMENT

We are indebted to the Science Research Council for financial support during the course of this work.

NOMENCLATURE

- d_e Equivalent spherical droplet diameter (single droplets).
- \bar{d}_e Mean equivalent spherical droplet diameter (multidroplet systems).
- D_N Nozzle diameter.
- E_I Average inducing field strength at the nozzle.
- E_B Average bulk field strength between the electrodes.
- E_{Nom} Nominal field strength.
- f_1 -- f_5 Functions.
- g Acceleration due to gravity.
- L Inter-electrode distance.
- L_d Volumetric flowrate of the dispersed phase.
- Q Droplet charge.
- U_s Velocity of a single charged droplet relative to the continuous phase.
- U_s^* Average velocity of a population of charged droplets relative to the continuous phase.
- V_d, V_c Dispersed and continuous phase superficial velocities respectively.
- x Fractional holdup of the dispersed phase.
- \varnothing Denotes physical properties.

REFERENCES

1. Bailes, P. J., and Thornton, J. D., Proceedings of the International Solvent Extraction Conf., April 1971, p 1431.
2. Stewart, G., Ph.D. Thesis, Newcastle University, Newcastle upon Tyne (G.B.) 1970.
3. Thornton, J. D., Chem. Eng. Sci., 1956, 5, 201. (Cf also Hughmark, G.A., Ind. Eng. Chem. Fundamentals, 1967, 6, 408.
4. Bailes, P. J., Paper presented at CHISA, Czechoslovakia, September 1972.

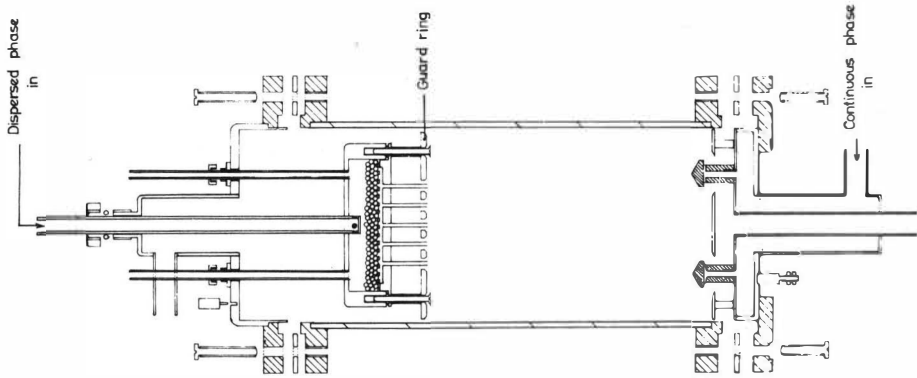


FIGURE 1 Multiple nozzle extraction cell

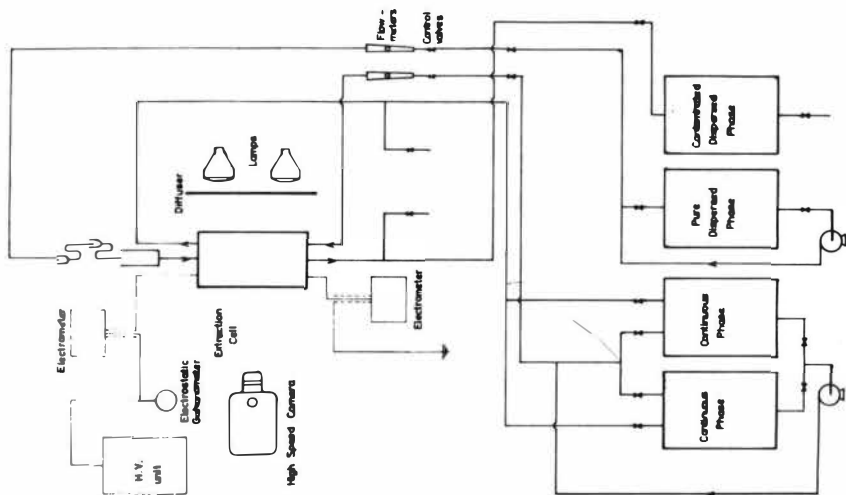


FIGURE 2 Schematic Diagram of Experimental Apparatus

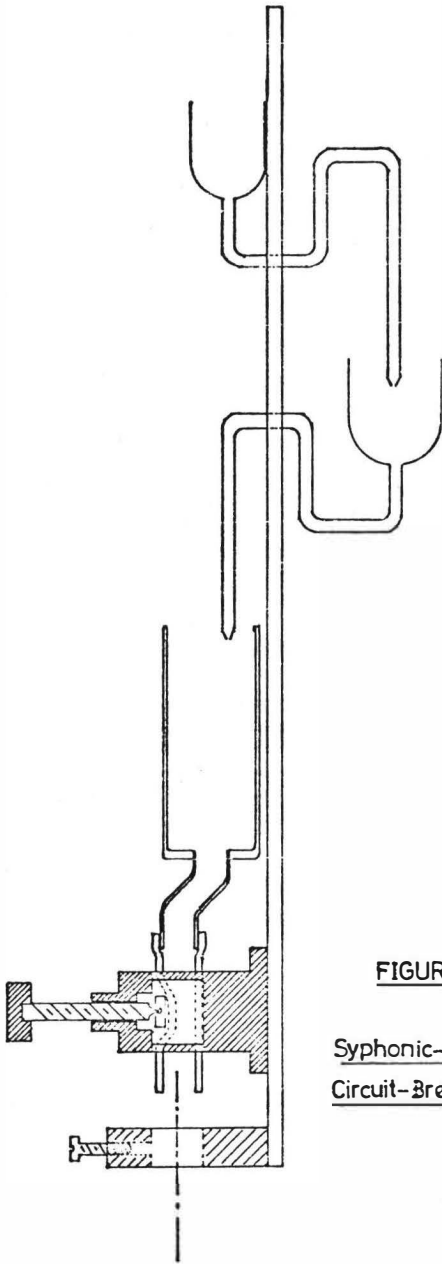


FIGURE 3

Syphonic-Action, Electrical
Circuit-Breaker

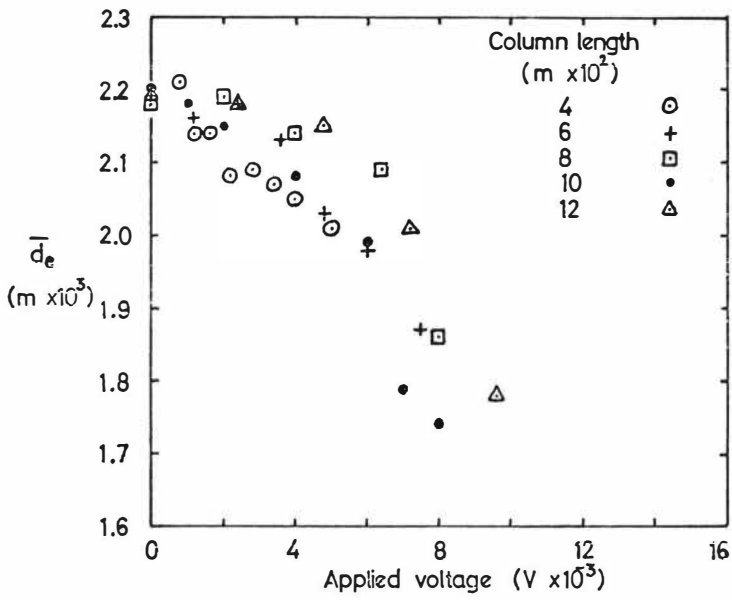


FIGURE 4 Effect of applied voltage on mean droplet size for different column lengths

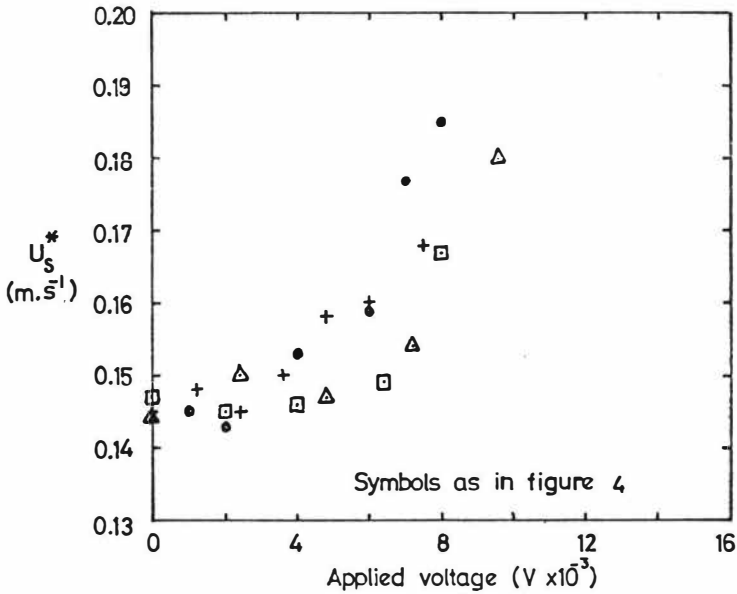


FIGURE 5 Mean slip velocity plotted against applied potential difference for various column lengths

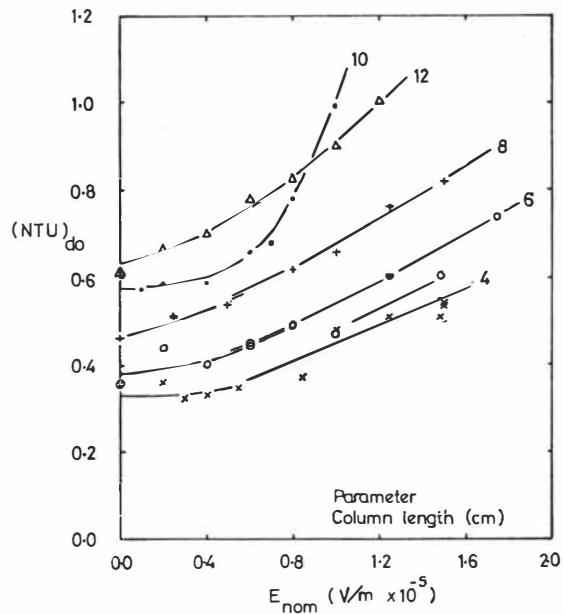


FIGURE 6 Number of dispersed phase transfer units plotted against nominal field strength for different column lengths

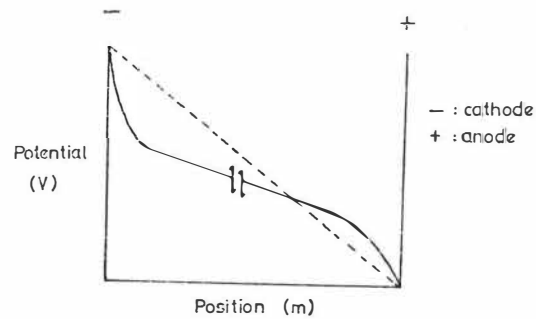


FIGURE 7 Potential distribution in a liquid dielectric

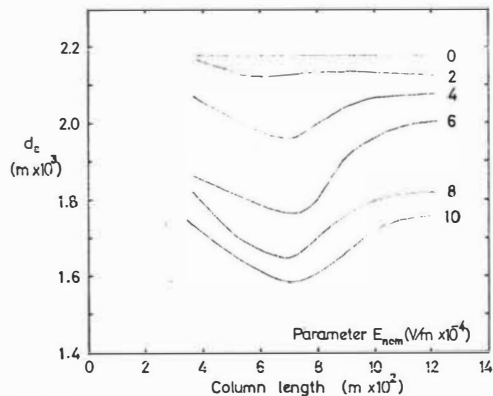


FIGURE 8a Interpolated droplet size data showing optimum column length for single droplets

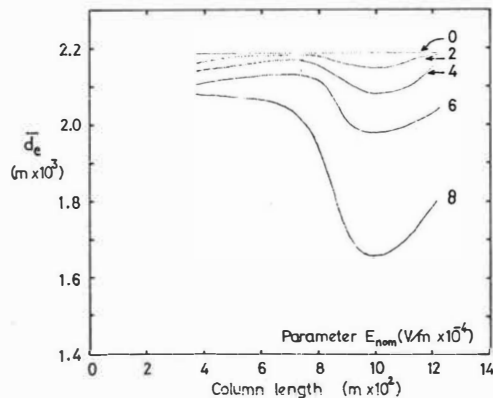


FIGURE 8b Interpolated mean droplet size data showing optimum column length for multidroplets

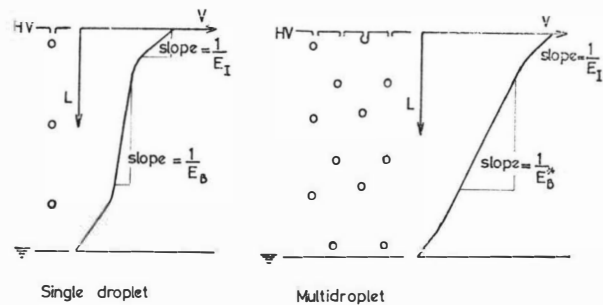


FIGURE 9 Hypothetical voltage profiles in both single and multidroplet situations

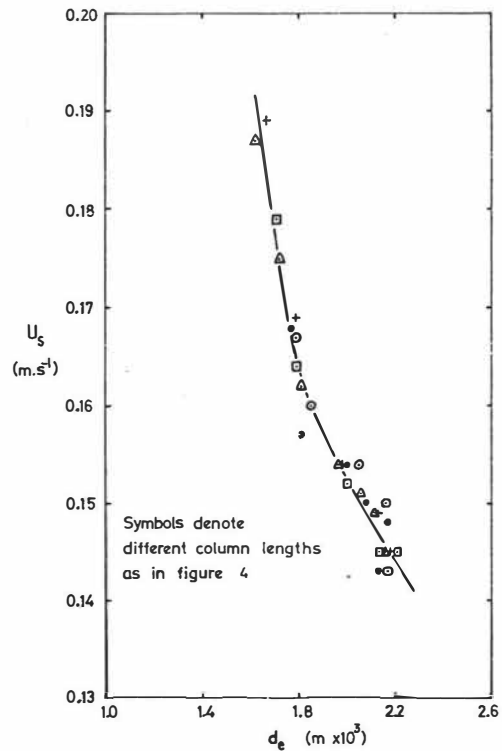


FIGURE 10a Single droplet velocity plotted against droplet diameter

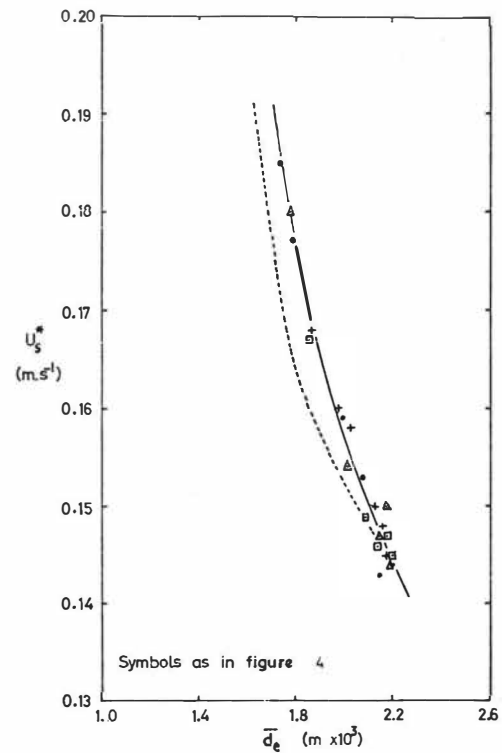


FIGURE 10b Mean slip velocity plotted against mean droplet diameter
(---- Single droplet curve)

Effect of electric field on mass transfer
across a plane interface

P.V.R. Iyer* and H. Sawistowski

Department of Chemical Engineering and Chemical Technology

Imperial College of Science and Technology

London, SW7

Synopsis: It is shown that under suitable conditions the presence of electric charges in the interface may lead to the appearance of Marangoni-type phenomena and hence to intensification of the rate of mass transfer. The presence of the phenomena has been confirmed visually by observation in a scalieren field and experimentally by their effect on mass transfer coefficients determined in a horizontal laminar contactor for transfer in partially miscible binary systems and of solute between two immiscible solvents. Increases in mass transfer rates of 20% to 1000% were observed depending on type of system, direction of transfer and polarity of interfacial charges. The mechanism of transfer was found to be more complex than anticipated by movement of charges in the bulk of the non-conducting phase.

*Present address: Department of Chemical Engineering,
Indian Institute of Technology,
New Delhi

Introduction

The rate of mass transfer in liquid-liquid extraction is proportional to the mass transfer coefficient, the interfacial area and the driving force. At a fixed driving force any attempt to increase the transfer rate must, therefore, be directed towards increasing the other two factors. In equipment with unsupported interfacial area, the area can be increased by the formation of smaller drops and hence producing a better surface to volume ratio. In contactors with supported interfacial area the same effect is obtained by spreading the film over a large support area. Mass transfer coefficients can in turn be increased by the application of mechanical energy as, for instance, in pulsed columns or stirred vessels. There is also the well known fact of a spontaneous increase in mass transfer coefficients due to the presence of the Marangoni effect.

The Marangoni effect is a surface flow resulting from the appearance in the interface of an interfacial tension gradient. Since interfacial tension γ is a function of solute concentration C at the interface, of interfacial temperature θ and of the surface density σ of electric charges, therefore

$$d\gamma_{\infty} = (\partial\gamma_{\infty}/\partial C) dC + (\partial\gamma_{\infty}/\partial\theta) d\theta + (\partial\gamma_{\infty}/\partial\sigma) d\sigma \quad (1)$$

$$\begin{aligned} \text{and} \quad d\gamma_{\infty}/dy &= (\partial\gamma_{\infty}/\partial C)(dC/dy) + (\partial\gamma_{\infty}/\partial\theta)(d\theta/dy) + \\ &+ (\partial\gamma_{\infty}/\partial\sigma)(d\sigma/dy) \end{aligned} \quad (2)$$

Hence, a gradient of static interfacial tension γ_{∞} will appear, which will be equal to the gradient of the dynamic interfacial tension γ if the interface is Newtonian and dynamic effects of compression and dilation can be neglected, when there exists in the interface a concentration

gradient, a temperature gradient and/or a gradient of density of electrostatic charges. Under suitable conditions, when local perturbations in solute concentration, temperature and/or density of electrostatic charges become amplified, the resulting gradients in interfacial tension produce a surface-tension induced or Marangoni instability. This spontaneous phenomenon leads to significant intensification of mass transfer rates.

Effect of charges on interfacial tension

The variation of static surface tension with electrostatic charge can be predicted theoretically for certain geometric configurations, e.g. for an isolated charged drop carrying a charge Q it is¹

$$\gamma_{\infty} = \gamma_{\infty}' - 5\sigma^2 d/4\epsilon\epsilon_0 \quad (3)$$

where γ_{∞}' is the static surface tension at $Q = 0$, d is the drop diameter, ϵ is the dielectric constant and ϵ_0 is the permittivity of free space.

The results of an experimental estimation² of the dependence of interfacial tension on applied voltage is shown in Fig. 1. This is the so-called electrocapillary curve. A drop of water was formed at the tip of a capillary placed centrally in a cubical glass enclosure filled with benzene. A wire passing centrally through the capillary formed one electrode while the second electrode, which was earthed, was created by a thin film of carbon deposited on the glass. The interfacial tension was estimated from photographs using the method of Andreas, Hauser and Tucker³. It was noted that Marangoni-type disturbances occurred at voltages above 1500V caused probably by non-uniformity of the field and deviation of the drop from spherical shape.

Effect of electric field on mass transfer in binary systems

The application of electric field towards intensification of mass transfer rates has already been reported^{4,5} in literature. It relied on the fact that the maximum drop size decreased on decrease in effective interfacial tension due to increase in charge density. This produced a higher surface to volume ratio and, in addition, for a given drop size promoted drop oscillations thus leading to higher mass transfer coefficients. The latter was also improved by increase in drop velocities resulting from electrical forces of attraction exerted on the drop in the direction of its motion.

The type of phenomena described above were not investigated in the present work. It was limited exclusively to the application of electric potential across a flat interface. In a system consisting of a conducting and a non-conducting phase such applied charges accumulated in the interface. Conditions are thus established in which, as a result of the electrocapillary effect, any perturbation in σ could lead to Marangoni instabilities. This proposition was initially tested on four binary systems⁶: cyclohexanol/water, isobutanol/water, aniline/water and ethyl acetate/water. In the absence of the field the systems were stable or weakly unstable. It was found that application of potential across the interface, that is between the interface and the upper electrode, produced interfacial activity of very high intensity, which resulted in up to a tenfold increase in mass transfer coefficients (Fig. 2). The mass transfer coefficients were determined in a horizontal countercurrent contactor fitted with two electrodes placed about 30 mm above and below the interface. The lower electrode was charged and the upper electrode earthed. The flow of the two phases was laminar throughout. The contactor was placed in a schlieren field to facilitate simultaneous visual observation.

In general the results seemed to support the supposition of introduction or intensification of Marangoni instabilities by application of electrostatic field. However, certain evidence was produced which did not support such a simple explanation. Thus, as expected, interfacial turbulence was initiated at the interface (Fig. 3) and stayed there for low values of applied potential. But, in the aqueous-organic systems employed, it even then seemed to be confined largely to the organic phase. Increase in applied potential led predominantly to further expansion of the zone of interfacial turbulence into the organic phase (Fig. 4 and 5). Consequently, additional work was required for further elucidation of the phenomena involved. This took the form of studying the effect of polarity of the lower electrode and of investigating the phenomena in ternary systems, that is for transfer of a solute between two immiscible solvents.

Effect of polarity of interface

A qualitative and quantitative investigation was conducted of the effect of polarity of the lower electrode. In the qualitative study a schlieren cell, 77 mm high, 99 mm long and 49 mm wide, was employed⁷ for visual observation in a schlieren field. The cell was fitted with flat copper gauze electrodes, the lower electrode resting on the cell floor and the upper suspended horizontally near the top of the cell. The interface was usually positioned centrally about 30 mm from each electrode. Charge was applied to the lower electrode from a constant-voltage photomultiplier power supply unit, Brandenburg model 471R, and the upper electrode was earthed. An electrostatic voltmeter, in series with a resistor of $1M\Omega$, was connected across the cell to measure the applied voltage. The circuit was also fitted with an ammeter.

Twelve binary systems were selected for qualitative studies. Nine of these were organic/water systems, with the organic phase being amyl

acetate, n-butyl acetate, ethyl acetate, methyl acetate, cyclohexanol, isobutanol, n-butanol, n-hexanol and amyl alcohol. The remaining three systems were hexane/aniline, toluene/formic acid and benzene/formic acid. Observations were made for each system at various voltages. Photographs of observed phenomena were taken using a box camera and employing R20 panchromatic film at exposure time of 0.005s. The experiments were repeated by presaturating each of the phases in turn and also by changing the polarity of the lower electrode.

All systems which were interfacially stable in the absence of a field showed interfacial instabilities on application of an electric field of 0.5 kV (0.7 kV for cyclohexanol/water). Higher voltages resulted generally in stronger instabilities which progressed to turbulence in the non-conducting phase. Similarly, for systems which were already unstable in the absence of a field, introduction of charge at the interface made the instabilities more pronounced. In most cases instabilities were initiated by the applied voltage at the interface. There were, however, systems in which they originated in the bulk, as e.g. in the toluene phase of the system toluene/formic acid. The system n-butanol/water represented an interesting case in this respect: for negative polarity disturbances first appeared in the bulk at 400 V, but for positive polarity they originated at the interface at 1000 V.

No general trend was noticed with respect to polarity. The behaviour of some systems was independent of polarity, some showed stronger disturbances with positive polarity (isobutanol/water, amyl alcohol/water, methyl acetate/water), while others exhibited stronger disturbances with negative polarity (n-butyl acetate/water). There existed also a directional effect observable with presaturation of one of the phases. Thus, e.g. transfer of amyl alcohol into water was less affected by the field than transfer of water into amyl alcohol.

The mass transfer experiments were conducted in a countercurrent contactor 149 mm long, 13.5 mm wide and 61 mm high. The low width was conditioned by the optical demands of a schlieren field. Very low flow rates were employed (Reynolds number around 20) to obtain measurable values of mass transfer coefficients and their volumetric values were kept approximately the same in both phases to ensure central positioning of the interface. Figs. 6 to 9 show the results obtained for the systems isobutanol/water and ethyl acetate/water for conditions of presaturation of either phase. With the isobutanol phase presaturated (Fig. 6), that is transfer of isobutanol into water, the mass transfer coefficient was affected very little. Disturbances were noticed in the bulk of the organic phase at 0.5 kV which did not affect the interface. (The potential quoted is the applied field voltage. Its limited range of 0.7 kV is due to a flow of current of 2 mA which reduced the voltage produced by the power supply unit.) For the transfer of water from the presaturated aqueous phase into isobutanol (Fig. 7) there was a pronounced effect of positive polarity but weak effect of negative polarity. Visually, positive polarity produced interfacial turbulence restricted to interfacial regions at 0.3 kV (Fig. 5) which increased in intensity with increase in applied potential and gradually extended into the bulk of the organic phase. With negative polarity bulk disturbances were noticed at a field voltage of 0.5 kV which, beyond 0.7 kV, extended to the interface. The interfacial turbulence was however much less vigorous.

In the system ethyl acetate/water the mass transfer coefficient increases with applied potential in both directions of transfer. However, there was no effect of polarity in the transfer of water but a measurable difference for the transfer of the ester. For the latter eddies were observed to appear in the bulk of the organic phase at 0.3 kV and move across the interface thus continually renewing it. The intensity of

this movement increased with applied potential. For the transfer of water interfacial turbulence appeared at 0.9 kV for positive polarity and weak turbulence in the bulk of the organic phase for 0.6 kV negative polarity. Both effects increased with applied voltage.

Visual observations of the effects of direction of transfer and polarity indicate thus that there exist at least two separate phenomena affecting the rate of mass transfer: interfacial turbulence and movement of charges. Their relative contribution to the net effect, is however, still obscure.

Effect on mass transfer in ternary systems

As in the previous study quantitative work was supported by qualitative observation⁸. For the latter a schlieren set up was employed using the same cell as previously described. The system toluene/water was selected with propionic acid and acetone as solutes. The assessment of results is complicated in such systems since in addition to Marangoni instability there may also exist a gravitational instability. Thus, e.g. the transfer of propionic acid from water into toluene is gravitationally stable but Marangoni unstable, as predicted by the Sternling-Scriven criterion⁹. Conversely, transfer of propionic acid in the reverse direction is Marangoni-stable but gravitationally unstable in both phases. In both cases the presence of additional effects due to the applied electric field is thus to a certain extent obscured. However, mild interfacial turbulence was observed at 0.3 kV for transfer into toluene, which gradually spread into the bulk of the toluene phase with increased voltage. The effect was more pronounced for positive than negative polarity. For transfer into water interfacial turbulence was observed at 1.0 kV and there was little difference between positive and negative polarity. However, the presence of interfacial turbulence seemed to reduce

the intensity of gravitational instability in the toluene phase (Fig. 10).

For the transfer of acetone from toluene into water the system is Marangoni stable and gravitationally stable in both phases. The reverse direction of transfer is gravitationally unstable in both phases as well as Marangoni unstable. In such a case it is difficult to observe any effects due to electric charges but additional interfacial turbulence seemed to have appeared at 1.0 kV. For the transfer of acetone into water interfacial instability was first observed at 0.4 kV which increased in intensity with applied voltage. However, it also became time dependent and gradually disappeared.

The quantitative work was conducted in a cylindrical countercurrent glass contactor 258 mm long and 52 mm in diameter. The contactor was fitted with flat stainless steel electrodes held in position by means of short tungsten rods fused into the glass. Again the top electrode was earthed. The mass transfer results obtained are shown in Figs. 11 to 14. The intensification of mass transfer was much less pronounced than in the case of binary systems particularly for the non-polar acetone. For the transfer of acetone from toluene into water there also appeared a local maximum in the variation of mass transfer coefficient with applied voltage. This was connected with the time decay of charge-induced interfacial activity previously observed at high applied potentials. No improvement in performance was obtained by on-off application of voltage or the use of multipoint electrodes¹⁰.

Conclusions

The results obtained from the study of polarity and directional effects in the application of electric field across an interface under conditions of mass transfer indicate that the initial supposition of introduction or intensification of Marangoni instabilities is unable alone to explain the

observed phenomena. Their concentration in the nonconducting phase together with the effect of polarity and direction of mass transfer indicates the presence of additional effects such as ionization and movement of charges. The increase in mass transfer coefficients is the net result of all such effects and their interaction is not yet sufficiently understood to produce a criterion for selection of systems in which mass transfer could be maximised by the application of electric field.

Nomenclature

C	molar concentration
d	drop diameter
K_{OT}	overall mass transfer coefficient based on toluene phase
K_{OW}	overall mass transfer coefficient based on aqueous phase
K_1	mass transfer coefficient in the organic phase
K_2	mass transfer coefficient in the aqueous phase
V	applied potential
y	direction in the plane of the interface
γ_∞	static interfacial tension
ϵ	dielectric constant
ϵ_0	permittivity of free space
θ	temperature
σ	surface density of electric charges

References

1. Jeans, J., Mathematical Theory of Electricity and Magnetism, 5th Edn, 1951 (Cambridge: Cambridge University Press).
2. Dodson, M.G. and Harrison, G.W., B.Sc. report, Imperial College, London, 1968.

3. Andreas, J.M., Hauser, E.A., and Tucker, W.B., J. Phys. Chem. 1938, 42, 1001.
4. Stewart, G., and Thornton, J.D., Chem. Engng. Symp. Ser. Instn Chem. Engrs, 1967, 26, 29.
5. Stewart, G., and Thornton, J.D., Chem. Engng. Symp. Ser. Instn Chem. Engrs, 1967, 26, 37.
6. Austin, L.J., Banczyk, L., and Sawistowski, H., Chem. Engng Sci., 1971, 26, 2120.
7. Benebo, T.E.T., M.Sc. report, Imperial College, London, 1970.
8. Iyer, P.V.R., M.Sc. report, Imperial College, London, 1971.
9. Sternling, C.V., and Scriven, L.E., A.I.Ch.E. Jl, 1959, 5, 514.
10. Holland, P.J., and McNee, I.C., B.Sc. report, Imperial College, London, 1972.

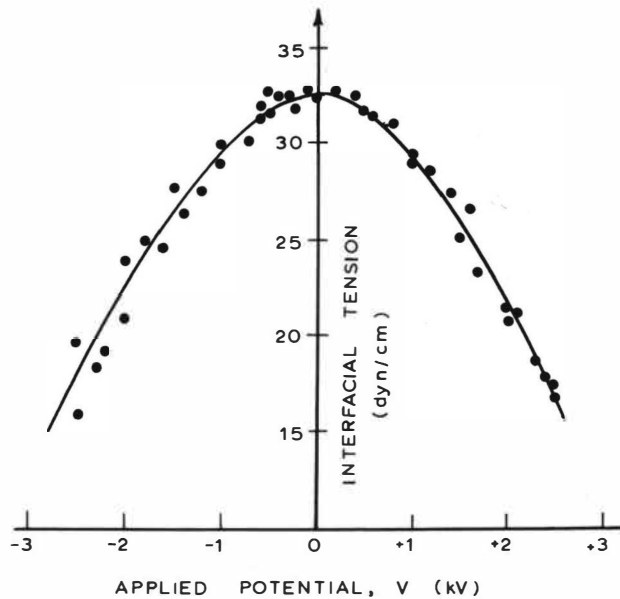


FIG. 1. ELECTROCAPILLARY EFFECT FOR THE SYSTEM BENZENE/WATER.

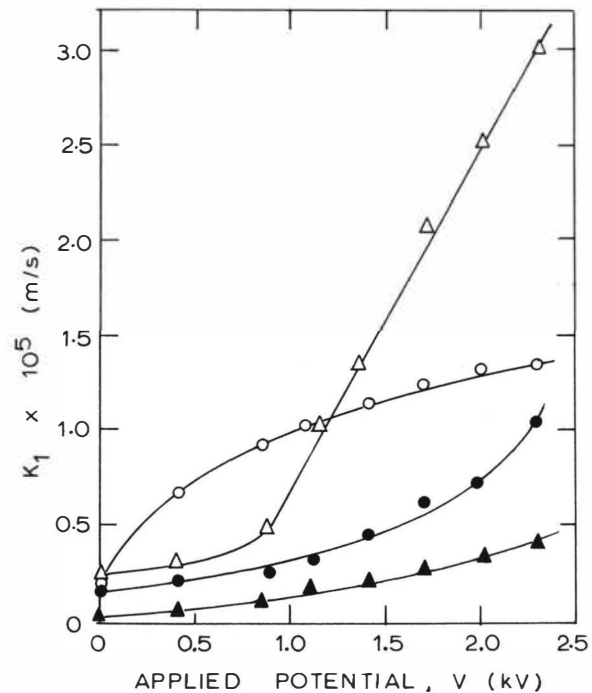


FIG. 2. EFFECT OF APPLIED VOLTAGE ON MASS TRANSFER COEFFICIENT OF WATER IN THE ORGANIC PHASE. (▲ CYCLOHEXANOL/WATER, ● ISOBUTANOL/WATER, ○ ANILINE/WATER, △ ETHYL ACETATE/WATER)

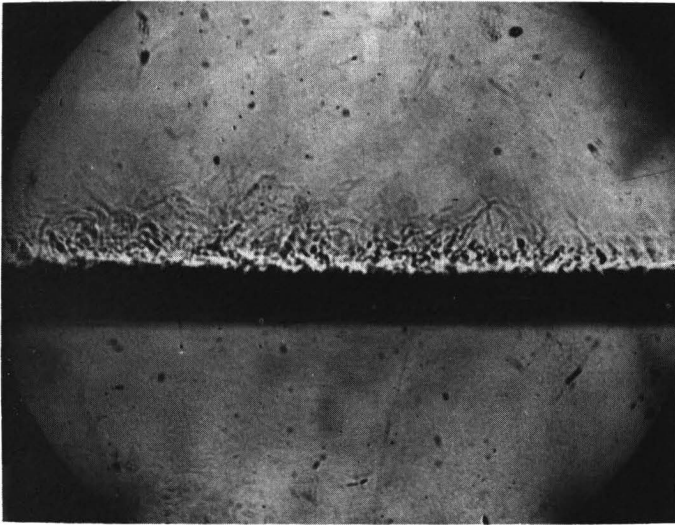


FIG. 3. SCHLIEREN PHOTOGRAPH OF MASS TRANSFER IN ISOBUTANOL/
WATER SYSTEM AT 0.45 KV.

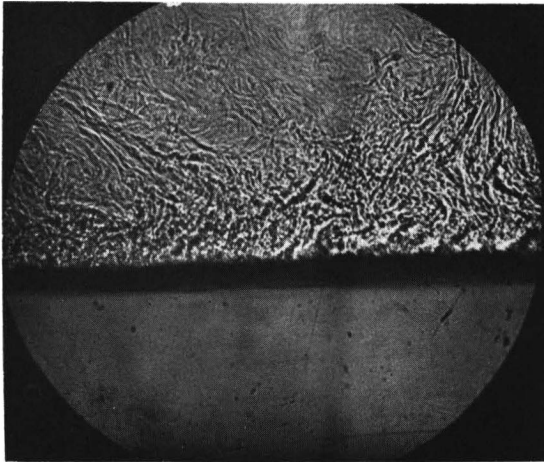


FIG. 4. SCHLIEREN PHOTOGRAPH OF MASS TRANSFER IN ISOBUTANOL/
WATER SYSTEM AT 0.85 KV.

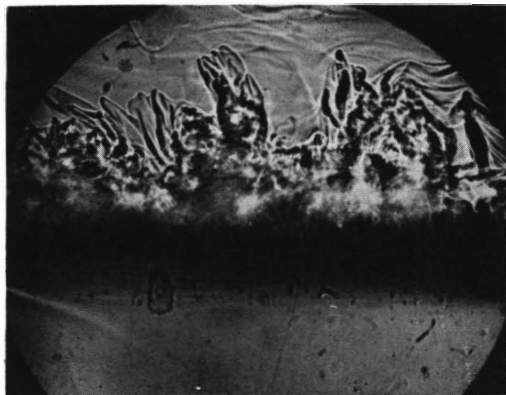


FIG. 5. SCHLIEREN PHOTOGRAPH OF MASS TRANSFER IN CYCLO-
HEXANOL/WATER SYSTEM AT 0.80 KV.

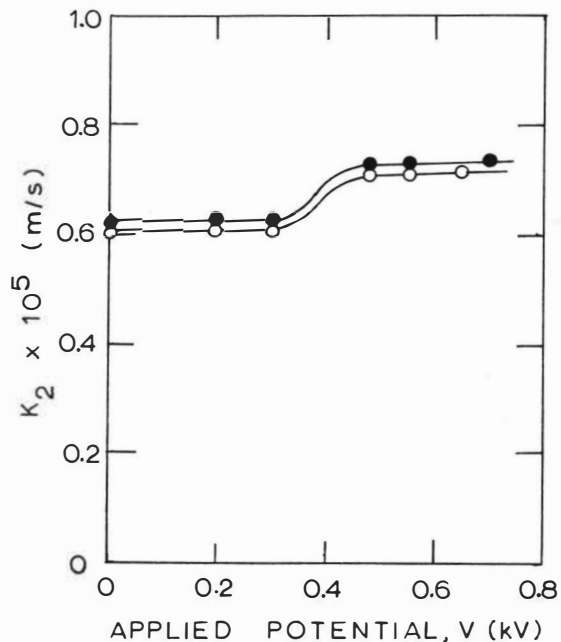


FIG. 6. MASS TRANSFER COEFFICIENT OF ISOBUTANOL
FOR TRANSFER INTO SOLUTE-FREE WATER FROM A PRESAT-
URATED ISOBUTANOL PHASE. (O POSITIVE POLA-
RITY, ● NEGATIVE POLARITY)

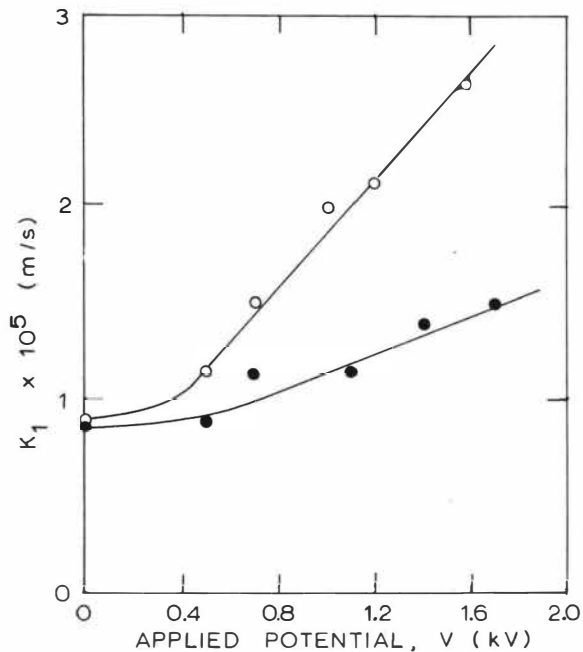


FIG. 7. MASS TRANSFER COEFFICIENT OF WATER FOR TRANSFER INTO SOLUTE-FREE ISOBUTANOL FROM A PRESATURATED AQUEOUS PHASE. (○ POSITIVE POLARITY, ● NEGATIVE POLARITY)

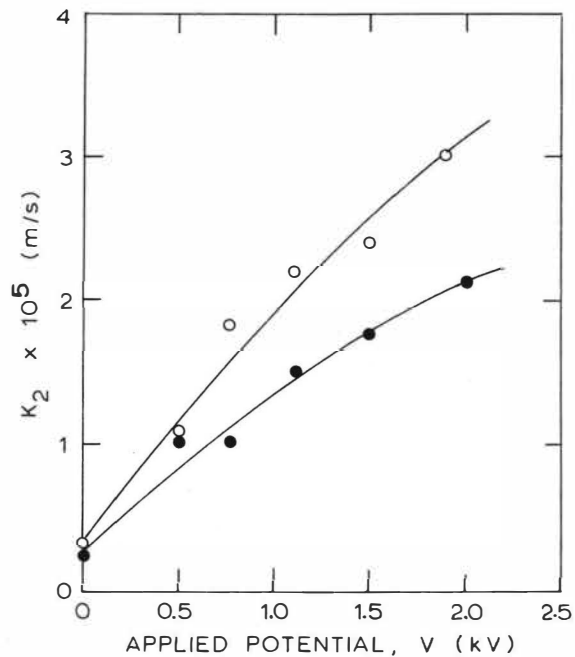


FIG. 8. MASS TRANSFER COEFFICIENT OF ETHYL ACETATE FOR TRANSFER INTO SOLUTE-FREE WATER FROM A PRESATURATED ETHYL ACETATE PHASE. (○ POSITIVE POLARITY, ● NEGATIVE POLARITY)

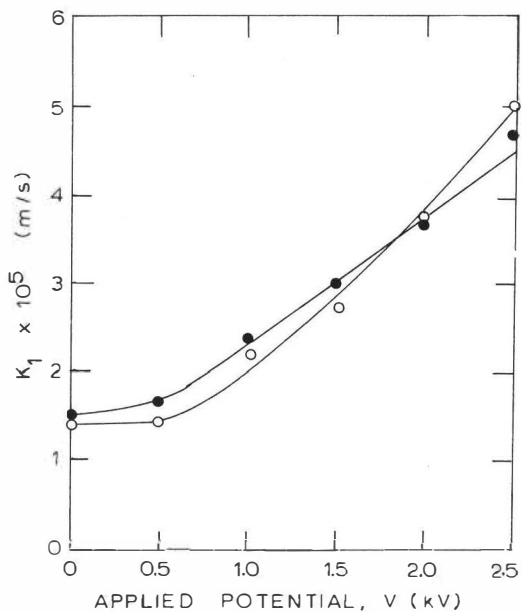


FIG. 9. MASS TRANSFER COEFFICIENT OF WATER FOR TRANSFER INTO SOLUTE-FREE ETHYL ACETATE FROM A PRESATURATED AQUEOUS PHASE. (○ POSITIVE POLARITY, ● NEGATIVE POLARITY)

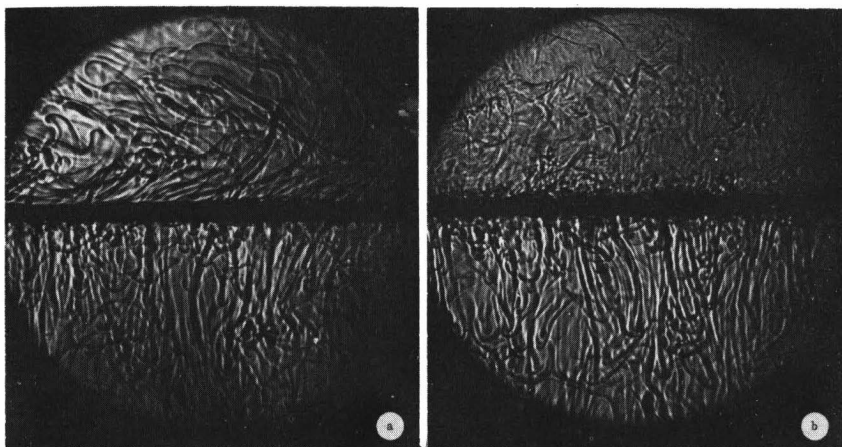


FIG. 10. SCHLIEREN PHOTOGRAPH FOR THE TRANSFER OF PROPIONIC ACID FROM TOLUENE INTO WATER AT APPLIED POTENTIAL OF (a) 0 V,

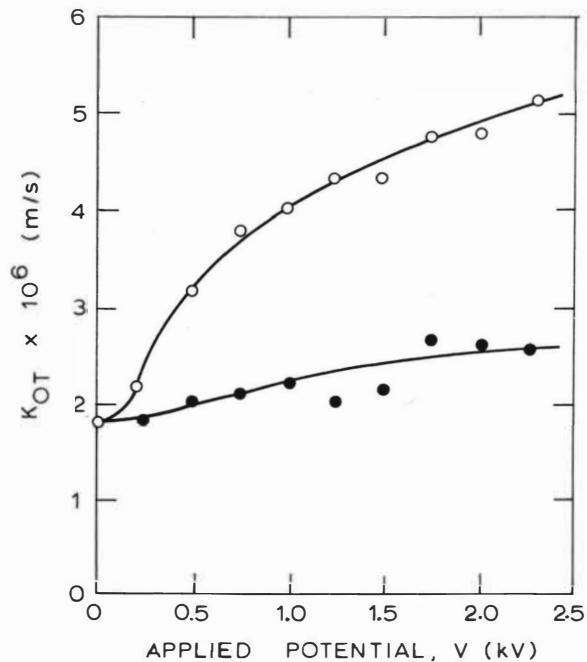


FIG. 11. EFFECT OF APPLIED VOLTAGE ON OVERALL MASS TRANSFER COEFFICIENT FOR THE TRANSFER OF PROPIONIC ACID FROM 1.0 M SOLUTION IN WATER INTO INITIALLY SOLUTE-FREE TOLUENE. (O POSITIVE POLARITY, ● NEGATIVE POLARITY)

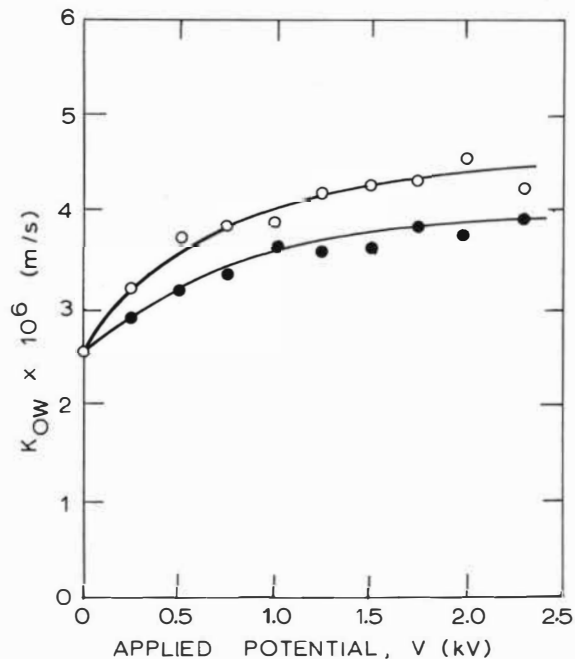


FIG. 12. EFFECT OF APPLIED VOLTAGE ON OVERALL MASS TRANSFER COEFFICIENT FOR THE TRANSFER OF PROPIONIC ACID FROM 0.66 M SOLUTION IN TOLUENE INTO INITIALLY SOLUTE-FREE WATER. (O POSITIVE POLARITY, ● NEGATIVE POLARITY)

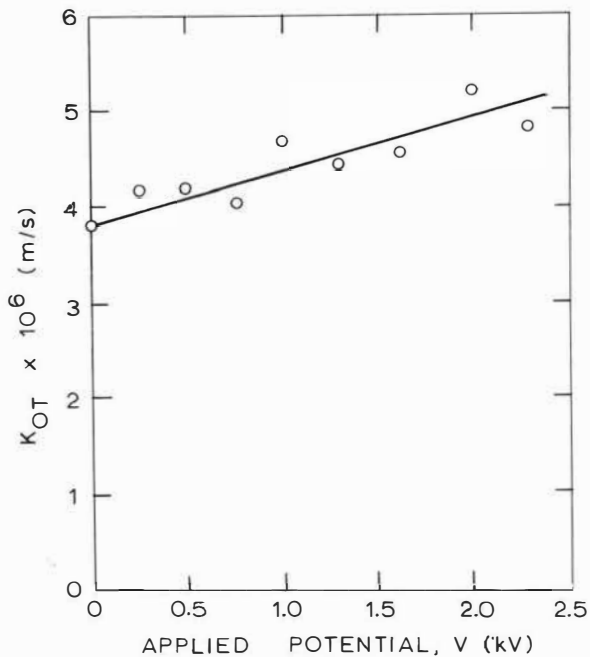


FIG. 13. EFFECT OF APPLIED VOLTAGE OF POSITIVE POLARITY ON OVERALL MASS TRANSFER COEFFICIENT FOR THE TRANSFER OF ACETONE FROM 0.7 M SOLUTION IN WATER INTO 0.06 M SOLUTION IN TOLUENE.

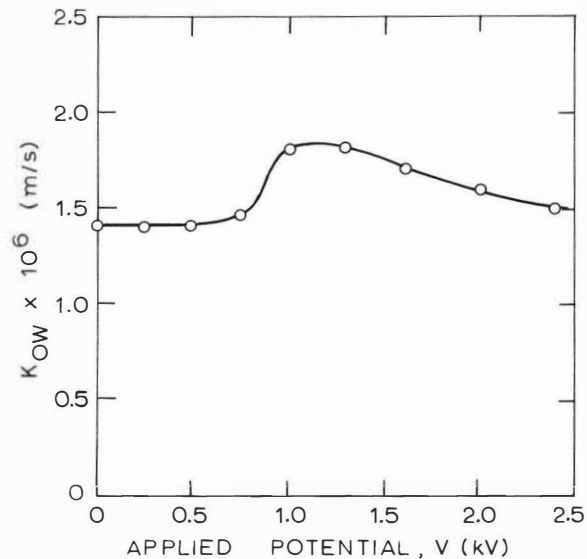


FIG. 14. EFFECT OF APPLIED VOLTAGE OF POSITIVE POLARITY ON OVERALL MASS TRANSFER COEFFICIENT FOR THE TRANSFER OF ACETONE FROM 0.45 M SOLUTION IN TOLUENE INTO INITIALLY SOLUT-FREE WATER.

SINGLE DROP OSCILLATIONS AND MASS TRANSFER

P. Nekovář and V. Vacek

Chem. Eng. Dept., Prague Institute of Chemical Technology and
Institute of Inorganic Chemistry, Czech Academy of Sciences, Řež

An investigation of drop shapes and drop velocity was carried out for single oscillating drops falling through a stationary liquid continuous phase. Mutually saturated two component systems were studied as well as systems with a third component transferring from the drops. A novel technique was used to determine mass transfer rates.

Introduction

In certain cases of steady drop motion through motionless continuous phase, drop shape periodically changes. Drop shapes are complex and reveal complicated flow fields inside as well as outside the drop. A theoretical analysis does not exist at the present time^(1,2) which enables us to decide whether a given drop will oscillate, and to predict the frequency and the intensity of these oscillations. The frequency is usually correlated by empirical relationships^(2,3), which are based on theoretical analyses of infinitesimally small oscillations of motionless liquid spheres^(4,5). There is no information in the literature on the effect of a third, transferring component on frequency and intensity of oscillation. Further, no experimental data are available for the time dependence of the drop surface area during the oscillation period. The following relation is mostly assumed⁽⁶⁾ to hold:

$$A(t) = A_0 (1 + E \sin(\pi t/T)) \quad t \leq T \quad (1)$$

The value of the parameter $E = (A_{max} - A_0)/A_0$ is based on the maximum area of the spheroid. Drop volume V and the parameter E (which is defined as ratio of maximum horizontal to vertical diameters) are considered to be the same as for a spheroid. A_0 is the area of the sphere. From the general evaluation of theoretical treatments⁽⁶⁾ of mass transfer between oscillating drops and their surroundings we can assume that time variable area should be incorporated into these models to improve significantly agreement between empirical and theoretical data.

In this paper some experimental results on oscillating drops are presented. Two component systems without mass transfer as well as systems with the presence of a third component were studied. In addition to conventionally measured quantities such as average terminal velocity of the drop, v_t , and the drop oscillation period T , the time variations were determined of the instantaneous drop velocity, v , the parameter E and the surface area, A , during one oscillation period. The mass transfer coefficient over one oscillation period was also measured. In this paper we tried to compare the measured data with consequences of the approximation of the drop shape by a spheroid.

Theoretical part

The dependence of steady velocity of an oblate or prolate spheroid upon the parameter E was given by Luiz⁽⁷⁾. Assuming that the velocity of the oscillating drop motion at every moment equals the velocity of a spheroid with the same volume and E , then

$$\begin{cases} V(t) = v_t F(\bar{E}) / F(E(t)) & (2) \\ \text{where } \left\{ \begin{aligned} F(E) &= \frac{(E^2)^{1/2} - E \arcsin(1-E^2)^{1/2}}{\arcsin(1-E^2)^{1/2} - E(1-E^2)^{1/2}} \cdot \frac{1}{E} & , E < 1 \\ F(E) &= \frac{(E^2-1)^{1/2} - E \operatorname{arccosh} E}{\operatorname{arccosh} E - E(E^2-1)^{1/2}} \cdot \frac{1}{E} & , E > 1 \end{aligned} \right. \end{cases}$$

$$\bar{E} = (1/T) \int_{t_0}^{t_0+T} E(t) dt, \quad V_e = (1/T) \int_{t_0}^{t_0+T} V(t) dt$$

The spheroid area is given by the expression

$$A = 2\pi (3V/4\pi E)^{2/3} [1 + E^2(1-E^2)^{-1/2} \operatorname{arctgh} (1-E^2)^{1/2}], E < 1$$

$$A = 2\pi (3V/4\pi E)^{2/3} [1 + E^2(E^2-1)^{-1/2} \arcsin (E^2-1)^{1/2}/E], E > 1$$

We suppose that the oscillating drop as well as its surroundings are ideally mixed and concentrations inside and outside the drop are c_1 and c_2 , respectively. A film of thickness $x = r_2 - r_1$ exists at interfacial drop surface in which only molecular diffusion can occur. For a spherical drop with radius r_2 , the diffusion equation

$$\frac{\partial c}{\partial t} = D \left(\frac{\partial^2 c}{\partial r^2} + \frac{2}{r} \frac{\partial c}{\partial r} \right) \quad (4)$$

with conditions

$$C(r < r_1, t > 0) = C_1, \quad C(r_1 < r < r_2, t = 0) = C_1, \quad C(r > r_2, t \geq 0) = C_2 \quad (5)$$

has the following solution^(8,9,10)

$$C = \frac{2}{\pi r} \sum_{n=1}^{\infty} \frac{r_2(C_2 - C_1) \cos(n\pi r)}{n} \cdot \sin\left(\frac{n\pi(r - r_1)}{x}\right) \cdot e^{-n^2\pi^2 D t / x^2} + r_1 C_1 / r + (r_2(C_2 - r_1 C_1)(r - r_1) / x r} \quad (6)$$

The average interfacial flux N is defined

$$N = \frac{1}{T} \int_{t_0}^{t_0+T} N(t) dt = \frac{1}{T} \int_{t_0}^{t_0+T} D \frac{\partial c}{\partial r} \bigg|_{r=r_2} dt \quad (7)$$

We shall consider only the case when $c_2 = 0$; then

$$\frac{\partial c}{\partial r} \bigg|_{r=r_2} = -\frac{C_1}{x} \left[\frac{r_1}{r_2} + 2 \sum_{n=1}^{\infty} e^{-(n^2\pi^2 D t / x^2)} \right] \quad (6a)$$

From the measured values of the function $A(t)$ we can calculate the flux N as well as the mass transfer coefficient K , defined as

$$K = \bar{N} / C_1 \bar{A}, \quad \bar{A} = \frac{1}{T} \int_{t_0}^{t_0+T} A(t) dt \quad (8)$$

The interfacial film thickness can be estimated from Levich⁽¹¹⁾ equation, which was recommended for a similar case by Marsh⁽⁹⁾.

$$x = 2.5\eta / \sqrt{V_e} \quad (9)$$

Experimental part

The oscillating drop shapes were determined by filming drops moving through a glass cylindrical column. The description of the experimental apparatus was published earlier⁽¹²⁾. Liquids used were twice redistilled and the apparatus was kept scrupulously clean. The results presented were obtained mainly for the system benzene (as continuous phase) - water (as dispersed phase) - acetic acid (component transferring from water to benzene). Drop volumes were 0.08 - 0.10 cm³. At any chosen point in the column, the drop was seized and isolated in a teflon bowl of volume 0.43 cm³. At the bottom of the bowl were affixed electrodes for conductometric determination of acetic acid concentration. The root mean square deviation of ten measurements was 5%. This method, even when a number of calibrations are needed, makes possible quick and precise determination of the transferring component's concentration inside the drop at any position in the column.

Results

Measured frequencies of drop oscillations were best fitted by the empirical correlation of Edge and Grant⁽²⁾, see Fig. 1 where measured values of one oscillation period times are compared with values calculated^(3,4,5). The correlation was derived for water continuous phase only⁽²⁾. Further it was found that this correlation fits the measured dependence of oscillation frequency on the volume of the drop well⁽¹²⁾.

The different drop shapes which occur during one oscillation period are shown in Fig. 2. This figure relates to a water drop (volume 0.120 cm^3) moving through benzene. However, the same type of drop shape changes was observed in other low viscosity systems, e.g. water - n hexane, water - n heptane, water - cyclohexane, water - toluene, carbon tetrachloride - water (first mentioned phase is dispersed). The smaller the drop, the less is the amplitude. At a certain critical size, the oscillation becomes indiscernible. The amplitude of oscillation is very sensitive to the purity of the chemicals used. However, for systems with twice redistilled liquids (originally of the analytical purity), the amplitudes were found perfectly reproducible.

As it can be seen from Fig. 2, the drop shapes are very complex and we did not attempt to find their analytical description. Measured time dependence of the parameter E, characterizing simply the drop shape, is shown in Fig. 2. Here again, the smaller the drop, the less is the difference between maximum and minimum E value. In the water - benzene system, amplitude damping was not observed over the first six periods. However, according to the theory of Miller and Scriven⁽⁵⁾, amplitude damping is small and lies within experimental error limits for the system. Measured values of terminal velocity, v_t , were well described by the empirical correlation given by Thorsen, Stordalen and Terjesen⁽¹³⁾, see Fig. 3. This correlation was also based only on experiments with water as the continuous phase.

The comparison of the instantaneous drop velocity measured (full line) and calculated (dashed line) according to the relationship⁽²⁾ is given in Fig. 2. The quite similar course of the lines seems to confirm that the velocity of the drop is greatly determined by the instantaneous drop shape. More detailed results were published in our previous paper⁽¹⁴⁾.

In Fig. 2, the measured time-dependent surface area of the drop, which was determined by numerical integration of the drop picture meridional profile, is shown (full line). The dashed line represents a surface area of the joined spheroid, which was calculated from expression (3). It is evident that the approximation of the drop area by a spheroid significantly underestimates the real values. The average real value is 1.14 cm^2 , the average value based on spheroid approximation is 1.04 cm^2 . It is noteworthy that values of published mass transfer coefficients are based on spheroid approximation of drop shapes.

The addition of a third component may change the physical properties of the system. Mass transfer across the interface can also cause changes in drop behaviour. The measured effect of acetic acid concentration on the drop behaviour is summarised in Table 1. Maximum values of E decrease almost linearly with the concentration, whereas minimum values of E as well as oscillation frequency remain almost constant. Velocity v_t decreases with increasing concentration. It is a consequence of the opposing effects of decreasing drop size⁽¹³⁾ and increasing intensity of mass transfer across the interface⁽¹⁵⁾. The character of drop shapes and their changes remain almost unchanged up to an initial concentration 3 mole/l. For higher concentrations the shapes become much more rounded.

Mass transfer coefficients averaged over one oscillation period were measured for three concentration levels. All results obtained were the same and $K = 0.0131 \text{ cm/s}$ for real average area; the value based on spheroid approximation makes $K = 0.0144 \text{ cm/s}$. The coefficient calculated from

Table 1 The effect of the presence of acetic acid on drop behaviour

Initial concentration of acetic acid in drop c mole/l.	Volume of drop V cm ³	Terminal velocity of drop motion v _t cm/s	Time of oscillation period T s	Ratio of maximum vertical to horizontal diameters of oscillating drops during one oscillation period		
				E _{max}	E _{min}	\bar{E}
0	0.105	18.5	0.104	1.30	0.45	0.82
0.266	0.096	18.6	0.102	1.27	0.44	0.80
0.397	0.092	18.3	0.098	1.24	0.44	0.79
0.606	0.086	17.9	0.094	1.21	0.43	0.78
1.04	0.070	17.8	0.093	1.17	0.43	0.75
1.98	0.055	17.4	0.092	0.90	0.44	0.65
2.98	0.041	17.2	0.092	0.82	0.43	0.61
3.82	0.035	16.8	0.091	0.69	0.44	0.55
4.59	0.030	16.6	0.092	0.56	0.45	0.50

All drops were formed at the tip of the nozzle, the wetted diameter was 0.1375 cm. Flow rate of the dispersed phase was constant 0.0121 cm³/s.

Table 2. Mass transfer coefficients in benzene - water - acetic acid system

Mass transfer coefficient K cm/s	Origin	Note
0.0131	this work:	measured value
0.0128	"	calculated value
0.0144	"	measured value
0.0124	"	calculated value
		} based on spheroid approximation
0.012	Angelo et al ⁽¹⁸⁾	theory
0.012	Brunson and Wellek ⁽⁶⁾	theory
0.011	"	alternative theory
0.016	"	modified Highbie theory
0.020	"	modified Handlos-Baron theory
0.030	Wellek and Skelland ^(6,17)	empirical correlation
0.032	"	" "
0.059	Ellis ⁽¹⁶⁾	semi empirical correlation

equations (6a), (7), (8), using experimentally measured values of $A(t)$ is $K = 0.0128$ cm/s; assuming the drop to be a spheroid to determine $A(t)$, the same equations give $K = 0.0124$ cm/s. Using measured $A(t)$ in the model, and in the determination of K from observed mass transfer rates, gives good agreement between the model and experiment; using a spheroid approximation of $A(t)$ in the model and in the experimental determination of K gives poor agreement. The spheroid approximation introduces errors into experimental as well as calculated coefficients, so that the agreement between measured and calculated values becomes worse.

Mass transfer coefficients, calculated according to correlations recommended in the literature^(6,17,18,19) are given in Table 2. It is surprising that the simple model presented here gives, for our case, better results than other models.

It seems likely that similar conclusions could be valid, if we consider various approximations of $A(t)$, using an expression of type (1). The parameter characterizing variation of the surface area (parameter in equation (1)) should be based on the real function $A(t)$, and not to a spheroid approximation of this function.

Conclusions

During the oscillation period, the drop shapes are of a much more complex character than is supposed by spheroid approximation. Area variation was found to be significantly higher than is supposed by using the spheroid approximation. This should be noted in the evaluation of experimental as theoretical mass transfer data.

Symbols

A	area
A_0	area of sphere
c	concentration
D	diffusion coefficient
E	parameter defined in text
F	function defined in text
K	overall mass transfer coefficient
n	natural number
N	flux
r	radial coordinate
r_1	= $r_2 - x$
r_2	radius of spherical drop
v	instantaneous velocity of drop motion
v_t	terminal velocity of drop motion
V	volume of drop
x	film thickness
t	time
T	time of drop oscillation period
π	ratio of circumference to diameter of circle
ϵ	parameter of surface area variation
η	viscosity of dispersed phase
ρ	density of dispersed phase

References

- 1 Winnikow S., Chao B.T. Phys.Fluids 9 50 (1966)
- 2 Edge R.M., Grant C.D. Chem.Engng.Sci. 26 1001 (1971)
- 3 Schroeder R.R., Kintner R.C. A.I.Ch.E.J. 11 5 (1965)
- 4 Lamb H. Hydrodynamics Dover New York 1932
- 5 Miller A.C., Scriven L.E. J.Fluid Mech. 32 417 (1968)
- 6 Brunson R.J., Wellek R.M. Can.J.Chem.Eng. 48 267 (1970)
- 7 Luiz A.M. Chem.Engng.Sci. 22 1083 (1967) and 24 119 (1969)
- 8 Crank J. Mathematics of diffusion Clarendon Press Oxford 1964
- 9 Marsh B.D. Ph.D.Thesis, University of Washington, Seattle 1966
- 10 Marsh B.D., Heideger W.J. Ind.Eng.Chem.Funds. 4 129 (1965)
- 11 Levich V.G. Physicochemical hydrodynamics Prentice Hall 1962
- 12 Vacek V., Nekovář P. Paper presented at IV Congress CHISA Prague 1972
- 13 Thorsen G., Stordalen R.M., Terjesen S.G. Chem.Engng. Sci. 23 413 (1968)
- 14 Nekovář P., Vacek V. Paper presented at XVIII Conference CHISA Brno 1973
- 15 Sawistowski H. in Hanson C. (ed) Recent advances in liquid-liquid extraction Pergamon Press Oxford 1971
- 16 Ellis W.B. Ph.D.Thesis, University of Maryland 1966
- 17 Skelland A.H.P., Wellek R.M. A.I.Ch.E.J. 12 751 (1966)
- 18 Angelo J.B., Lightfoot E.N., Howard D.W. ibid. 10 491 (1964)

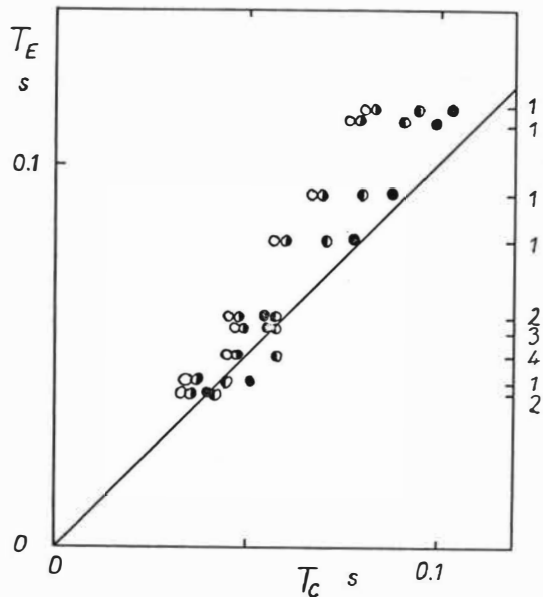


Fig. 1 Comparison of oscillation period times measured (T_E) and calculated according to Lamb⁽⁴⁾ ○, Miller and Scriven⁽⁵⁾, ●, Schroeder and Kintner⁽³⁾ ●, Edge and Grant⁽²⁾ ● ;
 Systems used were 1 water - benzene
 2 water - n hexane
 3 water - n heptane
 4 water - diethylether

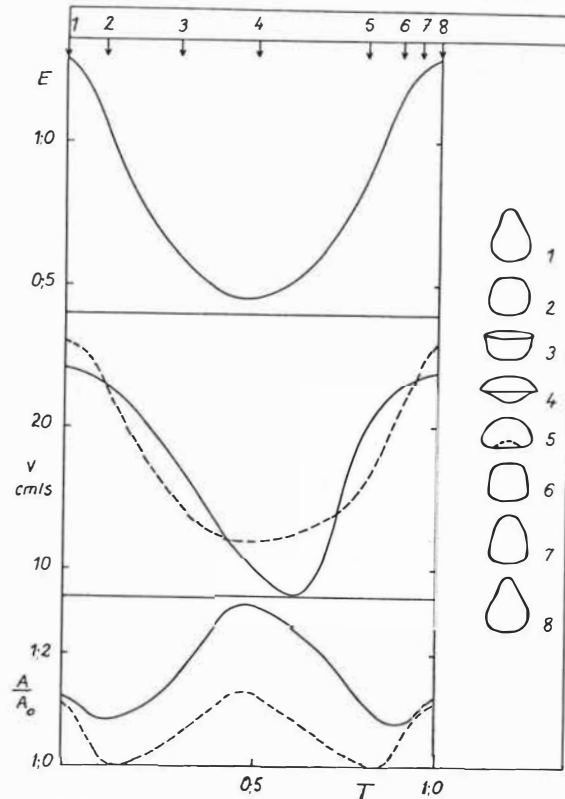


Fig. 2 Variation of instantaneous drop motion velocity, surface area and of parameter E during one oscillation period.
 — measured values
 - - - values calculated for the spheroid approximation

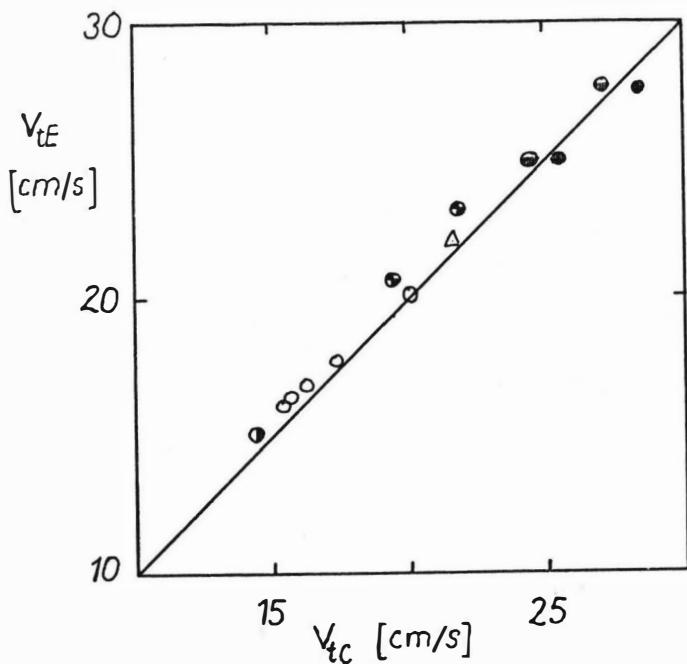


Fig.3 Comparison of measured (v_{tE}) and calculated⁽¹³⁾ (v_{tC}) terminal velocities of oscillating drop motions. Systems used were

○	water - benzene ,	⊖	water - n heptane,
⊙	water - diethylether,	⊕	water - cyclohexane,
●	water - n hexane,	△	carbon tetrachloride - water.

SESSION 10

Tuesday 10th September: 14.00 hrs

C H E M I S T R Y O F E X T R A C T I O N

(Rare Earths of Transplutonium Elements)

Chairman:

Ing. O. Braaten

Secretaries:

Dr. D.F.C. Morris

Mr. P. Patigny

State Institute for Rare Metals,
B. Tolmachevsky, 5
Moscow

EXTRACTION OF THE RARE EARTH ELEMENTS WITH PHOSPHINE-
AMINE-, AND SULPHOXIDES

Abstract

The extraction of rare earth nitrates by neutral oxygen containing extractants increases along the series TBP \leftarrow DOSO \leftarrow HTSO \leftarrow DAMP \leftarrow NPO TOAO \leftarrow TAPO at pH 5.5, and at pH 1.0 along the series TOAO \leftarrow TBP DOSO \leftarrow HTSO \leftarrow NPO \leftarrow DAMP \leftarrow TAPO.

The difference in the sequence of the extractants is due to changes in the amount of nitric acid extracted.

The data obtained on metal - and water - distribution and IR spectra showed that rare earths are extracted by phosphine-, amine- and sulphoxides (excepting TOAO) as anhydrous trisolvates $\text{Ln}(\text{NO}_3)_3 \cdot 3\text{S}$.

When rare earths are extracted by neutral oxygen-containing extractants of the same class the extractant strength and selectivity change in parallel. Generally when extractants of different classes (e.g. sulphoxides and amine-oxides) are compared, there is no correlation between extractant strength and selectivity.

The features in the shape of the plots of distribution coefficient vs. rare earth element atomic number (tetrad effect) for five extraction systems are discussed. Conclusions concerning the influence of the tetrad effect on the separation factors for adjacent rare earth elements in systems of different type are formulated.

INTRODUCTION

Among neutral phosphorganic compounds, trialkyl-phosphineoxides possess the greatest extractant strength with respect to rare earth elements¹. Therefore, it is desirable to study the extraction of rare earths with organic oxides in which the O atom is bonded to an atom other than phosphorus and in particular to a nitrogen or sulphur atom.

In this paper the extraction behaviour of rare earth elements with phosphine-, amine-, and sulphoxides has been investigated. The results obtained are compared with results for neutral phosphorganic compounds. The form of distribution isotherms as a function of atomic number are also discussed and conclusions have been drawn concerning the influence of the te trad effect on the separation factor for adjacent elements in different systems.

EXPERIMENTAL

Triisoamylphosphineoxide (TAPO), tri(1-methylheptyl)phosphineoxide (TMHPO), n-nonylpyridine-N-oxide (NPO) tri-n-octylamine-N-oxide (TOAO), di-n-octylsulphoxide (DOSO), ~~☛~~ n-heptylthiophane sulphoxide (HTSO), diisoamylmethylphosphonate (DAMP), diisooctylmethylphosphate (DOMP) and tri-n-butylphosphate (TBP) were used as extractants. The purity of the compounds was >99%.

All experiments were carried out at room temperature ($22 \pm 2^\circ\text{C}$).

The experimental procedure has been described previously².

RESULTS AND DISCUSSION

Extractant strength. The extractant strength of investigated extractants for a case of the extraction of tracer amounts of thulium are given in fig.1. At pH 5.5, the thulium distribution coefficients increase along the series TBP \leftarrow DOSO \leftarrow HTSO \leftarrow DAMP \leftarrow NPO \leftarrow TOAO \leftarrow TAPO while at pH 1.0 the order is TOAO \leftarrow TBP \leftarrow DOSO \leftarrow HTSO \leftarrow NPO \leftarrow DAMP

TAPO. The difference in the sequence of the extractants in the series is due to the extraction of nitric acid. The higher the nitric acid extraction equilibrium constant (K_{HNO_3}), the greater effect of nitric acid. This effect should increase along the series TBP \leftarrow DOSO \leftarrow HTSO \leftarrow NPO \leftarrow TOAO³⁻⁵. As fig. 2 shows the reduction in the thulium distribution coefficients as the pH decreases follows that order. At high (pH 5) pH values, the decrease in the extraction is caused by hydrolysis.

As the pH increases (pH 2), a plateau appears on the isotherms due to the fact that the bond between the extractant oxygen and acid breaks. For TAPO liberation, a pH 3 is required ($K_{\text{HNO}_3} = 8.5$) to rupture this bond. At this pH value the plateau becomes narrower. This explains why a plateau is absent and one does not fully exploit the potential extractant strength of TOAO.

The shift of the right hand plateau boundary into the range of higher pH values in the case of the NPO extractant (in comparison with TBP extractant) is apparently attributable to the amineoxides of ability to extract hydrolysed forms.

As far as extractant strength is concerned with respect to rare earth elements, dialkylsulphoxides take their place between trialkylphosphates and trialkylphosphonates, and cyclic sulphoxide and amineoxide, that is, close to trialkylphosphonates.

Extractant concentration dependence. Fig.3 illustrates the dependence of distribution coefficients (D) for tracer amounts of neodymium and thulium on the sulphoxide concentration in carbon tetrachloride and benzene. The tangent of the slope of the D V (sulphoxide) plots was equal to 3 for all extractants, i.e. the dependence of D on extractant concentration (follows the same) third power law as was found earlier for phosphineoxides⁶. Hence it would appear that rare earth nitrates are extracted as trisolvates.

Distribution isotherms. The distribution isotherms for rare earth nitrates are shown in fig.4. In the case of NPO and TAPO, the corresponding isotherms have plateaus brought about by maximum loading by rare earth nitrates. The plateau range begins at the lowest salt concentrations in the case of TAPO on account of its greater extractant strength.

On curve 4 (fig.4) the maximum loading capacity has not been attained owing to relatively low DOSO extractant strength. However, when a salting-out agent (4M lithium nitrate) was introduced into the aqueous phase, a distinct horizontal region appeared on the distribution isotherm (curve 3).

At maximum loading capacity, the molar ratio of extractant to metal was equal to approximately to 3:1. This fact provides support for the conclusion that all of the organic oxides studied extract rare earth nitrates as trisolvates.

Water behaviour. IR spectra of extracts. Extraction mechanism. The behaviour of water has been studied in the extraction of lanthanum, neodymium and erbium nitrates with DOSO and TAPO. The water content in the organic phase decreases sharply with increasing salt concentration. When the maximum loading capacity of 0.5M TAPO in m-xylene is achieved, the water concentration is approximately one third of the metal concentration. This proves that anhydrous trisolvates are extracted. The residual water in the extracts apparently influences liquid structure formation in highly concentrated solutions.

IR spectral measurements also prove that anhydrous trisolvates are formed in the extraction of neodymium nitrate with a 0.5M DOSO solution in CCl_4 . The bonded water absorption band intensity in the 3200-3600 cm^{-1} range decreases with increasing salt concentration in the extracts and this absorption disappears completely when saturation loading is attained. The S=O group absorption band at 1050 cm^{-1} disappears simultaneously and a band appears at 1002 cm^{-1} due to bonded S=O groups. The considerable displacement (48 cm^{-1}) of the S=O band indicates that the metal is directly coordinated to the oxygen atom of the extractant. Bands, characteristic of coordinated bidentate nitrate-groups (1291 and 1497 cm^{-1}), are observed in the spectrum. It therefore seems reasonable to suppose that the coordination number of neodymium in $Nd(NO_3)_3 \cdot 3DOSO$ solvate is equal to 9, as in the case of the $La(NO_3)_3 \cdot 3TBP$ solvate⁷.

Thus, the mechanism for the extraction of rare earth nitrates with organic oxides can be written as



As the metal is transferred from the aqueous into the organic phase, the water molecules are completely displaced from the metal coordination sphere by the extractant and nitrate ions. This conclusion does not apply to TOAO. Evidently, the mechanism of the extraction of rare earths with tri-n-octylamineoxide is more complicated and required thorough investigation.

The relationship between extractant strength and selectivity. The distribution coefficients for lanthanum, cerium, praseodymium, and neodymium nitrates for extraction with 0.1M solutions of sulphoxides and amineoxides in benzene are shown in fig.5. The distribution coefficients for all of these solvents increase from La to Nd which is typical of extraction with neutral oxygen-containing compounds. The selectivity (curve steepness) increases as one passes from DOSO to HTSO. For example, the separation factor for neodymium and lanthanum, β^{Nd-La} , is 4.3 and 6.7 for DOSO and HTSO respectively.

Sulphoxide solvent selectivity for the elements at the beginning of the rare earth series increases as the extractant strength increases.

In case of amineoxides, β_{Nd-La} is higher for NPO than for TOAO, but NPO and TOAO cannot be compared because the mechanism of the extraction of rare earths with these extractants is not, apparently, the same.

It should be pointed out that although the extractant strength of NPO is slightly higher than that of HTSO (fig.1), β_{Nd-La} for NPO is lower than that for HTSO.

Fig.6 shows the correlation between the cerium and lanthanum, and also the neodymium and praseodymium separation factors for extraction from nitrate solutions with neutral phosphororganic compounds and the Kabachnik constants β^r which express the quantitative influence of substituent groups on the phosphorus atom on the reactivity of the compound.⁸ The data for TBP and DAMP

x) The separation factor for a pair of elements is equal to the ratio of their distribution coefficients, $\beta_{Nd-La} = D_{Nd}/D_{La}$. are taken from the previous works^{9,10}.

The separation factors for all of the solvents have been obtained approximately under the same conditions: the concentration with respect to the sum of the metals in the aqueous phase was 0.6-0.9M, and the concentration of the aluminium nitrate salting-out agent was 6N. The magnitudes of the separation factor increase along the TBP \leftarrow DAMP \leftarrow TAPO series and there is an approximately linear correlation between the values of β and the β^r Kabachnik constants.

The data obtained suggest that the extractant strength and selectivity vary in a similar manner in the trialkylphosphate \leftarrow trialkylphosphineoxide series for the extraction of rare earth nitrates.

It is confirmed by comparing the results for sulphoxides, amineoxides and neutral phosphororganic compounds that the extractant strength and selectivity change similarly for the extraction of the rare earth elements by neutral oxygen-containing extractants of the same class. However, extractant strength and selectivity are not inter related in case of extractants of different classes, such as sulphoxides and amineoxides, for example.

The peculiarities of the distribution of rare earth elements in extraction systems. The te trad effect. Plots of the system (compound) properties vs. 11-16, show that the rare earth group is subdivided into four subgroups (te trads) with 4 elements in each one. This phenomenon, called the te trad effect^{11,12} has been theoretically explained on the basis of specific peculiarities in the structure of the electron shells for 4f- and 5f-elements ^{17,18}.

The phenomenon of the te trad effect was originally established in 4 rare earth extraction systems. Experimental results for 5 more extraction systems which exhibit a well-defined te trad effect are cited in this section.

Fig.7 (table 1) shows that dependence of the rare earth distribution coefficients for extraction with neutral phosphororganic compounds from chloride and mixed chloride-thiocyanate solutions. In the systems investigated the distribution coefficient values are slightly along the series from lanthanum to lutecium vary. Under these conditions four subgroups of elements (four te trads) La-Md, Pm-Gd, Gd-Ho and Er-Lu are distinctly visible on the $\log D Z_{Ln}$ plot. The junction of the first and the second subgroups occurs between Nd and Pm and the third and fourth subgroups join between Ho and Er. The second and the third subgroups come into contact at Gd. Gd being the last element of the second subgroup, is also the first element of the third subgroup.

The four subgroups mentioned above should be designated by the first element in the subgroup i.e. as the lanthanum (the first te trad), promethium (the second te trad), gadolinium (the third te trad) and erbium (the fourth te trad) subgroups. The occurrence of the te trad effect in the distribution of rare earth elements in two-phase systems used for separating the rare earth elements helps us to understand the peculiar variations in the separation factor values for adjacent elements, e.g. why β_{Tb-Gd} and β_{Ce-La} are comparatively high while β_{Nd-Pr} , β_{Gd-Eu} and β_{Ho-Dy} are low for the extraction of rare earths with di(2-ethylhexyl)phosphoric acid¹⁹.

Fig. 8 shows the arrangement of the main types of distribution coefficient (or equilibrium constants of reactions, e.g. complexation reactions) vs. atomic number plots for all the rare earth subgroups. The following examples of the above mentioned types of curves.

Type Ia (ascending-convex curve) - extraction with di(2-ethylhexyl) phosphoric acid¹⁹, all the four subgroups.

Type Ib (descending-concave) - extraction with di-n-nonylnaphthalene-sulfonic acid in the presence of ethylenediaminetetraacetic acid²⁰, the lanthanum subgroup.

Type IIa (ascending-concave curve) - complexation with hydroxyethylethylenediaminetriacetic acid²¹, the europium subgroup.

Type IIb (descending-convex curve) - extraction of nitrates with TBP⁹, the gadolinium and erbium subgroups.

Type IIIa (horizontal-convex curve) - extraction of chlorides with DOMP (fig.7), curve 3), the lanthanum and promethium subgroups.

Type IIIb (horizontal-concave curve) - complexation with hydroxyethylethylenediaminetriacetic acid²¹, the gadolinium subgroup.

Fig. 8 shows that the influence of the te trad effect on the separation factors of adjacent elements is as follows:

If the rare earth distribution coefficients change with increasing atomic number of the elements in the subgroup according to type I, then the value of the separation factor will be a maximum for the adjacent second and first elements and a minimum for the adjacent third and fourth elements.

If the distribution coefficients change according to type II, the opposite behaviour will result: maximum β for the adjacent fourth and third elements and minimum β for the adjacent second and first elements.

When the plots of $\log D Z_n$ are of type III, a minimum value of β can be found between the adjacent third and second elements in the subgroup. Whether the values of β will be equal between the second and the first and between the fourth and the third elements in the subgroup or one of them will be greater than the other, depends on the specific properties of the system.

These results of the te trad effect are summed up in table 2. It is natural that in all the systems the distribution coefficient values will be intermediate in the range between promethium and neodymium, and between erbium and holmium (the elements where the junction of the subgroups takes place).

The conclusion drawn about the influence of the te trad effect on the separation factors for the adjacent elements can be utilised when choosing systems for the separation of rare earth elements, especially adjacent elements which are difficult to separate.

As the tetrad effect is found not only in the case of the 4f-elements but also for 5f-ones^{12,18}, analogous arguments can be employed in choosing separation systems for actinides.

REFERENCES

1. Blake C.A., Baes C.F. et al., "Proc. Sec. Int. Conf. Peaceful Uses Atomic Energy. Geneva, 1958. Select. Articles Foreign Scientists", 1959, v.7, p.393 (Moscow, Atomizdat).
2. Mikhailichenko A.I., Pimenova R.M., Radiokhimiya, 1969, 11, 8.
3. Mikhailov V.A., Torgov V.G. et al., Int. Conf. Extraction Chemistry, Haag, 1971, paper 196.
4. Rozen A.M., Nikolotova Z.I. et al., in "Chemistry of the Extraction Processes", 1972, p.41 (Moscow, Nauka).
5. Rozen A.M., Murinov Ju.I., Nikitin Ju.E., Minyaeva N.Z., Radiokhimiya, 1972, 14, 750.
6. Goffart S., Duyckaerts G., Analyt. Chim. Acta, 1969, 49, 91.

7. Ferraro J.R., Cristallini C., Fox I., J. inorg. nucl. Chem., 1967, 28, 139.
8. Mastryukova T.A., Kabachnik M.I., Uspekhi Khimii, 1969, 38, 1751.
9. Korpusov G.V., Eskevich I.V. et al., in "Extraction", 1962, v.2, p.117 (moscow, Atomizdat).
10. Mikhlin E.B., Korpusov G.V., Zh Neorgan. Khimii, 1965, 10, 2787.
11. Peppard D.F., Mason G.W., Lewey S., J. inorg. nucl. Chem., 1969, 31, 2271.
12. Peppard D.F., Bloomquist C.A.A., Hortwitz E.P., Lewey L., Mason G.W., J. inorg. nucl. Chem., 1970, 32, 339.
13. 13. Fidelis E., Siekierski S., J. inorg. nucl. Chem., 1966 28, 185.
14. Siekierski S.? J. inorg. nucl. Cjem., 1970, 32, 519.
15. Fidelis E.3 Siekierski S.? J. inorg. nucl. Chem., 1971, 33, 3191.
16. Siekierski S.? Fidelis I.? J. inorg. nucl. Chem., 1972, 34, 2225.
17. Jrgensen C.K., J. inorg. nucl. Chem., 1970, 32, 3127.
18. Fidelis I., Siekierski S., "Periodicity of some properties of lanthanides and actinides", 1970 (Warszawa, Inst. Badan Jadrowych).
19. Pierce T.B.? Peck P.F.? Analyst, 1963, 88 (1044), 217.
20. Werner G., in "Solvent Extraction Chemistry". Proc. Int. Conf. held at Gothenburg, 1966", 1967, p.54 (Amsterdam, Noth-Holland Publ. Comp.).
21. Thompson L.C., Loraas J.A., Inorg. Chem., 1963, 2, 89.

TABLE 1

Conditions employed for the extraction of rare earths with 50% solution of extractants in m-xylene from chlorides and mixed chloride-thiocyanate solutions. Distribution coefficients are given in fig.7. The composition of the initial concentrate (w.t.% was: La 8.2, Ce 5.2, Pr 5.4, Nd 6.6, Sm 6.2, Eu 6.3, Gd 7.7, Tb 6.8, Dy 7.7, Ho 7.3, Er 8.0, Tm 8.0, Yb 8.1, Lu 8.5; in experiment N3: Y 98.6, other rare earths 0.1 (each).

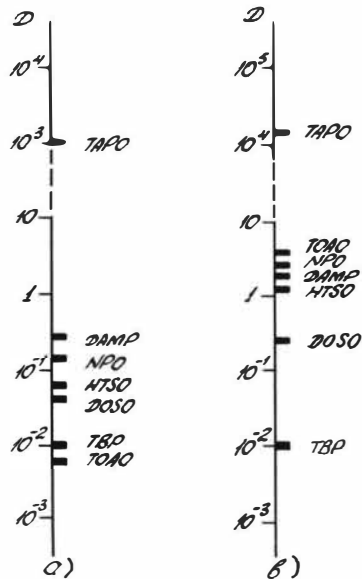
NN	: Extractant :	Starting solution				: pH :	Concentration of rare earths in	
		Concentration, M					equilibrium phases, M	
		: LnCl ₃ :	: LiCl :	: NH ₄ NCS :	:		: aqueous :	: organic
1	DOMP	1.56	4.0	-	3.0	1.42	0.142	
2	DOMP	1.02	-	0.48	2.8	0.874	0.146	
3	DOMP	1.45	4.0	-	3.0	1.27	0.180	
4	TBP	1.02	-	0.48	2.8	0.917	0.103	
5	TMHPO	1.56	4.0	-	3.0	1.20	0.362	

table 2

Limiting values for the separation factors of adjacent rare earth elements in the systems of different types.

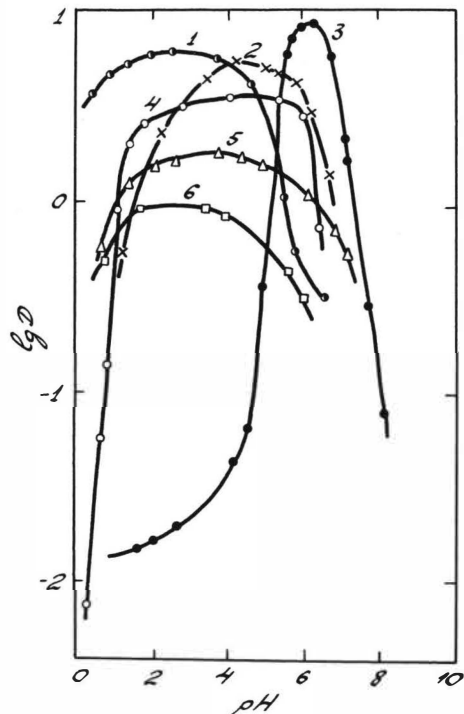
Separation factor	Sub group (tetrad)	Type of log $D Z_{Ln}$ plot in subgroup	I	II	III
			a) ascending-convex b) descending-concave	a) ascending- concave b) descending- convex	a) horizontal- convex b) horizontal- concave
Maximum	Lanthanum (I)		Ce-La	Nd-Pr	Ce-La or Nd-Pr
	Promethium (II)		Sm-Pm	Gd-Eu	Sm-Pm or Gd-Eu
	Gadolinium (III)		Tb-Gd	Ho-Dy	Tb-Gd or Ho-Dy
	Erbium (IV)		Tm-Er	Lu-Yb	Tm-Er or Lu-Yb
Minimum	Lanthanum (I)		Nd-Pr	Ce-La	Pr-Ce
	Promethium (II)		Gd-Eu	Sm-Pm	Eu-Sm
	Gadolinium (III)		Ho-Dy	Tb-Gd	Dy-Tb
	Erbium (IV)		Lu-Yb	Tm-Er	Yb-Tm

Fig.1. Distribution coefficients of thulium nitrate at the extraction with 0.1M extractant solutions.



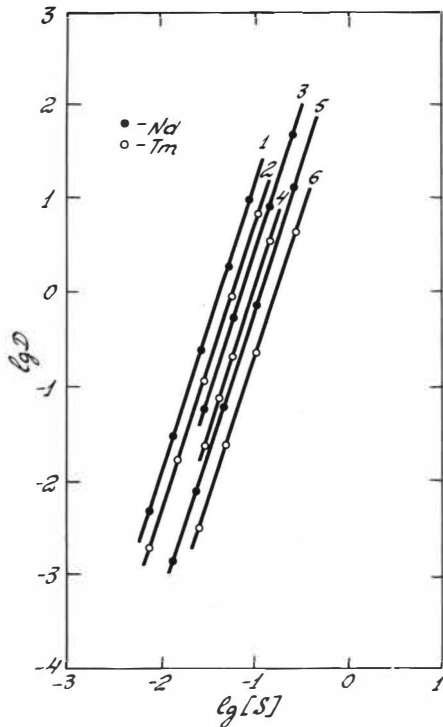
- a) salting-out agent - 5.9N $\text{Al}(\text{NO}_3)_3$, pH 1.0, diluent CCl_4 ,
 b) salting-out agent - 6.0M LiNO_3 , pH 5.5, diluent C_6H_6 .

Fig.2. Distribution coefficients of thulium nitrate vs. pH equilibrium aqueous phase.



- 1 - 0.5M TBP, 2 - 0.005M TAPO, 3 - 0.1M TOAO,
 4 - 0.1M NPO, 5 - 0.1M HTSO, 6 - 0.1M DOSO in benzene.
 Salting-out agent - 6M LiNO_3 .

Fig. 3. Distribution coefficients of thulium and neodymium vs. extractant concentration in diluent.

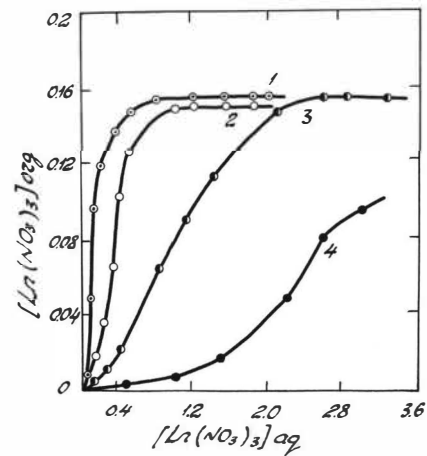


1,2 - HTSO in CCl_4 , 6.6M LiNO_3 , pH 3.0.

3, 4 - NPO in C_6H_6 , 6.0M LiNO_3 , pH 2.3.

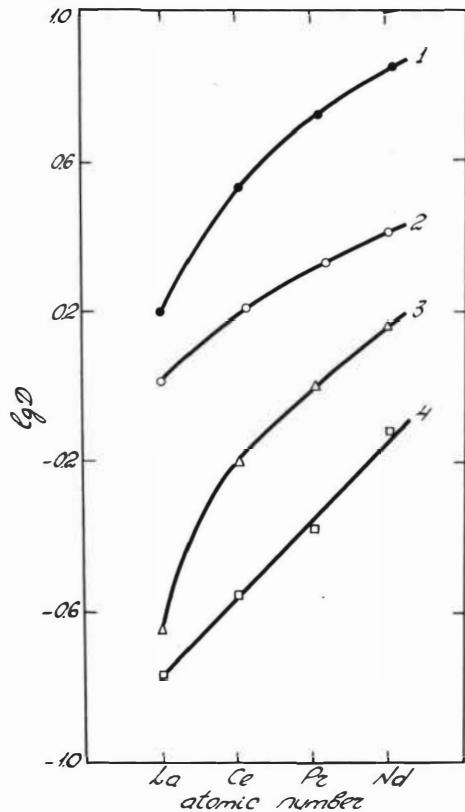
5,6 - DOSO in CCl_4 , 6.0M LiNO_3 , pH 3.0.

Fig. 4. Distribution isotherm of lanthanum and neodymium nitrates at the extraction with 0.5M extractant solutions in benzene.



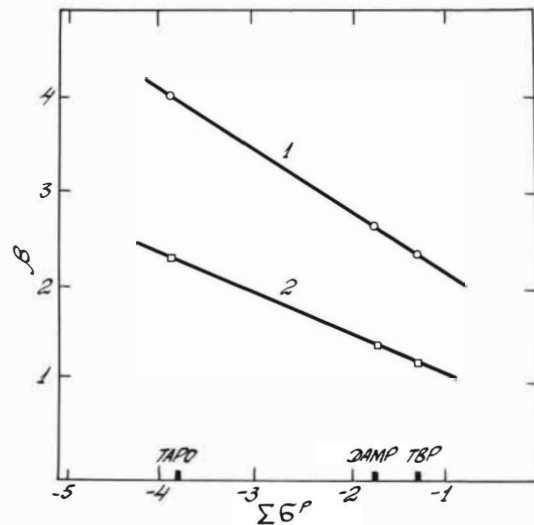
1 - La, DOSO, 2 - Nd, NPO, 3 - La, DOSO, salting-out agent - 4M LiNO_3 , 4 - La, TAPO, pH - 3.0.

Fig.5. Distribution coefficients of rare earths at the extraction with 0.1M extractant solutions in benzene.



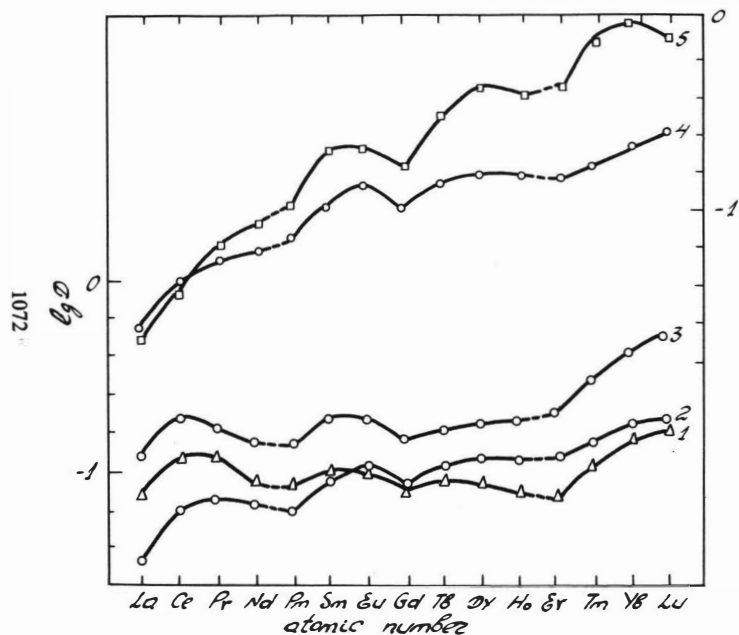
1 - DOSO, 2 - HTSO, 3 - TOAO, 4 - NPO.

Fig.6. Separation factors of $\beta_{\text{Ce-La}}$ and $\beta_{\text{Nd-Pr}}$ on rare earth nitrates extracting with neutral phosphororganic compounds vs. the sum of σ^p Kabachnik constants of the substitution radicals of phosphorus atom. Aqueous phase: 0.6 - 0.9M $\text{Ln}(\text{NO}_3)_3$, salting-out agent - 6N $\text{Al}(\text{NO}_3)_3$.



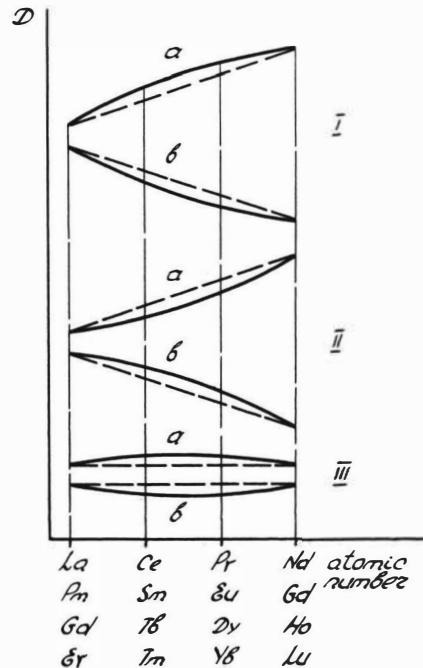
1 - $\beta_{\text{Ce-La}}$; 2 - $\beta_{\text{Nd-Pr}}$.

Fig.7. Distribution coefficients of rare earths at the extraction with neutral phosphororganic compounds from chloride and mixed chloride-thiocyanate solutions.



The experimental conditions are given in table 1. The numbers of the systems in fig.7 correspond to the numbers of the systems in table 1.

Fig.8. The scheme of main types of curves describing the distribution coefficients vs. the atomic number of the element (for all four rare earth subgroups).



I, a - ascending-convex, b - descending-concave);
 II, a - ascending-concave, b - descending-convex;
 III, a - horizontal-convex, b - horizontal-concave.

DOUBLE-DOUBLE EFFECT IN THE FREEENERGY AND ENTHALPY CHANGES
OF THE EXTRACTION OF HEAVY LANTHANIDES IN THEHDEHP - HNO₃
SYSTEM

by - Irena Fidelis, Department of Radiochemistry,
Institute of Nuclear Research, Warsaw, Poland.

ABSTRACT - The extraction coefficients and separation factors of lanthanides in the HDEHP - HNO₃ system were determined over the range 10-50°C. The relative free energy and enthalpy changes were estimated. It was found that the monotonic decrease in the enthalpy changes determined for the series of heavy lanthanides (Gd-Lu) follows the known pattern of regularities i.e. double-double effect. Regular changes in the separation factors (the double-double effect in the first form of presentation) are observed over the whole investigated temperature range.

INTRODUCTION

The paper forms part of a general program of investigation of the trends in the thermodynamic functions associated with the extraction of lanthanides by organophosphorus ligands. This program is, in its turn one of the directions of study of the double-double effect first revealed in 1964 when 2-ethylhexylphenyl phosphonic acid, HEH/P was used as the extractant¹. The particular order of the separation factors, for the investigated systems, which results from a definite variation the standard free energy changes, ΔG^0 , with Z was initially used as an index of the effect^{1,2}.

The double-double effect infers some stabilization of the f^3 , f^4 and f^{10} , f^{11} configurations in addition to the well known stabilization of the f^0 , f^7 and f^{14} configurations. From a phenomenological point of view the double-double effect consists of a main division of the whole series of the f^0 - f^{14} elements into two groups f^0 - f^7 and f^7 - f^{14} , together with a further subdivision of each of these two groups at the central pairs: $f^{3,4}$ and $f^{10,11}$, respectively.

This is illustrated in Fig.1, in which the mean free energy of complex formation, $\overline{G^0}$, calculated from stability constants for many different ligands^{3,4} is plotted as a function of Z. In fig.1 the changes in the mean separation factors are also shown. An analogous plot for extraction by HEH/P was used for the first presentation of the effect, which was introduced as a function of stability constants¹.

The effect has usually been presented as a definite pattern of periodical changes in the free energy or in another property related to the free energy. However, it can be demonstrated by certain other properties not necessarily directly related to the free energy change; lattice parameters⁴⁻⁷ are an example of such a property.

Determination of the trends in the enthalpy and entropy terms associated with the extraction of lanthanides with organophosphorus ligands, has formed the subject of our study for a few years. Starting with HEH/P, for a complete set of extraction coefficients and separation factors for adjacent lanthanides and the corresponding thermodynamic functions have been determined^{2,8-12} for commonly employed organophosphorus extractants, such as trinitylphosphate (TBP) and di-(2-ethylhexyl)-phosphoric acid (HDEHP). The present paper reports data for dibutylphosphate (HDBP).

EXPERIMENTAL

Extraction experiments were carried out using radioactive tracer techniques. The radioisotopes used were obtained by irradiation of the respective oxides of spectral purity with thermal neutrons in the Polish reactor, except for ^{152,154}Eu and ¹⁴⁷Pm, which were obtained from the Radiochemical Centre, Amersham. Radiochemical purity of the tracers was verified chromatographically, as well as by γ -spectrometry and by half-life measurements. The concentration of the lanthanide carrier in the aqueous phase was below 10^{-4} M.

Equal volumes of the diluted HDBP and an aqueous solution of HNO_3 of appropriate concentration were shaken for 5 min in a separatory funnel which was fitted with a water jacket and connected to a thermostat. The extraction coefficients were measured generally at 10, 17, 25, 35 and 50°C. The temperature was kept constant to within $\pm 0.1^\circ\text{C}$. The concentration of HDBP in the organic phase was 0.1M, and HDBP supplied by Koch-Light and Co., was used without further purification. All the other reagents were of standard analytical purity. Other experimental details have been described previously⁸.

RESULTS AND DISCUSSION

Extraction coefficients, D , for heavy lanthanides at different temperatures are presented in Table 1; these are mean values from at least five independent measurements. A decrease in magnitude of extraction coefficient with increase of temperature is observed for the heavy lanthanides from Tb to Lu. The plots of $\log D$ against $1/T$ were found to be straight lines for the temperature range investigated. These are presented in Fig. 2. The slopes of the plots were estimated by the least-squares analysis.

The separation factors, β , defined by the following equation

$$\beta = D_{Z+1}/D_Z \quad (1)$$

were calculated from interpolated values of extraction coefficients. The influence of temperature on the separation factors is presented in Table 2. When the variation in β as a function of the atomic number is taken into consideration, the pattern of the double-double effect is observed, thus, is shown in Fig. 3, the plots display the known pattern of the effect over the whole investigated temperature range; this is also the case for all of the other organophosphorus extractants, HEHP ^{2,8}, TBP ⁹, and HDEHP ¹² studied. It can be seen that for all these extractants, the values of the relative free energy changes when plotted against Z conform to the pattern shown in the upper plot in Fig. 1.

Some plots of ΔG_r° vs Z, for HEHP², TBP⁹ and HDEHP¹² are presented in Fig.4.

In the case when MDBP is used the extractant, the results show the same pattern of the variation of the ΔG_r° values with Z. In respect to the enthalpy changes, however, the behaviour of the light and heavy lanthanides is essentially different. The lanthanides from La to Gd show an endothermic interaction with the ligands and the logD vs 1/T plots are not always rectilinear.

The results obtained for heavy lanthanides are similar to those reported earlier for HEHP, TBP and HDEHP. That is, the plots of logD vs 1/T are linear correspond to an exothermic interaction of the lanthanide ions with the extractant. The monotonic decrease in the enthalpy term observed along the series from Tb to Lu, is equal to about 4 kcal/mole. (Fig.5). The upper half of the double-double pattern is displayed both by the plots of enthalpy term and by the plot of the free energy change; The latter is presented in Fig.6.

The relative free energy and enthalpy changes have been evaluated by means of Equations (2) and (3) respectively, as was done previously².

$$\Delta G_{Z+1}^\circ - \Delta G_Z^\circ = -RT \ln \beta \quad (2)$$

$$\Delta \log D / \Delta 1/T = \Delta H^\circ / 2.303 R \quad (3)$$

The statistical significance of the results is more or less the same as that reported earlier for the other extractants⁸⁻¹⁰.

Table 3 lists the values of the separation factors for heavy lanthanides as determined at 25°C for acidic organophosphorus extractants. The data for HDEHP and HEHP are taken from the previous paper¹².

Acknowledgements - The author is indebted to Professor S. Siekierski for helpful discussion and to Mrs. R. Osinska for her assistance.

TABLE 1

Values of the extraction coefficients at different temperatures

	Gd	Tb	Dy	Ho
10°C	0.0412	0.341	1.041	2.29
17	0.0414	0.332	0.977	2.15
25	0.0417	0.321	0.903	2.00
35	0.0426	0.302	0.837	1.80
50	0.0430	0.273	0.737	1.55

	Er	Tm	Yb	Lu
10°C	6.58	24.9	82.9	172
17	6.03	22.1	70.5	141
25	5.26	19.9	61.3	126
35	4.74	16.4	52.0	102
50	4.02	13.2	39.4	77.0

TABLE 2

The separation factors at different temperatures

	10°C	17°C	25°C	35°C	50°C
Gd-Tb	8.28	8.02	7.70	7.08	6.35
Tb-Dy	3.05	2.93	2.81	2.77	2.69
Dy-Ho	2.19	2.20	2.20	2.15	2.10
Ho-Er	2.87	2.80	2.63	2.62	2.59
Er-Tm	3.80	3.70	3.79	3.46	3.32
Tm-Yb	3.32	3.19	3.07	3.16	2.97
Yb-Lu	2.07	2.00	2.06	1.94	1.95

TABLE 3

The comparison of the separation factors of heavy lanthanides for acidic organophosphorus extractants

	HDBP	HDEHP	HEHOP
Gd-Tb	7.70	5.66	6.96
Tb-Ly	2.81	2.79	3.22
Dy-Ho	2.20	2.07	2.19
Ho-Er	2.63	2.42	2.74
Er-Tm	3.79	3.85	4.02
Tm-Yb	3.07	3.61	3.76
Yb-Lu	2.06	1.92	1.99

REFERENCES

1. Fidelis, I., Siekierski, S., J.inorg.nucl.Chem., 1966, 28, 185
2. Fidelis, I., Siekierski, S., J.inorg.nucl.Chem., 1967, 29, 2629
3. Siekierski, S., J.inorg.nucl.Chem., 1970, 32, 519.
4. Fidelis, I., Siekierski, S., Institute of Nuclear Research, Report No.1212/V/C, Warsaw 1970.
5. Fidelis, I., Bull.Acad.Polon.Sci., Ser.Sci.Chim., 1970, 18, 681.
6. Siekierski, S., J.inorg.nucl.Chem., 1971, 33, 377.
7. Siekierski, S., Fidelis, I., J.inorg.nucl.Chem., 1972, 34, 2225
8. Fidelis, I., Nukleonika, 1967, 12, 477
9. Fidelis, I., J.inorg.nucl.Chem., 1970, 32, 997
10. Fidelis, I., Proc.Intern.Solvent Extraction Conf., The Hague 1971, 2, 1004
11. Fidelis, I., Institute of Nuclear Research, Report No.1393/V/C, Warsaw 1972.
12. Fidelis, I., Institute of Nuclear Research, Report No.1394/V/C, Warsaw, 1972.

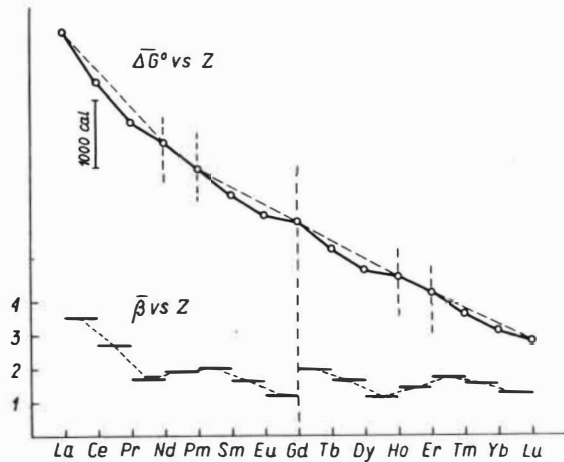


Fig. 1. The double-double effect in the form of a plot of mean standard free energy changes (upper curve) and of the variation of mean separation factor (lower plot) with Z .

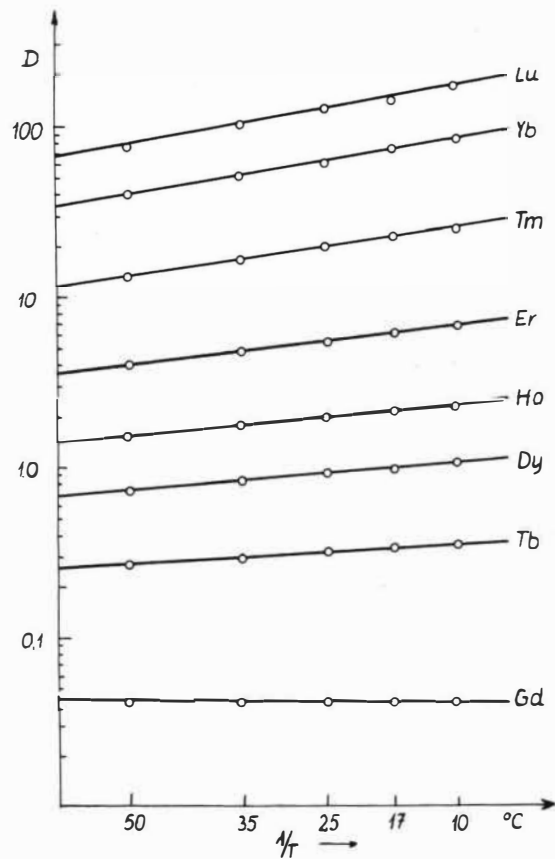


Fig. 2. Effect of temperature on the distribution of heavy lanthanides.

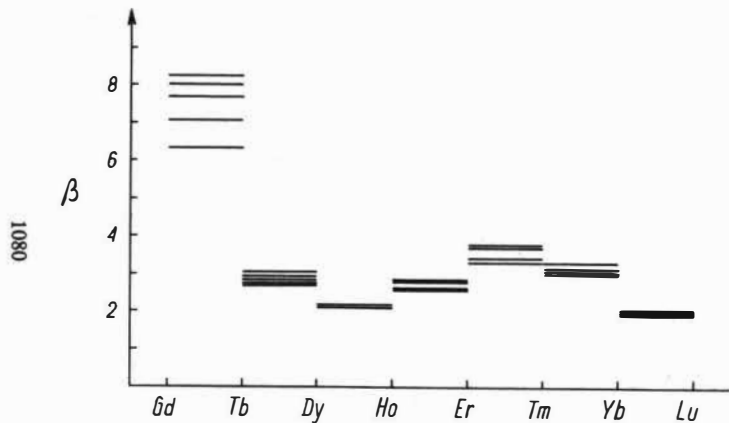
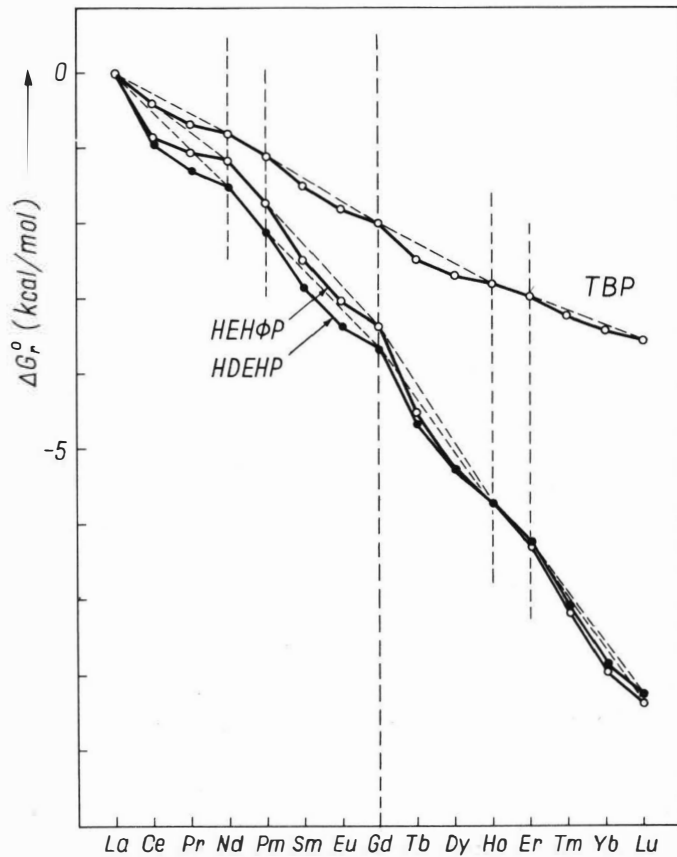


Fig.3. Variation of the separation factors of heavy lanthanides, determined at 10, 17, 25, 35 and 50°C.

Fig.4. Double-double effect illustrated by the variation of the relative free energy changes for lanthanide and various different organophosphorus extractants.



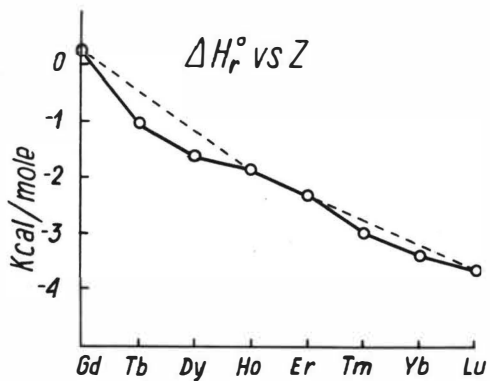


Fig.5. Variation of the relative enthalpy changes for heavy lanthanides in the case of HDBP as extractant.

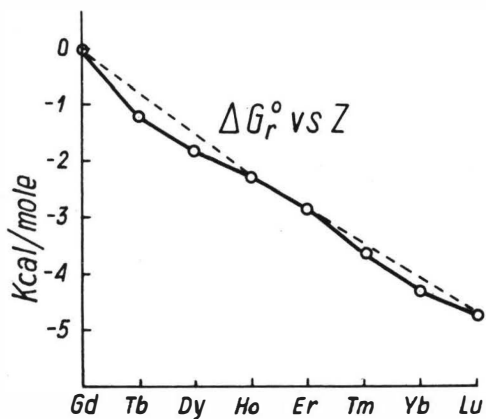


Fig.6. Variation of the relative free energy changes for heavy lanthanides in the case of HDBP as extractant.

International Solvent Extraction Conference 1974

Lyon, 8th-14th September 1974

A COMPARATIVE STUDY OF THE RARE EARTH ELEMENTS IN EXTRACTION BY
HDEHP/SHELL SOL T FROM NITRIC AND SULFURIC ACID SOLUTIONS

by

J Alstad, J H Augustson, T Danielssen, L Farbu
Department of Chemistry, University of Oslo, Oslo 3, Norway

ABSTRACT

Extraction equilibrium data for tracer amounts of all the rare earths (lanthanum series) and yttrium have been measured at acidities of HNO_3 and H_2SO_4 up to about 15 N at 25°C. At $a_{\text{H}^+} = 1.0$, the extraction constants for the light rare earths are found to be higher with HNO_3 rather than H_2SO_4 in the aqueous phase.

The influence of the aqueous rare earth nitrate- and sulfato- complexes on the D-values is discussed.

The tetrad effect is found to show up distinctly in the slope analysis, and, with nitric acid in the aqueous phase, anomalies consistent with the presence of the +4 state are found for both Ce and Tb.

The rate of extraction, as measured by the AKUFVE technique, is found to be greater with HNO_3 than with H_2SO_4 . In the latter case, the time for equilibrium attainment varies with (H_2SO_4), (HDEHP), and Z of the heavier rare earths and of Y.

INTRODUCTION

The main advantages of using di(2-ethylhexyl) phosphoric acid (HDEHP) in separating rare earth elements by solvent extraction are the high separation factors obtained together with high extraction equilibrium constants. From the latter it follows that the distribution ratios for the various rare earth elements, at least the heaviest, are high even when extraction is performed from relatively high concentrations of mineral acid in the aqueous solutions.

Shaw and Bauer (1) showed that, in extraction by HDEHP, the distribution ratio of Ce(III) as a function of the aqueous nitric acid concentration passes through a minimum at 5 M. However, in their early studies on the extraction by HDEHP, Peppard et al. (2, 3) found that the distribution ratio of rare earth elements is inversely dependent on the third power of the acid concentration. Thus the increase in distribution ratio for Ce(III) above 5 M acid, as observed by Shaw and Bauer, was attributed to a change in extraction mechanism. As high acid concentrations in the aqueous phase promote the back extraction of rare earth elements, many workers have been concerned with the extraction behaviour of a selection of these elements from various strong mineral acids. With respect to the number of rare earth elements studied, the most comprehensive works are those of Mikhailichenko and Pimenova (4) and Qureshi et al. (5). The general trend from these works is that the effect of a change in extraction mechanism appears most prominently in nitric acid media, less in hydrochloric acid and is intermediate in perchloric acid. It is further seen that the acid concentration for the minimum in the distribution ratio increases with increasing Z of the rare earth element.

From sulfuric acid media the extraction by HDEHP of Y, Er, Yb at initial metal concentrations 0.014 M seems to be even less influenced by change of extraction mechanism than from hydrochloric acid media. The work of Michelsen and Smutz (6), from which the above conclusion can be drawn, shows that a minimum in the distribution ratio is found at ~ 15 N H_2SO_4 , which is about twice the analogous concentration observed for the other mineral acids.

In the present work the extraction behaviour of all the rare earth elements and yttrium (RE), present as tracers in nitric as well as sulfuric acid media, is studied in some detail. Acid solutions of mixtures of rare earth nitrates or sulfates are common as feeds for the separation of these elements by solvent extraction. The preparation of ultra pure grade elements by this technique requires a knowledge of the extraction behaviour of the metal ions even at tracer levels.

In order to accumulate adequate distribution data on all the elements at various acid concentrations, a considerable number of measurements has to be performed. In the present case this could be satisfactorily accomplished by use of the AKUFVE extraction technique (7). This method is found especially suitable and reliable for the present extraction systems with HDEHP and acidic aqueous phases.

EXPERIMENTAL

Apparatus

Continuous solvent extraction experiments were carried out by means of an AKUFVE 100, delivered by Incentive Research and Development AB, Stockholm. This apparatus consists of a 1.4 l mixing vessel (mixer) and an H-centrifuge (8), the rate of rotation of which is adjusted by a high frequency induction motor. The mixer is mounted above the centrifuge and these are interconnected by viton tubing. The liquid volume in the centrifuge is 150 ml. The separated phases flow through 6 mm i.d. viton tubing for on-line measurements in glass flow-cells using radiometric detectors, and back to the mixer making a closed cycle. The liquid volume in the tubing is 75 ml for each phase.

The centrifuge, stirrer, top and bottom of the mixer and tube joints are all made of titanium metal, while the walls of the mixer as well as flowmeters are of glass.

The detectors used for radiometric determinations consist of two 3 in x 3 in well-type NaI(Tl) scintillation crystals. Two Philips FW 4280 single channel analyzers, serving for energy-selective discrimination of the radiation, and a Philips time-programmed high-speed counter arrangement for the simultaneous accumulation of counts in two measuring channels, with a printout device, facilitate the recording of metal distributions between the two phases.

Reagents

Technical grade HDEHP was obtained from Farbenfabriken Bayer, AG, Leverkusen. Titration of a sample with NaOH in 80 wt % ethanol - 20 wt. % solvent showed a content of (96.6 ± 0.2) wt % di-ester. The mono-ester was not detectable (less than 0.2 wt %).

Stock solutions of ~ 1 M extractant were prepared by dissolving HDEHP, as obtained, in Shell Sol T. This diluent is composed essentially of iso-paraffins boiling around 180-215°C, and has a sp. gr. of 0.760 g/cm³. The final concentration of extractant was determined by titration as 0.97 M HDEHP in extractions from nitric acid solutions, and as 0.92 M HDEHP in the similar extractions from sulfuric acid solutions.

All other reagents used were analytical grade or better.

Radioactive tracers

The radionuclides ¹⁴¹Ce, ¹⁴⁷Pm and ¹⁵³Gd were supplied by the Radiochemical Centre, Amersham. All others, viz. ¹⁴⁰La, ¹⁴²Pr, ¹⁴⁷Nd, ¹⁵³Sm, ^{152,154}Eu, ¹⁶⁰Tb, ¹⁶⁹Dy, ¹⁶⁹Er, ¹⁷⁰Tm, ¹⁶⁶Ho, ¹⁶⁹Yb, ¹⁷⁷Lu and ⁹⁰Y, were obtained by neutron activation of the respective rare earth oxides. The radiochemical purity of the tracer was in all cases checked by γ -spectrometry using a Ge(Li)-detector with a 4000 channel analyzer.

Procedure

Starting volumes of the organic and aqueous phases were each 500 ml. After attainment of complete phase separation (centrifuge speed 7000 rpm) and constant temperature (25.0 ± 0.2) °C, a suitable amount of the radioactive tracer was added. Distributed in one phase only, the radioactivity amounted to ~ 200000 cpm and a metal concentration of $\leq 10^{-5}$ M.

The acid concentration was changed by incremental addition of small volumes of a concentrated acid solution. After each addition a series of activity measurements, usually with a counting period of 1 min, was made until equilibrium was established. The equilibrium concentration of acid in the solutions was determined on small volumes withdrawn from the two phases. The possible retention of radioactivity in the detector cells during a run was checked by counting simultaneously-withdrawn samples of the two phases with an off-line NaI(Tl) well-type detector.

The distribution ratios for the highest nitric acid concentrations (> 9 N HNO₃) were measured by shaking the two phases in separating funnels. Preconditioning of organic phase was performed in most cases. The acid concentration at equilibrium was, however, determined by titration. 2 ml volumes of each phase were counted for a sufficient time to obtain $\leq 1\%$ standard deviation.

The ratio of the detection efficiencies in the two phases for each of the actual rare earth radionuclides was determined for each of the counting systems by means of standard radiochemical calibration procedures.

Treatment of data

The experimental data for log D vs. log HNO₃ concentration were treated by a linear least square method to fit the polynomial

$$\log D = \sum_{n=0}^{n=4} a_n \cdot (\log (\text{HNO}_3))^n \quad (1)$$

where a_n ($n = 0 - 4$) are constants and (HNO_3) is the measured nitric acid concentration.

On the assumption that the log D-values are subject to normally distributed random errors, the relative standard deviation in D is given by

$$\frac{s_D}{D} = \ln 10 \cdot \frac{\sum (\log D_{\text{obs}} - \log D_{\text{calc}})^2}{f}$$

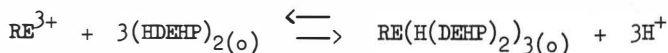
where f is the number of degrees of freedom.

The standard deviation is a measure of the experimental reliability of the D-values from which the coefficients of equation (1) have been calculated. The calculated equation is only adopted as a local approximation. All values for the relative standard deviation are less than 1 per cent, with the exception of 1.3 per cent for Ce.

The evaluated equation (1) may be used for obtaining interpolated D-values and various slopes of the log D vs. log (HNO₃) curves.

Dependence of the distribution ratio on the HDEHP concentration

The accepted extraction reaction between aqueous rare earth ions and HDEHP in a diluent such as Shell Sol T is expressed as:-



Accordingly D, which should correspond to $\frac{(\text{RE}(\text{H}(\text{DEHP})_2)_3(o))}{(\text{RE}^{3+})}$,

is dependent upon the third power of $[(\text{HDEHP})_2]$. This dependency is verified by Peppard et al. (9) for Y, La, Pm and Tm in 0.2 M HClO₄ when extracted with $(\text{HDEHP})_2$ up to 0.15 M in toluene. In the present work deviations from the third-power dependency are observed even below 10^{-2} M $(\text{HDEHP})_2$. On a plot of log D vs. log $[(\text{HDEHP})_2]$, the slope of the curves for various rare earth ions decreases with increasing $[(\text{HDEHP})_2]$, as shown for Tb in Fig 1. Similar curves are obtained for either of the two acids in the aqueous phase and for different acid strengths (0.5 N HNO₃ and 4 N H₂SO₄). If the slope of 3 is considered to be the dependency in an ideal system, the deviation may be interpreted as an increasing solute-solvent interaction with increasing HDEHP concentration. The observation is consistent with the measurements of the apparent molecular weight of HDEHP in n-hexane by Ferraro et al. (10), as they deduced that the state of aggregation of HDEHP appears to be strongly concentration-dependent.

The deviation from a line with slope of 3 for log D vs. log $[(\text{HDEHP})_2]$ (Fig. 1) may be considered as an effect of differences between activity and concentration of $(\text{HDEHP})_2$ in the organic phase. The activity coefficient, γ , may be calculated as a function of $[(\text{HDEHP})_2]$, and log $\gamma_{(\text{HDEHP})_2}$ is approximately linear

with respect to $\sqrt{[(\text{HDEHP})_2]}$ (Fig. 2):

$$\log \gamma_{(\text{HDEHP})_2} = -A\sqrt{[(\text{HDEHP})_2]}$$

with A = 0.83 in the concentration range 4.7×10^{-3} M to 0.5 M (dimeric form).

As will be shown below, the extraction mechanism changes when the nitric acid concentration in the aqueous phase increases above a certain value. The change is supposed to be completed at the highest concentration used, 14.45 N, and a study of the relationship between $\log D$ and $\log ((\text{HDEHP})_2)$ for Lu at this acid strength discloses a linear dependency with slope = 2.0 (Fig 3). The uptake of nitric acid in the organic phase will influence the interaction between $(\text{HDEHP})_2$ and Shell Sol T. If the activity coefficient of $(\text{HDEHP})_2$ in the organic phase varies little in the presence of HNO_3 , the slope of $\log D$ vs. $\log (\text{HDEHP})_2$ indicates an extracting species of formula $\text{Lu}(\text{NO}_3)_3 \cdot 2(\text{HDEHP})_2$.

Distribution ratio as a function of acid concentration

Compared with HNO_3 in the aqueous phase the extraction system with H_2SO_4 shows a less complex picture of $\log D$ vs. \log acid normality. The slopes are here approximately -3 for La and the lighter lanthanides, but for the heavier ones, where D-values at higher acid concentrations could be measured, the slopes approach -4 (Fig 4).

With nitric acid in the aqueous phase the trend in the plots of $\log D$ vs. \log acid concentration (Fig 5) can be examined by use of the fitted polynomial Eq. (1). If the slope

$$n = \frac{d(\log D)}{d(\log(\text{HNO}_3)_{\text{aq}})}$$
 is plotted as a function of atomic number,

several interesting effects are disclosed (Fig 6). For a given acid concentration the slope varies considerably with Z, and a typical tetrad effect is found. The tetrad grouping seems also justified in the region of positive slopes, but in these cases anomalously high slopes show up for Ce and Tb. For Ce this anomaly is easily explained by the presence of a fraction of Ce in +4 state, but the consequence would be a similar situation for Tb. Such an effect for Tb in solution has hardly been observed earlier.

By means of the polynomial it is possible to determine the concentration of aqueous nitric acid for which the minimum value of D is obtained. This $(\text{HNO}_3)_{\text{aq}}$ is found to vary along the series of elements in a manner that exhibits tetrad grouping. Again anomalies with respect to tetrad effects are found for Ce and Tb (Fig 7).

In these studies on extraction behaviour, Y seems to behave as a rare earth element between Ho and Er, except at the higher concentrations of HNO_3 where D-values of Y exceed those of Ho and Er.

Variation of log D with log a_{H^+} or H

The deviation from a slope of -3 for the plots of log D vs. log N H_2SO_4 , and of log D vs. log M HNO_3 , for concentrations below 5 M may arise from the large difference between the normality of the acids and the H^+ -activity. If an extended pH scale based on potentiometric titrations (11) or the Hammett acidity function, $-H_0$ (12), is applied in the plots instead of the log normality of acid, great changes appear in the log D curves. For example the log D plot for La with H_2SO_4 in the aqueous phase, exhibiting a linear slope of -3 on the concentration basis, results in a curve with slope ~ -8 at low acidity and about -1.5 at higher values of the acid concentration. For heavier metals where higher acid concentrations are used, the negative slopes become less and less. The large deviation from ideality may be due to an increase in dissolved extractant in the aqueous phase with increasing acidity.

Influence of the anions in aqueous phase

The concentration of the anions in aqueous solutions of HNO_3 and H_2SO_4 as a function of the acid concentration is known (13) and may be used to correct for the formation of complexes of rare earth ions in the aqueous phase. As the concentration of sulfate ions is 1/3 or 1/5 of the concentration of nitrate ions at a given acid molarity (Fig 8), but the first formation constant is 10 to 20 times larger for $RE(SO_4)^+$ than for $RE(NO_3)^{2+}$ (14, 15, 16), the degree of complex formation by the rare earth elements in aqueous solution should be higher for sulfuric acid. The formation of metal ion complexes in the aqueous phase causes a lowering of the D-values compared with a similar system in which no metal complexes are formed in the aqueous phase. Thus addition of the NH_4 -salts of the respective acids to the aqueous phase in order to increase the anion concentration should have a greater depressive effect on the D-value in the sulfate than in the nitrate system. One sees, however, a distinct increase in the D-value for the sulfate system, but a decrease, as expected, for the nitrate system, Fig 9. As the second protolysis step for sulfuric acid is of medium strength, addition of sulfate anions will reduce the free H^+ -concentration and the D-value will become higher. This illustrates some of the complexity involved in the use of sulfuric acid in the aqueous phase.

Variation of extraction with atomic number

The extraction equilibrium constants for various rare earth elements may be calculated with the use of D-values at a given H^+ -activity and of the activity of 0.5 M (HDEHP)₂ in Shell Sol T. Thus with neglect of possible influences of metal complexing by the anions in the aqueous phase, and of the effect of introducing activities instead of concentrations of free metal ions and the extracted metal complexes, extraction constants, K, may be calculated:

$$K = D \frac{(a_{H^+})^3}{(\text{HDEHP})_2^3 (\text{HDEHP})_2}$$

At $a_{H^+} = 1.0$ (ionic strength $I = 1.3$ for both acids) the K-values for Gd are 2.64 and 2.59 with HNO_3 and H_2SO_4 , respectively. In comparison, Peppard et al. (17)²₄, measured $K = 2.02$ for Gd with 0.106 M HDEHP in n-heptane diluent in contact with 0.25 M HCl (at 22°C).

As K is proportional to D, the trend in the K-values at $a_{H^+} = 1.0$ is seen from a plot of log D at this H^+ -activity vs. atomic number, Fig 10. For the second octad of lanthanides, and for yttrium, the log D values for HNO_3 and H_2SO_4 fall on the same curve. For the first octad, however, the values for the extraction with HNO_3 in the aqueous phase are the higher ones, and the difference increases with decreasing Z. As a consequence of the tetrad grouping, a poor separation is obtained for Nd and Pm in the HNO_3 system. A possible enhancement of Ce extraction is seen when compared with a smooth tetrad grouping.

In concentrated HNO_3 ($M = 14.45$) the increase in log D with increasing Z is lower than at $a_{H^+} = 1.0$, indicating poorer separation efficiency in this system. The tetrad effect is present with anomalies in the behaviour of Ce and Tb. In 7 M HNO_3 (corresponding to minimum D) separation efficiencies are even less. This seems to be a consequence of the strange variation in (HNO_3) for D_{\min} along the series of metals (Fig 7). At a high H_2SO_4 concentration (10 N) log D increases faster with Z than at $a_{H^+} = 1.0$ (Fig 10).

Kinetic studies

The experimental procedure applied so far does not allow us to measure rates of extraction with half-lives less than one minute. To obtain a reasonable statistical significance, the half-life should be $\gtrsim 1.5$ min (rate constant $k \lesssim 0.5 \text{ min}^{-1}$). Besides this limitation, the distribution ratio at equilibrium should not deviate from unity by more than a factor of approximately 50 if a measurement is to be reliable.

In our experiments, the rate of extraction from nitric acid was too fast to be observed. In the sulfuric acid system, however, a measurable rate of extraction could be observed under certain conditions.

On the assumption of a first-power dependence on metal concentration, the measured time-dependent extraction data were used to test the following rate expression:

$$\ln \frac{R_t - R_{e0}}{R_0 - R_{\infty}} = kt$$

where

R_0 is the metal ion concentration at time $t = 0$,

R_t is the metal ion concentration at time t ,

R_{∞} is the metal ion concentration at equilibrium,

k is the overall rate constant.

All the recorded data, when treated according to equation (2), yielded straight lines. A typical set of such lines is shown in Fig 11. As a matter of convenience, the constant denominator $R_0 - R_{\infty}$ is omitted throughout the calculation of the rate constants.

The variation in the rate constant with the sulfuric acid normality is shown in Fig 12. The shape of this curve is characteristic for all the heavier rare earths (atomic number greater than 64) and for yttrium. For the lighter rare earths, the rate of extraction is too fast to be observed.

The slope in Fig. 12 is about -1.7 in the lower acidity region, indicating an inverse 1.7 power dependency on the sulfuric acid concentration. The data corresponding to the higher acidity region are difficult to obtain, owing to the low distribution ratios.

The normality of H_2SO_4 for the minimum rate constant is found to increase with increasing atomic number. Furthermore, the minimum value of the rate constant decreases with increasing Z.

The rate constant is found to vary with the (HDEHP), Fig 13. Furthermore, the (HDEHP) at which the rate constant passes its minimum depends on the (H_2SO_4).

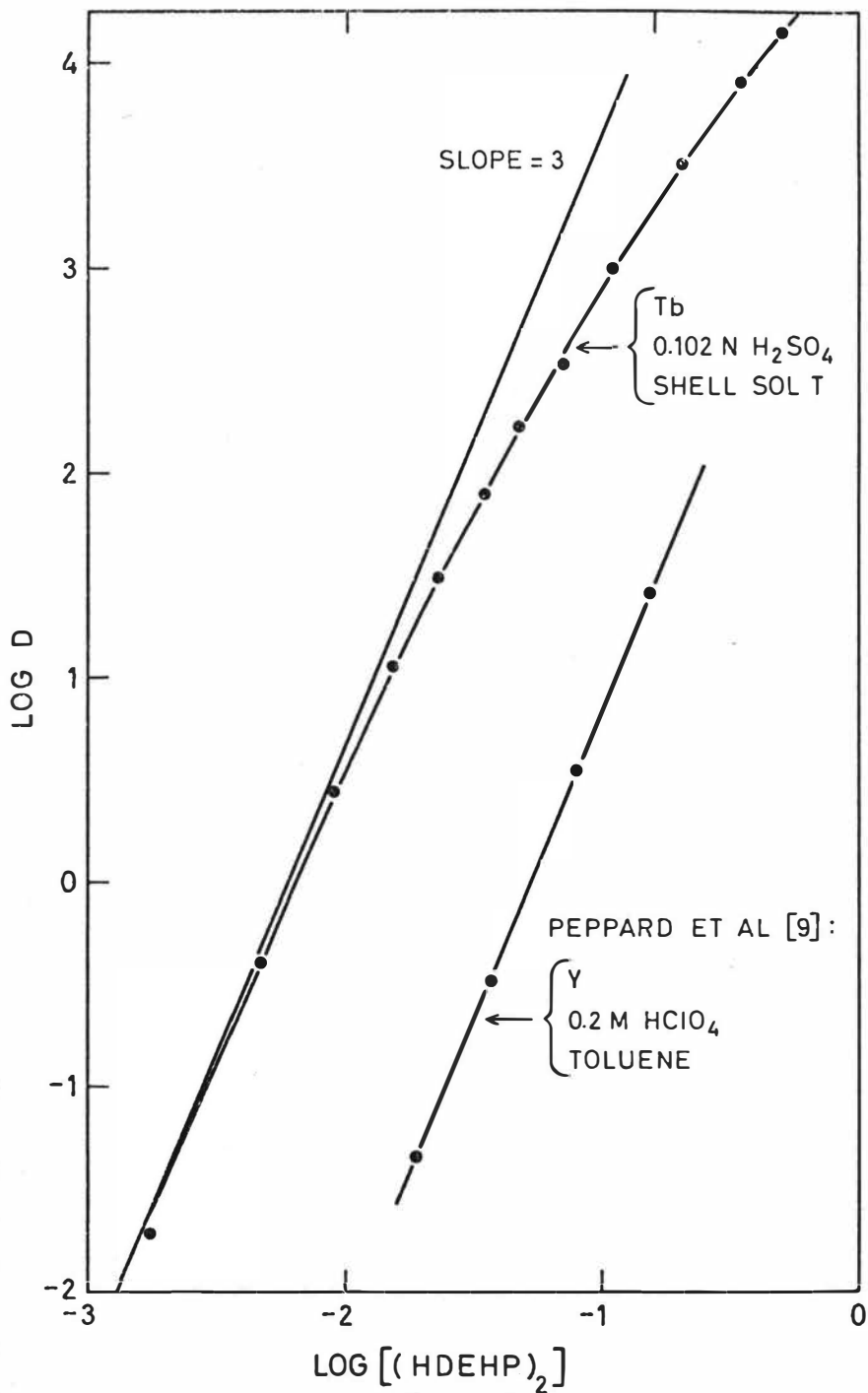
From the kinetic experiments the conclusion so far is that the rate expression for a given rare earth is a highly complex function. As effective phase contact is obtained over a very large interfacial area in the AKUFVE apparatus, the rate is considered to be chemically controlled. It is strongly dependent on the presence of sulfuric acid.

Acknowledgement

The authors wish to express their gratitude to Professor A C Pappas for his stimulating interest and for helpful discussions pertaining to this work. Financial support from Forskningsgruppe For Sjeldne Jordarter is gratefully acknowledged.

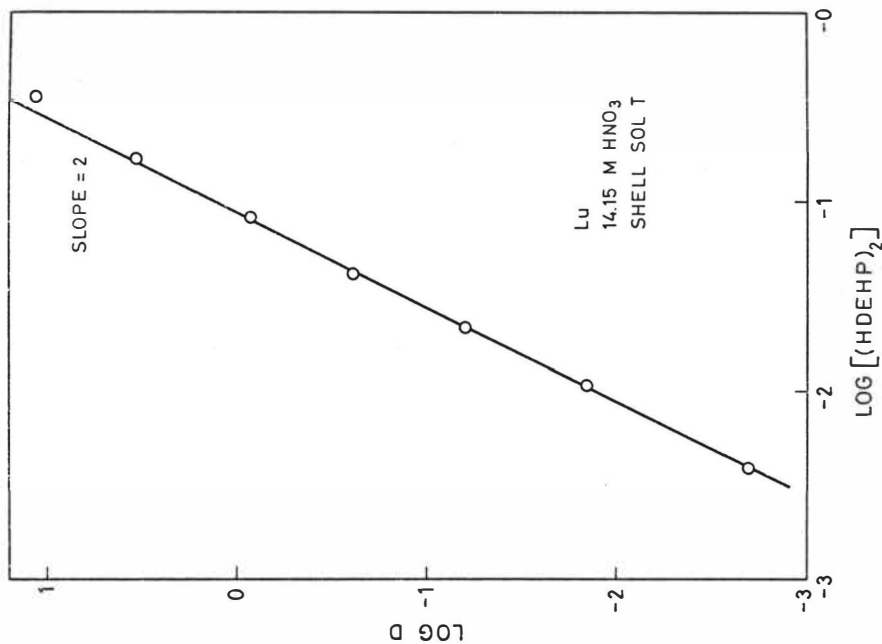
REFERENCES

1. V E Shaw and D J Bauer, USA Rept. R.I.-7691, Bureau of Mines (1964).
2. D F Peppard, G W Mason, J L Maier and W J Driscoll, *J. inorg. nucl. Chem.* 4, 334 (1957).
3. D F Peppard, G W Mason and I Hucher, *ibid.* 18, 245 (1960).
4. A I Mikhailichenko and R M Pimenova, *Radiokhimiya* 11, 8 (1969).
5. I H Qureshi, L T McClendon and P D LaFleur, *Radiochim. Acta* 12, 107 (1969).
6. O B Michelsen and M Smutz, Paper 28, ISEC 1971.
- 7a. J Rydberg, *Acta Chem. Scand.* 23, 647 (1969).
- 7b. C Andersson, S O Andersson, J O Liljenzin, H Reinhardt and J Rydberg, *ibid.* 23, 2781 (1969).
8. H Reinhardt and J Rydberg, *ibid.* 23, 2273 (1969).
9. D F Peppard, G W Mason, W J Driscoll and R J Sironen, *J. inorg. nucl. Chem.* 7, 276 (1958).
10. J R Ferraro, G W Mason and D F Peppard, *ibid.* 22, 285 (1961).
11. L Michaelis and S Granick, *J. Am. Chem. Soc.* 64, 1861 (1942).
12. M A Paul and F A Long, *Chem. Rev.* 57, 1 (1957).
13. Y Marcus and A S Kertes, *Ion Exchange and Solvent Extraction of Metal Complexes*, p. 227, Wiley-Interscience 1969.
14. R G De Carvalho and G R Choppin, *J. inorg. nucl. Chem.* 29, 725 (1967).
15. D F Peppard, G W Mason and I Hucher, *ibid.* 24, 881 (1963).
16. G R Choppin and W F Strazik, *Inorg. Chem.* 4, 1250 (1965)
17. D F Peppard, C A A Bloomquist, E P Horwitz, S Lewey and G W Mason, *J. inorg. nucl. Chem.* 32, 339 (1970).

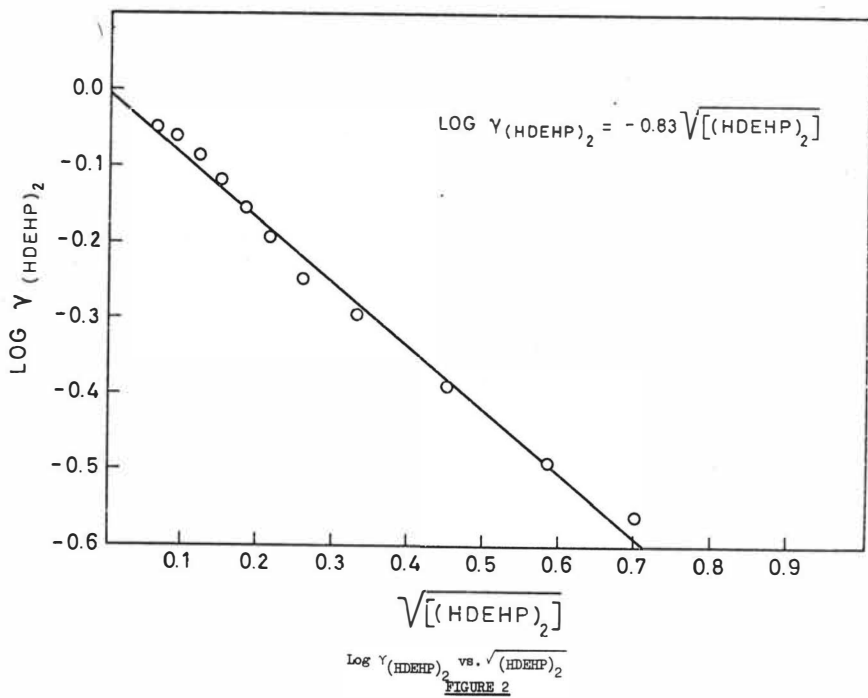


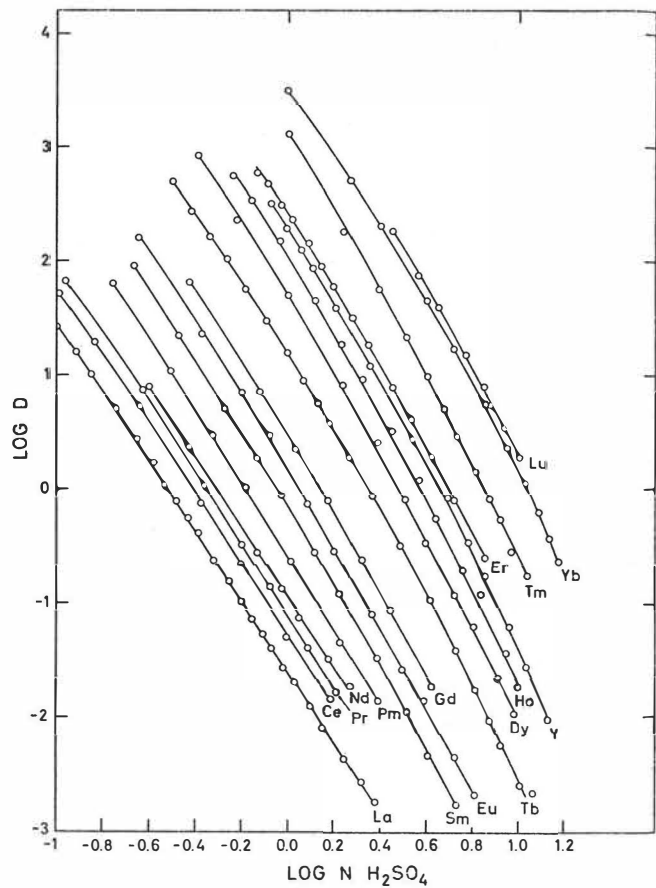
Log D vs. log [(HDEHP)₂] for Tb

FIGURE 1



Log D vs. $\log [(HDEHP)_2]$ for Lu at 14.15 N HNO₃ aqueous phase
FIGURE 3

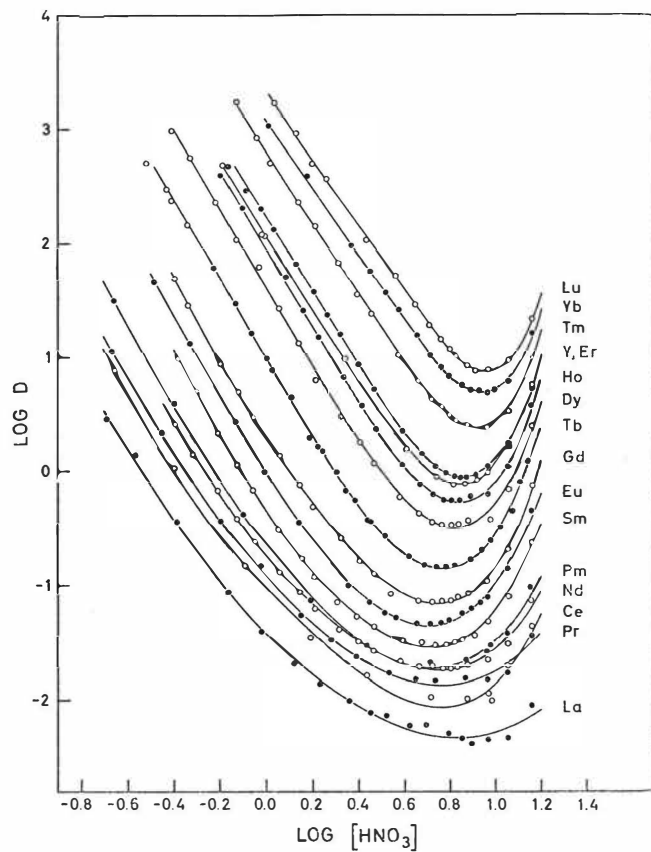




Log D vs. log N H₂SO₄

FIGURE 4

1197



Log D vs. log M HNO₃

FIGURE 5

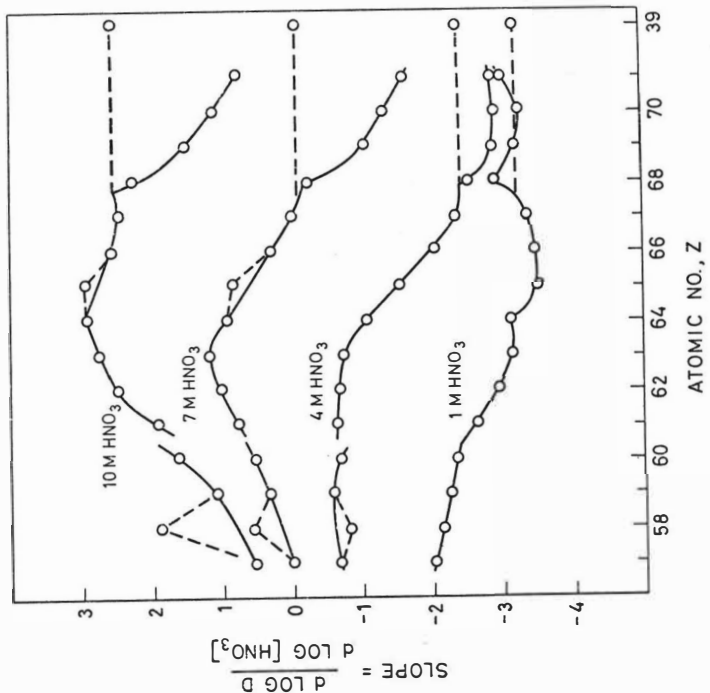


FIGURE 5
 $n = \frac{d(\log D)}{d \log [HNO_3]}$ vs. atomic no., Z.

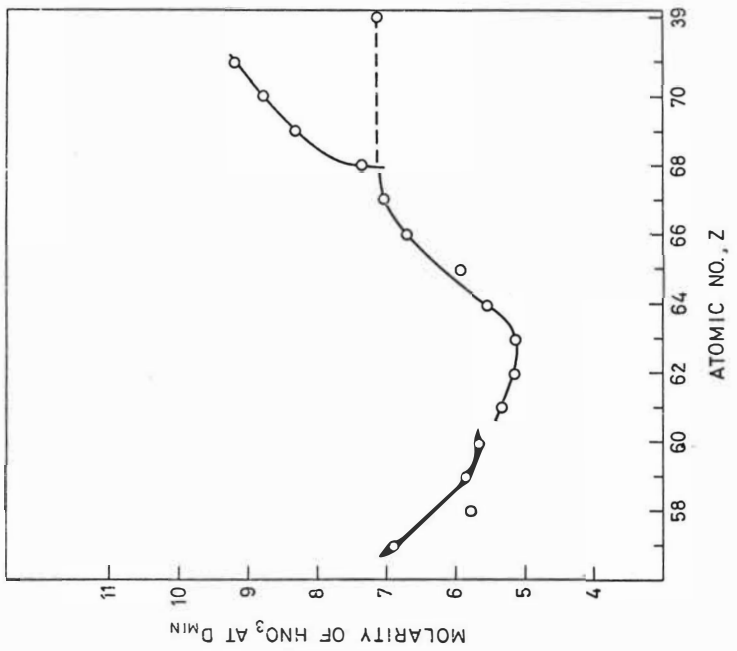
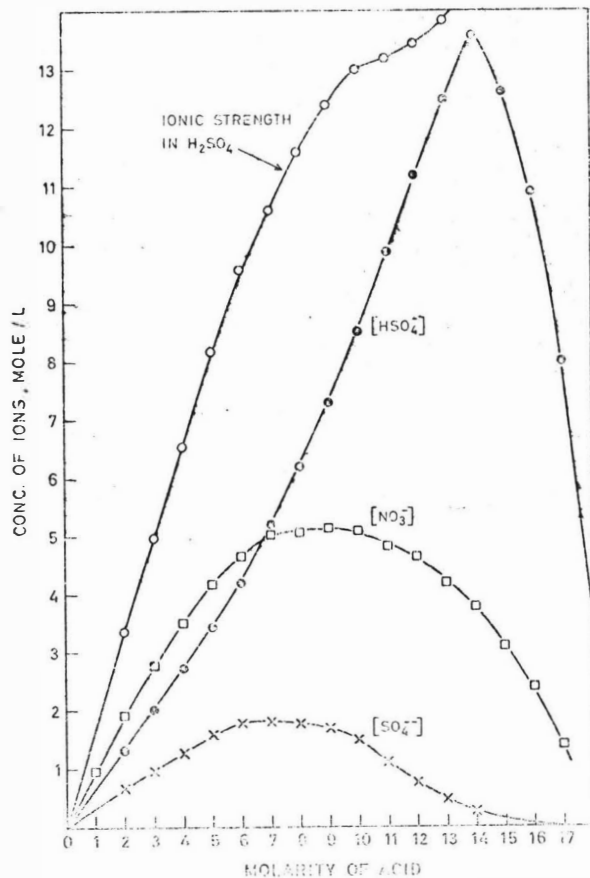


FIGURE 7
 $[HNO_3]_{at D_{min}}$ vs. atomic no., Z.



Sulfate and nitrate concentration as a function of the respective acid concentration

FIGURE 8

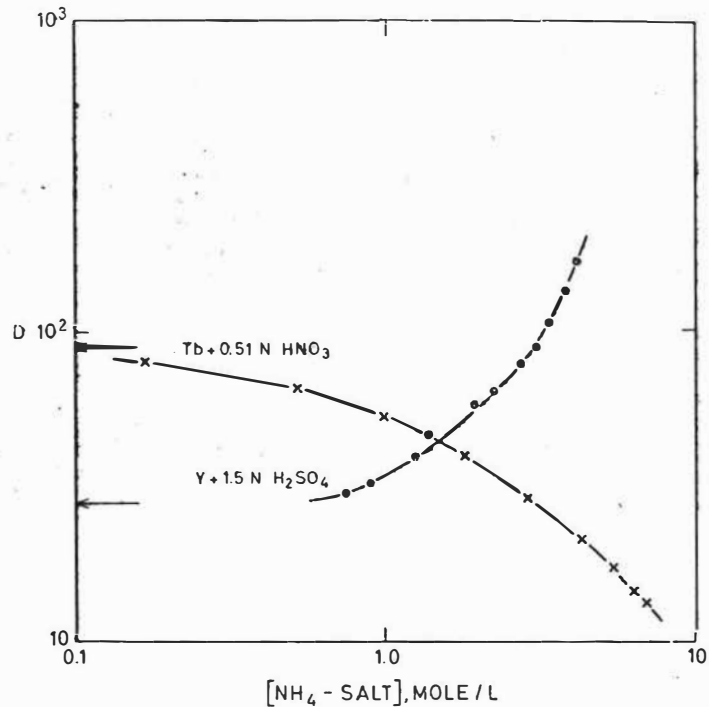
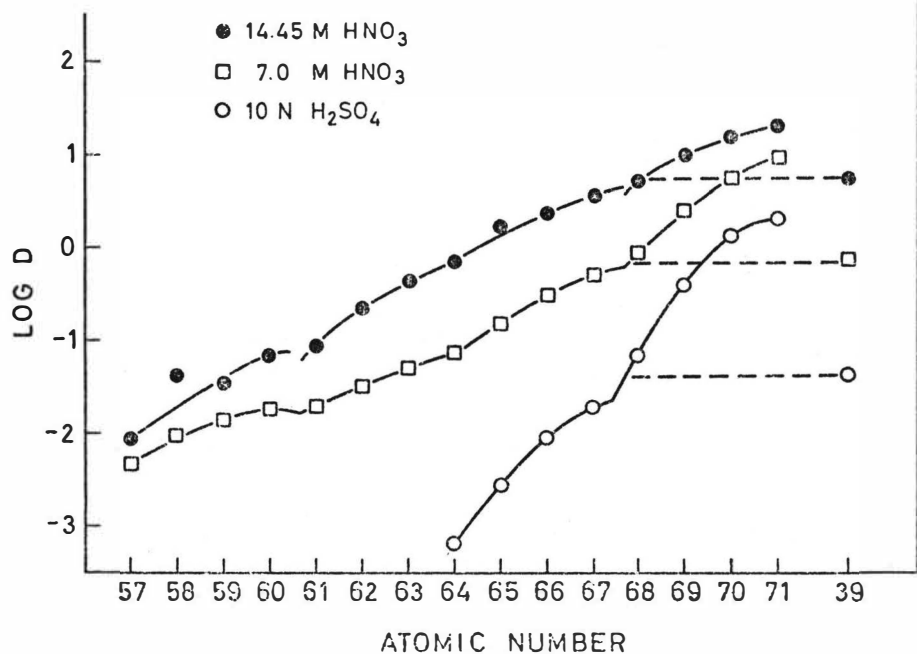
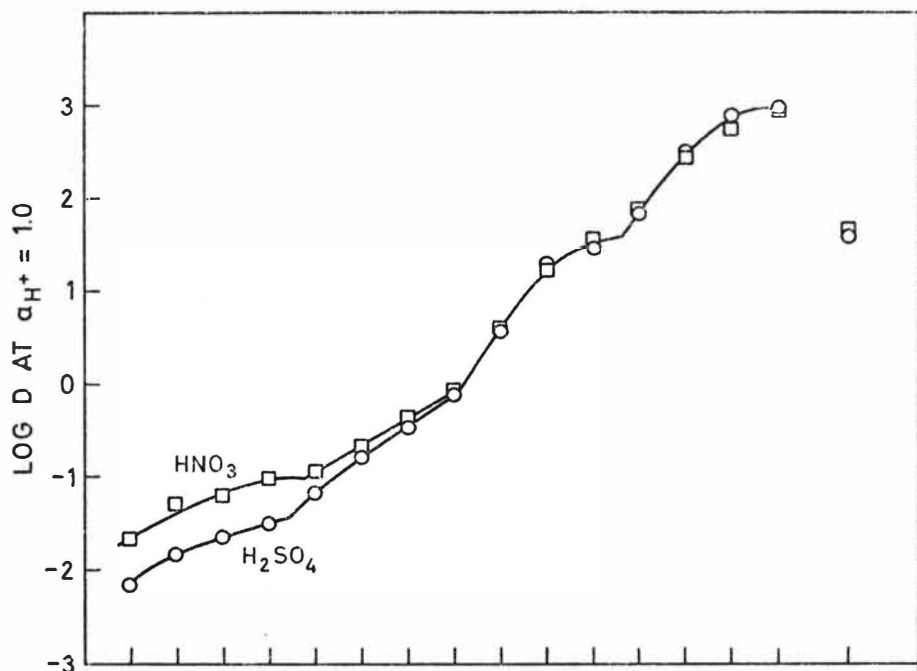
D-values of Tb and Y as function of $[NH_4NO_3]$ and $[(NH_4)_2SO_4]$, respectively

FIGURE 9



Log D vs. atomic no., Z, at various acid concentrations

FIGURE 10

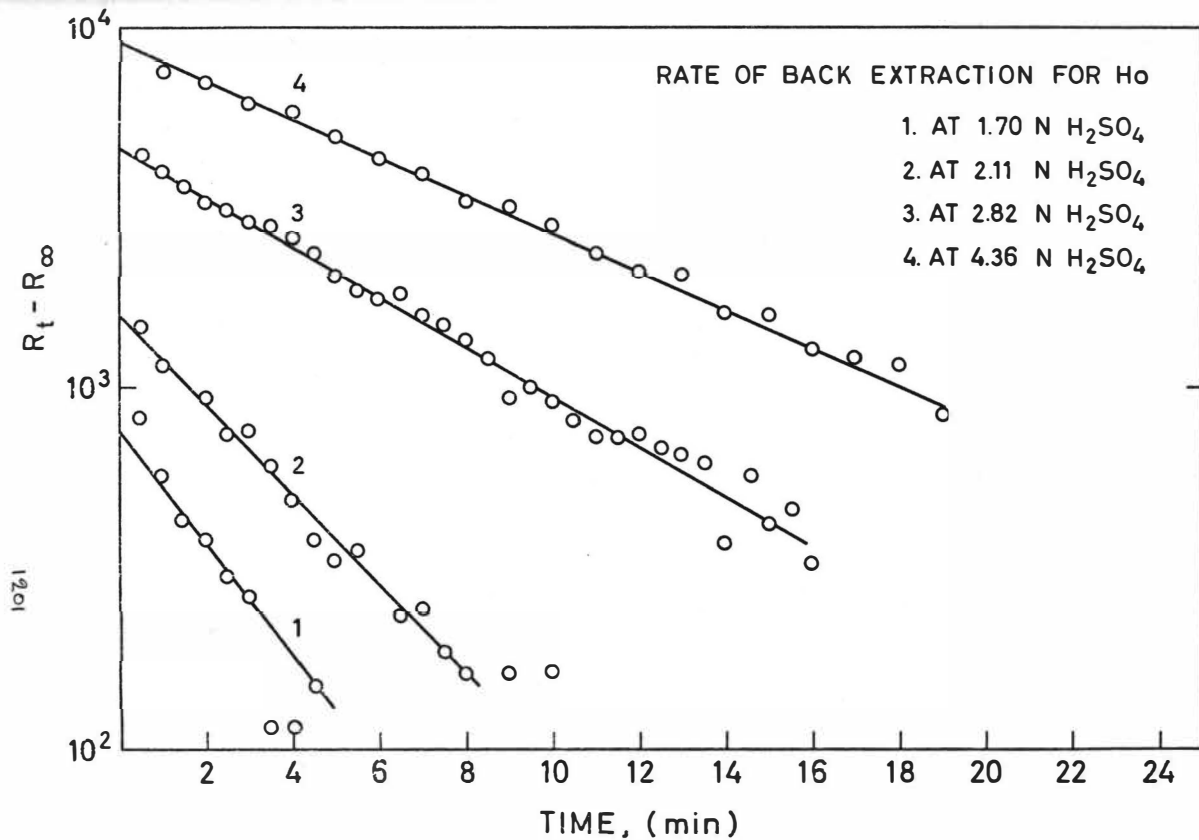
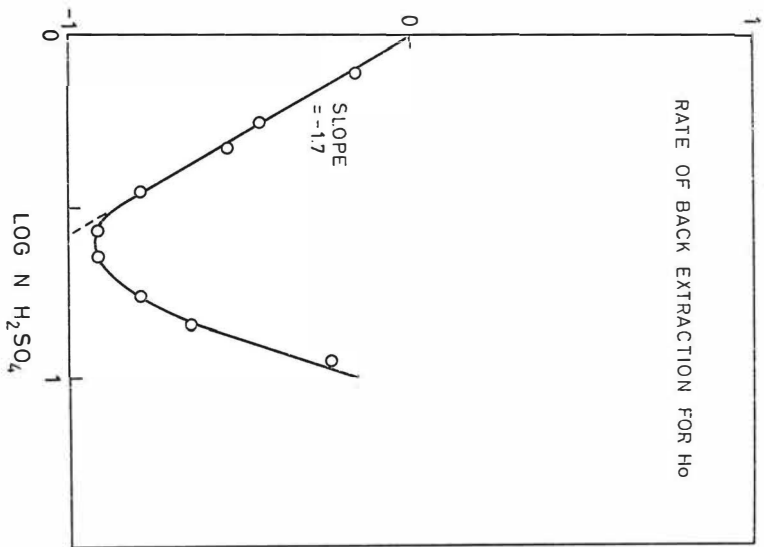


FIGURE 11

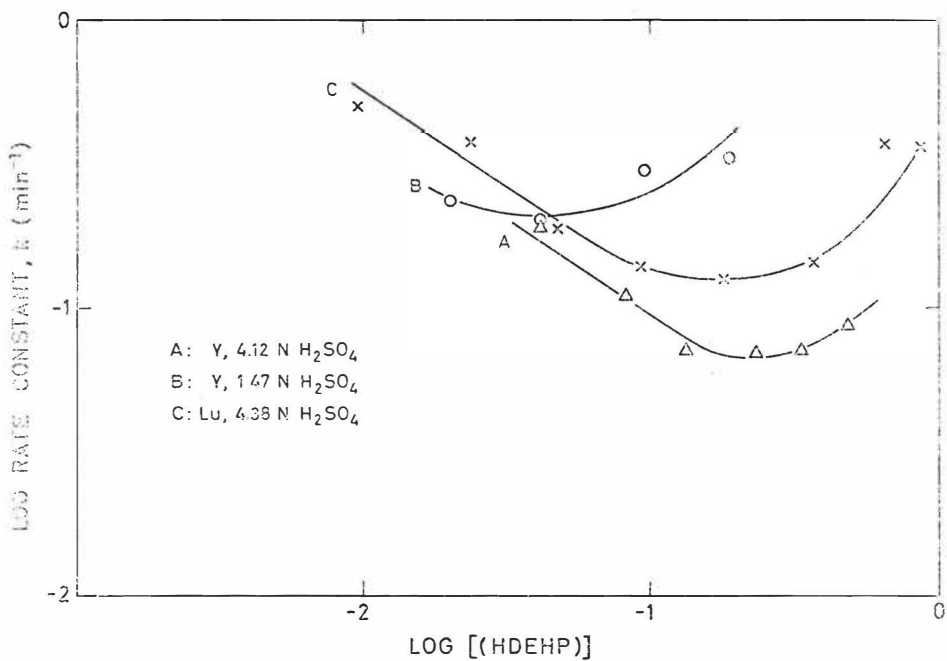
 $\ln (R_t - R_\infty)$ vs. time in min

LOG RATE CONSTANT, k (MIN^{-1})



Rate constant, k , vs. $N H_2SO_4$

FIGURE 12



Rate constant, k , vs. [HDEHP]

FIGURE 13

EXTRACTION OF TRIVALENT TRANSPUTONIUM ELEMENTS AND EUROPIUM
BY A MIXTURE OF DI-2-ETHYLHEXYLORTHOPHOSPHORIC ACID AND
PHOSPHORUS PENTOXIDE FROM STRONGLY ACID MEDIA

B.F. Myasoedov, M.K. Chmutova, H.E. Kochetkova, G.A. Pribylova
V.I. Vernadsky Institute of Geochemistry and Analytical
Chemistry, USSR Academy of Sciences, Moscow

The extraction of trivalent transplutonium elements and europium from solutions of inorganic acids by a mixture of di-2-ethylhexylorthophosphoric acid (D2EHPA) and P_2O_5 in cyclohexane has been investigated. It is shown that the proposed mixture of reagents quantitatively extracts Am and Eu from solutions of acids of sufficiently high concentration. Large amounts of aluminium and ammonium nitrates, at D2EHPA and P_2O_5 concentrations equal to 0.3M and 0.1M respectively, do not interfere with extraction. The extractant exhibits low-selectivity with respect to trivalent transplutonium elements (TPE).

We have used a solution of a di-2-ethylhexylorthophosphoric acid (D2EHPA) and phosphorus pentoxide in cyclohexane as an extractant for trivalent transplutonium elements and europium.

The mixture of D2EHPA and P_2O_5 displays an unusually high extraction capacity with respect to Am and Eu; by dissolving a mixture of low concentration in cyclohexane these elements may be quantitatively extracted from 1-2M HNO_3 and H_2SO_4 , 1-5M $HClO_4$ and 1-11M HCl . From 2-12M HNO_3 and 2-7M H_2SO_4 more than 90% of Am and Eu are extracted (fig.1). Data on the extraction of trivalent Am, Cm, Bk, Cf and Eu from solutions of nitric acid by a mixture of these reagents in cyclohexane are listed in table 1. It can be seen from table 1 that extractant exhibits a low selectivity for trivalent TPE; the distribution coefficients being very similar. Eu is somewhat better extracted.

The dependence of trivalent americium extraction from 5M nitric acid on the D2EHPA and P_2O_5 concentrations has been investigated (fig.2).

In the first case (curve 1) the concentrations of both components of the reagent were simultaneously changed, but their ratio was kept constant and equal to three (dilution of the initial mixture by cyclohexane).

In the second case (curve 2) only the P_2O_5 concentration was changed and the D2EHPA concentration was maintained constant and equal to 0.03M (dilution of the initial mixture by 0.03M of D2EHPA solution in cyclohexane). It is of interest to note that, for the series of experiments which were carried out, distribution is lower, for a fixed concentration of P_2O_5 , when the D2EHPA concentration is higher.

The influence of aluminium and ammonium nitrates on americium extraction from 1M and 5M nitric acid was investigated.

It can be seen from figure 3, that aluminium nitrate does not lower americium extraction from 1M and 5M nitric acid, if the D2EHPA concentration equals 0.3M and the P_2O_5 concentration - 0.1M (curves 1 and 2).

When the concentration of the reagents is decreased a hundred times, aluminium nitrate noticeably suppresses americium extraction (curves 3 and 4). According to preliminary data, the mixture of extractants in cyclohexane which has been employed also extracts appreciable amounts of aluminium. Therefore, when there is a great excess of aluminium present, americium extraction is suppressed due to the binding of the reagents by aluminium.

Even large amounts of ammonium nitrate do not change the distribution of coefficients of americium, (10M (in 1M HNO_3) and 7M (in 5M HNO_3)). Hence, the nitrate-ion does not exert an appreciable influence on the extraction.

The extractive properties of the D2EHPA P_2O_5 mixture decrease with time. The dependence of Am extraction by mixtures containing different D2EHPA concentrations in cyclohexane on the time, which had elapsed after preparation of the solution has been investigated. The distribution coefficient of americium sharply decreases during the two first days, it then falls off less sharply and after 5 days the distribution coefficient remains almost constant (fig.4).

Fig.1 (curve 5) shows the dependence of americium extraction by a solution of 0.003M D2EHPA and 0.001M P_2O_5 in cyclohexane on nitric acid concentration on the sixteenth day after the solution had been prepared. The extraction decreases, but the character of the distribution coefficient dependence on nitric acid concentration does not change.

The use of a freshly prepared solution of the reagent mixture ensures good reproducibility in the results.

On the basis of the results which have been presented it may be assumed that the high distribution coefficients for the trivalent transplutonium elements and europium are the results of the formation of a new compound which is formed during the dissolution of phosphorus pentoxide in di-2-ethylhexylorthophosphoric acid and which possesses a high extraction capacity.

TABLE 1

The dependence of trivalent Am, Cm, Bk, Cf, Eu extraction by a solution of 3.10^{-4} M D2EHPA and 1.10^{-4} M P_2O_5 in cyclohexane on HNO_3 concentration

HNO_3 M	Distribution coefficient				
	Am	Cm	Bk	Cf	Eu
1	27.4	-	-	48.5	-
3	2.1	1.8	1.8	1.9	4.5
5	0.7	0.7	0.6	0.6	1.2
7	0.3	0.3	0.4	0.3	0.6
9	0.2	-	-	0.2	-
12	0.3	-	-	0.3	-

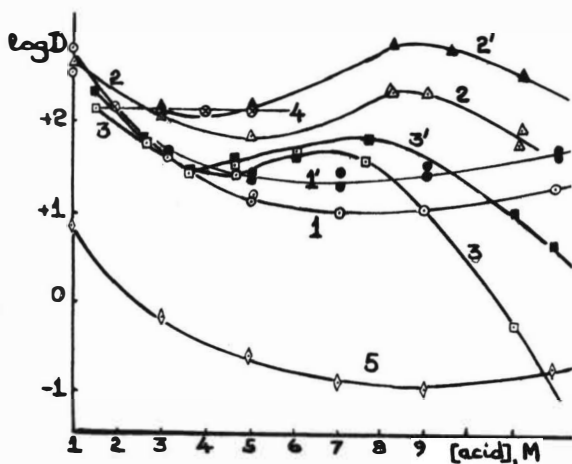


Fig. 1. Dependence of Am(III) and Eu(III) extraction by a solution of 0.003M D2EHPA and 0.001M P_2O_5 in cyclohexane on the acid concentration.

- | | | |
|---|------|-----------|
| 1 - Am | 2-Am | 3-Am |
| HNO_3 | HCl | H_2SO_4 |
| 1 - Eu | 2-Eu | 3-Eu |
| 4 - Am, $HClO_4$ | | |
| 5 - Am, HNO_3 (on the 16th day after preparation of the extractant solution). | | |

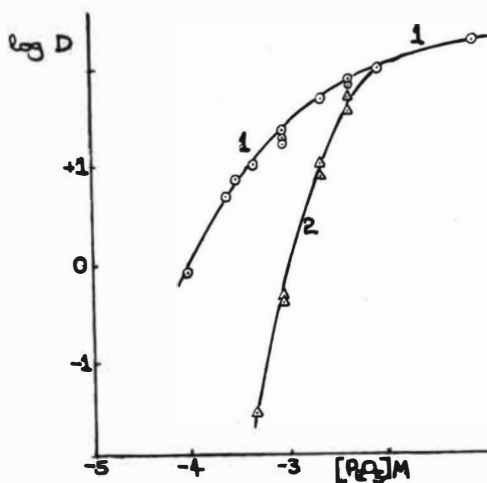


Fig. 2. Dependence of Am(III) extraction by D2EHPA and P_2O_5 mixtures in cyclohexane from 1M HNO_3 on the extractant dilution

- 1 - Dilution by cyclohexane; D2EHPA: P_2O_5 = 3:1
- 2 - Dilution by 0.03M D2EHPA solution;
D2EHPA = const = 0.03M.

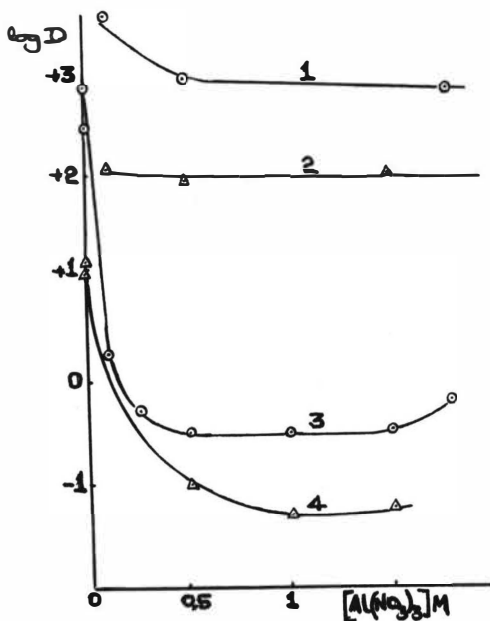


Fig.3. Dependence of Am(III) extraction by D2EHPA and P_2O_5 mixtures in cyclohexane from solutions of 1M and 5M HNO_3 on aluminium nitrate concentration

1 - 1M HNO_3	0.3M D2EHPA - 0.1M P_2O_5
2 - 5M HNO_3	
3 - 1M HNO_3	0.003M D2EHPA - 0.001M P_2O_5
4 - 5M HNO_3	

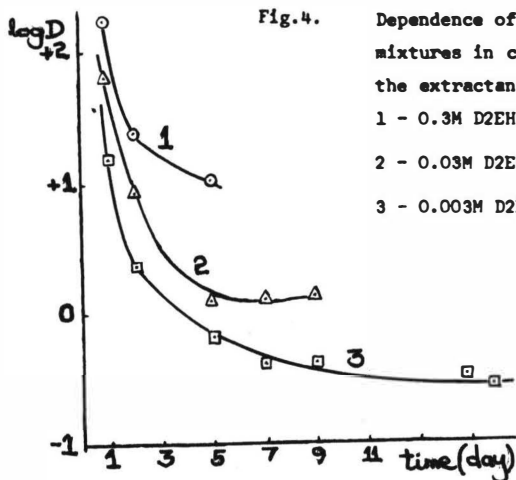


Fig.4. Dependence of Am(III) extraction by D2EHPA and P_2O_5 mixtures in cyclohexane from 5M HNO_3 on the time for which the extractant has been left standing after preparation

1 - 0.3M D2EHPA - 0.1M P_2O_5
2 - 0.03M D2EHPA - 0.01M P_2O_5
3 - 0.003M D2EHPA - 0.001M P_2O_5

INVESTIGATION OF RARE-ELEMENTS EXTRACTION WITH
DIFFERENT CARBOXYLIC ACIDS

G.V. Korpusov, N.A. Danilov, Yu.S. Krylov, R.D. Korpusova,
A.I. Drygin, and V.Ya. Shvartsman

Institute of Physical Chemistry of the Academy of
Sciences of the U.S.S.R., Moscow, U.S.S.R.

At present carboxylic acids are rather successfully used in rare-earth elements separation /1-3/. But the data published mainly refer to the technical mixtures of changeable composition /4-9/. However it is necessary to study the extraction of individual systems to obtain data on process operating parameters. So in this paper a comparative investigation of extraction systems has been carried out based on monocarboxylic acids with different hydrocarbon radicals attached to the carboxylic group.

Special attention has been paid to ~~o~~-branched carboxylic acids. Having the branching near the carboxylic group, they may be expected to have a greater selectivity.

EXPERIMENTAL

The main physico-chemical properties of carboxylic acids under investigation are given in Table 1. For carboxylic acids we used the following diluents: n-heptane, dodecane, benzole, toluole, 4-hydrogen chloride, n-decanole, n-heptanol and synthin. We used standard reagents produced in the USSR and as a rule they were not additionally purified.

Solutions of rare-earth elements salts (chlorides, nitrates and sulphates) were prepared by dissolving oxides of individual lanthanides, of not less than 99.9% purity, in corresponding mineral acids.

Equilibrium distribution of lanthanides in the extraction system was as a rule reached in 2-3 min (Fig.1). But in case of need of stirring was carried out for 1h. The investigation of the distribution of individual lanthanides between aqueous phase and carboxylic acids was performed by a two-phase titration method /13/ in presence of indicator quantities of lanthanide radioactive isotopes.

The accuracy of pH measurements was $\pm 0.005p$.

In a number of cases to stabilize the extraction system and avoid the necessity of precise pH adjustment the extract was used as 'prepared in advance' lanthanum soap of predetermined concentration. Solutions of lanthanide salts of known concentration were used as the aqueous phase.

In this case lanthanum served as a macrocomponent and the distribution of other lanthanides was determined against this background. The content of water in the extracted compounds was determined by titration with Fisher's reagent /14/.

Distribution of α, α' -Dialkyl Carboxylic Acids between Water and Different Diluents.

Data on carboxylic acids distribution as well as on their state in the organic phase are necessary for a proper understanding of the extraction mechanism. Such data is not available for α, α' -dialkylcarboxylic acids.

We investigated two samples of α, α' -dialkylcarboxylic acids with 8 and 9 carbon atoms in the molecule. Beforehand we had determined the solubility of these carboxylic acids in water; their ionization constants in water were $pK_{(C_8)} = 4.92 \pm 0.08$ and $pK_{(C_9)} = 4.94 \pm 0.02$ (Table 1).

It can be seen that the values of ionization constants of α, α' -branched carboxylic acids are close to those for non-branched carboxylic acids with the same number of carbon atoms in the molecule ($pK_{C_8} = 4.89$ and $pK_{C_9} = 4.85$ /10/). Dimerization constants of the investigated samples of α, α' -acids and the constants of their distribution between water and n-heptane, benzene, toluene, 4-hydrogen chloride and decanole were determined by the distribution method (Fig.2).

The values of distribution constants regularly increase and the values of dimerization constants regularly decrease with increase in diluent polarity. These regularities are typical for all acid extracts. But the absolute values of dimerization constants of α, α' -dialkylcarboxylic acids are much lower than those for n-carboxylic acids with the same number of carbon atoms in molecule. This could be explained by the presence of branching in the α -position creating spatial difficulties in dimer formation.

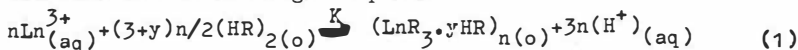
TABLE 2

Distribution and Dimerization Constants of α, α' -Dialkylcarboxylic Acids in Different Diluents

diluent permittivity	ϵ	α, α' -dialkylcarboxylic acid (C_8)		α, α' -dialkylcarboxylic acid (C_9)	
		distribution constant K_p	dimerization constant K_{dim}	distribution constant K_p	dimerization constant K_{dim}
n-heptane	1.92	60.0	24.3	380.0	57.0
4-hydrogen chloride	2.23	140.0	14.9	540.0	13.3
benzene	2.27	150.0	9.17	890.0	1.72
toluene	2.43	250.0	6.58	1130.0	1.25
n-decanole	8.1	780.0	0	2870.0	0

Regularities of Individual Lanthanides Distribution in Extraction Systems with Carboxylic Acids

In the general case of lanthanides extraction with acid extracts, the $(LnR_3 \cdot 3HR)_n$ compound formed by the reaction below, can transfer to the organic phase



The extraction constant may be represented as

$$K = ((LnR_3 \cdot yHR)_n(o) \cdot (H^+)^{3n} / (Ln^{3+})^n \cdot ((HR)_2)^{(3+y)n/2} \quad (2)$$

or in logarithmic form

$$\lg C_{Ln(o)} = n(\lg C_{Ln(aq)} + 3pH) + \lg nK + n(3+y)/2 \lg ((HR)_2(o)) \quad (3)$$

The degree of polymerization of the compound in the organic phase may be found from the slope of the curve in coordinates

$$(\lg C_{Ln(o)}) - (\lg C_{Ln(aq)} + 3pH), \text{ at } ((HR)_2) = \text{const}$$

then the distribution coefficient may be expressed as

$$\lg D = \lg K + n(3+y)/2 \cdot \lg ((HR)_2(o)) + 3pH \quad (4)$$

At constant values of the distribution coefficient and concentration of lanthanum in the aqueous phase the change in pH depends only on the concentration of $(HR)_2$ in the organic phase

$$pH = \lg D - \lg K / n(3+y) / 2 - \lg ((HR)_2(o)) \quad (5)$$

As the concentration of acid in the organic phase increases, the pH shifts to more acid values and the shift increases with the degree of polarization of the diluent (Fig. 3a, 3b). The shift to more alkaline values when using polar diluents (n-heptanol $\epsilon = 11.1$) in comparison with nonpolar n-heptane ($\epsilon = 1.92$) can be attributed to the greater strength of the proton bond in the carboxylic acid and H.R.S alcohol as compared with the bond strength in dimerized molecules of carboxylic acids.

The presence of 'salting out' agents like LiNO_3 in extraction with α, α' -acids shifts the pH to more acid values (Fig.3c). This is due to the fact that the 'salting out' agent increases the activity coefficient of lanthanide ions in the aqueous phase. The slope of the curve in Fig.3c decreases with increase in lanthanide concentration in the aqueous phase. The presence of electronegative chlorine atoms in the α -position relative to the carboxylic group shifts lanthanide extraction to the more acid pH values (Fig.3b).

Raising of the temperature shifts lanthanide extraction with α, α' -dialkylcarboxylic acids to the more acid pH area (Fig.4). It is due to increase in the ionization constants of the extract and decrease of its dimerization constant. At the same temperature extraction from sulphate solutions occurs at higher values of pH as compared with extraction from chlorine and nitrate solutions. It is connected with the greater complexing ability of sulphate ions in aqueous solutions. Similar results were obtained earlier in the investigation of the influence of temperature on extraction of praseodymium chloride and sulphate with technical mixtures of carboxylic acids of the fat series, (C₇-C₉) /15/.

Extractive Compounds of Lanthanides with Carboxylic Acids

To determine the composition of the extracted species we chose the last two elements of the lanthanide series, lanthanum and lutecium. We used n-capric acid, α, α' -dialkylcarboxylic acid (C₉) and individual naphthenic acid, C₁₃H₂₄O₂, as extractants.

In all cases (Fig.5) the slope of curves in coordinates $(\lg C_{\text{Ln}(o)} - (\lg C_{\text{Ln}(aq)} + 3\text{pH}))$ is close to 1. This indicates the absence of polymerization of extracted compounds in the organic phase ($C_{\text{Ln}(o)} 3 \cdot 10^{-3} \text{M}$). At the same time the slope of the curve is equal to 3 (Fig.6) in coordinates $(\lg C_{\text{Ln}(aq)} + 3\text{pH}) - (\lg (\text{HR})_2)$ i.e. the compound, $\text{LnR}_3 \cdot 3\text{HR} \cdot x\text{H}_2\text{O}$, transfers to the organic phase.

Determination of water in extracted compounds of La, Nd, Gd, Yb, Lu, and Y showed that in the case of n-capric acid and α, α' -dialkylcaroxylic acid (C_9) the hydration number was not constant. It ranged from 2 to 1 on changing the lanthanum concentration in the organic phase from 0.05 to 0.88 M (Fig.7), i.e. the extracted compound may be written as $LnR_3 \cdot 3HR \cdot xH_2O$, where $x=2-1$. At the same time water is absent in solid carboxylates.

We calculated "seeming" constants of lanthanide extraction with α, α' -dialkylcaroxylic acid (C_9) and naphthenic acids by equation (4). Dependence of lanthanide extraction constants on their atomic number (Fig.8) is similar to that observed with complexes with acetate ion /16/.

Increase in concentration of the lanthanide extracted compound in the organic phase to certain limits results in their precipitation in the form of carboxylates. We determined the maximum content of the lanthanides in different carboxylic acids in equilibrium with carboxylate precipitates. As the number of carbon atoms in the carboxylic acid molecule increases (Fig.9) the solubility of lanthanide carboxylates in the organic phase drops. Maximum solubility was observed for Nd and Sm and minimum for Gd to Er.

The rather low solubility of yttrium is worth attention. It is necessary to point out that the capacity of α, α' -dialkyl carboxylic acids is much higher than that for nonbranched carboxylic acids. For example, the solubility of yttrium soap in 100% α, α' -dialkylcaroxylic acid (C_9) is 0.523M and of n-capric acid (C_8) is 0.0309M. The high maximum concentration of lanthanide soaps in α -acids indicates the possible formation of compounds such as, LnR_3 and $Ln(OH)_x R_{3-x}$. For example, the samarium concentration in solution of α, α' -dialkylcaroxylic acid (C_9) in n-heptane (3.07M) was 1.56M, indicating an extracted compound having the composition, $Sm(OH)R_2$ (beforehand we had confirmed the absence of $C1^-$ ion in organic phase).

The melting points of precipitates of the caprylates of La, Ce, Nd, Sm, Gd, Lu, Y, and the salts of these lanthanides with α , α' -dialkylcarboxylic acid (C_9) range from 50 to 80°C and their decomposition temperatures from 285 to 375°C.

By means of chemical analysis of solid carboxylates we found that the molar ratio of lanthanum to carboxylate-anion was close to 1:3 for carboxylic acids of the fatty series and less than stoichiometric in the case of α , α' -acids (C_9) (Table 3).

TABLE 3

Molar Ratio $Ln^{3+}:R^-$ in Lanthanides Carboxylates

Element	capric acid		α, α' -acid (C_9)	
	thermogravimetric method	chemical analysis	thermogravimetric method	chemical analysis
La	1:2.64	1:2.8		
Ce	1:2.98	1:3.0		
Nd	1:3.18	1:2.96	1:2.4	1:2.45
Sm	1:2.93	1:2.75	1:1.05	1:0.98
Gd	1:3.3	1:3.2		
Lu	1:2.66	1:2.7	1:2.61	1:2.7
Y	1:3.2	1:3.2	1:2.2	1:2.05

This was confirmed by the thermogravimetric method.

Precipitation of the salts of α , α' -dialkylcarboxylic acid (C_9) differing in their stoichiometric composition, is easy to explain as the production of precipitates was performed at higher values of pH of the equilibrium aqueous phase. At these pH values partial hydrolysis of lanthanides ions is possible. Spatial difficulties, (branching in the α -position) also makes formation of mixed compounds easier.

We did not observe any noticeable content of water in the samples of lanthanide carboxylates dried at 50°C and kept on a desiccator. Lanthanide carboxylates are practically insoluble in water and many other organic diluents but are easily dissolved in mineral acids with formation of the salt of the mineral acid and lanthanide and the carboxylic acid.

The distribution of multicomponent Mixtures of Rare-Earth Elements

To determine selectivity in the extraction of lanthanides with carboxylic acids we determined distribution with multicomponent mixtures in the presence of 'salting out' agents with varying concentrations of rare-earth element nitrates and chlorides in the aqueous phase. To compare data in the lanthanide series, the majority of the experiments were carried out with microquantities of lanthanide isotopes against a background of macroquantities of lanthanum in the aqueous and organic phases. The organic phase consisted of different carboxylic acids (Fig.10-11) containing 0.2M lanthanum soap.

Individual n-carboxylic acids and iso-acids (with branching in positions other than the α -position) extract lanthanides with little selectivity, separation coefficients being somewhat higher for solution of carboxylic acids in polar diluents (alcohols). Separation coefficients slightly increase in the presence of 'salting out' agents.

Naphthenic acids extract lanthanides more selectively (Fig.11). At low concentration of lanthanides or 'salting out' agents in the aqueous phase, rare-earth elements are not selectively extracted. Selectivity of carboxylic acids increases considerably with branching in the α -position relative to the carboxylic group (Fig.10,11).

Both diluent and type of 'salting out' agent influence selectivity to a smaller degree than in the case of α, α^L -dialkyl-carboxylic acids.

It should be pointed out that the position of yttrium in extraction systems with carboxylic acids is rather changeable and ranges from La to Er depending on aqueous phase concentration. At low concentrations of nitrates in the aqueous phase yttrium ranges from La to Nd, at high concentrations (of both lanthanides and 'salting out' agents) its position shifts to Gd-Er. We observed this in extraction with n-carboxylic acids, iso-acids, naphthenic acids, and secondary α -acids.

In the case of extraction with tertiary α, α' -branched acids the yttrium position was more stable and ranged from Tb to Er not depending on concentration and composition of the aqueous phase.

It is worth while noting that in the extraction of lanthanides with carboxylic acids, of all investigated types, the yttrium position is most likely to be between La and Nd.

Use of Complexing Agents in Systems with Carboxylic Acids.

All the acids studied either show little selectivity or their selectivity is limited to a group of rare-earth elements. In this case to make separation more effective we introduced complexing agents to aqueous solutions. Earlier /17,7/ we had considered the features of using such systems for phospho-organic extracts and carboxylic acids of the fatty series. So in the paper we gave only some practical results.

To successfully use complexing agents we should make the most of its capacity and, in the absence of complexing agents, of moderate values of extraction coefficients (20-50). Separation coefficient values decrease with increase in concentration of lanthanides in the aqueous phase. In the case of high values of distribution coefficients (100-1000) the rate of reaching equilibrium decreases.

Besides, the pH values for carboxylic acid extraction and complex formation in the aqueous phase might not coincide. So it is necessary that complex formation in the aqueous phase should occur at lower pH values than those necessary for extraction. If this is not the case than complete neutralization of extracts may be necessary which might result in: precipitation of carboxylates, loss of extract due to high solubility of sodium or ammonium carboxylates, lowering kinetics, and so forth.

To separate lanthanides of the cerium series the use of carboxylic acids of the fat series is preferable as they are less selective when compared with naphthenic acids (Fig.10,11).

For the separation of yttrium lanthanides, naphthenic acids should be used. They have greater capacity and less selectivity when compared with other reagents.

We tested some complexing agents: nitriletriacetic (NTA), ethylenediaminetetraacetic (EDTA) and diethylenetriaminopentaacetic (DPTA) acids. We used complexing agents under conditions to make the most of their capacity (pH 4), with high lanthanide concentrations in the organic phase. In case of NTA the value of the equilibrium pH of the aqueous phase exceeded 5-5.5 but was not equal to 6, as at pH 6 kinetics of the lanthanide exchange reaction complexes decreased sharply. In our experiments both binary lanthanide mixtures and normal rare-earth mixtures were used.

Table 4 and Fig.12 give the values of lanthanide separation coefficients when we used carboxylic acids of the fat series and naphthenic acids as extracts in the presence of complexing agents in the aqueous phase.

As may be seen from results given in this paper, extraction systems can be successfully used for lanthanide separations as well as for their purification.

Now we can conclude that monocarboxylic acids having branching in the α -position, are as a rule more selective and have other advantages such as: good compatibility with organic diluents, high solubility of carboxylates in organic diluents, and so on.

As pointed out, practically all lanthanides may be isolated in pure form when using only carboxylic acids as extracts. If cerium lanthanides may be successfully isolated with α -branched carboxylic acids, then yttrium lanthanides may be isolated with carboxylic acid-complexing agent systems, while using, for example carboxylic acids of the fat series or iso-acids.

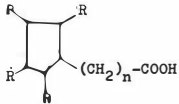
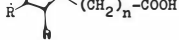
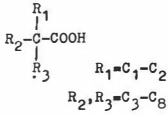
TABLE 4

Distribution Coefficients of Lanthanides in System: Carboxylic Acids - Aqueous Solution of Complexing Agent /7/.

/NTA/ M	Ln(NO ₃) ₃ -g/1 on Ln ₂ O ₃		β Ln ₁ /Ln ₂					
	aqueous phase	organic phase	La-Ce	Ce-Pr	Pr-Nd	Ce-Nd	Pr-Sm	Nd-Sm
0.3	Ln-25	Ln-96	5.8	2.0	2.2			
0.5	Ln-44	Ln-65	4.25	2.68	1.91			
0.3	(La,Ce)-21	(La,Ce)-96	5.50					
0.5	(La,Ce)-38.5	(La,Ce)-86	5.40					
0.5	(La,Ce)-45	(La,Ce)-100	5.00					
0.5	(La,Ce)-32	(La,Ce)-50	4.60					
0.3	(Ce,Pr)-23	(Ce,Pr)-100		2.50				
0.5	(Ce,Pr)-40	(Ce,Pr)-100		2.85				
0.5	(Ce,Pr)-45	(Ce,Pr)-100		2.30				
0.5	(Ce,Pr)-32	(Ce,Pr)-50		2.50				
0.3	(Pr,Nd)-24	(Pr,Nd)-96				2.15		
0.50	(Pr,Nd)-41	(Pr,Nd)-95				2.0		
0.5	(Pr,Nd)-45	(Pr,Nd)-100				2.0		
0.5	(Pr,Nd)-32	(Pr,Nd)-50				2.10		
0.3	(Ce,Nd)-23	(Ce,Nd)-95						
0.5	(Ce,Nd)-39.5	(Ce,Nd)-84						
0.5	(Ce,Nd)-47	(Ce,Nd)-98				6.50		
0.5	(Ce,Nd)-42	(Ce,Nd)-99					4.13	

Table 1

Some Properties of Carboxylic Acids and their Mixtures*

carboxylic acid	formula	boiling temperature °C	density g/cm ³	average molecular weight	dissolution in water	pK
n-capric acid	CH ₃ (CH ₂) ₄ -COOH	208.5	0.929	116.15	9.68	4.94
n-caprilic acid	CH ₃ (CH ₂) ₆ -COOH	239.7	0.910	144.21	0.68	4.94
n-caprincic acid	CH ₃ (CH ₂) ₈ -COOH	270.0	0.895 ³⁰	172.26	0.15	
naphthenic acids separated from oil fraction			0.9800	210	0.018	5.0
naphthenic acids separated from the water accompanying oil			1.0220	200	1.21	6.5
individual naphthenic acid	C ₁₃ H ₂₄ O ₂	125-130 (p=5 mm Hg)	0.980	210	-	6.6
β,β' -carboxylic acid (C ₈)	CH ₃ -(CH ₂) ₂ -CH-COOH C ₂ H ₅	124-125* (p=15mm Hg)	0.9053*	148.5*	1.21*	4.92* 0.08
α,α' -acids (C ₉)	CH ₃ -(CH ₂) ₃ -CH-COOH CH ₃ C ₂ H ₅	135-137 (p=10mm Hg)*	0.9001	166.1*	0.476*	4.94* 0.02
technical mixture of acids		-	0.8744*	215*	-	4.9*

* This table is based on the known literature data /10-12/ as well as on our experimental data.

REFERENCES

- 1) G.V.Korpusov, A.B. Loginov, R.D. Korpusova, E.N. Patrusheva, Avtorskoye svidetelstvo No 158419, 1962.
Byulleten isobretenii i tovarnykh znakov No 21, 55 (1963)
- 2) I.N. Plaksin et al., "Metallurgiya i gornoe delo", No 6, (1964).
- 3) L.G. Sherrington, W.P. Kemp, U.S. patent, N 3, 514, 267 cl. 23-312, May 26 (1970)
- 4) J.M. Fletcher, "Purification by Solvent Extraction" Paper 2 in Extraction and Refining of Rarer Metals, The Institution of Mining and Metallurgy, London, 1957.
- 5) I.N. Plaksin, V.S. Strizhko, Yu. S. Fedotov, DAN SSSR, 171, (6) 1348 (1966).
- 6) I.N. Plaksin, V.S. Strizhko, Yu. S. Fedotov, DAN SSSR, 174, (1) 162 (1967).
- 7) G.V. Korpusov, R.D. Korpusova, G.L. Vax, Z. neorg. khimii XIV, 7, 1912, (1969).
- 8) R.A. Alekperov, S.S. Geibatov, DAN SSSR, 178 (2), 349 (1968).
- 9) E.B. Mikhlina, A.I. Mikhailichenko, I.B. Berengard, Z. neorg. khimii XVII, 2, (1972).
- (10) G. Kortum, W. Vogel and K. Andrussov, "Dissociation Constants of Organic Acids in Aqueous Solutions", Butterworth, London (1961).
- 11) R.A. Alekperov, "Extractsiya naphtenatov" doktorskaya dissertatsiya Baku (1969).
- 12) E. Back, B. Sternberg, Acta Chem. Scand., 4, 810 (1950).
- 13) W.J.McDowell and C.F. Coleman, J. Inorg. Nucl. Chem., 27, 1117 (1965).
- 14) K. Fischer, Angew. Chem. 48, 394 (1935).
- 15) I.N.Plaksin, M.D. Ivanovsky, V.S. Strizhko et al., v sbornike "Problemy metallurgii", Metallurgiya, M., (1968).
- 16) K.B. Yatsimirsky, N.A. Kostromina, Z.A.Sheka et al., "Khimiya kompleksnykh soedineniy redkozemnykh elementov", Naukova dumka, Kiev (1966).
- 17) G.V. Korpusov, E.N. Patrusheva, N.P. Petrakova, V.F.Sokolova, v sbornike "Redkozemelnye elementy", p. 224-239, Izd, AN SSSR, M., (1963).

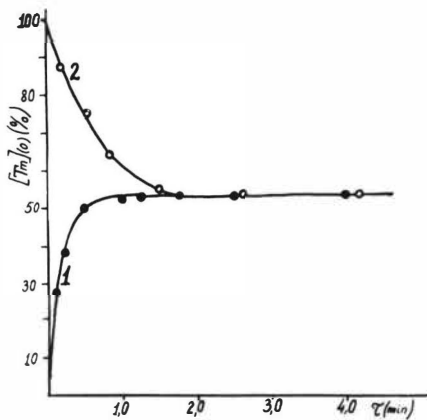


Fig.1. Time of reaching equilibrium in system:

1. aqueous phase - 0.15M Tm(NO₃)₃
organic phase - 0.15M Er(NO₃)₃
2. aqueous phase - 0.15M Er(NO₃)₃
organic phase - 0.15M Tm(NO₃)₃

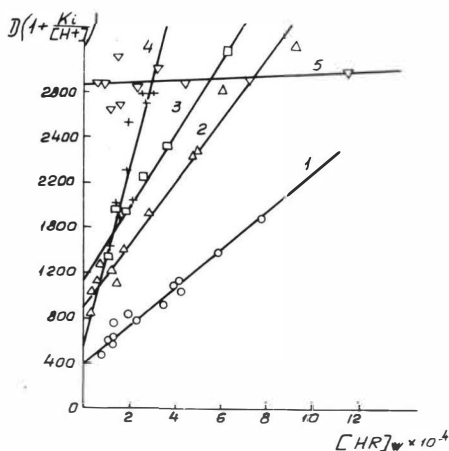


Fig.2. Distribution of α, α' -dialkylcarboxylic acid (C₉) between water and different diluents:

- 1 - n-heptane; 2 - benzole; 3 - toluole; 4 - 4-hydrogen chloride; 5 - decyl alcohol.

Fig.3. Distribution of lanthanides at different pH of equilibrium aqueous phase:

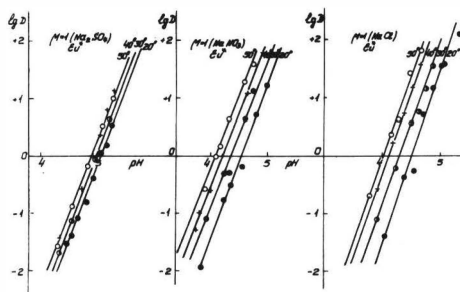
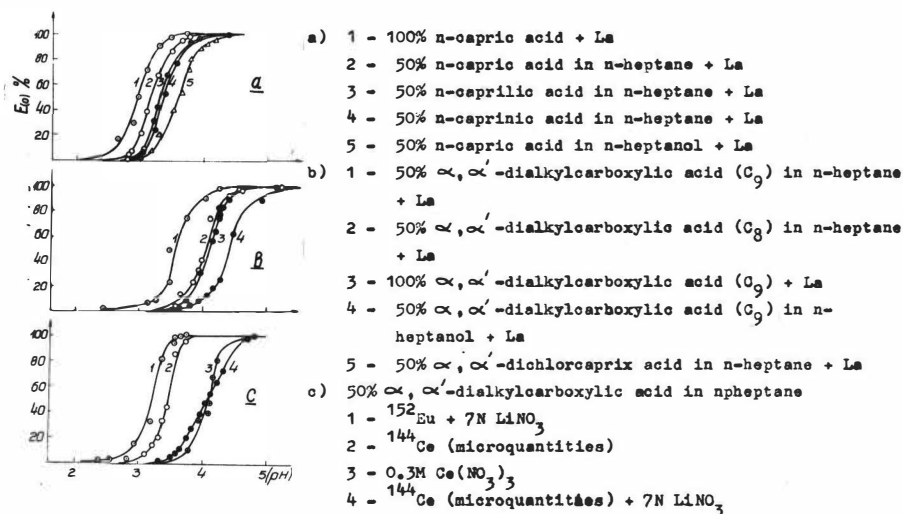


Fig.4. Distribution of ^{152}Eu microquantities at extraction with $0.99\text{M } \alpha, \alpha'$ -dialkylcarboxylic acid (C_9) from chloride, nitrate, and sulphate media at different temperatures.

1274

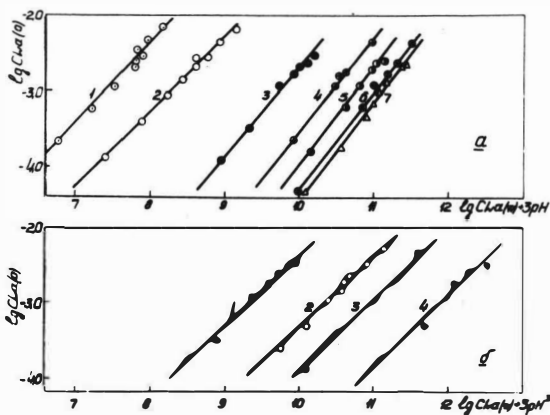


Fig.5. Distribution of lanthanum (initial concentration is $3.5 \cdot 10^{-3} M$) at extraction with:

a) n-capric acid in n-heptane

1 - $3.58 M$; 2 - $2.1 M$; 3 - $9.83 \cdot 10^{-1} M$; 4 - $5.02 \cdot 10^{-1} M$;
5 - $4.6 \cdot 10^{-1} M$; 6 - $3.64 \cdot 10^{-1} M$; 7 - $2.6 \cdot 10^{-1} M$

b) α, α' -dialkylcarboxylic acid in n-heptane

1 - $3.2 M$; 2 - $1.63 M$; 3 - $1.17 M$; 4 - $6.2 \cdot 10^{-1} M$

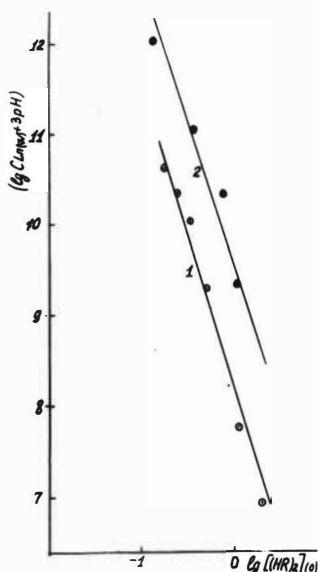
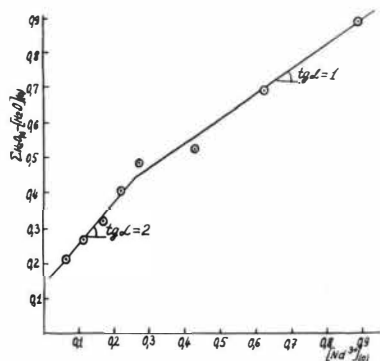


Fig.6. Distribution of lanthanum between aqueous and organic phases at extraction with:

1 - α, α' -dialkylcarboxylic acid in n-heptane

2 - n-capric acid in n-heptane

at $C_{Ln(a)} = \text{const.}$



$\Sigma[H_2O]$ - total content of water in organic phase
 $[H_2O]_o$ - concentration of water dissolved in α, α' -dialkylcarboxylic acid (C_9)

Fig. 7. Content of water in organic phase at different concentrations of α, α' -dialkylcarboxylic acid in organic phase.

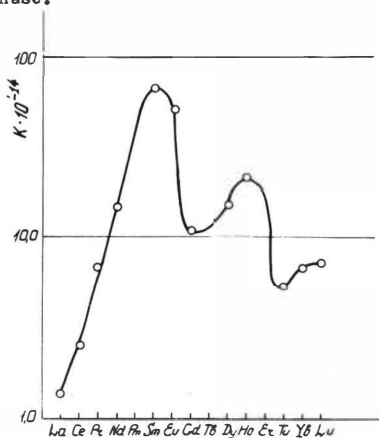
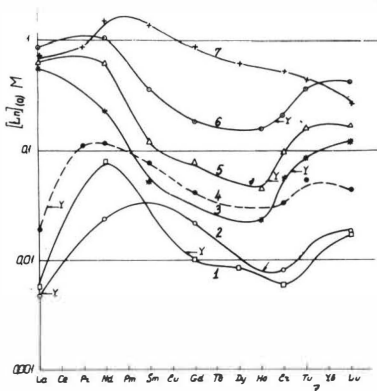


Fig. 8. Constants of lanthanides extraction with α, α' -dialkylcarboxylic acid (C_9) (3.07M in n-heptane).



- 1 - 50% n-caprillac acid in n-heptane
- 2 - 50% n-capric acid in n-heptane
- 3 - 100% n-capric acid in n-heptanoil
- 4 - 100% n-caprillac acid
- 5 - 50% n-capric acid in n-heptane
- 6 - 100% n-capric acid
- 7 - 100% α, α' -dialkylcarboxylic acid (C_9)

Fig. 9. Content of lanthanides (M) in carboxylic acids equilibrium with lanthanides carboxylates precipitate:

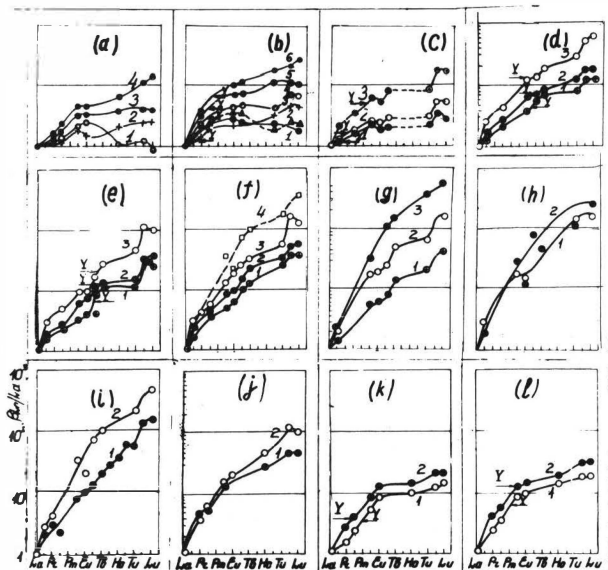


Fig.10. Distribution coefficients of lanthanides (β Ln/La) relatively lanthanum.

- a) 50% n-capric acid in n-heptane + 0.2M La
Aqueous phase: 1 - 2M LaCl_3 ; 2 - 2M $\text{La}(\text{NO}_3)_3$; 3 - 6N $\text{Ca}(\text{NO}_3)_2$ + 0.3M $\text{La}(\text{NO}_3)_3$; 4 - 6N LiNO_3 + 0.3M $\text{La}(\text{NO}_3)_3$
- b) 50% n-capric acid in decanole + 0.2M La.
Aqueous phase: 1 - 0.3M $\text{La}(\text{NO}_3)_3$; 2 - 2M LaCl_3 ; 3 - 100% n-capric acid - 2M $\text{La}(\text{NO}_3)_3$; 4 - 2M $\text{La}(\text{NO}_3)_3$; 5 - 6N $\text{Ca}(\text{NO}_3)_2$ + 0.3M $\text{La}(\text{NO}_3)_3$; 6 - 6.5N LiNO_3 + 0.3M $\text{La}(\text{NO}_3)_3$
- c) 50% iso-acids in synthin; -d), e), f), g), i) - 50% dialkylcarboxylic acids (C_7), (C_8), (C_9), (C_{13}), (C_{16}) in synthin.
Aqueous phase: 1 - 1.0M $\text{La}(\text{NO}_3)_3$; 2 - 1.5M $\text{La}(\text{NO}_3)_3$; 3 - 2.0M $\text{La}(\text{NO}_3)_3$; 4 - 6N LiNO_3 + 0.3M $\text{La}(\text{NO}_3)_3$
- j) 50% α, α' -dialkylcarboxylic acid (C_9) + 0.2M La.
Aqueous phase: 1 - 0.3M $\sum \text{REE}$ + 6N LiNO_3 ;
2 - 0.3M $\text{La}(\text{NO}_3)_3$ + 6M LiNO_3
- k) 50% α, α' -dialkylcarboxylic acids (C_9) in decanole.
Aqueous phase: 1 - 0.3M $\text{La}(\text{NO}_3)_3$
2 - 2.0M $\text{La}(\text{NO}_3)_3$
- l) 50% α, α' -dialkylcarboxylic acid (C_9) in n-heptane
Aqueous phase: 1 - 0.3M LaCl_3
2 - 2.0M LaCl_3

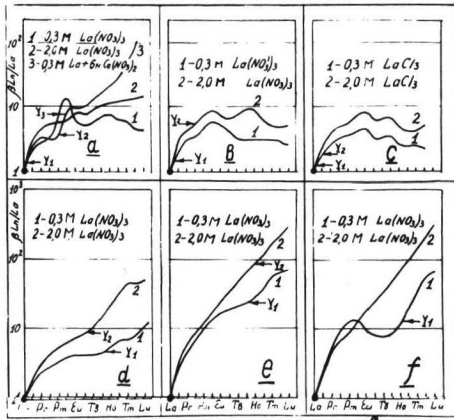


Fig. 11. Lanthanides distribution coefficients (β in β_{La}) relatively lanthanum at extraction with 50% solutions of different carboxylic acids in dodecane.

- a) naphthenic acids separated from oil fractions
- b) and c) naphthenic acids separated from water accompanying oil.
- d) high branched carboxylic acids (C₇-C₉)
- e) high branched carboxylic acids (C₉-C₁₅)
- f) high branched carboxylic acids (C₁₅-C₂₅)

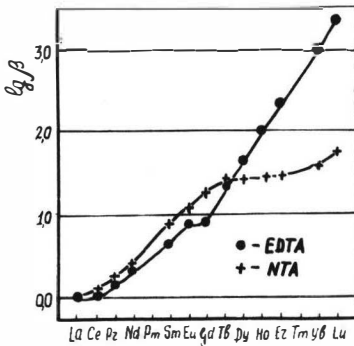


Fig. 12 Distribution Coefficients of rare-earth elements in system: naphthenic acids - complexing agent; $Ln(NO_3)_3$

THE EXTRACTION OF AMERICIUM, THORIUM AND EUROPIUM
WITH CAPRYL-HYDROXAMIC ACID (CHA)

M F Pushlenkov, V G Voden, M E Obukhova
V G Khlopin Radium Institute, Leningrad

Abstract

Capryl-hydroxamic acid (CHA) association in octyl alcohol and the rate of its hydrolysis under the influence of nitric acid have been investigated.

The compositions of precipitates formed by europium and thorium with CHA in aqueous-alcoholic solutions are defined.

The influence of CHA concentration, acetate ions and pH value on the behaviour of europium and americium with CHA solution in octyl alcohol have been studied.

Americium and europium extraction mechanisms with CHA are proposed; the argument for such mechanisms is based on the compositions of the mixed salts being formed and the distribution data.

Introduction

Alkyl- and arylhydroxamic acids, RCONHOH, easily form complex compounds with polyvalent elements; they are used for weight (1-3) and colorimetric determination of these compounds (3-8).

Colorimetric determination is often carried out after extraction of the complex (5, 6, 9-11). The conditions for complex formation by some cations with acetyl and benzylhydroxamic acids have been investigated and the stability constants have been determined (12-22).

According to their stability constants the cations can be arranged in a series: $\text{Ca}^{2+} < \text{Fe}^{2+} < \text{rare earths} < \text{Al}^{3+} < \text{Th}^{4+} < \text{U}^{4+} < \text{Fe}^{3+} < \text{Pu}^{4+}$ (20, 22).

It is evident that the complex stability increases with increase of the cationic charge. The use of the hydroxamic acids is possible only for solutions with rather high pH-values because of weak dissociation of these acids ($\text{pK} \approx 8-10$ (23)).

Higher alcohols, chloroform and aromatic compounds are frequently used as solvents for the hydroxamic acids.

Because of the high solubilities of acetylhydroxamic and benzylhydroxamic acids in aqueous solutions, capryl-hydroxamic acid, $\text{C}_8\text{H}_{19}\text{CONHOH}$ (CHA), which does not have this drawback, is proposed as the extractant.

There are no data in the literature on the association and hydrolysis of the higher aliphatic hydroxamic acids. CHA association in octyl alcohol has therefore been investigated as has its hydrolysis by nitric acid.

Precipitates formed between americium, thorium and europium and CHA have been analysed to determine the compositions of the europium, americium and thorium complexes being formed; the dependence of europium and americium distribution on CHA concentration, on acetate ion concentration and on pH of the aqueous solution have also been considered.

Experimental

Methods

Experiments on CHA hydrolysis were carried out at room temperature ($20 \pm 2^\circ\text{C}$) by contacting a 0.05M solution of CHA in n-octyl alcohol with aqueous solutions of nitric acid at different concentrations. The rate of hydrolysis was determined from the change of CHA concentration with time. Depending on the

nitric acid concentration in the aqueous solution the time of phase contact was varied from some minutes to 300 hours. To eliminate the influence of the aqueous phase composition the ionic strength was kept constant and equal to 4. Samples were periodically taken from the organic phase and were analysed for CHA content⁽²⁴⁾.

The method of isomolar series was used to obtain data on the compositions of europium and thorium compounds with CHA. Samples of thorium nitrate and CHA were dissolved separately in the minimum quantities of ethyl alcohol. The solutions obtained were mixed together, and a white precipitate was deposited immediately. The precipitate was centrifuged and the mother solution removed, leaving the precipitate with a small part of the mother solution.

The method of Shreinemakers⁽²⁵⁾ was used to determine the composition of the precipitate. Precipitate and mother solution were analysed for the metal ion, for nitrate ion and CHA. The metal content of the precipitate was determined by a weight method involving calcination of the precipitate at 950°C.

Nitrate ion concentration was determined by means of nitron⁽²⁶⁾. The metal and CHA concentrations in the mother solution were determined colorimetrically⁽²⁶⁾. The hydrogen ion concentration in the mother solution was determined by volume titration.

The solution obtained by dissolution of americium trioxide in perchloric acid was used as the aqueous feed solution in studies on the distribution of americium; and the americium concentration used was 10^{-5} - 10^{-6} g/l.

The aqueous europium feed solution consisted of a mixture of the stable and radioactive europium isotopes at a concentration of 10^{-4} - 10^{-5} M. Constant ionic strength ($I=0.1$) in the aqueous solution was maintained by sodium perchlorate and the pH of the aqueous solution was controlled by means of sodium acetate and acetic acid with an accuracy of ± 0.05 units of pH. The extraction was carried out by a CHA solution in octyl alcohol which was equilibrated with the aqueous solution ($pH=3-9$) at room temperature ($20 \pm 2^\circ C$). The extraction reaction goes slowly, therefore it took three hours to achieve equilibrium. The phase volumes after contact were unchanged because of the low solubilities of water in the organic phase and of CHA in water (3.4×10^{-4} M).

All results are averages from three parallel experiments. The experimental data were treated by the method of the least squares.

Reagents

CHA was synthesized from capryl chloride and hydroxylamine by the method in reference 27. Its purification was carried out by means of copper salt precipitation and by threefold recrystallization from ethyl alcohol. The purity was 99.5%, the remaining 0.5% being due to capric acid. CHA analysis was carried out by hydrolysis followed by hydroxylamine and capric acid determination⁽²⁸⁾. Other reagents used were chemically pure.

Results

Investigation of CHA association in n-octyl alcohol

CHA distribution between octyl alcohol and 0.1N sodium perchlorate was investigated to determine CHA association in octyl alcohol.

The distribution data are shown in Table 1.

TABLE 1

CHA distribution between n-octyl alcohol and 0.1N NaClO₄ with varying CHA concentration in the organic phase pH=4.2 at equilibrium

$(\text{CHA})_0 \times 10^2$ M	CHA distribution coefficient D
9.15	1165
7.27	1005
4.50	760
3.70	670
2.23	557
1.25	420
1.05	350
0.55	220

An approximate representation of CHA association is given by the relation $\lg(\text{CHA})_0 = f(\lg(\text{CHA})_{\text{aq}})$, which, when plotted, gives a straight line of slope equal to 2.

In order to obtain further information about the associated forms of CHA, it is necessary to express the distribution coefficient as a function of the CHA concentration in the aqueous phase.

An empirical equation for the dependence of the distribution coefficient (between octyl alcohol and 0.1N NaClO₄) on aqueous CHA concentration has the form:

$$D = 82 + 6.84 \times 10^6 C_{aq} + 8.58 \times 10^{10} C_{aq}^2, \dots\dots\dots 1$$

where C_{aq} is the CHA concentration in the aqueous solution.

C₀ is the CHA concentration in the organic phase.

In addition, the equation for the material balance in the organic phase,

$$C_0 = (HR) + 2(H_2R_2) + 3(H_3R_3) + \dots\dots\dots$$

where (HR), (H₂R₂) and (H₃R₃) are the concentrations of the monomeric, dimeric and trimeric forms of CHA, shows that the dependence of the CHA distribution coefficient on CHA concentration in the aqueous solution can be written,

$$D = D_m + 2D_m^2 \cdot K_d \cdot C_{aq} + 3D_m^3 K_t \cdot C_{aq}^2 + \dots\dots\dots 2$$

where D_m = (HR)₀ / (HR)_{aq} is the distribution coefficient for the monomeric form of CHA between octyl alcohol and 0.1N NaClO₄;

K_d = (H₂R₂) / (HR)² is the dimerisation constant for CHA in octyl alcohol;

K_t = (H₃R₃) / (HR)³ is the trimerisation constant for CHA in octyl alcohol.

Equation 2 is true when CHA association does not occur in the aqueous solution. With an equilibrium pH equal to 4.2, the degree of CHA dissociation is insignificant and it can be neglected. As was determined in our work by the method of reference 23, the CHA dissociation constant is 2.2 x 10⁻¹⁰.

It follows from the equations 1 and 2 that $D_m = 82$, $K_d = 508$ and $K_t = 51900$. From the values of the dimerisation and trimerisation constants, we have estimated the concentrations and the percentage ratios of the monomeric, dimeric and trimeric forms of CHA in octyl alcohol.

CHA hydrolysis

It is known that hydroxamic acids are hydrolysed under the influence of mineral acids resulting in carboxylic acids and hydroxylamine salts⁽²⁸⁾.

We determined the rate of CHA hydrolysis in octyl alcohol in the presence of nitric acid. Values of reaction half-times and rates of hydrolysis are given in Table 2.

It can be concluded from the linear relationship obtained, that the hydrolysis reaction is second order of the type II⁽²⁹⁾; the kinetic equation has the form:

$$d(\text{HR})/dt = -K(\text{HR})(\text{HNO}_3) \quad \dots\dots\dots 3$$

The mean value of K for the concentration range used is $(2.7 \pm 0.3) \times 10^{-4} \text{ l/mole sec}$.

TABLE 2

Reaction half-times and rates for CHA hydrolysis in octyl alcohol

(HNO ₃) in the organic phase M	Reaction half-time T (min)	CHA hydrolysis rate, V, 1/sec
0.86	97	1.2×10^{-4}
0.27	222	5.2×10^{-5}
0.075	570	2.0×10^{-5}
0.028	970	1.2×10^{-5}
0.001	32000	3.6×10^{-7}

It is evident, over the range of nitric acid concentrations in octyl alcohol studied, that below 0.01M CHA hydrolysis occurs rather slowly, which permits the use of CHA as an extractant for certain elements from aqueous nitrate solutions containing not more than 0.1M nitric acid.

Compositions of thorium and europium precipitates with CHA

The results from the determination of compound compositions are given in Table 3.

When the molar ratio Th:CHA changes over the range 2 to 0.05, the precipitated compounds are found to have average compositions corresponding to the stoichiometric formulae $\text{Th}(\text{NO}_3)_2 \cdot \text{R}_2$

(Calc Th = 31.9%; NO_3 = 17.0%; CHA = 51.2%) and $\text{Th}(\text{NO}_3)\text{R}_3$

(Calc Th = 27.2%; NO_3 = 7.3%; CHA 65.5%).

TABLE 3

Compositions of thorium precipitates with CHA in ethyl alcohol

Molar ratio Th:CHA	Composition of precipitate (%)			Filtrate Composition (g/l)		
	Th	NO_3	CHA	Th	NO_3	CHA
2.00	36.5	14.3	49.8	23.5	24.2	5.9
1.00	33.9	17.2	51.2	14.1	15.9	3.9
0.44	32.8	18.5	50.0	4.9	6.7	7.9
Average composition	34.4	16.7	50.3			
0.16	26.3	7.6	68.8	0.52	8.0	29.8
0.11	23.6	9.0	62.0	1.6	6.4	50.2
0.08	26.8	7.3	66.7	1.3	5.8	60.8
0.05	25.9	6.5	70.4	0.06	3.7	67.0
Average composition	25.7	7.6	68.0			

Under similar conditions, except that sodium acetate was present, a precipitate was also obtained with europium and CHA. The compound had the following composition: Eu = 23.6%, Ac = 10.5%, CHA = 63.4%, which corresponds to the compound EuAcR_2 (calc Eu = 26.1%, Ac = 10.1%, CHA = 63.8%).

Two thorium compounds with CHA are formed (see Table 3), $\text{Th}(\text{NO}_3)_2\text{R}_2$ and $\text{Th}(\text{NO}_3)\text{R}_3$. Even with a considerable excess of CHA (Table 3, experiment 7), nitrate ion is not entirely displaced from the precipitate formed. An attempt has been made to shift the equilibrium for the thorium complex formation reaction with CHA so that the CHA content of the precipitate is increased, by means of the addition of alkaline alcohol immediately after precipitation. A CHA:Th ratio of 1:1 was chosen. Neutralisation of the filtrate was carried out successively with determination of the hydrogen ion concentration. Final analysis of the precipitate gave the following composition (%): Th = 30(33.9), NO_3 = 14.0(17.3), CHA = 54.8(51.2). The corresponding values for the precipitate formed without neutralisation of the filtrate are given in brackets. Hence it appears that neutralisation of the filtrate with alkaline alcohol shifts the equilibrium insignificantly in the direction of lower nitrate content in the $\text{Th}(\text{NO}_3)_2\text{R}_2$ complex. Similar experiments were carried out with the molar ratio CHA:Th = 6:1. Neutralisation of the filtrate did not shift the equilibrium to lower nitrate content in the precipitated $\text{Th}(\text{NO}_3)\text{R}_3$ complex.

From the data of Table 3 the proximal intervals and proximal probabilities for the percentage composition of two compounds, $\text{Th}(\text{NO}_3)_2\text{R}_2$ and $\text{Th}(\text{NO}_3)\text{R}_3$, have been calculated and are given in Table 4.

TABLE 4

Proximal intervals and proximal probabilities for the percentage composition of the compounds $\text{Th}(\text{NO}_3)_2\text{R}_2$ and $\text{Th}(\text{NO}_3)\text{R}_3$

Th (in %)		NO_3 (in %)		CHA (in %)	
$x \pm \Delta$	x^{\propto}	$x \pm \Delta$	α	$x \pm \Delta$	α
$\text{Th}(\text{NO}_3)_2\text{R}_2$					
31.9 ± 2.4	0.80	17.0 ± 1.6	0.80	51.2 ± 1.6	0.72
$\text{Th}(\text{NO}_3)\text{R}_3$					
27.2 ± 2.0	0.80	7.3 ± 1.0	0.80	65.5 ± 2.9	0.85

$x \pm \Delta$ is the proximal interval

α is the proximal probability

Americium and europium distribution between aqueous solution and
CHA in octyl alcohol

The aqueous solution of americium perchlorate used contained acetate ions to prevent the precipitation of americium and europium hydroxides when the pH of the solution was increased. To determine the degree of americium complex formation with acetate ion in the aqueous solution, the stepped stability constants were estimated by the method of extraction. Extraction was carried out by a 0.05M solution of thenoyl trifluoroacetone (TTA) in benzene, from the acetate solution. The data obtained are given in Table 5.

TABLE 5

Americium extraction by 0.05M TTA in benzene from acetate (Ac) solutions. Ionic strength = 0.1, pH = 0.5

(Ac) (M)	Am distribution coefficient
0.10000	27
0.03160	138
0.01000	470
0.00316	850
0.00300	930

The values of the complex formation constants with one, two and three acetate ions are $K_1 = 95 \pm 7M^{-1}$; $K_2 = (2.2 \pm 0.2) \times 10^3 M^{-2}$; $K_3 = (5.4 \pm 0.5) \times 10^3 M^{-3}$. These values are in accordance with similar constants that were estimated by the ion-exchange method⁽³¹⁾, i.e. $K_1 = 98.5 \pm 3M^{-1}$; $K_2 = (1.9 \pm 2) \times 10^3 M^{-2}$; $K_3 = (5.4 \pm 0.5) \times 10^3 M^{-3}$.

The dependence of americium distribution on the concentrations of: (a) hydrogen ions, (b) CHA and (c) acetate ions was investigated in order to determine the solvate composition and to evaluate the stoichiometry of americium extraction with CHA.

The dependence of the americium distribution coefficient (lg D) on hydrogen ion concentration has the form of a straight line. The slope of this straight line for (Ac) = 0.1M is 2.06 and for (Ac) = 0.01M, 2.88.

The data showing the dependence of the americium distribution coefficient on CHA concentration in octyl alcohol are given in Table 6.

TABLE 6

The dependence of americium distribution on CHA concentration in octyl alcohol

CHA concentration in octyl alcohol (M x 10 ³)	CHA monomer concentration in octyl alcohol (M x 10 ³)	Americium distribution coefficient	
		(Ac) = 0.1M	(Ac) = 0.01M
100	6.36	3.09	850.0
75	5.62	1.58	251.0
50	4.80	0.49	122.0
38	4.06	0.27	72.0
25	3.37	0.10	15.9
12	2.32	0.03	-
10	2.20	0.03	0.8
5	1.53	0.0044	-

The dependence of the logarithm of the americium distribution coefficient on the logarithm of the total concentration has the form of a straight line of slope equal to 2.2, and the similar dependence on the logarithm of the monomer concentration results in a straight line of slope 5.3 when (Ac) is 0.1M and 6.8 when the acetate ion concentration is 0.01M.

For the other forms of capryl hydroxamic acid, linear relationships are not found.

To determine the composition of the europium complex with CHA, the relationships between the europium distribution coefficient and hydrogen ion concentration in the aqueous solution and CHA concentration in the organic phase have been investigated. The experimental data obtained are given in Tables 7 and 8. Between the logarithm of the europium distribution coefficient and the logarithms of the hydrogen ion and CHA concentrations, there exist linear relationships with slopes of 2.6 and 4.8 respectively.

TABLE 7

The dependence of europium distribution on the hydrogen ion concentration ($(\text{CHA}) = 0.05\text{M}$)

pH	Eu Distribution coefficient
3.5	0.0145
4.6	14.6
4.8	53.4
5.0	92.0
5.5	1600.0

TABLE 8

The dependence of europium distribution on the CHA concentration in octyl alcohol (pH of the equilibrium aqueous solution is 5.0)

(CHA) (M)	(HR) ^{*x} (M x 10 ³)	(H ₂ R ₂) ^{*x} (M x 10 ³)	Eu distribution coefficient
0.010	2.2	3.00	1
0.025	3.37	7.10	16
0.038	4.06	10.48	47
0.050	4.80	14.00	92
0.075	5.62	19.00	215
0.100	6.36	24.40	543

* (HR) and (H_2R_2) are the concentrations of the monomeric and dimeric forms of CHA.

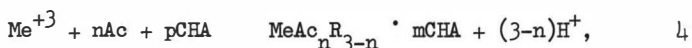
Discussion

Analysis of the compositions of compounds formed by CHA with thorium and europium nitrates shows that these compounds include various anions. Even neutralisation does not result in complete nitrate substitution in the thorium compounds.

Europium, in the presence of sodium acetate, forms a compound with the formula EuAcR_2 .

The mode of dependence of americium and europium extraction on hydrogen ion concentration suggests that extraction occurs with the elimination of two hydrogen atoms when the acetate ion concentration is 0.1M and 2.88 atoms when (Ac) diminishes to 0.01M, with the simultaneous binding of two or more molecules of CHA.

These results can be represented by the following summary equation for the extraction reaction



where Me = metal ion,

Ac = acetate ion,

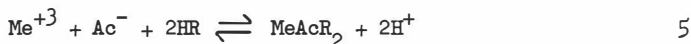
CHA = capryl hydroxamic acid

R = CHA anion and

n, p, m = whole positive numbers: $0 < n < 3$, $0 < p$, $0 < m$, $p > m$.

When $n = 3$ extraction does not occur, when n diminishes to 2, 1 and 0, Am distribution coefficients increase. With increase in the total CHA concentration the distribution coefficient increases because CHA not only enters into the composition of the salt, but also solvates the compound obtained. The number of hydrogen ions eliminated should increase when the acetate ion concentration diminishes, and this has been observed in the course of experiment.

The calculation of separate reaction constants from the summary equation is difficult because of the numerous solutions possible. Therefore, from the observed compositions of the europium compound (EuAcR_2) and the americium compounds (AmAcR_2 and AmR_3) formed, and the dependence of the distribution coefficients of the elements on hydrogen ion concentration, the most probable reactions for europium and americium extraction are as follows:



At least three CHA forms coexist in the organic phase; monomeric, dimeric and trimeric (and their relative proportions are dependent upon the analytical concentration of CHA), therefore the slope of the function $\lg D = f(\lg C_0)$ does not correspond to the solvation number of the complex being extracted. Taking into account that the slopes of the linear function $\lg D = f(\lg (\text{HR}))$ found empirically exceed 2-3 (numbers of CHA molecules that enter the complexes according to reactions 5, 6), it can be supposed that the excess CHA molecules arise from solvation of these compounds. On the basis

of the CHA association data obtained, it is considered most probable that the complexes are solvated by CHA dimer. The estimated formation constants for the complexes are given in Table 9.

TABLE 9

Estimated formation constants for Am and Eu complexes with CHA

Complex	K
$\text{AmAcR}_2 \cdot \text{H}_2\text{R}_2$	0.0170
$\text{AmAcR}_2 \cdot 2\text{H}_2\text{R}_2$	2.0000
$\text{AmR}_3 \cdot 2\text{H}_2\text{R}_2$	0.0220
$\text{EuAcR}_2 \cdot \text{H}_2\text{R}_2$	5.9000
$\text{EuR}_3 \cdot \text{H}_2\text{R}_2$	0.00024

Conclusions

1. CHA association in n-octyl alcohol has been studied by investigation of CHA distribution between octyl alcohol and 0.1N NaClO_4 .
2. The rate constant for CHA hydrolysis has been estimated from data on CHA hydrolysis under the influence of nitric acid; this constant is $(2.7 \pm 0.3) \times 10^{-4}$ l/mole sec.
3. Reaction mechanisms for americium and europium extraction in CHA-nitric acid systems have been proposed. Formation constants for the reactions of americium and europium with CHA in these systems have been estimated, taking into account solvation.

References

1. Rjazanov I P, Badeeva T I, Molot L A. Proceedings of the Saratov State University, 1951, 25, ed. chim. 18.
2. Bhaduri A S, Z Anal Chem, 1956, 151, 109.
3. Brandt W W, Rec Progr, 1960, 21, 159.
4. Musante C, Gazz. chim. ital, 1948, 78, 536.
5. Bhaduri A S, Ray P, Z. Anal. Chem., 1957, 154, 103.

6. Minczewski J, Skorco-Trybula Z, Talanta, 1963, 10, 1063.
7. Shome S C, Anal. Chem., 1951, 23, 1186.
8. Alimarin I P, Borzenkova N P, Shmatko R I, Zh. Analyt. Khim., 1963, 18, 342.
9. Wise W M, Brandt W W., Anal. Chem., 1955, 27, 1932.
10. Meloan C E., Dissertation abstracts, 1959, 10, 52.
11. Meloan C E., Holkeboer P., Brandt W W., Anal. Chem., 1960, 32, 791.
12. Rjazanov I P., Molot L A., Plant Lab., 1952, 18, 3, 271.
13. Sakai T., Y Zasshi, 1963, 83, 44.
14. Baroncelli F., Grossi G., J. Inorg. Nucl. Chem., 1965, 27, 1085.
15. Maggio F, Romano V, Cefalu R, J. Inorg. Nucl. Chem., 1966, 28, 1979.
16. Dyrssen D., Acta Chem. Scand., 1956, 10, 353.
17. Bhaduri A S., Grosh N N., Z. anorg. allg. Chem., 1958, 297, 73.
18. Chmutova M K., Zolotov Ju A., Radiokhimiya, 1964, 6, 6, 640.
19. Schwarzenbach G, Schwarzenbach K., Helv. Chim. Acta., 1963, 46, 1390.
20. Anderegg G., L' Eplattenier F., Schwarzenbach G., Hev. Chim., 1963, 46, 1400.
21. Bagreev V V., Petruchim O M., Rakovskii E E, Zolotov Ju;A., Chemical basis of the extraction method for elements separation. 1966, Ed. "Nauka", (M).
22. Barocas A., Baroncelli F., Biondi G B., Grossi G., J. Inorg. Nucl. Chem., 1966, 28, 2961.
23. Wise W W., Brandt W W., J. Am. Chem. Soc., 1955, 77, 1058.
24. Voden V G, Obukhova M E., Pushlenkov M F., Radiokhimiya, 1969, 11, 644.
25. Falinski M., Ann. chim., 1941, 16, 237.

26. Gillebrand V F., Practical recommendations on nonorganic analysis. 1967, 556, 795, Goschimisdat, (M).
27. Renfrow W R., Jr, Hauser C.R., J.Am. Chem Soc., 1937, 59, 2312.
28. Rol E T., Swern D., Anal. Chem., 1950, 22, 1160.
29. Benson S., Chemical kinetics fundamentals. 1964, Ed. "Mir", (M).
30. Laidel A M., Elementary estimations of measurement mistakes. 1965, Ed. "Nauka", (M-L).
31. Grenthe I., Acta Chem. Scand., 1962, 16, 1699.

SESSION 11

Tuesday 10th September: 14.00 hrs

E X T R A C T I O N T E C H N O L O G Y

(Common Metals)

Chairman:

Dr. R. Blumberg

Secretaries:

Mr. A.L. Mills

Mr. P. Claudy

THE SOLVENT EXTRACTION OF ANIONS FROM
CHROMIUM BEARING LIQUORS - BINARY EQUILIBRIA

by

M.A. Hughes and T.M. Leaver

ABSTRACT

The equilibria established between Aliquat 336 and various metal anions involving chromium, vanadium, and the chloride and hydroxide anions are considered. The results are presented for all possible binary combinations in the system above for extraction from alkaline media.

Binary equilibria have been mathematically modelled and good results are obtained in all systems other than those involving the vanadium containing species.

The work is of consequence to the extraction of the above anions from chromate liquors.

School of Chemical Engineering,
Bradford University,
Bradford.

INTRODUCTION

The present route to chromium chemicals involves the oxidation roast of the chromite ore with sodium carbonate to produce a hot fritte which, when leached with water, gives a strongly alkaline sodium chromate liquor and an insoluble residue. All of the iron and some of the aluminium is removed in the precipitate and subsequent acidification and lime treatments can remove all the aluminium and vanadium respectively. Final pH adjustment gives valuable acid dichromate liquors which are used for electroplating purposes.

A typical leach liquor may contain the sodium salts of chromate, aluminate, vanadate and hydroxide in the ratio 300:20:2:40; very little sodium carbonate is left unreacted.

The several stages in the process outlined above give a variety of liquors which are amenable to solvent extraction. In addition, certain effluents containing chromium may be treated in this way.

This paper describes an investigation into the binary equilibria developed in systems involving alkaline solutions of chromate, vanadate and hydroxide and the quaternary amine Aliquat 336 (General Mills Co.).

EXPERIMENTAL

All experiments were carried out at $22 \pm 2^{\circ}\text{C}$.

Chemicals. The reagents used for analysis were AR grade. Simulated liquors were made up from laboratory grade sodium chromate, vanadate and aluminate.

The extractant was used for forward extraction in the chloride form, as received. Various diluents and modifiers were tested but economic consideration finally dictated that kerosene with 4% w/w decanol should be used as the carrier solvent. Furthermore the maximum loading of the Aliquat in the carrier solvent was limited to 0.5 M because of viscosity problems at higher concentrations. The extractant was found to be stable to alkali chromate but was slowly oxidised when acid conditions prevailed. A thorough search of reagents has not yielded an extractant stable to acid chromate liquors over long periods.

Analysis. Metals were determined by atomic absorption spectroscopy (Pye SP90A) or by classical volumetric procedures. Water in the organic phase was determined by the Karl Fisher method; this last technique could not be applied to organic solutions loaded with oxidising metal anions.

Preliminary equilibria experiments

Kinetics. Before embarking on equilibrium shake-out tests it was necessary to establish that the reaction kinetics were not significantly slow so as to affect the results. The extractions of chromium seemed to be very fast under both acid and alkali conditions, See TABLE 1.

TABLE 1
RATE OF EXTRACTION OF Cr(VI)

Contact time Seconds	E%	
	pH 1.2	pH 11.6
1	35.6	37.5
3	99.8	59.6
30	99.6	60.4
120	99.6	60.5
900	99.7	61.5

$$E\% = \text{percentage of chromium extracted} = \frac{Cr_o \times 100}{Cr_{aq}}$$

Aqueous feed: Chromate, .025 M, aliquat chloride 0.05 M

Similar fast kinetics were found for higher concentrations of chromate and vanadate in contact with aliquat 336 chloride solutions stronger than 0.05 M, e.g. 0.5 M. It was decided that all shake-out tests would include a three minute agitation time.

Water uptake. It is to be expected that amines, particularly quaternary amines, will take up water through either micelle or salt formation. In this work, significant volume changes were observed during shake-out tests, with the organic phase volume increasing by up to 6%. TABLE 2 is typical of many measurements on 0.5 M aliquat 336.

TABLE 2
WATER UPTAKE BY THE ORGANIC PHASE, EQUILIBRIUM VALUES

Organic concentration Chromate, g/l	% increase in organic phase volume	Organic concentration Vanadate, g/l	% increase in organic phase volume
8.80	6.0	25.50	5.0
5.16	6.0	22.00	4.75
3.99	5.0	12.21	5.0
2.70	5.0	4.23	5.25
1.50	5.0		

Infrared spectra demonstrate that the water bound in the organic phase is strongly hydrogen bonded; (broad band at 3380 cm^{-1}). Further, the ratios of the O-H (3380 cm^{-1}) peaks to the C-H (2920 cm^{-1}) peaks for various amine molarities contacted with 1M NaCl solutions, show a linear relationship with the molarity values, therefore, the amine is the only component in the organic phase which markedly affects the water transfer.

Quantitative analysis of water in the organic phase shows that each amine takes up about four molecules of water.

A consequence of the above observations is that equilibrium data have been corrected to a water free organic basis.

The pH dependence of the extraction

The variation of the extraction with pH for both chromate and vanadate is shown in Figs. 1 and 2. It can be seen that a drop in the extractive capacity of the Aliquat 336 occurs at pH7 and it will be seen later that this corresponds to a change of chromium (VI) species existing in the aqueous phase. At pH7 the species present is predominantly CrO_4^{2-} . Electronic spectra taken on the organic phase identified the CrO_4^{2-} ion (peaks at 275 and 375 m μ) suggesting that no change of species occurred once the chromate was removed from the aqueous environment.

The change in extraction with pH for the vanadate system is more complicated and reflects the complex nature of the species of vanadium occurring in both the acidic and alkaline media. It was not found possible through spectroscopic techniques to identify the exact species of vanadium which were extracted into the organic phase.

Aluminium. The aluminate ion was not found to extract when present in the quantities found in leach liquors and therefore this metal was not considered in further studies.

EQUILIBRIUM STUDIES

The nature of the species existing in solution

(1) Chromium

Pourbaix¹ has demonstrated the various domains of predominance of chromium (VI) ions and several reports exist citing the stability constants for each species. We have used the following data² to predict concentrations of ions in existence at various pH conditions:

$$\frac{[\text{Cr}_2\text{O}_7^{2-}]}{[\text{HCrO}_4^-]^2} = 98, \quad \frac{[\text{H}^+][\text{CrO}_4^{2-}]}{[\text{HCrO}_4^-]} = 3.2 \times 10^{-7}, \quad \frac{[\text{H}^+][\text{HCrO}_4^-]}{[\text{H}_2\text{CrO}_4]} = 1.21,$$

$$\frac{[\text{H}^+][\text{Cr}_2\text{O}_7^{2-}]}{[\text{HCr}_2\text{O}_7^-]} = 0.85, \quad \frac{[\text{H}^+][\text{HCr}_2\text{O}_7^-]}{[\text{H}_2\text{Cr}_2\text{O}_7]} = 10^6$$

A computer programme was written to predict concentration changes and the results have been plotted in Fig. 3.

(11) Vanadium

Rossotti and Rossotti³ have already reported and calculated the distribution of the vanadium species in the acid pH range.

For studies of alkaline media other workers⁴ have indicated the presence of HVO_4^{2-} , $\text{HV}_2\text{O}_7^{3-}$, H_2VO_7^- , $(\text{V}_3\text{O}_9)^{3-}$ and VO_4^{3-} . Fig. 4 presents the features of the alkaline side of the equilibria computed from the constants⁵;

$$\frac{[\text{HVO}_4^{2-}]}{[\text{VO}_4^{3-}][\text{H}^+]} = 3.98 \times 10^{12},$$

$$\frac{[\text{HV}_2\text{O}_7^{3-}]}{[\text{H}^+][\text{HVO}_4^{2-}]^2} = 3.98 \times 10^{10},$$

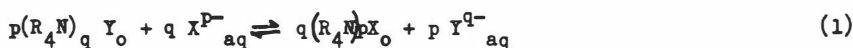
$$\frac{[\text{H}_2\text{VO}_7^-]}{[\text{H}^+][\text{HVO}_4^{2-}]} = 5.012 \times 10^7,$$

$$\frac{[\text{V}_3\text{O}_9^{3-}]}{[\text{H}^+]^3[\text{HVO}_4^{2-}]^3} = 5.012 \times 10^{30}.$$

The results demonstrate the predominance of the $\text{V}_3\text{O}_9^{3-}$ ion in the region pH 7-9.

The binary extraction equilibria

The general equation for the binary interaction is



The binary equilibria data are represented by the distribution ratio expressions of the type;

$$D = K_1^1 \left\{ \frac{[\text{C} - p(\text{R}_4\text{N})_p \text{X}]_o}{q[\text{Y}^{q-}]_{\text{aq}}} \right\}^{p/q} \quad (2)$$

where K_1^1 is an overall constant incorporating the activity factors, and C is the total loading of the reagent in the organic phase. Substituting for D, and rearranging gives

$$\frac{[(\text{R}_4\text{N})_p \text{X}]_o}{[\text{C} - p(\text{R}_4\text{N})_p \text{X}]_o} = K_1^1 \frac{[\text{X}^{p-}]_{\text{aq}}}{q[\text{Y}^{q-}]_{\text{aq}}^{p/q}} \quad (3)$$

$$\text{or } [(\text{R}_4\text{N})_p \text{X}]_o = f_1 [\text{X}^{p-}, \text{Y}^{q-}]_{\text{aq}} \quad (4)$$

Equation (4) demonstrates that the binary equilibrium will be represented by a surface in three dimensional space, Fig. 5, in which the axes are $[(\text{R}_4\text{N})_p \text{X}]_o$, $[\text{X}^{p-}]_{\text{aq}}$ and $[\text{Y}^{q-}]_{\text{aq}}$. The limits of the surface are fixed by the equilibrium equation such that:

$$\text{when } \frac{[\text{Y}^{q-}]_{\text{aq}}}{[\text{X}^{p-}]_{\text{aq}}} = 0, \quad [(\text{R}_4\text{N})_p \text{X}]_o = \frac{\text{C}}{p}$$

and when $\frac{[Y^{q-}]_{aq}}{[X^{p-}]_{aq}} = \infty$, $[(R_4N)_pX]_o = 0$.

The term $\frac{C}{p}$ represents the maximum organic loading of the metal X; it is assumed that the maximum organic loading is independent of $[Y^{q-}]$. Hence the surface may only be applied to one organic feed molarity, C, a change in this resulting in the introduction of a fourth variable. The line dg is the equilibrium line under the condition of a constant $[Y^{q-}]_{aq}$. Every such line will tend to the i-j saturation plane ($\frac{C}{p}$)

as $\frac{[X^{p-}]_{aq}}{[Y^{q-}]_{aq}}$ becomes large, for example, line fh on the lower $[Y^{q-}]_{aq}$ plane.

One point on the surface will satisfy simultaneously this plane, a constant $[X^{p-}]_{aq}$ and a constant $[(R_4N)_pX]_o$ plane. This follows from the total differential of equation (4);

$$d[(R_4N)_pX]_o = \left(\frac{\partial [(R_4N)_pX]_o}{\partial [X^{p-}]_{aq}} \right)_{[Y^{q-}]_{aq}} \cdot d[X^{p-}]_{aq} + \left(\frac{\partial [(R_4N)_pX]_o}{\partial [Y^{q-}]_{aq}} \right)_{[X^{p-}]_{aq}} \cdot d[Y^{q-}]_{aq} \quad (5)$$

Thus for any change in $[(R_4N)_pX]_o$, there must be a change in either $[Y^{q-}]_{aq}$ or $[X^{p-}]_{aq}$ or both, corresponding to a shift to a second point on the equilibrium surface.

In a steady state solvent extraction process, feed of known and constant composition will be introduced and since anion exchange only is taking place; the concentration of the aqueous phase cation and thus its equivalent anion will remain constant throughout the process. The equilibrium tie line PQ is therefore of interest to flow sheet design. Known as the constant cation or equivalent anion concentration line, it describes any aqueous phase composition of a two anion system derived from a specific feed point R. The components at any point on line PQ will always sum as:

$$p[X^{p-}]_{aq} + q[Y^{q-}]_{aq} = [R]_{aq}$$

where $[R]_{aq}$ = total anion concentration (moles/litre) in the aqueous phase. The projection of the line PQ of the plane $[(R_4N)_pX]_o = 0$ will subtend an angle θ with the $[X^{p-}]_{aq}$ axis, the tangent of which represents the stoichiometry of the exchange reaction. Thus when the $[X^{p-}]_{aq}$ and $[Y^{q-}]_{aq}$ axes are equally divided and represent moles/l of each anion, $\tan \theta = \frac{q}{p}$.

It is possible to condense the surface onto a two dimensional diagram where a family of equilibrium lines, representing slices through the surface at constant $[Y^{q-}]_{aq}$, $[X^{p-}]_{aq}$ or $[(R_4N)_pX]_o$, lie between axes representing the remaining component concentrations.

Experimental design and procedure

Since all systems considered in this work contain at least two of the anions, Cl^- , CrO_4^{2-} , $(VO_3)_3^-$ (and other vanadium species), and OH^- ,

it was necessary to obtain binary data for every pair.

The experimental determination of the data required to produce an equilibrium surface is complicated by the unique nature of any particular point. It is not possible to fix a desired aqueous phase composition unless prior knowledge of the distribution is available. Consequently, feed concentrations required to obtain equilibrium points over a useful range of aqueous phase concentrations were established by a minimum of trial equilibrations. Variations in the equilibrium aqueous phase concentration of the extracted anion was achieved by altering the feed concentration of that anion (i.e. varying R in Fig. 5) and changes in aqueous phase counter-anion concentrations were effected by phase ratio adjustment (i.e. moving down line PQ for each value of R).

For use in graphical design methods and rapid interpolation it was necessary to express the equilibrium data in the more convenient two dimensional diagrammatical form (fh, dg, Fig. 5).

DISCUSSION

Characteristics of the binary data

(i) Chromate - chloride equilibrium data

Since chromium was the principal element under investigation, a substantial amount of data was collected to ensure a full description of its extraction by the extractant in its supplied anionic form. Fig. 6 illustrates the results obtained. The data suggest slightly better extraction of the chloride ion from the binary aqueous mixture. The equilibrium lines are smooth curves and show no abnormalities. The curves have been smoothed out through interpolated data points.

Fig. 7 presents data obtained for the suggested back extractant NH_4Cl and illustrates the effect of higher chloride loadings on the equilibrium. A high proportion of chromate exists in the aqueous phase at chloride concentrations of 0.12 moles/l. At lower chloride concentrations the equilibrium lines are very similar to those in Fig. 6. In practice, due to the formation of a second organic phase it is necessary to add a quantity of NH_3 solution, and binary $\text{CrO}_4^{2-} - \text{NH}_4\text{Cl}$ data can no longer be used as a reliable description of the back extraction process.

(ii) Vanadate - chloride equilibrium data

The results obtained from this system are shown in Fig. 8. From pH measurements of the aqueous phases, it is assumed that the vanadate (VO_3^-)₂ ion is in predominance (Fig. 4). There is a marked affinity of the extractant for this ion demonstrated by the high organic concentrations even at high aqueous chloride concentration.

(iii) Chromate - hydroxide equilibrium data

The closeness of the hydroxide ion concentration contours to the saturation line, (organic chromate 0.25 molar), Fig. 9, at low aqueous chromate ion concentrations reflects the preferential ion association of the extractant with the chromate ion.

(iv) Chloride - hydroxide equilibrium data

The results (Fig. 10) show a similarity to system (iii) above with the extractant preferentially associating with the chloride ions.

(v) Chromate - vanadate equilibrium data

Data in Fig. 11 suggest a strong affinity of the extractant for vanadium. Again the aqueous phase pH indicates that $(VO_3^-)_3$ is the predominant species. The data indicate that a mixture of the two metals in solution may therefore be easily separated, and that if an organic vanadium solution were contaminated with chromate, a scrub using relatively dilute solutions of vanadate would be sufficient to purify it.

(vi) Vanadate - hydroxide equilibrium data

It can be seen from Fig. 12 that although at low hydroxide and vanadate ion concentrations the organic phase concentration of vanadium increases almost linearly with aqueous vanadate ion concentration in favour of vanadium extraction, there is a change in the equilibrium characteristics with increasing ion concentrations. This effect is due to the increasingly complex nature of the aqueous vanadate solution as the hydroxide ion concentration, and thus the pH, increases. The nature of the extractable vanadium species changes with pH, see Fig. 4.

Stripping

Various ammonium salts might be used to strip the loaded organic phase and thereby produce the valuable chemicals, ammonium vanadate and ammonium chromate. The tests on possible stripping reagents, TABLE 3 show that an ammonium chloride/ammonia system would be satisfactory, the data confirm some results reported⁶ by the General Mills Co.

TABLE 3

STRIPPING TESTS ON CHROMIUM LOADED REAGENTS

Reagent	% Cr removed	Observation
NH_4Cl , 1.5M	49	
$(NH_4)_2SO_4$, 1.5M	25	2nd organic phase with interfacial crud formation
NH_4NO_3 , 1.5M	71	
NH_4Cl + 1.5M NH_3	79	clean two phase system
$(NH_4)_2SO_4$ + 1.5M NH_3	46	clean two phase system
$(NH_4)NO_3$ + 1.5M NH_3	93	2nd organic phase

Other tests showed that vanadate could also be readily stripped with the NH_4Cl/NH_3 or $(NH_4)_2SO_4/NH_3$ reagents.

Models for binary data

The organic phase concentration is

$$C = p \left[(R_4N)_p X \right] + q \left[(R_4N)_q Y \right] \quad (6)$$

and by substitution into equation (3) we obtain for the counter anion distribution,

$$\frac{[C - q [(R_4N)_q Y]_o]}{p[(R_4N)_q Y]_o^{p/q}} = \frac{K_1^{-1} [X^{p-}]_{aq}}{[Y^{q-}]_{aq}} \quad (7)$$

In the case where $p = q$, the above equation reduces to

$$p[(R_4N)_q Y]_o = \frac{c[Y^{q-}]_{aq}}{K_1^{-1} [X^{p-}]_{aq} + [Y^{q-}]_{aq}} \quad (8)$$

thus

$$[(R_4N)_p X]_o = \frac{c}{p} \left\{ \frac{c[Y^{q-}]_{aq}}{p(K_1^{-1} [X^{p-}]_{aq} + [Y^{q-}]_{aq})} \right\} \quad (9)$$

When $p \neq q$, the contents of the bracket $\{ \}$ in equation (9) would be the appropriate roots of a p/q order equation.

Such equations have been fitted to the experimental data given in Figs. 6-12 and a summary of the results is given in TABLE 4. We also present typical computer plots from the curve fitting programme CARROT[®] in Fig. 13; in these Figs. (+) represents experimental points and the solid line is the isotherm predicted by the best equation.

We have found our models give good agreement with experimental results for those systems not involving the vanadium bearing ions. The complex chemistry of the vanadate systems suggests that a more sophisticated equation than the types indicated in TABLE 4 will be necessary to obtain good results by this approach.

We have confirmed that for systems involving large amounts of chromium, the binary data discussed above explain the extraction of the chromium in counter-current solvent extraction processes. Thus it has been possible to step off across Fig. 6 in the manner indicated by Robinson and Paynter⁷ for the ion exchange system L1X64N/Cu²⁺.

Further work with the chromate systems has been concerned with the ternary and quaternary equilibria and will be reported elsewhere.

[®] Bradford University Computer Library.

TABLE 4 Summary of equations to fit binary data

Extraction reaction	General extraction equation	Best extraction parameters										
$2(R_4N)Cl + CrO_4^{=2} \rightleftharpoons (R_4N)_2CrO_4 + 2Cl^-$	$[(R_4N)_2CrO_4]_o = \frac{C}{2} - \left\{ \frac{-1 + \sqrt{1 + 8CK^I [CrO_4^{=2}]_{aq} / [Cl^-]_{aq}^2}}{8K^I [CrO_4^{=2}]_{aq} / [Cl^-]_{aq}^2} \right\}$	<table border="0"> <tr> <td>$[Cl^-]_{aq}$</td> <td>K^I</td> </tr> <tr> <td>0.09</td> <td>0.539</td> </tr> <tr> <td>0.17</td> <td>0.405</td> </tr> <tr> <td>0.27</td> <td>0.419</td> </tr> <tr> <td>0.34</td> <td>0.396</td> </tr> </table>	$[Cl^-]_{aq}$	K^I	0.09	0.539	0.17	0.405	0.27	0.419	0.34	0.396
$[Cl^-]_{aq}$	K^I											
0.09	0.539											
0.17	0.405											
0.27	0.419											
0.34	0.396											
$(R_4N)Cl + VO_3^- \rightleftharpoons (R_4N)VO_3 + Cl^-$	$[(R_4N)VO_3]_o = C - \left\{ \frac{C[Cl^-]_{aq}}{K^{II} [VO_3^-]_{aq} + [Cl^-]_{aq}} \right\}$	<table border="0"> <tr> <td>$[Cl^-]_{aq}$</td> <td>K^{II}</td> </tr> <tr> <td>0.34</td> <td>190.0</td> </tr> <tr> <td>0.51</td> <td>33.9</td> </tr> <tr> <td>0.68</td> <td>22.3</td> </tr> <tr> <td>0.85</td> <td>9.8</td> </tr> </table>	$[Cl^-]_{aq}$	K^{II}	0.34	190.0	0.51	33.9	0.68	22.3	0.85	9.8
$[Cl^-]_{aq}$	K^{II}											
0.34	190.0											
0.51	33.9											
0.68	22.3											
0.85	9.8											
$(R_4N)_2CrO_4 + 2OH^- \rightleftharpoons 2(R_4N)OH + CrO_4^{=2}$	$[(R_4N)_2CrO_4]_o = \frac{C}{2} - \left\{ \frac{-1 + \sqrt{1 + 8CK^{III} [CrO_4^{=2}]_{aq} / [OH^-]_{aq}^2}}{8K^{III} [CrO_4^{=2}]_{aq} / [OH^-]_{aq}^2} \right\}$	<table border="0"> <tr> <td>$[OH^-]_{aq}$</td> <td>K^{III}</td> </tr> <tr> <td>0.25</td> <td>329.0</td> </tr> <tr> <td>0.5</td> <td>412.1</td> </tr> <tr> <td>1.0</td> <td>439.1</td> </tr> <tr> <td>2.0</td> <td>531.8</td> </tr> </table>	$[OH^-]_{aq}$	K^{III}	0.25	329.0	0.5	412.1	1.0	439.1	2.0	531.8
$[OH^-]_{aq}$	K^{III}											
0.25	329.0											
0.5	412.1											
1.0	439.1											
2.0	531.8											
$(R_4N)Cl + OH^- \rightleftharpoons (R_4N)OH + Cl^-$	$[(R_4N)OH]_o = C - \left\{ \frac{C[Cl^-]_{aq}}{K^{IV} [OH^-]_{aq} + [Cl^-]_{aq}} \right\}$	<table border="0"> <tr> <td>$[Cl^-]_{aq}$</td> <td>K^{IV}</td> </tr> <tr> <td>0.034</td> <td>0.046</td> </tr> <tr> <td>0.068</td> <td>0.022</td> </tr> <tr> <td>0.137</td> <td>0.025</td> </tr> <tr> <td>0.205</td> <td>0.029</td> </tr> </table>	$[Cl^-]_{aq}$	K^{IV}	0.034	0.046	0.068	0.022	0.137	0.025	0.205	0.029
$[Cl^-]_{aq}$	K^{IV}											
0.034	0.046											
0.068	0.022											
0.137	0.025											
0.205	0.029											

TABLE 4 CONTINUED

Extraction reaction	General extraction equation	Best extraction parameter										
$2(R_4N)VO_3 + CrO_4^{=2} \rightleftharpoons (R_4N)_2CrO_4^{=} + 2VO_3^{=}$	$[(R_4N)_2CrO_4]_o = \frac{C}{2} - \left\{ \frac{-1 + \sqrt{8CK^V [CrO_4^{=2}]_{aq} / [VO_3^{=}]_{aq}^2}}{\epsilon K^V [CrO_4^{=2}]_{aq} / [VO_3^{=}]_{aq}^2} \right\}$	<table border="0"> <tr> <td>$[VO_3^{=}]$</td> <td>K^V</td> </tr> <tr> <td>0.098</td> <td>0.037</td> </tr> <tr> <td>0.196</td> <td>0.100</td> </tr> <tr> <td>0.382</td> <td>0.302</td> </tr> <tr> <td>0.585</td> <td>0.536</td> </tr> </table>	$[VO_3^{=}]$	K^V	0.098	0.037	0.196	0.100	0.382	0.302	0.585	0.536
$[VO_3^{=}]$	K^V											
0.098	0.037											
0.196	0.100											
0.382	0.302											
0.585	0.536											
$(R_4N)_2HVO_4 + CrO_4^{=2} \rightleftharpoons (R_4N)_2CrO_4 + HVO_4^{=}$	$[(R_4N)_2CrO_4]_o = \frac{C}{2} - \left\{ \frac{0.50 [HVO_4^{=}]_{aq}}{K^{VI} [CrO_4^{=2}]_{aq} + [HVO_4^{=}]_{aq}} \right\}$	<table border="0"> <tr> <td>$[HVO_4^{=}]$</td> <td>K^{VI}</td> </tr> <tr> <td>0.098</td> <td>0.175</td> </tr> <tr> <td>0.196</td> <td>0.241</td> </tr> <tr> <td>0.382</td> <td>0.335</td> </tr> <tr> <td>0.585</td> <td>0.423</td> </tr> </table>	$[HVO_4^{=}]$	K^{VI}	0.098	0.175	0.196	0.241	0.382	0.335	0.585	0.423
$[HVO_4^{=}]$	K^{VI}											
0.098	0.175											
0.196	0.241											
0.382	0.335											
0.585	0.423											
<p style="text-align: center;">pH 6.9</p> $(R_4N)VO_3 + OH^- \rightleftharpoons (R_4N)OH + VO_3^{=}$	$[(R_4N)VO_3]_o = C - \left\{ \frac{C [VO_3^{=}]}{K^{VII} [OH^-]_{aq} + [VO_3^{=}]_{aq}} \right\}$	<table border="0"> <tr> <td>$[OH^-]_{aq}$</td> <td>K^{VII}</td> </tr> <tr> <td>0.284</td> <td>2.090</td> </tr> <tr> <td>0.588</td> <td>2.38</td> </tr> <tr> <td>1.175</td> <td>1.855</td> </tr> <tr> <td>1.765</td> <td>1.950</td> </tr> </table>	$[OH^-]_{aq}$	K^{VII}	0.284	2.090	0.588	2.38	1.175	1.855	1.765	1.950
$[OH^-]_{aq}$	K^{VII}											
0.284	2.090											
0.588	2.38											
1.175	1.855											
1.765	1.950											

TABLE 4 CONTINUED

Extraction reaction	General extraction equation	Best extraction parameters				
$9 < \text{pH} < 12.5$ $(R_4N)_2HVO_4 + 2OH^- \rightleftharpoons 2(R_4N)OH + HVO_4^-$	$[(R_4N)_2HVO_4]_o = \frac{C}{2} - \left(\frac{-1 + \sqrt{1 + 8K^{VIII} [HVO_4^-]_{aq} / [OH^-]_{aq}^2}}{8K^{VIII} [HVO_4^-]_{aq} / [OH^-]_{aq}^2} \right)$	$[OH^-]_{aq}$ <table border="0"> <tr> <td style="text-align: right;">1.175</td> <td style="text-align: right;">38.56</td> </tr> <tr> <td style="text-align: right;">1.765</td> <td style="text-align: right;">20.34</td> </tr> </table>	1.175	38.56	1.765	20.34
1.175	38.56					
1.765	20.34					
$\text{pH} > 12.5$ $(R_4N)_3VO_4 + 3OH^- \rightleftharpoons 3(R_4N)OH + VO_4^{=}$	$[(R_4N)_3VO_4]_o = \frac{C}{3} - \frac{1}{3} \left[\alpha + \frac{(\alpha/4)^3 + (\alpha/2)^2}{4} \right]^{1/3} + \left[\alpha - \sqrt{\frac{(\alpha/4)^3 + (\alpha/2)^2}{4}} \right]^{1/3}$ $\alpha = C[OH^-]_{aq}^3 / 6K^{IX} [VO_4^{=}]_{aq}$	K^{IX} <p style="text-align: right;">940.5</p>				

REFERENCES

1. Pourbaix, M., "Atlas of electrochemical equilibria in aqueous solution", publ. Pergamon, 1966.
2. Deptula, C., Inst. Nucl. Res. Dept., No. 772 (Warsaw), 1966.
3. Rossotti, F., Rossotti, H., Acta. Chem. Scand., 10(6), 957, 1956.
4. Griffith, W.P., Wickins, T.D., J.C.S.(A), 1087, 1966.
5. Sillen, L.G., Quart. Revs., 13, 160, 1959.
6. General Mills Inc., C.D.S. 1-61, "Chromium", 1961.
7. Robinson, C.G., Paynter, J.C., Proceedings of ISEC 71, Vol. II, paper 214, Society of Chemical Industry, London, 1971.

Acknowledgements

The authors are grateful to the Albright and Wilson Company (Great Britain) for the financial support of this project.

LIST OF FIGURES

- Fig. 1 Variation of vanadium extraction with pH.
- Fig. 2 Variation of chromium extraction with pH.
- Fig. 3 Distribution of the chromium (VI) species existing at a concentration of 0.25M Cr (VI).
- Fig. 4 Distribution of the vanadium (V) species existing at a concentration of 0.25M V(V).
- Fig. 5 The constant equivalent ion line.
- Fig. 6 Chromate-chloride equilibrium data.
- Fig. 7 Back extraction equilibrium data, chromate-ammonium chloride.
- Fig. 8 Vanadate-chloride equilibrium data.
- Fig. 9 Chromate-hydroxide equilibrium data.
- Fig. 10 Chloride-hydroxide equilibrium data.
- Fig. 11 Chromate-vanadate equilibrium data.
- Fig. 12 Vanadate-hydroxide equilibrium data.
- Fig. 13 Computed $\text{CrO}_4^{=}\text{.Cl}^-$ equilibria.

List of Symbols

[]	= concentration
C	= total extractant concentration, organic phase
R	= total anion concentration, aqueous phase
Y, X	= counter anions
p, q	= charge on anions X and Y
R ₄ N	= quaternary amine cation, aliquat 336
$K^I, K^{II}, K^{III},$ $K^{IV}, K^V, K^{VI},$ $K^{VIII}, K^{VIII}, K^{IX} .$	} = "reaction constants"
E%	= percentage extraction
D	= distribution ratio
subscript o	= organic phase
subscript aq	= aqueous phase

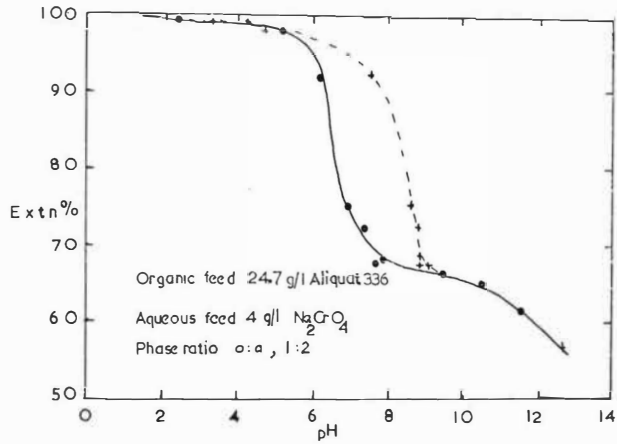


Fig 1 VARIATION OF CHROMIUM EXTRACTION WITH pH
(●) feed pH (+) raffinate pH

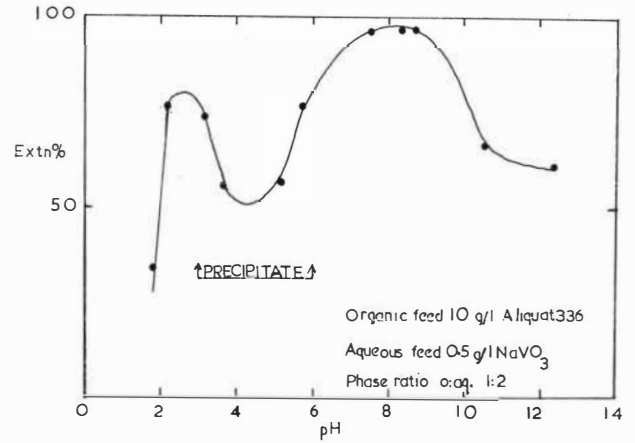


Fig 2 VARIATION OF VANADIUM EXTRACTION WITH pH

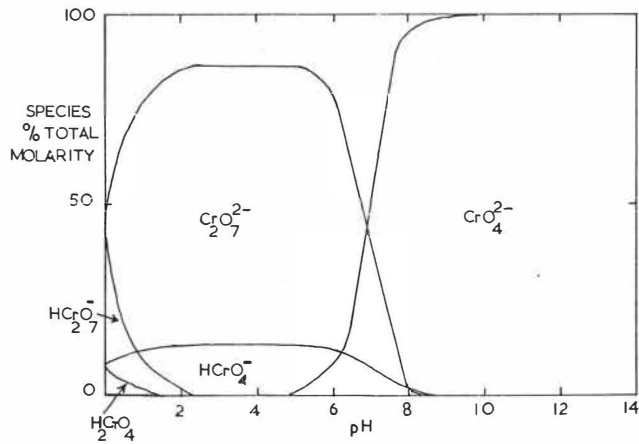


Fig 3. DISTRIBUTION OF THE CHROMIUM(VI) SPECIES
EXISTING AT A CONCENTRATION OF 0.25M Cr(VI)

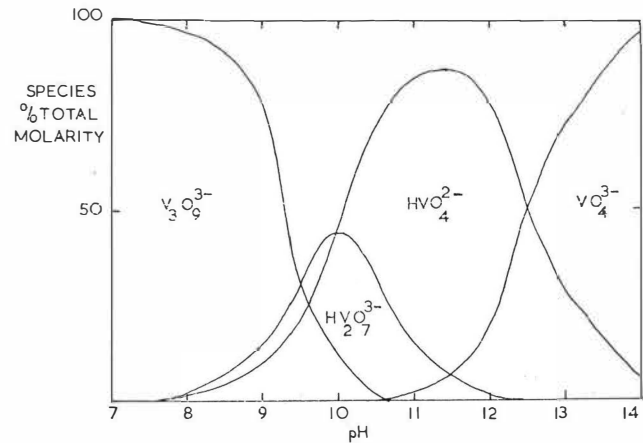


Fig 4 DISTRIBUTION OF THE VANADIUM(V) SPECIES
EXISTING AT A CONCENTRATION 0.25 M V(V)

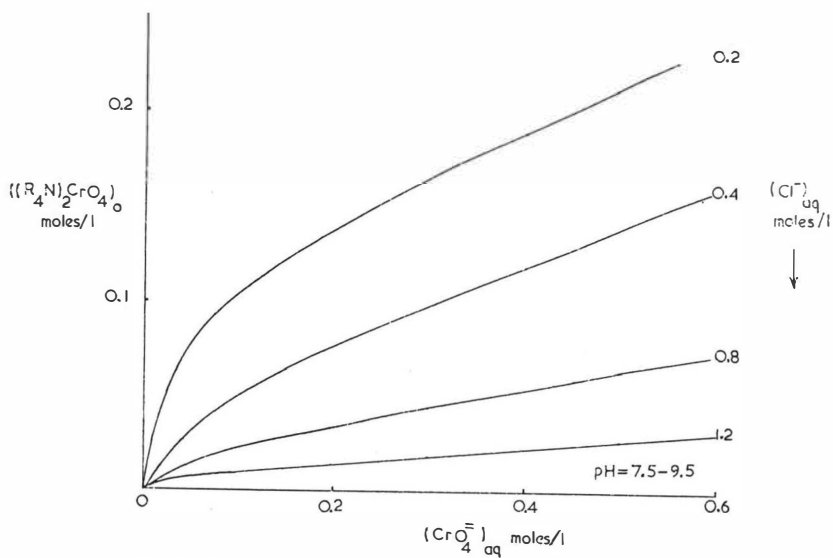


Fig 7 BACK EXTRACTION EQUILIBRIUM DATA, CHROMATE · AMMONIUM CHLORIDE

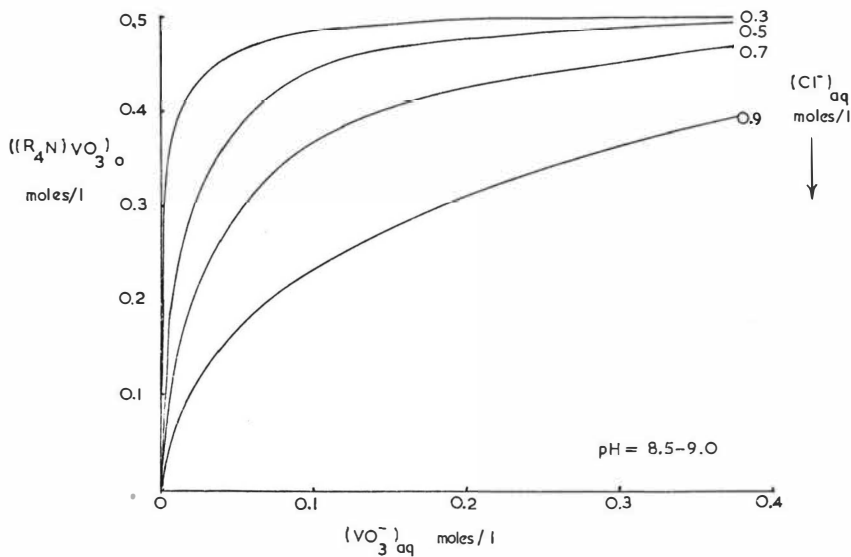


Fig 8 VANADATE · CHLORIDE EQUILIBRIUM DATA

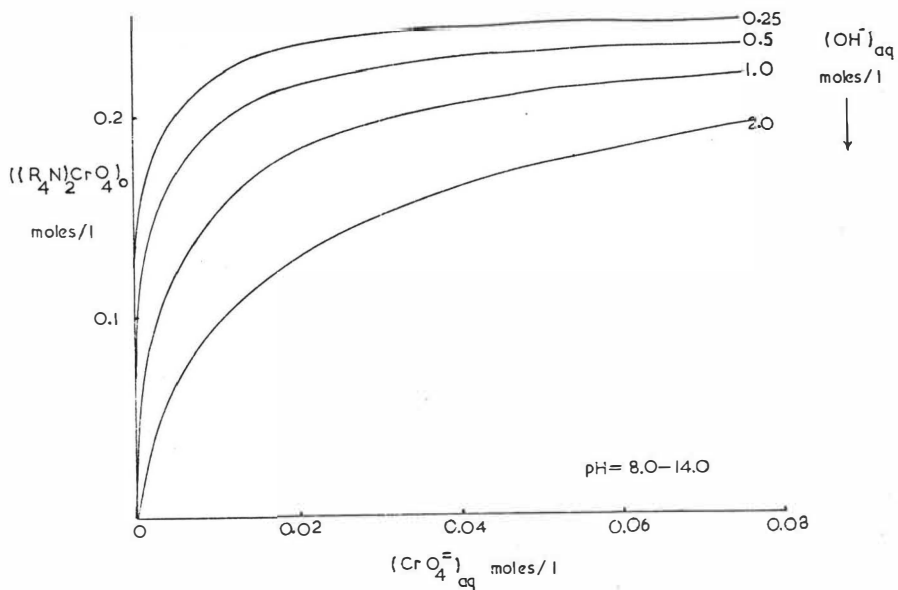


Fig 9 CHROMATE · HYDROXIDE EQUILIBRIUM DATA

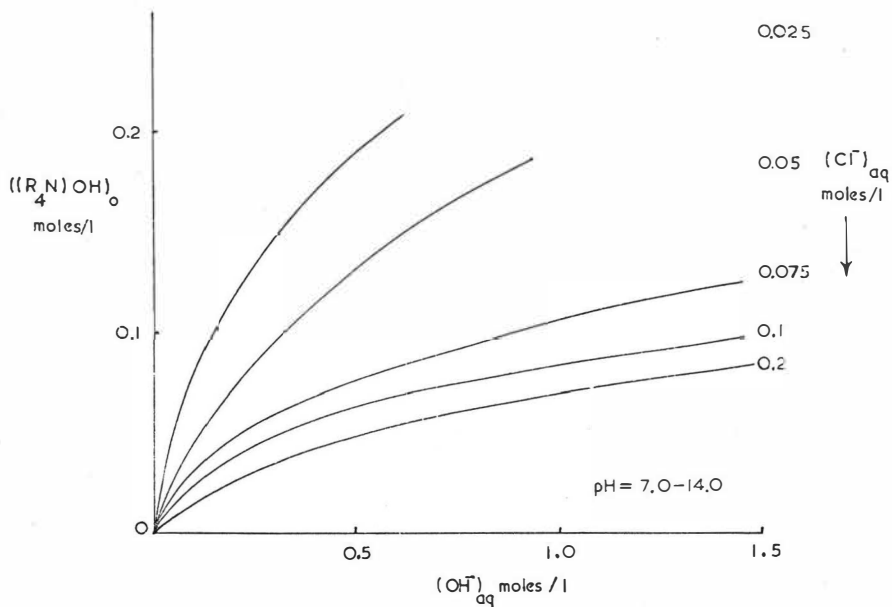


Fig 10 CHLORIDE · HYDROXIDE EQUILIBRIUM DATA

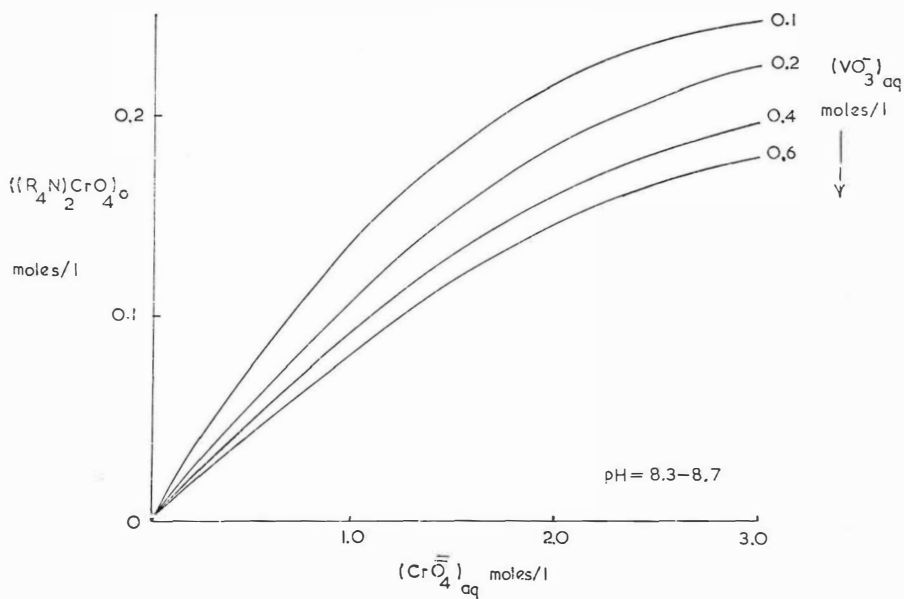


Fig 11 CHROMATE · VANADATE EQUILIBRIUM DATA

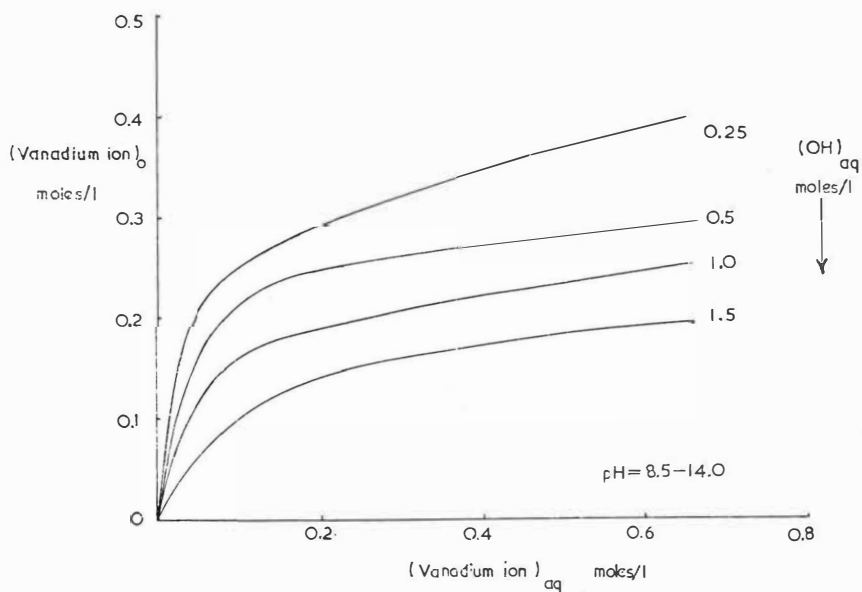


Fig 12 VANADIUM · HYDROXIDE EQUILIBRIUM DATA

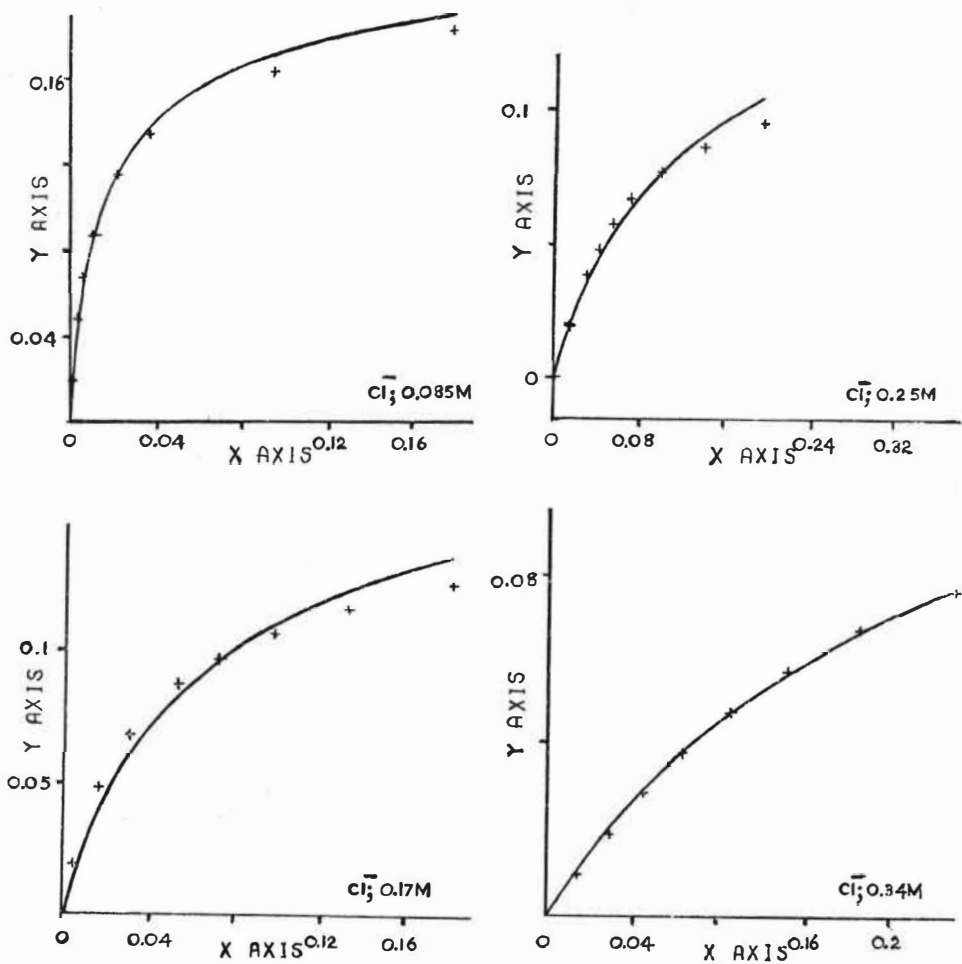


Fig 13 COMPUTED $\text{CrO}_4^{=}$ · Cl^- EQUILIBRIA

X : $(\text{CrO}_4^{=})_{\text{aq}}$

Y : $(\text{R}_4\text{N})_2\text{CrO}_4$

The Extraction of Cadmium(II) and Zinc(II) from
Sulphate and Chloride Solutions with Kelex 100 and
Versatic 911 in Kerosene

by

V.I. Lakshmanan and G.J. Lawson

(Wolfson Secondary Metals Research Group, Department of Minerals
Engineering, The University of Birmingham, U.K.)

Abstract

The separation of cadmium and zinc is of commercial importance, and the applicability of the commercial extractants Kelex 100 and Versatic 911 to this separation has been examined. Each extractant in kerosene will extract the metals readily and reversibly, but Kelex affords a much better separation. The separate extractants both extract cadmium at pH values near to neutrality, where pH control is difficult, and zinc at slightly lower values, but if they are mixed the extraction of both metals is shifted to lower, more readily controlled pH levels. When chloride is substituted for sulphate as the aqueous phase anion the extraction of cadmium takes place at more alkaline, and that of zinc at more acid, pH levels and separation is thus enhanced. Extraction of cadmium and zinc from chloride aqueous media with the mixed extractants thus allows a clear separation within a useful range of pH.

Introduction

Interest in the application of solvent extraction in extractive metallurgy has increased rapidly in recent years following the development of selective extractants for copper. Increased prices for metals and growing objection to the atmospheric pollution associated with some smelting operations have also made solvent extraction more attractive economically. Cadmium and zinc are two metals which merit examination in a solvent extraction system because of their prices; they are usually associated in orebodies, and their separation by solvent extraction forms the subject of this paper.

Fletcher *et al.*⁽¹⁾ reported the separation of zinc and cadmium using TBP and naphthenic acid as extractants, while Rice and Smith⁽²⁾ have made an extensive study of the behaviour of these metals with such extractants as TBP, TOPO, Alamine and Aliquat 336. In the present investigation the extraction of cadmium and zinc from sulphate and chloride media was studied using the commercial extractants Kelex 100 and Versatic 911 in kerosene as diluent, either singly or mixed in various proportions.

Experimental

Kelex 100 was kindly supplied by the makers, Ashland Chemical Corporation, and was purified as described earlier⁽³⁾. Versatic 911 was kindly supplied by Shell Chemicals Ltd. and was used as supplied. Radioactive tracers ^{115m}Cd and ^{65}Zn were supplied by the Radiochemical Centre, Amersham. Kerosene was 'kerosene white' supplied by Hopkins and Williams Ltd. All other reagents were of analytical quality.

Standard aqueous solutions of Cd(II) and Zn(II) were prepared by dissolving the corresponding sulphates or chlorides in water and determining the metal concentrations by the oxinate and pyrophosphate methods respectively⁽⁴⁾. Aqueous phases for extraction experiments were prepared from appropriate amounts of standard metal solution and sodium sulphate or chloride to maintain the anion concentration, usually at 1.0M; for experiments in which the concentrations of these anions were varied, appropriate amounts of sodium sulphate or chloride were taken to give the desired anion concentration and the total ionic strength was adjusted to 4.0M by addition of sodium nitrate. Organic phases were prepared by dissolving appropriate amounts of Kelex 100 and/or Versatic 911 in kerosene.

The AKUFVE-110 instrument, which was used for the extraction experiments, has been described in detail elsewhere⁽⁵⁾. It was fitted with two flow-through scintillation counters (Nuclear Enterprises Ltd), one in each phase recycle loop, which measured the metal concentration in each phase by the activity due to ^{115m}Cd or ^{65}Zn . The outputs were fed into differential counting equipment connected to a printer which printed out values of the metal distribution coefficient, D , repeatedly and automatically. The pH of the aqueous phase was continuously monitored by a combined glass electrode placed in the aqueous phase recycle loop and connected to a pH meter which also formed part of a pH-stat control unit (Radiometer Ltd.); this unit controlled the aqueous phase pH at any predetermined value by the automatic addition of acid or alkali. To determine a $\log D - \text{pH}$ relationship equal volumes (450ml) of selected aqueous and organic phases were introduced into the mixing chamber of the AKUFVE-110 and the centrifuge was started. When equilibrium had been established, usually after about 1 min., several readings of D were taken, to ensure statistical accuracy, and the pH of the aqueous phase was checked by withdrawing a small sample for measurement with an independent Pye model 290 pH meter, the sample being afterwards returned to the mixer. The pH-stat was then set to a new pH value and the procedure repeated to obtain a series of readings from which a $\log D - \text{pH}$ graph was constructed. The pH was controlled by addition of sodium hydroxide or an appropriate acid; for work with 1M chloride or sulphate solutions HCl or H_2SO_4 respectively was used, while for experiments with 4M ionic medium but various concentrations of chloride or sulphate nitric acid was employed. At the end of a set of measurements the total increase in volume of the aqueous phase caused by addition of acid and alkali did not exceed ten per cent. During the experiments cold tap water was circulated through the heat exchangers fitted to the AKUFVE; the phase temperature was thus controlled within 1°C on any one day, but over the whole series of experiments the temperature varied between about 8° and 12°C due to seasonal change in tap water temperature.

Results and Discussion

These investigations form a part of the programme of the Wolfson Secondary Metals Research Group in which the separation of various combinations of metals occurring in secondary sources, by solvent extraction with commercial extractants, is being examined. It is anticipated that solutions for treatment would arise from dissolution of mixed secondary metals in sulphuric or hydrochloric acid, so that in the present work the extraction of cadmium and zinc from both sulphate and chloride aqueous media was examined, using the extractants Kelex 100, an oxine derivative, and Versatic 911, a carboxylic acid, in kerosene diluent, with the object of determining conditions for the most effective separation of the two metals.

A typical extraction equilibrium involving a metal ion M^{n+} and an extractant HX may be written:



from which may be derived:

$$\log D = \log K + npH + m \log [HX]$$

where K is the extraction equilibrium constant. Consequently the slope of a $\log D - pH$ graph for conditions of constant extractant concentration, i.e. with $[HX] \gg [M^{n+}]$ will be equal to n . Similarly the value of $pH_{0.5}$, the pH at which $\log D = 0$, is given by:

$$pH_{0.5} = -\frac{1}{n} \log K - \frac{m}{n} \log [HX]$$

so that from the slope of a graph of $pH_{0.5}$ vs $-\log [HX]$ is determined, and hence m .

For metals which show the same value of slope n in a particular extraction system the corresponding values of $pH_{0.5}$ give a useful indication of the ease with which they may be separated, since this increases with increase in the difference between the two values.

In Tables 1 and 2 are shown values of slope and $pH_{0.5}$ for $\log D - pH$ relationships for the extraction of cadmium with Kelex - Versatic organic phases of various compositions from aqueous phases maintained at 1M concentration with respect to sulphate and chloride respectively. Concentrations of the individual extractants up to 10% were used, and the initial metal ion concentrations were varied between $5 \times 10^{-4}M$ and $10^{-2}M$. For a typical $\log D - pH$ line about 10 individual experimental points were recorded, which in all but a few cases fitted a linear relationship with a regression coefficient of 0.997 or better.

The results indicated a second power dependency of extraction on pH for both sulphate and chloride systems, corresponding to the extraction of Cd^{2+} . In some experiments considerable variation in slope value from 2.0 was found, although most results were reasonably close; however no account was taken of possible hydrolysis of the cadmium ion, which could affect the slope value and probably occurred at higher pH levels. Extraction behaviour appeared to be independent of metal ion concentration. The value of $\text{pH}_{0.5}$ decreased with increase in the concentration of either extractant, as was expected; overall, the $\text{pH}_{0.5}$ values in sulphate media were less than the corresponding values for chloride media by about 0.3 pH units. The extraction of cadmium with carboxylic acids has been reported by other workers^(1,6), and so only a few confirmatory experiments were carried out with Versatic 911 alone; in a typical experiment with $1.0 \times 10^{-3}\text{M}$ cadmium in 1M chloride and 1% Versatic in kerosene a slope of 2.2 and $\text{pH}_{0.5}$ value of 7.14 were obtained.

The most striking result was the decrease in $\text{pH}_{0.5}$ caused by mixing the two extractants; e.g. extraction of $1.0 \times 10^{-3}\text{M}$ cadmium with 2% Kelex in kerosene gave a $\text{pH}_{0.5}$ value of 7.55, while with 1% Kelex + 1% Versatic the value was 6.16. The molecular weight of Kelex is about 310, and that of Versatic dimer about 340; thus, although the 'percentage' solutions were not strictly comparable on a molar basis, the differences in $\text{pH}_{0.5}$ to be expected from concentration differences were far less than the reduction of 1.3 - 1.4 pH units found for comparable cases. It therefore appears that the extractants act together synergistically.

Using the above results graphs of $\text{pH}_{0.5}$ vs log (extractant concentration) were constructed, with respect to variation of the concentration of Kelex (HX) or Versatic (HA), and corresponding values of m were calculated. For extraction with Kelex alone a value of $m = 3$ was obtained, corresponding to an extracted complex of the type $\text{CdX}_2 \cdot \text{HX}$, while for the mixed extractants values of $m = 2$ and $m = 1$ were obtained with respect to Kelex and Versatic (Table 3), indicating a complex of the form $\text{CdX}_2 \cdot \text{H}_2\text{A}_2$. Substitution of chloride for sulphate appeared to have no effect on the values of m . It is assumed that neither hydrolysis of metal ions nor formation of chloride or other complexes in the aqueous phase was significant.

The effects of varying the concentration of sulphate or chloride in a salt medium of overall concentration 4M on the extraction of $5 \times 10^{-4}\text{M}$ cadmium with 2% extractant solutions are shown in Table 4. Extraction with Versatic was virtually

unaffected by sulphate concentrations up to 0.3M, while with Kelex a small change in $pH_{0.5}$ to higher values was noted; increase in chloride concentration however produced a marked increase in $pH_{0.5}$. Under the experimental conditions it was not possible to examine sulphate concentrations greater than 0.3M because they caused phase disengagement problems.

The extraction of zinc(II) with Kelex and Versatic in kerosene has not yet been examined as extensively as that of cadmium, and detailed results will be published later, but typical values of slope and $pH_{0.5}$, for various extractant concentrations and two concentrations of zinc in 1M sulphate or chloride, are shown in Table 5. These results indicate that the behaviour of zinc is opposite to that of cadmium in two respects; under comparable conditions zinc is extracted by Versatic at higher $pH_{0.5}$ values than by Kelex, while the reverse is true for cadmium, and the substitution of 1M chloride for 1M sulphate causes a reduction in $pH_{0.5}$ of about 0.4 units for zinc, whereas $pH_{0.5}$ for cadmium is increased by about 0.3 units. The opposite effects of chloride media in the extraction of cadmium and zinc were reported earlier by Flett⁽⁷⁾ for extraction with naphthenic acid, and result in increased separation between the two metals. From the present results it may be deduced, very approximately, that for extraction with 1% extractant of small concentrations of zinc and cadmium in 1M sulphate or chloride Versatic with sulphate would give very little separation, and Versatic with chloride would give a separation of about 0.7 units at $pH_{0.5}$; the corresponding separations with Kelex would be 1.7 and 2.2. Thus Kelex with chloride would offer the best separation, but in a pH range, 5.7 - 7.9, difficult to control and likely to cause hydrolysis of the metal ions. However, Table 5 shows a similar synergistic reduction in $pH_{0.5}$ for zinc when extracted with Kelex + Versatic as was observed for cadmium, and consequently by extracting with the mixed extractants from chloride media a useful separation may be achieved in a more acid pH range. Table 6 shows the effect of increasing chloride concentration, in a salt medium of 4M total concentration, on the extraction of zinc by 2% Kelex or 1% Kelex + 1% Versatic; a small increase in $pH_{0.5}$ was observed, less than that found for cadmium. The synergistic effect in the mixed extractants is also evident from these results.

It appeared that a separation of cadmium and zinc should be obtainable in a useful pH range by taking advantage of the separations in chloride media and the synergistic effect of the mixed extractants. This was demonstrated by extracting an aqueous

solution containing 1×10^{-3} M cadmium and 1×10^{-3} zinc in 1M chloride with 5% Kelex + 5% Versatic in kerosene; a clear separation resulted (Fig.1), with respective values of $pH_{0.5}$ of 5.2 and 3.9, corresponding to a separation coefficient of about 450.

Both cadmium and zinc were readily recovered from the organic solution by stripping with an acid aqueous solution of pH 2. When nitric acid was used for stripping and the resulting solution treated with silver ions no chloride could be detected, indicating that chloro-complexes of the metals had not been extracted into the organic phase.

Conclusions.

1. Kelex 100 in kerosene is an effective extractant for cadmium and zinc, affording larger separation factors than carboxylic acids. Cadmium appears to be extracted as the species $CdX_2 \cdot HX$.
2. Mixtures of Kelex 100 and Versatic 911 show a synergistic effect, extracting cadmium and zinc with lower $pH_{0.5}$ values than either extractant separately. Cadmium appears to be extracted as the species $CdX_2 \cdot H_2A_2$.
3. Kelex and Kelex-Versatic mixtures extract cadmium at higher pH values in chloride than in sulphate media; the reverse is true for zinc, so that extraction from chloride media is attended by increased separation factors.
4. Separation of cadmium and zinc at more easily controlled pH values is best achieved by extracting with Kelex-Versatic mixtures from chloride media.
5. Increase in chloride ion concentration leads to a small increase in $pH_{0.5}$, less for zinc than for cadmium.

Acknowledgements.

Grateful acknowledgement is made to Professor S.G. Ward for his interest, to Mr. G. Harrison for experimental assistance, to Dr. J. Hartlage of Ashland Chemical Corporation for a supply of Kelex 100, and to Shell Chemicals Ltd. for a supply of Versatic 911.

References

1. Fletcher, A.W., Flett, D.S, Pegler, J.L., Pepworth, D.P. and Wilson, J.C. "Advances in Extractive Metallurgy", p.686, The Institution of Mining and Metallurgy, London, 1967.
2. Rice, N.M. and Smith, M.R. Canadian Metallurgical Quarterly, 1973, 12, 341.
3. Lakshmanan, V.I. and Lawson, G.J. J. inorg. nucl. Chem., 1973, 35, 4285.
4. Vogel, A.I. "Textbook of Quantitative Inorganic Analysis", pp. 389, 533. Longmans, London, 1962.
5. Reinhardt, H and Rydberg, J. International Symposium on 'Solvent Extraction in Metallurgical Processes', p.31, Technologisch Instituut. K.VIV, Antwerpen, May 1972.
6. Spitzer, E.L.T.M. ibid., p.16
7. Flett, D.S. Nature, 1963, 200, 465.

Initial Cd(II) concn. $\times 10^3$	Kelex concn. %	Versatic concentration, %											
		0		0.5		1.0		2.0		5.0		10.0	
		P	S	P	S	P	S	P	S	P	S	P	S
0.5	0.5	8.02	1.4	6.26	1.9	6.22	2.0	6.21	1.7	5.89	1.9	5.52	2.1
1.0		8.11	1.7	6.26	1.9	6.14	1.9	6.05	1.9	5.84	2.0	5.53	2.1
0.5	1.0	7.59	1.3	5.90	1.8	5.79	1.8			5.48	1.8		
1.0		7.71	1.7	5.98	1.8	5.75	1.9	5.67	1.9	5.47	1.9	5.17	1.9
2.5					5.92	1.9	5.72	2.4	5.69	1.9	5.49	1.8	5.20
1.0	2.0	7.11	2.1	5.66	2.0	5.49	2.0	5.38	2.0	5.23	2.0	5.10	2.0
2.5		7.15	1.7	5.64	2.0	5.51	1.9	5.32	1.9	5.14	1.8	5.09	1.9
5.0		7.20	1.8	5.65	2.0	5.55	1.8	5.35	1.8	5.15	1.8	5.10	1.8
1.0	5.0	6.60	2.5	5.22	2.1	4.97	2.0	4.93	1.9	4.81	2.0	4.70	2.0
2.5		6.60	2.0	5.29	1.7	5.13	2.0	4.98	1.8	4.79	2.0	4.66	2.3
5.0		6.68	2.1	5.33	1.8	5.17	1.9	5.01	2.0	4.80	2.0	4.71	1.9
10.0		6.71	1.7					5.03	1.9	4.82	2.0	4.73	1.8
1.0	10.0	6.19	1.8	5.11	1.8	4.92	2.0	4.79	1.9	4.57	2.0	4.41	2.0
2.5		6.10	2.4	5.11	1.9	4.89	1.9	4.72	2.0	4.53	2.0	4.41	2.0
5.0		6.08	2.3	5.07	2.0	4.97	1.9	4.71	2.0	4.54	2.0	4.41	2.1
10.0		6.16	1.6					4.73	2.0	4.55	1.9	4.41	2.0

Table 1. Extraction of Cadmium(II) from 1M sulphate solution with Kelex 100 and Versatic 911 in kerosene; $pH_{0.5}$ (P) and slope (S) values of log D - pH relationships.

Initial Cd(II) concn. $\times 10^3$ M	Kelex concn. %	Versatic concentration, %											
		0		0.5		1.0		2.0		5.0		10.0	
		P	S	P	S	P	S	P	S	P	S	P	S
0.5 1.0	0.5			6.55	1.8	6.50	1.9	6.37	1.9	6.14	2.0	6.02	2.0
				6.54	1.8	6.51	1.9	6.37	1.9	6.13	2.0	5.95	2.0
0.5 1.0 2.5	1.0	7.93	2.0	6.32	1.7	6.17	1.9	6.02	1.9	5.82	2.0	5.69	2.0
				6.32	1.7	6.16	2.0	6.03	1.9	5.80	1.9	5.67	2.1
				6.27	1.8	6.16	1.8	6.02	1.9	5.79	2.0	5.68	2.1
1.0 2.5 5.0	2.0	7.55	2.1	5.94	1.9	5.8	1.9			5.50	2.0	5.39	2.0
		7.49	2.1	5.92	1.8	5.8	1.9	5.67	1.9	5.49	1.9	5.39	1.9
		7.49	2.3	5.93	1.9			5.66	2.0	5.49	1.9	5.40	1.8
1.0 2.5 5.0 10.0	5.0	6.74	1.8	5.54	1.8	5.40	1.9	5.28	2.0	5.13	1.8	4.99	1.9
		6.77	1.7			5.40	1.8	5.27	1.9	5.08	1.9	5.00	2.0
		6.77	1.8	5.55	1.7	5.40	1.9	5.28	1.8	5.10	1.8	4.99	2.0
		6.81	1.7					5.28	1.8	5.08	1.8	4.99	1.9
1.0 2.5 5.0 10.0	10.0			5.31	1.9	5.19	1.8	5.07	1.8	4.87	1.8	4.77	1.9
		6.42	1.7	5.31	1.8	5.17	1.8	5.07	2.0	4.87	2.0	4.76	1.9
		6.45	2.0	5.32	1.8	5.17	1.8	5.04	1.9	4.91	1.9	4.77	1.9
		6.41	1.9					5.04	1.8	4.90	2.0	4.74	1.9

Table 2. Extraction of Cadmium(II) from 1M Chloride solution with Kelex 100 and Versatic 911 in kerosene; $\text{pH}_{0.5}$ (P) and Slope (S) values of $\log D - \text{pH}$ relationships.

Initial Cd(II) concn. M	Unvaried Extractant concn. %	Value of m	
		1M sulphate	1M chloride
1×10^{-3}	Kelex		
	1.0	1.2	1.0
	2.0	0.8	0.8
2.5×10^{-3}	10.0	1.1	0.9
	2.0	0.9	0.8
	5.0	1.0	0.8
5.0×10^{-3}	5.0	1.0	0.9
1.0×10^{-3}	Versatic		
	0.5	2.0	2.1
	1.0	2.0	2.1
	2.0	2.0	2.0
	5.0	1.9	1.9
10.0	1.6	1.8	
2.5×10^{-3}	5.0	1.9	1.9
	10.0	1.7	1.9

Table 3. Extraction of Cadmium(II) with Kelex 100 and Versatic 911 in kerosene from Sulphate and Chloride Media. Values of m derived from graphs of $\text{pH}_{0.5}$ vs. log (extractant concentration).

Extractant	Anion concentration (M)													
	0		0.05		0.1		0.2		0.3		0.5		4.0	
	P	S	P	S	P	S	P	S	P	S	P	S	P	S
	Sulphate medium:													
2% Kelex	5.42	1.8	5.49	1.8	5.54	1.8	5.59	1.8	5.65	1.9				
2% Versatic	6.42	1.9	6.39	1.8	6.39	1.9	6.43	1.7	6.46	1.7				
1% Kelex + 1% Versatic	5.23	1.7	5.30	1.9	5.35	1.9	5.41	1.9	5.46	1.9				
	Chloride medium:													
2% Kelex											5.97	1.8	6.86	2.0
2% Versatic	6.42	1.9	6.52	1.9	6.56	1.9			6.81	1.8	6.93	1.8		
1% Kelex + 1% Versatic	5.23	1.7	5.36	1.8	5.46	1.8			5.66	1.9	5.80	1.8		

Table 4. Effects of Sulphate and Chloride Concentration on Extraction of Cadmium(II) with Kelex 100 and Versatic 911 in kerosene. Initial Cadmium Concentration $5 \times 10^{-4} \text{M}$. Total Salt Concentration 4M. P = $\text{pH}_{0.5}$, S = Slope of log D - pH lines.

Kelex concentration %		Versatic concentration, %											
		0		0.5		1.0		2.0		5.0		10.0	
		P	S	P	S	P	S	P	S	P	S	P	S
0	a			6.78	2.3	6.71	2.4	6.58	2.3	6.36	2.3		
0.5	a	6.06	1.3							5.02	2.0		
	b	5.91	1.9							4.88	1.9		
	c	6.19	1.7										
1.0	a	5.57	1.6							4.65	2.0		
	b	5.66	2.0							4.59	2.0		
	c	5.97	2.1										
2.0	a	5.09	1.9							4.37	1.9		
	b	5.25	1.7							4.32	2.0		
	c	5.49	2.1										
5.0	a	4.51	1.9	4.30	1.9	4.19	2.1	4.09	2.0	3.93	2.0	3.86	2.0
	b	4.83	1.7	4.29	1.9	4.15	2.0	4.05	1.7	3.94	2.1	3.80	2.2
	c	5.18	2.0	4.76	2.0	4.62	2.1	4.49	2.0	4.33	2.0	4.22	2.1

Table 5. Extraction of Zinc (II) with Kelex 100 and Versatic 911 in kerosene; $\text{pH}_{0.5}$ (P) and slope (S) values of $\log D - \text{pH}$ relationships.

a - $2.5 \times 10^{-3} \text{M}$ Zn(II) in 1M chloride medium.

b - $5 \times 10^{-4} \text{M}$ Zn(II) in 1M chloride medium.

c - $5 \times 10^{-4} \text{M}$ Zn(II) in 1M sulphate medium.

Extractant	Chloride ion concentration (M)									
	0.05		0.1		0.5		1.0		4.0	
	P	S	P	S	P	S	P	S	P	S
2% Kelex	4.98	1.6	4.95	1.7	5.02	1.7	5.13	1.8	5.29	1.8
1% Kelex + 1% Versatic	4.57	1.7			4.55	1.8	4.65	2.0	4.86	2.1

Table 6. Effect of chloride concentration on extraction of Zinc(II) with Kelex 100 and Versatic 911 in kerosene. Initial Zinc Concentration $5 \times 10^{-4} M$. Total Salt concentration 4M. P = $pH_{0.5}$, S = slope of log D - pH lines.

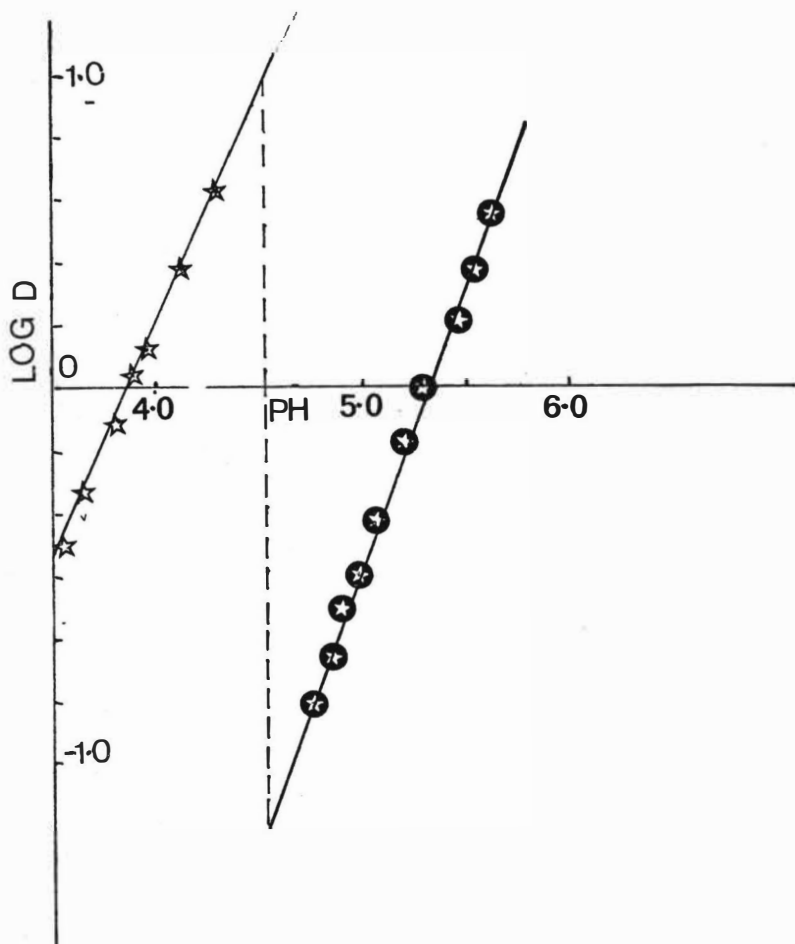


FIGURE 1

SEPARATION OF CADMIUM AND ZINC BY EXTRACTION FROM 1M CHLORIDE SOLUTION WITH KELEX 100 - VERSATIC 911 IN KEROSENE.

Cd (II) ● Zn(II) ☆

INITIAL METAL CONCENTRATIONS $1 \times 10^{-3}M$
 CONCENTRATION OF EACH EXTRACTANT 5%.

THE TECHNIQUES OF SOLVENT EXTRACTION APPLIED TO THE
TREATMENT OF INDUSTRIAL EFFLUENTS

J.P. CUER - W. STUCKENS - N. TEXIER

Produits Chimiques UGINE KUHLMANN - PARIS - FRANCE

SUMMARY

Liquid-Liquid extraction of various industrial acid effluents by means of organic solvents allows recovery of the contained chromium (Cr VI).

In a comparison between amine solvents and TBP, the latter has shown much promise in its high extraction capacity under strong acid conditions, its stability in an oxydising medium and the ease of recovery of the extracted chromium.

The process which is described permits recovery, under economically advantageous conditions, of 99,5% of chromium Cr VI contained in industrial effluents of various origins.

INTRODUCTION

The object of this article is to show that, in inorganic chemistry, the technique of solvent extraction does not have to apply only to the treatment of liquors resulting from the leaching of minerals but may also provide the preferred solution to the recovery of products contained in industrial waste liquors.

As an example we have chosen the recovery of chromium (Cr VI) contained in waste liquors originating in plants producing chromic anhydride (CrO_3) and in shops using this product (chromium plating and metal treatment).

The profitability of the process depends on numerous factors such as simplicity of the equipment, stability of the solvent in oxydizing media, negligible solubility of the solvent in aqueous phases containing the ions, and ease of operation of the installation.

STARTING MATERIALS

The main starting material containing recoverable chromium (Cr VI) is a byproduct of the manufacture of chromic anhydride.

Chromic anhydride is often produced through the treatment of sodium dichromate, anhydrous or the dihydrate, with concentrated sulfuric acid. The reaction leads to formation of chromic anhydride together with a mixture of sodium hydrogen sulfate and chromic anhydride. It is desirable to recover the latter component of this mixture.

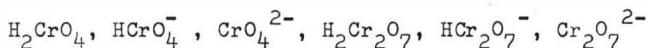
Chromium plating baths, on the other hand, contain chromic acid, sulfuric acid and various additives.

The overall mixture of these byproducts contains, in addition to Cr VI, non negligible quantities of Cr III, vanadium, iron and sulfate, which prevent its reuse. Addition of water dissolves the different constituents. The resulting liquor has an adjusted acid concentration of about 4N. Often, it contains in suspension materials which settle with difficulty.

The desired product is the most concentrated solution of Cr VI obtainable with the least amount of SO_4^{2-} ions and without Cr III or heavy metal cations.

CHOICE OF SOLVENT

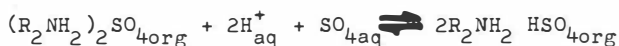
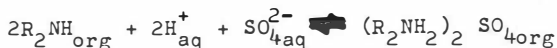
Depending on the acidity of a solution, chromium (Cr VI) is present in various forms:



As may be seen from the equilibrium constants of these compounds (1)(2), the chromate ions do not exist below a pH of 4. Furthermore, in concentrated and acid solutions, $\text{Cr}_2\text{O}_7^{2-}$ exists in the form of polymers.

Anions containing Cr VI may be extracted from the aqueous sulfuric acid phase by means of various extractants with a basic nature, like secondary or tertiary amines (di-lauryl or tri-n-octyl amine) or tributyl phosphate (TBP).

In contact with a sulfuric acid medium, the amine functions of the extractant form acid or neutral sulfate through reactions of the following type:

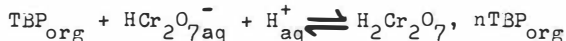
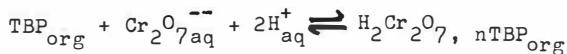


The amine salt, in the presence of a chromate solution, transforms the group SO_4 into Cr_2O_7 by substitution (3):



Thus, there is competition between SO_4^{2-} ions and those containing Cr VI.

Chromium (Cr VI) may be extracted by TBP from strongly acid aqueous solutions (2 to 4 N) in which chromium is mainly in the form of anions $\text{Cr}_2\text{O}_7^{2-}$ or $\text{HCr}_2\text{O}_7^{-(4)}$.



We have studied the following three extractants: TnOA (alamine 336 of General Mills), DLA (LA 2 of Rohm and Haas) and TBP.

ESTABLISHING COMPARISONS AMONG THE THREE CHOSEN SOLVENTS

The amines TnOA and LA 2 are diluted with xylene (in general 0.1 M amine).

TBP is used as such.

4.1. Stability of the solvents loaded with chromium.

In the process considered, the solvents are in contact with a strongly oxidizing medium.

When technical quality solvents are used, it is necessary to distinguish the decomposition of the extracting molecule proper and that of the other constituents: diluent, additive or impurity contained in the solvent.

In the present case, solvent stability is followed by determining the quantity of Cr VI reduced to Cr III and the residual concentration of extractant in the solvent.

The solvent is loaded with chromium by contacting an acid solution containing Cr VI. To avoid photochemical acceleration of decomposition indicated by numerous authors, the loaded solvent is kept in darkness. At given intervals, a sample is removed and analyzed.

TABLE I

Stability of Cr VI extracted by an amine solvent TnOA (0.1 M), diluted with xylene, loaded with chromium from a solution of H^+ , 2N ; Cr vI, 7.6 g/1

Time hr	Cr VI g/1	Cr Total g/1	Cr III g/1	Total % of Cr reduced
0	7.20	7.20	0	0
72	6.60	6.92	0.32	9.2
144	6.32	6.52	0.30	12.2

TABLE 2

Stability of Cr VI extracted by an amine solvent LA 2 (0.1 M), diluted with xylene, loaded with chromium from a solution of H^+ , 2N ; Cr VI, 3.8 g/1

Time hr	Cr VI g/1	Cr total g/1	Cr III g/1	Total % of Cr reduced
0	5.43	5.44	0	0
24	5.31	5.34	0.03	2.2
170	5.10	5.12	0.02	6.1

TABLE 3

Stability of Cr VI extracted by TBP

Pure TBP loaded with chromium from a solution of H^+ , 4N ;

Cr VI, 7.7 g/l

Time hr	Cr VI g/l	Cr total g/l	Cr III g/l	Total % of Cr reduced
0	23.6	23.6	0	0
6	23.6	23.6	0	0
24	23.5	23.6	0.1	0.3

Chromium (Cr III), in addition to that present in the organic phase in concentrations shown in tables 1 and II, collects in the aqueous droplets separating on the bottom of vessels in which are kept the solvents.

In our experiments we have found no tangible destruction of the amine function but only a reduction of Cr VI by compounds present in the solvents. Analyses have shown disappearance of a certain number of functions due to impurities contained in the solvent.

Yet, this phenomenon of decomposition is troublesome in the industrial application of the process ; for, in continuous operations of long duration, it leads to a stabilisation of emulsions formed in the mixers.

TBP, even in a very acid medium (4 N instead of 2N), seems to be more stable than the amine solvents. A contact time of 1000 hours at normal temperature with a 4N sulfochromic acid solution has shown a remarkable stability of the solvent. Even more, the decomposition products, if there are any, do not seem to stabilize water-solvent emulsions.

4.2. Distribution coefficient and chromium between the aqueous phase and the various solvents

The distribution isotherms of Cr VI between the aqueous and the organic phases are shown for the following three solvents:

- MnOA, 0.099 M in xylene, pretreated with a solution of sodium hydrogen sulfate.
NaHSO₄ ($H^+ = 1.58 N$) ; concentration of acid in the aqueous phase, 2.16 N (Fig.1)
- LA 2, 0.1M in xylene, pretreated with a solution of sodium hydrogen sulfate ($H^+ = 1.58 N$) ; concentration of acid in the aqueous phase, 2 N (Fig.2).
- Pure TBP, acid concentration in the aqueous phase, 1 to 2 and 4 N (Fig.3).

The distribution coefficients of chromium for a solvent in contact with a 0.2 g/1 Cr solution are shown in table 4.

a comparison of these indicates that :

- a) It is the amine solvent which extracts Cr VI better from dilute solutions.
- b) The extraction capacity of amine solvents diminishes when the acidity of the aqueous phase increases from 0.01 to 2N. In the case of TBP, on the contrary, this phenomenon is the reverse. Here, the distribution coefficient is very high even with 4 N acid solution.
- c) the chromium loading capacity at saturation of TBP (30 g/1) is much greater than that of the other two solvents (5.75 and 7.00 g/1) when at equilibrium with a 2N acid solution.

TABLE 4

Comparison of effectiveness of various solvents in the extraction of Cr VI

Solvent	Acidity of the aqueous phase	K_A^0 for an aqueous phase of 0.2 g Cr/1	Loading capacity g/1
TnOA	0.099 M	2.16	25
	0.193 M	2.16	42
LA 2	0.1 M	0.01	29
		0.25	29
		2.0	17
TBP pure		1	5.75
		2	1.5
		4	6.0
		4	12.5
			30.0
			55.0

4.3. Separation factor of SO_4 - Cr VI

A solvent contacting a solution containing SO_4^{2-} and $Cr_2O_7^{2-}$ ions extracts both of them simultaneously. The ratio of Cr/ SO_4 extracted into the solvent depends on the acidity of the medium and the relative concentrations of SO_4^{2-} and $Cr_2O_7^{2-}$ ions.

Amine solvents

For LA 2 (0.1 M) in presence of an aqueous sulfuric acid (1 M) containing chromium, the relationship between the concentrations of Cr VI and SO_4 in the solvent is expressed by an approximately linear equation

SO_4 m mole = -0.73 Cr m mole + 80 represented in Fig.4.

TBP

In the presence of an aqueous sulfochromic acid solution of constant acidity (due to H_2SO_4) the relationship between the concentrations of H_2SO_4 and $H_2Cr_2O_7$ in the solvent phase has not been established with precision. Nevertheless, it seems that high concentrations of chromium in the aqueous phase inhibit the extraction of sulfuric acid from 4 N solutions (Table 4 bis).

On the other hand, TBP, in contact with aqueous sulfuric acid of various concentrations (between 0.2 and 2 M) containing 5 g of Cr VI/1, extracts simultaneously sulfuric acid and Cr VI. Similarly to the concentration of Cr VI, the concentration of sulfuric acid in the organic phase increases in proportion to its concentration in the aqueous phase, i.e. in parallel with the acidity (Fig.5).

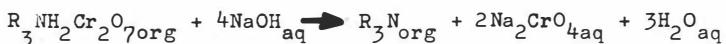
TABLE 4bis

Relationship between H_2SO_4 and $H_2Cr_2O_7$ in TBP contacting a 4 N sulfochromic acid solution.

Experiment No.	1	2	3	4
Cr VI g/1	13.6	15.81	23.35	25.3
SO_4 g/1	6.8	7.00	3.8	3.0

4.4. Recovery of chromium extracted by a solvent Amine solvents

The recovery of chromium may be carried out by contacting the solvent with an alkaline solution in order to allow the following reaction to take place:



The results of experiments are shown in Table 5.

TABLE 5

Stripping of Cr VI by caustic from LA 2 diluted with xylene (0.1 M).

The solvent was loaded with 0.330×10^{-3} mole/l of H_2SO_4 and various concentrations of chromium (about 2×10^{-3} moles of Cr VI).

NaOH/Cr VI introduced 10^{-3} moles	3.45	1.98	1.62	1.27	0.82
% SO_4 recovered	100	100	97	95.5	88
% Cr recovered	100	100	95	81	41.5
SO_4 /Cr VI redovered	0.12	0.12	0.12	0.14	0.26

According to the results expressed in Table 5, SO_4^{2-} ions are stripped in preference to those of Cr VI.

Total stripping of Cr VI necessitates the use of nearly two moles NaOH for each mole of Cr VI which is then recovered principally in the form of CrO_4^{2-}

TBP

Stripping of Cr VI is complete when the solvent comes in contact with sufficient caustic to form sodium chromate (2 NaOH for 1 Cr VI). As with the amines, the aqueous phase after stripping step has a pH of nearly 8.

Meanwhile, the extraction isotherms of Cr VI with TBP seen previously (Fig,3) show that Cr VI is not extracted any further from weakly acidic solutions. This allows a prediction that stripping is possible under these conditions.

Experimentally, chromium is stripped from the organic phase when the aqueous reaches a pH of 4 and the quantity of sodium hydroxide introduced is one half of that which corresponds to the chromate (Table 6). Chromium, then, is stripped in the form of sodium dichromate.



TABLE 6

Stripping by NaOH of Cr VI extracted with TBP. Solvent loaded with 18.8 g Cr VI/1 and 0.82 g SO₄/1

<u>NaOH introduced</u> Cr VI in the solvent)) moles	0.90	1.35	1.80
<u>Cr VI stripped</u> Total Cr VI		0.89	1.0	1.0

This possibility is of interest because sodium dichromate is an industrial product serving as starting material for the manufacture of numerous chromium salts.

In addition, it should be possible then to strip Cr VI by means of a solution of sodium chromate, already in existence in plants producing sodium dichromate.



Experiments have shown that it is possible to strip Cr VI extracted with TBP without expenditure of caustic.

Solubility of solvents in the aqueous phase

This is an important criterion in the choice of a solvent. The economic feasibility of a solvent extraction process depends on the small losses of solvent during the production cycle.

Long chain amines of the LA 2 or TnOA type are claimed to be slightly soluble in water. Measurements carried out on hydrogen sulfate solutions (2 M) in contact with LA 2 show a solubility of 4 mg amine/l. While using amine solvents, it is necessary to take into consideration the solubility of the diluent in the aqueous phase.

TBP is quite soluble in water (390 mg/l), but it is less so in salt containing solutions. The solubility was found to be about 10 mg/l in a solution of sodium hydrogen sulfate (2 M).

INDUSTRIAL CONSIDERATIONS

All the above results, as well as a thorough study in laboratory equipment permitting continuous runs have permitted to develop an original process using TBP as the solvent. We found the following reasons persuasive :

- acceptable stability in the absence of light
- high loading capacity for chromium in highly acid solutions.
- possibility of stripping chromium by means of a solution of sodium chromate.
- relative facility (while taking certain precautions) of coalescence of emulsions

The treatment process for acid chromium effluents using TBP as a solvent does not permit to lower the chromium content of the raffinate nearly to 1 ppm, something that is possible with the amines, but it affords the capability of economic recovery of close to 99.5% of chromium contained in the wastes.

The industrial scale up unit constructed in FRANCE by Produits Chimiques UGINE KUHLMANN⁽⁵⁾ uses TBP and consists of the following stages :

- extraction of Cr VI
- stripping of Cr VI
- solvent regeneration

This process is of an original design and permits the treatment of sulfochromic acid solutions of various origins, either clarified or containin solids in suspension.

The regulation and control systems have been chosen so as to allow a large degree of flexibility and ease of operation.

Acceptable impurities are admissible : Cr III, Fe³⁺, Co²⁺, Ni²⁺. The solutions of Cr VI produced is fed to the sodium dichromate unit. Its concentration of Cr VI may reach 200 g/l. The quantity of Cr III present does not exceed 200 mg/l.

Solvent losses are limited by choice of an appropriate continuous phase at each stage and of suitable equipment for the plant. The raffinate, still quite acid, may be used in various production steps requiring a large supply of sulfuric acid.

REFERENCES

1. W.G. DAVIS et J.E. PRUE, Trans. FARADAY Soc. 51, 1, 45 (1955)
2. J.Y. TONG, E.L. KING, J.Am. Chem. Soc. 51, 1145 (1955)
3. C. DEPTULA, J. Inorg. Nucl. Chem. 30, 1309-16 (1968)
4. D.G. TUCK et R.M. WALTERS, J. of Chem. Soc. p 1111 - 1120 (1963)
5. F.P. 72 13318, April 14th 1972, N. TEXIER, J.P. CUER, M. GABRIEL (Produits Chimiques UGINE KUHLMANN - FRANCE)

Fig. 1 - Cr VI extraction with ThOA (0,099 M in xylene)
from acidic aqueous phase (2,16 N)

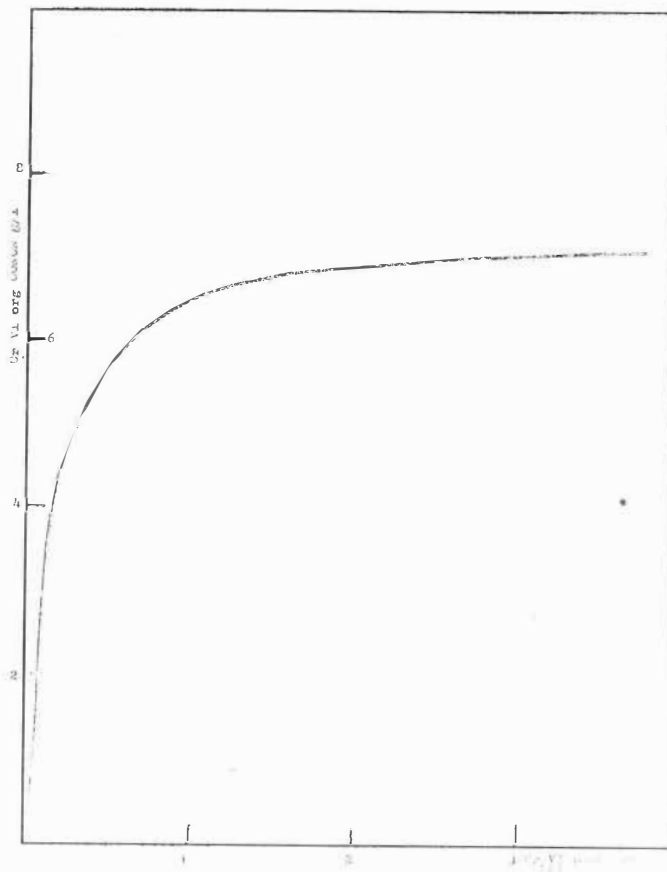
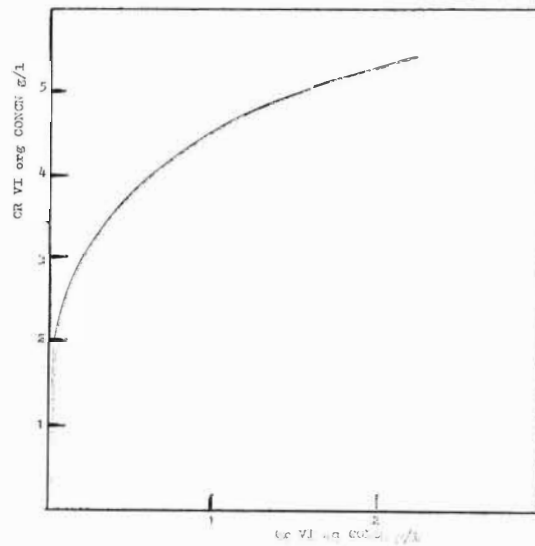


Fig. 2 - Cr VI extraction with LA 2 (0,1 M in xylene) from
acidic aqueous phase (2 N)



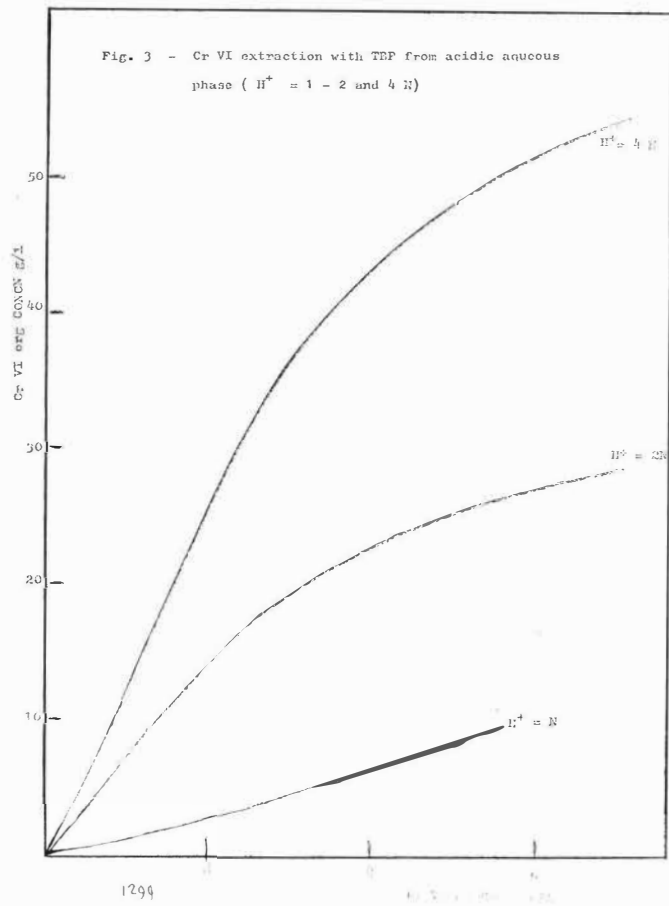


Fig. 4 - Simultaneous extraction of Cr VI and SO_4 with LA 2 ($0.1 M$ in xylene) from acidic aqueous phase ($2 N$)

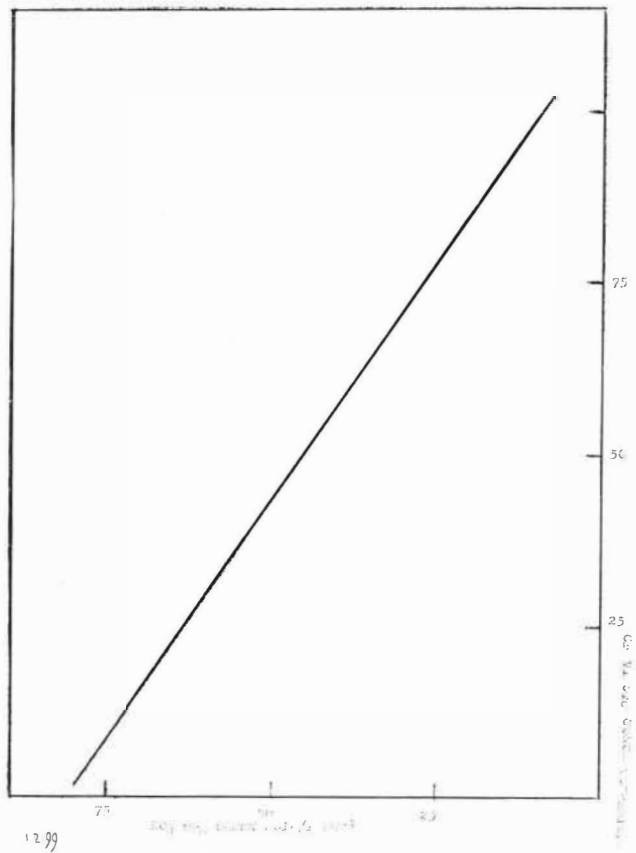
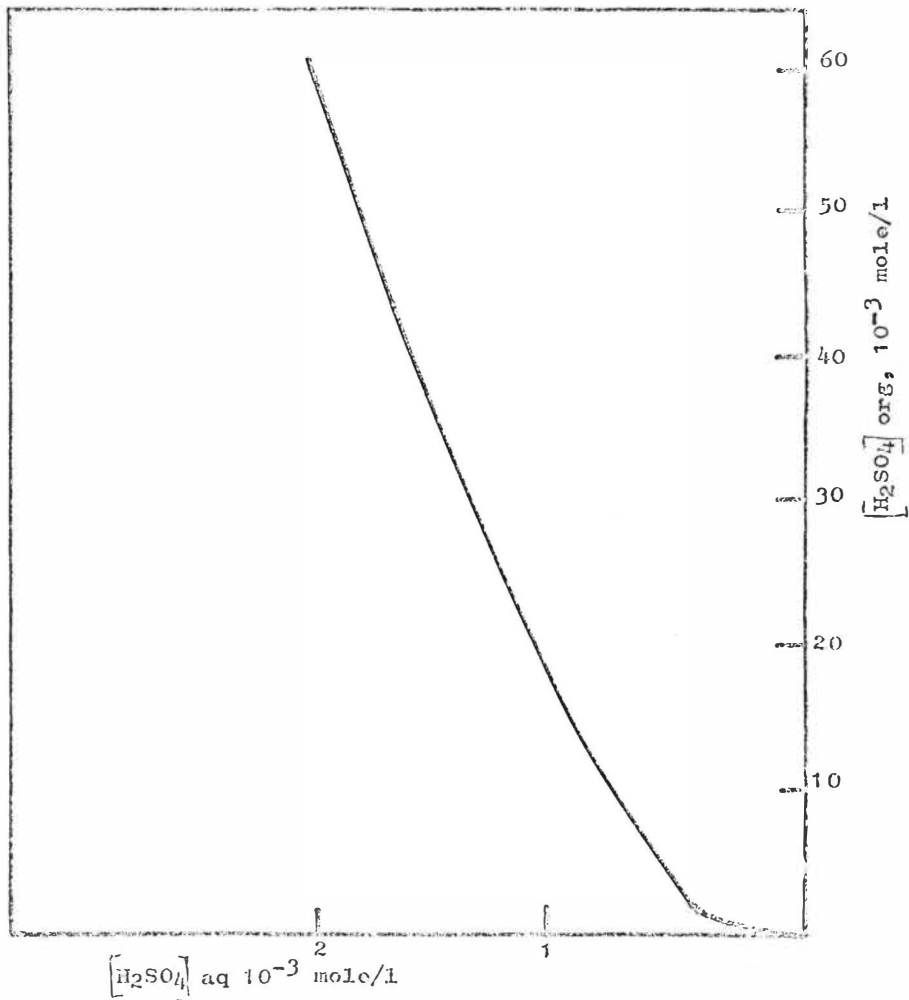


Fig. 5 - H_2SO_4 extraction with TBP from acidic aqueous phase
charged with 5 g Cr VI/l



RECOVERY OF NICKEL AND COBALT
FROM METALLURGICAL WASTES
BY SOLVENT EXTRACTION

by - C. Bozec, J.M. Demarthe and L. Gandon

SYNOPSIS

A metallurgical waste consisting of metallic chlorides chlorides is dissolved in water and treated by liquid-liquid extraction with amines in order to separate nickel, cobalt and iron.

Laboratory and small scale pilot plant experiments are described. The flexibility of this process, as a function of metal contents in the waste, is studied by a graphical method.

INTRODUCTION

The use of liquid-liquid extraction in the treatment of metal salt solutions has increased over the past ten years and we have applied this technique to some of our metallurgical processes.

The present paper describes the recovery of nickel and cobalt from the slag obtained after cobalt removal from a crude nickel matte by chlorination.

Origin of the crude material, source of nickel and cobalt

Until 1968 Souete Le Nickel at Le Havre produced only one grade of pure nickel, the slag from the separation contained about 0.5% Co and 0.12% Ni. The nickel metal is obtained from a matte containing about 78% Ni, 0.40% Co, 0.10% Fe and results from a heavy smelting operation in the Doniambo smelter (New Caledonia). The removal of iron and cobalt by this technique is limited by the loss of nickel to the slag, these slags cannot be further treated to recover the nickel and cobalt.

In 1970 after laboratory and small scale pilot plant studies SLN built a semi-industrial plant in which a partially refined matte was purified in a molten state by chlorine injection (1).

Three main objectives of this operation were:

- producing purer nickel : Co 0.30% - Fe < 0.10%,
- improving the total nickel recovery,
- for the first time in SLN operations the recovery and valorisation of cobalt was considered.

The chlorine treatment consists of an injection of gaseous chlorine into the molten matte under a layer of molten sodium chloride. This latter acts as a solvent for the iron, cobalt and nickel chlorides formed during this operation. At the end of the chlorine injection period, the sodium chloride slag contains in the one homogeneous phase these three metallic chlorides. It can be readily dissolved in water either by direct pouring into water, or by leaching of cold ingots.

Table 1 gives analysis of a solution obtained from this slag:

Table 1 - Analysis of the crude solution

	Ni	Co	Fe	Cu	Na
E/1	56	21.6	36.4	0.15	55

EXPERIMENTAL

Requirements of the liquid-liquid extraction operation

They are:

- separating the metals Ni/Co/Fe
- recovering a solution of $\text{NiCl}_2 + \text{NaCl}$
- recovering a solution of CoCl_2

These last two solutions can be afterwards treated to valorise nickel and cobalt in different forms: carbonate, oxide, salts or metal.

The present paper considers the theoretical aspects of the process together with laboratory and small scale pilot plant work on liquid-liquid extraction. The flexibility of the process as a function of variations in the crude feed composition is also considered.

Selection of the extractants

The Ni/Co/Fe separation is achieved by amine extractants acting in liquid phase as ion exchangers. The considered anions are the "chloro-complexes" formed by transition metals as eg.

Zn, Fe(III), Cu(II), Co, Mn, Fe(II), Ni
with chloride ions provided that the chloride ion concentration is sufficiently high (2) (3).

Many alkylamines are now available in industrial quantities. We have examined some of them by determining the distribution isotherm of the metallic impurities between the aqueous phase containing nickel chloride and the organic phase consisting of the extractant diluted in an organic solvent with a high aromatic content.

The metallic impurities considered were:

Zn, Cu, Fe(III), Co

Criteria used for selection of the solvent were -

- 1) the loading capacity of the solvent, expressed in grammes, of metallic ion extracted by one liter of solvent containing 0.30 moles of amine.
- 2) the selectivities of the solvent which can be expressed by the ratio of the concentration of the impurity to the concentration of the metal in the loaded solvent - a poor selectivity gives a significant loss of nickel.

- 3) the case of stripping the metallic ion from the solvent phase.
- 4) the rate of phase disengagement during the settling periods; it affects the mechanical entrainment of one phase into the other and the dimensioning of the equipment.

From these considerations, we have chosen two extractants, the first for Ni, Co/Fe separation and the second for Ni/Co separation. These extractants are:

AMBERLITE LA2 for iron removal

ADGEN 381 for cobalt removal

LA2 is a secondary amine (lauryl) made by ROHM and HAAS

AD.381 is a tertiary amine (triisooctyl) made by ASHLAND CHEMICALS

The observations we have made on these two extractants are collected in table 2.

Table 2 - Observations of LA.2 and Ad.381 (behaviour)

	Amberlite LA.2 0.30M in naphtha	Adogen 381 0.30M in naphtha + octylol (3%)
Zn	loading capacity 7 g/1 complete extraction possible very high selectivity complete stripping possible very good phase disengagement	loading capacity 9 g/1 complete extraction possible poor selectivity <u>complete stripping very</u> difficult slow phase disengagement
Fe(III)	loading capacity 10 g/1 complete extraction possible high selectivity complete stripping possible very good phase disengagement	loading capacity 10 g/1 complete extraction possible very high selectivity <u>complete stripping</u> <u>difficult</u> good phase disengagement
Cu	loading capacity 6 g/1 complete extraction difficult very high selectivity complete stripping possible very good phase disengagement	loading capacity 8 g/1 complete extraction possible very high selectivity complete stripping possible very good phase disengagement.
Co	loading capacity 3 g/1 <u>complete extraction very</u> <u>difficult</u> very high selectivity complete stripping possible very good phase disengagement	loading capacity 8 g/1 complete extraction possible very high selectivity complete stripping possible very good phase disengagement

Selection of diluent:

Naphtha 90/160 has been selected as diluent, this has the following physical properties :

- specific gravity (20°C) = 0.872 - 0.876
- aromatic content : \approx 99%
- melting point : 36 - 40°C

For dilution of Adogen 381 we have used an octylol made by SHELL as a third phase inhibitor. This octylol was used at 3% (by volume) of the total organic phase.

Description of the bench scale tests

Two continuous tests have been carried out on the same crude nickel solution using different concentrations of extractant in the solvent phase.

- Products :

- aqueous feed : see analysis in table 4
- solvents : table 3 (see below)

test reference	I	II
Iron removal by Amberlite LA.2	0.30M in naphtha	0.60M in naphtha

- Equipment :

A set of mixer-settlers made by Etablissements PALY (France). Each mixer compartment was equipped with a mechanical agitator driven by an electric motor, the speed of which can be modified by a thristor system. In the settling compartments it was possible to adjust precisely the interface level by a weir. The circulation of liquids was achieved by the pumping action of the agitators.

- Operating procedure :

The mixer-settlers were arranged as shown in figures 1 (test 1) and 2 (test II).

- Analytical results:

Table 4 shows the chemical analysis of samples taken just before the end of the tests.

Table 4 - Bench scale tests chemical analysis

	Ni	Co	Fe	Cu	Na	H ⁺	Cl ⁻
	g/l	g/l	g/l	g/l	g/l	N	N
aqueous feed	56	21.6	36.4	0.15	55	0.2	7.3
purified solution	1) 55	0.09	0.004	0.001	55	0.2	4.6
	II) 55	0.15	0.004	n d	55	0.2	4.6
Fe strip liquor	1) 0.20	0.07	32	0.12	0.20	n d	1.8
	II) 0.14	0.28	30	n d	n d	n d	1.7
Co strip liquor	1) 1.25	47.0	0.002	0.050	1.10	n d	1.6
	II) 1.10	54.8	0.002	n d	n d	n d	1.9

nd = no determined

DISCUSSION

During the tests we have noticed imperfections such as poor phase separation, this caused aqueous phase entrainment in the organic phase which was then carried forward to the stripping stages. The scrubbing stage did not give complete iron removal.

In the cobalt removal section the effect was more accentuated, this is shown by the Ni and Na contents in the Co strip liquors.

The phenomena are explained as follows:

- TEST 1 - the ratio O/A was too high, this promoted the entrainment of aqueous in the organic phase,
TEST 2 - the viscosities of organic phases were higher because of the higher extractant concentrations.

Cobalt removal is not complete, there being about 0.1 g/l left in the "purified" solution.

Description of the pilot plant test

(This test was run continuously for 14 days)

Products

- aqueous feed: see analysis in table 5.

The solution after Fe removal is concentrated by evaporation in order to increase the chloride content, hence the medium is more complexing than that used in the laboratory tests, and one may expect an improved extraction of cobalt.

- solvents : for iron removal : Amberlite LA.2 diluted in naphtha, 0.49M initially - 0.54M finally.

for cobalt removal : Adogen 381 diluted in naphtha and octylol (3% with respect to the total volume), 0.51M initially, 0.58M finally.

Table 5 - Analysis on the pilot test

	Ni	Co	Fe	Cu	Na	H ⁺	Cl ⁻
	g/l	g/l	g/l	g/l	g/l	N	N
aqueous feed to Fe removal	46	21.0	32.0	0.23	47	0.20	6.2
aqueous feed to Co removal	65	29.7	0.001	n d	66	0.28	6.4
purified solution	60	0.002	0.001	0.001	61	0.24	4.9
Fe strip liquor	0.020	0.020	23.0	0.08	0.05	n d	1.3
Co strip liquor	0.040	75	0.001	0.17	0.05	0.13	2.7

- Equipment :

A set of 24 mixer-settlers made by Denver Equipment.

- Operating procedure:

The mixer-settlers were arranged as shown in figure 3.

Some modifications have been made to the scheme used on bench scale, in order to decrease the entrainment of Ni and Na in the stripping steps.

Internal recycling of aqueous phases was used at the scrubbing stages in order to induce to the ratio O/A at about 3 in the mixers.

Each impeller in mixing compartment could be rotated at a selected speed.

Temperature was maintained at about 25°C for the two phases.

- Analytical results:

Analysis in table 5 are for samples taken during the last days of the test.

DISCUSSION

Poor settling was obtained, this led to significant entrainment of solvent in the aqueous phase. The relatively high concentration of the extractant and the consequent high viscosity essentially accounted for this situation.

The phase volume ratio O/A in the Co strip section (9.7) was too high for satisfactory mechanical operation of the equipment, internal recycling of the aqueous phase will be necessary to adjust O/A nearer to unity in the mixing compartments in order to increase the Co content in the Co strip liquor.

The levels of minor elements in the product was determined at the end of the test run (table 6).

Table 6 - Analysis including minor elements (results in g/l)

	Ni	Co	Fe	Cu	Na	Mn	Zn
crude solution	46	21.0	32.0	0.23	47	0.0054	0.0037
purified solution	60	0.0020	0.0010	0.0010	61	0.0020	0.0001

	Pb	Sb	As	Mg	Ca	Al	SO ₄
crude solution	0.0025	0.0042	0.0020	0.026	0.29	0.021	0.050
purified solution	0.0006	0.0042	0.0022	0.035	0.40	0.029	0.065

- Consumption of organics

The amines entrained by solubilisation in aqueous solution have been determined in the following liquors:

- Fe stripping liquor = $3 \text{ mg} \cdot 1^{-1}$ (C1⁻H1.3N)
- Co stripping liquor = $3.5 \text{ mg} \cdot 1^{-1}$ (C1⁻H2.7N)
- purified solution = $3.0 \text{ mg} \cdot 1^{-1}$ (C1⁻H4.9N)

This minimum consumption related to 1 kg purified nickel gives:

330 mg amines/kg Ni

The true organic material balance on the complete test, taking into account the mechanical entrainments and some accidental leaks, leads to:

38 g amines/kg Ni

We consider that in industrial operation, we shall not consume more than:

1 g amine/kg Ni

The loss of diluent by evaporation, seen in the enhancement of the extractant content in the solvents between the beginning and the end of the test, is not negligible viz:

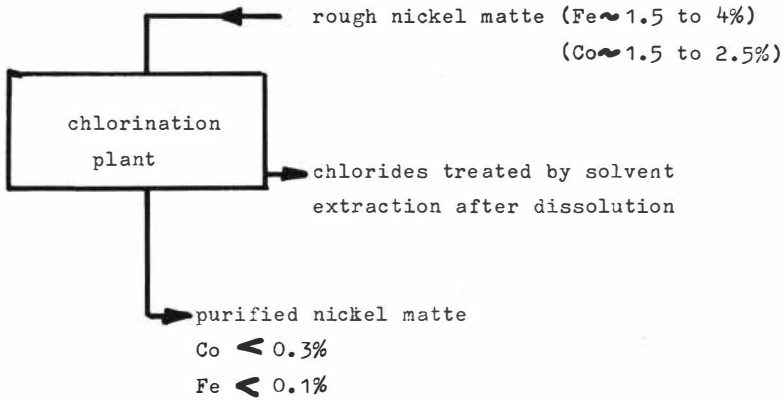
- about 80 litres or about 0.2 liters/kg purified nickel

This high value is due to operation at relatively high temperature (25°C) and to the existence of ventilation and slight suction above the settlers during the test. On an industrial scale this loss could be considerably decreased by a condenser placed in the vessel ventilation circuit.

For further work on industrial scale, we intend to use the scheme of the figure 4 in which the extractants are used 0.30M in SOLVESSO 150 this diluent having given good phase disengagement results in recent laboratory tests.

FLEXIBILITY STUDY

The solvent extraction process must have a sufficient flexibility to cope with variation in the chlorination residues



It can be seen from the above diagram that the fluctuations, which are due to the raw material or to the perturbations of the chlorination plant, have repercussions on the content of the chlorides' slag; their interaction on the cobalt and iron extractions is difficult to estimate. Under these conditions, we will first define the limit of interest in the solvent purification, then determine the maximum variations that can be absorbed by the hydrometallurgical plant.

Notations:

- [Ni] : nickel concentration moles l^{-1} after leaching of the slag
- [Co] : cobalt -do- -do-
- [Fe] : iron -do- -do-
- [Na] : sodium -do- -do-

Limitations:

1) Iron extraction

a) Minimum chloride level

The distribution coefficient of ferric chloride between water and LA₂ is dependent upon the chloride concentration of the aqueous phase.

The chloride level of the aqueous phase corresponding to nickel, cobalt and sodium, which is expressed by:

$$2([\text{Ni}] + [\text{Co}]) + [\text{Na}] \text{ must be greater than a minimum value } L_1 \quad (1)$$

b) Loading capacity of solvent : LA₂ = 0.3M

LA₂ (0.3M has a limited ultimate capacity (10 g/1 of solvent) for iron, which is not dependent on the chloride level. The iron concentration in the solvent has been limited to 8 g/1 for the commercial plant. So in considering the phase ratio for iron extraction, the iron concentration must be under 0.57.

$$[\text{Fe}] < 0.57 \quad (2)$$

c) Solubility limit of the aqueous phase

Sodium chloride at high concentration has a depressive effect on the solubility of the nickel, cobalt and iron chlorides. Under these conditions, the concentration of iron, cobalt and nickel is dependent on the sodium concentration

$$[\text{Ni}] + [\text{Co}] + [\text{Fe}] \leq f([\text{Na}]) \quad (3) \text{ (fig.6)}$$

* The inequality $[\text{Ni}] + [\text{Co}] + [\text{Fe}] \leq f([\text{Na}])$ is determined by the solubility curve at 60°C.

The inequalities (1), (2) and (3) represent all the limitations that must be observed to assure good conditions for iron extraction.³³³

2) Cobalt extraction

The raffinate coming from the iron extraction is concentrated to increase the chloride level (k is the concentration factor). Under these conditions, the feed for cobalt extraction has the following composition:
 $k(\text{Ni})$: nickel moles l^{-1} ; $k(\text{Co})$: cobalt moles l^{-1} ; $k(\text{Na})$: sodium moles l^{-1}

a) Minimum chloride level

We consider two hypotheses corresponding to two different commercial products :

Hypothesis 1: production of very pure nickel

$$H(1) \quad (\text{Co/Ni} < 20 \text{ ppm})$$

The chloride concentration corresponding to nickel and sodium (non extractable species) must be over 5M.

Hypothesis 2: production of pure nickel

$$H(2) \quad (\text{Co/Ni} < 500 \text{ ppm})$$

The chloride concentration must be over 4.5M.

This limitation is expressed by the following inequality

$$k(2) ([\text{Ni}] + [\text{Na}]) < L_2 \quad \begin{array}{l} L_2 = 5M \quad H(1) \\ L_2 = 4.5M \quad H(2) \end{array} \quad (4)$$

b) Loaded capacity in cobalt of TIOA 0.3M

The loaded capacity is limited to $6 \text{ g } l^{-1}$, which represents 70% of the ultimate theoretical capacity. In regard of the phase ratio, the inequality (5) has to be satisfied.

$$k(\text{Co}) < 0.52 \quad (5)$$

³³³ good conditions of extraction imply that :- phase ratio has a constant value,
 - iron removal is sufficient.

c) Solubility Limitation

$$k ([Ni] + [Co]) < \phi (k [Na]) \quad (6)$$

Adaption of the solvent extraction process

- 1) Flexibility of iron extraction (principle limitation: loaded capacity). The inequalities (1) to (3) define the limits of $[Fe]$ and $([Ni] + [Co])$ as a function of Na . (fig.5 and 6)

It is important to note that the loading capacity of the solvent is the principle limitation

- 2) Flexibility of cobalt extraction

Hypothesis 1 : very pure nickel (principle limitation : chloride level).

To produce very pure nickel by this process, the sodium concentration $[Na]$ must be under 3M. (fig.7)

Hypothesis 2 : pure nickel principle limitation: loaded capacity). (fig.7 and 8)

In that case, there is no limitation on the sodium concentration.

- 3) Consequences of the maximum variations of the slag's

composition. The inequalities (1) to (3) are used to determine a relation between $([Ni] + [Co]) / [Na]$ and $([Fe] / [Na])$ (7) (Fig.9).

The inequalities (4) to (6) define two relations between $[Ni] / [Na]$ and $[Co] / [Na]$ corresponding to the hypothesis (1) or (2).

$$[Ni] / [Na] > g_i \quad ([Co] / [Na]) \quad \begin{matrix} H(1) \quad i = 1 \\ H(2) \quad i = 2 \end{matrix} \quad (8)$$

All the inequalities (1) to (6) are verified when the relations (7) and (8) are satisfied. (fig.10).

By using this diagram, it is possible to determine if a given slag can be treated in a commercial plant using this process; in fact, it is sufficient to know $[Fe] / [Na], [Co] / [Na], [Ni] / [Na]$ to define the representative point of the solution to purify (noted M on the diagram). (fig.10)

M over the straight line of equation: $\frac{(Fe)}{[Na]} - \frac{(Co)}{[Na]}$	M under the straight line equation: $\frac{(Fe)}{[Na]} - \frac{(Co)}{[Na]}$	
Complete iron extraction	Complete iron extraction: impossible	
M over $g^1 \frac{(Co)}{[Na]}$	M between $g^1 \frac{(Co)}{[Na]}$	M under $g^2 \frac{(Co)}{[Na]}$
	and $g^2 \frac{(Co)}{[Na]}$	
Very pure nickel production (M ₁)	Pure nickel production (M ₂)	Bad cobalt extraction (M ₃)

Examples (slag's contents in %)

	Ni	Co	Fe	Na
Very pure nickel production	15.9	0.8	9.5	15.6
and cobalt exempts from iron	21.2	2.9	8.9	10.3
M ₁	24.2	4.4	8.4	5.8
Pure nickel	13.5	3.07	8.9	15.4
M ₂	18.8	4.06	8.9	10.7
	23	5.8	8.4	6.9
Bad cobalt extraction	11.8	5.8	8.9	15.2
M ₃	14.7	6.9	9.8	11.5
	21.2	6.9	8.4	6.9

CONCLUSION

This process has proved to be very flexible; this is a very important point with respect to the possible variations in the composition of the slag. The choice of operating conditions is such as to permit the process to cope with these variations and to give high purity cobalt and nickel as separate products. Nickel contained in the raffinate can be separated easily from sodium for instance by precipitation of the carbonate. Cobalt can be also obtained in a pure form, (except for copper), but this latter impurity can be removed easily, if required, by cementation on cobalt powder or by sulfide precipitation. Nickel and cobalt recoveries are very high and make this process very attractive in comparison with the pyrometallurgical process described in the introduction of the present paper.

Extension of this process on industrial scale is foreseen for the near future. Recently we have run some successful pilot tests in pulsed columns but, at the moment, the choice of the technology is not defined.

BIBLIOGRAPHY

- (1) French patent 2 067 106
- (2) Brooks P.T., Rosenbaum J.B.,
R.I.6159 - U.S. Bur. of Mines 1963.
- (3) Tougarinoff B., Willekens M., Van Peteghem A.
36e Congres International de Chimie industrielle - 1967

LIST OF FIGURES

- Fig.1 and 2 Circuits for bench scale tests
- Fig.3 Circuit for the pilot tests
- Fig.4 Circuit retained for further developments
Ni/Co/Fe separation
- Fig.5 Limitations related to the iron extraction.
(limitation related to the chlorides solubility
- nickel, cobalt, iron, sodium and to the necessity to maintain a sufficient chloride level for the iron extraction.)
- Fig.6 Limitation related to the chloride level required for the iron extraction
- Fig.7 Limitation related to the chloride solubility and level.
Hypothesis 1 (nickel of very high purity :
Co in Ni 20 ppm).
- Limitation related to the cobalt solvent capacity
- Limitation related to the solubility and chloride level (5M) of the solution before cobalt extraction (nickel of high purity - Co 500 ppm).
- Fig.8. Limitation related to the minimum level chloride (5M) for cobalt extraction (obtainment of very pure nickel).
- Fig.9 and 10 Molar ratio.

FIG. 1
Test I

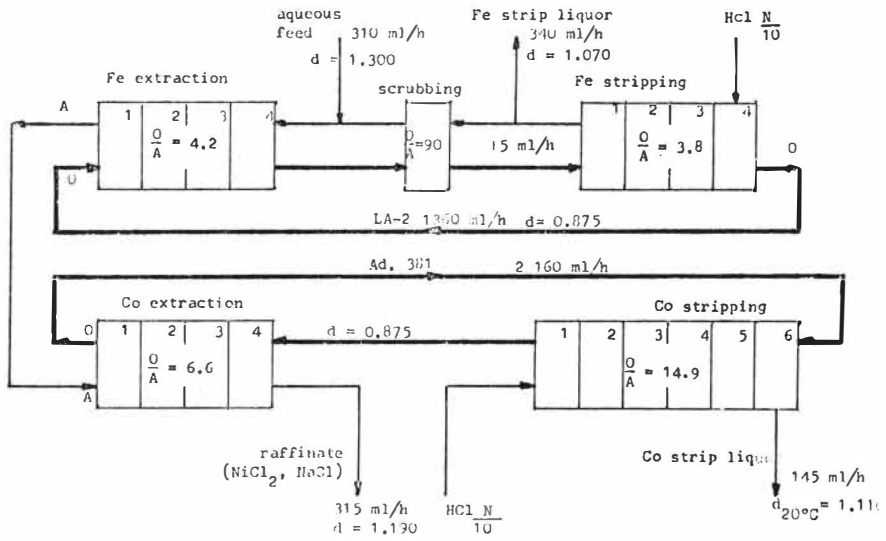


FIG. 2
Test II

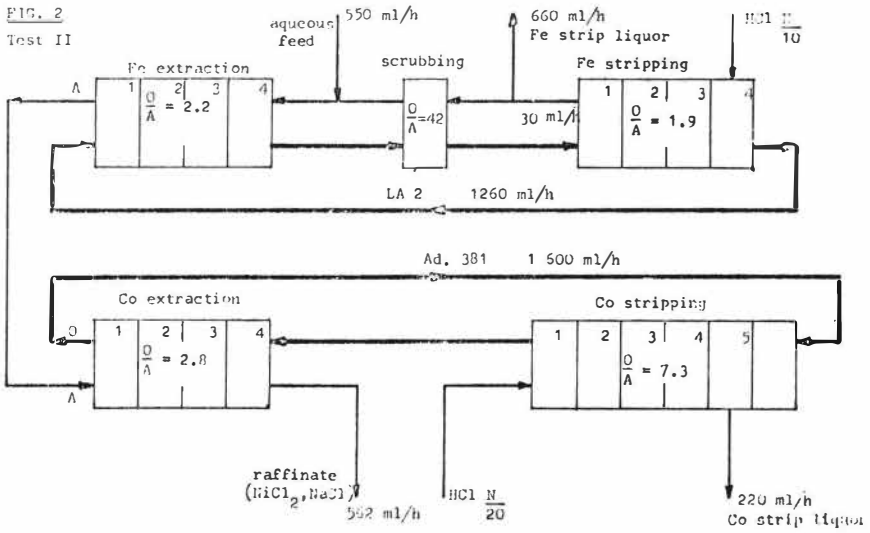


FIG 3 - CIRCUIT FOR THE PILOT TEST.

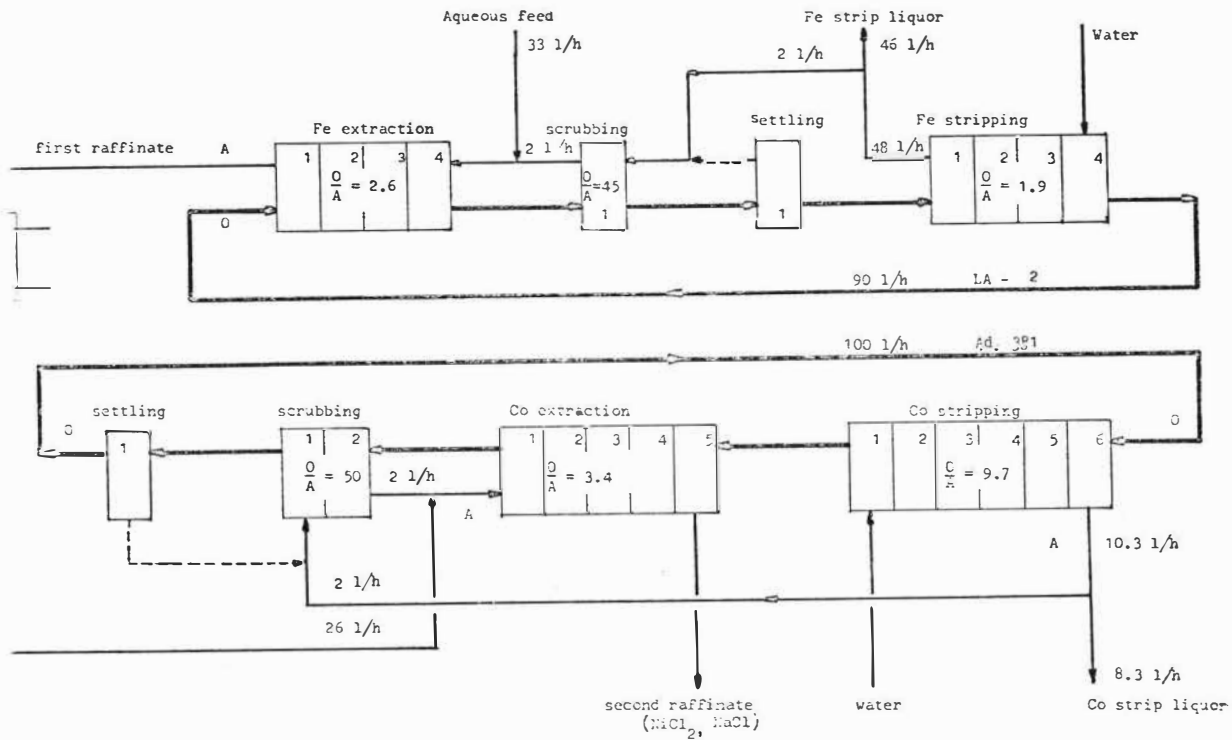
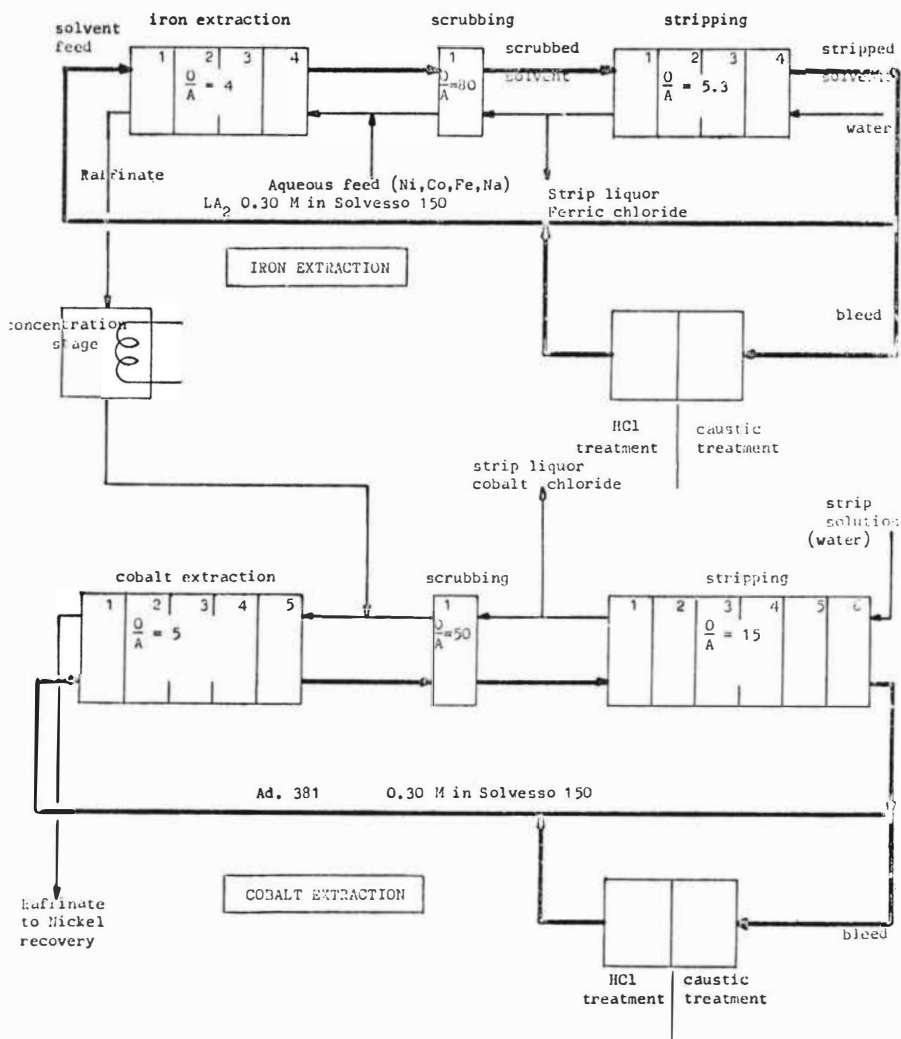
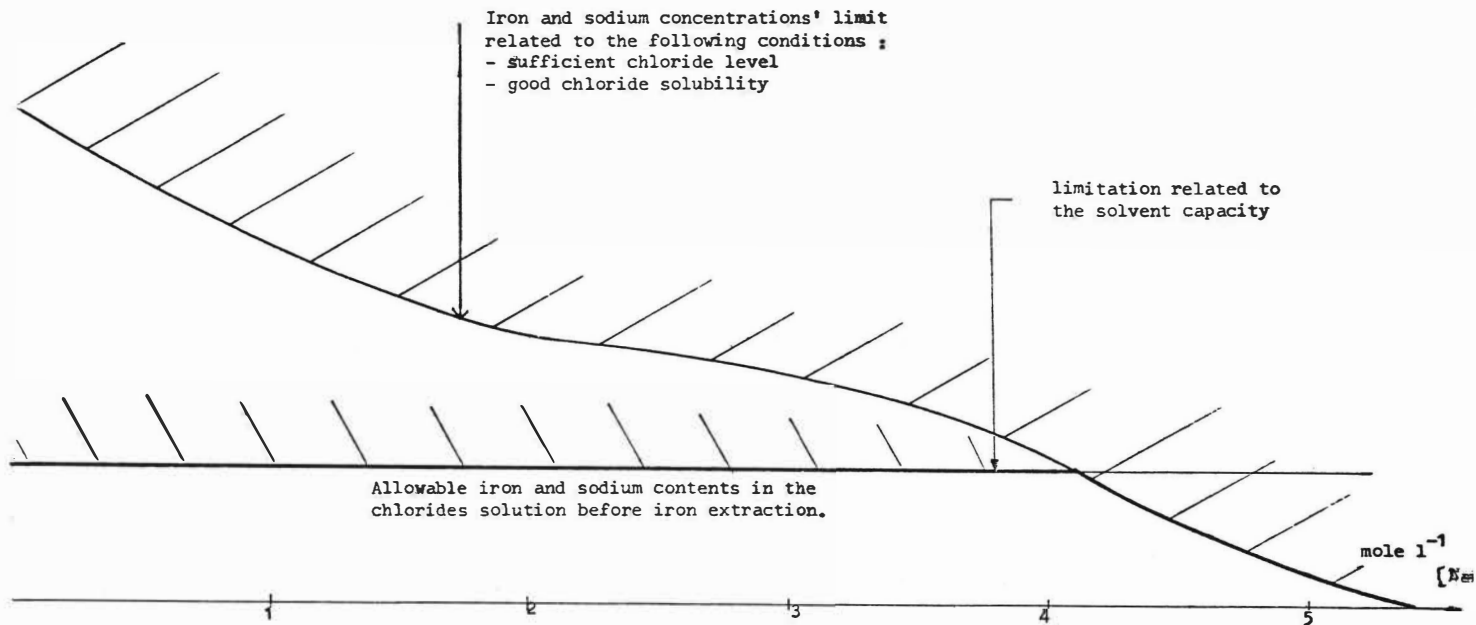
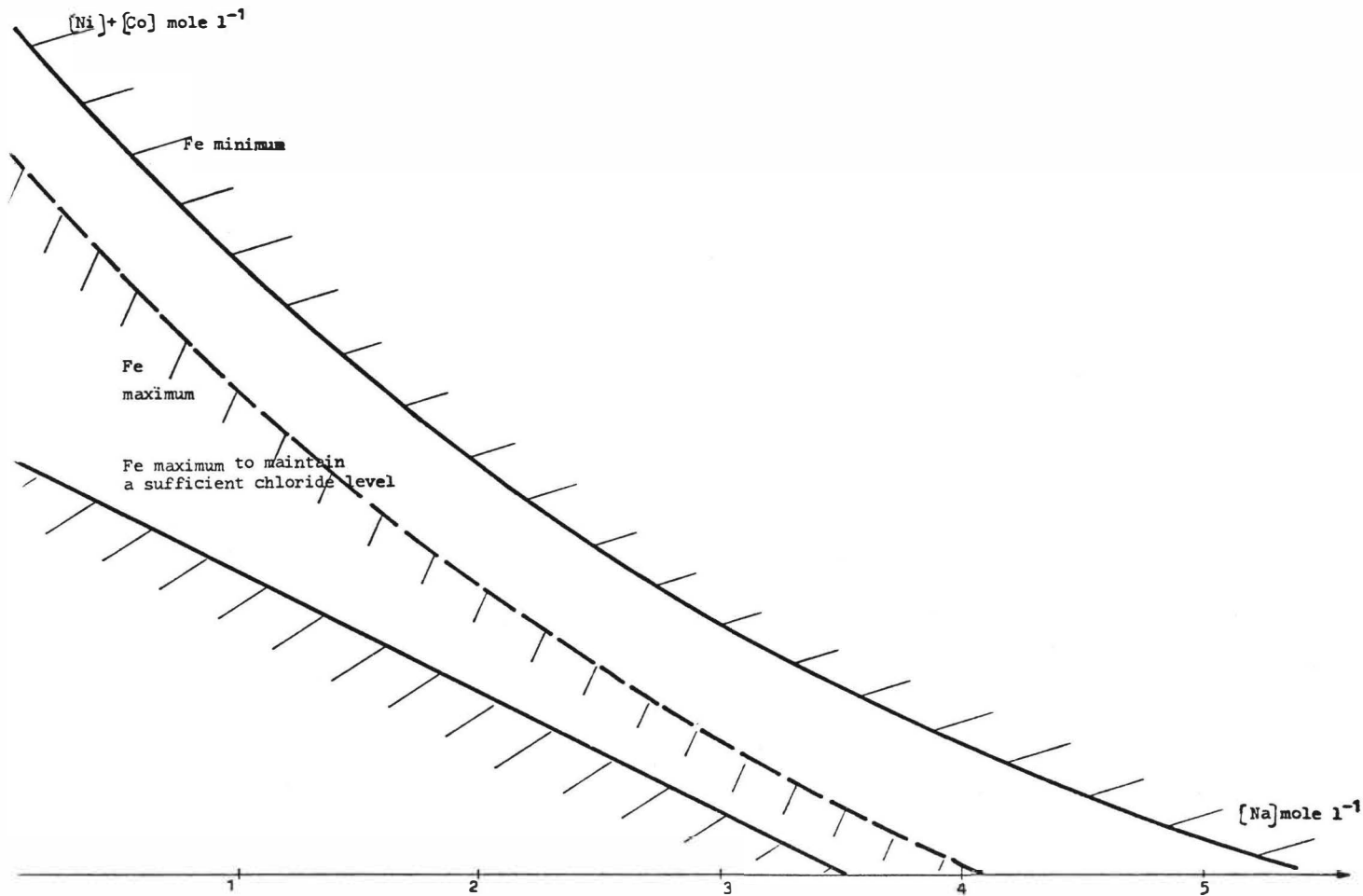


FIG. 4 - CIRCUIT RETAINED FOR FURTHER DEVELOPMENTS
Ni/Co/Fe separation.



[Fe] mole l⁻¹





$x [\text{Co}] \text{ mole l}^{-1}$

Cobalt concentration before
extraction of it by TIOA

Limitation related to the chloride solubility and level
Hypothesis (1) (Nickel of very high purity : Co in Ni < 20 ppm)

Limitation related to the cobalt solvent capacity

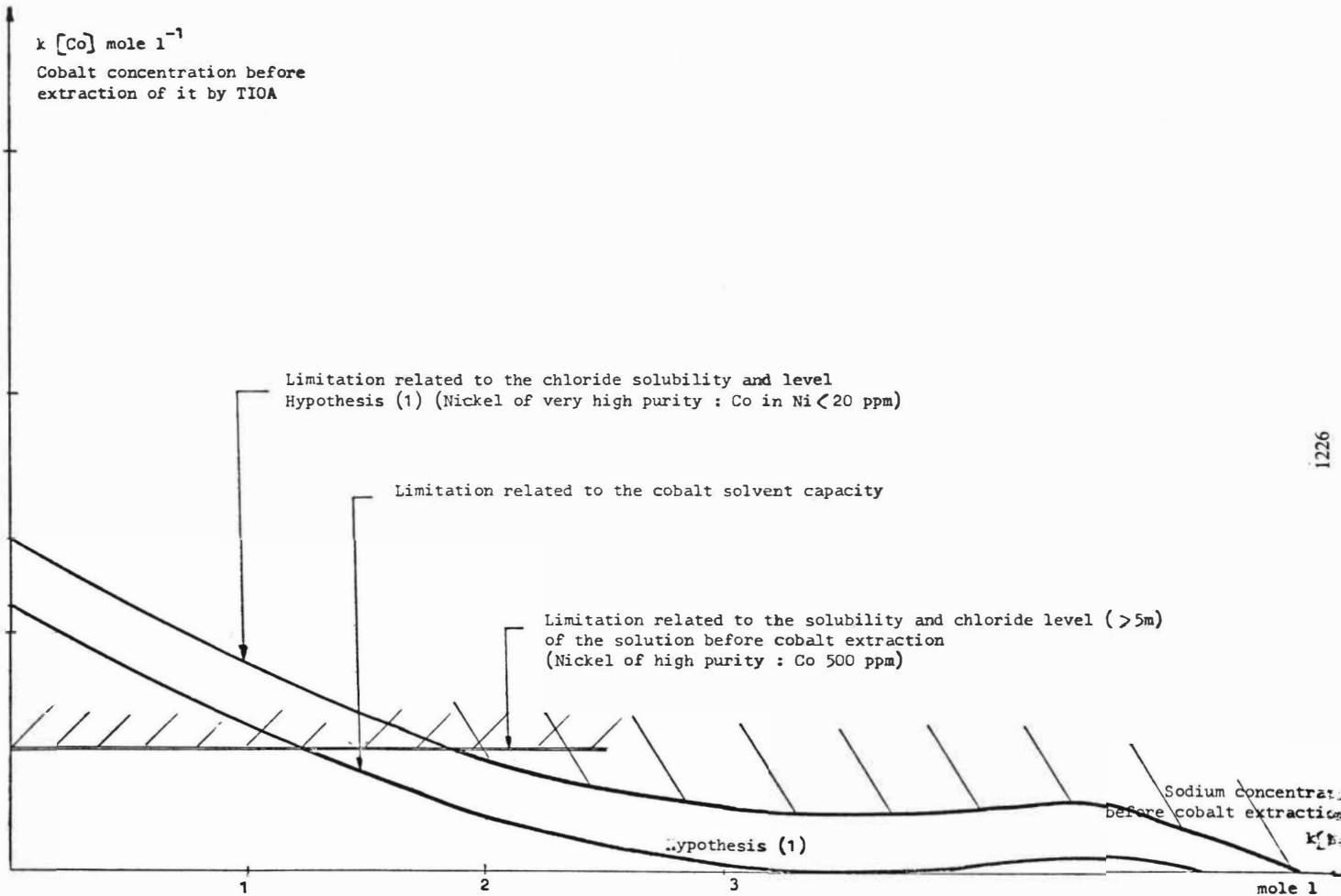
Limitation related to the solubility and chloride level (>5m)
of the solution before cobalt extraction
(Nickel of high purity : Co 500 ppm)

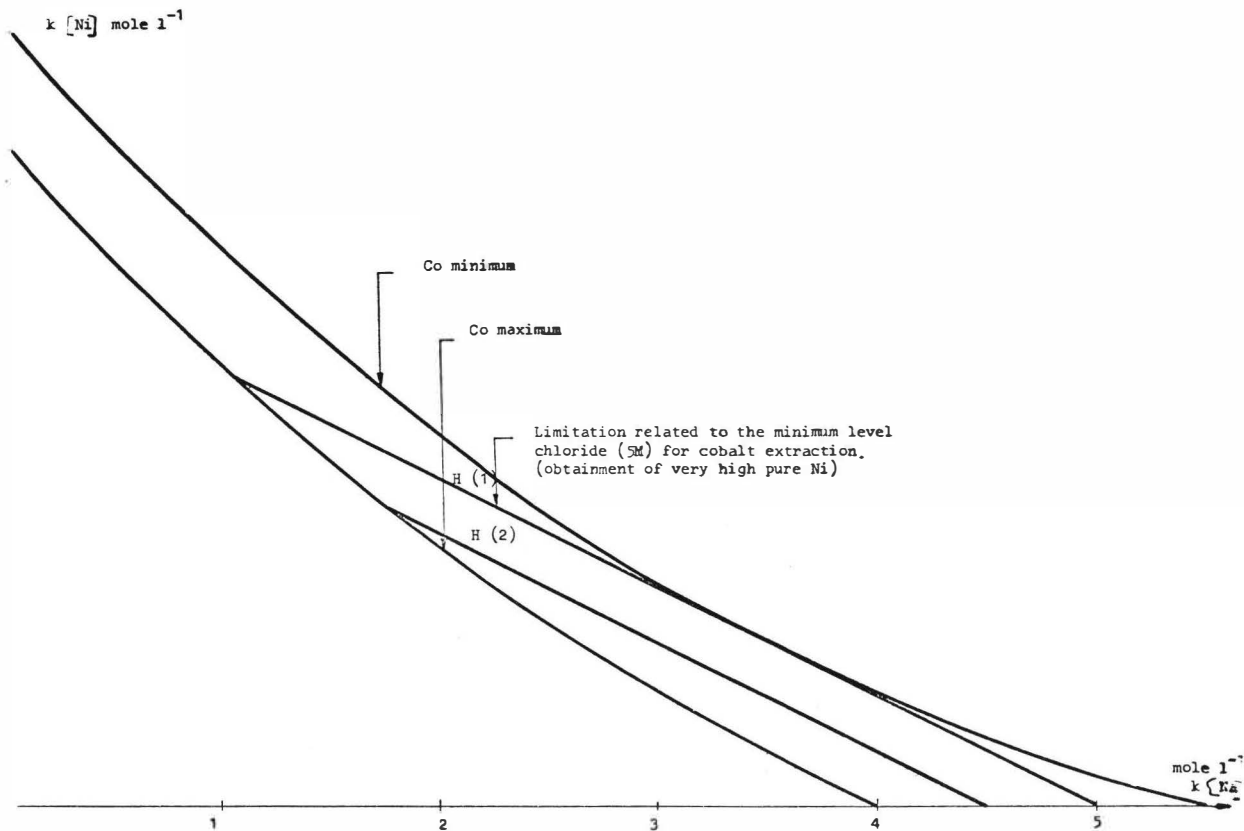
Sodium concentrat.
before cobalt extraction

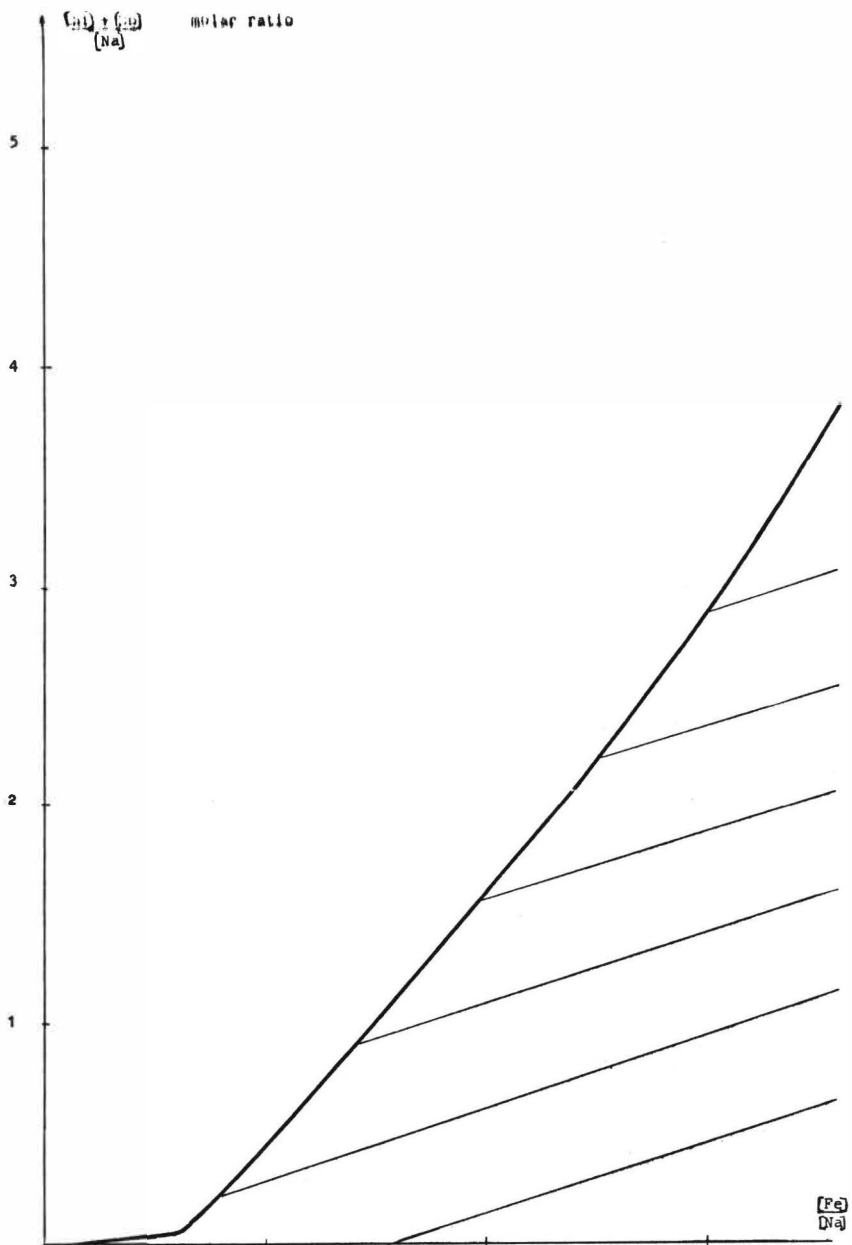
Hypothesis (1)

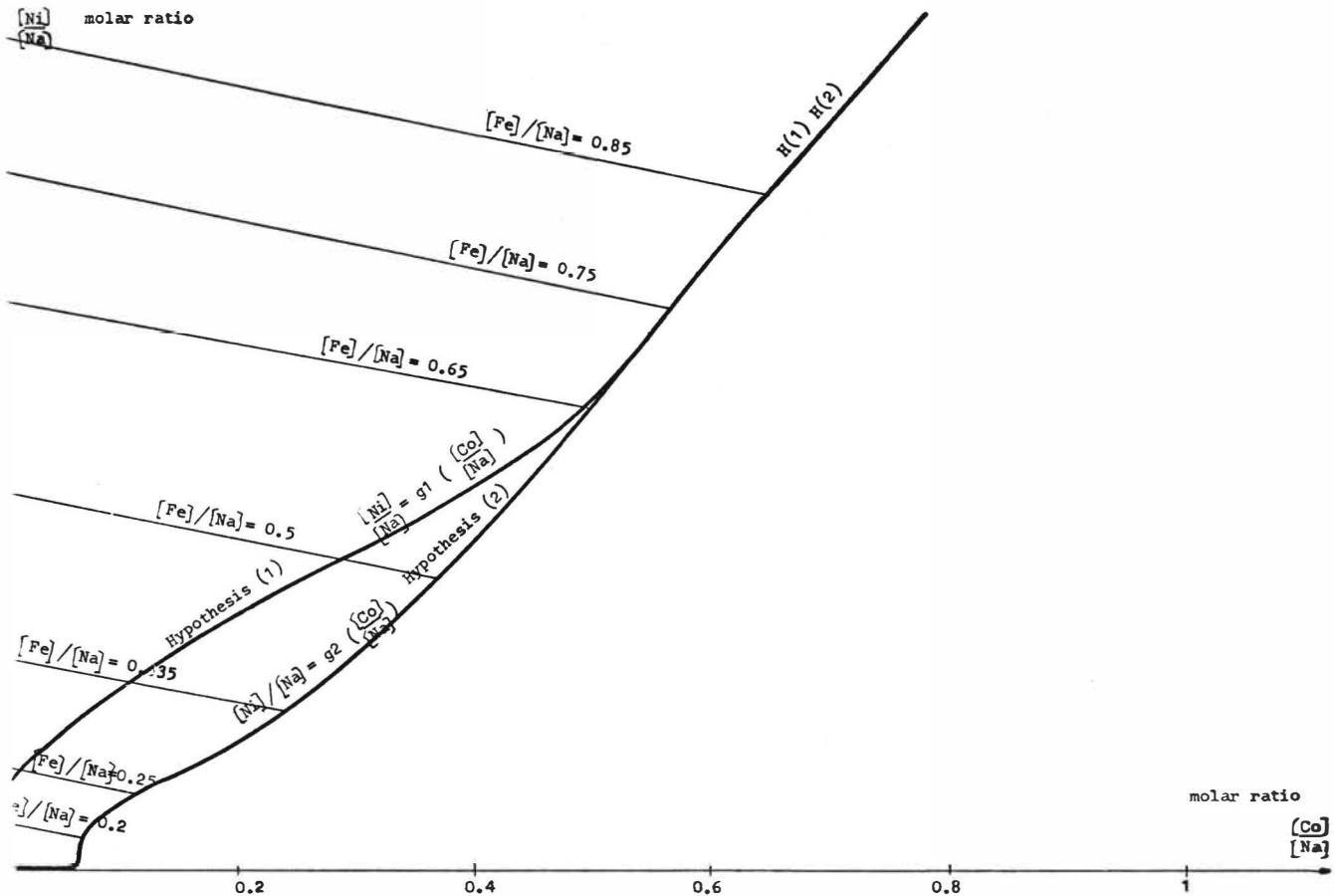
k_f

mole l









The Separation and Recovery of Nickel and Copper from a Laterite-Ammonia Leach Solution by Liquid Ion Exchange

by - R.C. Merigold and W.H. Jensen

General Mills Chemicals, Inc., Minerals Industries, 1712 West Grant Road, Tucson, Arizona 85705, U.S.A.

Increased interest on an international scale is directed toward developing new lateritic ore bodies by a number of mining companies. Looking toward future environmental and economic considerations, new methods are required for lower cost, non-polluting techniques to more efficiently separate and recover the metals of interest. Solvent extraction techniques meet these requirements with the added advantage of producing salable electrowon cathodes at the mine site.

INTRODUCTION

In 1973 General Mills Chemicals, Inc., presented a paper describing the separation of copper and nickel from a synthetic ammoniacal leach liquor.¹ The purpose of this investigation was to prove the feasibility of the solvent extraction recovery process while varying the nickel and copper concentrations and ratios and to illustrate the economics of the system. At that time no specific leach liquor was under consideration.

The success of this study attracted a number of mining companies, and subsequently we were asked by one company to evaluate a synthetic leach liquor according to their specifications in view of a New Caledonian laterite ore body which would produce approximately 12,500 tons of nickel and 62 tons of copper per year. This paper includes the results of that study, including capital investment and operating cost estimates.

Test Objectives

The leach solution for testing was prescribed as follows:

<u>Metal</u>	<u>Concentration - g/l</u>
Ni	25.5
Cu	0.10
Co	0.021
Mn	< 0.004
Zn	0.0022
Pb	0.05 to 1.00
Cr	Trace
Sn	< 0.002
Sb	< 0.002
As	Trace
Al ₂ O ₃	54
Ca ₂	51
pH	~ 9.25

The objective of the test program was to produce a nickel electrolyte suitable for electrowinning processing. Solution requirements for the nickel pregnant electrolyte from solvent extraction to electrowinning were prescribed as follows:

<u>Metal</u>	<u>Concentration - g/l</u>
Ni	100
Cu	< 0.002
Zn	< 0.010
Pb	< 0.005
Sn	< 0.005
Sb	< 0.005
Mn	< 0.020
Others	as low as obtainable
H ₂ SO ₄	pH 3.0 to 3.5

The spent electrolyte from nickel electrowinning to solvent extraction was prescribed at 75 g/l Ni and approximately 40 g/l H₂SO₄.

Both the leach liquor and spent electrolyte were prepared synthetically using reagent grade chemicals. The raffinate from solvent extraction was discarded. The nickel pregnant electrolyte containing about 100 g/l Ni at pH 3 to 3.5, was diluted with water back to 75 g/l Ni and acidified to 40 g/l H₂SO₄. By this method we were able to provide a fresh spent electrolyte back to the solvent extraction circuit without the additional contaminants common to the original reagent grade chemicals.

No attempt was made to actually electrowin nickel during the test program due to a lack of the appropriate equipment.

Typically, our synthetic leach solution contained the following:

<u>Metal</u>	<u>Concentration - g/l</u>
Ni	38 - 40
Cu	0.15 to 0.16
Co	0.015 to 0.019
Mn	0.00013
Zn	0.0005 to 2.95
Pb	0.00153
Cr	Not Assayed
Sn	0.055
Sb	0.0011
Mg	Not Assayed
NH ₄	~ 75
CO ₃	~ 75
pH	10.0 to 11.6

It should be noted that our ammonia and carbonate concentrations are greater than originally prescribed. These greater concentrations were used due to the difficulty in dissolving the reagent nickelous carbonate at ambient temperature and atmospheric pressure. Also, contaminants such as Mn, Pb, Cr, Sn, Sb, and Mg were present in the reagent grade nickelous carbonate

and were not added separately. In addition to the nickelous carbonate, we included reagent grade cobaltous carbonate, cupric carbonate, ammonium hydroxide, and ammonium carbonate.

The original nickel spent electrolyte contained:

<u>Metal</u>	<u>Concentration - g/l</u>
Ni	72 to 75
Cu	0.0010
Co	0.0015
Zn	0.0003
H ₂ SO ₄	~ 40

The above contaminants, Cu, Co, and Zn, were present in the reagent grade nickel sulfate and were not intentionally added separately.

Preliminary Test Procedures

Very little preliminary testing was done in separatory funnel shakeout tests. Most of the background work necessary for this evaluation was derived from a previous similar test program reported in our publication, "Recovery of Nickel by Liquid Ion Exchange", by C.R. Merigold and R.B. Sudderth, a paper presented at the AIChE Annual Meeting in Chicago during February 25 through March 2, 1973. However, some initial exploratory work was included for the evaluation of some carrier solvents.

Included in these tests were Escaid 200 made by Exxon and Napoleum 470 made by Kerr-McGee Corporation.

The Escaid 200 contains a very low aromatic concentration (about 0.6%) and exhibited very fast phase disengagement. However, the lack of aromatic (we believe) caused the precipitation of a metal-organic reagent complex at reagent (LIX 64N) concentrations greater than 20 volume percent when the organic phase was loaded to its maximum capacity. Escaid 200 plus an aromatic diluent (Napoleum 140A) allowed greater LIX 64N concentrations without precipitation; but the aromatic portion of the organic phase slowly dissolved our acrylic mixer-settler units,

and its use had to be discontinued. Finding the best physical behaviour with Napoleum 470, most of our circuit evaluation was done with this carrier. However, some precipitation of organo-metallic complexes was found when the organic phase was loaded to its maximum loading capacity if reagent concentrations in excess of 30 to 35 volume percent were used. Consequently, LIX 64N concentrations greater than 30 volume percent are not recommended in Napoleum 470. Any investigation considering the use of other diluents should include a study of the solubility of the organo-metallic complexes prior to laboratory or pilot circuit evaluations.

The precipitated "metal-LIX 64N" complex should not be confused with degradation products. The precipitate is due to super-saturation, and it can be readily redissolved in kerosine and reused in the solvent extraction circuit.

Since a number of different kerosine diluents are available on the market today, each exhibiting slightly different primary and secondary (entrainment) phase disengagement rates, we did not attempt to define precise phase disengagement rates in our test program. We would prefer to run these tests after the customer has chosen the diluent he intends to use in his pilot or commercial plant operation.

Laboratory Circuit Test Procedures

Initially, the laboratory circuit was installed according to the flow-sheet shown in Figure 1. The circuit consists of a number of mixer-settler units, as illustrated in Figure 2. Each mixer contains a volume of 200 ml. Both mixing and inter-stage pumping are achieved with the pumping impellers. The organic-aqueous interface in each settler is maintained externally with a glass "Jackleg". All mixer-settlers used aqueous recycles (where necessary) to provide mixer organic:aqueous input ratios of 1:1. For example, when an organic flow rate of 36 ml/min. and a feed (leach liquor) flow rate of 5 ml/min. were used, an aqueous recycle of 31 ml/min. was used to provide the mixer input flow ratio of 1:1. The use of this recycle permits optimization of the chemical and physical properties of the system.

Once the leach liquor was prepared it was filtered to remove all suspended solids. The leach liquor, or feed, was then pumped to two extraction stages, and the nickel and copper barren raffinate was discarded. In these two extraction stages we attempted to load the organic to approximately 80 percent of its maximum loading capacity so that a nickel and copper barren raffinate could be obtained. Although our raffinate was discarded, it would actually be recycled back to leach for renewed leaching.

A second stream of filtered feed was contacted in another mixer-settler stage to load the organic phase to its maximum loading capacity. The purpose of this stage is two-fold. First, the loading of nickel and copper to the reagent's maximum loading capacity tends to "crowd off" some of the zinc that might tend to load in the two previous extraction stages where loading sites are available for the zinc. Second, the crowding stage provided a constant concentration of nickel in the loaded organic prior to stripping. More will be discussed on the purpose of the crowding stage later in this report. The aqueous from this stage, still containing most of its metal values, was discarded during our tests. In actual practice, however, this aqueous would normally be returned to the feed holding tank.

The loaded organic phase, now loaded to its maximum loading capacity, can contain a small amount of entrained aqueous (leach solution) containing metal values and strong ammonia. Previous test work has also shown that the loaded organic can contain dissolved NH_3 gas and actually some loaded NH_3 . Such loading is typical with organic or petroleum products (kerosine) and is not necessarily unique to the reagent. Since it is necessary not to carry ammonia to the nickel strip circuit, the loaded organic from the crowding stage was contacted in a mixer-settler wash stage. Our previous publication (cited above) suggested scrubbing the organic with a solution containing 10 g/l Na_2SO_4 . This system was less than desirable since it potentially allowed the entrainment transfer of sodium to the strip circuit. A water wash alone could not be used since the NH_3 bearing loaded

organic provided an aqueous phase after mixing containing NH_4OH , insufficient in anion content for optimum phase disengagement. As an alternative, we prepared an aqueous wash solution containing 20 g/l H_2SO_4 and neutralized this solution with NH_4OH to a neutral pH of 7. This dilute $(\text{NH}_4)_2\text{SO}_4$ solution then contained sufficient anions to provide good phase separation after mixing while eliminating the risk of transferring unwanted cations to the strip circuit. In a separate surge tank (large beaker), the aqueous from the wash stage was heated to approximately 40 to 45°C to drive off excess NH_3 gas. In a commercial system this gas would be recovered for renewed leaching. Of course, the SO_4^{--} remains in the wash solution eliminating the need for further anion make-up.

As an alternative to using dilute $(\text{NH}_4)_2\text{SO}_4$ as the scrub solution, CO_2 gas bubbled into the wash aqueous surge tank works very well in scrubbing the organic of ammonia and providing good phase separation. In this case the wash solution would have to be bled to control the build-up of excess ammonium carbonate. This bleed would be used in leaching, but one should first determine the bleed required against leach make-up requirements to avoid a water imbalance problem.

Our "water wash" stage (using dilute $(\text{NH}_4)_2\text{SO}_4$) removed approximately 96 to 97 percent of the total ammonia from the loaded crowded organic.

It was then necessary to remove the remaining 3 to 4 percent NH_3 from the organic phase. This was achieved in two aeration stages, shown in Figure 3. This figure illustrates the aeration system and the water wash surge tank. The wash aqueous from the wash stage enters beaker "A" which is placed on a magnetic stirrer hot plate. The temperature of the aqueous was controlled at 40 to 42°C. Agitation was achieved with the magnetic stir bar, and aeration was achieved with the air dispersion tubes. This agitation and aeration provided the control required for subsequent renewed washing. The first organic aeration surge beakers were supported in the aqueous wash beaker. This method allowed some heat to the organic phase for improved NH_3 scrubbing.

The organic from the wash stage entered beaker "B", where aeration occurred, and overflowed into beaker "C". The organic in beaker "C" was then syphoned (continuously) into beaker "D" which was the second aeration stage. As before, the organic overflowed into a larger beaker, "E". These two stages removed the remaining 3 to 4 percent of the ammonia, and any entrained aqueous from the wash stage, providing a clean loaded organic for pumping to the strip circuit. In a commercial system, a bank of flotation cells would be recommended for the purpose of aerating the organic.

An alternative to air scrubbing the loaded and washed organic would be a mixer-settler stage, washing with water at an equilibrium pH of about 5.5. This pH value would scrub the remaining 3 or 4 percent ammonia without stripping copper and nickel. It could also be a better "guarantee" towards scrubbing all of the ammonia from the loaded organic in a continuous operation. Testing of these various methods in a pilot plant would be recommended to better determine the various efficiencies and economics of each system.

The loaded organic then proceeded to four stages of nickel and copper stripping. As previously mentioned, our spent electrolyte contained approximately 75 g/l Ni and 40 g/l H_2SO_4 and our objective was to produce a nickel pregnant electrolyte containing 100 g/l Ni at pH 3.0 to 3.5. The extreme acid concentrations between the nickel spent electrolyte and nickel pregnant electrolyte required a recovery and control method for removing copper values from the system. Two copper extraction stages were installed in the circuit for this purpose (again refer to Figure 1). The first copper extraction stage was installed to avoid the accumulative build-up of copper in the overall system (organic phase used in the nickel extraction-stripping circuit). The second copper extraction stage removed trace amounts of copper from the final nickel pregnant electrolyte. This flowsheet was the initial test scheme evaluated in the laboratory solvent extraction circuit.

During the course of this valuation we found that although the practice of including the separate copper circuit as seen in Figure 1 was technically sound, it was not necessarily the most economical approach.

Commercially, the copper recovery solvent extraction circuit would have to be sized according to the flow rate of the nickel electrolyte stream to maintain the proper organic: aqueous flow ratios. Although this circuit would be smaller than the nickel extraction-stripping circuit, it would still be expensive in terms of a copper production rate of 345 pounds of copper per day. Comparative capital investment economics will be discussed later in this report.

The alternative to the above copper solvent extraction circuit included the precipitation of copper cement onto gaseous reduced nickel shot. One precipitation stage was placed between the fourth and third nickel stripping stage, and the other precipitation stage was placed after the first nickel stripping stage -- which is the final pregnant electrolyte. (To avoid confusion, the nickel electrolyte flow proceeds from the electro-winning tankhouse to the fourth stripping stage, on to the third, the second, and through the first before it results as the final nickel pregnant electrolyte. The organic phase flows counter-currently, entering the first stripping stage as the loaded organic, proceeds to the second, the third, through the fourth, and leaves the fourth stripping stage before entering the second extraction stage as the stripped organic). This system worked very well, controlling the copper content in the organic phase of the nickel solvent extraction system at about 0.7 g/l Cu. Also, no copper was detected in the nickel pregnant electrolyte by this method.

Commercially, nickel cathode chips could be used for this system. In this way there would be no net loss of nickel production, since the copper replaces the nickel; and it would not be necessary to purchase nickel shot from a supplier. It is recommended, however, that the copper precipitation system should be installed as a "ball mill" plant. The cathode chips would serve as the balls, and the abrasive action of the rolling mill would continuously expose the surface of the nickel cathode chips for renewed precipitation. The copper cement produced from this system can then be leached in a separate ammoniacal leach operation, at ambient temperature and atmospheric pressure, and the resulting leach solution is then processed in a separate, very small, solvent extraction-electro-winning system. The economics for this approach will also be reviewed later in this report.

Our next process for controlling copper build-up and recovery was the most successful. The nickel shot system was removed from the circuitry, and we then installed an electro-winning cell between the fourth and third nickel stripping stages (see Figure 4). The aqueous electrolyte flowing from the fourth nickel strip stage contained approximately 80 to 35 g/l Ni, 0.30 to 0.50 g/l Cu, and 25 to 35 g/l H₂SO₄. At this location in the flowsheet we find the greatest concentration of copper in the nickel electrolyte and here we placed the electro-winning cell. Our intention was to electrowin enough copper from this aqueous solution to provide the control necessary to maintain a low copper concentration in the recirculating organic phase. We used four copper starter sheets in the electro-winning cell, five lead anodes, and employed a current of 1.0 amps (current density of about 0.5 amps/ft²).

Although copper was electrowon, the deposit was a loose, dark, spongy deposit with the characteristic appearances of cement copper. In this case, the copper recirculating in the organic phase was reduced to 0.2 to 0.3 g/l Cu, and no copper was reporting in the nickel pregnant electrolyte. Commercially, the copper cement thus produced can be processed in a separate ammonia leach-solvent extraction-electrowinning system similar to the case cited above.

After several days of operating the above flowsheet in the laboratory circuit, the cement copper was removed from the electro-winning cell. It was then washed with water and dried. Once dried the cement copper was leached in 30 g/l NH₄ and 30 g/l CO₃ for approximately one hour. The resulting solution contained copper ammine carbonate and no nickel or zinc.

The original copper cement, however, contained 97 percent Cu, 0.17 percent Ni, zero percent Zn, and 2.68 percent insoluble material (insoluble in HNO₃). The insoluble material was most likely PbO₂ which is commonly found in our laboratory electro-winning cell while using non-alloyed lead anodes. In a full-scale plant greater current densities could be employed to reduce the size or number of copper electro-winning cells needed.

Studies are currently underway to better determine the efficiency and economics of this recovery approach at higher current densities. At the time of this writing efficiencies are found to be greatly enhanced by providing high recirculation rates in the electrowinning cell while heating the electrolyte to temperatures normally involved in nickel electrowinning processes.

Additionally, stainless steel blanks could be used as the cathodes. DSA or other insoluble anodes could be used rather than antimonial lead. The cost of such anodes should not be prohibitive because of the low inventory requirement.

Circuit Chemistry

The laboratory circuit was finally operated according to the flowsheet shown in Figure 4. The organic phase contained 20.4 volume percent LIX 64N in the kerosene diluent, Napoleum 470. The extraction organic:aqueous flow ratio was 6.9:1 to provide a nickel loading of approximately 70 percent of its maximum loading capacity. (Commercially, we would recommend loading to 80 or 90 percent of maximum). Aqueous recycles were used in all stages where required to maintain mixer input organic:aqueous flow ratios of 1:1. A single crowding stage was used with an organic:aqueous flow ratio of 3.6:1. (Again, an aqueous recycle was used for a mixer input ratio of 1:1). One wash stage was used with an originating organic:aqueous ratio of 1:1. So, no recycle was used here. Mixing time in all stages was approximately 2.7 minutes. Normally we would test and recommend two minutes. The longer mixing time was actually used to conserve our leach liquor (which was quite expensive). Following the wash stage the organic was "aerated" in two stages.

As briefly mentioned earlier in this report, the single crowding stage performs a very important function. Once the organic phase is loaded with nickel, it is subsequently stripped with the aqueous electrolyte. The stripping chemistry involves hydrogen ion exchange such that the nickel "released" from the organic phase is replaced with the hydrogen ion from the aqueous phase. Thus, the build-up of nickel into the aqueous electrolyte results in a "loss" of acidity from the aqueous phase by a factor of 1 g/1 Ni replacing 1.67 g/1 equivalent acid. Since we are attempting to provide a pregnant electrolyte within a pH range of 3.0 to 3.5, and since slight variations in acidity appreciably changes the solution pH at, above, or below this range (see Figure 5), it is important to provide the strip circuit with a loaded organic of constant nickel concentration. Without a crowding stage constant loading conditions would have to be achieved in the two extraction stages. At constant flow rates, this presupposes a constant nickel concentration in the leach liquor at all times. If we further consider no crowding stage, and slight variations of nickel concentration in the leach liquor, constancy would have to be provided by purposely varying flow ratios to achieve the same goal. This method of control is not recommended in commercial practice. The crowding stage is, therefore, recommended to simplify commercial plant operation.

Also, briefly mentioned earlier was the recommendation for the wash stage and the aeration stages. During the circuit operation analyses were run to prove this need:

Sample	g/1 NH ₃
Leach Liquor	73.44
Crowded Loaded Organic	1.88
Washed Organic	0.472
Organic Following First Aeration	0.172
Organic Following Second Aeration	not detectable

Commercially, a bank of flotation cells would serve this function nicely. The impellers in the flotation cells would provide good agitation and aeration for optimum performance. This system would prevent the transfer of ammonia to the nickel electrolyte, which if allowed to accumulate could subsequently allow the strip circuit. Also, the transfer of ammonia would artificially influence the pH of the nickel pregnant electrolyte from the strip circuit.

The "cleaned" loaded organic then proceeds to the nickel strip circuit where it flows countercurrent to the aqueous nickel electrolyte flow in four stripping stages. The equilibrium data for this test are shown in Table 1.

The data show that some nickel is actually stripped from the crowded loaded organic in the wash stage. This is of no concern since the nickel that is stripped will reach equilibrium with the ammonium sulfate in the wash water. To reiterate, our wash water was originally 20 g/l H_2SO_4 neutralized with ammonium hydroxide to pH 7. Therefore, the nickel in this wash water could reach approximately 10 to 12 g/l Ni, although we never exceeded 2.4 g/l Ni in the laboratory test. As nickel and other impurities accumulate in the wash water by entrainment from the crowding stage, a very small bleed can be taken from the wash water surge tank and added to the leach liquor entering the extraction circuit. The ratio of water bleed to the leach liquor flow would be sufficiently low to prevent any significant change in the blended leach liquor composition.

The data in Table 1 also show some loading of cobalt onto the organic phase. It was found, however, that once the cobalt concentration reached about 0.0005 to 0.0012 g/l Co, additional cobalt loading was not found with the continued recycling of the organic phase in contact with new leach liquor. Therefore, cobalt is not considered a problem.

Zinc loading was insignificant in this test. The data show that the synthetic spent electrolyte prepared for the strip circuit contained more zinc than could be traced by extraction. Although the crowding stage was not required in this case for "crowding off" zinc, it was required for the other reasons cited above.

TABLE 1

Circuit Profile Analyses

Assay	Analyses - g/l									
	Wash Surge	Wash Stage		Crowd Stage		Leach Liquor	Extraction #1		Extraction #2	
	Aqueous	Aqueous	Organic	Aqueous	Organic	Aqueous	Aqueous	Organic	Aqueous	Organic
Ni	1.20	1.40	9.14	31.6	9.07	39.0	10.2	6.35	0.0183	2.24
Cu	0.0011	0.0009	0.272	0.0046	0.268	0.162	0.0015	0.230	N.D.	0.210
Co	---	---	0.0005	---	0.0005	0.019	---	0.0005	0.030	---
Zn	0.0002	---	Trace	---	Trace	0.0005	---	Trace	0.0006	---
Pb	---	---	---	---	---	---	---	---	---	---
NH ₃	7.65	9.33	---	---	---	---	---	---	---	---
H ₂ SO ₄	---	---	---	---	---	---	---	---	---	---
pH	9.19	9.37	---	---	---	11.80	---	---	---	---

Assay	Analyses - g/l									
	Ni Spent Electrolyte	Strip #4		Electrowinning Cell	Strip #3		Strip #2		Strip #1	
	Aqueous	Aqueous	Organic	Aqueous	Aqueous	Organic	Aqueous	Organic	Aqueous	Organic
Ni	72.7	79.2	0.36	76.9	83.9	1.90	96.3	3.53	98.6	7.58
Cu	0.0024	0.294	0.210	0.036	0.250	0.296	0.015	0.343	0.0006	0.266
Co	N.D.	N.D.	0.0005	N.D.	---	---	---	---	N.D.	---
Zn	0.0009	0.0008	Trace	0.0008	0.0007	Trace	0.0007	Trace	0.0007	Trace
Pb	N.D.	---	---	---	---	---	---	---	N.D.	---
NH ₃	0.858	---	---	---	---	---	---	---	1.08	---
H ₂ SO ₄	40.4	33.0	---	33.7	23.3	---	6.2	---	---	---
pH	0.48	0.59	---	0.56	0.68	---	1.45	---	3.18	---

Note: N.D. - not detectable by atomic absorption analysis.

The data also show some transfer of ammonia on the organic to the aqueous electrolyte--approximately 0.07 g/1 NH₃ on the organic while stripping at an organic:aqueous flow ratio of 3.1:1. A third aeration of flotation stage would have eliminated this transfer (we recommend five or six flotation cells in the commercial plant).

We also see some copper (0.6 ppm) reporting in the nickel pregnant electrolyte. This was found at a nickel pregnant electrolyte pH of 3.18. Figure 6 shows the amount of copper that might be found in the nickel pregnant electrolyte at various pH's. The data show that at pH values between 2.8 and 3.2, less than one ppm copper is found in the nickel pregnant electrolyte. At pH values above 3.2, no copper is found. Of course, the reason for this is that LIX 64N re-extracts all of the copper that might be present in the nickel pregnant electrolyte when the pH is at or above 3.2. When the pH is lower than 3.2, there is enough acidity to strip a slight amount of copper from the organic phase.

During the course of the test period we sampled various solutions to determine the selectivity of extraction and calculated the transfer of metal contaminants to the electrolyte. The results are shown in Table 2. Examining Table 2, the 27.9 g/1 Ni transferred should be added to the 72.7 g/1 Ni in the spent electrolyte resulting in a pregnant electrolyte concentration of 100.6 g/1 Ni.

The calculated copper concentration of 0.077 g/1 Cu actually does not exist at all since the difference in copper concentrations between the crowded loaded organic and the stripped organic (the transfer concentration) reports to the electrowinning-precipitation cell within the nickel strip circuit and does not report to the nickel pregnant electrolyte.

The zinc concentration in the electrolyte might be real, but according to atomic absorption analysis of the pregnant electrolyte the zinc concentration was actually less than 0.01 ppm.

There was no transfer of Mg, Cr, or Sb that could be detected. The tin was the greatest impurity found, but it should be remembered that our

TABLE 2

Metal Transfer by Extraction

<u>Metal</u>	<u>Feed</u>	<u>Raffinate</u>	<u>Crowded Loaded Organic</u>	<u>Loaded Organic</u>	<u>Stripped Organic</u>	<u>Calculated Concentration to Pregnant Electrolyte</u>
Ni	40.8	0.0158	10.3	7.9	1.30	27.9
Cu	0.183	<0.00003	0.540	0.458	0.463	0.077
Co	0.0085	0.0378*	0	0	0	0
Zn	0.00113	0.00108	Trace	Trace	Trace	0.0007
Mg	0.0050	0.0051	0	0	0	0
Cr	0.00023	0.00025	0	0	0	0
Sb	0.0011	<0.00004	<0.0001	<0.0001	<0.0001	N.D.
Sn	0.055	<0.0005	0.037	0.027	<0.005	0.099
Mn	0.00013	<0.00003	0.000105	0.000075	0.00001	0.00029
Pb	0.00153	0.00010	0.00075	0.00063	0.00001	0.00229

Stripping Organic:Aqueous Ratio - 3.10:1

*Experimental Error

synthetic leach solution contained 0.055 g/l Sn while the prescribed leach liquor contains less than 0.002 g/l Sn. In this case, Sn reporting to the pregnant electrolyte would still be less than originally prescribed.

Mn loading was inconsequential. Although the transfer calculation showed Pb in the electrolyte, it could not be detected analytically. We suspect that most or all of the lead which is stripped as lead sulfate is essentially insoluble, precipitating out of solution as it is stripped. It was, therefore, not detected by atomic absorption.

Based on the indicated transfer of metal contaminants to the electrolyte, we can compare the solvent extraction-electrolyte composition against the prescribed objective (see Table 3)--again realizing that our Sn concentration in our leach liquor was 27.5 times greater than prescribed.

TABLE 3

Comparative Data Between Actual Nickel Pregnant
Electrolyte Produced and Original Objective

Metal	Electrolyte Analyses - g/l	
	"Real" Concentration	Objective
Ni	100	100
Cu	Not Detectable	<0.002
Co	Not Detectable	Not Given
Zn	<0.0007	<0.010
Mg	Not Detectable	Not Given
Cr	Not Detectable	Not Given
Sb	Not Detectable	0.005
Sn	< 0.099	<0.005
Mn	< 0.00029	<0.020
Pb	Not Detectable	< 0.005
pH	3.18	3.0 to 3.5

It can be seen in both Table 3 and the profile analyses in Table 1 that we have met and even bettered our original objectives.

We should also note here that common nickel electrolyte additives such as H_3BO_3 were not used in our tests. Previous work has shown that H_3BO_3 neither helps nor hinders the solvent extraction process, so there was no point in including this material in our tests.

One major advantage of employing the solvent extraction process with the ammonia leach process is the ability to recycle the ammonia pregnant raffinate back to the leaching process. This allows the reuse of the raffinate stream and allows the accumulative build-up of zinc and cobalt for subsequent recovery. Speculating that it might be desirable to accumulate up to 30 g/l Co in the recycling ammonia solution, we next investigated the effect of the corresponding increase in zinc concentration on the extraction circuit. Since our prescribed leach liquor contained 0.021 g/l Co and 0.0022 g/l Zn, an accumulative concentration of 30 g/l Co represents a (theoretical) zinc concentration of 3.1 g/l Zn.

So, our next laboratory circuit test included the original leach solution plus 2.95 g/l Zn. Cobalt was not added to a 30 g/l Co concentration because of the difficulty of dissolving cobalt carbonate at that concentration at ambient temperature and atmospheric pressure and because we have already shown that oxidized cobalt does not load.

Once equilibrium was obtained in the circuit, organic and aqueous samples were analyzed. The results are shown on Table 4. The data does show that the crowding stage does effectively remove some of the zinc from the loaded organic by approximately 42 percent. Although such crowding is not completely effective, it still allowed us to produce a nickel pregnant electrolyte below the initial prescribed objectives.

If for some reason the zinc in the nickel pregnant electrolyte were to exceed specifications, it could be treated in a single extraction stage with D2EHPA without extracting nickel. A single strip stage could be used to strip the zinc from the D2EHPA using a weak H_2SO_4 solution, and the zinc could be subsequently electrowon. According to our laboratory investigation, however, this system should not be required; and its application should be considered provisional.

During the course of the above test run, we learned from our potential customer that it is not desirable to allow the accumulation of cobalt to reach 30 g/l since this high concentration tends to prohibit re-leaching of cobalt once the raffinate has been recycled back to leach. So, although the above test was not really necessary, it does provide additional data for when and where it might apply.

As a final and rather "uncontrolled" test, we took some of the raffinate from the above test run for further processing. The raffinate contained 2.92 g/l Zn and 0.010 g/l Co at a pH of approximately 9.87. This raffinate was heated for several hours with agitation. Ignoring evaporation of the aqueous, approximately 84 percent of the zinc precipitated out of solution,

TABLE 4

Circuit Analyses While Using Elevated
Zinc Concentration in the Leach Liquor

<u>Assay</u>	<u>Leach Liquor Aqueous</u>	<u>Raffinate Aqueous</u>	<u>Wash Solution Aqueous</u>	<u>Growd Stage Organic</u>
Ni	38	0.01	2.2.	8.2
Cu	0.205	0.0001	0.0004	0.43
Co	0.007	0.007	---	0.0002
Zn	2.95	2.33	---	0.0021
pH	11.41	--	---	---

<u>Assay</u>	<u>Loaded Organic</u>	<u>Stripped Organic</u>	<u>Spent Electrolyte Aqueous</u>	<u>Pregnant Electrolyte Aqueous</u>
Ni	6.85	0.29	73	96
Cu	0.36	0.34	0.003	N.D.
Co	0.0002	0.0002	0.001	0.001
Zn	0.0036	N.D.*	0.0007	0.008
pH	---	---	---	4.0

but none of the cobalt precipitated. Final pH was about 3.3. As mentioned above, this was not a closely controlled test; but the results indicate that zinc could be selectively separated from the cobalt by distillation, evaporation, etc. The cobalt could then be recovered by H₂S precipitation. Thus, we achieve the separation of nickel, copper, cobalt, and zinc from our original leach solution.

Economic Consideration

Our first objective in this area is an economic comparison between the flowsheet of Figure 1 (using solvent extraction recovery of copper within the nickel strip circuit) and the flowsheet of Figure 4 (using the electrowinning-precipitation stage followed by a separate copper cement leach, solvent extraction system). All calculations will be based according to the concentration of metals in the leach liquor and the anticipated annual production rate of 12,500 tons of nickel per year. Given this much, we find the following fixed operating conditions:

Production Rate = 69,500 lbs. Ni/day

345 lbs. Cu/day

Leach Solution Flow Rate = 150 gpm*

Aqueous Recycle Flow Rate (where applicable) = 850 gpm

Organic Flow Rate = 1,000 gpm

Electrolyte Flow Rate = 325 gpm

Aqueous Recycle Flow Rate = 675 gpm

*Flow rates are rounded off to the nearest 5 gpm for calculation purposes.

In case one we find our only fixed condition is the electrolyte flow rate of 325 gpm. The organic phase of the copper solvent extraction circuit is recommended at 2.5 volume percent LIX 64N. A total of two extraction stages are required plus two stripping stages. While extracting copper at an organic:aqueous ratio of 1:1, the total flow to the circuit is 650 gpm.

The capital investment cost for the circuit, ready for start-up, is \$135,900.00 (U.S.) Considering a 10 year amortization period, this cost represents 11.1 cents per pound of copper produced. The organic inventory is 11,515 gallons at a cost of \$8,207.00.

The second case includes the electrowinning-precipitation stage followed by ammonia leaching and solvent extraction. The leaching system would produce a liquor containing 20 g/l Cu using 30 g/l NH_3 and 30 g/l CO_2 . At a production rate of 345 lbs. of copper per day, the leach solution flow rate would be only 1.44 gpm. Thirty volume percent LIX 64N would be used at a flow rate of 5.7 gpm for an originating extraction organic:aqueous flow ratio of 4:1. Using aqueous recycles, the total flow to the solvent extraction circuit would be 11.4 gpm. The capital investment cost for this circuit would be relatively insignificant compared to case one, or a cost of \$12,000.00. The cost for the single electrowinning cell and rectifier would be about \$17,250.00 for a total capital investment cost of \$29,250.00.

The final single electrowinning cell for the copper cathode production was not included in the above cost comparison since this cost would be the same in both cases (\$17,250.00).

Perhaps a third alternative would be the direct leaching of the cement copper with H_2SO_4 , thus, avoiding the small solvent extraction circuit. Of course, this decision depends on the production objectives of the user.

The next objective is the capital investment cost and operating costs for the entire recovery system. It is not our objective to include leaching costs of the laterite ore, filtration costs of the leach liquor prior to solvent extraction and the cost of heating the nickel electrolyte (if required) prior to electrowinning since these areas are not within our experience.

The major items which are included under capital investment costs are:

1. Nickel solvent extraction circuit
2. Nickel circuit organic inventory
3. Heat exchanger (for water wash system)
4. Organic aeration-flotation circuit
5. Nickel electrowinning circuit
6. Micro-flotation circuit
7. Activated carbon column
8. Copper precipitation-electrowinning cell
9. Copper production electrowinning cell
10. Copper solvent extraction circuit
11. Copper circuit organic inventory

Nickel Solvent Extraction Circuit: The total circuit contains eight mixer-settler stages, i.e. two extraction stages, one crowding stage, one wash stage, and four stripping stages. Two minute mixer retention times are recommended for each stage. As mentioned earlier in our report, we did not attempt to measure phase disengagement rates. However, a phase disengagement rate of 1.5 gpm/ft^2 should be quite realistic for a four-inch dispersion band. So, this figure will be used for calculation purposes.

Our cost estimates for the nickel solvent extraction circuit are based on calculations derived from actual costs obtained from several commercial solvent extraction circuits built within the last five year period.

The capital investment cost for the complete nickel solvent extraction circuit, including pumps, piping, instrumentation, mixer motors, and impellers, etc., is \$1,247,355.00.

Nickel Circuit Organic Inventory: The total organic inventory, containing 20 volume LIX 64N and 72 volume percent kerosine, represents a cost of \$514,822.00. This inventory includes a 25 percent surge capacity.

Heat Exchanger: The heat exchanger is used in the water wash system to heat the wash aqueous from the water wash mixer-settler from about 35°C to about 42°C. We are also assuming that heat energy for this unit is available from elsewhere in the plant. The cost for the heat exchanger is about \$2,500.00, and the operating cost is estimated at about 0.01 cents per pound of nickel produced. Once the wash aqueous is heated, aeration is achieved in a six cell water treatment flotation circuit. This system is self aspirating so that blowers are not required. Each of the six cells contains a 748 gallon volume. The capital investment cost for this item is \$15,000.00, and the only operating cost would be power costs for three 7.5 HP motors.

Organic Aeration-Flotation Circuit: This circuit would be identical to the one above for a cost of \$15,000.00. Data obtained from a pilot plant operation would provide additional information in regard to cell size, number of cells required in terms of retention time required, etc., for scale-up to the commercial plant. The operating cost in terms of cost per pound of nickel produced would be insignificant.

Nickel Electrowinning Circuit: After contacting a number of "Authorities" in the field with nickel electrowinning experience, we obtained a wide range of costs for the electrowinning plant. So, for purposes of cost estimating this section of the plant we are using the average cost presented to us, or \$75.00 per pound of nickel produced per day. At a production rate of 69,500 pounds of nickel produced per day, our capital investment cost is \$5,212,500.00.

Micro-Flotation Circuit: Some experts in the field have suggested that it is imperative that the nickel pregnant electrolyte must be free of organic impurities prior to electrowinning. Apparently trace quantities of organic can tend to lubricate the nickel starter sheet and prevent good plating characteristics. With a properly designed solvent extraction circuit, the nickel pregnant electrolyte would normally contain about 40 ppm entrained organic. The use of micro-flotation would reduce the organic content from 40 ppm to about 5 ppm. The capital investment cost for this item is \$32,000.00.

Activated Carbon Column: Following micro-flotation, the nickel pregnant electrolyte would be treated with activated carbon to remove the final 5 ppm organic (although we have been told that an organic content of 2 to 4 ppm is permissible). Considering a carbon column five feet in diameter and 18 feet high containing 3,500 pounds of 12 x 14 mesh activated carbon, the capital investment cost would be about \$10,000.00. The cost of the activated carbon is 20 cents per pound. The 3,500 pounds of carbon would collect 55 gallons of 'oil' (entrained organic). This 55 gallons represents 11,000,000 gallons of electrolyte treated, or an operating cost of 0.11 cents per pound of nickel produced--assuming that the spent activated carbon is discarded rather than regenerated.

Copper Precipitation-Electrowinning Cell: We have already shown that the cost of this cell, including the rectifier, is about \$17,250,000. Optimization of this system should also be achieved in the pilot plant evaluation.

Copper Production Electrowinning Cell: This cell would be identical to the above at a cost of \$17,250,000. In this case pretreatment of the copper pregnant electrolyte is not required.

Copper Solvent Extraction Circuit: Also shown above was the cost for the copper solvent extraction circuit. This cost was \$12,000.00.

Copper Circuit Organic Inventory: The organic inventory for the copper circuit would be \$5,220,000.

Leaching of the cement copper would be done in a single tank containing a flotation type impellor. This impellor would provide both the agitation and the oxidation required. The capital investment cost for this item would be about \$10,000,00.

A summary of the capital investment costs is shown in Table 6. It can be seen that we have not included any operating costs for the copper recovery circuit. This system is so small that the operation and maintenance of this circuit can be administered by the personnel in the nickel solvent extraction-electrowinning plant. One should also notice that no credit has been given for the recoverable cobalt and zinc which would make the total economic picture even more attractive.

TABLE 5
Summary of Capital Investment Costs

Nickel Circuit:

<u>Item</u>	<u>Cost</u>
Solvent Extraction Circuit	1,247,355
Organic Inventory	514,822
LIK 64N Inventory = 26,547 gallons	
Kerosine Inventory = 63,263 gallons	
Heater Exchanger	2,500
Aqueous Aeration	15,000
Organic Aeration	15,000
Electrowinning Plant	5,212,500
Micro-Flotation Plant	32,000
Activated Carbon Column	<u>10,000</u>
Total Capital Investment Cost =	<u>\$7,049,177</u>

Capital Investment Cost vs. Amortization = 0.0282/1b. Ni (10 year amortization period).

Copper Circuit:

Item	Cost
Copper Precipitation-Electrowinning Cell	\$17,250
Copper Production Electrowinning Cell	17,250
Solvent Extraction Circuit	12,000
Organic Inventory	5,220
Copper Cement Leaching	<u>10,000</u>
Total Capital Investment Cost	\$61,720

Capital Investment Cost vs. Amortization = \$0.049/lb. Cu (10 year amortization period).

TABLE 6

Summary of Operating Costs

Nickel Circuit:

Item	Cost c/lb. Ni
Labor	0.66
Solvent Extraction.	0.05
Electrowinning.	0.61
Power	1.44
Solvent Extraction.	0.16
Electrowinning.	1.28
Misc. Power, Labor, Services, Repair, Etc.	0.15
Administrative Overhead	0.90
Chemicals (make-up)	0.46
LIX 64N	0.08*
Kerosine.	<0.01*
Acid.	<0.01
NH ₃	0.25
Activated Carbon.	0.11
Total Operating Cost	<u>3.61c/lb. Ni</u>

*Based on total organic loss rate of 40 ppm, although much of this "loss" is recoverable in the micro;flotation circuit.

DISCUSSION

Success for the realization of a new process in reaching commercial practice depends primarily on whether the laboratory evaluation achieves the original objectives of the test program. A second and equally important measure of success is the economic picture of the total process package. Other measures might include additional considerations such as recyclability or percent of reuse of the chemicals used in the process, disposal of waste materials (if necessary), legislative environmental considerations, and so on-- all of which have to be compared against existing or other new process techniques. If these and other parameters are the true measure of success, then we must consider this program a complete success.

Our first and major objective (and achievement) was the complete separation of nickel from the mother liquor followed by the complete separation of copper. Our final liquor (raffinate) , now void of nickel and copper, was still in the original form (unaltered by expensive chemical change) allowing the separations and recovery of zinc and cobalt. This was all achieved by the solvent extraction of nickel by LIX 64N followed by simple re-leaching of cement copper and solvent extraction of copper for the production of prime grade cathode copper. Solution recycling is possible in all areas. Percent recycling, or percent bleeding, is a function of re-leaching requirements as dictated by the build-up and control of impurities in the recycling leach liquor. Of course, electrolyte recyclability is greater in this process than any other process used today since the solvent extraction circuits provide the cleanest and most complete separations. This advantage results in decreased impurity processing costs.

One of the major capital investment costs prior to plant start-up is the organic inventory. Since the organic phase is nearly 100.0 percent recyclable (losses due to entrainment), the loss of organic is one of the lowest operating costs.

So, it can be seen that the "cleanliness", or high rate of solution reuse, eliminates the discharge of chemicals to the environment and waterways since the extremely low (potential) discharge of bleed streams can be handled by solar evaporation or other similar inexpensive artificial techniques.

Other incentives make the total package even more attractive. One is in the area of leaching laterites and sulfides with ammonia. Some investigators have improved the recovery of metals from laterites by the Nicaro process, increasing percent recovery from 30 percent to 90 or 95 percent. The U.S. Bureau of Mines has done some interesting work in this area too. Perhaps the newest and most exciting work in this area is the development of the **Arbiter Process by Anaconda**.

Another breakthrough is the development of the new so-called "DSA" anodes being developed by DeNora, Electrode Corporation, TiFab, and Texas Instruments. Some of these anodes, fairly priced, eliminate the additions of impurities (mostly lead) in the electrowon product. Some have also shown lower voltage requirements, resulting in lower power costs, making these anodes quite competitive to the usual antimonial lead anodes. The addition of cobalt, as 50 to 70 ppm Co, to copper electrolytes has once again allowed the use of lead anodes with less than 5 ppm lead reporting to the finished copper cathode.

Although some of the techniques and systems recommended in this report are somewhat novel from current practices, they need not be considered a "pioneering" concept. Today there are several major producers of metals using solvent extraction-electrowinning as well as other new plants on the drawing boards. As of this writing, the total copper produced per year via solvent extraction-electrowinning is now at least 15,300 tons of copper per year. Once the plants now on the drawing boards are under construction or completed, the total annual copper production will exceed 212,000 tons of copper per year. We might also note that all of these plants do now use or have committed to use General Mills Chemicals' reagents (LIX 64N or LIX 65N).

Of course, our second objective was to provide a recovery system at low capital investment and operating costs. This too was achieved, resulting in a capital investment cost (not including laterite leaching and filtration) of 2.82 cents per pound of nickel produced and 4.9 cents per pound of copper produced (10 year straight line amortization period). The total operating cost was 3.61 cents per pound of nickel produced. No credit was included in our cost analyses from the sale of zinc and cobalt since their respective production costs are beyond our experience.

The capital investment cost for the nickel electrowinning section of the plant might be debated since we were not successful in obtaining two like opinions on such costs from the industry. Other capital investment costing data, however, is believed to be accurate according to up-to-date cost information at U.S. prices. Also, power and labor costs were measured according to U.S. costs. So, these can vary in different parts of the world. Variations in these items, however, would be insignificant when all costs are considered as a whole.

Acknowledgements

The authors want to express their gratitude to the staff of the Centre de Recherches Le Nickel Penarroya Mokta for their assistance and contribution in providing solution parameters and recovery requirements as they would apply to a commercial system.

References

1. Merigold, C. R., Sudderth, R. B., "Recovery of Nickel by Liquid Ion Exchange Technology", Presented at the A.I.M.E. Annual Meeting, Chicago, Illinois, February - March, 1973.

1261

Figure 3

Aeration-Flotation Circuit Diagram

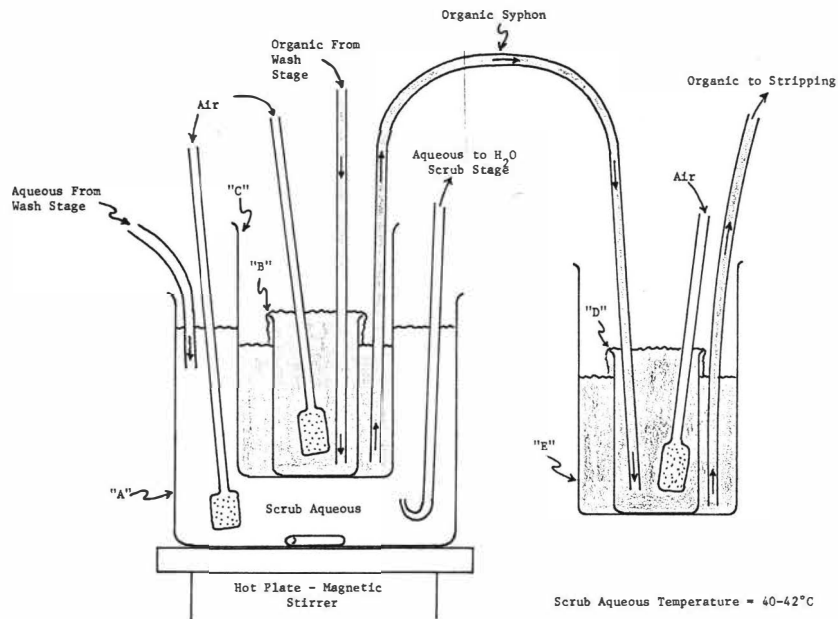


Figure 4

Final Laboratory Solvent Extraction Circuit Flowsheet

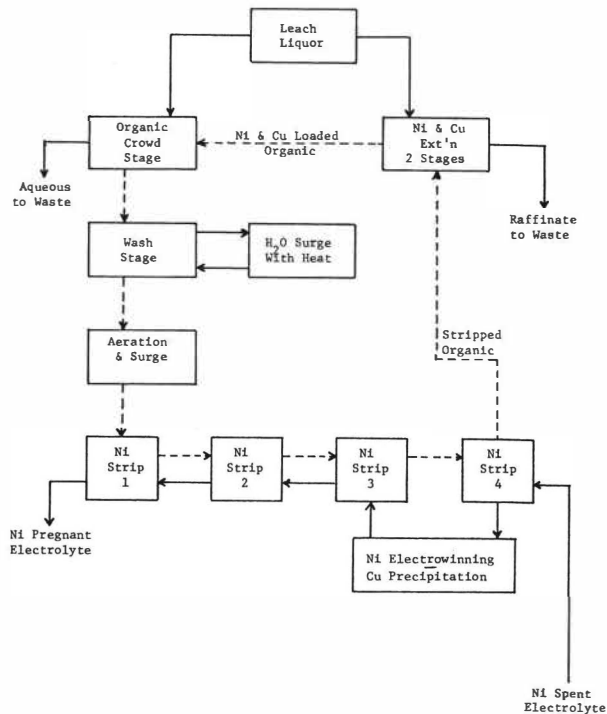


Figure 5

Nickel Electrolyte - H_2SO_4 Concentration vs. pH
(Initial Spent Electrolyte: 75 g/l Ni, 40 g/l H_2SO_4)

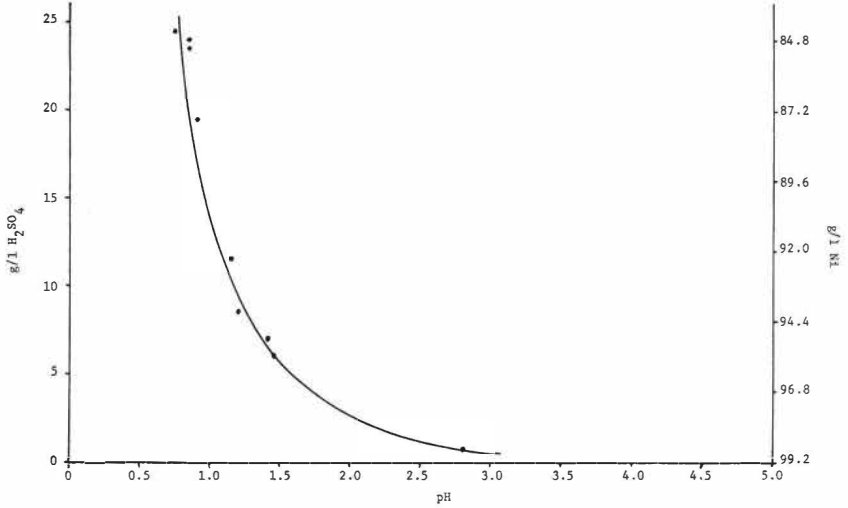
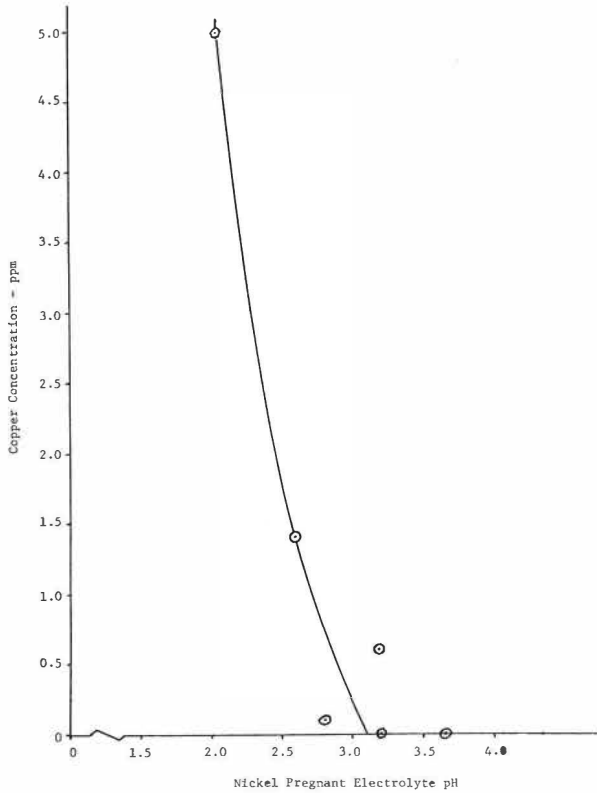


Figure 6

Nickel Pregnant Electrolyte - Copper Concentration vs. pH



Design of a Process for the Purification of Cobalt
by means of Di-2-ethylhexyl Phosphoric Acid

P. Mihalop
Charter Consolidated Ltd., Ashford, Kent, U.K.

and

Mrs. C.J. Barton, D.H. Logsdail, H.A.C. McKay and D. Scargill
Atomic Energy Research Establishment, Harwell, Didcot, Berks. U.K.

Abstract

Chemical data have been obtained in order to write a flowsheet for decontamination of a Co stream, arising from a copper plant, from Zn by means of HDEHP. Careful pH control proves to be an essential feature. Computer predictions of different possible systems have been made, and the favoured system has been successfully tested.

1. Introduction

The work described here was undertaken in order to remove zinc impurity from a cobalt stream consisting of raffinates from a copper solvent extraction plant. After treatment, the stream is of the following composition:

Co	40.0 g/l	0.68M
Zn	0.02	0.31mM
Cu	0.05 or 0.002	0.79 or 0.03mM
Mn	2.50	0.046M.
Mg	15.0	0.62M
Fe ²⁺	0.01	0.18mM
Ca	0.55 (saturated)	0.014 M

The medium is sulphate, the pH can be controlled, and operation at temperatures up to 60°C is possible. The requirement is for decontamination from Zn down to a level of 0.0004 g/l or 0.006mM, i.e. by a factor of 50. Removal of Mn and Cu is not a requirement, but it is useful to have knowledge of their behaviour in the system chosen.

On the basis of L.F. Cook and W.W. Szmokaluk's work⁽¹⁾, it appeared that solvent extraction with HDEHP (di-2-ethylhexyl phosphoric acid) might be suitable. Escaid 100 was chosen as diluent for the HDEHP, since this is the diluent used in the copper plant.

2. Experimental Techniques

HDEHP from Albright and Wilson Ltd. was purified to >99%, with no detectable mono-ester, by formation and decomposition of the copper salt, as described by J.A. Partridge and R.C. Jensen⁽²⁾. Escaid 100 was used as received from Rutpan Ltd., the U.K. supplier. HDEHP/Escaid 100 mixtures were prepared by making up weighed amounts of extractant to known volumes with diluent.

Aqueous phases were prepared by mixing together stock solutions of the salts and diluting as necessary. Cu was sometimes omitted, as its effect would be small. Saturation with CaSO₄ was achieved by agitating for at least 2 h with solid CaSO₄. The final pH was adjusted by addition of NaOH, and radioactive tracers were added as required. The tracers used were:

⁶⁰Co (5.27 y) as CoCl₂ in dilute HCl.

⁶⁵Zn (245 d) as Zn metal (later dissolved in dilute H₂SO₄).

⁶⁴Cu (12.8 h) as anhydrous CuSO₄.

⁵⁴Mn (291 d) as MnCl₂ in dilute HCl.

⁴⁵Ca (165 d) as CaCl₂ in dilute HCl.

The quantities of chloride added were trivial (generally <10⁻⁴M) and would not have affected the extractions.

Extractions were carried out by stirring or shaking the phases together at room temperature, under the various conditions indicated below. After separation, the phases were centrifuged, and samples were analysed. pH measurements were made with the aid of an E.I.L. general purpose dual electrode. Metals were determined either by atomic absorption spectrophotometry or radio-metrically. Organic phases were backwashed with 0.25 - 0.5M H₂SO₄ for the former method. Radiometric measurements were made by gamma-counting of liquid samples, except in the case of ⁴⁵Ca, when solid samples were beta-counted.

3. Distribution Coefficients

The distribution coefficients obtained by equilibrating synthetic cobalt feed with HDEHP/Escaid 100, are given in Figs.1 and 2. The following conditions were used throughout:

Organic/aqueous (O/A) ratio	1:1
Temperature	23-24°C
Stirring time	2-3 min

Separate tests showed that equilibrium was established in <0.2 min, so it would be possible to operate with very short contact times between the phases.

It will be observed from the curves that log D is approximately a linear function of pH at the lower pH's, while at the higher pH's the curves tend to level off, and in the case of Ca, they pass through a maximum at pH 3.2. Since all the metals are divalent, one might have expected the slopes of the linear parts of the curves to be 2, but in fact those for Co and Mg are close to unity, most lie between 1 and 2, and only that for Zn with 0.1M HDEHP approximates to 2. However the data are hardly adequate to establish the true limiting slopes, which may in fact be 2 in all cases.

At the higher pH's the organic phase becomes increasingly highly loaded with the extracted metals, and this is presumably the reason for the extraction being less than extrapolation of the linear portions of the curves would indicate. With 0.1M HDEHP and a 1:1 O/A-ratio, the millimolarities of the metals in the organic phase at various pH's are:

pH	Co	Zn	Cu	Mn	Mg	Ca	Total
2.5	0.5	0.3	<0.1	2.3	0.9	2.8	6.8
3.0	1.4	0.3	<0.1	4.8	2.2	4.1	12.8
3.5	3.5	0.3	<0.1	7.4	4.0	3.8	19.0
4.0	9.0	0.3	<0.1	9.6	4.8	2.5	26.2
4.5	(16.0)	0.3	<0.1	11.3	6.0	1.5	(35.1)

and at least twice these concentrations of DEHP must be combined with the metals, which would leave at most 86, 74, 62 and 48% respectively of the HDEHP free. If species of such formulae as MH(DEHP)₃ or MH₂(DEHP)₄ are formed, the proportion of free HDEHP must be still smaller. Indeed from the extent to which the curves level off or turn over as the pH rises, it seems necessary to postulate such species.

The dependence of D on the HDEHP concentration cannot be clearly established from the limited data available, although for Cu, Mn, Mg and Ca, D appears to be proportional to $[\text{HDEHP}]^2$ at the lower pH's. Since HDEHP exists mainly as dimer in the organic phase, this indicates formation of species of the formula $\text{MH}_2(\text{DEHP})_4$, as just suggested. Of practical significance to flowsheet design is the fact that D_{Zn} is less sensitive to HDEHP concentration than are the D-values of the other metals. Extraction of Zn relative to the other metals is thus favoured by lowering the HDEHP concentration, and raising the pH.

The results indicate that it should be possible to obtain a Co/Zn separation without difficulty at a pH of, say, 2.5. For 0.1M HDEHP, D_{Zn} is then 6.2, which is ample for extraction of the Zn, while D_{Co} is only 7.7×10^{-4} , so that Co losses are very small.

4. pH Control during Extraction

The D-values are sensitive to pH changes, and it is necessary to keep the latter within a suitable range during the extraction. Some tests were therefore made of the pH changes that actually occur on adding 0.1M NaOH to the synthetic cobalt feed. Fig.3 shows the results in the absence of HDEHP phase, and Fig.4 the results with an equal volume of an HDEHP phase present.

Fig.3 also includes the titration curve calculated for a dilute strong acid of the same initial pH as the synthetic cobalt feed. Comparison of the two curves shows that 2.75 times as much alkali is required to produce a given pH change in the cobalt feed as in the strong acid. This implies that in the cobalt feed, the stoichiometric concentration of hydrogen ions is 2.75 times the concentration of free (pH-controlling) hydrogen ions. Presumably the remainder of the hydrogen ions are complexed as HSO_4^- . This is not unreasonable in view of the fact that the stoichiometric sulphate concentration is as high as 1.36M; a value of 1.75 for the ratio $[\text{HSO}_4^-]/[\text{H}^+]$ is broadly compatible with known sulphate complexation constants, although an exact calculation is not feasible in such concentrated solutions. Furthermore we may expect the ratio to remain essentially constant so long as the concentrations of the major constituents of the solution do not change appreciably, a condition which is met by the flowsheets under development.

To shift the pH much above the highest value in Fig.3 requires substantial further amounts of alkali. This may be ascribed to cobalt hydrolysis. It appears, however, that this is not a significant effect below pH 6.1.

The additional alkali requirements in presence of an HDEHP phase, as indicated by a comparison of Figs.3 and 4, are due to displacement of hydrogen ions by metals entering the organic phase. For 0.1M HDEHP the amounts displaced are given by twice the total metal concentrations in the organic phase in the table given earlier. These agree satisfactorily with the observed additional alkali requirements:

pH	Alkali requirements, mM/litre			H ⁺ displaced by metals mM/litre
	0.1M HDEHP phase present	No HDEHP phase present	Difference	
3.0	28	4	24	26
3.5	46	5	41	33
4.0	60	6	54	52
4.5	73	6	67	70

The conclusions from these results can be summed up in the equations:

$$2.75 [H^+]_{\text{free}} = [H^+]_{\text{stoichiometric}}$$

and

$$\Delta [H^+]_{\text{stoichiometric}} = -2\Delta [M^{2+}]$$

It is a fortunate feature that the free hydrogen ion concentration changes less than the stoichiometric, since this means that the pH falls less than might have been expected as the metals enter the organic phase.

5. Computer Modelling of the System

The complications introduced by pH changes would make it difficult to represent the system by means of McCabe-Thiele diagrams, although a method could no doubt be devised. Instead the appropriate equations were incorporated in a computer programme, which was run on an IBM 360 computer.

By way of illustration, consider three counter-current extraction stages, the aqueous feed being to stage 1 and the solvent feed to stage 3. Let aqueous concentrations be denoted by c , and organic phase concentrations by Dc , where D is the actual distribution coefficient, assumed equal to the measured equilibrium distribution coefficient. Let the stages be denoted by subscripts, c_1, D_1 etc. and the feed by subscript 0.

Then according to the usual theory:

$$c_0 + e_2 c_2 = c_1 + e_1 c_1$$

$$c_1 + e_3 c_3 = c_2 + e_2 c_2$$

$$c_2 = c_3 + e_3 c_3$$

where $e = Dr$ is an extraction factor, and r is the organic/aqueous phase volume ratio. This gives a decontamination factor

$$c_0/c_3 = 1 + e_1 + e_1 e_2 + e_1 e_2 e_3$$

In the pilot plant runs referred to below the solvent feed was not completely barren, because some Zn remained in the solvent from the stripping (solvent purification) cycle, and the same situation would arise in a full-scale plant. This is readily dealt with by adding a term to the left-hand side of the mass-balance equation for stage 3.

Now in the system under investigation, the D-values and hence the e-values are functions of $[H^+]$, as given by Figs.1&2. Furthermore, the $[H^+]$ values are related to the metal concentrations by the equations given at the end of the previous section. These lead to the result that

$$2.75[H^+]_{\text{free}} + 2\sum c,$$

where \sum refers to summation over all the (divalent) metal species concerned, has a constant value throughout the system, i.e. in the feed and in each of the stages. $-\log[H^+]_{\text{free}}$ can, of course, be identified with the pH.

We have thus $s(n + 1)$ relations between the $s(n + 1)$ unknown concentrations, where s is the number of stages and n is the number of metals concerned, so a complete solution is possible. Solving of the $s(n + 1)$ equations has been effected by an iterative technique of successive approximation in which the final result was estimated, the equations were solved using this estimate, and the feed composition calculated was compared with the actual feed; the estimate was then continuously revised until the system stabilised.

In order that a preliminary financial evaluation could be conducted, a series of predictions were made, in which the number of stages s , the phase volume ratio r , and the pH of the feed were varied. (It would also be possible to vary the concentrations of minor constituents of the feed, such as Zn, but not those of major constituents, because this would affect all the D-values, as well as the 2.75 factor included above.) Typical results for a three-stage, 0.05M HDEHP/Escaid 100 system, with a feed pH of 6.0, were as follows:

Stage number	r = 0.5				r = 1			
	pH	D _{Zn}	DF _{Zn}	[Co] _{org}	pH	D _{Zn}	DF _{Zn}	[Co] _{org}
1	3.09	10.6	5.1	0.56mM	2.89	8.0	8.1	0.39mM
2	2.85	7.4	21	0.37	2.67	4.6	39	0.25
3	2.62	4.0	65	0.22	2.45	2.45	136	0.17

On the basis of these predictions, a system of three extraction and two stripping stages, with $r = 1$, but using 0.03M HDEHP/Escaid 100, was selected for further study, and some experimental results are reported in the next section. The lower HDEHP concentration was chosen because, as already noted, extraction is less affected by changes in this parameter than is the extraction of the other metals concerned. The fall in D_{Zn} can readily be counteracted by a slight rise in pH (ca. 0.2 unit), and the lower extractions of the other metals then lead to reductions in HDEHP inventory and in strip acid requirement.

Further work to optimise the flowsheet conditions will be attempted in due course, when the pilot-plant runs have been completed.

6. Three-stage Countercurrent Extraction

In order to check the conclusions reached, two manually operated, three-stage, countercurrent extraction runs at 25°C were carried out simulating flowsheet conditions. The three stages were filled initially with 0.05M (first run) or 0.03M (second run) HDEHP/Escaid 100 and synthetic cobalt feed at an O/A ratio of 2:1. In stages 1 and 2, the cobalt feed had previously been shaken once with an equal volume of fresh HDEHP/Escaid 100, in order to start the experiment a little nearer to the final steady state than would otherwise have been the case; but in stage 3, the cobalt feed was untreated. First, the three stages were stirred for 2 min to bring them to equilibrium. Next, the organic phases were each moved onwards one stage in the 1 → 3 direction, fresh solvent being added to stage 1, and the aqueous phases were moved in the opposite direction, fresh cobalt feed being added to stage 3. A second equilibration was then carried out, and so on. The pH and the Zn level of the aqueous phase from stage 1 were measured after each operation, with the following results ($DF_{Zn} = [Zn]_{initial} / [Zn]_{emerging}$):

Equilibration number	First run (0.05M HDEHP)		Second run (0.03M HDEHP)	
	pH	DF_{Zn}	pH	DF_{Zn}
1	2.42	28	2.72	7
2	2.28	103	2.44	97
3	2.28	93	2.43	103
4	2.28	219	2.49	199
5	2.28	236	2.49	184
6	2.28	287	2.50	228
7	2.30	327	2.50	271
8	-		2.49	312

At the end of each run, further measurements were made with results as follows (computed figures for first run in brackets):

Stage number	First run (0.05M HDEHP)			Second run (0.03M HDEHP)		
	pH	D_{Zn}	Co in solvent (ppm)	pH	D_{Zn}	Co in solvent (ppm)
1	2.30 (2.29)	1.6 (1.4)	5.2 (7.4)	2.48	1.6	5.2
2	2.43 (2.49)	3.1 (2.9)	9.2 (10.9)	2.70	3.2	9.6
3	2.72 (2.71)	5.4 (5.2)	6.5 ? (16.2)	2.92	5.9	15.7

It will be noted that the pH values levelled off quite quickly in both runs, indicating that a steady state had been reached as regards the major constituents of the system. The pH's remained high enough to give reasonable Zn extraction throughout, with decontamination factors well above the required value of 50, and still rising at the end of each run; the computed value for the first run was 237. Loss of Co to the solvent was very low.

Further tests have been made in a mixer-settler pilot plant, with three extraction and two stripping stages. The results at the end of a typical run are shown in Fig. 5. As a matter of operational convenience the stripping solution was recycled throughout the run, so the Zn built up continuously in the stripping cycle, and an increasing quantity of Zn was fed back to the extraction cycle in the organic solvent. Despite this, a decontamination factor of 82 was still being achieved at the end of the run. In actual plant operation, a fraction of the strip liquor would be bled off continuously, and this would limit the build-up of Zn. Co losses were <0.1%. The results are generally in accordance with expectation, although a full comparison with theory is not possible at the time of writing because distribution data for 0.03M HDEHP are incomplete.

7. Conclusion

The results show that the Co stream can be purified from Zn at the level tested, under conditions similar to those of the run in Fig.5.

Engineering data for mixer-settler design and phase entrainment data are being obtained in conjunction with the chemical information. Estimates of operating costs, based on the data so far to hand, are in the range £2-3 per tonne of Co treated.

Acknowledgements

The authors thank Charter Consolidated Limited for permission to publish this paper.

Reference

- (1) L.F. Cook and W.W. Szmokaluk, ISEC - 71, p. 451.
- (2) J.A. Partridge and R.C. Jensen, J. Inorg. Nucl. Chem., 31, 2587 (1969).

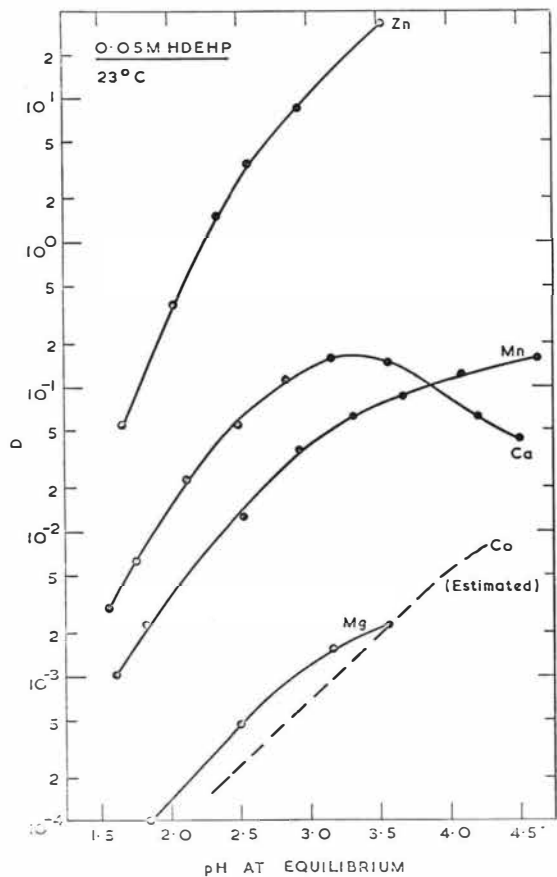


FIG. 2. EXTRACTION FROM COBALT FEED SOLUTION.

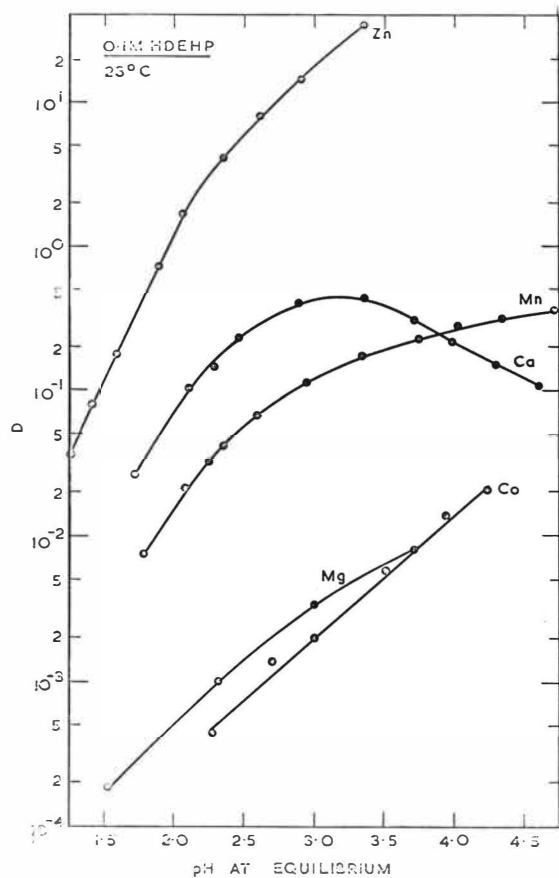


FIG. 1. EXTRACTION FROM COBALT FEED SOLUTION.

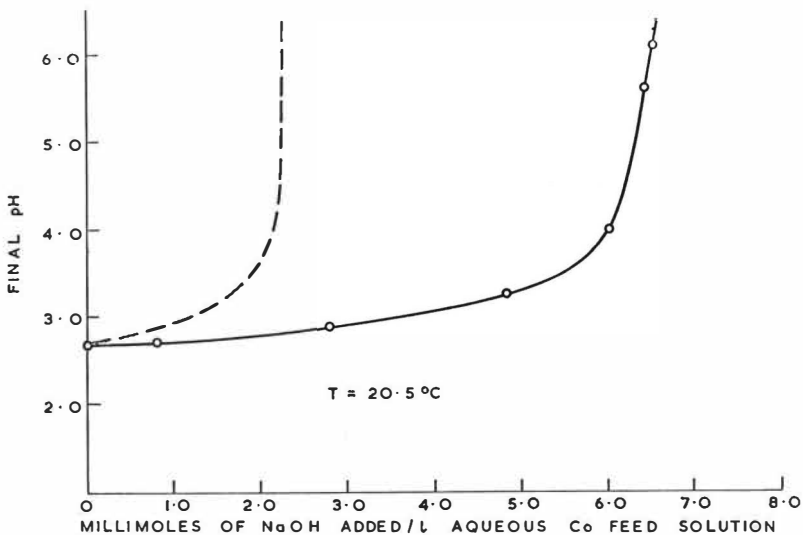


FIG. 3. ADDITION OF ALKALI TO COBALT FEED SOLUTION.

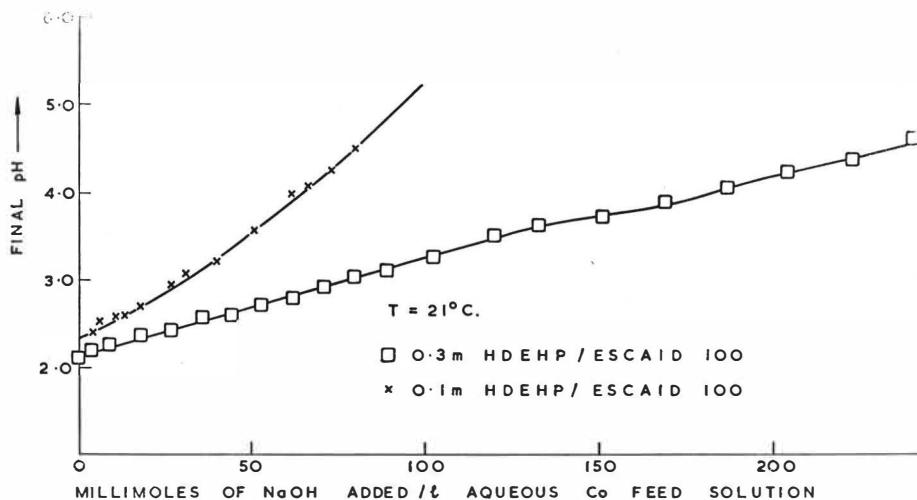


FIG. 4. ADDITION OF ALKALI TO COBALT FEED SOLUTION IN THE PRESENCE OF EQUAL VOLUME OF HDEHP.

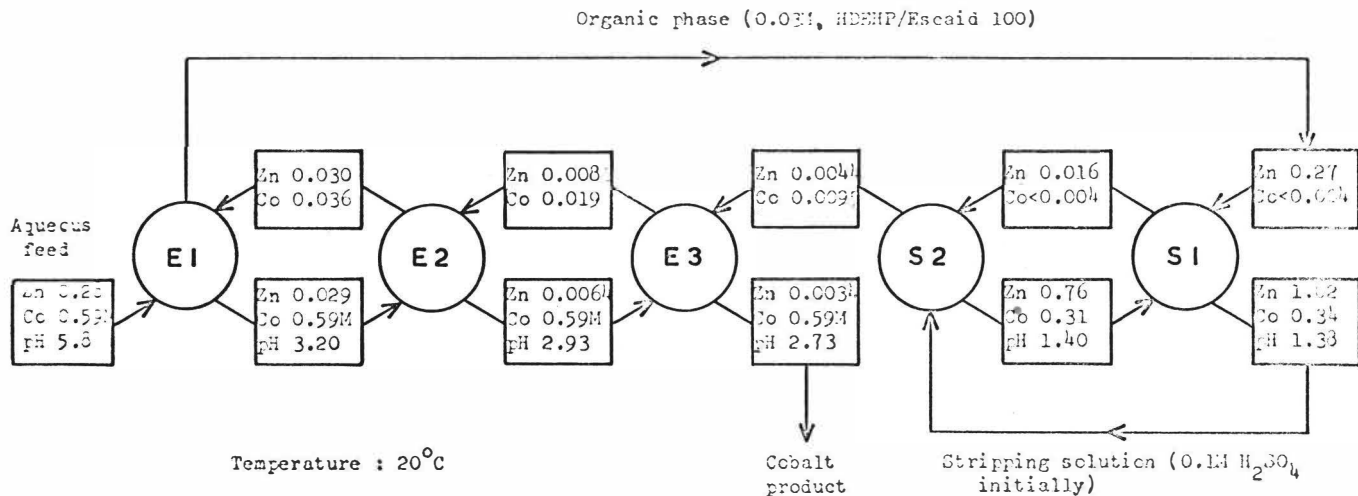


FIG. 5. RESULTS AT THE END OF A TYPICAL PILOT-PLANT RUN. Zn AND Co CONCENTRATIONS IN mM, EXCEPT WHERE OTHERWISE INDICATED. AQUEOUS FEED ALSO CONTAINED Mn, 0.042M; Mg, 0.37M; AND Ca, SATURATED WITH Ca SO₄.

EXAMPLE OF NITRIC ACID RECOVERY
BY SOLVENT EXTRACTION

J.M. DEMARTHE - M. TARNERO - P. MIQUEL - J.P. GOUMONDY

Commissariat a l'Energie Atomique
Department de Genie Radioactif

C.E.A.
B.P. No. 6
92260 - Fontenay-aux-Roses
FRANCE

ABSTRACT

A process for the recovery of nitric acid by solvent extraction from nickel sulphate solutions containing this acid is described. The solvent is TBP 50% - dodecane. The process includes one extraction, and two stripping, producing HNO_3 1.5 N and HNO_3 3 to 5 N. Bench-scale tests, with mixer settlers, pilot tests with pulsed columns and an asymmetric rotating disc contactor (ARDC-Luwa) have shown that the cost of solvent losses is less than 0.02 F/kg of nickel.

INTRODUCTION

The industrial recovery of acids by solvent extraction was proposed as early as 1948. At that time Smith and Page (1) were already mentioning that long chain amines could be used to extract hydrochloric acid from the hydrolysates of gelatin and casein. A process for the recovery of hydrofluoric acid, giving an anhydrous acid by trilaurylamine was developed in Great Britain (2) (3). Israel Mining Industries (I.M.I.) uses a mixture of alcohols in $\text{C}_4 - \text{C}_5$ to extract the phosphoric acid produced by the hydrochloric attack of phosphate rocks; other industrial processes also use various solvents to extract phosphoric acid for the purpose of purification (4). The extraction of HCl by amyl alcohol is used by I.M.I. in the industrial production of potassium nitrate; the $\text{KCl} + \text{HNO}_3 \xrightarrow{1} \text{KNO}_3 + \text{HCl}$ reversible reaction is made total in direction (1) by extracting the HCl produced with alcohol (5). Finally Crittenden and Hixson (6), have suggested a process for the recovery of hydrochloric acid comprising the extraction of this acid with iso-amyl alcohol.

The Societe Le Nickel and the C.E.A. have jointly developed in the laboratory, and tested in a pilot plant, an extraction process for denitrifying a nicheliferous solution resulting from the nitric attack of a sulphide concentrate. This denitrification forms part of a project for processing nickel that comprises the stages shown in the simplified diagram of figure 1.

A preliminary examination showed that the HNO_3 extraction and stripping operation with tributyl phosphate seemed to be technically and economically feasible, providing that:

- the right operational mode was found to recycle all the nitric acid in the sulphide solubilisation process ;
- sulphuric acid was added to the nickel solution to displace the nitrates ;
- an extraction apparatus that could be sealed up for high throughputs was available.

We sought a scheme compatible with the constraints, determined the optimum operational conditions on a computer, carried out experiments in laboratory mixer-settlers (to a scale of 1:30,000), before testing the scheme finally chosen by an extended test in a 1:3,000 scale pilot plant. Lastly, we began the work on the study of extrapolating the type of liquid-liquid extractor chosen.

1. DEFINITION OF A PROCESS ADAPTABLE ON AN INDUSTRIAL SCALE

The definition process sought is the one which, allowing for the various industrial constraints, enables one to obtain maximum yield at minimal operational costs. In point of fact, this generally results in finding a compromise solution from among the various technical and economic considerations.

Thus, in the case of HNO_3 extraction and stripping, the problem amounts to setting two essential targets :

1. first sufficiently denitrifying the nickeliferous solution; the maximum permissible concentration of nitrates in the nickel solution intended for electrolysis is around 500 mg/l;
2. then recovering the stripped nitric acid for re-use attacking the sulphides.

These objectives lead us to consider the constraints of the entire nickel production process and, inter alia, those linked to the sulphide attack conditions and the constraints inherent in the physical and chemical nature of the tributyl phosphate-nitric aqueous phase system.

A) Adapting the process of the constraints

1) Constraints on the process as a whole

Figure 2 shows the general diagram for acid attack. The nitric acid must be 8 N and it is maintained at this normality by the direct additions of acid and the returns from the recovery column of nitrous gases (HNO_3 , 14 N). (The solving of the balance equations shows the need to use highly concentrated nitric acid at the intake of the attack tanks (3 to 5 N) and the advantage of adding diluted acid to the columns).

2) Constraints at solvent extraction level

For obvious reasons of economy, over 90% of the nitric acid must be recycled, but the considerations mentioned above show that most of the recycled acid must have a concentration of 3N (3 to 5N). Therefore it will be necessary to obtain a large recovery of acid at this concentration by adjusting the ratio of the aqueous phase-organic phase volumes, the excess sulphuric acid added on extraction, the number of extraction stages, the temperature, etc.

B) Extraction and stripping scheme

Owing to the above mentioned constraints, a "reflux" scheme must be used at the extraction stage comprising of the recycling of part of the acid at the hydration while at the stripping stage, a scheme with intermediate drawing off the diluted acid (figure 3) is necessarily employed.

This is the general diagram that we are going to define in detail in the following lines.

c) Determining the optimum conditions

1) Isotherms for the division of the nitric acid between the tributyl phosphate and the HNO_3 , H_2SO_4 and NiSO_4 for various sulphuric acidities

It emerges from the above considerations that there are two parameters based on which it is possible to adjust the denitrification process : i.e. the reflux and the amount of H_2SO_4 added before extraction.

The reason for this is that the nitric acid partition isotherms determined experimentally at the C.E.A. (figure 4) show that the addition of sulphuric acid assists HNO_3 extraction, giving nitric recovery at high concentration. But it can become an economic disadvantage ^x which must be reduced to a minimum. Thus, in order to obtain sufficiently concentrated nitric acid at the first stripping (3 to 5N) - see section A-1), it is necessary to work very close to the solvent saturation point.

Two variables are available for this:

- the reflux of part of the nitric acid stripped on hydration
- the addition of sulphuric acid to increase the extraction.

2) Optimisation of the process

Linear programming and computer calculations which need no describing here have been used for determining the optimum conditions of the extraction and double stripping schemes, making due allowance for the various technical and economic constraints. Only the main conclusions stemming from this optimisation are mentioned here.

Acid at two different concentrations must be recovered on stripping : 1.5N and 3 to 5 M according to the amount of nitrate coming from the attack.

The concentration of the necessary excess sulphuric acid must not be less than 1.5N. It will be necessary to exceed this concentration, i.e. around 2 to 3N.

In any case the total number of stages required is very high (30 to 35), unless it is possible to add a high sulphuric acid excess on hydration.

The complete recovery of the nitrates coming from the tanks seems possible; yet, as could be foreseen, the greater the amount to be recovered, the more difficult it is to achieve optimum conditions. If the quantity of nitrates to be recovered is of the order of 2M on coming from the attack, these nitrates can be recycled by adding a quantity of sulphuric acid of the order of 1.5 N. Extraction and stripping are done at ordinary room temperature in banks totalling 30 stages.

On the other hand, if the quantity of nitrate to be recovered is around 3 M on coming from the attack, it will be necessary to add much more sulphuric acid (2.5 N) or accept losing some of the nitric acid used in the process.

The reduction in the hydration flow appears to facilitate the recovery of the nitrates,

At this stage of the study, the conclusions emerging from the calculations have still to be checked experimentally, and the predictable solvent losses evaluated.

D) Experimentation of the optimum scheme in a mixer-settler bank to a scale of 1:30.000.

1) Operating conditions

The experiment was made in AT.1 mixer settlers (capacity 2 -2 1/h). The solvent used, TBP 50% diluted in dodecane, has a low enough specific gravity to ensure good hydraulic working of the mixer-settlers and sufficient enough dilution to limit to the minimise any entrainments and losses in the aqueous phase.

The experiments is kept going continuously for at least 48 hours for the mass equilibria balances to be reached and 200 hours at the most to test the process and examine the subsidiary phenomena and the reliability of the process.

2) Characteristics of the tests carried out

Many approach tests were carried out, but mention will be made only of the most important, particularly the tests annotated I and II on figure 5, which enabled us to adjust or check the temperature conditions, the number of stages, the flow ratio or the sulphuric acid concentrations by changing the concentration of nitric acid to be extracted.

The extended experiment was undertaken with flow diagram I, the solvent was recycled without passing through a basic processing stage.

3) Results

In general the results confirmed the calculation data.

During the extended test we were particularly able to verify:

- a) that the concentration profiles in the stages agree with the results expected; all the stages used are necessary and the diagram is optimum:
- b) that the system is stable; nitrate leaks in the raffinate never exceeded 500 mg/l
- c) that the silica precipitations in the inter-phases are avoided by the addition of HF,
- d) that solvent losses are low. These losses measured in:
117 l of raffinate (extraction)
37 l of concentrated acid and
60 l of diluted acid (stripping)

were respectively 25, 50 and 50 mg/l by solubility and 7 mg/l, 1 mg/l and 1 mg/l by entrainment, which finally represent losses of less than 1 g of tributyl phosphate per kilogram of processed nickel.

During test II, confirmation was obtained that there is total recovery of the nitric reagent when nitrate concentration before hydration is around 3N.

II - PILOT PLANT TEST

- A) Experimentation of the optimum flow scheme in pulsed columns to a scale of 1:3,000

1) Equipment

The extraction, and stripper I and stripper II columns with an internal diameter of 45 mm and 6, 4 and 6 m long respectively are fitted with perforated stainless steel trays 50 mm apart and 23% perforations. Pulsation is ensured by compressed air pressure on a side leg. Stripping column II is heated to 40°C by five 200 mm long double jackets, regularly spaced along the column, with hot water circulation.

The extraction column functions in continuous organic phase (interphase at the bottom) and the stripping columns in continuous aqueous phase (interphase at the top of the column).

Finally a single stage mixer-settler ensures the alkaline treatment of the solvent (between stripper II and recycling for extraction).

2) Operating conditions

Short-duration preliminary tests enabled us to determine the operating conditions of the columns (pulse amplitude and frequency giving the theoretical number of stages to make the optimum scheme defined by calculation and experiment in the mixer-settlers. These conditions are shown in table 1.

TABLE 1

Operating conditions of the pulsed columns and the mixer-settler

Conditions	Pulsed columns			Mixer-settler
	Extractor	Stripper I	stripper II	(solvent treat- ment)
Pulse amplitude (cm)	2,5	1	1	--
Pulse frequency (mm min)	100	50	100	--
Aqueous phase flow (1/h)	8,9	3	7,55	7,55
Solvent flow (1/h)	15,1	15,1	15,1	7,55
Operating temp- erature (°C)	average 23°C (heating due to chemical reactions)		ambient 40°C	ambient

3) Results - Solvent losses

The preliminary tests were followed by an extended test (62 hours) to test the stability of the scheme, assess the solvent losses by physical entrainment and degradation, and to study the gradual formation of the interphase precipitates, or "sludge" on extraction. The main results were as follows:

a) Extraction

The average value of the nitrate concentration in the raffinate was 190 mg/l, under the set limit of 500 mg/l. The corresponding number of theoretical stages is between 13 and 14, or a height equal to a theoretical height (HETS) of 43 to 46 cm.

b) Stripper 1

The stripped nitric acid is 3.13 N, corresponding to a theoretical number of stages of 7, to 8, or an HETS between 50 and 56 cm.

c) Stripper II

The stripped nitric acid has an average concentration of 1.43 N, the used solvent coming out at less than 10^{-3} of HNO_3 . This corresponds to over 9 theoretical stages, or an HETS of less than 67 cm.

d) Solvent losses

The TBP lost by solubility and that lost by solubility plus physical entrainment was determined. With the pulsed columns and mixer-settler used, the losses by entrainment were less than 10 mg/l. The losses by solubility for the first stripping, the second stripping and the extraction were respectively: 220 mg/l, 270 mg/l and under 75 mg/l. During the TBP concentration time no increase was found in the sodium carbonate of the solvent degradation. The solvent losses vary between 2 g and 2.5 g of TBP per kg of nickel product.

4) Conclusion

These pulsed column tests provided information on the chemistry of the process, particularly on solvent losses. On the other hand, in view of the maximum permissible flows in pulsed columns ($10 \text{ m}^3/\text{h}$), there is no question of envisaging this type of extraction equipment for use on an industrial scale. This is why for this reason we also made extraction-stripping tests in the optimum scheme conditions with a stirred column of the ARD-LUWA type with which total flows exceeding $100 \text{ m}^3/\text{h}$ may be achieved.

B) Experimentation of the optimum scheme in a 1:300 scale
ARD-LUWA column

1) Description of the apparatus

The ARD extractor is composed of a vertical cylindrical column (in glass for the pilot apparatus used). This column is separated into two parts by a vertical partition that defines a mixing area and a peripheral phase separation area. Each of these area is itself divided into several compartments by horizontal flanges.

In the middle of each mixing compartment there is an horizontal disc.

All these discs are fixed to a vertical spindle which revolves and stirs the phases, this spindle being off centre in relation to the column.

Characteristics of the apparatus used

The pilot apparatus used is an ARD 150-3000 having the following dimensions:

- total height of the column : 4.7 m - diameter 150 mm
- height of the stirred area (effective height): 3m
- upper settler: 1 m - lower settler: 0.7 m
- stirring discs : 75 mm diameter, apportioned along the stirring spindle at the rate of 25 per metre, Rotation rate between 125 and 1000 rev. min.
- height of mixing and settling compartments : 40 mm

The column has two taps for drawing samples.

The diagram of the apparatus and its main dimensions are shown in figure 7.

2) Height transfer units-extrapolation

The change in the efficiency of the extractor has been determined in terms of the rate of rotation ω for two specific flows of 1 and 1.5 l/h and organic flow ratios of 1.7 and 2. aqueous

For this number of theoretical stages (NTS) and the height equivalent of a theoretical stage (HETS) as well as the mean height of transfer unit (HTU) and the number of transfer units (NTU) were determined from the experimental results.

The results obtained are shown on tables II, III and IV.

The height of transfer unit, which is already linked to the over-all transfer coefficient and the specific exchange area, may be expressed in terms of the stirring power per volume unit.

Hence:

$$HTU_{(a)} = Cte \left(\frac{D^{0.4} \omega^2}{D_c \gamma_{hm} s} \right) C \quad (2)$$

where $HTU_{(d)}$ = height of transfer unit for the dispersed phase
(in this case the aqueous phase)

D_r = diameter of stirring discs

D_c = diameter of the column

h_m = height of a mixing compartment

= rate of rotation

$\alpha, \beta, \gamma, S^M$

= numerical constants depending on the hydrodynamic operating regime.

If the HTU in terms of the rate of rotation for the three tests is entered on the co-ordinate, a linear relation is in fact obtained, as shown in figure 9. Constant C, which enables the change in efficiency of the diameter to be calculated, is determined from the slope of these straight lines.

There is in fact an equation of the following type:

$$\frac{HTU_{D_2}}{HTU_{D_1}} = \left(\frac{D_2}{D_1} \right)^{-C}$$

for two appliances working at the same specific flow and same dispersion regimes.

HTU_{D_1} being the height of transfer unit of the D_1 diameter extractor

HTU_{D_2} being the height of transfer unit of the D_2 diameter extractor

For the system considered, it was found that the height of transfer unit varied significantly with the square root of the diameter.

These results would theoretically enable the design of columns 1.5 m in diameter to be calculated which would be suitable for industrial scale production. Nevertheless several comments must be made:

- the experimental column used has only 3 meters of effective height. But, it has been noticed that the dispersion of one phase in the other took place over a relatively important height of between 0.5 and 1 m.

- the play between the horizontal partitions and the cylinder of the column, which is in non-graduated glass, creates preferential passages detrimental to efficiency. The relative importance of this play increases as the diameter of the column diminishes.
- the Extraction and stripping schemes are "pinching" hence an error in the number of transfer units (NTU) can be very significant if the HNO_3 distribution curves chosen for the calculation stray, even in a small way, from actual operational conditions, for instance because of the temperature changes along the column or due to chemical reactions or for any other reason. Because of this possibility of error we were unable, inter alia, to calculate the NTU's and HTU's for stripping conditions, where the "pinching" between equilibrium curve and the operating line is the most sensitive.

For all these reasons, it is probable that the results obtained are pessimistic; it would be advisable to check them with a larger apparatus by making a tight seal between the trays and the walls of the column and by improving the quality of dispersion on intake and by choosing extraction or stripping/scheme for the tests leading to greater accuracy with respect to the calculation of the NTU's.

3) Solvent losses

These losses are under 75 mg/1 on extraction and 220 mg/1 on each stripping (losses by entrainment plus solubility). This is equal to 2 g of TBP per kg of treated nickel. The values found are appreciably equal to those obtained with pulsed columns.

III - GENERAL CONCLUSIONS

A process by denitrification to solvent solutions of nickel sulphate containing nitric acid has been developed in the laboratory and in a pilot unit. To meet the many constraints of the process as a whole, a computer optimisation programme was necessary. The resultant scheme, based on the utilisation of TBP 50% - dodecane, produced denitrified solutions at under 500 m/1 of nitrate. Further it comprises a double stripping stage, allowing the nitric acid to be recovered at two concentrations.

In the laboratory, in mixer-settlers, as in pilot units (pulsed columns, ARD-LUMA extractors) solvent losses amount to less than 0.02 F par kg of treated nickel.

Allowing for the prescribed flow rates, it seemed worthwhile using ARD-LUMA columns on an industrial scale. A start was therefore made on the extrapolation studies of these equipments to a scale of 1:300: determination of the height of transfer units ; experimental determination of the constants enabling the results found to be extrapolated.

TABLE 2

Extraction test 1 - $V_c + V_d = 1 \text{ l/h cm}^{-2} - \frac{0}{A} = 1.7$

NTS , HETS, NTU and HTU changes with the rotation rate ω

ω in rev/min	NTS	HETS in cm	NTU	HTU in cm
160	2,2	136	4,2	71
224	2,8	107	5,3	57
288	3,5	86	6,7	45
352	4,7	64	9,4	32
416	6,2	48	12,5	24
480	6,7	45	14	21,5

TABLE III

Extraction test 2 - $V_c + V_d = 1 \text{ l/h. cm}^{-2} - \frac{0}{A} = 2$

NTS, HETS, NTU and HTU changes with rotation rate

ω in rev/min	NTS	HETS in cm	NTU	HTU in cm
250	3,5	86	7,1	42
325	4,6	65	10	30
400	7	43	13,6	22
475	8	37	15,8	19
550	8	37	16,7	18

TABLE IV

$$\text{Extraction test 3} - V_c + V_d = 1.5 \text{ 1/h cm}^{-2} - \frac{0}{A} = 2$$

NETS, HETS, NTU and HTU changes with the rotation rate ω

ω in rev/min	NETS	HETS in cm	NTU	HTU in cm
175	2,3	130	5	60
250	3,5	86	6,7	45
325	5	60	9,5	31,5
400	6,5	46	12,2	24,5
475	7,7	39	15,8	19

BIBLIOGRAPHICAL REFERENCES

1. E.L. SMITH - J.E. PAGE
The acid binding properties of long-chain aliphatic amines
J. Soc. Chem. Ind. (London) 67, 48-51 (1948)
2. Anonymous
Brit. Chem. Engng 6 (10) 670 (1961)
3. W.H. HARDWICK - P.F. WACE
Hydrofluoric acid recovery by amine solvent extraction
Chem. and Proc. Engng. 46, 283-93 (1965)
4. R. SLUMBERG
Industrial extraction of phosphoric acid. Solvent extraction
Revs. 1 (1) 93-104 (1971)
5. J. INGHAM
Solvent extraction in Israel. Chem. and Ind. 44 1863-7
(Nov.4, 1967)
6. E.G. CRITCHEMEN - A.N. HIXSON
Extraction of hydrogen chloride from aqueous solutions.
Ind. and Eng. Chem. 46, 265 (1954)
7. T. NISEK - J. HAREK
Asymmetric rotating disc extractor.
Brit. Chem. Engng. 15, 202 (1970)

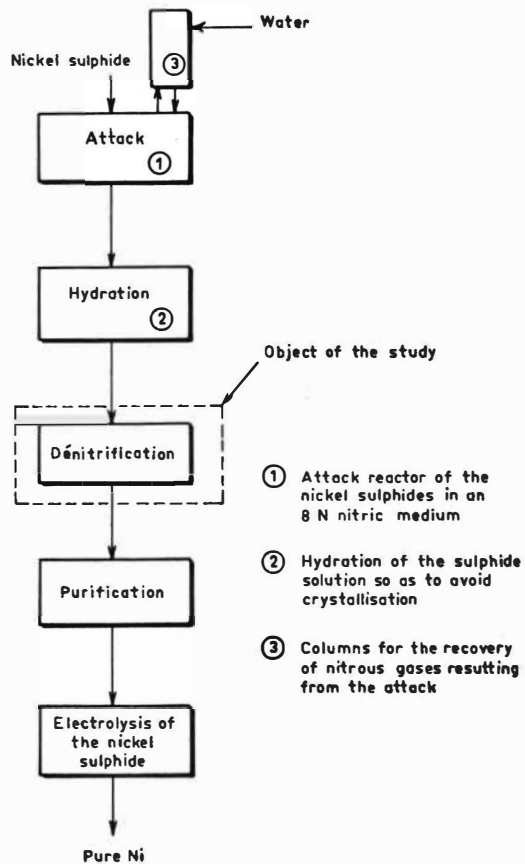


Fig.1. Diagram for the preparation of nickel from sulfide concentrates

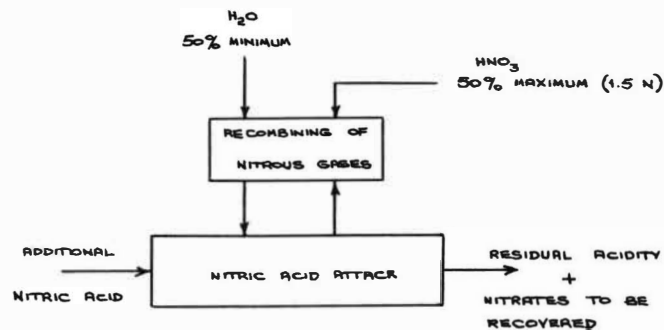


Fig.2. Dissolution process

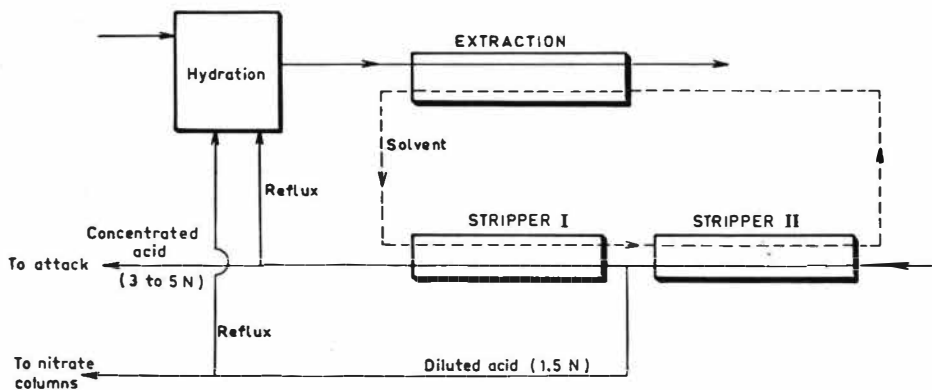
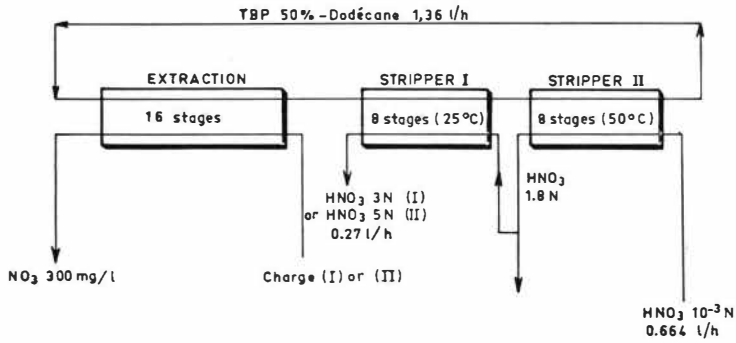


FIG. 4. Extraction and re-extraction of nitric acid.



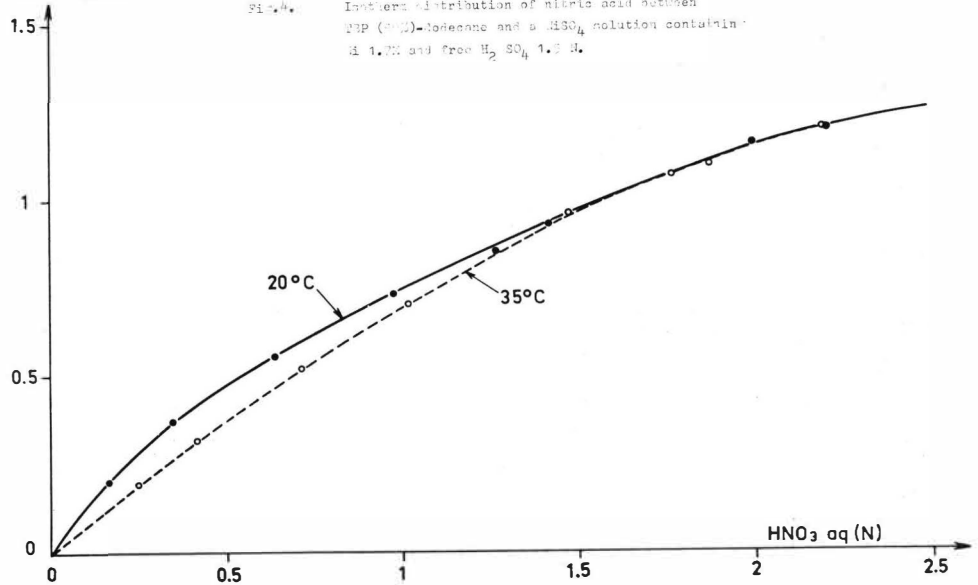
Scheme I - Charge: H_2SO_4 1.52 N free
0.8 l/h

Minimum recovery case

Scheme II - Charge: H_2SO_4 2,5 N-2.6 N free
0.8/h

Maximum recovery case

HNO_3 org. (N)



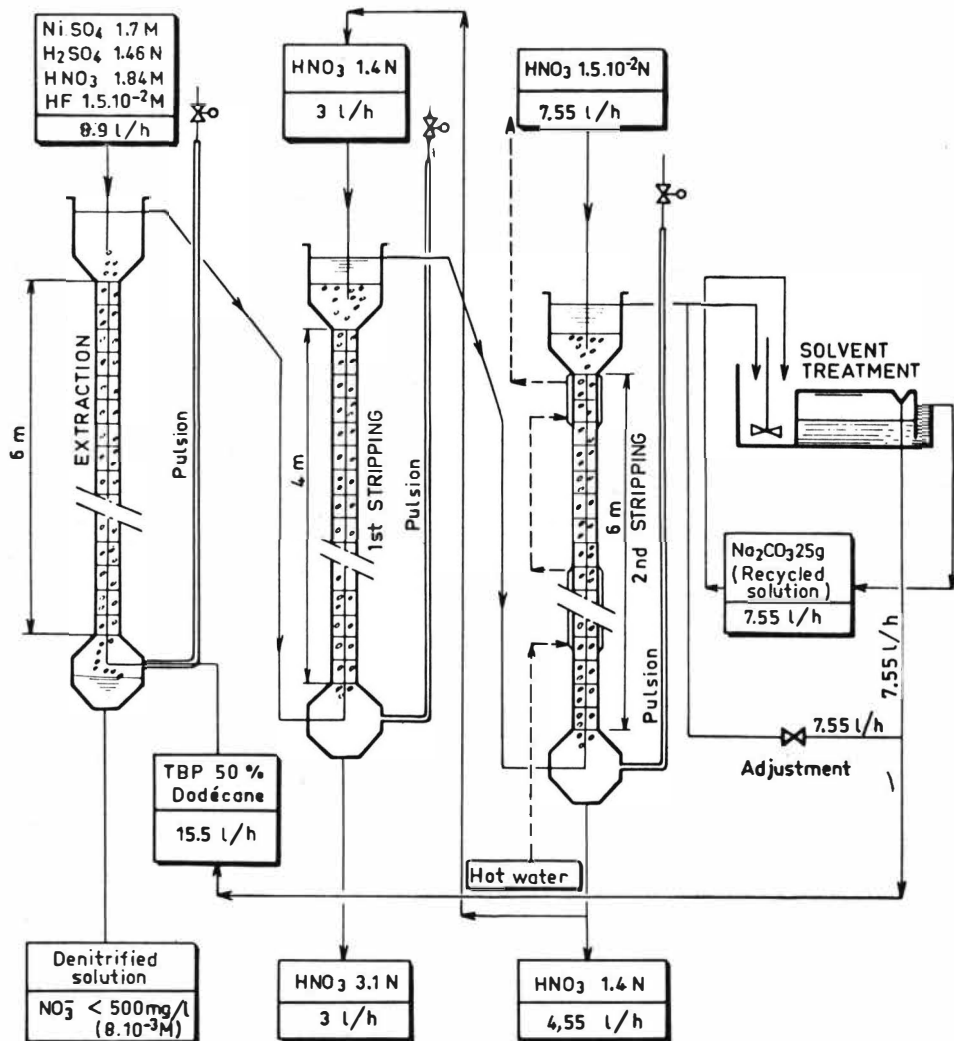


Fig. 5. Scheme used in pulse columns

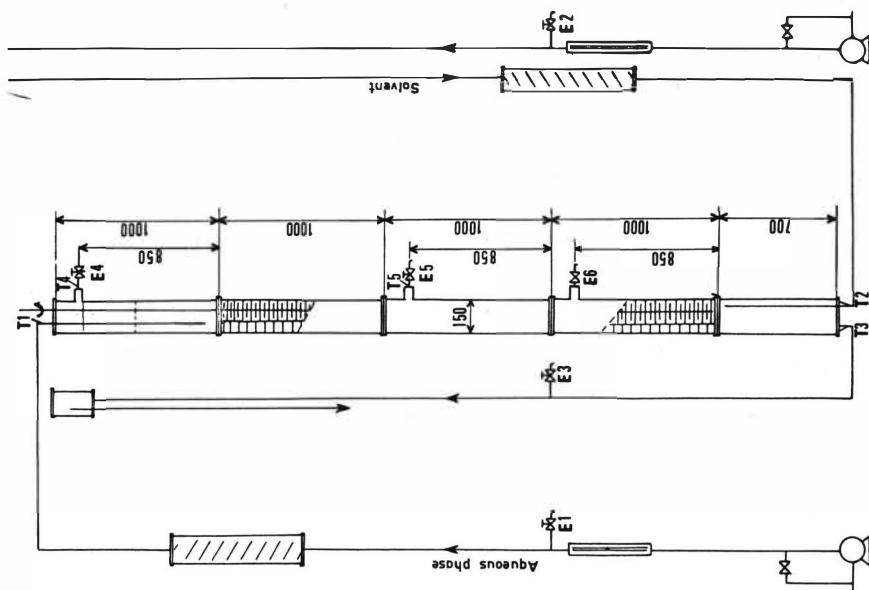


Fig. 7
Column LUT-A 150/3000

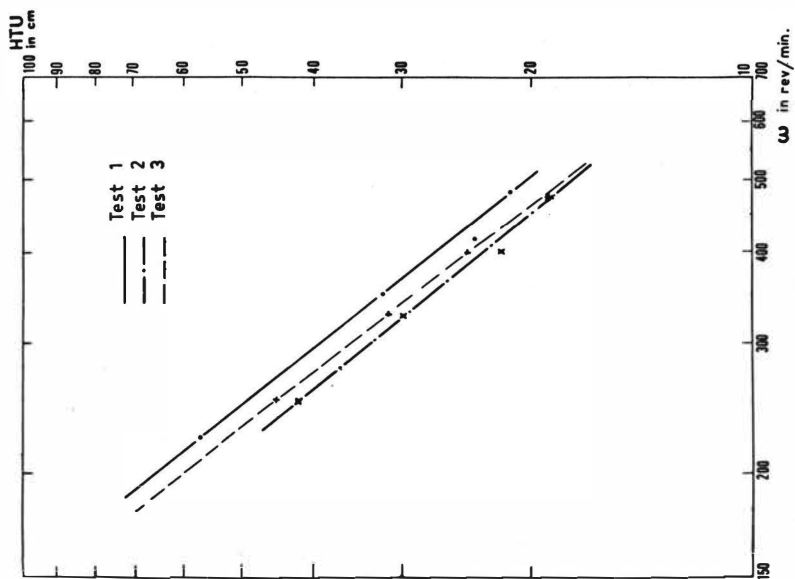


Fig. 8
Variation of HTU with ω

SESSION 12

Tuesday 10th September: 14.00 hrs

E Q U I P M E N T

(Axial Mixing Phenomena)

Chairman:

Professor G.V. Jeffreys

Secretaries:

Dr. J. Ingham

Mr. M. Perrut

Backmixing in a Kühni Liquid-Liquid Extraction Column

by

J. Ingham*

J.R. Bourne**

A. Nögli***

Abstract

New data on the continuous phase backmixing in a 150 mm diameter Kühni liquid-liquid extraction column are presented for conditions of both single phase and two-phase countercurrent flow operation. The results show similar tendencies to those found previously for other types of mechanically agitated column.

* Post-graduate Schools of Chemical Engineering,
The University of Bradford, UK.

** Technisch-Chemisches Laboratorium,
E.T.H. Zurich, CH 8006

*** Kühni AG, Basle, CH 4123

December, 1973

Summary

Preliminary studies of the continuous phase backmixing characteristics of a mechanically agitated liquid-liquid Kuhn extraction column with variable stator plate and rotor geometry have been carried out, based on the system deionized water-odourless kerosene. The results, when correlated by the one-dimensional axial diffusion model, show similar characteristics to those found in other forms of mechanically agitated extractor. The continuous phase backmixing in the two phase system is well correlated, over the normal range of operating conditions, by the equivalent single phase backmixing relationship when modified by the inclusion of an average holdup value for the dispersed phase. Measurements of the average dispersed phase holdup were also well correlated through the characteristic velocity relationship proposed by Misek (1).

1. Introduction

The deleterious effects of backmixing on the mass transfer performance of liquid-liquid extraction equipment is now generally well known. Considerable advances have been made in the development of relevant mathematical models and appropriate calculation procedures, allowing for the effects of backmixing. These have been well reviewed recently by Misek and Rod (2). Two forms of model are most commonly employed for solvent extraction applications. These are the stagewise model, with backmixing, and the axial dispersion flow model. Although both models give approximately equal results under the highly dispersive conditions commonly encountered in agitated column extractors, the axial dispersion flow model is most commonly preferred (3,4,5,6,7). In this model, the various contributions causing deviations from plug flow are all assumed to follow an eddy diffusion relationship, analogous in form to Ficks Law for

molecular diffusion, but in which the dispersion is characterised by a constant value of an eddy diffusion coefficient, appropriate to the given conditions. Unfortunately there still remains a considerable dearth of information concerning the extent of backmixing in many types of contactor. The Kuhni liquid-liquid extraction column represents an apparatus of considerable industrial importance for which a substantial amount of other fundamental operating data have been obtained (8,9,10, 11,12). A correct scale up of pilot scale laboratory results requires full allowance for the effects of backmixing. It was therefore decided to study the backmixing characteristics of a 150 mm diameter extractor of the scale most commonly used for preliminary process studies. Unfortunately it was necessary to restrict the work initially to a consideration of the water-kerosene system although it is realised that potentially important effects of differing system physical properties may have been neglected. It is hoped that a systematic study of the effect of physical property changes on the backmixing in agitated contactors will be carried out later under the programme proposed by the European Federation of Chemical Engineering (13).

2. Experimental

The main apparatus consisted of a standard E150/13 pilot plant extraction column of Kuhni type construction, 150 mm in diameter and containing 18 compartments, each of height 68.5 mm. The agitation in the compartments was effected by means of centrally located shrouded turbine type impellers of the type illustrated in Fig. 1. Three sets of rotors with varying heights of turbine blade, as shown in Fig. 1, were employed. The geometry of the stator plates, bounding each of the column compartments, was also varied during the course of the experiments in order to give differing free areas for flow. These are

illustrated in Fig. 2. A typical arrangement of impeller and adjoining stator plates is shown in Fig. 3.

The liquid system consisted of deionized water and Shellsol K odourless kerosene. In all experiments, water was the continuous phase and kerosene was dispersed. The physical properties for the mutually saturated fresh liquid-liquid system at a temperature of 293 K are given in Table 1.

The flow system followed a normal countercurrent arrangement. The water and kerosene feeds to the column were supplied from separate feed tanks via centrifugal pumps, fitted with flow by-pass control arrangements, and rotameters; the dispersed kerosene phase entering at the base of the column through an inlet distributor. The exit kerosene was allowed to overflow by gravity from the top part of the column and to recirculate to kerosene storage. This was fitted with a cooling coil for temperature control purposes. Water leaving the base of the column was regulated by a pneumatic valve, actuated by a float control operating in the liquid-liquid interface, and allowed to discharge to drain.

The degree of backmixing in the column was measured using the steady state tracer injection technique, described many times previously in the literature (4,14,15,16). In this case, a steady and continuous stream of an aqueous sodium chloride tracer solution was injected into the bottom compartment of the column using a metering pump. Under steady state conditions, the concentration of tracer at any point in the column above the point of injection is determined by a steady state balance between the rate of backmixing of the tracer and the rate at which it is swept out of the column by the bulk flow of aqueous phase. Simple relationships may then be easily derived on the basis of the appropriate flow model, from which the relevant backmixing parameters can be determined,

from measurements of the resulting steady state concentration profile of backmixed tracer along the length of the column. For the axial dispersion flow model, it is easily shown that:-

$$\ln \left[\frac{c}{c_0} \right] = - \frac{Uz}{E} \quad (1)$$

The concentration profile of the backmixed tracer was determined by allowing the samples of continuous phase to drip continuously from nozzles located at various positions along the length of the column. On the achievement of steady state conditions, usually following 4-5 column mean residence times, the samples were collected and the concentration of tracer determined by conductivity measurement. Both the rate of tracer injection and the total rate of sample removal were kept at values of less than 1% of the continuous phase feed rate so as not to disturb the column operating conditions unduly.

Average fractional holdup values for the dispersed phase, required in the correlation of the two phase backmixing results, were obtained by measurement of the pressure differential occurring between the extraction column operating under two phase conditions and an equivalent manometric balancing leg of water representing the pressure drop across the effective length of column under single phase operation and equal stirring speed. A detailed description of a more highly refined version of this method, which was used to investigate axial variations of holdup in the Kuhni column, is given by Fischer (12).

3. Results and Discussion

From equation (1), a logarithmic plot of the dimensionless tracer concentration versus distance upstream along the column should give a straight line plot, from the slope of which the eddy dispersion coefficient is easily determined. The excellent experimental agreement so

obtained was taken as sufficient justification for the use of the axial flow model. The steady state injection method for the determination of backmixing is convenient and extremely simple when compared to other methods involving the analysis of unsteady state stimulus-response curves, or the analysis of steady state solute concentration profiles during two phase mass transfer. It should be noted, however, as pointed out by Bleicher (17) that this technique is capable of measuring only those flow mechanisms that are actually capable of causing physical backflow of material, and that therefore some mechanisms contributing to the overall non-ideal flow behaviour may not be detected by this method. For mechanically agitated contactors operating at normal working conditions, however, backmixing is usually dominant. The steady state injection method therefore represents both a convenient and realistic measure of the flow non-idealities in the type of system presently considered.

3.1 Single Phase Backmixing

Fig. 4 shows the variation in the eddy dispersion coefficient with respect to rotor speed. The results in Fig. 4 apply for constant water flowrate and are shown for the four alternative stator plate designs and the standard impeller design with blade height equal to 10 mm. In all cases, the backmixing coefficient was found to increase linearly with increasing rotor speed, with the resulting straight line plots passing approximately through the origin. Fig. 5 shows a plot of the eddy dispersion coefficient versus varying aqueous phase flowrate and constant rotor speed, for the four same compartment geometries. In all cases, the dispersion coefficient was found to be independent of the flowrate of the continuous phase. The behaviour shown in Fig. 4 and 5 is in good agreement with that found previously for RDC (3,4,5) and Oldshue-Rushton contactors (6,7), thus confirming the mechanism of backmixing in mechanically agitated contactors to be rotor dominated. In Fig. 6, the results for

the four same compartmental geometries are correlated on the basis previously found to be suitable for the RDC and Oldshue-Rushton column. The results of the least squares linear regression analysis of the data shown in Fig. 6 are listed in Table 2. As with other forms of mechanically agitated contactor, the degree of backmixing increases with an increase in available free area of stator plate. The relationship however, is not linear, since the backmixing shows a progressive tendency to increase with increasing area. Gutoff (14) showed that, for an Oldshue-Rushton column, the backmixing tends to increase progressively with increasing proximity of the flow opening to the column wall, owing to the strong vertical circulation currents caused there by the deflection of the impeller discharge. The results are rather more difficult to characterise in the Kuhni column, owing to the somewhat variable nature of the stator plate hole arrangement, as shown in Fig. 2. Since this represents an important design characteristic, giving additional flexibility of operation, such that different plate arrangements can be chosen to suit particular process conditions, no attempt has been made to combine the results of the four particular plate designs into a single correlating expression. A further design variable that may be altered to suit particular process conditions is the height of the impeller turbine blades. Table 2 includes results, obtained using the single stator plate opening $Q = 0.236$, and three heights of turbine blades $T = 10, 20, \text{ and } 30 \text{ mm}$ respectively. As expected, increasing the height of the turbines increases the degree of backmixing, but to an extent which is less than that expected from a proportional increase in the rate of turbine discharge.

3.2 Two Phase Backmixing

The continuous phase backmixing studies, under two phase operating conditions, were limited to the two stator plate geometries, $Q = 0.236$,

and 0.41, using the standard turbine impellers of height, $T = 10$ mm. The effect of increasing rotor speed was found to be similar to that previously observed in an Oldshue-Lushton Column (7). This is shown in Fig. 7. At zero or very low rotor speeds, appreciable backmixing in the continuous phase occurred, which was attributable to the entrainment of continuous phase in the wakes of the rising drops of dispersed phase. At higher rotor speeds, the effects of the wake mechanism are reduced, and the effect of the rotor then becomes dominant. At higher rotor speeds approaching flooding conditions, the holdup of dispersed phase builds up very rapidly causing a final reduction in the backmixing. Under normal operating conditions, the degree of backmixing was always found to be less than the corresponding single phase value. The separate effects of increasing continuous and dispersed phase velocities on the degree of backmixing are more difficult to characterise than that of rotor speed. Under normal conditions of agitation, both increasing continuous and dispersed phase velocities cause some reduction in the extent of the backmixing. At very high rotor speeds, increasing dispersed phase velocity causes a correspondingly rapid decrease in the backmixing. It was found, however, that over the normal range of operating conditions, the effects of the two phase operation could be taken into account by the inclusion of an average holdup term in the form of correlation, previously used for the single phase results. The resulting correlation of results for the two phase operating region are shown and listed in Fig. 8 and Table 3 respectively. The agreement in the coefficients of the equations for the single and two phase conditions for the two respective stator plate openings found by the least squares analysis of the results is noteworthy. It should be noted however that the average holdup term represents a very approximate and empirical correction factor. Work by Fischer (12) has confirmed the existence of substantial variations

in the axial holdup for the dispersed phase in the Kuhn column, as found in RDC and Oldshue-Rushton contactors. Average values of dispersed phase holdup, therefore, have only limited theoretical value.

5.3 Correlation of Holdup

The average holdup values were correlated on the basis of the characteristic velocity equation proposed by Kisek (1).

$$\frac{U_{dK}}{X} + \frac{U_{dc}}{1-X} = U_0 (1-X) \exp \left(- \left(4.19 - \frac{Z}{m} \right) X \right) \quad (2)$$

where U_0 represents the equivalent unhindered free fall velocity of a single drop falling in infinite continuous medium, and the term $\frac{Z}{m}$ represents a measure of the coalescence characteristics of the actual droplet swarm. Fig. 9 shows a typical plot of the holdup results, according to equation (2), obtained by keeping rotor speed constant and progressively varying the continuous and dispersed phase flow-rates. Equivalent values of U_0 and $\frac{Z}{m}$ can then be determined from the vertical intercepts and slopes of the respective plots. No attempt was made to correlate these quantities in terms of fundamental droplet behaviour, owing to the restriction of the use of only one liquid-liquid system in these experiments.

Notation

c	concentration of tracer at distance z	kg mol/m^3
c_0	concentration of tracer in feed compartment	kg mol/m^3
CR	least squares linear regression coefficient	
E	backmixing eddy dispersion coefficient	m^2/s
H	axial height of compartment	m
N	rotor speed	s^{-1}
Q	fractional free area for flow of stator plates	
R	diameter of turbine impeller	m
T	height of turbine impeller blades	m
U	superficial phase velocity	m/s
U_W	superficial aqueous phase velocity	m/s
U_K	superficial velocity of kerosene phase	m/s
X	fractional holdup of dispersed phase	
z	distance from tracer injection point	m

References

1. Misek, T., Colln. Czech. Chem. Commun. 28 1631 (1963).
2. Misek, T., and Rod, V., 'Recent Advances in Liquid-Liquid Extraction' Ed. C. Hanson, Pergamon Press, London, (1971).
3. Westerterp, K.R., and Landsman, P., Chem. Engng. Sci. 17 363 (1962).
4. Westerterp, K.R., and Reyberg, W.H., Chem. Engng. Sci. 17 373 (1962).
5. Strand, O.P., Olney, R.B., and Ackermann, G.H., A.I.Ch.E.Jl. 8 252 (1962).
6. Bibaub, R.B., and Treybal, R.L., A.I.Ch.E.Jl. 12 472 (1966).
7. Ingham, J., Trans. Inst. Chem. Engrs. 50 372 (1972).
8. Mögli, A., Chem. Ing. Technik, Nr. 3 210 (1965).
9. Mögli, A., and Gusset, J., Verfahrenstechnik 1 357 (1967).
10. Fischer, A., Verfahrenstechnik 5 360 (1971).
11. Fischer, A., Chemische-Rundschau Nr. 19 1 (1973).
12. Fischer, A., Ph.D. Thesis, Diss. Nr. 5016 ETH/Zürich
13. Misek, T., Meeting of European Federation of Chemical Engineering Working Party on Distillation, Absorbtion and Extraction, Prague, April 1970.
14. Gutoff, B.B., A.I.Ch.E.Jl. 11 712 (1965).
15. Landau, J., Prochazka, J., and Souhrada, F., Colln. Czech. Chem. Commun. 31 1377 (1966).
16. Hartland, J., and Wise, G.D., Trans. Instn. Chem. Engrs. 45 T353 (1967).
17. Gleicher, C.A., A.I.Ch.E.Jl. 6 529 (1960).

Table 1: Physical Properties for Saturated De-Ionized Water/Shellsol K at 293 K

Interfacial Tension	28.8	x	10 ⁻³	N/m
Density of Kerosene	0.777	x	10 ⁺³	kg/m ³
Viscosity of Kerosene	1.54	x	10 ⁻³	N s/m ²

Table 2: Correlation of Single Phase Backmixing Results

Q	T mm	a	b	CR
0.124	10.0	0.056	0.0115	0.997
0.236	10.0	0.062	0.0131	0.997
0.236	20.0	0.079	0.0146	0.999
0.236	30.0	0.048	0.0160	0.999
0.296	10.0	0.054	0.0166	0.994
0.41	10.0	0.005	0.0186	0.997

$$\frac{E}{U_w H} = a + b \frac{RN}{U_w}$$

Table 3: Correlation of Two-Phase Backmixing Results

Q	T mm	a	b	CR
0.236	10.0	0.031	0.0128	0.976
0.41	10.0	-0.038	0.0192	0.980

$$\frac{E}{U_w H} = a + b(1 - X) \frac{RN}{U_w}$$

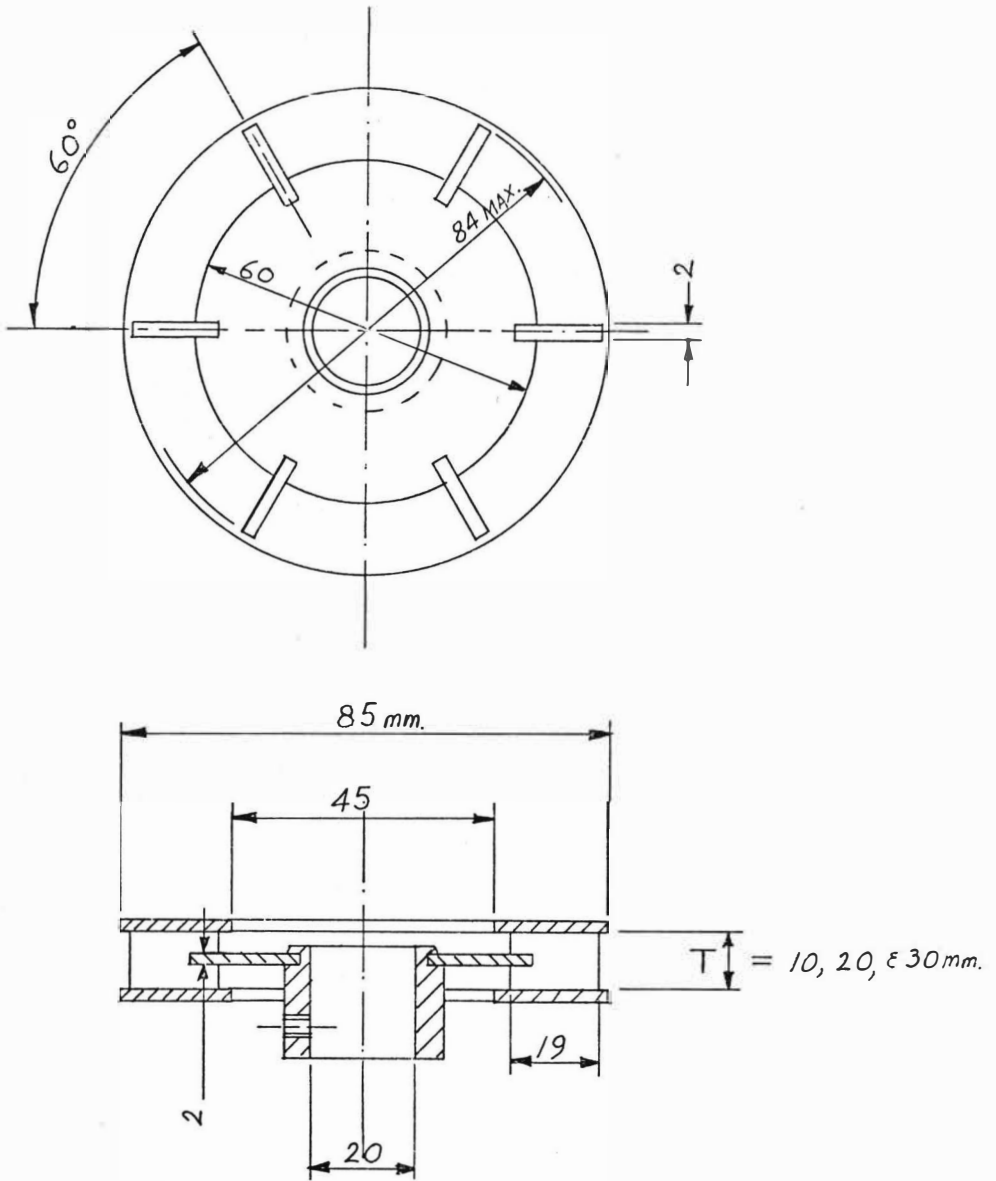
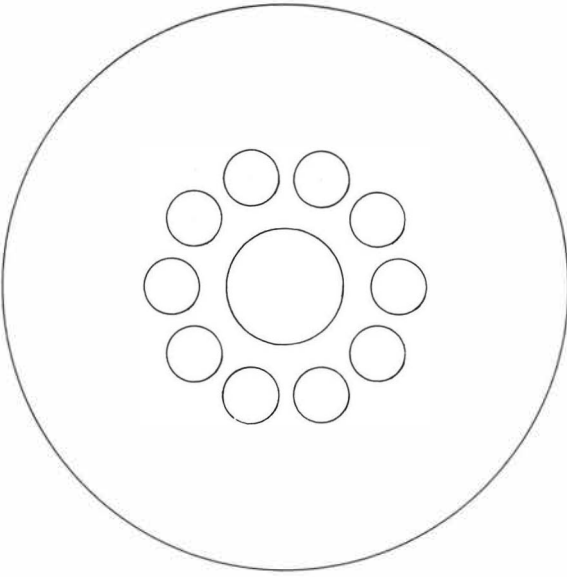
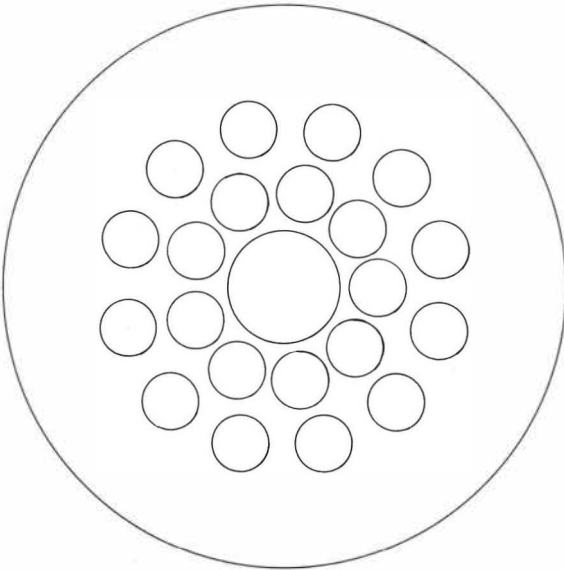


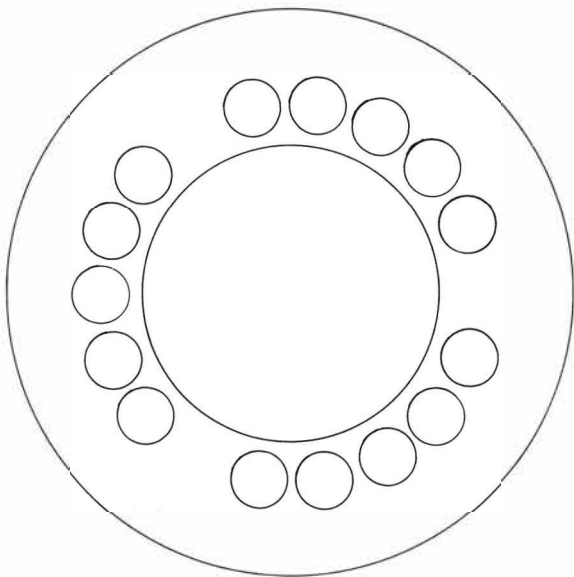
Figure 1 : Arrangement of Turbine Impeller



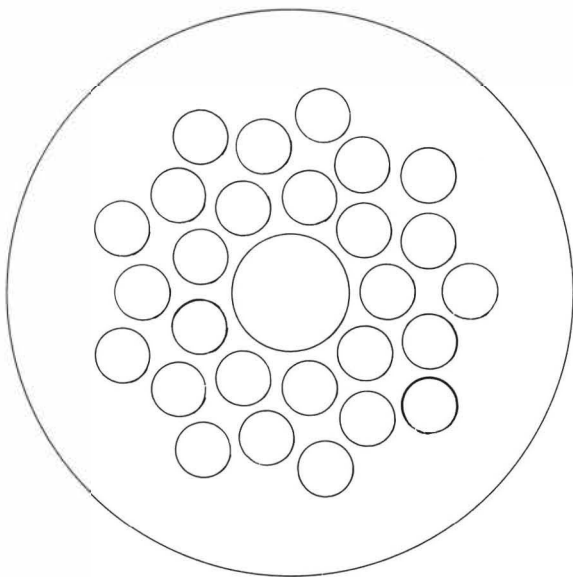
Free Area of Flow, $Q = 0.12$



Free Area of Flow, $Q = 0.236$



Free Area of Flow, $Q = 0.41$



Free Area of Flow, $Q = 0.296$

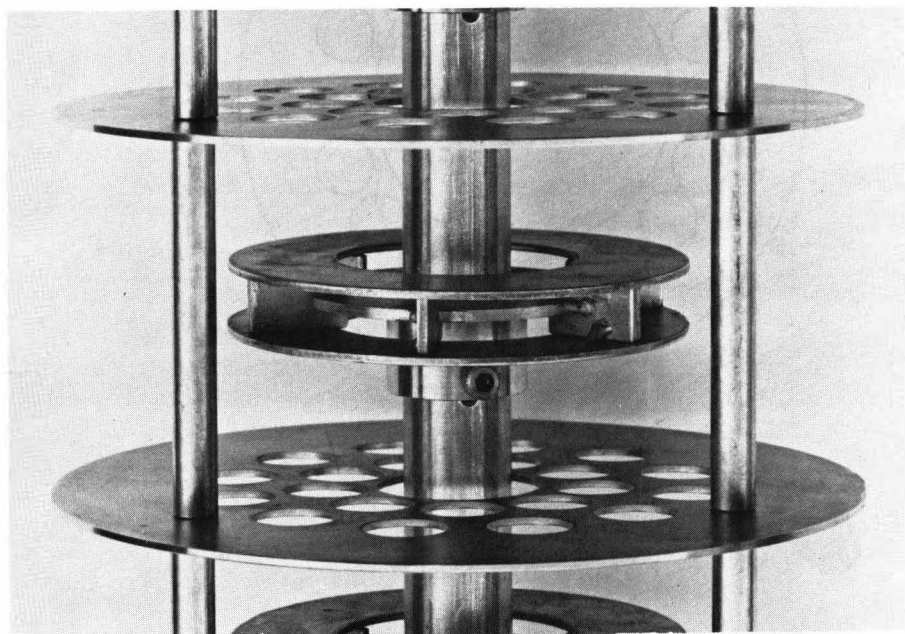


Figure 3 : Typical Compartmental Geometry.

Fig. 4. SINGLE PHASE BACKMIXING: EFFECT OF ROTOR SPEED

HEIGHT OF IMPELLER = 10 mm

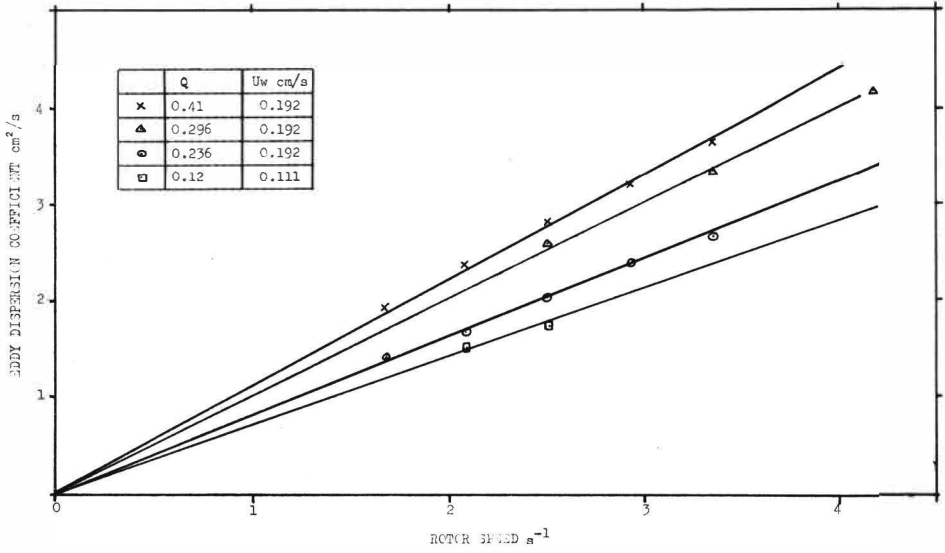


Fig. 5. SINGLE PHASE BACKMIXING: EFFECT OF PHASE VISCOSITY

HEIGHT OF IMPELLER = 10 mm

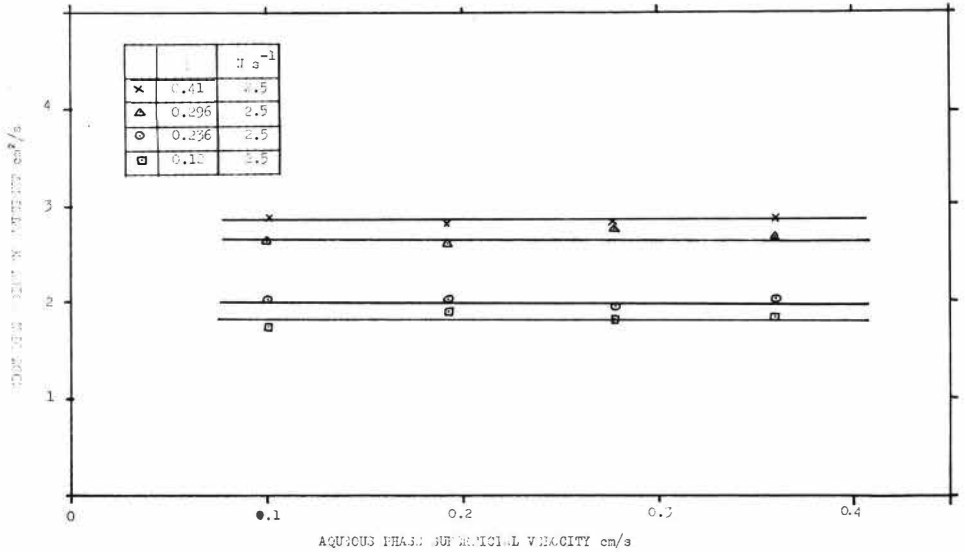


Fig. 6 CORRELATION OF SINGLE PHASE BACKSLIDING RIGHEITS
 HEIGHT OF TURBINES = 10 mm

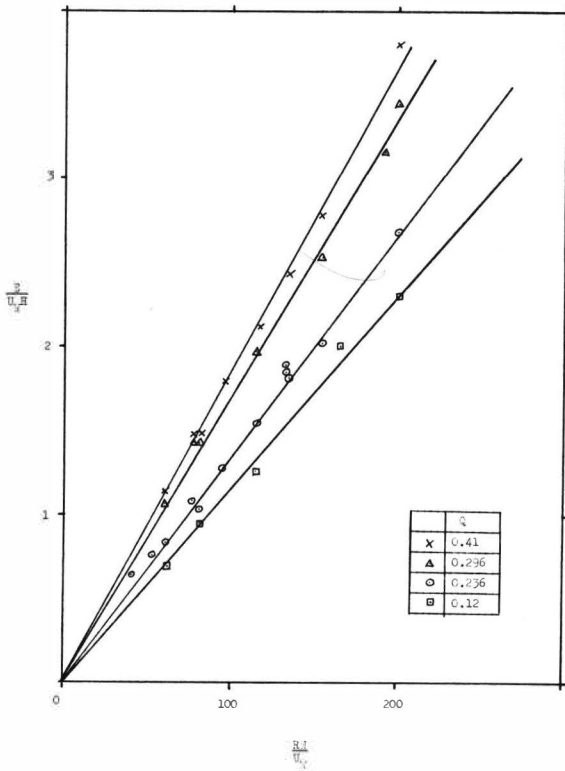


Fig. 7 TWO PHASE BACKSLIDING: HEIGHT OF ROTOR SPEED

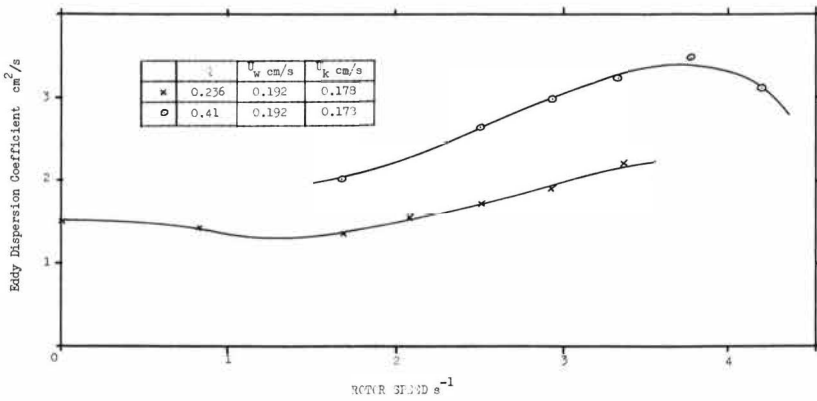


Fig. 9. THE BUILDUP OF DEFERRED PEAK BUILDUP USING VARIOUS VALUES OF α

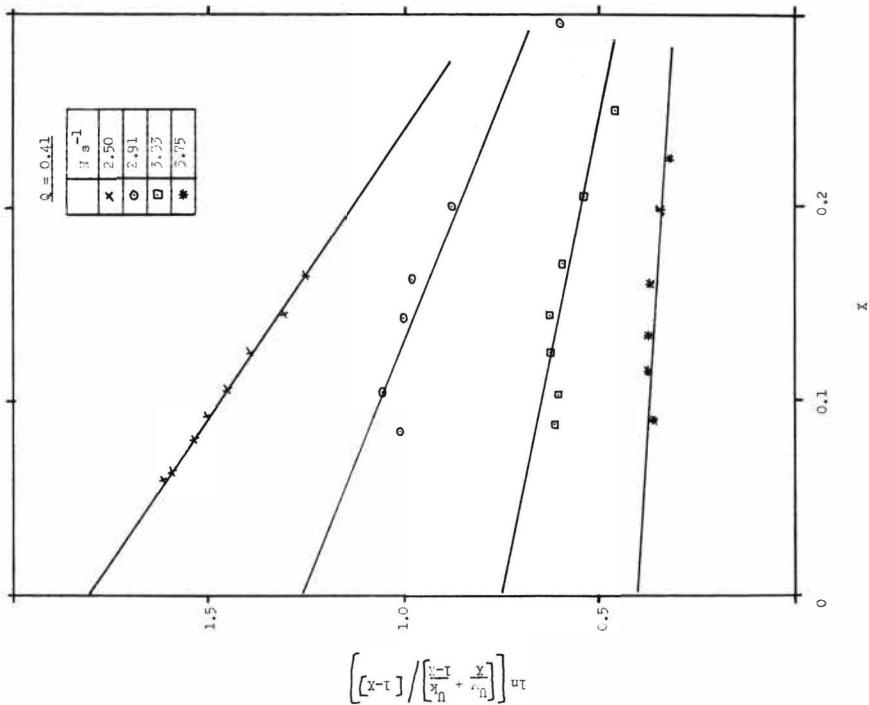
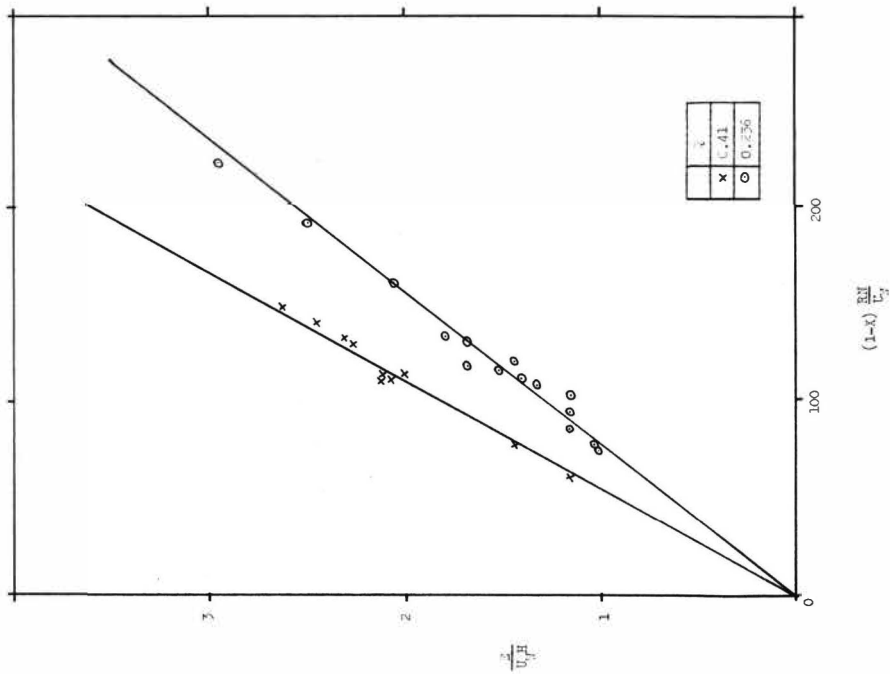


Fig. 10. A LINEAR PLOT OF $\frac{1-X}{X} \frac{dN}{dX}$ VERSUS $\frac{1-X}{X}$ FOR $\alpha = 10$ AND $\alpha = 100$



P. R. Choudhury¹; P. T. Ambrose²; G. S. McNab³; L. W. Fish; and S. D. Cavers

*Department of Chemical Engineering, The University of British Columbia,
Vancouver 8, B. C.*

Concentration profiles have been measured for both phases in the axial direction for spray liquid-liquid extraction columns operating at steady state. Measurements have been made for 38-mm I.D. columns of various lengths. Numerical integration has been used to obtain the true number of transfer units between the nozzle tips and the column interface. From these results a factor has been derived to correct the logarithmic mean driving force for axial mixing. Information has been obtained also with respect to abrupt changes in concentration resulting from agitation of the drops at the top of the column prior to coalescence. Heights of transfer units corrected for this end effect and for axial mixing are reported.

1. INTRODUCTION

The behaviour of spray liquid-liquid extraction columns has been the subject of a large number of investigations extending over roughly the last thirty years. It has been found possible to produce both dispersed and dense packings of drops in such columns^{1,2}. The observations of the present investigators have been confined to the dispersed type of packing.

The qualitative behaviour encountered has been found to depend greatly on whether solute is being extracted from the continuous into the dispersed phase or vice versa³. For transfer out of the continuous phase into the dispersed phase the drops rising up the column do not coalesce until they reach the main interface at the column top (*the column interface*). Even here coalescence is slow, and the drops remain in turbulent agitation³ for a time. In 38-mm I.D. columns there is little or no evidence of backmixing of the dispersed phase as distinct from axial dispersion in general, which would result, for example, because of varying rates of drop rise whenever a range

¹P. R. Choudhury now is with Westinghouse Research and Development Center, Beulah Rd., Churchillboro, Pittsburg, Pa.

²P. T. Ambrose now is with Imperial Oil Ltd., Ioco, B. C.

³G. S. McNab now is with Dept. of Engineering Science, University of Oxford, Oxford, England.

of drop sizes is present. On the other hand, when mass transfer takes place from the dispersed phase to the continuous, coalescence of the drops takes place within a short distance of the formation of the spray at the bottom of the column. Large drops are produced, with rapidly changing irregular shapes. Many of the drops produced by coalescence are so large as to be unstable and break apart. Evidently in these circumstances axial dispersion of the dispersed phase must be considerable.

The present paper is restricted to 38-mm I.D. columns in which solute was transferred from the continuous to the dispersed phase. Gier and Hougen⁴ suggested that the ratio of column diameter to column height would be an important parameter influencing the extent of axial mixing. Work with 3 different column lengths is reported in the present study. However, it appears that it is column diameter and not the ratio of length to diameter which is important in determining the axial dispersion coefficient in the continuous phase⁵. Following the example of Gayler and Pratt⁶ for the continuous phase of a packed liquid-liquid column, and Epstein⁷, for packed beds, the present paper proposes factors for correcting the logarithmic mean driving force of the plug-flow model for axial dispersion.

2. EXPERIMENTAL

The system investigated was water/acetic acid/4-methyl-2-pentanone. This system was chosen in order to facilitate comparison with earlier work. The ketone was technical grade, the acetic acid was reagent grade, and the water used was either laboratory distilled or deionized. The ketone phase always was dispersed and always was water-saturated. The water phase similarly always was saturated with ketone.

Figure 1 is a typical schematic flow diagram of the Elgin-design columns used. These were closely similar to apparatus described previously^{3,8}. Operation was always at room temperature and at steady state. The fluids contacted only glass, graphite, polyethylene, Saran, aluminum, chromium,

stainless steel, and asbestos. (Some asbestos gaskets and packing may have contained a partially soluble bonding agent.) Feed tanks A and D were used to store continuous and dispersed phase respectively. These phases were pumped from these tanks to constant head tanks, E and F, each vented at V. Continuous phase passed to the column through rotameter G. Dispersed phase entered through rotameter H and spray nozzle S. Drops were formed by passing the dispersed phase through stainless steel tubes (6.4 mm in length) press-fitted into the top plate of the nozzle. These tubes were chamfered at 45° on the outside to a sharp edge (Figure 2). Continuous streams of fluid extended for a short distance above the nozzle tips, and drops were formed by the break-up of these streams. The distributor plate shown in Figure 5 of the earlier work³ was not present in the experiments reported here. Various nozzle tips were capped off so as to maintain a constant linear velocity of the fluid in the tips during runs at different dispersed phase superficial velocities.

In the early runs stable operation was achieved, with the total flow divided evenly between the various nozzle tips, when bulk velocities of 77.7 - 91.3 mm/s were used in the nozzle tips. However, to maintain similar stable behaviour in later runs, it was found necessary to increase this velocity to 108.8 mm/s, which is above the value of 100 mm/s recommended by Hayworth and Treybal⁹, but is in accord with the recommendations of Johnson and Bliss¹⁰ (up to 127 mm/s), and of Keith and Hixson¹¹ (up to 115 mm/s).

Drop size distributions have been measured⁵ for the highest nozzle tip velocity used. These show maxima at drop sizes of about 3.4 mm and 0.6 mm. Although there are a large number of the smaller drops present, they contribute only a small percentage of the total dispersed phase volume. According to the correlation of Null and Johnson¹² the drop sizes predicted for the system in use are 4.2 mm and 3.6 mm, corresponding to velocities in the nozzle tips of 77 and 109 mm/s respectively. The Hayworth and Treybal⁹ correlation predicts corresponding drop sizes of 3.7 and 3.1 mm.

Sampling tubes were lowered into the column from the top in order to remove samples at various elevations above the nozzle tips. These tubes were of similar design to those described in detail in an earlier paper³. They are shown in Figure 2 of the present paper, the funnel probe being used to sample the dispersed phase, and the hook probe to sample the continuous phase. Controlled suction was used for removing the samples. Care was taken to purge the lines connecting the probes to the sample bottles. In order not to disturb the steady-state operation of the column, samples ordinarily were taken at rates which were only about 3 to 4% of the respective total rates of flow of the phases in the column. However in some runs higher sampling rates were used.

Runs were made by bringing the apparatus to steady-state, and taking the requisite samples. Holdup was determined by measuring the rate of rise of typical drops in the column and applying the equation

$$H = \frac{L_k}{U} (100\%) \quad (1)$$

The holdup was not measured in all runs. Missing values were obtained by fitting a polynomial to H in terms of L_w and L_k for similar velocities of dispersed phase in the nozzle tips.

Samples were analysed by titration with standard sodium hydroxide solution containing 0.1 kgmole/m^3 of the reagent. One-percent phenolphthalein was used as the indicator, and ethanol was mixed with each ketone sample before titration so that only one phase was present during analysis. Samples of the continuous phase contained no noticeable ketone entrainment. However, the samples of the dispersed phase were approximately 10% by volume water, and mass transfer continued after the samples had been collected. Therefore it was necessary to correct the measured concentration of acetic acid in each ketone sample to the value which obtained as the drops passed into the funnel probe. Equation 2 was used for this purpose.

$$C_{ki} = \frac{V_w (C_{wf} - C_{wi}) + V_k C_{kf}}{V_k} \quad (2)$$

Table 1 gives the range of variables investigated^{3,13,14}. Figure 3 shows typical measurements¹³, and in addition a water phase profile (shown dashed) calculated in a way to be described presently on the basis of an assumption of no axial mixing. The experimental points plotted at the upper and lower end of each concentration profile arise from column feed and effluent samples taken outside the column proper: at W, K, WO, and KO in Figure 1. The intermediate points in each of the solid-line profiles of Figure 3 arise from samples taken from within the column. There can be large end effects in the concentration profiles of both phases at the end of the column where continuous phase enters and drops coalesce; see, for example, CE and AB in Figure 3.

Inspection of the drops of dispersed phase within the column showed that no backmixing occurred of the rising drops toward the bottom of the column, except for some of the very small drops present.

3. MODEL AND GENERAL METHODS OF CALCULATION

Cavers and Ewanchyna³ adopted a simplified model to describe operating spray columns. The model is summarized and clarified in what follows. It is assumed that continuous phase enters the column just above a bed of agitating and coalescing drops at the column interface. At entry the continuous phase has a concentration labeled C in Figure 3. Due to the agitation of the drops during their coalescence into the column interface, and due to the time involved in this coalescence, the concentration of the dispersed phase changes during this operation (e.g. from B to A in Figure 3). The solute required for this last concentration change comes from the continuous phase, with the result that the concentration of that phase decreases (e.g. from C to D). As the continuous phase emerges from the bed of coalescing drops it is diluted by the addition to it of backmixed continuous phase which has been carried

toward the top of the column, presumably in the wakes of rising drops. See, for example, the fall in concentration DE in Figure 3. Thus there is one end effect in the dispersed phase: AB, and two end effects in the continuous phase: CD and DE. These last two combine to produce the total end effect CE in the continuous phase.

Evidently this model is a simplified description of what happens in the columns of the present work. In these the continuous phase enters near the bottom of the Elgin head and then flows upward, and over the top of the glass pipe forming the column proper. The continuous phase then flows on down the column. The entering continuous phase encounters drops rising to the interface, as well as drops at the interface. Also, since the model includes the implications of drawing the concentration profiles as they appear in Figure 3, the fall in concentration of the continuous phase from C to E occurs infinitesimally below the column interface. However, both the agitation end effect CD and the backmixing end effect DE must in reality occur over a finite height. In addition, these end effects are not events which happen to the continuous phase in series with respect to time; rather they are events which happen more or less in parallel, and occur in regions of the column which at least overlap. Nevertheless, as will be seen later in this paper, it is of necessity the simplified model which is used in most of the calculations. Also, the model provides a reasonably adequate description of spray column behaviour, particularly if the calculated water-phase profiles now to be described are included, and a comparison between the calculated and measured concentration of the continuous phase used as a qualitative indication of backmixing.

The calculated continuous-phase profile shown dashed in Figure 3 was obtained on the assumption that both the phases pass through the column in plug flow, and that the concentrations at the bottom of the column were those shown in Figure 3. Equation 3 then gave the calculated water phase profile in terms of the measured ketone phase profile.

$$C_w = \frac{L_k (C_k - C_{kb})}{L_w} + C_{wb} \quad (3)$$

In Figure 3 AB and CD are related by Equation 4 below:

$$(AB) (L_k) = (CD) (L_w) \quad (4)$$

Since an overall solute balance must be satisfied with respect to the terminal concentrations of the phases, and since subtraction of Equation 4 from such an overall balance must result in a particular case of the material balance represented by Equation 3, the value of C_w corresponding to point D in Figure 3 can be calculated from Equation 3 by substituting the value of C_k corresponding to point B.

In order to calculate a factor to correct the logarithmic mean driving force for axial mixing it was necessary to have a measure of the rate of mass transfer across the interface between drops and continuous phase in an increment of column height. As mentioned earlier, little or no backmixing of the dispersed phase took place within the column. Therefore the change in ketone phase concentration observed in an element of column height is the result solely of mass transfer across the interface between phases. On the other hand, the measured water phase concentrations result, not only from transfers of this sort, but also from axial mixing. It is important, then, to use the measured ketone phase profiles as measures of interfacial transfer for the purpose of calculating mass transfer coefficients and heights of transfer units. Values of the latter were obtained from Equation 5 below:

$$HTU'_{Ok} = \frac{h}{\int_b^B \frac{dC_k}{C_k^* - C_k}} \quad (5)$$

in which the denominator is evaluated most easily by numerical integration of the measured profiles. This integration is carried out only to point B on the dispersed phase concentration profile in order to eliminate the agitation end effect mentioned previously. Equation 5 involves the assumption that the

solutions are dilute (and L_k and $K'_k a$ constant). The HTU of Equation 5 is the measured value mentioned by Miyauchi¹⁵. If an assumption of no axial dispersion of the dispersed phase is valid this will also be close to Miyauchi's true value.

If plug flow of each of the phases can be assumed, as well as constant superficial velocity of each phase, constant overall capacity coefficient: $K_k a$, and constant value of the partition coefficient (m) describing the ratio of solute concentrations in the two phases at equilibrium, Equation 6 results.

$$N = K'_k a S h (C_k^* - C_k)_{lm} \quad (6)$$

Equation 7 gives the value of HTU_{Ok} corresponding to the circumstances assumed.

$$HTU_{Ok} = \frac{L_k S}{K'_k a S} = \frac{h (C_k^* - C_k)_{lm}}{C_{kB} - C_{kb}} \quad (7)$$

In Equations 6 and 7 the log mean driving force $(C_k^* - C_k)_{lm}$ is calculated on the basis of the present model from the concentrations at D and B in Figure 3, and from C_{wb} and C_{kb} . The HTU_{Ok} calculated from Equation 7 then is consistent with the HTU'_{Ok} obtained by Equation 5 except that the value from Equation 7 involves the assumptions of plug flow (and of constant L_w and m).

Next, Equation 6 can be rewritten as follows:

$$N = K'_k a S h (C_k^* - C_k)_{lm} F_m \quad (8)$$

in which $K'_k a$ now is the measured mass transfer coefficient corresponding to HTU'_{Ok} , and where the factor F_m has been included to correct for the fact that backmixing of the continuous phase does take place in the actual column, as shown, for example, by the fact that the calculated and the measured concentration profiles of the continuous phase do not coincide in Figure 3. Notice that it is necessary to have removed the agitation end effect from the total end effect in the continuous phase before using Equations 6, 7, and 8, basically because agitation and backmixing are such different phenomena.

The factor F_m corrects for the reduction in driving force due to the

backmixing. Its value in principle cannot exceed unity. (F_m would include the effect of the system not obeying assumptions involved in Equation 7, but not in Equation 5. Thus the effects of the slight variations in L_w and in the partition coefficient are thrown into F_m .)

The corrected height of a transfer unit corresponding to the corrected log mean driving force will be given by

$$HTU'_{Ok} = \frac{L_k S}{K'_k a S} = \frac{h (C_k^* - C_k)_{lm} F_m}{C_{kB} - C_{kb}} \quad (9)$$

which is of the form of Equation 7. Dividing Equation 9 by Equation 7 produces the following expression for F_m :

$$F_m = \frac{HTU'_{Ok}}{HTU_{Ok}} \quad (10)$$

Equation 10 indicates that F_m can be determined by evaluating the right-hand sides of each of Equations 5 and 7, the ratio of the results being F_m .

An overall capacity coefficient for agitation at the column interface was calculated by

$$K_{kA} = \frac{\text{Rate of mass transfer at the column interface due to agitation}}{\text{Average overall driving force at the column interface}} \quad (11)$$

4. DETAILED METHODS OF CALCULATION

Many of the experimental runs contained too few measured concentrations for reliable direct numerical integration of Equation 5. Therefore, for each of the profiles of each run, smooth, hand-drawn curves were constructed from the elevation corresponding to the nozzle tips to that of the column interface. C_{wb} and C_{kb} were weighted most heavily because these were based on multiple samples (taken at W0 and K in Figure 1), whereas only one internal sample was available to provide the value of each concentration obtained between the nozzle tips and the column interface.

Digitized concentrations were recorded from the dispersed-phase profile

and from the continuous-phase profile at equal intervals of 0.02 times the column height from tips to interface. The resulting concentration pairs then were arranged into five groups of 11, with the final pair of a given group appearing as the first pair of the next group. Least squares regression analyses produced, for each phase, polynomials relating concentration to height for each group. That degree of polynomial which had the minimum standard error of estimate was selected as the best. The maximum degree permitted was four.

Points E and B in Figure 3 were calculated from the respective polynomials evaluated at the interface height. Two values of the concentration corresponding to point D were calculated, one from each of Equations 3 and 4. If both such values were within the range CE (Figure 3), the average of the two was taken; if either was outside this range, the other was used. In two runs both values of D as calculated lay below E. The value of D nearer to E was used in each of these cases.

To evaluate C_k^* in the integrand of Equation 5 one needs the equilibrium partition of acetic acid between the ketone and water as a function of C_w . The following polynomial has been derived¹⁶ to fulfill this purpose.

$$C_k^* = 0.4487 C_w + 0.1162 C_w^2 - 0.01861 C_w^3 + 0.001987 C_w^4 \pm 0.032 \quad (12)$$

(In this paper the \pm values are standard errors of estimate.)

For evaluating HTU'_{Ok} Equation 5 was rewritten as follows, with the total height of the column divided into 10 equal-height sections (j).

$$HTU'_{Ok} = \frac{h}{\sum_{j=1}^{10} \left[\int \frac{dC_k}{C_k^* - C_k} \right]_j} \quad (13)$$

In applying Equation 13 analytical differentiation of the fitted polynomials giving C_k was used to provide expressions for dC_k in terms of height above the nozzle tips as independent variable. Similarly in the denominator of the integrand appearing in Equation 13 the fitted polynomials were used to pro-

vide expressions for C_k^* and C_k in terms of height. The integration was carried out over the height range of each section j by using the polynomial functions appropriate to the particular section. The numerical integration procedure adopted was a "cautious adaptive Romberg extrapolation"¹⁷ with maximum absolute and relative error limits prescribed.

In order to calculate the overall capacity coefficient K_{kA} for mass transfer at the column interface due to agitation, the numerator of the right-hand side of Equation 11 was evaluated by multiplying the superficial velocity of the ketone phase by the end effect corresponding to agitation; i.e. the numerator was obtained by evaluating the following

$$F L_k (C_{kA} - C_{kB}) \quad (14)$$

The denominator of Equation 11 was evaluated by obtaining the arithmetic average overall driving force based on the model described previously. The following expression gave this average

$$\frac{(C_{kC}^* - C_{kA}) + (C_{kD}^* - C_{kB})}{2} \quad (15)$$

Cavers and Ewanchyna³ calculated K_{kA} as described above except that in the last expression C_{kD}^* was replaced by C_{kE}^* on the basis that this would be a more realistic concentration to represent the situation in the water phase just below the interface. This would seem to be true; on the other hand Expression 15 is consistent with the model for spray column operation described earlier, which assumes that the agitation end effect, and the end effect due to backmixing, occur in series.

5. RESULTS

Multiple linear regression analysis was carried out on the values of F_m obtained from the various experimental runs. Potential independent variables included the superficial velocity of the water phase, the superficial velocity of the ketone phase, the bulk velocity of the ketone phase in the nozzle

tips, the dispersed phase holdup, and the column height (nozzle tips to interface). Each of these potential independent variables was included in the analysis as the variable to the first power and as the variable squared. The following is the relationship recommended for obtaining F_m in spray columns of approximately 38-mm I.D.

$$F_m = 0.4552 - 0.04290 h + 190.4 L_w - 16.310 L_w^2 \pm 0.051 \quad (16)$$

The squared multiple correlation coefficient (R^2) associated with Equation 16 was 0.845. [With $1/F_m$ used instead of F_m , R^2 changed only a little (as might have been expected), to 0.854; the slight improvement in R^2 is offset by the inconvenience of using the reciprocal.]

An attempt was made to obtain a better correlation by regressing the natural logarithm of $1-F_m$, against the same variables. R^2 was 0.639. An attempt also was made to relate F_m to the ratio of the superficial velocity of the water phase to that of the ketone phase, and this ratio raised to the second power; R^2 was 0.610.

In reporting F_m values for the continuous phase of a packed column Gayler and Pratt⁶ showed F_m as a function of the following

$$\frac{L_w H}{L_k (1 - H)} \quad (17)$$

where the notation of the present paper has been used. The correlation of F_m versus this group and its square was attempted; R^2 was 0.737.

Finally an attempt was made to correlate F_m in terms of the two quantities defined below

$$\frac{C_{kB} - C_{kb}}{C_{kD}^* - C_{kb}} = n = \text{approach to equilibrium} \quad (18)$$

$$\frac{C_{kD}^* - C_{kb}^*}{C_{kB} - C_{kb}} = z = \frac{\text{fall}}{\text{rise}} \quad (19)$$

This approach is based on correction factors for the log mean temperature driving force in shell and tube heat exchangers. It was found that F_m is

linearly related to Z with an associated R^2 of 0.659. As with heat exchangers¹⁸ F_m decreases as Z increases. Variable η was found to be not significant at the 0.95 probability level. Indeed F_m appeared to increase with η whereas it decreases in the case of heat exchangers.

Figure 4 shows F_m plotted against L_w with column height as parameter. The lines appearing on Figure 4 were calculated from Equation 16 using respectively the average height for the 19 run group and that of the 15 run group from Table 1. Inspection of Figure 4 shows that approximately doubling the column height decreases F_m by an amount comparable to the standard error of estimate (0.051) associated with Equation 16. In other words, data are rather badly scattered with respect to height. For example, notice the position of the point representing the single run at a column height of 0.41 m. This point falls more or less in the middle of a group of runs made with a column height averaging 1.16 m. Based on the work of Choudhury¹³ and on measurements of axial mixing coefficients⁵, it had been concluded that axial mixing was not affected by column height. The scatter of points in Figure 4 leaves the matter still unsettled. Accordingly, the following equation is reported to enable the prediction of F_m in spray columns of 38-mm I.D. independent of the column height.

$$F_m = 0.3754 + 194.2 L_w - 16.360 L_w^2 \pm 0.056 \quad (20)$$

The value of R^2 is only slightly less than for Equation 16, 0.808 instead of 0.845. Both Equations 16 and 20 indicate a parabolic relationship between F_m and L_w , with a decreasing F_m above an L_w value of about 0.006 m/s. However one would expect F_m to approach unity asymptotically at high L_w values.

As is true for most mass transfer results the values of HTU'_{Ok} showed considerable scatter. Probably the main cause is that the phases were near equilibrium at one end of the column or the other for perhaps 8 of the experimental runs (e.g. Figure 3). In these circumstances considerable chance for error arises in evaluating the integral of Equation 13. The scatter, of

course, carries over to the F_m results, particularly since a similar problem arises with Equation 7. The dimensional equation appearing below seemed to be about the best that could be obtained ($R^2 = 0.500$) from the present data.

$$HTU'_{Ok} = 0.3617 + 0.6745 h - 0.2070 h^2 - 2.910 v_N - 22.92 L_w \pm 0.063 \quad (21)$$

The effects of v_N and L_w in this equation seem reasonable. Thus in the case of v_N , increasing v_N reduces drop size and increases a , the area of dispersed phase per unit volume of column. Increasing L_w also increases a by causing the residence time of the drops to increase. Increasing a reduces HTU'_{Ok} (Equation 9).

As might be expected the values of $K_k A$ showed considerable scatter as well. Regression results are given in the following two equations, the first based on point D (Figure 3), and the second on point E

$$(K_k A)_D = 3.462 \times 10^{-4} L_w + 3.602 \times 10^{-4} L_k \pm 6.5 \times 10^{-7} \quad (22)$$

$$(K_k A)_E = 3.278 \times 10^{-4} L_w + 3.916 \times 10^{-4} L_k \pm 6.5 \times 10^{-7} \quad (23)$$

(R^2 values were 0.622 and 0.632 respectively.) Notice that, as would be expected, $K_k A$ increases with L_k , more drops being available for agitation at the interface. $K_k A$ also increases with L_w , presumably as a result of increased mixing as the water phase enters the column.

It is interesting that a similar agitation end effect is absent in a spray column heat exchanger^{19,20}.

6. APPLICATION TO COLUMN DESIGN

Small-diameter liquid-liquid spray columns can be designed in the following way. Suppose for example, that a feed of given concentration and flow rate is to be extracted to a given raffinate concentration by a dispersed phase of known entering concentration. The ratio of dispersed to continuous phase superficial velocity would be obtained by economic considerations. Then one could proceed as follows to determine the column height, assuming an Elgin

design of column, and that the dispersed phase enters at a value of v_N of about 0.109 m/s through nozzle tips of inside diameter 2.6 mm. One first calculates the composition of the dispersed phase leaving the column (A in Figure 3) by an overall material balance. The next step is to obtain point B and point D by a trial and error procedure. Thus one estimates the continuous-phase concentration at D and applies Equation 4 to obtain the corresponding point B. Based on the assumed value of D, the arithmetic average driving force applicable to mass transfer during agitation of drops at the column interface now is calculated according to Expression 15 given earlier. This driving force then is used with a value of $K_k A$ obtained from Equation 22 to give the rate of mass transfer taking place due to agitation. This rate equals the product of the continuous-phase superficial velocity, the column internal cross-sectional area, and the difference in concentration between points corresponding to C and D. D can be calculated from this equality and compared with the value assumed. With D located, Equation 9 is used along with Equations 16 and 21 to obtain h by trial and error. It should be remembered that considerable caution should be exercised in applying the equations of the present work to design columns for other than the present system, and for values outside the ranges given in Table 1.

7. CONCLUSIONS

The separation of agitation and backmixing end effects at the continuous phase entrance to liquid-liquid spray extraction columns seems to be a useful device for clarifying spray column behaviour, and for providing a basis for design. More work needs to be done with different chemical systems and with columns of different diameters and heights, in order to provide more-general correlations describing mass transfer due to agitation at the interface, heights of transfer units corrected for axial mixing effects, and correction factors for the log mean driving force.

Acknowledgements

Financial support from the National Research Council, and from the Dean's Committee on Research, Faculty of Graduate Studies, The University of British Columbia, is gratefully acknowledged. Thanks are due to J. S. Forsyth for many helpful suggestions, and to Georges Bergeron for making one of the experimental runs.

References

1. Letan, R.; Kehat, E. *A.I.Ch.E. Jl* 1967, 13, 443.
2. Perrut, M.; Loutaty, R.; Le Goff, P. *Chem. Engng Sci.* 1973, 28, 1541.
3. Cavers, S. D.; Ewanchyna, J. H. *Can. J. chem. Engng* 1957, 35, 113.
4. Gier, T. E.; Hougen, J. O. *Ind. Engng Chem.* 1953, 45, 1362.
5. Henton, J. E.; Cavers, S. D. *Ind. Engng Chem. Fundamentals* 1970, 9, 384.
6. Gayler, R.; Pratt, H. R. C. *Trans. Instn chem. Engrs* 1957, 35, 267.
7. Epstein, N. *Can. J. chem. Engng* 1958, 36, 210.
8. Henton, J. E.; Hawrelak, R. A.; Forsyth, J. S.; Cavers, S. D. Proc. Int. Solvent Extraction Conference 1971, II, 1302.
9. Hayworth, C. B.; Treybal, R. E. *Ind. Engng Chem.* 1950, 42, 1174.
10. Johnson, H. F. Jr.; Bliss, H. *Trans. Instn chem. Engrs* 1946, 42, 331.
11. Keith, F. W. Jr.; Hixson, A. N. *Ind. Engng Chem.* 1955, 47, 258.
12. Null, H. R.; Johnson, H. F. *A.I.Ch.E. Jl* 1958, 4, 273.
13. Choudhury, P. R. M.A.Sc. Thesis, The University of British Columbia, 1959.
14. Bergeron, G. M.A.Sc. Thesis, The University of British Columbia, 1963.
15. Miyauchi, T.; Vermeulen, T. *Ind. Engng Chem. Fundamentals* 1963, 2, 113.
16. Fish, L. W.; Errico, J. E.; Lim, J.; Cavers, S. D. submitted for publication.
17. Immerzeel, G. UBC CADRE, The University of British Columbia Computing Centre, July 1972.
18. McAdams, W. H. *Heat Transmission*, Edition 3, p. 194, McGraw-Hill, New York, 1954.
19. Letan, R.; Kehat, E. *A.I.Ch.E. Jl* 1968, 14, 398.
20. Loutaty, R.; Vignes, A.; Le Goff, P. *Chem. Engng Sci.* 1969, 24, 1795.

Nomenclature

A	interfacial area of ketone drops at the column interface, plus any free area of the column interface (m^2)
a	interfacial area per unit volume of the column (m^2/m^3)
C	concentration ($kgmole/m^3$)
C_k^*	concentration of a ketone phase in equilibrium with a water phase of concentration C_w ($kgmole/m^3$)
$(C_k^* - C_k)_{lm}$	log mean of the overall driving force between the phases at the bottom of the column and the phases at points D and B in Figure 3 ($kgmole/m^3$)
F_m	factor correcting $(C_k^* - C_k)_{lm}$ for axial mixing of the continuous phase (dimensionless)
H	holdup, the volume percent of the column occupied by dispersed phase
h	height of the column (nozzle tips to interface) (m)
HTU_{Ok}	overall height of a transfer unit based on $(C_k^* - C_k)_{lm}$ (m)
HTU'_{Ok}	overall height of a transfer unit calculated by numerical integration of the $(C_k^* - C_k)$ driving force, and with the agitation end effect eliminated (m)
K_k	except when used with A, overall mass transfer coefficient based on $(C_k^* - C_k)_{lm}$; when used with A the driving force is that of Expression 15, or that described in the text following that expression (m/s)
K'_k	overall mass transfer coefficient corresponding to HTU'_{Ok} (m/s)
L	superficial velocity of a phase flowing in the column (m/s)
m	equilibrium partition coefficient, C_k^*/C_w
N	rate of interfacial mass transfer ($kgmole/s$)
R^2	squared multiple correlation coefficient
S	cross-sectional area of the column (m^2)
U	average velocity of rise of the ketone drops, relative to the column wall (m/s)
V	volume of a phase of a ketone internal sample (m^3)
v_N	bulk velocity of the ketone phase in the nozzle tips (m/s)
Subscripts and limits of integration	
A,B,C,D,E	corresponding to the designated points in Figure 3

b bottom of the column
f final value, at time of analysis
i initial value, at time of sampling
k ketone phase
N bulk value, in the nozzle tips
O overall
w water phase

Superscripts

* corresponding to equilibrium

TABLE 1. Ranges of variables investigated

Column inside diameter	38 mm	
Nozzle tip inside diameter	2.5 - 2.6 mm	
Column height (nozzle tips to interface)		
	0.41 m	1 run
	1.13 - 1.20 m (ave. = 1.16)	19 runs
	2.23 - 2.26 m (ave. = 2.24)	<u>15</u> runs
	Total	35 runs
Inlet water phase, acetic acid concentration	0.711 - 0.854 kgmole/m ³	
Inlet ketone phase, acetic acid concentration	0.082 - 0.126 kgmole/m ³	
Acetic acid material balance, absolute value of 100(in - out)/in	0.065 - 1.74	
Water phase superficial velocity	0.96 - 7.20 mm/s	
Ketone phase superficial velocity	1.55 - 7.55 mm/s	
Average velocity of ketone phase in nozzle tips	77. - 109. mm/s	
Holdup of dispersed phase	0.017 - 0.119 volume fraction	

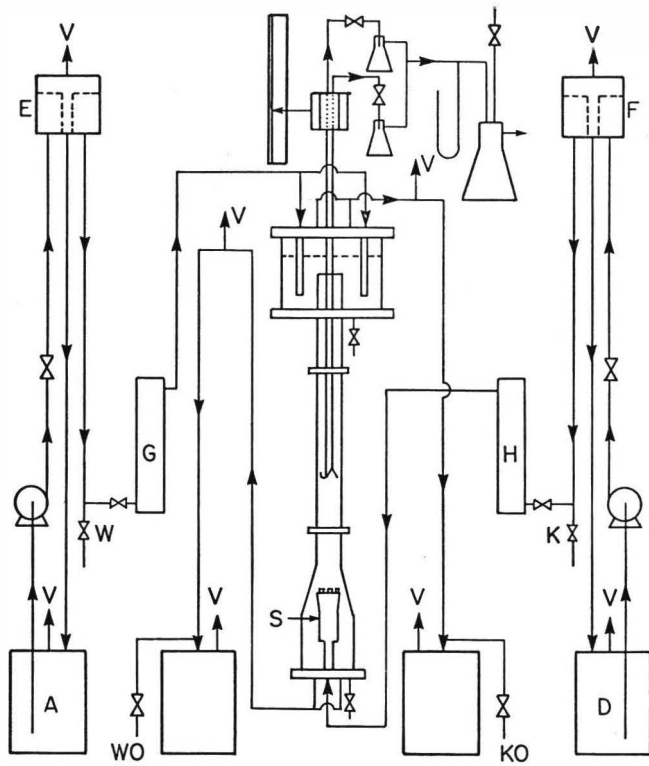


Figure 1. Schematic flow diagram.

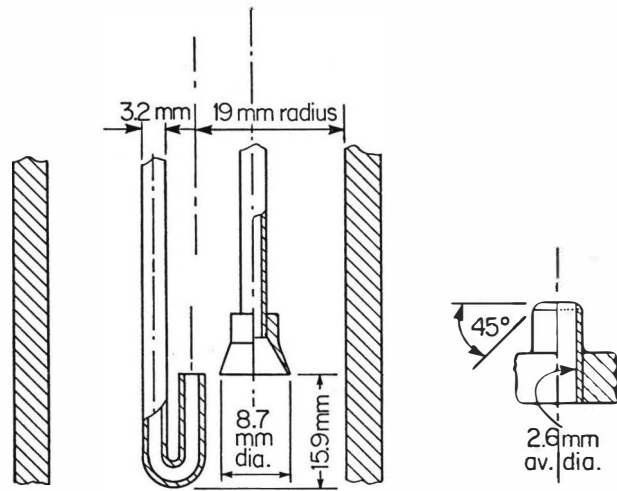


Figure 2. Sample probes and nozzle tips.

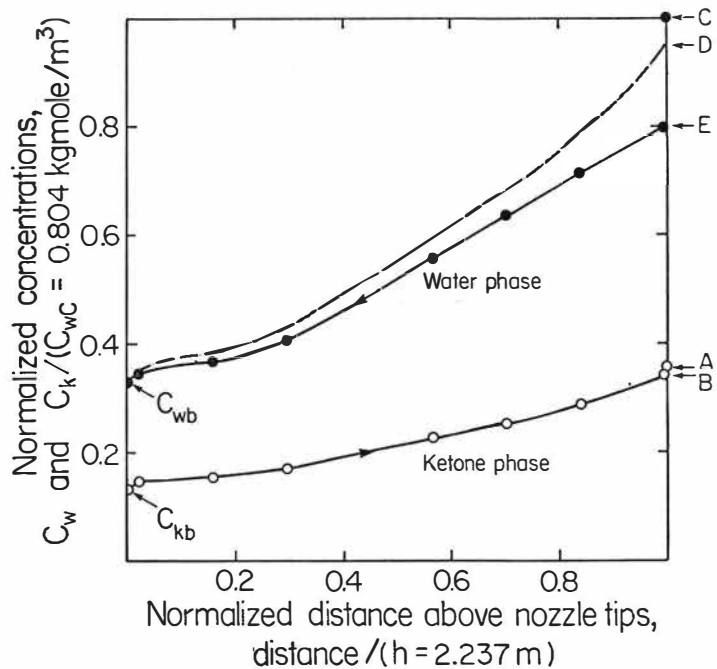


Figure 3. Concentration profiles for Run 69.

$$L_w = 1.54 \times 10^{-3} \text{ m/s}$$

$$L_k = 4.63 \times 10^{-3} \text{ m/s}$$

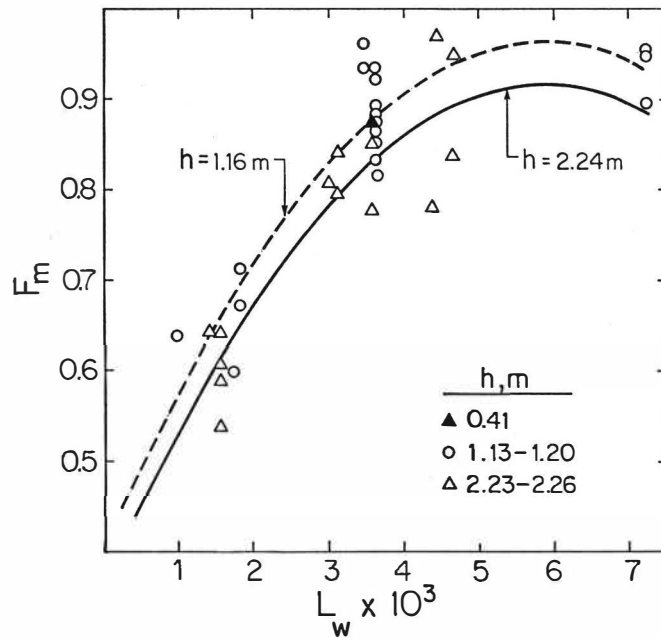


Figure 4. Values of F_m .

CONTRIBUTION OF THE DISPERSED PHASE TO
THE LONGITUDINAL MIXING IN A ROTATING DISC CONTACTOR

by
A. BORRELL - G. MURATET - H. ANGELINO

LABORATOIRE ASSOCIE C.N.R.S.
INSTITUT DU GENIE CHIMIQUE
31078 TOULOUSE CEDEX - FRANCE

SUMMARY

In the first part of this work the hold-up of the dispersed phase was determined under different experimental conditions and from these results the mean residence time and the average flow velocities were deduced.

In the second part the technique of tracer pulse injection was employed and PECLET number Pe and mean residence time \bar{t} were computed using the dispersed plug flow model. To solve the equations three methods were developed :

- moments of the responses curves,
- least square fit of the response curves in the time domain,
- least square fit of the response curves in the frequency domain.

I - INTRODUCTION

Operating conditions of a rotating disc contactor (RDC) have been studied using the techniques of response characteristics to a tracer pulse injection.

The hold-up of the dispersed phase was determined under different conditions and was used to compute average flow velocities and mean residence times. The remainder of this work concerns the continuous phase. As a first step it was shown that the residence time distribution for this phase was well represented by the dispersed plug flow model with a Peclet number, Pe , and a mean residence time, \bar{Z} , as parameters. Then the influence of the flow rate of the continuous and of the dispersed phase was investigated as well as the effect of the rate of rotation of the discs.

Peclet numbers were determined by means of three different methods

- use of the moments of the responses or break-through curves ;
- least square fit of the response curves in the time domain ;
- least square fit of the response curves in the frequency domain.

2 - APPARATUS

A flow diagram of the pilot plant is shown on fig. 1.

The one meter extraction section was made of a 50 mm diameter glass tube. The column was equipped with 40 equispaced stator rings of 35 mm inside diameter and 1 mm thick, forming a series of compartments agitated individually by a centrally located disc. These equisized flat rotor discs were 30 mm in diameter and 1 mm thick. The discs were mounted on a centrally rotating drive shaft 8 mm in diameter. The speed of rotation could be adjusted by means of an electronic variator coupled with a direct current motor. The speed of rotation could be varied from 300 to 3000 rpm and the value was determined with an accuracy of 3 %.

The heavy and light phases were supplied to the column from two constant level tanks.

Experimental work was performed using distilled water as the heavy continuous phase and isopropyl ether as the light dispersed phase with no mass transfer occurring.

In a RDC column the determination of the hold-up of the dispersed phase is much more complicated than in other equipment due to the presence of the shaft and the difficulty in separating the extraction zone from the other regions. In order, to determine the hold-up, a calibrated glass tube was set on top of the extraction column (50 mm in diameter, 300 mm long) with a lateral evacuation by overflow for the organic light phase. Two electromagnetic valves positioned on the organic phase entrance and exit pipes, served to stop the flow of the above phase through the extraction column. The hold-up was deduced by the difference between the total volume measured after decantation and the volume in the upper decantation zone.

Longitudinal mixing was evaluated using the method of tracer injection during steady state operation. The dynamic method viz injection of a pulse of an electrolyte into the system and measurement of the time dependence of the tracer concentration at a fixed point downstream from the point of injection was employed. The tracer employed was 1.5NHCl contained in a tank 8 m above the equipment. The injection was done by using an electromagnetic valve (fig. 2) connected to the tank by a teflon tube 5 mm in diameter. The tracer was injected at the upper interface level through a stainless steel needle 2 mm in diameter. This device avoided an upstream diffusion. The time dependence of the conductivity was subsequently measured 900 mm downstream. The system was thus considered a closed-open system (1). In order to avoid the existence of a trail due to the diffusion of the remaining tracer inside the injection tube, a second electromagnetic valve was used. This valve opened when the first one closed and the remaining tracer was eliminated through that second valve and replaced by continuous phase. Both valves were controlled by using a relay with a variable time constant. Opening periods were adjusted to $1/10$ s which corresponded to the injection of 1 cm^3 . Injections performed with the above device were assumed to be ideal Dirac pulses.

Changes in conductivity corresponding to the flow of the electrolyte were detected by means of two cylindrical platine electrodes, 10 mm in

diameter and 1 mm thick. These electrodes were connected to a conductimeter and the break through curves were registred by an "Histomat S". This apparatus allowed a direct sampling of the curves, giving the results on a perforsted ribbon, readily available for computer work.

4 - DETERMINATION OF THE HOLD-UP

The hold-up of the dispersed phase allowed the calculation of the various flow cross section areas, average velocities and mean residence times for both dispersed and the continuous phases.

Forty-eight runs were performed and the results are shown in figures 3-4. Two different total flow rates were used, with 4 different dispersed to continuous phase flow rate ratios and 6 speeds of rotation of the discs. The conclusions obtained are as follows :

- the hold-up remained almost constant in the range 8-10 % until a speed of rotation of 1500 rpm (2.4 m/s) was reached : the hold-up then began to increase rapidly ; this phenomenon occured for all flow rate ratios.

- for a given speed of rotation and a given flow rate ratio, hold-up increased with the total flow rate. This might be related to a higher drag force resulting from the increase of the counter-current flow rate.

5 - PECLET NUMBER EVALUATIONS

The dispersed plug flow model was used. This model is characterised by a piston flow with solute transfer by a diffusional process from zones of higher concentrations towards zones of lower concentrations. Assuming that this diffusion is the same along the apparatus and making a mass balance, an equation analogous to Fick's Law of diffusion has been established. Using reduced variables this equation is written

$$\partial c / \partial \theta = - \partial c / \partial X + 1 / Pe. \partial^2 c / \partial X^2$$

From a theoretical point of view, the work of DANCKWERTS (2), MIYAUCHI and VERMEULEN and SLEICHER (4) contributed to the formulation and to the solution of the problem.

In reduced coordinates, two parameters characterise this model : τ , the mean residence time between the entrance point and the measurement point and Pe , the Peclet number for the phase considered.

5.1 - Use of the moments of the "C" curve

Let us suppose that the experimental response curve to a perturbation introduced in a system is known, the most reliable method of verifying a theoretical model would consist in solving the equations describing the model and in comparing theoretical and experimental curves. This method is quite often tedious. One of the most attractive method is the use of the various moments of the distribution of the "C" curve. The interesting property of the moments of a distribution is that they completely define the distribution : hence they can be used to compare the distribution without comparing the curves themselves. LEVENSPIEL and SMITH (5) were the first to point out the relation between the moments and the dispersion coefficient, the form of the relation depends on the boundaries conditions. VAN DER LAAN (6) generalized the calculations using the transform curves.

As a general rule all the moments are necessary to describe any sort of curve but if a given phenomenon can be described by a model using "n" parameters then "n" moments are independent. Usually only the two first moments are used because of the errors due to the lack of accuracy for higher times, and therefore the mathematical model shall have only two parameters.

Let us consider $s(t)$ the response function to a perturbation. The first moment about the origin is defined for a continuous distribution as

$$\mu_1 = \frac{\int_0^{\infty} t s(t) dt}{\int_0^{\infty} s(t) dt} \quad (2)$$

The second moment about the mean or variance is defined as

$$\sigma^2 = \frac{\int_0^{\infty} (t - \mu_1)^2 s(t) dt}{\int_0^{\infty} s(t) dt} \quad (3)$$

The precise relationship between the first moment and the variance of a "C" curve and Peclet number found by LEVENSPIEL and SMITH (5) and VAN DER LAAN (6) depends on the end conditions. In the case under investigation the relations are

$$\mu_1 = \bar{t}/\tau = 1 + 1/Pe \quad (4)$$

$$\sigma^2 = \sigma_t^2/\tau^2 = 2/Pe + 3/Pe^2 \quad (5)$$

$$\sigma^2/\mu_1^2 = 2Pe + 3/(Pe + 1)^2 \quad (6)$$

As it was already mentioned the mean residence time can be deduced from hold-up experiments and therefore using equations (4) or (5) a Peclet number may be evaluated. It is important to note that in the case of equation (6), experimental mean residence time is not necessary. Results are presented in tables 1-3. Peclet numbers calculated using only the first moment were quite different from the others because of the high sensitivity of the method to errors on the residence time. The figures 5,6,7 illustrate the variations of Peclet numbers calculated from relation (6) as a function of ω , the speed of rotation of the disc with either one or two phases in the column : Peclet numbers decrease smoothly and ω increases. Comparison of the various results demonstrates the important contribution of the dispersed phase in the back mixing of the continuous phase.

5.2 - Least square fit of the response curves in the time domain and in the frequency domain.

The identification of the two parameters \bar{t} and Pe of the model was done using an optimization method which is a modification of HOOKE and JEEVES method (7). Usually the research of the optimum requires 30 to 50 calculations of the criterion function.

The transfer function of the model used is the following

$$C(p) = \exp (Pe/2) \cdot Pe^{1/2} \cdot \exp \left[-Pe^{1/2} (Pe + p)^{1/2} \right] / (Pe)^{1/2}/2 + (Pe/4 + p)^{1/2} \quad (7)$$

The analytical expression of the pulse response is

$$C(\theta) = (Pe/\pi\theta)^{1/2} \exp \left[-Pe(1-\theta)^2/4\theta \right] - Pe/2 \exp Pe \operatorname{erfc} \left[(Pe/\theta)^{1/2}(1 + \theta/2) \right] \quad (8)$$

The above expression may be calculated using the method developed elsewhere (8) and the result is

$$C(\theta) = (Pe/\pi\theta)^{1/2} \exp \left[-Pe(1-\theta)^2/4\theta \right] - Pe/2(\pi)^{1/2} \int_{Pe(1-\theta)^2/4\theta}^{\infty} (Pe+U)^{-1/2} \exp(-U) du \quad (9)$$

The calculation of the integral which appear in equation (9) was done using SIMPSON'S method after having verified that the resulting curve may be assimilated to a 3rd degree conical.

Choice of the criterion

The first reproductibility of the data was verified in the range of conductivity used, then best fit model was obtained by minimization of a non-weighted least square criterion.

In the time domain the criterion is expressed by the integral

$$Z = \int_0^{\infty} [CT(t) - CE(t)]^2 dt$$

with

CT = reduced theoretical concentration

CE = reduced experimental concentration

Z = square of the error surface

The corresponding criterion in the frequency domain is found by means of PARSEVAL theorem

$$Z = 1/\pi \int_0^{\infty} [(\Delta R)^2 + (\Delta I)^2] d\omega$$

with ΔR = difference between the real parts of the transfer function of the model and of the experimental curve

ΔI = difference between the imaginary parts of the transfer function of the model and of the experimental curve.

ω = angular frequency

One advantage of working in the frequency domain is that the analytical expression of the transfer function is simpler than that of the pulse response. In order to calculate easily FOURIER's transform of experimental curves the F.F.T. algorithm was employed (9-10).

6 - DISCUSSION OF THE RESULTS

Results are given in tables 4-9 with two typical graphs (fig. 8-9). The results concern experiments with one phase as well as with two phases. In both cases the value of \bar{T} and Pe , deduced from time or frequency domain identification, are identical. The agreement between experimental and theoretical curves obtained by the use of the optimal values is quite good (fig. 8-9).

Comparison of theoretical and experimental curves shows that Pe obtained by optimization are not very different from the initial values corresponding to the method of the moment : the above proves the good quality of the recorder output and the low noise level. The noteworthy improvement of the criterion depends mainly on the existence of errors in the experiments and especially on the erroneous values of the residence time of the dispersed phase deduced from hold-up measurements.

7 - CONCLUSIONS

Results concerning the hold-up of the dispersed phase showed a strong dependence on the speed of rotation of the discs above a certain speed.

As the speed of rotation was increased the Peclet number for the continuous phase decreased. In the presence of a dispersed phase the back mixing of the continuous phase becomes more important, this tendency being accentuated at low speeds of rotation.

- S Y M B O L S -

C	Reduced concentration
CE	Experimental reduced concentration
CT	Theoretical reduced concentration
DT	Total flow rate
p	LAPLACE parameter
P, Pe	PECLET number
P ₁	PECLET number calculated using first moment
P ₂	PECLET number calculated using variance
P ₂₋₁	PECLET number calculated using the ratio between the variance and the square of the first moment.
Q _c	Continuous phase flow rate
Q _d	Dispersed phase flow rate
s(t)	Response function to a perturbation
t	Time
\bar{t}	Center of gravity of the response curve
W	Speed of rotation of the discs (rpm)
X	Reduced distance
Z	Criterion function : square of the error surface.



ΔR	Difference between the real parts
ΔI	Difference between the imaginary parts
Φ	Hold-up of the dispersed phase
Θ	Reduced time = t/τ
τ	Mean residence time : volume/flow rate
ω	Angular frequency
μ_1	First moment
μ_{1t}	First moment in time unit
σ^2	Variance
σ_t^2	Variance in time unit

Theoretical curves agree with experimental results and the assumed model describes adequately the flow behaviour and hence more realistic value of the hold-up may be deduced from the computed mean residence time.

Identification of the two parameters τ and Pe in the frequency domain is as accurate as in the time domain but approximately 35 times faster.

LITERATURE

- 1 - O. LEVENSPEIL , Chemical Reactor Engineering, Wiley, N.Y. 1962
 - 2 - P.V. DANCKWERTS, Chem. Eng. Sci., 2, 1,(1953)
 - 3 - T. MIYAUCHI and T. VERMEULEN, Ind. Eng. Chem. Funds, 2, 113 et 304,(1963)
 - 4 - C.A. SLEICHER, A.I. Chem. E. Journal, 5, 145, (1959)
 - 5 - O. LEVENSPIEL and W.K. SMITH, Chem. Eng. Sci., 6, 227, (1956)
 - 6 - E.T. VAN DER LAAN, Chem. Eng. Sci., 7, 187, (1958)
 - 7 - D.J. WILDE, Methodes de Recherche d'un Optimum, Dunod, Paris, 1966
 - 8 - J. VILLERMAUX and W.P.M. VAN SWAAYI, Chem. Eng. Sci., 24, 1097, (1969)
 - 9 - P.W. MURRILL, Chem. Eng., Aug. 25, (1969)
 - 10 - A. BORREL, G. MURATET and H. ANGELINO, (à paraître in Chem. Eng. Sci.)
-

FIGURES LIST

Fig. 1 - Apparatus

1. electrical motor
2. constant level tank for the light phase
3. constant level tank for the heavy phase
4. light phase storage
5. heavy phase storage
6. pump
7. rotameter
8. overflow for the heavy phase
9. sampling of the two phases
10. drain-pipe
11. purge-valve
12. pipe to solvent regeneration
13. electromagnetic valve
14. heavy phase sampling

Fig. 2 - Tracer injection system

1. electrical motor
2. tracer storage tank
3. injection electromagnetic valve
4. evacuation electromagnetic valve
5. platine electrodes
- A. operational amplifier
- C. conductimeter
- H. histomat S
- T. relay

Fig. 3 - Liquid hold-up. Total flow rate = 40 l/hr

Fig. 4 - Liquid hold-up. Total flow rate = 45 l/h

Fig. 5 - PECLET numbers (one phase)

Fig. 6 - Continuous phase PECLET numbers. Total flow rate = 40 l/h (two phases)

Fig. 7 - Continuous phase PECLET numbers. Total flow rate = 45 l/h (two phases)

Fig. 8 - Comparison between experimental and theoretical curves $Q_c = 6$ l/h

$$W = 500 \text{ mn}^{-1}$$

Fig. 9 - Comparison between experimental and theoretical curves $Q_c = 6$ l/h

$$W = 1000 \text{ mn}^{-1}$$



TABLE LIST

- Table 1 - PÉCLET NUMBER FOR EXPERIMENTS WITH ONE PHASE.
- Table 2 - PÉCLET number for experiments with two phases
Total flow rate = 40 l/h
- Table 3 - PÉCLET number for experiments with two phases
Total flow rate=45 l/h
- Table 4 - Optimization in the time domain. Experiments with one phase
- Table 5 - Optimization in the time domain. Experiments with two phases
Total flow rate = 40 l/h
- Table 6 - Optimization in the time domain. Experiments with two phases
Total flow rate = 45 l/h
- Table 7 - Optimization in the frequency domain. Experiments with one phase
- Table 8 - Optimization in the frequency domain. Experiments with two phases
Total flow rate = 40 l/h
- Table 9 - Optimization in the frequency domain. Experiments with two phases
Total flow rate = 45 l/h.
-

TABLE 1

PECLET NUMBER FOR EXPERIMENTS WITH ONE PHASE

	P_1	P_2	P_{2-1}		P_1	P_2	P_{2-1}
<u>$Q = 5 \text{ l/h}$</u>				<u>$Q = 6 \text{ l/h}$</u>			
$W = 500$	19.50	53.64	57.17		32.52	56.02	57.46
1000	14.82	37.28	40.33		20.73	39.90	41.74
1500	20.40	29.25	30.11		22.47	30.47	31.17
2000	19.45	22.86	23.20		30.61	25.64	25.32
2500	22.13	21.16	21.07		53.43	23.7 4	22.67
<u>$Q = 6.77 \text{ l/h}$</u>				<u>$Q = 8 \text{ l/h}$</u>			
$W = 500$	9.32	53.27	63.02		24.68	58.51	61.26
1000	8.08	36.48	43.74		16.38	48.58	52.55
1500	8.47	29.47	34.55		19.30	36.72	38.53
2000	9.93	26.95	30.42		26.70	31.19	31.52
2500	11.59	24.78	27.06		23.43	22.21	22.11
<u>$Q = 9 \text{ l/h}$</u>				<u>$Q = 10 \text{ l/h}$</u>			
$W = 500$	7.29	50.67	63.14		38.52	64.70	66.06
1000	6.60	39.40	49.82		15.76	56.64	61.90
1500	5.79	31.09	40.27		17.73	46.57	49.85
2000	7.08	27.54	33.51		17.57	38.47	40.86
2500	7.48	23.70	28.13		25.18	33.71	34.38

TABLE 2

PECLET NUMBER FO EXPERIMENTS WITH TWO PHASES

Total flow rate = 40 l/h

	P_1	P_2	P_{2-1}		P_1	P_2	P_{2-1}
$\underline{Q_d/Q_c = 3}$				$\underline{Q_d/Q_c = 4}$			
W = 0	6.40	36.15	45.90	7.12	32.39	39.75	
500	6.57	31.40	39.28	7.56	31.75	38.37	
1000	5.76	30.32	39.15	9.12	32.12	37.27	
1500	6.43	30.15	37.85	7.27	29.24	35.48	
2000	5.64	25.83	33.33	7.63	26.43	31.50	
2500	6.61	26.96	33.33	7.38	24.33	29.05	
 $\underline{Q_d/Q_c = 5,7}$				 $\underline{Q_d/Q_c = 7}$			
W = 0	9.23	29.75	34.29	13.79	25.53	27.23	
500	9.82	28.86	32.80	12.91	26.02	28.05	
1000	13.17	28.56	30.90	10.66	23.17	25.53	
1500	9.45	25.84	29.36	12.64	22.32	23.85	
2000	9.81	23.64	26.48	12.40	18.72	19.72	
2500	10.49	21.21	23.25	10.91	17.53	18.73	

TABLE 3

PECLET NUMBER FOR EXPERIMENTS WITH TWO PHASES

Total flow rate = 45 l/h

	P_1	P_2	P_{2-1}		P_1	P_2	P_{2-1}
<u>$Q_d/Q_c = 3$</u>				<u>$Q_d/Q_c = 4$</u>			
W = 0	6.86	31.74	39.29		6.68	24.73	30.31
500	5.45	30.25	39.87		5.83	24.77	31.54
1000	5.03	27.33	36.73		6.29	22.44	27.75
1500	5.70	26.36	33.95		16.34	28.08	29.52
2000	5.22	24.42	32.15		5.34	17.40	22.07
2500	4.70	20.43	27.50		5.18	16.89	21.58
<u>$Q_d/Q_c = 5,7$</u>				<u>$Q_d/Q_c = 7$</u>			
W = 0	6.57	22.74	27.82		5.91	16.94	20.76
500	6.31	21.11	25.94		5.64	15.21	18.69
1000	5.89	19.60	24.40		7.98	17.54	19.95
1500	6.75	19.05	22.78		6.70	15.99	18.79
2000	5.94	17.16	21.03		6.63	16.36	19.34
2500	4.94	15.62	20.11		5.71	14.96	18.27

TABLE 4

OPTIMIZATION IN THE TIME DOMAIN. EXPERIMENTS WITH ONE PHASE

	Initial values			Final values		
	P	τ	$z \cdot 10^2$	P	τ	$z \cdot 10^2$
<u>$Q = 5 \text{ l/h}$</u>						
W = 500	57.17	20.24	3.25	53.95	21.00	0.22
1000	40.33	20.24	3.09	38.82	21.25	0.15
1500	30.11	20.24	0.49	29.73	20.62	0.11
2000	23.20	20.24	0.13	24.07	20.37	0.05
2500	21.07	20.24	0.11	21.73	20.11	0.09
<u>$Q = 6 \text{ l/h}$</u>						
W = 500	57.46	16.87	1.22	61.77	17.19	0.22
1000	41.74	16.87	1.46	42.52	17.40	0.22
1500	31.17	16.87	0.49	30.20	17.19	0.19
2000	25.32	16.87	0.41	28.17	16.76	0.19
2500	22.67	16.87	0.29	22.53	16.55	0.12
<u>$Q = 6.77 \text{ l/h}$</u>						
W = 500	63.02	14.95	19.42	59.08	16.35	0.13
1000	43.74	14.95	13.00	42.37	16.45	0.14
1500	34.55	14.95	8.10	33.69	16.35	0.14
2000	30.42	14.95	4.62	28.14	16.07	0.17
2500	27.06	14.95	2.35	25.37	15.79	0.14
<u>$Q = 8 \text{ l/h}$</u>						
W = 500	61.26	12.65	1.35	65.09	12.89	0.10
1000	52.55	12.65	4.06	49.59	13.20	0.27
1500	38.53	12.65	1.42	35.64	13.05	0.23
2000	31.52	12.65	0.32	31.72	12.81	0.20
2500	22.11	12.65	1.82	29.57	12.57	0.38
<u>$Q = 9 \text{ l/h}$</u>						
W = 500	63.14	11.25	29.77	65.11	12.59	0.06
1000	49.82	11.25	25.38	49.20	12.73	0.12
1500	40.27	11.25	22.86	39.77	12.94	0.12
2000	33.53	11.25	11.19	32.67	12.52	0.10
2500	28.13	11.25	6.82	26.37	12.37	0.12

...

$$Q = 10 \text{ l/h}$$

W = 500	66.06	10.12	0.78	67.30	10.25	0.17
1000	61.90	10.12	5.77	58.42	10.63	0.28
1500	49.85	10.12	3.03	45.49	10.50	0.31
2000	40.86	10.12	2.07	37.54	10.50	0.21
2500	34.38	10.12	1.01	29.87	10.31	0.33

TABLE 5

OPTIMIZATION IN THE TIME DOMAIN. EXPERIMENTS WITH TWO PHASES

Total flow rate = 40 l/h

	Initial values			Final values		
	P	τ	$z \cdot 10^2$	P	τ	$z \cdot 10^2$
$Q_d/Q_c = 3$						
W = 0	45.90	9.30	22.28	43.89	10.52	0.09
500	39.29	9.30	16.95	39.53	10.46	0.08
1000	39.15	9.29	22.27	37.44	10.68	0.11
1500	37.85	9.25	17.49	37.38	10.46	0.13
2000	33.33	9.10	17.36	30.62	10.47	0.14
2500	33.33	8.70	13.02	31.87	9.79	0.12
$Q_d/Q_c = 4$						
W = 0	39.75	11.57	14.80	38.01	12.94	0.12
500	38.37	11.56	12.49	36.21	12.86	0.15
1000	37.27	11.54	8.31	33.78	12.55	0.18
1500	35.48	11.52	12.09	35.26	12.82	0.11
2000	31.50	11.22	8.73	27.96	32.41	0.17
2500	29.05	10.69	7.86	26.33	11.83	0.15
$Q_c/Q_d = 5,7$						
W = 0	34.29	15.39	6.64	30.65	16.74	0.19
500	32.80	15.38	5.35	29.93	16.33	0.19
1000	30.90	15.32	2.30	29.93	16.09	0.11
1500	29.36	15.26	4.85	26.24	16.50	0.18
2000	26.48	14.77	3.60	23.50	15.88	0.17
2500	23.25	13.95	1.95	22.23	14.73	0.13
$Q_c/Q_d = 7$						
W = 0	27.23	18.47	1.47	24.85	19.28	0.14
500	28.05	18.46	1.97	25.35	19.38	0.16
1000	25.53	18.34	2.78	23.14	19.49	0.17
1500	23.85	18.26	1.46	21.47	19.06	0.16
2000	19.72	17.69	0.73	18.12	18.35	0.10
2500	18.73	16.73	1.08	16.97	17.46	0.14

TABLE 6

OPTIMIZATION IN THE TIME DOMAIN. EXPERIMENTS WITH TWO PHASES

Total flow rate = 45 l/h

	Initial values			Final values		
	P	τ	$z \cdot 10^2$	P	τ	$z \cdot 10^2$
<u>$Q_d/Q_c = 3$</u>						
W = 0	39.29	8.21	14.52	37.33	9.19	0.07
500	39.87	8.21	37.45	43.61	99.65	0.42
1000	36.73	8.21	24.65	34.20	9.60	0.31
1500	33.95	8.19	16.39	32.25	9.37	0.07
2000	32.15	7.98	18.29	28.53	9.28	0.10
2500	27.50	7.50	17.11	25.27	8.77	0.40
<u>$Q_d/Q_c = 4$</u>						
W = 0	30.31	10.25	9.50	29.93	11.40	0.06
500	31.54	10.23	13.45	29.57	11.64	0.07
1000	27.75	10.23	8.78	25.50	11.44	0.14
1500	29.52	10.18	1.10	26.94	10.50	0.11
2000	22.07	9.92	8.02	22.48	11.16	0.05
2500	21.58	9.35	8.23	21.31	10.58	0.04
<u>$Q_d/Q_c = 5,7$</u>						
W = 0	27.82	13.58	8.21	25.21	15.11	0.08
500	25.94	13.58	7.75	23.35	15.19	0.76
1000	24.40	13.52	8.01	22.11	15.21	0.07
1500	22.78	13.44	4.86	20.64	14.78	0.08
2000	21.03	12.97	5.74	18.93	14.43	0.07
2500	20.11	11.96	8.19	17.72	13.75	0.08
<u>$Q_d/Q_c = 7$</u>						
W = 0	20.76	16.30	5.29	20.24	18.03	0.08
500	18.69	16.30	4.54	16.59	18.13	0.18
1000	19.95	16.25	2.73	17.08	17.47	0.09
1500	18.79	16.12	3.30	16.79	17.63	0.07
2000	19.34	15.56	3.76	16.80	17.02	0.09
2500	18.27	14.27	4.69	15.99	15.88	0.08

TABLE 7

OPTIMIZATION IN THE FREQUENCY DOMAIN. EXPERIMENTS WITH ONE PHASE

	Initial values			Final values		
	P	τ	$Z(\pi/\Delta\omega)$	P	τ	$Z(\pi/\Delta\omega) 10^3$
<u>$Q = 5 \text{ 1/h}$</u>						
$\omega = 500$	57.17	20.24	0.1029	53.95	21.00	6.64
1000	40.33	20.24	0.0978	38.82	21.25	4.52
1500	30.11	20.24	0.0156	29.73	20.62	3.30
2000	23.20	20.24	0.0403	23.93	20.49	1.52
2500	21.07	20.24	0.0033	21.73	20.11	2.66
<u>$Q = 6 \text{ 1/h}$</u>						
$\omega = 500$	57.46	16.87	0.0461	61.77	17.19	8.24
1000	41.74	16.87	0.0549	42.26	17.40	7.82
1500	31.17	16.87	0.0184	30.00	17.19	6.81
2000	25.32	16.87	0.0154	28.17	16.76	7.39
2500	22.67	16.87	0.0111	22.53	16.55	4.71
<u>$Q = 6.77 \text{ 1/h}$</u>						
$\omega = 500$	63.02	14.95	0.8007	59.08	16.35	4.75
1000	43.74	14.95	0.5569	42.37	16.45	5.22
1500	34.55	14.95	0.3466	33.69	16.35	4.88
2000	30.42	14.95	0.1981	28.14	16.07	6.67
2500	27.06	14.95	0.1003	25.20	15.79	5.10
<u>$Q = 8 \text{ 1/h}$</u>						
$\omega = 500$	61.26	12.65	0.0678	65.09	12.89	4.79
1000	52.55	12.65	0.2056	49.59	13.20	12.69
1500	38.53	12.65	0.0720	35.64	13.05	11.38
2000	31.52	12.65	0.0160	31.72	12.81	9.75
2500	22.11	12.65	0.0917	29.57	12.57	19.29

...

$$Q = 9 \text{ l/h}$$

$w = 500$	63.14	11.25	1.6952	65.11	12.59	3.13
1000	49.82	11.25	1.4449	49.20	12.73	5.72
1500	40.27	11.25	1.3012	39.77	12.94	5.65
2000	33.51	11.25	0.6373	32.67	12.52	4.90
2500	28.13	11.25	0.3886	26.37	12.37	5.91

$$Q = 10 \text{ l/h}$$

$w = 500$	66.06	10.12	0.0479	67.30	10.25	9.36
1000	61.90	10.12	0.3647	58.42	10.63	16.40
1500	49.85	10.12	0.1920	45.49	10.50	18.59
2000	40.86	10.12	0.1303	37.28	10.50	17.99
2500	34.38	10.12	0.0638	29.65	10.31	20.32

TABLE 8

OPTIMIZATION IN THE FREQUENCY DOMAIN. EXPERIMENTS WITH TWO PHASES

Total flow rate = 40 l/h

	Initial values			Final values		
	P	τ	$Z(\eta/\Delta\omega)$	P	τ	$Z(\eta/\Delta\omega) \cdot 10^3$
<u>$Q_d/Q_c = 3$</u>						
W = 0	45.90	9.30	1.5352	43.89	10.52	4.97
500	39.28	9.30	1.1672	39.53	10.46	5.00
1000	39.15	9.29	1.5359	37.44	10.68	6.22
1500	37.85	9.25	1.2107	37.38	10.46	7.85
2000	33.33	9.10	1.2219	30.41	10.46	8.65
2500	33.33	8.70	0.9584	31.87	9.79	7.57
<u>$Q_d/Q_c = 4$</u>						
W = 0	39.75	11.57	0.8195	38.01	12.94	5.83
500	38.37	11.56	0.6919	36.21	12.86	6.89
1000	37.27	11.54	0.4612	33.78	12.62	8.95
1500	35.48	11.52	0.6722	35.26	12.82	5.56
2000	31.50	11.22	0.4986	27.96	12.41	8.77
2500	29.05	10.69	0.4710	26.33	11.83	7.75
<u>$Q_d/Q_c = 5,7$</u>						
W = 0	34.29	15.39	0.2754	30.65	16.74	7.07
500	32.80	15.38	0.2229	29.93	16.53	7.18
1000	30.90	15.32	0.0964	29.93	16.09	4.34
1500	29.36	15.26	0.2038	26.24	16.50	6.89
2000	26.48	14.77	0.1564	23.50	15.88	6.90
2500	23.25	13.95	0.0694	22.23	14.73	5.38
<u>$Q_d/Q_c = 7$</u>						
W = 0	27.23	18.47	0.0509	24.85	19.28	4.63
500	28.05	18.46	0.0685	25.93	19.38	5.16
1000	25.53	18.34	0.0972	23.14	19.49	5.42
1500	23.85	18.26	0.0512	21.47	19.06	5.33
2000	19.72	17.69	0.0264	18.12	18.35	3.13
2500	18.73	16.73	0.0413	16.86	17.46	5.23

TABLE 9

OPTIMIZATION IN THE FREQUENCY DOMAIN. EXPERIMENTS WITH TWO PHASES

Total flow rate = 45 l/h

	Initial values			Final values		
	P	τ	$Z(\eta/\Delta\omega)$	P	τ	$Z(\eta/\Delta\omega) \cdot 10^3$
<u>$Q_d/Q_c = 3$</u>						
W = 0	39.29	8.21	1.1327	37.33	9.19	4.98
500	39.87	8.21	1.1913	37.13	9.49	20.08
1000	36.73	8.21	1.8573	33.29	9.60	7.65
1500	33.95	8.19	1.2870	32.25	9.37	4.91
2000	32.15	7.98	1.4684	28.53	9.28	6.63
2500	27.50	7.50	1.4489	25.27	8.81	16.03
<u>$Q_d/Q_c = 4$</u>						
W = 0	30.31	10.25	0.5935	29.93	11.40	2.95
500	31.54	10.23	0.8419	29.37	11.64	3.84
1000	27.75	10.23	0.5494	25.50	11.44	7.42
1500	29.52	10.18	0.0695	26.94	10.50	6.88
2000	22.07	9.92	0.5179	22.48	11.16	2.86
2500	21.58	9.35	0.5639	21.31	10.58	2.65
<u>$Q_d/Q_c = 5,7$</u>						
W = 0	27.82	13.58	0.3872	25.21	15.11	3.45
500	25.94	13.58	0.3657	23.35	15.19	3.11
1000	24.40	13.52	0.3798	22.11	15.21	2.89
1500	22.78	13.44	0.2317	20.64	14.78	3.49
2000	21.03	12.97	0.2834	18.93	14.43	3.03
2500	20.11	11.96	0.4385	17.72	13.75	3.41
<u>$Q_d/Q_c = 7$</u>						
W = 0	20.76	16.30	0.2080	20.24	18.03	2.61
500	18.69	16.30	0.1786	16.47	18.13	6.35
1000	19.95	16.25	0.1078	17.08	17.47	3.14
1500	18.79	16.12	0.1313	16.79	17.63	2.64
2000	19.34	15.56	0.1550	16.68	17.12	3.15
2500	18.27	14.27	0.2106	15.87	15.88	3.23

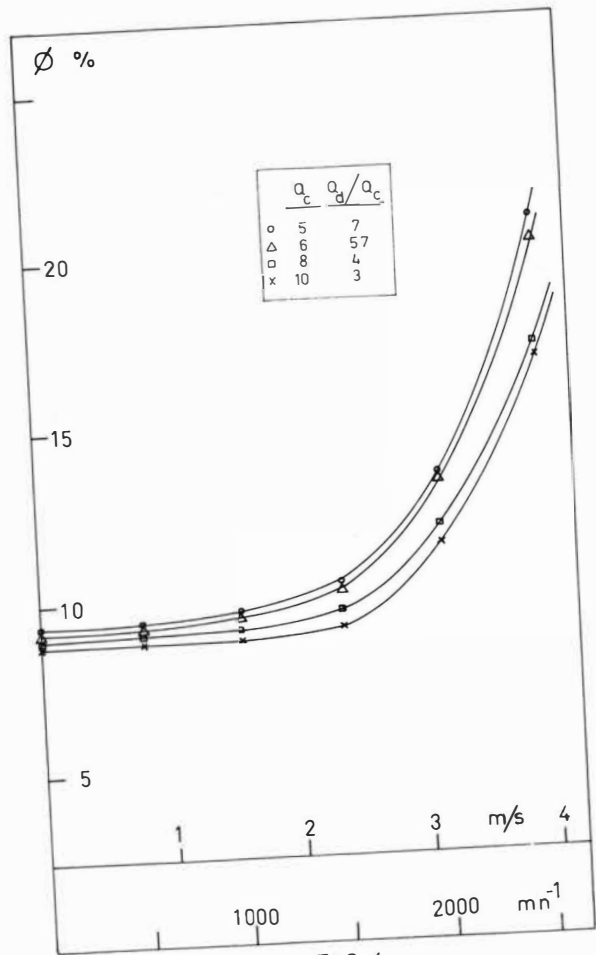


FIG 4

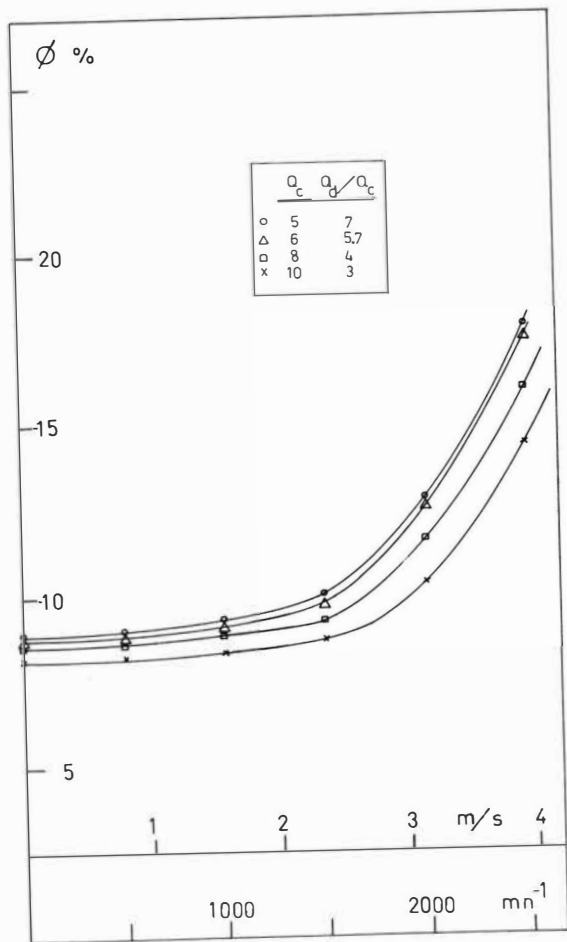


FIG 3

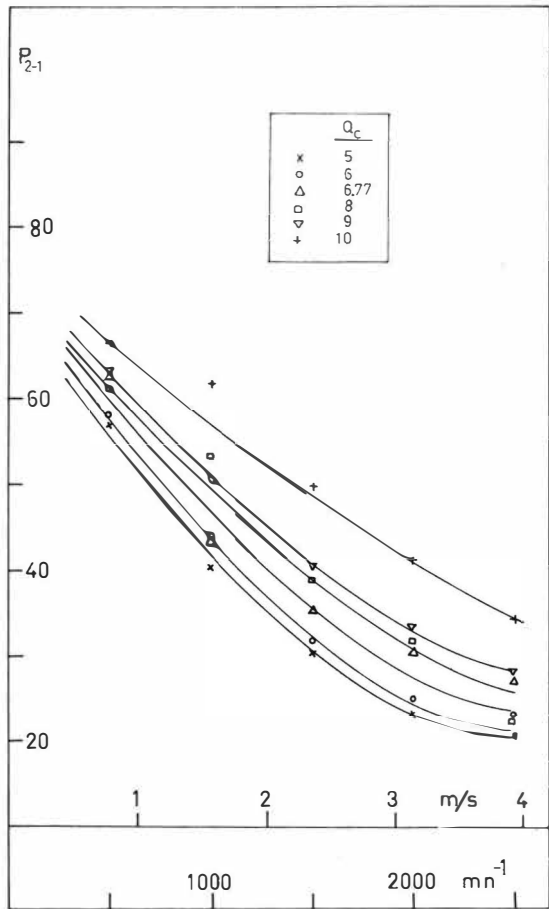


FIG 5

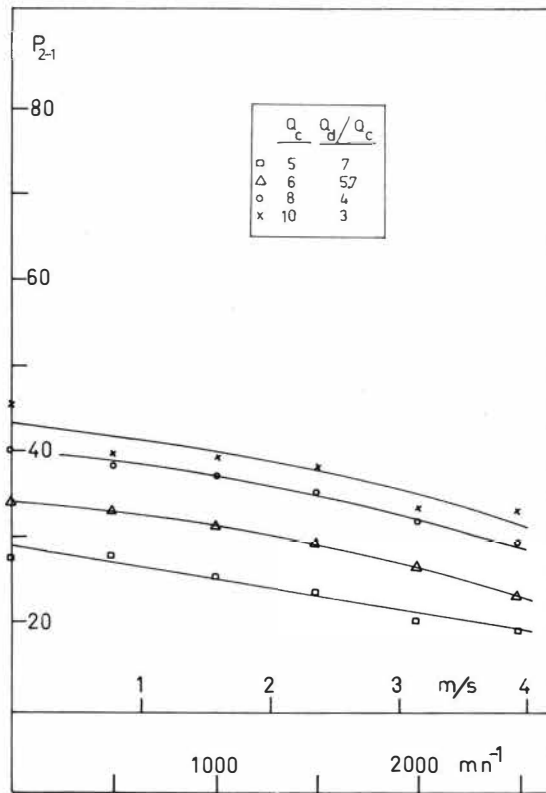


FIG 6

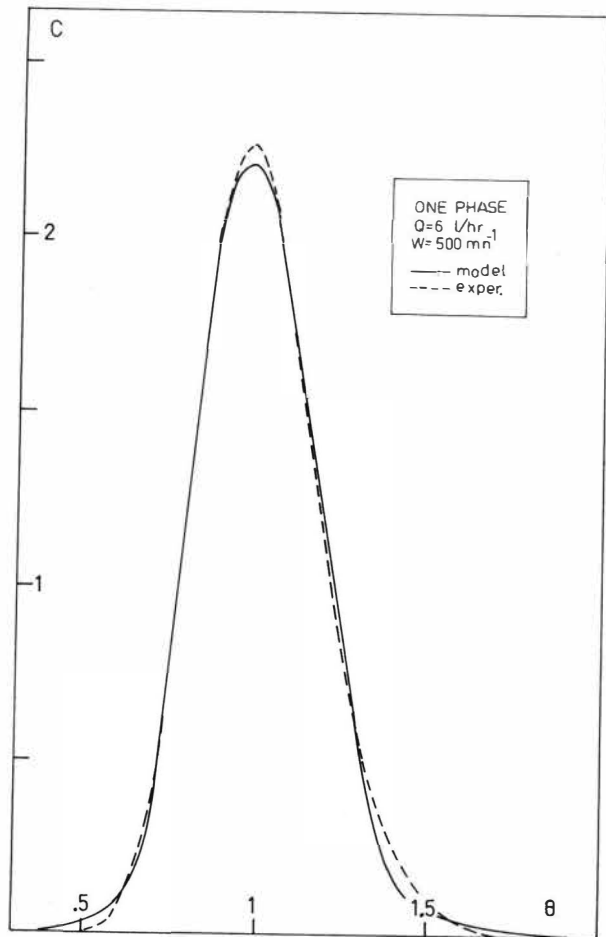


FIG 8

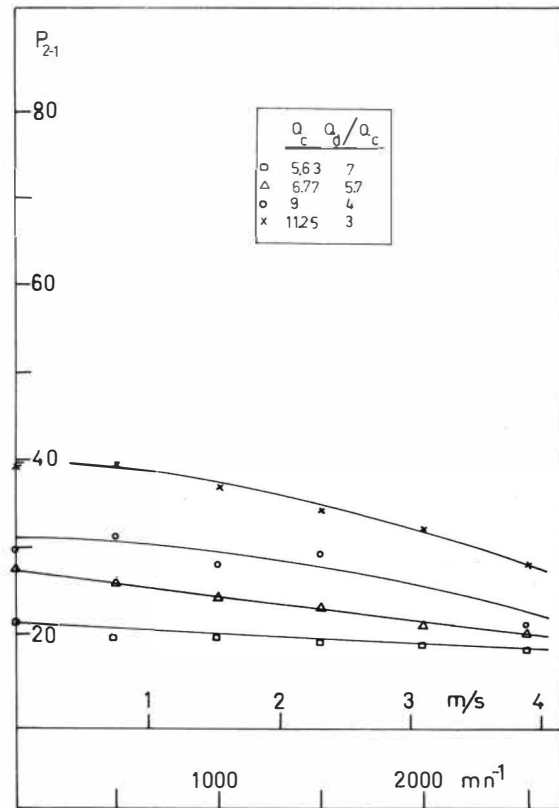


FIG 7

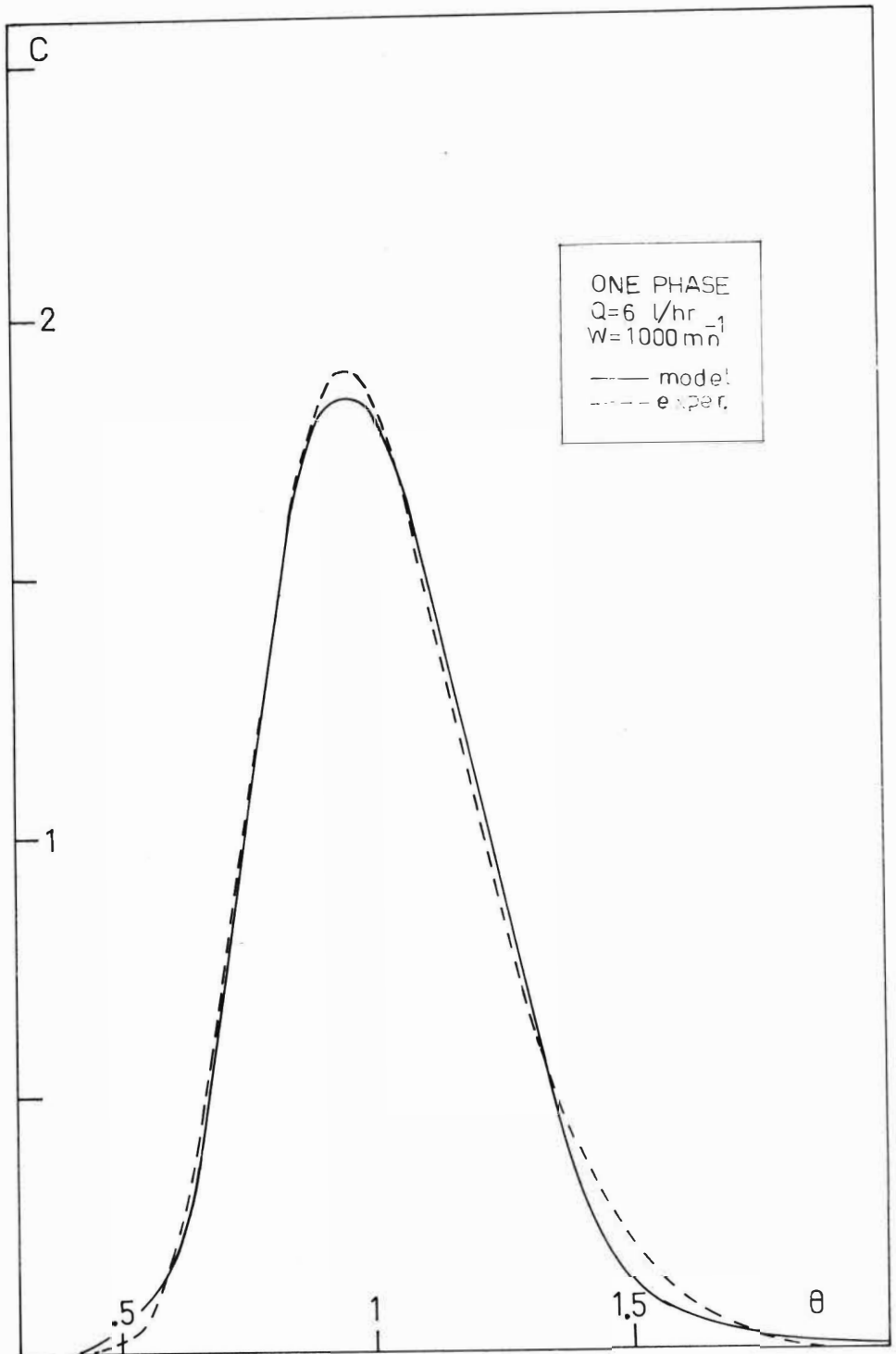


FIG 9

Hydrodynamic Behavior of Packed Liquid-Liquid Extraction
Columns with Fluids of Different Densities*

J. S. Watson
L. E. McNeese

Oak Ridge National Laboratory
Oak Ridge, Tennessee 37830

Abstract

Flooding rates and axial dispersion in packed columns are examined using new data covering a wide range of physical properties especially density difference. A new correlation for flooding rates is developed and shown to be significantly more accurate than previous correlations. Axial dispersion data for high density fluids are satisfactorily described by an existing correlation.

* Research sponsored by the U. S. Atomic Energy Commission under contract with the Union Carbide Corporation.

Introduction

Past studies of countercurrent flow in packed columns have been concerned, for the most part, with systems using organic solvents and aqueous solutions, since these types of fluids have been used in most solvent extraction applications. In recent years, however, applications requiring high-density fluids such as liquid metals and/or molten salts have received increased attention.¹⁻³ Watson and McNeese¹ and Johnson and coworkers³ showed that conventional correlations developed from data on organic-aqueous systems were of little help in estimating the hydrodynamic behavior of systems consisting of high-density (or high-density-difference) fluids. Correlations that give similar predictions in the case of low-density fluids give widely divergent predictions for high-density fluids and thus cannot be extrapolated to conditions far removed from those observed in conventional systems. Watson and McNeese reported a correlation to predict flooding rates or capacities for columns operating with mercury and water. However, this correlation cannot be extrapolated to low-density systems since systematic variations of fluid properties were not included in that study. More recent measurements reported by Watson, McNeese, Day, and Carrod⁴ have provided information on variations in physical properties in systems of high density difference, as well as data for high-density halocarbons (CCl_4 and CH_2Br_2). These new results made it possible to develop a general correlation covering a wide range of physical properties. Such a correlation is needed as solvent extraction applications incorporating a wide range of conditions become increasingly important. The general correlation, even if it does not fit either the conventional low-density data or the high-density data as well as correlations based upon a narrow range of conditions,

would permit a higher degree of reliability in extrapolating or interpolating to new conditions of interest.

Flooding Rates

Literature Review

Correlations for predicting flooding rates in packed columns have been reviewed by Nemunaitis *et al.*⁵ and more recently by Watson and McNeese. Breckenfeld and Wilke⁶ measured flooding rates with several low-density fluids and 0.635-cm (1/4-in.) Raschig rings and Berl saddles. They developed a correlation which can be written as

$$(v_{c,f}^{1/2} + v_{d,f}^{1/2})^2 = 32.5 \frac{\Delta\rho^{0.98} \epsilon^{1.98}}{a^{0.82} \mu_c^{0.32} \sigma^{0.26}} \quad (1)$$

Crawford and Wilke⁷ used additional data from larger Raschig rings to develop two similar equations. For

$$\frac{(v_{c,f}^{1/2} + v_{d,f}^{1/2})^2 \rho_c}{a \mu_c} > 50, \quad (2)$$

flooding occurs when

$$(v_{c,f}^{1/2} + v_{d,f}^{1/2})^2 = \frac{69.4 \Delta\rho \epsilon^{1.5}}{\rho_c^{0.8} a^{0.5} \sigma^{0.2}} \quad (3)$$

For values less than 50, flooding occurs when

$$(v_{c,f}^{1/2} + v_{d,f}^{1/2})^2 = \frac{79.7 \Delta\rho^{1.33} \epsilon^2}{\rho_c^{0.73} a \mu_c^{0.33} \sigma^{0.27}} \quad (4)$$

Ballard and Piret⁸ proposed the correlation

$$\begin{aligned} & [v_{d,f}^{1/2} + 1.7 \left(\frac{\rho_c}{\rho_d}\right)^{0.3} v_{c,f}^{1/2}]^2 \\ & = \frac{0.3025 \epsilon^{0.55} \Delta\rho^{0.43}}{\rho_d^{0.83} \mu_d^{0.1}} \left(\frac{\epsilon}{a^{0.65}} \left(\frac{\sigma_{da} + \sigma_{ca}}{\sigma} \right)^{0.4} \right), \end{aligned} \quad (5)$$

and Dell and Pratt⁹ used data from several fluids and several packing materials to develop the correlation

$$[V_{c,f}^{1/2} + 0.835 \left(\frac{\rho_d}{\rho_c}\right)^{1/4} V_{d,f}^{1/2}]^2 = C_2^2 \left(\frac{a}{g \epsilon^3}\right)^{-1/2} \left(\frac{\rho_c}{\Delta \rho}\right)^{-1/2} \sigma^{-1/3}. \quad (6)$$

All of the above expressions represent a straight line on a plot of $V_{d,f}^{1/2}$ vs $V_{c,f}^{1/2}$, as do most experimental data. Hoffing and Lockhart,¹⁰ however, proposed a different type of expression:

$$V_c = \left[\frac{\phi \left(\frac{V_{d,f}}{V_{c,f}} \right) \Delta \rho^{1/2}}{\rho_d^{0.22} \rho_c^{0.1} \mu_d^{0.08} \mu_c^{0.1} \left(\frac{\sigma}{\sigma_{ca}} \right)^{0.5} \left(\frac{a}{\epsilon^{1.2}} \right)^{0.67}} \right]^{1.25} \left(\frac{V_{d,f}}{V_{c,f}} \right)^{1/4}, \quad (7)$$

where the function $\phi \left(\frac{V_{d,f}}{V_{c,f}} \right)$ is presented in their paper. This equation does not yield a straight line on a plot of $V_{d,f}^{1/2}$ vs $V_{c,f}^{1/2}$, but for conventional low-density systems, it is in agreement with other correlations.

Conventional low-density systems were used in all of the studies mentioned above. Watson and McNeese,¹ who reported flooding rates with mercury and water and 3/16- to 3/8-in. Raschig rings could be represented by,

$$V_{c,f}^{1/2} + V_{d,f}^{1/2} \sim K, \quad (8)$$

where K is proportional to the column void fraction and to the packing (Raschig ring) diameter. Few data and no correlation existed to link the conventional low-density data with the new high-density results. The new results recently reported by the authors makes it possible to develop a more general correlation encompassing both sets of data.

Summary of Available Data

Most of the flooding data chosen for use in the present study (see Table 1) were taken from five sources: Dell and Pratt, Breckenfeld and Wilke, Crawford

and Wilke, Ballard and Piret, and Watson, McNeese et al. The first three sources contain data from conventional low-density systems plus a small amount of information on CCl_4 and water. The last source provides data for high-density systems (mercury and water) and a few data for intermediate-density systems (CH_2Br_2 or CCl_4 with water). Hannaford et al.¹¹ have reported results for liquid bismuth and a molten fluoride salt, while Johnson et al. have reported results for Woods metal and water.

The column packing in this study was restricted to Raschig rings. Although considerable data are available for other packing materials, especially Berl saddles, there is not sufficient information on any other single packing to permit an analysis and correlation of the magnitude presented here. It appears likely that other materials will show a similar dependence upon fluid properties and packing dimensions; hence the results of this study should be useful in extrapolating data from other packing materials to the systems of interest. Several authors⁶⁻¹⁰ have reported correlations which use the packing external surface area per unit packing volume rather than packing diameter as a parameter. For a single type of packing, such as Raschig rings, this parameter is approximately proportional to $1/d_p$, where d_p denotes packing diameter. The only advantage of using packing area instead of d_p as a correlating parameter is that the resulting correlation may possibly describe results from several types of packing, such as Raschig rings and Berl saddles. When the interaction between the two phases occurs over the surface of the packing (such as gas-liquid systems with packing wet by the dispersed liquid phase), there is some theoretical basis for such a parameter; for example, the area of contact and drag between the two phases is essentially equal to the area of packing surface. On the other hand, liquid-liquid systems

usually operate with the packing not wet by the dispersed phase. In these cases, the dispersed phase travels up or down the column in the form of droplets, and there is no justification for such a single correlation for all packing shapes. The interacting surface area is that of the droplets, not that of the packing. In any case, there is little reason to use packing area rather than the more easily measured packing diameter as a parameter in correlating data from a single packing shape.

Examination of each set of data listed in Table 1 indicated that flooding data can be approximated reasonably well as a straight line when the square root of the superficial flow rate of one phase is plotted against the square root of the other flow rate. This behavior has also been reflected in several previous correlations (see Equations 1, 3, 4, 5 and 6). The new correlation was developed on this basis. The flooding points from each data set were fit to a straight line with the form

$$V_{c,f}^{1/2} + k_1 V_{d,f}^{1/2} = k_2 \quad (9)$$

The resulting parameters k_1 and k_2 for each set of data were evaluated by a least-squares regression, and the results are shown in Table 1. Only those sets where the uncertainties in k_1 or k_2 did not exceed 30% of their most probable value are listed. This criterion eliminated a few sets of scattered data, but, in general, they were sets containing only one or two data points. The reliability of the eliminated data could not be quantitatively confirmed.

Results

The parameters of Equation 9, k_1 and k_2 , are functions of fluid and packing properties; the significant variables were identified and the functional dependences were evaluated. It was convenient to use the intercepts of $V_{c,f}^{1/2}$ -vs- $V_{d,f}^{1/2}$

plots rather than k_1 and k_2 for the dependent variables of the correlation. These intercepts are related directly to k_1 and k_2 as follows:

$$V_{c,o}^{1/2} = k_2 \quad (10)$$

and

$$V_{d,o}^{1/2} = \frac{k_2}{k_1} \quad (11)$$

Several independent variables were investigated; among these were fluid density difference, $\Delta\rho$; packing diameter, d_p ; packing void fraction, ϵ ; continuous-phase viscosity, μ_c ; and interfacial tension, σ . Both $V_{c,o}^{1/2}$ and $V_{d,o}^{1/2}$ were correlated with all of these parameters; however, some of the parameters did not significantly affect one or both of the dependent variables. The correlations were improved by discarding some parameters. The resulting correlations were compared using the F ratio as a figure of merit:

$$F = \frac{\Sigma(y - y_{\text{mean}})^2/n_{\text{coefficient}}}{\Sigma(y - y_{\text{predicted}})^2/(n_{\text{data}} - n_{\text{coefficient}})} \quad (12)$$

The higher the F ratio, the better the correlation.

The best fits to the data were:

$$V_{c,o}^{1/2} = (23.8 \pm 0.6)\Delta\rho^{0.269 \pm 0.015} d_p^{0.494 \pm 0.046} \mu_c^{-0.084 \pm 0.030} \epsilon^{0.50}, \quad (13)$$

$$V_{d,o}^{1/2} = (28.2 \pm 2.1)\Delta\rho^{0.124 \pm 0.017} d_p^{0.196 \pm 0.062} \epsilon^{1.28 \pm 0.18}. \quad (14)$$

All of the regression coefficients are given above, along with their standard error, except in the case of ϵ in Equation 13. The first regressions gave an exponent of 0.35 ± 0.15 . Fixing the exponent at 0.5, however, resulted in a higher F ratio, or a better fit. Additional regressions were made with fixed exponents of 0.45 and 0.55, both of which gave lower values for the F ratio. This means that a minimum sum of residual squares occurs when the value of this exponent is near 0.50. Thus, this value was chosen for the correlation.

The scatter of data around the correlations is illustrated in Figures 1 and 2. These are common log plots of the predicted intercepts vs the experimental or measured values. The scatter in the results is significant but not unreasonable for flooding data. The F ratios for the $V_{c,o}^{1/2}$ and $V_{d,o}^{1/2}$ correlations were 133 and 32, respectively. These values suggest a high confidence in the validity of the correlations (greater than 99%).

Equations 13 and 14 can be combined into the more convenient single form of equation 9:

$$\begin{aligned}
 V_{c,f}^{1/2} + (0.844\Delta\rho^{0.145} d_p^{0.298} \mu_c^{-0.084} \epsilon^{-0.078}) V_{d,f}^{1/2} \\
 = 23.8\Delta\rho^{0.269} d_p^{0.494} \mu_c^{-0.084} \epsilon^{0.5}.
 \end{aligned}
 \tag{15}$$

This flooding correlation is based upon more extensive data and a wider range of physical properties than has been the case for any previous correlation. Thus it should be more reliable in predicting flooding rates for new systems where no data exist. Its advantages will be most evident when systems with higher density differences are used. Since it is not a dimensionless correlation, however, care must be taken to choose correct units.

Discussion of Results

Comparison of the New Correlation with Previous Correlations. — In Table 2, the fit of this new correlation to the data in Table 1 is compared with some of the previous correlations. The measured and predicted intercepts of flooding curves are compared for conventional low-density data ($\Delta\rho < 0.5$), for high-density data ($\Delta\rho > 0.5$), and for all of the data listed in Table 1. For each intercept, the fractional "error", e_f , in each correlation has been evaluated:

$$e_f = \frac{V_{\text{calc}}^{1/2} - V_{\text{meas}}^{1/2}}{V_{\text{meas}}^{1/2}} \quad (16)$$

The fractional error for each correlation listed in Table 2 is defined as:

$$\Delta_f = \sqrt{\frac{\sum e_f^2}{n-1}} \quad (17)$$

The fractional error is written to resemble a standard deviation. Since the same number of data points was used for each correlation, n is of no importance in comparing correlations for any set of data. However, the normalization achieved by the denominator $n-1$ allows the relative accuracies of the correlations for low-density, high-density, and all data to be compared.

The new correlation, Equation 15, is in good agreement with both low-density- and high-density-difference data. It is more accurate than any of the other three correlations listed in Table 2 for both high- and low-density data. The fractional errors in $V_{c,o}^{1/2}$ and $V_{d,o}^{1/2}$ range from 0.20 to 0.30. The most accurate of the previous correlations, that of Dell and Pratt, gives significantly larger fractional errors. At low values of V_d , e.g. at the $V_{c,o}^{1/2}$ intercept their error is from 0.30 to 0.40. On the other hand, the accuracy of their correlation diminishes further at high V_d values. Both of the other correlations tested were considerably less accurate. Their fractional errors range from approximately 0.88 to 0.90. The new correlation is clearly better.

The differences between the new correlation and previous expressions also can be illustrated by comparing the dependence of flooding rates on several parameters, i.e., the exponents of these parameters. Exponents of Δp are approximately unity in Equations 1, 3, and 4, while the exponent is near 0.5 for Equations 5 and 6. The latter value is in agreement with the new results. The

exponent for the specific packing area, a , is near -0.5 for Equations 3, 5, and 6, but near -1 for Equations 1 and 4. The new correlation agrees with the latter value. Similar differences are observed for the exponents of μ_c and ϵ . Since the new correlation is based on a wider range of experimental conditions, it should be more reliable than previous ones. It is evident from comparisons of exponents that differences in correlations could be important if extrapolations to conditions far from those encountered in conventional systems are required. The differences between the new, proposed correlation and previous correlations are significant and justify the use of the new correlation in estimating flooding rates with new fluids or in extrapolating data with other packing materials.

Interpretation of Results. — We have examined the power dependence of flooding rates on some parameters shown in Equations 13, 14, and 15 and attempted to rationalize the results from qualitative knowledge of countercurrent flow patterns in packed columns. At high continuous-phase and low dispersed-phase flow rates, the dispersed phase moves up or down the column in the form of small droplets. The dependence of flooding rates on density difference and void fraction is essentially what one would expect from settling rates of separate spheres. In the inertial region, spheres settle with an approximately constant drag coefficient; therefore, the settling (slip) velocity is proportional to the square root of the density difference. In Equation 15, the dependence (0.538) is near the value. Furthermore, in the inertial region, the flooding rate should not be a strong function of continuous-phase viscosity, i.e., power dependence on viscosity should be considerably less than unity. The dependence as shown in Equation 15 is significant but small (0.168), which is not inconsistent with the physical model just described.

At high dispersed-phase flow rates, the droplets coalesce into larger droplets, which fill some of the packing openings. It is more difficult to rationalize the dependence of $V_{d,0}$ on the significant parameters with physical interpretations. In this range of flow rates, interaction of the dispersed phase with the packing is increased. The viscosity of the continuous phase should, then, have a decreased effect. This proved to be true in subsequent observations; the correlation was even improved by eliminating μ_c as a parameter. The flooding rate shows less dependence on packing diameter but a strong dependence on void fraction. This latter term for Raschig rings does not vary over a wide range; nevertheless, it is statistically significant.

Axial Dispersion

Axial dispersion is another hydrodynamic property of packed columns that has not been previously studied over a wide range of physical properties. The principal study of dispersion in packed columns was made by Vermeulen, Moon, Hennico, and Miyauchi,¹² who reported and correlated dispersion coefficients for a variety of packing materials and low-density (difference) fluids. These authors pointed out that their data did not cover a sufficiently wide range of differences in fluid densities to permit evaluation of the effects of this parameter.

In order to determine the effects of fluid densities, dispersion measurements were made in packed columns during the countercurrent flow of mercury and water.¹³ A copper nitrate optical tracer was continuously injected near the top of the column, and the steady-state concentration profile was measured down the column (upstream from the injection point). A small aqueous stream

was removed from the column, circulated through a photo cell for analysis, and returned to the column at the same elevation from which it was removed. The steady-state concentration down the column was fit to the relation

$$\ln \frac{C}{C_{\text{inlet}}} = - \frac{D_e}{V_c Z},$$

where E is the dispersion coefficient, Z is the distance down the column from the tracer inlet, and c_{inlet} is the concentration of tracer in the column at the point of injection.

The experimental results are summarized in Figure 3. The dimensionless plot is the type suggested by Vermeulen et al., and the line through the data is a correlation developed from the earlier low-density data. The agreement of the new high-density data with the earlier correlation is excellent. The scatter of the data is not significantly greater than that observed for the earlier data. Thus, axial dispersion with both high- and low-density fluids can be described well by an existing correlation.

Conclusions

A new correlation has been proposed and tested which predicts flooding rates for Raschig-ring-packed columns with significantly greater accuracy than previous correlations over a wide range of fluid properties. The earlier correlations were developed from data covering a more narrow range of low-density difference systems. Although the new correlation was developed solely from data for Raschig rings, it can also be used to extrapolate measurements made with other packing materials (e.g. Berl saddles). The dependence of flooding rates on parameters such as density difference, viscosity, packing (nominal) diameter, etc. should be similar for many other packing materials.

Axial dispersion data are presented for high-density fluids which show that an existing correlation is satisfactory.

1. Watson, J. S., and McNeese, L. E., A.I.Ch.E. J. (1973), 19, 230.
2. The Development Status of Molten-Salt Breeder Reactors, ORNL-4812 (August 1972).
3. Johnson, T. R., Pierce, R. D., Teats, F. G., and Johnston, E. F., A.I.Ch.E. J. (1971), 17, 14.
4. Watson, J. S., McNeese, L. E., Day, J., and Carrod, P., submitted for publication.
5. Nemunaitis, R. R., Eckert, J. S., Foote, E. H., and Rollison, L. R., "Capacity and Efficiency Behavior in Packed Liquid-Liquid Extractors," paper presented at the 68th Annual A.I.Ch.E. Meeting, Houston, Texas (1971).
6. Breckenfeld, R. R., and Wilke, C. R., Chem. Eng. Progr. (1950), 46, 187.
7. Crawford, J. W., and Wilke, C. R., Chem. Eng. Progr. (1951), 47, 423.
8. Ballard, J. H., and Piret, E. L., Ind. Eng. Chem. (1950), 42, 1088.
9. Dell, F. R., and Pratt, H. R. C., Trans. Inst. Chem. (1951), 29, 89.
10. Hoffing, E. H., and Lockhart, F. J., Chem. Eng. Progr. (1954), 50, 94.
11. Hannaford, B. A., Watson, J. S., Kee, C. W., and Cochran, H. D., "Hydrodynamics and Mass Transfer in Packed Columns," paper presented at the 72nd Annual Meeting of the A.I.Ch.E., St. Louis, Missouri (May 1972).
12. Vermeulen, T., Moon, J. S., Hennico, A., and Miyauchi, T., Chem. Eng. Progr. (1966), 62, 95.
13. Watson, J. S., and McNeese, L. E., Ind. Eng. Chem., Process Design Develop. (1972), 11, 120.

NOTATION

a	= cm^2 of packing surface/ cm^3 of packing volume
A, B, C, r, s	= constants used in particular correlations
C	= concentration of tracer, mol/cm^3
D_e	= axial dispersion coefficient, cm^2/sec
d_p	= diameter of packing
g	= gravitational acceleration ($980 \text{ cm}/\text{sec}^2$)
V_c	= superficial velocity of the continuous phase, cm/sec
V_d	= superficial velocity of the dispersed phase, cm/sec
$V_{c,f}$	= superficial continuous-phase velocity at flooding, cm/sec
$V_{d,f}$	= superficial dispersed-phase velocity at flooding, cm/sec
Z	= axial position in the column, cm

Greek Letters

α, β	= constants used in particular correlations
$\Delta\rho$	= difference in densities of dispersed and continuous phases, g/cm^3
ϵ	= void fraction of the packed column, dimensionless
μ	= viscosity, poise
ρ	= density, g/cm^3
σ	= interfacial tension between the continuous and dispersed phases, dynes/cm (subscripts c_a and d_a refer to the interfacial tension between the continuous or dispersed phase and air, for example, surface tension)
ν	= kinematic viscosity of continuous phase (water)
ψ	= sphericity, dimensionless

Subscripts

c, d	= subscripts denoting continuous and dispersed phases, respectively
o	= subscript representing intercept value; flow rate of other phase approaching zero

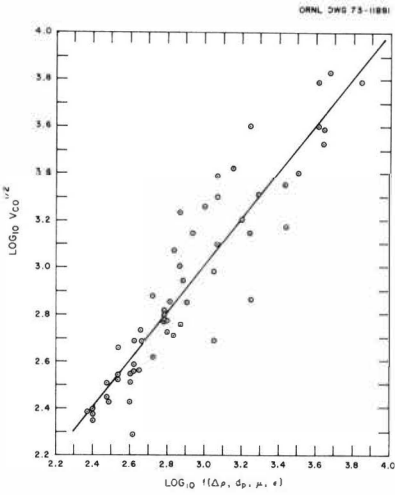


Fig. 1 Comparison of Measured and Predicted Values of $V_{CO}^{1/2}$

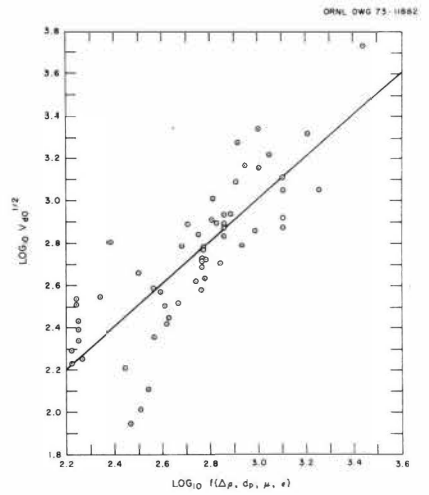


Fig. 2 Comparison of Measured and Predicted Values of $V_{g0}^{1/2}$

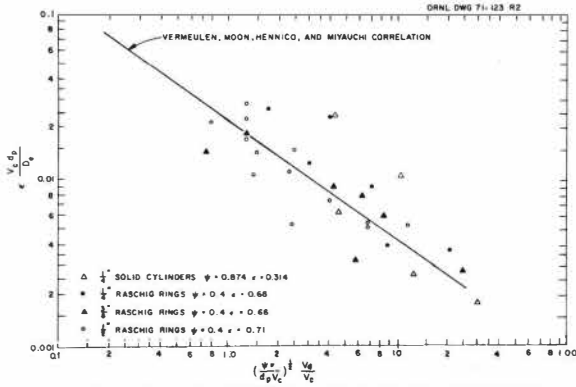


Fig. 3 Comparison of Mercury-Water of Axial Dispersion Data in Packed Columns with Vermeulen, Moon, Hennico, and Miyauchi Correlation

Table 1. Summary of Available Flooding Data

Packing Diameter (cm)	Fluids	Void Fraction	Viscosity of Continuous Phase (cP)	Density Difference (g/cm ³)	$k_1 = \frac{V}{c_0} \cdot \frac{1}{2}$ (cm/sec)	k_2	Reference
0.6	Benzene-Water	0.725	1.0	0.12	9.07 ± .35	0.865 ± .064	Dell and Fratt
1.0	Benzene-Water	0.785	1.0	0.12	11.28 ± .26	0.748 ± .035	Dell and Fratt
1.0	Benzene-Water	0.795	1.0	0.12	11.70 ± .57	0.771 ± .072	Dell and Fratt
0.635	Benzene-Water	0.745	1.0	0.12	9.32 ± .33	0.764 ± .058	Dell and Fratt
0.453	Benzene-Water	0.674	1.0	0.12	9.10 ± .10	0.688 ± .017	Dell and Fratt
1.27	Methylisobutyl Ketone-Water	0.748	1.0	0.195	17.16 ± .28	0.850 ± .028	Dell and Fratt
1.27	Dibutylcarbitol-Water	0.618	1.0	0.113	13.60 ± .45	0.957 ± .064	Dell and Fratt
1.0	Dibutylcarbitol-Water	0.797	1.0	0.113	11.26 ± .66	0.810 ± .101	Dell and Fratt
1.0	Dibutylcarbitol-Water	0.781	1.0	0.113	10.75 ± .39	0.816 ± .058	Dell and Fratt
0.635	Dibutylcarbitol-Water	0.745	1.0	0.113	9.32 ± .23	0.813 ± .048	Dell and Fratt
0.600	1-octane-Water	0.725	1.0	0.308	12.29 ± .59	0.763 ± .071	Dell and Fratt
1.0	1-octane-Water	0.8	1.0	0.308	13.93 ± .78	0.638 ± .074	Dell and Fratt
1.0	Butylacetate-Water	0.79	1.0	0.117	11.69 ± .16	0.730 ± .021	Dell and Fratt
1.0	Butylacetate-Glycerol Solution	0.79	1.65	0.157	11.37 ± .09	0.622 ± .012	Dell and Fratt
1.0	Butylacetate-Glycerol Solution	0.79	2.32	0.184	12.88 ± .09	0.715 ± .010	Dell and Fratt
1.0	Butylacetate-Glycerol Solution	0.79	5.7	0.237	13.50 ± .24	0.722 ± .026	Dell and Fratt
1.0	Chlorex-Water	0.795	1.0	0.22	14.40 ± .42	0.852 ± .052	Dell and Fratt
1.0	Chlorex-Water	0.795	1.0	0.22	14.69 ± .21	0.836 ± .028	Dell and Fratt
1.0	Chlorex-Water	0.795	1.0	0.22	14.00 ± .27	0.780 ± .037	Dell and Fratt
1.0	Chlorex-Water	0.793	1.0	0.22	14.13 ± .43	0.80 ± .059	Dell and Fratt
1.6	CCl ₄ -Water	0.798	1.0	0.6	17.36 ± .73	1.00 ± .075	Dell and Fratt
1.905	Benzene-Water	0.755	1.0	0.12	19.87 ± 1.59	1.33 ± .18	Dell and Fratt
2.5	Benzene-Water	0.777	1.0	0.12	25.71 ± 1.49	1.59 ± .14	Dell and Fratt
2.5	Dibutylcarbitol-Water	0.753	1.0	0.114	12.55 ± 1.17	0.668 ± .136	Dell and Fratt
1.905	Methylisobutyl Ketone-Water	0.753	1.0	0.195	21.65 ± .12	1.088 ± .011	Dell and Fratt
1.27	Methylisobutyl Ketone-Water	0.725	1.0	0.195	21.18 ± .73	1.340 ± .079	Dell and Fratt
0.635	Gasoline-Water	0.534	1.0	0.16	8.67 ± .36	0.934 ± .094	Breckenfeld and Wilke
0.635	Gasoline-Water	0.534	1.0	0.16	8.16 ± .05	0.827 ± .013	Breckenfeld and Wilke
0.635	Gasoline-Water	0.534	1.0	0.2	8.78 ± .23	0.805 ± .054	Breckenfeld and Wilke
0.635	Gasoline-Water	0.534	1.0	0.2	9.0 ± .28	0.87 ± .061	Breckenfeld and Wilke
0.635	Methylisobutyl Ketone-Water	0.534	1.0	0.2	10.0 ± .19	0.839 ± .041	Breckenfeld and Wilke
0.635	Toluene-Glycerol Solution	0.534	2.77	0.23	7.94 ± .29	0.842 ± .067	Breckenfeld and Wilke
1.27	Naphtha-Water	0.74	0.98	0.15	12.91 ± .04	0.848 ± .007	Breckenfeld and Wilke
1.27	Naphtha-Water	0.74	0.98	0.15	13.53 ± .11	0.903 ± .017	Breckenfeld and Wilke
1.27	Gasoline-Water	0.707	0.88	0.215	14.24 ± .43	0.835 ± .052	Crawford and Wilke
3.81	Gasoline-Water	0.679	0.88	0.215	19.25 ± 1.00	0.730 ± .082	Crawford and Wilke
2.54	Gasoline-Water	0.74	0.88	0.215	19.66 ± .31	0.830 ± .027	Crawford and Wilke
2.54	CCl ₄ -Water	0.728	0.44	0.58	25.10 ± .66	1.008 ± .054	Crawford and Wilke
2.54	CCl ₄ -Glycerol Solution	0.722	0.41	0.44	23.79 ± .50	1.016 ± .046	Crawford and Wilke
0.635	Bismuth-Molten Salt	0.84	12.0	6.28	15.87 ± 2.43	0.755 ± .195	Hannaford
0.635	Wood's Metal-Water	0.94	0.33	8.67	32.8 ± .95	0.789 ± .121	Johnson et al.
0.635	Toluene-Water	0.559	0.894	0.117	7.79 ± .14	0.635 ± .025	Ballard and Firt
0.635	Toluene-Water	0.559	0.894	0.117	7.59 ± .11	0.601 ± .017	Ballard and Firt
0.635	Petroleum Ether-Water	0.559	0.894	0.26	7.15 ± .21	0.561 ± .030	Ballard and Firt
0.635	CCl ₄ -Water	0.559	0.894	0.543	10.42 ± .22	1.206 ± .04	Ballard and Firt
1.27	Petroleum Ether and CCl ₄ -Water	0.603	0.894	0.154	13.07 ± .45	1.76 ± .22	Ballard and Firt
1.27	Petroleum Ether and CCl ₄ -Water	0.603	0.894	0.55	23.16 ± .34	1.87 ± .04	Ballard and Firt
1.27	Petroleum Ether and CCl ₄ -Water	0.603	0.894	0.4	20.45 ± .68	1.777 ± .093	Ballard and Firt
1.27	Petroleum Ether and CCl ₄ -Water	0.603	0.894	0.2	14.32 ± .38	1.754 ± .082	Ballard and Firt
1.27	Petroleum Ether and CCl ₄ -Water	0.603	0.894	0.111	10.32 ± .72	1.486 ± .18	Ballard and Firt
0.953	Petroleum Ether and CCl ₄ -Water	0.603	0.894	0.26	16.71 ± .46	1.496 ± .075	Ballard and Firt
0.953	CH ₂ -Water	0.595	1.0	1.485	27.5	1.536	This study
0.953	CCl ₄ -Water	0.595	1.0	0.60	19.5	1.50	This study
0.953	Hg-Glycerol Solution	0.656	15.0	12.4	29	1.57	This study
0.953	Hg-Water	0.656	1.0	12.5	35	1.67	This study
0.635	Hg-Water	0.757	1.0	12.5	31	1.13	This study

Table 2. Fractional Error of the Proposed Flooding Rate Correlation and Previous Correlations

Investigators	All Data		Low $\Delta\rho$, $\Delta\rho < 0.5 \frac{g}{cm^3}$		High $\Delta\rho$, $\Delta\rho > 0.5 \frac{g}{cm^3}$	
	$\Delta_{V_{c,o}}^{1/2}$	$\Delta_{V_{d,o}}^{1/2}$	$\Delta_{V_{c,o}}^{1/2}$	$\Delta_{V_{d,o}}^{1/2}$	$\Delta_{V_{c,o}}^{1/2}$	$\Delta_{V_{d,o}}^{1/2}$
	Watson and McNeese, (this study)	0.276	0.209	0.293	0.213	0.204
Breckenfeld and Wilke	0.825	0.829	0.842	0.857	0.795	0.746
Crawford and Wilke	0.903	0.904	0.926	0.935	0.847	0.811
Dell and Pratt	0.324	0.628	0.309	0.574	0.394	0.844

SESSION 13

Wednesday 11th September: 9.00 hrs

C H E M I S T R Y O F E X T R A C T I O N

(Thermodynamics)

Chairman:

Professor A.S. Kertes

Secretaries:

Dr. N.M. Rice

Mr. Buero

THERMODYNAMIC CHARACTERISTICS OF THE EXTRACTION
OF ANIONS

I.M.Ivanov, L.M.Gindin, G.N.Chichagova.

The reactions of interphase extraction exchange of a series of organic and inorganic anions have been investigated. ΔG , ΔH and ΔS of anion extraction equilibria have been determined.

Institute of Inorganic Chemistry of the Siberian Branch of the Academy of Sciences, Novosibirsk, 90, USSR.

It is well known that anions fall into a stable sequence of increasing extractability. We have previously determined the quantitative increasing extractability line for single-charged, double-charged and co-ordination anions [1-3]. A linear relation was found between the logarithms of the exchange constants and the differences of the energies of enthalpies of hydration of the two partitioned ions (see Table 1). It is noteworthy that the ΔH_h values of the ions studied earlier were proportional to the ΔG_h values. Presumably, there took place complete or partial compensation of the entropy term in the exchange of some inorganic anions. Obviously, this compensation is not a general feature of all the exchange reactions, and the strongest deviations from the $\lg K_{ex}$ and ΔH_h correlation should be the case with organic acid anions. For example, benzoate ion is extracted much better than would follow from its hydration heat.

The present communication is concerned with the results of the studies of the thermodynamic characteristics of extractive anion exchange. Generally, the following interphase exchange reactions were studied:



and the extraction equilibrium constant (exchange constant) was defined as follows:

$$K_{ex} = \frac{[K_t B]_o [A^-]_a}{[K_t A]_o [B^-]_a} \quad (2)$$

Table 1

Interphase exchange constants

 K_{A^-}/OH^- and the anion hydration parameters

A n i o n	- ΔG h. hydration in water, kcal/g-ion	- ΔH h. hydration in water, kcal/g-ion	lg K_{ex} A^-/OH^-	pK_a of acid
OH^-	111	122	0.00	
F^-	107	116	0.60	-3.5
CH_3COO^-		101	1.34	-4.8
HCO_3^-		91	1.50	
$HCOO^-$		99	1.74	-3.8
$C_2H_5COO^-$		101	1.84	-4.9
$C_3H_7COO^-$			2.35	
HS^-		82	2.65	
HSO_4^-		72	2.66	
$C_4H_9COO^-$			2.72	-4.9
Cl^-	79	84	2.80	2.50
$C_5H_{11}COO^-$			3.52	
$C_6H_{13}COO^-$			4.15	
Br^-	72	76	4.16	4.0
$C_6H_5COO^-$		87	4.20	
$C_7H_{15}COO^-$			4.79	-4.9
NO_3^-	69	74	4.80	
$C_8H_{17}COO^-$			5.23	
$C_9H_{19}COO^-$			5.94	
I^-	64	67	5.80	6.0
ClO_4^-	50	54	7.50	9.5
CO_3^{2-}	313	332	2.75	
SO_4^{2-}	249	265	3.35	
MoO_4^{2-}		231	4.25	
WO_4^{2-}		218	4.23	

The anion exchange was performed at a constant ionic strength, 0.1 mole/l in the aqueous phase. The concentration of the extractant tetraalkylammonium salt in the organic solvent did not exceed 0.1 mole/l. Due to the anion exchange character of the reactions, the ionic strength did not change during the extraction. For these reasons it was assumed that the activity coefficient ratio in the aqueous phase was close to unity, and that the γ_0 value was constant over the range of concentrations in the organic phase employed. The apparent extraction equilibrium constants were calculated using the Equation 2 from the experimental data on the distribution of anions. The thermodynamic characteristics of the anion exchange reactions were calculated from the reaction isobars which were found by measuring the extraction equilibrium constants at 15, 25, 35, 45°C.

Table 1 presents the values of the extraction equilibrium constants and of the hydration parameters of some organic and inorganic anions. It is seen that the K_{ex} values of inorganic anions monotonously increase with decreasing energy of enthalpy of their hydration. As for the anions of aliphatic acids, the hydration enthalpies are known of only the first three members of the series, and it is impossible to look for the correlation between the $\lg K_{ex}$ and the ΔH_h values. However, it is seen, that the extraction equilibrium constants in this series continuously increase with an increasing number of carbon atoms in the anions. Only the formate anion falls out of this line. The better extractability of formate ion compared with acetate is due to the smaller hydration enthalpy of the former (99 and 101 cal/g-ion, respectively [4]). The extraction behaviour of formate ion is in accord with the strength of the corresponding acids: formic acid is stronger than acetic acid, presumably due to the smaller enthalpy of formate ion hydration. There is a strict correlation between the extractabilities of inorganic anions and the strengths of the corresponding acids. Comparison of the inorganic anions exchange series [1] with the acids strength series [5] shows that the correlation between them is linear. This regularity does not seem surprising because there also is a practically

linear dependence between the anions' hydration enthalpies and their proton affinities; the two effects are determined by the charges, the sizes and the structures of the anions [6].

In the series studied previously, the exchange constant values are in good correlation with the ΔH_h and ΔG_h values, i.e., the contribution of the entropy term is small. Somewhat different behaviour is characteristic of organic anions, particularly of the monocarboxylic acid anions. For example the benzoate anion. These anions have two moieties - a hydrophobic one, and a hydrophilic one. The hydrophilicity of the carboxyl group $-\text{COO}^-$ changes insignificantly with increasing length of the hydrocarbon chain, beginning with acetate ion; (N.B. the strength of all the carboxylic acids of the aliphatic series is almost the same, beginning with acetic acid). It is known that the solubility of carboxylic acid decreases with increasing number of carbon atoms in their molecules, i.e. there is a decrease of the energy of ions hydration. Studies of the interphase exchange reactions reveals as well that the interphase exchange constants increase with increasing size of the hydrophobic moieties i.e., with decreasing free energy of hydration (see Table 2). The data on the exchange reactions for the nine ions studied are described by the general equation

$$\log K_{ex} = \log K_2 + A(n_c - 1) \quad (3)$$

where K_2 is the exchange constant of acetate ion, A is a constant, and n_c is the number of carbon atoms in the hydrocarbon moiety. The hydrophilicity of the carboxyl being practically constant, decrease of the free energy of anion hydration with increasing number of carbon atoms is presumably due to the predominant increase of the entropy term of the hydrophobic moiety of the molecule. Studies of the thermodynamic characteristics of the exchange reactions revealed that, within the accuracy of the measurements, the enthalpy of carboxylate ion exchange (with the exception of formate ion) was $\Delta H_{ex} = 1.18 \pm 0.12$ kcal/g-ion. The constancy of the ΔH_{ex} value suggests either the constancy of the ΔH_h (hydration) and ΔH_s (solvation) values for all the aliphatic acid anions, or compensation of hydration enthalpies and solvation enthalpies during the exchange.

Table 2

Thermodynamic characteristics of anion extraction

Reaction eq. 1	Diluent	$-\Delta G_{\text{ex}}$ kcal/g- -ion	$-\Delta H_{\text{ex}}$ kcal/g- -ion	ΔS_{ex} entropy units	$\delta\Delta G_s$ kcal/ g-ion	$\delta\Delta H_s$ kcal/ g-ion
$\text{HCOO}^-/\text{Cl}^-$	toluene	-1.42	-0.60	-2.76		-14.4
$\text{CH}_3\text{COO}^-/\text{Cl}^-$	toluene	-2.02	-1.18	-2.84		-15.8
$\text{C}_2\text{H}_5\text{COO}^-/\text{Cl}^-$	toluene	-1.29	-1.18	-0.87		-15.8
$\text{C}_3\text{H}_7\text{COO}^-/\text{Cl}^-$	toluene	-0.72	-1.18	1.52		
$\text{C}_4\text{H}_9\text{COO}^-/\text{Cl}^-$	toluene	0.09	-1.18	4.28		
$\text{C}_5\text{H}_{11}\text{COO}^-/\text{Cl}^-$	toluene	0.70	-1.18	6.29		
$\text{C}_6\text{H}_{13}\text{COO}^-/\text{Cl}^-$	toluene	1.88	-1.18	10.24		
$\text{C}_7\text{H}_{15}\text{COO}^-/\text{Cl}^-$	toluene	2.63	-1.18	12.76		
$\text{C}_8\text{H}_{17}\text{COO}^-/\text{Cl}^-$	toluene	3.28	-1.18	14.95		
$\text{C}_9\text{H}_{19}\text{COO}^-/\text{Cl}^-$	toluene	4.41	-1.18	18.74		
$\text{Br}^-/\text{NO}_3^-$	toluene	-1.04	-0.30	-2.47	-1.96	-1.7
Br^-/Cl^-	toluene	1.64	0.83	2.71	5.36	7.17
Br^-/Cl^-	chloro- benzene	1.72	0.92	2.67	5.28	7.08
Br^-/Cl^-	trichloro- benzene	1.68	0.65	3.44	5.32	7.35
Br^-/Cl^-	methylhexyl- ketone	1.35	0.45	3.01	5.65	7.55
Br^-/Cl^-	phenetol	1.54	0.61	3.12	5.46	7.39

No compensation of the entropy term occurs, there takes place an increase of the ΔS_{ex} value. Generally, assuming that the enthalpies of the ionic pairs solvation are the same, the enthalpy of the anions 1 and 2 exchange is equal to the difference of the hydration and solvation enthalpies of these anions in the two phases, i.e.,

$$\Delta H_{ex} = (\Delta H_{h1} - \Delta H_{h2}) - (\Delta H_{s1} - \Delta H_{s2}) = \delta \Delta H_h - \delta \Delta H_s \quad (4)$$

where indexes "h" and "s" refer to hydration and solvation, respectively. The ΔH_s value can be calculated from the experimental data. The data presented in Table 2 suggest that for toluene $\delta H_s = 0.9 \delta \Delta H_h$; both organic and inorganic anions fall into this correlation. The high ΔH_s values cannot be explained by the properties of the pure diluent like its dielectric constant, dipole moment, etc. Moreover, the $\delta \Delta H_s$ value for the Br^-/Cl^- pair is approximately constant and independent of the nature of the diluent (see Table 3). Of considerable importance in the systems discussed is the distribution of water. The content of water in the organic phase depends to a large extent on the nature of the anion and of the diluent (see Table 3). The hydrate numbers increase with increasing enthalpies of anions hydration. At the same time, the hydrate number of given anion depends to a strong extent on the nature of the diluent. Generally, the greater the solubility of water in the pure diluent, the higher the hydrate number of the anion. Presumably, the anion has a combined hydrate-solvate coating in the organic phase, and this explains the high $\delta \Delta H_s$ values and their constancy in different solvents which is the case in spite of the difference of the hydrate numbers.

The different solubility of water in different solvents may be interpreted in terms of the difference in water activity coefficients because the activity of water in water-saturated pure solvents is the same. Hence, the greater the solubility of water in pure diluent, the greater is the extent of its association with the solvent. For this reason, the greater number of water molecules is necessary to build the hydrate-solvate coating, the smaller is its activity coefficient.

In this type of solvent, water interacts with both the ion and

Table 3

Hydration numbers of anions in organic solvents.

Diluent	Trichloro- benzene	CCl ₄	Chloro- benzene	Tolu- ene	Phene- tol	Metyl- hexyl- ketone
Solubility of water in pure diluent, mole/l.	0.0067	0.009	0.018	0.019	0.051	0.37
Anion hydra- tion numbers						
Br ⁻	0.65	0.44	1.3	1.3	1.4	2.9
HSO ₄ ⁻	0.60	1.5	1.0	1.8	1.6	4.3
Cl ⁻	2.5	1.1	2.4	2.6	2.7	4.9
C ₃ H ₇ COO ⁻	3.2	3.6	4.4	4.7	4.4	7.8
C ₆ H ₁₃ COO ⁻	3.6	3.9	4.6	4.7	4.2	7.2
CH ₃ COO ⁻	4.7	4.6	4.9	5.6	5.3	8.4
SO ₄ ²⁻	5.9	6.2	6.0	6.9	6.3	10.2

the diluent.

REFERENCES

1. I.M.Ivanov, L.M.Gindin, T.N.Chichagova, *Izv. Sib. otd. Acad. Nauk SSSR, ser. khim. nauk*, issue 3, 100 (1967)
2. I.M.Ivanov, L.M.Gindin, T.N.Chichagova, "The Chemistry of Extraction Processes", Nauka, 1972, p.207
3. G.N.Chichagova, L.M.Gindin, I.M.Ivanov, *Izv. Sib. otd. Acad. Nauk SSSR, ser. khim. nauk*, issue 2, 58 (1973)
4. K.P.Mischenko, T.N.Poltoratsky, "The Problems of Aqueous and Nonaqueous Electrolyte Solutions Thermodynamics and Structure", *Khimia*, 1968
5. A.I.Shatenshtein, "Theory of Acids and Bases", Goskhimizdat, 1949, p.87
6. N.A.Izmaylov, "Electrochemistry of Solutions", *Khimia*, 1966.

A THERMODYNAMIC ACTIVITY MODEL FOR A SINGLE LANTHANIDE NITRATE
LIQUID-LIQUID EXTRACTION SYSTEM

William G. O'Brien and Renato G. Bautista

Ames Laboratory-USAEC and Department of Chemical Engineering

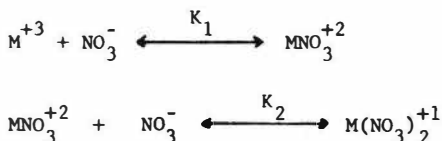
Iowa State University, Ames, Iowa 50010

ABSTRACT

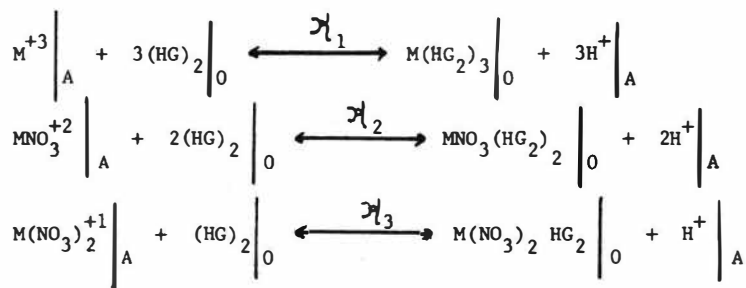
A thermodynamic model for a single component extraction system has been developed by making use of the thermodynamic activity of the various species, the stability constants of the inorganic complexes formed and by defining the solvent extraction equilibrium constants. The liquid-liquid extraction of a lanthanide from an acidic lanthanide nitrate solution by di(2-ethylhexyl) phosphoric acid can be represented by the equation:

$$K_D = \frac{[(HG)_2]_0}{[H^+]_A^3 \left\{ 1 + K_1[NO_3^-]_A + K_1 K_2 [NO_3^-]_A^2 \right\}} \left\{ \mathcal{X}_1 [(HG)_2]_0^2 + \mathcal{X}_2 K_1 [NO_3^-]_A [H^+]_A [(HG)_2]_0 + \mathcal{X}_3 K_1 K_2 [NO_3^-]_A^2 [H^+]_A^2 \right\}$$

where K_D is the distribution coefficient of the metallic species between the organic and the aqueous phase, $[H^+]_A$ the hydrogen ion activity in the aqueous phase, $[NO_3^-]_A$ the nitrate ion activity in the aqueous phase and $[(HG)_2]_0$ the activity of the di(2-ethylhexyl) phosphoric acid dimer in the organic phase. The quantities K_1 and K_2 are the stability constants for the formation of the following lanthanide-nitrate complexes in the aqueous phase:



The quantities \mathcal{K}_1 , \mathcal{K}_2 and \mathcal{K}_3 are the solvent extraction equilibrium constants for the various metallic species existing in the aqueous phase:



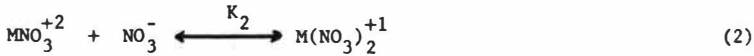
INTRODUCTION

The separation of several lanthanides by liquid-liquid extraction from concentrated aqueous solution have previously been correlated from the equilibrium concentrations of each lanthanide in the organic and aqueous phase. These empirical relationships based on their equilibrium data have been formulated to predict the distribution coefficients of the various components (1, 2, 3).

In this paper, a thermodynamic activity model of the extraction of a single lanthanide in di(2-ethylhexyl) phosphoric acid is presented. The formation of the lanthanide-anion complexes in the aqueous phase and the subsequent extraction of these complexes into the organic phase is examined. The formation of the lanthanide-anion complex is characterized by their complex stability constants.

THERMODYNAMIC MODEL

The model for the distribution coefficient of a single lanthanide specie has been formulated by defining liquid-liquid equilibrium constants for the extraction of each of the single component lanthanide complexes. The lanthanide nitrate inorganic complexes existing in aqueous solution have been shown by several investigators (4, 5, 6) to form by the following reactions:



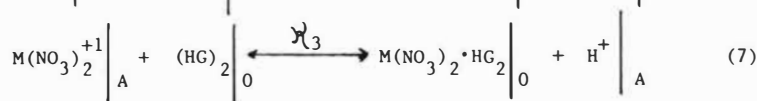
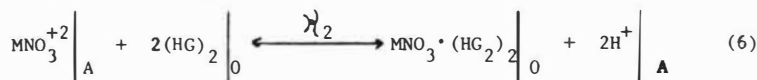
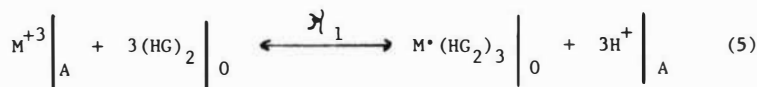
The complex stability constants K_1 and K_2 are defined by:

$$K_1 = \frac{[MNO_3^{+2}]}{[NO_3^-][M^{+3}]} \quad (3)$$

$$K_2 = \frac{[M(NO_3)_2^{+1}]}{[NO_3^-][MNO_3^{+2}]} = \frac{[M(NO_3)_2^{+1}]}{K_1[M^{+3}][NO_3^-]^2} \quad (4)$$

where the brackets denote thermodynamic activity. The existence of the neutral species, $M(\text{NO}_3)_3^0$, in the aqueous phase is neglected because the complexes are outer sphere in nature ⁽⁶⁾ (layer of water molecules surrounding the lanthanide ion) and the upper concentration limit of solutions studied is far from the solubility limit where the neutral species predominate.

The extraction of these complexes along with the trivalent lanthanide ion by organo-phosphorous acids such as di(2-ethylhexyl) phosphoric acid (HDEHP) has recently been studied by several investigators ^(7, 8) and the following extraction mechanisms have been proposed:



M represents the metal lanthanide ion, and $(\text{HG})_2$ represents the dimeric form of di(2-ethylhexyl) phosphoric acid. The presence of the dimeric form of HDEHP and the deprotonated HDEHP dimer (HG_2) in various hydrocarbon diluents has been verified by Peppard, Ferraro and Mason ⁽⁹⁾.

The liquid-liquid extraction equilibrium constants \mathcal{K}_1 , \mathcal{K}_2 and \mathcal{K}_3 are defined as follows:

$$\mathcal{K}_1 = \frac{[M(\text{HG}_2)_3]_0 [\text{H}^+]_A^3}{[M^{+3}]_A [(\text{HG})_2]_0^3} \quad (8)$$

$$\mathcal{K}_2 = \frac{[\text{MNO}_3(\text{HG}_2)_2]_0 [\text{H}^+]_A^2}{[M(\text{NO}_3)^{+2}]_A [(\text{HG})_2]_0^2} \quad (9)$$

$$\mathcal{K}_3 = \frac{[M(\text{NO}_3)_2 \cdot \text{HG}_2]_0 [\text{H}^+]_A}{[M(\text{NO}_3)_2^{+1}]_A [(\text{HG})_2]_0} \quad (10)$$

Any model which attempts to describe liquid-liquid extraction over a wide concentration range must take into account the complex formation and the eventual extraction of the complex. The distribution coefficient, K_D , is defined for a single component system by the ratio of the total concentration of metallic species in the organic phase to the total concentration of the metallic species in the aqueous phase:

$$K_D = \frac{\Sigma(M)_O}{\Sigma(M)_A} \quad (11)$$

The total activity of the metallic species in the organic phase can be written:

$$\Sigma[M]_O = [M \cdot (HG)_2]_3 + [MNO_3 \cdot (HG)_2]_2 + [M(NO_3)_2 \cdot HG_2]_0 \quad (12)$$

Equation 12 can be rewritten by using the definitions for the liquid-liquid extraction equilibrium constants given in Equations 8, 9 and 10.

$$\begin{aligned} \Sigma[M]_O &= \mathcal{K}_1 [M^{+3}]_A [(HG)_2]_0^3 / [H^+]_A^3 & + \\ &\mathcal{K}_2 [M(NO_3)^{+2}]_A [(HG)_2]_0^2 / [H^+]_A^2 & + \\ &\mathcal{K}_3 [M(NO_3)_2^{+1}]_A [(HG)_2]_0 / [H^+]_A & \end{aligned} \quad (13)$$

Equations 3 and 4 for the lanthanide nitrate complex stability constants are substituted in Equation 13 to yield:

$$\begin{aligned} \Sigma[M]_O &= \mathcal{K}_1 [M^{+3}]_A [(HG)_2]_0^3 / [H^+]_A^3 & + \\ &\mathcal{K}_2 K_1 [M^{+3}]_A [NO_3^-]_A [(HG)_2]_0^2 / [H^+]_A^2 & + \\ &\mathcal{K}_3 K_2 K_1 [M^{+3}]_A [NO_3^-]_A^2 [(HG)_2]_0 / [H^+]_A & \end{aligned} \quad (14)$$

Similarly the total activity of the metallic species in the aqueous phase can be written:

$$\Sigma[M]_A = [M^{+3}]_A + [M(NO_3)^{+2}]_A + [M(NO_3)_2^{+1}]_A \quad (15)$$

The following is obtained by again substituting Equations 3 and 4 for the lanthanide nitrate complex stability constants in Equation 15.

$$\Sigma[M]_A = [M^{+3}]_A + K_1[M^{+3}]_A[NO_3^-]_A + K_2K_1[M^{+3}]_A[NO_3^-]_A^2 \quad (16)$$

On the assumption that the concentration ratio of the total metallic species in the organic to the aqueous phases is approximately equal to the activity ratio of total metallic species in the organic to the aqueous phases, the distribution coefficient is given by Equation 17.

$$K_D = \frac{\Sigma(M)_O}{\Sigma(M)_A} \approx \frac{\Sigma[M]_O}{\Sigma[M]_A} \quad (17)$$

Substituting Equations 14 and 16 into Equation 17 and rearranging, gives:

$$K_D = \frac{[(HG)_2]_O}{[H^+]_A^3 \left\{ 1 + K_1[NO_3^-]_A + K_1K_2[NO_3^-]_A^2 \right\}} \left\{ \alpha_1 [(HG)_2]_O^2 + \alpha_2 K_1[NO_3^-]_A [H^+]_A [(HG)_2]_O + \alpha_3 K_1K_2[NO_3^-]_A^2 [H^+]_A^2 \right\} \quad (18)$$

The nitrate and hydrogen ion activities of the equilibrium aqueous phase can be measured by the nitrate and pH electrodes. The reliability of the nitrate electrode for activity measurements can be established by calibration against known concentration of aqueous solutions of sodium nitrate. The activity of the nitrate ion in these standards can be estimated by using the chloride convention as suggested by Bates and Alfenaar (10).

The activity of the free HDEHP dimer, $[(HG)_2]_O$, in the organic phase can be estimated from a knowledge of the free dimer concentration and the dimer activity coefficient, $\alpha(HG)_2$, in the equilibrium organic phase. The concentration of the free dimer in the organic phase can be determined from the initial dimer concentration, the total metallic concentration in the organic phase, the total nitrate concentration in the organic phase, and from the stoichiometry of the solvent extraction reactions. If no lanthanide nitrate complex is formed, the free HDEHP dimer concentration is equal to its initial concentration minus three times the organic metal concentration due to the extraction reaction. The presence of the nitrate complex reduces the amount of dimer necessary to

complete the lanthanide extraction. Therefore, the following relation must hold:

$$m_{(HG)_2} = m_{(HG)_2}^* - 3m_M^{ORG} + m_{NO_3}^{ORG} \quad (19)$$

where $m_{(HG)_2}$ and $m_{(HG)_2}^*$ represent the equilibrium and the initial dimer concentration respectively, m_M^{ORG} is the total metal concentration of the organic phase and $m_{NO_3}^{ORG}$ is the total nitrate concentration of the organic phase.

The organic phase metal concentration can be determined by back extracting the organic phase with strong nitric acid and titrating the back extract with EDTA. The organic phase nitrate concentration can be determined by back extracting the organic phase with strong sulfuric acid and analyzing the aqueous back extract by the nitrate electrode.

The activity coefficient of the $(HG)_2$ dimer in the organic phase can be obtained from solution vapor pressure measurements. Assuming only the $(HG)_2$ dimer and the specific diluent comprise the organic phase, we have from regular solution theory:

$$y_i P_T = \gamma_i x_i P_i^* \quad (20)$$

where y_i is the mole fraction of the i th species in the vapor phase, P_T the total pressure, γ_i the activity coefficient of the i th species, x_i the mole fraction of the i th species in the liquid phase and P_i^* the vapor pressure of the i th species. Thus by measuring y_i , P_T , x_i and P_i^* the activity coefficient of the i th species can be determined. The free dimer activity is given by Equation 22.

$$[(HG)_2] = \gamma_{(HG)_2} \cdot m_{(HG)_2} \quad (21)$$

In order to measure the activity coefficient of the $(HG)_2$ dimer in the organic phase, the diluent for the HDEHP solvent must be a pure compound. Where the diluent is a mixture of aliphatic hydrocarbons (Amsco Oderless Mineral Spirits), as in the extraction of lanthanide nitrates in HDEHP diluted with Amsco the $(HG)_2$ dimer activity coefficient cannot be determined experimentally.

In this particular case, the $(\text{HG})_2$ dimer activity will be assumed equal to the free dimer concentration as measured by the nitrate electrode.

The distribution coefficient K_D at a specific extraction condition can be determined by analysis of the metal concentration in the aqueous and organic phase. When all of the above information is available, the liquid-liquid extraction equilibrium constants \mathcal{K}_1 , \mathcal{K}_2 and \mathcal{K}_3 can then be estimated by linear regression analysis.

After the values of the liquid-liquid extraction equilibrium constants are established, the distribution coefficients at other experimental conditions can be calculated given the information on the hydrogen and nitrate ion activity and the total ionic strength of the aqueous phase.

CONCLUSION

The model as developed allows for a complete thermodynamic analysis of the liquid-liquid extraction of a lanthanide in di(2-ethylhexyl) phosphoric acid.

It also makes possible the prediction of the distribution coefficients at other experimental conditions when the hydrogen and nitrate ion activity and the total ionic strength of the aqueous phase are specified. The results of experiments to verify this model will be reported in due time. This method of analysis is presently being extended to binary and multicomponent systems and will be reported in a subsequent paper.

REFERENCES

- (1) Ioannou, Tom K., Smutz, Morton and Bautista, Renato G., "Single and Multicomponent Equilibrium Data for the Extraction of SmCl_3 , NdCl_3 , and CeCl_3 in Acidic Chloride Solutions with Di(2-Ethylhexyl) Phosphoric Acid." *Met. Trans.*, 1972, Vol. 3, pp. 2639-2648.
- (2) Ioannou, Tom K., Bautista, Renato G. and Smutz, Morton, "Correlating Multicomponent Equilibrium Data for the Extraction of Lanthanides with Di(2-Ethylhexyl) Phosphoric Acid as the Solvent." *Proc., Int. Solvent Extraction Conf.*, 1971, Vol. II, pp. 957-956, Society of Chemical Industry, England, 1972.
- (3) Thomas, Norman, "Separation of Lutetium, Ytterbium, and Thulium in Acidic Chloride Solution by Fractional Solvent Extraction," Ph.D. Thesis, Iowa State University, Ames, Iowa, 1974.
- (4) Peppard, D. F., Mason, F. W. and Hucher, I., "Stability Constants of Certain Lanthanide and Actinide Chloride and Nitrate Complexes." *J. Inorg. Nucl. Chem.*, Vol. 24, pp. 881-888, 1962.
- (5) Goto, T. and Smutz, M., "Stability Constants of Lighter Lanthanide and Chloride Complexes by a Potentiometric Method." *J. Inorg. Nucl. Chem.*, Vol. 27, pp. 663-671, 1965.
- (6) Choppin, G. R. and Strazik, W. F., "Complexes of Trivalent Lanthanide and Actinide Ions." *Inorg. Chem.*, Vol. 9, pp. 1250-1254, 1965.
- (7) Kosinski F. E. and Bostian, H., "Lanthanum Solvent Extraction Mechanism Using Di(2-Ethylhexyl) Phosphoric Acid." *J. Inorg. Nucl. Chem.*, Vol. 31, pp. 3622-3631, 1969.

- (8) Rozen, A. M., Martynov, B. V. and Anikin, V. E., "Mechanism of the Extraction of $UO_2(NO_3)_2$ from Nitric Acid Solutions by Organophosphorus Acids." Radiokhimiya, Vol. 15, pp. 24-30, 1973.
- (9) Peppard, D. F., Ferraro, J. R. and Mason, G. W., "Hydrogen Bonding in Organo-Phosphoric Acids." J. Inorg. Nucl. Chem., Vol. 7, pp. 231-244, 1958.
- (10) Bates, R. G. and Alfenaar, M., "Activity Standards for Ion Selective Electrodes;" In Ion Selective Electrodes, ed. R. Durst, pp. 191-214, N.B.S. Publication 314, Washington, D. C., 1969.

THERMODYNAMICS OF EXTRACTION OF SALTS WITH NOBLE GAS IONS.

K.S. KRASNOV, T.S. KASAS, V.S. KUZNETSOV.

(Institute of Chemistry and Technology, Engels Street 7,
EVANOV, USSR).

This paper presents the results of investigating the thermodynamics of extraction of alkali metal halides MeHal and alkali earth metals MeHal₂ halides by isoamyl alcohol. The distribution of salts was studied in a wide range of concentrations and temperatures. The hydration and solvation numbers of salts in an organic phase have been determined. Extraction equilibrium constants K and the change of free energy ΔG° at different temperatures have been estimated by the extrapolation zero concentration.

The heat of extraction ΔH_{ex} at different concentrations and the extrapolated value at infinite dilution were estimated by direct measurements in a specially constructed differential microcolorimeter. The changes of entropy ΔS_{ex}° have been calculated. The relations found between thermodynamic characteristics of extraction and the structure of ions have been discussed.

Alkali halides and alkali earth halides which are salts with noble gas ionic structure a good model for investigating the influence of size and charge of ions upon the thermodynamic characteristics of extraction.

Crystallochemical radii and other parameters of noble gas ions of these salts are known and this favours the comparison of thermodynamic and structural characteristics of extraction and the generalisation of results for other salts with noble gas ions.

The physical properties of the extractant/, isoamyl alcohol/, are also sufficiently known (1) compared with the properties of other higher alcohols. Previous investigations dealt with a very small number of salts mainly MeHal and were carried out at one temperature (2) or over a range of 5° (3).

The distribution of MeHal between water and secondary butanol has been investigated (4). However, the extrapolation to infinite dilution was carried out without taking into account the change of activity coefficients. As far as we know, investigations such as these for MeHal₂ over a wide temperature range have not been carried out and therefore we have investigated the distribution of halides LiCl, NaCl, KCl, KI, MgCl₂, CaCl₂, CaBr₂, CaI₂, SrCl₂, SrBr₂, SrI₂, BaCl₂.

Distribution.

The distribution has been studied at 25°C and 50°C and in some cases at 12° and 70°C and over a wide concentration range; NaCl and KI were studied only at 25°C.

On the base of the experimental data the distribution coefficients $D = y/x$ and the extraction equilibrium constants, K of salts were obtained, where

$$K = \frac{y^n a_w^n}{x^n a_o^n} = (D \gamma_o^n / \gamma_w^n)^n \frac{1}{a_w} \quad (1)$$

where y and x - the salt concentration in organic and aqueous phases in moles per 1000 g solvent; γ_o and γ_w - are the average ionic activity coefficients; n - the number of salt ions, a_w - water activity in aqueous solution of salt, and h - hydration number in the organic phase.

From the experimental data, it follows that the distribution coefficient of the halides varies with concentration in different ways. The distribution coefficient of all halides, except KCl and BaCl₂ increases with the rise of concentration especially abruptly at large concentrations. $D(KCl)$, $D(SrCl_2)$ and $D(BaCl_2)$ were slightly changed with the concentration. The temperature effect on extractibility is also different. In the range of

low concentrations in the organic phase the distribution of all halides, except CaI_2 and SrI_2 does not depend on temperature. In the range of higher concentrations the distribution coefficient of KCl , SrCl_2 and BaCl_2 increases but in the case of the other salts decreases with the change of temperature.

Hydration and Solvation Numbers

Hydration numbers h of salts MeHal_2 and some MeHal were determined experimentally by the method described in (5). It was established that NaCl , KCl and LiCl are extracted as nonhydrated ion pairs, whereas, MgCl_2 and all the salts CaHal_2 were extracted as hydrated species.

For the determination of solvation numbers, the dilution method described in (6) was used. All the investigated salts MeHal_2 were solvated in the organic phase; SrCl_2 and BaCl_2 were solvated by the six molecules and the remainder by three and four molecules. The total number of molecules of alcohol and water in hydrosolvates of calcium halides in the organic phase increases in the sequence of chloride < bromide < iodide.

Extraction Equilibrium Constant.

Isoamyl alcohol dissolves water during extraction (34.9% mol. water at 25°C in the absence of salt, the dielectric constant being 14.34 (1)). In such media halides dissociate. The extraction equilibrium constant, K , may be determined from the equation (1), which after transformation and taken logarithms gives:

$$\lg Q = 1/n \lg K - \lg \gamma_{\text{O}^{\pm}}$$

where $Q = D \gamma_{\text{B}}^{\pm} \pm a_{\text{B}}^{1/n}$.

In the range of very low concentrations \log_0^+ depends linearly upon the root of ionic strength of the solution, μ . Therefore, the dependence $\log Q = f(\sqrt{\mu})$ in this range becomes linear. The parameters $\log K$ of this straight-line dependence for each salt are determined by the least-squares method. The values of K are given in the Table (the value of K (LiCl) taken from the work (2) is also given there).

Cation effect

It is seen from the Table that extraction constants, which are very low, are reduced by some orders, when passing from single charged ions Me^+ to doubly charged ions Me^{2+} . However, the difference in the distribution coefficient D_0 at infinite dilution is not so marked e.g. D_0 (KCl) = 2.75×10^{-3} , and D_0 (CaCl₂) = 4×10^{-4} . This is explained by the fact that in the calculation of K the dissociation of molecules into three ions in the case of $MeHal_2$ and into two ions in the case of $MeHal$ is taken into account. K (LiCl) $>$ K (NaCl) \approx K (KCl). In reference (2) this fact was explained in terms of electrostatic considerations by the larger size of the highly hydrated lithium ion as compared with the non-hydrated potassium ion. The extraction equilibrium constants of the corresponding halides of calcium, strontium and barium within the experimental errors are equal, and one order lower than the extraction equilibrium constant of $MgCl_2$. The reason of this is because highly hydrated magnesium ions become larger than less hydrated Ca^{2+} , Sr^{2+} , and Ba^{2+} ions, the relative sizes of the latter ions being decreased by hydration. All this affects the extraction as well as other physical properties, for example the close values of the ion mobility of Ca, Sr and Ba in water. Thus, the ion mobility of the highly hydrated ion Mg^{2+} appears to be lower than of its analogues (7).

Anion effect

For anions Cl^- , Br^- and I^- in contrast to highly hydrated cations, the hydration cannot counteract the difference in crystallographic radii, therefore, the increase of the latter in Cl, Br and I series results in the increase of the constants.

Enthalpy of Extraction (heat distribution effect)

That the extraction constants of salts, except iodides, do not depend on the temperature within the experimental errors (Table) indicates that $\Delta H_{\text{ex}}^{\circ} \approx 0$. (The error in $\Delta H_{\text{ex}}^{\circ}$ determination according to the second law does not exceed ± 2 kcal/mole).

This fact maybe explained as follows:

The heat of extraction must be equal to the difference of heats of dilution (or solvation) of a salt in isoamyl alcohol and in water. The data on the heats of solution (or solvation) in isoamyl alcohol are not available; but the difference in the heats of solvation of the alkaline metal halides in other alcohols and in water is approximately constant and has a value of $\sim 3-4$ kcal/mole (8). It is evident that during mutual saturation of the alcohol with water and water with alcohol, which takes place during the extraction, this difference will be much less. Unfortunately, similar data for 2-1 electrolytes are not available in the literature but a different result seems to be improbable here. The difference of the heats of solvation for iodides is to some extent higher than for other halides, namely - 6 kcal/mole (8). Therefore, the observed exothermic effect expressed in the relation of K to temperature is not striking for the iodides of the alkaline earth metals.

To obtain ΔH_{ex} and ΔS_{ex} values of high accuracy for heat effects close to zero, direct calorimetric measurements of the extraction heats were made. With this end in view, the differential microcalorimeter for small heat effects was constructed and tested. The sensitive differential thermobattery provides a threshold of detectability 5×10^{-5} cal. The heat of reaction is compensated by supplying current into calibrated heaters and the non-compensated part is registered by a recorder. The heats of mixing in the water-isoamyl alcohol system at 25°C which are necessary for the measurement of distribution enthalpy have been determined and the differential heats of dilution of water in isoamyl alcohol and isoamyl alcohol in water have been calculated.

The developed procedure gave the possibility of determining the heat extraction effects over a wide range of salt concentrations in aqueous and organic phases at 25°C . (in the experiments heats of the order 0.5 - 0.005 cal. were registered). The experimental heat effects were in good agreement with those calculated according to the equation of the isobar within experimental error. The heats of extraction at the infinite dilution $\Delta H_{\text{ex}}^{\circ}$ were determined from experimental heat effects. It follows from our data that the heats of solution of the salts MeIal and MeIal_2 which have not previously been studied for isoamyl alcohol, saturated with water, are closer to their heats solution in water, except for iodides. The closeness to zero of the heat effects for extraction by isoamyl alcohol has also been observed for the extraction of salts by triphenylmethane dyes (9). This phenomenon seems to be characteristics of salt extraction by the higher alcohols in all cases but that where we observe specific interaction between the salt and alcohol. In our case such a specific donor-accepting interaction takes place between the iodide ion and alcohol. Experiments on paramagnetic resonance clearly prove this (10).

The Entropy of extraction

As $\Delta H_{\text{ex}}^{\circ}$ in most cases under consideration is close to zero, the entropy factor $T \Delta S_{\text{ex}}^{\circ}$ causes the main changes of the free energy. This phenomenon is of great importance, and as we have previously indicated (11,12) $\Delta S_{\text{ex}}^{\circ}$ calculated on the basis of extraction equilibrium constants K_{ex}° and $\Delta G_{\text{ex}}^{\circ}$ are given in the Table. It follows from the table the change of standard distribution entropy ($\Delta S_{\text{ex}}^{\circ}$) for all halides is negative. The decrease of entropy during the distribution between water and alcohol is the result of differences in the structural properties of the phases. Water is a more ordered solvent than alcohol, which is why the effect on the orientation of the molecules of a solvent by the electrostatic ion field with attendant entropy decrease is greater for alcohols than for water. This causes negative values $\Delta S_{\text{ex}}^{\circ}$ for the distribution. The extraction entropy of the halides of the alkaline-earth metals, is more negative than for the salts of the alkali metals. This maybe explained by the greater ordering effect which is created by divalent cations compared with monovalent and the increase of the ion number of a salt from two to three. Values found for the distribution entropy of the halides of alkali metals S_{ex}° which are equal for KCl and LiCl at -22 cal $\text{K}^{-1}\text{mol}^{-1}$ are in good agreement with the difference of the KCl solvation entropy in water and in alcohol which contain the same quantity of water (34.9 mol.%) as does our organic phase, namely -20.8 cal $\text{K}^{-1}\text{mol}^{-1}$ (methanol) (13) and -21.5 cal $\text{K}^{-1}\text{mol}^{-1}$ (ethanol) (14). Thus it appears that the increase of the number of carbon atoms of alcohols will not greatly affect the changes of extraction entropy for the same quantity of water in alcohol phase, although the decrease of entropy takes place in $\text{C}_1 - \text{C}_2 \dots \text{C}_5$. As the higher alcohols C_6, C_7 etc. dissolve less water with an increasing number of carbon atoms, S_{ex}° will decrease in the same way as in the case of salts of crystal violet (9).

For the alcohols which dissolve practically no water, ΔS_{ex}° of the distribution equals the difference of the dissolution entropy (or solvation entropy) in anhydrous alcohols and water. Data necessary for the higher alcohols are not available in the literature, but in terms of the data on ΔS° for the solvation of KCl in ethanol, the difference of dissolution entropy in alcohol and water $\Delta S^{\circ} = 37.9 \text{ cal K}^{-1} \text{ mol}^{-1}$ or $45.2 \text{ cal K}^{-1} \text{ mol}^{-1}$. Taking ΔS_{ex}° for the distribution equal to $\text{cal mol}^{-1} \text{ K}^{-1}$ with $\Delta H_{ex}^{\circ} = 0 \pm 2 \text{ kcal/mole}$, we obtain the value $\sim 10^{-9}$ for the extraction equilibrium constant of KCl with the higher alcohols, immiscible with water. That is why higher alcohols which do not dissolve water, should be extremely ineffective as extractant of the salts of KCl type.

For the salts being investigated of I - I type the extraction entropy does not depend upon the nature of the salt and equals -22 to $-24 \text{ cal mol}^{-1} \text{ K}^{-1}$. Similarly, for the salts of the 2 - I type (except iodides), ΔS_{ex}° in the range of the experimental does not depend upon the nature of a salt and equals -43 to $-49 \text{ cal K}^{-1} \text{ mol}^{-1}$. From these data it follows that the solvation entropy of I-I salts in infinitely dilute solutions while passing from water to the higher alcohols decreases by one and the same value irrespective of the nature of the salt. If one applies this to separate ions as well, one obtains for mono-di- and trivalent ions respectively $\Delta S_{ex}^{\circ} = 12, -24, -36 \text{ cal K}^{-1} \text{ mol}^{-1}$ so that for a $\beta - 1$ electrolyte we would expect $\Delta S_{ex}^{\circ} = -72$ and with $\Delta H_{ex}^{\circ} = 0$, the extraction equilibrium constants will be of the order $\sim 10^{-15}$, and $D_0 \sim 10^{-5}$ respectively.

In conclusion we would like to state the following. During the extraction of noble-gas like ions in the absence of a specific interaction with the solvent, the changes of the extraction entropy in similar salts are constant, as one would expect (16). But in contrast to what was expected in (16), ΔH° for the extraction is close to zero in all cases (except iodides) and a large change of the extraction equilibrium constants in similar compounds was not observed.

Table. Thermodynamic Characteristics of Extraction.

Salt	K ₂₉₈	K ₃₂₃	ΔH_{ex}^0 ₂₉₈ cal/mole	ΔS_{ex}^0 ₂₉₈ cal/mole ⁻¹
LiCl	1.45×10^{-5} $\pm 0.17 \times 10^{-5}$	1.45×10^{-5} $\pm 0.17 \times 10^{-5}$	165 ± 48	21.6 ± 0.4
NaCl	2.3×10^{-6} $\pm 0.3 \times 10^{-6}$		385 ± 104	-24.5 ± 0.6
KCl	4.0×10^{-6} $\pm 0.6 \times 10^{-6}$	4.0×10^{-6} $\pm 0.6 \times 10^{-6}$	870 ± 191	-22 ± 1
KI	6×10^{-6} $\pm 2 \times 10^{-6}$		-4520 ± 723	-39 ± 2
MgCl ₂	2.0×10^{-11} $\pm 1.5 \times 10^{-11}$	2.0×10^{-11} $\pm 1.5 \times 10^{-11}$	260^{**}	-48
CaCl ₂	7×10^{-12} $\pm 4 \times 10^{-12}$	7×10^{-12} $\pm 4 \times 10^{-12}$	997 ± 249	-48 ± 2
CaBr ₂	8.0×10^{-11} $\pm 2.6 \times 10^{-11}$	8.0×10^{-11} $\pm 2.6 \times 10^{-11}$	795 ± 203	-43 ± 1
CaI ₂	1.0×10^{-9} $\pm 0.6 \times 10^{-9}$	4.1×10^{-10} $\pm 2.6 \times 10^{-10}$	-5640 ± 338	-60 ± 3
SrCl ₂	1.0×10^{-11} $\pm 0.7 \times 10^{-11}$	1.0×10^{-11} $\pm 0.7 \times 10^{-11}$	1750 ± 455	-49 ± 3
SrBr ₂	9.0×10^{-11} $\pm 2.4 \times 10^{-11}$	9.0×10^{-11} $\pm 2.4 \times 10^{-11}$	0^{***}	-46
SrI ₂	3.8×10^{-10} $\pm 1.6 \times 10^{-10}$	1.6×10^{-10} $\pm 0.7 \times 10^{-10}$	-6600^{***}	-65
BaCl ₂	6×10^{-12} $\pm 3 \times 10^{-12}$	6×10^{-12} $\pm 3 \times 10^{-12}$	1990 ± 717	-47 ± 3

* Our estimate.

** Value is found according to the second law.

From all the salts which were studied the iodides have relatively greater heat effect and greater negative entropy. This shows a specific interaction of iodide ion with the solvent.

Acknowledgement

We are sincerely indebted to I.A. Chanova, laboratory assistant for the help she has given us in the carrying out of the experimental work.

THERMODYNAMICS AND SOLVENT INFLUENCE IN ZINC AND COPPER ACETYLACETONATE EXTRACTION.

B. Allard, S. Johnsson and J. Rydberg.

Department of Nuclear Chemistry, Chalmers University of Technology, Fack, S-402 20 Göteborg 5, Sweden.

From distribution measurements partition coefficients have been determined for copper and zinc acetylacetonate complexes. From the temperature dependency of the partition coefficient the entropy and enthalpy changes have been calculated. The influence of the ionic strength of the aqueous phase and of the nature of the diluent have been studied. The results are discussed in terms of the regular solution theory. Indications of hydration in the aqueous phase and solvation in the organic phase giving changes in the coordination numbers have been found from thermodynamic data.

Introduction

In several investigations efforts have been made to determine and describe fundamental factors governing the partition of an extractable species between two immiscible phases. The regular solution theory¹ has been used to interpret the effect of the diluent on the extraction. In some cases, correlations between partition coefficients and formation constants for complexes of different metals have been established and systematic size dependencies have been observed.²⁻⁷ However, very little is known about the enthalpy and entropy changes in distribution equilibria and about the correlation between such thermodynamic data and diluent properties, structure, etc.⁸ The purpose of this study was to investigate if systematic determinations of ΔH and ΔS can give any qualitative explanation to the particular interactions which govern the partition coefficients of the complexes. The systems selected were zinc(II)- and copper(II) acetylacetonate in sodium perchlorate - organic solvent. These complexes have been chosen because of their limited distribution coefficient in the systems of interest, ease of preparation and chemical stability. Unlike several other bivalent metal acetylacetonate complexes, monomeric complexes form preferentially. Moreover formation constants and distribution data are to some extent well known.^{6,9} The theory

of regular solutions has been successfully used for other similar systems.⁴⁻⁷

Experimental

Chemicals

Sodium perchlorate and acetylacetone were prepared and purified according to conventional methods.¹⁰ For the distribution measurements ⁶⁵Zn and ⁶⁴Cu were used. The radiochemical purity was checked by gamma spectrometry. All other chemicals were of p.a. quality and used without further purification.

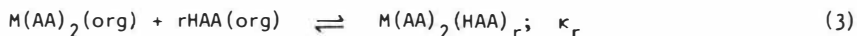
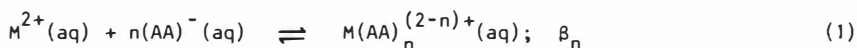
Distribution measurements

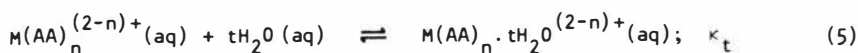
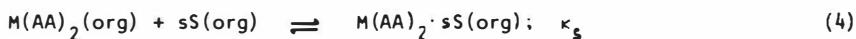
The distribution experiments were carried out in an AKUFVE-apparatus.^{11,12} To the organic phase acetylacetone (HAA) was added corresponding to a total initial concentration of 0.485 M. The aqueous phase was 1.00 M [Na, HClO₄], except in the experiments with variation of the ionic strength of the aqueous phase. Equal phase volumes were used. The metal was added to the aqueous phase as radio tracer. To avoid adsorption losses in the apparatus some carrier was added. The total initial metal concentration was between $5 \cdot 10^{-4}$ and $5 \cdot 10^{-5}$ M. The initial pH was low (pH \approx 2) in order to prevent hydrolysis. During each experiment pH was increased by addition of [NaOH, ClO₄] of suitable concentration until the pH-independent plateau region (pH \approx 7.5) was reached.⁹ For each system distribution coefficients were determined at different constant temperatures between 10°C and 40°C. The temperature, pH and metal concentration were continuously determined according to the AKUFVE-technique.¹¹ At each selected temperature ten measurements were made and the mean value was calculated. In this way, the distribution equilibrium could be confirmed. For comparison, measurements were made by conventional batch technique giving results equal to the results from the AKUFVE-experiments within estimated error limits.

Results and discussions

The chelate extraction process

The distribution process (with corresponding equilibrium constants) can be expressed by





where S is the diluent. The formation of polymer complexes and hydrolysis have been neglected, and all solvates with water and diluent are assumed to be found in the aqueous and organic phases respectively. Since no adduct formation with HAA takes place⁹ the following expression for the distribution coefficient D_M is valid; all charged species assumed to be in the aqueous phase. For species in the organic phase the index org is used; for the aqueous phase no index is given. Brackets are used to indicate concentrations.

$$D_M = \lambda_2 \beta_2 [AA]^2 (1 + \sum \kappa_s [S]_s^{\text{org}}) / (1 + \sum \beta_n [AA]^n (1 + \sum \kappa_t [H_2O]^t)) \quad (6)$$

$$s + t + n \leq N \quad (7)$$

where N is the coordination number.

In the pH-independent region mainly uncharged species exist, i.e. $n = 2$. Thus the measured value will correspond to λ_2 , if solvates according to reaction (4) and (5) are neglected.

Variation of diluents

The partition coefficient λ_2 has been determined for both polar and non-polar diluents, all with a molar volume around 100-150 cm³/mole. In Fig. 1 the temperature dependency of $\log \lambda_2$ is shown for some of the systems, and in Table 1 thermodynamic constants are given. The thermodynamic quantities ΔH and ΔS were calculated by the usual procedure from $\log \lambda_2$ vs $1/T$ using a linear least squares method.

According to the theory of regular solutions,^{1,4} and taking differences between the molar volumes of solute and solvent into account, the partition coefficient for a component A at equilibrium between an organic and an aqueous phase can be expressed as

$$RT \cdot \ln \lambda_A = V_A (\delta_{\text{aq}} + \delta_{\text{org}} - 2\delta_A) (\delta_{\text{aq}} - \delta_{\text{org}}) + RT \cdot V_A (1/V_{\text{org}} - 1/V_{\text{aq}}) \quad (8)$$

where λ_A is given in terms of molar concentration, V is the molar volume and δ is the solubility parameter. In equation (8) the expression for the activity of A valid for the regular organic phase has been mechanically applied also to the aqueous phase. An empirical value of $\delta_{\text{aq}} = 17.5$ for the aqueous phase calculated from equation (8), has been determined for similar systems.⁴ As long as this empirical value is used and a constant aqueous

phase is assumed the partition coefficient of component A is represented approximately by equation (8).^{4,5}

Equation (8) can be rewritten as

$$\log \lambda_A / (\delta_{aq} - \delta_{org}) = (V_A / RT \cdot \ln 10) (\delta_{aq} + \delta'_{org} - 2\delta_A) \quad (9)$$

$$\delta'_{org} = \delta_{org} + RT / (\delta_{aq} - \delta_{org}) (1/V_{org} - 1/V_{aq}) \quad (10)$$

Fig. 2 shows $\log \lambda_2 / (\delta_{aq} - \delta_{org})$ as a function of δ'_{org} . A linear relationship is obtained for similar systems and from the slope of the line the molar volume in inert solvents $V_{Zn(AA)_2} = 148 \text{ cm}^3/\text{mole}$ and $V_{Cu(AA)_2} = 185 \text{ cm}^3/\text{mole}$ are obtained. The cyclohexane values have not been included, the relative errors being larger for these measurements than for the others.

δ'_{org} has been calculated from the equation given below¹

$$\delta' = ((\Delta H^V - RT) / V)^{1/2} \quad (11)$$

where ΔH^V is the heat of evaporation at 25°C obtained from the literature.¹⁴

For the partition coefficient k_d of the chelating agent HAA the following equation is valid:⁵

$$\log \lambda_2 = (V_{M(AA)_2} / V_{HAA}) \cdot \log k_d + \text{const.} \quad (12)$$

Fig. 3 shows $\log \lambda_2$ as a function of $\log k_d$. From the slope of the straight line the values $V_{Zn(AA)_2} = 156 \text{ cm}^3/\text{mole}$ and $V_{Cu(AA)_2} = 175 \text{ cm}^3/\text{mole}$ are obtained using the value $V_{HAA} = 103 \text{ cm}^3/\text{mole}$.⁴ The results are in good agreement with the values calculated from equation (9). From density measurements⁶ the value $172 \text{ cm}^3/\text{mole}$ has been calculated for $Cu(AA)_2$. The molar volume for $Zn(AA)_2$ is apparently smaller than for $Cu(AA)_2$ indicating a tetrahedral distortion of the structure in comparison with the square planar coordination of $Cu(AA)_2$.

The equations (8)-(12) are only strictly valid for systems that obey the requirements of the regular solution theory. In these systems interactions are mainly of dispersion type. No chemical interaction between solute and solvent molecules and no change in states of association and orientation by mixing should occur. As stated before the equations might even be applied to systems containing an aqueous phase if an empirically found value for δ_{aq} is used. The validity of the regular solution theory with this semi-empirical adjustment for correlation of partition data seems to be satisfactorily

proved for systems with an inert non-polar organic phase as can be seen from Fig. 2 and 3 and has been shown in other investigations.⁴⁻⁶ Any major deviations from parameters predicted by the theory might as a consequence be looked upon as indications of chemical interactions where the solute is involved and would give rise to larger changes in ΔH and/or ΔS for the extraction process.

From Fig. 2 and 3 it seems evident that the oxygen containing solvents and chloroform deviate from the regular solution behaviour indicating a certain solvent interaction.

From equation (9) the solubility parameters for $M(AA)_2$ have been calculated using the molar volumes $V_{Cu(AA)_2} = 175 \text{ cm}^3/\text{mole}$ and $V_{Zn(AA)_2} = 156 \text{ cm}^3/\text{mole}$, and the values are given in Table 2. The calculated values are higher than those calculated from the empirical equation¹⁵

$$\delta_{M(AA)_n} = \delta_{HAA} (n/n^*)^{1/2} \quad (13)$$

where $n^* \approx 0.95 n$ for $n = 2$ and with the value $\delta_{HAA} = 10.6$, which has been obtained empirically for acetylacetone in an aqueous system.⁴ From equation (13) the value $\delta_{M(AA)_2} = 10.7$ could be expected. A solvated molecule $M(AA)_n \cdot mB$ would have the value given by¹⁵

$$\delta_{M(AA)_n \cdot mB} = ((n \cdot \delta_{HAA}^2 \cdot V_{HAA} + m \cdot \delta_B^2 \cdot V_B) / (n \cdot V_{HAA} + m V_B))^{1/2} \quad (14)$$

According to equation (14) the value 11.8 will be obtained for a water adduct $M(AA)_2 \cdot H_2O$, which is in remarkable agreement with the values found for $\delta_{Zn(AA)_2}$ in non-polar solvents. For a solvent adduct the value will be lower, e.g. $\delta_{M(AA)_2 \cdot CHCl_3} = 10.8$. The mean of the measured values as given by Table 2 of $\delta_{M(AA)_2}$ for the inert solvents is 11.9 for $Zn(AA)_2$ and 11.3 for $Cu(AA)_2$. For the diluents dibutylether, hexone and chloroform the mean value is 11.6 for $Zn(AA)_2$ and 11.2 for $Cu(AA)_2$. These values may indicate that for systems with an inert organic phase the complexes are more or less hydrated in the aqueous phase, at least for $Zn(AA)_2$, while for systems with an organic phase containing donor diluents the complexes might also be solvated to some extent in the organic phase.

Variation of ionic strength

Partition coefficients have been determined at various ionic strengths in the system $Zn(AA)_2$ -benzene- $NaClO_4$. The values of $\log \lambda_2$, ΔH and ΔS are given in Table 3 and $\log \lambda_2$ vs $1/T$ in Fig. 4. For $\log \lambda_2$ as a function of $[NaClO_4]$ a linear relationship is obtained in the concentration range investigated as

shown in Fig. 5. No obvious significant trend in the variation of the ΔH and ΔS -values with $[\text{NaClO}_4]$ can be observed. Errors in one parameter will naturally influence the other parameter due to the interdependence in the method of determination. It can, however, be proved that the error for $\Delta H/T\Delta S$ would be considerably smaller. A plot of $\Delta H/T\Delta S$ as a function of $\ln \lambda_2$ as given by

$$\Delta H/T\Delta S - 1 = -R/\Delta S \cdot \ln \lambda_2 \quad (15)$$

gives a straight line indicating that ΔS is essentially constant in the investigated concentration range.

Studies are reported, where the influence of the concentration of certain organic donor solvents on the formation of solvated complexes according to reaction (4) has been studied.⁷ In a similar way, the formation of a hydrated species, e.g. in systems with inert organic diluents, might be detected if the concentration of "free" water, that is uncoordinated water available for coordination to any other species in the aqueous phase, could be estimated. If the number of water molecules coordinated to every Na^+ ion in the aqueous phase is regarded as constant the concentration of "free" water is proportional to the NaClO_4 -concentration. From the function $-\log \lambda_2 = f(\log [\text{H}_2\text{O}])$ a value for t in reaction (5) might then be determined. The limiting slope for $[\text{NaClO}_4] = 0$ should be 2 for a square planar $\text{M}(\text{AA})_2$ species, where the coordination number would increase from 4 to 6. At least for zinc the preferred coordination number seems to be 5 rather than 4, and 6-coordination is also well established.¹⁶ If a limiting slope of 2 is assumed the required concentration of "free" water would correspond to a number of hydration for NaClO_4 of 14-16, and a limiting slope of 1 will give a hydration number of 25-28. As comparison can be mentioned that if Na^+ and H_2O are considered as hard spheres the first coordination sphere around Na^+ will be occupied with 4 H_2O -molecules and the second with 10, assuming most favourable geometric close packing. A continuous decrease of the number of water molecules from 2 or 1 to 0 attached to the $\text{M}(\text{AA})_2$ -complex in the aqueous phase should, however, give significant changes for at least ΔH , which is not contradictory to our data, as can be seen in Table 3.

Thermodynamic parameters and coordination

From equation (8) the terms corresponding to changes of the partial molar enthalpy and partial molar entropy can be calculated assuming regular solution behaviour with the empirical modifications mentioned before. These

calculated values are given in Table 4 as well as the excess values obtained as the difference between measured and calculated values.

For a distribution process it is reasonable to divide ΔH and ΔS into different parts.

1. Solvation. The existence of hydrated species in the aqueous phase would give a positive contribution to ΔH corresponding to the energy required for breaking the bonds between the complex and the hydrate water; ΔS would have a positive value as well; solvated species in the organic phase would give a negative contribution to ΔH and ΔS .
2. Hole formation. The hole formation in the organic phase and filling up of the volume in the aqueous phase corresponding to the volume of the complex molecule will effect at least ΔH . The influence would probably be much less than changes caused by solvation.
3. Breaking of hydrophobic bonds. Destruction of the ordered water molecule layer around the complex in the aqueous phase would give a positive contribution to ΔS , while any formation of a similar layer of diluent molecules in the organic phase would give a negative contribution, but of much smaller magnitude than for the water phase. Assuming regular solution behaviour, measured and calculated parameters would coincide. For a two phase system, where one of the phases is aqueous, one might consequently expect an excess ΔS -term in the measured values caused by breaking this "hydrophobic bond".

In systems where hydration occurs in the aqueous phase an excess ΔH -term would be expected, while in systems where solvation occurs only in the organic phase the result would be a negative excess ΔH -term of the enthalpy. Copper has a preferred coordination number of four, both in solid compounds and in solutions. Very strongly basic ligands may form 5-coordinated species,

but these compounds easily decompose in solvent systems.¹⁶

For zinc, however, the coordination number five seems to be dominant, at least in solid compounds, even if 4- and 6-coordination also are well established.¹⁶ Several 5-coordinated base adduct complexes that are stable, e.g. in benzene solutions, have been prepared. It is therefore reasonable to assume, that the copper complex in the acetylacetonone system investigated preferably would be unsolvated and 4-coordinated, while the zinc complexes might be solvated leading to a coordination number of five or maybe even six, if coordination is not hindered for steric or other reasons. In the aqueous phase one might expect a hydration with one or maybe two water mole-

cules while for donor solvents solvation in the organic phase might be expected.

The values for the excess ΔH and ΔS as given in Table 4 could very well be explained if such coordination changes are assumed. For $\text{Cu}(\text{AA})_2$ 4- coordination seems to be maintained in both phases for all systems but chloroform, where a solvation in the organic phase might take place. $\Delta H_{\text{exc.}}$ is almost zero while $T\Delta S$ is constant possibly indicating the breaking of hydrophobic bonds in the aqueous phase. For $\text{Zn}(\text{AA})_2$ a hydration might take place in the aqueous phase for all the investigated systems and besides a solvation seems probable in the organic phase for the solvents hexone, chloroform and benzonitrile. The energy involved in solvation in the organic phases seems to be around 10-20 kJ/mole.

It is interesting to note that the energy required for breaking a water hydrogen bond is $\Delta H \approx 10$ kJ/mole and $T\Delta S \approx 11$ kJ/mole.

Conclusions

It is evident that calculations of thermodynamic parameters based on the regular solution theory with some semi-empirical modifications might give interesting information concerning the behaviour of complex species in different chemical systems as well as give indications of coordination changes when compared with measured data. The diluents in distribution equilibria seem to play two roles:

1. The diluent may be coordinated to the complex forming solvates depending on its donor ability.
- 2: The diluent will act as a medium for the distribution of the complex, with properties mainly depending on the cohesive forces between the complex and the diluent molecules.

It is also evident, that the amount of energy involved in these interactions is comparatively small. Very accurate data must be obtained for these changes to be properly explained. Complementary spectroscopic experiments might give valuable information concerning the specific kinds of interactions involved.

Acknowledgements

The authors are indebted to Drs. S.Andersson and J.O.Liljenzin for valuable and stimulating discussions and never failing interest in this project. Financial support from the Swedish Atomic Research Council is gratefully acknowledged.

References

1. Hildebrand, J.H. & Scott, R.L., "Solubility of Non-electrolytes", 1964, 3rd Ed. (New York, Dover Publ. Inc.).
2. Siekierski, S., J. Inorg. Nucl. Chem., 1962, 24, 205.
3. Siekierski, S. & Olszer, R., J. Inorg. Nucl. Chem., 1963, 26, 1351.
4. Wakahayashi, T., Oki, S., Omori, T. & Suzuki, N., J. Inorg. Nucl. Chem., 1964, 26, 2255.
5. Omori, T., Wakahayashi, T., Oki, S. & Suzuki, N., J. Inorg. Nucl. Chem., 1964, 26, 2265.
6. Mitchell, J. & Banks, C., J. Inorg. Nucl. Chem., 1969, 31, 2105.
7. Suzuki, N. & Akiba, K., J. Inorg. Nucl. Chem., 1971, 33, 1897.
8. Hopkins, P. & Douglas, B., J. Inorg. Nucl. Chem., 1964, 3, 357.
9. Liljenzin, J.O., Stary, J. & Rydberg, J., "Solvent Extraction Research", (Eds. Kertes, A.S. & Marcus, Y.), 1969, p. 21 (New York, Wiley & Sons Inc.).
10. Liljenzin, J.O. & Rydberg, J., "Physico-Chimie du Protactinium", 1966, p. 255 (Paris, Ed. du Centr. National de la Recherche Scientifique).
11. Reinhardt, H. & Rydberg, J., "Solvent Extraction Chemistry" (Eds. Dyrssen, D., Liljenzin, J.O. & Rydberg, J.), Proc. Int. Conf. on Solv. Extr. Chem., Göteborg, 1967, p. 18 (Amsterdam, North-Holland Publ. Co.).
12. Andersson, C., Andersson, S.O., Liljenzin, J.O., Reinhardt, H. & Rydberg, J., Acta Chem. Scand., 1969, 23, 2781.
13. Andersson, S., unpublished results.
14. Riddick, J. & Bunger, W., "Organic Solvents", Techniques of Chemistry, Vol. 11, 1970 (New York, Wiley-Interscience).
15. Tanaka, M., Proc. ISEC 71, Vol. 1, 1971, p. 18 (London, Society of Chemical Industry).
16. Gaudon, J.P., Coord. Chem. Rev., 1969, 4, 1.

Figure 1. $\log \lambda_2$ for $\text{Zn}(\text{AA})_2$ (filled symbols) and $\text{Cu}(\text{AA})_2$ (open symbols) as a function of $1/T$. (System data and numbers as in Table 1).

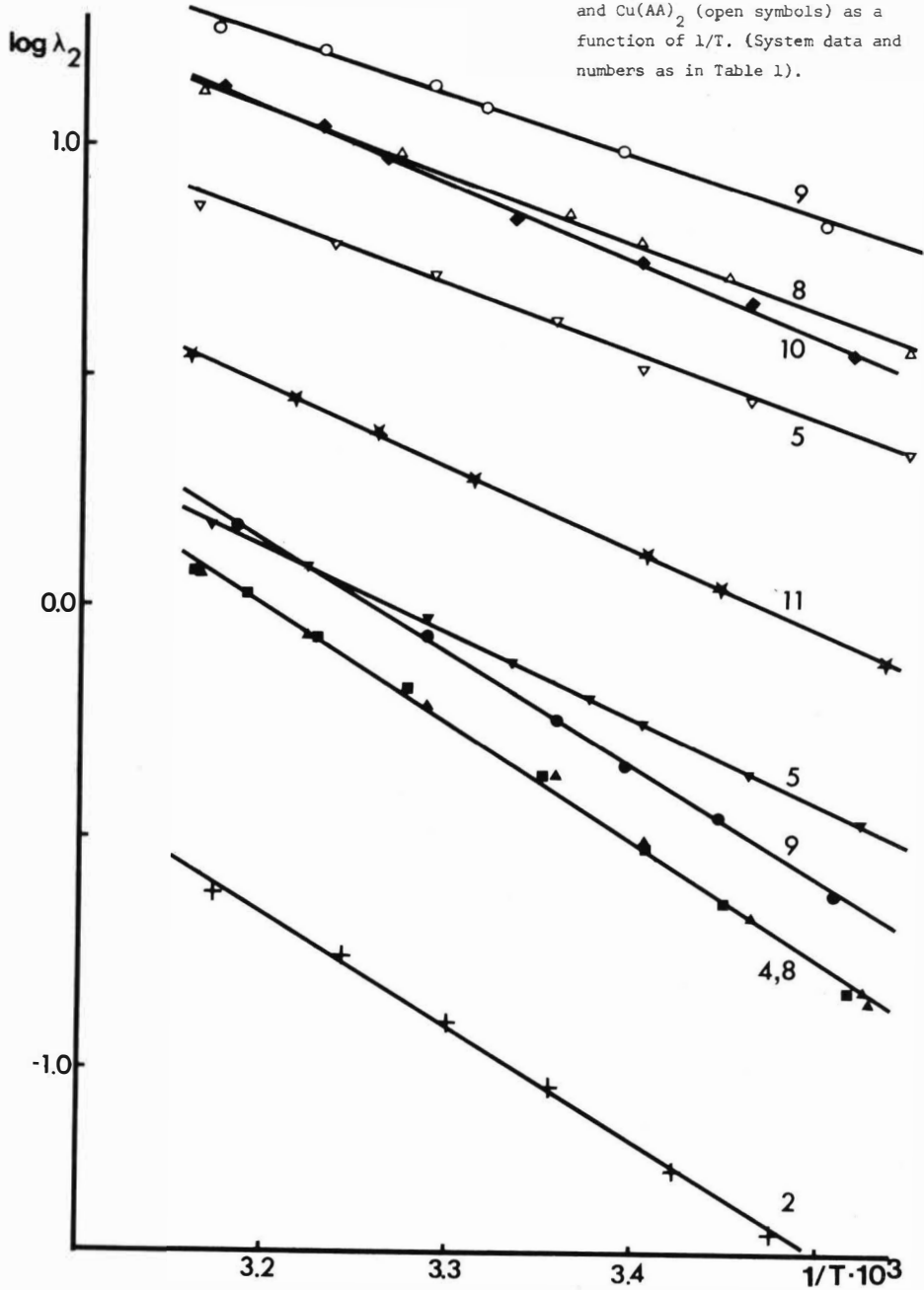


Figure 2. $\log \lambda_2'(\delta_{aq} - \delta_{org})$ for $Zn(AA)_2$ (filled symbols) and $Cu(AA)_2$ (open symbols) as a function of δ for the diluent at 25°C. (System data and numbers as in Table 1).

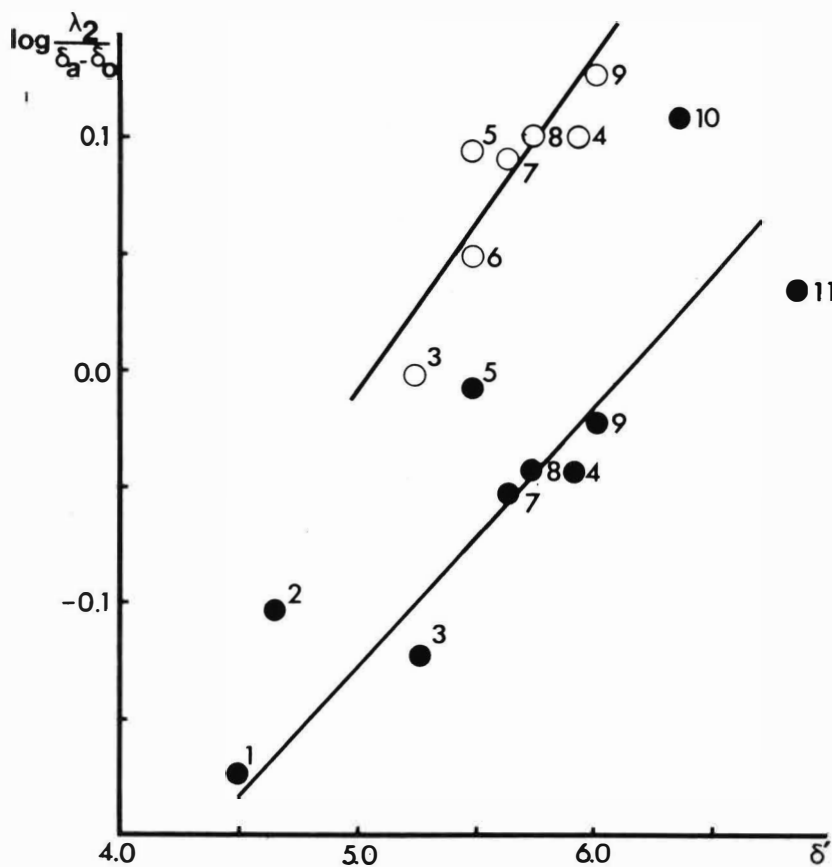


Figure 3. $\log \lambda_2$ for $\text{Zn}(\text{AA})_2$ (filled symbols) and $\text{Cu}(\text{AA})_2$ (open symbols) as a function of $\log k_d$ for HAA at 25°C. (System data and numbers as in Table 1).

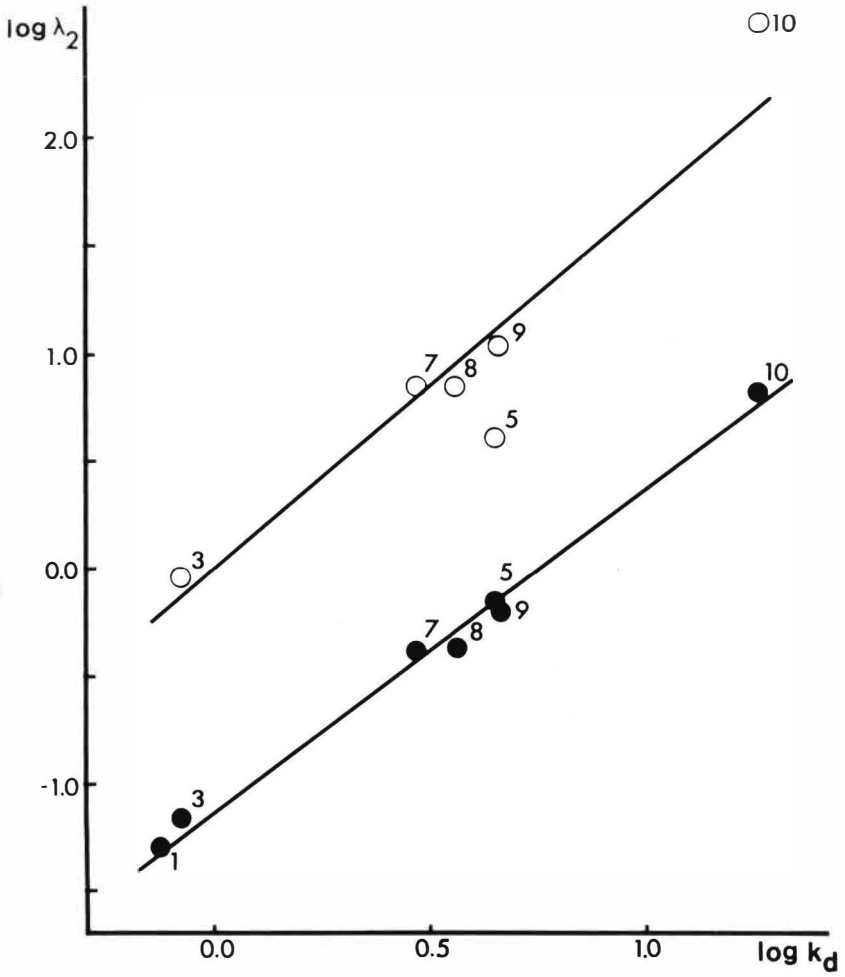


Figure 4. $\log \lambda_2$ for $\text{Zn}(\text{AA})_2$ as a function of $1/T$ with benzene as organic diluent and various ionic strength in the aqueous phase. (System data and numbers as in Table 3).

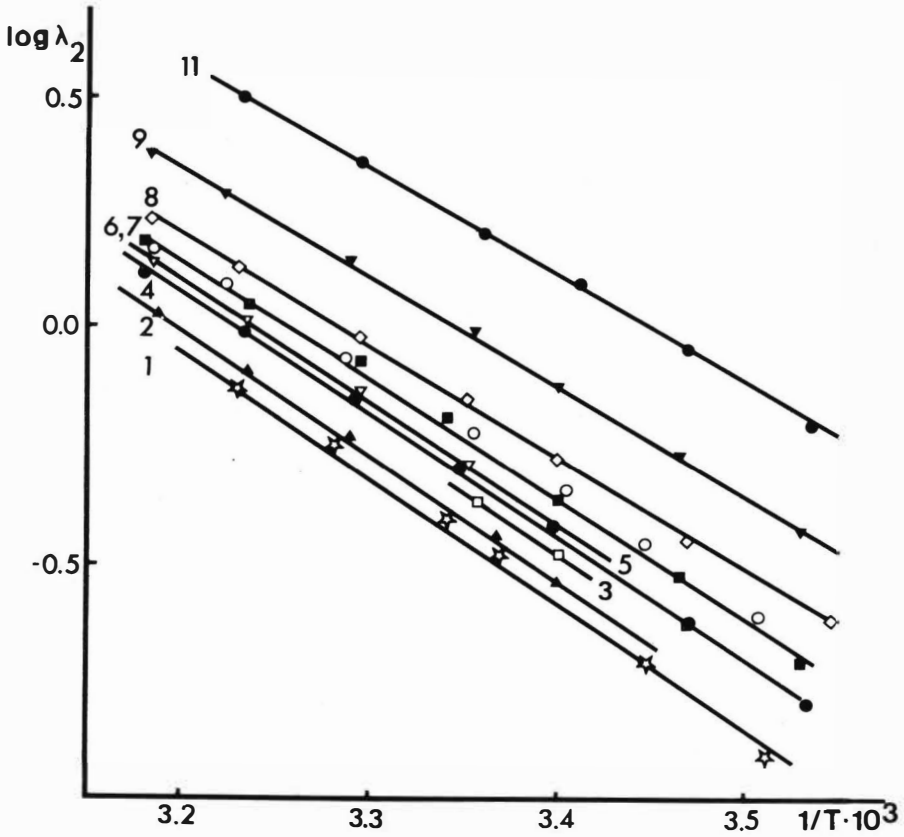
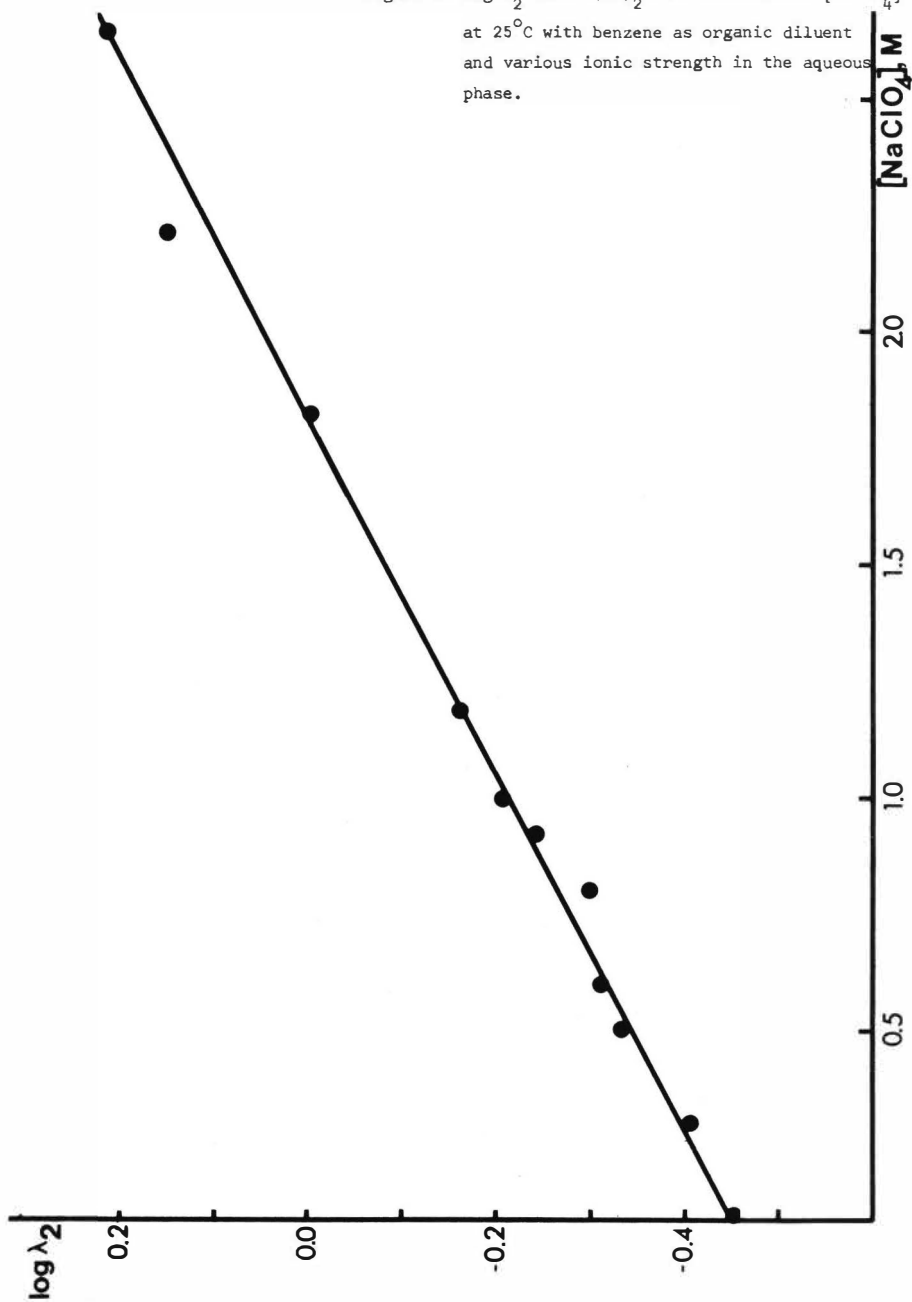


Figure 5. $\log \lambda_2$ for $\text{Zn}(\text{AA})_2$ as a function of $[\text{NaClO}_4]$ at 25°C with benzene as organic diluent and various ionic strength in the aqueous phase.



CORRELATION OF EXCESS ENTHALPIES OF MIXING
IN TRIBUTYLPHOSPHATE - N-ALKANE SYSTEM

L. Tsimering and A.S. Kertes
Institute of Chemistry, The Hebrew University
Jerusalem, Israel

Abstract

Excess enthalpies of mixing of tributylphosphate with n-alkanes have been evaluated from experimental data in TBP-hexane and TBP-dodecane systems at 303.15 K by using a model involving the lattice theory of mixtures and group and molecular interchange enthalpies of interacting surfaces.

We have reported recently⁽¹⁾ direct calorimetric data on the heat of mixing of tri-n-butylphosphate with n-hexane, n-dodecane and benzene at 303.15 K, and compared these new sets of excess enthalpies with those in the literature⁽²⁻⁴⁾. In continuation of the project, we now report a quantitative interpretation of our experimental data in terms of a simple statistical thermodynamic model previously used for alkyl-amine-hydrocarbon systems⁽⁵⁾, which is based on a combination of the group interaction model and the zeroth approximation form of the lattice theory of mixtures for molecules of different sizes at a completely random arrangement.

The model⁽⁵⁾ requires that each molecule, \underline{i} , consists of \underline{m}_i segments, each occupying one site on a lattice of coordination number \underline{z} . The number of contact points for each type of molecule \underline{i} is thus given by

$$\underline{s}_i = \underline{m}_i (\underline{z}-2) + 2 \quad (1)$$

Each segment on the surface of the molecule has a characteristic capability of interaction which is proportional to a group cross section \underline{s}^u and \underline{s}^v of u and v type surfaces of molecule \underline{i} . The combined molecular cross sections are thus given as

$$\underline{s}_i = \sum \underline{m}_i^u \underline{s}^u \quad (2)$$

representing the sum of the appropriate group cross sections

of the molecule. The corresponding molecular coverages are defined by the ratio

$$\alpha_{\underline{i}\underline{s}} = \frac{m_{\underline{i}}^u s^u}{s_{\underline{i}}} \quad (3)$$

For the binary systems of tributylphosphate and the normal alkane diluents under consideration we have the simplest possible combination that the surface of the tributylphosphate molecule (component 1) is composed of aliphatic (CH_3 and CH_2) and phosphatic (PO_4) elements, and that

of the normal aliphatic hydrocarbons (component 2), of aliphatic elements only. Thus, in terms of the theory, the two interacting surfaces are the aliphatic (u) and the phosphatic (v), assuming that the methyl and methylene surfaces are of the same kind.

The experimentally determined excess enthalpy of mixing per mole of mixture is defined as:

$$H^E = s_1 s_2 \frac{x_1 x_2}{s_1 x_1 + s_2 x_2} A_{12} \quad (4)$$

where x is the mole fraction of components 1 and 2, s the corresponding molecular cross section, and A_{12} the molecular interaction parameter defined as:

$$A_{12} = -k^{uv} (\alpha_1^u - \alpha_2^u) (\alpha_1^v - \alpha_2^v) \quad (5)$$

where k^{uv} is the molar interchange enthalpy per conventional unit area of the interacting aliphatic (u) and phosphatic (v) surfaces. Since the sum of all molecular coverages for any

given molecule is equal to unity

$$\alpha_1^u + \alpha_1^v = \alpha_2^u + \alpha_2^v = 1 \quad (6)$$

and $\alpha_2^v = 0$, eq. (5) reduces to

$$\underline{A}_{12} = \underline{k}^{uv} (\alpha_1^v)^2 \quad (7)$$

The group and molecular cross sections were calculated by adopting a lattice coordination number $\underline{z} = 8$, thus an area of 0.125 for each bond. Accordingly, each methyl and methylene group constitutes one section which would have a value of unity in the isolated state, but have the values of $\underline{s}^{\text{CH}_2} = 0.750$ and $\underline{s}^{\text{CH}_3} = 0.875$ when chemically bonded. In the tributylphosphate molecule, the phosphatic group has the value of $\underline{s}^{\text{PO}_4} = 0.625$ (three bonds per group). From these values of group sections, the molecular cross sections are calculated by simple addition: that for tributylphosphate is $\underline{s}_{\text{TBP}} = 10.00$, and the corresponding molecular coverage, $\alpha_1^v = \underline{s}^{\text{PO}_4} / \underline{s}_{\text{TBP}} = 0.0625$; that for n-hexane is $\underline{s}_{\text{C}_6} = 4.75$ and for n-dodecane $\underline{s}_{\text{C}_{12}} = 9.25$.

The molar interchange enthalpy, \underline{k}^{uv} , as derived from the experimental data⁽¹⁾ for TBP-hexane and TBP-dodecane systems by eqs. (4) and (7) has the value of $\underline{k}^{uv} = 130,600 \pm 6400 \text{ J mol}^{-1}$. The fit of the calculated \underline{H}^E values is shown in Figure 1 along with the experimentally determined points⁽¹⁾. While the agreement is satisfactory in the TBP-hexane system, the deviation from the experimental points at low TBP content

in the TBP-dodecane system may be as high as 20%. A better agreement may be expected by employing a more sophisticated model which will take into account the cross sections and interchange parameters of the etheric oxygen and the phosphoryl group in TBP separately, rather than the overall phosphatic group as in the present model. We are now engaged in generating additional heat of mixing data, which then will enable calculations based on the more elaborate model.

In the meantime, we have calculated the excess enthalpies of mixing of tributylphosphate with several n-alkanes at 303.15 K using the k^{uv} value derived here. The results, estimated to be reliable to $\pm 5\%$, are given in Table 1 at 0.1 mole fraction intervals.

References

1. L. Tsimering and A.S. Kertes, J. Chem. Thermodyn., 6, 000 (1974).
2. K. Schwabe and K. Wiesener, Z. Elektrochem., Ber. Bunsenges. physik. Chem., 66, 39 (1962).
3. V.V. Fomin and T.I. Rudenko, Radiokhimiya, 7, 33 (1965).
4. Yu. A. Afanasiev, A.V. Nikolaev and T.I. Koroleva, Radiokhimiya, 8, 696 (1966).
5. A.S. Kertes and F. Grauer, J. Phys. Chem., 77, 3107 (1973).

Table 1

Excess enthalpies of mixing of tributylphosphate with n-alkanes calculated using eqs. (4) and (7).

x_{TBP}	$H^E \text{ J mol}^{-1}, 303.15 \text{ K}$			
	n-Pentane $\underline{s} = 4.00$	n-Heptane $\underline{s} = 5.50$	n-Octane $\underline{s} = 6.25$	n-Nonane $\underline{s} = 7.00$
0.1	399	424	433	440
0.2	628	701	729	751
0.3	739	860	908	949
0.4	765	874	987	1045
0.5	729	904	980	1050
0.6	644	821	900	974
0.7	522	681	754	824
0.8	371	493	551	607
0.9	195	264	310	331

x_{TBP}	n-Decane $\underline{s} = 7.75$	n-Undecane $\underline{s} = 8.50$	n-Tetradecane $\underline{s} = 10.75$	n-Hexadecane $\underline{s} = 12.25$
	0.1	446	449	462
0.2	771	788	828	847
0.3	985	1017	1094	1133
0.4	1097	1143	1259	1321
0.5	1113	1172	1321	1404
0.6	1042	1107	1277	1376
0.7	890	953	1126	1229
0.8	662	715	864	956
0.9	364	396	490	550

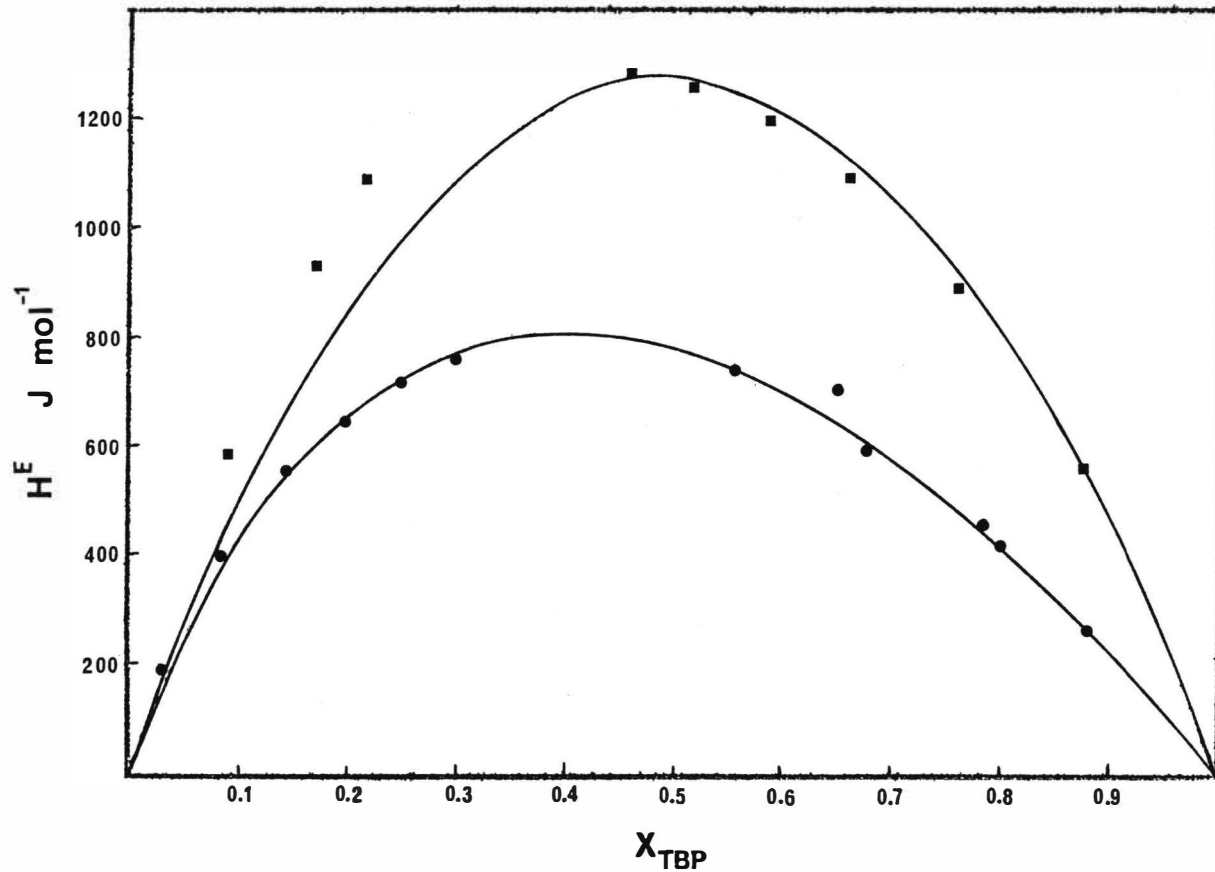


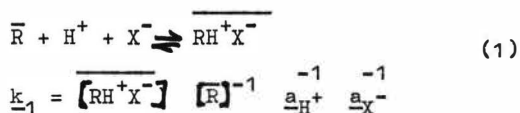
Figure 1. Comparison of theory with experiment for the excess enthalpies of mixing of tri-n-butylphosphate with hexane (●) and dodecane (■) at 303.15 K. Points show experimental results, full lines predicted by the theory.

F. Grauer* and A.S. Kertes , Institute of
Chemistry, The Hebrew University, Jerusalem, Israel

ABSTRACT

The formation constants of tri-n-octyl, tri-n-decyl- and tri-n-dodecylammonium chlorides have been determined in anhydrous benzene by direct calorimetry at 30°C. The values obtained, $\log k_2 = 2.19, 2.38$ and 2.48 respectively, have been corrected for the competitive reaction which takes place between benzene and hydrogen chloride, $\log k_3 = 0.80$. These values were compared with those in the literature obtained from partition data, with due correction to the extent of hydration of both the amine-base and the ammonium chloride in wet benzene. The conclusion has been reached that the presence of water stabilizes the formation of the ionpairs.

The most characteristic reaction of long-chain alkylamine bases is that with strong mineral acids to form salts. In water-immiscible, low polarity and low dielectric constant organic solvents, which are practical as diluents in solvent processes, the alkylammonium salts form ionpairs. The ionpairs, however, are only exceptionally stabilized as such. Depending on the nature of the diluent and that of the salt and its concentration, ionpairs may dissociate to ions RH^+ and X^- (R-alkylamine, X^- anion), or associate into higher aggregates $(RH^+ X^-)_n$. In most nonionizing solvents, at low solute concentrations, there is presumably a certain, but always limited, concentration range in which the alkylammonium salt is predominantly in the form of the undissociated monomeric ionpair, RH^+X^- . When these conditions are met, and only then, the simple equilibrium of salt formation



holds true, and the semi-thermodynamic equilibrium constant in terms of activities a and molarities ($()$) may be determined experimentally. Existing literature data on these formation constants for several tri-n-alkylammonium salts in various diluents have recently been compiled and critically evaluated¹.

All available formation constants according to eq. (1) refer to an equilibrium condition in the presence of water, implicit by the methods of experimentation employed. When a mineral acid is extracted from an aqueous solution by a high-molecular weight alkylamine in a diluent, or when an organic solution of the corresponding alkylammonium salt is equilibrated with water or an aqueous electrolyte solution, varying amounts of water pass into the organic phase. With due corrections for the solubility of water in the diluent alone, the quantity of extracted water depends on the nature of the amine and its salt, and their concentration, as well as the nature of the acid, its aqueous concentration, and to a significant extent also on the water activity in the aqueous solution²⁻¹¹. Though several attempts have been made to correlate water extraction with various experimental parameters^{5,7,8,12}, the effect of coextracted water on the formation constant of alkylammonium salts could not be properly assessed since no data for comparison are available on such formation constants in anhydrous systems.

In spite of the facts that the bulk dielectric constant of the organic medium containing the amine and/or the ammonium salt is not significantly different in the presence or absence of water⁸, and that the dissolved water is not osmotically active¹⁰, it can be assumed that in the highly involved two-phase multicomponent reaction of salt formation the presence is bound to produce a measurable effect upon the formation constants derived.

With this aim in mind, we have determined the formation constants of three tri-n-alkylammonium chlorides in anhydrous benzene, and report here our first results. For the sake of a complete analysis, we will review the available information, and wish to offer a preliminary explanation of the effect water plays in the process of alkylammonium salt formation.

RESULTS

For the formation of tri-n-alkylammonium chloride using tri-n-octyl, tri-n-decyl and tri-n-dodecylamine and gaseous hydrogen chloride, all dissolved in anhydrous benzene, the equilibrium constants of the reaction



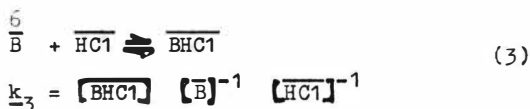
were determined calorimetrically at $30.000 \pm 0.001^\circ\text{C}$ using a Tronac Model 1000 A continuous automatic titration calorimeter, by a technique ^{13,14} and method ¹⁵ described elsewhere. From the experimentally determined heat effects upon neutralization of the base by the acid, the pertinent thermodynamic functions were computer calculated ¹⁵ by a modification of a procedure described in the literature ¹⁶ for entropy titration data. The corresponding equilibrium constants according to eq. (2), obtained from the free energy changes derived previously ¹⁵, $\ln k_2 = G/RT$, are compiled below, along with the concentration range of the reactants in the three sets of experiments at 30°C .

Chloride	Concentration range, 10^2M		$\log k_2$
	Amine base	Acid	
Tri-n-octylammonium	1.10	0.53-1.73	2.19 ± 0.01
tri-n-decylammonium	0.82	0.21-1.34	2.38 ± 0.01
Tri-n-dodecylammonium	1.00	0.20-1.26	2.48 ± 0.01

DISCUSSION

For a meaningful comparison of the present equilibrium constants according to eq. (2) in a single phase system of (dry) benzene, with those according to eq. (1) in a two-phase system of (wet) benzene, a number of additional equilibria should be considered. We will thus first review briefly the available information on systems pertinent to our discussion.

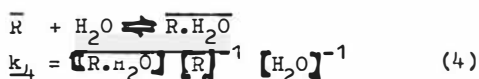
Benzene-Hydrogen Chloride. From the freezing-point diagram ¹⁷ of liquid hydrogen chloride and benzene in the temperature range between -130° and 0°C evidence was found for the formation of a 1:1 complex attributed to the weak hydrogen bonds formed between the components. Strong confirmation comes from the observed shift of the infrared band for H-Cl ¹⁸. More recently, Gerrard ¹⁹, and Brown and Melchiorre ²⁰ have reviewed earlier literature, and the latter provided additional spectral evidence for the formation of the equimolar complex. From Henry's Law constant for the solubility of hydrogen chloride in benzene, the equilibrium constant for the reaction



has been determined at -45.2 , -63.5 and -78.5 . The enthalpy of formation of the complex was found to be $\underline{H} = 1.99$ kcal mole⁻¹. We have extrapolated these data by the van't Hoff equation, and estimate that $\log k_3 = 0.80$ at 30°C .

The low enthalpy value suggests that in complexes formed between hydrogen chloride and benzene, there is no complete transfer of the proton to the aromatic ring. This is in line with the findings ²¹ that hydrogen chloride is virtually unionized in benzene.

Benzene-Tri-n-alkylamine-Water. Roddy and Coleman ⁵ studied the distribution of water between pure water (activity of unity) and a benzene solution of tri-n-octylamine, when the concentration of the latter varies between 0.01 and 0.5M, at 25°C . The solubility of water in the organic phase increases owing to the presence of the amine-base in benzene. When corrected for the amount of water soluble in benzene alone (0.0363 M), the excess water varies linearly with the concentration of the base, and the equilibrium constant of the reaction.



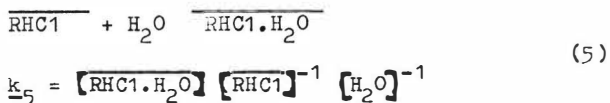
has a value of $\log k_4 = 0.07$ at 25°C for the trioctylamine. The linear relationship has been interpreted to mean that not more than one water molecule is associated with each amine-base monomer, thus no dimer hydrate can be present in significant quantities.

Benzene-tri-n-alkylammonium chloride-water. When anhydrous solid trilaurylammonium chloride is dissolved in dry benzene, and the resulting organic solution equilibrated with pure water, the solubility of water, after being corrected for its solubility in pure benzene, is directly proportional to the salt concentration over a 0.02-0.5M range. The water-to-salt molar ratio is $0.95 \pm 25^\circ\text{C}$ ¹¹.

In a comparable set of experiments but with a benzene solution of trioctylammonium chloride⁵, the water-to-salt ratio varies between 0.93 at a salt level of 0.01M to 1.22 at 0.5M at 25°C . The solubility of water (activity of unity) in a 0.1M TOA.HCl follows Henry's Law, consistent with the formation of a monohydrate. The variation of the ratio has been interpreted by assuming that the extracted water is held both as a definite monohydrate, and in the form of simple solution. The two kinds of attachment for water differs in bond strength: in the first case, water is rather strongly bound to the amine salt and is not affected by the variation of the salt concentration, while in the second case, the rather weakly bound water shows considerable dependence upon the concentration of the amine salt. It should be emphasized that the authors⁵ have found no evidence for an interaction between water and the alkylammonium cation, RH^+ . This is a confirmation of earlier findings¹¹ in the similar TLA.HCl/benzene system saturated with water, where the hydration of the cation alone has been ruled out on the basis of infrared spectral data. There is though strong indication that the water is indeed bound to the salt, probably in the form of a monohydrate. The consensus seems to be^{5,7,11,12} that the water is mainly associated with the chloride ion.

Further supporting evidence for the existence of the trialkylammonium monohydrate in benzene (and some other solvents, though by no means all¹¹) has been obtained from partition data under comparable experimental conditions^{2,7,22-24}.

Regardless the way in which water is associated with the trialkylammonium chloride molecule, it is relevant for the present discussion to accept the experimental evidence that the salt in benzene is a monohydrate. From the available data^{5,11} we have thus calculated the equilibrium constant of the reaction.



and will use the value of $\log k_5 = -0.02$ at 25°C for the alkylammonium salts under consideration.

Benzene-Trialkylamine-Hydrochloric acid-Water. Such are, of course, the actual solvent extraction systems, which have been extensively studied by various authors, and from the experimentally determined partition data the equilibrium constants k_1 , eq. (1), have been calculated under a variety of conditions. The available numerical data have recently been reviewed and critically assessed¹, and we will use the recommended values of $\log k_1 = 4.14 \pm 0.05$ for trioctylammonium and $\log k_1 = 4.18 \pm 0.08$ for trilaurylammonium chloride in benzene at 25°C .

Our only concern now is to illustrate and discuss the effect of dissolved water upon the formation of trialkylammonium chlorides in benzene solutions.

In dry systems there is a complex formation between hydrogen chloride and benzene. Consequently, the process of salt formation under anhydrous conditions, between the amine-base and the hydrogen chloride should be regarded as a competitive reaction between equilibria (2) and (3), meaning that the formation constant k_2 should be corrected by k_3 to describe the actual salt formation reaction

$$\overline{\text{BHC1}} + \overline{\text{R}} \quad \overline{\text{RHC1}} + \overline{\text{B}}$$

$$k_{23} = \frac{[\overline{\text{RHC1}}][\overline{\text{R}}]}{[\overline{\text{BHC1}}]^{-1}[\overline{\text{R}}]^{-1}} \quad (6)$$

$$= k_2 k_3^{-1}$$

The numerical values at 30°C are then $\log k_{23} = 2.99, 3.18$ and 3.28 for trioctyl- tridecyl- and tridodecylammonium chloride respectively.

In wet systems, the formation of the salt has been assumed to proceed according to the two-phase equilibrium (1), and the formation constant k_1 calculated accordingly. In view of the evidence that both, the alkylamine-base and the alkylammonium chloride form monohydrates in benzene when in equilibrium with water (activity unity), equilibrium (1) should be corrected to this effect. Thus, the actual overall two-phase equilibrium occurring when a dilute aqueous solution of hydrochloric acid is equilibrated with a benzene solution of a trialkylamine, can be expressed as

$$\overline{\text{R.H}_2\text{O}} + \text{H} + \text{C1} \quad \overline{\text{RHC1.H}_2\text{O}}$$

$$k_{145} = \frac{[\overline{\text{RHC1.H}_2\text{O}}]}{[\overline{\text{R.H}_2\text{O}}]^{-1} a_{\text{H}^+}^{-1} a_{\text{C1}}^{-1}} \quad (7)$$

$$= k_1 k_5 K_4^{-1}$$

assuming that the formation constants of the amine base monohydrate, k_4 , and that of the ammoniumchloride monohydrate, k_5 , are not significantly affected ^{5,11} by the length of the alkyl chains, the numerical values of $\log k_{145}$ are 4.23 ± 0.05 and 4.19 ± 0.08 for trioctyl - and trilauryl-ammonium chloride monohydrate, respectively. These corrections are not large, and are within the experimental errors of the k_1 values.

We can now arrive to the conclusion that the stability of the trialkylammonium chloride ionpair formed in presence of water in benzene is by an order of magnitude higher than in the same medium but in absence of water. It is thus tempting to assume that water plays a significant role in stabilizing the ion pair, perhaps by linking the ions together and hence promoting salt formation.

References

1. A.S. Kertes, IUPAC Report, Commission on Equilibrium Data, Pure and Applied Chem., to appear 1974.
2. O.I. Zakharov-Nartsissov and A.V. Ochkin, Russ. J. Inorg. Chem., 7, 337 (1962).
3. W.E. Keder and A.S. Wilson, Nucl. Sci. Eng. 17, 287 (1963).
4. L. Kuca and E. Högfeltdt, Acta Chem. Scand., 21, 1017 (1967).
5. J.W. Roddy and C.F. Coleman, J. Inorg. Nucl. Chem., 31, 3599 (1969).
6. R. Bac, J. Inorg. Nucl. Chem., 32, 3655 (1970).
7. J.F. Desreux, Anal. Chim. Acta, 52, 207 (1970).
8. A.S. Kertes, in "Recent Advances in Liquid-Liquid Extraction", C. Hanson, ed., Pergamon, Oxford, 1971, p. 15.
9. C. Deptula and S. Minc, Nukleonika, 10, 355 (1965).
10. J.J. Bucher and R.M. Diamond, J. Phys. Chem., 69, 1565 (1965).
11. W. Müller and R.M. Diamond, J. Phys. Chem., 70, 3469 (1966).
12. V.S. Shmidt, "Amine Extraction", Atomizdat, Moscow, 1970. English transl., IPST, Jerusalem, 1971.
13. A.S. Kertes and E.F. Kassierer, Inorg. Chem., 11, 2108 (1972).
14. A.S. Kertes and F. Grauer, J. Phys. Chem., 77, 3107 (1973).
15. A.S. Kertes and F. Grauer, J. Phys. Chem., to appear.
16. J.J. Christensen, R.M. Izatt, L.D. Hansen and J.A. Partridge, J. Phys. Chem., 70, 2003 (1966).

17. D. Cook, Y. Lupprien and W.G. Schneider, *Can. J. Chem.*, 34, 964 (1956).
18. M.L. Josien and G. Sourisseau, *Bull. Soc. Chim. France*, 178 (1955).
19. W. Gerrard, *J. Chim. Phys.*, 61, 73 (1964).
20. H.C. Brown and J.H. Melchior, *J. Am. Chem. Soc.*, 87, 5269 (1965).
21. G.J. Janz and S.S. Danyluk, *Chem. Rev.*, 60, 209 (1960).
22. R.R. Grinstead and J.C. Davis, *J. Phys. Chem.*, 72, 1630 (1968).
23. U. Bertocci and G. Rolandi, *J. Inorg. Nucl. Chem.*, 23, 323 (1961).
24. G. Duyckaerts, J. Fuger and W. Müller, *Euratom Report*, EUR-426 (1963).

SESSION 14

Wednesday 11th September: 9.00 hrs

E X T R A C T I O N T E C H N O L O G Y

(Nuclear Processes I)

Chairman:

Dr. W. Schuller

Secretaries:

Mr. A.L. Mills

Mr. P. Patiguy

EXPERIENCES OF HIGHLY ENRICHED URANIUM
REPROCESSING IN THE EUREX PILOT PLANT.

by S. CAO, H. DWORSCHAK*, A. HALL

ABSTRACT

The results of the reprocessing campaign of irradiated MTR fuel elements with long-chain tertiary amines as extractant in the Eurex pilot plant in Italy are discussed. Besides the U recovery and the FP decontamination performances particular emphasis is given to the U/Pu separation, which was achieved in two steps, first by addition of sulfuric acid as Pu(IV) complexant to the 2nd cycle extraction and scrubbing sections and secondly by the treatment of the concentrated U final product with an organic diluent soluble hydroxamic acid (HX). Np was mainly separated from U by the HX process.

Finally a brief description is given of the results obtained with a 5% TBP - kerosene flowsheet, still for highly enriched U recovery from MTR elements, at Eurex.

CNEN-Eurex plant, Saluggia, Italy

*Commission of the European Communities, D.G. III/B1

INTRODUCTION

The Eurex plant, built in the frame of a joint CNEN-Euratom programme, is a multipurpose pilot reprocessing plant for irradiated nuclear fuel elements, with the aim of performing operations under industrial-like plant conditions.

The plant was started with active operation in October 1970, with the reprocessing of irradiated Material Testing Reactor (MTR) fuel elements with a 90% ^{235}U initial enrichment, from Italian and Euratom research reactors.

In this paper the flowsheet performances of a two years operation period are emphasized, during which at first tertiary amines (Alamine 336, TCA) and later TBP have been used as U extractants.

HEAD-END

The treated fuel elements are made up of a series of plates of Al-cladded U-Al alloy within an aluminium channel with a rectangular cross-section of 75.8 x 76.1 mm.

After cutting off the inactive terminals the elements have a length of 645 ± 5 mm and a weight of about 4.5 kg. The average U content of the treated elements has been 185 g. The burn-up varied from a minimum of 11.6% to a maximum of 34.3%.

Because of the rather long cooling the residual activity was mainly due to the long lived fission products like ^{137}Cs and ^{90}Sr , whereas ^{95}Zr - ^{95}Nb have been virtually absent in a good deal of the treated elements.

Figure 1 gives a schematical representation of the head-on section with an overall material balance for a batch dissolution of 3 fuel elements.

U and fission products were dissolved together with cladding and structural aluminium at 100°C by feeding continuously 7M nitric acid

*) EURATOM-CNEN Convention Nr. 001-64-11 RCI I with variable amounts of mercuric nitrate as catalyst. An overall dissolution rate of about 1 mg/cm² min may be roughly estimated.

A fumeless dissolution is performed by the reoxidation of nitrous oxide with air, which is added to the dissolver off gases, also for H₂ dilution. The recovered nitric acid is refluxed directly into the dissolver.

For each mole of dissolved Al, an average of 3.8 moles nitric acid was consumed; 21% of this acid was lost to the dissolver off gas. 3/4 of these losses were incondensable gases released to the stack, the remaining part was recovered in the dissolver off gas wash tower.

The presence of up to 120 g Si/batch led to the formation of colloidal silica in the acid feed liquor. By addition of gelatine and heating of the solution to 80°C the silica was coagulated. The precipitate was separated by centrifugation.

Only with feed liquor purified in this way, a satisfactory hydraulical behaviour of the extraction battery could be guaranteed. Periodically, after the washout of the fissile material, the precipitate in the centrifuge was suspended and discharged to the High Level Waste storage tanks.

When these wash solutions were fed to the extraction battery, in some occasion difficulties like interface instability and flooding were encountered. Peptization of part of the precipitate might be the reason, perhaps because of gelatine degradation.

SOLVENT EXTRACTION

The first aim of the MTR-reprocessing campaign at Eurax had been to demonstrate the feasibility of a flowsheet using tertiary amines as extractant for U recovery. Successively the plant was run with a TBP flowsheet, still for highly enriched U purification.

Amine flowsheet

The project flowsheet¹, developed in 1963, was based on two separate extraction cycles; in both cycles the organic phase was a 4% A-lamine 336 solution in an aromatic hydrocarbon diluent, preferentially Solvesso 100.

The salting out action in the second cycle should have been provided by adding aluminium nitrate to the scrub solution.

The higher selectivity and radiation stability of the amine solvent was expected to permit higher decontamination factors and therefore a reduction of the number of extraction cycles, resulting finally in capital and operating costs savings.

Difficulties emerged in U/Pu separation, for which a DF_{Pu} of about 10^5 had to be realized in order to meet the USAEC specification for the residual transuranium alpha activity ($\leq 15\ 000$ dpm/gU).

After an extensive study of the behaviour of Pu under the process conditions² and its kinetics in stripping³ a revised flowsheet for the plant start-up was elaborated (fig.2 and 3).

U/Pu separation work was extended from the 2nd cycle, as foreseen initially, to both cycles.

In particular the 1st cycle strip conditions were chosen to get a Pu-to-organic/U-to-aqueous partition. In the 2nd cycle the addition of ANN was suppressed. The lack of salting-out action was compensated by a higher TCA concentration in the solvent. In tests with laboratory scale countercurrent equipment, the prefixed DF_{Pu} couldn't be realized. Considering however that with the kinetics involved in the Pu separation the results are strongly depending on the equipment efficiency, and that the plant mixer-settlers efficiency was clearly superior to that of the mixer-settlers used in the laboratory tests, this flowsheet was chosen for the not operation start-up. The first results showed immediately that not even in the plant the U specifications would be achieved. The 1st and the 2nd cycle DF_{Pu} have been respectively ~ 3 and ~ 20 . A new flowsheet concept was adopted, reserving the 1st cycle to fission products decontamination only and optimizing the 2nd cycle conditions for U/Pu separation. A post-purification extraction process, operated batch-wise with a highly selective Pu(IV) and Np(IV) complexing agent (HX) was introduced for the final purification of the concentrated U product from these alpha emitters.

A total of 14.5 kg U have been treated with this combined amine-HX flowsheet⁴.

The overall U losses of this campaign have been exceptionally high, amounting to 3.8%, mainly due to the frequent recycling during flowsheet adjustments.

First Extraction Cycle

Acid conditions in extraction and scrubbing have always been the choice for the amine flowsheet. Studies with irradiated solvent and a hot laboratory countercurrent test run indeed shown heavy crud formation with acid-deficient aqueous feed solutions.

The flowsheet conditions, as finally adopted for standard plant operation, are given in figure 4.

In accordance with the tendency of the DF_{β} to increase with the acidity¹, the nitric acid concentration was increased as far as possible, taking into account that first the U distribution drops with increasing acid concentration and secondly the solvent flow rate had to be kept low. Beside general considerations on economics, the latter was necessary in order to get acceptable U concentrations for the 2nd cycle aqueous feed by the stripping, in the absence of an intercycle U evaporator.

Of great utility for the flowsheet optimization has been a computer programme for a stage-by-stage calculation of the U and nitric acid concentrations. The programme was based on empirically established functions from the experimental equilibrium lines⁵.

Gradually, all modifications introduced for the flowsheet optimization were checked, prior to their realization in the battery, by this programme. Based on the stage-by-stage U distribution during the trial runs a 100% stage efficiency in extraction was assumed for the calculations.

Table 1 gives the theoretical U distribution in the scrubbing and extraction stages for the finally adopted standard flowsheet.

Table 1

Stage-by-stage U distribution in the 1st cycle extraction and scrubbing batteries.

stage number	aqueous phase U g/1	organic phase U g/1
1	0.00016 (1AW)	0.00036
2	0.00069	0.0015
3	0.0023	0.0050
4	0.0076	0.016
5	0.024	0.051
6	0.076	0.16
7	0.24	0.51
8	0.75	1.43 (1AP)
<hr style="border-top: 1px dashed black;"/>		
9	2.40 (1BR)	1.44
10	2.41	1.44
11	2.41	1.44
12	2.41	1.44
13	2.41	1.43
14	2.39	1.43
15	2.36	1.41
16	2.28	1.37
17	2.17	1.26
18	1.51	0.95 (1 BP)

In these conditions the real plant U losses were, on average, 0.5 mg/1 in the 1AW stream, which show indeed, when compared with the calculated values in table 1, a nearly theoretical efficiency of the Eurex extraction battery.

As to fission products' decontamination the gradual acidity adjustments influenced particularly the DF_{Ru} as shown in table 2.

Table 2Plant DF_{Ru} in function of the nitric acid concentration

Scrubbing - extraction aq. ph. compn. ANN/HNO ₃ , M	Over-all 1st cycle DF _{Ru}
0.7/1.3 - 1.37/1.3	200 - 30
0.7/2.0 - 1.37/1.55	1200
0.6/3.0 - 1.37/1.8	4000 - 6000

DF of about 10^6 - 10^7 were found for ¹³⁷Cs and ¹⁴⁴Ce. These values were too high to allow an evaluation of whether they were influenced by the acid concentration modifications or not.

First Cycle Uranium Stripping

As to the Uranium stripping in the first cycle, during the amine campaign, two facts have emerged worthy of being discussed more in detail. Already during the operations with unirradiated natural uranium, using the 0.5M start-up flow-sheet strip acidity as well as 0.1M and 0.01M concentrations, incomplete stripping was observed. After a few recyclings of the solvent the U concentration in 10W seemed to reach a steady state value of about 20 mg/l. A stage-by-stage analysis showed that the bulk of U had been stripped within 4-5 stages, whereas in the remaining stages of the battery 12-11 its concentration had been stationary.

With a new solvent charge the same phenomenon was observed at the hot operation start up.

Hypotheses like bad solvent quality delivered by the manufacturer, U(IV) in the feed or generated in the battery, and radiation damage, at least as primary reason, had to be excluded.

Finally the investigations were directed toward the effects of nitrous gases, which are easily generated in concentrated aluminium nitrate/nitric acid solutions like those of the 1st cycle feed. This hypothesis was supported by the fact that the U retention had never been observed in the 2nd cycle, where ANN was not present. Table 3 shows the results of stripping tests using fresh solvent and solvent treated with nitrous gases.

Table 3

Influence of nitrous acid on U distribution coefficients in stripping; phase ratio A/O = 0.1; initial aq. U conc. 1.4 g/l

strip. soln.	HNO ₃ , 0.5N		HNO ₃ /H ₂ SO ₄ , 0.8/0.6N	
	fresh	HNO ₂	fresh	HNO ₂
4% TCA				
stage 1	0.059	0.059	0.054	0.045
" 2	0.026	0.057	0.032	0.030
" 3	0.020	0.23	0.047	0.039
" 4	0.023	1.83	-	-

An increasing distribution coefficient can be observed with nitric acid alone, whereas with sulfuric acid present in the strip solution no differences between fresh and treated solvent are noted. Stripping was therefore performed with a nitric acid/sulfuric acid mixture. The choice of the HNO₃/H₂SO₄ normality ratio of 55/45 % was determined by the slope of the U distribution coefficients, which shows a minimum in the range from about 25 to 60% sulfuric acid⁶. As the U distribution coefficient at the chosen acid ratio was found nearly independent from the total acid concentration, the flowsheet value was fixed such to introduce all the sulfuric acid required successively for the 2nd cycle feed stream, already with this strip solution.

As long as diluted nitric acid was used for stripping, the impeller speed had to be reduced from 900 to 750 rpm in order to avoid an aqueous phase entrainment by incomplete settling. The same speed was maintained initially for the sulfonitric strip. In these conditions still U losses were observed, which this time, however, depended on a low stage efficiency.

Table 4 summarizes the results at the 750 and 900 rpm impeller speeds.

Table 4

Efficiency and U-losses in 1st cycle stripping battery (16 effective stages). $D_U = 0.04$; $A/O = 0.18$.

Impeller speed, rpm	750	900
1CW, U mg/l	14	≤ 0.5
loss in % of throughput	~ 1.5	≤ 0.05
theor. stages required	2.9	5.1
battery eff. %	18	≥ 32

The difference in stage efficiency between extraction and stripping were mainly due to the following two facts:

- the use of low A/O ratios, which allow good U concentration in the stripping step, due to its low distribution factors with the amines,
- the aqueous-in-oil emulsion, which is formed generally in the Eurex mixers, because of their geometry (cylinders of 100 mm diameter with a liquid height of 380 mm) and the centrifugal pump-mix impeller type used.

Consequently the solute transfer in stripping from an excess of continuous solvent phase to a small quantity of dispersed aqueous phase was slow, leading to a low stage efficiency.

Second Extraction Cycle

Pu extraction, from an aqueous phase containing a reducing agent like ferrous sulphamate (FeSM), with tertiary amines reaches rapidly an equilibrium corresponding to an apparent Pu(III) partition coefficient. From literature data⁷ and from our own experience it is however known that the extracted Pu behaves in the organic layer in all aspects like Pu(IV).

The stripping of this Pu into an aqueous phase containing a reducing agent results the slower, the higher is the corresponding Pu(IV) partition coefficient^{4,8}. At equilibrium the two distribution coefficients will tend to the same value, with the Pu stripping as the rate controlling step.

Whether this conditions can be fulfilled in a counter-current process, depends, at given chemical conditions, on the stage efficiency, i.e. on the mixing efficiency and residence time.

Steady state conditions had evidently not been realized in the Eurex batteries under the start-up flowsheet conditions, especially in the scrub section, for the reason outlined already above, i.e. for the formation of a poor aqueous-in-oil emulsion.

Therefore the chemical conditions had to be adjusted to the equipment performance, in order to make work the U/Pu separation, by the reduction of the Pu(IV) partition coefficient introducing a complexing compound.

Among a series of reagents sulphuric acid was chosen since its influence on equipment corrosion (stainless steel AISI 304L), and on U and FP distribution was known the best from all considered compounds⁹.

The flowsheet conditions are reported in figure 5.

In the 11 extraction stages and the first 7 scrub stages the aqueous phase was built of a 85/15 % nitric acid/sulphuric acid mixture at a 3.5N total acid concentration. The reducing reagent, FeSM, was introduced exclusively by the 2BS1 scrub solution.

A 4 stages scrub section with nitric acid alone, prior to the solvent overflow to the stripping battery, prevented the strip liquor from being contaminated by entrained iron and sulphuric acid.

By the addition of the sulphuric acid the Pu(IV) partition coefficient was reduced, with respect to the nitric acid flowsheet (figure 3), from ~ 380 to about 30 and the Pu stripping rate in the presence of FeSM was markedly increased as can be seen from figure 6.

This figure illustrates, at the same time, that the apparent Pu(III) equilibrium is influenced, if at all, only marginally by the presence of the complexant.

In these conditions the DF_{Pu} reached values of 10^4 and higher, confirming the primary importance of the Pu(IV) partition coefficient on Pu extraction and stripping, also in the presence of a reducing reagent.

Two more things of interest for Pu separation were noted in this amine campaign:

- the DF_{Pu} were the same, independently from whether the feed solution was adjusted with FeSM prior to its feeding to the battery or not. For operational convenience FeSM was thereupon introduced exclusively with the scrub stream.
- the second point is that above a 3.5N acid concentration FeSM becomes too instable to guarantee a good Pu reduction.

When an attempt was made to operate the 2nd cycle at a 4N total acid concentration in order to reduce U losses in the aqueous waste solution, the U/Pu separation broke down.

The 2nd cycle, too, was indeed operated at its extreme limits of U recovery in order to favour the Pu elimination. The introduction of sulphuric acid had also slightly reduced the U(VI) partition coefficients, as shown in figure 7. The comparison of the calculated U losses, being 1.3 mg/1 for 11 theoretical stages, with the experimental average value of 1.5 mg/1 with the same number of real stages shows again the excellent efficiency of the Eurex mixers in extraction. The U stripping in this cycle was done with dilute nitric acid. The impeller speed had to be kept at 750 rpm, because at the projected 900 rpm heavy aqueous phase entrainment had been observed. A battery efficiency of about 28% was calculated from the average 1.5 mg/1 losses in the stripped solvent.

As to the fission products only Ru was still present at appreciable levels, the 2nd cycle satisfied the requirement to reduce the residual activity to the USAEC specification levels.

The fate of Neptunium

The Np concentration in the feed solution was of the same order of the Pu concentration, corresponding, for its lower specific activity, to about 700 000 dpm/gU on average. A DF_{Np} of at least 100 was therefore required to meet the final U product specifications.

According to the known behaviour of Np in nitric acid solutions¹⁰, it should be present in the dissolver product at the 6+ valency state. It has been however shown¹¹, that in tertiary amine solutions the Np tends to transform from its higher valency states to the 4+ state. Table 5 gives a Np balance based on 21 kg U treated.

	Solution	Np, dpm x 10 ⁹
Input:	1 AF	14.7
	(LLW (from 1st (and 2nd cycle (Solv.	
Output	(regen.)	3.2
	(2AW	3.9
	(conc.final U prod.	2.6
Input-output = 1AW		5

For lack of a separate analysis, the Np in the organic waste streams should be equally divided between the two cycles. Based on this assumption the DF_{Np} in both extraction sections results in about 1.5-2. This conformity lets suppose that nevertheless its initial 6+ oxidation state and the absence of FeSM the Np had been transformed to Np(IV) also in the 1st cycle extraction battery.

As a consequence of this behaviour the 2nd cycle U product contained on average a residual Np activity of 170 000 dpm/gU, which contrarily to Pu could hardly be brought to the required values by simple recycling.

Final Product Purification

A new extraction process was therefore introduced at Eurex for a batch-wise purification of the concentrated U solution, based on the capacity of a highly organic diluent-soluble hydroxamic acid (HX) to extract selectively Pu(IV) and Np(IV) from a nitric acid solution. Hx had been developed in the CNEN's laboratories at Casaccia¹²⁻¹⁴. It is a compound of the general type:



In order to guarantee a sufficiently high organic diluent solubility a minimum of 10 carbon atoms is required. Branching increases this solubility, but its main effect consists in the stabilization of the hydroxylamine group against hydrolysis in acid medium, probably by steric hindrance.

At pH=0 the following ions are extracted by a 0.1M HX solution with distribution coefficients $\gg 1000$: Pu(IV), Np(IV), Zr(IV), Nb(V), Fe(III). U becomes sensibly extracted only at $\text{pH}=4$.

In the evaporator concentrate, with 205 g/l U and 4.7M HNO_3 concentrations on average, Pu was present in the 4+ and Np in the 5+ oxidation state. The reduction of the latter to the extractable 4+ state could have been obtained by the HX itself. The overall reaction rate however is very slow and requires intensive mixing over the whole period because of the low solubilities of Np(V) in the organic layer and of HX in the aqueous layer, respectively.

The following procedure was therefore adopted: The U nitrate solution was adjusted with hydrazine ($\sim 0.01\text{M}$). This reagent had the double function of scavenger of nitrous acid, which is the only reagent that destroys the hydroxamic acid immediately, and of reductant for Np(V). The adjusted solution was immediately contacted for 15 minutes with a 0.1M HX solution in Solvesso 100 at a A/O ratio of 5. After settling the phases were separated. The aqueous phase was allowed to digest for about 24 hours for Np reduction and was then extracted by a second contact with fresh solvent as above.

The organic layers were stripped for U recovery ($D_{\text{U(VI)}} \approx 0.013$) with 1M HNO_3 . The strip solution was joined to the U product. In this way a final U product solution was obtained with a residual alpha transuranium activity of about 10 000 dpm/gU, mainly due to Np, probably because its reduction had not been complete.

TBP Flowsheet

The hot MTR fuel elements reprocessing campaign was continued in 1973 with a flowsheet using a 5% TBP solution in kerosene as solvent in both extraction cycles.

Experience with amines had governed the choice of some important parameters in this new flowsheet, for example:

- acid conditions in the extraction as well as in the scrub section of the first cycle;
- limitation of the nitric acid concentration to a maximum of 3.5M in the sections where FeSM was present;
- no direct feed adjustments with FeSM, which was introduced exclusively as a separate stream to the scrub.
- The main point was however that on the basis of the U/Pu separation experiences with the amines, the most best system for the realization of a high DF_{Pu} was a flowsheet with a low extractant concentration also for the 2nd cycle, in order to keep the Pu(IV) partition coefficients as low as possible.

The 1st and 2nd cycle flowsheet conditions are shown in the figures 8 and 9.

The results have been extremely satisfactory.

For an initial experimental period the use of FeSM was limited to the 2nd cycle only; the corresponding U product had a residual Pu activity of maximum 7300 dpm/gU, indicating a DF_{Pu} of about 10^5 in one cycle.

Also in the 1st cycle a DF_{Pu} of 10^3 was obtained, when operated later with FeSM. Consequently the residual Pu activity in the 2nd cycle U product dropped to the routine analysis sensitivity limits. The same can be said for Np. Its initial activity of 1.2×10^6 dpm/gU was reduced to about 3×10^4 dpm/gU in the product stream of the 1st cycle, operated with FeSM. In the 2nd cycle the residual Np activity was brought to about 1000 dpm/gU.

As to the fission products decontamination, table 6 gives for the 3 most important of them those activity levels of this campaign, which can be considered the most representative ones in the main aqueous process streams.

Table 6

Fission products decontamination in the 5% TBP campaign

	^{137}Cs	^{144}Ce	^{106}Ru
1AF $\mu\text{Ci/gU}$	500 000	60 000	12 000
1CU/2AF $\mu\text{Ci/gU}$	5	0.1	0.5
2CU $\mu\text{Ci/gU}$	0.01	$\ll 0.01$	0.1 - 0.01
1st cycle DF	10^5	6×10^5	$\sim 2.5 \times 10^4$
overall DF	5×10^7	$> 6 \times 10^6$	10^5 10^6

The 2nd cycle DF's have not been indicated. They would in any event be much lower than those of the 1st cycle. This fact however, does not indicate a lower separation capacity of the 2nd cycle, but depends mainly on the rather low final activity level, which could be considered in a certain way almost a background contamination of reprocessing plant equipment.

The capacity for fission product decontamination in the 2nd cycle became evident on two occasions due to flooding in the 1st cycle, when the activity level in the 1CU stream reached 1/10 of that in the 1AF solution.

After the feeding of this solution to the 2nd cycle without recycling, the residual activities in the 2CU stream were, in the most unfavourable case, only about a factor 10 higher than the values reported in table 6, nevertheless the feed activity had been nearly 10^5 times above the normal level. This demonstrates a quite good buffer capacity of the 2nd cycle, also in view of the treatment of shorter cooled elements.

No problems at all were found with U losses in this flowsheet.

The residual concentrations were <0.5 mg/1 in all effluents. A reduction of the U losses in this flowsheet, compared to that with amines, resulted from the sensible flow rates reductions of all process streams, except the 1st cycle aqueous feed of course; they were possible for the higher U affinity of the TBP. As a further consequence of this fact the theoretical number of stages for the required U recovery could be kept below the existing number of real stages. Table 7 summarizes some pertinent data of the conditions in the extraction.

Table 7

Extraction conditions in the 5% TBP flowsheet

	1st cycle	2nd cycle
D_U	20 - 50	2
A/O	3.2	0.71
U loss, mg/1	<0.1	<1
theor. stage n.	4.2	6.2
AP saturn, %	33	27

Stripping worked at a 800 rpm impeller speed and at room temperature without appreciable entrainments of the aqueous phase, probably also because of the increased residence time in the settlers as a consequence of the general flow rates reduction.

The overall losses from about 32 kg U, treated with the 5% TBP flowsheet, were 1.5%, which however had been due only for the minor part to the extraction cycles. The quality of the final product obtained from this two-cycle treatment can be considered rather high. The residual transuranium alpha activity, due to Pu, Np, and Am, has been <5000 dpm/gU. Of course no further purification was necessary.

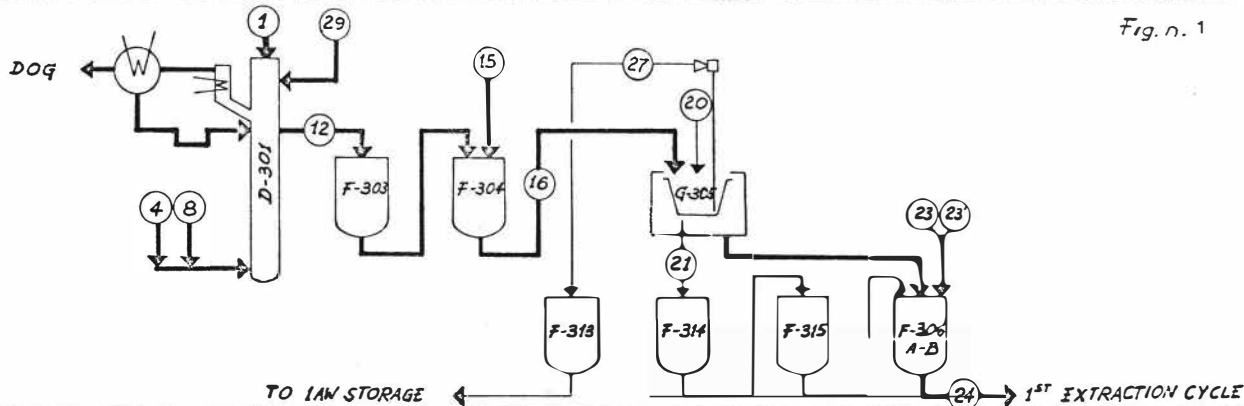
ACKNOWLEDGEMENTS

We thank F. Pozzi, head of the EUREX Analytical Group, for the valuable collaboration and the Industrial Chemistry Laboratory of the CSN-Casaccia-CNEN for the development of the HX process.

References:

- 1) Baroncelli F., Calleri G., Moccia A., Scibona G., Zifferero M., Nucl. Sci. Eng. (1963) 17, p. 298-308
- 2) Dworschak H., Euratom Communication 21.1-2412 (1969)
- 3) Dworschak H., Barocas A., CNEN - RT/CHI (69)19
- 4) Cao S. Dworschak H., Hall A., EUREX 13(73)
- 5) Baroncelli F., CNEN - RT/CHI (70)31
- 6) Bathellier A., Koehly G., Perez J.-J., Chesné A., CEA-R 2594(1964)
- 7) Horner D.E., Coleman C.F., ORNL 3051(1961)
- 8) Champion J., Chesné A., CEA-R 2607(1964)
- 9) Barocas A., Baroncelli F., Dworschak H., Proc. Int. Solvent Extn. Conf., The Hague, April 1971, p. 1174
- 10) Koch G., KFK 976(1969)
- 11) Basili N., Delle Site A., CNEN - RT/CHI (71)15
- 12) Baroncelli F., Grossi G., CNEN - RT/CHI (70)26
- 13) Grossi G., CNEN - RT/CHI (70)27
- 14) Baroncelli F., Grossi G., Italian Patent 48741 A/71
- 15) Jenkins I.L., McKay H.A.C., Shorthill C.G.C., Wain A.G., AERE-R - 4440 (Part 2)(1965)

Fig. n. 1



STREAM	1*	4	8	29	12	15	16	23	23'	24	20**)	21	27
DESCRIPTION	Fuel charge	Dissolvent	Air	DP	GR	DDP	Adj. Reagent	1AF	CR	CL	CSW		
Volume	l	190	90		243	5	var.	var.	290	100			
Density		1.2	1.24		1.32	1.0	1.5	1.0	1.31	1.3			
Flow	l/h	50		25000					7.63				
Al	M	473			1.95				1.7	1.7			
U	g/l	555			2.3				2.0				
Pu	mg/l	573			2.35				2.1				
Activity	ci/l	1335			5.5				5				
HNO ₃	M	7	7		0.1			15.6	1.3	1.3			
Hg(NO ₃) ₂	mM		50		10								
Gelatine	%/‰					0.5							
Si	g	120											

Remarks (●) 3 MTR fuel elements / charge

(●●) After 10 clarification operations

Figure 2

I CYCLE START UP FLOWSHEET

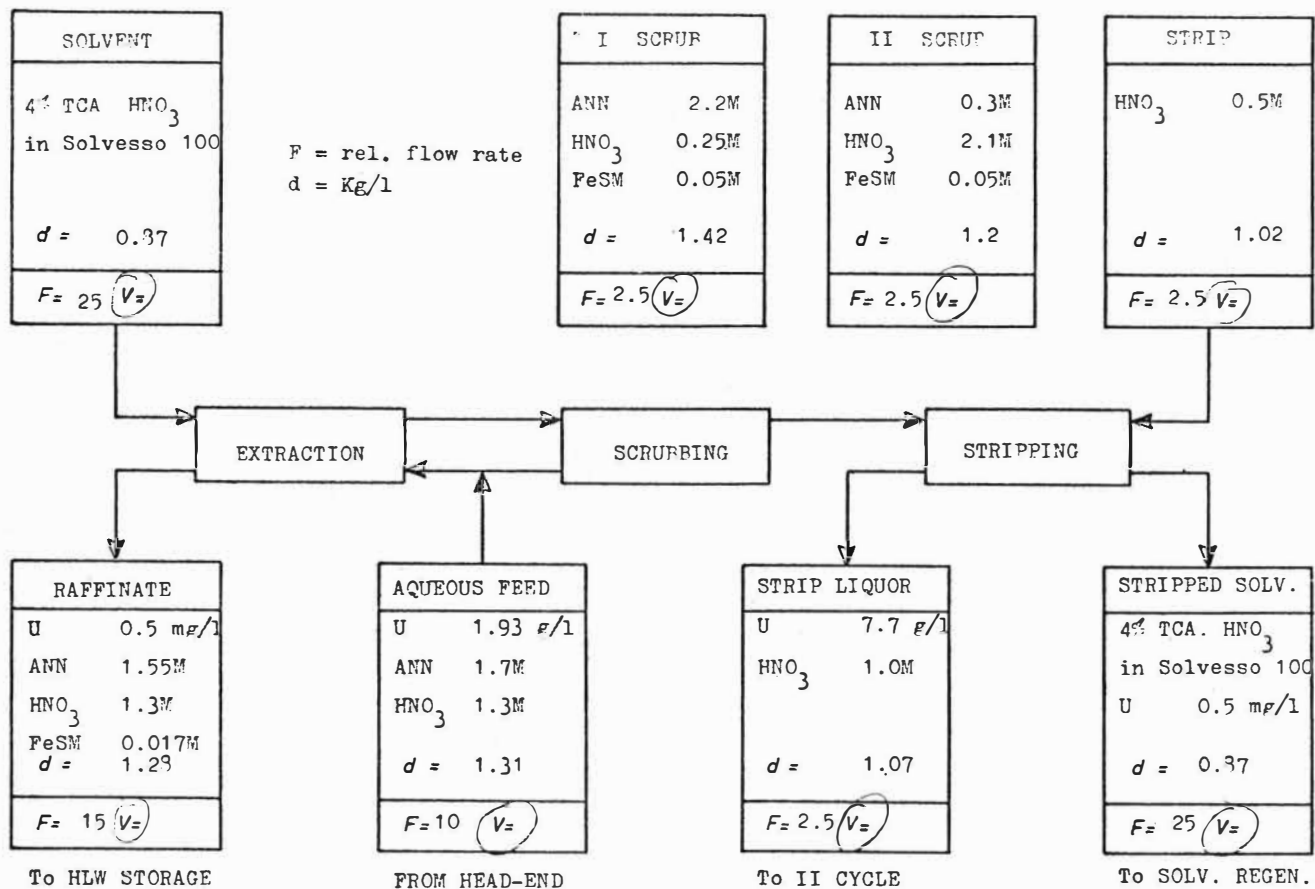


Figure 3

II CYCLE START UP FLOWSHEET

1475

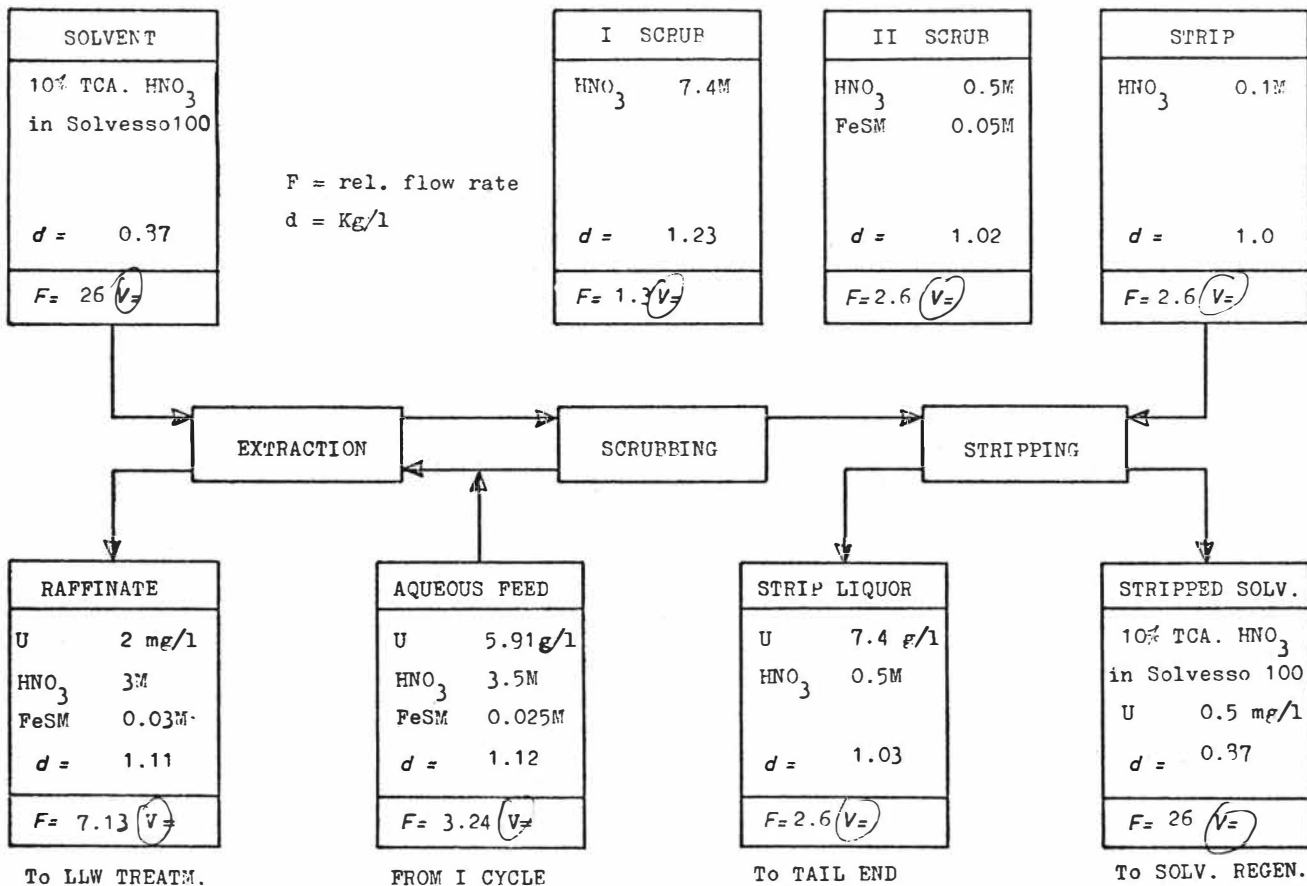
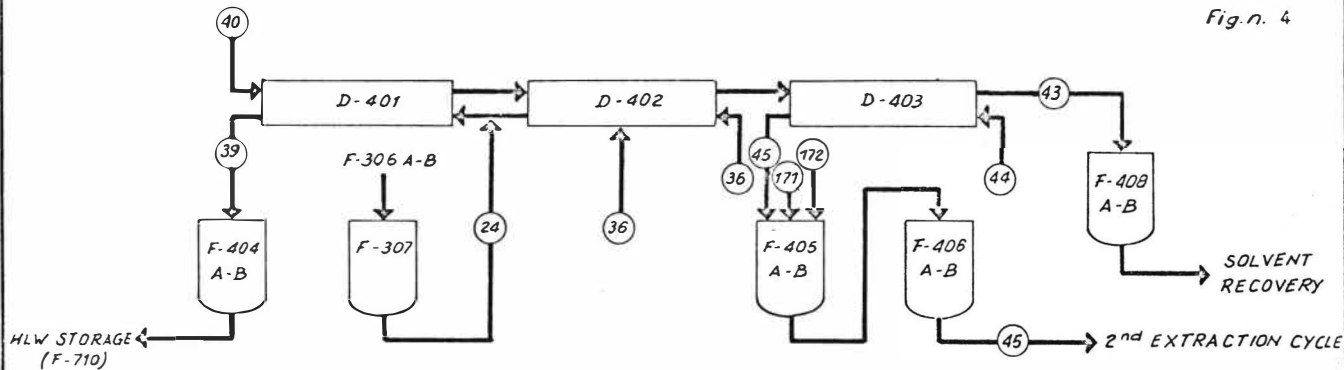


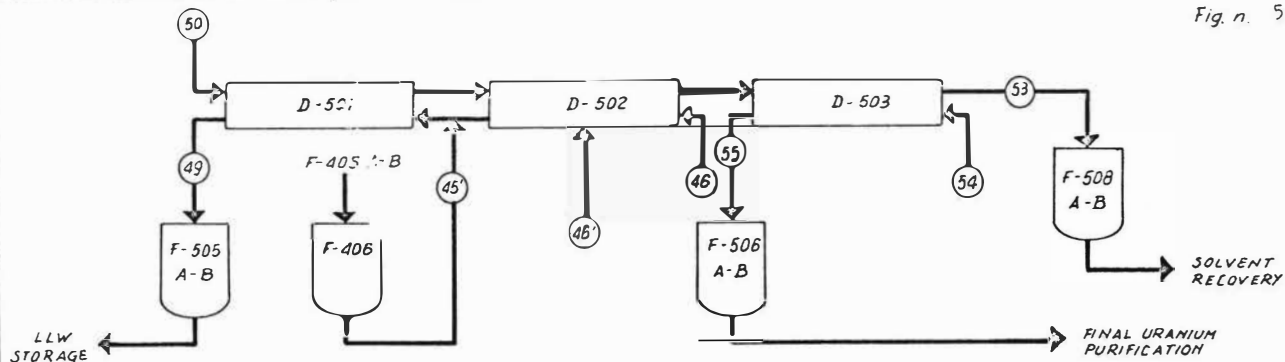
Fig. n. 4



STREAM	24	36'	36	40	44	39	45	43	171	172	45'									
DESCRIPTION	1AF	1BS'	1BS	1AX	1CX	1AW	1CU	1CW	Adj. Reagent	2AF										
Volume	l/d	123.1	76.9	334	63.5	260	63.5	394	20.3											
Density		1.31	1.19	0.97	1.05	1.25	2.35	0.97	1.3											
Flow	l/h	7.63	3.2	16	2.35	10.8	1.06	16												
Al	M	1.7	0.6			1.37														
U	g/l	2.0				0.5*	5.3	0.5*												
Pa	mg/l	2.1																		
Activity	C/l																			
HNO ₃	M	1.3		3.0	0.9	1.6	0.9	0.02	10											
FeSM	M																			
TCA	%/‰				4			4												
H ₂ SO ₄	N					0.65		0.65												
Remarks		* mg/l																		

1476

Fig. n. 5



STREAM	45'	46'	46	50	54	49	55	53											
DESCRIPTION	2AF	2BS'	2BS	2AX	2CX	2AW	2CU	2CW											
Volume	l/d	88.9	77.5	35	710	71	202.3	71	710										
Density		1.12	1.15	1.02	0.97	1.00	1.114	1.027	0.97										
Flow	l/h	3.7	3.23	1.5	29.6	2.96	8.43	2.96	29.6										
U	g/l	1.15					1*	5.2	0.5*										
Pu	μg/l	4000					<10 ⁵ *	Traces											
Activity	μCi/l	30					1												
MNO ₃	M	3.0	3.7	0.5	Traces	0.1	2.5	0.5	Traces										
H ₂ SO ₄	M	0.5	0.9				0.5												
TCA	%				10				10										
Fe SM	M		0.13				0.05												
Remarks		(*) mg/l		(**) dpm/gU for α emitters															

1477

Fig. 6

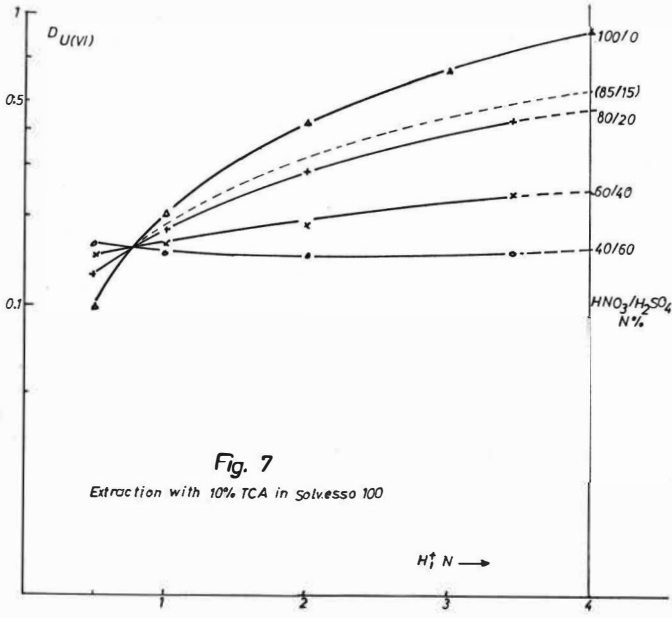
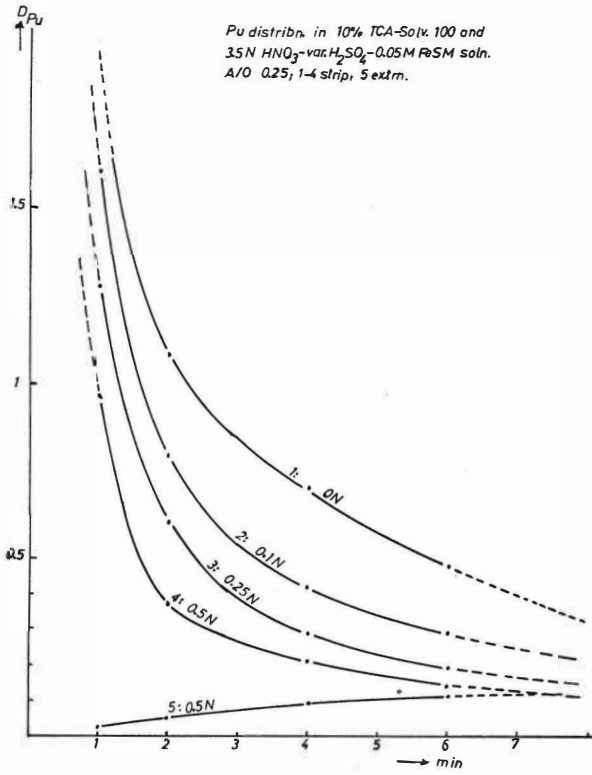


Figure 8

I CYCLE TPP FLOWSHEET

1479

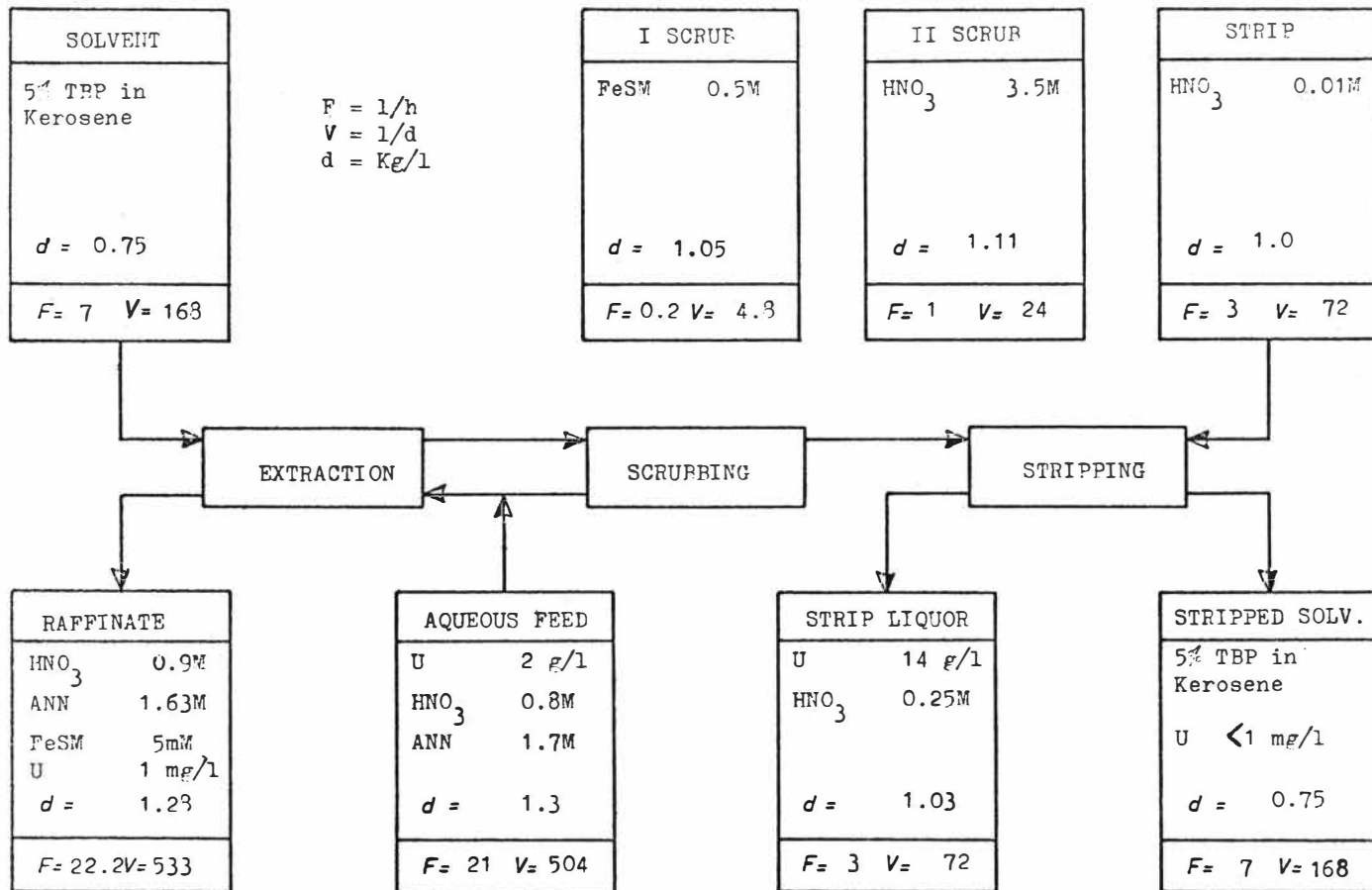
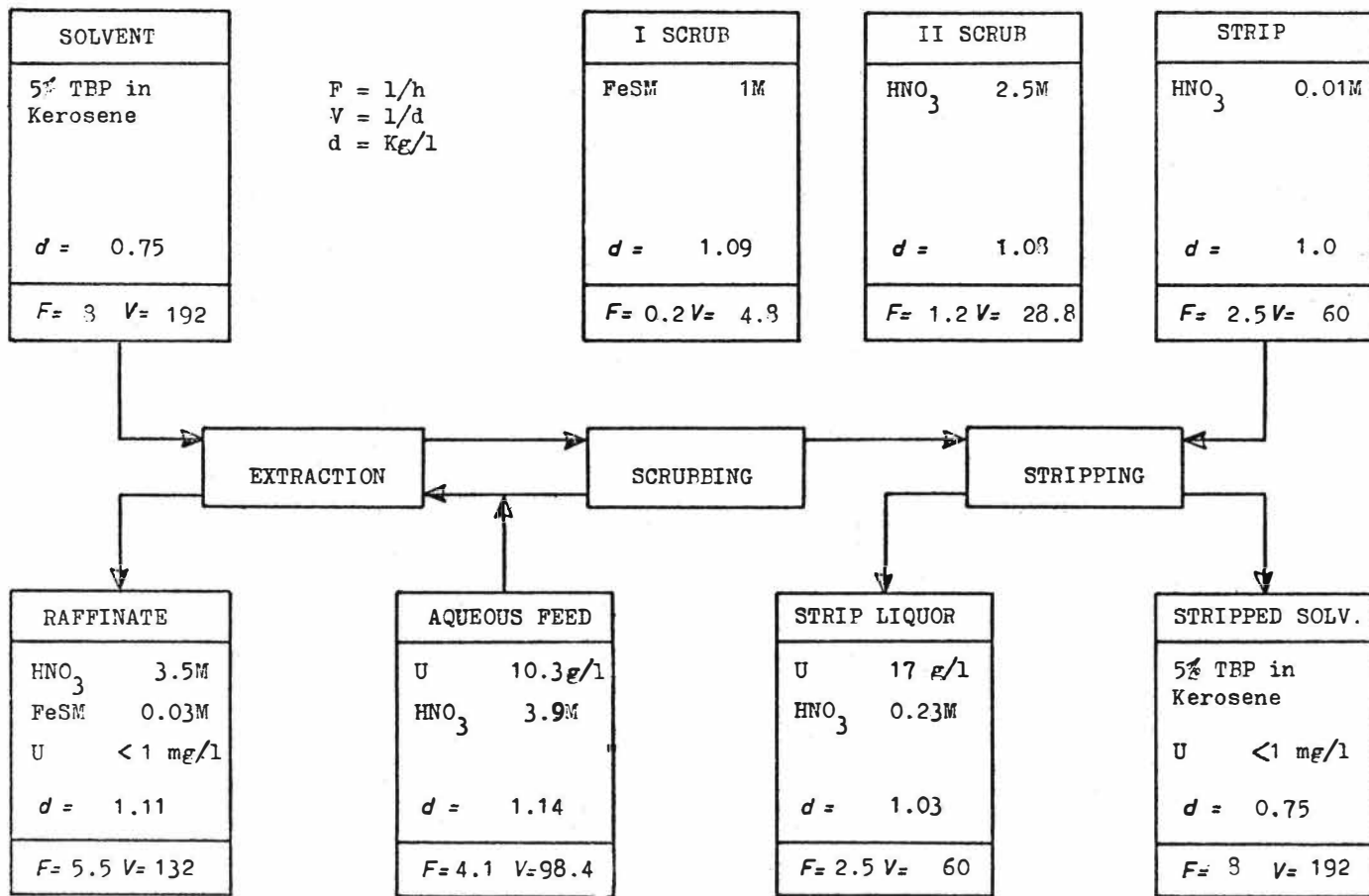


Figure 9

II CYCLE TBP FLOWSHEET



A REVIEW OF THE SUITABILITY OF SOLVENT EXTRACTION FOR THE
REPROCESSING OF FAST REACTOR FUELS

B F Warner, A Naylor, A Duncan and P D Wilson

Abstract

The application of solvent extraction to the reprocessing of Fast Breeder Reactor fuel has previously been questioned on the grounds of radiation damage to the solvent. However, calculations suggest that in pulsed columns or centrifugal contactors, residence times and exposure to radiation would be low enough to permit satisfactory operation. The validity of this prediction has been largely confirmed by a small-scale counter-current trial in which a fuel solution containing over 5000 curies of fission products per litre was successfully processed through a first cycle incorporating the separation of plutonium from uranium.

British Nuclear Fuels Limited, Windscale and Calder Works,
Seascale, Cumberland, United Kingdom.

Introduction

It is probable that several power stations based on Fast Breeder Reactors (FBR's) will be installed in Britain by the end of the century. The fuel will comprise a core of mixed uranium and plutonium oxides, together with axial and radial breeder regions of uranium oxide alone to be partly transmuted into plutonium. The first plutonium charges will naturally have to be derived from thermal reactors, but to maintain supplies it will eventually be necessary to re-cycle plutonium from spent FBR fuel, and so to reprocess material with a very much higher plutonium content and fission product activity than any other presently or prospectively treated at Windscale. This will still be true even if core material is diluted by the simultaneous reprocessing of axial breeder fuel.

TABLE 1. Plutonium and fission product content of various fuels

Cooling time = 180 days

Fuel type	Irradiation MWd/te	Rating MW/te	Pu g/kg	Heat Release W/kg	Fission Products Ci/g
Magnox	4000	2.67	2	1.6	0.5
CAGR*	20000	20	~6	5	1.3
FBR ⁺	43000	77.5	~100	36	9

*CAGR = Civil Advanced Gas-cooled Reactor

+Blended core and axial breeder fuel

The method generally used for thermal reactor fuels, after dissolution in nitric acid, is solvent extraction with tributyl phosphate (TBP) in a hydrocarbon diluent⁽¹⁾. The suitability of this method for FBR fuels has been questioned in the past, chiefly because of the expected radiolytic damage to the solvent, and alternatives based on volatility or on pyrometallurgical principles have been developed at

considerable expense. However, at Windscale it was decided to examine first the possibility of building upon the experience already gained with solvent extraction. In 1968, estimates of radiation dose and extrapolations from existing data on radiation effects indicated that the use of contactors with a short residence time might well limit solvent degradation to tolerable levels. Active small-scale trials were undertaken in 1969, and in 1972 culminated in the successful reprocessing of a short-cooled oxide fuel pin (irradiated in the Dounreay fast reactor), when the solution fed to the solvent extraction process contained over 5000 curies of fission products per litre. Although problems remain, this trial together with supporting information is considered to have confirmed the choice of solvent extraction for the reprocessing of FBR fuel.

Process Requirements

The extent of problems in reprocessing FBR fuel depends largely on the cooling time (the period elapsed since discharge from the reactor), the choice of which has to be based on several factors involving reactor discharge schemes, transport to a central plant, and the effects of short lived nuclides such as ^{131}I (see Table 2).

TABLE 2. Effect of cooling time on FBR fuel irradiated to 43,000 MWd/te at 77.5 MW/te

Cooling time (days)	^{131}I (Ci/kg)	Heat release (W/kg)
30	210	119
50	37	89
90	1.2	59
180	5×10^{-4}	36
360	1×10^{-10}	15

It is probable that the early stages of the FER programme will accommodate cooling times of perhaps 90-180 days, although in the more distant future there could be advantages in reducing the cooling time, perhaps in conjunction with the use of "island" sites comprising reactors with reprocessing and fuel fabrication plant. To cover this possibility, the use of solvent extraction after cooling periods as short as 50 days has been considered, and it was necessary to test such a process with fuel cooled for as short a time as was feasible.

It is envisaged that core and associated axial breeder material would be processed together. The fuel (metal oxides in stainless steel tubes) would be cut into short pieces, leached with nitric acid and clarified, to give a feed solution containing perhaps 270 g uranium, 30 g plutonium and several thousand curies of fission products per litre of 3M nitric acid. Among the major fission products which cause problems through being appreciably extracted by TBP would be ruthenium (0.014M) and zirconium (0.015M). A process for treating this solution must fulfill the following requirements:-

- (a) Plutonium must never be allowed to accumulate, even under conditions of maloperation, to an extent at which a criticality incident might occur. For this reason, and to avoid economic losses, the quantity of plutonium remaining in undissolved solids must be kept as low as possible.
- (b) To assist in minimising losses to raffinate, it is desirable that plutonium in the feed solution should be in its most extractable (tetravalent) state.
- (c) Radiolysis of the solvent must not detract excessively from its extractive or settling properties.

- (d) Plutonium concentrations must not reach the point of forming a second organic phase, which would interfere with hydraulic operation and complicate criticality control.
- (e) Plutonium and uranium must be separated adequately (this becomes more difficult at high plutonium concentrations) and decontaminated so far as to minimise problems in storage and refabrication.
- (f) To prevent unnecessary expansion of the requirements for waste storage, the introduction of extraneous salts should be avoided as far as possible.
- (g) Heat released by fission products must be dispersed safely at all relevant stages.
- (h) The fission products themselves must be contained.

There is of course a considerable body of valuable experience gained in the reprocessing of early fast-reactor fuels at Dounreay (2,3). However, the process there is on a much smaller scale than would be necessary for a large power reactor programme. Because the concentration of waste solutions is a less serious consideration, it is possible to reduce the effects of solvent degradation by means of a heavily iron-loaded scrub solution, which would not be acceptable on a large scale. Any comparison between Dounreay and Windscale processes should therefore take due account of the differences in conditions and constraints.

Preliminary Assessment

The first problem to be considered, because the most fundamental to the viability of a solvent extraction process, was that of solvent degradation. The intense radiation from fission products during the first extraction causes TBP to decompose successively to dibutyl and monobutyl phosphoric acids (DBP and MBP) and orthophosphoric acid. All are deleterious, but DBP particularly so.

- (i) With some fission products, notably zirconium, it forms extractable complexes which reduce the degree of decontamination attainable⁽¹⁾, and at high concentrations can be precipitated in quantities so great as to interfere with operation⁽⁴⁾.
- (ii) During back-extraction it can form inert plutonium complexes which are strongly retained in the solvent⁽¹⁾.

The diluent is also degraded, but this causes less acute problems which will be examined later. However, the two cannot be considered in complete isolation, since the radiosensitivity of TBP depends markedly on the diluent; thus in the very stable n-paraffins, TBP is degraded far more readily than in rather less inert diluents, so that the presence of some electron sinks is beneficial. The choice of diluent is also influenced by hydraulic properties. In preliminary work at Windscale, the use of odourless kerosene (OK) has been assumed, although it need not be the ultimate choice.

The effects of radiation were assessed for mixer-settlers, pulsed columns and centrifugal contactors. Of course, it was essential to use values for the radiolytic yield (G) measured under realistic conditions, with an appropriate aqueous phase present; and to avoid the common error of neglecting the contribution from the radiolysis of TBP dissolved in the aqueous phase, which is sometimes the principal source of DBP. The

method of calculation depended to some extent on the assumed solvent composition, since in 20% TBP/OK the G value is the same as in the aqueous phase, so that the distribution of absorbed dose between the phases is immaterial⁽⁵⁾, whereas with 30% TBP/OK this is not so.

In mixer-settlers with appropriately large dimensions, all the β and 80% of the γ energy were assumed to be absorbed internally. (The α -contribution was found to be relatively small). Doses were calculated separately for mixers, and in the settlers for the emulsion band and disengaged solvent and aqueous phases. Over 70% of the total equivalent dose to the solvent (i.e. the dose which, if absorbed solely in the solvent, would have produced the same concentration of DBP) was estimated to be received in the settlers.

In pulsed columns, radiation losses would be more significant, and the estimate of absorbed dose was derived from an average over the range of possible positions and directions in which radiation could be emitted. The solvent phase was assumed to be continuous to minimise the hold-up of aqueous phase and so of fission products. With 30% TBP it was necessary to allow for the absorption of β -energy largely within the 2.5 mm aqueous droplets. Doses were calculated separately for the plated section of the column, in which mixing was assumed to be uniform, and the end settler regions which with either solvent composition were estimated to contribute about half of the total equivalent dose to the solvent.

In centrifugal contactors, allowance again had to be made for radiation losses. The mixer regions were treated as containing a homogeneous mixture of the two phases with dose distributed in the ratio of the electron densities. In this case, with centrifugally-aided phase separation requiring only a small volume, settlers contributed only a sixth of the total equivalent dose.

Once the extent of DBP formation had been calculated, its effect on $DF_{Zr/Nb}$ (DF_{Ru} is less sensitive) was estimated by extrapolation of data obtained when the Magnox pilot plant was operated with a range of added DBP concentrations⁽⁶⁾. Specimen results are shown in Table 3. It was assumed in all the calculations that on average, fuel would be irradiated to 43000 MWd/te at a rating of 77.5 MWd/te, and cooled for 50 days. Calculations on pulsed columns were based on the use of either 20% or 30% TBP/OK, but those on mixer-settlers were limited to the lower concentration, assumed in engineering assessments: for the sake of comparison, results are therefore given for 20% TBP. Decontamination factors refer to extraction plus scrub contactors.

TABLE 3. Solvent degradation in various types of contactor

Contactor Type	Radiation dose, Wh/l			$\frac{[DBP]_{\text{organic}}}{M}$ (calculated)	$DF_{Zr/Nb}$ (E + S) (estimated)
	Solvent	Aqueous	Equiv. to Solvent		
Mixer-Settler	1.02	3.78	2.84	5.3×10^{-4}	10
15 cm pulsed column	0.114	0.267	0.190	3.6×10^{-5}	300
Centrifugal	0.035	0.060	0.064	1.2×10^{-5}	500

It should be emphasised that the estimates of decontamination factor were derived from data on the reprocessing of Magnox fuel, where DBP would form complexes mainly with uranium⁽¹⁾. Plutonium at the higher concentrations appropriate to CFR fuel would be likely to form the predominant DBP complexes, so that direct comparison is at best an approximation. Nevertheless, it is clear from Table 3 that

mixer-settlers would be unsuitable, but that pulsed columns or centrifugal contactors warrant further investigation. Because of their relative simplicity and cheapness, pulsed columns were chosen for practical tests.

Considerations on practical trials

The practice at Windscale is to develop any large-scale process by way of a conceptual flowsheet which enables the size of major equipment to be determined. Engineering tests are performed at full scale with inactive materials, while the process chemistry is verified at full radioactivity, with any modifications which may prove necessary, on a miniature plant scaled to give correct residence times in countercurrent operation. For the purpose of demonstration only, a flowsheet of the type shown in Figure 1 was chosen for fuel breakdown and the first cycle of reprocessing, including the separation of plutonium from uranium. The feed stream to an FBR reprocessing plant could not be adequately simulated by a synthetic solution, and for an active trial it would be necessary to use irradiated fuel. This is scarce, expensive and difficult to handle in large quantities, so that operating the miniature plant for a useful length of time would necessitate a very small scale. That eventually adopted was 1:3500, which allowed active operation for sixteen hours with fuel containing 350 g (U + Pu).

Despite difficulties due to wall effects in some types of miniature pulsed column, it was found that glass columns of the design shown in Figure 2, with perforated plates spaced 2.5 cm apart, could be operated satisfactorily over a useful range of conditions with either phase continuous. Preliminary experiments, in which uranium or plutonium was extracted or back-extracted in column sections of various heights, indicated the actual heights necessary for the required performance; the volume was determined as that of the full-scale equipment reduced by the scale factor, and so the diameter could be calculated.

Since the principal intention at this stage was to establish that uranium and plutonium could be adequately decontaminated from a high concentration of fission products by solvent extraction, it was not necessary to optimise the rest of the first cycle, but only to demonstrate that it was operable. To separate plutonium from uranium, the well-tried method of selective back-extraction aided by complex formation with sulphuric acid was therefore adopted, although because of corrosion problems and production of an intractable waste it is not certain to be used in the full-scale plant. The flowsheet of the first cycle is outlined in Figure 3. In Column 1, uranium and plutonium are extracted from the aqueous feed into 30% TBP/OK, and the loaded solvent is scrubbed with fresh acid. It then passes to Column 2 for back-extraction of plutonium by an aqueous stream containing dilute sulphuric acid: inevitably some uranium is also back-extracted, and is removed from the aqueous product by scrubbing with fresh solvent. Eventually the uranium is back-extracted with very dilute nitric acid in Column 3.

To simplify construction and installation, Columns 1 and 2 were made composite, with the scrubbing functions performed in separate units. Before installation, columns were tested with inactive solutions for operating stability and efficiency in their intended purpose. Column 1 was operated with a continuous solvent phase to minimise the aqueous content and so the radiation level; in the other columns the aqueous phase was continuous for ease of operation.

Active Trials

There have been two active trials, each preceded immediately by a period of inactive operation with a feed of uranyl nitrate in nitric acid to establish a steady state. The first, with a mixture of long-cooled oxide fuels (mean plutonium content 8.5%) which gave a feed solution of activity 0.3 Ci/ml, permitted some necessary adjustments to be made to the flowsheet; it was encouraging that at least

under these favourable conditions, with an equivalent radiation dose to the solvent of only 0.008 Wh/l, good decontamination factors could be obtained (Table 4).

TABLE 4. Decontamination factors in the long-cooled fuel test

Col or cycle	DF _{Ru}	DF _{Zr}	DF _{Zr/Nb}
Col 1 (extraction + scrub)	1900	3300	7500 (predicted >1000)
1st cycle (U)	6×10^3	1.4×10^5	2.3×10^5
1st cycle (Pu)	5.3×10^4	3.3×10^3	7.5×10^3

In the second active trial, the fuel used was of co-precipitated UO₂ (85%) and PuO₂ (15%), irradiated discontinuously to a total of 4% burn-up at a mean operating rating of 143 watts/g. It was cut into lengths of 2.5 cm at Dounreay. On arrival at Windscale it was leached with nitric acid at temperatures gradually raised from 35 to 108°C. The solution was cooled, conditioned with nitrogen oxides to convert tri- or hexavalent plutonium to the tetravalent state, and undissolved solids in suspension were removed by filtration to 2 microns. After addition of washings and adjustment of acidity, the feed to the solvent extraction process contained 238 g U/l, 40.5 g Pu/l (98.7% Pu(IV)) and was 3.4M in nitric acid. Despite the intense radioactivity, the proportion of Pu(IV) appeared stable over the two days between conditioning and use. The fission product content amounted to 5.5 Ci/ml (β) and 2.8 Ci/ml (γ) after 38 days' cooling, when the active trial started. Enough gas was generated by radiolysis to prevent the use of diaphragm pumps, but positive-displacement metering pumps proved satisfactory despite the formation of gas bubbles in the feed lines.

Solvent was prepared from Windscale stocks of TBP and Odourless Kerosene. Before use it was passed through a cycle of uranium extraction, back extraction and washing with aqueous alkali, as this treatment had previously been found to eliminate an unidentified impurity which interfered with decontamination from ruthenium. Spent solvent from Column 3 was not recycled, since the object was to examine effects of short-term radiolysis (chiefly of TBP) rather than those of long-term diluent degradation.

The system was operated with the active feed for sixteen hours, corresponding in Column 1 to 51 aqueous throughputs in the extraction section, 14 in the scrub, and 64 throughputs of solvent in either. Equilibrium with respect to uranium and plutonium was established in nine hours, and with respect to zirconium in eleven; it might have been reached earlier but for disturbances due to a failure in an ancillary system. Some crud collected at the bottom interface of Column 1 extraction section, but did not interfere with operation, and during run-down at the end of the trial it was washed out with the aqueous raffinate.

Plant performance during the highly-active trial

Losses to the first-cycle aqueous raffinate were found to be less than 0.08% plutonium or 0.03% uranium. Losses on back-extraction were only 0.0025% plutonium and 0.003% uranium. Decontamination factors for various contaminants are given in Table 5.

TABLE 5. Decontamination factors in the highly-active trial

Column or cycle	DF _{Ru}	DF _{Zr}	DF _{Zr/Nb}	DF _U	DF _{Pu}
Col 1 (extraction + scrub)	700	52	80*	-	-
Col 2 (U)	1.1	182	95	-	4 x 10 ⁴
Col 3 (U)	10	12.4	12.3	-	1
1st cycle (U)	7700	1.2 x 10 ⁵	9.4 x 10 ⁴	-	4 x 10 ⁴
Col 2 (Pu)	16.8	1.0	1.0	2.3 x 10 ⁴	-
1st cycle (Pu)	12000	52	80	2.3 x 10 ⁴	-

*Niobium appeared to be only very slightly extracted.

Decontamination factors on the plutonium stream are very much lower than during the trial with long-cooled fuel; zirconium and niobium in Column 2 follow the plutonium stream, imparting to it an activity less than an order of magnitude below that of the highly-active feed to the present main reprocessing plant at Windscale. Nevertheless, in the extraction and scrub columns the degree of decontamination from these elements taken together (80) is in the region predicted (80-100) from the calculated equivalent dose to the solvent (0.17 Wh/l, i.e. 90% of that estimated for the large-scale reprocessing of 90-day-cooled fuel), and so supports the validity of the method used for prediction. There is good reason to suppose that further purification by conventional means would be adequate, particularly as past experience suggests that a loss of decontamination efficiency in a first cycle may be at least partially recovered later in the process.

Implications for future work

The results of this highly-active trial encourage the belief that it will be feasible to reprocess fast reactor fuel by solvent extraction: an acceptable degree of decontamination from fission products has been achieved in the first cycle, and plutonium has been separated satisfactorily from uranium, although by a method which may well be superseded. However, caution is necessary for several reasons and much work remains to be done.

- (1) In the run described, solvent was used once only and not recycled. Conventional methods of purification would remove the degradation products of TBP but not all those of the diluent, which would therefore deteriorate progressively until the formation of degradation products was balanced by the combination of partial purification and the inevitable losses of solvent. Diluent degradation products can hinder decontamination by forming complexes with fission products, or interfere with operation of the plant by promoting emulsification. While experience suggests that these effects should be less serious than those of DBP, confirmatory tests are required. These will probably take the form of a single-pass run with degraded solvent in pulsed columns, supplemented by a careful analysis of the results to be obtained from the DERE mixer-settler plant during the processing of PFR fuel.
- (2) Although the fuel used in the highly-active run had been cooled for only 38 days before solvent extraction, most of the fission product energy (including practically all of the γ -contribution) was lost from the miniature columns so that the absorbed dose of radiation corresponded closely to the large-scale reprocessing of fuel cooled for 90 days. Processing through pulsed columns therefore seems likely

to be feasible if the reactor cycles call for a cooling period of not less than 90 days, particularly as the flowsheet has not yet been optimised. Shorter-cooled fuel could perhaps be processed similarly, but success would be more probable with the still shorter residence times attainable in centrifugal contactors.

- (3) Sulphuric acid, used in the trials described to separate plutonium from uranium, is corrosive towards metallic equipment and makes more difficult the ultimate disposal of wastes. Alternative methods of separation are therefore being investigated.
- (4) It will be necessary to ensure that cruds (of the type observed in Column 1 during the highly-active trial) are not allowed to interfere with operation of the plant.
- (5) A reliable means must be found to remove undissolved solids on an industrial scale from suspension in the fuel solution. These solids consist largely of segregated fission products with a high specific activity, and if allowed to enter the solvent-extraction equipment they would exacerbate problems due to heat release, irradiation of solvent and accumulation of solid material.

Conclusions

The successful, if brief and small-scale, reprocessing of short-cooled FBR fuel has largely vindicated predictions that solvent extraction in short-residence contactors would be a suitable technology for reprocessing the fuel from FBR power stations. Valuable experience has also been gained in dissolving such fuel and conditioning feed solutions. It remains to be established that comparable performance can be achieved over a longer period and on the larger scale which would eventually be required.

Acknowledgements

The authors wish to thank Mr G D C Short for preparing the flowsheet on which the pilot-plant trials were based; Dr P G M Brown for calculating radiation doses and the consequent DBP concentrations; Mr A L Mills and colleagues for information on experience in fuel reprocessing at Dounreay; the glass blowers of Technical Department, Windscale, for making the pulsed columns; staff of DERE and Windscale Reactor Group, for providing the irradiated fuel; Mr D B Clatworthy and Mr D Drysdale for help in the design, construction and operation of the miniature plant; Dr A Tognarelli, Mr R Ivens and Mr W Smith for operational assistance; and Analytical Services Department, Windscale, for performing analyses.

References

1. A Naylor and M J Larkin, Proc. Int. Conf. Solv. Ex. 1971, p 1356.
2. I G Wallace in "Solvent Extraction Chemistry of Metals", ed H A C McKay et al, p 41 (1965).
3. R H Allardice and I G Wallace, J. Brit. Nuclear Energy Soc. 4, 13 (1965).
4. P Faugeras and X Talmont, 11th Int. Conf. Coord. Chem (1968).
5. R J W Streeton and H A C McKay, unpublished work.
6. W Baxter and A Naylor, unpublished work.

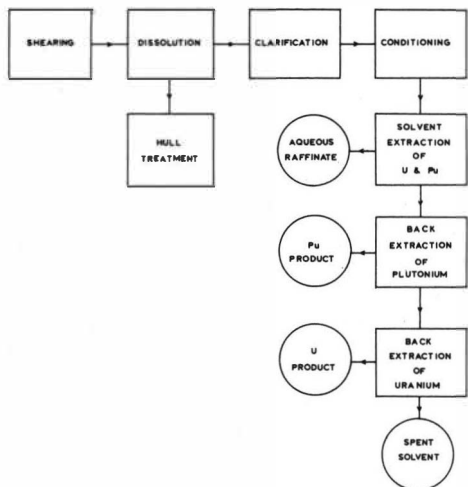


FIGURE 1. FEED PREPARATION AND FIRST CYCLE (SCHEMATIC)

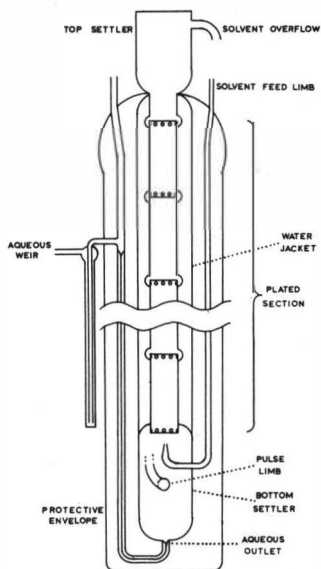


FIGURE 2. MINIATURE PULSED COLUMN (NOT TO SCALE)

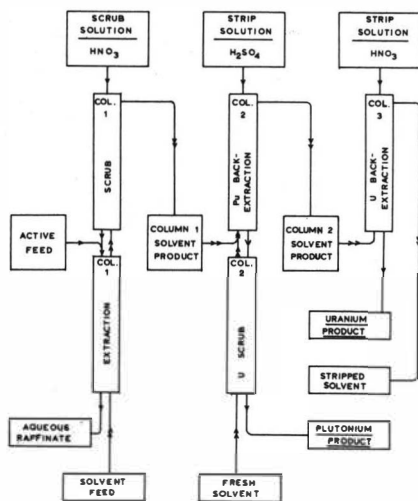


FIGURE 3. OUTLINE FLOWSHEET OF FIRST CYCLE

A REVIEW OF METALLIC FAST REACTOR FUEL REPROCESSING AT DOUNREAY

by

A L Mills and E Lillyman
Process Plants Division
Experimental Reactor Establishment
Dounreay
Caithness
Scotland

SYNOPSIS

6, 20, 25 and 30% tri-n-butyl phosphate in odourless kerosene have all been used as first cycle solvents in the Purex type reprocessing of Dounreay Fast Reactor Fuels. The superior performance of the 6% TBP system is attributed to the physical properties of the solvent and to the formation of a hitherto unreported solvate $\left[\text{UO}_2(\text{NO}_3)_2 \right]_a \left[\text{HNO}_3 \right]_b \left[\text{TBP} \right]_c$.

INTRODUCTION

Irradiated fuel from the Dounreay Fast Reactor (DFR) has been reprocessed at Dounreay in 30 campaigns over the past 12 years. U235-Cr was the first reactor charge to be processed; all subsequent charges have consisted of U235-Mo with varying molybdenum contents. During the period under review the fuel burn-up has steadily increased to 3.0% (maximum) and cooling times prior to reprocessing have been decreased to 85-90 days at the commencement of a campaign.

The original Purex-type flowsheet utilised 20% (vol) tri-n-butyl phosphate (TBP) in odourless kerosene (OK) in three cycles of decontamination. The present flowsheet uses one cycle of 6% TBP/OK and one cycle of 25% TBP/OK. Before the current flowsheet was designed both 30% TBP/OK and 25% TBP/OK were used as first cycle solvents.

The present paper describes the flowsheet changes and philosophy which have led to the acceptance of the "dilute" TBP flowsheet for metallic fast reactor fuel reprocessing.

DFR FUEL CHARACTERISTICS

The original U-Cr DFR fuel was used for reactor physics studies (in one irradiation period) only and is therefore not discussed further. All "driver" charge fuel subsequent to this first charge has been a U235-Mo alloy with the molybdenum content varying from 20 atomic % to the present value of 15 atomic %. The driver charge is irradiated in single pins clad in niobium. Fuel improvements have permitted the average burn-up to be increased to 3.0% (heavy atoms) in certain sections of the reactor. This is equivalent to 35,000 MWD/te with a fuel rating of about 200 watts/gm.

REPROCESSING PLANT DESCRIPTION

Fuel is brought from the reactor to the reprocessing plant at an initial cooling time of 90 days. At the reprocessing plant the clad fuel pins are cropped into 1" lengths into a stainless steel basket for batch dissolution. An average batch size is 10 kgm fuel. The fuel dissolution reagent is 5.5M HNO₃ with 1.0M ferric nitrate, the fuel being dissolved to give a uranium concentration of about 125 gm/l U in 3M HNO₃. The ferric nitrate moiety of the dissolution agent is included to dissolve the molybdenum as "ferric molybdate".

After the vigorous dissolution the liquor is syphoned into the plant feed vessel. The metal hulls from the cladding are retained in the basket from which they are discharged after washing.

The solvent extraction plant consists of a series of cascades of "nuclearly eversafe" pulsed mixer settlers (Figs 1 and 2).

SOLVENT EXTRACTION PROCESS FLOWSHEETS

The original 20% TBP/OK solvent extraction flowsheet has been previously described and was used with some minor modifications until 1968.

30% TBP/OK Flowsheet

During the period up to 1968, one campaign was attempted with 30% TBP/OK as the process solvent in the first decontamination cycle. The plant proved quite unstable with this solvent, the desired solvent loading could not be achieved and the resulting first cycle decontamination factors were quite unacceptable.

In addition to a poor chemical performance the use of 30% TBP gave rise to excess solvent carry over and poor aqueous/solvent phase separation. These "mechanical" effects were probably caused in the main by plant design: the lack of performance of the 30% TBP flowsheet cannot be attributed solely to the use of 30% TBP.

Experience with the standard 20% TBP/OK flowsheet and the 30% TBP/OK first cycle system led to a re-examination of the possible use of solvent concentrations other than 20% that might give rise to improved plant performance.

Criteria for Plant Performance

- a. The plant throughput (Kgm U/day) must be significantly enhanced, when the feed is of about 130g/l U with its associated molybdenum and ferric iron content.
- b. The overall plant decontamination factor (DF) must be at least as high as that obtained with 20% TBP/OK, and the first cycle DF must be at least similar to the DF obtained in the first cycle of the 20% TBP/OK process.
- c. The TBP concentration chosen must be satisfactory from a "mechanical" point of view (phase disengagement, solvent carry over etc).

Consideration of the "Ideal" Solvent Concentration

A consideration of the solvent extraction process in a given plant shows that a number of factors such as the chemical condition of both solvent and diluent, fission product species present, temperature etc govern the DF obtained, but the major contribution to the DF in any process is due to the "solvent loading" obtained. That is, the greater the amount of solvent which is combined with the solute or solutes it is required to extract, or conversely the smaller the amount of "free" solvent in a given system, the higher the DF. Clearly it is not possible to achieve 100% solvent utilisation in an extractor but for the highest DF one requires the highest possible solvent utilisation at the feed plate of the extraction section.

In the DFR process the plutonium level is trivial and can be ignored; uranyl nitrate and nitric acid are the only solutes to be considered. If it may be assumed that uranyl nitrate forms a di-solvate with TBP, then for 20, 25 and 30% TBP systems (0.73; 0.91 and 1.1M respectively) the maximum uranium loadings are 80, 97 and 112g/l. However, based upon plant experience, solvent loadings of 50, 75 and 90g/l U for the above systems were chosen. After allowance for nitric acid monosolvate formation it was shown theoretically that the percentage of "free" TBP was least in the 25% TBP system, with the 20 and 30% TBP systems having approximately equal amounts of free TBP.

Pilot plant trials of 20, 25 and 30% TBP systems validated the assumptions made for solvent utilisation. With the values of uranium loading accepted as optimum for plant control purposes, 25% TBP/OK was chosen as the solvent concentration that would give an optimum first cycle performance based on the criteria listed above.

25% TBP/OK Flowsheet

A major problem arising from the use of 25% TBP/OK is that although one could achieve an enhanced metal throughput in the first extraction cycle and have a final solvent product loading of 75gm/l U, there were insufficient stages in the backwash system to utilise the 0.05M HNO_3 back-extraction process at a 1:1 ratio. Further, if a nitric acid back-extraction system could be used, the subsequent cycles of the plant would be unable to cope with the enhanced volume of liquor such a scheme would require; thus use of a nitric acid back-extraction would require a reduction in the active feed flowrate and hence would negate the possible advantages offered by the use of 25% TBP/OK.

Substituting sulphuric acid for nitric acid in the strip solution enabled a back-extracted product of 75gm/l U to be obtained, thus maintaining the high uranium concentrations in the plant. Re-extraction from sulphuric acid can be accomplished by acidification of the sulphate stream with nitric acid to about 4.0M.

The final (third) cycle back-extraction was achieved with nitric acid in order to provide a final uranyl nitrate product.

Laboratory tests showed that, provided trace quantities of nitric acid were present in the sulphate cycles, corrosion levels in the 18.8.1 stainless steel plant were low and acceptable. This has been confirmed during routine inspections of the plant itself.

The 25% TBP process gave an enhancement of metal throughput; overall DFs (per gram of uranium) of 1.17×10^6 Beta and 1.11×10^7 Gamma were obtained with first cycle DFs of 6.9×10^3 Beta, 2.3×10^3 Gamma, 3×10^3 Ru, 1.4×10^3 Zr/Nb. The mechanical performance of the plant was in no way inferior to that obtained with 20% TBP/OK.

Fig 3 shows cycles I and II for the 25% TBP flowsheet.

6% TBP/OK Flowsheet

An examination of the process used at Downreay for the reprocessing of Materials Testing Reactor (MTR) fuels in 1969 showed that 6% TBP/OK could be used in the first cycle of the DFR fuel process provided:

1. that the hourly metal throughput could at least be maintained,
2. that flowsheet modifications could be made to enable the first cycle back-extraction and subsequent cycles to cope with any enhanced mass or volume throughput that might arise from the use of 6% TBP/OK in the first cycle.

Full scale plant trials with inactive feeds showed that high solvent-plus-aqueous feed rates could be handled with 6% TBP/OK as solvent. The mechanical performance of the extractor box was adequate.

The back-extraction problem of the 6% TBP/OK flowsheet was solved by use of sulphuric acid to give a product of 90 g/l U, and 25% TBP/OK was then used in the subsequent extraction cycles. The final backwash system used nitric acid in order to provide a product suitable for the metal recovery process.

Owing to a lack of distribution data for 6% TBP/OK systems, several pilot plant runs were carried out to give solvent product concentrations of 12.5, 15, 17.5, 20 and 22 gm/l U respectively in 6% TBP/OK. Table 1 gives details of these runs and Figs 4-8 show both the uranium profiles and the calculated solvent utilisation figures based upon $UO_2(NO_3)_2 \cdot 2TBP$ and $HNO_3 \cdot TBP$ in the solvent phase. In each run sulphuric acid was used as a stripping agent to give an aqueous product of 90gm/l U. The concentration profile data were used to provide distribution data relevant to the processes being examined.

All five flowsheets were stable and easy to control; in each case raffinate values were satisfactory ($<0.005 \text{ gm/l U}$). Each profile shows a sharp drop in the uranium concentration in the solvent phase beyond the feed plate and into the extract section of the box. The scrub profiles are even with little variation in U concentration along the profile.

One consequence of the higher profile in the scrub-section solvent is that the uranium "distribution coefficient" falls in the scrub section - feed plate region because of the "squeeze effect" which causes these higher profiles. If taken to the limit a breakthrough of uranium to the raffinate would occur.

In all the various flowsheets examined, the total solvent utilisation is high and fairly constant along the whole of the unit, with slightly more variation in the 12.5 and 15 gm/l flowsheets than at higher uranium concentrations. This would suggest for dilute TBP at high saturation $(\text{TBP})_{\text{U}} + (\text{TBP})_{\text{H}} \approx \text{constant}$, where $(\text{TBP})_{\text{U}}$ and $(\text{TBP})_{\text{H}}$ are the mole fractions of TBP complexed by uranyl nitrate and nitric acid respectively. In this system the free TBP is minimised all the way along the extraction unit by uptake of either uranyl nitrate or nitric acid. This should give minimum recycle of fission products in the extraction section, unlike the 20-25% TBP systems where some fission product recycle probably occurs under "squeeze" conditions.

For the feed plate region, in all but the 12.5 gm/l product flowsheet, the total solvent utilisation is about or in excess of 100% when calculated on a basis of $\text{UO}_2(\text{NO}_3)_2 \cdot 2\text{TBP}$ and $\text{HNO}_3 \cdot \text{TBP}$. Repeat analyses of selected samples confirmed the original uranium and acid values and it was therefore postulated that a new solvated species was present in the solvent phase. No third phase was found in any of the samples or in the mixer settler. Table 2 gives relevant details of the infra-red spectrum of samples of the solvent phase where the apparent utilisation is in excess of 100%. Other similar spectra were obtained but dilutions of these specimens were not examined. It should be noted from the table that the absorbance due to NO and UO_2^{++} at 935 cm^{-1} decreases with dilution but that it is not halved by each dilution. The shoulder appearing in the x_1 dilution at 988 cm^{-1} is due to the appearance of the P-O-C vibration, but it is not known why there is a decrease in absorbance at 1030 cm^{-1} for this sample on dilution. At 1184 cm^{-1} the absorbance due to P = O bonded uranyl nitrate decreases, but again not as a simple function of dilution. At 1350 cm^{-1} and 1370 cm^{-1} there is a significant increase in absorbance with dilution except for the x_1 dilution at 1370 cm^{-1} where the absorbance is greater than for the undiluted sample, but less than for the x_2 dilution. These two bands are assigned to asymmetric stretching of NO_2 in HNO_3 . There is also a decrease in absorbance with dilution at 1530 cm^{-1} . There is a decrease in absorbance at 935, 1184 and 1530 cm^{-1} with dilution,

but the absorbance is not halved for each dilution. This can be ascribed to a change in the composition of the complex occurring on dilution rather than a straight dilution effect. At 1350 and 1370 cm^{-1} the absorbance increases markedly with dilution, this can be accounted for if nitric acid, bonded in some way in the original sample is being released from one complex to form say $\text{HNO}_3 \cdot \text{TBP}$ when excess TBP is available. It is postulated therefore that a complex $(\text{UO}_2(\text{NO}_3)_2)_a \cdot (\text{HNO}_3)_b \cdot (\text{TBP})_c$ is formed at these high solvent utilisations but breaks down to the usual di-solvate and monosolvate on dilution, but clearly more work must be carried out to confirm this statement.

One of the objectives of any flowsheet designer or engineer concerned with high burn-up fuels is to minimise the solvent residence time in the highly active side of the plant. Various mechanical solutions such as pulsed columns, centrifugal contactors and so on are available but the present work utilises a more simple solution, that is to dilute the solvent (the TBP) and to increase the throughput rate.

By reduction of the TBP concentration to 6% and an increase in the TBP/OK throughput (for a 20 gm/l product) by 3.75, the effective residence time of one mole of TBP is reduced by a factor of about 20 per pass through the mixer settler unit.

During the Pilot Plant runs it was noticeable that there was a complete absence of mixed phase wedge in the settlers; settling appeared to be instantaneous at the mixed phase port.

The first active run took place in March 1969 when 331 Kgm of 74.4% enriched uranium were reprocessed. The average fuel burn up was 1.2% and fuel cooling time at the commencement of the run was 95 days. The feed liquor activity was 4470 Ci Beta and 3425 Ci Gamma per Kgm U with the feed uranium concentration 125 gm/l U. The overall average DFs of 1.4×10^6 Beta and 1.3×10^7 Gamma were deemed to be satisfactory.

In subsequent 6% TBP/OK runs it was found that on a change of cycle 1 solvent/aqueous ratios, the third cycle of decontamination became effectively redundant and it is now not run, the second cycle backwash being changed to nitric acid to give the required nitrate product.

Experiments with the cycle 1 scrub composition showed that, if 1M ferric nitrate in 3M nitric acid is used as the scrub, the ruthenium DF for the first cycle is significantly enhanced: values as high as 1.5×10^7 have been obtained. The ruthenium in the first cycle product is so low that difficulty is often experienced in detecting it by gamma spectrometry.

The improved hydraulic performance of the plant is ascribed to the following changes:

- a. the viscosity of the solvent and mixed phases is greatly reduced, thus reducing pressure drops in the mixed phase ports and solvent passages.
- b. the interfacial tensions are increased giving an improved separation factor.
- c. the density of the mixed phase is reduced from 1.14 to 0.94; this allows the strip feed to enter the extractor box readily. (A hydraulic problem has always existed in D1206 owing to the large difference between the aqueous feed and the strip, i.e. 1.45 to 1.1). Consequently, aqueous levels in the strip box have remained consistently below the mixed phase port and the box hydraulics greatly improved.
- d. the density difference between solvent and aqueous phases is enhanced owing to the lower solvent density.

COMPARISON OF PLANT PERFORMANCE FOR DIFFERING SOLVENT TBP CONCENTRATIONS

Table 3 compares decontamination factors for 6, 20, 25 and 30% TBP systems (value of solvent concentration quoted refers to cycle 1 feed). Current 6% flowsheets operate on two cycles only. It can be seen that the 6% TBP/OK first cycle system is superior to the other flowsheets used. For this reason and also due to the ease of operation of this flowsheet the "dilute" TBP system is the preferred flowsheet for DFR fuel reprocessing.

CONCLUSIONS

6, 20, 25 and 30% TBP/OK have been used as first cycle solvent concentrations in the Dounreay Fast Reactor fuel reprocessing plant. Over a series of campaigns it has been found that 6% TBP/OK gave the best performance. This is attributed to the physical or mechanical properties of the solvent, that is low density, low viscosity, high interfacial tension etc. With 6% TBP/OK a "bonus" was obtained owing to the formation of a hitherto unknown solvate of uranyl nitrate, nitric acid and TBP. The experiences reported above are not quoted as the panacea to all reprocessing problems but they do suggest a new train of thought.

TABLE 1

MIXER SETTLER RUNS IN PILOT PLANT

NOTES

1. Total volumetric throughput about 2.5 l/hr aqueous + solvent.
2. In all the runs the U feed flow was fixed and the solvent loading was achieved by adjustment of the solvent feed flow rate.
3. The scrub to solvent flow ratio was fixed at 1:30.
4. The feed was prepared by dissolving U-7 atomic % Mo in $\text{HNO}_3/1\text{M Fe}(\text{NO}_3)_3$ to give a feed solution about 110g/l U; 3M HNO_3 plus associated iron and molybdenum.

<u>Run</u>	<u>Scrub</u>	<u>Solvent Product</u>
1	0.5M $\text{HNO}_3/1\text{M Fe}(\text{NO}_3)_3$	12.5 g/l U 0.06M HNO_3
2	0.5M $\text{HNO}_3/1\text{M Fe}(\text{NO}_3)_3$	15 g/l U ca 0.03M HNO_3
3	0.5M $\text{HNO}_3/1\text{M Fe}(\text{NO}_3)_3$	17.5 g/l U ca 0.02M HNO_3
4	0.5M $\text{HNO}_3/1\text{M Fe}(\text{NO}_3)_3$	20 g/l U ca 0.02M HNO_3
5	0.5M $\text{HNO}_3/1\text{M Fe}(\text{NO}_3)_3$	22.5 g/l U ca 0.02M HNO_3

The solvent product was back-extracted with 0.25M H_2SO_4 to give a back-extracted product of 90 gm/l U.

TABLE 2
INFRA RED SPECTRA DATA OF TBP SAMPLE

Sample No	Ug/l Acid(M)	% Utilisation	Wave Number cm ⁻¹																
			720	835	910	935	988	1030	1115	1143	1184	1350	1370	1450	1530	1638	2340	2840	2930
685	23.6 0.03	102.3	←———— absorbance —————→																
685(a)	685 dil x 2 ⁽²⁾		0.14	0.04	-	0.21	-	0.57	-	-	0.31	0.85	0.85	0.8	0.30	-	0.06		
685(b)	685 dil x 4 ⁽²⁾		0.16	0.085	0.06	0.12	0.17 ^{sh}	0.42	-	0.09	0.21		1.22	0.95	0.18	0.05	0.06		
Assignment of wavelength						NO ⁺ UO ₂	P-O-C	P-O-C	CH	CH	P = O bonded U nitrate	NO ₃ asymmetric HNO ₃	NO ₃ asymmetric HNO ₃		ONO ₂ asymmetric U nitrate			CH stretching of n C ₄ H ₉	CH stretching of n C ₄ H ₉

- NOTES: 1. Utilisation based on true TBP concentration, nominal value 6% TBP.
2. 6% TBP/OK used for dilution.

TABLE 3

COMPARISON OF DF's

Run	CI 6% +		CI 6% +	CI 6% o	CI 25% x	CI 30% x	Best 20% x
	Run DF	Daily Average					
CI Ext/Strip only	β	2.6×10^4	2.8×10^4	3.8×10^3	6.6×10^3	4.2×10^3	6.2×10^3
	γ	6.4×10^3	2.5×10^3	1.3×10^3	1.6×10^3	6.0×10^2	8.6×10^2
	Ru		1.6×10^4	1.5×10^7	9.0×10^6	7.5×10^2	1.7×10^3
	Zr/Nb		1.3×10^4	6.0×10^2	3.5×10^3	8.8×10^2	6.4×10^2
CI	β		2.1×10^4	8.4×10^2	1.8×10^3	6.9×10^3	1.3×10^4
	γ		1.0×10^4	3.8×10^2	1.2×10^3	2.3×10^3	2.5×10^3
	Ru		2.6×10^4	5.7×10^7	4.7×10^7	3.0×10^3	5.3×10^3
	Zr/Nb		9.8×10^3	3.8×10^2	6.6×10^3	1.4×10^3	1.9×10^3
Overall	β	$1.5 \times 10^{7*}$	$3.3 \times 10^{7*}$	$2.6 \times 10^{5\theta}$	1.4×10^6	1.2×10^{6x}	5.6×10^5
	γ	$7 \times 10^{7*}$	$\sim 5.5 \times 10^{5\theta}$	$\sim 3.3 \times 10^{6\theta}$	$\sim 1.3 \times 10^7$	$\sim 1.1 \times 10^7$	$\sim 7 \times 10^6$
	Ru	$> 4.4 \times 10^7$	$> 5.9 \times 10^7$	4.1×10^7	3.7×10^7		2.7×10^7
	Zr/Nb	6.3×10^7	9.0×10^7	3.5×10^7	7.6×10^7	2.9×10^7	3.5×10^6

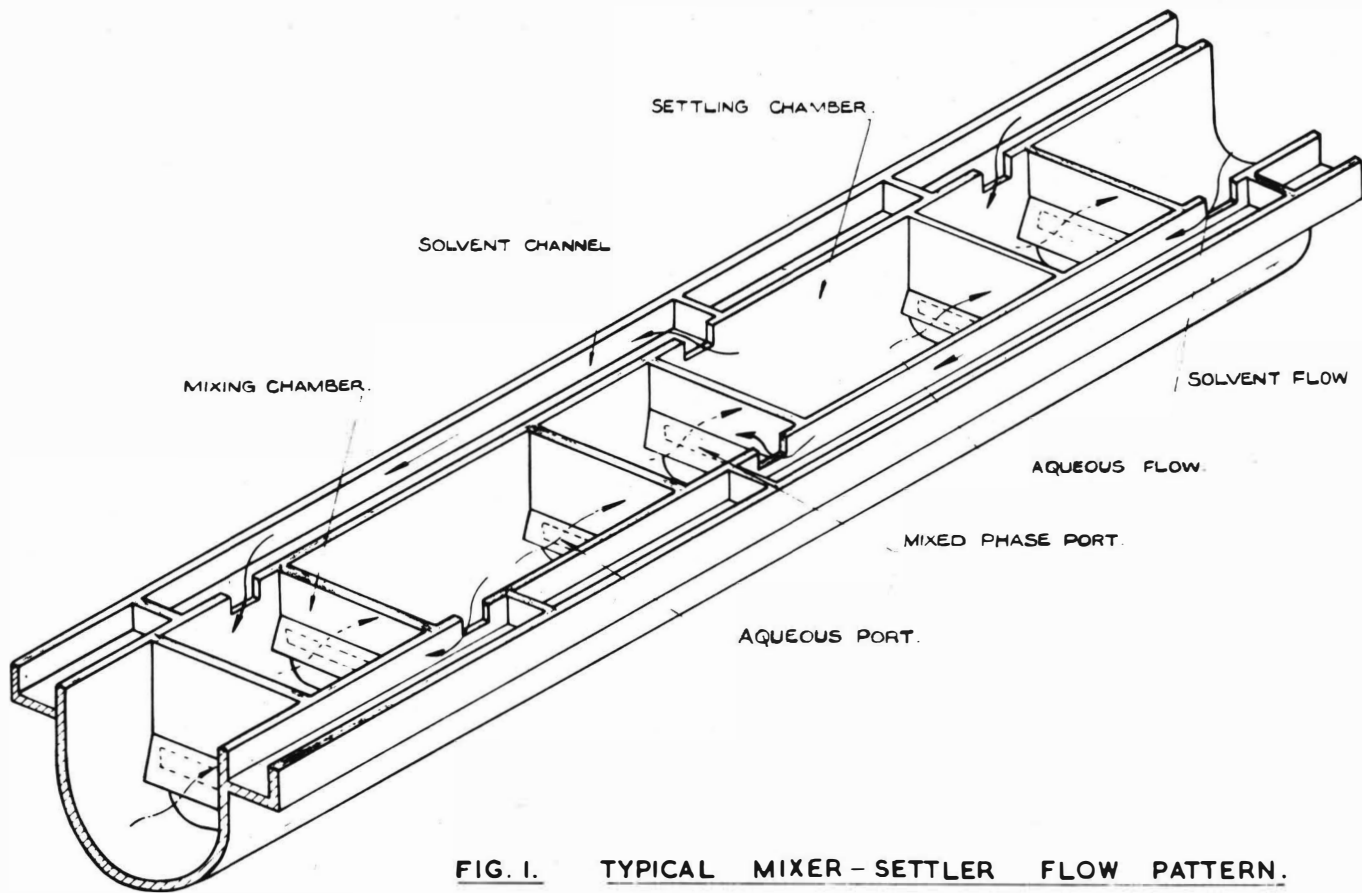
NOTES: + - Large amount U237 present.

x - No U237 present.

θ - No allowance for U237

o - Some U237 present

* - Correction made for U237



1510

FIG. 1. TYPICAL MIXER - SETTLER FLOW PATTERN.

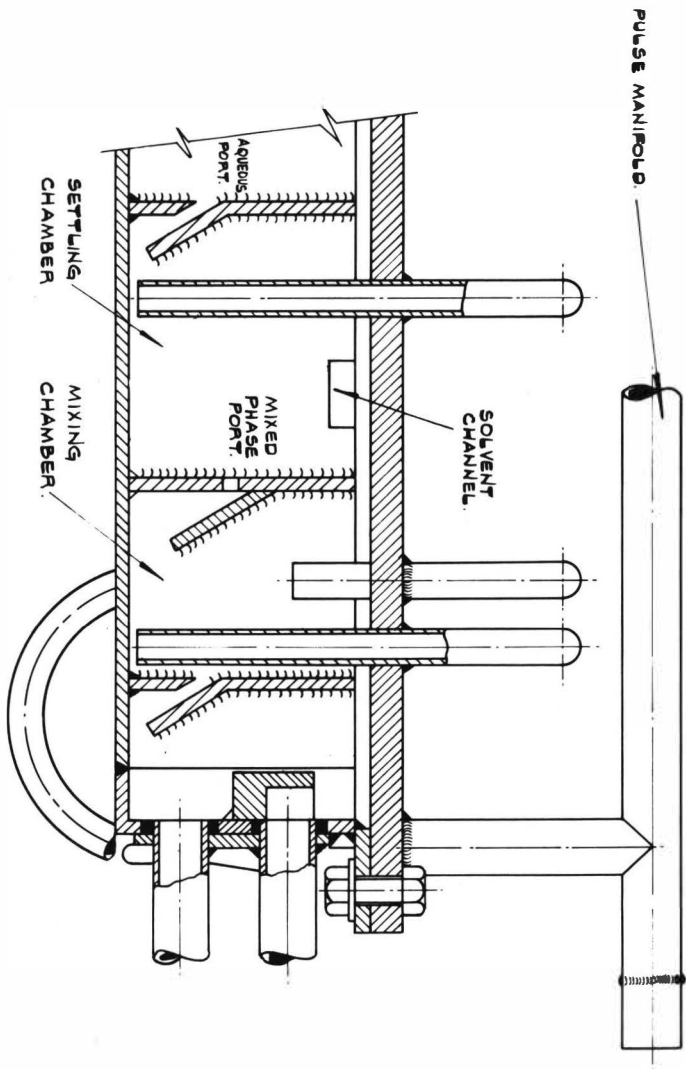


FIG. 2. TYPICAL MIXER SETTLER.

1611

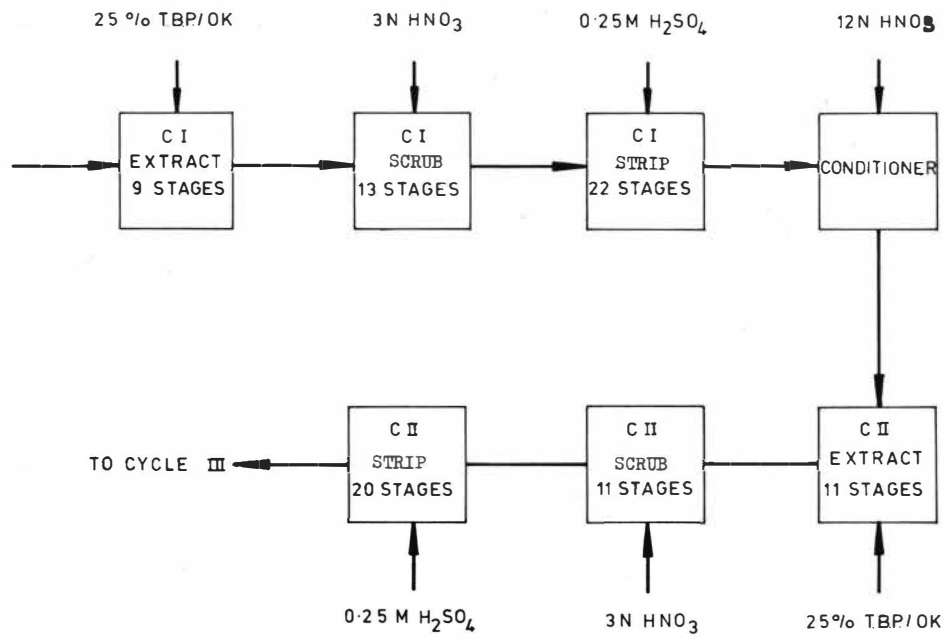


FIG. 3. 25% TBP FLOWSHEET CYCLES I & II.

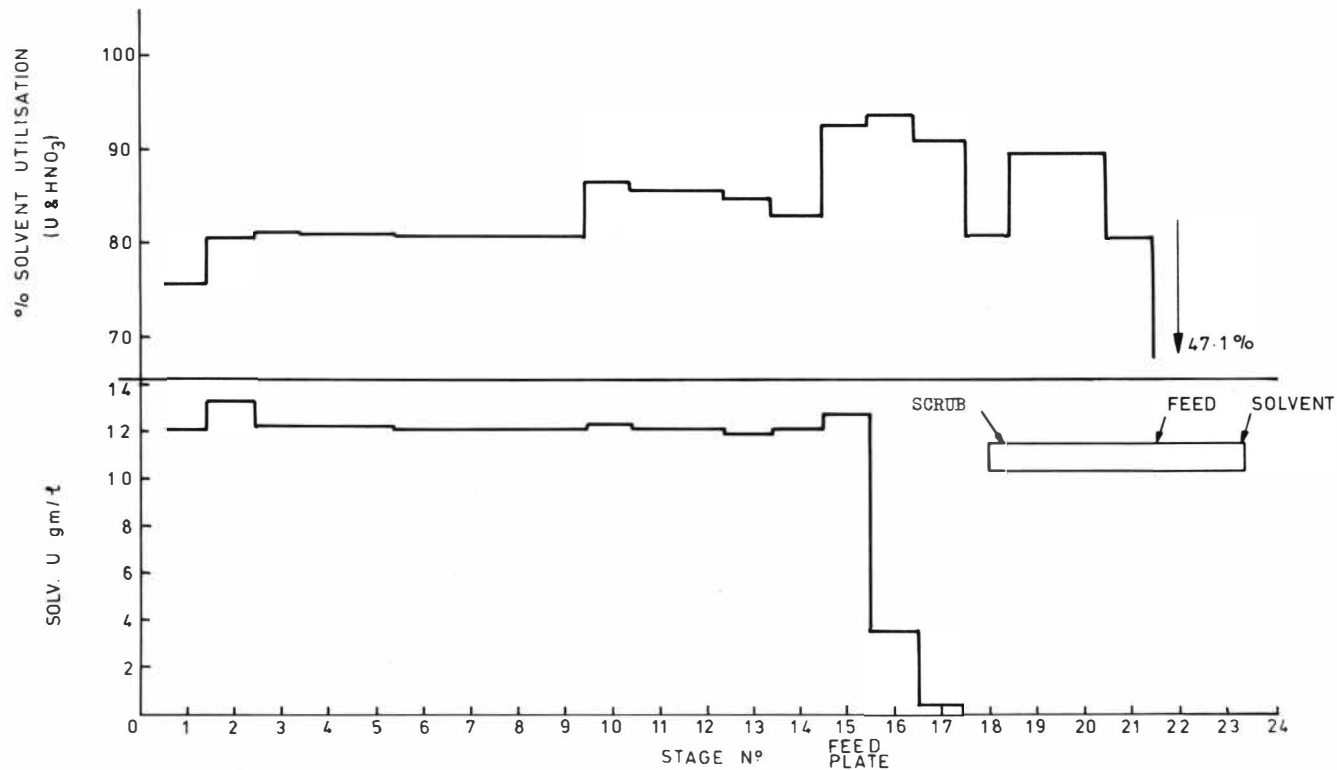


FIG. 4. PROFILE OF SOLVENT LOADING & % SOLVENT UTILISATION
6% T.B.P. 12.5 gm/l U PRODUCT.

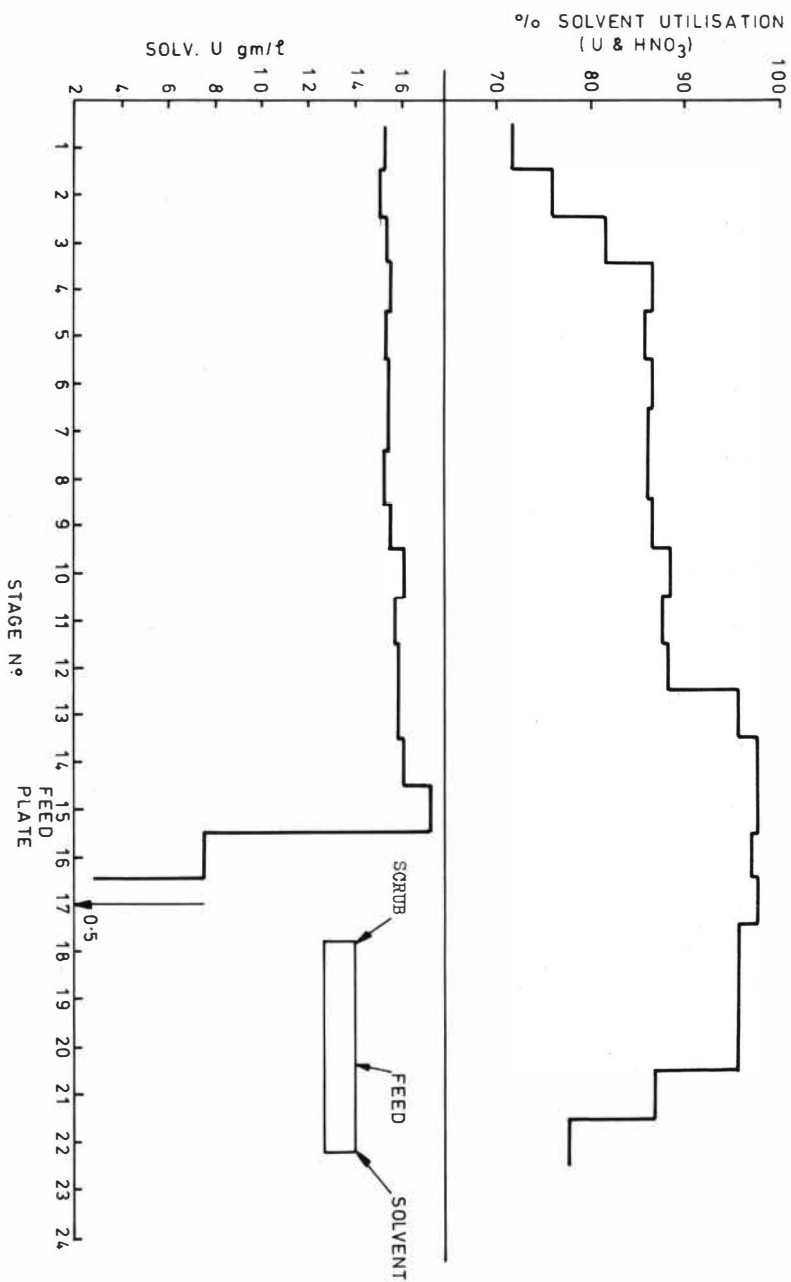


FIG. 5. PROFILE OF SOLVENT LOADING & % SOLVENT UTILISATION
6% T.B.P. 15 gm/ℓ U PRODUCT.

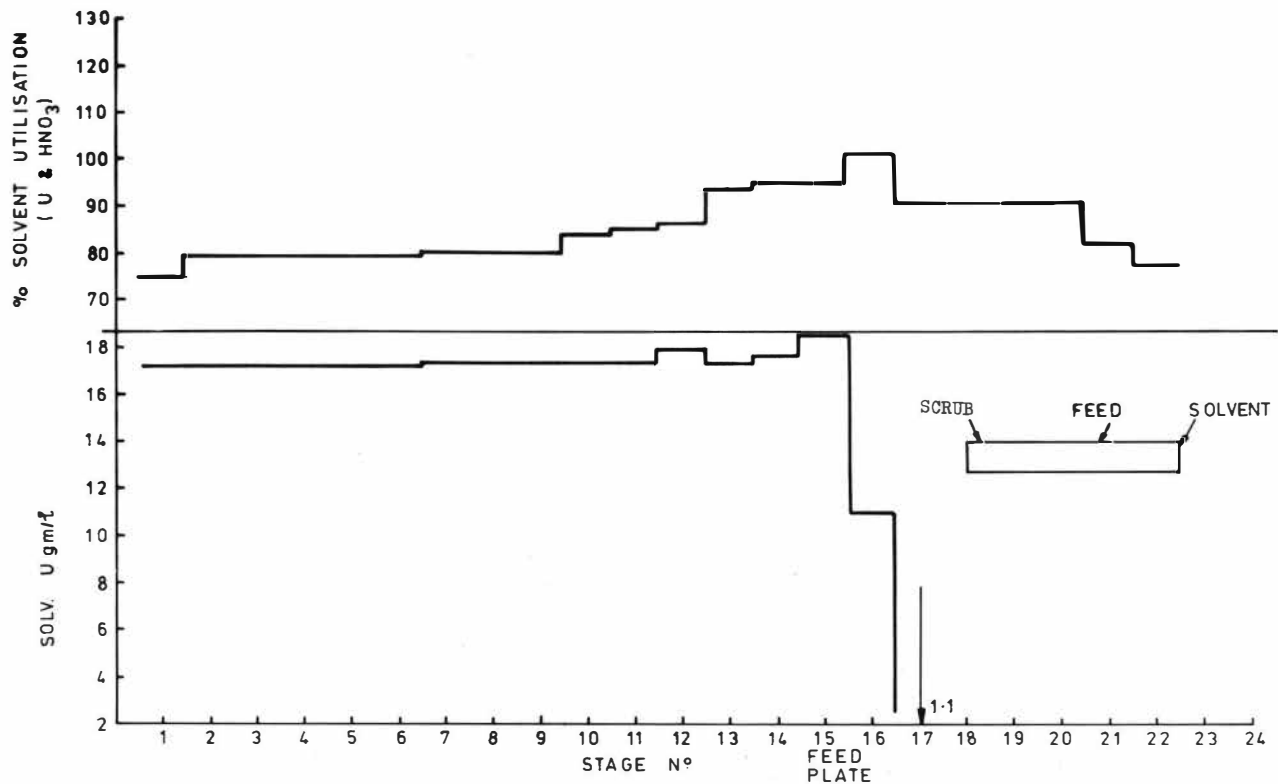


FIG. 6. PROFILE OF SOLVENT U LOADING & % SOLVENT UTILISATION
 6% T.B.P. 17.5 gm/l U PRODUCT.

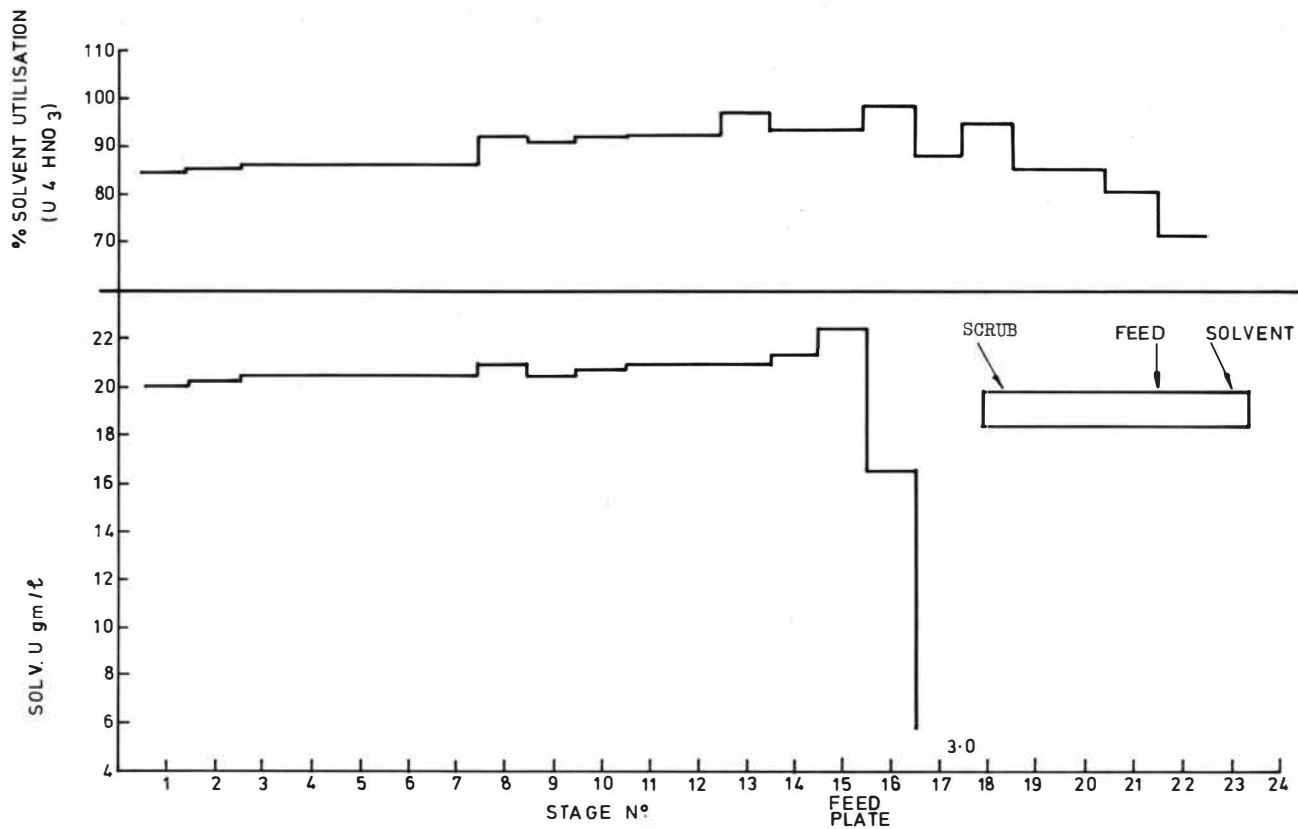


FIG. 7. PROFILE OF SOLVENT U LOADING & % SOLVENT UTILISATION
6% T.B.P. 20 gm/t U PRODUCT.

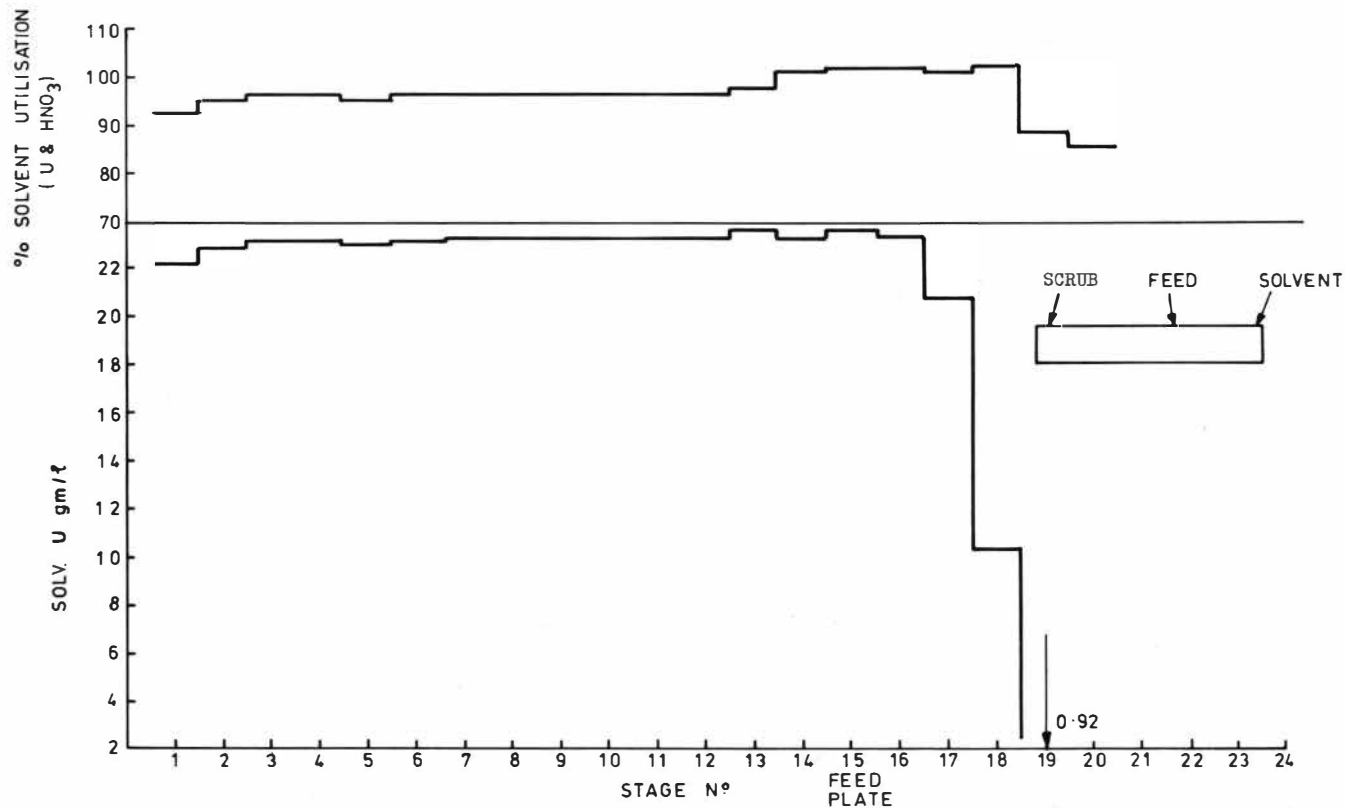


FIG. 8. PROFILE OF SOLVENT U LOADING & % SOLVENT UTILISATION

6% T.B.P. 22 gm/l U PRODUCT.

THE RECOVERY OF URANIUM FROM URANTHORIANTITE AT THE PALABORA
MINING COMPANY LIMITED

T.H. TUNLEY*

V.W. NEL**

SYNOPSIS

Uranthorianite is present in the Palabora Igneous Complex and the orebody is exploited as a low-grade copper deposit.

The National Institute for Metallurgy, in association with the Atomic Energy Board, undertook research on behalf of the Palabora Mining Company into the most suitable methods of chemical extraction applicable to the uranthorianite concentrate produced in a pilot plant at the Palabora Mining Company.

A full-scale plant produced uranium oxide for the first time in August, 1971.

This paper describes the operation of the plant, which produces an extremely pure grade of uranium from a very low-grade deposit.

* National Institute for Metallurgy, Johannesburg, South Africa.

** Palabora Mining Company Limited, Phalaborwa, South Africa.

INTRODUCTION

The separation of uranium and thorium by solvent extraction from nitric acid solution with tri-butyl phosphate is a well-established and well-documented technique. However, the application of this process to the recovery of uranium from the ore mined at Phalaborwa includes some interesting features, and it is the purpose of this paper to describe the process and the plant used.

The presence of the radioactive mineral uranothorianite in the Palabora Igneous Complex in the Eastern Transvaal Lowveld of the Republic of South Africa, was established in 1952 by a geological unit of the South African Atomic Energy Board, which was attached to the South African Geological Survey. Investigation showed the deposits of radioactive minerals to be economically unattractive but led to the discovery of a very large low-grade copper orebody and the subsequent exploitation of this orebody by Palabora Mining Company (P.M.C.). The presence of considerable quantities of the zirconia mineral, baddeleyite, was also established.

No attempts were made to exploit the radioactive-mineral deposits until 1967, when studies undertaken by P.M.C. into possible methods of recovery led to the establishment of a gravity-concentration plant for the investigation of the recovery of heavy minerals from copper-concentrator tailings. Concurrently with that work, the National Institute for Metallurgy (NIM), in association

with the Atomic Energy Board, undertook research on behalf of P.M.C. into the most suitable methods of chemical extraction applicable to the uranothorianite concentrates produced in the pilot concentrator.

Towards the end of 1969, following the development of novel and successful gravity-concentration and chemical-extraction techniques, feasibility studies were completed and the construction of a full-scale plant commenced. This was completed by mid-1971, and production of uranium oxide began in August of that year.

DESCRIPTION OF THE PLANT

Gravity Concentration

The entire output of tailings from the copper concentrator, after desliming in hydroseparators, removal of magnetite, and further desliming in hydrocyclones, is processed through this plant, the average daily feed to the plant being some 22 000 tonnes of dry solids.

Gravity concentration is carried out in Reichert cone concentrators to give a 40- to 50-fold concentration of the heavy-minerals fraction.

Magnetite is removed by magnetic drum separators, and the cone concentrate is fed to shaking tables, where separation into three product streams is achieved: a uranothorianite concentrate, (which constitutes the feed to the chemical-extraction section), a baddeleyite (ZrO_2) concentrate (which is stockpiled), and table tailings.

Leaching of Uranium

The uranothorianite concentrate, which consists of approximately 5 per cent U_3O_8 , 14 per cent ThO_2 , and 65 per cent ZrO_2 , is processed through the chemical extraction plant, shown diagrammatically in Figure 1. The extraction of uranium and thorium is achieved by leaching with hot nitric acid. The hot leach pulp is filtered on stainless-steel tilting-pan filters, and the leach residue containing 90 to 95 per cent ZrO_2 joins the main stream of baddeleyite concentrates from the shaking tables. Fume (oxides of nitrogen) from the leaching operation is scrubbed with ammonium hydroxide solution to produce an ammonium nitrate scrubber effluent.

The unclarified pregnant liquor is settled and then polished through a centrifuge before being fed to the solvent extraction section.

Solvent Extraction

The pregnant liquor fed to the solvent-extraction section contains 30 to 40 g of U_3O_8 , 120 to 140 g of ThO_2 , and 80 to 100 g of free nitric acid per litre. This solution is fed to a six-stage counter-current mixer-settler unit, where the uranium and some thorium are extracted from the liquor with 10 per cent tri-butyl phosphate (TBP). From here, the solvent is fed to a four-stage unit, where the traces of thorium are scrubbed from the solvent with pure uranyl nitrate

solution. The solvent is then stripped with warm water in an eight-stage unit, to produce a solution containing 30 to 50 g of U_3O_8 per litre. This solution is treated in the usual way with ammonia gas to produce ammonium diuranate. Some of the strip liquor is used as a scrubbing medium since it does not cause excessive stripping of uranium in the scrubbing stages.

The solvent is scrubbed with sodium carbonate solution, followed by dilute nitric acid, each in a single stage, before being returned to the solvent storage tank.

THEORY

The uranyl nitrate and thorium nitrate complexes are extracted by TBP as $UO_2(NO_3)_2 \cdot 2TBP$ and $Th(NO_3)_4 \cdot 2TBP$ respectively. However, as shown in Figure 2, the distribution ratio for uranium is higher than that for thorium. These results are reported by Sato. (1)

When the uranium and thorium are together as a mixture, the distribution ratio of each element is enhanced since the total nitrate concentration is higher. In the solution at P.M.C., the total nitrate is approximately 4M and hence the distribution ratio of uranium is high.

The other elements can be separated by saturation of the solvent phase, which "squeezes out" the thorium.

1623

LABORATORY AND PILOT-PLANT TESTS

Laboratory work to prove that the uranium and thorium could be separated by solvent extraction was conducted in the NIM laboratories. Pilot-plant tests were conducted in mixer-settlers, each mixer having a volume of 6 litres and each settler having an area of 450 cm².

The object of the tests was the extraction of only uranium nitrate, and a solvent of low TBP strength was chosen (12 per cent) since the separation factor decreases as the TBP strength increases.

Tests had shown that it was possible to extract the uranium and thorium together and to separate them by scrubbing. However, this system was considered to be more complex, and would be suitable only if thorium was to be recovered as a product. Since thorium cannot be sold under present marketing conditions, the process for the extraction of uranium alone was chosen.

Typical results for the pilot-plant tests are given in Table 1. These tests showed that it was possible to produce pure uranium diuranate having a thorium content of less than 200 p.p.m. (on a uranium basis).

The equilibrium curves for uranium are given in Figures 3 and 4.

DESIGN OF THE SOLVENT-EXTRACTION PLANT AT P.M.C.

The mixer-settlers used in the plant are constructed in 316L stainless steel and have the following dimensions (in mm)

Mixer: 300 by 300 by 1000

Settler: 2400 by 300 by 1000

The extraction and scrubbing units are arranged together as a ten-stage unit (six extraction and four scrubbing stages).

The stripping mixer-settler is an eight-stage unit with provision for the heating of each stage. The feed (water) is heated by steam heat exchanger. The temperature in the stripping stages is maintained at between 40 and 50°C.

OPERATION OF THE PLANT

The main operating parameters are given in Table 2.

TABLE 2 OPERATING PARAMETERS

Aqueous feed	16 l/min.
Solvent	25 to 30 l/min.
Scrub feed	2 to 5 l/min.
Strip feed	20 to 30 l/min.

Specific gravity of solvent in:

Stripped solvent	0,900
1st extraction stage	0,927 to 0,934
3rd extraction stage	0,935 to 0,940
6th extraction stage	0,954 to 0,958

Steady operation of the plant is promoted by the maintenance of a constant flowrate of aqueous feed. This is made possible by the relatively large size of the feed tank for pregnant liquor (153 000 litre). No alteration is made to the flowrate of the aqueous phases, and, if the level in the tank becomes low, the solvent-extraction plant is shut down.

The flowrate of the solvent is adjusted according to the specific gravity of the solvent in the first extraction stage. This is a good indication of the extent of loading of the solvent and is also sensitive to changes in the concentration of the feed liquor. This stage is maintained at a specific gravity between 0,928 and 0,932, and the loaded solvent is then constant at approximately 0,957.

Only a part-time operator is required to run the plant. The maintenance of maximum loading as indicated by the specific gravity is important, since the thorium is squeezed out of the solvent. (The specific gravity of unloaded solvent is 0,900).

The raffinate concentration is approximately 0.3 g/l, giving a uranium recovery of 99 per cent.

The solvent circulating in the plant is stable, and the concentration of TBP is approximately 10 per cent. The diluent used is SHELLSOL R because this hydrocarbon mixture has a very high flash point.

SEPARATION OF THORIUM

As an illustration of the separation of thorium from uranium, a series of samples was taken from the mixer-settlers for analysis. (Table 3). Thorium is shown to be extracted along with the uranium but is later squeezed out of the solvent as the uranium loading increases. Further decontamination of thorium from the solvent is seen to take place in the scrubbing stage. The use of the uranyl nitrate stripping liquor is important in providing a means of saturating the organic phase with uranium.

The very low concentration of thorium in the final liquor (0.01 g/l) proves the effectiveness of the extraction and scrubbing techniques. The amount of thorium present in the final ammonium diuranate is less than 0.6 per cent (on U_3O_8 basis).

CONCLUSIONS

Although there were some deficiencies in the equipment which became apparent at the start up of the plant, no process problems of any sort were encountered. Once the mechanical problems had been overcome, the plant operation soon duplicated the pilot-plant results and there was no difficulty in obtaining a product of exceptional purity, as shown by the typical assay given in TABLE 4.

The successful operation of this plant has demonstrated that it is possible to produce an extremely pure solution of uranyl nitrate when the feed liquor contains more than three times as much thorium as uranium. This is the more remarkable when it is considered that no additives are used to complex the thorium as has been done in similar separations elsewhere.

ACKNOWLEDGEMENTS

This paper is presented by permission of the Management of Palabora Mining Company Limited; the Director of the Extraction Metallurgy Division, Atomic Energy Board; and the Director General of the National Institute for Metallurgy.

REFERENCE

1. SATO, T. J. Appl. Chem., 15th Nov., 1965. p. 489.

TABLE 1RESULTS OF PILOT-PLANT TESTS

<u>Flow</u>	<u>Solvent</u>	<u>l/min</u>
	Pregnant liquor	0.4 to 0.9 l/min
	Stripping solution	0.5 to 0.7 l/min
	Scrubbing solution	0.05 l/min

Specific gravity

Fresh solvent	0.80
Loaded solvent	0.85 to 0.86
Scrubbed solvent	0.842 to 0.850

U₃O₈

Loaded solvent	38 to 42 g/l
Scrubbed solvent	40 to 50 g/l
Raffinate	0.005 to 0.03 g/l
Strip liquor	60 to 75 g/l

ThO₂

Loaded solvent	0.7 to 10 g/l
Scrubbed solvent	0.001 to 0.03 g/l

TABLE 3
ANALYSIS OF SAMPLES TAKEN FROM EXTRACTION
AND SCRUBBING MIXER-SETTLERS

Stage no.	Duty	Aqueous phase		Organic phase	
		U_3O_8 g/l	ThO_2 g/l	U_3O_8 g/l	ThO_2 g/l
1	Extraction	1.1	59.8	0.3	8.9
2	"	0.7	75.6	0.4	9.6
3	"	0.9	87.8	0.3	8.4
4	"	0.9	82.8	1.3	9.8
5	"	2.2	82.8	8.2	1.6
6	"	11.8	71.5	28.9	3.4
7	Scrub	69.1	11.3	34.9	1.0
8	"	106.0	1.4	29.8	0.9
9	"	98.3	0.2	29.9	0.2
10	"	83.2	0.1	23.3	0.3

Pregnant liquor: $U_3O_8 = 29.7$ g/l $ThO_2 = 100.2$ g/l

Strip liquor : $U_3O_8 = 36.0$ g/l $ThO_2 = 0.2$ g/l

(and scrub solution)

T A B L E 4

TYPICAL ASSAY OF URANIUM OXIDE PRODUCED AT PMC

ELEMENT	PARTS FOR MILLION
Al	25
As	<3
B	0.3
Bi	<1
Co	<1
Cd	0.3
Cu	9
Fe	60
Mg	40
Mn	<1
Mo	0.5
Ni	<1
Pb	17
Sb	<3
Sn	<3
Si	<300
V	<1
Zn	<10

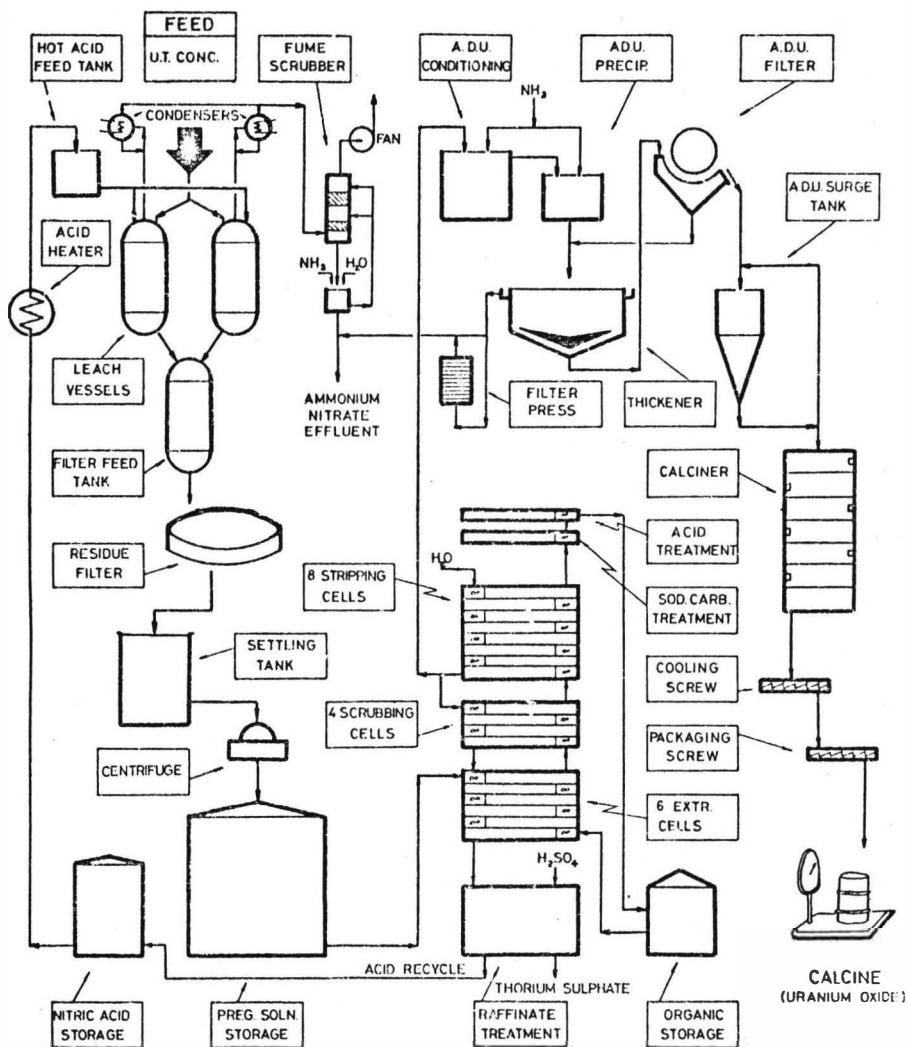


FIGURE 1
 CHEMICAL EXTRACTION PLANT AT P.M.C.

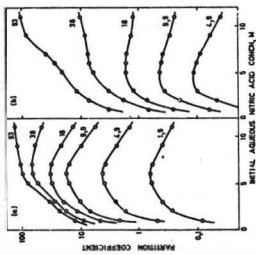


Figure 2 Extraction of uranium(VI) and thorium from nitric acid solutions by BP in kerosene (a) Uranium (VI), (b) Thorium concentrations, 2) (figures on curves are the concentrations, 3) (after Sato)

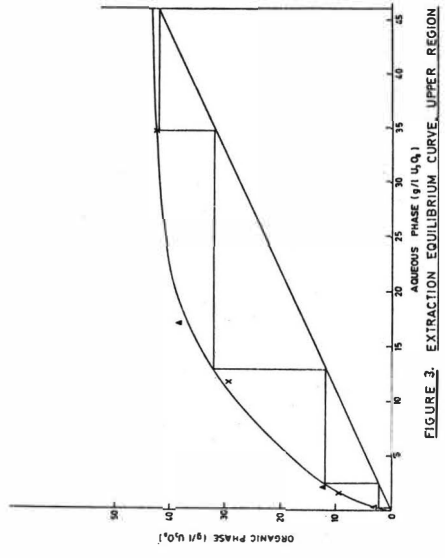


FIGURE 3. EXTRACTION EQUILIBRIUM CURVE, UPPER REGION

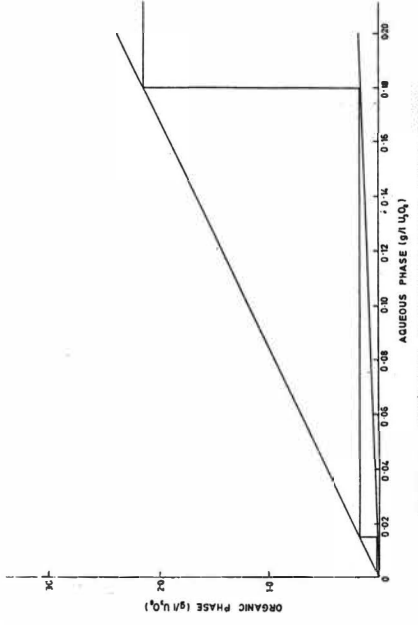


FIGURE 4. EXTRACTION EQUILIBRIUM CURVE, LOWER REGION

FISSION PRODUCT BEHAVIOR IN A TWO-SOLVENT EXTRACTION

SYSTEM FOR ENRICHED URANIUM

L. C. Lewis

K. L. Rohde

ABSTRACT

At the Idaho Chemical Processing Plant operated by Allied Chemical Corporation for the USAEC, the first solvent extraction cycle for uranium recovery uses tributyl phosphate in hydrocarbon diluent; the second and third cycles use methyl isobutyl ketone as the solvent. Data for decontamination of uranium from fission products will be displayed for aluminum alloy fuels, zirconium fuels, zirconium-aluminum alloy fuels blended, and stainless steel clad fast reactor fuels to indicate the performance of the two-solvent system. Decontamination factors will be compared to those for the Purex, Redox, and Hexone-25 processes. There are no process problems associated with the presence of two solvent systems in the same plant.

Idaho Chemical Processing Plant

Allied Chemical Corporation

Idaho Falls, Idaho U.S.A.

FISSION PRODUCT BEHAVIOR IN A TWO-SOLVENT EXTRACTION
SYSTEM FOR ENRICHED URANIUM

INTRODUCTION

The Idaho Chemical Processing Plant located at the United States National Reactor Testing Station near Arco, Idaho is a government owned, multipurpose, reprocessing facility for fuels containing highly enriched uranium. As such it consists of dissolution, extraction, product packaging facilities plus the necessary support areas: fuel storage, liquid waste storage, waste calciner, solidified waste storage, analytical, maintenance, and technical support facilities.

Routinely processed fuels at the ICPP include stainless steel clad, zirconium clad, and aluminum clad reactor fuels. Enrichments before burnup vary from 52% to 93% although limited amounts of lower enriched fuels have been processed on a small scale, non-routine basis. In the near future, a facility will be installed to process graphite-based, high temperature, gas cooled reactor fuel.

Historically, the plant was designed as a Redox-type facility with three cycles of solvent extraction using methyl isobutyl ketone (MIBK). For reasons of economy and safety, a first cycle of larger columns was installed during the middle 1950's for use with tributyl phosphate (TBP) in a hydrocarbon diluent. The MIBK columns were retained for final decontamination and cleanup. Utilization of the larger columns and the TBP/hydrocarbon solvent (Amsco 125-90W) permitted the use of higher acid flowsheets and greater throughput.

The facility has no current capability for processing plutonium fuels because of the lack of packaging and ventilation safeguards necessary for this type of processing. A limited capability for the recovery of certain fission product isotopes does exist.

ICPP PROCESSES

A schematic diagram of the fuel recovery process employed at the ICPP is shown in Figure 1. It consists essentially of four phases. The initial phase in the process is the fuel preparation process where any excess cladding metal which would reduce throughput and increase waste volumes is physically removed and discarded to solid waste. Any batching required by the process is done at this time.

The second phase is the extraction feed preparation phase or basically the dissolution of the fuel. This phase will be dealt with in somewhat greater detail later.

The third phase of the total process is the extraction of the dissolved fuel. It consists of an extraction with TBP/hydrocarbon followed by two extractions with MIBK. This phase of the operation will also be dealt with in much greater detail.

The final phase of the process is the product and waste handling phase. The uranyl nitrate product from the extraction system is denitrated in a fluidized bed denitrator to the trioxide (UO_3) for shipment as a solid from ICPP. The waste from the process is concentrated and solidified in a fluidized bed calciner to a predominantly oxide, granular, solid which is stored in stainless steel bins.

DISSOLUTION

The feed for the extraction system is derived from the dissolution process. In the currently existing aqueous processes which furnish greater than 95% of the feed for the extraction systems, the fuel elements are charged to one of three primary dissolution processes. The entire fuel element is dissolved except for relatively minor amounts of insoluble residues. The three primary dissolution processes are the continuous aluminum dissolver which uses a mercuric ion catalyzed nitric acid dissolvent; the zirconium dissolver

which uses a hydrofluoric acid dissolvent; and the stainless steel dissolver which uses nitric acid in the presence of an electric field. In order to achieve practical geometries and throughputs some of these dissolvent streams are poisoned with either boric acid or gadolinium nitrate to assure criticality safety.

In processing fluoride containing solutions from the zirconium dissolvers in stainless steel equipment, it is necessary to complex the fluoride--usually with aluminum nitrate. A practical source of aluminum nitrate for this purpose is from aluminum dissolver product. Thus, if the aluminum fuel is available, co-dissolution and extraction (co-processing) of aluminum and zirconium based fuels is carried out to minimize the waste volume which would otherwise be caused by the addition of cold aluminum nitrate. The extraction of this feed stream takes place in the TBP extraction system with only minor changes to the flowsheet. The economic savings realized by this co-processing are considerable because of the very high costs of handling nuclear wastes.

Another source of feed to the extraction system is an infrequent neptunium recovery operation. After partitioning the neptunium from the uranium product in the first MIBK extraction cycle, the raffinate containing the neptunium and associated small quantities of plutonium is recycled to the TBP extraction system where the neptunium and plutonium, after reoxidation to the extractable hexavalent state, are recovered as a product, concentrated, and accumulated until a sufficient quantity exists to make a recovery operation economically feasible. At that time the feed is adjusted, a second MIBK uranium partition cycle frees the neptunium product of uranium followed by an acid MIBK extraction to remove accumulated ^{233}Pa and associated fission products.

The dissolution processes result in the fission products going into solution in most cases. A notable exception is cerium which is insoluble in

fluoride systems. Cerous fluoride (CeF_3) can be found deposited on the walls of the vessels and adsorbed onto solid residues. Any other fission products which are insoluble or become adsorbed onto solid residues are removed from the extraction feed by a centrifuge.

EXTRACTION SYSTEM

A typical flowsheet for the first cycle extraction system is shown in Figure 2. It consists of four pulsed columns. The extraction from the adjusted dissolver product takes place into a TBP/hydrocarbon solvent. The aqueous raffinate from this column containing most of the fission products and the dissolved cladding goes directly to the high level waste tanks.

The organic phase containing the uranium passes into the scrub column where it is scrubbed with acid-deficient aluminum nitrate. The aqueous raffinate contains a significant quantity of uranium and is recycled to the extraction column feed tank where it is blended with incoming dissolver product. The scrub column removes extracted acid and some of the entrained fission products.

After scrubbing, the uranium product still in the organic phase goes to the stripping column where a gadolinium poisoned, dilute nitric acid solution strips the uranium from the organic phase. The stripped organic goes to a bank of three mixer settlers, the first of which washes the organic with the same solution used in the stripping column which is then recycled. The organic phase is then washed with 0.5M sodium carbonate and then with dilute nitric acid before being recycled to the extraction column. Both of these latter aqueous solvent cleanup solutions are concentrated and then discarded to the intermediate level liquid waste tanks for ultimate calcination.

The uranium product goes to the fourth column where it is washed with a hydrocarbon diluent to remove any residual TBP. The hydrocarbon is steam distilled and then burned.

An approximately hundred-fold concentration of the aqueous product from this extraction cycle takes place in a thermosyphon evaporator. This results in a feed for the first MIBK extraction cycle which is about 300 g/l uranium, 2 g/l gadolinium and 0.5M nitric acid. The gadolinium, added at a 20 ppm level in the stripping reagent, is present as a secondary criticality safeguard to prevent a criticality which conceivably could occur in the head of the thermosyphon evaporator.

The second solvent system consists of two cycles of MIBK extraction. A typical flowsheet for this extraction is shown in Figure 3.

Each cycle of MIBK extraction consists of two packed columns. The extraction column is an approximately 10 transfer unit column. The feed enters above the center of the column and is scrubbed by an acid deficient aluminum nitrate solution which contains a ferrous sulfamate reductant for partitioning the neptunium and plutonium. The organic phase containing the uranium is stripped with dilute nitric acid. The aqueous phase is then concentrated in a small thermosyphon evaporator and fed to the second MIBK extraction cycle.

The partitioned neptunium and plutonium are collected with the fission product containing raffinate for later TBP extraction to recover the neptunium and plutonium it contains.

The concentrated uranyl nitrate is fed to the final MIBK extraction system. The feed is fed above the center of the column, and an acid deficient aluminum nitrate scrub is fed part way up which may contain ferrous ion if an optional water scrub is fed near the top of the column. The uranium containing organic phase is stripped with a dilute nitric acid solution, concentrated and finally denitrated.

The water top-scrub is a recently installed anti-entrainment modification to reduce the amount of inorganic contaminants (notably iron and aluminum) and fission products carried through the final extraction by entrained aqueous phase.

The scrubbed MIBK solvent is steam stripped in a counter-current contactor. Caustic flows counter-current to the steam - MIBK azeotrope and removes any actinides and many fission products by precipitation. Organic residues from the TBP extraction cycle have higher boiling points than the MIBK - water azeotrope and are thus discarded to waste with the caustic stream.

FISSION PRODUCT DECONTAMINATION

Fission products are removed from the process solutions at many places in the process. Advantage is taken of the different fission product-to-uranium separation factors for certain fission products with the two solvents to yield greater overall decontamination than would be possible with three cycles of a single solvent. Examples of these are the desirable separation factors for ruthenium in a TBP extraction but relatively poorer separation in an MIBK extraction and desirable separation factors for zirconium in an MIBK extraction with poorer separation factor for a TBP extraction. Advantage is also taken of the chemical behavior of cerium in a fluoride system to yield a greater decontamination because of the low solubility of CeF_3 . This yields a decontamination factor for cerium of about 10 for this part of the process.

Another indicator of rare earth fission product behavior in the MIBK system is the uranium product quality. Gadolinium is deliberately added to the first cycle stripping reagent at a level of about 20 mg per liter to insure criticality safety in one of the vessels. It is concentrated by factor of about 100 and then in two subsequent extraction steps is reduced to a concentration below the maximum allowable concentration for soluble neutron poisons (approximately 2 mg per kg U). This is equivalent to a decontamination factor of at least 3×10^3 over the two MIBK extraction cycles.

Another decontamination process which has a relatively minimal effect on radionuclide decontamination but plays a large part in chemical decontamination is the use of the top water scrub in the final MIBK extraction. This

scrub minimizes entrainment of the normal aluminum nitrate scrub and permits the use of a ferrous scrub for greater alpha decontamination in that cycle without compromising the chemical purity of the product. The fission product decontamination factor improvement as the result of this modification is relatively small because at that point there are not large concentrations of fission products still present in the feed. The added cycle of transuranic reductant is significant in the transuranic alpha content of the final product. The decontamination factor for the chemical contaminant, aluminum, is 34 as the result of the use of the top water scrub. For transuranic alpha this added cycle of reductant yields a decontamination factor of about 1.3×10^3 .

Two fission product elements are more significant decontamination problems in the two solvent system than any others except for the bred-in transuranic elements as can be seen from Table 1. These elements are ruthenium which is not as readily removed by the MIBK extraction, probably because of an extractable complex formed with the MIBK, and zirconium which forms extractable complexes with TBP and with the degradation products from the TBP. Thus, for ruthenium, good decontamination (decontamination factor $\sim 10^3$) is obtained in the TBP cycle with relatively poorer decontamination in the MIBK cycles (total decontamination factor ~ 100 for both cycles). With zirconium a decontamination factor of about 30 is obtained for the TBP cycle and about 10^5 for both MIBK cycles. With the two systems together the decontamination factors are a respectable 10^5 for ruthenium and 10^7 for zirconium.

A comparison of the β, γ decontamination factors for the two-solvent system with various fuels commonly processed at ICPP is shown in Table 2. Gross gamma activity in reprocessing streams is due predominantly to ^{95}Zr - ^{95}Nb . In a TBP system using the common nitrate feed, zirconium is not normally well separated from the uranium product. However, in a fluoride system the decontamination factor for zirconium is nearly three orders of magnitude better

TABLE 1
THE DECONTAMINATION OF ALUMINUM FUELS

	Log_{10} Decontamination Factors			
	β	γ	Ru	Zr
ICPP TBP cycle	3.2	2.7	3.6	1.3
ICPP MIBK two cycles acid deficient scrub	3.3	3.3	2.0	5.6
ICPP overall decontamination	6.5	6.0	5.6	6.9

TABLE 2
A COMPARISON OF β, γ DECONTAMINATION OF THE COMMONLY
PROCESSED ICPP FEEDS

	Feed Stream							
	<u>Aluminum</u>		<u>Stainless Steel</u>		<u>Zirconium</u>		<u>Co-processing</u>	
	Log_{10} decontamination factors							
	β	γ	β	γ	β	γ	β	γ
ICPP TBP	3.2	2.7	3.7	3.5	5.0	6.0	3.9	3.8
ICPP MIBK two cycles acid deficient scrub	3.3	3.3	1.7	1.7	1.5	1.9	2.2	2.0
ICPP overall	6.5	6.0	5.4	5.2	6.5	7.9	6.1	5.9

than in a pure nitrate system. In the co-processing extraction, which uses a blended nitrate-fluoride feed, the zirconium decontamination factor is slightly better than the pure nitrate feeds but much less than the pure fluoride feed. The extractable zirconium nitrate complexes are responsible for this behavior. In the pure fluoride system the nitrate complexes never form during the dissolution step and are tightly complexed by the fluoride during the aluminum nitrate complexing step. Thus, no extractable nitrate complexes can form. In the co-processing system where part of the feed is from a nitric acid dissolver, complexing of the fission product zirconium with fluoride during the blending step is not complete prior to extraction as seen from the significantly lower gross gamma decontamination factor. This is probably associated with the driving force of the low concentration of zirconium that is just not great enough to fully complex, with fluoride, the extractable zirconium. Thus, the fission product zirconium derived from the fluoride system is fully complexed and the aluminum system zirconium is slightly complexed resulting in slightly better separation factor than for the pure nitrate system.

Decontamination factors are influenced by the quantity of radionuclide present. Accordingly, the low burnup of the EBR-II fuel does not indicate that the process is performing very satisfactorily. In reality, the 10^5 decontamination factors indicated are more than adequate to meet product purity specification.

Table 3 shows a comparison of transuranic alpha to the gamma decontamination factors. With the exception of the fluoride systems in which only a part of the plutonium is extracted in the TBP cycles, decontamination from transuranic elements occurs in the first MIBK cycle. This is sufficient to meet the normal shipping specification. The specification is that an α -ratio $\frac{\text{gross } \alpha\text{-activity of product}}{\text{transuranic } \alpha\text{-activity}}$ be greater than 750. The α -ratio normally starts low and increases as the duration of the run increases. The α -ratio

of the stainless steel fuel-derived product is greater than the others because of the use of a reductant in this cycle was made possible by the dual scrub system which prevented iron contamination of the final product. Occasional use is made of the reductant, hydroxyl amine sulfate in the second MIBK cycle for slightly improved transuranic decontamination. It is not as effective as ferrous ion, but does not require use of the dual scrub. It does not appreciably contaminate the final product since it is decomposed in the product denitration system.

TABLE 3
A COMPARISON OF ALPHA DECONTAMINATION OF THE COMMONLY
PROCESSED ICPP FEEDS

	Log ₁₀ decontamination factors							
	Aluminum		Stainless Steel		Zirconium		Co-Processing	
	γ	α	γ	α	γ	α	γ	α
ICPP TBP	2.7	0	3.5	0	6.0	2.0	3.8	0.1
ICPP MIBK Fe reductant in 1st MIBK cycle	3.3	3.2	1.7	5.2	1.9	2.6	2.0	3.7
ICPP overall	6.0	3.2	5.2	5.2	7.9	4.6	5.9	3.8

α-ratio (1) 10³-10⁴ 10⁴-10⁵(2) 10³-10⁴ 10³-10⁴

(1) α-ratio = $\frac{\text{gross } \alpha\text{-activity of product}}{\text{transuranic } \alpha\text{-activity}}$

(2) An additional cycle of reductant was used as the result of the use of the dual scrub system in the third cycle.

Table 4 shows the decontamination of specific isotopes obtained in a special application of one cycle of the MIBK system. This application was the acidic scrub-MIBK purification of a neptunium by-product stream salvaged from the normal second MIBK extraction of uranium feed stacks. Ruthenium decontamination is not as great in an acidic-scrubbed MIBK extraction as it is in the normal acid-deficient scrub. This is due to extractable ruthenium complexes.

TABLE 4
DECONTAMINATION FACTORS FOR AN ACID-MIBK EXTRACTION USING A
NEPTUNIUM BY PRODUCT FEED STREAM

<u>Fission Product</u>	<u>Log₁₀ Decontamination Factor</u>
¹³⁷ Cs, ¹³⁴ Cs	4.1
¹²⁵ Sb	2.2
¹⁴⁴ Ce	>4.6
¹⁰⁶ Ru	1.6

Table 5 makes a comparison of the decontamination efficiencies for various commonly used processes. For the ICPP with its wide diversity of fuels, an overall decontamination factor for all fuels was obtained. This factor is 1×10^6 for γ and 2×10^6 for β activity.

The Purex process normally uses a reductant, ferrous sulfamate, for the partitioning of Pu from the U. The ICPP process has no need for this step. The Purex process is a 30% TBP/hydrocarbon diluent process. Nitric acid is the salting agent.

TABLE 5
COMPARISON OF DECONTAMINATION EFFICIENCIES FOR
COMMON REPROCESSING SYSTEMS

Process	<u>Log₁₀ decontamination factor</u>	
	β	γ
Overall ICPP for all fuels, two-solvent system	6.3	6.0
Purex	6.1	6.8
Redox	6.3	6.5
Hexone 25		
2 cycles	5.7	5.0
3 cycles	6.4	6.1

The Redox process is a MIBK process for the separation and purification of uranium and plutonium. This process obtains its Ru decontamination by volatilization of the RuO₄ species during feed preparation.

The Hexone 25 process is a two column per cycle MIBK extraction for essentially Pu-free feed systems.

CONCLUSION

Each of the ICPP processes discussed achieves the total decontamination factors necessary to meet product purity specifications. The two-solvent system used at ICPP takes advantage of the acid tolerance of the TBP system to simplify acid control of the dissolution and extraction feed portions of the first cycle. Acid control is much easier to achieve in the later cycles because it is a function of the stripping reagent concentration and the

intercycle concentration factor. The use of the two solvents alleviate some decontamination problems that would be present with one or the other solvent such as the ruthenium and zirconium problems. The interface between the TBP and the MIBK systems is through the first intercycle evaporator. Any organic residues (from the diluent, solvent, or degradation products of either) which remain with the product through the intercycle evaporator are soluble in the MIBK and are disposed of in the solvent cleanup system for the MIBK. There is no conceivable way for direct back cycling of any stream contaminated with MIBK into the TBP system. Evaporators used for concentrating salvage streams such as the transuranic containing second cycle raffinate are very efficient in removing the residual MIBK in that stream. There are no process problems that have been encountered due to the use of two distinct solvents in the system over the operating history of the plant. The problems that have been encountered are those arising in the operation of a complex chemical plant with hazardous starting material, wastes and final product.

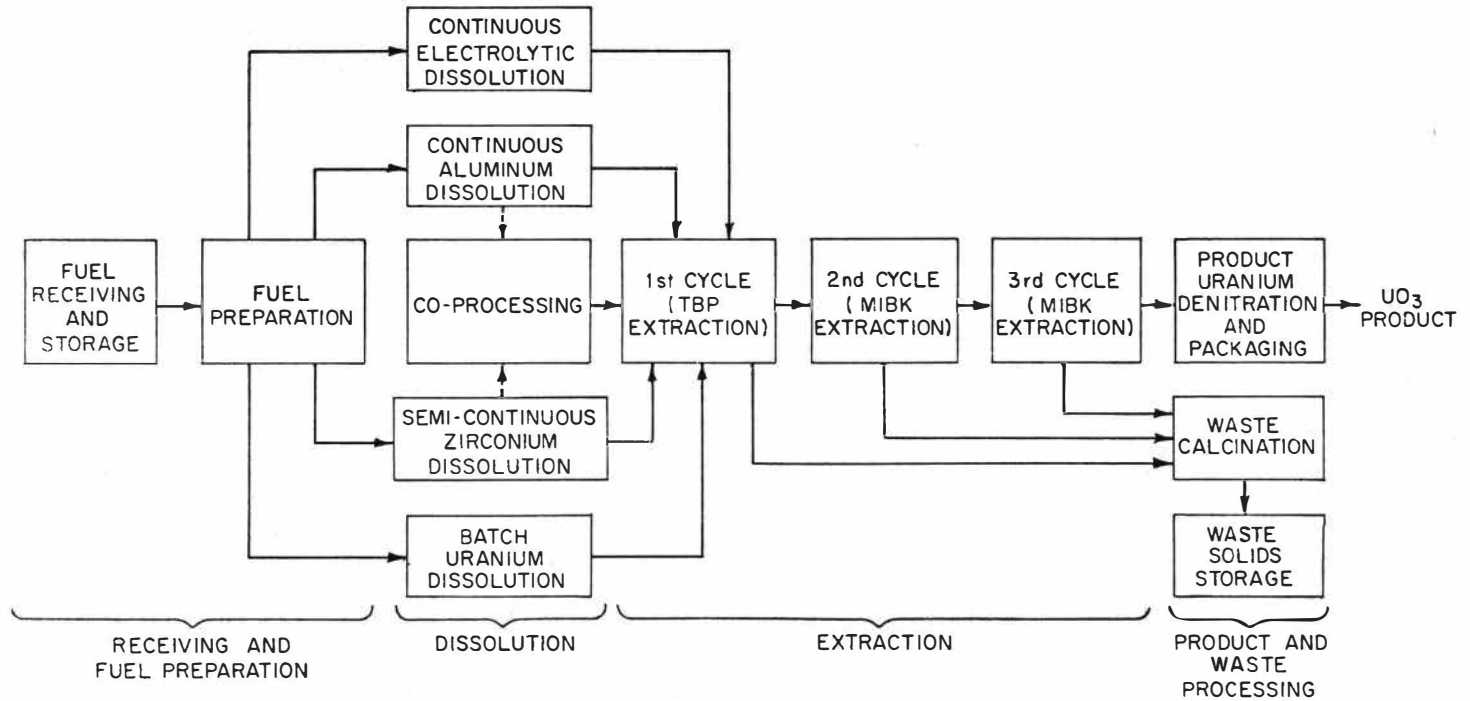
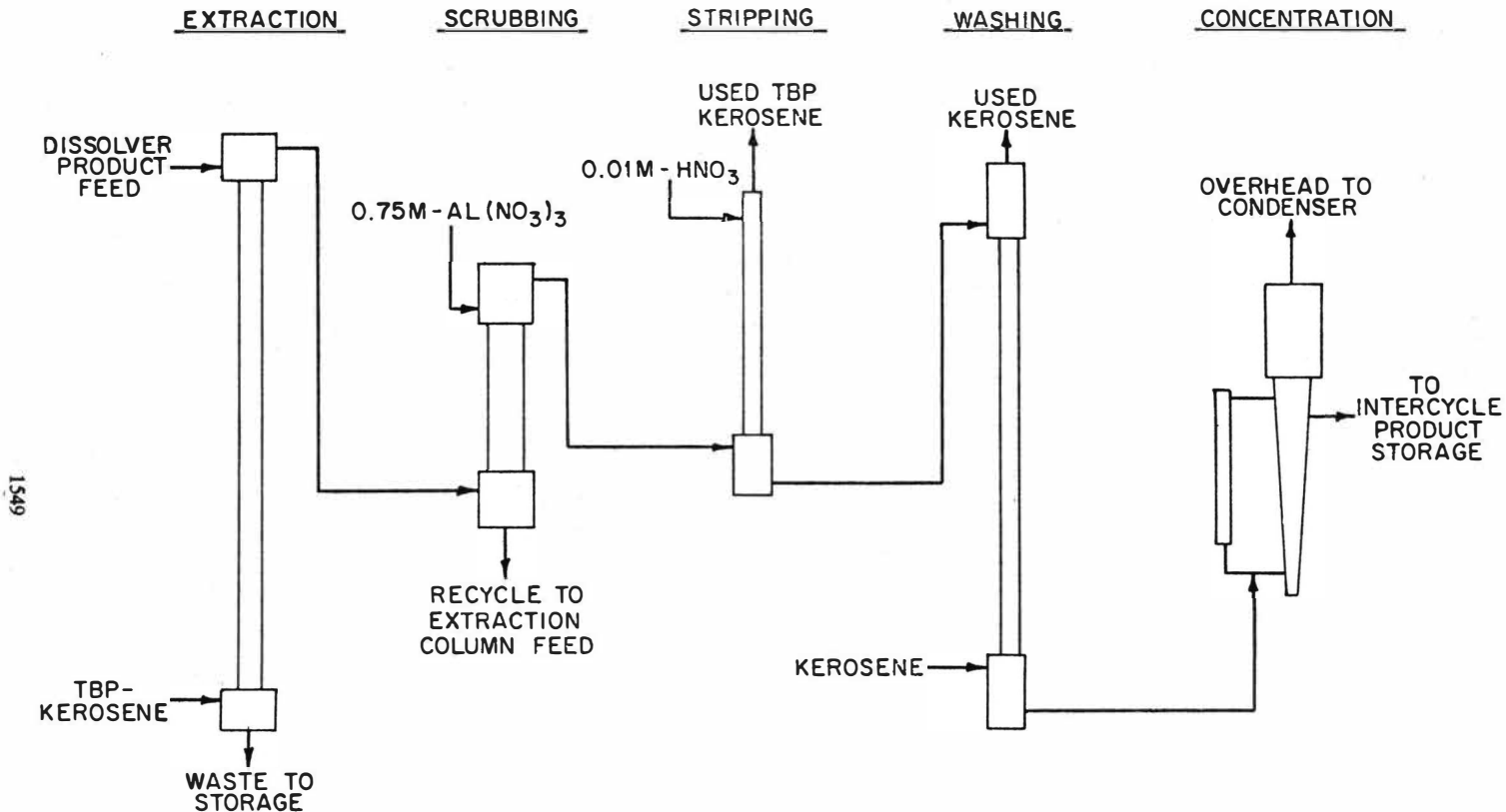
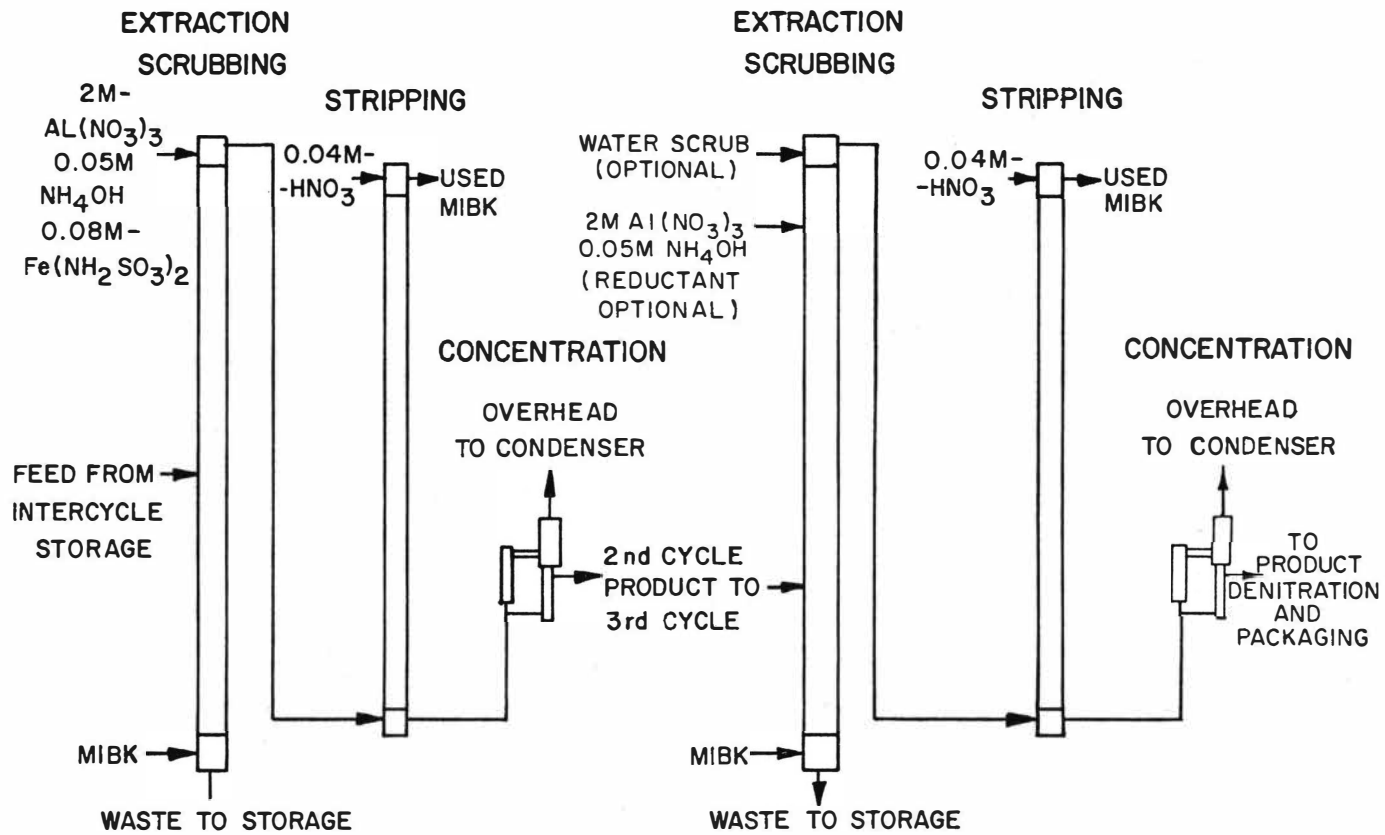


FIG.1: SCHEMATIC DIAGRAM OF ICPP FUEL AND WASTE PROCESSES



1549

FIG.2: SCHEMATIC DIAGRAM OF FIRST (TBP) EXTRACTION CYCLE



1550

FIG.3: SCHEMATIC DIAGRAM OF THE SECOND AND THIRD CYCLE (MIBK) EXTRACTION SYSTEM

ADAPTATION OF THE PUREX PROCESS TO
THE REPROCESSING OF FAST REACTOR FUELS

by

J C BOUDRY⁺⁺ and P MIQUEL⁺

ABSTRACT

The enhanced fission product content of highly irradiated fuels tends to reduce the selectivity of TBP with respect to the extraction of plutonium nitrate and uranyl nitrate. Some new improvements are required in such areas as feed clarification, the design of liquid-liquid contactors, and process chemistry.

In a process utilising existing plant, small amounts of hydrogen fluoride (HF) were added in the first extraction feed to eliminate the very bad effects due to the zirconium. This process has been in use since 1968 for the reprocessing of metallic fuels in the Marcoule plant. It has been successfully adapted for the reprocessing in the AT.1 pilot plant at La Hague of fast reactor fuels irradiated up to 80 000 MWd/t.

⁺CENTRE D'ETUDES NUCLEAIRES
Division de Chimie - Fontenay-aux-Roses (France)

⁺⁺COMMISSARIAT A L'ENERGIE ATOMIQUE
Atelier AT.1 - Centre de LA HAGUE (France)

I. INTRODUCTION

Studies related to the processing of irradiated fast reactor fuels began in France with the construction project for the experimental reactor Rapsodie. The fuel originally foreseen was a ternary U-Pu-Mo alloy, but this was abandoned in favour of the mixed oxide UO_2 - PuO_2 , clad in stainless steel, which in its composition (25-50% PuO_2 , 70-75% UO_2) is typical of fast reactor fuel save for uranium enrichment of from 60% to over 90%. It is this composition which led to the construction of a plant for the separate processing of the core fuel (1). The burn-up limit of the fuel was originally fixed at 50000 Mwd.t⁻¹, but numerous experimental assemblies were irradiated to over 80000 Mwd.t⁻¹.

The method chosen is derived from the "Purex" process, based on the separation of uranyl and plutonium nitrates by tributyl phosphate extraction. From the results obtained at the Marcoule plant and from many foreign publications, it was estimated that three extraction cycles were required to give a sufficiently decontaminated product. For reasons of simplicity we developed a process avoiding:

- (a) uranium-plutonium separation in the first cycles, although in the fast reactor programme this appears to be necessary particularly if the core and at least the axial blankets are processed simultaneously. However, this separation problem is now quite solved, notably in France, by the use of uranous nitrate, hydroxylamine nitrate or in-line electrolysis, and no purpose would have been served by trying it out in active operation;
- (b) plutonium valency adjustments, so that it is necessary to extract U(VI), Pu(IV) and Pu(VI) jointly;
- (c) concentration between cycles by evaporation requiring unacceptable capital expenditure for a small capacity plant (1 kg.d⁻¹).

The process was studied in the Chemistry Division at Fontenay-aux-Roses, in the "Cyrano" cell (2) for the tests on irradiated fuels.

The irradiated fuel processing plant (AT.1) is at the La Hague Centre. Its first tests were carried out at the beginning of 1969 and since then it has processed over 400 kg of highly irradiated fuel.

The possibility of studying in the laboratory the problems arising in the reprocessing plant made it possible to define a process particularly well suited for fast reactor fuels.

II. DISSOLUTION OF THE FUEL AND CLARIFICATION

II.1 Dissolution rate

The dissolution rates were first measured on small non-irradiated UO_2 - PuO_2 ceramic pellets as a function of:

- the PuO_2 content
- the nitric and hydrofluoric acid concentrations of the attacking solution.

The results were somewhat scattered, depending on the different batches of pellets used for these tests. Nevertheless they showed that industrial conditions could be defined so that the dissolution of the oxide would be complete in 6 hours, given:

- a PuO_2 concentration below 35%
- a nitric acid concentration higher than 8 moles litre⁻¹.

In these conditions there is no need to add hydrofluoric acid, and this proves that although a powder mixture is used, the fabrication method produces pellets composed of a fairly homogeneous solid solution.

Tests on irradiated oxides showed the dissolution rates to be considerably increased by irradiation, one of the reasons for which must be fragmentation of the irradiated oxides. During the last tests carried out in the Cyrano cell on pins irradiated to 75000 MWd.t⁻¹, it was nevertheless observed that the dissolution of the oxide, at first very fast, had to be prolonged for over 10 hours in concentrated nitric acid (11 moles l⁻¹) to achieve a sufficiently complete dissolution of the fissile matter.

II.2 Behaviour of non-gaseous fission products

Whatever the procedure, dissolution is always incomplete, leaving:

- highly corroded cladding sections devoid of fissile matter, retained in a stainless steel basket;
- residues of polymetallic alloys that are essentially composed of Mo, Ru, Rh, Pd and Tc and small amounts of uranium, plutonium and corrosion products. The weight of these non-soluble residues increases rapidly with the burn-up of the oxide as shown in Figure 1. Their considerable specific activity and their very fine particle size ($<0.5\mu$) give rise to extremely difficult problems at the clarification stage which has always proved to be necessary to avoid deposits and degradation of the solvent in the mixer-settlers (Fig 1).

II.3 Clarification of the dissolver solution

The clarification of dissolver solutions pre-diluted with normal nitric acid was first carried out with a conventional static stainless steel filter with 40μ pores. But it soon became apparent that this filter was inefficient and clogged up too often to be satisfactory. It had to be replaced by a filter with a periodical clearing system, also called "pulsed filter", the operation of which is shown schematically in Figure 2. This arrangement, comprising a filtering candle with 3μ pores, placed in a vessel fed by the solution to be filtered, was designed to avoid the irreversible migration of the particles into the pores. Filtration occurs by forward motion of the solution through the filter, periodically stopped and replaced by reverse flow to release the particles caked on the filter wall and encourage their settling. The frequency and duration of the clearing operation, as well as the flow rate of the clearing solution, are adjusted according to the characteristics and behaviour of the suspensions to be clarified.

This periodical clearing filter has given good results in the AT.1 plant and in the Cyrano cell and has enabled the most radioactive solutions and those with the highest levels of suspended solids to be clarified at a very high and fairly constant rate.

The sludges collected in the settling pot are, nevertheless, very radioactive and cause swelling and reactions very troublesome to the filtering operation. They must be removed very frequently. Their rinsing and drying give rise to problems which are difficult to solve. Attempts are now being made to improve this "pulsed filter" to make it suitable for use on an industrial scale and to compare it with centrifugal clarification.

III. EXTRACTION

III.1 Extraction diagram (Figure 3)

III.1.1 Concentration of the tributyl phosphate solvent

A concentration of 30% by volume was chosen for the following reasons:

- this is the composition for which the most experimental data were available on the distribution coefficients of uranium, plutonium and fission products;
- it is quite close to the 25 to 27% figure for which the maximum uranium yield is obtained at maximum loading in pulsed columns (3);
- since the distribution coefficient of plutonium (IV) increases with the tributyl phosphate concentration with an exponent greater than one, the greater this concentration, the smaller the ratio of the tributyl phosphate flow rate to the plutonium flow rate needed to achieve a given yield with a given number of stages. This should reduce the radiolysis of tributyl phosphate.

It was established experimentally that with the flowsheet selected there was virtually no risk of a second organic phase, since the plutonium concentrations in this phase were sufficiently far below those at which this phenomenon occurs.

The diluent used was that normally employed in France, i.e. hydrogenated tetra-propylene, commonly called "dodecane", since no comparative study has proved the superiority of any other diluent, such as normal dodecane in particular.

III.1.2 Relationships of flow rate to nitric acid concentrations

These were first determined for plutonium extraction at valency IV. As the tests proceeded, they had to be modified to allow for the formation of plutonyl nitrate by dismutation during dissolution and back-extraction, mainly in a weak acid solution. The solvent flow rates were increased, as were the nitric acid concentrations at extraction.

The plutonium extraction yields achieved during the AT.1 active tests were 99.999% in the first cycle and 99.98% for each of the next two cycles.

III.2 Behaviour of fission products during extraction

III.2.1 Degree of solvent saturation

The solvent is saturated to 55% of the theoretical limit at the end of the first cycle scrubbing, and slightly less for the following cycles. The distribution coefficients of the fission products at this value are distinctly greater than those corresponding to the extent of saturation reached during the processing of irradiated natural or slightly enriched uranium. However, this effect is offset by the higher dilution of the aqueous phases which enables a lower solvent/aqueous phase flow rate ratio to be achieved.

III.2.2 Effect of acidity

To extract the plutonium quantitatively without having to adjust the valency, we were obliged to increase the nitric acid concentrations during extraction (4N HNO₃) and scrubbing (3N HNO₃). The distribution coefficient of ruthenium is known to decrease when the acidity rises. This is all the more favourable since the ¹⁰⁶Ru yield during the fission of plutonium by fast neutrons is around 10 times greater than that achieved during the fission of uranium 235 by thermal neutrons.

The effect on rare earths is less, and the increase in their distribution coefficients can be offset by increasing the loaded solvent scrubbing rate.

It is mainly for zirconium that a high acidity is detrimental. However, at the radioactivity levels encountered in the reprocessing of fast reactor fuel, it is not the extraction of zirconium with tributyl phosphate that determines the decontamination factor for this element, but its reactions with the radiolysis products of tributyl phosphate, namely, di- and monobutyl phosphoric acids.

III.2.3 Complexing of zirconium by hydrofluoric acid

Extractors favourable to decontamination, such as pulsed columns, could not be used in the AT.1 plant and we had to resort to the "hydrofluoric acid method" to avoid precipitation of zirconium butylphosphates in the first extractor, as the processing of oxides irradiated to more than 50000 MWd.t^{-1} in mixer-settlers, without eliminating or complexing the zirconium, is quite out of the question.

This "HF method" was described at the last solvent extraction international conference (4) and has been applied with success since 1968 at the Marcoule factory.

As will be remembered it consists of adding an amount of HF to the feed, so calculated that there is no corrosion or complexing detrimental to the extraction of fissile matter.

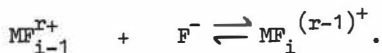
The aim in fact is to form as far as possible the inextractable complexes of zirconium (ZrF_2^{2+} , ZrF_3^+) with an amount of HF determined by consideration of the degrees of formation of the fluoro-complexes (X_M) in the aqueous phase of the extractor stages, containing the elements (U, Zr, Pu, H^+M). This X_M function represents the quantity of complexing agent (F_M) neutralised by a cation. It is linked to the product of the equilibrium constants of the fluoride addition reactions and to the concentration of ionised fluorine (F^-) by the equations:

$$(1) \quad X_M = \frac{F_M}{M} = \frac{\sum_{i=0}^n i(MF_i)}{\sum_{i=0}^n (MF_i)} = \frac{\sum_{i=0}^n i \cdot P_i (F^-)^i}{\sum_{i=0}^n P_i (F^-)^i} \equiv f(F^-)$$

where i is the number of fluoride ions in the complex MF_i

n is the maximum fluoride number per cation and

P_i the product of equilibrium constants ($P_i = K_1 \times K_2 \times K_3 \times \dots \times K_i$) of fluoride addition reactions of the type:



It was thus possible to calculate and plot the functions $X_M = f(F^-)$, and the distribution of the corresponding complexes, from the equilibrium constants given in the literature, as shown in Figure 4. These X_M functions depend on each other and are linked by definition through the formula:

$$(2) \quad F_t = (F^-)^* + X_M C_M + X_M' C_M' + \dots$$

where F_t represents the total concentration of fluoride in the medium.

Equations (1) and (2) provide the data needed to calculate the total fluoride required in the extraction for a chosen degree of complexing X_M , or conversely to calculate the value of X_M and the concentrations of the complexes ($X_M C_M$) corresponding to the total HF concentration (F_t) and the concentration C_M of the ions present.

Choice of the degree of zirconium complexing

The ZrF_3^+ complexes are extractable and in order to reach the required goal it is necessary to convert as much zirconium as possible into ZrF_2^+ .

Unfortunately the depressive effect of the complexing agent on the extraction of plutonium limits the concentration of fluoride which may be added, and in extraction this concentration must correspond to the range $1.8 < X_{Zr} < 2.2$, as shown in Figure 4.

In actual fact, in order to obtain a useful concentration of fluoride in an extractor, it is necessary to operate so as to obtain $X_{Zr} > 1.8$ in the aqueous phase at the feed stage and $X_{Zr} > 2.2$ in the more dilute stages.

To obtain these degrees of complexing, it is sometimes necessary to add aluminium with the HF in the feed, since it has practically no effect at the feed stage but on the other hand acts as a buffer in the more dilute stages.

8.

* In the theory, the fluoride is ionised only to a small extent, and the concentration (F^-) is insignificant in equation (2).

The HF is added to the feed rather than in the scrub solution to avoid its being extracted into the solvent and disseminated throughout the process. In theory it is sufficiently complexed in the extractor and in the fission product concentrator which follows to prevent corrosion. But it is, nevertheless, necessary to confine it in the concentrator and prevent its presence in the vapour phase by running a solution of aluminium nitrate down the column above the evaporator, and by maintaining low acidity (2N) through the continuous addition of formaldehyde to the boiler.

All these considerations caused us to add for instance $3.5 \times 10^{-2}M$ HF in the feed (to extractor 1) resulting from the dissolution of fuel irradiated to 80000 MWd.t⁻¹ (see Figure 3).

III.3 Decontamination results achieved

During the active tests the following results were achieved in the 1st cycle during the processing of fuel irradiated to 35-85000 MWd.t⁻¹.

$$\begin{array}{l} \text{DF (Ru)} : 5 \quad \times \quad 10^4 \\ \text{DF (Nb)} : 4.3 \quad \times \quad 10^4 \end{array}$$

The zirconium decontamination factor was such that this element could not be measured by gamma spectrometry (Ge-Li) simultaneously with the measurement of ruthenium and niobium. The next two cycles worked in more normal conditions. The UO₃ + PuO₂ oxide mixture produced contained $2.5 \times 10^{-2} \mu\text{Ci}$ of ⁹⁵Nb and $2.5 \times 10^{-2} \mu\text{Ci}$ of ¹⁰³Ru + ¹⁰⁶Ru per gram of U + Pu and this is distinctly less than the microcurie per gram required. No other gamma emitters were found.

III.4 Treatment of the solvent

In the first AT.1 cycle this is simply five stages of alkali treatment, and gives fairly good results. Not surprisingly an accumulation of ruthenium is observed.

Experiments are now being carried out with similar processes to those recommended by Schulz (5) and contactors that allow optimum contact time between alkaline phases and the solvent.

IV. CONCLUSION

In the light of the many tests effected in the Chemistry Department Laboratories at Fontenay-aux-Roses, and the satisfactory results of the active tests in the reprocessing plant for Rapsodie-irradiated fuel, it can justifiably be considered that the aqueous processing route will provide a satisfactory method for the processing of $UO_2 - PuO_2$ mixed oxides irradiated in fast reactors.

Nevertheless the studies will have to be continued to improve the process and extend its possibilities. We consider that the efforts should be directed to the search for better dissolution conditions; pre-treatments that would enable, for instance, some of the troublesome fission products to be eliminated before extraction (Zr, Ru, Nb, I, 3H); and to a treatment of the solvent which does not involve the introduction of foreign elements such as sodium into the process, with the aim of using at every point of the process clean reagents that do not give rise to an increased amount of radioactive waste.

The development of chemical processes will probably be pursued in the Cyrano cell and in the AT.1 plant, whilst new techniques (centrifuges for clarifying feed solutions, centrifugal extractors, pulsed columns, crushing-sieving for the separation of powders before dissolution, fission gas traps) will be tested in the Marcoule pilot plant by processing batches of fuel from the Rapsodie and Phenix reactors.

BIBLIOGRAPHICAL REFERENCES

- (1) P AMAURY - X TALMONT
AT1, maillon du programme d'étude de la filière surrégéné-
ratrice française.
Energie Nucleaire - Vol. 9 n° 2 Mars/avril 1967
- (2) G LEFORT - R PAQUIS
Cyranol. A new type of chemistry cell for high specific
activity at Fontenay-aux-Roses.
Proceedings of the 12th conference on remote systems
technology. ANS Nov. 1964, pp. 15-24
- (3) J DURANDET - X TALMONT
Influence de la variation des propriétés physiques sur le
fonctionnement des colonnes à pulsation.
Bulletin d'informations scientifiques et techniques n° 42
Juillet/Aout 1960
- (4) Ch BRESCHET - P MIQUEL
Improvement of the procedure used to treat highly irradiated
fuels.
Paper 195 pp. 565-576. International solvent extraction
conference La Hague April 1971. Soc. of Chemical Industry,
London.
- (5) W N SCHULZ
Macroreticular ion-exchange resin clean-up of purex process
tributylphosphate solvent.
Paper 179 pp. 175. Proceeding International Solvent
Extraction Conference La Hague 1971 - Soc. of Chemical Industry,
London.

FIGURE LEGENDS

- Fig 1 Weight of non-soluble residues in terms of the specific burn-up of fast reactor oxide fuels (Dissolution in 9N nitric acid).
- Fig 2 Flow diagram of a periodic-clearance filter.
- Fig 3 Flowsheet for the reprocessing of Rapsodie fuel (Burn-up 80000 MWd.t^{-1}).
- Fig 4 Proportions of fluoride complexes as functions of free fluoride.

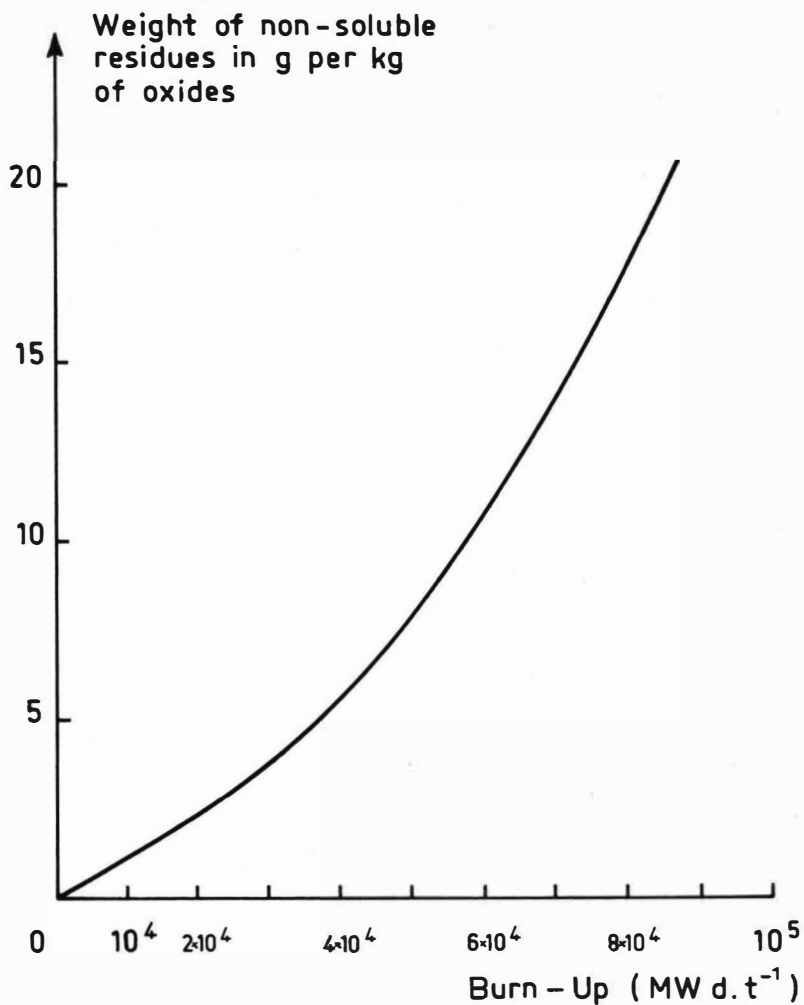


FIG. 1. WEIGHT OF NON-SOLUBLE RESIDUES

in terms of the specific burn-up of fast reactor oxide fuels (dissolution in 9 N nitric acid).

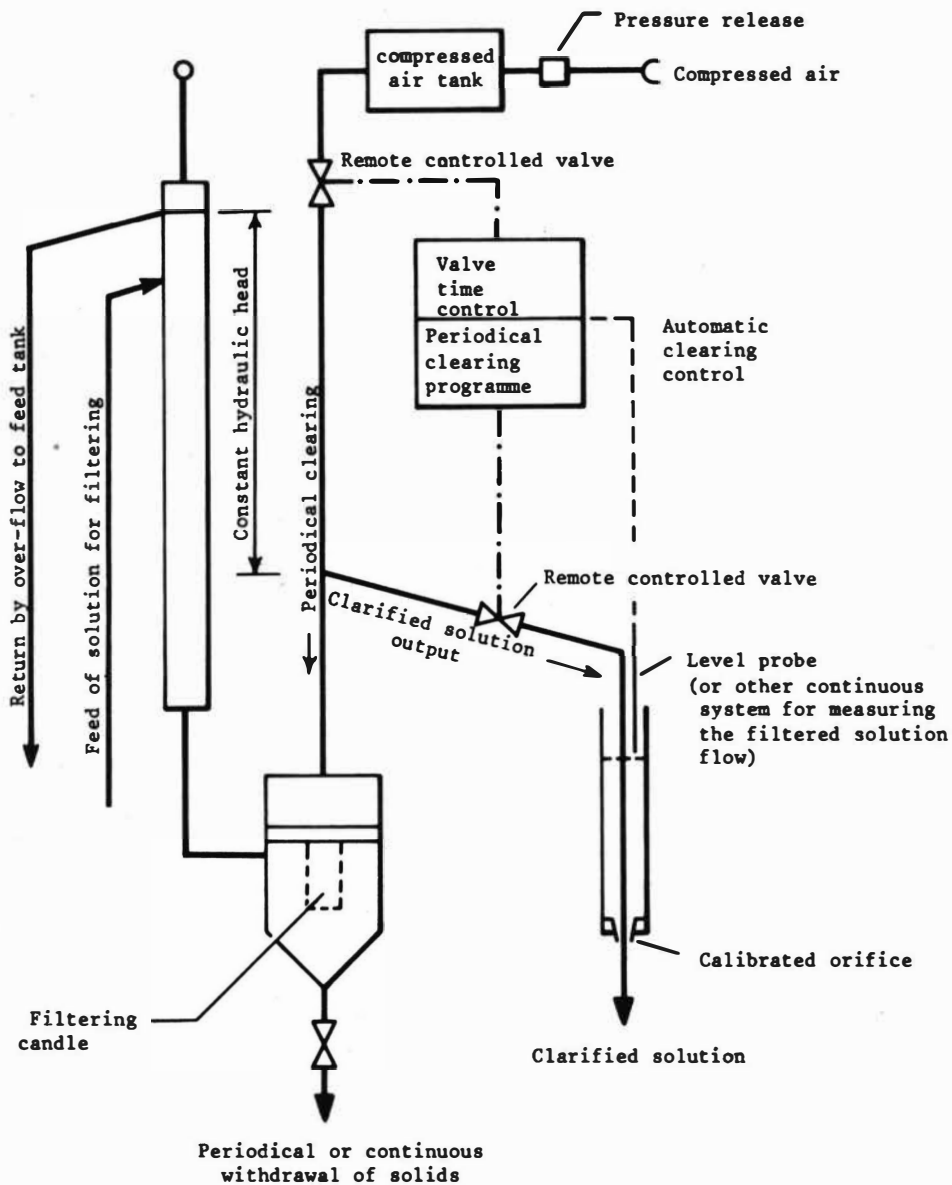


FIG. 2. FLOW DIAGRAM OF A PERIODIC-CLEARANCE FILTER.

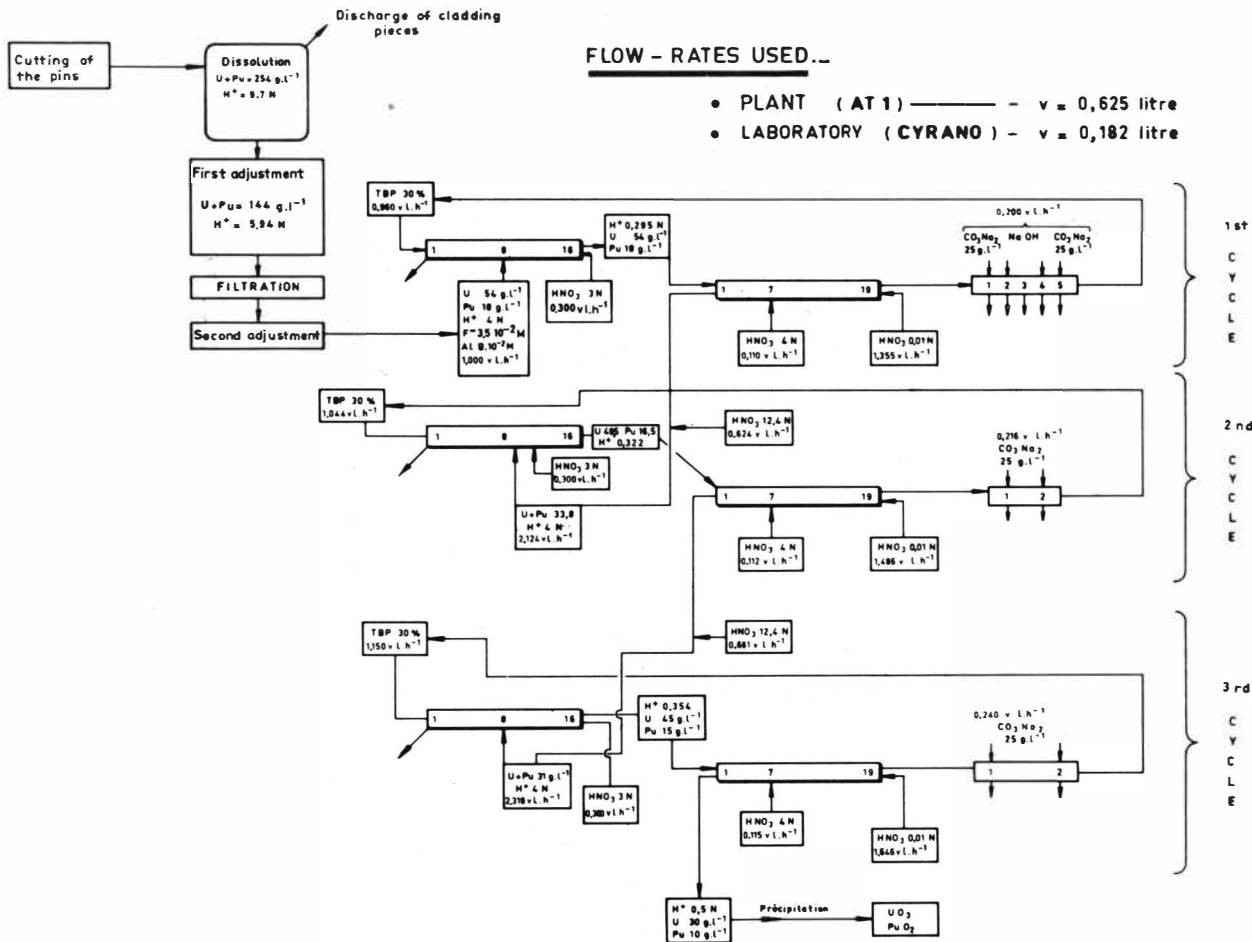


FIG. 3. FLOWSHEET FOR THE REPROCESSING OF RAPSODIE FUEL (BURN-UP 80 000 MWd. t⁻¹).

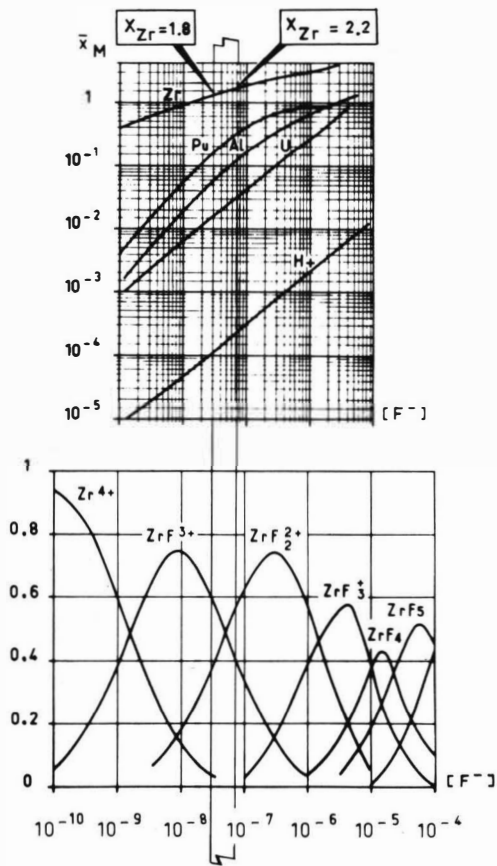


FIG. 4. PROPORTIONS OF FLUORIDE COMPLEXES AS FUNCTIONS OF FREE FLUORIDE.

SESSION 15

Wednesday 11th September : 9.00 hrs

EQUIPMENT

(Contractor Performance I)

Chairman:

Mr. A. Trambouze

Secretaries:

Dr. C.J. Mumford

Mr. H. Van. Landeghem

AIR PULSING TECHNIQUES FOR EXTRACTIOⁿ COLUMNS

R.N.I. Baird* and G.M. Ritcey**

Available techniques for air-pulsing of extraction columns are reviewed. The advantages of operating at the natural frequency of the system are described and theoretical predictions of frequency and air consumption are compared with data for a 15.3 cm diameter perforated plate column. The design of large air pulsed columns is discussed.

* McMaster University, Hamilton, Canada

** Department of Energy, Mines and Resources (mines Branch)
Ottawa, Canada

Countercurrent solvent extraction is greatly enhanced by external agitation, either in the form of rotary agitation or pulsing. The choice between the various forms of agitation has been discussed by Reman¹ and Hanson² among others and the present review will be confined to recent developments in air pulsing*. This technique is particularly applicable to large columns because of the small or even non-existent role of mechanical moving parts. With increasing emphasis on high throughputs (e.g. in the extraction of non-ferrous metals) air pulsing is expected to grow in popularity.

Historical review

Air pulsing has been practiced on a large scale for over 70 years in the coal mining industry³. In the Baum hydraulic washer, air is supplied intermittently by means of a rotary valve to a chamber communicating with a stream of water carrying coal and gangue. The resulting vertical oscillations of the suspension help to separate the coal particles from the heavier gangue.

However, pulsed solvent extraction as first proposed in 1935 by Van Dijk⁴ called for mechanical oscillation of an assembly of plates in a column. In later developments, oscillations were transmitted directly from a piston or bellows to the continuous phase in the column which contained stationary packing or plates⁵.

It was not until 1954 that Thornton⁶ pointed out the advantages of isolating the pulser from the liquid contents of the extraction column by means of an air space. Another advantage of air pulsing was the absence of cavitation problems. He pulsed two columns, 7.6 cm and 15.3 cm diameter, by means of air-driven reciprocating pistons connected to the main column by a 5 cm diameter air line. Weech and Knight⁷ successfully pulsed a 26 cm diameter column 12.4 m in height, using a pair of air injection and exhaust valves controlled by rotating cams.

* The term "air pulsing" as used in this article can be taken to include special cases where gases other than air must be used as the pulsing medium.

Design equations were presented requiring numerical (computer) solution. Air pulsing developments with pistons and rotating valves in the U.S.S.R. have been reviewed by Karpacheva et.al.⁸ Recently, Uhle⁹ has reported on an 80 cm diameter, 10 m high packed extraction column, pulsed by nitrogen via a rotary valve.

Figures 1a and 1b respectively show typical arrangements for air pulsing by means of a piston and a rotary valve.

The natural frequency of an air-pulsed column

An air-pulsed column possesses inertia due to the liquid column and compressibility due to the enclosed air space connecting the liquid phases to the pulser. Consequently it possesses a natural frequency. If the column is operated at an arbitrary frequency other than the natural frequency, it can be difficult to obtain a sinusoidal waveform. This is apparent in Figure 5 of the paper by Weech and Knight⁷. However a column being pulsed at its natural frequency will tend to oscillate sinusoidally, even if the "drive" provided is not sinusoidal. A simple analogy is that of a person on a swing, being kept in essentially sinusoidal motion by a series of short pushes applied at the end of each cycle. The advantage of a sinusoidal waveform is not significant from a mass transfer point of view, but it is reproducible for a given amplitude and frequency and it imposes a minimum of pressure surges on the column walls.

Another advantage of operating a column at its natural frequency is the saving in energy required. At the natural frequency, the air space is able to store and release energy in such a way as to help accelerate and decelerate the liquid column, so that the energy supply need only be sufficient to meet frictional losses. The air space performs the role of the "flywheel" advocated by Jealous and Johnson¹⁰ in their study of energy requirements in pulsed columns.

A case in which the set frequency coincides with the natural frequency of the system appears in Figure 6a of Thornton's early paper⁶. The pulsation amplitude attainable in the column for a given piston displacement is seen to reach a maximum at a frequency of 0.25 Hz. Unfortunately the data in the paper⁶ are not sufficient for a precise calculation of the natural frequency of the column, but the approximately calculated frequency is of the same order of magnitude as that observed.

Several workers have intentionally designed columns to operate at the natural frequency. Baird¹¹ developed a pulsed gas absorption column controlled by a solenoid valve which could be linked electrically to a liquid level sensing device. The positive feedback so obtained caused the oscillations to build up and be maintained (figure 1c). Vermijs¹² described a pulsed packed extraction column, 30 cm in diameter, in which the liquid movement was transmitted through a membrane and a mechanical linkage to the controlling air valve. Carstens et.al.¹³ have operated an oscillatory flow test tunnel at its natural frequency of 0.288Hz and obtained amplitude up to 40 cm. A "resonating pulse reactor" patented by Spence et.al.¹⁴ was driven by a piston which was carefully tuned to the natural frequency (between 0.36 and 0.62Hz) of the reactor and the accompanying gas spaces.

An air pulsing technique requiring neither a piston nor a mechanical valve has been proposed by Baird¹⁵. This is the so-called "water-blow" pulsation technique (Figure 1d). The pulse leg is provided with a small discharge orifice and air is constantly supplied to it. With proper sizing of the discharge orifice, air and liquid discharge from it alternately, and the liquid level surges up and down at the natural frequency. The behaviour of this type of column is not easily treated theoretically, but a performance correlation is available¹⁵ and a numerical simulation procedure has been developed¹⁶.

The technique has been applied¹⁷ to a simple extraction process (acetic acid from kerosene to water) in a 7.6 cm diameter packed column. It is presently being applied to a 13 m high, 5.1 cm diameter perforated plate column at the Department of Energy, Mines and Resources, Ottawa, Canada. Uranium is being extracted from an aqueous continuous to an organic dispersed phase at pulse amplitudes and frequencies in the order of 1 cm and 1 Hz respectively. A fuller report on this work will be published in due course.

Theory

The behaviour of an air pulsed column has been examined theoretically by many previous workers^{7,11,12,14,16}. It can be considered by referring to the simplified diagram in Figure 2.

The pressure and volume of the gas space between the pulser and the liquid column are taken to have time-averaged values \bar{P} and \bar{V} which corresponds to a static equilibrium, in other words \bar{P} is the sum of the atmospheric pressure and the hydrostatic head of the supported liquid column.

Now consider the conditions at some instant during the pulsation cycle. Let the displacement of the liquid column from equilibrium be v . The gas space volume at that instant is then effectively $(\bar{V} - v_1 + v)$ and the gas pressure can be found from the equation of state of the gas:

$$\bar{P} \bar{V}^r = P(\bar{V} - v_1 + v)^r \quad (1)$$

where the exponent r can vary between 1 (for isothermal gas behaviour) and c_p/c_v (for adiabatic gas behaviour). If the volume displacements are small compared to \bar{V} , the above equation can be written:

$$P - \bar{P} = r\bar{P} (v_1 - v)/\bar{V} \quad (2)$$

This excess pressure can be equated to the sum of three terms representing the change in head due to the liquid displacement, the frictional pressure drop due to the rate of displacement and the inertial pressure drop due to the acceleration in the rate of displacement.

$$r \bar{P}(v_1 - v)/\bar{V} = g v (\rho_s / s_s + \rho_c / s_c) + R |\dot{v}| \dot{v} + \ddot{v} (\rho_s H_s / s_s + \rho_c H_c / s_c + \rho_p H_p / s_p) \dots \dots \dots \mathbf{3}$$

The liquid column is considered as three different regions, the pulse leg, the unpacked portion of the main column and the packed portion of the main column, denoted respectively by subscripts S, C and P. The liquid density may differ in each part of the column because of the effect of the dispersed phase holdup. The effective cross-sectional area of the packed portion of the column is less than the total cross-sectional area¹² and this is also the case for perforated plate columns and baffled columns¹⁸. The frictional constant R has the units Nm⁻⁸s⁻², it being assumed that energy is dissipated in turbulent flow. R depends not only on the height and nature of the packing, but on the configuration of the pulse leg (elbows, enlargements, etc).

For a given column geometry and liquid-liquid system, equation (3) can be expressed in the simple form:

$$k_1 \ddot{v} + k_2 |\dot{v}| \dot{v} + k_3 v = v_1 \tag{4}$$

This resembles the well known equation for the response of an electrical circuit to an applied voltage, except that the damping term is not linear in v. Weech and Knight⁷ derived a similar equation except that the right hand term was the air pressure in the pulse leg, rather than the column displacement as in equation (4). The general solution of such an equation necessitates the use of a computer⁷, but a more explicit solution is possible for a system operating at the natural frequency.

Consider a liquid column oscillating sinusoidally with a volume displacement amplitude of v' .

$$v = v' \sin \omega t \quad (5)$$

At the natural frequency, given by

$$\omega = (k_2/k_1)^{1/2} \quad (6)$$

the first and third terms in equation (4) cancel out and it becomes:

$$k_2 (v')^2 \cos^2 \omega t = v_1 \quad (7)$$

This gives the interesting result that a squared sine wave function is necessary to generate sinusoidal liquid oscillations; However it has been found experimentally¹⁹ that an essentially sinusoidal liquid motion can be generated by an air pulser with a switched valve which alternately injects and exhausts air to and from the pulse leg., equivalent to a saw-toothed waveform for v_1 . The volume of air V_c admitted to the air space by an air pulsing system in one cycle is the difference between the maximum and minimum values of v_1 :

$$V_c = 2k_2 (v')^2 = 2R\bar{V} (v')^2 / r\bar{P} \quad (8)$$

The volumetric air flow rate, brought to atmospheric pressure, is given by

$$Q_A = V_c \bar{P} / (2 P_A) = R\bar{V}^3 (v')^2 / r P_A \quad (9)$$

This equation resembles that obtained by Vermijs,¹² by a different route, for the case where $r = 1$ (isothermal gas behaviour). However, observation¹¹ suggests that adiabatic behaviour, with $r = 1.4$ for air, is a more realistic approximation. The natural frequency is given from equation (6) as

$$f = \frac{1}{2\pi} \left[\frac{r\bar{P}/\bar{V} + g(\rho_s/s_s + \rho_c/s_c)}{\rho_s^H/s_s + \rho_c^H/s_c + \rho_p^H/s_p} \right] \quad (10)$$

Case Study

To illustrate the use of equations (9) and (10), some data has been obtained with a 15.3 cm nominal diameter extraction column that has recently been constructed at the University of Queensland, Australia. The column is shown schematically in Figure 3 and the main parameters are listed in Table 1. The continuous phase was water (at zero throughput in this case) and the dispersed phase was kerosene flowing at a superficial velocity of 0.3 cm s^{-1} . Air pulsing was carried out by means of a 3-way solenoid valve (3.2 mm orifice triggered by a photorelay attached to the pulse leg. The exhaust air from the solenoid valve normally flowed to a vacuum line, but in the present tests it was discharged at atmospheric pressure and measured by collection in an inverted water-filled graduate cylinder.

Two operating frequencies were established by using different average volumes \bar{V} , namely 3.1 and 19.9 l. The larger volume was obtained by connecting an air-filled bottle to the pulse leg without altering any of the other system parameters shown in Table 1. The observed frequencies at the two values of \bar{V} were respectively 1.37 and 0.655 Hz. The frequencies calculated from equation (10) were respectively 1.366 and 0.668 Hz.

Some air consumption data at the two frequencies is shown in Figure 4. In applying equation (9) it was necessary to evaluate the resistance factor R and the data in Perry²⁰ were used. It was assumed that the open area of the perforated plates had an orifice coefficients of 0.75, whence their contribution to R was found to be $2.6 \times 10^8 \text{ Nm}^{-8} \text{ s}^{-2}$. The pulsing leg contains a long radius elbow, a tee junction and a step enlargement to the main column diameter. It was estimated²⁰ that these losses amounted to 2.85 velocity heads, corresponding to a pulse leg contribution of $4.3 \times 10^{-8} \text{ Nm}^{-8} \text{ s}^{-2}$. Thus the total resistance R is $6.9 \times 10^8 \text{ Nm}^{-8} \text{ s}^{-2}$.

This value of R was substituted in equation (9) which was then used to calculate the air consumption as a function of the superficial amplitude (v'/S_c) in the main column. Figure 4 shows that the measured air consumption tends to agree with equation (9) at the highest amplitudes but is greater at low amplitudes. The slope of the logarithmic plot is experimentally about 1.6 as against 2.0 predicted from equation (9). It is thought that these discrepancies are due to laminar drag effects in the pulse lag; such effects would become less important as the pulse amplitude is increased.

Design of large air-pulsed columns

The largest air-pulsed column reported in the literature⁹ has a diameter of 80 cm but there seems to be no reason why the technique should not be used in even larger sizes. However there are certain design aspects which become increasingly important as the size and therefore costs of a column are increased.

The major recommendation is that the column should be operated at its natural frequency. The advantages are:

Minimum energy and air consumption for given pulse intensity
Sinusoidal and therefore reproducible and smooth waveform
Energy and air requirements easy to predict

The designer as faced with a choice of methods of operating the column at its natural frequency. A self-triggered control system such as that shown in Figure 3 will always ensure operation at the natural frequency. However a large air control valve would need to be pilot operated and the control system would require an automatic shut-off in case of failure of one of the components. The same criticism applies to the mechanically linked system proposed by Vermijis¹². Fane and Alfredson²¹ have recently reviewed air pulsing techniques for nuclear fuel reprocessing plants, and the possible maintenance problems with self-triggering systems^{11,12} were the main reason for their preference for a rotary valve drive for the pulser, as described by Weech and Knight.⁷

The advantages of operating at the natural frequency can be combined with the reliability of a rotary air valve if the frequency of rotation is carefully adjusted to coincide with the natural frequency of the system. Alternatively, the expense of a variable speed motor for the rotary valve can be avoided by tuning the air-pulsed column itself to the frequency at which the valve is driven. This could be done by connecting to the air space a surge vessel, the effective volume of which could be varied at will by the addition or removal of a suitable non-volatile liquid.

The simplest air-pulsing system, involving no moving parts or valves, is the "water-blow" system (Fig. 1d). Although considerable development work is still needed, the development costs might be more than offset by the savings in valves and other components.

A comment has been made²² about hydraulic nonuniformity in large pulsed columns. There seems to be no specific published evidence that nonuniformity of the pulse itself is a problem, but in large diameter columns there is a tendency towards channeling of the dispersed phase²³, which can be remedied by the inclusion of distributor baffles.

For obvious reasons of cost and space, the pulse leg is made narrower than the main column: pulse leg to column diameter ratios have been reported between 0.29⁷ and 0.5⁹. However if the pulse leg is very narrow, the velocities in it can become so large that frictional losses in the pulse leg can exceed those in the main column (for example, see Case Study). Losses can be reduced by the use of long radius bends, diffusers, etc., but the most effective parameter is the pulse leg diameter. For a given design, there will be an optimum diameter determined by a balance between higher frictional losses at small diameters and higher piping costs and space requirements at large diameter ratios. A possible approach might be to abandon the traditional pulse leg concept and build the air space as an annulus around the base of the main column¹⁷.

Acknowledgement

One of us (M.H.I.B.) is grateful to the University of Queensland for financial support while this article was being prepared.

LIST OF SYMBOLS

c_p	specific heat of gas at constant pressure
c_v	specific heat of gas at constant volume
f	frequency
g	acceleration due to gravity
H	liquid column length
k_1	constant in equation (4)
k_2	constant in equation (4)
k_3	constant in equation (4)
P	pressure
P_A	atmospheric pressure
\bar{P}_A	time-average air space pressure
Q_A	air flow at atmospheric pressure
T	exponent in equation of state
R	resistance constant, see equation (3)
S	cross-sectional area
v	volume displacement of liquid column free from equilibrium
v'	extreme value of v
v_1	volume displacement due to pulser
V_c	volume of air admitted to system in one cycle
\bar{V}	time-average volume of air space

Greek

ρ	liquid density
ω	angular frequency = $2\pi f$

Subscripts

S	denotes pulse leg
P	denotes packing or plates
C	denotes unobstructed portion of main column

References

1. Reman, G.K., Chem.Eng.Progr., 1966, 62, (9), 56
2. Hanson, C., Chem.Engng., 1968, 75, (18), 76
3. Hughes, H.W., "A Text-Book of Coal-Mining" p539, 5th Edn., 1904 (London: Charles Griffin and Co.)
4. Van Dijck, W.J.D., U.S. Pat., 2 011 186 (Aug. 13, 1935)
5. Sege, G. and Woodfield, F.W., Chem.Eng.Progr., 1954, 50,396
6. Thornton, J.D., Chem.Eng.Progr.Symp.Ser., 1954, 50 (13), 39
7. Weech, M.E. and Knight, B.E., Ind.Eng.Chem.Proc.Des.Devel. 1967, 6, 480
8. Karpacheva, C.M., Zakharov, E.N., Raginskii, P.C. and Muratov, B.M., "Pulsating Extractors", 1964 (Moscow: Atomizdat)
9. Uhle, K., Chem.Ing.Tech., 1970, 42, 841.
10. Jealous, A.C., and Johnson H.F., Ind.Eng.Chem., 1955, 47, 1159
11. Baird, M.H.I., Proc.Joint A.I.Ch.E./I.Chem.E.Symp., Lond., 1965 (6), 53.
12. Vermijs, W.J.W., Proc.Joint A.I.Ch.E./I.Chem.E.Symp.,Lond., 1965 (6), 98
13. Carstens, M.R., Neilson, F.M. and Altinbilek, H.D., Tech. Memo Coastal Res.Centre, Washington, 1969, No.28
14. Spence, S.P., Marshall W.R., and Steen, H.W., U.S.Pat. 3 167 395 (Jan 26, 1965)
15. Baird, M.H.I., Brit.Chem.Eng. 1967, 12, 1877
16. Milburn, C.R. and Baird, M.H.I., Ind.Eng.Chem.Proc.Des.Dev., 1970, 2, 629
17. Baird, M.H.I., Gloyne A.R., and Meghani, M.A.N., Can.J. Chem.Eng., 1968, 46, 249.

18. Baird, M.H.I. and Garstang, J.H., Chem.Eng.Sci., 1967, 22, 1663.
19. Garstang, J.H., Ph.D.Thesis, University of Edinburgh, 1970
20. Perry, J.H., (ed) "Chemical Engineers' Handbook" p5-32, 4th Edn., 1964 (New York: McGraw Hill)
21. Fane, A.G. and Alfredson, P.G., Aust.At.Energy.Common. Rept., 1970, No.AAEC/TM547.
22. Akell, R.B., Chem.Eng.Progr., 1966, 62 (9), 50
23. Woodfield, F.W. and Sege, G., Chem.Eng.Progr.Symp. Ser., 1954, 50, (13), 14.

Table 1: Air Pulsed Column Parameters

$$H_s = 1.14 \text{ m} \quad S_s = 18.2 \text{ cm}^2 \quad \rho_s = 1000 \text{ Kg/m}^3$$

$$*H_c = 1.00 \text{ m} \quad S_c = 179.3 \text{ cm}^2 \quad \rho_c = 1000 \text{ Kg/m}^3$$

$$H_p = 1.50 \text{ m} \quad * S_p = 109.3 \text{ cm}^2 \quad \dagger \rho_p = 980 \text{ Kg/m}^3$$

$$\bar{P} = 1.20 \times 10^5 \text{ N/m}^2 \quad P_A = 10^5 \text{ N/m}^2$$

$$\bar{V} = 3.1 \text{ l or } 19.9 \text{ l}$$

$$r = 1.4 \text{ (assumed)}$$

Number of perforated plates : 56

Perforation diameter: 14.3 mm

Percentage open area : 61%

* Calculated as "water equivalent" height with correction for density of upper kerosene layer.

* Taken as the open area of the column

† A kerosene holdup of 10% is assumed

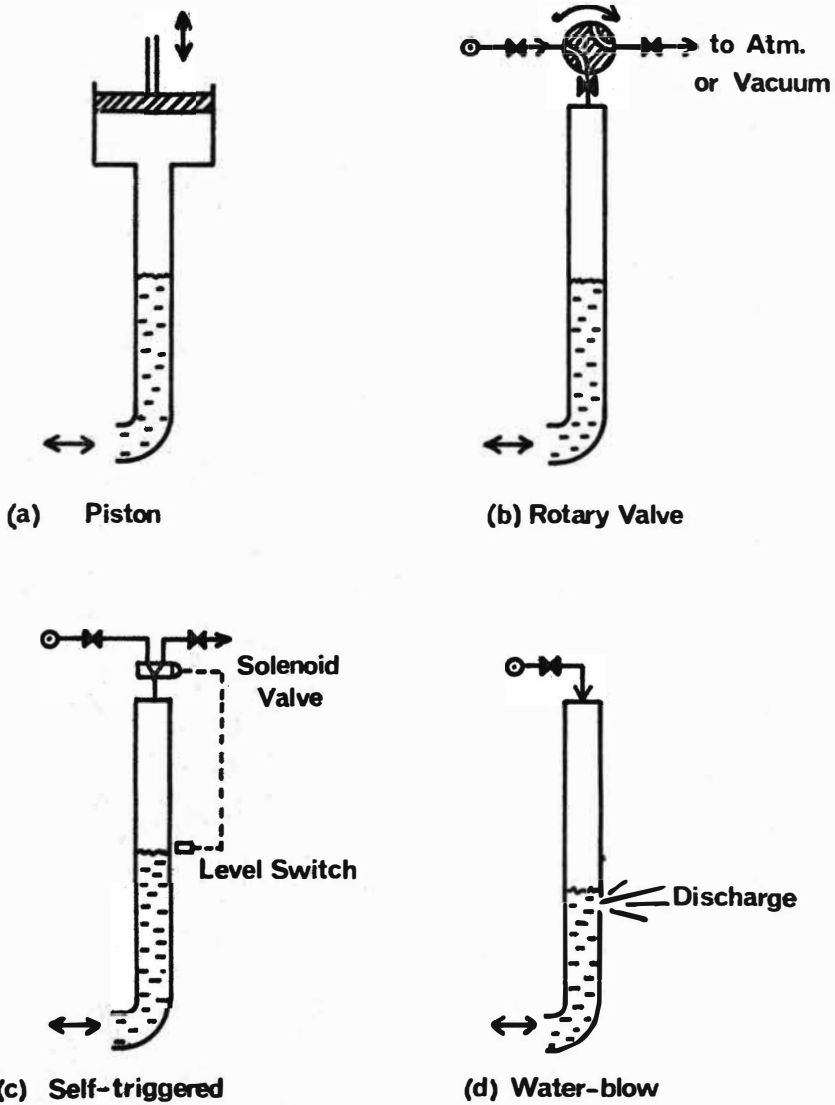


Figure 1 Air pulsing methods (detail of pulse leg only)

- (a) Piston
- (b) Rotary valve
- (c) Self-triggered
- (d) Water-blow

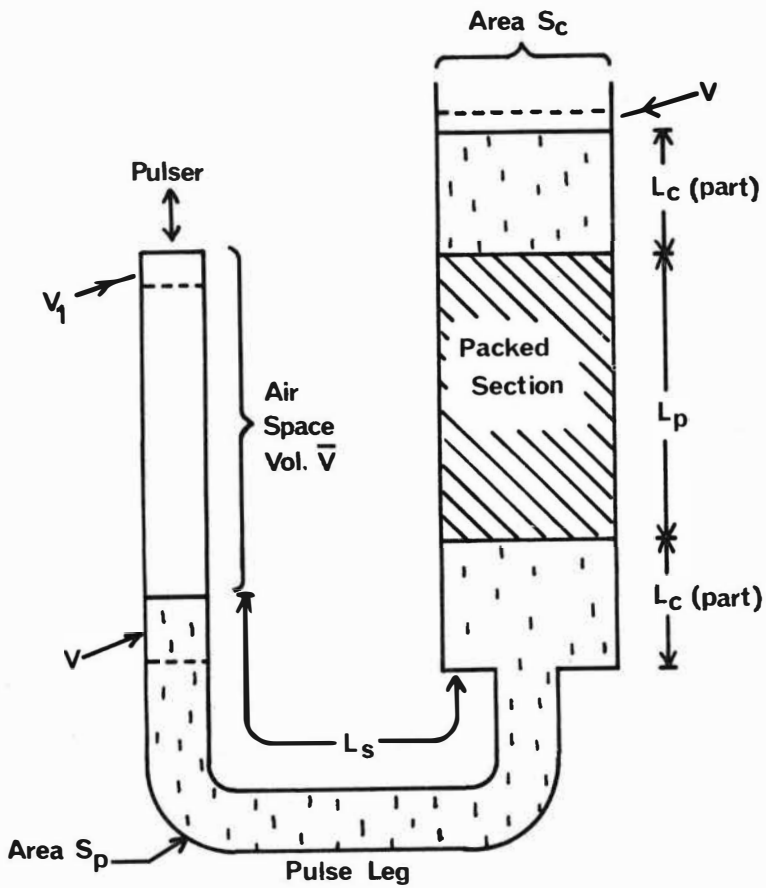


Figure 2 Theoretical model of pulsed column



liquid phases



displaced interface positions

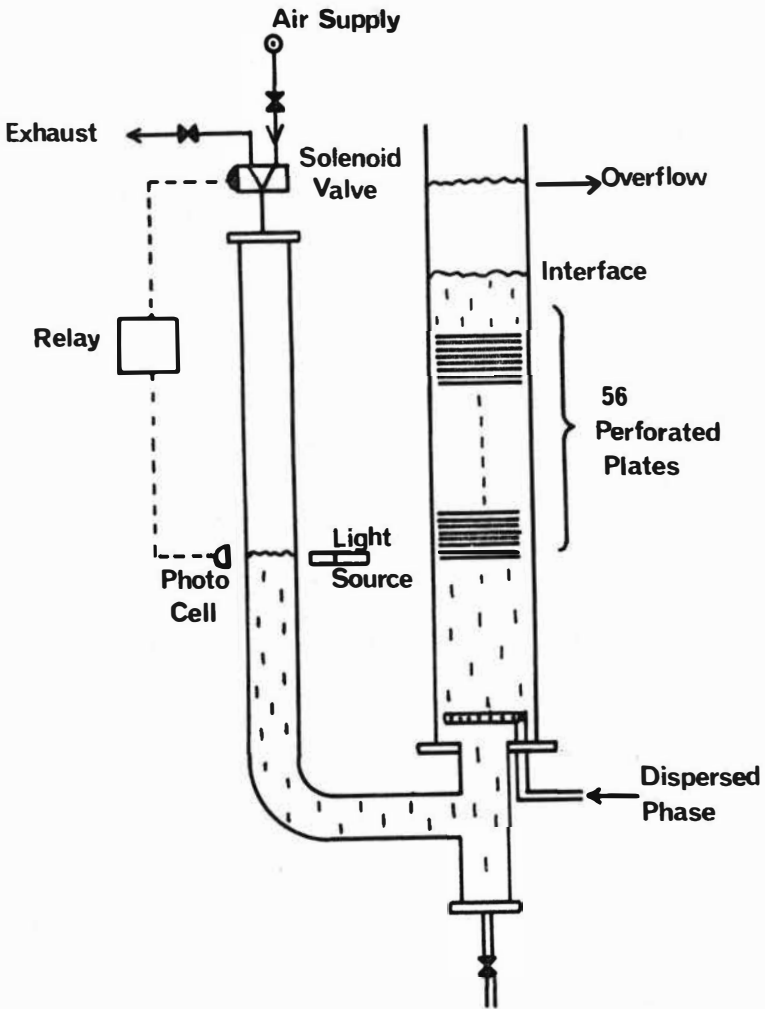


Figure 3 15.3 cm diameter perforated plate column

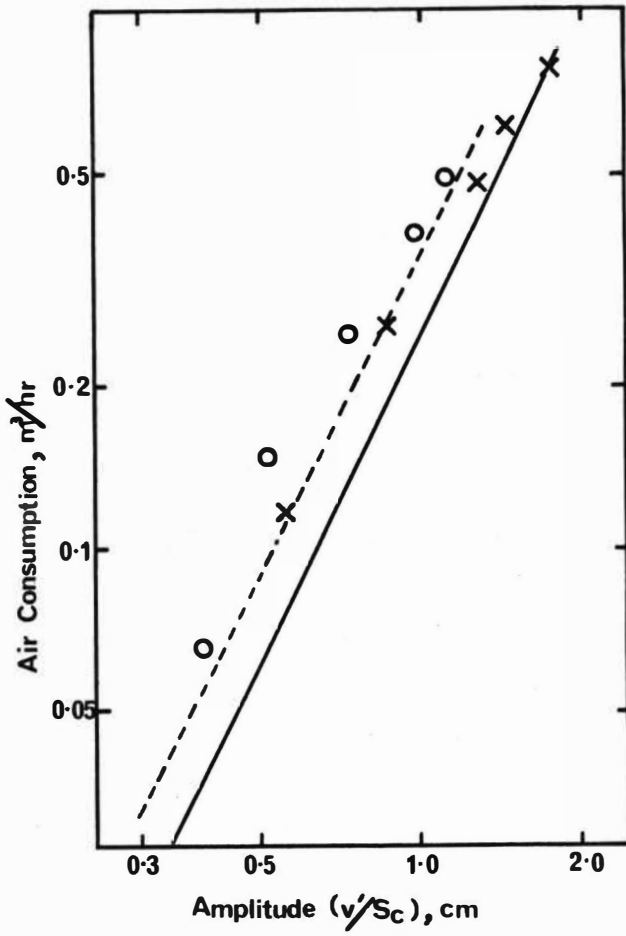


Figure 4 Air consumption data and theory

At 0.655 Hz, data x, theory ———

At 1.37 Hz, data o, theory - - - - -

The Effect of Wetting Characteristics
upon the Performance of a Rotating
Disc Contactor

C. J. Mumford and A.A.A. Al-Hemiri

A 4 inch diameter, 6 feet high R.D.C. was used to investigate droplet hydrodynamics and mass transfer efficiencies with a range of 5 liquid-liquid systems.

Hold-up and volumetric capacity were found to vary with operating parameters as previously reported. Axial point hold-ups were determined directly and correlated by,

$$x = \left(0.0013N + 0.38(V_d - 1)\right) (h-h^2) + 0.076 (1-1/V_d)$$

Mean drop size decreased with column height and the results were correlated by,

$$d_{32}/R = 4.7 \times 10^{17} \left(\frac{NR^2 \rho_c}{\mu_c}\right)^{-3.33} \left(\frac{\mu_d}{\mu_c}\right)^{0.23} \left(\frac{NR \mu_c}{\sigma_i}\right)^{2.0} \left(\text{EXP}.0.4 \left(\frac{n}{z}\right)^{0.225}\right)$$

Correlations of similar form were obtained with discs selected to be 'wetted' by the dispersed phase and with 'wetted' cones. The latter novel design employed polypropylene cones to eliminate the dispersed liquid vortex produced by enhanced coalescence when solute transfer was out of this phase. Original observations were made of phase inversion in countercurrent contact; this phenomenon was used to characterise limiting capacities.

Mass transfer data were interpreted by comparing observed mass transfer coefficients with values calculated assuming the oscillating drop model. Although different coalescence-redispersion mechanisms pertained, disc-wetting properties had no significant effect on efficiency. Compared to non-mass transfer operation, axial mixing in both phases was greatly reduced when transfer was from the dispersed to the continuous phase, because of enhanced coalescence, and greater with transfer in the opposite direction due to inhibition.

Department of Chemical Engineering
 University of Aston in Birmingham

INTRODUCTION

The terms 'wetting' and 'non-wetting' are generally used to describe whether or not a liquid spreads on a particular solid surface. For a solid adsorbed surface film the spreading coefficient is given by,

$$S_{C(S)} = \gamma_S - \gamma_{SL} - \gamma_{LV} \quad 1$$

where γ_{SV} , γ_{SL} and γ_{LV} denote the solid-gas, solid-liquid and liquid-gas interfacial tensions respectively.

In many instances when a liquid is placed upon a surface it will not completely wet it, but remain as a drop exhibiting a definite contact angle between the liquid and the solid. The spreading coefficient is defined in terms of the contact angle and the surface tension of the liquid (1, 2).

$$S_{C(SV)} = \gamma_{LV}(\cos \theta - 1) \quad 2$$

Thus for a liquid to spread as a very thin film on a solid surface, i.e. condition for a positive spreading coefficient, θ is finite. γ_{SL} and γ_{LV} should be as small as possible in order to achieve good spreading. This may be promoted by the addition of a surfactant to the liquid (3). Alternatively, the liquid and solid may be chosen such that spreading will occur.

A difference has been observed between the advancing and receding contact angles. Generally, however, wetting means that the contact angle is zero, and non-wetting represents an angle greater than 90° . High surface energy materials, e.g. most metals and glass, are wetted by liquids with a high surface tension such as water whilst low surface energy materials, e.g. plastics, are wetted by liquids with low surface tension including most organic liquids.

Since efficiency of mass transfer in any liquid-liquid extractor is dependent upon interfacial area and the turbulence in either or both of the phases, the degree of wetting exhibited by contactor internals, i.e. walls, stators, packings or rotors may have a significant effect. However studies summarised in Table 1. have yielded conflicting results. It is generally accepted nevertheless that best efficiency is obtained when the

Type of extractor		Dispersed phase	Transfer direction	Types & wettability of internals	Efficiency	Ref
Perforated plate column	Toluene-Diethylamine	Water	d → C	Metal plates	Low	4
		Water	d ← C	Metal plates	Low	
		Water	d → C	Polyethylene plates	High	
		Water	d ← C	Polyethylene plates	High	
Pulsed sieve plate column	Ketone-Acetic acid Water	Water	d → C	S. Steel plates	Low	9
		Water	d → C	Polyethylene plates	Low	
		Water	d ← C	Polyethylene plates	High	
		Water	d ← C	Alternating s. steel & polyethylene plate	Moderate	
Packed column	_____	_____	d ↔ C	Dispersed phase wetted packing	Low	10
			d ↔ C	Continuous phase wetted packing	High	11 12
Packed column	_____	Aqueous	_____	Dis. or Cont. phase wetted packing	High	13
		Non-aqueous	_____	Dis. or Cont. phase wetted packing	Low	
Packed column	MIBK-acetic acid-water	Either	MIBK → water	plastic packing	High	14
			MIBK → water	ceramic packing	Low	
			MIBK ← water	plastic packing	Low	
			MIBK ← water	ceramic packing	High	
Pulsed packed column	Toluene-Benzoic acid-water	Toluene	d → C	Polyethylene packing	High	15
		Toluene	d → C	Unglazed ceramic	Low	
		Toluene	d → C	Alternating bands of polyethylene & ceramic packing	Moderate	
Pulsed plate column				Dispersed phase wetted plates	Low	16
				Continuous phase wetted plates	High	
Pulsed plate column				Dispersed phase wetted plates	Low	17
				Continuous phase wetted plates	High	
				"Dual plates"	Moderate	

TABLE 1. Summary of Published Data

continuous phase wets the internals. (3, 4, 5, 6).

Thus in a Rotating Disc Contactor with dispersed phase wetted internals, Davies et al (3) showed that the transfer rate of phenol from dispersed water to a kerosine phase was less than that achieved using a conventional R.D.C. Under normal conditions a uniform dispersion of small droplets is obtainable rather than the films and globules produced by coalescence of dispersed phase on the wetted internals. However it has been suggested that an R.D.C. with selected internals, e.g. rotors, wetted by the dispersed phase could be more efficient when the dispersed phase film resistance is controlling (5) since at low flow rates of the dispersed phase extremely small droplets may be formed from the tip of the wetted disc in a manner similar to that described for disc atomizers (7) and rotating cups (8).

A reduction in the volumetric capacity of an R.D.C. with wetted discs has been reported(5, 18).

This result is contrary to that which would be expected at low disc speeds since the increased coalescence promoted by the wetting effect should result in bigger drops having higher settling velocities.

In the Scheibel and Oldshue-Rushton column sections the wettability of the turbine agitator was not important. The use of wetted mesh packing in the Scheibel column produced a pool of the dispersed phase over the packing and very small drops in the agitated compartment at conditions prior to flooding. At lower hold-ups drop phenomena were similar to those for non-wetted packings (5).

It has frequently been observed that preferential wetting of the column internals by the continuous phase deteriorated with time. This resulted in a change in the mode of operation of the equipment, possibly at the expense of extraction efficiency. The effects were noted in a laboratory scale Pulsed Plate column by Coggan (15), who observed different types of dispersions at different times.

In a later study using an aqueous continuous phase and organic dispersions in R.D.C., Scheibel column and Oldshue-Rushton column sections, a variation was observed in the wetting properties (in the form of increased coalescence of the dispersed phase) on the glass and stainless steel column internals. This was attributed to the deposition of dirt or impurities on the column internals (5).

Any distributor plate should preferentially be wetted by the continuous phase to produce a continuous stream of drops of fairly constant size. In a study of the formation of droplets from a circular orifice at varying contact angles Haynes et al (19) found that as the contact angle was increased, i.e. the dispersed phase wetted the plate, the dispersed phase tended to spread along the plate surface and form relatively large droplets before breaking away under the action of gravity. Conversely liquids with small contact angles formed from the orifice without spreading. Thus for organic droplets formed from an orifice an increase in size up to 10 fold has been reported for p.t.f.e. compared with metal plates (19).

There is no published data on the effect of wettability of the column internals on the drop size distribution although it has been generally observed that large globules formed by a drip point mechanism from static wetted internals (5, 16). In practice the tendency for dispersed phase coalescence is influenced by the direction of solute transfer.

On the basis of the above, the behaviour of an R.D.C. in which the discs were wetted by the dispersed phase appeared to be of practical significance. This study set out to investigate the magnitude of wetting phenomena and their effect on hydrodynamics and mass transfer in a pilot scale R.D.C. In the event enhanced coalescence under specific conditions described later resulted in large drops and a liquid vortex beneath each disc. Therefore a novel design of rotor in the form of a dispersed phase wetted (polypropylene) cone was introduced to displace and disperse the vortex.

EQUIPMENT & LIQUID SYSTEMS

A flow diagram of the equipment, comprising a 4 inch diameter pilot scale glass R.D.C. with 19 compartments each 2 inches high, is shown in Figure 1. The diameter of the discs was 2 inches and of the stator rings 3 inches in accordance with normal designs (21, 22). Five sampling points were provided at 9 inch intervals along the column; additional sampling points were provided at each of the respective inlets and outlets of the two phases. The stator rings were of stainless steel and were precision machined to obtain a close fit at the column walls; they were supported by means of

3 equispaced pieces of 1/24 inch stainless steel wire. The discs were fabricated from either 1/16 inch stainless steel or p.t.f.e. and had straight edges.

The heavy phase which was the continuous phase in all cases, was introduced into the column at a point just above the top compartment, and left via a bottom outlet. The dispersed phase entered the column via a brass or stainless steel distributor plate designed to Treybal's recommendations (6). The rotors were driven by a 1/4 H.P. (0-3000 r.p.m.) A.C. motor shaft via a flexible rubber joint. The other end was attached via a flexible drive to a permanent tachometer mounted on the control panel and the speed was controlled by means of a voltage regulator.

The liquids could be recirculated to any one or between two, of 4, 50 liter reservoir vessels using by-passes on the transfer pumps.

The systems used are listed in Table 2.

Table 2 Systems Studied

System	
1.	Toluene - Water
2.	Liquid paraffin - water
3.	Toluene-(60% Glycerine) water
4.	(25% Toluene) Liquid paraffin-water
5.	(37% Toluene) Liquid paraffin-water
6.	Toluene-Acetone-Water
7.	Liquid Paraffin-M.E.K.-Water

EXPERIMENTAL PROCEDURES & RESULTS

The method used to determine average values of hold-up involved operating the column under the desired conditions and when steady state was reached rapidly closing the inlet and outlet valves, (23, 24). After stopping the agitator and allowing complete phase separation the height of the dispersed phase below a previously marked interface, and the overall operating height of the column, were measured by reference to a fixed graticule.

To determine the variation of hold-up along the column axis point hold-up measurements were made using a sampling tube positioned at a point midway between the rotor and upper stator and between $S/2$ and $R/2$ from the centre. (25).

In this work flooding was characterised by the complete rejection of the dispersed phase as a dense layer of droplets. Flooding rates were determined by establishing steady conditions at a fixed rotor speed and then increasing the flow of the dispersed phase slowly, with the continuous flow rate kept constant, until flooding occurred. The assessment of flooding points presented greatest difficulty in the wetted disc and cone columns. Since dispersed phase was ejected from these rotors as a dense sheet, which in turn disintegrated into large drops possessing high relative velocities, little or no drop rejection occurred from the mixed section. Therefore in these cases the criterion for maximum capacity was taken as the point at which 'phase inversion' first occurred. Phase inversion rates were determined in a similar manner to flooding rates, i.e. fixing the rotor speed and continuous phase flow then slowly increasing the dispersed phase flow rate until phase inversion occurred. This was characterised by the continuous phase becoming dispersed and vice versa.

Preliminary observations confirmed that as reported by other workers (5, 24, 26), drop size distribution was not directly affected by continuous phase flow rate. Therefore observation and photography of droplet phenomena and drop sizes without mass transfer were carried out with a stationary continuous phase. For each condition two or three photographs were taken after hydrodynamic equilibrium was attained. The criterion for equilibrium was taken as a steady interface level and its attainment normally required about 5 minutes. Drop size measurements were taken from prints with approximately $2 \times$ magnification. A Carl Zeiss Particle Size Analyser TG.Z. 3(27) and an S.P.R.I.

Particle Size Analyser Type II (28) were used to count and measure droplets. Ellipsoids were recorded as spheres of equivalent diameter.

DISCUSSION OF RESULTS

Hold-up

In general hold-up increased with increasing dispersed phase flowrate with all the systems and designs used. The results are plotted in Figs. 2, 3, and 4.

'Wetted' disc, viz. p.t.f.e. and polypropylene cone columns gave lower hold-up values than the 'non-wetted' disc columns. This was expected since coalescence was enhanced by the 'wetted rotors' and thus larger drops with higher terminal velocities were produced.

The variation of hold-up along the column was in agreement with the earlier findings of Rod (29) and Strand et al (30), i.e. hold-up increased to a maximum value at a point approximately midway up the column and subsequently decreased. The accuracy of point hold-up values was found however to be dependent on the position of the sampling tube, wettability of the column internals and homogeneity of the dispersion. Therefore, since average hold-up values do not differ greatly from the mean of the "point" hold-ups, it would appear that many practical difficulties can be avoided by considering average rather than point hold-ups. Contrary to this Strand et al and other workers have stressed the importance of 'point' hold-up measurements for better mass transfer predictions (29, 30). However close examination of the data of the two former authors and that obtained in this study tends to support the argument proposed here. Excluding the top and bottom points, all points in the column had approximately equal hold-up values (20). The low values at the two extreme points were due to end effects, viz. the presence of larger drops with higher terminal velocities than for the characteristic size in the rest of the column.

Rod (29) suggested a design modification to increase the hold-ups at these points.

Theoretically hold-up profiles would be expected to follow drop size profiles. The data suggest therefore that the characteristic drop size first decreased to a minimum value at a point corresponding to a maximum hold-up value and then increased towards the exit. This however was found not to be the case and the drop size decreased progressively up the column.

The point hold-up results were reasonably correlated by Equation 3 arrived at by means of simple extrapolation.

$$x = \left(0.0013N + 0.38(V_d - 1) \right) (h - h^2) + 0.076 \left(\frac{1}{V_d} \right) \quad 3.$$

Mass transfer runs were performed with the systems toluene-acetone-water and liquid paraffin-MEK-water with the solutes acetone and MEK giving a distribution coefficient of 0.75 and 0.5 respectively.

The column was operated with flow rates between 50% and 60% of those causing flooding under non-mass transfer conditions, as recommended by Treybal (6). Both directions of transfer were investigated. In all but a few cases the initial raffinate concentration was approximately 10% by weight and the initial extract concentration was between 0-0.5%.

After steady conditions were reached, normally after 15 mins., 10 to 20 c.c.s. samples were taken from sample ports at the respective phase outlets. The samples were analyzed by measuring their refractive indices using an ABBE A 60 refractometer. Separate runs were carried out to determine the operating lines, by analysing samples taken from the five sample ports along the column and the inlet and outlet concentrations of the respective phases.

In mass transfer runs, higher hold-up values were observed when the direction of transfer was from the continuous to the dispersed phase, than for the opposite direction of transfer. This was attributable to the different rates of coalescence for the different transfer directions, i.e., for $d \rightarrow C$, increased coalescence caused the mean drop diameter to increase and the residence time to be shorter resulting in lower hold-ups. For $d \leftarrow C$, the reduction, or absence of, coalescence resulted in smaller drops with longer residence times, and hence higher values of hold-up.

Clearly, therefore, hold-up values obtained under non-mass transfer conditions should not be used to predict practical values during mass transfer. However for the case $d \leftarrow c$, hold-up values are only about 10 - 15% higher than those for non-mass transfer runs. Hold-up values obtained for $d \rightarrow c$ were in most cases about half of those obtained for non-mass transfer runs. The above findings were generally the same irrespective of the rotors wetting properties, suggesting that the different break-up mechanisms and droplet behaviour resulting from the different directions of mass transfer override the effect of rotor wettability.

Flooding

With either p.t.f.e. discs or cone columns it was not possible to characterise flooding as normally defined because of enhanced coalescence. In practice however increase in dispersed phase flow rate beyond a certain value for a given continuous phase flow rate led to the former becoming continuous, i.e. "phase inversion. Therefore for columns with wetted rotors the phenomena of "phase inversion" was taken to define limiting capacities. This was possible with the system toluene-water. With liquid paraffin-water however the column flooded; the flooding rates were approximately the same whether or not the rotors were 'wetted'. This was attributed to the fact that the later system was inherently difficult to coalesce. The onset of phase inversion occurred in the bottom compartment giving rise to a very large 'slug', possessing a high terminal velocity, which travelled up the column and eventually dispersed in higher compartments. This phenomenon was indicated by the increased intensity of a non-surfactant dye added to the dispersed phase. Typical 'flooding' and 'phase inversion' data for the various designs and systems are given in Figs. 5, 6, 7 & 8. A model was developed to provide a criteria for the onset of phase inversion and this is described elsewhere (20, 31).

Flooding rates in the presence of mass transfer in the direction $d \rightarrow c$ were higher than, or similar to, those for non-mass transfer runs with the same systems. For transfer in the direction $c \rightarrow d$ however lower flooding rates were obtained in accordance with the observed reduction in mean drop diameter.

Typical results are reproduced in Fig. 9.

Mechanisms of Droplet Break-up and Drop-Size Distribution

Generally droplet break-up on the "non-wetted" disc occurred by a discrete drop undergoing deformations and finally break-up due to velocity gradients at the tip of the disc. At low rotor speeds, e.g. $Re < 2.15 \times 10^4$, few drops were observed to break-up by collision with the edge of the stator.

With the "wetted" discs and cones, drops coalesced on the "wetted" rotor surface and redispersion followed by two different mechanisms similar to those described by Hinze (32) and Dombrowski et al. (33).

These were,

- (i) drip point, which occurred at the rotors tip, at dispersed phase flow rates approximately $< 0.1 \text{ cm s}^{-1}$.
- (ii) from the periphery of the sheet; this generally occurred at dispersed phase flow rates $> 0.1 \text{ cm s}^{-1}$.

Whilst this was true for the "easy coalescing" system, toluene-water, ($\sigma = 34.1 \text{ dynes/cm}$ and $\mu_d = 0.6 \text{ c.p.}$) discrete drop break-up at the disc's tip was the predominant mechanism with the more "difficult coalescing" system, viz. liquid paraffin-water, ($\sigma = 50 \text{ dynes/cm}$ and $\mu_d = 170 \text{ c.p.}$) irrespective of the wetting characteristics of the rotor. However, with p.t.f.e. discs little of the liquid paraffin coalesced on the disc particularly at low rotor speeds viz. $Re < 2.5 \times 10^4$ so that drip point formation occurred. At higher rotor speeds increased hold-up prevented visual observation. Other systems used in this section of the work are listed in Table 2.

Under mass-transfer conditions the mechanisms of drop break-up were practically independent of the rotor's wetting properties but strongly dependent upon the direction of mass transfer. Break-up was by sheet or drip point formation for the case $d \rightarrow c$ and by discrete drop break-up at the tip of the disc for $d \leftarrow c$. The different mechanisms of

droplet break-up are illustrated in Fig. 10. Though less obvious with the liquid-paraffin M.E.K. - water system, increased coalescence was detected for the case $d \rightarrow c$ by the reduction of axial mixing. Axial mixing was present in non-mass transfer runs and was made worse by transfer in the direction liquid paraffin \leftarrow water. d_{32} decreased with increasing column height.

Experimental values of d_{32} were compared with those obtained using the correlations of Misk (34). Although all experimentation was in the transition region, for which $10^4 < Re < 6 \times 10^4$, all three correlations were considered. None of the correlations gave reasonable agreement with experimental d_{32} values. In general d_{32} values were much greater than values predicted from Equations for the turbulent and transition regions respectively and much smaller than those from the laminar region correlation.

The poor performance of these correlations was not surprising since they take no account of the variation of d_{32} with column height, dispersed phase flow rate and hold-up. Therefore a correlation, for d_{32} , was developed to take account of these factors considering d_{32} as a function of the physical properties of the system, the operating conditions and the column geometry. The correlation is given by:

$$\frac{d_{32}}{R} = 4.7 \times 10^{117} \left(\frac{NR^2 \rho_c}{\mu_c} \right)^{-3.33} \left(\frac{\mu_d}{\mu_c} \right)^{0.23} \left(\frac{NR \mu_c}{\sigma_i} \right)^{2.0} (X)^{0.225} \left(\text{EXP } 0.40 \left(\frac{H}{Z} \right) \right) \quad (4)$$

Values of d_{32} for non-mass transfer runs were generally larger than those for the case $d \leftarrow c$ and lower than those $d \rightarrow c$. This was expected and can again be attributed to the reduction, or absence of, coalescence in the former case and its increase in the latter.

Correlation of Mass Transfer Data

Two different operating mechanisms were observed in the column dependent upon direction of mass transfer. With transfer dispersed \rightarrow continuous phase, coalescence was promoted giving rise to vortex and sheet formation and hence conditions of repeated coalescence and redispersion. For the opposite direction of transfer,

i.e. continuous \rightarrow dispersed phase, coalescence was greatly reduced and the column operated as a discrete drop contactor. The two different operating mechanisms are illustrated in Fig. 10. The effect of transfer direction on coalescence caused by the change in interfacial gradient, i.e. coalescence is reduced or promoted dependent upon whether this gradient is negative or positive (35) was fully discussed elsewhere (20). Vortex and sheet formation was only observed in the case of the "easy coalescing" system, toluene acetone-water. In the case of the "difficult-coalescing" system, liquid-paraffin-MEK-water, vortex and sheet formation did not occur. However the increase in coalescence for the case paraffin \rightarrow water was detected by the substantial reduction in axial mixing and entrainment which occurred under non-moss transfer conditions and with the opposite direction of mass transfer. The above findings may be of practical significance since axial mixing can be substantially reduced by the appropriate choice of which phase is dispersed and the direction of mass transfer. The experimental data were interpreted in terms of an overall mass transfer coefficient, K_{exp} . This was then compared with theoretical values assuming the oscillating drop model using diffusivities calculated by the Wilke-Chang (36) correlation. Although this has not been tested for high viscosity liquids, e.g. liquid paraffin, it is considered to be the most reliable correlation.

The oscillating drop coefficient varied between 1.1 and 34 times K_{exp} for the system liquid paraffin-MEK-water irrespective of transfer direction. This wide range may be because the "difficult coalescing" drops of high viscosity, persist as small discrete drops which are more likely to circulate or be stagnant than oscillate; with the second system, viz. toluene-acetone-water larger drops were produced. Thus the oscillating drop coefficient K_o , was in this case closer to K_{exp} .

In the disc columns, the values of K_{exp}/K_o were greater in the case toluene-water than water-toluene. This may be attributable to the surface area estimation by photography which may not give accurate representation of the effective transfer area. Dependent upon the mechanism of mass transfer the effective interfacial area may be larger or smaller than actually suggested by photographs. Therefore either photography is not a sufficiently accurate method of area estimation or the mass transfer mechanisms differed. For example, in one case, viz. toluene-water, a 'surface renewal' mechanism existed whilst in the other case, a different mechanism might be postulated e.g., a process of surface ageing'. Thus a higher transfer coefficient was observed in the former case.

Replacement of the discs by cones eliminated the liquid vortex and sheet and resulted in reduction in drop size for the case toluene-water. For the cone column d_{32} values for toluene \rightarrow water

were in most cases comparable to those for the case water \rightarrow toluene. Thus the ratios K_{exp}/K_o are comparable for both transfer directions.

It is concluded from the above that, under practical conditions, the rotor "wettability" had no significant effect upon mass transfer efficiency. This is confirmed by Fig. 11 in which the mass transfer coefficients for wetted and non-wetted rotors are of similar magnitude under given conditions.

However at rotor speeds well below the practical range, viz. < 300 r.p.m., the drops coalesced with and then broke off the wetted discs. This phenomenon illustrated in Fig. 12 may have been the cause of some misleading expectations (5) at higher speeds where the short contact time between the drop and disc does not allow coalescence to take place.

CONCLUSIONS

It has been shown that drop size and volumetric capacity measurements made under mass transfer conditions may differ greatly from those under non-mass transfer conditions. Furthermore these measurements are dependent upon the direction of interfacial tension increase with solute concentrations; in the one case coalescence is increased, thus increasing the drop size and capacity but in the other case solute transfer results in reduced coalescence and subsequently drop size and capacity. With most common systems the former case occurs when the transfer direction is from the dispersed to continuous phase and the later one occurs for the opposite direction. The main conclusions are:

1. Non-Mass Transfer Studies

- (i) Drop size Correlation - The effect which the main parameters, viz. interfacial tension, density difference, hold-up and rotor speed have upon drop size was confirmed. However the following factors also affected d_{32} .
 - a - Dispersed phase viscosity. An increase in μ_d resulted in lower rates of break-up (and coalescence) thus increasing the mean drop size.
 - b - Column height - The mean drop size produced in any compartment decreased with increasing number of the compartment from the dispersed phase inlet.
 - c - Disc wettability - d_{32} was larger for wetted than for non-wetted discs, particularly at lower rotor speeds.

- (ii) Axial hold-up Profile - The results obtained in this study confirm the earlier findings of Rod (79) and Strand et al (74), i.e. hold-up increased to a maximum value at about half way up the column and then decreased towards the top.

- (iii) Limiting Capacity - The phenomenon of phase inversion was found to be a better criteria to define limiting capacity than the rather ambiguous flooding phenomena. Phase inversion occurred first in the bottom compartment and travelled upwards until other compartments reached their inversion hold-up. Extraction columns can be operated efficiently near

the maximum capacity limits so defined without the loss in efficiency formerly believed to occur due to the apparent reduction in surface area caused by the increase in coalescence frequency.

2. Mass Transfer Study

(i) Effect of Wetting - No significant difference was observed between the efficiency of wetted and non-wetted disc columns. The mode of column operation was mainly dependent on the mass transfer direction and rotor speed.

(ii) Direction of Mass Transfer - With the systems studied transfer from the dispersed to continuous phase enhanced coalescence and transfer in the opposite direction reduced it. The former mechanism improved mass transfer and substantially reduced axial mixing. Therefore the proper selection of transfer direction should provide improved mass transfer efficiencies in practical extractors.

Nomenclature

d_{32}	Sauter mean drop diameter	L
D_D	Dispersed phase diffusivity	$L^2 T^{-1}$
h	Dimensionless column height	
n	Number of compartments	
N	RPM	T^{-1}
Pe	Peclet number = $\frac{ud_{32}}{D_D}$	
R	Disc diameter	L
Re	Reynolds number	
Sc	Spreading coefficient	
u	Drop velocity	LT^{-1}
V	Volumetric flow rate	$L^3 T^{-1}$
x	point hold-up	
X	Overall average hold-up	
Z	Total number of compartments	

Greek Letters

ρ	Density	ML^{-3}
μ	Viscosity	$ML^{-1} T^{-1}$
σ_i	Interfacial tension	MT^{-2}
γ	Surface tension	MT^{-2}
θ	Contact angle	

Subscripts

d	dispersed phase
c	continuous phase
LV	Liquid-vapour
SL	Solid-liquid
SV	solid-vapour

References

1. Adamson, A.W., Physical Chemistry of Surfaces, Interscience Publishers, Inc. 1960
2. Osipow, L.I. "Surface Chemistry" Reinhold Publishing Corp. 1962
3. Davies, J.T. et al. Trans. Instn. Chem. Engrs. 38, 331, (1960)
4. Garner, F.H., S.R.M. Ellis and J.W. Hill, A.I.Ch.E. Journal 1, 185, (1955) and Trans.Instn.Chem.Engrs. 34, 223, (1956)
5. Mumford, C.J., Ph.D. Thesis, University of Aston (1970)
6. Treybal, R.E., Liquid Extraction, 2nd Edition (1963) McGraw-Hill
7. Friedman, S.J., Gluckert, F.A. and Marshall Jr. W.R., Chem.Eng.Prag. 48, 181 (1952)
8. Fraser, R.P., Dombrowski, N. and Routley, J.H. Chem.Eng.Sci., 18, 323, (1968)
9. Sobic, R.H. and D.M. Himmelblau, A.I.Ch.E. Journal 6, 619 (1960)
10. Appel, F.J. and Elgin, J.C. Ind.Eng.Chem., 29, 451 (1937)
11. Meisner, H.P. Stokes, C.A., Hunter, C.M. and Morrow, G.M. Ind.Eng.Chem. 36, 917 (1944)
12. Treybal, R.E. Ind.Eng.Chem. 51, 262 (1960)
13. Berg, C., Manders, M. and Switzer R., Am.Inst.Chem.Engr., Los Angeles Calif., March 9, 1949
14. Osmon, F.O. and Himmelblau, D.M. Journal of Chemical Engineering Data, 6, 551 (1961)
15. Jackson, M.L., Holman, K.L. and Grove, D.B., A.I.Ch.E. Journal 8, 659 (1962)
16. Coggan, G.C., Instn. of Chem.Engrs. Symp. on Liquid-Liquid Extraction, April, 1967
17. Sege, G. and Woodfield, F.M. Chem.Eng.Progr. 50, 396 (1954)
18. Misek, T. Chem.Eng. 68, 58 (1961) and Czechoslovakian Patent No. 88, 415 A.R.D. Extractor-Technoexport, Prague and Luqa (U.K.) Literature
19. Haynes, L.G., D.M. Himmelblau and R.S. Schechter, I. & E.C. Process Design and Development, 7, 508 (1968)

20. Al-Hemiri, A.A.A., Ph.D. Thesis, University of Aston, 1973
21. Reman, G.H. and Olney, R.B., Chem.Eng.Prog., 51, 141, (1955)
22. Misek, T. Rotacni Diskove Extraktory, Statni Nakadelstri Literatury, Prague 1964
23. Logsdail, D.H., Thornton, J.D. and Pratt, H.R.C., Trans.Instr. Chem.Eng. 35, 301 (1957)
24. Misek, T., Coll.Czech.Chem.Comm. 28, 1631, (1963)
25. Kung, E.Y., and Bekmann, R.B., A.I.Ch.E. Journal, 7, 319 (1961)
26. Honekemp, J.R. and L.E. Burkhardt, Ind.Eng.Chem.Proc.Design and Dev., 1, 3, 177, (1962)
27. Carl Zeiss, Oberkochen/wuertt, West Germany
28. Sondes Place Research Institute, Dorking Surrey, U.K.
29. Rod, V., Paper Presented at 3rd International Congress on Chem.Eng., Marianske Lazne, Sept. 1969, and Brit.Chem.Eng., 16, 617 (1971)
30. Strand, C.P., Olney, R.B. and Ackerman, G.H., A.I.Ch.E. Journal 8, 525, (1962)
31. Al-Hemiri, A.A.A., and Mumford, C.J. to be published
32. Hinze, J.O., A.I.Ch.E. Journal 1, 289 (1955)
33. Dombrowski, N. and Johns, W.R. Chem.Eng.Sci., 18, 203, (1963)
34. Misek, T. Coll.Czech.Chem.Comm., 28, 426 and 570, (1963)
35. McFerrin, A.R. and R.R. Davison, A.I.Ch.E. Jour. 17, 1021, (1971)
36. Wilke, C.R. and Pin Chang, A.I.Ch.E. Jour. 1, 264 (1955)

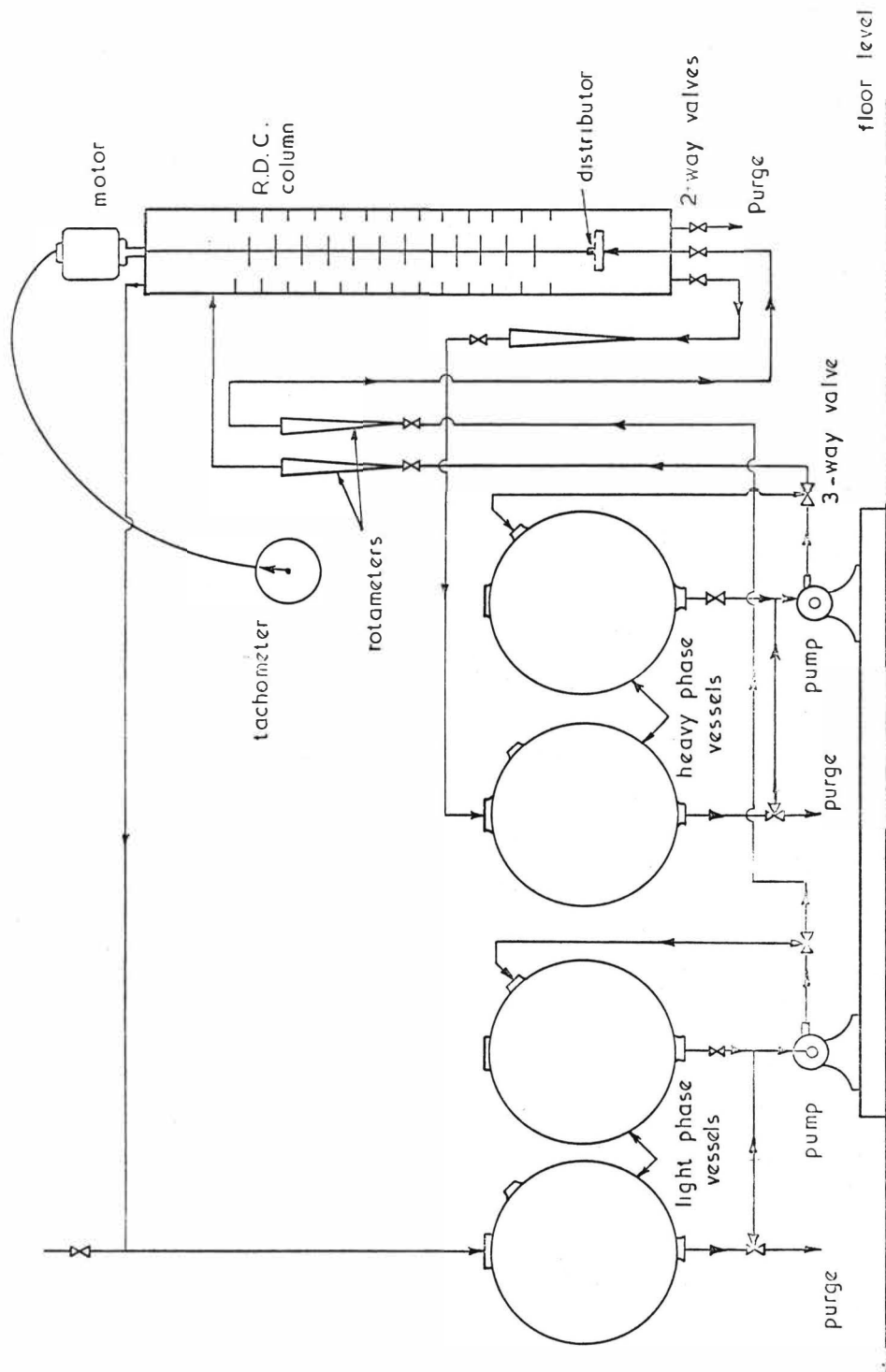


Fig. 1. Flow diagram

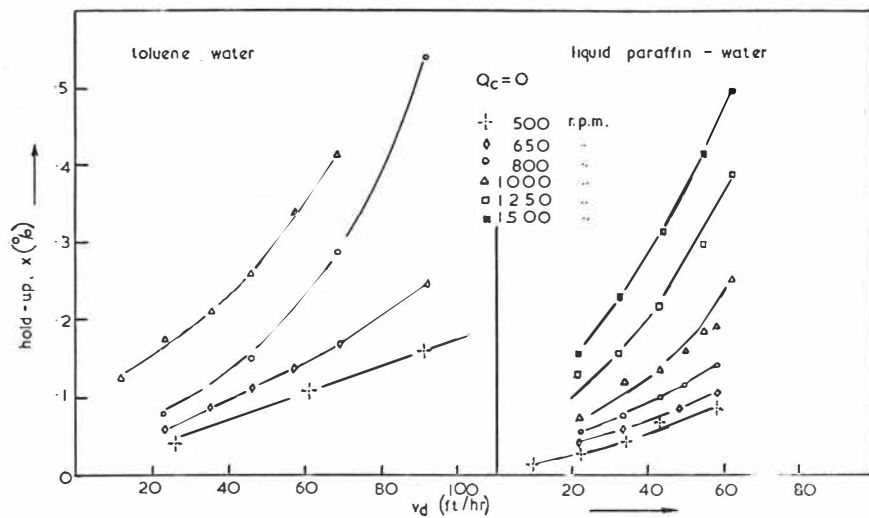


Fig. 2. Hold-up vs. dispersed phase flow rate in an rdc with stainless steel discs

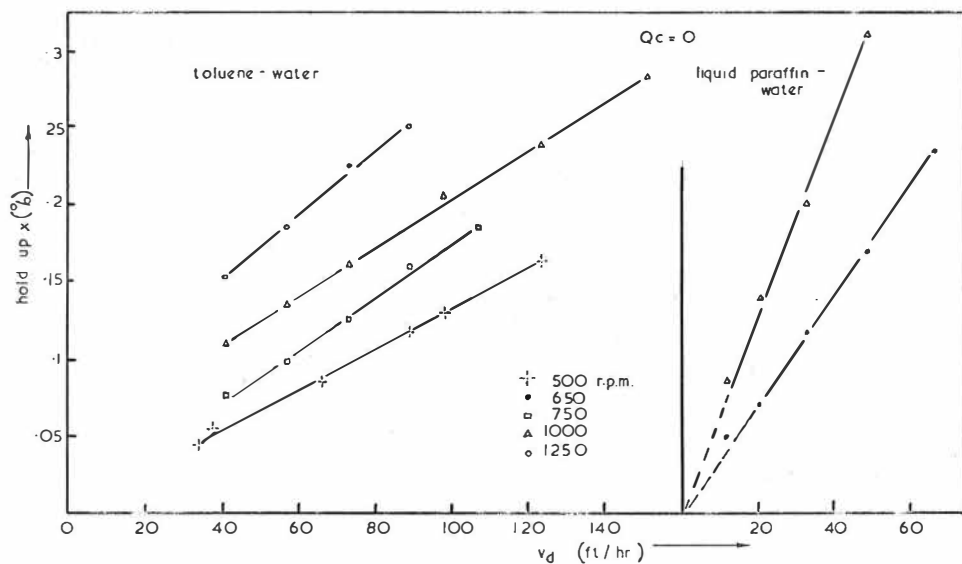


Fig. 3. Hold-up vs dispersed phase flow rate for a wetted disc column

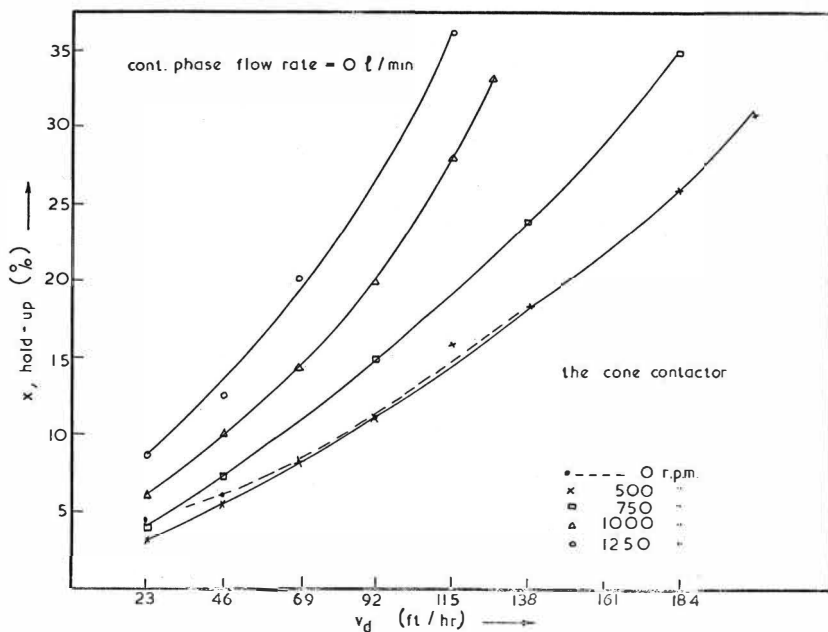


Fig. 4. Hold-up vs dispersed phase flow rate

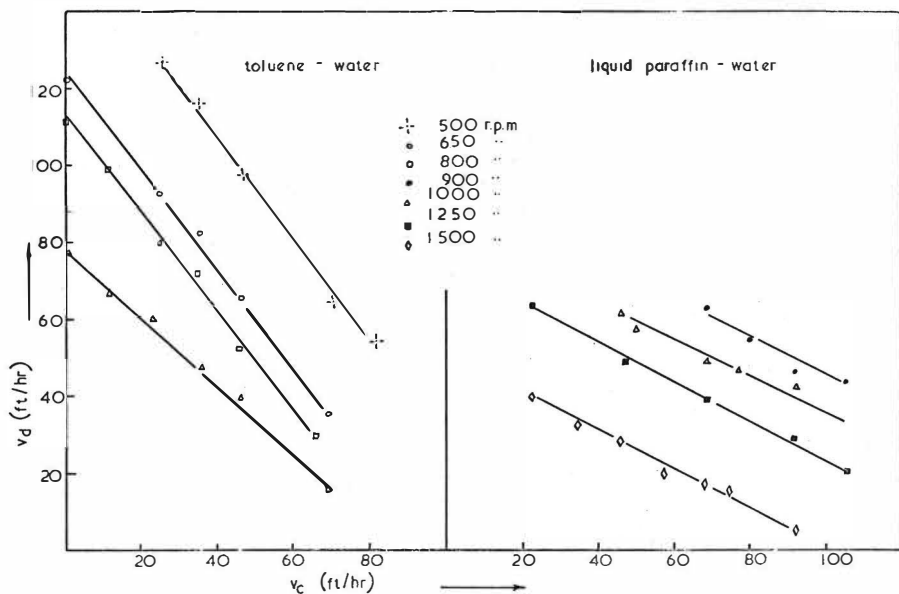


Fig. 5. Flooding curves for a non wetted disc column

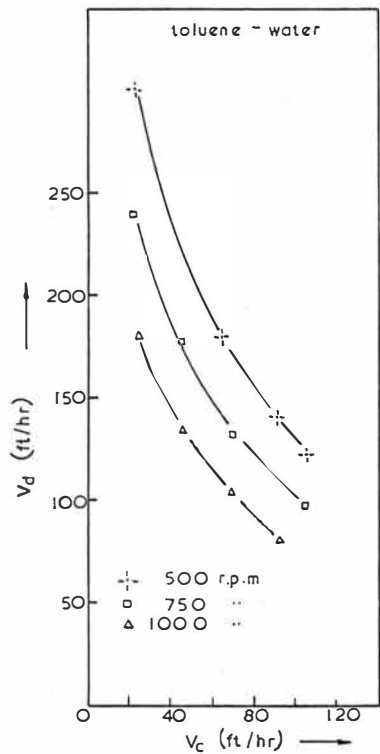


Fig. 6. Phase inversion curves for a non-wetted disc column

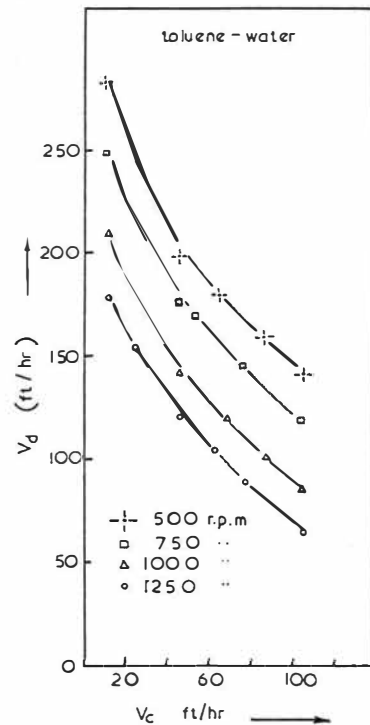


Fig. 7. Phase inversion curves for a wetted (ptfc) disc column

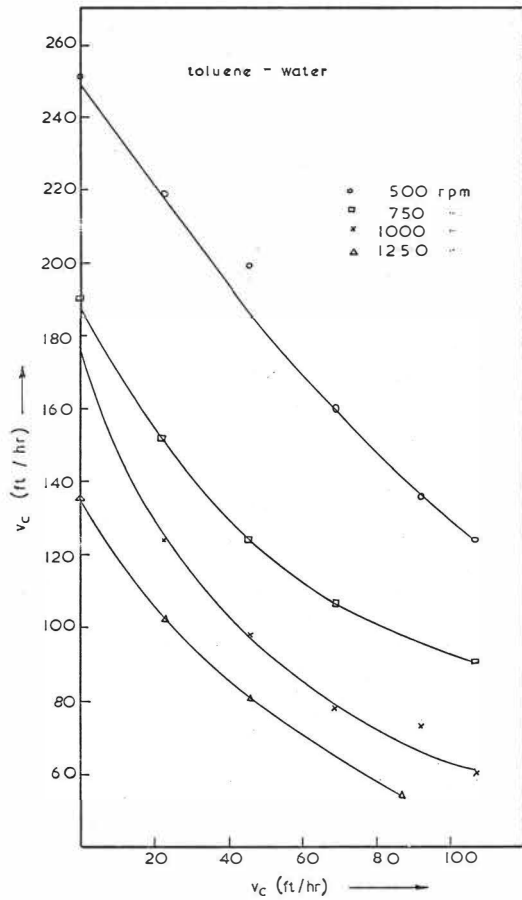


Fig. 8. Phase inversion characteristics of the cone column.

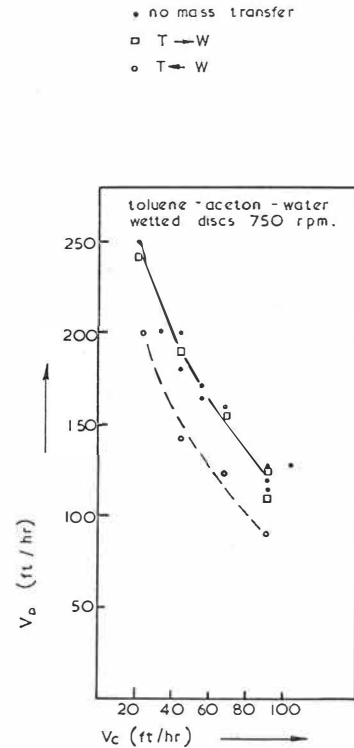


Fig. 9. The effect of mass transfer on flooding rates in an R.D.C.

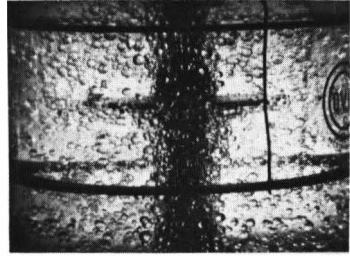
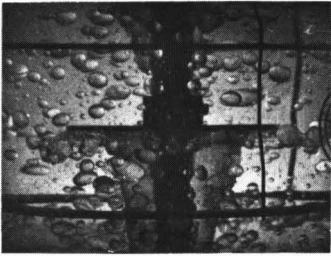


Fig. 10. The Effect of Mass Transfer Direction on Column Behaviour

Top Left: T \rightarrow W 1000 rpm

Top Right: T \leftarrow W 1000 rpm

Bottom Left: T \rightarrow W 0 rpm

Bottom Right: T \leftarrow W 0 rpm

Δ cone column

○ non wetted disc column

□ wetted disc column

empty symbols dispersed → continuous

solid symbols continuous → dispersed

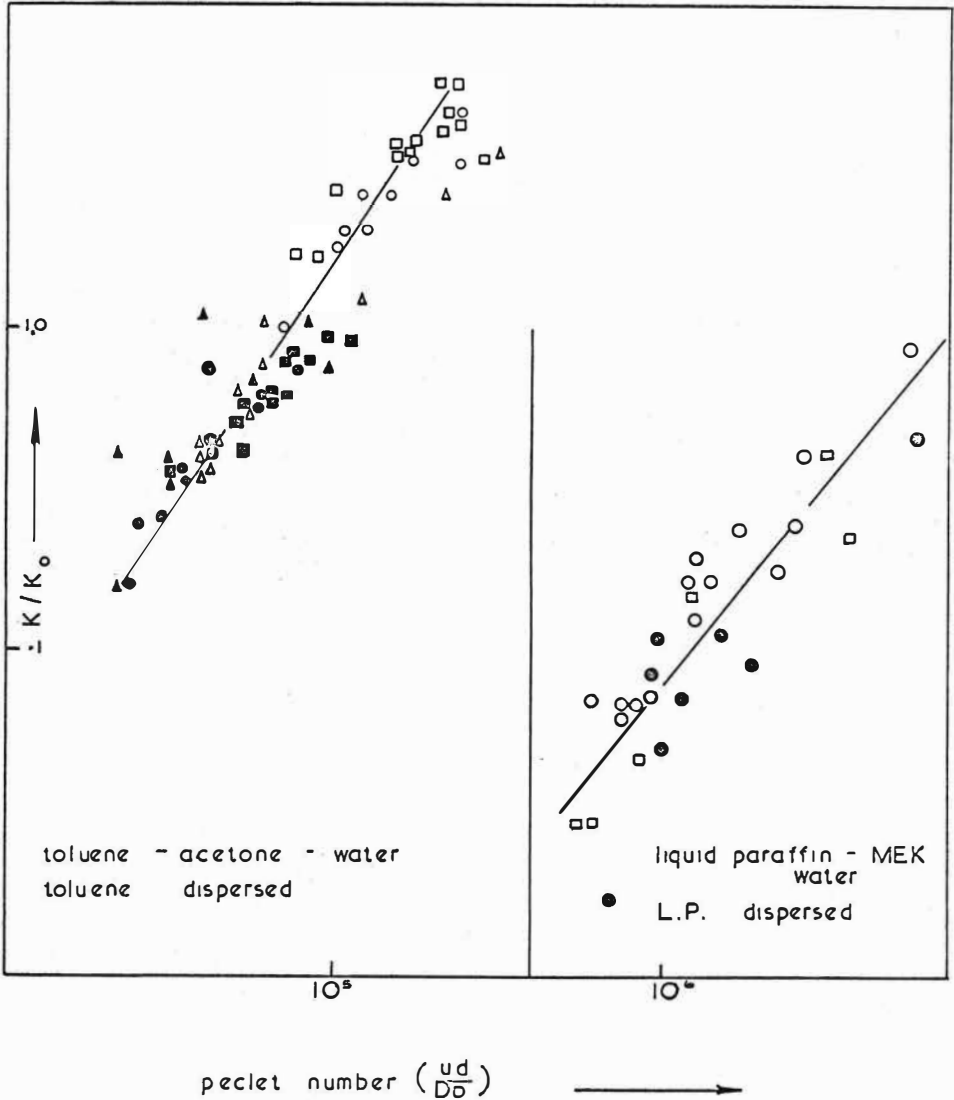


Fig. 11. Correlation of oscillating drop mass transfer coefficient

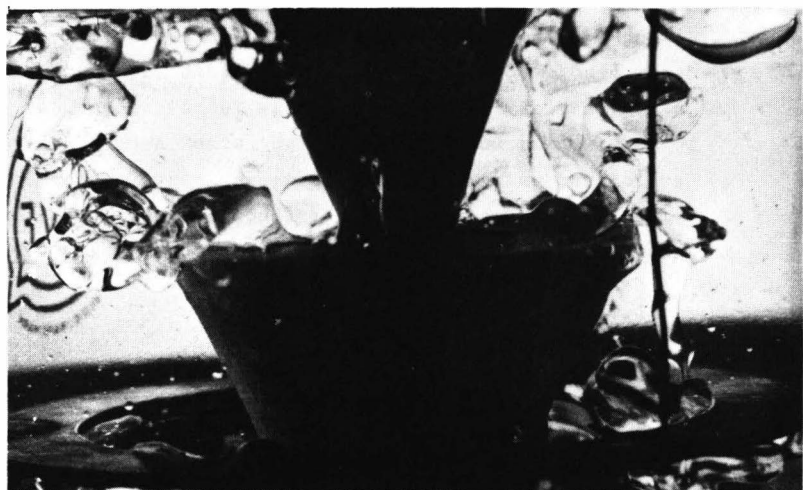
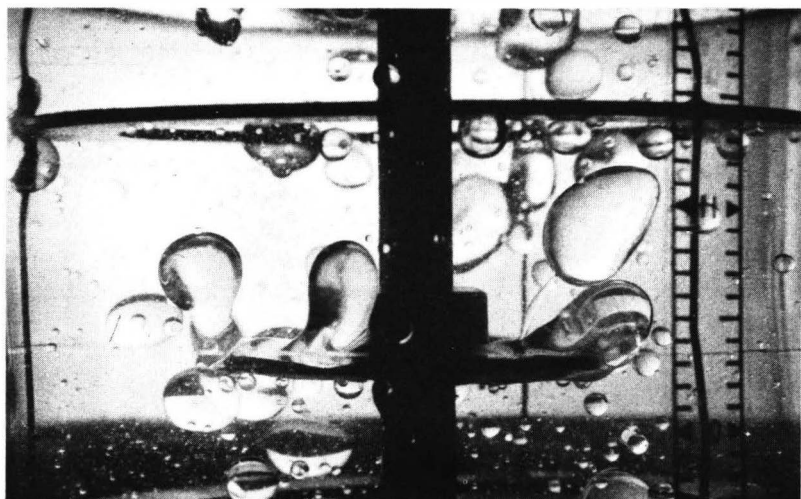


Fig. 12. Illustration of Wetting Effects on Drop Formation at Low Rotor Speed (250 rpm).

Top Plate: ptfе discs

Bottom Plate: Polypropylene Cones

DROPLET SIZE DISTRIBUTION AND INTERFACIAL AREA IN
AGITATED CONTACTORS

D.R. Arnold, C.J. Mumford and G.V. Jeffreys
Department of Chemical Engineering, University of Aston
in Birmingham, United Kingdom. December 1973.

ABSTRACT

The prediction of drop sizes and interfacial areas in rotary agitated contactors is discussed, together with the shortcomings of usual methods especially with regard to the extension of mathematical models for batch systems to continuous ones. An empirical design equation has been developed which enables the prediction of mean drop sizes at various points in the Oldshue-Rushton Contactor to be made from a knowledge of column geometry, system properties and operating parameters where non-mass transfer conditions approximate to the real situation. Experimental results are correlated by the equation

$$\left(\frac{d_{32}}{D}\right) = 2.44 \left(\frac{H}{H_T}\right)^{-0.06} \left(\frac{v_I^2 D \rho_m}{\sigma_i}\right)^{-0.63} \left(\frac{v_K}{v_I}\right)^{0.18}$$

for the system toluene-water in a six inch diameter 16 compartment pilot scale unit.

The changes in drop size distribution up the column have been recorded for a range of operating conditions, and the distribution is shown to be log-normal.

Flooding of the column was investigated for a wide range of operating conditions. It is concluded that phase inversion normally takes place before flooding in the Oldshue-Rushton Column.

INTRODUCTION

In liquid-liquid, or gas-liquid, contactors maximisation of the area offered by one phase to the other assists in the attainment of the greatest possible rate of mass transfer. Therefore in the design of liquid-liquid extraction equipment attention has generally been focussed on the creation of a large interfacial area, at the expense of throughput and back-mixing. Comprehensive reviews of equipment for liquid extraction have shown that many designs of varying geometric complexity have been proposed and used^{1,2}.

In rotary agitated contactors dispersion of one phase as droplets within the other (continuous) phase is achieved by the transmission of kinetic energy from the agitator to the continuous phase and thence by various means to the dispersed phase, causing droplet distortion and subsequent break-up.

For rotary agitated contactors operating at an impeller Reynolds' Number below 10^4 , where the flow regime of the bulk of the continuous phase is predominantly laminar, energy mainly is transmitted from the continuous phase to the dispersed phase by viscous shear. At higher Reynolds' numbers, above the laminar - turbulent transition, transmission energy is by inertial forces, i.e. the impact of turbulent continuous phase eddies on the surface of the drop. Hinze³ has illustrated how these different mechanisms of energy transfer may cause break-up.

The power input to the agitator is thus transferred into the kinetic, surface, potential and heat energy of the droplets. Designs of rotary agitated contactors may therefore be classified in terms of the rate of energy input per unit volume of continuous phase, measured by the familiar equation

$$E = K N^3 D^5 \rho_c$$

where E is the energy input per unit volume, N is the agitator speed, D is the agitator diameter, ρ_c the continuous phase density and K is a constant which depends only on system geometry, for $Re_I > 10^4$.

Thus the Rotating Disc Contactor is a low energy device with a value of $K = 0.1$, whereas the Oldshue-Rushton or Scheibel column has a K value = 4.4 and is consequently a high energy device. Therefore fundamental differences exist between the mechanisms of energy transfer to the dispersed phase in these units.

An attempt has been made⁵ to derive equations for the prediction of drop sizes in the R.D.C., using Kolmogorov's theory of isotropic turbulence together with a mathematical model of flow patterns around a rotating disc derived by Cochran⁶. These predictions agreed well with experimental values despite deviation of the experimental conditions from the underlying assumption of Kolmogorov⁷ concerning local isotropic turbulence.

The advances in design data and mathematical analysis since the publications of Reman⁸ relating to the R.D.C.^{4,47} have not been matched for the high energy contactors. Studies of the Oldshue-Rushton Column⁹ have been limited to analyses of hydrodynamics based on the prediction of drop sizes as an extension of studies in stirred tanks¹⁰, or the interpretation of mass transfer data in terms of H.T.U.'s or H.E.T.S., with the obvious attendant limitations of this approach¹¹. Interstage or Axial mixing has also received some attention^{9,12,13,14,15}, albeit under non-mass transfer conditions. Therefore a detailed study has been made of the performance of this type of extraction column, including measurements of drop size distributions, volumetric hold up, and associated variables, over a wide range of operating conditions. This has covered non-mass transfer conditions and transfer in both directions⁴⁸. The work under non-mass transfer conditions is described in this paper, including original observations of phase inversion phenomena in continuous flow.

The Oldshue Rushton Column

The energy required to break-up droplets in a mechanically agitated rotary extraction column is provided by the agitator. Since droplets are suspended in the continuous phase an analysis of energy distributions and flow patterns is necessary prior to the consideration of actual mechanisms of break-up.

The Oldshue-Rushton Contactor is neither a compartmental or truly continuously differential device, but has some properties of both. Compartments are separated by horizontal stator rings and the vertical component of velocity of any droplet within each stator opening determines whether or not it moves to the next compartment. Each compartment may be regarded as a stirred tank in its own right. The motion of droplets between compartments is therefore dependent upon droplet size, the physical properties of the phases, the phase flowrates and the agitator speed, for a fixed geometry system. The correlation of these variables therefore involves an examination of fluid flow patterns within each compartment, and between adjacent compartments⁴⁸.

The sizes of the droplets within each compartment depends upon similar variables, and, since the drop size distribution of the dispersion passing through the stator opening is determined by conditions within the previous compartment, it is droplet behaviour within the circulating flow of each compartment that determines column operating characteristics.

Droplet Sizes in Agitated Tanks

Droplet sizes in fully baffled, stirred tanks have been studied extensively. Theoretical analyses of droplet break-up have resulted in predictions of minimum, mean, and maximum droplet diameters at volumetric hold-up values ranging from zero to 30 per cent. The dependence of drop diameter on system properties in stirred vessels is summarised in Table 1.

TABLE 1
EXPONENTS FOR SINGLE TANKS

	Authors	N	D	Reference
*	Kolmogorov	-1.2	-2.0	16
*	Obukhov	-1.2	-2.0	17
+	Vermeulen et.al.	-1.2	-0.8	18
+	Rea et.al.	-1.0	-1.5	19
+	Kafarov and Babanov	-1.1	-0.7	20
+	Pavlushenko et. al.	-1.0	-1.65	21
+	Rodger et. al.	-0.72	-0.75	22
+	Yamoguchi et. al.	-1.5	-2.45	23
+	Pebalk and Mishev	-0.912	-1.624	24
+	Calderbank	-1.1	-0.7	25
*	Shinnar	-1.2	-0.8	26
*	Shinnar and Church	-1.2	-0.8	27
+	Brown and Pitt	-1.2	-0.8	28
*	Hinze	-1.2	-2.0	3
*	Taylor	-1.5	-1.0	29
+	Mylbeck and Resnick	-1.2	-0.8	30
+	Giles et.al.	-1.2		31
+	Giles et. al.	-1.0		31
+	Luhning and Sawistowski	-1.2		32

+ Experimental Data

* theoretical

Significantly the exponent of the impeller speed N varies between -1.5 and -0.72 , and the exponent of the impeller diameter D between -2.45 and -0.70 . For experimental studies these large differences may be explained by the use of different systems which cannot be characterised solely in terms of density, viscosity and interfacial tension. It is not clear in some cases whether the systems were in thermodynamic equilibrium. Finally the expression of drop size in terms of a limited number of variables may be invalid.

A notable exception in the table is the correlation of Rodger et. al.²² which gives $d \propto N^{-0.72}$. The dimensional analysis of their results contains a group to account for the degree of contamination of the drops by surfactants expressed as a ratio of the settling time of the dispersion to that of the pure liquid. However in addition to surfactant concentration, settling time must be dependent on drop size, due to the differing buoyancy of the drops, and therefore the precise dependence of d on N is difficult to determine from the correlation.

Detailed consideration of theoretical models for droplet sizes is beyond the scope of this paper. However, it is of interest to examine the relevance of Kolmogorov's Theory of isotropic turbulence to droplet analysis in stirred tanks, since all the models relate droplet sizes to both impeller speed and diameter, and hence to energy input to the system.

The two basic postulates of the theory concern the relationship between the mean square relative velocity $\overline{u^2(r)}$ between any two points a distance r apart and the energy per unit mass in the fluid.

Thus

$$\overline{u^2(r)} = C_1 E^{\frac{2}{3}} r^{\frac{2}{3}} \quad \text{for } L \gg r \gg z \quad (1)$$

$$\overline{u^2(r)} = \frac{C_2 E r^2}{D} \quad \text{for } L \gg z \gg r \quad (2)$$

where the symbols have their usual meanings.

The familiar development then leads to the two equations

$$r_{sd} = K_1 \left(\frac{\sigma_i}{\rho_c} \right)^{0.6} \left(\frac{1}{E} \right)^{0.4} \quad (3)$$

$$\text{and } r_{sd} = K_2 \left(\frac{\sigma_i \mu_c}{\rho_c^2} \right)^{1/3} \left(\frac{1}{E} \right)^{1/3} \quad (4)$$

For fully turbulent flow the power number is constant and $E \propto N^3$. Hence,

$$r_{sd} \propto N^{-1.2} \quad (5)$$

$$\text{and } r_{sd} \propto N^{-1.0} \quad (6)$$

These relationships were verified experimentally³¹ for the nitration of toluene. For this system it was argued that which of equations (5) and (6) was applicable was dependent only on the value of the volumetric hold-up. No attempt was made to estimate the microscale of turbulence. Levins and Glastonbury³³ investigated mass transfer from solid particles in a stirred tank and determined the requirements for local isotropic turbulence. From a consideration of equations by which the size of the particles in a stirred tank may be compared with the size of the turbulent eddies present, the dependence of d on N was evaluated theoretically for specific cases of liquid-liquid systems at steady state, they concluded that equation (1) was of doubtful validity.

Microscales of turbulence in the Oldshue-Rushton column have been calculated⁴⁸ from Kolmogorov's definition

$$z = \left(\frac{\nu^3}{E} \right)^{1/4} \quad (7)$$

together with

$$E = \frac{4.4 N^3 D^5 \rho_c}{M} \quad (8)$$

where M is the mass of continuous phase in the tank. Values of the microscale are for a standard fully baffled mixing vessel of identical geometry to a single compartment of the Oldshue-Rushton column containing water. These are given in Table 2. Cutter's³⁴ ratios of E'/\bar{E} for the impeller region ($E'/\bar{E} = 7.7$) and for other lower energy regions ($E'/\bar{E} = 0.26$) were used to obtain the higher and lower limits. The magnitude of the calculated microscales is of the same order as the droplet diameters commonly encountered in mixer-settlers, the Oldshue-Rushton and similar high energy contactors, and therefore the use of equations (3) or (4) requires caution. Shinnar and Church²⁷ have derived an expression for mean drop size related to the Weber number and Brown & Pitt²⁸ have correlated drop size with hold-up by an equation of the form

$$\frac{d_{32}}{D} = k_1 (1 + k_2 x_d) We^{-0.6} \quad (9)$$

for low hold-up values between 0.05 and 0.3

Bouyatiotis and Thornton found that for both batch and continuous operation with four different systems (including toluene-water) the measured distribution approximated to a normal one. Similar results for different systems have been reported by Chen and Middleman⁴² and Brown and Pitt²⁸. Pelbalk and Mishev²⁴, however, reported that for a variety of liquid-liquid systems, including kerosine-water as used by Brown & Pitt²⁸, the drop size distribution in a stirred tank was log-normal. Giles et al³¹ reported a log-normal distribution during the nitration of toluene in a stirred tank.

Whether the drop size distribution is normal or log-normal is of practical significance in an extraction column. For a fixed volumetric throughput, a comparison of the two types of dispersion is illustrated in Table 3.

TABLE 2Microscales of Turbulence for Water

N (r.p.m.)	\bar{E} ($\text{cm}^2 \text{s}^{-3}$)	Impeller region	Z (mm) Circulation Zone
200	39.6	0.075	0.176
300	134	0.056	0.130
400	317	0.045	0.105
500	620	0.038	0.089
600	1070	0.033	0.077

TABLE 3

<u>Property of dispersion</u>	<u>Normal</u>	<u>log-normal</u>
Proportion of smaller droplets	Lower	Higher
mean m.t. coeffs.	Higher because more drops are circulating	Lower - more stagnant drops
Interfacial area	Lower	Higher
Settling rate	Higher	Lower
Tendency to flood column	Higher	Lower

From the point of view of predicting hydrodynamic and mass transfer performance the preferred distribution is a mono-dispersion with a consequent standard deviation of zero. Although this is impracticable in an extractor, a distribution where the mode is equal to the mean results in more drops being nearer the mean size than with a log-normal distribution. Droplet characteristics are thus more predictable in a normal distribution. Therefore it is desirable to obtain a normal distribution around a certain mean drop diameter rather than a log-normal one.

All models developed to date to predict drop sizes in stirred tanks are restricted to batch operations or continuous operations with either one or both of the phases flowing in a single tank. Fluids enter and leave the tank via many diverse geometric arrangements, which affect the hydrodynamics of operation. For example the geometry used by Thornton¹⁰ resulted in the drop size being independent of flowrate, i.e. the mean residence time of the dispersed phase was large compared with the flowrate, and thus the dynamic equilibrium between droplet break-up and coalescence remained unaffected. Operation was therefore effectively batchwise.

In rotary agitated columns, entrance and exit mechanisms are very important. Larger drops have a greater vertical velocity than smaller ones and are less affected by small scale disturbances in other directions. Classification therefore occurs between compartments resulting in a tendency for the smaller drops to remain in a compartment and larger ones to pass to the next.

The positive skewness in the drop size distribution noted by Giles et. al.³¹, is therefore less significant in the column, and a negative skewness would be expected. Oldshue-Rushton column designs based upon a mean drop size throughout the length of the column in which the drop size correlations are themselves based on data from single stirred tanks are therefore open to criticism.

The effect of hold-up on mean drop size in the column could be expected to follow the general form of Thornton's correlation,

$$d_{32} = d_o (1 + m x_d) \quad (10)$$

This would only be expected to hold for any compartment at constant volumetric flowrate.

Phase Inversion

Phase inversion in liquid-liquid systems was first recorded by Ostwald³⁵; the phase ratio at which it occurred was 3:1 and became known as "Ostwald's Ratio". Recently the phenomenon has received attention from Luhnig and Sawistowski³² for a single stirred tank operating batchwise, and Quinn and Sigloh³⁶. The existence of an ambivalent range is well known, as is its dependence on agitator speed. The effect of mass transfer on the ambivalent region has been briefly studied³².

Phase inversion will occur in a batch system only when the rate of coalescence of drops is greater than the rate of break-up. In a continuous system additional factors have to be taken into account. In a continuous single stirred tank both phases are in flow and as mentioned earlier the geometric arrangement for the entrance and exit of each phase will affect the dynamics of operation. The volumetric hold-up of dispersed phase reaches a steady state value in each compartment when the column is operating normally. This is achieved only when the input of each phase is equal to the output, and this is particularly important with reference to the dispersed phase.

A complex situation exists between consecutive compartments, because the droplets exist in a distribution of diameters, not as a monodispersion. Thus a polydispersion of droplets is flowing by buoyancy through the stator opening against the flow of continuous phase. Superimposed on the varying terminal velocities of the droplets in the dispersion is the turbulent flow mainly across the opening generated by the impellers at the centre of each compartment. When hold-up in the Oldshue-Rushton contactor is large, (about 0.6 - 0.8) phase inversion occurs and has the effect of relieving the imminent flooding situation. Phase inversion occurs in preference to flooding.

In any two phase counter current operation therefore there is a limit above which normal operation is not possible as either flowrate is increased incrementally. Under certain operating conditions flooding in the usual sense of the word takes place.

EXPERIMENTAL

Experimentation was performed in the sixteen-compartment, six inch diameter Oldshue-Rushton column. The glass column has stainless steel internals and the stators were machined to an exact fit inside the column. Sampling points in each compartment consisted of stainless-steel ports sealed by "teflon" "O" rings in holes drilled with an ultrasonic drill. The agitator and shaft were made of stainless steel, supported by a p.t.f.e. bearing at each end of the column. A brass bearing was installed in the centre of the column. The agitator shaft was driven by a $\frac{1}{4}$ h.p. electric motor controlled by a "Torovolt" variable voltage device, and its speed monitored by a directly coupled tachometer. Standard four blade disc turbines of identical dimensions to those used by Oldshue and Rushton were employed; the energy input of this geometric arrangement having been measured¹¹. Fluid was transferred from the stainless steel 40 gallon storage tanks to the column by stainless steel centrifugal pumps with viton 'A' seals, controlled by a variable voltage device. All transfer lines were of 0.5 in. i.d. borosilicate glass or 5/8" dia. p.t.f.e. tubing. A variable height overflow leg was incorporated in the continuous phase outlet line to control the position of the interface. The unit was operated at ambient temperature, ($18 \pm 2^{\circ}\text{C}$).

The system toluene (commercial, redistilled grade) - distilled water was selected³⁸. Toluene was the dispersed phase.

A photographic technique for recording the dispersions in the compartments was developed.

An Asahi-Pentax 35 mm still camera with a N⁰ 1 single extension tube was used to record the drop size distribution at the wall in several compartments on Kodak Plus X pan film. Enlargement of the negative and printing on Kodak grade 4 "Bromesko" paper gave sufficient magnification and contrast for the drops to be counted on a Carl Zeiss T.G. 3 particle size analyser and the distribution obtained. Figures 3 and 4 show typical photographs. Due to the high quality of the photographs produced, drop sizes as low as 0.12 mm could be recorded accurately. A Honeywell 316 digital computer was used to process the measurements to produce a comprehensive statistical analysis of the distribution. At least 300 drops were used for each distribution measurement obtained from three separate negatives for each compartment, giving a statistical accuracy better than 3%⁴¹.

Hold up of the dispersed phase was measured by sampling of several compartments via the Simplifix toggle valves. Accuracy of this technique was checked by comparison of the overall hold-up when the agitator was stopped and the column isolated. Three samples for each compartment were taken and these were generally consistent to within \pm 5%. Both phases were mutually presaturated and the interfacial tension was checked by Wilhelmy's method prior to each run. The column was precleaned with a 2 per cent "Decon 90" solution and rinsed with distilled water.

RESULTS

Drop-size

The nature of the drop size distribution in various parts of the column was investigated.

Figure 5 (a) is a typical ogive for the toluene-water system, and as shown in Figure 5 (b) this conforms well with a log-normal distribution. At all impeller speeds (200 - 600 rpm) and at all points in the column the distribution of drop sizes was log-normal.

The interacting effects of drop size, volumetric hold-up, column height and agitator speed on dispersions of toluene in water under non-mass transfer conditions is demonstrated in Figures 6-11.

Figures 6 and 7 show the variation of d_{32}^0 with position in the column at flowrates of 0.25 and 0.5 kg/sm². Although the mean drop size decreased up the column, a false picture would be gained from considering this in isolation. Figures 8 and 9 show the relationship of hold up to height up the column, and figure 10 depicts the typical variation of hold-up with agitator speed.

The variation of drop size with hold up in figure 11, is in agreement with the work of Thornton and Bouyatosis¹⁰, in as much as the mean drop size is a linear function of hold-up, for fixed agitator speed and column compartment. They found that m was a function of physical properties only,

i.e.

$$m = 1.18 \cdot \left(\frac{\sigma_i^2}{\mu_c^2 g} \right) \cdot \left(\frac{\Delta p \cdot \sigma_i^3}{\mu_c^4} \right)^{-0.62} \cdot \left(\frac{\Delta p}{\rho_c} \right)^{0.05} \quad (10)$$

$$\text{and} \left(\frac{d_{32}^0 \rho_c^2 g}{\mu_c^2} \right) = 29.0 \left(\frac{\left(\frac{E}{M} \right)^3 g_c^3}{\rho_c^2 \mu_c^4} \right)^{-0.32} \left(\frac{\rho_c^3 \sigma_i}{\mu_c \cdot g} \right)^{0.14} \quad (11)$$

The units of m are those of length, and for the toluene/water system the value of m from equation (10) is $2.62 \times 10^{-4} m$, compared with a mean of $2.49 \times 10^{-3} m$ for the data figure 11 at 300 rpm. Further experimental data revealed that m is independent of impeller speed in the Oldshue Rushton Column as predicted by equation (10), but that values of d_{32}^0 extrapolated from the curves of figure 11 do not show d_{32}^0 to be proportional to $(E)^{1/3}$ as would be expected from equation (11).

A dimensional analysis was carried out to correlate all 15 dependent variables which may effect the drop size distribution and the mean drop size. These are listed in Table 4. A full dimensional analysis based on all these variables has not been completed, since those marked with an asterisk in the figure were maintained constant, and a "short" analysis results. Thus the drop size may be expressed as a function of height up the column, impeller speed, flowrates, physical properties and impeller diameter. Height up the column (i.e. compartment) is expressed as a fraction of the total height, as opposed to H/D as would be normally required in a formal analysis. The flowrates are expressed as a single quantity V_k , which is a common expression of characteristic velocity for two phase flow,

$$V_k = \frac{V_d (1 - x_d)}{x_d} + V_c \quad (12)$$

TABLE 4

Variables Considered in the Dimensional
Analysis

<u>Quantity</u>	<u>Symbol</u>	<u>Dimensional Formula</u>
Drop Size	d_{32}	L
Impeller Tip Speed	V_I	$L T^{-1}$
Column Height	H	L
Mean Viscosity	μ_m	$M L^{-1} T^{-1}$
Mean Density	ρ_m	$M L^{-3}$
Drop Characteristic velocity	V_K	$L T^{-1}$
Interfacial Tension	σ_i	$M T^{-2}$
Compartment Height	H	} Combined as a geometric factor"
Column Diameter	D_T	
Baffle Width	B	
Blade height	b_h	
Blade width	b_w	} Fg, dimensionless
Impeller diameter	D	L
Coalescence factor	C	-
Break-up factor	R	-
Buoyancy	$\Delta\rho/\rho$	-

Total number of variables = 16

Number of fundamentals = 3

∴ Number of dimensionless groups = 9

For a countercurrent system V_c is a negative quantity if V_d is regarded as positive. Mean densities are expressed by ρ_m ,

$$\rho_m = (1-x_d)\rho_c + x_d\rho_d \quad (13)$$

which has been shown in this form to be arealistic measure of mean density.⁴³

Thus

$$\left(\frac{d_{32}}{D}\right) = C \left(\frac{H}{H_T}\right)^p \left(\frac{V_i^2 D \rho_m}{\sigma_i}\right)^r \left(\frac{V_K}{V_i}\right)^s \quad (14)$$

for the range of variables considered under normal operation.

where $\frac{H}{H_T}$ is the fractional height up the column

$$V_I = \pi ND$$

$$V_K = V_d \cdot \frac{(1-x_d)}{x_d} + V_c$$

$$\rho_m = (1-x_d)\rho_c + x_d\rho_d$$

The exponents p, r & s and the constant C were evaluated experimentally, to yield

$$\left(\frac{d_{32}}{D}\right) = 2.44 \left(\frac{H}{H_T}\right)^{-0.06} \left(\frac{V_i^2 D \rho_m}{\sigma_i}\right)^{-0.63} \left(\frac{V_K}{V_i}\right)^{0.18} \quad (15)$$

Phase Inversion

As the dispersed phase flowrate was increased at very low rotor speeds e.g. less than 250 rpm, droplets were rejected from the inlet end of the column, and a build-up of dispersed phase droplets occurred below the lowest stator ring. At high rotor speeds e.g. greater than 700 rpm and at high continuous phase flowrates, greater than $4.0 \text{ Kg/m}^2 \text{ s}$, droplets which entered from the distributor ruptured, due to the high level of turbulence in the first compartment and since the terminal velocity of the daughter droplets was lower than the downward velocity of the continuous phase and they were carried out of the contactor as a fine dispersion in the continuous phase, i.e. conventional 'flooding' occurred.

In between these two extremes, before flooding was reached, phase inversion was observed. No reference was found concerning inversion in liquid-liquid extraction columns, although during the course of this work Al-Hemiri³⁷ and Jillood³⁸ have observed a characteristic but dissimilar effect in an R.D.C.

Compartments of the column have been observed to invert individually so that 'slugs' of coalesced dispersed phase progressed up the column. The compartment in which inversion first took place as flowrates were increased was reproducible, and may be predicted from experimental results. These results are recorded elsewhere⁴⁸.

Inversion points were determined precisely by allowing the column to attain hydrodynamic steady-state conditions at values of dispersed and continuous phase flowrates below those for inversion at a fixed impeller speed. The dispersed phase flowrate was then incrementally increased by between 2 - 5% and time allowed for steady-state to be obtained at the each new value. This usually required 10 - 20 minutes depending on the total flowrate. As soon as phase inversion began to occur on a cyclic basis, and a pseudo-steady-state was established with a steady frequency of the inversion, the dispersed phase flowrate was decreased by intervals of about 1% until the cycling ceased and phase inversion was eliminated.

At this point a slight increase in the dispersed phase flowrate caused the column to invert at one particular compartment, and this value was taken to be the characteristic flowrate for phase inversion. The particular compartment in which the inversion first occurred was recorded. Measurements of the volumetric hold-up of dispersed phase were made via the sampling point in the compartment immediately before and after phase inversion.

Inversion occurs when the input flowrate of either of the phases means that steady-state conditions are not able to cope with the flow. This situation is represented in figure 12 where flowrate of dispersed phase (G_d) is plotted against impeller speed (N) for various values of continuous phase flowrate (G_c). Characteristically these curves all tend towards a common asymptotic value of impeller speed between 200 and 250 rpm. The corresponding impeller Reynolds numbers with regard to continuous phase physical properties were between 0.858×10^4 and 1.075×10^4 . Since the commonly accepted Reynolds' Number of transition from laminar to turbulent flow is 1.0×10^4 , it appears that phase inversion is precluded by operation in the laminar region. The change in apparent fluid properties (such as density) corresponding to dispersed phase hold-up would result in lower Reynolds' Numbers^{43,18,44,45} so that the transition from laminar to turbulent would occur at a slightly higher value of Reynolds Number. This is in agreement with the experimental results. Phase inversion could not be generated below an impeller speed of 225 rpm under any flowrate conditions, since at such low values of Re there was stratification of droplets in the compartment; when phase inversion occurred the coalesced dispersed phase therefore occupied only the upper half of the compartment.

Increasing flowrates at low impeller speeds, below 250 rpm, resulted in flooding in the generally accepted sense. Dispersed phase droplets were rejected from the first compartment and flowed out of the column via the continuous phase outlet.

According to Figure 13 phase inversion should be possible at negative values of G_d and G_c , especially at high impeller speeds e.g. 500 rpm. At zero flowrate of continuous phase, phase inversion could be obtained at impeller speeds of 350 rpm and greater. Extrapolation of these curves suggests that phase inver-

-sion could in theory occur during co-current operation.

Measurements of hold-up of dispersed phase immediately before and after phase inversion occurred were made in certain compartments for certain runs. The values of x_d for various flowrates, impeller speeds and positions in the column followed the general pattern up to the point of the limit of steady-state operation, after which the hold-up began to increase up to the phase inversion value. Figure 14 shows a typical phase inversion curve for the system toluene/water in the absence of mass transfer. As would be expected, the results show no variation of hold-up at phase inversion with changing flowrate of either phase. Each point on the figure is an arithmetic mean of the hold-up values obtained for each impeller speed, although the maximum deviation from the mean was only 5 per cent, the same order of magnitude as the experimental error of each reading.

In figure 14 the upper curve shows the hold-up immediately prior to inversion. The column was operated under conditions where inversion takes place periodically, and the hold up was measured in the compartment in which inversion was initiated. The hold-up value necessary for inversion to occur decreases with increasing rotor speed. This is in concert with the findings of Lunning & Sawistowski. The hold up of the residual phases after inversion, i.e. when the 'slug' of inverted fluids had passed to the next compartment, is shown as the lower curve.

CONCLUSIONS

Drop sizes in the Oldshue Rushton Column were related by equation (15) for the system toluene/water under non-mass transfer conditions. The dependence of d_{32} on $We^{-0.63}$ in equation (15) is in very good agreement with all preceding investigations in stirred tanks. The effects of column geometry are expressed in the other two terms in the equation, although there are more terms in the full analysis⁽⁴⁸⁾. Some modification is necessary in the presence of mass transfer or varying interfacial tension but for dilute systems where major surfactant effects are absent, equation (15) serves as a guide to drop sizes for design purposes. Interfacial areas may be calculated directly from the familiar equation

$$a = \frac{6x_d}{d_{32}} \quad (16)$$

for incremental column heights.

Phase inversion is an important feature of operation of the contactor which has to date received insufficient attention. Phase inversion can occur in any agitated contactor, and indeed operation under inverted conditions may improve mass transfer rates due to better mixing of the phases.

When phase inversion does not take place, equation (15) may be used to provide an estimate of drop size and mass transfer coefficients calculated^{46,47}. Column performance is then evaluated bearing in mind the backmixing correlations.

The effects of mass transfer on the operating characteristics of the Oldshue-Rushton Column, and scale-up procedures are reported in detail elsewhere⁴⁸.

NOMENCLATURE

a	interfacial area
C_1, C_2	constants in equations (1) and (2)
D	impeller diameter
E	energy
d	drop diameter
G	mass velocity
g	gravitational constant
H	column height
K_1, K_2	constants in equations (3) and (4)
k_1, k_2	constants in equations (9)
L	Lagrangian macroscale of turbulence
M	mass
m	parameter in equation (10)
N	agitator speed
n	number of drops
\bar{r}	radius of drop
$u^2(r)$	mean square velocity
V	Velocity
We	Weber Number
x	volume fraction
z	microscale of turbulence
μ	viscosity
ν	Kinematic viscosity = $\frac{\rho}{\mu}$
ρ	density
σ	interfacial tension

Subscripts

C	continuous phase
d	dispersed phase
I	Impeller
S.d	Stable drop
T	total
o	Zero hold-up
32	sauter mean

References

1. Mumford C.J. Brit. Chem. Eng. 1968 13 981.
2. Bailes P.J. and Winward A. Trans. Instn. Chem. Engrs. 1972 50 240.
3. Hinze J.O. A.I.Ch.E.Jnl 1955 1 289.
4. Misek T 'Rotating Disc Contactor' 1964 (Prague : Statni Nakadelotri Technicke Literatury).
5. Jeffreys G.V. and Mumford C.J. 1971 Proc. I.S.E.C. '71 S.C.I. The Hague (1971).
6. Cochran W.E. Proc. Camb. Phil. Soc. 1934 30 365.
7. Kolmogorov A.N. Dokl. Akad. Nauk. S.S.S.R. 1949 66 825.
8. Reman G.H. Proc. 3rd World Petr. Congr. Hague 1951.
9. Bibaud R.E. and Treybal R.E. A.I.Ch.E.Jnl 1966 12 472.
10. Bouyatiotis B.A. and Thornton J.D. Ind. Chem. 1963 39 298.
11. Oldshue J.Y. and Rushton J.H. Chem. Eng. Progr. 1952 48 297.
12. Gutoff E.B. A.I.Ch.E.Jnl. 1965 11 712.
13. Ingham J. Ph.D. Thesis University of Bradford 1972 and Trans. Instn. Chem. Engrs. 1972 50 372.
14. Haug H.F. A.I. Ch.E . Jnl 1971 17 585.
15. Lelli, U. et al Chem. Engng. Science 1972 27 1109.
16. Kolmogorov A.N. Dokl. Acad. Nauk. S.S.S.R. 1941 32 19.
17. Obukhor A.M. ibid 1941 32 22.
18. Vermeulen T et. al. Chem. Engng Progr. 1955 51 85F.
19. Rea H.E. and Vermeulen UCRL - 2123 1953 cited in
20. Kafarov V.V. and Babanov D.M. Zh. Prikl. Khim. 1959 32 789.
21. Pavlushenko I.S. and Yanishevskii A.V. Zh. Prikl. Khim 1958 31 1348.

40. Mylneck Y. and Resnick W. Can. J. Chem. Engng. 1972 50
134.
41. B.S. 3406 Part 4 1963 p. 35.
42. Chen H.T. and Middleman S. A.I.Ch.E.Jnl 1967 13 989.
43. Laity D.S. and Treybal R.E. A.I.Ch.E.Jnl 1957 3 177.
44. Miller S.A. and Mann C.A. Trans. A.I.Ch.Engng 1944 40 709.
45. Vanderkeem J.H. M.Sc. Thesis Univ. of California 1960.
U.C.R.L. 8722.
46. Jeffreys G.V. Chem. Proc. Engng 1962 March p. 117.
47. Hanson C. (Editor) Recent Advances in Liquid-liquid Extraction
Pergamon 1971.
48. Arnold D.R. Ph.D. thesis, University of Aston 1974.

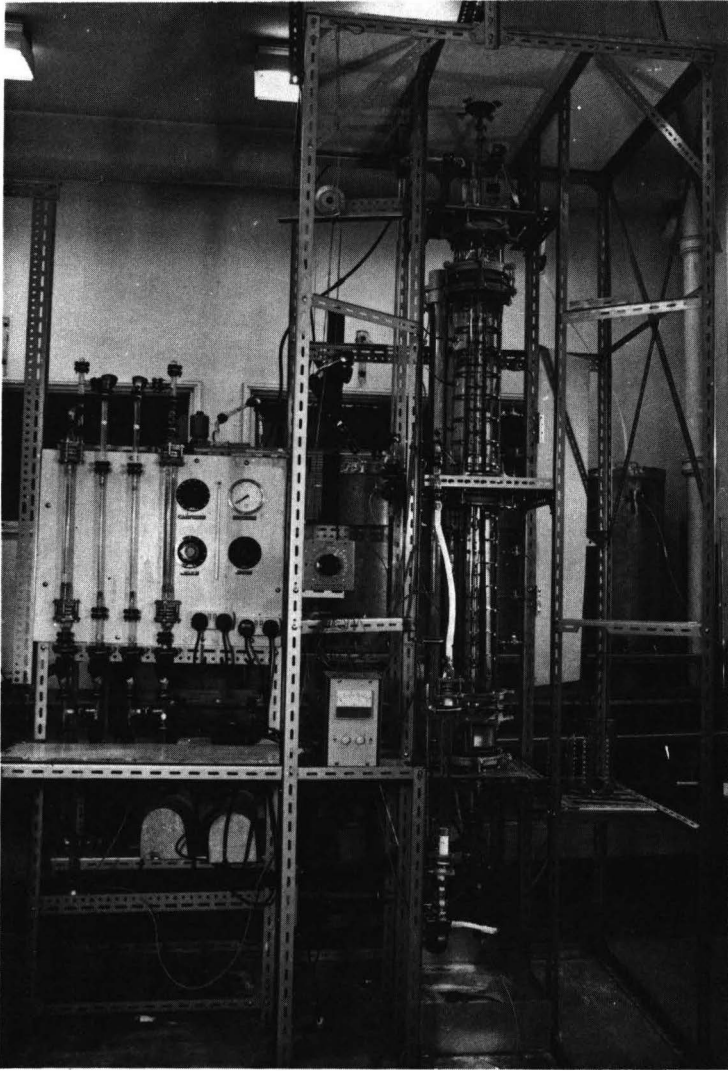


FIGURE 1
The Oldshue— Rushton Column

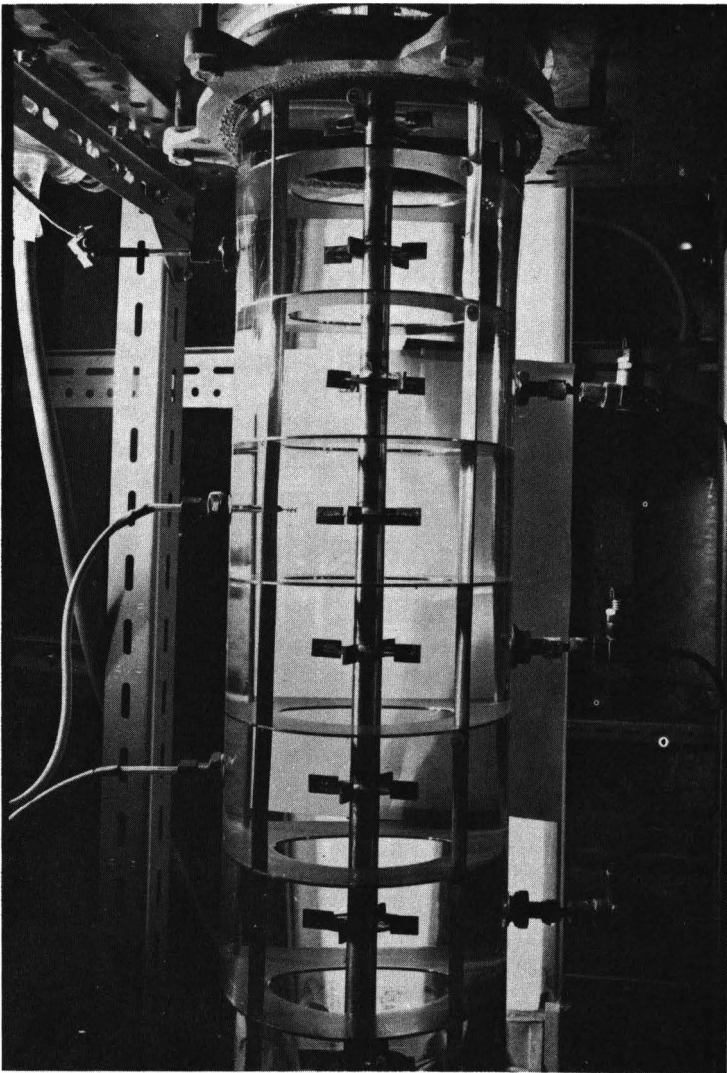


FIGURE 2

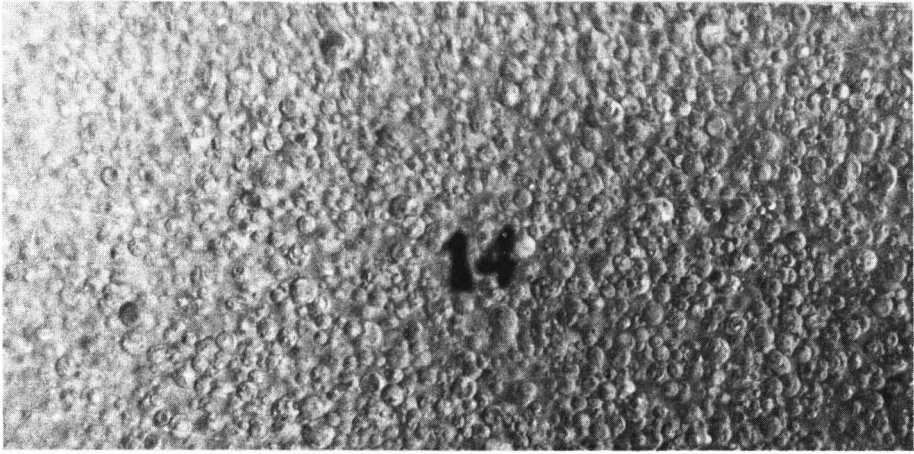


FIGURE 3
Dispersion in compartment 14 (near top)

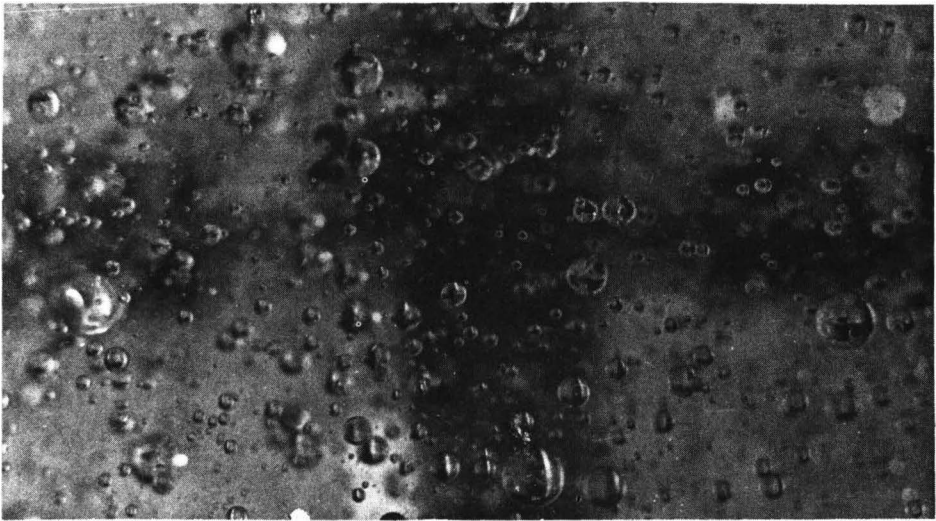
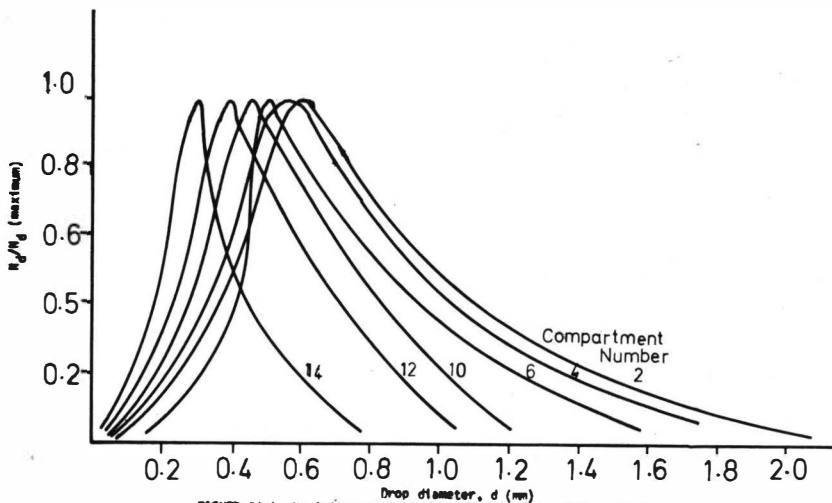


FIGURE 4
Dispersion in compartment 2 (bottom)



Drop diameter, d (mm)

FIGURE 5(a) Variation of drop size distribution with compartment number
 $N = 400$ r.p.m. $G_c = G_d = 0.5 \text{ Kg/m}^2$ system: toluene/water

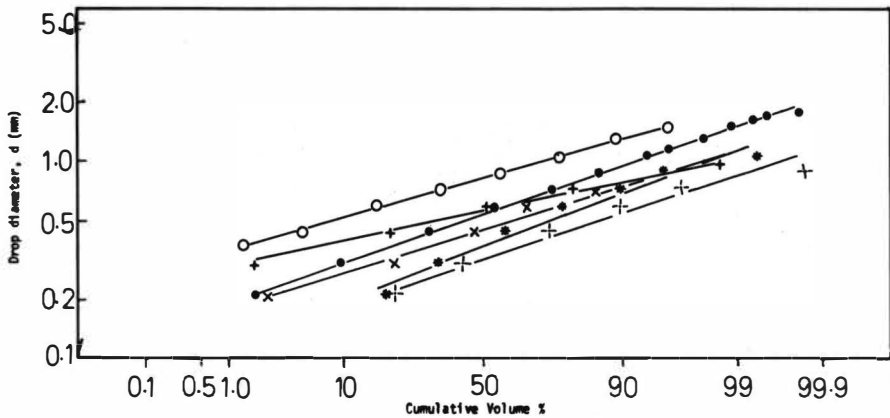
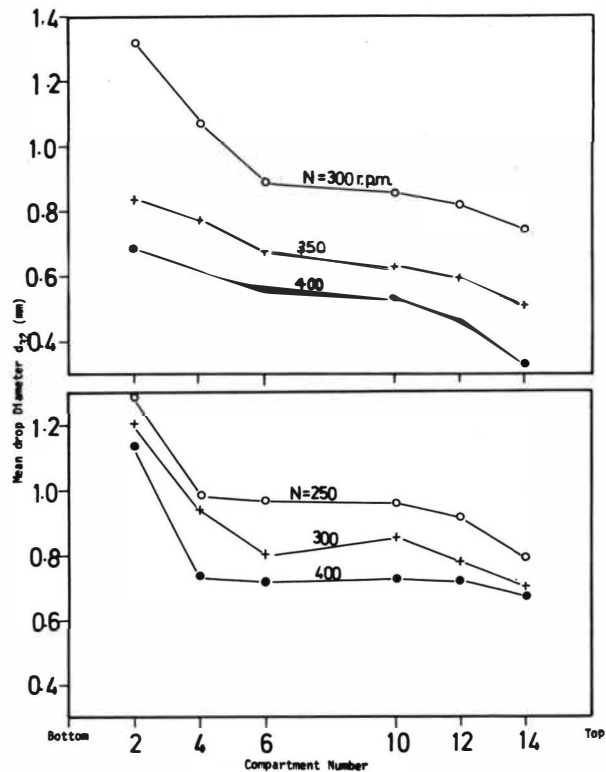
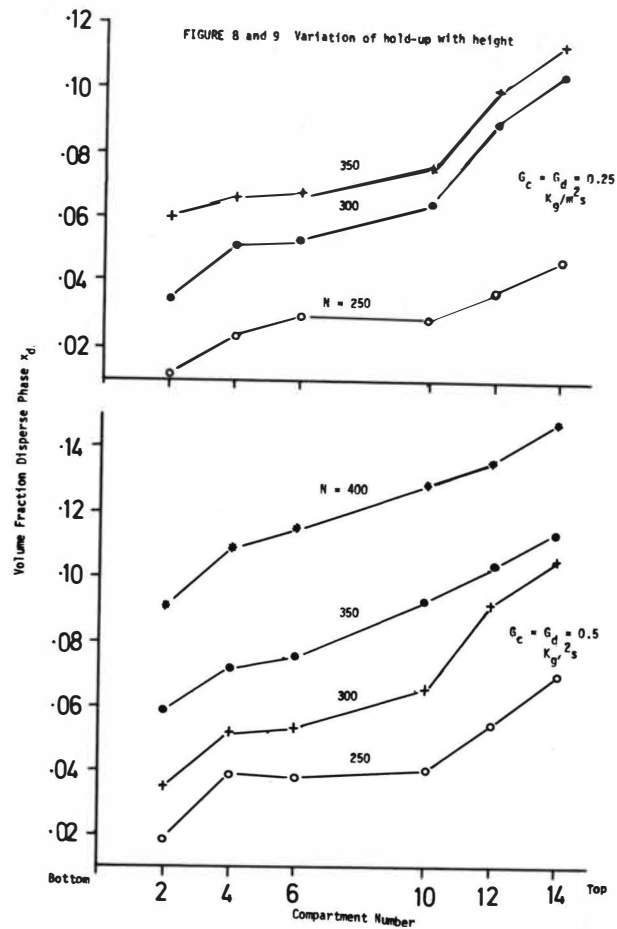


FIGURE 5 (b) Log-normal drop size distribution in the column
 $N=400$ r.p.m. $G_c = G_d = 0.5 \text{ Kg/m}^2$ system; toluene/water

FIGURE 6 and 7. Variation of mean drop size with height



1647



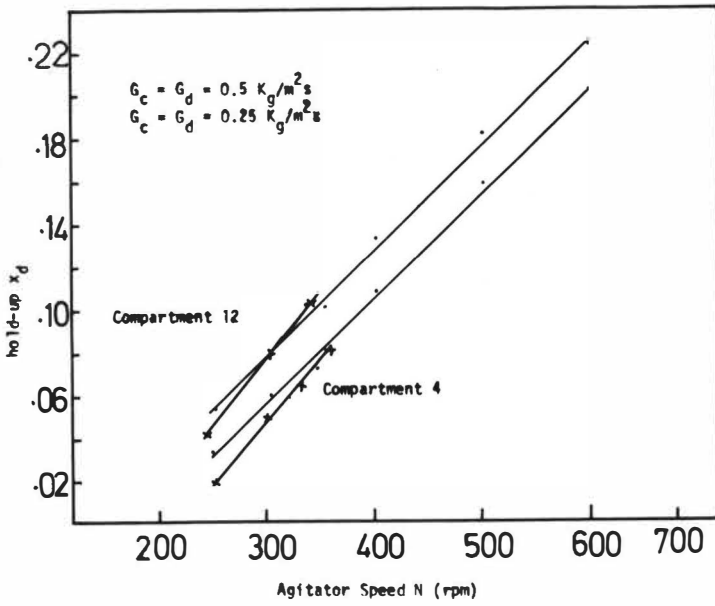


FIGURE 10 Variation of volume fraction, dispersed phase with agitator speed

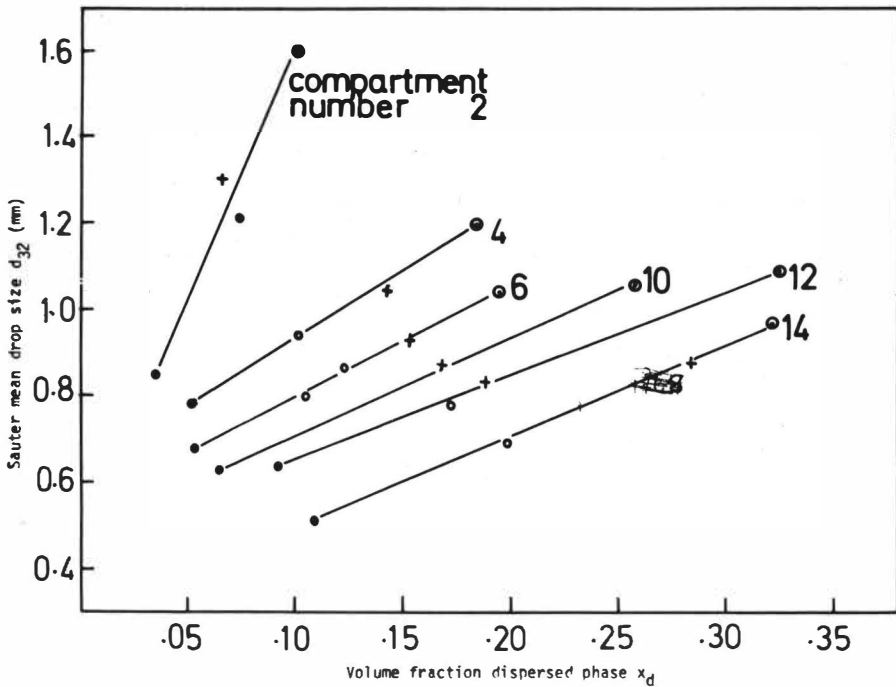
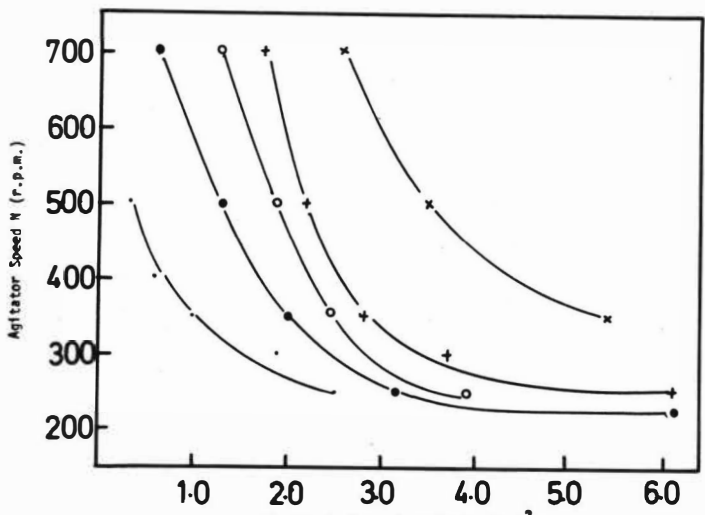


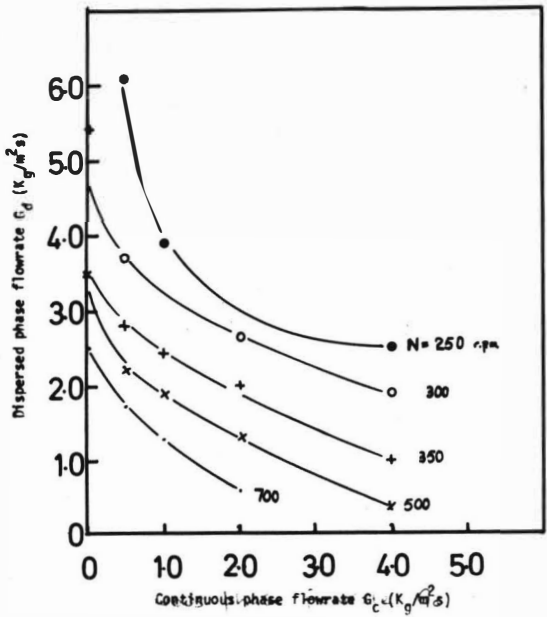
FIGURE 11. Mean drop size vs hold-up $G_c = G_d$

- \bullet = 0.25 $\text{Kg/m}^2 \text{s}$
- \circ 0.50 "
- $+$ 0.75 "
- \square 1.00 "
- \bullet $N = 300 \text{ rpm}$



Dispersed phase flowrate G_d ($\text{Kg}/\text{m}^2\text{s}$)

FIGURE 12 G_d vs N at phase inversion $G_c =$ 0.00 $\text{Kg}/\text{m}^2\text{s}$ x
 0.25 " o
 0.50 " +
 0.75 " •
 1.00 " •



Dispersed phase flowrate G_d ($\text{Kg}/\text{m}^2\text{s}$)

FIGURE 13 G_d vs G_c at phase inversion

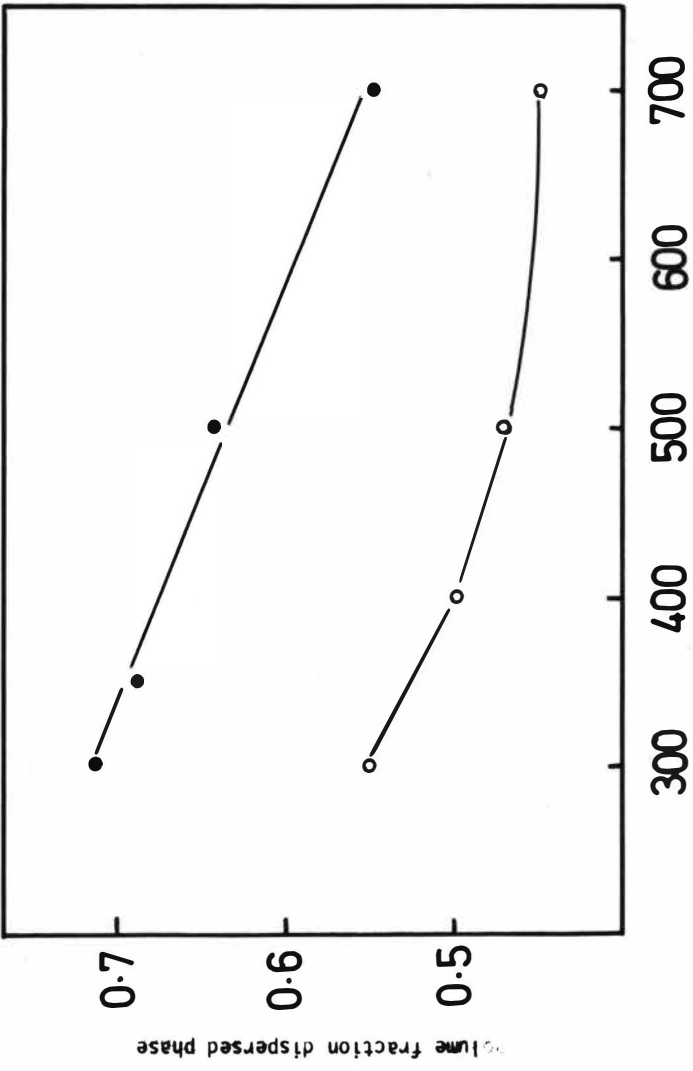


FIGURE 14 Phase inversion hold up vs impeller speed

J. Y. OLDSHUE, MIXING EQUIPMENT COMPANY, INC., ROCHESTER,
NEW YORK, U.S.A.

F. HODGKINSON, LIGHTNIN MIXERS LIMITED, POYNTON, CHESHIRE, ENGLAND.

J. C. PHARAMOND, LIGHTNIN MIXERS LIMITED, COMPIEGNE, FRANCE

ABSTRACT

The use of multi-stage mixer columns, illustrated by the Oldshue-Rushton Column, involves a consideration of the effect of mixing in each of the stages. Mixing affects the throughput, the mass transfer rate and the interstage mixing. Full scale columns can have various proportions for the same extraction performance, and differ in geometry from small pilot plant columns. Batch emulsion break times can be used to qualitatively predict column throughput.

On scale up, pumping capacity and individual fluid shear rates scale up with different relationships.

Mixing Equipment Co., Inc., Rochester, New York
A unit of General Signal

Agitated liquid-liquid extraction columns have been in use since the early 1950's (5) At that time, three types of columns were introduced, the rotating disc column, the York-Scheibel Column and the Oldshue-Rushton Column. They contrast to the previously available columns which obtained mass transfer by flowing streams across a packing, or through perforated plates, bubble caps, or spray nozzles.

Three characteristics of mixer columns are important:

1. Improved volumetric mass transfer rates by using a controlled mixing regime.
2. The ability to scale up accurately, since the dispersion is produced by rotating impellers with known characteristics. Using the flowing energy of liquid streams for dispersion can cause problems in liquid distribution, changing wall effects on scale-up, and channeling.
3. One or both phases may contain solids, Agitated columns are essentially self-cleaning, and can be used on a wide variety of process streams.

The two open-type columns, the RDC and the Oldshue-Rushton Column, differ from the original York-Scheibel Column. The latter had individual mixing and packed settling stages. This meant that higher mixer power levels could be used and higher mass transfer rates could be obtained in the mixing zone, but then there had to be provided a lower power level and lower mass transfer rate in the settling zone. The net result was about equal performance in terms of total stage height from either type. The open type column offers construction simplicity, and only one interface to consider. A frequent requirement for alloy construction in large columns further constrains the type of internal complexity that is economically justified.

Another type of system is the mixer-settler. A high mass transfer rate can be obtained in the mixer, since there is a settling tank provided to separate the two phases.

In general, comparisons of all extractor types have to be made on cost estimates, since rarely is there the same process operating simultaneously on two different types of equipment. Cost estimates can have considerable variation. Usually, however, the total volume in all the different systems is quite similar, and the major cost difference revolves around the cost of land, the necessity of multiple column units, because of the plant size involved, and whether the mixer-settlers have to be enclosed in a structure.

When mixer-settlers get very large, and interstage pumping requirements are added to mixing requirements, the increased fluid shear stresses associated with developing high lift heads may bring the mixer regime farther into an area of high mixer horsepower producing a dispersion which cannot be adequately compensated for by additional settler volume. Figure 1 illustrates this situation. The remaining discussion in this paper concerns the Oldshue-Rushton extractor.

SCALE-UP PRINCIPLES

A large scale extractor will usually be quite different in several regards than the small pilot plant unit used for study. A 6" diameter column with a 3" stage height, and a 2- $\frac{1}{4}$ " diameter stage opening similar to that shown in Figure 2, and reported in Reference 6, is often used to obtain pilot plant data.

By separating the several mixing factors involved, it is possible to scale up the extraction results to end up with any desired geometry, which can then be costed out and economic comparisons made to carry out overall evaluation. Figures 3 and 4 show some of the properties that change on scale up. In the pilot plant, the usual measurement is the number of theoretical stages obtained in the equipment. It is then possible to calculate the stage efficiency.

The most reliable scale up technique is to determine the mass transfer coefficient, $K_L a$, which is normally based on the dispersed phase. In the pilot plant, the effect of interstage mixing is evaluated, the effect of the ratio of the slope of operating line to equilibrium equipment line is evaluated, and the $K_L a$ determined for the residence time in the small scale equipment. Interstage mixing is a flow induced by the mixer which is in addition to the fluid throughput, and tends to reduce concentration gradients. Scale up can then be made to several different geometries on full scale. For any chosen geometry, the effect of residence time ratio of fluid shear rates, blend time, interstage mixing of the undispersed phase, degree of mixing of the dispersed phase, and the effect of power level is considered.

Actually, many different combinations of geometry are possible to accomplish the same degree of extraction. For example, a given capacity can be obtained with large openings in a small diameter column, or smaller openings in a larger diameter column, Figure 5. Also, different stage heights can be considered, which vary the number of mechanical stages required further. In general, the stage efficiency will be considerably higher on full scale than it is on small scale, as shown in Figure 6.

Stage Efficiency

Overall extraction stage efficiency is determined by interstage mixing, (1,2,3) which is related to the interstage mixing stage efficiency, residence time, and mass transfer rate. It is also a function of concentration driving force. Any mixing of the dispersed phase tending to reduce its concentration gradient will decrease column performance. It is normally assumed that the undispersed phase is completely mixed and essentially has no concentration gradient. This is less true as column scale up is increased. The larger the opening between the stages the lower the stage efficiency, and the greater the throughput. There is also the function of the impeller size to tank size ratio, and impeller size to opening size ratio.

In addition, allowing the radial flow impeller to establish a dual flow pattern in each stage does establish some desirable concentration gradients in the system.

Fluid Shear Stresses

The role of shear stress is quite important, and among other things, determines what is going to happen on full scale to entrainment. Figure 7 shows that as we scale up, there is a tendency for the maximum shear rate in the impeller zone to increase while the average shear rate throughout the impeller zone tends to decrease (4). If droplet size is proportional to shear stress, then we will have a greater distribution of droplet sizes from the shear stresses shown in Figure 7 than we have in the small scale unit. We may have the same average mass transfer coefficient, but there will be a difference in droplet size in the dispersed phase.

COLUMN THROUGHPUT

There is no way at the present time to calculate the throughput capacity of a full size liquid-liquid extraction column without making a small scale test. The test purpose is to get the capacity through a standard set of geometry conditions so that extrapolation can be made to other geometry options. Table 1 indicates how capacity changes with different stage openings in a small unit for one chemical system. Normally, the low volume phase is dispersed, and the higher viscosity phase is dispersed. These two requirements may not be possible in every case. One important criterion is to determine the performance under throughput turn-down conditions. Figures 8 and 9 show that depending upon the relative mass transfer characteristics in the system, turn-down ratios can either help or hurt the overall column performance. It is essential that these turn-down ratios be specified, and a suitable test be made in the pilot plant to determine their effect on column performance. At a lower throughput, the increased residence time may either be important or insignificant. The increased interstage mixing lowers performance. Normally, the performance of a high $K_L a$ system is lowered with turn-down, while the performance of a low $K_L a$ system is enhanced.

In general the dispersed phase has less entrainment than the continuous phase. Therefore, special separators have to be placed in the continuous phase withdrawal zone to prevent mixing energy "leaking out" of the last mixing stage.

Many studies have been conducted to try and compare break-time studies with capacity of liquid-liquid extraction columns. In a later section, examples of some of these break-time studies will be illustrated related to column capacity.

PILOT PLANTING

It is very helpful in analyzing column performance to have batch extraction tests as well as batch break-time tests. These batch studies should be done with impellers that simulate the shear rate that will be obtained in the full scale unit. This means the use of non-geometrically similar impellers as well as special runs designed to duplicate certain shear rate parameters in the system.

Break-time studies involve measuring the time for coalescence to occur after certain RPM and residence time runs in the batch system. For these tests, phase ratios are chosen as the feed ratio, even though the column hold-up may not be that value.

It is important to make runs with each of the phases dispersed, even though it is customary in the continuous column to have the small volume phase dispersed. As long as the small volume phase is not less than $1/3$ of the large volume phase flow rate, it is possible for the lower flow rate phase to be the undispersed phase.

Figure 10 indicates methods of predicting which phase will be dispersed in the batch experiments.

In the pilot column, normally a minimum of four flow rates are required. At a speed of about 300 rpm, flow rates are adjusted upward until the column just begins to flood. At this point, the flow rate is reduced to 80% of this value and extraction tests performed. Speed is then increased by approximately 20% and the flooding point determined. The flow rate is then reduced to 80% of that value and the extraction test performed.

The flow is then cut in half at the same mixer speed and the extraction performance measured. In addition, the speed is raised to a flood point, and then backed off to about a 7% lower value to determine what effect increased power would have during the turn-down condition.

An example of a scale-up calculation is shown. In a 6" diameter column, a 29% stage efficiency was obtained. This is now corrected for interstage mixing as well as the ratio of operating line to equilibrium line. A $K_L a$ value of 16.2 was obtained.

This $K_L a$ is now scaled up to a full sized column 10' diameter with a 6' high stage. A 3 HP impeller is determined to be compatible with desired capacity relationships. The effect of interstage mixing in both the continuous and discontinuous phases is determined, and an overall stage efficiency of 85% calculated. A suitable design factor is then applied.

Another example starts with a 4% stage efficiency on the 6" diameter column. This is now corrected for interstage mixing as well as the ratio of operating line to equilibrium line. A $K_L a$ value of 4.6 was obtained.

This $K_L a$ is now scaled up to a full sized column 10' diameter with the same 6' high stage. A 4 HP impeller is required. The overall stage efficiency is now 65%. Again, a suitable design factor can be applied.

BATCH-BREAK-TIME STUDIES

Solute concentration can have a large effect on break time. Therefore, break-time studies should be run simulating the rich end of the column as well as conditions simulating the lean end of the column. The approximate volumetric phase ratio in the feed streams should be used, but in no case greater than 2 to 1.

A 6" diameter jar with a 2" diameter turbine and a 6" total liquid level is typical. The impeller should be placed to give each phase dispersed in successive tests. Several speeds are run and break time is measured. Observing break time with various mixer and system variables can give a qualitative picture of the effect on column throughput.

Figure 11 shows the relationships between break time and mixer impeller speed for the water, acetic acid, methyl isobutyl ketone (MIBK) system. One of the peculiarities found was that under certain conditions there was a decrease in break time with an increase in mixer speed. However, even though the break time was slower, there was a cloudiness in the dispersed phase so that there was considerably more entrainment in that phase.

Another observation which illustrates the importance of temperature in column performance is a curve of break time versus temperature. Figure 12 shows this relationship and indicates that temperatures must be carefully specified for full scale design and properly controlled during continuous flow performance experiments.

R E F E R E N C E S

1. Bibaud, R., Treybal, R.
AIChE Journal, 12(3), 472 (1966)
2. Haug, H.F.,
AIChE Journal, 17, 3, 585 (1971)
3. Ingham, J.,
Trans. Instn. Chemical Engineers, 50, 372 (1972)
4. Oldshue, J.,
Blotech and Bioeng., VIII 1, 3 (1966)
5. Oldshue, J.,
Sol. Ext. Revs. 2, 185 (1971)
6. Oldshue, J., Rushton, J.,
Chem. Eng. Progress, 48(6), 297 (1952)

TABLE 1

EFFECT OF SIZE OF OPENING BETWEEN COMPARTMENTS

Typical Data for Operation With:

Methyl Isobutyl Ketone, Water, Acetic Acid
 4 Stages, 4 Inches Stage Height, 152 mm Diameter Column
 Extraction, W K

<u>Compartment</u> <u>Opening</u>	<u>Maximum</u> <u>Stage</u> <u>Efficiency</u>	<u>Minimum</u> <u>H.E.T.S.</u> <u>Inches</u>	<u>Flow Rate</u> <u>KG/SEC/SQM</u> <u>(Constant</u> <u>(Flow Rate)</u>
0	100	101	0 *
54 mm	83	122	2.9*
82 mm	52	195	2.9
152 mm	38	265	2.9
			(At Maximum) (Efficiency)
0	100	101	0 *
54 mm	83	122	2.9*
82 mm	67	152	5.4*
152 mm	38	265	6.0*

* Optimum Flow Rate

TABLE 2
BREAK-TIME DATA

System Methyl Isobutyl Ketone-Water

Tank 152 mm Diameter
Four Baffles 13 mm Wide
152 mm Liquid Level

Impeller 51 mm Diameter, Mounted at Interface,
Stainless Steel, Four Flat Blades

Break Point
Level 6 mm Above Interface

Interface 76 mm

R.P.A.	Break Time, Seconds				
	Time of Mixing (Seconds)				
	5	10	15	30	60
300	38	47	52	58	60
400	59	77	87	99	104
500	83	108	116	118	120
600	110	134	138	136	136
700	137	142	141	138	140
800	142	145	146	147	146
1000	141	124	123	117	126

TABLE 3
BREAK-TIME TEMPERATURE DATA

System Methyl Isobutyl Ketone-Water
 Tank 305 mm, Four Baffles, 25 mm Wide
 305 mm Liquid Level
 Impeller 101 mm Diameter, Mounted at Interface,
 Stainless Steel, Four Flat Blades
 Break Point Level 13 mm Above Interface
 Interface 101 mm
 Turbine Speed 400 R/M

Time of Mixing (seconds)	Break Time (seconds)	Temperature C°
5	55.5	12
10	58.1	12
20	57.1	12
30	56.5	12
40	55.2	13
5	53.6	14
10	55.6	14
20	54.8	14
30	54.5	14
40	54.0	15
5	50.6	18
10	52.7	18
20	52.8	19
30	52.1	19
40	52.3	19

TABLE 3 (continued)

Time of Mixing (seconds)	Break Time (seconds)	Temperature C ^o
20	49.9	20
30	49.9	20
40	49.5	21
5	46.9	21
10	49.4	21
5	45.0	23
10	47.4	23
20	47.2	23
30	46.6	24
40	46.5	24
5	42.8	26
10	45.4	26
20	45.4	27
30	45.2	27
40	45.2	27
5	38.9	30
10	42.7	30
20	42.8	30
30	42.5	30
40	42.8	31
5	38.9	32
10	41.5	32
20	41.3	32
30	41.5	32
40	41.5	32

MASS EXTRACTED/TOTAL SYSTEM VOL.

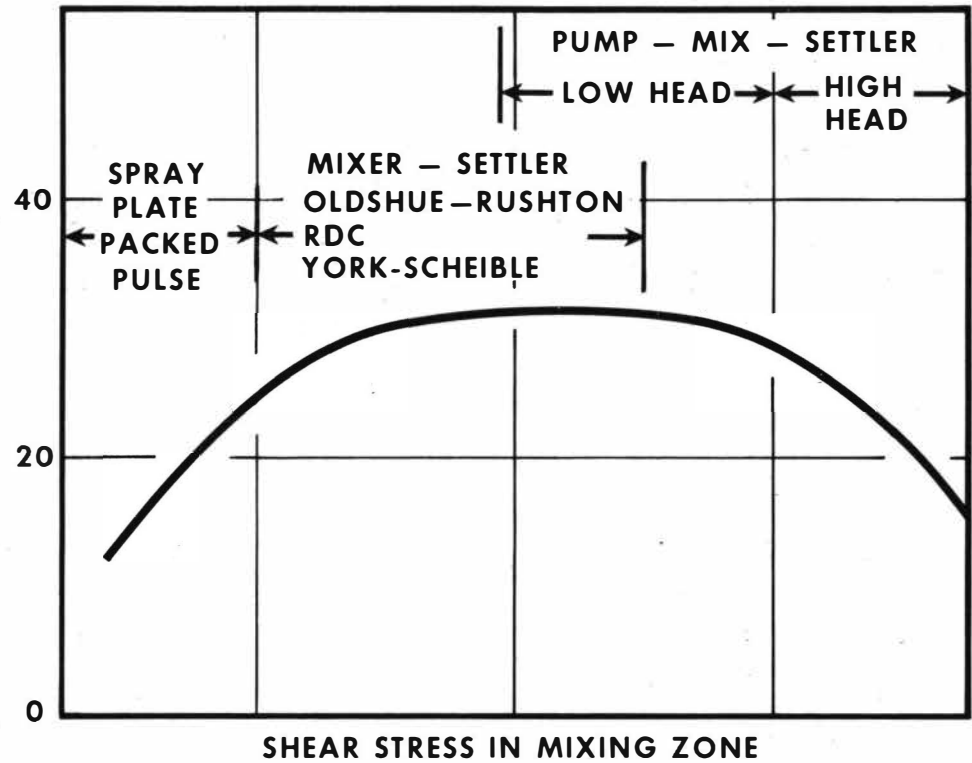


FIGURE 1
EFFECT OF SHEAR STRESS IN MIXING ZONE ON
OVERALL EXTRACTOR PERFORMANCE

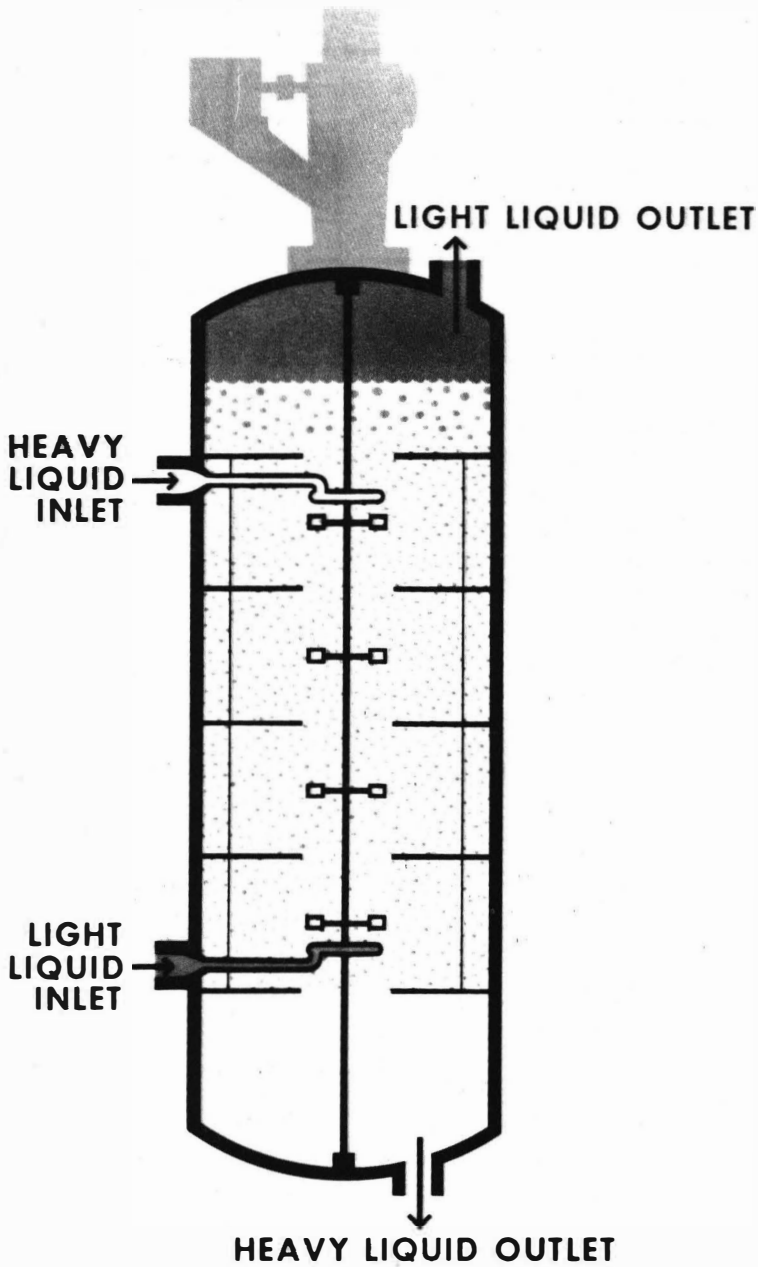
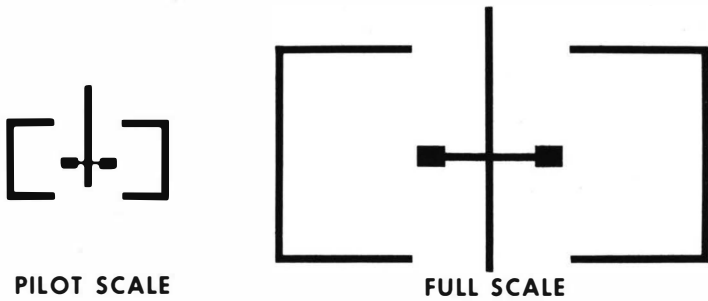


FIGURE 2
SCHEMATIC OF OLDSHUE – RUSHTON EXTRACTOR



FULL SCALE COMPARED TO PILOT SCALE

RESIDENCE TIME	HIGHER
BLEND TIME, UNDISPERSED	LONGER
INTERSTAGE MIXING, UNDISPERSED	DIFFERENT
INTERSTAGE MIXING, DISP.	DIFFERENT
CONCENTRATION GRADIENT, DISP.	HIGHER
MAX. IMPELLER ZONE SHEAR RATE	HIGHER
AVE. IMPELLER ZONE SHEAR RATE	LOWER
AVE. TANK ZONE SHEAR RATE	LOWER
TURBULENT SHEAR RATES	DIFFERENT

FIGURE 3
MIXING FACTORS COMPARED FOR PILOT AND FULL SCALE

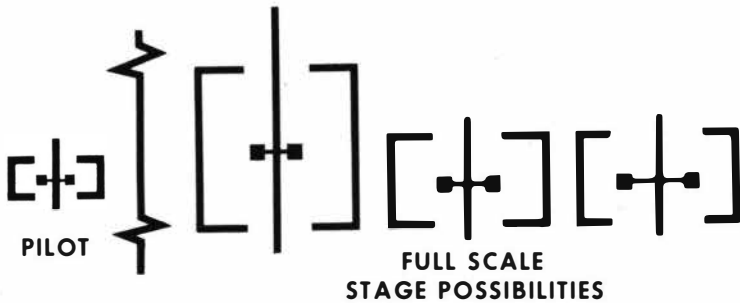


FIGURE 4
POSSIBLE FULL SCALE EXTRACTOR GEOMETRY

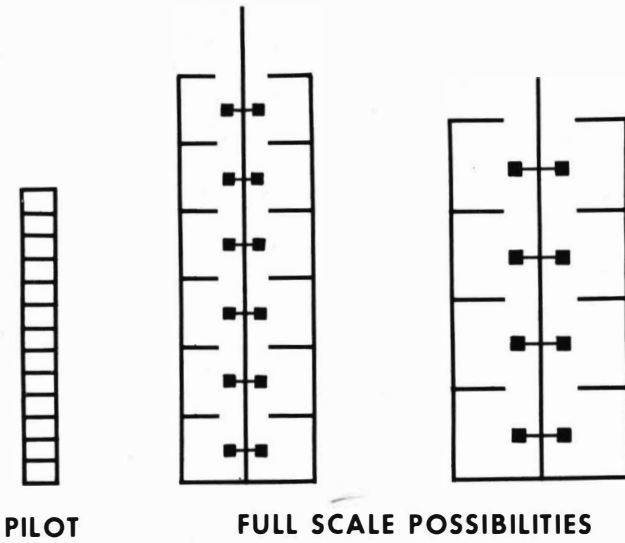


FIGURE 5
 POSSIBLE FULL SCALE COLUMN
 GEOMETRIES FOR SAME PERFORMANCE

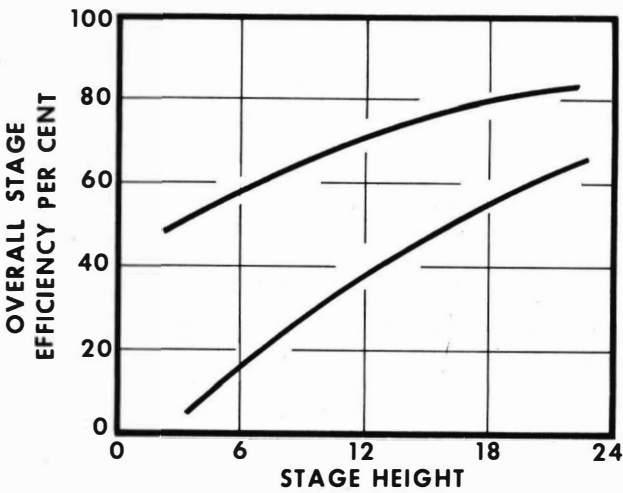


FIGURE 6
 EFFECT OF STAGE HEIGHT ON STAGE EFFICIENCIES FOR
 OLDSHUE-RUSHTON COLUMN

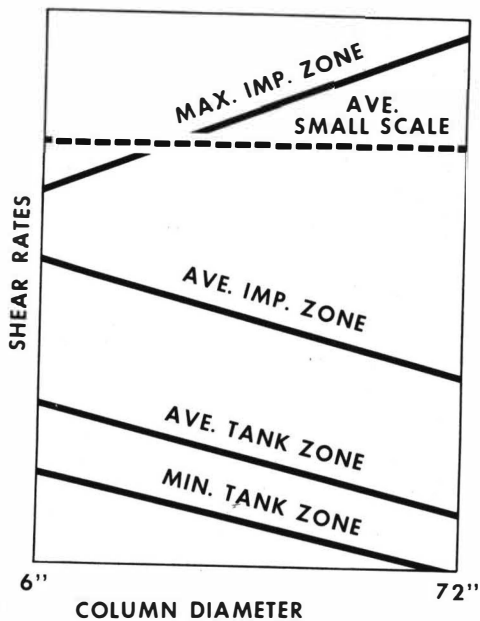


FIGURE 7
EFFECT OF SCALEUP ON SELECTED SHEAR RATES

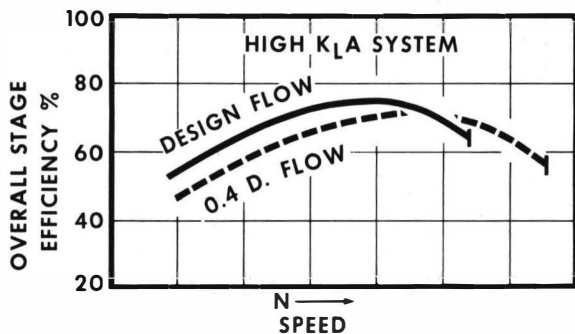


FIGURE 8
EFFECT OF THROUGHPUT TURNDOWN RATIO
ON STAGE EFFICIENCY FOR HIGH $K_L a$ SYSTEM

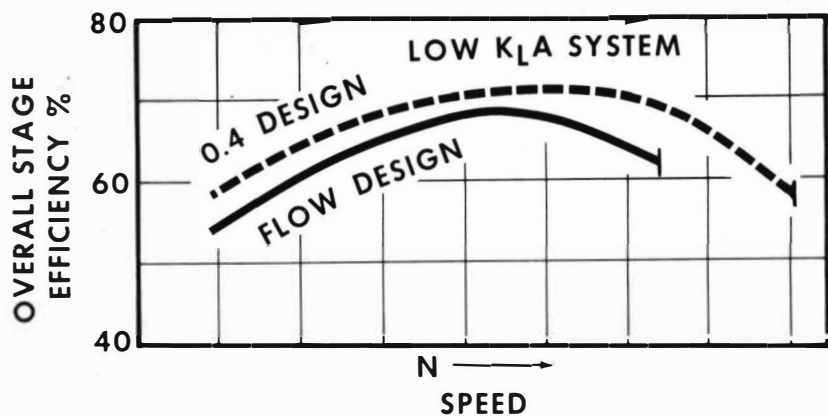


FIGURE 9

EFFECT OF TURNDOWN RATIO ON STAGE EFFICIENCY FOR LOW K_LA SYSTEM

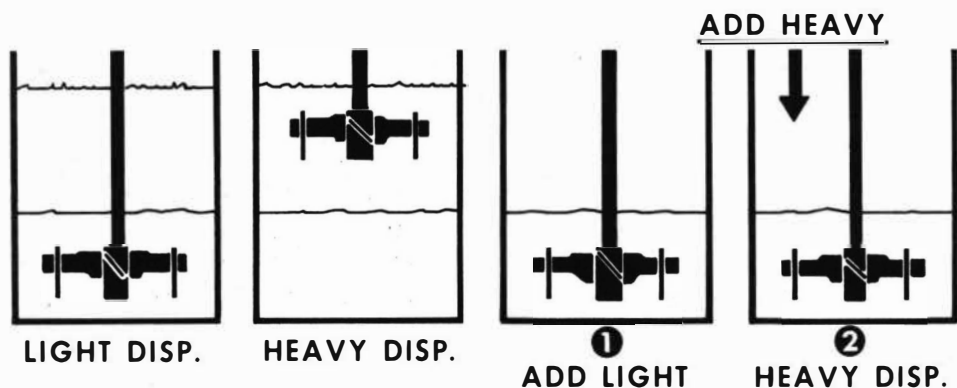


FIGURE 10

METHOD OF CONTROLLING WHICH PHASE IS DISPERSED IN BATCH EXTRACTIONS

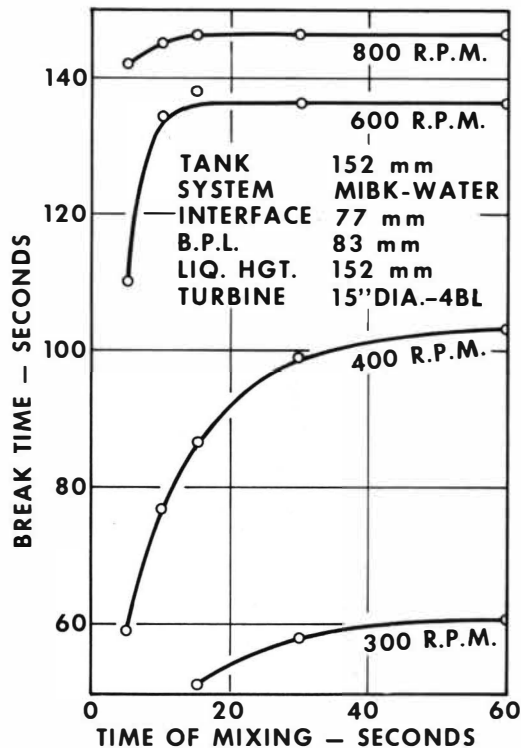


FIGURE 11
 BREAK TIME AS A FUNCTION OF
 TIME OF MIXING AND SPEED

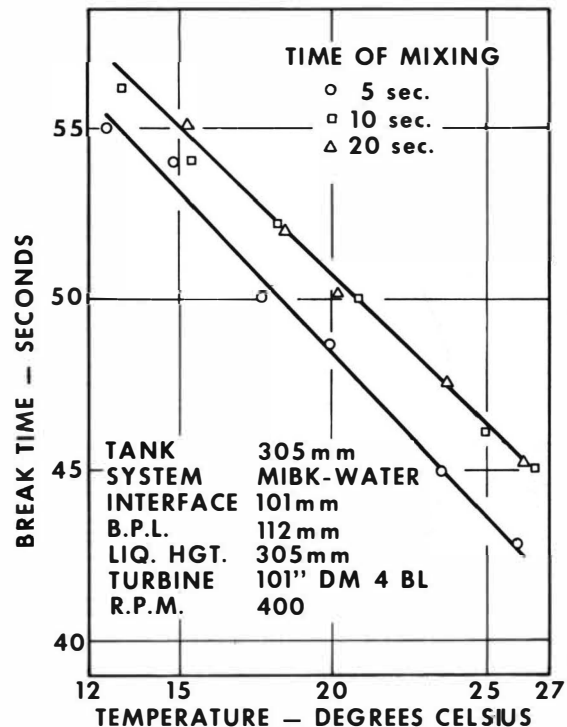


FIGURE 12
 EFFECT OF TEMPERATURE ON BREAK TIME

HOLD-UP AND FLOODING IN RECIPROCATING-PLATE EXTRACTORS

M.M.Hafez, N.Nemecek and J. Prochazka

Mean drop size, hold-up of dispersed phase and flooding have been measured in two models of a reciprocating-plate extractor. The system used was water-trichloroethylene. Three different regimes of flow could be distinguished and special attention has been paid to the dispersion regime in the case of hold-up and the corresponding transition regime in the case of flooding, respectively. A new correlation of the drop size has been proposed, based on the concept of homogeneous, isotropic turbulence. The close connection between the hold-up and power input has been emphasized. New types of correlation of hold-up data in the transition and emulsion type regions have been proposed. A comparison of results for three main types of perforated plates has shown distinct features of the individual types and the similarity of behaviour of the reciprocating and pulsed extractors with the same construction of plates.

Czechoslovak Academy of Sciences, Prague, Czechoslovakia,
Institute of Chemical Process Fundamentals.

INTRODUCTION

The reciprocating-plate extractors were put into industry only recently³. They proved to have a very good efficiency combined with unusually high throughputs. Also their easy adaptability to widely differing demands indicates that a variety of applications of this extractor can be expected. Under these circumstances the need of data on hydrodynamics and mass transfer in this equipment, as well as its mechanical behaviour, is evident.

Previous work was concerned mainly with longitudinal mixing^{4,5} in the reciprocating extractors and with the dynamic effects, including the power input, in this apparatus⁶⁻⁸. It has been also shown that the behaviour of the reciprocating-plate extractors is in some respects similar to that of a pulsed column, as long as the geometry of their trays is identical. The main differences are of mechanical nature and here also lies the superiority of the principle of moving plates to that of pulsating liquid. Consequently the data on hydrodynamics in the reciprocating column can be compared with those obtained in pulsed columns under similar conditions.

When analysing the hydrodynamics of the reciprocating and pulsed plate columns three hydrodynamics regimes can be distinguished: the so called mixer-settler type (MS) dispersion type (D) and emulsion type (E) regimes. The first and the last one have been well described^{9,10}. In this paper the dispersion type regime has been introduced as it has been found that both the hold-up and the flooding velocity correlations display distinct features in this region. Qualitatively the dispersion region can be defined either statically or dynamically. According to the first definition the whole mass of the dispersed phase in the stage consists of droplets but the local hold-up shows a marked gradient in axial direction. The dynamic description follows the gradual transition from the (D) type to the (E) type with increasing pulse velocity. At first the originally continuous layer of the dispersed phase on the plate changes to a layer of densely packed droplets and this layer then gradually expands under the influence of the pulsating jets of the continuous phase streaming from the openings of the plate. The transition regime changes to the emulsion type one when the expanding layer reaches the next plate.

Three main types of the reciprocating plate geometry have been reported and each of them has its place among the pulsed plate columns. These are: 1. the plates with perforations of uniform size and so small, that the surface tension practically prevents the flow with no pulsation¹¹; 2. the plates with very large openings and large free areas¹²⁻¹⁴; 3. the plates with downcomers for the continuous phase^{3,15}. As can be expected, there are principal differences in hydrodynamic characteristics of the above mentioned types of plates in the sense, that not all of them exhibit all three hydrodynamic regimes. Some evidence for this opinion has been found in the course of this work.

Experimental

The experiments have been performed in glass reciprocating-plate columns of 50 and 85 cm inner diameters, 2 m long in which a set of horizontal perforated brass plates mounted on a common rod was situated. An electronically controlled variable speed DC motor connected with an adjustable eccentric imparted the reciprocating motion to the plates. The ranges of amplitudes and frequencies used were $a(0-0.8 \text{ cm})$, $f(0-4\text{c/s})$. The liquids used were distilled water and trichloroethylene mutually saturated at 25°C, the organic phase dispersed.

The total hold-up⁹ was measured using the method of abrupt closing the inlets of both phases and the outlet of the organic phase and reading the increase of the interface level at the bottom of the column. In some cases, especially those in which the total number of plates was not high enough, local holdups in the midst of the column were determined. This was done by reading the level of the layer of the dispersed phase on the plate, which formed when the vibrations were interrupted at the same time as the flows. With the used system of liquids and range of hole diameters no appreciable leakage has been observed. In the majority of measurements a sufficient overall number of plates was used to ensure¹⁶ a practically uniform axial hold-up profile throughout the column. The flooding points were determined visually according to the commonly accepted definitions. The approach to flooding was either increasing the dispersed phase flow-rate, or increasing the frequency of reciprocating with other variables kept constant.

In the course of experiments also the size of drops has been determined by taking photographs of the dispersion. The Sauter diameter d_{32} has been used as the characteristic mean value.

Finally also measurements of power input were performed using the methods of the capacitance probe recording of the pressure wave at the bottom of the column and the tension line indication of the force wave on the rod, respectively. Both methods have been described elsewhere^{1,7}.

Mean drop size

A suitable form of correlating d_{32} with the pertaining variables can be found by simple theoretical considerations. Let us suppose that the drop splitting is caused predominantly by the dynamic pressure forces of the turbulent flow in the vicinity of the vibrating plate, under noncoalescing conditions. Following Hinze¹⁷ the turbulent fluctuations responsible for the splitting are expected to have a wave length of the order of d_{32} and to belong to the inertia subrange of locally isotropic homogeneous turbulent field. For the mean square of the fluctuation velocity difference then holds

$$\overline{u^2} \sim (E d_{32})^{2/3} \quad (1)$$

With the given system, in which u_D is small and ρ_c is large, the viscosity group $\frac{\mu_D}{\rho_c D^{d_{32}}}$ is expected to be small and hence the Weber number can be assumed constant

$$We = \frac{\rho_c \overline{u^2} d_{32}}{\sigma} = \text{const.} \quad (2)$$

Combining this expression with (1) one has

$$d_{32} \sim (\sigma / \rho_c)^{3/5} E^{-2/5} \quad (3)$$

To evaluate the turbulent energy dissipation measurements of the mean power consumption were undertaken and an empirical correlation obtained.

$$N = n \cdot 3.73 \times 10^{-4} \cdot 2^{af} \cdot \rho_c^{2.92} E^{-2.01} + 0.131 (u_D / 2^{af})^{0.138} \quad (4)$$

It can be readily shown that for high values of 2^{af} formula (4) is in accord with

$$\frac{N^2}{(2^{af})^3 \rho_c D^2} = \text{const.} \quad (5)$$

which may be deduced from dimensional analysis. From this follows for the energy input per unit mass

$$E \sim \beta^{3/h}; \quad \beta = \frac{2^{af}}{\rho_c^{2/3}} \quad (6)$$

If the height of the region where intensive splitting occurs, h is assumed to be constant, the final expression for the drop diameter results

$$d_{32} \sim \left(\frac{\sigma}{\rho_c} \right)^{3/5} \cdot \beta^{-6/5} \quad (7)$$

Fig.1 shows the results of our measurements. For the emulsion regime they follow formula (7). The correlation d_{32} vs β gives a straight line for the other regimes, too, but with a slope differing from $-6/5$. The respective formulae are

$$d_{32} = 0.28 H^{0.11} \beta^{-0.34}; \quad \beta < 9.0 \quad (8)$$

$$d_{32} = 0.29 \left(\frac{\sigma}{\rho_c} \right)^{3/5} \beta^{-6/5}; \quad \beta \geq 9.0 \quad (9)$$

In Fig.1. there are also drawn the lines representing the data of Miyauchi and Oya¹⁸ as well as a line representing Eq.(9) for the system MIBK - water used in the cited work ($\sigma_{\text{MIBK-H}_2\text{O}} = 10.3 \text{ dyn/cm}$; $\sigma_{\text{tri-H}_2\text{O}} = 31.2 \text{ dyn/cm}$).

Holdup

The general form of the dependence of the holdup on the pulse velocity (Fig.2) corresponds to that of a pulsed plate column. The holdup decreases in the (MS) region and increases in the other two regions. As was expected, in the (D) and (E) regions the holdup correlates well with the drop size

$$X = \begin{matrix} 0.074 & 0.61 & u_D^{1.5} & ; & 6.0 \leq \beta \leq 13.0 \\ 3.5 \times 10^{-5} & \beta^{3.6} & u_D^{1.5} & ; & \beta > 13.0 \end{matrix} \quad (10)$$

The results of this correlation are shown in Fig.3.

In the (MS) region where the distribution of the dispersed phase within the stage is rather nonuniform, the holdup in the bulk of the stage contributes but little to the average holdup, the latter being predominantly determined by the dense packed layer on the plate. In other words the residence time of the dispersed phase in the layer exceeds that in the rest of the stage. Now the fraction of the cycle, during which the layer exists, decreases with increasing pulse velocity $2af$ and is independent of the geometry of the plate. These considerations help to explain the form of correlation for the (MS) region found (Fig.4)

$$X = 0.15 (2af)^{-1.57} u_D^{1.5} ; 2af \leq 0.75 \quad (11)$$

The region in the figure described by Eq.(11) is followed by a section of constant holdup linking it to the true (D) regime.

$$X = 0.215 u_D^{1.5} \quad (12)$$

This phenomenon can be qualitatively explained as follows. Starting from a certain value of the pulse velocity the layer of densely packed drops begins to expand, which is caused by the increasing velocity of the jets of continuous phase penetrating it as well as by the decreasing drop diameter. Under these conditions the increasing pumping capacity of the plate is counter-balanced by the decreasing concentration of the dispersed phase within the layer.

Simultaneously the relative importance of the holdup in the bulk of the stage gradually increases. It is clear that the exact balance of these phenomena expressed by Eq.(12) cannot be expected to hold for widely differing conditions, as can be seen from Fig.5. This figure shows another promising way of correlating the holdup data, namely against the power consumption - Straight lines in semi-log coordinates result in this case.

It has been suggested for the RDC columns¹⁹, and pulsed plate columns with large openings of the plates¹⁴, that the average falling velocity of drops equals that of rigid spheres but only a proportionality has been confirmed by indirect measurements. In the case of the vibrating plate column of the Karr type (i.e. with large openings of perforations) Pavasovic et. al.²⁰ have found an increase of the apparent drag coefficient of 8 to 25%. In our case of the plates with small holes it exceeded the values for infinitely diluted rigid spheres more than twice. The hindering effect of the plates could apparently be an explanation of this fact.

Flooding

The form of the flooding curve of the vibrating plate column with a small diameter of perforations (Fig.6) corresponds to that for a pulsed column of similar construction. A comprehensive survey of the work done in correlating the flooding data on pulsed plate columns has been given by McAllister et al.¹⁰. Two regions are distinguished, the region of flooding by insufficient pulsation and that of flooding caused by excessive intensity of pulsations. Little attention has been paid to the transition region, as it is called in this paper. This region is defined as that part of the flooding curve between the apex and the point, where the curve starts to deviate from the line described by the pertaining equation for the flooding by insufficient pulsation. This region may be comparatively wide under some conditions.

The term "flooding by insufficient intensity of pulsation" has its origin in thinking of a process of decreasing the pulse velocity at constant throughput. For the description of the transition region the process of increasing the velocity of dispersed phase at constant pulse velocity is more suitable. When starting this process at a point within the (B) region (see Fig.6) a layer of fully coalesced dispersed phase commences to build up on the plate during a part of the cycle. As u_D increases, this layer persists for an increasing fraction of that part of the cycle, when the direction of flow in the openings of the plate equals that of u_D . The flooding point corresponds to that value u_{Df} , at which for entire part of the cycle mentioned the plate is covered by said layer. The equation describing the flooding velocity in the case of continuous feeding and withdrawing of the phases is as follows¹⁰

$$u_{Df} = 4\pi af \cos \phi / \pi + 2\phi + r (\pi - 2\phi) \quad (13)$$

$$\phi = \sin^{-1}(u_c - u_D) / 2\pi af; \quad r = u_c / u_D$$

If the process starts in the (D) region, there is no longer a continuous layer of the dispersed phase on the plate. Instead a more or less densely packed layer of drops appears. So at the moment of flooding in the transition region a mixture of dispersed and continuous phases is pumped through the plate, the fraction of the dispersed phase in it X_D being determined by the local holdup in the layer. Increasing the pulse velocity the layer expands into the stage and its holdup decreases. This is the cause of a still stronger deviation of the flooding curve from the line given by (13). The apex will be arrived at when the expanding layer reaches the next plate. The model just described can be formalised by multiplying the right-hand side of (13) with a function of the pulse velocity, $X_D(2af)$. A simple linear function has proved satisfactory, which is determined by two points, $(2af)_{MS}$, 1 and $(2af)_E$, X_E respectively. Fig.7 shows examples of the transition curves calculated in this way and the corresponding experimental points.

The equation for the region of flooding by excessive intensity of pulsations given by McAllister¹⁰ is implicit in both u_{Df} and $2af$. In this work a simple relation has been found to hold between these variables of the form

$$u_{Df} = A - B \log 2af \quad (14)$$

The data obtained in this work are plotted on semilogarithmic coordinates in Fig.8. As the straight lines corresponding to different values of μ , d are parallel, it can be inferred that the slope of these lines is a function of the properties of the liquid system only. In Fig.9 the data of other authors using different systems are shown.

Among the data collected in the figures 8 and 9 are two sets belonging to plates of different types. In Fig.9 it is the set denoted as Baird¹³, which represents the Karr type plates, in Fig.8 the line labelled "downcomers" concerning the plates with special large openings for continuous phase provided with tubular mouths (see Fig.10). It can be seen that (14) holds for these types as well.

In conclusion a comparison has been made between the flooding curves for plates with and without downcomers. The results are shown in Fig.11. The total free area of both plates is equal and so is the diameter of the small perforations. Apparently the throughput of the plate with downcomers is considerably higher, especially in the region of low pulse velocities due to the presence of the downcomers. The main reason for this is the fact that the throughputs in the mixer-settler regime are not limited by the pumping capacity of the plate.

A similar shape of the flooding curves, as that for plates with downcomers, has been reported for the Karr plates by Baird¹³. Here the mixer settler regime is apparently absent as the plates are unable to bear the coalesced layer.

Conclusions

1. The mean drop size in the emulsion type region could be predicted on the basis of a model using the assumption of homogeneous isotropic turbulence of the continuous phase in the vicinity of the plate.

2. Both the mean drop size and the fractional holdup of the dispersed phase have been found to be simple functions of the energy consumption.

3. New ways of the correlation of flooding in the transition region and the excessive pulsation flooding region have been proposed.

4. Similar hydrodynamic behaviour of reciprocating-plate and pulsed extractors with identical plate construction has been found. The plates with downcomers have been found to be superior to those having only small perforations.

Symbols

a	amplitude, (cm)
d	diameter of plate perforation, (cm)
d_{32}	Sauter mean drop diameter, (cm)
D	column diameter, (cm)
f	frequency, (s^{-1})
h	height of region of intensive splittin \bar{g} , (cm)
H	height of stage, (cm)
n	overall number of plates
N	mean power consumption, (W)
u	superficial velocity of flow, ($cm\ s^{-1}$)
$\overline{u^2}$	mean square of fluctuation velocity, ($cm\ s^{-1}$)
We	Weber number
X	fractional holdup of dispersed phase

Greek letters

ϵ	fractional free area of plate
μ	dynamic viscosity, ($g\ cm^{-1}\ s^{-1}$)
ρ	density, ($g\ cm^{-3}$)
σ	interfacial tension, ($dyn\ cm^{-1}$)
E	turbulent energy dissipation per unit mass, ($cm^2\ s^{-3}$)

Subscripts

C	continuous phase
D	dispersed phase
f	flooding

L I T E R A T U R E

1. Hafez M.M., PhD Thesis, Czechoslovak Academy of Sciences, 1973.
2. Nemecek M., PhD Thesis, Czechoslovak Academy of Sciences, 1973.
3. Prochazka J., Landau J., Souhrada F., Heyberger A., Brit.Chem.Eng. 1971, 16, 42
4. Novotny P., Prochazka J., Landau J., Canad.J.Chem.Eng. 1970, 48, 405
5. Nemecek M., Prochazka J., Canad.J.Chem.Eng. - in press
6. Prochazka J., Hafez M.M., Collection Czech.Chem.Comm., 1972, 37, 3725
7. Hafez M.M., Prochazka J., Chem.Eng.Sci. - in press
8. Hafez M.M., Prochazka J., Chem.Eng.Sci. - in press
9. Sege G., Woodfield F.W., Chem.Eng.Progress 1954, 50, 396
10. McAllister R.A., Groenier W.S., Ryon A.D., Chem.Eng.Sci. 1967, 22, 934
11. Van Dijek W.J.D., US Pat. 2,011,136 (1935)
12. Karr A.E., A.I.Ch.E. Journal 1959, 5, 446
13. Baird M.H., McGinnis R.G., Tan G.C.: Proc.of ISEC 71
14. Misek T.: Collection Czech.Chem.Comm., 1964, 29, 1767
15. Goldberger W.M., Benenati R.F.: Ind.Eng.Chem. 1959, 51, 641
16. Bell R.L., Babb A.L.: Ind.Eng.Chem.ProcessDes. Develop. 1969, 8, 392
17. Hinze J.O.: A.I.Ch.E.Journal 1955, 1, 289
18. Miyauchi T., Oya H.: A.I.Ch.E.Journal 1965, 11, 395
19. Misek T.: Collection Czech.Chem.Comm. 1963, 28, 570
20. Pavasovic V., Misek T., Perunicic., Ristic S.: 4th Int. CHISA Congress, Prague 1972
21. Thornton J.D., Logsdail E.: Trans.Inst.Chem. Engrs (London) 1957, 35, 331

Fig. 1 Mean drop diameter

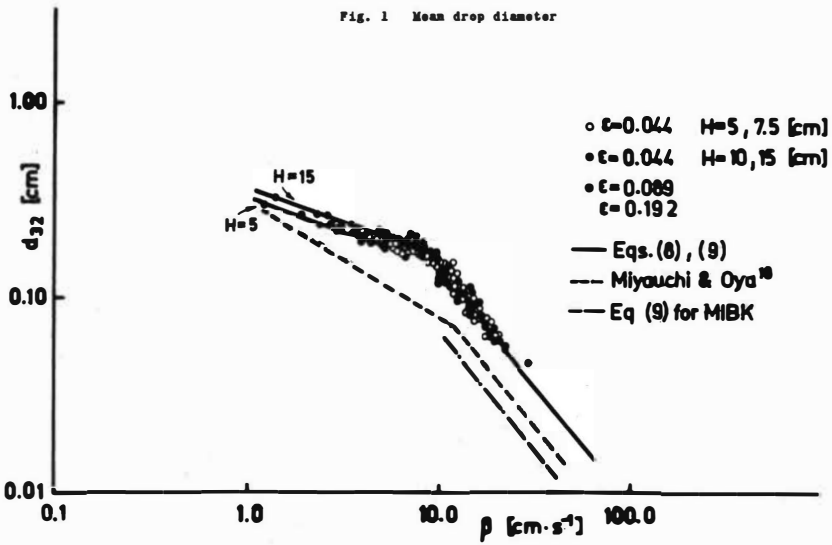


Fig. 2 Holdup vs. pulse velocity

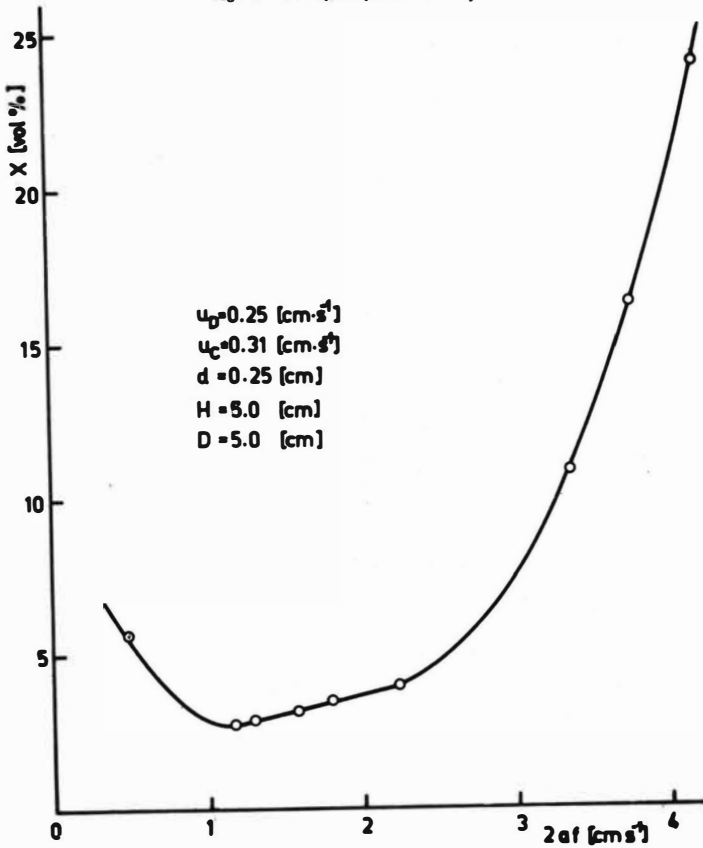


Fig. 3 Holdup in (D) and (E) regions

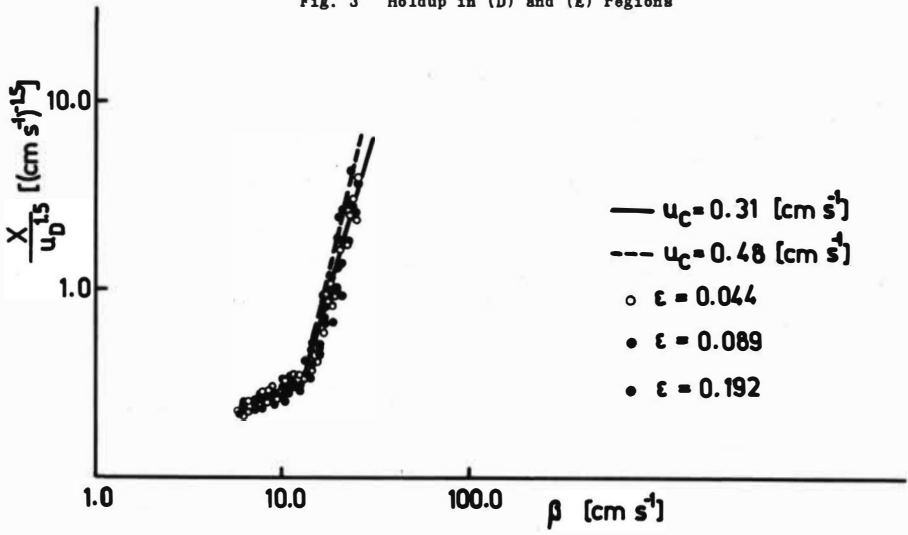


Fig. 4 Holdup in (MS) region

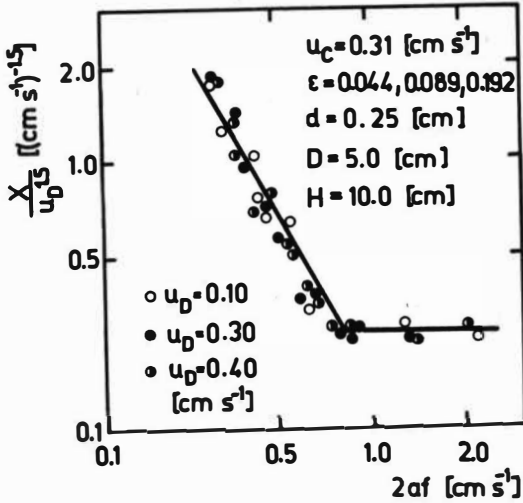


Fig. 5 Holdup vs. power input

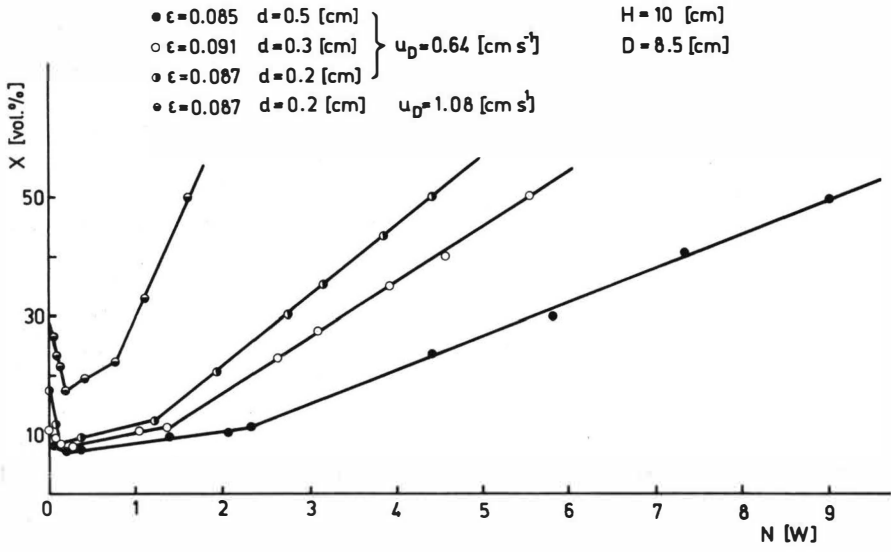


Fig. 6 Flooding curve

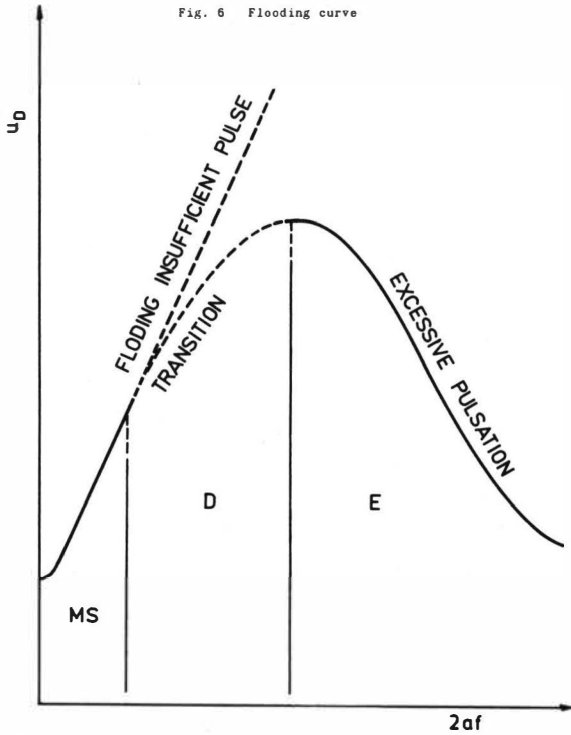


Fig. 7 Transition region of flooding

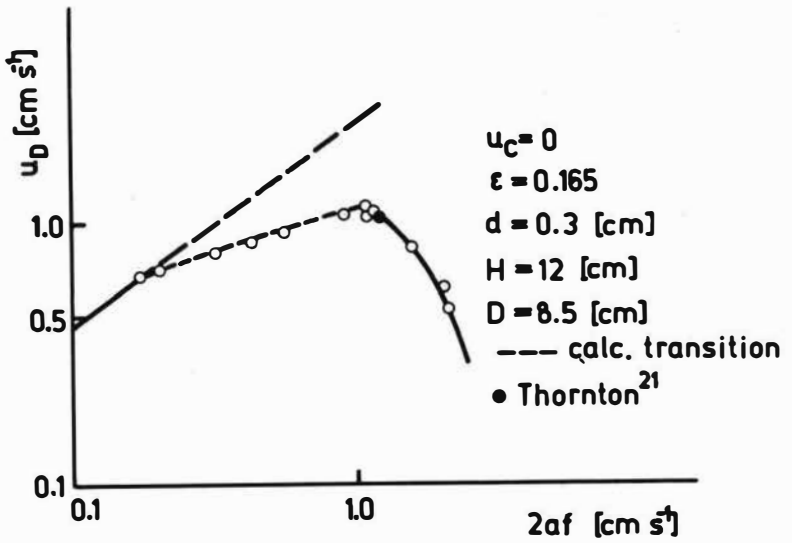


Fig. 8 Region of excessive pulsations, this work

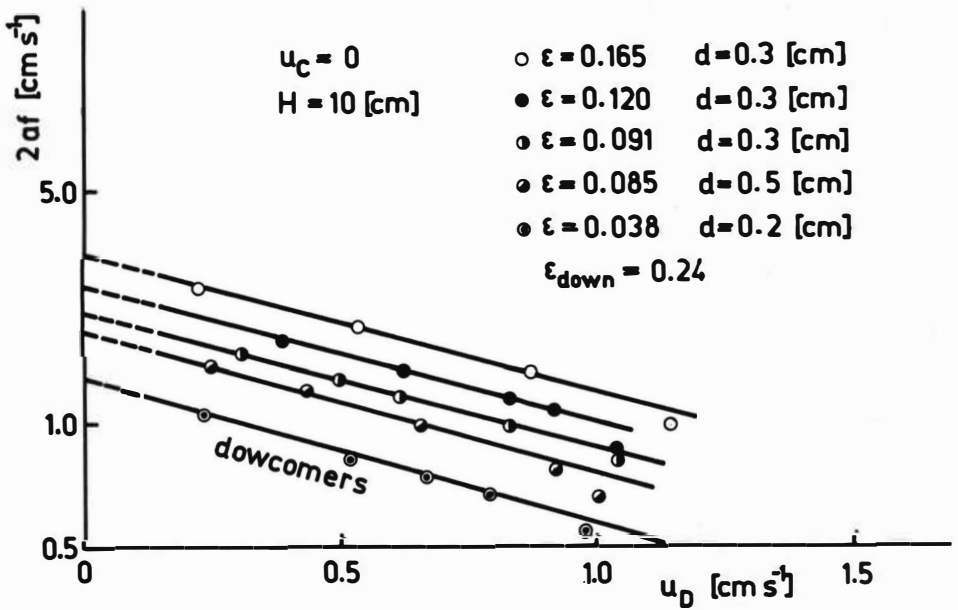


Fig. 9 Region of excessive pulsations, other authors

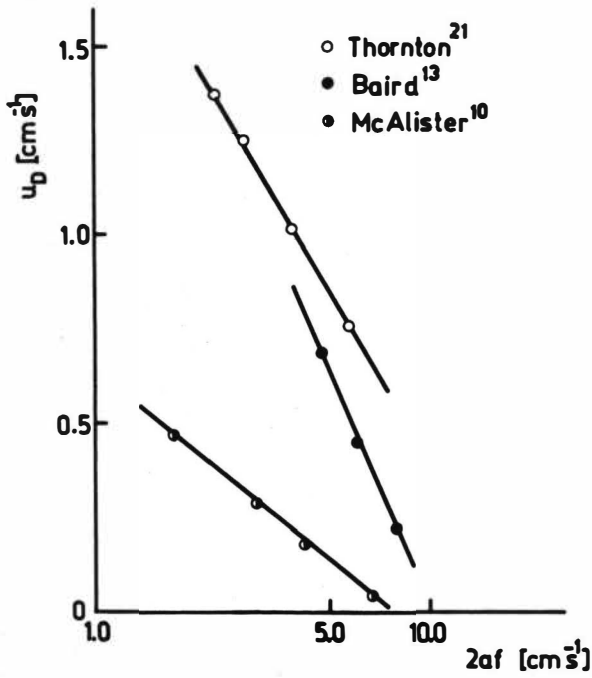


Fig. 10 Plate with downcomers

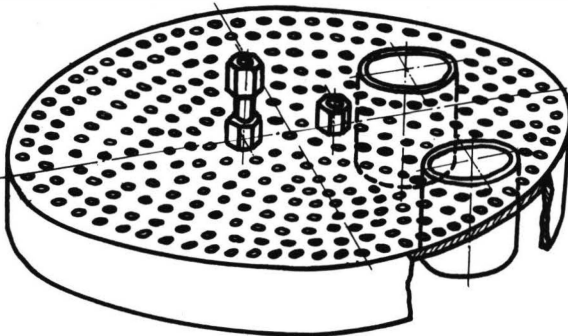
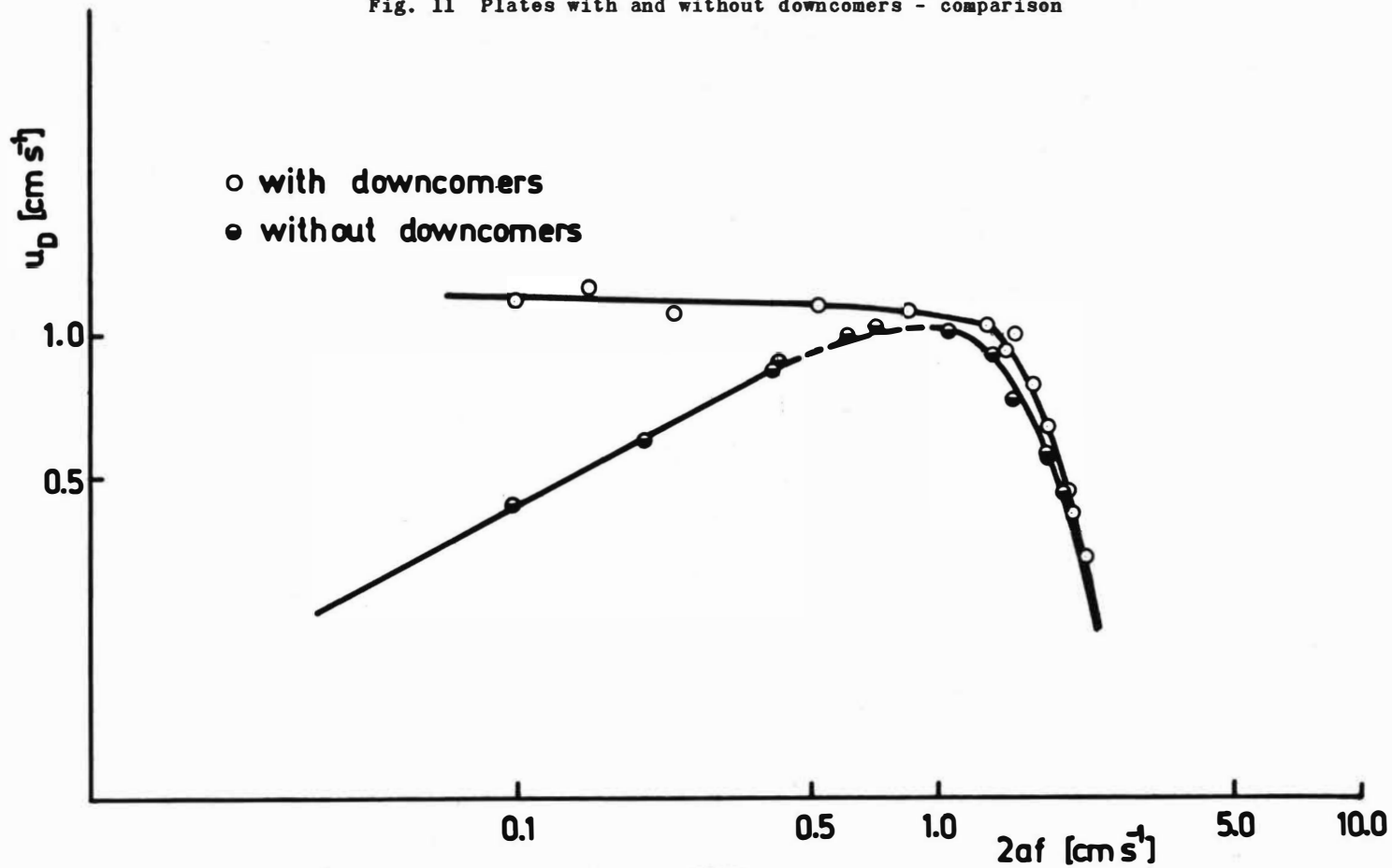


Fig. 11 Plates with and without downcomers - comparison



SESSION 16

Wednesday 11th September: 14.00 hrs

C H E M I S T R Y O F E X T R A C T I O N

(Common Metals)

Chairman:

To be appointed

Secretaries:

Dr. V. Lakshmanan

Mr. C.P. Battu



DISTRIBUTION CHARACTERISTICS OF IRON(III) AS BENZOIC
 ACID COMPLEX BETWEEN BENZENE AND 1.0M (Na,H)ClO₄
 AQUEOUS SOLUTION

Hisahiko EINAGA

Abstract

Studies have been made on the distribution characteristics of iron(III) as benzoic acid complex between benzene and aqueous solution of 1.0M (Na,H)ClO₄. Iron(III) is distributed from the aqueous to organic phase as benzoate complex in the form of monomeric species according to the following equilibrium:



The values $K_{\text{eq } 10}$ and $K_{\text{ex } 10}$ for the equilibrium $\text{Fe}^{3+} + 3\text{L}^- \rightleftharpoons \text{FeL}_3 \text{ org}$ were determined to be $10^{-6.33}$ and $10^{10.37}$, respectively, at 25°C. Distribution characteristics of the extractant benzoic acid (HL) were also studied and the value K_{exL} for the equilibrium $2\text{H}^+ + 2\text{L}^- \rightleftharpoons \text{H}_2\text{L}_2 \text{ org}$ was determined to be $10^{11.13}$ under the same condition.

National Institute for Researches in Inorganic
 Materials, Kurakake, Sakura-mura, Niihari-gun,
 Ibaraki-ken, 300-31, Japan.

Carboxylic acids are known to extract metal ions from aqueous to organic phases and many examples have already been reported^{1,2)}. Systematic treatments of the extraction equilibria and elucidation of the distribution mechanism have however little been made until recently³⁾. It became evident from the recent investigations that carboxylic acids tend to form extractable complex species of the forms of $(ML_2OH)_n$ and $(ML_3(HL)_m)_n$ for trivalent metal ions (In(III)⁴⁾, Al(III)⁵⁾, and Ga(III)⁶⁾) by extraction with aliphatic monocarboxylic acids (HL), which are sparingly soluble in water, such as capric acid. For the extraction of iron(III), both FeL_3 and $FeL_3 \cdot HL$ in the form of monomeric state are reported to be formed and extracted with fatty acids of 7 to 9 in their carbon number, but $(FeL_3)_3$ in the trimeric form with capric acid^{2,7)}. To deduce general conclusions on the extraction characteristics of metal ions with carboxylic acids, it must be necessary to obtain more information for various types of carboxylic acids and metal ions. The present study was undertaken to obtain such information for aromatic carboxylic acids with moderately soluble in water and iron(III) and benzoic acid system was chosen for the present purpose. It is reported that iron(III) can be extracted with sodium benzoate into ethyl acetate, methyl, and amyl alcohols¹⁾, no systematic study has been made on the extraction characteristics of iron(III) with benzoic acid from aqueous solution into benzene.

DISTRIBUTION CHARACTERISTICS OF BENZOIC ACID

It is necessary first of all to know acid-base and distribution characteristics of the extractant benzoic acid to elucidate distribution characteristics of the iron(III)

complex.

Acid dissociation constant, k_a , of benzoic acid (HL) in a constant ionic medium of 1.0M (Na,H)ClO₄ was determined spectrophotometrically on the fact that electronic absorption spectrum of benzoic acid in the ultraviolet region is shifted hypsochromically by its dissociation. Absorption measurements at 285 nm for solutions containing 1.07×10^{-3} M of benzoic acid with varied $-\log [H^+]$ and calculation by equation (1) led to the value of $k_a = 6.03 \times 10^{-5}$ ($pK_a = 4.22$) as summarized in Table 1.

$$pK_a = \log \frac{E_{285} - E_{285}^{\min}}{E_{285}^{\max} - E_{285}} - \log [H^+] \quad (1)$$

In equation (1) the terms E_{285}^{\max} and E_{285}^{\min} are absorbances due to undissociated and dissociated forms of benzoic acid, respectively. Thermodynamic acid dissociation constant of benzoic acid has been reported to be $k_a = 6.339 \times 10^{-5}$ at 25°C⁸).

It is known that monocarboxylic acids generally form dimerized species in nonpolar organic solvents. Dimerization constant and partition coefficient of monomeric species of benzoic acid was therefore determined by the following treatment. In this case it was assumed that monomeric species of benzoic acid was distributed from aqueous into organic phases followed by dimerization in the organic phase and that the dimerization in aqueous phase of benzoic acid could be made negligible as compared with the monomeric and deprotonated species because concentration of benzoic acid is considerably low. All the assumptions made above may be considered appropriate in the present study. Under the conditions specified above, the distribution ratio of benzoic acid, D_L , may be re-

presented as shown in equation (2).

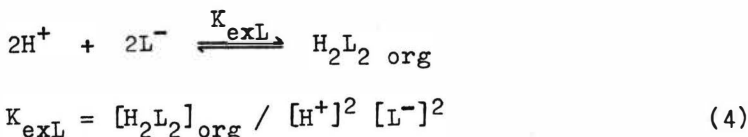
$$D_L = \frac{2 [H_2L_2]_{org} + [HL]_{org}}{[HL] + [L^-]} \quad (2)$$

Rewriting of equation (2) by using P_L , the partition constant of monomeric species, K_{dm} , the dimerization constant in the organic phase, and k_a with appropriate rearrangement leads to equation (3).

$$D_L(1 + k_a/[H^+]) = P_L + 2P_L^2 K_{dm} [HL] \quad (3)$$

Equation (3) indicates that there should stand a linear relation between distribution ratio of benzoic acid corrected for by hydrogen ion concentration and concentration in the aqueous phase of monomeric species with an intercept of P_L and a slope of $2P_L^2 K_{dm}$, from which P_L and K_{dm} can easily be calculated. Experimental data were shown in Fig. 1, and the values of 2.31 for P_L and 90.5 for K_{dm} were obtained as summarized in Table 1.

Extraction constant of benzoic acid may be defined as follows:



The constant K_{exL} in equation (4) may further be rewritten by using the terms of P_L , K_{dm} , and k_a as shown in equation (5):

$$K_{exL} = P_L^2 K_{dm} k_a^{-2} \quad (5)$$

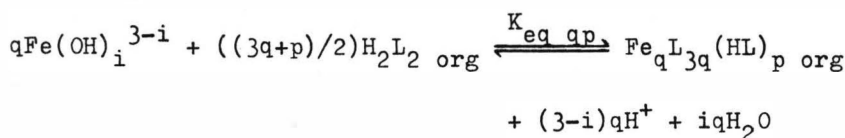
The value of K_{exL} was then calculated and $\log K_{exL} = 11.13$ was obtained as summarized in Table 1.

DISTRIBUTION CHARACTERISTICS OF THE IRON(III) AS BENZOIC ACID COMPLEX

In the acidic aqueous solution with no auxiliary or secondary ligands, iron(III) presents in the form of aquoion, $\text{Fe}(\text{OH}_2)_6^{3+}$, hydroxo complex species, such as $\text{Fe}(\text{OH})^{2+}$, $\text{Fe}(\text{OH})_2^+$, etc.

For aliphatic monocarboxylate complexes of iron(III), it has been reported as stated earlier that both monomeric and polymeric species of the general form $(\text{ML}_3(\text{HL})_m)_n$, where m and n are integer, were distributed into nonpolar organic phase.

In the present study species contributing to the distribution equilibrium were therefore assumed to be $\text{Fe}(\text{OH})_i^{3-i}$ for iron(III) in the aqueous phase and $\text{Fe}_q\text{L}_{3q}(\text{HL})_p$ for the iron(III) complex in the organic phase. Distribution equilibrium can then be represented as follows:



$$K_{\text{eq } qp} = \frac{[\text{Fe}_q\text{L}_{3q}(\text{HL})_p]_{\text{org}} [\text{H}^+]^{(3-i)q}}{[\text{Fe}(\text{OH})_i^{3-i}]^q [\text{H}_2\text{L}_2]_{\text{org}}^{(3q+p)/2}} \quad (6)$$

Now let us define distribution ratio, D_M , and apparent distribution ratio of iron(III), D_M' , which may easily be obtained experimentally, as follows: $D_M = q[\text{Fe}_q\text{L}_{3q}(\text{HL})_p]_{\text{org}} / [\text{Fe}(\text{OH})_i^{3-i}]$ and $D_M' = q[\text{Fe}_q\text{L}_{3q}(\text{HL})_p]_{\text{org}} / C_{\text{Fe tot}}$, where $C_{\text{Fe tot}}$ is the total concentration of iron(III) in aqueous phase. Equation (7) can be obtained by using the term D_M' with further appropriate rewriting of equation (6).

$$\log D_M' = \log qK_{\text{eq } qp} - q \log \alpha_{(\text{H})} + (3q+p)/2 \log [\text{H}_2\text{L}_2]_{\text{org}} - (3-i)q \log [\text{H}^+] + (q-1) \log C_{\text{Fe tot}}$$

$$\alpha_{(H)} = (1/k_{hi}[\text{OH}^-]^i) \sum_0^i k_{hi} [\text{OH}^-]^i \quad (7)$$

where the k_{hi} are the hydrolysis constants of iron (III)

Equation (7) implies that under the constant condition of both $[\text{H}_2\text{L}_2]_{\text{org}}$ and $[\text{H}^+]$ there should be a linear relation between $\log D_M'$ and $\log C_{\text{Fetot}}$ with a slope of $q-1$, from which polymerization number of iron(III) in the complex may be determined. There should also be other linear relations between $\log D_M'$ and $\log [\text{H}_2\text{L}_2]_{\text{org}}$ under the constant condition of both $[\text{H}^+]$ and C_{Fetot} with a slope of $(3q+p)/2$ and again between $\log D_M'$ and $-\log [\text{H}^+]$ under the constant condition of both $[\text{H}_2\text{L}_2]_{\text{org}}$ and C_{Fetot} with a slope of $(3-i)q$, from which both p and i may be determined.

Extraction constant, $K_{\text{ex } qp}$, of the iron(III) complex, which can be defined as follows:

$$q\text{Fe}^{3+} + (3q+p)\text{L}^- + p\text{H}^+ \xrightleftharpoons{K_{\text{ex } qp}} \text{Fe}_q\text{L}_{3q}(\text{HL})_p \text{ org}$$

$$K_{\text{ex } qp} = \frac{[\text{Fe}_q\text{L}_{3q}(\text{HL})_p]_{\text{org}}}{[\text{Fe}^{3+}]^q [\text{L}^-]^{(3q+p)} [\text{H}^+]^p} \quad (8)$$

may further be rewritten in terms of $K_{\text{eq } qp}$ and K_{exL} as shown in equation (9).

$$\log K_{\text{ex } qp} = \log K_{\text{eq } qp} + (3q+p)/2 \log K_{\text{exL}} \quad (9)$$

Distribution experiments were carried out for systems containing 0.448×10^{-4} — 1.790×10^{-4} M of iron(III), 0.0247 — 0.247 M of benzoic acid, and $-\log [\text{H}^+]$ of 2—3. For the relation between $\log D_M'$ and $\log C_{\text{Fetot}}$ at a specified values of $[\text{H}_2\text{L}_2]_{\text{org}}$ and $-\log [\text{H}^+]$, it was found that $\log D_M'$ was independent on $\log C_{\text{Fetot}}$ under the conditions studied. This fact concludes that the value of q is equal to unity, hence no polymerization as for iron(III) is observed in the present study.

Figure 2 shows the results on the relation between $\log D_M'$

+ q log $\alpha_{(H)}$ and $-\log [H^+]$ at a specified value of $[H_2L_2]_{org}$. In this case $k_{hl} = 10^{11.0}$ and $k_{h2} = 10^{10.7}$ were used for the calculation¹⁰⁾. A linear relation is obtained as shown in Fig. 2 with a slope of 3, indication that i is equal to 0. Relation between $\log D_M'$ and $\log [H_2L_2]_{org}$ at a specified value of $[H^+]$ is presented in Fig. 3, from which it can be seen that the slope of a linear relation $(3q+p)/2$ is equal to 1.5. Hence p is equal to 0.

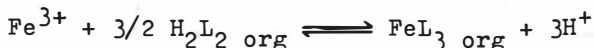
Summarizing these results leads to the conclusion that Fe^{3+} and not hydroxo species participates to the distribution equilibrium and that the iron(III) complex of the form of FeL_3 is present in the organic phase. Equations (7) and (9) can further be simplified as follows:

$$\log D_M' = \log K_{eq} 10 + 3/2 \log [H_2L_2]_{org} - 3 \log [H^+] \quad (7')$$

$$\log K_{ex} 10 = \log K_{eq} 10 + 3/2 \log K_{exL} \quad (9')$$

The values of $\log K_{eq} 10$ and $\log K_{ex} 10$ were calculated by using the data from Figs. 2 and 3 and -6.3 and 10.4 were obtained as summarized in Table 2.

In conclusion, iron(III) is extracted from aqueous phase by benzoic acid according to the following equilibrium:



and the extraction constant is $\log K_{ex} 10 = 10.4$.

Iron(III) has been extracted with capric acid from aqueous solution (ionic strength: 0.04) into benzene to form trimeric complex species of the form of $(FeL_3)_3$ with an equilibrium constant of $K_{eq} 30 = -9.9$ at $25^\circ C$ ⁷⁾. Results of the present study on the extraction with benzoic acid reveals on the contrary that monomeric species is formed and extracted into benzene. These differences might in part be due to the struc-

tural change of the extractant, but further study should be made from structural standpoint.

Adduction of benzoic acid in its undissociated form to the neutral iron(III) complex is in this case not practical and coordination of carboxylic groups by way of two oxygen atoms per group constituting three four-membered rings is concluded structurally because iron(III) has generally a coordination number of six.

EXPERIMENTAL

Iron(III) solution was prepared by dissolving metallic iron in nitric acid followed by converting to perchloric acid solution with slightly acidic to avoid hydrolytic precipitation of iron(III). Benzoic acid was recrystallized twice from water and dried over anhydrous phosphoric acid. m.p.: 122°C^8).

Distribution ratio of benzoic acid was determined by using electronic absorption characteristics in the ultraviolet region (270 nm). Adherence to Beer's law for benzoic acid was ascertained. Absorbance of benzene was also corrected. Distribution ratio of iron(III) was determined by using a spectrophotometric method with 8-hydroxyquinoline. In this case, completion of ligand substitution reaction of the extracted iron(III) complex with 8-hydroxyquinoline in benzene was also ascertained¹¹). Hydrogen ion concentration, $-\log [\text{H}^+]$, was determined potentiometrically with glass and saturated calomel electrodes and a solution containing 0.990M of sodium perchlorate and 0.0100M of perchloric acid was defined to be $-\log [\text{H}^+] = 2.00$.

All the experiments were carried out at a solution temperature of 25°C . Absorption measurements were carried out with

a spectrophotometer, model 139, of Hitachi Ltd., Japan, with matched quartz cells. A pH meter, model F-5, of Horiba Ltd., Japan, was used to obtain potentiometric data. Equilibration was carried out with a Universal Shaker, model V-D, of Iwaki Ltd., Japan, at a rate of 300 strokes per minute. Shaking of more than 10 minutes was sufficient to attain equilibration.

REFERENCES

- 1) Morrison, G. H., and Freiser, H., Solvent Extraction in Analytical Chemistry, 1957, p.145(New York, Wiley).
- 2) Marcus, Y., and Kertes, A. S., Ion Exchange and Solvent Extraction of Metal Complexes, 1969, p.537(New York, Wiley-Interscience).
- 3) Jaycock, M. J., and Jones, A. D., Solvent Extraction Chemistry, 1967, p.160(Amsterdam, North-Holland).
- 4) Tanaka, M., Nakasuka, N., and Yamada, H., J. Inorg. Nucl. Chem., 1970, 32, 2759.
- 5) Ibid., 1970, 32, 2791.
- 6) Yamada, H., and Tanaka, M., Ibid., 1973, 35, 3307.
- 7) Tanaka, M., Nakasuka, N., and Goto, S., Solvent Extraction Chemistry, 1967, p.154(Amsterdam, North-Holland).
- 8) Furukawa, J., and Onishi, A., Series of Comprehensive Organic Chemistry(Dai Yuki Kagaku), 1958, vol.9, p.367 (Tokyo, Asakura).
- 9) Tanaka, M., Nakasuka, N., and Sasane, S., J. Inorg. Nucl. Chem., 1969, 31, 2591.
- 10) Ringbom, A., Complexation in Analytical Chemistry, 1963, p.298(New York, Wiley-Interscience).
- 11) Einaga, H., to be published.

Table 1. Acid-Base Properties and Distribution Characteristics of Benzoic Acid in the System of Benzene—
1.0M (Na,H)ClO₄ Aqueous Solution.

pK_a	P_L	K_{dm}	$\log K_{exL}$
4.22	2.3	90.5	11.1

Table 2. Distribution Characteristics of the Iron(III) as Benzoic Acid Complex in the System of Benzene—
1.0M (Na,H)ClO₄ Aqueous Solution.

Formula of the extracted complex	$\log K_{eq\ 10}$	$\log K_{ex\ 10}$
FeL ₃	-6.3	10.4

cf. The constant $K_{ex\ 10}$ is equal to $P_C\beta_{30}$, where P_C is the partition constant and β_{30} the over-all formation constant in the aqueous phase of the iron(III) complex FeL₃.

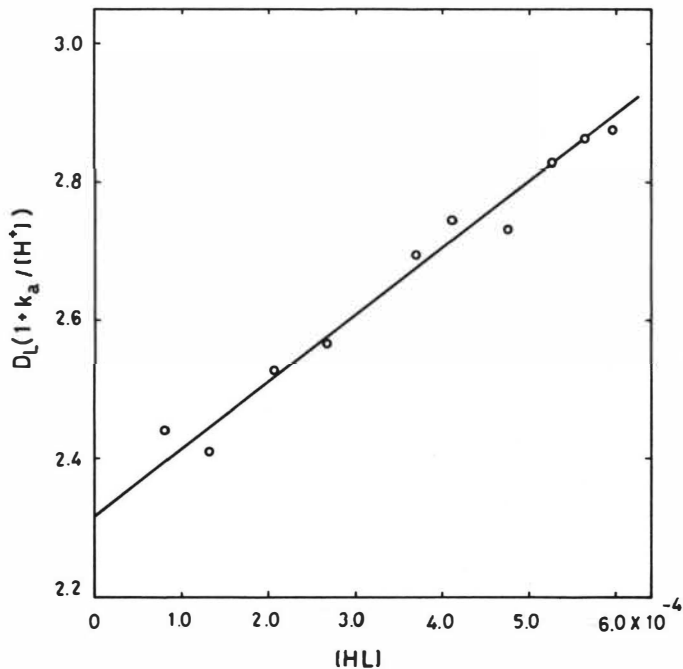


Fig. 1. Relation between $D_L(1 + K_a/[H^+])$ and $[HL]$ in the System of Benzene—1.0M $(Na,H)ClO_4$ Aqueous Solution. Total concentration of benzoic acid: 0.00267M. V_{org}/V_{aq} : 1 (V_{aq} : 20.0 ml).

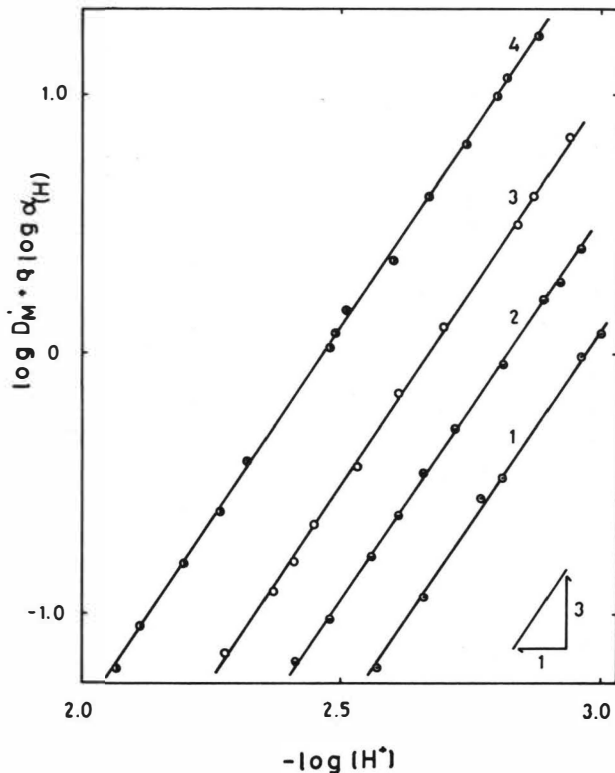


Fig. 2. Relation between $\log D_M' + b \log \alpha_{(H)}$ and $-\log [H^+]$ in the System of Benzene—1.0M $(Na,H)ClO_4$ Aqueous Solution. Total concentration of benzoic acid: 1—0.0247M, 2—0.0494M, 3—0.0988M, 4—0.247M. Total concentration of iron(III): $0.895 \times 10^{-4}M$.

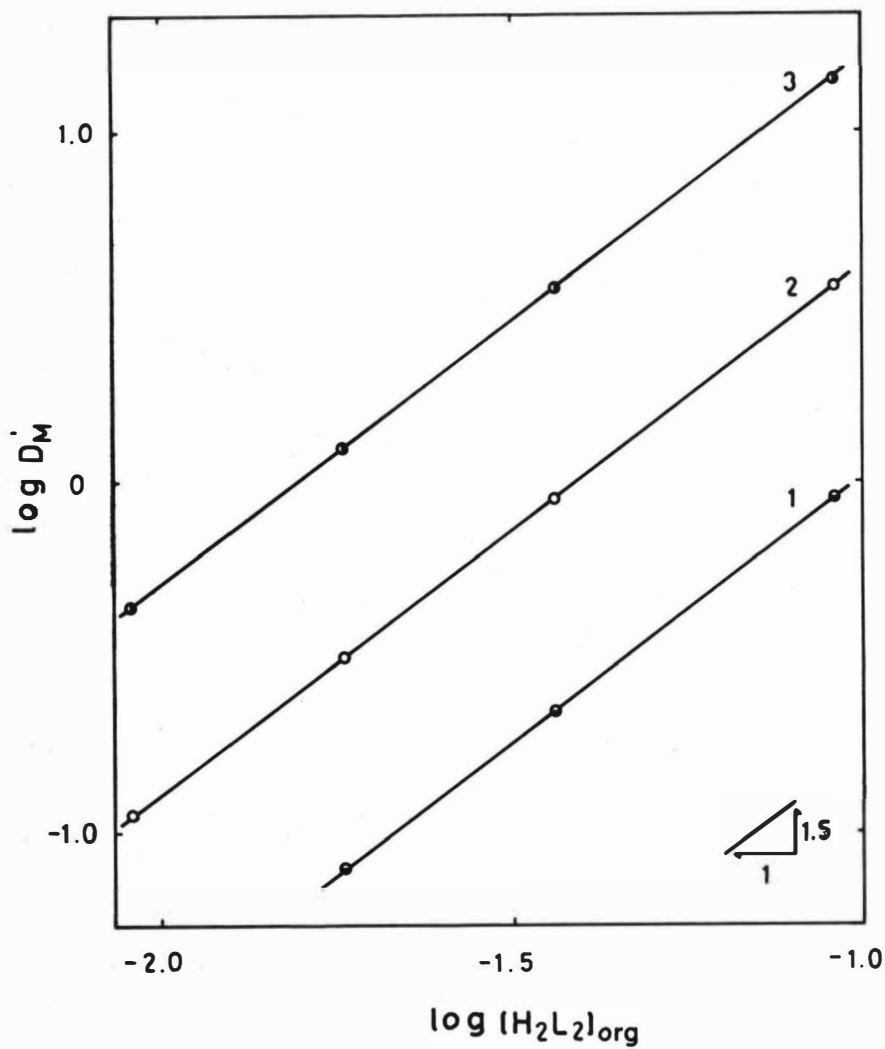


Fig. 3. Relation between $\log D_M'$ and $\log [H_2L_2]_{org}$ in the System of Benzene-1.0M (Na,H)ClO₄ Aqueous Solution. $-\log [H^+]$: 1-2.45, 2-2.65, 3-2.85. Total concentration of iron(III): $0.895 \times 10^{-4}M$.



Extraction of some univalent and bivalent metals in the presence
of macrocyclic polyether

J. Rais, M. Kyrš and L. Kadlecová¹

Institute of Nuclear Research, Czechoslovakia

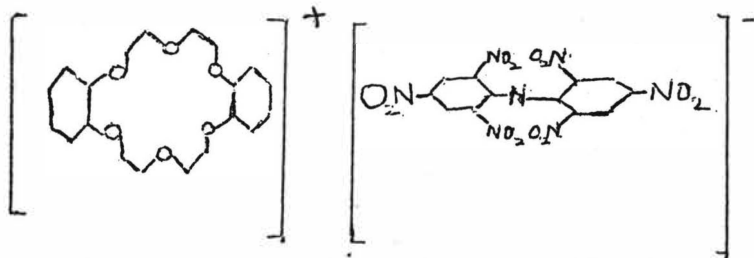
Ever increasing amount of information on macrocyclic ligands and their complexes with alkali metal and alkali earth cations [1-3] predetermines the search of their practical applications in some branches of chemistry. It seems that the use for ion selective electrodes is the main area investigated at present. So, e.g. highly selective electrode for K^+ ion based on valinomycin has been proposed [4] and is now commercially available. The information on this area of practical use may be gained from review papers [5,6].

Solubilisation properties of the cyclic polyethers vs. the alkali metal cations in organic solvents made possible to prepare a number of organic solutions of simple salts up to now not obtainable which, subsequently, may be used for new reactions. E.g. the solution of $KMnO_4$ formed in benzene after solubilisation in the presence of dicyclohexyl-18-crown-6 may be used as an oxidation agent in the organic phase [7].

Extraction behaviour in the presence of the metal cations and cyclic polyethers has been studied mainly for the characterisation of the polyether, most often being measure the distribution ratio of picrate anion between water and organic solvent in the presence of polyether and an excess of alkali metal hydroxide [8]. The quantitative analysis of the extraction equilibria has been given by EISENMAN [9,10] and FRENSDORFF [11]. Generally speaking, the extraction in the presence of polyethers may be characterised as "ion pair extraction". This is due to the cationic form of the complex, the charge of the cation being unchanged upon complexing. Equilibrium may be described by the stability constant of the complex in one of the phases, the extraction constant of the complexed salt in either dissociated or undissociated form, dissociation constant of the ion pair in the organic phase and distribution of the polyether itself between water and organic solvent. It is usually assumed that ion pairs are not formed in the aqueous phase [11].

From the point of view of possible practical separation of alkali metals or alkaline earths the distribution ratios attainable with picrate anion are too low. We have used in our recent work

[12] as a counter ion of complexed alkali metal cation large hydrophobic anion of the type dipicrylaminato (DPA^-) and it has been found that the salts of the following type:



M^+ dibenzo-18-crown-6 dipicrylaminato MC^+DPA^- strongly prefer the organic phases. In comparison with simple M^+DPA^- which are extracted only into polar organic solvents (the highest selectivity being reached in nitrobenzene [13]) for complexed MC^+DPA^- the solvent of choice may be also some slightly polar solvent as CH_2Cl_2 , CHCl_3 etc.

It seemed to us that the study of the influence of organic solvent on the selectivity of extraction in the presence of macrocyclic polyethers is of primary importance for further development. In this work the selectivity of extraction of microamounts of Na^+ and Cs^+ ions in the presence of Li^+DPA^- and into six organic solvents has been studied. In other experiments the extraction of Ca^{2+} , Sr^{2+} and Ba^{2+} in the presence of polyhedral borate sandwich anion $(\text{B}_9\text{C}_2\text{H}_{11})_2\text{Co}^-$ [14] has been investigated. In all experiments the macrocyclic polyether has been dibenzo-18-crown-6.

Experimental

All reagents were of A.R. purity. The solvents used were also of this grade and were before use equilibrated several times with fresh portions of distilled water. The following radioisotopes were used: ^{22}Na , ^{137}Cs , ^{133}Ba , ^{85}Sr and ^{45}Ca , the purity of which has been checked γ -spectrometrically or by β -absorption and half-life (^{45}Ca).

The sample of polyhedral borate sandwich anion in the form of caesium salt $\text{Cs}^+(\text{B}_9\text{C}_2\text{H}_{11})_2\text{Co}^-$ has been obtained from Institute of Inorganic Chemistry, Rez by Prague. This salt has been converted into H-form after dissolution in nitrobenzene (10^{-2}M) by 12 fold equilibration with 4N H_2SO_4 by a procedure which will be given in full detail elsewhere [15]. The anion has shown similar properties as DPA^- in view of its extractibility into organic solvents [15].

The synthesis of dibenzo-18-crown-6 has been performed according to the method published by Pedersen [7] and purity tests corresponded to those reported in [7,12].

Extraction experiments were performed with 2ml of each phase during 30 minutes at $25 \pm 1^\circ\text{C}$. Aliquots of both phases were measured on standard β and γ -equipment.

Results and Discussion

Although, if equilibrated, the main portion of M^+DPA^- initially present in the aqueous phase passes into dibenzo-18-crown-6 solution in chloroform almost immediately it is doubtful whether a true equilibrium is attained at short time interval of about 30 minutes. This has reflected in some spread of experimental results not permitting the precise quantitative evaluation of respective constants in extraction of alkali metal dipicrylamines. Two factors are operating in our opinion: slow kinetics of dissolution of dibenzo-18-crown-6 in water and aqueous solutions of alkali metal nitrates and partial hydrolysis of DPA^- anion present in chloroform layer which probably increases with the time of the contact due to the formation of HCl. The first factor had been studied to some extent with another intention. It had been hoped that from the solubility data of dibenzo-18-crown-6 in aqueous solutions of varying concentration of say alkali metal chloride an information on the composition and stability constants of respective complexes in the aqueous phase may be relatively easily obtained. The solubility of crown really increased with increasing molarity of KCl, but equilibrium values have not been obtained even after two weeks of equilibration. Further experiments in this direction were not performed. Eventually, the lack of the true equilibrium in extraction experiments for the times 1-2 hours was proved by the following experiment: a relatively concentrated ($10^{-2}M$) solution of CsDPA in chloroform solution of crown was prepared and diluted to a sample for extraction. Another sample of the same composition contained CsDPA initially in the aqueous phase. With the first sample always slightly higher distribution ratios of DPA were obtained. Regardless of the small kinetic effects discussed we have used in all experiments a time experimentally suitable-30 minutes - of extraction.

The selectivity of the extraction of microamounts of Na and Cs in the presence of LiDPA is given in Figs. 1 and 2. It may be seen that the highest distribution ratios D_{Cs} are obtained with chlorinated solvents. As shown in Fig.2 for these solvents also the selectivity increases with crown concentration. On the other hand for nitrobenzene, where in the absence of crown the separation factor D_{Cs}/D_{Na} is 1000 [16], the selectivity of the extraction is about two orders suppressed in the presence of this cyclic polyether. In propylene carbonate the values of D_{Cs} and D_{Na} are small and selectivity ratio is very close to 1.

To throw some light on the results obtained, several comments should be made at first. Alkali metal dipicrylamines are totally insoluble in chlorinated solvents used ($D_{CS} < 10^{-3}$ for CsDPA and chloroform or chlorobenzene) indicating very low ability of the molecules of these solvents to coordinate with alkali metal cations. In these solvents the latter may be present only in complexed form. In other solvents with higher basicity and dielectric constant alkali metal dipicrylamines are soluble and in the organic phase both complexed and uncomplexed forms may be present. The dissociation of MC^+DPA^- compounds may occur to some extent in slightly polar solvents (the dissociation constant of KC picrate in CH_2Cl_2 as found by FRENSDORFF [11] is $K_d = 4.4 \times 10^{-6}$) and may be supposed almost total in nitrobenzene (see further text), nitromethane and propylene carbonate (all with dielectric constant > 30). The composition of Na^+ with dibenzo-18-crown-6 is supposed to be 1:1, whereas in methanol the formation of CsC^+ and sandwich CsC_2^+ with comparable formation constants was proved [17]. It may be reasonably supposed that the constants of stability of the respective complexes are several orders lower in water than in the organic media due to the competition of water molecules for ligand. Similar effect has been experimentally verified for dicyclohexyl-18-crown-6 [17].

Considering that water is the strongest electron pair donor solvent in the systems involved in Fig.2 and that the affinity of the cation towards the donor molecule increases with decreasing radius it may be concluded rather schematically that the water content in the organic phase should be one from the controlling factors of extraction selectivity [13]. This idea should apply both to the uncomplexed cations and cations in 1:1 complexes, as solvent contacts are possible probably also in the direction perpendicular to the plane of the ring [17]. The results obtained in this work are consistent with this criterion, the water content decreasing in the sequence propylene carbonate $>$ nitromethane $>$ nitrobenzene $>$ CH_2Cl_2 $>$ $CHCl_3$ $>$ C_6H_5Cl and in the same sense increasing the selectivity of the extraction. If this effect is operative, it may be further expected that with increasing complexing the solvation of cation by water molecules will decrease and ultimately if both cations will be present in their 1:2 complexes and hence not susceptible to further contact with water molecules the selectivity will be independent of the water solubility in the organic phase. This state has not been apparently reached in our experiments.

The main factor influencing the selectivity is evidently the composition and stability of the respective complexes in both phases. There is a lack of data in the literature on stability constants of dibenzo-18-crown-6 in solvents used in this work.

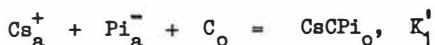
At first sight the reported higher stability constant for Na^+ ion in methanol than for Cs^+ ion 1:1 complexes [17] is in contradiction with our finding that Cs^+ ion is invariably better extracted by six organic solvents than Na^+ ion. It must be remembered, however, that there will be probably a compensation of two factors: complexation and extraction selectivity. E.g. for nitrobenzene, the ion Cs^+ will be preferred in comparison with Na^+ , similarly as Cs^+ ion is preferred over Na^+ , but presumably in lesser extent (isosteric NaC_2^+ and CsC_2^+ should be extracted almost equally [16]). Even if Na^+ ion in nitrobenzene is more strongly complexed than Cs^+ , the resulting effect may be that $D_{\text{Cs}}/D_{\text{Na}} > 1$. The discussed effects are probably responsible for observed decrease of separation factor of Cs and Na in nitrobenzene upon addition of crown (Fig.2.)

The increase of $D_{\text{Cs}}/D_{\text{Na}}$ with crown concentration for chlorinated solvents may be connected with the transformation of Cs^+ 1:1 complex to 1:2 complex. If it is so, the formation of 1:2 complex in nitrobenzene should occur only at higher concentrations of crown. To verify this opinion the distribution of pure caesium picrate from water into dibenzo-18-crown-6 solution in chloroform and nitrobenzene has been studied (Fig.3.) In this case the overall equilibrium may be simplified, giving for DCs ($v_a = v_o$):

$$D_{\text{Cs}} = \frac{[\text{Cs}^+]/o + [\text{CsC}_2^+]/o + [\text{CsCPI}]/o + [\text{CsC}_2\text{PI}]/o}{[\text{Cs}^+]_a}$$

$$= K_1/C/o + K_2/C/o^2 + \frac{K_1' c_{in}/C/o}{D_{\text{Cs}} + 1} + \frac{K_2' C_{in}/C/o^2}{D_{\text{Cs}} + 1}$$

where C denotes crown, c_{in} is the initial concentration of CsPI in the aqueous phase and following equilibria are involved:



Some terms in equation (1) may be neglected for real systems.

For chloroform it has been found previously that CsC_2 complex is formed for $C_{\text{crown}} > 10^{-2}M$ [12], hence only terms with K_2 and K_2' will apply. The experimental set of curves for $CHCl_3$ has been fitted with $K_2 = 1-2$ and $K_2' = 1-3 \cdot 10^5$ (the agreement of the theoretical and experimental curves was not perfect for $C_{\text{crown}} > 5 \cdot 10^{-2}M$ where theoretical curves became more curved upwards). The calculated dissociation constant of CsC_2Pi in $CHCl_3$ / $K_d = K_2/K_2' = 3 \cdot 10^{-6} - 2 \cdot 10^{-5}$ is of a comparable magnitude as that reported for $KCPi$ in CH_2Cl_2 ($K_d = 4.4 \cdot 10^{-6}$ [11]).

In nitrobenzene the dependence $\log D_{Cs}$ vs. $\log C_{\text{crown}}$ are near to the straight line with a slope $+0.5$ (Fig 3). Considering also the relative independence of D_{Cs} of c_{in} , it is obvious that dissociated CaC^+Pi^- is extracted (term with K_1) and only at high concentrations of crown this is transformed to 1:2 complex. From the curve for $c_{in} = 1 \cdot 10^{-4} M$ the value of K_1 may be evaluated as $K_1 \sim 400$. This value is of about four orders of magnitude higher than that for uncomplexed Cs^+Pi^- into the same solvent ($K = 1.2 \cdot 10^{-2}$ [18]) and shows a large gain in hydrophobicity of Cs^+ ion upon complexing. From the values of K_1 and K_0 the formation constant of CsC^+ in nitrobenzene may be estimated as $\log K_{CaC^+} = \log K_1 - \log K_0 = 4.5$. This is of one order higher than the same constant in methanol [17]. It is not quite clear why the 1:2 complexing in nitrobenzene is so suppressed in comparison with chloroform, but perhaps the same factors as discussed above may have an influence, i.e. the stronger competition of molecules of solvent and water molecules for second ligand in nitrobenzene than in chloroform.

In view of some signs of the complexing of bivalent metals with crown compounds [7] and determined stability constant of dibenzo-18-crown-6 with Ba^{2+} ion ($\log K_{BaC^{2+}} = 4.28$ in methanol [19]) it seems interesting to find out what is the influence of the polyether studied in this work on the extraction of alkaline earth cations. The results for Ca, Sr and Ba are given in Fig.4. In all cases the curves pass through maximum, indicating perhaps some competition of more stable BaC^{2+} for less stable HC^+ [20] formed at higher concentrations of crown. The position and shape of the maximum is more evident from Fig.5 where Na^+ is the competing cation in its turn transformed into much better extractable NaC^+ (compare CsC^+ and Cs^+ discussed above). In the latter case the competition mechanism seems to be proved by the fact that the decrease of D_{Ba} values was accompanied by rapid increase of the concentration of DPA anion in the organic phase in the same region of C_{crown} . Curve 2 in Fig.5 gives the distribution of Ba into chloroform in otherwise identical conditions. Why in this case the curve lies much lower and maximum does not occur is not possible to decide on the basis of the experimental results.

Conclusion.

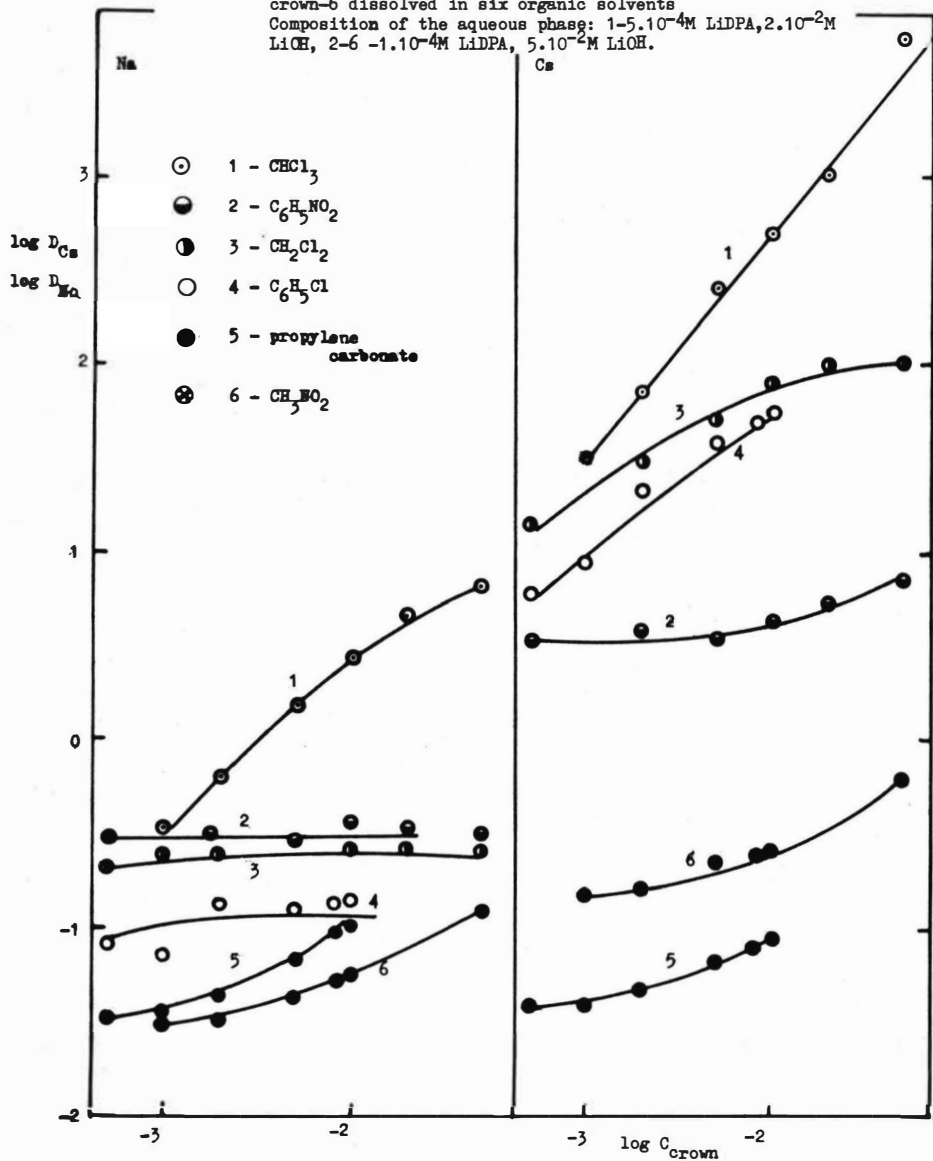
The use of macrocyclic polyethers opens certainly broad possibilities in extraction isolation and separation of some elements. It may be supposed that selectivity can be varied appreciably by the choice of polyether and solvent. The price and availability of more complicated ligands may be a limiting factor for practical use, but for simple compounds as used in this work is not of primary importance.

On the other hand, the extraction selectivity for these compounds may be often in direct connection with potentiometric selectivity if their solutions in organic solvents are used as ion selective electrodes. E.g. the potentiometric selectivity Cs/Na for dibenzo-18-crown-6 in nitrobenzene as found by RECHNITZ and EYAL [21] (~ 6.5) is almost identical with our extraction selectivity (~ 10). Also in this direction the study of the extraction behaviour of cyclic polyethers may be useful.

Literature

1. C.J. Pedersen and H.K. Frensdorff: *Angew. Chem.* 84, 16 (1972).
2. B.Dietrich, J.M.Lehn and J.P.Sauvage: *Tetrahedron* 29, 1647 (1973).
3. A.Leveque and R.Rossett: *Analisis* 2, 219 (1973).
4. L.A.R. Piode, V.Stankova and W.Simon: *Anal.Lett.* 2, 665 (1969)
5. J.Koryta: *Iontove selektivni membranove elektrody*, CSAV-Academia, Praha, 1972.
6. G.Eisenman: *Theory of membrane electrode potentials*, Chapt.1 from *Ion selective electrodes* (R.A. Durst ed.), Washington, 1969.
7. C.J. Pedersen: *J.Am.Chem.Soc.* 89, 7017 (1967)
8. C.J. Pedersen: *Fed.Proc.* 27, 1305 (1968)
9. G.Eisenman; S.M.Ciana and G.Szabo: *Fed.Proc.*27, 1289 (1968).
10. G.Eisenman, S.Ciani and G.Szabo: *J.Membrane Biol.* 1, 294 (1969).
11. H.K. Frensdorff: *J.Am.Chem.Soc.* 93, 4684 (1971).
12. J.Rais and P.Selucky: *Radiochem.Radioanal.Lett.* 6, 257 (1971)
13. P.Selucky, J.Rais and J.Krtil in *International Solvent Extraction Conference, The Hague, 1971*, paper 79, p.616.
14. M.F. Hawthorne: *Pure Appl. Chem.* 29, 547 (1972).
15. J.Rais, P.Selucky and M.Kyrs: *J.inorg.nucl.Chem.*, to be published.
16. J.Rais: *Coll.Czech.Chem.Comm.*: 36, 3253 (1971).
17. H.K. Frensdorff: *J.Am.Chem.Soc.* 93, 600 (1971).
18. J.Rais and P.Selucky: *Coll.Czech.Chem.Comm.* 36, 2766 (1971).
19. Reference 114 in R.Scholer: *Thesis, Juris Druck-Verlag Zurich*, 1972.
20. E.Shchori and J.J.Grodzinski: *J. Am.Chem.Soc.* 94, 7957 (1972).
21. G.A. Rechnitz and E.Eyal: *Anal.Chem.* 44, 370 (1972).

Fig.1. Extraction of microamounts of Na^+ and Cs^+ by dibenzo-18-crown-6 dissolved in six organic solvents
 Composition of the aqueous phase: $1-5 \cdot 10^{-4}\text{M}$ LiDPA, $2 \cdot 10^{-2}\text{M}$ LiOH, $2-6 - 1 \cdot 10^{-4}\text{M}$ LiDPA, $5 \cdot 10^{-2}\text{M}$ LiOH.



1813

Fig.2. Selectivity of extraction of microamounts of Na^+ and Cs^+
 Constructed from Fig.1, the same numbering of the systems.

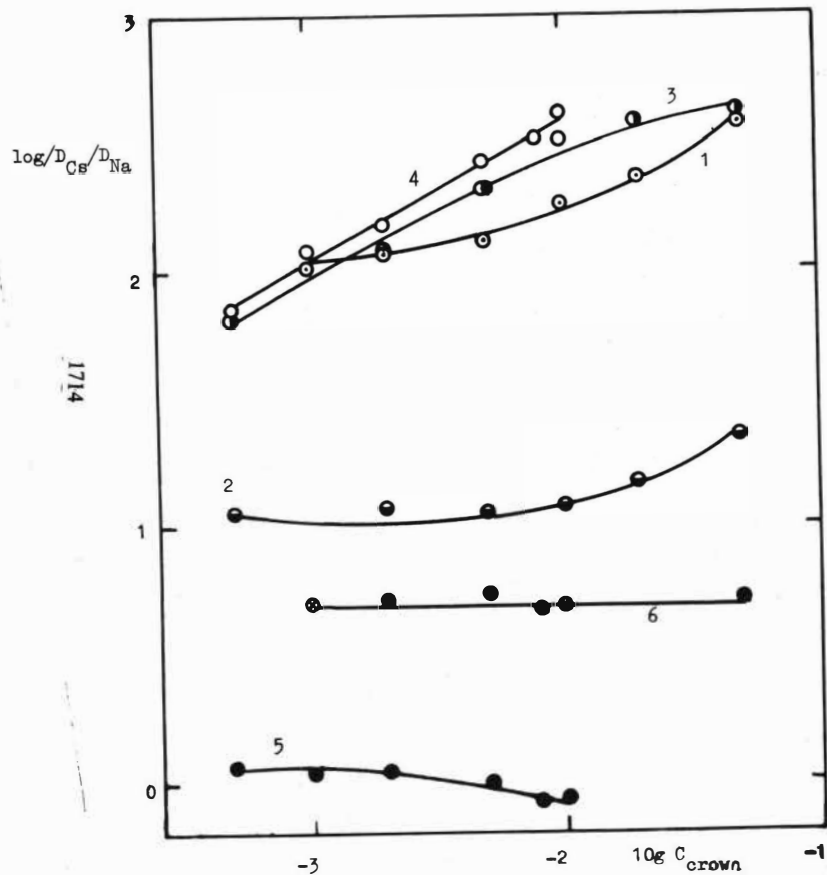


Fig.3. Extraction of caesium picrate into nitrobenzene and chloroform. Each three curves correspond from top to bottom to the concentrations of $\text{CsPi}: 1.10^{-3}\text{M}$, 5.10^{-4}M and 1.10^{-4}M

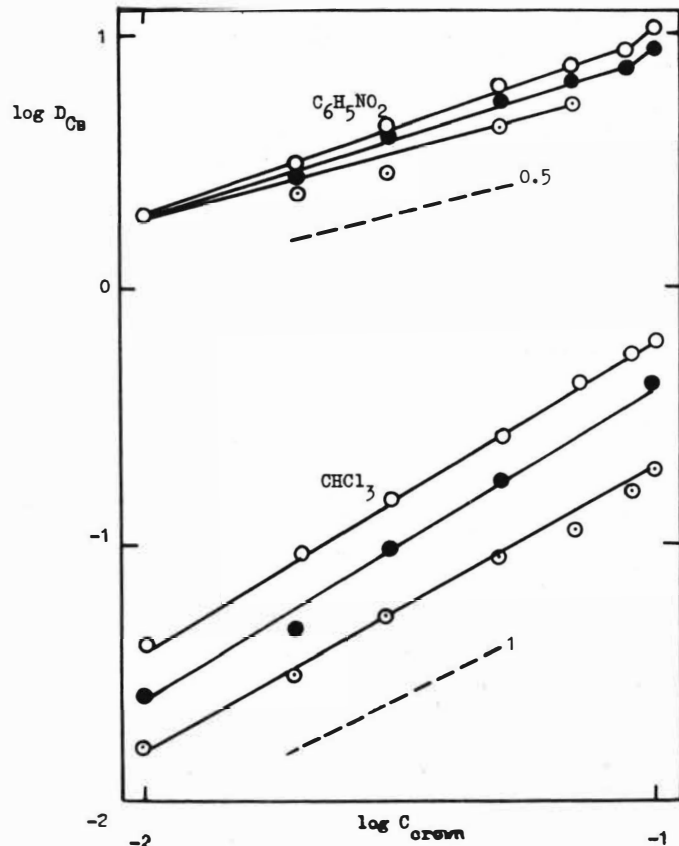


Fig.4. Extraction of Ca, Sr and Ba into nitrobenzene in the presence of crown and polyhedral borate anion $1.10^{-2}M H^+ (B_3O_3H_1)_2Co^-$ in nitrobenzene, $0.5M HNO_3$ in the aqueous phase.

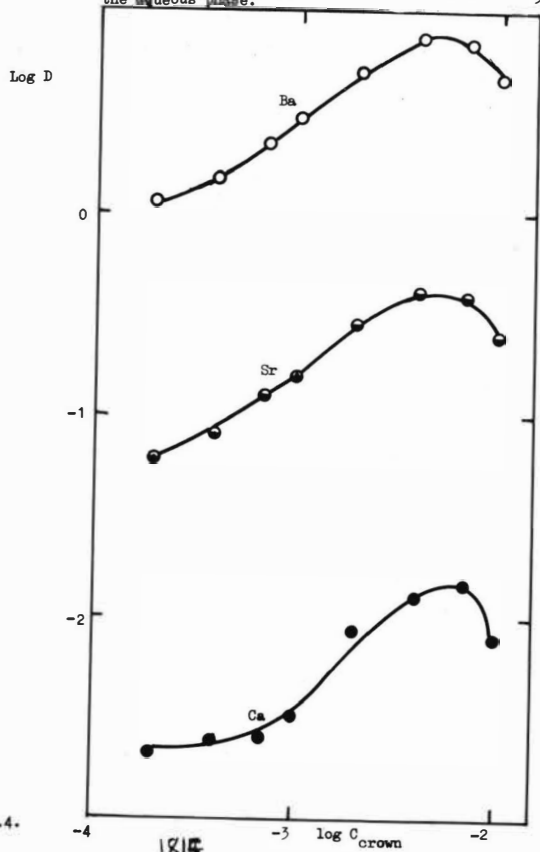


Fig.4.

Fig.5. Extraction of Ba into nitrobenzene and chloroform in the presence of dipicrylamine in the presence of dipicrylamine $1.10^{-3}M NaDPA$ and $5.10^{-4}M NaOH$ in the aqueous phase 1 - nitrobenzene, 2 - chloroform.

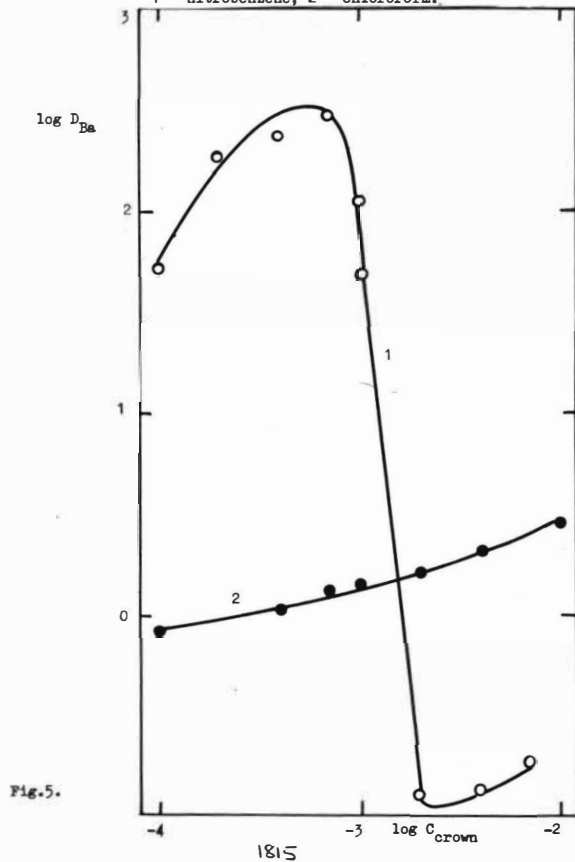


Fig.5.



Investigations on the mechanism of Fe(III) extraction
by n-caprylic acid

P. Mühl, L.M. Gindin, A.I. Kholkin, K. Gloe and K.S. Luboshnikova

Central Institute of Solid State Physics and Material Research,
Dresden, Academy of Science, GDR, and

Institute of Inorganic Chemistry, Novosibirsk, Siberian Branch
of the Academy of Science, USSR

Abstract:

A trimer iron(III) caprylate $[\text{Fe}(\text{C}_7\text{H}_{15}\text{COO})_3 \cdot \text{H}_2\text{O}]_3$ is formed
in the organic phase in the extraction of iron(III) by solutions
of n-caprylic acid in n-decane.

Constants for the following extraction equilibrium have been
determined:



Under the experimental conditions there do not exist hydrolyzed
species in the organic phase.

The influence of various diluents on the extraction behaviour
of Fe(III) is discussed.

Investigations on the mechanism of Fe(III) extraction
by n-caprylic acid

P. Mühl, L.M. Gindin, A.I. Kholkin, K. Gloe and K.S. Luboshnikova
Central Institute of Solid State Physics and Material Research,
Dresden, Academy of Science, GDR, and
Institute of Inorganic Chemistry, Novosibirsk, Siberian Branch
of the Academy of Science, USSR

Results published till now on the composition of extracted iron(III) compounds in systems involving monocarboxylic acids are contradictory, though there is a great number of publications¹⁻⁶⁾ concerning the mechanism of iron(III) extraction. This is based on the fact that, in the case of the extraction of iron(III) with monocarboxylic acids and compared with the extraction of many other metals, there occurs a number of additional interactions in the organic and aqueous phase.

In this paper results of investigations are given concerning the extraction equilibria of iron(III) in systems with n-caprylic acid and various diluents. The composition of the extracted iron(III) complexes in the organic phase was determined comprehensively using n-decane as diluent.

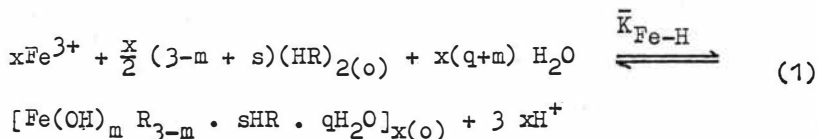
Extractions were carried out partly in the extraction apparatus AKUFVE, partly by usual shaking at $25 \pm 0,1^\circ\text{C}$ with a volume ratio of 1:1. The organic phases consisted of solutions of n-caprylic acid in n-decane and other diluents; the aqueous phases were solutions containing FeCl_3 and $\text{NH}_4\text{Fe}(\text{SO}_4)_2$ of various concentrations. Usually the ionic strength was kept constant by addition of Na_2SO_4 . The pH values were adjusted by addition of NaOH resp. H_2SO_4 . IR and electron spectra were taken for the completion of the thermodynamic analysis of the results.

Previous experiments confirmed that, in the case of iron(III) extraction by n-caprylic acid in n-decane, the equilibrium for extraction and reextraction was obtained by 15 min. shaking. After that the distribution coefficient remains constant, also for longer mixing times. However, if the mixing time exceeds four hours, a small increase of the iron(III) concentration in the aqueous phase and therefore a decrease of D_{Fe} can be observed. After some time the aqueous phase evolves a hydroxide precipitation. Such a behavior of the iron(III) is corresponding to the results of ARDEN ⁷⁾, who pointed out, that the equilibrium of the soluble hydrolyzed Fe(III) species in the aqueous solutions is obtained relatively quickly, whereas the formation of the solid iron hydroxide takes place very slowly.

In figs. 1 and 2 the experimentally determined $\lg D_{Fe}$ values are plotted against the equilibrium pH values of the aqueous phases. The values were obtained with variable initial Fe(III) concentrations and constant extractant concentration and constant ionic strength (fig. 1) resp. with variable initial concentrations of n-caprylic acid in n-decane and constant initial Fe(III) concentration (fig. 2). The figures show the increase of the distribution coefficients with increasing pH values of the aqueous phase, according to the cation exchange mechanism. A further increase of pH causes precipitations in the organic phases, which could be identified as basic ferric caprylates by means of IR spectroscopy and chemical analysis.

The curves of the plots of $\lg D_{Fe}$ vs. pH are bent to some extent. In the range of low D_{Fe} values the slopes of the curves are essentially larger than the charge of the Fe^{3+} cations. This fact, and further the shift of the curves for the plots of D_{Fe} vs. pH value in the direction of larger pH values with decreasing initial Fe(III) concentrations (fig. 1) point to polymerisation of the extracted iron compounds ⁸⁾.

The extraction of iron(III) by n-caprylic acid, taking into account solvation, hydration, polymerisation of the extracted compounds, and formation of hydrolyzed species, in the organic phase, may be described by the following equation:



where HR - n-caprylic acid
 x - degree of polymerisation
 s - solvation number
 m - degree of hydrolysis
 q - hydration number.

The subscript (o) denotes the organic phase; the aqueous phase is without subscript.

It could be proved by chemical analysis, that anions of inorganic acids are not present in the extracted complex. As iron(III) in aqueous solution is exposed very strongly to the complex formation with anions of inorganic acids and to hydrolysis, the overall Fe(III) concentration in the aqueous phase is not equal to the concentration of free Fe^{3+} -cations. According to BJERRUM resp. FRONAEUS the relation between these two concentrations is defined by

$$c_{\text{Fe}} = c_{\text{Fe}^{3+}} \left(1 + \sum_1^n \beta_n (\text{A})^n \right) = c_{\text{Fe}^{3+}} \phi \quad (2)$$

where c_{Fe} - overall Fe(III) concentration in the aqueous phase
 $c_{\text{Fe}^{3+}}$ - concentration of free (uncomplexed) Fe^{3+} -cations in the aqueous phase
 (A) - anion ligand concentration
 n - ligand number in the complex
 β_n - overall stability constant of the n-th complex
 ϕ - complexity function

Thereby the complexity function ϕ is available under the given conditions by means of the formation constants of the sulphate resp. chloro complexes and the hydrolysis constants of the soluble hydrolyzed Fe(III) compounds. The needed constants were taken from 9). Therefore the equilibrium constant of the exchange Fe-H is given according to equation (1) as

$$\overline{K}_{\text{Fe-H}} = \frac{c_{\text{Fe}(o)} a_{\text{H}^+}^{3x} 2^{\frac{x}{2}(3-m+s)} \phi^x}{x \cdot c_{\text{Fe}}^x c_{\text{HR}(o)}^{x/2(3-m+s)}} \quad (3)$$

where $c_{\text{HR}(o)}$ - analytical concentration of the free n-caprylic acid in the organic phase
 a_{H^+} - hydrogen ion activity
 $c_{\text{Fe}(o)}$ - analytical concentration of Fe(III) in the organic phase; on the assumption that there is only one Fe(III) compound in the organic phase

The activity constants of the compounds as well as the water activity may be regarded as constant under the chosen experimental conditions and with the assumption, that all interactions of the extracted compound are taken into consideration in equation (1).

Using equation (3) it is possible to evaluate the solvation number and the degree of polymerisation from the experimental results. For that the values of the plots given in fig. 1 and 2 are used. From equation (3) it follows

$$\lg D_{\text{Fe}} = \lg K_1 + 3x \text{pH} - x \lg \phi + (x-1) \lg c_{\text{Fe}} + \frac{x}{2}(3-m+s) \lg c_{\text{HR}(o)} \quad (4)$$

With D_{Fe} and $c_{\text{HR}(o)} = \text{const.}$, equation (4) leads to the expression

$$\text{pH} - 1/3 \lg \phi = K_2 - \frac{x-1}{3x} \lg c_{\text{Fe}} \quad (5)$$

The slope of the plot of pH vs. $\lg c_{Fe}$ according to equation (5) gives the degree of polymerisation 3. The linearity indicates a constant degree of polymerisation for variable values of $c_{Fe(o)}$. A further indication of constant degree of polymerisation is the constancy of the molar extinction coefficient of the absorption band at 348 nm in the electron spectrum of the organic phases with Fe(III) concentrations 0.0001-0.003 molar/l [extractant 1 m HR in n-decane; $\epsilon_{348} = (2.0 \pm 0.1) \cdot 10^3$].

The obtained results point out the extracted Fe(III) compound to be a trinuclear complex in the investigated concentration range and confirm TANAKA's results⁶⁾ on the extraction of Fe(III) by n-capric acid in benzene.

A possible solvation of the iron complex by n-caprylic acid molecules can be proved by thermodynamic analysis of the values given in fig. 2. Using equation (4) the dependence of the equilibrium pH value on extractant concentration with D_{Fe} and $c_{Fe} = \text{const.}$ yields

$$\text{pH} - 1/3 \lg \bar{\Psi} = \frac{1}{6} (3-m+s) \lg c_{HR(o)} \quad (6)$$

A value $s-m=0$ was determined from the slope of the plotted entities according to equation (6). However, this points out in accordance with TANAKA and COWORKERS⁶⁾, that the thermodynamic analysis of the extraction equilibria only does not provide a proof of the existence of hydrolyzed caprylates.

The degree of hydrolysis of the extracted compounds was determined titrimetrically using KARL FISCHER's method.^{+) Hydroxyl groups}

+) It has been shown by means of spectrophotometric investigations, that in the absence of inorganic iron salts there is either no reduction of Fe(III) to Fe(II) in the organic phases by KARL FISCHER solution or an extremely slow reduction rate, possibly caused by the great stability of the trinuclear complex. Therefore, iron(III) in organic phases has no influence on the determination of water and hydroxyl groups.

were found in few samples only (possibly a partial hydrolysis during the drying process⁺⁺), the maximal concentration being < 5 % relating to the Fe(III) concentration.

It can be concluded from these results, that the extraction of Fe(III) by solutions of n-caprylic acid in n-decane yields the neutral salt FeR_3 . According to the established value for the degree of hydrolysis $m=0$ it can easily be derived now from equation (6), that $s=0$, i.e., the ferric caprylate in the organic phase is not solvated by n-caprylic acid.

In this connection the hydration of the extracted iron compound in this system was investigated, too. As the iron compound has not any hydroxyl groups, the water concentration in the organic phase could easily be determined by KARL FISCHER's method. The hydration number was estimated in the usual manner according to the equation

$$c_{H_2O} = c_{H_2O}^0 + q c_{Fe(o)}, \quad (7)$$

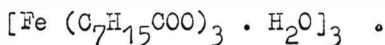
c_{H_2O} being the analytical concentration of water in the organic phase, and $c_{H_2O}^0$ the solubility of water in the initial n-caprylic acid solution² in n-decane at the corresponding water activity.

A plot of $c_{H_2O} - c_{H_2O}^0$ vs. $c_{Fe(o)}$, obtained by extraction of Fe(III) by 1m caprylic acid in n-decane from 0.163 m $FeCl_3$ solution at constant ionic strength, but at variable pH values, gave a slope of nearly 1; i.e., the hydration number is unity in relation to one metal cation (accordingly 3 in the trinuclear complex). The constancy of the hydration number at various values for a_{H_2O} indicates a relatively weak bonding of the H_2O molecules in the complex; probably they are not directly bonded with the metal atom.

Thus the composition of the extracted iron compound in the system with n-caprylic acid in n-decane may be given by the following

⁺⁺) Extracts with relatively high pH values were pretreated to eliminate the water by 3h vacuum drying at 70°C.

Formula:



Comparing the $\lg D_{\text{Fe}}\text{-pH}$ -plots for extraction from 0.163 m FeCl_3 (fig. 2) resp. from aqueous sulphate solutions (fig. 1) it can be deduced, that the introduction of sulphate ions into the system yields a significant shift of the curves in the direction of larger pH values. Thus the half pH value $\text{pH}_{0.5}$ is 1.70 in the extraction of iron(III) by 1 m caprylic acid in n-decane from 0.163 m FeCl_3 solution, whereas it increases to 2.28 in the extraction under the same conditions, but with the addition of 0.78 moles/l Na_2SO_4 to the aqueous phase. The strong shift of $\lg D = f(\text{pH})$ in the direction of larger pH values in the second case is undoubtedly connected with the stronger complex formation of the iron in sulphate medium.

The equilibrium constants $\bar{K}_{\text{Fe-H}}$ were evaluated for the two cases considering the complex formation in the aqueous phase. According to the determined composition of the extracted compound and by use of equation (3) the following values were obtained:

$\lg \bar{K}_{\text{Fe-H}}$	Extraction from
- 10.1 \pm 0.2	0.163 m FeCl_3 , without Na_2SO_4
- 10.4 \pm 0.2	0.163 m FeCl_3 + 0,78 m Na_2SO_4

These results confirm, that the shift of the curves for $\lg D = f(\text{pH})$ in this case is caused only by the complex formation in aqueous solution.

The influence of the diluent was investigated extracting Fe(III) by n-caprylic acid in n-decane, benzene, carbon tetrachloride, 1,2,4-trichlorobenzene, nitrobenzene + CCl₄(ratio 5:1), i-amyl alcohol, diisopropyl ketone, and i-amyl acetate.

Fe(III) was extracted by 1 m n-caprylic acid solutions in various diluents from aqueous solutions containing 0.5 m Na₂SO₄ + 0.02 m Fe(III). In all cases the slopes of the plots of lg D_{Fe} vs. pH were considerably larger - with the exception of i-amyl alcohol - than 3, indicating polymerisation of the extracted compound in those diluents. The half pH values were determined as follows;

decane	2.52
benzene	2.51
CCl ₄	2.58
nitrobenzene + CCl ₄	2.57
1,2,4 trichlorobenzene	2.60
iso-amyl alcohol	2.73
iso-amyl acetate	2.97
diisopropyl ketone	3,02

The pH_{0.5} values point out, that the systems involving diluents with weak electron donor properties are characterized by similar pH_{0.5} values in the range of 2.5-2.6. The systems with i-amyl alcohol, i-amyl acetate, and diisopropyl ketone show larger pH_{0.5} values. Probably this may be attributed to a stronger influence of the extractant-diluent interaction. It should be emphasized, that i-amyl alcohol having the strongest electron donor properties of all diluents investigated in this work yields a smaller pH_{0.5} value than i-amyl acetate and diisopropyl ketone. Probably, this is due to a significant interaction between the diluent and the extracted compound (solvation). It is possible, that this interaction effects partial or total destruction of the trinuclear complexes in the organic phase. This statement is supported by the smaller slope of the lg D -pH-plot; ^{and} too, by the smaller molar extinction coefficient ($\epsilon_{348} = 1.5 \cdot 10^3$) in

the electron spectra of the organic phases, compared with the corresponding ϵ values using the other diluents ($\epsilon_{348} = 2.1 \pm 0.2 \cdot 10^3$). Distinctions are shown by the IR spectra, too. Only in the system involving i-amyl alcohol a large quantity of water is coextracted with the Fe(III).

For interpretation of the IR spectra of the organic phases containing various diluents, above all IR spectra were taken from solutions of neutral Fe(III) caprylate in n-decane resp. of basic Fe(III) caprylate in benzene, furthermore from precipitations of the latter compound. Thereby, in the case of the neutral caprylate two bands of antisymmetrical stretching vibrations of the COO^- -ion appear at ≈ 1610 resp. 1560 cm^{-1} , which are shifted to 1590 resp. 1535 cm^{-1} in the case of the basic caprylate samples. Thus one can easily distinguish the neutral and the basic Fe(III) caprylate.

In the IR spectra of the iron(III) extracts with various diluents only the neutral compound FeR_3 could be detected. Thus it may be concluded that, on conditions of having investigated the extraction equilibria, the neutral Fe(III) caprylate predominates in the organic phase.

The investigations on the mechanism of Fe(III) extraction in systems involving monocarboxylic acids are not only of interest with regard to theory, but they have already contributed to the creation of an extraction process for the preparation of purest iron compounds¹⁰).

References

- 1) KARPACHEVA, S.M., ADAMSKII, N.M., and BORISOV, V.V., Radiokhimiya, 1961, 3, 291
- 2) RICE, N.M., Proceedings of the International Solvent Extraction Conference, The Hague, 1971, paper 146 (Society of Chemical Industry London)
- 3) FLETCHER, A.W., FLETT, D.S., and WILSON, J.C., Trans. Instn. Min. Metall., 1964, 73, 765
- 4) BOLD, A., and FISEL, S., Analele stiintifice ale univ. din Jasi, 1971, Sec. 1c, 17, 19 (Roumania)
- 5) PIETSCH, R., Anal. chim. acta, 1971, 53, 287
- 6) TANAKA, M., NAKASUKA, N., and GOTO, S., Solvent Extraction Chemistry, 1967, p. 154, (North-Holland, Amsterdam)
- 7) ARDEN, T.V., J. chem. Soc., 1951, 350
- 8) GINDIN, L.M., and KHOLKIN, A.I., Izv. Sibirsk. Otd. Akad. Nauk SSSR, 1969, No. 2, Ser. Khim. Nauk No. 1, 90
- 9) SIMLEN, L.G., and MARTELL, A.E., Stability constants of metal-ion complexes, 1964, (The Chemical Society, London)
- 10) MÜHL, P., et. al., GDR Patent, 1972, 93 758

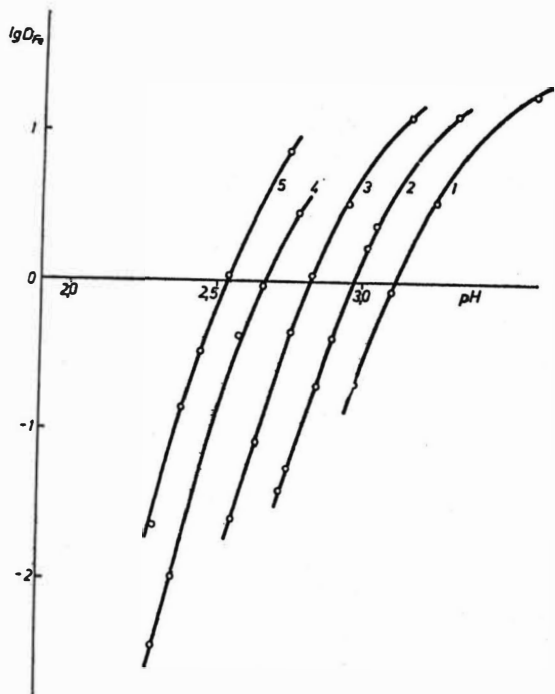


Fig.1. Extraction of Fe(III) from solutions of different Fe(III) concentrations

$c_{\text{HR}(o)} = 1\text{m}$; ionic strength = 4 (Na_2SO_4).

c_{Fe} : curves 1, $2 \times 10^{-4}\text{m}$; 2, $5 \times 10^{-4}\text{m}$;
3, $2 \times 10^{-3}\text{m}$; 4, $1 \times 10^{-2}\text{m}$;
5, $5 \times 10^{-2}\text{m}$

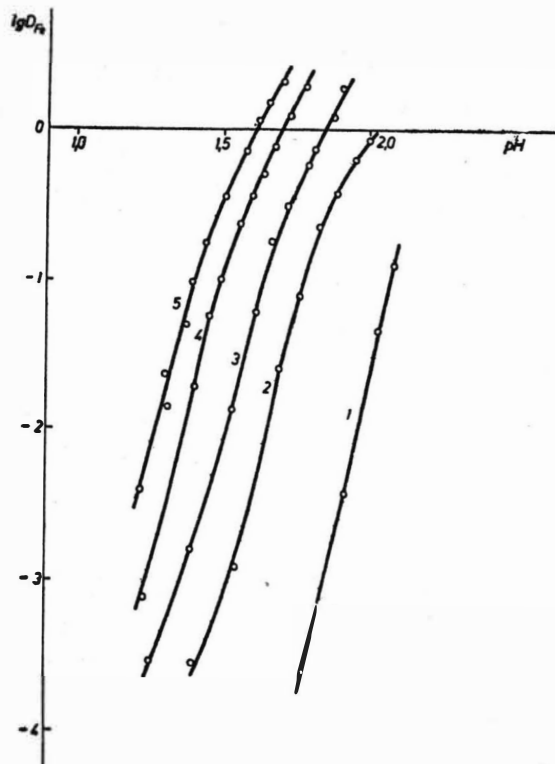


Fig.2. Extraction of Fe(III) at various n-caprylic acid concentrations in n-decane

$c_{\text{Fe}} = 1.63 \cdot 10^{-1}\text{m}$. x

$c_{\text{HR}(o)}$: curves 1, $1 \times 10^{-1}\text{m}$; 2, $3 \times 10^{-1}\text{m}$; 3, $6 \times 10^{-1}\text{m}$;
4, 1m; 5, 1,5m. x

SALTING OUT EFFECT OF SOME METAL-CHLORIDES ON FeCl_3 EXTRACTION
FROM AQUEOUS PHASE WITH METHYL ISOBUTYL-KETONE

I. Eger

Extraction of iron chloride from aqueous solution with Methyl Isobutyl-Ketone was studied, using metal chlorides as salting out agents. Partition coefficients of FeCl_3 in the presence of hydrochloric acid in varied concentrations were used as references.

The salting out effect greatly increases when the salting out agent is hydrophilic. The highest values were obtained by using MgCl_2 , CaCl_2 or AlCl_3 for salting out.

University of the Negev

Research & Development Authority

P.O.B. 1025

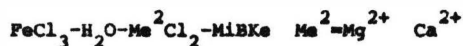
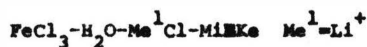
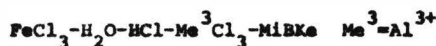
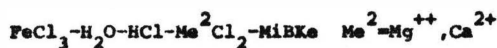
Beer Sheva

ISRAEL

The present work concerns the separation conditions of FeCl_3 from a chloride mixture of AlCl_3 , CaCl_2 , MgCl_2 , NaCl , KCl etc. in aqueous solutions.

The reason for studying this reaction has been the fact that to obtain AlCl_3 from clays by acid leaching, the problem of FeCl_3 separation from a system of chlorides has great importance. Due to the high concentration of the chlorides, the distribution coefficient between the aqueous and methyl-isobutyl-ketone (MIBKe) phase is much increased, a fact that led us to a systematic examination of the partition coefficient variation as a function of the HCl salting out agent and FeCl_3 concentration in the mixture.

The following system of metal chlorides has been tested:



Extraction of FeCl_3 from hydrochloric acid solutions by organic solvent has been studied by various authors (1-5) chiefly for analytical purposes. A number of works treat the extraction mechanism, that is the forming of the FeCl_4^- complex, the dependence of extractibility on the acid concentration of the ferric-ion, and the nature of the solvent used (6,7,8,10,11).

Work based on infra-red spectroscopic analysis has identified the FeCl_4^- ion in the system, proving that FeCl_4^- was formed in the aqueous phase (8). This complex ion is extracted by the organic solvent to an equilibrium stage in a very short time.

The capacity of the organic oxygenated solvent to extract FeCl_3 increases in the following sequence:

Ethers - alcohols - organic acids - esters - ketones - aldehydes (9). We used MIBK as an extractant to obtain FeCl_3 from aqueous solutions, adding various metal chlorides to the above mentioned system.

In our work we used the same quantity of salting out agent, namely 3 equivalent Cl^- from the salt, for each liter of solution, but the ratio of hydrochloric acid was varied between 1 to 6 mols/liter.

Method

Constant amounts of FeCl_3 solution (8,4 g Fe_2O_3 /lit) were introduced in a measuring flask and brought to constant volume and to desired salting out agent and acid concentrations. Then the content of the flask was contacted with MIBK in a volume ratio of 1:1 between organic and aqueous phase.

Prior to this operation the samples were introduced in a thermostat to maintain their temperature at 25°C.

Samples in ferrous complex form were tested by spectrophotometry at pH 3,5 with α - α dipiridil at λ 520 nm using Beckmann apparatus, after reducing Fe^{3+} and Fe^{2+} with hydrochinon.

Interpretation of Results

The values of the partition coefficient of the FeCl_3 were considered as a reference system for FeCl_3 extraction with MIBKs from aqueous solutions with increasing concentration of HCl . The resulting values are introduced in column 2 of Table 1, and are in accordance with the data communicated by Specker and Beckmann.

It can be seen that the partition coefficient is small up to a concentration of 2 M/HCl, but rises to thousands at 6 M/lit HCl concentration.

Table 1, columns 3-10 shows the values of FeCl_3 partition coefficients between MIBKs and the aqueous phase obtained by adding metal chlorides as salting out agent of valence 1 to 4 in which the Cl^- concentration is 3 equivalents/l. (Salts with a solubility lower than this value, are marked with asterisks).

As conclusions of these results we are mentioning the following:

A marked increase in the partition coefficient was observed in all cases in the presence of chlorides.

The partition coefficient increases in most cases only in the presence of acid.

The systems with the salting out agents LiCl , MgCl_2 and CaCl_2 show at high concentration high values for the partition coefficient also in the absence of acid. (Table 2 columns 1,2,3). In all the other cases studied, when extraction was tried without adding the acid, the value of the partition coefficient is negligible.

From the dates in columns 3 to 6 it can be seen that the valence of the anionic and the ionic strength of the salting out agent has no influence upon the extractibility of the iron chloride with MINKe.

From columns 7 to 10 we can see the powerful influence of $MgCl_2$, $CaCl_2$, $AlCl_3$ and $TaCl_5$. This fact is doubtless the consequence of the great affinity of this cation for water.

Values of K very near to that for $MgCl_2$ and $CaCl_2$ are the result of the fact that both salts are highly hydrophilic.

Examining column 1 and columns 7 to 10 for the concentration ranges 1-3 Mol HCl/l we can see that the values of K are increasing more than two orders of magnitude due to the great salting out effect of the hydrophilic chlorides.

There is no need to stress the importance of this effect for separation of $FeCl_3$ from other chlorides in HCl solutions, resulting from hydrochloric acid decomposition of minerals and alloys. The iron chloride separation from these elements can be completed in this condition with relatively low hydrochloric acid concentration in aqueous solutions.

Acknowledgement

The author gratefully acknowledges the assistance of Mrs. Sonia Corcos, for carrying out the measurements of this work.

References

- Rothe, J.W. Stahl u. Eisen, 12, 1052 (1892).
- Langmuir. J. Am. Chem. Soc., 22, 102 (1900).
- Wolfe, R.A. and Fowler, R.G. J. Apt. Soc. Am. 35, 86 (1945).
- Ashley, S.E. and Murray, W.M. Ind. Eng. Chem. Anal.
- Wachtrieb, M.H. and Conway, J.G. Ed. 10, 367 (1938). J. Am. Chem. Soc. 70, 3547 (1948).
- Rabinowitch, E. and Stockmayer, W.H. J. Am. Soc. 335 (1942).
- Dodson, R.W., Forney, G.Y. and Swift, E.H. J. Am. Chem. Soc. 58, 2573 (1936)
- Friedman, H.L. J. Am. Chem. Soc. 74, 5 (1958)
- Kuznetsov, V.I. Zh. Obshch, Khim. XVII, 2, 175 (1947)
- Miller, W. Chemiker Zeitung, 11, 499 (1971)
- Zolotov, Yu. A. et al. Zh. Neorg. Khim. 7, 1197 (1962)
- Bankmann, E. and Specker, H. Z. Anal. Chem. 162, 18 (1959)

TABLE 1

Partition coefficients of FeCl_3 between aqueous HCl solutions
and organic solvent MIBKe (volume 1:1) by using varied
salting out agents

Concentration HCl/ M/l	Without salting out agent	LiCl 127.2 g/l	NaCl 175.3 g/l	KCl 223.3 g/l	NH_4Cl 160.5 g/l	MgCl_2 142.8 g/l	CaCl_2 166.5 g/l	AlCl_3 133.35 g/l	ThCl_4 162 g/l	Remarks
1M	0.034	4.98	4.45	1.2	1.36	6.75	5.6	5.3	3.2	The concentration of the salting out agent is 3g equivalent Cl ⁻ /lit, the working temperature 25°C. The concentration of iron 8.4 g/l Fe_2O_3 .
2M	0.45	71.0	46.5*	8.0*	14.2	146.5	158.8	147	57.3	
3M	3.42	426.8	390.0*	62.0*	105.3*	1005.0	1152	795	560	
4M	37.3									
5M	389.0									
6M	3285.0									

TABLE 2

Partition coefficients of FeCl_3 between aqueous solutions and organic solvent MIBKs (volume 1:1) by using varied salting out agents (without acid HCl)

Conc. of the salting out agent equiv. $\text{Cl}^-/1$	LiCl	MgCl_2	CaCl_2
1	0.051	-	-
2	0.07	-	-
3	0.51	-	-
4	3.00	0.25	0.20
5	31.90	1.55	1.54
6	169.00	12.30	8.40
7	462.50	73.50	67.00

INVESTIGATION OF EXTRACTION AND SOME PROCESSES OF
SEPARATION OF ALKALI-EARTH ELEMENTS

N.E.Brezhneva, G.V.Korpusov, N.P.Prokhorova, Yu.Z.Prokopchuk,
V.I.Svetlakov, and S.Ya.Trukhanov

Institute of Physical Chemistry of the Academy of Sciences
of the U.S.S.R., Moscow, U.S.S.R.

At present not enough consideration has been given to extraction methods of alkali-earth elements (AEE) separation, although all of them are effective and may be successfully used.

Among the papers published only the works on radioactive strontium-90 isolation with D2EHPA /1-4/ are worth while mentioning. Yet, most of data on the regularities of extraction with analytical bias /5-8/.

Earlier we published data on AEE extraction with oxine, its haloid derivatives, and salicyl aldoxime /9-11/. The latter, having good capacity, gives higher values of separation coefficients of calcium-strontium, and strontium-barium as compared with D2EHPA. But this reagent is not produced on a large scale.

Present paper deals with possibilities of other extracts use, such as TBP, D2EHPA, and some others, mainly different carboxylic acids. They are inexpensive and available in unlimited quantities.

EXPERIMENTAL

Table 1 gives the list of investigated extracts.

To study regularities of distribution we used radioactive indicators:

^{45}Ca ($T=164$ days, β); ^{89}Sr ($T=50.5$ days, β);

^{140}Ba ($T=12.8$ days, β, γ); ^{133}Ba ($T=7.5$ years, γ).

^{45}Ca and ^{133}Ba had no impurities and were not additionally purified.

^{89}Sr , containing small amount of ^{90}Sr , was purified from the latter by extraction of 0.5M solution of D2EHPA in kerosene from aqueous solutions of 0.3M on nitric acid. ^{140}Ba was separated from ^{140}La also by extraction with D2EHPA but in 0.1M solution of HNO_3 .

We used standard reagents which were not additionally purified.

INVESTIGATION OF EXTRACTION SYSTEMS

We aimed to study regularities of AEE extraction to choose optimal conditions for AEE separation. So we estimated systems under investigation from the standpoint of their selectivity, technological effectiveness, extract capacity and some other parameters.

I. Extraction of AEE with D2EHPA

D2EHPA solution in hydrogen chloride diluent is known to extract calcium, strontium, and barium in the range of pH values from 1 to 3 (Fig.1), at pH equal to 1.5-2 separation coefficient of calcium-strontium ($\beta_{\text{Ca/Sr}}$) having maximum value ~ 20 . This fact is used in technology of radioactive strontium isolation: strontium is separated from calcium on the stage of reextraction with solution of citrate-poiser (pH $\sim 1.8-2$) /1/. Citric acid is used only to

Table 1

List of Investigated Extracts

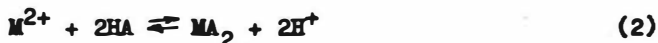
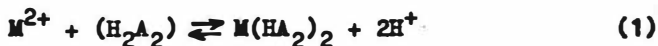
extract	formula	molecular weight	dissolution in water g/100g H ₂ O	dissociation constant
tributylphosphate (TBP)	$\begin{array}{c} \text{C}_4\text{H}_9\text{O} \backslash \\ \text{C}_4\text{H}_9\text{O} - \text{P} = \text{O} \\ \text{C}_4\text{H}_9\text{O} / \end{array}$	266.0	0.039	
diisoamyl ether of methyl-phosphonic acid (DAMPA)	$\begin{array}{c} \text{CH}_3 \backslash \\ \text{C}_5\text{H}_{11}\text{O} - \text{P} = \text{O} \\ \text{C}_5\text{H}_{11}\text{O} / \end{array}$	237.0	0.19	
trisoamylphosphin oxide (TIAPO)	$\begin{array}{c} \text{C}_5\text{H}_{11} \backslash \\ \text{C}_5\text{H}_{11} - \text{P} = \text{O} \\ \text{C}_5\text{H}_{11} / \end{array}$	260.3		
di-2-ethylhexyl-ortho-phosphoric acid (D2EHPA)	$\begin{array}{c} \text{C}_8\text{H}_{17}\text{O} \backslash \text{OH} \\ \text{P} \\ \text{C}_8\text{H}_{17}\text{O} / \end{array}$	322.7	~0.01	$1 \cdot 10^{-2}$
caprylic acid	$\text{CH}_3(\text{CH}_2)_6\text{COOH}$	144.22	0.25	$1.4 \cdot 10^{-5}$
naphthenic acids separated from oil (C ₁₀ -C ₁₃)	$\begin{array}{c} \text{R} \quad \text{R} \\ \diagdown \quad / \\ \text{C} \\ \diagup \quad \diagdown \\ \text{R} \quad \text{H} \end{array} (\text{CH}_2)_n\text{-COOH}$	~250	~0.009	$4 \cdot 10^{-7}$
-isobutyl - isopropylacrylic acid (α, β -acids).	$\begin{array}{c} \text{O} \\ \parallel \\ \text{C} - \text{C} = \text{CH} - \text{CH}_2 - \text{CH} - \text{CH}_3 \\ \quad \quad \\ \text{OH} \quad \text{CH} \quad \text{CH}_3 \\ \quad \\ \text{CH}_3 \quad \text{CH}_3 \end{array}$	169	0.0676	$1.86 \cdot 10^{-5}$
tertiary carboxylic acids C ₁₅ -C ₁₉ (-II)	$\begin{array}{c} \text{C}_2\text{H}_5 \\ \\ \text{R}_1 - \text{C} - \text{COOH} \\ \\ \text{R}_2 \end{array}$	215	-	$1.2 \cdot 10^{-5}$

stabilize pH value.

Changing of separation coefficient value is connected only with changing of pH (Fig.2) and does not depend on either pH of acetic, tartaric or citric acid changes.

At organization of the process of AEE separation, stable systems are of the greatest interest as they provide with complete use of extract capacity.

D2EHPA capacity is changeable in the range of pH of AEE extraction (pH=1-3). It also changes at higher values of pH in the area of extraction isotherm plateau (Fig.3). This fact is due to AEE ability to form two types of extractive compounds by two possible extraction reactions:



Reaction (1) is occurring at $pH \leq 3.5-4$ and corresponds to 50% of D2EHPA neutralization. At higher values of pH D2EHPA monomerises and we have reaction (2). Really (Fig.3) at pH ranging from 3.5 to 5 (monomerization is starting at approximately $pH=4.5$) D2EHPA capacity becomes two times as much.

In exchange systems under isotherm plateau the values of separation coefficients of calcium-stroncium and stroncium-barium are respectively: $\beta_{Ca/Sr} \approx 8-10$, $\beta_{Sr/Ba} = 2.0-2.5$. The last value is small and so great number of steps is required for the separation, But we found that when raising the concentration of sodium nitrate from 1M to 7M, $\beta_{Sr/Ba}$ increased from 1.5 to 6 (Table 2, Fig.4). It is quite natural as stability of nitrate complexing agents of AEE increases from Ca through Sr and to Ba.

Table 2

Separation coefficients of Stroncium-Barium at Different Concentrations of Sodium Nitrate. Extract - 0.5M D2EHPA; pH=3.3

[NaNO ₃], M	1	2	3	4	5	6	7
$\beta_{Sr/Ba}$	1.7	2.1	2.6	3.2	4	5	6

When using acetate poiser the difficulties are possible. One should not ignore them as at changing of relative content of nitrate-ion and acetate-ion the inversion of values of distribution coefficients of stroncium and barium (Fig.5) might take place.

We found as well that increase of TBP concentration in extraction system promoted selectivity of this extraction system (Table 3).

So, the above data show that using combined system, D2EHPA - TBP - NaNO₃, we may considerably raise the values of $\beta_{Sr/Ba}$ and make this system suitable for separation of mentioned elements.

2.4 Extraction of AEE with Neutral Phosphororganic Extracts

There is little information on extraction of AEE different salts with tributylphosphate /12-15/ and practically we have no data at all on AEE extraction with other neutral phosphororganic extracts.

In this paper we considered just for comparison AEE extraction with three representatives of neutral phosphororganic extracts: tributylphosphate, phosphonate, and phosphinoxide.

Above extracts form extractive compounds with AEE by well-known equation:

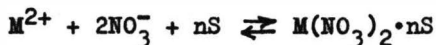


Table 3

AEE Distribution and Separation Coefficients for Different Organic Phase Compositions;
Composition of Aqueous Phase: 1, 3, 5M NaNO₃; 0.01M Ca; 0.01M Sr; 0.01M Ba; pH=4

Aqueous phase composition		1M NaNO ₃					3M NaNO ₃					5M NaNO ₃				
D2EHPA %	TBP %	D _{Ca}	D _{Sr}	D _{Ba}	$\beta_{Ca/Sr}$	$\beta_{Sr/Ba}$	D _{Ca}	D _{Sr}	D _{Ba}	$\beta_{Ca/Sr}$	$\beta_{Sr/Ba}$	D _{Ca}	D _{Sr}	D _{Ba}	$\beta_{Ca/Sr}$	$\beta_{Sr/Ba}$
100	0	>150	23	9.4	~6.5	2.4	~90	7	1.0	~12.8	—	106	3.5	1.0	30	3.5
80	20	~250	30	10	~8.3	3.0	~100	9	1.7	~11.1	5.3	127	6.7	0.9	19	7.4
60	40	~200	37	14	~5.4	2.6	~150	9	1.2	~16.6	7.5	118	8.0	1.10	15	7.3
40	60	~150	31	14	~4.8	2.2	~140	8	1.0	~17.5	8.0	143	5.5	0.9	26	6.1
20	80	~100	6.5	3.2	~15.3	2.03	~60	3.5	0.9	~17.1	3.9	110	2.1	0.34	52	6.2
0	100	0.1	0.04	0.03	2.5	1.3	0.5	<0.1	<0.1	~5	~1	0.8	0.25	0.11	3.2	2.3

where n is close to 2 for calcium (Fig.6) and somewhat less than 2 for strontium and barium.

At AEE extraction the general regularity of raising extraction ability from TBP to phosphinoxides was kept for considered extracts. The extraction order of main representatives of AEE: calcium, strontium, and barium corresponds to the one for above-considered extracts. Magnesium is extracted almost like strontium. Lead(II) is extracted with TBP worse than calcium, and in case of TIAPO better than it. Extraction of two last elements was checked as they are close in their properties to AEE and they are often present in the solutions from which strontium is extracted.

Effective constants calculated for AEE extraction with neutral phosphororganic compounds (TBP, DAMP, TIAPO) are changeable. So we do not give their values in the paper.

Extraction of AEE as well as other elements raises in 'salting out' agents presence (Fig.7).

Fig.8-12 show isotherms of distribution of calcium, strontium, barium, lead(II), and magnesium for TBP, DAMP, and TIAPO. The data obtained show that although neutral phosphororganic extracts extract nitrates of AEE less effective than trivalent elements, they can be still used for practical purposes. Neutral phosphororganic extracts may be used for AEE extraction from their saturated solutions ^{or} in presence of 'salting out' agents, for example, nitrogen nitrate or others. $\beta_{Ca/Sr}$ for TBP and phosphonates is approximately 5, for phosphinoxides $\beta_{Ca/Sr}$ is much lower.

3. Extraction of AEE with Carboxylic Acids

We chose four carboxylic acids representing main available types of carboxylic acids:

1. caprillic acid belonging to aliphatic monocarboxylic acids of normal series.
2. naphthenic acids produced from oil (C₁₀-C₁₃)
3. α -isobutyl- β -isopropylacrylic acid C₁₀ (α , β -acid)-branched carboxylic acid with double bond
4. tertiary α , α -branched carboxylic acids (C₁₅-C₁₉)

The properties of above extracts are given in Table 1.

Dependences of AEE distribution coefficients on pH of equilibrium aqueous phase were found for all acids (Fig.13). Fig. 13 shows that when passing from carboxylic acids of fat series to tertiary α , α -acids, $pH_{1/2}$ of AEE shifts to more alkali area, and extraction order changes as well (Table 4).

Table 4

Values of $pH_{1/2}$ of AEE at Extraction with Different Types of Carboxylic Acids

extract	$pH_{1/2}$ barium	$pH_{1/2}$ stroncium	$pH_{1/2}$ calcium
caprillic acid	3.8	4.22	4.37
naphthenic acids	4.68	4.97	5.26
α , β -acids	5.48	5.64	5.48
tertiary α , α -branched acids	6.01	6.09	5.83

If at the extraction with caprylic and naphthenic acids AEE extraction increases through the series $\text{Ca} < \text{Sr} < \text{Ba}$, then at extraction with tertiary α, α -acids extraction increases so that $\text{Sr} < \text{Ba} < \text{Ca}$.

It is seen from Fig.13 that tangent of angle of slope of curves in coordinates $\lg D$ -pH ranges from 1.7 to 2. This corresponds to the formation of extractive compounds of 2-charged cations. Depending on the conditions and types of carboxylic acids extractive compounds of AEE with both dimerization molecules of extract and monomer ones might be formed. At extraction of microquantities of AEE the formation of compounds with dimeric molecules is most characteristic for normal carboxylic and naphthenic acids. For branched carboxylic acids, which dimerization constants are small in organic diluents, the formation of extractive compounds with monomer molecules of extract is typical. Similar compounds are formed at high content of AEE in organic phase, under the conditions of complete neutralization of carboxylic acid. We did not observed noticeable polymerization of extractive compounds in organic phase.

Composition of AEE extractive compounds found for branched α, β -acids, $\text{MeA}_2 \cdot 4\text{HA}$, is close to that of strontium /16/.

Above acids have not great selectivity at AEE separation. But taking into account carboxylic acids high capacity, up to 1M and even higher, and convenience of different technological processes realization with carboxylic acids, we studied possibility of these acids use. for separation of strontium-barium which is the most difficult separating pair.

We mainly used two extracts: branched α, β -acids and naphthenic

acids which are inexpensive and quite available.

Fig.13 shows that at extraction of indicator quantities of strontium and barium with 50% solution of α, β -acids in dodecane separation coefficient $\beta_{Ba/Sr}$ is approximately 1.5-1.8.

When passing to macroquantities the value of separation coefficient $\beta_{Ba/Sr}$ gets somewhat lesser and makes up 1.28 ($\beta_{Sr/Ba}=0.81$). Dilution of carboxylic acids with tributylphosphate instead of dodecane was expected to increase selectivity of carboxylic acids like in case of D2EHPA. Really, at changing of extraction order separation coefficient of strontium-barium $\beta_{Sr/Ba}$ increases from 0.81 to 1.47 for 50% solution of carboxylic acids in TBP. Fig.14 shows that when increasing TBP concentration in organic phase from 0 to 70% the value of separation coefficient $\beta_{Sr/Ba}$ monotonically increases and reaches 2.28 for organic phase 70% TBP + 30% α, β -acid.

Like in case of D2EHPA, at increase of sodium nitrate concentration in aqueous phase from 0 to 5M (Fig.15) $\beta_{Sr/Ba}$ increases from 1.94 to 7.1. Apparently, concentration of sodium nitrate in aqueous phase should not be higher than 3M, as further increase of concentration does not result in increasing value of $\beta_{Sr/Ba}$, and only leads to decrease of solubility of $Sr(NO_3)_2$ and $Ba(NO_3)_2$, and it is not desirable.

Table 5 contains separation coefficients of strontium-barium for the following extraction system: 40% α, β -acid + 60% TBP - $Sr(NO_3)_2$ + $Ba(NO_3)_2$ + $3NaNO_3$ + H_2O . In this case values of separation coefficients for strontium-barium are much higher than those for D2EHPA. At strontium and barium extraction with naphthenic acids separation coefficient $\beta_{Sr/Ba}$ is 4 for

Table 5

Values of D_{Sr} , D_{Ba} , and $\beta_{Sr/Ba}$ for Different Compositions of Organic and Aqueous Phases

Phase composition	D_{Sr}	D_{Ba}	Sr/Ba
aq ph: 0.7M Sr+0.12M Ba+ 3M NaNO ₃ org ph: 40% α, β -acid + 60% TBP; 1.36M Sr	1.95	0.28	6.86
aq ph: 0.5M Sr + 0.1M Ba + 3M NaNO ₃ org.ph: 40% α, β -acid + 60% TBP; 1.25M Sr	2.5	0.25	10.0

indicator quantities and approximately 1.3 for macroquantities of elements. When introducing sodium nitrate in aqueous phase, like in case with α, β -acids, D_{Ba} decreases, D_{Sr} is approximately constant, and $\beta_{Sr/Ba}$ increases (Table 6).

In the investigated system concentration of barium nitrate should be not higher than 0.05M because of its slight solubility in the system.

So extraction system basing on naphthenic acids may be used only for purification of stroncium from small amounts of barium.

EXTRACTION METHODS

From above experimental data it is clear that neutral phosphates having great capacity, do not give high values of distribution coefficients. They are mainly used for separating calcium from stroncium from saturated solutions of AEE nitrates or solutions

Table 6

Values of D_{Sr} , D_{Ba} , and $\beta_{Sr/Ba}$ for Different Compositions of Aqueous Phase; Organic Phase: 50% solution of Naphthenic Acids in Dodecane; 0.7M Sr

Aqueous phase composition	D_{Ba}	D_{Sr}	Sr/Ba
1M Sr; barium indicator quantities	0.42	0.73	1.75
1.25M Sr; barium indicator quantities	0.28	0.59	2.13
1.25M Sr; 3M $NaNO_3$; barium indicator quantities	0.14	0.59	4.21
1.25M Sr; 0.1M Ba	0.27	0.7	2.59
1.25M Sr; 0.05M Ba	0.28	0.61	2.18

of AEE nitrates in presence of 'salting out' agents, for example, sodium nitrate.

Acid phosphororganic extracts, for example D2EHPA, which under standard conditions is effective at separation of calcium-stroncium cannot be used for separation of stroncium-barium, as the value of separation coefficient $\beta_{Sr/Ba}$ does not exceed 2. As it was pointed out, stroncium-barium separation might be considerably improved by introducing sodium nitrate in system and by dilution of extract with neutral phosphororganic compounds, for example TBP.

Low capacity (0.25M AEE for 1M solution of D2EHPA) of D2EHPA

as compared with carboxylic acids and neutral phosphororganic compounds is its fault.

We observed as well relatively high values of separation coefficients of strontium-barium $\beta_{Sr/Ba} = 10$ for some carboxylic acids, for example, for α -isobutyl, β -isopropylacrylic acid, when we used 'salting out' agents and at dilution of TBP. Carboxylic acids, as having lower molecular weight, own greater capacity in comparison with D2EHPA.

That is why when choosing an extract for separation of great quantities of AEE the preference is given to carboxylic acids.

So we have rather a good choice of extracts and extraction systems for AEE separation.

To perform the separation process different methods may be used. Great quantities of calcium nitrate, in case of its purification from strontium, might be extracted by periodic momentary process with phosphororganic extracts. And, of course, multiple-stage extraction processes should be used for deep purification of strontium from calcium and barium at their compared concentrations.

Semi-counter-current process is little suitable for separation of above elements.

In this case the method of total reflux or standard counter-current process is more effective. But in case of counter-current process for exchanged systems with fixed capacity of organic phase, to separate binary mixtures it is necessary to have at least two extraction cascades. For example, at strontium-barium separation we have pure strontium and the mixture of components on the first cascade, and on the second one there is pure barium and mixture of components.

Total reflux method allows to have two components in pure state with good yield. The only fault of it is that the yield of pure components depends proportionally on the number of extraction stages.

All extraction systems considered were checked in the processes of multiple-stage separation.

As an example confirming the effectiveness of extraction method of AEE separation there are results of experimental production of pure strontium with D2EHPA.

Separation process was carried out in 32-stage counter-current extractor of mixer-settler type with mechanical drive. Mixing and inleakage of phases were performed with spiral mixer. All the cells were isolated from each other. Light phase flowed over to next cells through top pouring and the heavy one through hydroseal. Working volume of every cell was 140 cm^3 , productivity with respect to the sum of phase currents was $600\text{-}1000 \text{ cm}^3$. The separation process was performed in the system: 0.5M solution of D2EHPA in kerosene neutralized by alkali at 50% - aqueous solution of AEE nitrates + 5M solution of NaNO_3 . For this system

$$\beta_{\text{Ca/Sr}}=30 \text{ and } \beta_{\text{Sr/Ba}}=3.5.$$

Separation process was carried out by total reflux method.

AEE concentrate containing 42% Sr, 42% Ba, and 16% Ca served as initial solution. Total content of AEE made up 17 g/l. To stabilize the system and not to fix pH we used as scrubbing solution the one containing NaNO_3 and $\text{Ca}(\text{NO}_3)_2$ which quantity was equivalent to the current of extract.

To conduct the process the extractor was filled in the following way: cells from 1 to 5 were filled with 5N solution of NaNO_3 , 6-16 cells - with initial mixture of AEE extracts,

17-24 cells - with the solution of $\text{Ca}(\text{NO}_3)_2$ of 3.4 g/l concentration.

Aqueous phase volume in every stage was 86 cm^3 .

Organic phase volume was 51 cm^3 .

Stroncium and barium contents were determined in raffinate, stroncium with radiometric method and barium with volumetric one. Stroncium and calcium contents were determined in extract. Aqueous phase pH was maintained constant and equal to 4.2.

After finishing the process practically all barium was scrubbed into raffinate and stroncium remained in the system, phase interface of calcium-stroncium being clearly visible. Fig.16 shows distribution of calcium and stroncium concentrations on cascade stages. Stroncium loss in the process of its purification was insignificant (Fig.17).

Pure fraction of stroncium was selected from 3-17 stages. In such a way stroncium of purity $> 99.95\%$ (barium $< 0.05\%$, calcium $< 0.01\%$) was produced.

Stroncium yield made up 96%.

Still more effective process of AEE separation may be carried out with carboxylic acids, which have much greater capacity at AEE separation coefficient value not less than for D2EHFA.

References

- (1) Beard S.J., Smith P.W., RI-SA-40, August 16, 1965 (to be presented at American Chemical Society Meeting in Atlantic City, New Jersey, September, 13-17, 1965).
- (2) Buttler F.A., Lamb E., Rupp A.F., Conf. on the Use of Radioisotopes in the Phys. and Ind. (Copenhagen, Ricc/204 (1961)).
- (3) McHenry R.E., Rosey J.G., Ind. Eng. Chem., 53, N 7-9, 131 (1961)
- (4) Burns R.E., Schulz W.W., Bray L.A., Nuclear Science and Engineering, 17, N 4, 567 (1963).
- (5) Zolotov Yu.A., Lambrev V.G., Radiokhimiya, 8, N 6, 627-632 (1966).
- (6) Zolotov Yu.A., Lambrev V.G., Zh. Analiticheskoi khimii, 20, N 6, 659-664 (1965).
- (7) Newman E.J., Watson S.A., Analyst, 88, 506 (1963).
- (8) Shevchenko F.D., Kuzina L.A., Ukrain. khim. zh., 33, N 10, 991 (1967).
- (9) Prokopchuk Yu.Z., Brezhneva N.E., Korpusov G.V., Radiokhimiya, 13, 2, 245 (1971).
- (10) Prokopchuk Yu.Z., Korpusov G.V., Brezhneva N.E., Radiokhimiya, 15, 1, 35 (1973).
- (11) Prokopchuk Yu.Z., Brezhneva N.E., Korpusov G.V., Prokhorova N.P. Radiokhimiya, 15, N 1, 42 (1973).
- (12) Mikhailichenko A.I., Klimenko M.A., Bulgakova V.B., Zh. Analiticheskoi khimii, 16, N 9, 2557 (1971).
- (13) Glubokov Yu.M., Korovin S.S., Reznik A.M., Rasskazova T.A., Izvestiya VUZov. "Khimiya i khimicheskaya tekhnologiya", 14, N 7, 983 (1971).
- (14) Lapitskaya E.V., Kuchkina E.D., Gorbenko F.P., ZNK, 13, N 10, (1968).

- (15) Shevchenko F.D., Ageev V.A., Sazhenyuk, ZNK, 16, N 1,
204 (1972).
- (16) McDowell W.J., Harmon H.D., J. Inorg. Nucl. Chem., 31, N 5,
1473 (1969).

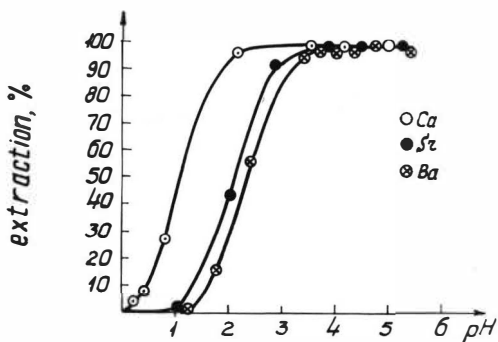


Fig.1. Dependence of calcium, strontium, and barium degree of extraction on pH of equilibrium aqueous phase.

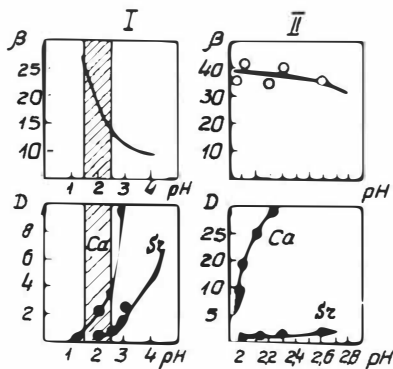


Fig.2. Dependence of distribution and separation coefficients of calcium-strontium on pH of equilibrium aqueous phase for acetate and citrate media.
1 - acetate medium. 2 - citrate medium

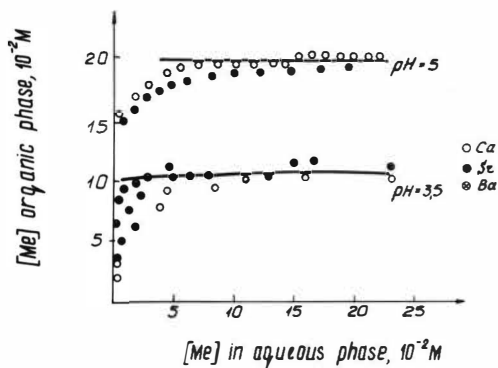


Fig.3. Isotherms of distribution of calcium, strontium, and barium in system: D2EHPA - AEE aqueous solution, at pH=3.5; 5.

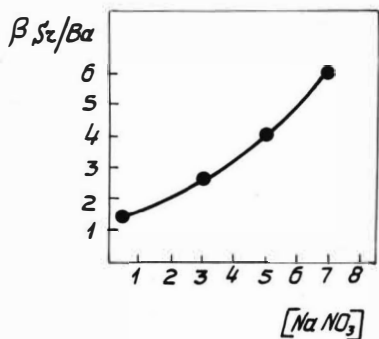


Fig. 4. Dependence of strontium-barium separation coefficients on the concentration of sodium nitrate in aqueous phase.

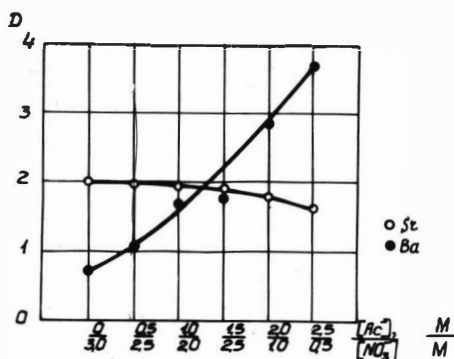


Fig. 5. Dependence of strontium-barium distribution coefficients on relative content of nitrate- and acetate-ion.

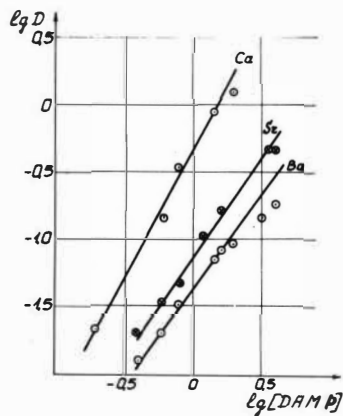


Fig. 6. Dependence of calcium, strontium, and barium distribution coefficients on extract concentration in coordinates $lgD-lg DAMP$.

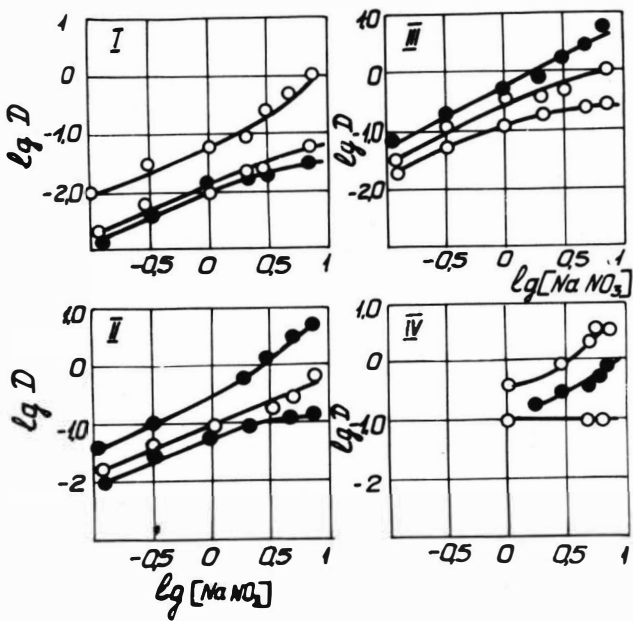


Fig.7. Dependence of calcium, strontium, and barium distribution coefficients on sodium nitrate concentration in aqueous phase in bilogarithmic coordinates for different extracts:

- 1 - TBP
- 2 - Phosphonate $\text{C}_7\text{-C}_9$
- 3 - DAMP
- 4 - TOPO

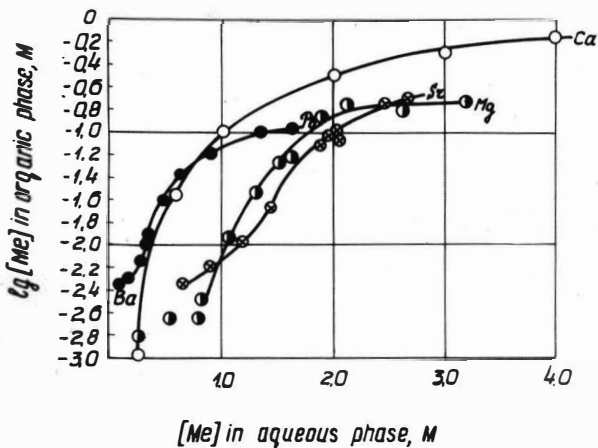


Fig.8. Isotherms of calcium, strontium, barium, lead and magnesium distribution in system: TBP-AEE aqueous solution in coordinates $\lg [\text{AEE}]$ in organic phase - $[\text{AEE}]$ in aqueous phase.

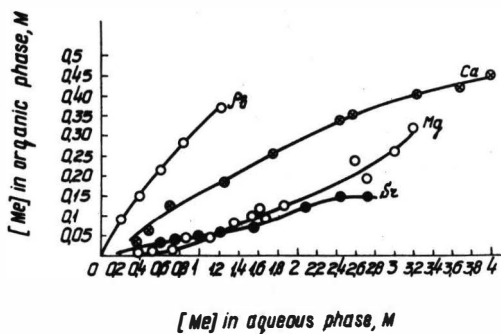


Fig.9. Isotherms of calcium, strontium, lead, and magnesium distribution in the system: TIAPO - AEE aqueous solution.

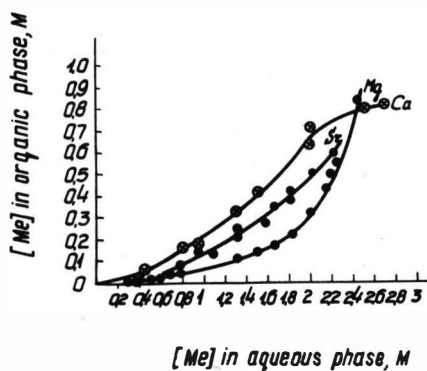


Fig.10. Isotherms of calcium, strontium, and magnesium distribution in the system: aqueous solution of nitrates - DAMP.

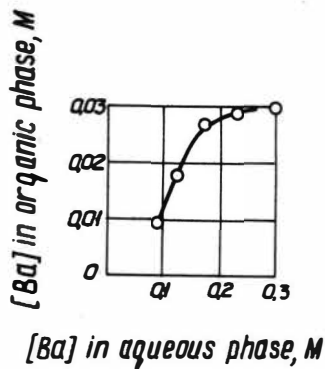


Fig.11. Isotherm of barium distribution in the system: aqueous solution of barium nitrate - DAMP.

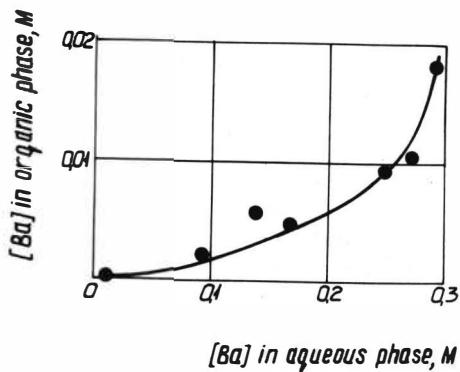


Fig.12. Isotherm of barium distribution in the system: aqueous solution of barium nitrate - TIAPO

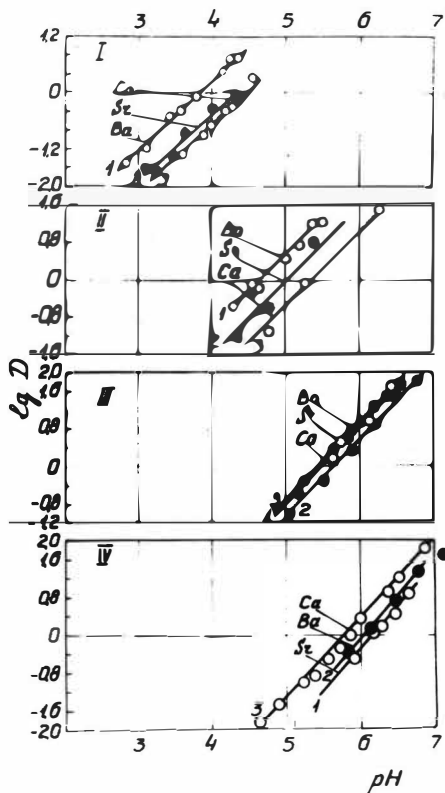


Fig.13.

Dependence of logarithm of calcium, strontium, and barium distribution coefficient on pH for different carboxylic acids:

1. caprylic acid
2. naphthenic acids
3. α -isobutyl- β -isopropyl-lactic acid.
4. tertiary carboxylic acids $C_{15}-C_{19}$

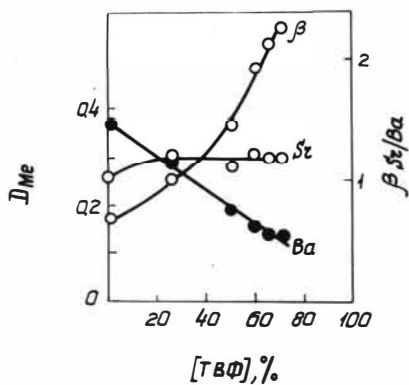


Fig.14. Dependence of D_{Sr} , D_{Ba} , and $\beta_{Sr/Ba}$ on TBP concentration in organic phase.

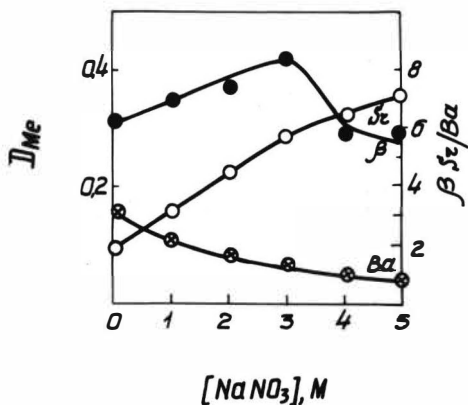


Fig.15. Dependence of D_{Sr} , D_{Ba} , and $\beta_{Sr/Ba}$ on sodium nitrate concentration in aqueous phase.

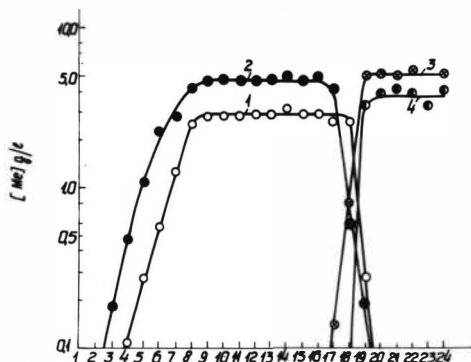


Fig.16. Distribution of calcium and strontium on extractor stages:
 1, Sr in aqueous phase. 2. Sr in organic phase.
 3. Ca in organic phase 4. Ca in aqueous phase.

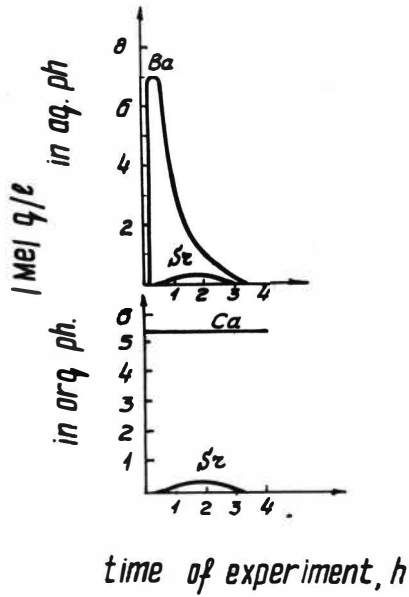


Fig.17. Yield curves of concentration of calcium and strontium in extract and of barium and strontium in raffinate.

ALKALI METALS EXTRACTION BY THE CYCLIC POLYETHER
DIBENZO-18-CROWN-6.

by

P.R. Danesi, H. Meider-Gorican, R. Chiarizia, V. Capuano and
G. Scibona.

C.N.E.N. Laboratorio di Chimica Industriale, C.S.N. Casaccia
Rome, Italy.

SYNOPSIS

The extraction of the alkali cations (Li^+ , Na^+ , K^+ , Rb^+ , Cs^+) by the neutral cyclic polyether dibenzo-18-crown-6 dissolved in various nitrobenzene-toluene mixtures has been studied. Thermodynamic data have been so obtained regarding both the alkali cation-cyclic polyether reaction as well as the ion pair formation in the organic phase. The affinity of the cyclic polyether for the alkali cations has been found to vary in the order $\text{K}^+ > \text{Rb}^+ > \text{Cs}^+ > \text{Na}^+ > \text{Li}^+$ for all the diluents compositions. Moreover the independence of the selectivity constant, defined as the equilibrium constant of the reaction:



(where M is the alkali cation, S the cyclic polyether, X the picrate ion and the bar indicates organic species) on the diluent composition, as well as the independence of the ion pair formation constant from the type of alkali cation, seem to indicate that the complexes formed with the cyclic polyether are isosteric i.e. with size, shape and external electronic distribution independent of the chemical nature of the cation.

INTRODUCTION

Solvent extraction studies of alkali metal cations by means of neutral cyclic polyethers can provide useful information in two fields of recent growing interest, i.e.:

- a) the design of liquid membrane ion selective electrodes responding to alkali cations
- b) the understanding of the mechanisms by which neutral carrier molecules make phospholipid bilayer membranes selectively permeable to cations.

Through solvent extraction experiments it is in fact possible to obtain thermodynamic data concerning the various biphasic equilibria which the alkali cations and the neutral polyether can give rise to.

The extent of selectivity of a given membrane electrode or of a phospholipid bilayer membrane, containing a neutral carrier molecule such as a neutral cyclic polyether, can then be quantitatively predicted.

Although some extensive studies have already appeared in the literature (1-5) concerning the complexing properties of the synthesized cyclic polyethers only one paper has up till now appeared (5) dealing quantitatively with the solvent extraction equilibria of these compounds. Moreover only the extraction of Na^+ and K^+ has been taken into consideration and no systematic study on the diluent effect has been reported.

Therefore in order to better characterize the biphasic equilibria which take place when the alkali cations are solubilized into an organic phase through complexation with a neutral cyclic polyether and to clarify what is the role of the diluent dissolving the polyether on the extent of selectivity of the extractant, we have studied the extraction properties of a neutral cyclic polyether i.e. dibenzo-18-crown-6 (DBC) dissolved in various nitrobenzene-toluene mixtures, covering a dielectric constant range 3.4-35, with respect to the following alkali metal cations: Li^+ , Na^+ , K^+ , Rb^+ , Cs^+ .

By using a similar approach to that previously followed by Pedersen (2,6) and Frensdorff (5) for the neutral cyclic polyethers and by Eisenman et al. (7,8) for the macrotetrolide actin antibiotics, thermodynamic data have been obtained concerning the complex formation reactions between DBC and the alkali cations.

The method used basically consists in studying the distribution of an alkali metal picrate between an aqueous and an organic phase, containing DBC, as function of various concentration variables. The presence of a large anion in the aqueous phase, such as the picrate, is required to make appreciably measurable the extraction of the alkali cations. Large anions, having low charge density and therefore low free hydration energy, are in fact more easily extracted into low dielectric constant solvents, thus favouring the solubilization of alkali cations into the organic phase as well.

EXPERIMENTAL

Reagents. Dibenzo-18-crown-6 (DBC) was prepared as reported in ref. (1,6). Nitrobenzene, toluene, picric acid, Li, Na, K, Rb, Cs chlorides and HCl were all Carlo Erba reagent grade products.

Tracers. ^{22}Na and ^{137}Cs (Amersham U.K.) were used to trace standard neutral solutions of NaCl and CsCl which total concentration had been determined by argentometric titrations.

Distribution Equilibria. Equal volumes of organic and aqueous phase were shaken for about 30 minutes at the temperature of 22 ± 1 °C. The phases were then separated by centrifugation and the Na and Cs concentrations determined by measuring the γ activity of both phases with a scintillation counting system. Rb, K and Li concentrations were determined by flame photometry using a Perkin Elmer spectrophotometer, model 303, at the wavelengths of 670, 780 and 760 $m\mu$ respectively. For Rb and K only the aqueous phase concentration was determined. In the case of Li the organic concentration was instead determined. To the purpose the organic phases were completely stripped with 10 ml of HCl 2M and then the total amount of Li determined by flame photometry.

The total concentration of picrate ions in the aqueous phase was determined, by first neutralizing the solutions with NaOH 0.05 M (to avoid the presence of picric acid), then shaking them with small portions of benzene (to remove traces of the interfering nitrobenzene) and finally measuring the optical density at 360 $m\mu$ by using a Beckman spectrophotometer model DK 2A. The equilibrium concentration of picrate ions in the aqueous phase was calculated by using the ionization constant of picric acid reported in ref. (9) $K=1.96 \cdot 10^{-1}$. The total concentration of the ions was kept constant in the experiments at 0.02 M,

i. e. $[H^+] + [Me^+] = [Pic^-] + [Cl^-] = 0.02$ M. Although, due to the extraction of some picric acid into the organic phase, the total concentration of ions was less than 0.02 M, the activity coefficients of the aqueous species have been assumed as constant in the calculations reported further on.

Organic solutions of DBC in the diluents: 100% nitrobenzene-0% toluene (dielectric constant $\epsilon = 35$), 50% nitrobenzene-50% toluene ($\epsilon = 15.6$), 30% nitrobenzene-70% toluene ($\epsilon = 10.6$), 5% nitrobenzene-95% toluene ($\epsilon = 3.4$), which dielectric constant had been measured by a WTW-DKOG multidecameter at 2 Mc, have been used to extract the alkali metal cations. We have in this way measured in each diluent mixture the distribution ratio, $D = \text{organic metal concentration} / \text{aqueous metal concentration}$, as function of the following variables:

M_{in} = initial aqueous metal concentration,

$M_{in} + H_{in}$ = initial aqueous total cation concentration,

S_{in} = initial organic extractant (DBC) concentration,

X_{in} = initial aqueous picrate concentration,

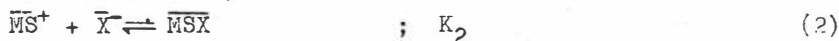
$[X^-]$ = equilibrium picrate concentration.

EQUATIONS DESCRIBING THE SYSTEM.

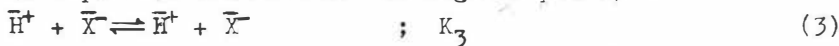
The equilibria taking place in our biphasic system can be represented by the following equations (the bar indicates organic species):



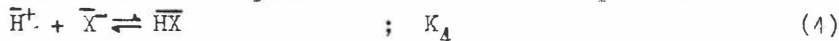
(complex formation between the alkali cation M^+ and the preferentially organic soluble cyclic polyether S-DBC, with the simultaneous transfer into the organic phase of the picrate counter ion X^-)



(ion pair association in the organic phase)



(distribution of picric acid between two phases)



(association of picric acid in the organic phase).

Equilibria 1-4 describe therefore the simultaneous distribution of both M^+ and X^- between the aqueous and the organic phases. They differ from the previously reported ones(8) by the presence of equilibria 3-4 which only occur in acidic solutions. In fact the need of using an easily extractable counter ion (X^-), introduces the further complication of dealing with a weak organic acid which can itself extract into the organic phase

when the aqueous phase is acidic. If the aqueous activity coefficients are assumed as constant, the association of aqueous picric acid properly taken into account (9) and the activity coefficients of organic species assumed equal to one, it follows for the metal distribution ratio D:

$$D = \left(\frac{K_1 c}{[\bar{X}]_{\text{tot}}} - K_2 K_1 a - K_3 K_4 b \right) (1 + K_2 ([\bar{X}]_{\text{tot}} - K_2 K_1 a - K_3 K_4 b)) \quad (5)$$

The variables a, b, c defined as:

$$a = [M^+][\bar{S}][X^-], \quad b = [H^+][X^-], \quad c = [\bar{S}][X^-] \quad (6)$$

are easily calculated for each D through the following mass balance equations:

$$[\bar{M}]_{\text{tot}} = [\bar{M}S^+] + [\bar{M}SX] = (D M_{\text{in}}) / (1 + D)$$

$$[M^+] = M_{\text{in}} - [\bar{M}]_{\text{tot}}$$

$$[\bar{S}] = S_{\text{in}} - [\bar{M}]_{\text{tot}}$$

$$[\bar{X}]_{\text{tot}} = X_{\text{in}} - [X^-]$$

$$[H^+] = H_{\text{in}} + M_{\text{in}} + [\bar{M}]_{\text{tot}} - [\bar{X}]_{\text{tot}}$$

where square brackets indicate concentrations.

It is worth mentioning that any bidimensional graphic representation of D (for example a $\log D$ vs. $\log M_{\text{in}}$ plot) will be only a projection on a plain of the multidimensional variable D. Therefore any function $D = D(K_1, K_2, K_3, K_4, a, b, c, [\bar{X}]_{\text{tot}})$ will be very likely to appear as a snake-like curve.

Due to the complex form of eq. 5 the constants K_1, K_2 and the product $K_3 K_4$ of equilibria 1-4 have been evaluated by computer through a minimization program. To the purpose the program LETAGROPVRID (10), with a specially written subroutine, was used. The function $U = \sum_i (D_{\text{exp}} - D_{\text{calc}})^2$ (i number of experimental points) was so minimized in the four dimensional space $U, K_1, K_2, K_3 K_4$ and the constants corresponding to the minimum U value assumed as the "best" set of constants describing the experimental data.

RESULTS AND DISCUSSION

Fig. 1 and 2 show some of the experimental results (11) obtained in the four diluent mixtures under the form of $\log D$ vs. $\log M_{\text{in}}$ plots. The black points of fig. 1 are reported as an example of a calculated curve obtained with the constants $K_1, K_2, K_3 K_4$ found by minimizing the error square sum U. Table 1 summarizes the constants $K_1, K_2, K_3 K_4$ (obtained from preliminary calculations (11)) for all

the systems studied. For the diluent mixture 5% nitrobenzene-95% toluene only the product K_1K_2 has been determined. In fact in this diluent, due to the negligible extraction of picric acid and to the very high value of the ion pair formation constant, as compared to K_1 , eq. 4 reduces to:

$$D = K_1K_2[S][X^-] \quad (7)$$

The K_1 values reported in table 1 show that, as expected, the extractability of the alkali metal cations decreases as the diluent composition is varied from pure nitrobenzene to pure toluene. Moreover the K_2 values show that the ion pair formation constants depend only on the diluent nature (the association increasing as long as the dielectric constant is lowered) and not on the nature of the alkali cation. This experimental evidence, giving also support to the hypothesis that the complexes are isosteric, i.e. with size, shape and external electron distribution independent of the chemical nature of the cation, allows to obtain a selectivity series, within a given diluent, by the comparison of either the K_1 or the K_1K_2 values. We observe then that, independently of the diluent, the affinity of DBC for the various alkali cations varies in the order $K^+ > Rb^+ > Cs^+ > Na^+ > Li^+$. A similar selectivity series had been found for other 18-crown-6 complexes in water and methanol by Frensdorff (3) although Na^+ and Cs^+ were found to have a closer affinity for the macrocyclic ring than in our case. A series equal to ours is also reported by Eisenman et al. (8) from solvent extraction studies (where the diluents used were CH_2Cl_2 , hexane and 64% hexane-36% CH_2Cl_2 mixture) in the case of monactin. However since the subject of selectivity of various macrocyclic polyethers for the alkali cations in a given medium, together its correlation with structural and solvation properties of both the ions and the polyether, has been widely discussed in the literature (1-6), it will not be discussed here. Emphasis will be instead put on the information it is possible to obtain by studying the influence that the diluent nature has on the selectivity of DBC for the alkali cations.

By defining as selectivity constant the equilibrium constant of the reaction:



where I^+ and J^+ stand for two different alkali cations, it follows:

$$\overline{K}_{IJ} = K_1(J)/K_1(I) \quad (9)$$

which is easily calculated when the K_1 are known. Alternatively

\overline{K}_{IJ} can be calculated from the ratio $K_1(J)K_2(J)/K_1(I)K_2(I)$ when the K_2 are the same for all the ions.

Table 2 reports the selectivity constants obtained in various diluents calculated with respect to Cs^+ . The absence of any systematic trend in the data reported in table 2 seems to indicate that the influence of the diluent on the selectivity of DBC for the alkali cations is negligible. In fact the differences between the selectivity ratios in the different solvents can be mainly attributed to the inevitably large errors present in the evaluation of K_1 and K_1K_2 . These errors are particularly large when dealing with the low dielectric constant diluents and low extractable metals where very small D values are measured.

The independence of the selectivity constant on the nature of the diluent therefore shows that, even in the case of the synthesized cyclic polyether DBC, we are dealing with isosteric complexes. The independence of the selectivity constant on the diluent nature, for isosteric complexes, had been already theoretically predicted by Eisenman et al. in ref. (8). The same experimental result had been obtained for the macrotetrolide actin antibiotics (8). However in this case, due to the very nature of the complexing molecule, it was easy to imagine the complexes as "a large sphere with the cation sequestered deep inside and with electronic distribution and orientation of side chains the same regardless of which cation species is at the centre of the complex" (8). The same result obtained for DBC is however somehow surprising considering that the complexes are likely to be shaped as planar with the alkali cations at their centre. Moreover the independence of the selectivity constant from the solvent requires that the hydration water of the cations to be completely removed when the complexation takes place or at least that the same number of water molecules is retained by all cations in the complexes with the macrocyclic polyether.

Concerning the consequences that the results of the present study have on the design of liquid membrane electrodes based on macrocyclic compounds sensitive to alkali cations, we can state that the use of high polarity water insoluble diluents is recommended. In fact the same selectivity can be achieved with a lower electrode impedance.

Moreover, if the extrapolation of the obtained results to bilayer biological model membranes using a neutral carrier for the alkali cations is legitimate, it follows that the selectivity to the alkali cations should be independent of the nature of the phospholipid (ruling the dielectric properties of the membrane) which constitutes the membrane structure.

REFERENCES

- 1) C.J. Pedersen, J. Am. Chem. Soc., 89, 7017 (1967)
- 2) C.J. Pedersen and H.F. Frensdorff, Angew. Chem. internat. Edit. 11(1), 16, (1972)
- 3) H.K. Frensdorff, J. Amer. Chem. Soc., 93, 600 (1971)
- 4) C.J. Pedersen, Fed. Proc., 27(6), 1305 (1968)
- 5) H.K. Frensdorff, J. Amer. Chem. Soc., 93, 4634 (1971)
- 6) C.J. Pedersen, J. Amer. Chem. Soc., 92, 391 (1970)
- 7) G. Eisenman, S.M. Ciani and G. Szabo, Fed. Proc., 27, 1289 (1968)
- 8) G. Eisenman, S.M. Ciani and G. Szabo, J. Membr. Biol., 1, 294 (1969)
- 9) J.F.J. Dippy, S.R.C. Hughes and J.W. Laxton, J. Chem. Soc., 2995 (1956)
- 10) N. Ingri and L.G. Sillen, Ark. Kemi, 23, 97 (1964)
- 11) all the experimental results obtained in the present investigation as well as definite values for the various constants will appear in a paper to be published.

Table 1

Equilibrium constants for the extraction of picric acid (K_3K_4), the formation of the cyclic polyether-alkali cation complexes (K_1) and the ion pair formation in the organic phase (K_2).

Diluent	ϵ	ION	K_3K_4	K_1	K_2	K_1K_2
Nitrobenzene 100%	35	K^+	$6.0 \pm 0.1 \cdot 10^2$	$(4.2 \pm 2) \cdot 10^3$	$(1.1 \pm 0.2) \cdot 10^2$	$4.6 \cdot 10^5$
		Rb^+	"	$(1.6 \pm 0.3) \cdot 10^3$	$(1 \pm 0.5) \cdot 10^2$	$1.6 \cdot 10^5$
		Cs^+	"	$(7 \pm 2) \cdot 10^2$	$(1.2 \pm 0.2) \cdot 10^2$	$8.6 \cdot 10^4$
		Na^+	"	$(1 \pm 0.2) \cdot 10^2$	$(1 \pm 0.5) \cdot 10^2$	$1 \cdot 10^4$
		Li^+	"	$(3 \pm 0.3) \cdot 10^{-1}$	$(1 \pm 0.5) \cdot 10^2$	$3 \cdot 10$
Nitrobenzene 50%	15.6	Cs^+	-	$(1.2 \pm 0.2) \cdot 10^2$	$(3.3 \pm 0.5) \cdot 10^3$	$4 \cdot 10^5$
Toluene 50%		Na^+	-	(5.2 ± 1)	$(3.8 \pm 0.4) \cdot 10^3$	$2 \cdot 10^4$
Nitrobenzene 30%	10.6	Cs^+	-	(5.8 ± 1)	$(2.2 \pm 0.6) \cdot 10^4$	$1.2 \cdot 10^5$
Toluene 70%		Na^+	-	$(1.7 \pm 0.3) \cdot 10^{-1}$	$(2.9 \pm 0.5) \cdot 10^4$	$4.9 \cdot 10^3$
Nitrobenzene 5%	3.4	K^+	-	-	-	$4.1 \cdot 10^4$
Toluene 95%		Rb^+	-	-	-	$1.7 \cdot 10^4$
		Cs^+	-	-	-	$1.8 \cdot 10^3$
		Na^+	-	-	-	$1.6 \cdot 10^{-2}$
		Li^+	-	-	-	4.0

Table 2

Equilibrium constants of the reaction $\text{Cs}^+ + \overline{\text{MSX}} \rightleftharpoons \overline{\text{CsSX}} + \text{M}^+$

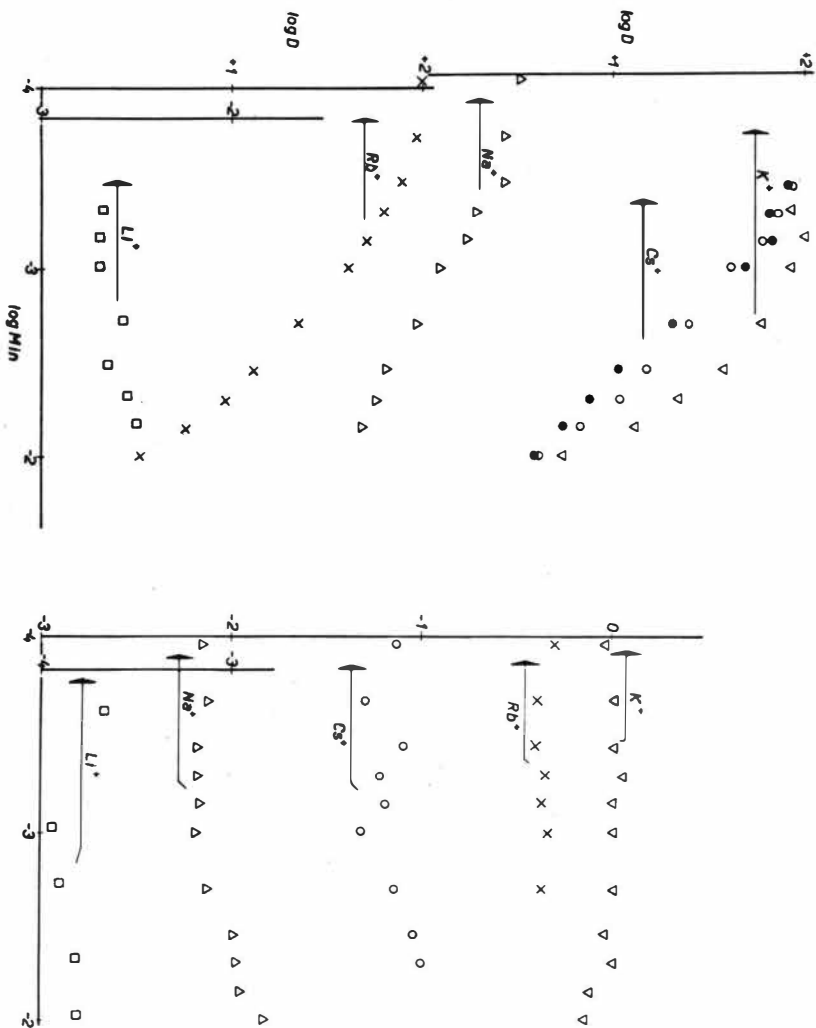
I^+/J^+	\overline{K}_{IJ} nitrobenzene	\overline{K}_{IJ} nitrobenzene 50% toluene 50%	\overline{K}_{IJ} nitrobenzene 30% toluene 70%	\overline{K}_{IJ} nitrobenzene 5% toluene 95%
Cs^+/K^+	$1.7 \cdot 10^{-1}$	-	-	$4.4 \cdot 10^{-2}$
Cs^+/Rb^+	$4.4 \cdot 10^{-1}$	-	-	$1.1 \cdot 10^{-1}$
Cs^+/Cs^+	1	1	1	1
Cs^+/Na^+	7	2.4 10	3.3 10	1.1 10
Cs^+/Li^+	$2.3 \cdot 10^3$	-	-	$4.5 \cdot 10^2$

FIGURES CAPTIONS

Fig.1. LogD vs. $\log M_{in}$ plots for K^+ (∇), Rb^+ (\times), Cs^+ (\circ), Na^+ (Δ), Li^+ (\square).

Fig.2. LogD vs. $\log M_{in}$ plots for Cs^+ (\circ), Na^+ (Δ)

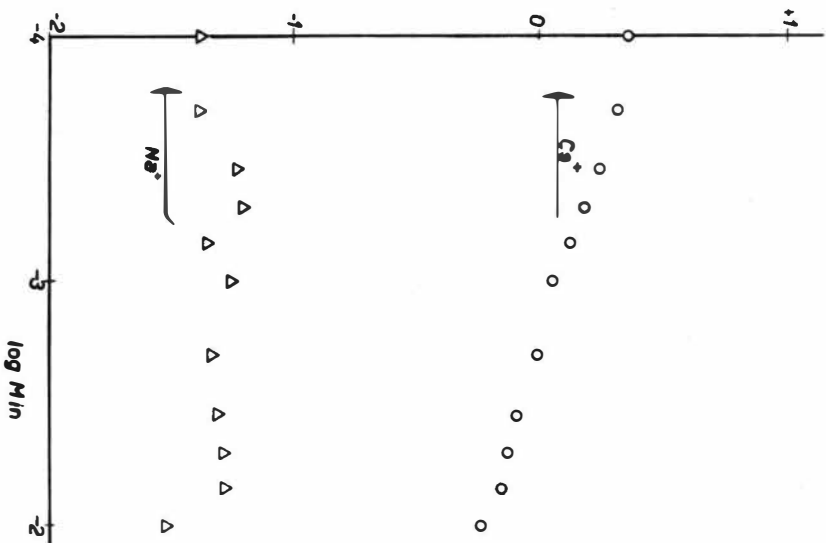
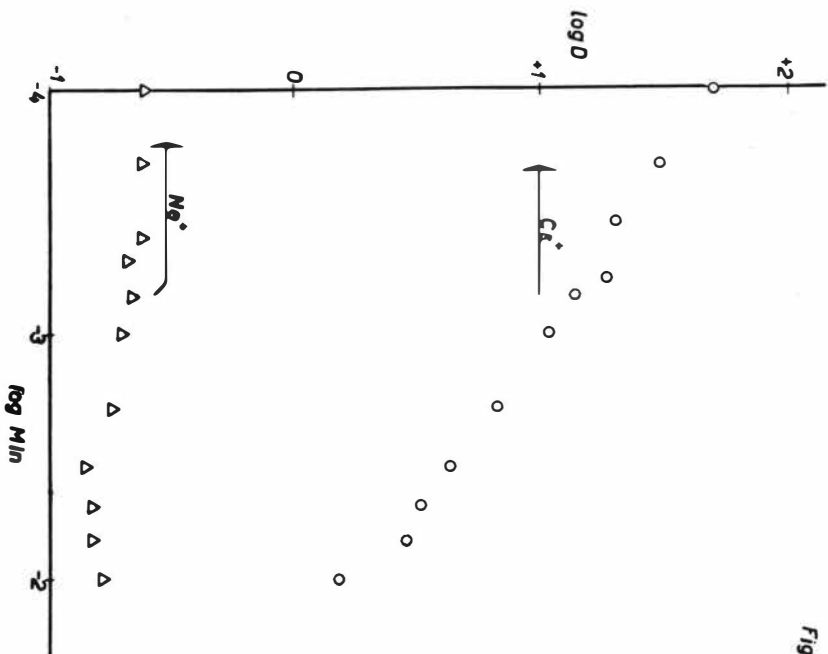
Fig 1



DILUENT = NITROBENZENE
 $\text{Min} = 0.05M$; $\text{Xin} = 0.01M$;
 $\text{Min} = \text{Min} = 0.02M$ (except Na^+ , $\text{Min} = \text{Min} = 0.015M$)

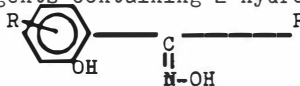
DILUENT = 5% NITROBENZENE + 95% TOLUENE
 $\text{Min} = \text{Min} = 0.02M$; $\text{Xin} = 0.01M$;
 $\text{Min} = 0.012M$ (Li^+ , K^+), $0.015M$ (Cs^+ , Na^+), $0.05M$ (Rb^+)

Fig 2



THE EFFECT ON STRUCTURE OF 2-HYDROXYPHENONOXIMES ON THE
FORMATION OF THEIR COPPER COMPLEXES

B.N. Laskorin, V.V. Yaksin, V.S. Ul'yanov, A.M. Mirokhin
The O.Yu. Shmidt Institute of Physics of the Earth
Academy of Sciences of the USSR, Moscow, USSR

The spatial and electronic structures of the copper extraction agents containing 2-hydroxyphenoximic group (HL) of the type  were studied by

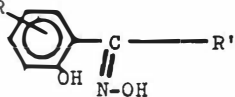
means of IR, UV and PMR spectroscopy using a consecutive isotopic substitution of the hydroxylic protons by deuterium.

The observed specific spectral behaviour of these compounds is explained by the formation of an intramolecular hydrogen bond and participation of the phenol hydroxyl proton and the lone electron pair of oximic group nitrogen.

Both in the solid phase and concentrated solutions 2-hydroxyphenoximes are associated via the intermolecular hydrogen bonds (IHB) with participation of oximic protons. The study of thermodynamic parameters of the association gives an estimate of IHB energy equal to 4-5 kcal/mol. Some factors manifest that the structure of the associated species in the organic solvents may be presented by a cyclic dimer (HL)₂.

The interaction of copper ions with (HL)₂ follows a cationic mechanism of an exchange to give the coloured extracting CuL complexes. The covalent ligand - copper bond in these complexes arises through the phenol oxygen. This was established by decomposition of CuL₂ with deuteriosulfuric acid (D₂SO₄). On the other hand the change in intensities and frequencies ν C=N of the ligand on complex formation lead to the conclusion of an additional coordination bond between oxime nitrogen and copper.

The compounds containing 2-hydroxyphenonoximic group of the type R where R is alkyl or



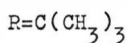
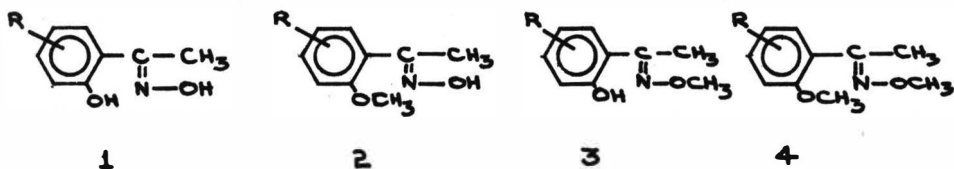
alkoxyl, R' is the aryl or alkyl are used widely in hydrometallurgy as the extraction agents for copper extraction, and purification (1,2). Study of the mechanism of copper extraction with these compounds is complicated by the absence of data on physical and chemical properties and structure of the 2-hydroxyphenonoximic group. Little information is also available on oximes behaviour in the organic solvents and their reactivity towards reactions with non-ferrous metals.

For investigating the spatial and electronic structures of these ligands we synthesized the derivatives listed in table 1. The compounds were prepared from alkylphenols or resorcicates and carboxylic acid chlorides by Friedel-Crafts reaction followed by oximation of the generated ketones using a common procedure.

The IR spectra of all investigated compounds were taken on a "Perkin-Elmer, 125" spectrophotometer in KBr pellets or liquid films. A broad intensive band was observed at $3250\text{-}3350\text{ cm}^{-1}$ the stretching mode of the hydroxyl associated in the hydrogen bond ($\nu_{\text{OH}}^{\text{as}}$). When the compounds were dissolved in CCl_4 and gradually diluted this band intensity decreased with an appearance of a narrow line at $3608\text{-}3615\text{ cm}^{-1}$ being the stretch of the free hydroxyl group ($\nu_{\text{OH}}^{\text{fr}}$).

Only the $\nu_{\text{OH}}^{\text{fr}}$ band was observed in CCl_4 at a concentration of 2-hydroxyphenonoximes below 0.002 M, 2-hydroxyphenonoximes being non-associated monomers under such conditions.

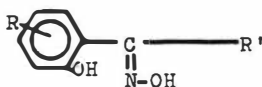
The ν_{OH} band observed in the IR spectra of 2-hydroxyphenoximes could be due to the stretching mode of phenol-hydroxyl and that of the oximic group or a result of overlap of these two bands. To resolve this question we prepared a number of the model compounds of 2-hydroxyacetophenoximes consecutively methylating the different hydroxygroups.



When the phenolic and oximic hydroxyls are methylated (compound 4) no inter or intramolecular association is possible. This enables assignment of the frequency of stretching vibration of the individual $C=N$ bond ($\nu_{C=N}$) in the oximes at 1676 cm^{-1} . A decrease of $\nu_{C=N}$ in compounds 1,3 with hydroxyl groups is evidence of their oximic nitrogen participation in the formation of additional bond with hydroxylic protons. This bond character is clearly pronounced in the comparison of IR spectra of compounds 2 and 3 in solid and CCl_4 solutions (table 2)

TABLE 1

The spectral properties of the substituted derivatives of 2-hydroxyphenoximes



Compound		IR spectrum liquid film		UV spectrum in methanol	
R	R'	$\nu_{C=N}$ cm^{-1}	ν_{OH} cm^{-1}	$n \rightarrow \pi^*$ λ_{max} nm	$\log \epsilon$
4- CH_3O	C_6H_5	1632	3355	302	3.69
4- C_2H_5O	C_6H_5	1629	3349	308	3.89
4- C_4H_9O	C_6H_5	1630	3367	306	4.19

/cont'd..

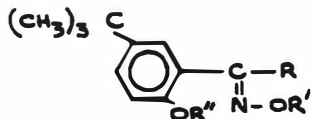
Cont'd..

4-C ₈ H ₁₇ O	C ₆ H ₅	1629	3359	300	4.17
4-C ₁₂ H ₂₅ O	C ₆ H ₅	1627	3370	305	4.12
4-iso-C ₈ H ₁₇ O	C ₆ H ₅	1631	3360	327	4.15
4-C ₂ H ₅ O	C ₈ H ₁₇	1634	3260	303	4.21
4-piso-C ₈ H ₁₇ O	C ₈ H ₁₇	1633	3272	302	4.14
5-CH ₃	C ₆ H ₅	1621	3349	317	4.04
5-tert-C ₄ H ₉	C ₆ H ₅	1637	3355	318	3.59
5-iso-C ₈ H ₁₇	C ₆ H ₅	1618	3348	313	4.63
5-C ₁₂ H ₂₅	C ₆ H ₅	1620	3347	315	3.88
5-iso-C ₈ H ₁₇	C ₈ H ₁₇	1634	3255	316	3.57

When the phenol hydroxyl in compound 2 is substituted by methyl the character of IR spectrum did not change with respect to that of I and in this case the ν_{OH} appears in the form of a broad intensive band at 3239 cm^{-1} ($\nu_{\text{OH}}^{\text{as}}$) in the solid compound shifting to 3615 cm^{-1} ($\nu_{\text{OH}}^{\text{fr}}$) in CCl_4 . This means that the oximic hydrogen takes part in the intermolecular hydrogen bond. This may explain the selfassociation of the oximes in the condensed phase and concentrated organic solutions.

TABLE 2

The spectral properties of



No.	Compound			IR spectra			UV spectra in CCl_4		
	R	R'	R''	Solid in KBr $\nu_{OH_{as}}$ cm^{-1}	$\nu_{C=N}$ cm^{-1}	0.002 M $\nu_{OH_{fr}}$ CCl_4 cm^{-1}	$\nu_{C=N}$ cm^{-1}	λ_{max} nm (log ϵ)	λ_{max} nm (log ϵ)
1	CH_3	H	H	3255	1634	3608	1624	255 (3.903)	316 (3.959)
2	CH_3	H	CH_3	3230	1635	3615	1625	292 (3.542)	-
3	CH_3	CH_3	H	-	1624 ^a	-	1646	260 (4.022)	319 (3.648)
4	CH_3	CH_3	CH_3	-	1676 ^a	-	1689	289 (3.482)	-
8	C_6H_5	H	H	3355	1637	3613	1622	260 (2.404)	318 (3.584)
9	$(CH_3)_3C$		H	3230	-	3631	-	276 (3.258)	-
10	CH_3		H	3310 3240	1640	3617	-	242 (4.052)	-

a - liquid film between the NaCl windows on UR-10 instrument

b - in methanol at 1=1 cm on cP-8 spectrometer

The structure of the associated species may be shown in the form of cyclic dimers "A" or linear polymers "2" (figure 1).

The self-association of 2-hydroxyphenonoximes is confirmed by measuring the molecular weight of compounds 1-4 by an isopiestic method on a "Hitachi-115" instrument in CCl_4 . At less than 0.001 M concentration the experimental molecular weights of 1 and 2 are close to those calculated, while for compounds 3 and 4 the molecular weight is constant at any concentrations.

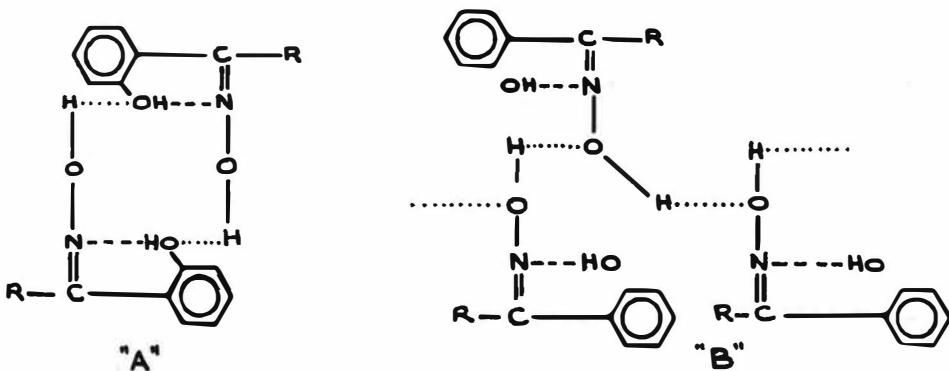


Fig. 1.

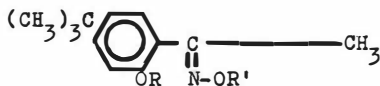
Temperature dependence of the intensities of $\nu_{OH_{fr}}$ and $\nu_{OH_{as}}$ studied on a Unicam SP-700A spectrophotometer at 30-70°C using a thermostatted block for 0.025 M solution in CCl_4 demonstrated that $\nu_{OH_{fr}}$ increases while $\nu_{OH_{as}}$ decreases with increasing temperature. At 70°C in CCl_4 these compounds are predominantly monomeric.

Quantitative treatment of the results in terms of (3) afforded the thermodynamic parameters of self-association of 2-hydroxyphenonoximes in CCl_4 (Table 4).

The study of the oximes self-association in other solvents shows that the hydrogen bond energy of formation decreases and the portion of monomeric molecules in solution increases with increase in solvent polarity.

TABLE 3

The spectral properties of deuterated derivatives

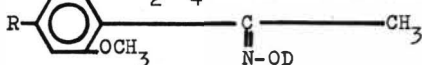


No.	Compound		IR spectra				UV spectra in CCl_4	
	R	R'	$\nu_{OD_{as}}$ cm^{-1}	$\nu_{C=N}$ cm^{-1}	$\nu_{OD_{fr}}$ cm^{-1}	$\nu_{C=N}$ cm^{-1}	λ_{max} nm	Log ϵ
5	CH_3	D	2382	1646	2556	1628	-	-
6	D	CH_3	2339	1641	2242	1642	320	3.625
7	D	D	2450	1635	2655		315	3.618
			2510		2500			

a - incomplete deuteration

Applying Pimental - McClellan's criteria⁽⁴⁾ to the systems under study $J_{as}/J_{fr}^2 = \text{const}$, where J_{as} and J_{fr} are in intensities of $\nu_{OH_{as}}$ and $\nu_{OH_{fr}}$ at the maximum absorption one may conclude that the cyclicdimer "A" is the most probable associate of 2-hydroxyphenoximes in CCl_4 .

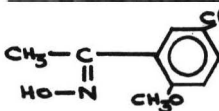
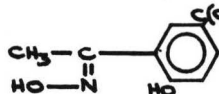
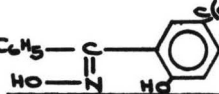
A prolonged refluxing of 2 with metallic sodium in toluene and the treatment of the reaction products with equivalent amount of D_2SO_4 afforded the deuterated compounds (5)



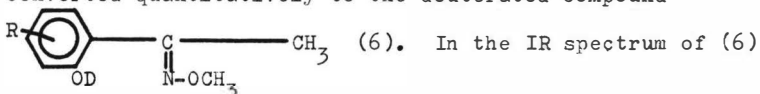
The low reactivity of the oximic group prevents the complete hydrogen deuterium exchange. IR spectrum of this solid compound displays the stretching bands of the OD bond ($\nu_{OD_{as}}$) (Table 3) at 2382 cm^{-1} shifting to 2656 cm^{-1} ($\nu_{OD_{fr}}$) in 0.01 M solution in CCl_4 . This may serve as evidence of inter/molecular hydrogen bond with an oxime proton participation in 2-hydroxyphenoximes.

TABLE 4

The thermodynamic parameters of self-association of 2-hydroxyphenoximes

Compound	K_{as}	$-\Delta H$ kcal/mol	$-\Delta S$ ent.u.	$-\Delta G_{298^\circ}$ kcal/mol
	42.29	5.0600	9.7872	2.1434
	12.36	4.6551	10.0383	1.6657
	50.77	4.2800	6.4189	2.3672

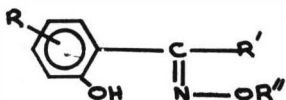
A comparison of spectral data of compound 3 which has a substituted oximic proton and compounds 1 and 2 demonstrated their different behaviour. Thus the IR spectrum of compound 3 reveals no hydroxyl stretching at $3700-3100\text{ cm}^{-1}$ in the condensed state or CCl_4 solution. Reaction with metallic sodium in toluene at room temperature gives the respective phenolate. The latter converted quantitatively to the deuterated compound



(table 3) the mode ν_{OD} appears at 2239 cm^{-1} in the condensed phase but it practically did not change upon dissolving in CCl_4 which is specific for the strong intramolecular hydrogen bond.

Taking into account the shift of OG with the isotopic hydrogen substitution by deuterium ⁽⁵⁾ on going from 3 to 6 one may estimate the wavelength of ν_{OH} for 3 at 3024 cm^{-1} . This value is in the region of the C-H phenyl ring stretching vibration. In addition we studied the IR spectrum of a 0.01 M solution of 6 in CCl_4 at $l = 4.012\text{ mm}$ where the comparison channel contained 0.01 M solution of 3 in CCl_4 at $l = 4.012\text{ mm}$.

The absence of absorption at $3700 - 2300\text{ cm}^{-1}$ shows that the ν_{OH} of phenyl hydroxyl does not appear in the IR spectra of 2-hydroxyphenoximes. Rasmussen ⁽⁶⁾ has called this phenomenon as "chelate conjugation". Earlier it has been observed for 2-hydroxyphenones ^(7,8) as a result of ν_{OH} broadening due to the intramolecular hydrogen bond formation ("chelate ring") between the phenol proton and oxime nitrogen



R = alkyl, alkoxy

R' = alkyl, aryl

R'' = H, alkyl

Formation of the "chelate ring" changes the electronic structures of the compounds decreasing the energy of the lowest antibonding π^* -orbital of the molecule ⁽⁹⁾. This shows itself in the presence of a strong band in the UV spectra of 2-hydroxyphenones corresponding to the $n \rightarrow \pi^*$ transition of the lone carbonyl oxygen electron pair ⁽¹⁰⁾. On going from the carbonyl group to its nitrogen analogues such as azomethynes, imines, semicarbazones, oximes etc., one should expect the change in the $n \rightarrow \pi^*$ band intensity with the character of heteroatomic lone pair hybridization. In oximes the $n \rightarrow \pi^*$ transition is forbidden by the local symmetry because of the high p-character of the lone nitrogen pair in these compounds. Thus oximes either show no $n \rightarrow \pi^*$ transitions in the UV spectra or this band intensity is rather weak. On the other hand the formation of strong intramolecular hydrogen bonds through the lone nitrogen pair may remove forbiddance by local symmetry and in this case the $n \rightarrow \pi^*$ transition would appear in the electronic spectra.

Thus the UV spectra of oximes containing an ortho-hydroxy group (table 2) display an intensive band at 300 nm which undergoes hypsochromic shift with increasing solvent polarity and thus could be assigned to the $n \rightarrow \pi^*$ transition. Its presence may be explained by participation of the nitrogen lone pair of the oxime group in the formation of an intramolecular hydrogen bond with the phenyl hydroxyl.

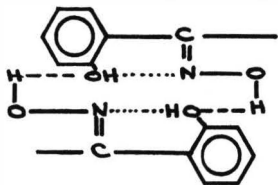
This assumption is favoured by the absence of shift of phenyl proton signal in 2-hydroxyphenonoximes in the PMR spectra on gradually diluting their CCl_4 solutions and by the fact that in compounds 2 and 4 with the alkyl radical instead of phenyl hydroxyl proton no $n \rightarrow \pi^*$ transition is observed in the UV spectra (table 2). This band has not been found in the spectra of α -diketone monooximes $R-C(=O)-C(=N-OH)-R'$,



their esters and amides⁽¹¹⁾, i.e. while the compounds 1 and 3 always show the strong $n \rightarrow \pi^*$ transition. In such case the proton in the "chelate ring" is more labile and may be more easily substituted by metals giving the complexes⁽¹²⁾.

The strength of the generated intramolecular hydrogen bond could be estimated from the IR spectra of these compounds as the temperature was increased. Above 100°C the IR spectra of 3 show the band $\nu_{OH_{fr}}$ at 3609 cm^{-1} increasing in intensity with temperature. The pattern of change of this band intensity with temperature enables estimation of the energy of the chelate ring (12-15 kcal/mol).

Thus the structures of 2-hydroxyphenonoximes could be presented in the form of a chelate ring with participation of the phenolic hydroxyl and oximic nitrogen which is a dimer in condensed phase and concentrated solutions owing to the intramolecular hydrogen bonds with participation of oximic hydroxyl protons:



where designates the intramolecular hydrogen bond,
 ----- means the intermolecular hydrogen bond.

Study of the structure of the 2-hydroxyphenonoxime complexes with copper ions is an important theoretical and practical problem. The compositions of the complexes extracted were investigated spectrophotometrically for different metal ligand ratios. Using the method of molar ratios and isomolar series and the tangent of slope of log D versus pH (D is the distribution coefficient of copper) we found that CuL_2 complex is extracted by the organic solvents from sulfuric acid and neutral solutions. The absence of water in the coordination sphere of the complex was demonstrated directly by Karl Fischer titration and by the absence of the band for free and combined water in the IR spectra. Some complexes were isolated in their pure forms and their physical, chemical and spectral properties are listed in Table 5.

TABLE 5

The spectral properties of 2 -hydroxyphenonoximates of copper CuL_2 .

No.	Initial compound	IR spectrum				UV spectrum		PMR spectrum δ_{HO}
		solid	0.02 M solution		λ_{max}	$\log \epsilon$		
		ν_{OH} cm ⁻¹	$\nu_{C=N}$ cm ⁻¹	ν_{OH} cm ⁻¹	$\nu_{C=N}$ cm ⁻¹	nm		ppm
11		3032	1624	3047	1627	680	3.04	12.6
12		2942	1631	2948	1639	640	2.77	13.1
13		3028	1629	3039	1637	660	2.82	12.9
14		2931	1634	2938	1640	650	2.88	13.2

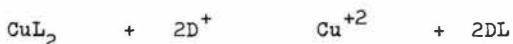
Formation of the covalent and dative ligand - metal bonds is an important question in determining the structures of complexes. Metal may replace both the phenol hydroxyl proton giving the donor bond with oximic nitrogen and the oximic proton in the iminoxide form producing the donor bond with phenol hydroxyl oxygen.

The oxime-iminoxide tautomery has been stated by some authors⁽¹³⁾ and employed for explanation of complexing ability of α -dioximes⁽¹⁴⁾, diimines⁽¹⁵⁾, α -ketoximes⁽¹⁰⁾, α -hydroxyoximes⁽¹⁶⁾ and pyridineketoximes^(17,18). In the most cases the iminoxide form could be detected by physical methods because of its low concentration and the preponderance of the oximic form. However the polar solvents and alkaline solvents should shift an equilibrium towards the more polar oxide form and its concentration would increase. Under such conditions the compound may react with metal in its iminoxide form.

To elucidate the structure of the copper complex and the position of the metal - ligand bond we used a decomposition of 2-hydroxyphenonoximates of copper with acids:



In this reaction the proton addition to the ligand may occur at the covalent Cu-L bond whose position may be established by means of deuterium



The reaction was carried out by means of a two hour contact with 10 ml of a 0.04 solution of copper complex of 5-(1',1',3',3'-tetramethylbutyl)-2-hydroxybenzophenonoxime in CCl_4 with 10 ml of a 20% solution of D_2SO_4 in D_2O at 0° . At first it was shown that no noticeable deuterioexchange occurs in the ligand molecule at the site of phenol. proton thus the deuteration site was determined by copper substitution with deuterium.

The IR spectrum of the decomposition product of the complex with D_2SO_4 in the condensed state shows the band at 2320 cm^{-1} retaining its place and intensity upon dissolving in CCl_4 . This means that in this reaction the phenol hydroxyl proton is substituted and the ligand - copper covalent bond in the complex forms through the phenol oxygen.

This assumption is confirmed by the absence of complexing ability in 2-alkoxyphenonoximes (compounds 2 and 4), with the phenol hydroxyl proton substituted by an alkyl radical and the oximic group remaining unchanged. The substitution of the oximic hydroxyl in 2-hydroxyphenonhydrazones



practically un-affects the complexing abilities of compounds.

It is known (19) that the structurally similar salicylimines produce copper complexes where the phenyl hydroxyl proton is substituted by the metal (ν_{M-O} $640-500\text{ cm}^{-1}$) and the coordination is achieved via the iminogroup nitrogen (ν_{M-N} $580-430\text{ cm}^{-1}$).

In the IR spectra of dimethylglyoxime complexes with different metals Randle and Parasol (20) have observed a considerable decrease in ν_{OH} of the oximic hydroxyl with respect to the starting compound. This phenomenon has been explained by formation of the strong intramolecular bond and Nakamoto has drawn the frequency - O---H...O distance plot which could be used in determining the structure of the complex. The distances shorter than 2.5 Å favour an iminonoxide structure of the complex while those greater than 2.9 Å specify an oximic form. The IR spectra of copper 2-hydroxyphenonoximates show the ν_{OH} at $3100-3028\text{ cm}^{-1}$ which corresponds to the distances 2.9-2.78 Å specific for the oxime form. Thus the mechanism of complex formation between 2-hydroxyphenonoximes and Cu^{+2} ions may be presented as a substitution of the phenol protons with metal ions in a dimer of the extracting agent which serves as a matrix for the complex generating: (figure)2)

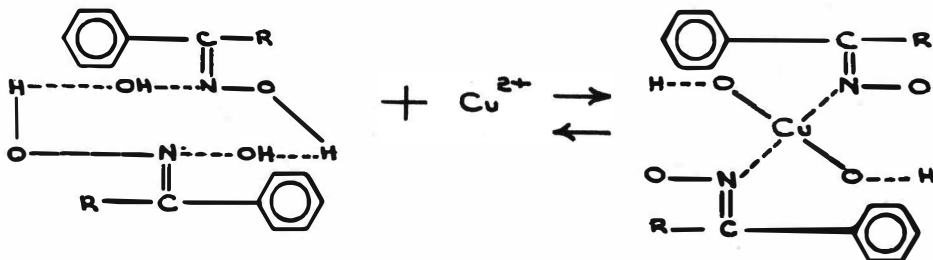


Fig.2.

In the complex generated, copper has its specific coordination number ⁽²²⁾ equal to four which is evident from the UV spectra: the complex 5-(1',1',3',3'-tetramethylbutyl)-2-hydroxybenzophenoxime - copper absorbs at $\lambda_{max} = 660 \text{ nm}$ ($\log \epsilon = 2.82$).

Complex configuration is either a distorted tetrahedron or planar which could be established by means of X-ray analysis.

REFERENCES

1. P.P.Swanson, USA Patent No. 3 428 449
2. B.N.Laskorin, Tsvet. Met. , 1971, 19
3. H.E.Affsprång, S.D.Christian, J.D.Worley, Spectrochim.Acta, 20, 1964, 1415
4. G.C.Pimentel, A.L.McClellan, "The hydrogen bond", San Francisco, 1960.
5. W.West, "Chemikal Applications of spectroscopy", London, 1956.
6. P.P.Rasmussen, D.D.Tannicliiff, J.Am.Chem.Soc., 71, 1068 (1949)
7. L.Joris, P.R.Schleyer, J.Am.Chem.Soc., 90, 4599 (1968)
8. E.B.Martin, Nature , 166, 474 (1950)
9. D.P.Graddon, G.M.Mokler, Austr.J.Chem., 21, No.7, 1769 (1969)
10. I.J.Bellamy, "The infra-red spectra of complex molecules", John Wiley & sons inc., New York.
11. J.Armand, J.-P.Guette, Bull.Chim.France, 1969, No.8, 2894
12. R.P.Patel, R.D.Patel, J. Inorg.Nucl.Chem., 32, N 8, 2894.
13. H.Dial, "The Applications of the Dioximes to Analytical Chemistry", "colombos", Ohio, 1940
14. L.E.Godycki, R.E.Randle, Acta Cryst., 6, 487 (1959)
15. K.Nakamoto, "Infrared spectra of inorganic and coordination compounds", John Wiley & sons, inc., New York, London.
16. USA Patent No. 3 224 873
17. John R.P.Pemberton, H.Dial, Talanta, 16, No.3, 393(1969)
18. A.A.Schilt, P.J.Taylor, Talanta, 16, No.3, 443(1969)
19. K.Ueno, A.E.Martell, J.Phys.Chem., 59, 998(1955), 60, 1270 (1956)

20. R.E.Randle, M.Parasol, J.Phys.Chem., 20,1487 (1952)
- 21.K.Nakamoto, M.Mergoshes, R.E.Randle,J.Am.Chem.Soc.,
77, 6480 (1955)
- 22.F.A.Cotton,G.Wilkinson,F.R.S., "Advanced inorganic chemistry,
John Wiley & sons, inc., New York.

SESSION 17

Wednesday 11th September : 14.00 hrs

CHEMISTRY OF EXTRACTION

(General & Other Interactions)

Chairman:

To be appointed

Secretaries:

Mr. T.V. Healy

Mr. P. Nichel

The hydration of organic phase components and its
influence on extraction equilibrium

Yu. G. Frolov and V. V. Sergievsky

The Mendeleev Institute of Chemical Technology, Moscow, USSR

Abstract

This report is a short review of the authors' investigation of the influence of hydration of organic phase components on extraction equilibrium. The activity of various extractants in ternary solutions, diluent-extractant-water, are tabulated. The equations connecting change of extractant activity when the extractant passes from its dry solution to the wet one are obtained. These equations are shown to be useful for quantitative description of water influence on extraction equilibrium. Application of the Taft equation to extraction systems has been found to ignore the difference in thermodynamic activity and standard states of extractants. The "anomalous" regularities of extraction of acids and metal salts by amines are explained. These results and conclusions are valid for systems including extractants of other classes.

Scientists' attention has previously been drawn to clearing up the question of effect of dissolved water in organic phases in extraction equilibrium. This interest is presumably due to Diamond's, Tuck's⁽¹⁾ and Zolotov's⁽²⁾ successful explanation of hydration influence on extraction of metal halides by neutral oxygen-containing extractants. Quantitative description of hydration is usually given according to the law of mass action on the assumption that⁽³⁻⁵⁾ molecules of extractant or extracted complex form stoichiometric compounds.

This article reviews the investigations of hydration influence on the reactants' activity in ternary solutions, diluent-extractant-water. That most of the results obtained concern amine systems⁽⁶⁾ is governed by the interests of the authors.^(7,8) At the same time, results and conclusions are for general systems and can be applied to extraction by reactants of other classes.

The activity determination is usually based on the Gibbs-Duhem equation. The equation for ternary homogeneous solution with constant molalities of solvent (m_1), extractant (m_2) and varying water concentration (m_3) is the following:

$$d \ln a_2 + \frac{m_1}{m_2} d \ln a_1 + \frac{m_3}{m_2} \left(\frac{\partial \ln a_2}{\partial m_3} \right) d m_3 = 0 \quad (1)$$

By integrating in limits from 0 to m_3

$$\ln \frac{a_2}{a_2^*} = \frac{m_1}{m_2} \ln \frac{a_1}{a_1^*} + \frac{1}{m_2} \int_0^{m_3} \frac{m_3}{a_3} \left(\frac{\partial a_3}{\partial m_3} \right) d m_3 \quad (2)$$

where a_i and a_i^* = activity of a component in binary and ternary solution.

If the distribution of water to extractant solutions occurs according to Henry's law, equation (2) transforms into:⁽⁶⁾

$$\ln \frac{a_2}{a_2^*} = \frac{m_3 - m_3^0}{m_2} = h \quad (3)$$

where h = degree of hydration of extractant and m_3^0 = solubility of water in the pure diluent.

Consequently, degree of hydration is a measure of the extractant activity change, the medium changing from anhydrous to wet. It should be noted that water distribution occurs, according to Henry's law for diluted solutions, in a great number of extractants: salts of substituted ammonium bases, (8-11) TBP in various diluents, (11) neutral organophosphorus compounds (12) and phenol and capric acid in toluene. (13) Therefore, equation (3) is presumed to be suitable for a great number of systems.

Equation (2) gives a simple opportunity for experimental determination of extractant activity in ternary solutions and for testing the validity of equation (3). It is suggested that a_2 and B_1 (the first term of equation (2)) be calculated according to data of cryoscopic measurements, the second B_2 - according to the data of water solubility dependence in extractant solutions of constant concentration on its absolute activity a_w , at the selected temperature of experiments. The results given in Table 1 show that the maximum changes in the activity of the systems studied by us (in three orders) are observed for benzene solutions of tetra-*n*-octylammonium sulphate. In most cases equation (3) conforms to experimental data. Considerable deviations are observed for systems in which water distribution is derived from Henry's law: tri-*n*-octylamine sulphate (TOA) and asymmetrical tertiary amine salts. It has been assumed that the reason for such deviations from Henry's law is the increase in extractant association in water wet solutions.

In all cases the contribution of the first term of equation (2) in extractant activity change is less than the value B_2 . Therefore for the systems not following Henry's law an approximate equation may be suggested:

$$\ln \frac{a_2}{a_2^*} = h_{int} = \frac{1}{m_2} \left[\int_0^{m_3} \frac{m_3}{a_3} \left(\frac{\partial a_3}{\partial m_3} \right) dm_3 - \int_0^{m_3^0} \frac{m_3^0}{a_3} \left(\frac{\partial a_3}{\partial m_3^0} \right) dm_3^0 \right] \quad (4)$$

It is clear that on sufficient dilution the value of the integral degree of hydration h_{int} numerically coincides with the value h . As can be seen, equation (4) conforms well with the experimental data (Table 1). Consequently equations (3) and (4) may be used for the calculation of extractant activity in ternary solutions, according to readily determinable experimental values of their activity coefficients in binary solutions, and the dependence of water solubility in the organic phase on its activity. These equations have been made the basis of subsequent consideration of the influence of organic phase component hydration on the extraction equilibrium.

Let us consider the case of extraction with formation of a chemical compound according to the reaction:



with extraction equilibrium constant:

$$K = \frac{[A_n B]_{org} \bar{\gamma}_{A_n B}}{[A]_{org}^n \cdot a_B \bar{\gamma}_A^n} \quad (5)$$

where A is extractant, B , extracted compound, n , solvate number, $\bar{\gamma}$, activity coefficients of organic phase components.

The principle of linear free energies (for example Taft equation) is usually used for determining the influence of reactants' structure on their extractive capability:

$$\ln \frac{a_i}{a_0} = \rho \Sigma G^* + \text{const} \quad (6)$$

where a_i and a_0 are distribution coefficients when extracting component B at constant concentration, i is the extractant and extractant taken for the standard one, ρ the constant of reaction series, σ the inductive constant of the substituent. The application of equation (6) to heterogeneous systems assumes the equality of chemical potentials of extractants of reaction series in given standard conditions. In general this condition is not observed because of the increase in the hydration of different extractants depending on their characteristics. In the case of the same standard state for series of extractants (solutions are in gaseous phase), equation (6) can be shown as follows:

$$\ln \frac{a_i}{a_0} = (\rho + \rho') \Sigma G^* + n \ln \frac{a_{Ai}}{a_{A_0}} - \ln \frac{\bar{\gamma}_{A_n B_i}}{\bar{\gamma}_{A_n B_0}} + \ln \frac{\gamma_{B_i}}{\gamma_{B_0}} \quad (7)$$

The last two terms of equation (7) may be neglected for the distribution of microcomponents. The second term of the equation reflects the difference in extractant activity in their binary solutions, coefficient ρ' includes the influence of hydration (difference in standard state of extraction systems usually infinitely diluted solutions, water saturated at a_w). Taking into consideration equation (3) at the preferable hydration of extractant in the organic phase, value ρ' is equal to:

$$\rho' = -n(h_i - h_0) \quad (8)$$

Consequently, the more the decrease in the dependence of $\ln a_i/a_0$ on ΣG^* and of other similar parameters, the greater the values n and the difference $\Delta h = h_i - h_0$. The value ρ' is small and the distribution coefficients increase with the rise of reaction capability of these compounds at small values of h_i , which occur, for example, in extraction by neutral organophosphorus compounds or by amine salts with monobasic acids.

The rise of value Δh in some cases results in inversion of a sequence of extractive capability as compared with the results expected on the basis of electronic theory for organic compounds. It has been shown⁽¹⁴⁾ that this occurs on extraction of metal salts by basic ammonium salts with different degree of substitution from sulphate solutions. The following sequence of extractive capability of bases is established for these systems (in contrast to the extraction from monobasic acid solutions): primary > secondary > tertiary > quaternary alkylammonium. Value $n = 7$ for the extreme terms of this series. As for sulphate systems, the extraction for example of uranyl gives $n = 3$. Because of the difference of hydration in this sequence, a decrease of distribution coefficient of about $5 \cdot 10^5$ times should be observed.

The difference in extraction of acids by symmetrical and methyl-substituted tertiary amines as well as regularity considered above, are usually connected with steric effects. Spectroscopic measurement data,⁽¹⁵⁾ however, show insignificant difference in the energy of acid-base interaction for these bases (methyl-substituted amines are slightly weaker bases). The coefficient in equation (8) has the opposite sign where preferable hydration of the compound formed occurs in the process of extraction, as takes place when acids are

extracted by amines. Methyl substituted tertiary amine salts in weakly polar diluents are hydrated more strongly than symmetrical aliphatic amine salts. The difference in logarithms of extraction equilibrium constants ($\Delta \lg K_{H,X}$) obtained from the standard state difference because of hydration, should n be equal to $0.434(h_1 - h_2)$. The values calculated for the extraction of hydrochloric and sulphuric acids are in good agreement with the experimental data (Table 2). The degree of hydration of nitrate salts differs negligibly, therefore, tri-*n*-octylamine extracts nitric acid with greater constancy than methyldioctylamine.⁽¹⁷⁾ So, hydration of extractant and extracted complex influence extraction equilibrium in opposite ways. Calculation of hydration is necessary in practice in all cases, because of the influence of reactant structure on extraction ability.

Dependences of distribution coefficients of complexes on extractant concentration are important to the understanding of the chemistry of extraction processes. They usually serve to determine extraction constants and composition of the complex formed. Recently, satisfactory results have been reported with equilibrium data, in extraction systems using activity coefficients of organic phase components, obtained in binary solutions in a diluent. Using this approximate method, for instance, Kertes and his co-workers⁽¹⁸⁾ calculated extraction equilibrium constants of monobasic acids by triaurylamine. In an investigation by Rosen,⁽¹⁹⁾ good agreement has been established between activity coefficients of some organic phase components, determined using distribution data, and independent physico-chemical measurements in TBP and di-2-ethylhexylphosphoric acid systems. According to equation (3) these factors should also be expected to exist for other systems where distribution of water varies slightly from Henry's law, degree of hydration is small and shows no dependence on concentration.

In the alternative case hydration influences not only the change of standard state but also the activity coefficients of components. Data on the activity of components in binary systems provide the fundamental basis for the description of extraction results. The influence of hydration in its simplified form may be calculated by equation (4).

In the systems studied by us, hydration is very important in extraction from sulphate solutions by amines. Even in the early reports on extraction of sulphuric acid,^(20,21) the "anomalous" behaviour of these systems was observed. Since then, they have attracted the attention of investigators but until recently they had not been explained satisfactorily. It is sufficient to mention the analysis of this problem carried out by Coleman and Roddy.^(9,22)

It was presumed^(23,24) that the slope of the curve in logarithmic coordinates showing the dependence of the acid concentration in the organic phase on the product $[R_3N]_{org} \cdot a_{HX}$ gives, at any point, the average degree of amine salt association. It has been established that, in these coordinates, dependences are "anomalous" for extraction of various monobasic acids by trilaurylamine: The tangent to the slope increases, reaches infinite value and then becomes negative. To a greater degree, this anomalous behaviour is typified in the extraction of sulphuric acid by benzene solutions of TOA.⁽⁶⁾ According to Muller and Diamond, the existence of a vertical asymptote to the curve, corresponds to the complete aggregation of salt into macrocolloid or to the formation of a new phase, which is not confirmed by the data of independent physico-chemical measurements. Incorrect conclusions about very strong salt association is due to the fact that the tangent to the slope has no physical sense in the degree of salt association ascribed to it. Association of salt is a specific value and is equal to the derivative only in the case of linear dependence. The form of curves is caused by the dependence of the effective constant of extraction on the concentration. The reason for this dependence is the change

of activity coefficients of organic phase components, caused not only by their association but also by their hydration.

Substitution of the activity coefficients of TOA sulphate (Fig. 1) determined with the help of equation (2), to the equation of the law of mass action, results in an essentially lesser dependence of extraction equilibrium constant on concentration.⁽⁶⁾ Weak residual dependence of this constant on the concentration of TOA sulphate occurs because activity coefficients are determined using equation (2) which is for a ternary solution, whereas the organic phase in the real extraction system contains four components.

Hydration may be taken into account by using the equation $a_2^* = m_2 e^{h_{int}}$ inasmuch as the activity coefficients of TOA sulphates in binary solutions are close to unity (Fig. 1). The value a_2^* is determined according to the standard state (infinitely diluted water-free solution). It is necessary to define the degree of hydration of components in the first instance at infinite dilution h_{∞} to pass into the standard state for extraction. The values of the extraction constants determined using this approximation (Table 3) are satisfactorily constant.

It should be noted that determination of the composition of the complex of uranyl sulphate and some other metals with sulphate TOA by the bilogarithmic method results in the proportion of the amine to the metal to be 1:1. Substitution of concentrations by activities of TOA sulphate, results in the proportion 5:6:1, which is close to the results obtained from the loading capacity experiments.

So, this work shows that the influence of hydration on organic phase components on extraction equilibrium is appreciable. It shows also that it is possible to account quantitatively for the effects of hydration using thermodynamic activity methods.

References

1. Tuck, D.G., Diamond, R.M., J.Phys.Chem., 1961, 65, 193
2. Zolotov, Yu.G., Usp.Khim., 1963, 32, 220
3. Lassetre, E., Chem.Rev., 1937, 20, 259
4. Christian, S.D., Taha, A.A., Gash, B.W., Quart, Rev., 1970, 24, 20
5. Komarov, E.V., Shpunt, L.B., Radiokhimiya, 1972, 14, 674
6. Frolov, Yu.G., Sergievsky, V.V., Zuev, A.P., Atomm. Energ., 1973, 35, 109
7. Frolov, Yu.G., Ochkin, A.V., Sergievsky, V.V., Atom. Energy Rev., 1969, 7, 71
8. Frolov, Yu.G., Ochkin, A.V., Sergievsky, V.V., Zuev, A.P., Proc. Int. Conf. Solvent Extraction, 1971, London, Society of Chemical Industry, v.2, p.1229

9. Roddy, J., Coleman, C., J.Inorg.Nucl.Chem., 1969, 31, 3599
10. Frolov, Yu.G., Sergievsky, V.V., Ochkin, A.V., Zuev, A.P., Radiokhimiya, 1972, 14, 643
11. Frolov, Yu.G., Sergievsky, V.V., Radiokhimiya, 1971, 13, 760
12. Frolov, Yu.G., Sergievsky, V.V., Zuev, A.P., Izv. Visch. Uchebn. Zav., Chim.Khim.Techn., 15, 59, 1972
13. Sergievsky, V.V., Fedjanina, L.B., Frolov, Yu.G., Izv.Visch. Uchebn. Zav., Khim.Khim.Techn., 1973, 16, 312
14. Frolov, Yu.G., Sergievsky, V.V., Zuev, A.P., Fedjanina, L.B., Zh. Fis. Khim., 1973, 47, 1956
15. Sergievsky, V.V., Frolov, Yu.G., Zh. Strukt. Khim., 1967, 8, 891
16. Shmidt, V.S., Ekstrakcija aminami (Extraction by amines), 1970, Atomizdat, Moscow
17. Shvedov, V.P., Kopyrin, A.A., Titov, V.S., J.Radioanal. Chem., 1972, 12, 421
18. Levy, O., Markovits, G., Kertes, A.S., J.Inorg.Nucl.Chem., 1971, 33, 551
19. Rozen, A.M., Yurkin, V.G., Fedoseev, D.A., Dokl. Acad.Nauk, SSSR, 1972, 207, 1165
20. Coleman, C.F., Brown, K.B., Moore, J.G., Crouse, D.J., Industr. and Engng. Chem., 1958, 50, 1756
21. Allen, K.A., J.Phys.Chem., 1956, 60, 239
22. Coleman C.F., Roddy, J.W., Solvent Extraction Chemistry (Dyrssen, D., Liljenzin, J.-O., Rydberg, J., Eds.), North-Holland Publishing Co., Amsterdam (1967), p. 363
23. Müller, W., Diamond, R.M., J.Phys.Chem., 1966, 70, 3469
24. Diamond, R.M., Solvent Extraction Chemistry (Dyrssen, D., Liljenzin, J.-O., Rydberg, J., Eds.), North-Holland Publishing Co., Amsterdam (1967), p. 426

Table 1

Influence of hydration on activity of extractants in 0,1 mol/l solutions in benzene at $a_w=1$

Extractant	B_2	B_3	$\ln a_2/a_2^*$	h	h_{int}
TBP	-0,276	0,350	0,073	0,13	
di-2-ethyl-hexyl-phosphoric acid	-0,198	0,419	0,22	0,21	
$(C_9H_{19})_2NH_2NO_3$	-0,158	0,355	0,197	0,145	
$(C_{12}H_{25})_3NHNO_3$	-0,211	0,416	0,205	0,20	
$(C_{12}H_{25})_3NH_2SO_4$	-0,204	0,949	0,745	0,705	
$(C_8H_{17})_4NNO_3$	-0,210	0,908	0,698	0,70	
$(C_8H_{17})_3NHCl$	-0,229	1,092	0,863	0,88	
$(C_9H_{19})_2NH_2SO_4$	-0,276	1,817	1,54	1,61	
$(C_8H_{17})_3NH_2SO_4$	0,079	3,294	3,37	4,99	3,30
$(C_8H_{17})_3NH_2SO_4^a$	0,269	3,93	4,19	5,0	3,92
$(C_8H_{17})_4_2SO_4$	-0,359	7,74	7,38	7,56	
$CH_3(C_8H_{17})_2NH_2SO_4^b$	-0,24	3,50	3,26	3,43	
$(C_8H_{17})_3NHCl^c$	0,063	1,24	1,30	1,52	1,24
$(C_8H_{17})_3NH_2SO_4^d$	0,687	3,64	4,32	5,14	3,46

a) $m_2 = 0,364$; b) $a_w = 0,4$

c) measurements are taken in cyclohexane

d) measurement are taken in p-xylene

Table 2

Extraction of acids by amines

Amine	$\lg K_{H_n X}$	Δh	$\Delta \lg K_{H_n X}$	
			exper.	calcul.
HCl				
$CH_3(C_{10}H_{21})_2N$	4,4	1	0,4	0,4
$(C_8H_{17})_3N$	4,0			
H_2SO_4				
$CH_3(C_8H_{17})_2N$	11,40	6	2,65	2,6
$(C_8H_{17})_3N$	8,75			

Table 3

Calculation of extraction equilibrium constant of sulphuric acid by benzene solutions of TOA at 6°C

m_{TOAS}	h_{int}	Δh	K_{eff}	K
0,048	3,02	1,02	13,53	4,89
0,034	2,75	0,75	7,51	3,54
0,056	3,09	1,09	16,49	5,54
0,059	3,11	1,11	8,95	2,96
0,089	3,31	1,31	15,62	4,23
0,110	3,42	1,42	20,24	4,94
0,122	3,53	1,53	26,20	5,76
0,157	3,75	1,75	40,84	7,10
0,225	4,05	2,05	30,55	3,94
0,290,	4,28	2,28	44,80	4,62

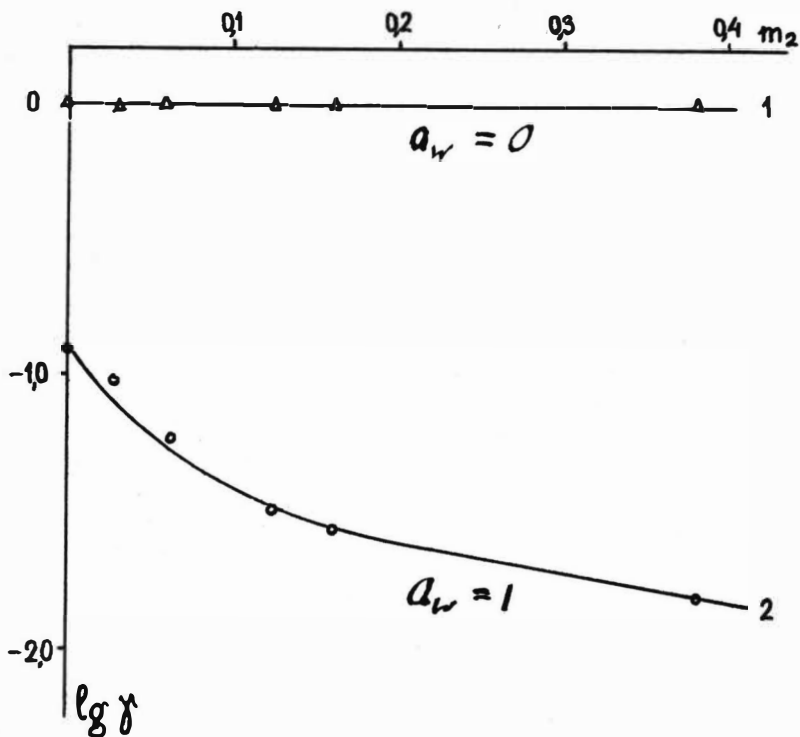


Fig. 1 Activity Coefficients of TOA sulphate in bg .



Effect of Inert Salts on the Solvent Extraction
of Metal Complexes

Tatsuya Sekine, Masakazu Kokiso, and Yuko Hasegawa

The extraction of mercury(II) complexes with chloride or bromide ions (X^-) into hexane containing tributylphosphate or into nitrobenzene was measured as a function of the ligand concentration when the aqueous phase was sodium perchlorate constant ionic medium at 0.5M, 1M, 2M, and 4M. The results were analyzed graphically and the formation constants for the HgX_3^- and HgX_4^{2-} complexes and the partition coefficients for the HgX_2 complex were determined. From these results, the effect of sodium perchlorate on the extraction behaviour of mercury(II) complexes was considered. It was concluded that both the stability constants and the partition coefficient are increased by the increase in the salt concentration but the effect is not very large. An extraction of $NaHgX_3$ species was also found in the bromide-nitrobenzene systems and the statistical treatment for this extraction was considered.

Department of Chemistry, Science University of Tokyo
Kagurazaka, Shinjuku-ku, Tokyo, JAPAN

The effect of a certain salt on the solvent extraction behaviour of a metal ion is related with both the stoichiometric and non-stoichiometric terms. In the present paper, the extraction of mercury(II) from sodium perchlorate constant ionic media containing chloride or bromide ions with tributylphosphate (TBP) in hexane or with nitrobenzene was measured and the results were analyzed from the standpoint of complex formation in the aqueous phase and the two phase partition of the complexes thus formed, and then the effect of this "inert" salt on these equilibrium constants was considered.

Experimental

All the experiments were carried out at 25°C. ^{203}Hg was employed for the determination of the distribution ratio of mercury(II). The procedures were similar to those described in the previous papers of our laboratory^{1,2} Stopped glass tubes (volume 20 ml) were used for the contact of the two phases. The aqueous phase contained mercury(II) labelled with the radioactive tracer, the ligand ion and sodium perchlorate and its ionic concentration was adjusted at a certain value. The organic phase was hexane containing 0.03M TBP or nitrobenzene. Five ml portions of each solution were placed in the tube. The pH of the aqueous phase was about 3 and the initial mercury(II) concentration was $1 \times 10^{-5}\text{M}$. The two phases were agitated mechanically and after an interval enough to establish the distribution equilibrium, they were centrifuged. A certain portion of aliquot was pipetted from each phase and the γ -radioactivity was measured. The distribution ratio was obtained as the ratio of the γ -count-rate of the two phases.

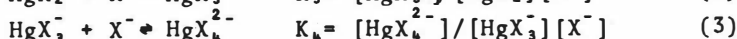
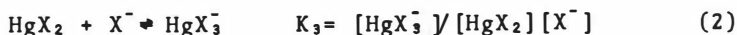
Statistical

The statistical treatment of the data was made as follows.

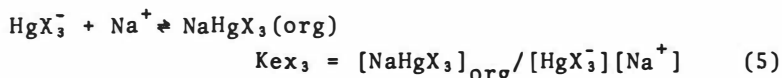
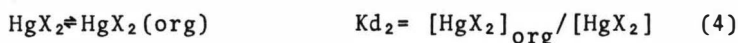
$$D = \frac{[\text{Hg(II)}]_{\text{org, total}}}{[\text{Hg(II)}]_{\text{total}}} \\ = \frac{([\text{HgX}_2]_{\text{org}} + [\text{HgX}_3^-]_{\text{org, total}} + \dots)}{\Sigma [\text{HgX}_n^{2-n}]} \quad (1)$$

Since the stabilities of the higher complexes are very large, the species Hg^{2+} and HgX^+ are negligible in the ligand concentration range of this study ($[\text{X}^-] \geq 10^{-4}\text{M}$).

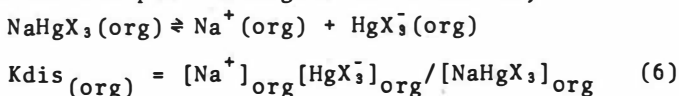
The formation equilibria of the aqueous complexes are;



The extraction equilibria of the complex species can be written as;



When the extracted ion-pair undergoes dissociation,



By introducing the above equations;

$$\begin{aligned} [\text{HgX}_3^-]_{\text{org, total}} &= [\text{NaHgX}_3]_{\text{org}} + [\text{HgX}_3^-]_{\text{org}} \\ &= K_3 K_{ex3} [\text{Na}^+][\text{X}^-](1 + K_{dis}(\text{org})[\text{Na}^+]_{\text{org}}^{-1})[\text{HgX}_2] \end{aligned} \quad (7)$$

From the electronic neutrality, the following relation can be written;

$$[\text{Na}^+]_{\text{org}} = [\text{HgX}_3^-]_{\text{org}} + [\text{X}^-]_{\text{org}} + [\text{ClO}_4^-]_{\text{org}} \quad (8)$$

However, when the mercury(II) concentration is low and the extraction of the ligand anion is much lower than that of perchlorate ion and moreover, when the ligand concentration is much lower than the perchlorate concentration, Eq. (8) may be regarded as;

$$[\text{Na}^+]_{\text{org}} \approx [\text{ClO}_4^-]_{\text{org}} = K[\text{ClO}_4^-] \quad (9)$$

here, K is the square root of the constant for the equilibria $\text{Na}^+ + \text{ClO}_4^- \rightleftharpoons \text{Na}^+(\text{org}) + \text{ClO}_4^-(\text{org})$. Then Eq. (7) may be described as;

$$[\text{HgX}_3^-]_{\text{org, total}} = K_3 K_{d3}' [\text{X}^-][\text{Na}^+][\text{HgX}_2] \quad (10)$$

$$= K_3 K_{d3} [\text{HgX}_2][\text{X}^-] \quad (11)$$

$$K_{d3} = [\text{HgX}_3^-]_{\text{org, total}} / [\text{HgX}_3^-] \quad (12)$$

Finally, by introducing the above equations, Eq. (1) can be written as;

$$D = (K_{d2} + K_3 K_{d3} [\text{X}^-]) / (1 + K_3 [\text{X}^-] + K_3 K_4 [\text{X}^-]^2) \quad (13)$$

Results and Discussion

Figure 1 shows the distribution ratio of mercury(II) as a function of the ligand concentration. These data were analyzed by a graphic method based on Eq. (13) in the same manner as was previously described¹. It was concluded from the analysis that the HgX_2 species is extracted in all the systems. In addition to this, an extraction of the HgX_3^- species as an ion-pair with

sodium ion was also concluded in the bromide-nitrobenzene system. The equilibrium constants thus obtained are given in Fig. 2 as a function of the concentration of the ionic medium.

The stability constants of mercury(II) halide complexes in 0.5M sodium perchlorate solution reported by Sillén³ and Marcus⁴ can be compared directly with the present results in the same ionic medium (for chloride complexes, $\log K_3$ is 0.85³ and 0.95⁴, $\log K_4$ is 1.00³ and 1.05⁴, for bromide complexes, $\log K_3$ is 2.41³ and 2.27⁴, $\log K_4$ is 1.26³ and 1.75⁴). The present results are approximately similar with these values and also with the values previously obtained in our laboratory¹.

As is described above, the solvent extraction of a metal ion, M^{m+} , as complexes with an anionic ligand L^- can be expressed in terms of the formation of metal complexes in the aqueous phase and of the two phase partition of the extractable complexes.

The complex formation is, of course, affected by the ligand concentration but it is also affected by the nature and the concentration of the coexisting electrolytes or by the total ionic concentration in the aqueous solution. Thus a constant ionic strength method or a constant ionic medium method is employed in order to avoid the difficulty due to the latter effect as was reviewed, for example, by Rossotti and Rossotti⁵.

The two phase distribution equilibrium of a certain uncharged molecular species is affected by the nature and the total concentration of the electrolyte in the aqueous phase as was described by Long and McDevit⁶. Such back-ground salt effects on the solvent extraction of metal ions are usually called "salting-out" effect, although the effect due to an increase in the ligand salt concentration is also called by this term in some cases. This salting-out effect should be regarded as the over-all effect of the salt on both of the equilibria, the complex formation and the two phase partition of the extractable species. However, not very much attempt seems to have been made to estimate the effect on individual equilibrium although the salt effect on the stability constants is one of the main subjects of the studies of metal complexes in aqueous solutions.

In the present study, the inert salt, sodium perchlorate, also causes an effect on the extraction of mercury(II) halides; the extraction curves in Fig. 1 are somewhat different when the perchlorate concentration is different. This effect can be considered more clearly from the equilibrium constants.

There is a general tendency that the stability constants of the halide complexes, K_3 and K_4 , increase by the increase in the salt concentration as is seen from Fig. 2 but the increase is not great. When the stability of the anionic complexes becomes higher, the distribution ratio becomes lower, especially in the higher ligand concentration range as is seen from Fig. 1.

The salt effect on the partition coefficient of the HgX_2 species given by Kd_2 in Eq. (4) can be regarded as a salt effect on the activity coefficient of this non-electrolyte. This kind of salt effect is fairly complicated as was described by Long and McDevit⁶, and no theory seems to have been quite successful in giving a general explanation for this effect.

The Kd_2 values of the mercury(II) complexes somewhat increase by the increase in the perchlorate concentration and thus the extraction is enhanced to some extent. However, this increase in Kd_2 due to the sodium perchlorate is not so large as is found in some other molecular substances in Table 2 which was previously obtained in our laboratory^{2,7-9}

The activity of uncharged metal complex in aqueous solutions should be affected in a more complicated manner than that of the simpler molecules in Table 2c but further accumulation of data seems to be necessary before we can give a clear explanation for this problem.

In the case of bromide extraction with nitrobenzene, an extraction of the ion-pair, $Na^+HgBr_2^-$, should be taken into account and thus sodium perchlorate is no longer an "inert" salt. Since the contribution of this species to the distribution ratio is not large, it seems to be rather difficult to estimate the salt effect on this ion-pair extraction. However, in the case of mercury(II) iodide extraction into polar solvents the extraction of such ion-pairs is important and a remarkable salt effect on the extraction of the ion-pairs was observed¹; it was found that the change in the total sodium ion concentration causes a serious change in the shape of the extraction curve of mercury(II) iodide into polar solvents.

References

1. Sekine, T. and Ishii, T. Bull. Chem. Soc. Japan 43, 2422(1970)
2. Sekine, T. and Ihara, N. Bull. Chem. Soc. Japan 44, 2942(1971)
3. Sillen, L. G. Acta Chem. Scand. 3, 539(1949)
4. Marcus, Y. *ibid.* 11, 329, 599, 610, 810(1957)
5. Rossotti, F. J. C. and Rossotti, H. "The Determination of

Stability Constants", McGraw-Hill, New York (1961)

6. Long, F. A. and McDevit, W. F. Chem. Rev. 51, 119(1952)
7. Sekine, T. and Yamasaki, A., Bull. Chem. Soc. Japan 38, 1110(1965)
8. Sekine, T., Nihon Kagaku Zasshi 90, 951(1969)
9. Sekine, T. and Hasegawa, Y. J. Inorg. Nucl. Chem. (in press)

Table 1. Effect of sodium perchlorate on the stability constants of mercury(II) halide complexes (cf. Eqs. (2) and (3)).

NaClO ₄ , M	HgCl _n		HgBr _n	
	logK ₃	logK ₄	logK ₃	logK ₄
0.5	0.65	0.95	2.13	1.77
1.0	0.66	1.00	2.14	1.78
2.0	0.72	1.12	2.16	1.80
4.0	0.80	1.40	2.26	1.90

Table 2. Effect of sodium perchlorate on the partition coefficients (cf. Eqs. (4) and (12))

a) Mercury(II) dihalide complexes (present work)

NaClO ₄ , M	HgCl ₂		HgBr ₂		HgBr ₃ ⁻ *
	0.03M TBP-hexane	nitro-benzene	0.03M TBP-hexane	nitro-benzene	nitro-benzene
0.5	-1.0	-0.28	0.11	0.62	-0.35
1.0	-0.99	-0.24	0.17	0.65	-0.35
2.0	-0.93	-0.19	0.20	0.73	-0.36
4.0	-0.70	0.00	0.47	1.00	-0.39

* These values are K_{d3} in Eq. (12)

b) Metal complexes previously reported

NaClO ₄ , M	In(SCN) ₃ *	Cu(AA) ₂ **	Cu(TFA) ₂ **	Cu(HFA) ₂ **	Zn(AA) ₂ **	Zn(TFA) ₂ **
0.1	--	0.70	1.24	0.90	-0.65	-1.84
1.0	1.00	0.83	1.40	1.39	-0.38	-1.44
2.0	1.34	--	--	--	--	--
3.0	1.80	3.00	1.81	1.76	0.17	-1.01
4.0	2.30	--	--	--	--	--

* ref.9 org. phase: hexane containing 0.03M TBP

** ref.2 org. phase: carbon tetrachloride

The abbreviations are described below.

c) Elementary molecules and weak acids

NaClO ₄ , M	Rn*	Br ₂ **	I ₂ **	SO ₂ **	AA***	TFA***	HFA***
0.1	--	--	--	--	0.51	-0.22	-1.92
0.5	1.85	1.49	1.94	-0.27	--	--	--
1.0	1.88	1.56	2.05	-0.27	0.40	-0.19	-1.74
3.0	2.26	1.83	2.32	-0.19	0.22	0.06	-1.40

* ref.7 org. phase: carbon tetrachloride

** ref.8 org. phase: carbon tetrachloride

*** ref.2 org. phase: carbon tetrachloride

AA: acetylacetone TFA: trifluoroacetylacetone

HFA: hexafluoroacetylacetone

organic phase: open-circles; hexane containing 0.03M TBP
 closed circles; nitrobenzene
 aqueous phase: $\text{Na}(\text{X}^-, \text{ClO}_4^-)$, constant ionic media
 The concentration of the ionic medium is 0.5, 1.0,
 2.0, and 4.0M from left to right.
 The solid curves are calculated curves by introducing the
 constants in Table 1 and 2a into Eq. (13).

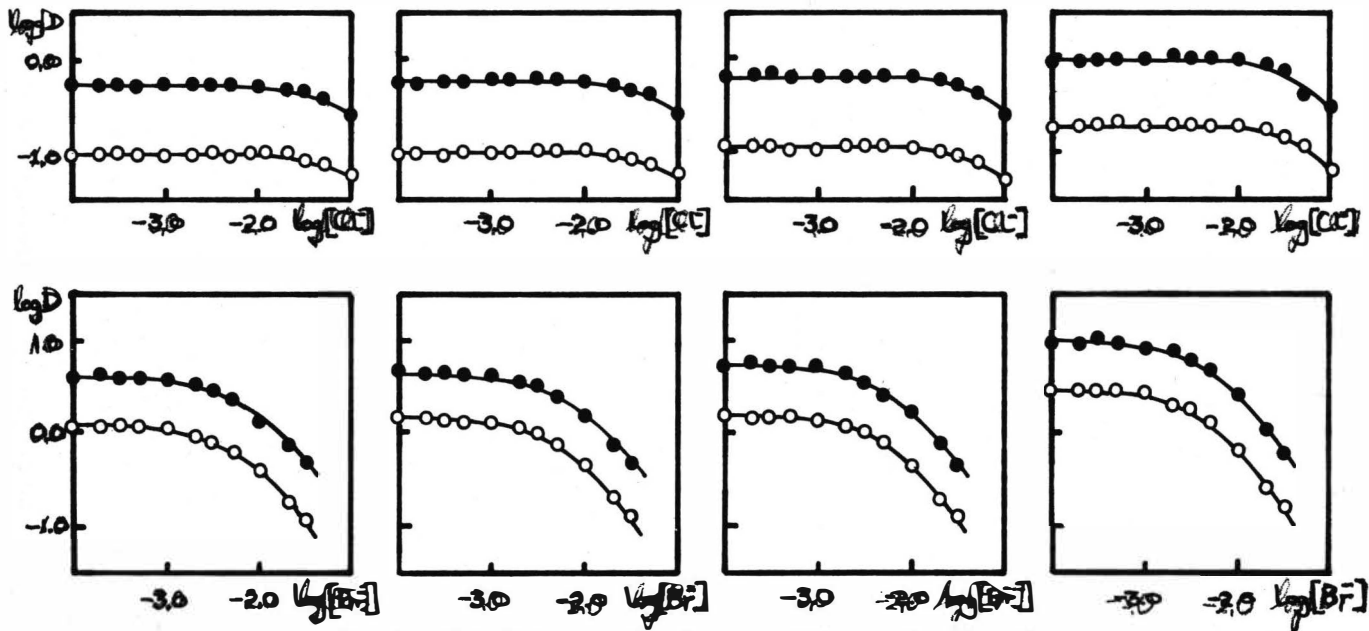


Fig. 1. Distribution ratio of mercury(II) as a function of ligand concentration

a) Partition coefficient

b) Stability constants

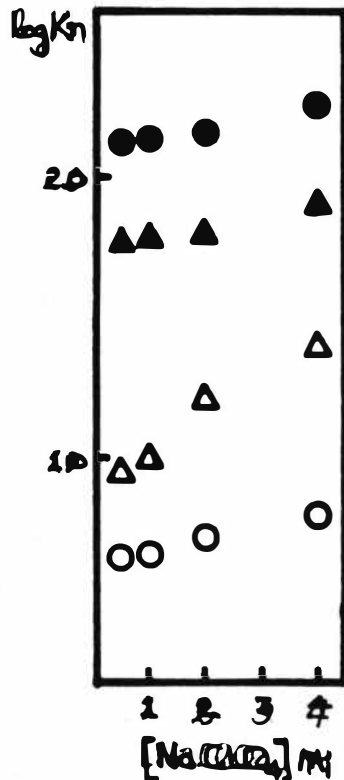
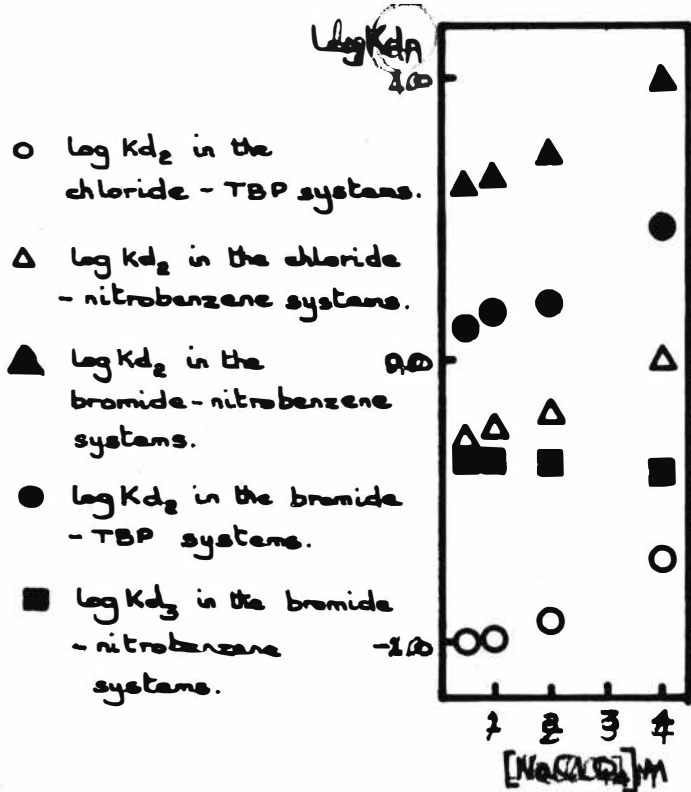


Fig. 2. Equilibrium constants as a function of the concentration of the ionic medium



PREDICTION OF MULTICOMPONENT
LIQUID EQUILIBRIA DATA

by

N. Ashton, L. de J. Soares and S.R.M. Ellis

Department of Chemical Engineering,
The University of Birmingham,
Birmingham.

January, 1974

SUMMARY

A miniature equilibrium still is described for phase equilibrium studies. Ternary tie line results are presented for the systems:

1 Hexene/Perfluoromethylcyclohexane / N Hexane at 6 and 9°C

and

N Heptane /Perfluoromethylcyclohexane / 1 Hexene at 6 and 20°C.

Methods are presented for the calculation of binary parameters for the non-random two-liquid (NRTL) equation and for the prediction of multicomponent tie line data using the NRTL equation.

It is shown that for the open (Type II) systems ternary tie line data can be predicted from binary data alone. For the closed (Type I) system, a reasonable accuracy of prediction can be achieved from binary data if vapour/liquid equilibrium results are used to evaluate the parameters for the miscible non-ideal binary. However, to obtain an ^{accuracy} ~~accuracy~~ of prediction comparable with that for the open systems some ternary data is required for the evaluation of the binary parameters.

INTRODUCTION

The design of liquid-liquid extraction equipment is dependent on the availability of accurate phase equilibria data. The experimental determination of such data is often difficult because of analytical difficulties, and consequently the design of liquid-liquid extraction units has often to be carried out with limited and sometimes inaccurate data. It is therefore highly desirable to have accurate correlating and predicting methods requiring only the minimum of data.

The Wohl type equations (1-9) and more recently the Renon and Prausnitz (10-13) NRTL equation have been applied in the prediction of ternary solubility and tie line data with reasonable agreement being achieved between predicted and experimental results. A paper (14) presented at the 1971 International Solvent Extraction Conference discussed the selection of binary parameters and illustrated the value of the NRTL equation in correlating and extrapolating limited scattered results in preliminary studies of perfluorocarbon and hydrocarbon systems. Current work has continued to demonstrate the usefulness of the NRTL equation for the correlation of phase equilibrium results for partially miscible systems (14-18).

The assessment of a correlating equation and specifically the NRTL type of equation requires the availability not only of binary mutual solubility data but also ternary tie line data and binary and ternary vapour-liquid equilibria at the same temperature. Rarely is

such data available for a specific system and in the past workers have been obliged to rely upon a variety of sources of information and/or extrapolate existing data with the uncertainties inherent to such extrapolations. Furthermore the number of systems for which quaternary liquid-liquid equilibria results are available is very limited.

Various hydrocarbon-perfluorocarbon mixtures have been studied on this comprehensive basis and the accuracy of the NRTL equation for correlating and predicting the data has been tested. Some experimental and predicted ternary liquid-liquid equilibria results are presented in this paper for the systems:

1 Hexene (1) / Perfluoromethylcyclohexane (2) / N Hexane (3) at 6 and 9°C
N Heptane (1) / Perfluoromethylcyclohexane (2) / 1 Hexene (3) at 6 and 20°C

An interesting feature of these mixtures is that over a small temperature range there is a change from a type II to a type I system.

EXPERIMENTAL PROCEDURE

Because of the limited availability and the cost of the pure hydrocarbons and perfluorocarbons, a miniature equilibrium still was developed for phase equilibrium studies (19). The still is suitable for both liquid-liquid tie line determinations and for the study of vapour-liquid equilibrium. When a vapour composition is required, a device for direct sampling of the vapour is used thus avoiding the difficulty of sampling a partially miscible condensate.

Apparatus

The general arrangement of the still is shown in Figure 1. A liquid charge of approximately 25 ml. is introduced into the conical chamber, A, which is enclosed in a constant temperature jacket B. This allows the operating temperature to be controlled at any desired value by recirculation of brine, water or oil. The vapour is condensed by condenser C and returned to the liquid chamber through the capillary D. The bulk liquid is mixed by an electromagnetic stirrer S and can be sampled through the port SL. Direct sampling of the vapour is made through the capillary sampling line SV which is connected to a chromatograph through a vapour injector of the type used by Packer (20). Temperatures are measured by thermistors inserted into the thermistor wells T_W for the liquid and T_V for the vapour. The additional point T allows control of the heating fluid temperature. Temperatures can be measured and controlled to within $\pm 0.05^\circ\text{C}$. The still can be operated at reduced pressures by connecting

the condenser vent to a vacuum line.

Operation

A liquid mixture of the required composition was charged to the still, the stirrer started and continued for 1 to 2 hours to attain equilibrium. The vapour was sampled directly into a gas/liquid chromatograph and liquid samples removed with a hypodermic syringe. If the liquid formed two phases at the operating temperature, then the bulk liquid was allowed to stand for up to 24 hours for the phases to settle out while the temperature was maintained at the required value.

Gas/liquid chromatography was used for all analysis of binary and multicomponent mixtures.

The still has been used for binary and multicomponent vapour/liquid equilibria determinations; for binary mutual solubility determinations over wide temperature ranges and for ternary and quaternary liquid/liquid tie line determinations.

EXPERIMENTAL RESULTS

Solubility curves and tie line data are given in Tables 1 and 2 for the system 1-Hexene (1) PFMCH (2) and N-Hexane (3) at 6 and 9°C respectively. Results for the system N-Heptane (1) PFMCH (2) and 1-Hexene (3) are given in Tables 3 and 4 for 6 and 20°C respectively.

It is interesting to note that the two systems are open (Type II) systems at 6°C but 1-Hexene/PFMCH/N-Hexane at 9°C represents a transition from an open to a closed (Type I) system as 9°C is the critical solution temperature for the binary PFMCH/N-Hexane. At 20°C the system N-Heptane/PFMCH/1-Hexene is a closed system.

CALCULATION PROCEDURES

In this work, the NRTL equation (10) has been used to correlate and predict liquid phase activity coefficients. In its multicomponent form this may be written as:

$$\ln \gamma_i = \frac{\sum_j^N \tau_{ji} G_{ji} X_j}{\sum_k^N G_{ki} X_k} + \sum_j^N \frac{G_{ij} X_j}{\sum_k^N G_{ki} X_k} \left[\tau_{ij} - \frac{\sum_l^N \tau_{lj} G_{lj} X_l}{\sum_k^N G_{kj} X_k} \right] \quad \dots (1)$$

where $\tau_{ji} = (g_{ji} - g_{ii})/RT$

$$G_{ji} = \exp(-\alpha_{ji} \tau_{ji})$$

Provided that the same standard state is used for both liquid phases, the thermodynamic equilibrium condition may be written in terms of component activities:

$$a_{i1} = a_{i2} \quad \dots (2)$$

where $i = 1 \dots N$ for each component

and a_{ij} is the activity of component i in liquid phase j .

Introducing the liquid phase activity coefficient, a simple re-arrangement leads to:

$$\ln \left(\frac{\gamma_{i1}}{\gamma_{i2}} \right) - \ln \left(\frac{X_{i2}}{X_{i1}} \right) = 0 \quad \dots (3)$$

In addition, the stoichiometric requirement in terms of the liquid composition for each phase is:

$$\sum_i^N X_{ij} = 1 \quad (j = 1, 2) \quad \dots (4)$$

The activity coefficients are functions of the NRTL parameters and the liquid phase composition so that equation (3) can be written as a system of N non-linear equations of the form:

$$F_i (A_1 \dots A_L; x_{11}, x_{12} \dots x_{N1}, x_{N2}) = 0 \quad \dots (5)$$

where $A_1 \dots A_L$ represent the NRTL binary parameters for each binary pair of components.

X_{ij} represents the liquid mole fraction of component i in the liquid phase j .

and $i = 1, N$

$j = 1, 2$

This system of non linear equations can be used for:

- a) the prediction of multicomponent solubility and tie-line data from a known set of binary parameters;
- b) the calculation of binary parameters from multicomponent tie-line data when a sufficient number of tie-lines are available;

c) the calculation of binary parameters from solubility data.

a) Prediction of Ternary Data

For the prediction of ternary tie line data from a known set of NRTL parameters, the approach used was to obtain x_{21} and x_{22} from equation (4) and substitute these values into the equation set represented by equation (5). This yields a set of three non linear equations of the form:

$$F_i(x_{11}, x_{12}, x_{31}, x_{32}; A_1 \dots A_L) = 0 \dots (6)$$

where $i = 1, 3$

As there are four unknowns ($x_{11}, x_{12}, x_{31}, x_{32}$) calculations were made by fixing the composition of the solute (component 3) in the liquid phase 1 ie. a value of x_{31} . The choice of which component should be treated as the solute and which phase should be defined as phase 1 is arbitrary. The set of equations was solved using a Newton-Raphson technique.

When predicting data for comparison with experimental values, the experimental value for x_{31} was taken as the fixed value and the remaining compositions calculated. Agreement between experimental and predicted phase compositions were expressed in terms of a Root Mean Square Deviation (RMSD) defined as:

$$\text{RMSD}(x_{11}) = \left[\frac{\sum_k^M (x_{11,c} - x_{11,e})^2}{M - 1} \right]^{\frac{1}{2}} \dots (7)$$

where subscript c refers to the calculated value
 subscript e refers to the experimental value
 and M is the total number of data points.

b) Calculation of Parameters from Ternary Data

When fitting the NRTL equation to a set of empirical ternary tie line data, the set of equations represented by equation (5) becomes three equations for each tie line. The approach used here to solve for the NRTL parameters was to minimise the sum of the squares of the residuals of the compositions ie,

$$\sum_{k=1}^M \sum_{i=1}^3 (x_{i,e} - x_{i,c})^2 \quad \dots (8)$$

The number of tie lines used should be such that

$$3M \gg L$$

where L is the number of parameters to be fitted.

M is the total number of experimental tie lines

For a ternary system, if all the binary pairs are treated as non ideal there results a maximum of 9 adjustable parameters. These can be calculated from a minimum of three tie lines.

c) Calculation of Parameters from Mutual Solubility Data

When calculating binary parameters from mutual solubility data, the set of equations represented by equation (5) becomes only two equations. This means that the third parameter χ_{ij} must be chosen

by some means eg. using the rules of Renon and Prausnitz (10), and then the parameters τ_{ij} and τ_{ji} can be calculated.

d) Other Sources

It is also possible to calculate the binary parameters from other types of phase equilibrium data. Soares (19) has reported methods using:

- i) Vapour/liquid equilibrium data;
- ii) Isobaric boiling point data
- iii) Isothermal total pressure data
- iv) Infinite dilution activity coefficients.

However the only other type of data used in this work on the perfluorohydrocarbons was isothermal vapour/liquid equilibrium data. For miscible binaries the NRTL parameters were calculated by fitting the equation to available vapour/liquid equilibrium data.

The technique used was a fit to total pressure minimising the sum of the squares of the residuals of the total pressure at each data point.

DISCUSSION OF RESULTS

Open (Type II) Systems.

At 6°C both systems are of the open type having two partially miscible binaries. For these systems the ternary tie line data were predicted using the NRTL equation with binary parameters for the two partially miscible binaries obtained from the mutual solubility data at the system temperature. The hydrocarbon/hydrocarbon binaries were treated as ideal mixtures. As discussed earlier, when using binary mutual solubility data to generate the NRTL parameters, the non-randomness parameter α_{ij} must be chosen separately. The rules of Renon and Prausnitz (10) for the choice of a value of α indicate a value of 0.4 for both partially miscible binary systems. For both systems, the tie line data were predicted for values of α varying from 0.375 to 0.425 and ~~the~~ ^{the} RMSD obtained are presented in Tables 5 and 6 together with the corresponding binary NRTL parameters. It can be seen that the values of $\alpha_{ij} = 0.4$ are similar to the best fit values.

The best fit values were used to generate the predicted compositions presented in Tables (1) and (3). The accuracy of prediction can be seen by referring to Figures 2 and 3 where a comparison is made between the experimental and predicted tie lines.

Closed Systems (Type I)

The system 1-Hexene/PFMCH/n-Hexane at 9°C as stated earlier represents a borderline case between closed and open systems

as 9°C is the critical solution temperature for the binary PFMCH/n-Hexane. In this case, the NRTL parameters were calculated by arbitrarily specifying mutual solubility compositions of the critical solution mole fraction ± 0.02 . The parameters for the other partially miscible binary, 1-Hexene/PFMCH, were calculated from the mutual solubility at the system temperature in the normal way for a range of values of the non-randomness parameter α_{12} . The RMSD values for the predicted compositions using values of α from 0.375 to 0.425 are given in Table 7. The rules of Renon and Prausnitz suggest a value of α of 0.4 for both binaries and it can be seen that good agreement is obtained using these values of α . However, a better fit can be achieved by treating α as an adjustable parameter. The best fit values of the parameters were used to generate the predicted results presented in Table 2. The accuracy of the predictions can be seen by referring to Figure 4.

The system n Heptane/PFMCH/1-Hexene at 20°C represents a closed (Type I) system and the prediction of ternary data from binary data alone becomes more difficult as less information is available on the non-ideal but miscible binary, PFMCH/1-Hexene.

To predict the ternary tie line data using only binary data, isothermal binary vapour/liquid equilibrium data at 55°C was used to obtain parameters for the non ideal miscible binary, PFMCH/1-Hexene. Using parameters obtained from the mutual solubility at the system temperature for the partially miscible binary n - Heptane/PFMCH, the ternary tie line data were predicted for values

of α_{12} varying from 0.2 to 0.47. The best fit was obtained with a value of $\alpha_{12} = 0.25$ and the resulting RMSD was 0.025.

This represented a much poorer fit to the experimental data than that obtained for the open systems.

The predicted results presented in Table 4 were generated using parameters obtained by fitting the NRTL equation to the experimental ternary data. As discussed earlier, if sufficient tie line data is available all nine binary parameters may be treated as adjustable parameters in a fitting routine. Soares (19) has previously studied the relative merits of treating from one to nine of the parameters as adjustable parameters and this study concluded that, for this system, the best agreement was achieved when α_{13} was fixed and the remaining eight parameters were fitted to the experimental data. The accuracy of the predicted data can be seen by referring to Figure 5.

QUARTERNARY DATA

Phase equilibrium data were determined by Soares (19) for the system

n-Heptane (1)/PFMCH (2)/ 1-Hexene (3)/ n-Hexane (4) at 6°C

A comparison was made between this experimental data and predicted values generated using parameters obtained from the mutual solubilities of the partially miscible binaries at the system temperature but treating the miscible binaries as ideal.

For a range of values of α_{ij} for the partially miscible

binaries, the overall RMSD obtained are presented in Table 8.

From the values of the overall RMSD obtained it appears that a reasonable accuracy of prediction is possible from binary data alone. Work is continuing to study the accuracy of prediction possible when using parameters obtained from the constituent ternary systems. Further work will also consider the prediction of closed (Type I) systems for multicomponent mixtures.

CONCLUSIONS

A miniature equilibrium still has been developed and it is suitable for both liquid/liquid and vapour/liquid phase equilibrium studies.

It has been shown that, for open (Type II) systems, it is possible to predict multicomponent tie line data from binary data alone, using the NRTL equation.

The prediction of data for closed (Type I) systems is less reliable but reasonable accuracy can be achieved when using binary parameters evaluated from vapour/liquid equilibrium results for the non-ideal miscible binary pair. If some ternary tie - line data is used to obtain binary parameters for the closed system, accuracy of prediction comparable with that for the open systems can be achieved.

NOMENCLATURE

A_1	Generalised binary NRTL parameter
a_{ij}	Activity of component i in liquid phase j
F_i	A defined function
G_{ij}	A defined function of the NRTL parameters
g_{ij}	Energy term in the NRTL equation
L	Total number of adjustable parameters
M	Number of experimental points
N	Number of components
R	Universal gas constant
T	System temperature
x_{ij}	Mole fraction of component i in liquid phase j (j may be omitted when dealing with a single liquid phase)
α_{ij}	Non-randomness parameter used in NRTL equation
$\hat{\tau}_{ij}$	Adjustable parameter in NRTL equation
γ_{ij}	Liquid phase activity coefficient of component i in liquid phase j (j may be omitted for a single liquid phase)

Abbreviations

PFMCH	Perfluoromethylcyclohexane
RMSD	Root mean square deviation

Subscripts

i	Property of component i
c	calculated value
e	experimental value
k	property at data point k

REFERENCES

1. Wohl, K. , Trans.Am.Inst. Chem. Engrs. 1946, 42, 215
2. Hildebrand, J.H. , "Solubility of Non-Electrolytes" 1936, 2nd Ed. Reinhold, New York.
3. Carlson, H. C. and Colburn, A. P. , Ind. Engng. Chem. 1942, 34, 581.
4. Treybal, R. E. , Ind. Engng. Chem. , 1944, 36, 875.
5. Kenny, J. W. , Chem. Engng. Sci. , 1957, 6, 116.
6. Ellis, S.R.M. , and Garbett, R.D. , Ind. Engng. Chem. , 1960, 52, 385.
7. Treybal, R. E. , "Liquid Extraction" 1963, McGraw-Hill, New York.
8. Brian, P. L. T. , Ind. Engng. Chem. Fund. , 1965, 4, 100.
9. Hala, E. , et al. "Vapour-Liquid Equilibrium" 1967, Pergamon Press, London.
10. Renon, H. and Prausnitz, J. M. , Am. Inst. Chem. Engrs. J. , 1968, 14, 135.
11. Renon, H and Prausnitz, J. M. , Ind. Engng. Chem. Proc. Des. and Develop. , 1968, 7, 221.
12. Renon, H. and Prausnitz, J. M. , Ind. Engng. Chem. Proc. Des. and Develop. , 1969, 8, 413.
13. Joy, D. S. and Kyle, B. G. , Am. Inst. Chem. Engrs. J. , 1969, 15, 298.
14. Soares, L. de J. S. et al. Proceedings of International Solvent Extraction Conf. 1971, Vol. 1, page 9, Soc. Chem. Ind. London.

15. Andiappan, A. and McLean, A. T., *Can. J. Chem. Engng.*, 1972, 50, 384.
16. Guffey, C. G. and Wehe, A. H. *Am. Inst. Chem. Engrs. J.*, 1972, 18, (5), 913.
17. Mandhane, J. M. and Heidemann, R. A., *Can. J. Chem. Engng.*, 1973, 51, 381.
18. Marina, J. M. and Tassios, D. P., *Ind. and Eng. Chem. Process Des. and Develop.*, 1973, 12 (3).
19. Soares, L. de J. S., Ph.D. Thesis, 1972, University of Birmingham.
20. Packer, L. G., et al. *Chem. Engng. Sci.*, 1973, 28, 597.
21. Othmer, D. F., and Tobias, P. E. *Ind. Engng. Chem.*, 1942, 34, 690.
22. Hand, D. B., *J. Phys. Chem.*, 1930, 34, 1961.

ACKNOWLEDGEMENTS

L. de J. S. Soares would like to thank the Gulbenkian Foundation for the financial support they provided.

The Authors thank Imperial Smelting Corporation Limited for providing the chemicals for this project.

TABLE I

Ternary Liquid Equilibria for the System

1-Hexene (1) / Perfluoromethylcyclohexane (2) / N- Hexane (3) at 6°C

Experimental Results				Predicted Results			
Hydrocarbon Phase		Solvent Phase		Hydrocarbon Phase		Solvent Phase	
X11	X31	X12	X32	X11	X31	X12	X32
0.8600	0.0001	0.3600	0.0000	0.8599	0.0001	0.3600	0.0000
0.8060	0.0420	0.3440	0.0200	0.8089	0.0480	0.3433	0.0210
0.7500	0.1000	0.3260	0.0420	0.7535	0.1000	0.3246	0.0444
0.6530	0.1900	0.2900	0.0740	0.6574	0.1900	0.2908	0.0365
0.5400	0.2940	0.2480	0.1360	0.5459	0.2940	0.2491	0.1379
0.4980	0.3320	0.2310	0.1560	0.5050	0.3320	0.2332	0.1575
0.4550	0.3720	0.2130	0.1780	0.4619	0.3720	0.2160	0.1786
0.4000	0.4225	0.1890	0.2060	0.4073	0.4225	0.1936	0.2060
0.3320	0.4860	0.1590	0.2420	0.3384	0.4860	0.1642	0.2417
0.2000	0.6080	0.0970	0.3170	0.2054	0.6080	0.1039	0.3148
0.1800	0.6260	0.0900	0.3260	0.1856	0.6260	0.0945	0.3261
0.0700	0.7280	0.0370	0.3920	0.0733	0.7280	0.0388	0.3934
NRTL Parameters:				RMSD Values:			
$\tau_{21} = 1.8318$	$\tau_{12} = 2.2833$	$\alpha_{12} = 0.425$		0.0051	-	0.0033	0.0014
$\tau_{32} = 2.1126$	$\tau_{23} = 1.6982$	$\alpha_{23} = 0.425$					

TABLE 2

Ternary Liquid Equilibria for the System
 1- Hexene (1) / Perfluoromethylcyclohexane (2) / N- Hexane (3) at 9°C

Experimental Results				Predicted Results			
Hydrocarbon Phase		Solvent Phase		Hydrocarbon Phase		Solvent Phase	
X11	X31	X12	X32	X11	X31	X12	X32
0.7720	0.0450	0.4026	0.0255	0.7708	0.0450	0.4026	0.0253
0.6123	0.1841	0.3480	0.1000	0.6111	0.1841	0.3409	0.1097
0.4660	0.3100	0.2790	0.1920	0.4637	0.3100	0.2771	0.1961
0.3790	0.3820	0.2360	0.2500	0.3776	0.3820	0.2363	0.2516
0.3650	0.3940	0.2300	0.2580	0.3631	0.3940	0.2291	0.2614
0.3150	0.4350	0.2040	0.2940	0.3130	0.4350	0.2036	0.2963
0.2990	0.4470	0.1870	0.3040	0.2982	0.4470	0.1958	0.3071
0.2550	0.4810	0.1730	0.3380	0.2556	0.4810	0.1727	0.3389
0.1990	0.5256	0.1400	0.3850	0.1983	0.5256	0.1399	0.3848
0.1520	0.5600	0.1118	0.4250	0.1522	0.5600	0.1118	0.4250
0.0483	0.6270	0.0404	0.5340	0.0484	0.6270	0.0404	0.5338
0.0190	0.6380	0.0160	0.5800	0.0194	0.6380	0.0173	0.5752

NRTL Parameters:

$\tau_{21} = 1.6998$

$\tau_{12} = 2.1703$

$\tau_{32} = 1.8816$

$\tau_{23} = 1.2458$

RMSD Values:

$\alpha_{12} = 0.4250$

0.0014

-

0.0035

0.0039

$\alpha_{23} = 0.4000$

TABLE 3

Ternary Liquid Equilibria for the System

N- Heptane (1) / Perfluoromethycyclohexane (2) / 1 - Hexene (3) at 6°C

Experimental Results				Predicted Results			
Hydrocarbon Phase		Solvent Phase		Hydrocarbon Phase		Solvent Phase	
X11	X31	X12	X32	X11	X31	X12	X32
0.9000	0.0002	0.1960	0.0000	0.8998	0.0002	0.1960	0.0000
0.8520	0.0485	0.1900	0.0100	0.8501	0.0485	0.1889	0.0115
0.7780	0.1215	0.1800	0.0280	0.7748	0.1215	0.1779	0.0297
0.6580	0.2400	0.1615	0.0620	0.6524	0.2400	0.1587	0.0622
0.4635	0.4265	0.1244	0.1300	0.4586	0.4265	0.1242	0.1227
0.3380	0.4980	0.1065	0.1620	0.3839	0.4980	0.1090	0.1502
0.2550	0.6220	0.0750	0.2200	0.2536	0.6220	0.0793	0.2059
0.1080	0.7590	0.0335	0.2945	0.1083	0.7590	0.0385	0.2847
0.0002	0.8600	0.0000	0.3580	0.0000	0.8600	0.0000	0.3596

NRTL Parameters Used:

$$\tau_{21} = 1.8529 \quad \tau_{12} = 2.3020 \quad \alpha_{12} = 0.4000$$

$$\tau_{32} = 2.2833 \quad \tau_{23} = 1.8318 \quad \alpha_{23} = 0.4250$$

RMSD Values:

$$0.0035 \quad - \quad 0.0030 \quad 0.0084$$

TABLE 4

Ternary Liquid Equilibria for the System

N- Heptane (1) / Perfluoromethylcyclohexane (2) / 1 - Hexene (3) at 20°C

Experimental Results				Predicted Results			
Hydrocarbon Phase		Solvent Phase		Hydrocarbon Phase		Solvent Phase	
X11	X31	X12	X32	X11	X31	X12	X32
0.7780	0.0420	0.3209	0.0197	0.3277	0.0187	0.7790	0.0439
0.6719	0.1319	0.3095	0.0649	0.3097	0.0649	0.6673	0.1340
0.5902	0.1965	0.3000	0.1081	0.3037	0.1081	0.5837	0.1969
0.5113	0.2508	0.2960	0.1529	0.3023	0.1529	0.5125	0.2455
0.4522	0.2799	0.3020	0.1936	0.3031	0.1936	0.4571	0.2781
0.4000	0.2830	0.3160	0.2300	0.3058	0.2300	0.4127	0.2985

NRTL Parameters Used:

$$\begin{aligned} \tau_{21} &= 1.9355 & \tau_{12} &= 2.2137 & \alpha_{12} &= 0.4255 \\ \tau_{31} &= 0.1366 & \tau_{13} &= 0.5283 & \alpha_{13} &= 0.3000 \\ \tau_{32} &= 1.8785 & \tau_{23} &= 1.3036 & \alpha_{23} &= 0.4510 \end{aligned}$$

RMSD Values:

$$0.0070 \quad - \quad 0.0071 \quad 0.0075$$

TABLE 5

RMSD (* 10²) values between experimental and calculated liquid compositions
using different values of the non-randomness parameter (α)

System - 1-Hexene (1)/ Perfluoromethylcyclohexane (2) / N-Hexane (3) at 6°C

α_{23} \ α_{12}	0.375	0.40	0.425
0.375	0.38	0.32	0.54
0.400	0.56	0.37	0.41
0.425	1.32	0.92	0.35

NRTL Parameters used

<u>Binary</u>	τ_{ji}	τ_{ij}	α_{ij}
1-2	1.2063	2.1210	0.375
	1.4076	2.1661	0.400
	1.8318	2.2833	0.425
2-3	1.9617	1.1355	0.375
	2.0043	1.3210	0.400
	2.1126	1.6982	0.425

Binary 1-3 Treated as Ideal

TABLE 6

RMSD ($\times 10^2$) Values between calculated and experimental liquid compositions
for different values of the non-randomness parameter (α)

System - N-Heptane (1) / Perfluoromethylcyclohexane (2) / 1-Hexene (3) at 6°C

$\alpha_{23} \backslash \alpha_{12}$	0.375	0.40	0.425
0.375	0.65	0.96	1.89
0.400	0.38	0.71	1.90
0.425	0.98	0.53	1.61

NRTL Parameters used

Binary	τ_{ji}	τ_{ij}	α_{ij}
1-2	1.6502	2.1999	0.375
	1.8529	2.3020	0.400
	2.2698	2.5123	0.425
2-3	2.1210	1.2063	0.375
	2.1661	1.4076	0.400
	2.2833	1.8318	0.425

Binary 1-3 Treated as Ideal

TABLE 7

RMSD ($\times 10^2$) values between calculated and experimental liquid compositions
for different values of the non-randomness parameter (α)

System - 1-Hexene (1) / Perfluorocyclomethylhexane (2) / N - Hexane (3) at 9°C

$\alpha_{23} \backslash \alpha_{12}$	0.375	0.40	0.425
0.375	0.88	0.42	0.42
0.400	1.76	0.85	0.30
0.425	3.46	2.44	0.71

NRTL Parameters Used

<u>Binary</u>	τ_{ji}	τ_{ij}	α_{ij}
1-2	1.1258	2.0318	0.375
	1.3165	2.0699	0.400
	1.6998	2.1703	0.425
2-3	1.8354	1.0799	0.375
	1.8816	1.2458	0.400
	1.9816	1.5904	0.425

Binary 1-3 Treated as Ideal

TABLE 8

Prediction of Quarternary Tie Line Data

α_{12}	α_{23}	α_{24}	RMSD x 10 ²
0.400	0.425	0.425	0.77
0.375	0.400	0.400	0.87
0.400	0.400	0.425	0.74
0.400	0.400	0.400	1.31

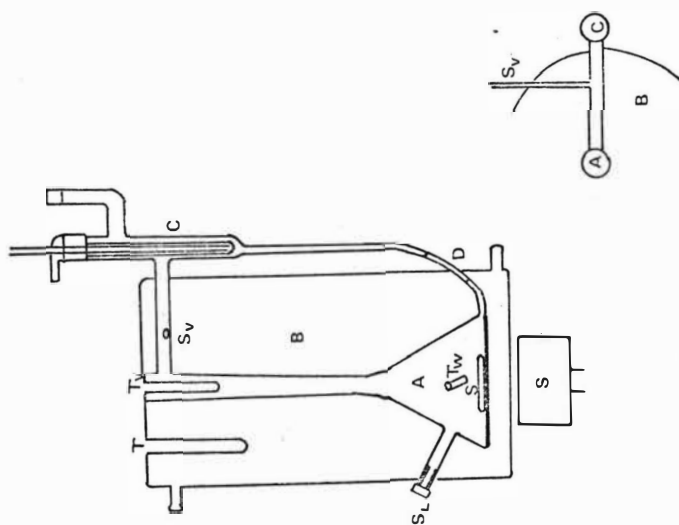


FIG 1 Miniature Equilibrium Still

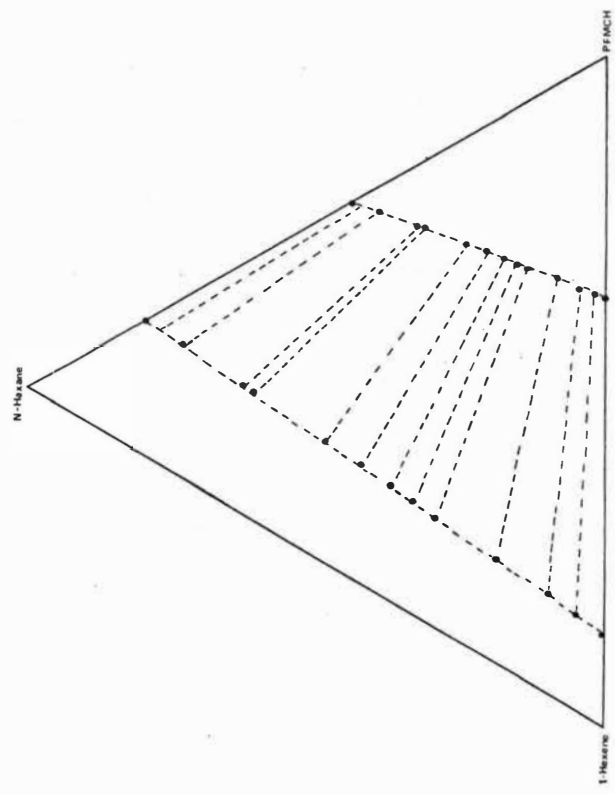


FIG 2 Experimental and Predicted Tie-Lines for the System 1-Hexene / PFMCH / N-Hexane at 8°C

● Experimental Points
 - - - - Predicted Data

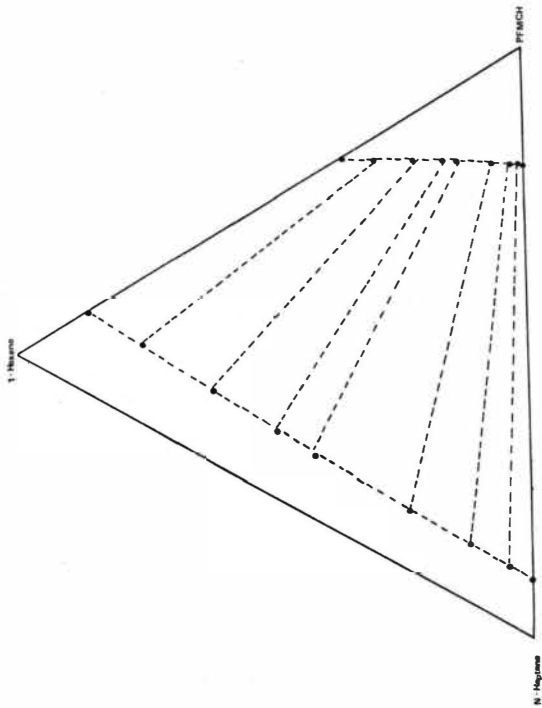


FIG 3 Experimental and Predicted Tie-Lines for the System
 N-Hexane / PMCH / 1-Hexane at 0°C
 ● Experimental Points --- Predicted Data

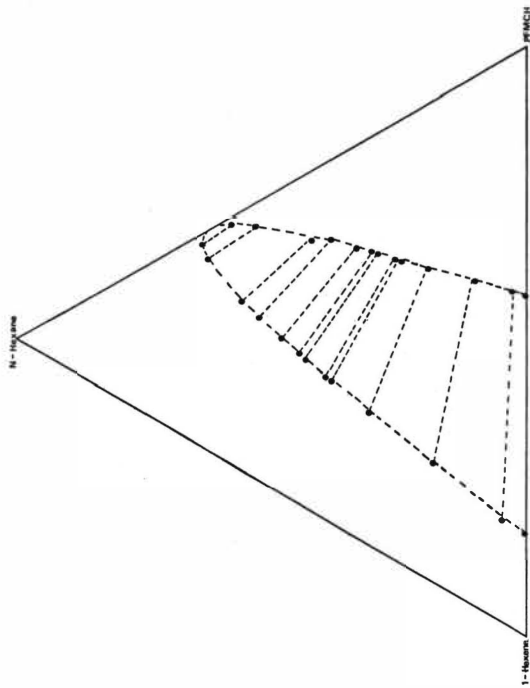


FIG 4 Experimental and Predicted Tie-Lines for the System
 1-Hexane / PMCH / N-Hexane at 0°C
 ● Experimental Points --- Predicted Data

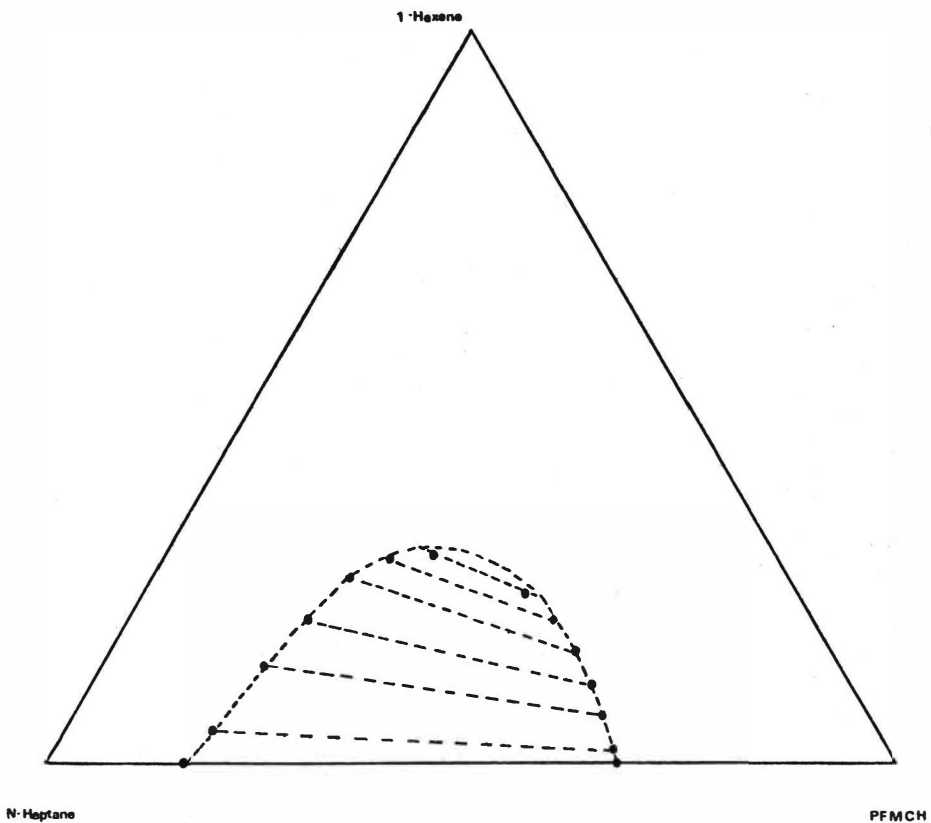


FIG 5 Experimental and Predicted Tie Lines for the System

N-Heptane, PFMCH / 1-Hexene at 20°C

● Experimental Points - - - - Predicted Data

Z. B. Maksimović and Lj. Miočinović

Chemical Dynamics Laboratory, Boris Kidrič Institute, Vinča,
POB 522 Beograd, Yugoslavia

Abstract

Solvent extraction of PETN and RDX from nitric acid solution with 1-nitro and 2-nitropropane has been investigated. Investigations were performed with respect to nitric acid, PETN, RDX and nitroparaffin concentrations at different temperatures. The results obtained show that PETN and RDX can be quantitatively extracted from nitric acid solution by using extracting agents.

Introduction

There are only a few published data⁽¹⁻⁴⁾ dealing with the removal of PETN and RDX from waste nitric acid with the aim of re-using them for industrial purposes. The investigations performed were based on decomposition of explosives in HNO_3 for several hours in autoclaves, at temperatures up to 200°C. However, no data are available on the use of a solvent extraction method for separation of explosives from waste nitric acid solutions. In our work we have used 1-nitro and 2-nitropropane as efficient extracting agents for the separation of PETN and RDX from waste nitric acid solutions. Investigations were performed with respect to the reacting components and temperature.

Experimental

Materials - The chemicals used were HNO_3 p.a. Merck, 1-nitro and 2-nitropropane, puris, Fluka, double distilled under low pressure and only the middle fraction used. Pentaerythritaltetranitrate (PETN) and cyclotrimethylenetrinitrate amine, (RDX), puris, were recrystallized several times from acetone solutions and dried at 60°C to constant weight. Pure crystals were kept in a dry box to prevent moisture access. All other chemicals were p.a., produced by Kemika and BDH.

Instruments - As well as a micro analytical balance, the instrument used for determination of PETN and RDX was a high resolution NMR spectrometer, Varian DA-60-IL. Measurements of proton signals were made with respect to TMS solvent, with the accuracy of ± 0.5 Hz. Frequency was controlled with a Varian V-3413 frequency meter. Sample temperatures were maintained within $\pm 1^\circ\text{C}$, using the Varian temperature controller, model V-4341/V-6040. The temperatures were controlled using methanol and ethylene glycol standards. Both PETN and RDX each gave one sharp line signal of CH_2 groups from acetone, 91.7 Hz and 374.9 Hz, respectively, to TMS. For determination of heat of PETN solubility in 2-nitropropane, an Isothermal twin-microcalorimeter from the Institute of Nuclear Research, Prague was used. For equilibration of the phases we used a Griffin and George vibrator while the solubility of PETN and RDX in nitroparaffins at different temperatures was determined with the accuracy of ± 0.05 , using an ultrathermostat type Colora.

Procedure - For determination of PETN, RDX and HNO_3 concentrations in the organic and aqueous phases we applied the analytical method described earlier⁽⁵⁾. The equilibration of equal volume of the two phases of different PETN, RDX, HNO_3 and nitroparaffin concentrations are carried and in glass stoppered test tube in a thermostated electric shaker at the desired temperature for 10 min. This time was sufficient to reach equilibrium at given temperatures. Necessary time for settling was 5 min. In order to determine RDX and PETN concentrations

in the organic phase the explosives were separated from nitric acid by one step stripping with water, and $10^{-4}M$ of HNO_3 remained in the organic phase. Nitroparaffins were distilled in an appropriate apparatus under a vacuum at up to 15 mm Hg at $50^\circ C$, and the dry residual, white crystals of the explosive, were quantitatively transferred by means of acetone into suitable crucibles, evaporated at $60^\circ C$ to constant weight.

In the other case, standard solutions of PETN and RDX from acetone solutions were measured at a known temperature on an NMR spectrometer. Measurements were based on the fact that both explosives have symmetrical molecular structure, giving only one sharp signal line in the spectrum, originating from the CH_2 group; in this way analytical determination is made easier. After extraction and distillation, the explosive samples were measured under the same conditions as the standard samples by the usual techniques. The accuracy of NMR measurements was $\pm 2\%$ with respect to PETN and RDX weights in the standard solutions.

Results and Discussion

In the first series of experiments PETN and RDX solubilities in nitroparaffin were determined in the temperature range from 20 to $50^\circ C$. In Fig. 1 it can be seen that this solubility linearly increases with increasing temperature, which means that the process is endothermal. The values obtained for PETN vary from 0.15-0.46M and those for RDX from 0.05-0.15M nitroparaffin. This proves the solubility of explosives to be equal in both solvents, with an accuracy of $\pm 3\%$. It can also be seen in the figure that in the given solvents the solubility of PETN can be 3-4 times higher than that of RDX depending on temperature.

Microcalorimetric measurements have shown that the mean value of the heat of solubility for the concentration $9.3 \times 10^{-4}M$ of PETN at $t = 25.000 \pm 0.003^\circ C$ is $H = 5.840 \text{ kcal.mole}^{-1}$. A positive value for heat of solubility also proves the reaction to be endothermal.

In the second series of experiments the extraction of nitric acid and solubility of 2-nitropropane were studied relative to the initial acid concentration over the temperature range $20-60^\circ C$. The results obtained are presented in Figs. 2(a,b) and 3(a,b). In Fig. 2a it can be seen that $\log D_{HNO_3}$ exponentially increases with increasing initial acid concentration in the range of 6-14M. With increasing temperature, in the range from $20-60^\circ C$ (Fig. 2b) the solubility of HNO_3 in 2-nitropropane increases linearly. The solubility of HNO_3 at $60^\circ C$ using an initial concentration of 11.2M is 4M. At the HNO_3 concentration of 14.4M and $20^\circ C$, equal volumes of the phases are completely miscible. The results have shown the extraction properties of 1-nitro and 2-nitropropane to be the same, so only 2-nitropropane was used for further investigations. Dependence of the solubility of 2-nitropropane on the initial concentration of 6-11.2M HNO_3 in the temperature range 20 to $60^\circ C$, is shown in Fig. 3(a,b). As can be seen in the figures, the solubility increases exponentially with increasing HNO_3 concentration (Fig. 3a) and linearly with increasing temperature (Fig. 3b). At equal initial volumes, at $20^\circ C$ and 14M HNO_3 , maximum solubility of 2-nitropropane in the aqueous phase is 1.6M.

In the third series of experiments, the extraction of PETN and RDX was examined relative to the initial concentration of nitric acid and 2-nitropropane at $20^\circ C$. Fig. 4 shows $\log D$ PETN and RDX dependent on the initial concentration of HNO_3 in the range 7-12M. The concentration of explosives in the corresponding solutions was 0.02M. The results presented in Fig. 4 show the distribution coefficients of PETN and RDX to be decreasing linearly with increasing initial concentrations of HNO_3 . They also show 2-nitropropane extracts PETN better than RDX under similar conditions.

Fig. 5 shows log distribution coefficients of HNO_3 , PETN and RDX relative to the initial concentration of 2-nitropropane diluted in n-hexane in the range 1-5M. Initial concentrations of the explosive and nitric acid were 0.02M and 11.77M, respectively. Investigations have shown the solubility of PETN and RDX in n-hexane at 20°C are less than 10 mg/l so that the diluent had no effect on the extraction of explosive with 2-nitropropane. The results obtained indicate that distribution coefficients $\log D$ PETN, RDX and HNO_3 linearly increase with increasing 2-nitropropane concentration in n-hexane. It can be seen in Fig. 5 that the distribution coefficients are higher by a factor of up to 10^2 in the case of PETN than in the case of RDX. The slopes of the straight lines show the competition between the explosive and nitric acid, which depends on their initial concentrations in the aqueous phase.

Fig. 6 shows the results of PETN and RDX extraction dependence on their initial concentration in the range of 10^{-3} to $4 \times 10^{-4}\text{M}$ at the constant concentration of 11M HNO_3 and 5M 2-nitropropane at 20°C . The solubility of PETN and RDX in 11M HNO_3 varied up to 0.02M. Above this concentration a suspension is formed in the aqueous phase which disappears after equilibration. Our measurements of nitric acid concentration in the organic phase show that irrespective of solubility, the increase of PETN and RDX concentration in the aqueous phase also increases the amount of these explosives in the organic phase, whereas the concentration of HNO_3 simultaneously decreases. It is also evident in Fig. 6 that $\log C_{\text{Org}}$ versus $\log C_{\text{Tot}}$ for the explosives gives a straight line which means that the concentration of the explosives increases on account of decreasing HNO_3 in the organic phase.

On the basis of the results shown it can be concluded that quantitative separation of PETN and RDX from nitric acid solution can be performed by extraction with nitroparaffins. The extraction of PETN is considerably greater than that of RDX due to the greater solubility of PETN in nitroparaffins. In practice both solvents are strong extractants of the explosives, but 2-nitropropane is better, having a lower B.P. (12°C less than 1-nitropropane). Also the loss of 2-nitropropane to the aqueous phase at a concentration of 8M HNO_3 and 20°C is 2%, i.e. negligibly small with respect to the amount of extracted explosive and HNO_3 . One step stripping with water practically eliminates HNO_3 from the organic phase which then contains pure explosive.

Conclusions

1. A new method for quantitative extraction of explosives from waste nitric acid by using nitroparaffins as extractants has been presented.
2. Extraction of PETN is double that of RDX which is in agreement with their solubility in nitroparaffins.
3. Nitric acid extraction is considerable, but this acid can be separated from the explosive by one step stripping with water.
4. From the results presented it is concluded that explosives can be equally successfully removed from nitric acid by solvent extraction, i.e. without using autoclaves at high temperatures.

Acknowledgements

The authors are indebted to Mr. S. Milonjić for microcalorimetric measurements. They also wish to express their gratitude to Mrs. D. Nemoda for skilled technical assistance.

References

1. Patentschrift, DBP 1030747 10 Dec., 1955.
2. Rodger I. and McIrvine J.D., *Cand. J. Chem. Eng.*, 1963, 41, 87.
3. Berlow E., Barth R. and Snow J., *The Pentaerythritols*, Reinhold Pub. Corp., 1958, London.
4. Anberteiu P. and Rehling R., *Mem. des Poudres.*, 1953, 35, 91.
5. Maksimovic Z. B., Miocinovic, Lj. and Nemoda D., to be published.

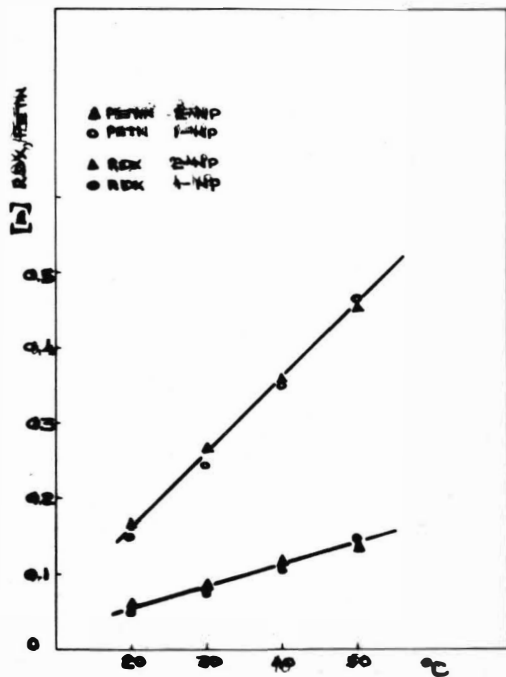


Fig. 1 Solubility of PETN and RDX in dependence of temperature and solvents.

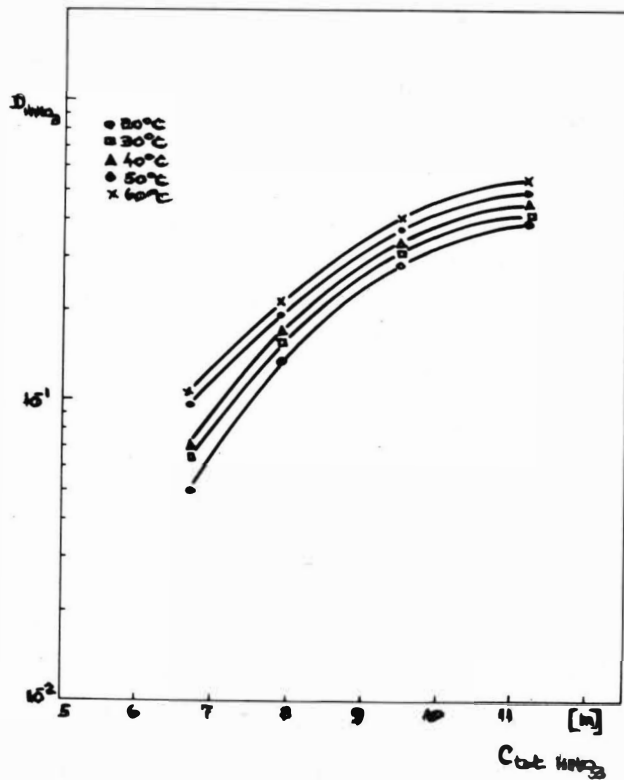


Fig. 2a Extraction of HNO_3 in dependence of their initial concentration with 2-nitropropane

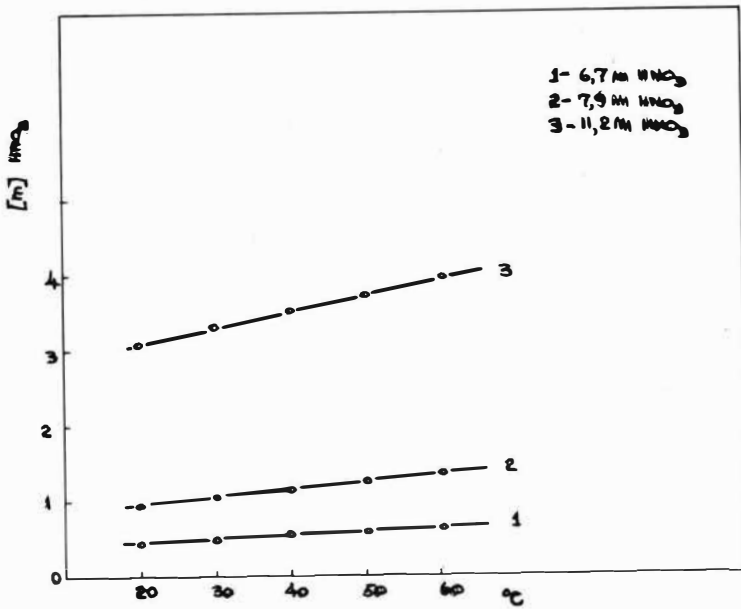


Fig. 2b Solubility of HNO₃ in organic phase 2-nitropropane in dependence of their initial concentration and temperatures.

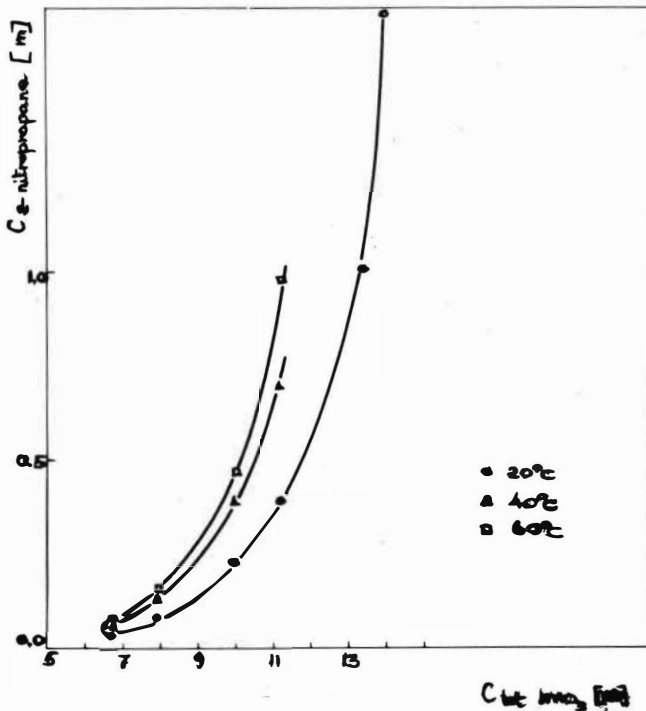


Fig. 3a Solubility of 2-nitropropane in aqueous phase HNO₃ in dependence of initial concentration of HNO₃.

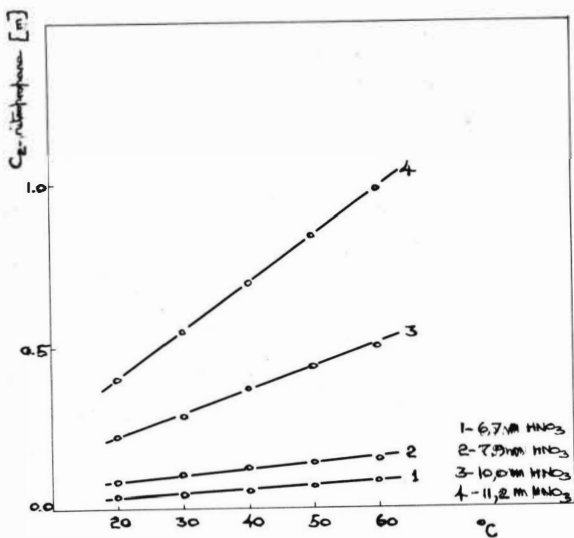


Fig. 3b Solubility of 2-nitropropane in aqueous phase HNO_3 in dependence of temperatures and HNO_3 concentration.

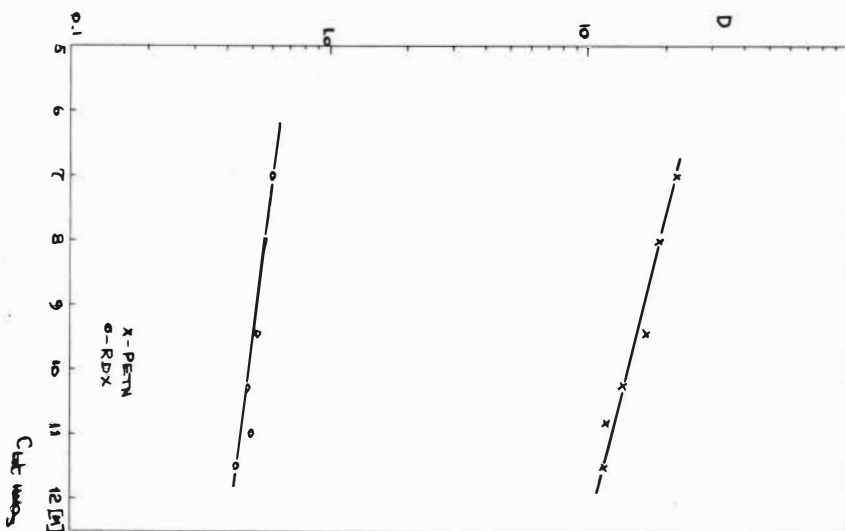


Fig. 4 Detection of PETN and RDX with 2-nitropropane in dependence of initial HNO_3 concentration.

Fig. 5 Extraction of PETN, RDX and HNO₃ in dependence of initial concentration of 2-nitropropane.

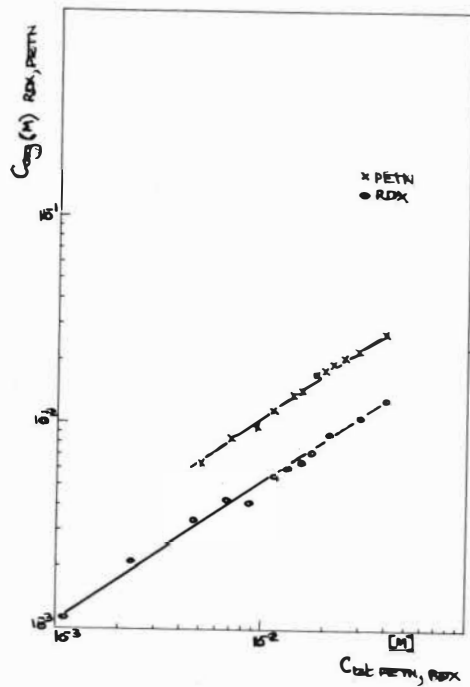
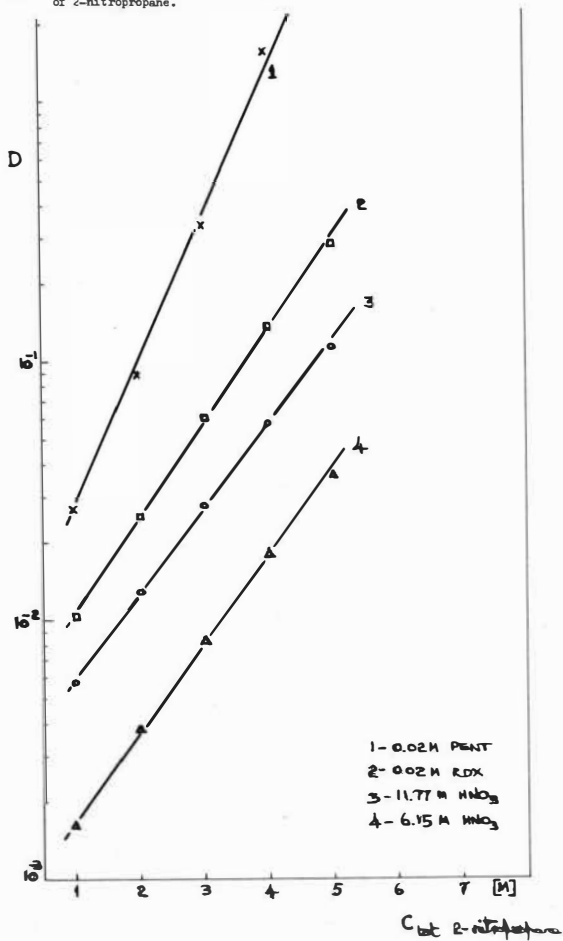


Fig. 6 PETN and RDX extraction by 5M 2-nitropropane distribution isotherms for 11M HNO₃.

PECULIARITIES OF SOLVENT EXTRACTION BY STRONGLY
ASSOCIATED REAGENTS

E V Komarov, V N Komarov

V G Chlopin Radium Institute, Leningrad; The A A Zdanov Leningrad State
University

Some specific difficulties arise in the interpretation of the results obtained when extractants that are capable of strong association in the nonpolar diluents that are used for the solvent extraction of metals and inorganic acids. It is shown in this work that the cause of such difficulties is the use of too simple models for characterising the organic phase which contains both the strongly associated extractant and some complexes of the extractant with the metal or acid as well. A variation of the molecular-static model of the solution is given which takes into account the main peculiarities of the extraction with strongly associated reagents.

I Introduction

When comparing the data on the state of the extractant in solution and the reaction stoichiometry for extractants capable of association with those of, for example phosphate esters, attention should be paid to the differences between these extractants.

Thus the following descriptions of the extraction with tertiary alkyl-ammonium salts may be found: the complete absence of association of the extractant¹; an average degree of association, \bar{f} , of the order of 2 - 6 (by cryoscopic studies of anhydrous solutions of trioctylamine, TOA,²; the existence of species with $\bar{f} = 40 - 60$, or data on the colloidal character of the organic phase^{3,4}.

The dependence of \bar{f} on the extractant concentration, S , calculated by the theory that the interaction of the various associated species with each other and with the medium are very weak (ideal associated solution, IAS) usually forms a curve with a maximum^{2,5}, which contradicts the thermodynamic properties of the model of the ideal associated solution.

For some systems the dependence of the distribution coefficient of the compound extracted on the concentration of the extractant, $\lg D = \psi(\lg S)$, is an extremely simple linear function in spite of the nonlinear dependence, $\bar{f} = \psi(\lg S)$.

As the difficulties shown are characteristic of systems with a pronounced association of components, the reason for such contradictions is naturally to be found in the fact that the model of the solution which is the basis of the interpretation of the experimental results does not correspond to the complex picture of interactions in the system. For the adequate description of the extraction systems with their pronounced heterodynamic interaction of particles, the model of the liquid to be used is that which takes into account the formation of associate or solvate species when the statistic sum of the binary mixture is obtained. Such a concept allows the use of experimental material obtained by the traditional way using the law of mass action, and IR-, UV-, and Raman-spectroscopy as well, to calculate the characteristics of the intermolecular interaction⁶.

II Experimental

Solutions of mono-n-octylphosphoric acid [MÓPA] in various solvents were investigated as the typical extraction system. The feed [MOPA] was obtained by reaction of n-octyl alcohol with phosphorus oxychloride followed by hydrolysis of the acid dichloride thus formed. Resultant purification of the reagent was carried out according to the published methods⁷.

1) Eu(III) extraction by the MOPA solutions

For the estimation of Eu distribution coefficients, $1\mu\text{C } ^{152,154}\text{Eu}$ (carrier free) was added to equal volumes of pre-equilibrated aqueous and organic phases. The solutions were shaken for 15 minutes at $20 \pm 1^\circ\text{C}$, and then the γ -activity of each phase was measured (in the gas counter with an aluminium filter 2mm thick). The results of the investigation of the extractant concentration dependence on the europium distribution coefficient are shown in Fig 1. For all the solvents investigated this dependence is linear with a slope of 1, and the absolute value of the distribution coefficients is quite similar for solvents with a wide variation in polarity. The reasons for such behaviour will be discussed below; here it should be noted that other associated extractants (dinonylnaphthalenesulphonic acid for example) behave quite similarly⁸. The data on the association of monoalkylphosphoric esters in organic solvents and the data on the role of water in the association process (which is of great importance) are quite fragmentary and contradictory; therefore isopiestic and cryoscopic studies of the system with MOPA were undertaken.

2) Isopiestic study of MOPA solutions in CCl_4 and CHCl_3

The activity of the solvent was measured by existing methods⁹. Tributylphosphate (TBP) was taken as the reference compound, and the data on CCl_4 and CHCl_3 activity in the reference systems are taken from published work¹⁰.

As a result of the measurements undertaken it is shown that the CCl_4 activity in CCl_4 - MOPA system at 25°C is described by the function:

$$\ln \gamma_{\text{CCl}_4} \approx 0.975 X_{\text{MOPA}} \quad (1)$$

for molar fractions $[\text{MOPA}]$ in the range 0.05 - 0.85.

A similar dependence is obtained for the system CHCl_3 - MOPA at 25°C in the molar fraction range 0.05 - 0.50.

$$\ln \gamma_{\text{CHCl}_3} \approx 0.860 X_{\text{MOPA}} \quad (2)$$

3) Cryoscopic study of MOPA solutions

Cryoscopic measurements were made by the Beckman method. Temperature measurements were reproducible to within the range 0.01 - 0.005°C.

In the experiments with MOPA solutions containing water the solution for cryoscopy was prepared from the feed 1M solution of MOPA in benzene, pre-equilibrated with 1M aqueous nitric acid, by dilution of the solution with the calculated quantity of benzene. The results are given in Table 1. Note each figure in the table is the result of three or four measurements.

S_{MOPA} mole/l	Δt °C	\bar{F} (IAS)
0.01	0.004	12
0.03	0.006	26
0.10	0.007	66
0.20	0.013	74
0.50	0.035	69
1.00	0.056	92

Table 1. Freezing point depression of the benzene solution of MOPA saturated with 1M aqueous nitric acid.

To investigate the influence of water on the MOPA association a measured quantity of water was added to 1M benzene solutions of MOPA until the solution separated into two phases (with the water content 12.8 mole/l). the data are given in Table 2.

S_{MOPA} mole/l	$S_{\text{H}_2\text{O}}$ mole/l	Δt °C	\bar{P} (IAS)
1.00	<0.01	1.037	5
1.00	0.1	0.869	6
1.00	0.3	0.671	8
0.98	0.85	0.431	14
0.97	1.90	0.243	23
0.93	4.10	0.110	42
0.91	5.91	0.084	53
0.86	9.25	0.060	69
0.81	12.8	0.055	75

Table 2. Dependence of the freezing point depression of MOPA solution on the concentration of added water.

The unexpected high solubility of water in benzene solutions of MOPA is to be noted (a similar phenomenon takes place in the other nonpolar solvents as well).

III Discussion

When the cryoscopic data are considered the great influence of water in the organic solution on the MOPA association becomes quite obvious. It follows that the data published on the average degree of association, $\bar{P} = 5 - 6$, which was found by cryoscopy of anhydrous solutions of monoalkyl-phosphates cannot be the basis of discussion of metal extraction mechanism as the actual extracting solutions are always saturated with water.

The second important point is the futility of using the ideal associated solution theory as the foundation for estimation of the average molecular weight from cryoscopic, isopiestic, and data from similar methods, for the description of the extraction systems. The actual extractant concentration often reaches 0.5 - 1M, and deviations from ideal behaviour are obviously significant. Non-ideality of the extracting solution is defined not only by

the formation of associative complexes but also to a great extent by the symmetry and size of the particles⁶. The latter is especially important for systems containing MOPA as its associates include scores of monomeric links the size of such aggregates is ten times larger than the size of the solvent particles. The increase of the difference in size between the particles results in a negative deviation from the ideal state and the solvent activity obtained experimentally is the result of two opposite processes. Thus, the degree of association that is estimated by the generally accepted methods is only the lower limit of the true value.

In order to take into account the influence of the size and shape of the particle and also the change of the properties of the medium during changes in the solution composition one should reject the simplified solution models in the description of extraction systems. One of the possible answers is to use the conclusions from the theory of associative equilibria⁶. Then the statistical sum of the binary system can be written as follows:

$$Q = g(N_A, N_B) \Psi_A^{N_A} \Psi_B^{N_B} \exp\left(-\frac{\sum_r N_r E_r}{kT}\right) \quad (3)$$

where:

- N_A is the number of molecules of the component A,
- N_r is the number of particles of the associated component (A),
- r is the measure of the associated component,
- E_r is the energy of r -measure formation,
- Ψ the statistical sum according to the inner states of the molecule.

The number of configurations in the mixture according to Guggenheim, g , is defined by the equation: (4)

$$\ln g = \sum_r N_r \ln \frac{\rho_r}{\sigma} - \ln \prod_r N_r! N_B! + \frac{z}{2} \ln \left(\sum_r q_r N_r + N_B \right)! - \frac{z-2}{2} \ln \left(R_A \sum_r r N_r + N_B \right)!$$

where:

- R_A is the number of junctions quazi-lattice in the solution that are occupied by the molecule of the associated component,
- ρ the number of ways of arranging a molecule according to R_A -junctions with one link being fixed,
- σ the symmetry factor of the molecule,
- q the average number of the neighbours of molecules for one coordinative place.

It follows from equations (3) and (4) that the chemical potential of the solvent μ_B is:

$$\mu_B = kT \left\{ \ln \frac{\rho_B}{\sigma_B} + \ln \frac{N_B}{N_B + \sum q_r N_r} + \left(\frac{z}{2} - 1 \right) \ln \frac{N_B + R_A \sum r N_r}{N_B + \sum q_r N_r} \right\} \quad (5)$$

where z is the average coordination number for the quazi-lattice of the solution.

It is possible to calculate the activity of the solvent or \bar{F} for any specific system if the form of the associated particles is given (linear, cyclic, branching chains, etc.) and the dependence of the value of the stepped constant K_r on the degree of association r is known.

Thus, if the associates have the form of unclosed chains and if $K_2 \approx K_3 \approx \dots \approx K_r$ then we have:

$$\left. \begin{aligned} \gamma_B &= \left(\frac{h_2}{X_A} \right)^{\frac{z}{2}} [1 + (R_A - 1)X_A]^{\frac{z}{2} - 1} \\ \frac{z - 2}{z} h_2 R_A + \frac{2}{z} h_1 + \frac{1 - X_A}{X_A} &= 1 \\ h_2 &= h_1 (1 + h_1 K_r) \end{aligned} \right\} \quad (6)$$

where X_A is the analytical concentration of the associated component, and h_1 and h_2 are the effective concentrations that are defined from conditions:

$$\left. \begin{aligned} h_1 &= \frac{\sum r N_r}{N_B + \sum q_r N_r} \\ h_2 &= \frac{\sum r N_r}{N_B + \sum q_r N_r} \end{aligned} \right\} \quad (7)$$

In Table 3 the results of calculation of the average degree of association r in the system $\text{CCl}_4 - \text{MOPA}$ at 25°C according to equation (6) and by the usual methods are compared. This comparison shows that the true value of \bar{F} for the given system is about an order of magnitude higher than it is in the literature^{7,11,12}.

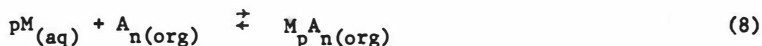
X_{MOPA} mole/l	$\ln \gamma_{\text{CCl}_4}$ exptl.	\bar{r} (IAS)	\bar{r} (6)	$\ln \gamma_{\text{CCl}_4}$ calc.
0.083	0.064	4.1	9.1	0.074
0.152	0.13	5.1	12.3	0.14
0.263	0.25	6.1	16.2	0.25
0.417	0.40	4.8	20.5	0.40
0.648	0.63	3.6	25.4	0.62
0.790	0.75	3.0	28.2	0.76

Table 3. Association of MOPA in CCl_4 by isopiestic measurements *

*Note: when the value of \bar{r} is estimated from equation (6) $z \rightarrow \infty$ and $R_A = 1$ are taken. With these parameters the experimental data are well described if $K_r = 1000$ is taken.

Cryoscopic studies of MOPA solutions in benzene were undertaken in the presence of water as the third component. It is difficult to calculate the size of the associate in the simple variant for the binary system that was considered above (equations 4, 5, 6 and 7). Therefore the interpretation of cryoscopic data (Table 1 and 2) is given with the ordinary formulae for the ideal associated solution, and the value of \bar{r} (IAS) defines only the lower limit of the degree of association. It is evident from Table 1 and 2 that the apparent degree of MOPA association is 10 - 15 times higher when the system is saturated with water and it increases with the increase in MOPA concentration. On the basis of results that were obtained for the anhydrous system MOPA - CCl_4 the conclusion can be drawn that the true values of \bar{r}_{MOPA} in benzene in the presence of water are $n \cdot \bar{r}$ (IAS), where the factor n varies from 1 - 3 depending on reagent concentration (in the investigated range of values).

The totality of reactions of the type:



is discussed to take into account the many types of interaction that occur.

If the composition of the reagent associate is designated as $A_{\bar{r}}$, and that of the complex extracted as $M_p A_{\bar{r}n}$, then the values of the coefficients \bar{n} and \bar{r} can differ as a result of the change in the bond strength A_1-A_1 in the associate under the influence of the penetrating particle M.

Beginning with the certain value of $n = m$, which is rather high, the constant of joining the link A_1 to complex MA_n will be equal to the constant of joining A_1 to A_n , and it can be written:

$$\left. \begin{aligned} \beta_n &= \frac{[MA_n]}{[A_1][MA_{n-1}]} \cdot \frac{\gamma_{mn}}{\gamma_1 \cdot \gamma_{m(n-1)}} \\ K_n &= \frac{[A_n]}{[A_1][A_{n-1}]} \cdot \frac{\gamma_n}{\gamma_1 \cdot \gamma_{(n-1)}} \end{aligned} \right\} \quad (9)$$

$$\lim_{n \rightarrow \infty} \beta_n = \lim_{n \rightarrow \infty} K_n = K_r$$

and the distribution coefficient of M in the system the equation can be written:

$$D = \beta_n \gamma_m \sum_{n=m}^{\infty} [A_n] W_r \frac{\gamma_n}{\gamma_{mn}} \quad (10)$$

where W_r is the statistical factor:

$$W_r = \frac{r/v!}{(r/v-p)! p!} \cdot \frac{1}{\sigma} \quad (11)$$

v is the number of monomeric links in the associate that form the single centre of reaction,

σ is the symmetry coefficient.

The case of the microconcentration of particles M being discussed and the assumption that the disturbance in the bond strength under the influence of the penetrating particle takes place in the three coordination spheres ($\beta_n/K_r = b$) that are nearest to M, then from the equation (10) can be obtained:

$$D = K_{mv} \left\{ [A_1]^v + \frac{1}{v(bK_r)^v} \sum_{j=1}^{3v} j (bK_r)^j [A_1]^j + \frac{b^{2v}}{vK_r^{2v}} \sum_{n=3v+1}^{\infty} n [A_1]^n K_r^n \right\} \quad (12)$$

where K_{mv} is the constant of the simplest complex MA_v formation.

The analysis of equation (12) indicates the possibility of some variation in the influence of M on the bond strength in the associate MA_n .

1) $b = 0$. Associate is destroyed with the formation of particles MA_v . On the concentration curve $D = \psi(S)$, where S is the total extractant concentration, a region exists where D does not depend on S.

2) $b = 1$. The bonds are not distorted. LgD has a linear dependence on LgS when $K_r \gg 1$.

3) $b > 1$. Bond strengthening. There is a region on the concentration curve where the slope is greater than v .

4) $0 < b < 1$. Bond weakening. Concentration curve has an intermediate character between the cases when $b = 0$ and $b = 1$.

Hence the important conclusions follow concerning the possible use of "the method of dilution" for the estimation of solvate numbers in associated systems:

a) Maintaining the slope of the concentration curve equal to v in some range of concentration cannot be evidence of the formation of a single compound MA_v . The slope equal to v can be conditioned by the same character of particles A_1 association in the complex MA_n and in the associate A_n .

b) The decrease of the slope of the concentration curve up to a value less than 1 cannot serve as evidence of polynuclear complex M_1A_j formation. One of the reasons of such formation can be the weakening of the bonds A_1-A_1 .

The detailed investigation of the case when $b = 1$, which takes place most frequently in practice, leads to the formation of the criterion:

$$[M]_{(org)} \ll \frac{S}{\bar{r}}, \quad (13)$$

maintenance of which allows the neglect of formation of the higher complexes M_2A_n , M_3A_n , and so on, when the totality of reactions (8) is discussed. Then it follows from equation (10), that the slope of the concentration curve must not depend on the nature of the particles M , on the law of the extractant association $K_r = \Psi(r)$, on the nature of the organic diluent, or on the nature of extractant. If the high degree of reagent association is retained the slope of the concentration curve approaches unity with the increase of concentration. The conclusion obtained becomes untrue when the concentration of the particles being distributed is commensurable with the value S/\bar{r} . The previously observed independence of distribution coefficient values of metal on the nature of the organic diluent is explained, according to the authors, by the extremely high degree of MOFA hydration as the metal particles pass from the entire aqueous phase into a disperse aqueous phase which consists of the hydrate shell of $OPO(OH)_2$ group of the extractant.

If the equation (13) is not followed in the course of the extraction of weight amounts M , then instead of equation (12) it follows:

$$D = \beta^2 K_r \frac{\gamma_m^2 [M] S^2}{v^2} \left\{ 1 - \beta \gamma_m [M] \left(1 - \frac{1}{v} \right) \right\} \quad (14)$$

i.e. a non-linear dependence of partition coefficient on the extractant concentration.

If the equation (13) is not followed as a result of the extractant behaving as a monomer in the solvent then the total concentration of component M in the organic phase is defined by the formula:

$$C_M = K_O [M^{z+}] S^v + K_1 [ML^{(z-1)+}] S^{v-1} + \dots, \quad (15)$$

where M can be extracted as complexes of the type MA_v , ML_{v-1} , ML_2A_{v-2} , and so on. It follows from equation (15) that the slope of the concentration curve increases with the increase of the reagent concentration up to a maximum value of v . Similarly the joint discussion of the equations:

$$S = \sum_{r=1}^{\infty} r [A_r] + \sum_{n=v}^{\infty} n [MA_n], \quad (16)$$

$$C_M = \sum_{n=v}^{\infty} [MA_n]$$

allows the determination of the principle condition for using the so-called "method of ultimate capacity" to define the stoichiometric coefficient $n/p = v$ in equation (8). Actually:

$$\frac{S}{C_M} = \frac{1 + \beta a_m}{\beta a_m} v \quad (17)$$

where a_m is the activity of the particles M in aqueous phase, and such condition will be:

$$\beta a_m \gg 1 \quad (18)$$

It emerges also from equation (17) that the estimation of the non-fractional values of v by "the method of ultimate capacity" is not indicative of the existence in solution of a single complex with the composition $M_p A_n$.

Thus, the proposed model of the extraction processes with the associated reagent leads to equations which combine the components' activity with the composition of the system. In most papers on extraction a comparatively narrow range of reagent concentration has been investigated, therefore it is rather difficult to determine the degree of agreement of the total character of the curve $\lg D = \Psi(\lg S)$ and that of the one discussed. Therefore the work of Awwal and Carswell¹³ on thorium extraction by alkylammonium sulphate solutions is of special interest. The authors obtained an S-shaped curve with a linear dependence $\lg D = \Psi(\lg S)$ with low extractant concentrations and a slope of 6; then with the increase of extractant concentration the slope decreases to zero, which, according to the authors, is indicative of formation of colloidal aggregates. With a further increase of concentration the slope increases again and reaches the value of approximately unity, and

the authors found it difficult to explain this phenomenon. As it is seen from Figure 2 such a dependence can be explained simply by a strong extractant association with the simultaneous weakening of the bonds in the associate under the influence of the particle being extracted.

IV Conclusions

On the basis of the investigation undertaken and on literature data the conclusion can be drawn that the use of the simplified model descriptions is the cause of most contradictions arising in the interpretation of experimental data on extraction by an associated reagent. Methods of evaluation of the average degree of reagent association or the characteristics of extraction equilibria that are based on assumptions of the ideal associated solution or of regular solution cannot reflect correctly the properties of systems with nondisperse interaction. It is difficult to foresee the consequences of many simplifications, therefore there always exists contradictions in the estimation of association obtained by different methods. Further progress on our theories concerning mechanism of extraction processes needs further accumulation of experimental data which must be obtained by different methods (cryoscopy, tensimetry, light dispersion, fluorescence depolarization, IR-, UV-, Raman spectroscopy, viscometry, extraction, etc.) under comparable conditions and with proper interpretation.

The methods of associative equilibria theory are, in the authors' opinion, most useful in the theoretical part of these studies.

Referencies

1. Boirie, Ch. Bull. Soc. Chim. France (1958), (7), 980
2. Fomin, V.V., Potapova, V.T. Zh. Neorg. Khim. (1963), 8(4), 990
3. Allen, K.A. J. Phys. Chem. (1956), 60, 239, 943; (1958), 62(9), 1119
4. Cattrall, R.W. J. Inorg. Nucl. Chem. (1967), 29(4), 1145
5. Vdovenko, V.M., Galkin, B.Ja., Chaikchorskii, A.A. Radiochimia (1961) 3(4), 448
6. Komarov, E.V. Radiochimia (1970), 12(2), 297, 312.
7. Peppard, D.F., Ferraro, J.R., Mason, G.W. J. Inorg. Nucl. Chem. (1958), 7, 231
8. Wang, S.M., Li, N.C. J. Inorg. Nucl. Chem. (1965), 27(9), 2093
9. Komarov, E.V. Radiochimia (1962), 4(6), 633
10. Shuvalov, O.N., Pushlenkov, M.P. Radiochimia (1963), 5, 536
11. Ferraro, J.R., Mason, G.W., Peppard, D.F. J. Inorg. Nucl. Chem. (1961), 22, 285
12. Ferraro, J.R., Peppard, D.F. J. Phys. Chem. (1961), 65(3), 539
13. Awwal, M.A., Carswell, D.J. J. Inorg. Nucl. Chem. (1968), 30(4), 1057

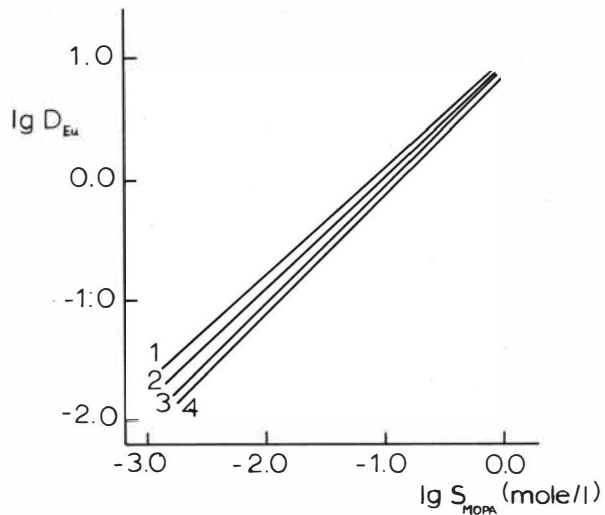


FIGURE 1. Eu(III) partition between MOPA solutions in benzene(1), chloroform(2), carbon tetrachloride(3), chlorobutylene(4), and 1M aqueous solution of nitric acid at 20°C.

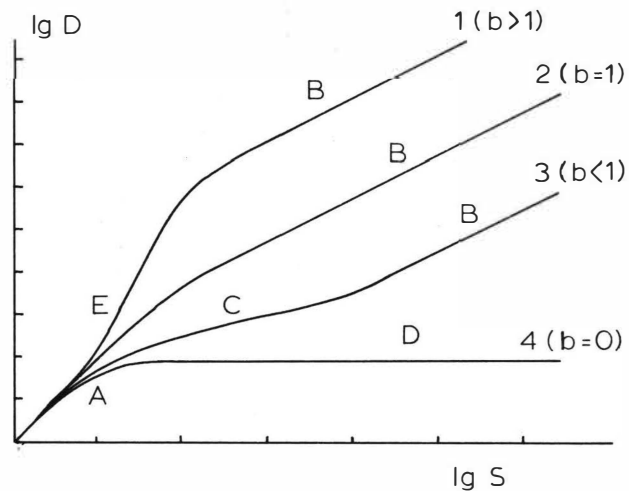
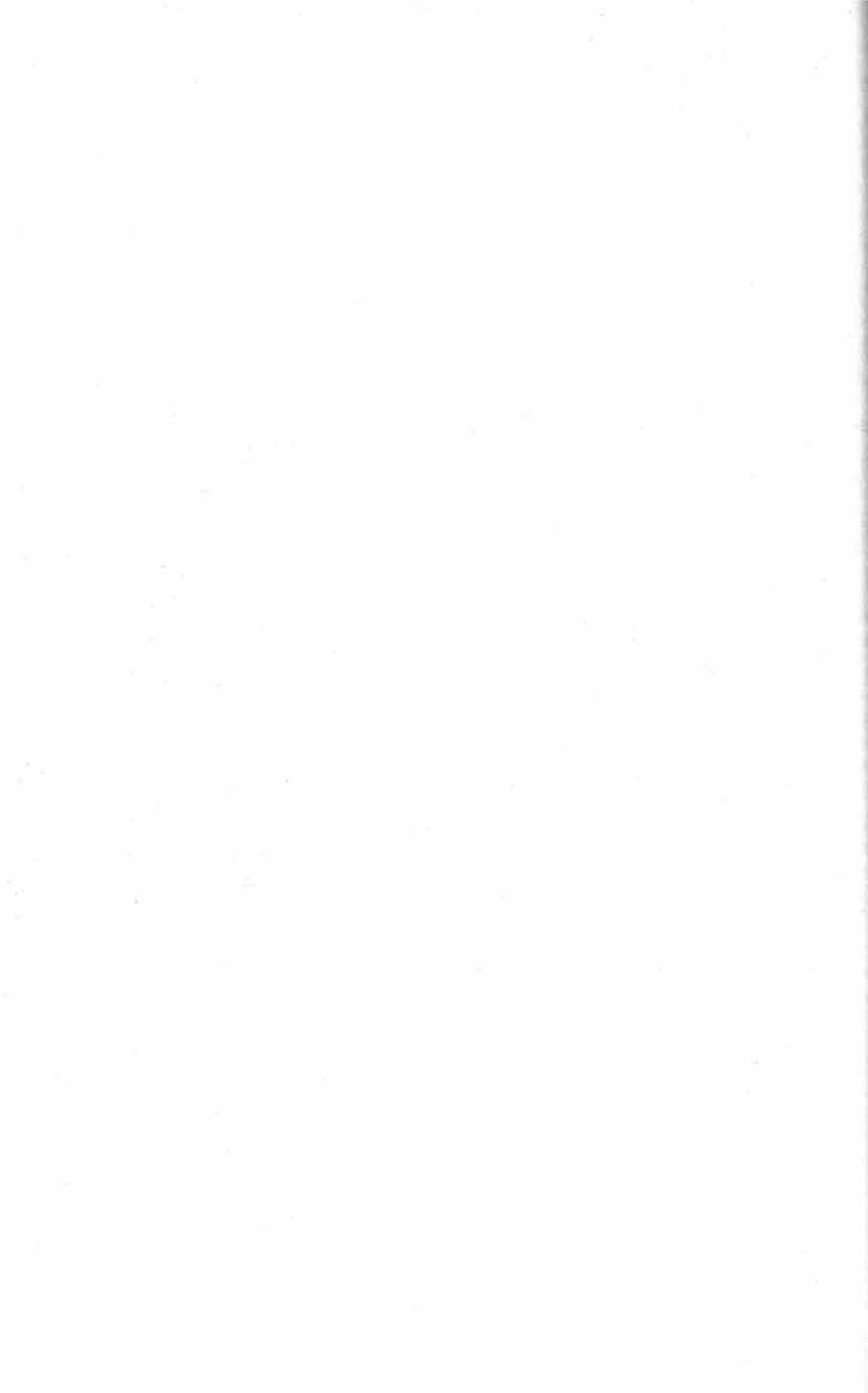


FIGURE 2. General variations of extractant concentration and partition coefficient with variation in parameter b . (Slope equals ν at A, 1 at B, $\langle \nu$ at C, 0 at D, and \gg at E).



PREDICTION AND ANALYSIS OF EXTRACTION SYSTEM PROPERTIES WITH
LINEAR FREE ENERGIES RELATIONSHIPS (LFER)

V S Shmidt, E A Mezhev, V N Shesterikov

In recent years the authors (1-12) and other Soviet researchers (13-18) have performed a series of studies, which show that characteristics of many extraction systems (defined by the extractant, the diluent and the basic anion acting as ligand in the system) may be described semiquantitatively or sometimes quantitatively, and predicted, on the basis of linear free energy relationships (LFER). This applies to a number of systems that differ in the nature of the element or compound being extracted.

The applicability of LFER requires that for each specific series of extraction systems in which only one of the variables changes (the extractant, the diluent, the ligand or the anion exchanging on extraction), relationships of the type

$$\lg K = \lg K_0 + aX \quad (1)$$

must be fulfilled, where K is the extraction constant in this system, K_0 is the extraction constant in the reference system, X is the quantity that characterizes quantitatively the effect of a varying parameter only and does not depend on the type of series, and a is the coefficient, constant for the given series of systems.

For series with different substituents, joined to the same basic functional group in the extractant molecule, the polar constants σ , σ^0 , σ^* (derived from theoretical organic chemistry (19) and expressing quantitatively the induction effects of substituents), or constants E_s characterizing their steric effects*), may be used as X .

Parameters BP and BP^* , as well as parameters E^T (21) derived from theoretical organic chemistry (20), may be used as X quantities for systems in which the diluent changes.

*) It appears that equations of type (1) with σ variables may be expected to apply only to the system series with E_s constant, and those with E_s variable to series with σ constant.

For systems in which the extraction of acids and metallic salts may be attributed to addition reactions (extraction of acids and metallic salts with amine salts, neutral organophosphorus compounds, amides etc), if the only varying parameter in a system series is the nature of the basic anion-ligand, then the anionic nucleophilicity parameter, H (derived from theoretical chemistry (19)) may be used as X quantity.

For systems in which the extraction of acids may be attributed to anion exchange reactions (with the anion displaced from the organic phase remaining unchanged), the free energies of hydration (or enthalpies of hydration, approximately proportional to them) of the extracted anions may be used as X quantities.

The applicability of relationships such as equation (1) simplifies the comparison between different series of extraction systems and permits a number of new regularities common to extractions (e.g. regularities defining the selectivity of extraction) to be revealed by the methods of correlation analysis.

To substantiate the possibility of predicting and analysing extraction systems by the above methods, we have mainly used experimental data obtained in studies of the extraction of acids and metallic salts by amines, amine salts and amides (1-14), and to some extent data obtained for neutral and acid organophosphorus extractants.

In a series of systems in which only one component (present at micro-concentrations) is extracted, extraction constants were replaced by distribution coefficients in equations of type (1).

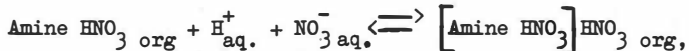
Effect of Extractant Structure

In 1965 the authors suggested (2) that in some extraction systems, including amines, relationships of the type

$$\lg K = \lg K_0 + \rho \Sigma \sigma \quad (2)$$

$$\text{and } \lg K = \lg K_0 + a \Sigma E_s \quad (3)$$

should be observed. The applicability of relationship (2) to extraction reactions may be illustrated (3) by comparison between the constants for extraction of nitric acid by nitrates of amines according to the reaction (22):



for the three series of tertiary amines (Fig 1). These have one varying substituent whose alteration leads to no significant change in steric factors. Fig 2 shows that for all three series of amines

investigated, the linear relationships between $\lg K_{\text{HNO}_3}$ and the quantity σ (σ^0 , σ^*) for the varying substituent, corresponding to eq. (2)*, are fully verified.

The validity of equation (3) was checked by application to the constants for the extraction of Pu (IV) and Np (IV) at micro-concentrations from nitric acid solutions. For the investigation trialkyl amines were chosen with from 10 to 20 carbon atoms in the chain. For these amines the changes in substituent inductive effects are small and the influence of amine structure on extraction is determined only by steric effects. Since E_s values for long chains are not known, we determined values satisfying equation (3) by studying one extraction series, and then constructed the relationships between $\lg K$ and E_s for different extraction series. The following values of E_s were found for different radicals:

$C_{10}H_{21}$, 0; $C_{12}H_{25}$, 0.028; $C_{14}H_{29}$, 0.045; $C_{16}H_{33}$, 0.078;

$C_{18}H_{37}$, 0.116; $C_{20}H_{41}$, 0.133. The relationships between $\lg K$ and ΣE_s are shown in Fig 3 for different systems; the figure shows these relationships to correspond with an equation of type (3)**.

These relationships open the way for prediction of amine extraction properties by use of the parameters σ (σ^0 , σ^* etc) and E_s values derived from theoretical organic chemistry.

In recent years some authors (10, 14-17, 20) have also shown the possibility of a similar approach to prediction of the extraction properties of neutral and acid organophosphorus compounds and of amides.

The construction of graphs of types (2) and (3) reveals the influence of factors, related to amine structure, on the extraction selectivity. Fig 4 shows the relationships between distribution coefficients ($\lg \alpha$) and σ^* for varying substituents. This is for the extraction of Zn-65 and Co-60 at micro-concentrations from chloride solutions with a series of tertiary amines that differ little in the steric effect of varying substituents. It follows from this figure that the extraction selectivity rises with an increase of σ , i.e. with a decrease of the positive inductive effect of a substituent; and Fig 3 shows (lines 1-2) that for a series of systems with varying steric

* A M Rozen and Z I Nagnibeda also showed the applicability of equation (2) to the quantitative comparison of extracting power between the groups of amines, i.e. tertiary, secondary and primary (13).

** The probability of observing the relationships of type (3) for ethers was also pointed out by Rozen A M (14).

effects and a practically constant substituent inductive effect, the selectivity rises with an increase of the steric hindrance due to substituents at a nitrogen atom. These theses are valid when the extracted compounds, from whose distribution the selectivity is estimated, have equal solvation numbers. If the less extractable compound has a lower solvation number, the selectivity of extraction is increased with the rise of positive inductive effects and with a decrease of steric hindrance by substituents (Fig 3, lines 2, 3).

Effect of Diluent

The applicability of a relationship of the type

$$\lg K = \lg K_0 + a \text{ BP} \quad (4)$$

was first shown for a large number of series of extraction systems in Reference 4, which established the scale of BP quantities, and then in more detail (for 35 series of systems) in Reference 1.

This relationship is applicable to systems in which extraction is not associated with a large change in the polarity of compounds in an organic phase, e.g. to acid extraction by an addition reaction and to metallic salt extraction by formation of a complex of the double salt type. Some examples illustrating the applicability of equation (4) are shown in Fig 5.

Construction of relationships of type (4) revealed the effect of diluent on selectivity in extraction with some dozens of series of extraction systems, as an example. It is established that the selectivity of extraction of metallic salts (see, for instance, Fig 5), as well as of acids, increases with a decrease of BP*.

Construction of relationships of type (4) also permits estimation of the influence of the diluent on the extractive power of extractants with different structures. It follows from Figs 6 and 7 that a decrease of BP is accompanied by a reduction in the differences between the constants for extraction of acids and metallic salts by salts of different amines, i.e. in extraction by addition reaction, the diluents with low BP values have a levelling effect on the extractive power of different extractants. The BP scale, although satisfactory in describing the influence of many diluents on the extraction of metallic salts and acids by addition reaction, is not fully applicable to amine extraction of acids by neutralization and anion exchange reactions. For reactions of this type, a large

* A decrease in BP corresponds to an increase in the ability of the diluent to solvate anions of amine salts, or nucleophilic groups of other extractants.

amount of data (Fig 8), available in the literature (21), is better described by means of the BP* scale (1, 5). This scale appears to be most useful in the description of the diluent effect on anion extractions if there is a considerable change in the polarity of compounds in an organic phase (Fig 9), and is also applicable to the effect of the diluent on extraction by cation exchange reactions (8)⁺.

Effect of Anion - Ligand

The validity of linear relationships of the type

$$\lg K = \text{const} + a H \quad (5),$$

for the series in which the only variable is the basic anion-ligand of the system, may be illustrated by data on the extraction of acids by salts of the same amine through addition reactions (Fig 10), and on extraction of some metals by the formation of complexes of the double salt type (Fig 11). Since the extraction constants vary in accordance with the H parameters, the scale of nucleophilicity parameters may be used to predict the influence of the anion-ligand on extraction.

Influence of the anion extracted by neutralisation of the amine or by ion-exchange with the amine salt

The validity of linear relationships of the type

$$\lg K = \text{const} + a \Delta H \text{ or } \lg K = \text{const} + a \Delta F \quad (6),$$

for series in which the only variable is the nature of the anion extracted from the aqueous phase by reactions of the type indicated, may be illustrated by the relationships (Fig 12) constructed on the basis of experimental data obtained from the literature. From comparison of the slopes of the lines in Fig 12, it follows that tertiary amines are more selective than secondary or primary ones in extraction by simple anion exchange.

Conclusions

The data presented show that many properties of extraction systems may be explained and predicted by means of formulae based on linear relationships of free energies. Construction of corresponding correlation graphs permits a more descriptive representation of some extraction regularities and reveals, for instance, factors influencing selectivity. Departures from the expected relationships in other systems may be considered to indicate some peculiarity of reaction in these systems.

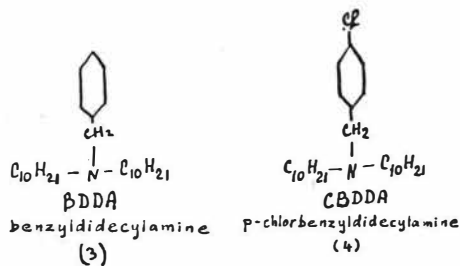
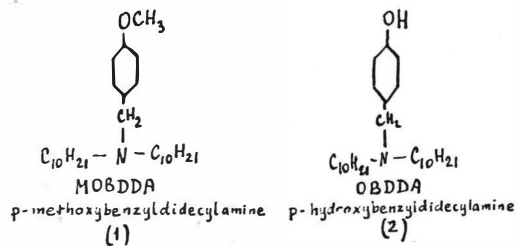
+ For such systems, not only the scale BP*, but also the scale of E_T parameters proportional to it may be used.

REFERENCES

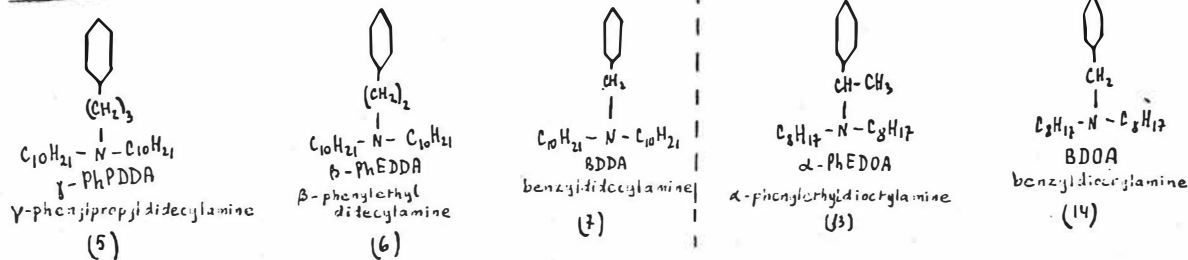
1. V S Shmidt, Ekstraktsija aminami, Atomizdat, Moscow, 1970.
2. V S Shmidt, E A Mezhov, Uspekhi khimii, 34, 1388 (1965).
3. V S Shmidt, E A Mezhov, V N Lisitsin, Z.neorgan.khim., 12, 571 (1971).
4. V S Shmidt, E A Mezhov, S S Novikova, Radiokhimiya, 9, 700 (1967).
5. V S Shmidt, E A Mezhov, Radiokhimiya, 12, 38 (1970).
6. V S Shmidt, V N Shesterikov, E A Mezhov, Radiokhimiya, 12, 399 (1970).
7. V S Shmidt, E A Mezhov, V N Shesterikov, Radiokhimiya, 12, 590 (1970).
8. V S Shmidt, V S Smelov, V N Shesterikov, Radiokhimiya, 12, 748 (1970).
9. V S Shmidt, V S Sokolov, Zh. phys. khim., 43, 1594 (1969).
10. V S Sokolov, E G Teterin, N N Shesterikov, V S Shmidt, Radiokhimiya, 11, 535 (1969).
11. V S Shmidt, V N Shesterikov, Radiokhimiya, 13, N 6, 815 (1971).
12. V S Shmidt, V N Shesterikov, E A Mezhov, Uspekhi khimii, 36, 2167 (1967).
13. A M Rozen, Z I Nagnibeda, Dokl. Akademii Nauk, 170, 855 (1966).
14. A M Rozen, Radiokhimiya, 10, N 3 (1968).
15. A M Rozen, N A Konstantinova, Radiokhimiya, 9, 1725 (1964).
16. V P Shvedov, Ju.F.Orlov, Zh.neorg.khimii, 10, 2774 (1965).
17. B N Laskorin, L A Fedorova, E P Buchikhin, in "Khimija processov ekstraktsii", "Nauka", Moscow, 1972, p.66.
18. Ju.G.Frolov, V V Sergievski, A V Ochkin, Atomic Energy Revs, IAEA 7, 71 (1969).
19. V A Palm, Osnovy kolichestvennoy teorii organicheskikh reaktsii, L, Chimia, 1937.
20. E Amis, Vlijanie rastvotitelja na skorost u mekhanizm khimicheskikh reaktsiy, Moscow, 1968.
21. Ju.G.Frolov, G V Makarov, Trudy of the Mendeleev's Moscow Institute of Chemical technology, N 54, 61, 56 (1967).
22. V B Shevchenko, V S Shmidt, E A Nenarokomov, Zh. neorgan. khimii, 5, 1852 (1960).

Fig. 1. THE STRUCTURE OF THREE AMINE SERIES

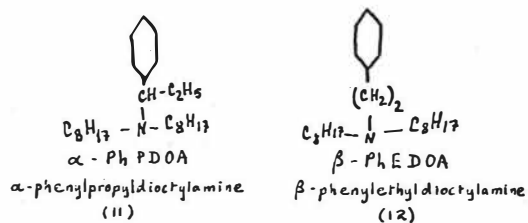
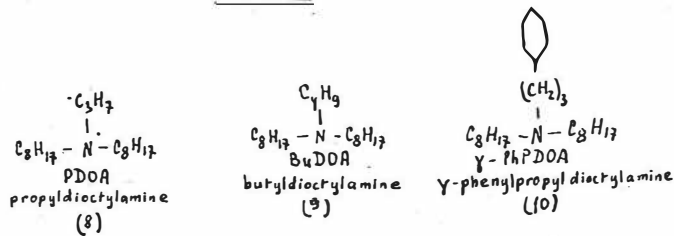
Series A



Series B



Series C



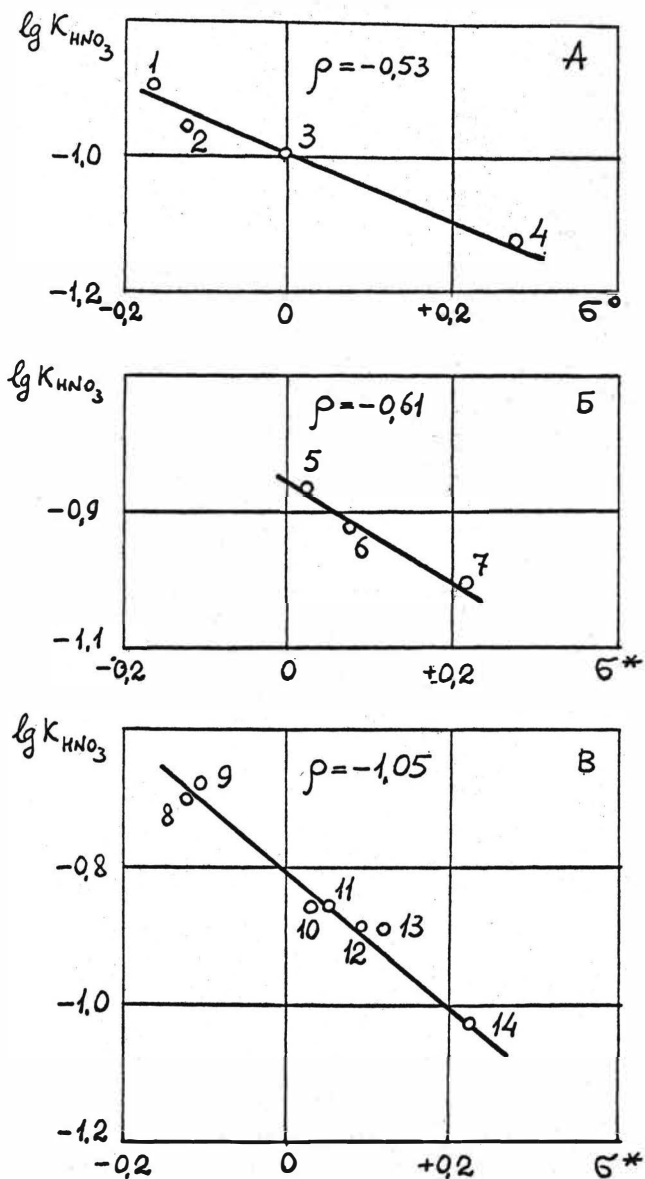


Fig. 2.

THE DEPENDENCE OF $\lg K_{\text{HNO}_3}$ ON σ (σ° , σ^*) FOR THE EXTRACTION OF HNO_3 BY 20% SOLUTIONS OF AMINE NITRATES IN *o*-XYLENE.

NUMBERS BESIDE THE POINTS CORRESPOND TO AMINES LISTED IN FIGURE 1.

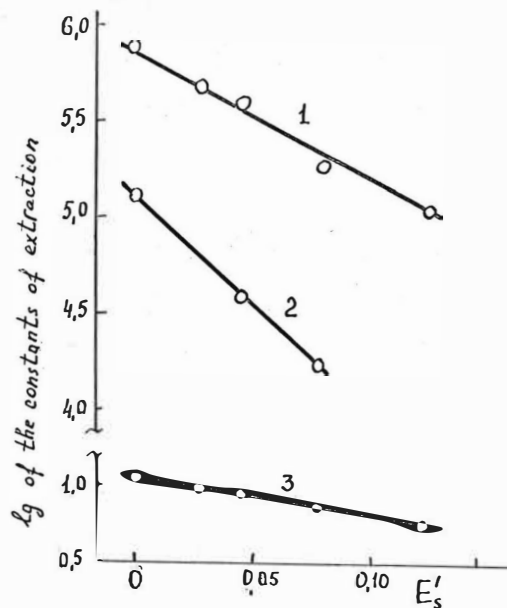


Fig. 3. DEPENDENCE OF EXTRACTION EQUILIBRIUM CONSTANTS ON E_s' VALUES, FOR SOLUTIONS OF AMINE NITRATES IN BENZENE. EXTRACTED SPECIES: 1, Pu(IV); 2, Np(IV); 3, HNO_3 .

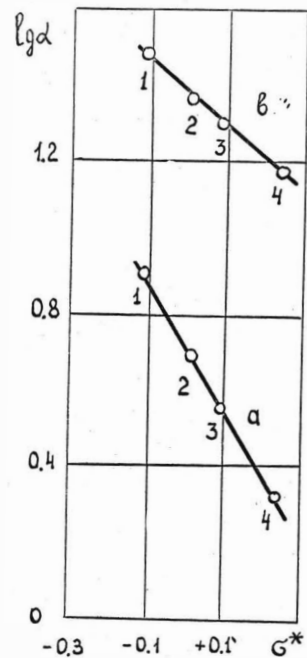


Fig. 4 DEPENDENCE OF THE DISTRIBUTION COEFFICIENTS FOR Co(II) (a) AND Zn(II) (b) ON THE σ^* VALUES OF VARIOUS SUBSTITUENTS IN THE AMINE MOLECULE.

EXTRACTANT: 0.02M TERTIARY AMINE SOLUTION.

AMINE: 1, PDDA; 2, PLDDA;
3, β -PLDDA; 4, BDDA.

AQUEOUS PHASE COMPOSITION:

FOR Zn, 2M HCl;

FOR Co, 3.6M $CaCl_2$.

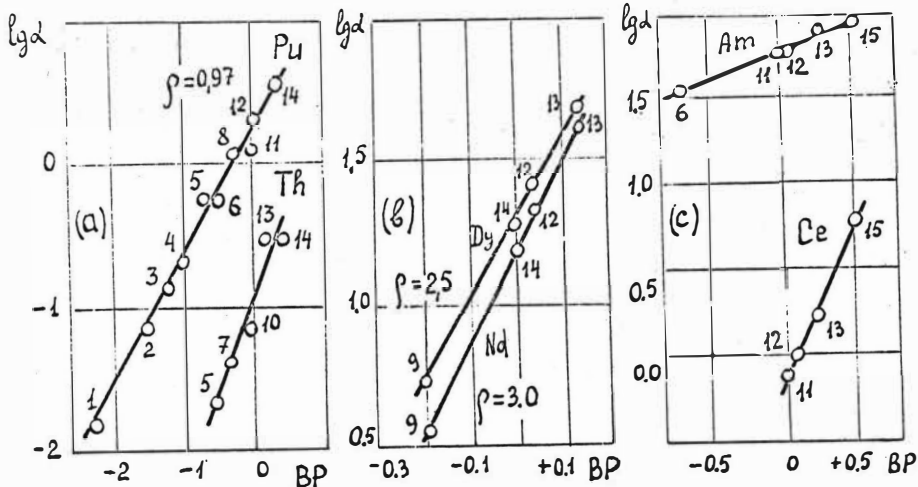


Fig.5

DEPENDENCE OF DISTRIBUTION COEFFICIENT ON BP VALUES OF DILUENTS.
 DISTRIBUTION OF (a) Pu (IV) AND Th (IV) BETWEEN 0.5M HNO_3 AND 0.1M TOA;
 (b) Nd (III) AND Dy (III) BETWEEN 7.1M $LiNO_3$ + 0.013M HNO_3
 AND 0.3M DI-ISOBUTYLAMINE;
 (c) Am (III) AND Ce (III) BETWEEN 4.0M NH_4SCN AND
 5% V/V METHYL TRIOCTYLAMMONIUM THIOCYANATE (MTOA).

- DILUENTS:
- (1) 80% $C_{10}H_{22}$ + 20% $C_8H_{17}OH$
 - (2) 80% $C_{10}H_{22}$ + 20% $CHCl_3$
 - (3) 85% $C_{10}H_{22}$ + 15% $CHCl_3$
 - (4) 85% C_6H_6 + 15% $CHCl_3$
 - (5) 90% C_6H_6 + 10% $CHCl_3$
 - (6) CCl_4
 - (7) C_6H_5Br + CCl_4 (1:1)
 - (8) 95% C_6H_6 + 5% $CHCl_3$
 - (9) 95% C_6H_6 + 5% $C_{10}H_{21}OH$
 - (10) C_6H_5Cl
 - (11) C_6H_6
 - (12) $C_6H_5CH_3$
 - (13) $C_6H_6(CH_3)_2$
 - (14) C_6H_6 + cyclohexane
 - (15) Cyclohexane

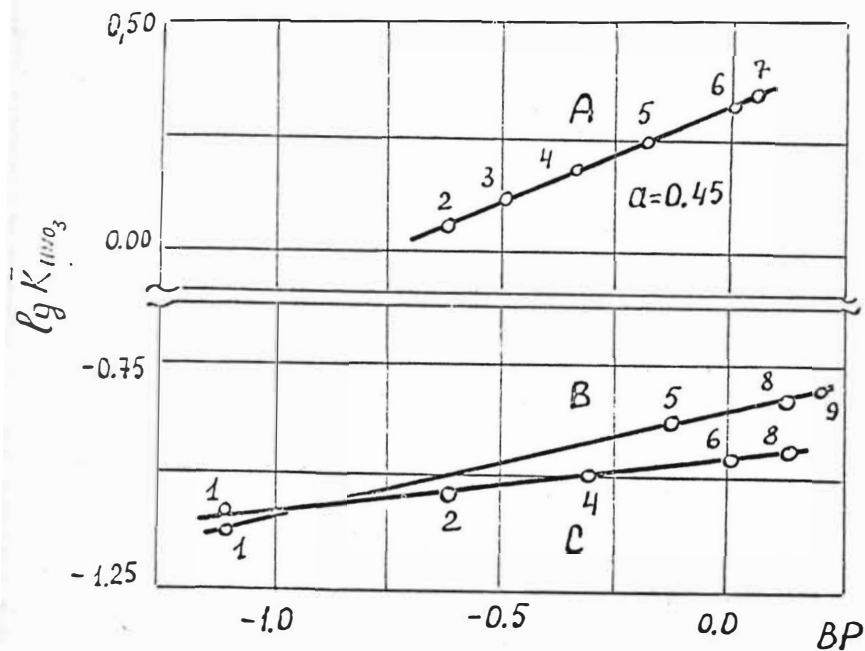


Fig. 6. DEPENDENCE OF EQUILIBRIUM CONSTANTS FOR EXTRACTION OF HNO_3 ON THE BP VALUES OF DILUENTS

EXTRACTANTS

- A 0.2 M MTOAN
- B 0.4 M TOA
- C 0.32 M TLA

DILUENTS

- (1) $C_6H_6 + CH_2Cl_2$ (4:1)
- (2) CCl_4
- (3) $CCl_4 + C_6H_5Br$ (1:1)
- (4) C_6H_5Br
- (5) C_6H_5Cl
- (6) C_6H_6
- (7) $C_6H_5CH_3$
- (8) $p-C_6H_4(CH_3)_2$
- (9) $C_6H_6 + \text{cyclohexane}$ (1:1).

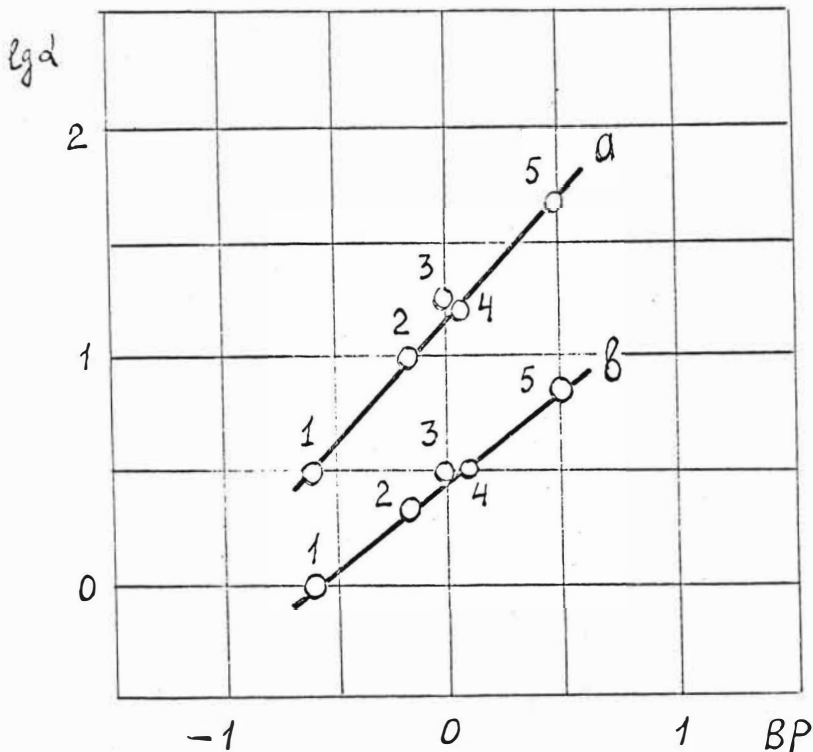


Fig. 7. DEPENDENCE OF DISTRIBUTION COEFFICIENT ON THE BP VALUES OF DILUENTS.

DISTRIBUTION OF CoCl_2 BETWEEN
 0.2M HCl + 7.8M LiCl and (a) 0.1M TOA HCl
 (b) 0.1M DOA HCl.

DILUENTS: (1) CCl_4 (2) $\text{C}_6\text{H}_5\text{Cl}$
 (3) C_6H_6 (4) $\text{C}_6\text{H}_5\text{CH}_3$
 (5) Cyclohexane.

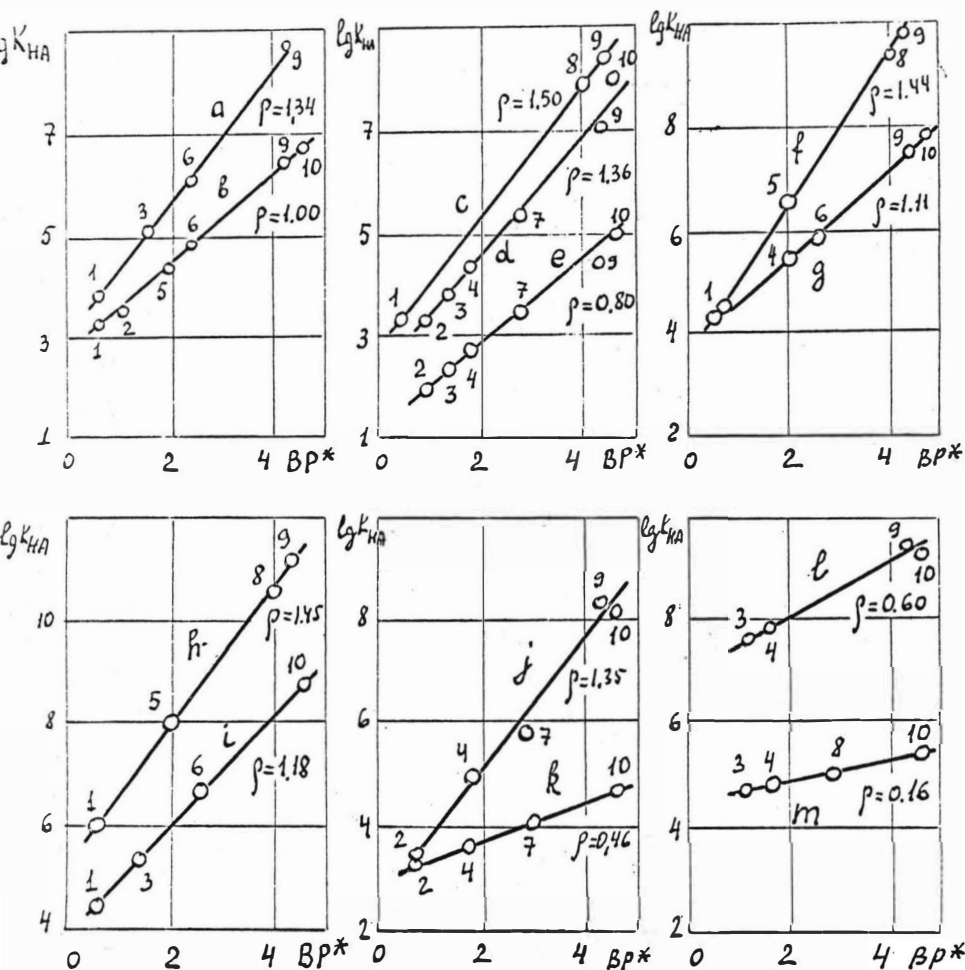


FIG. 8. DEPENDENCE OF $\lg K$ FOR NEUTRALISATION REACTIONS ON THE BP VALUES OF DILUENTS.

DILUENTS

- (1) Cyclohexane
- (2) $C_6H_4(CH_3)_2$
- (3) $C_4H_4 \cdot C_6H_5$
- (4) C_6H_4
- (5) $C_6H_5CH_3$
- (6) C_6H_6
- (7) $C_8H_{18} + 10\% C_8H_{17}OH$
- (8) $C_2H_7NO_2$
- (9) $C_6H_5NO_2$
- (10) $CHCl_3$

EXTRACTED SALTS

- (a) $TLA \cdot HI$
- (b) $TLA \cdot HCl$
- (c) $TOA \cdot HCl$
- (d) Benzyldinonylamine (BDNA) hydrochloride
- (e) Dibenzyl dodecylamine (DBDA) hydrochloride
- (f) $TOA \cdot HBr$
- (g) $TLA \cdot HBr$
- (h) $TOA \cdot HI$
- (i) $TOA \cdot HSCN$
- (j) $BDNA \cdot HNO_3$
- (k) $DBDA \cdot HNO_3$
- (l) $DBDA \cdot HClO_4$
- (m) $BDNA \cdot HClO_4$

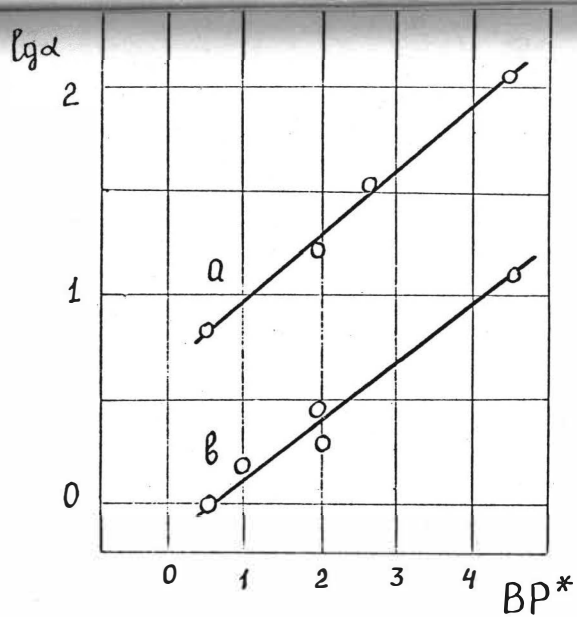


FIG. 9. DEPENDENCE ON DILUENT BP^* VALUES OF DISTRIBUTION COEFFICIENTS FOR TeO_4^- AND Cl^- AT MICRO-CONCENTRATIONS IN ANION-EXCHANGE EXTRACTION BY AMINE SALTS.

EXTRACTION SYSTEMS:

- (a). TeO_4^- - 0.001M dimethyldodecylammonium sulphate - 0.1M H_2SO_4 ;
 (b) Cl^- - 0.1M $(TOAH)_2SO_4$ - 0.1M H_2SO_4 .

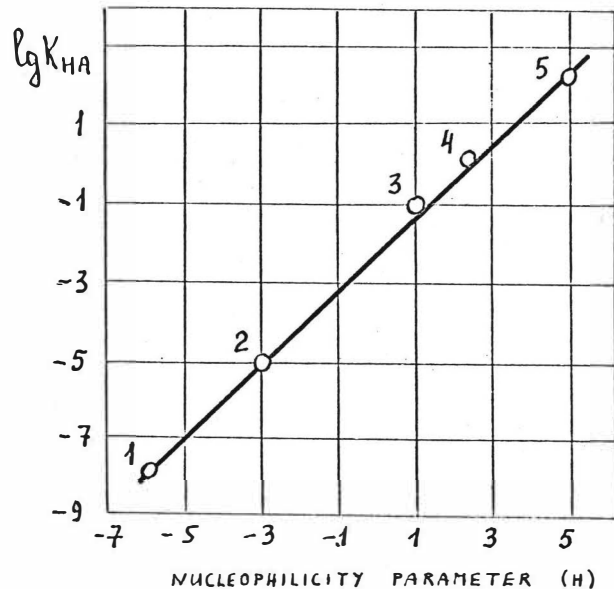


Fig. 10

DEPENDENCE OF EXTRACTION EQUILIBRIUM CONSTANTS FOR VARIOUS ACIDS ON THE NUCLEOPHILICITY PARAMETERS OF THE ACID ANIONS (IN EXTRACTION BY CORRESPONDING AMINE SALTS).

ACIDS: (1) HBr (2) HCl (3) HNO_3
 (4) CCl_3COOH (5) HF

EXTRACTANT: TOA.

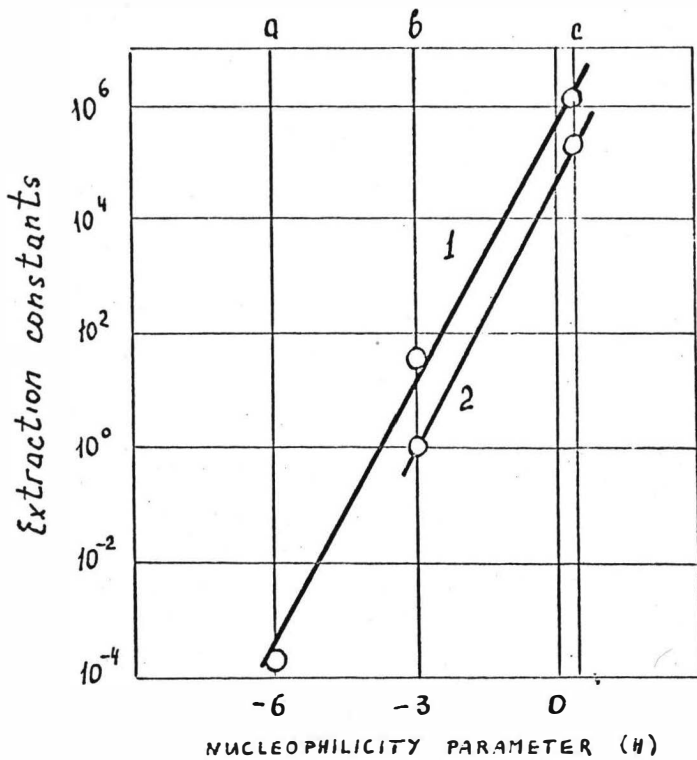


Fig. 11.

DEPENDENCE OF EXTRACTION EQUILIBRIUM CONSTANTS ON ANIONIC NUCLEOPHILICITY PARAMETER FOR EXTRACTION OF TWO METALS BY TOA - BENZENE SOLUTIONS.

(1) Pu(IV)

(a) Br⁻ (b) Cl⁻ (c) NO₃⁻

(2) Np(IV)

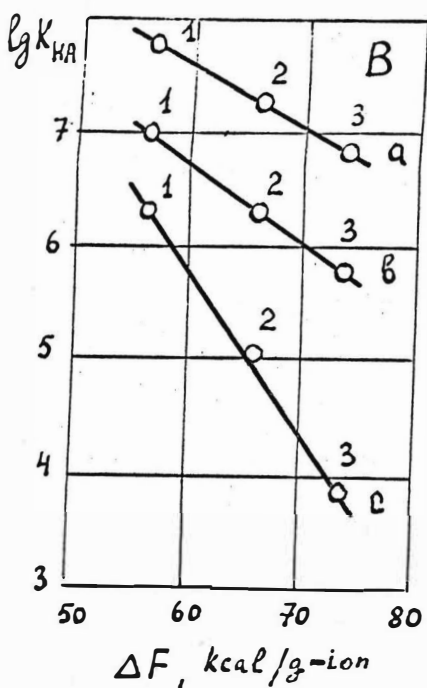
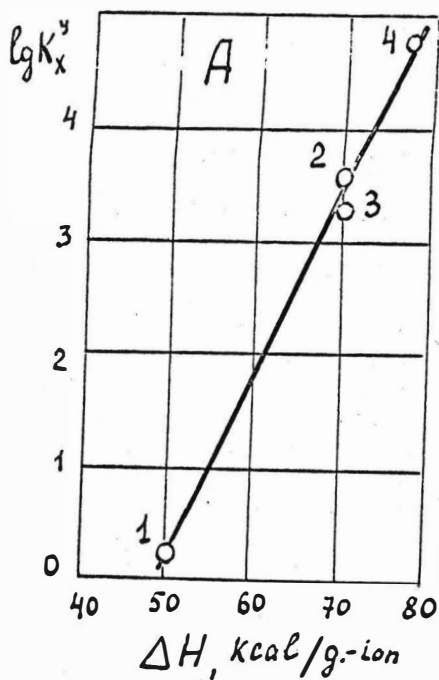


Fig. 12. (A) DEPENDENCE OF $\lg K$ ON THE ENTHALPY OF HYDRATION OF DISPLACED ANIONS, IN THE ION-EXCHANGE EXTRACTION OF ReO_4^- AT MICRO-CONCENTRATIONS.
DISPLACED ACIDS (1) HClO_4 (2) HBr (3) HNO_3 (4) HCl .

(B) DEPENDENCE OF $\lg K$ FOR ACID NEUTRALISATION EXTRACTION ON THE FREE ENERGY OF HYDRATION OF THE ANION.

ACIDS: (1) HI (2) HBr (3) HCl .

EXTRACTANTS: (a) Primary amine (Primene IMT)

(b) Secondary amine (LA-2)

(c) Tertiary amine (TLA)

DILUENT: Benzene.

Mutual Effects of Elements in the Extraction

by Long-chain Amine Salts

V. V. Bagreev, Yu. A. Zolotov, Yu. S. Tserlyuta,
L. M. Yudushkina and I. M. Kutryev

V. I. Vernadsky Institute of Geochemistry and Analytical
Chemistry, USSR Academy of Sciences, Moscow, USSR

C. Fischer and P. Mühl

Central Institute of Solid State Physics and Testing
of Materials, GDR Academy of Sciences, Dresden, GDR

Abstract

The influence of different factors on the extraction of microquantities of In, Tl, Fe, Cd, Co, Zn, W, Mo, Zr, Nb, Am and Eu (microelement) from halogen hydride solutions by amine salts as well as quaternary ammonium bases in the presence of macro-quantities of Fe, Ga, Co, Zn, Cd, Mo, Nb and Ta (macroelement) has been studied. Remarkable influences of macro-quantities of certain metals on the extraction of micro-quantities of other metals are found. In the majority of cases the distribution coefficients of microelements in the presence of extractable macroelements are found to decrease, i.e. suppression of the microelement extraction is observed. The dielectric constants and conductivities of organic solutions of metal species and their dependence on concentration have been measured. Some features connected with the mutual influence of elements in the extraction systems with amines are reported. The mechanism of this phenomenon is discussed.

Introduction

It is known that during extraction of complex metal halides by oxygenated solvents the mutual influence of extractable compounds is often observed. This is shown in the decrease in extraction of certain elements (extraction suppression) or inversely in the increase in extraction (co-extraction) of an element in the presence of other elements. The mutual influence in these systems is undoubtedly caused by interactions in the organic phase. The co-extraction observed in the solvents of low polarity is explained by the formation of mixed ionic associates. The suppression of extraction, when using solvents with a relatively high dielectric constant and/or with substantial donor capacity, are to be explained by the dissociation of extracting compounds in the organic phase and by the common ion effect.⁽¹⁻³⁾

Comprehensive and detailed investigation of this mutual influence in the process of extraction of complex metal species from halide and thiocyanate solutions by oxygenated solvents, leads to the conclusion that the mutual influence of elements is not a rare phenomenon and that similar effects are to be expected in other extraction systems, including the extraction of metal acidocomplexes by amines and quaternary ammonium salts.

The present authors investigated the extraction of many microelements (In, Tl, Fe, Cd, Co, Zn, W, Mo, Zr, Nb, Am, Eu) in the presence of large amounts of different metals (Fe, Ga, Co, Zn, Cd, Mo, Nb, Ta) with tri-n-octylamine, Aliquat-336 and other amines. A decrease in the extraction of microelements with macroelements has been shown to occur.

Experimental

The metals were extracted from solutions of halogen halides, mainly from

chloride solutions. Tri-n-octylamine ("Schuchard", West Germany) and Aliquat-336 ("General Mills Company", USA) were used as the solvents in different organic diluents. The concentrations of extractants were 0.1-0.5M. The phase distribution of microelements was controlled by means of radioactive isotopes. The concentration of microelements were kept at 10^{-6} - 10^{-4} M and concentration of macroelements, 0.1-0.4M.

Factors affecting the simultaneous extraction of micro- and macroelements were studied, including the concentration and nature of halogen halide, the nature of the organic solvent, the nature and concentration of macroelements, the amine concentration and others.

To help in understanding the extraction suppression mechanism, the dielectric constants and molar conductivities of the simple and metal-bearing amine salt extracts were measured and plotted against their concentrations. The dielectric constant measurements were carried out by means of dielcometer DK-Meter GK 68 ("F. Kuster", GDR). The data on conductivity of the same extracts were obtained on ICR-Meßbrücke 1521 (GDR).

Results and Discussion

A significant influence of macroquantities of certain metals on the extraction of other metals was found in all systems investigated. In the majority of cases, a decrease in microcomponent distribution coefficient in the presence of macrocomponents was observed. This phenomenon is called suppression of extraction. Many examples are given in the data in Table 1.

Table 1

Extraction of microelements from 6M HCl by 0.5M solution of tri-n-octylamine in benzene in the absence of other elements (D_1) and in the presence of macroelements (D_2)

Microelements	D_1	D_2	D_1/D_2
In the presence of Fe (0.4M)			
In	540	0.004	1.4×10^5
Cd	350	0.12	2.8×10^3
Zn	510	0.15	3.4×10^3
In the presence of Co (0.2M)			
In	540	101	5.4
Cd	350	29.5	12
Zn	510	19	27

The distribution coefficients of In, Cd, Zn (microelements) in the presence of iron(III) are decreasing by 3-4 orders of magnitude. In the presence of cobalt this decrease is less having a magnitude of 5-20 times. In the extraction of molybdenum and tungsten from dilute solutions of HCl and HBr, the

the co-extraction of microquantities of tungsten with molybdenum was observed (Fig. 1).

The influence of different factors on the degree of extraction suppression is discussed. The degree of suppression is determined as the ratio of the microelement distribution coefficient in the absence of the macrocomponent (D_1) to the corresponding value in the presence of this macrocomponent (D_2).

An example of the influence of acidity on the degree of suppression of extraction is illustrated in the data in Fig. 1, where the distribution values for tungsten in the absence and presence of macroamounts of molybdenum during their simultaneous extraction with tri-n-octylamine, are plotted against the concentration of HCl in the aqueous phase. The increase of the HCl concentration (higher than 3M) is accompanied by increasing suppression of the extraction of microelement tungsten by molybdenum. The same figure illustrates the extraction of macroquantities of molybdenum. It is not difficult to see that the degree of suppression increases with the increase of macroelement concentration in the organic phase, i.e. with the enhancement of its extraction. This phenomenon is typical of all the systems under investigation.

The degree of suppression of microelement extraction depends on the nature of the macroelements. The influence of this factor is given in Fig. 2. The extraction of indium in the presence of iron(III) is suppressed in much greater extent than in the presence of Cd, Zn and Co. A similar effect was obtained when gallium was used as the macroelement. The effect of iron, gallium and indium on the extraction of microamounts of cadmium and zinc is also higher than for instance the effect of cobalt above. Unicharge complex anions of macroelements (Fe, Ga) are found to suppress the microelements extraction to a greater extent than the doubly charged anions of macroelements (Cd, Zn, Co). Another aspect which affects this extraction suppression effect is observed in the differentiation in the influence of macroelements forming anions of the same charge.

On the other hand, the degree of suppression of the microelements extractable by amines in the form of doubly charged anions is less than that of the uncharged anion microelement complexes. As shown in Fig. 3, the degree of extraction suppression of zinc in the presence of macroquantities of iron is less than that of microelement indium. The same figure also illustrates the influence of the nature of the macroelement on the microelement's extraction. Iron is found to suppress the extraction of both microelements to a greater extent than cobalt. These effects are much greater in the case of uncharged anion complexes of microelements when compared with the doubly charged ones.

The effect of the nature of the organic solvent on the extraction of microquantities of tungsten and zirconium, in the presence of macroquantities of molybdenum and tantalum respectively, has been investigated using different diluents (Table 2).

The influence of macrocomponents on the extraction of microelements is specific to all diluents investigated. Correlation of the degree of suppression and the dielectric constants of organic solvents is observed, namely, increase of dielectric constant with increase in the degree of extraction suppression.

The influence of macroelement concentration on the extraction of micro- and macroelements has also been investigated. The distribution coefficients of metals are found to decrease more in the case of diluents with a relatively high dielectric constant (e.g. nitrobenzene) at the lower macrocomponent concentrations than in the case of diluents of low polarity (e.g. benzene).

Table 2

The degree of extraction suppression of W and Zr during their extraction with tri-n-octylamine from halogen hydride solutions in the presence of Mo and Ta

Diluents	ϵ	in the presence of Mo		in the presence of Ta from 1M HF
		from 6M HCl	from 6M HBr	
Cyclohexane	2.30	-	17	-
Toluene	2.38	14	22	926
Chloroform	4.81	2	17	280
Chlorobenzene	5.62	30	42	-
Ethylene chloride	10.5	-	-	946
B.B'-Dichloro- diethyl ether	21.2	-	-	950
Nitrobenzene	34.8	67	56	1031

The two observations (1) correlation of the degree of the extraction suppression and the solvent dielectric constant and (2) the difference of the dependence of the distribution coefficients of metals as a function of their concentration in the cases of benzene and nitrobenzene, serve as a basis for the assumption that the dissociation of the extractable compounds in the organic phase is one of the principal causes of the suppression of extraction. (This is shown in the extraction of metal-halides with oxygen-containing solvents.)

We obtained values of dielectric constant and molar conductivity of metal-bearing and metal-free amine salt organic phases as a function of their concentration. In Fig. 4 the data on the dielectric constant and conductivity of tri-n-octylamine salts containing Fe, Ga, In, Co, Cd and Zn extracted into benzene, are plotted against their concentration. Similar data for organic extracts of amine simple salts are shown. The sharp increase in dielectric constant is observed in solutions with metal concentration higher than 0.01M (Fig. 4a). The dielectric constant is found to increase earlier and sharper in the case of Fe, Ga, and In than that of Co, Zn and Cd. Presumably, even in benzene, the extractable amine salts are dissociated if their concentrations are high. The data on the conductivity of the same solutions (Fig. 4b) do not contradict this assumption. High molar conductivities are observed in high metal concentrations. The data of Fig. 4 show the following features: metals forming salts of uncharged anion complexes (e.g. Fe, Ga, In) are found to suppress the extraction of microcomponents in greater degree than metals forming the salts of doubly charged anions (Zn, Cd, Co). The former are more dissociated than the latter.

References

1. Zolotov Yu. A., and Golovanov V. I., Zh.neorg.Khim., 1971, 16, 2755.
2. Zolotov Yu. A., Reinststoffe in Wissenschaft und Technik. 3. Int. Symp. 4-8 May 1970 in Dresden. Plenar und Hauptvorträge Akademie-Verlag, Berlin, 1972, S. 655.
3. Zolotov Yu. A., and Golovanov V. I., Proc. of International Solvent Extraction Conference, ISEC 71, The Hague, 19-23 April, 1971, Vol. 1, London, Soc. Chem. Ind., 1971, p.625.

Figures

- Fig. 1 Extraction of molybdenum (0.2M), and tungsten (5.4×10^{-5} M) in the absence and in the presence of molybdenum, from hydrochloric acid solutions by 0.5M tri-n-octylamine in toluene.
- Fig. 2 Extraction of indium (1.4×10^{-5} M) by 0.5M tri-n-octylamine in benzene from hydrochloric acid solutions in the absence of other elements and in the presence of macroamounts of Fe (0.4M), Ga (0.4M), Cd (0.2M), Co (0.2M) and Zn (0.2M).
- Fig. 3 Indium and zinc extraction by 0.5M tri-n-octylamine in benzene from hydrochloric acid solutions in the absence and in the presence of iron (0.4M) and cobalt (0.2M).
- Fig. 4 Dielectric constants (a) and molar conductivity (b) of metal-bearing and metal-free tri-n-octylamine (TOA) salts in benzene as a function of their concentration.

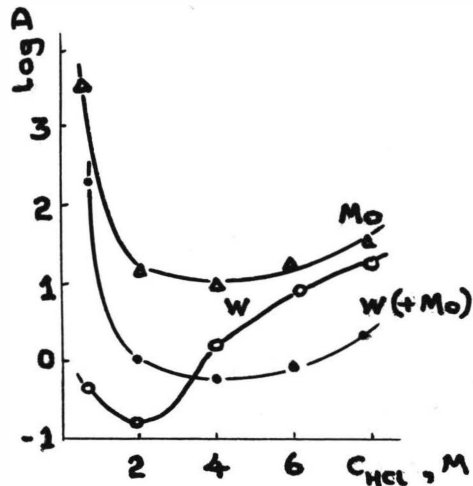


Fig. 1 Extraction of molybdenum (0.2%), and tungsten ($5.4 \times 10^{-5}\%$) in the absence and in the presence of molybdenum, from hydrochloric acid solutions by 0.5M tri-n-octylamine in toluene.

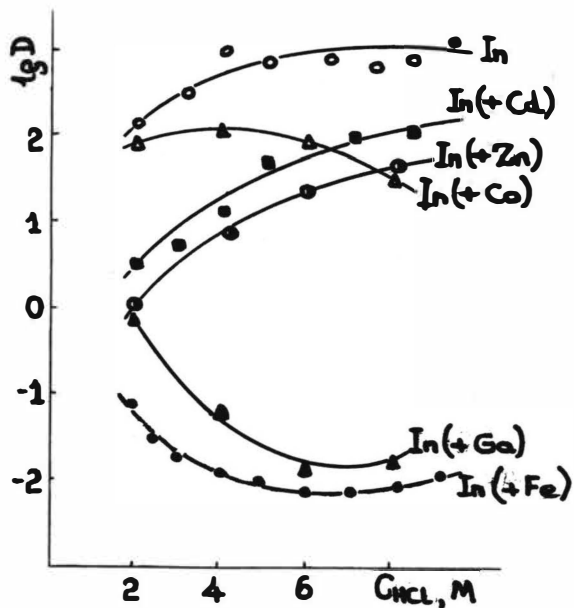


Fig. 2 Extraction of indium ($1.4 \times 10^{-5}\%$) by 0.5M tri-n-octylamine in benzene from hydrochloric acid solutions in the absence of other elements and in the presence of macroamounts of Fe (0.4%), Ga (0.4%), Cd (0.2%), Co (0.2%) and Zn (0.2%).

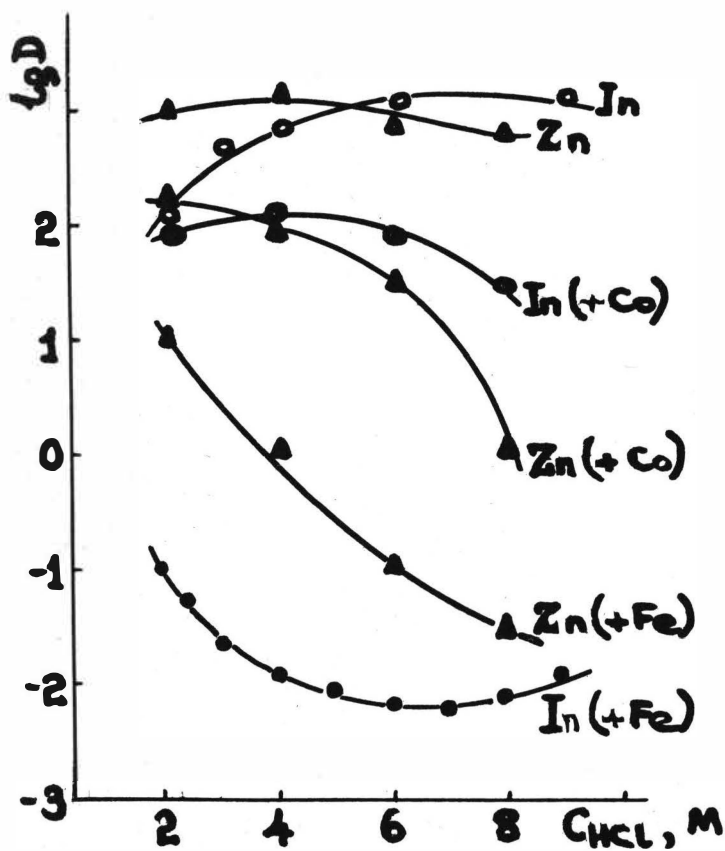


Fig. 3 Indium and zinc extraction by 0.5M tri-*n*-butylamine in benzene from hydrochloric acid solutions in the absence and in the presence of iron (0.4M) and cobalt (0.2M).

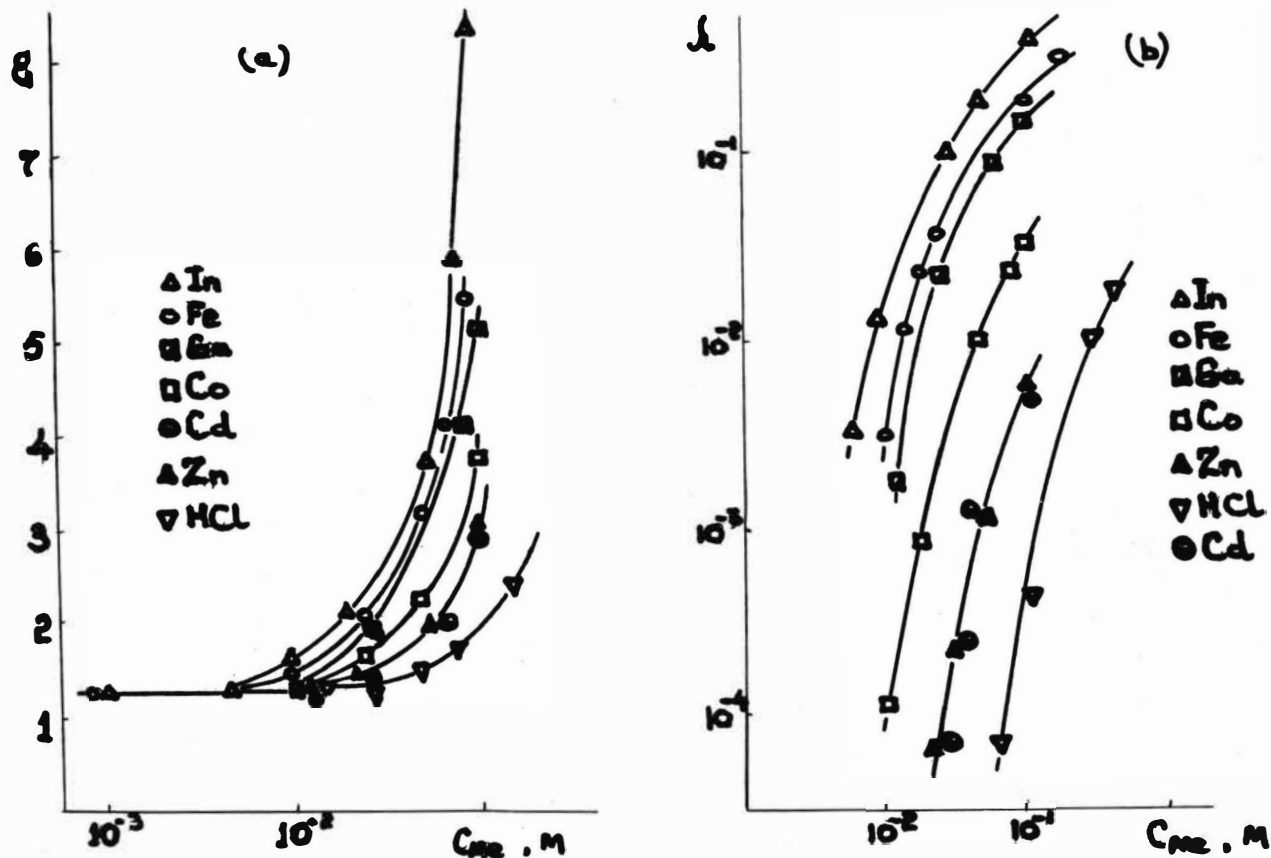


Fig. 4 Dielectric constants (a) and molar conductivity (b) of metal-bearing and metal-free tri-o-octylamine (TOA) salts in benzene as a function of their concentration.

SESSION 18

Thursday 12th September: 9.00 hrs

C H E M I S T R Y O F E X T R A C T I O N

(New & Unusual Extractants)

Chairman:

Mr. M. Parthault

Secretaries:

Dr. H. Cox

Mr. P. Joly



RECENT DEVELOPMENTS IN THE STUDY OF HETEROCYCLIC
AMINE EXTRACTION CHEMISTRY. APPLICATION OF THE
FORMATION OF INTRAMOLECULAR HYDROGEN BONDING
BETWEEN LIGAND AND COORDINATED ANIONS IN THE SALT
EXTRACTION

by V.M.Dziomko, O.V.Ivanov, V.N.Avilina, A.V.Iva-
shchenko, T.S.Kazakova

All-Union Scientific Research Institute of Chemical
Reagents and Ultra High Purity Chemical Substances,
Moscow, USSR

Heterocyclic amines involving NH-group capable of forming intramolecular hydrogen bonds with a coordinated anions such as 3,4,5-trialkylpyrazoles and bicyclic amidines make it possible to extract inorganic salts of transition metals. The maximum selectivity is observed in the sulfate and nitrate systems.

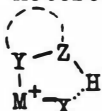
Introduction

STABILIZATION OF coordination compounds owing to the formation of intramolecular hydrogen bonds between coordinated ligands is of considerable interest for the extraction chemistry. The study of hydrogen bonds involving a heteroatom bonded directly to a metal is of special interest since it is the case when the extraction of salts formed by simple inorganic and organic anions is possible, particularly those having industrial value. Basing on the general principle that to reach high selectivity it is necessary to use ligands with an increased skeleton rigidity¹ we have undertaken the investigation of sys-

tems in which the formation of five- and six-membered metallo-cycles involving an intramolecular hydrogen bond between a rigid heterocyclic ligand and an anion bonded to a metal is possible.

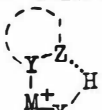
In general the systems investigated can be outlined as follows.

1. A heterocyclic ligand appears as a hydrogen donor



X is an inorganic anion or one of its atoms, OR, SR, SeR, TeR, NRR, etc.

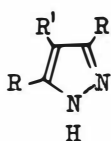
2. An anion is a hydrogen donor



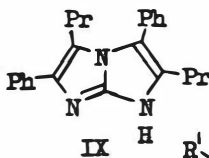
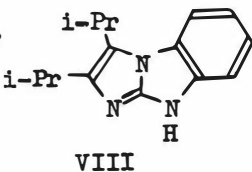
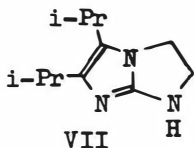
X is O, S, Se, Te, NR, etc. Y, Z are heteroatoms

W is C or a heteroatom. R, R are alkyls, aryls, acyls, etc.

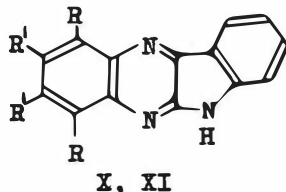
In the present work the investigation was made on heterocyclic extractants from the groups of 3,4,5-trialkylpyrazoles (I - VI) and bicyclic amidines with hydrogen atoms in different heterocycles (VII - XI).



	I	II	III	IV	V	VI
R	C ₂ H ₅	n-C ₃ H ₇	n-C ₄ H ₉	n-C ₅ H ₁₁	n-C ₆ H ₁₃	CH ₃
R'	CH ₃	C ₂ H ₅	n-C ₃ H ₇	n-C ₄ H ₉	n-C ₅ H ₁₁	n-C ₆ H ₁₃



X R=n-BuO; R'¹H
 XI R=H; R'¹n-BuO



Experimental

Reagents

3,4,5-Trialkylpyrazoles (I - V) were synthesized according to².

3,5-Dimethyl-4-heptylpyrazole (VI) was prepared by the interaction of 3-heptyl-2,4-pentanedione³ with hydrazine hydrate in ethanol. The yield is 88%, b.p. 169-170°/7 mm Hg.

All 3,4,5-trialkylpyrazoles were purified by fractional vacuum distillation.

2,3-Dihydro-5,6-diisopropyl-1(7)H-imidazo[1,2-a]imidazole (VII), 2,3-diisopropyl-1(9)H-imidazo[1,2-a]benzimidazole (VIII), 3,6-diphenyl-2,5-di-n-propyl-1(7)H-imidazo[1,2-a]imidazole (IX) were synthesized by known methods⁴⁻⁶.

1,4-Di-n-butoxy-6H-indolo[2,3-b]quinoxaline(X) and 2,3-di-n-butoxy-6H-indolo[2,3-b]quinoxaline(XI) were prepared by the interaction of isatine with 3,6-di-n-butoxy- and 4,5-di-n-butoxy-1,2-diaminobenzene respectively. The yield of X is 18%, m.p. 171.5-172.5°. The yield of XI is 40%, m.p. 242.5-243.5°.

Synthesis of Complexes

Dichlorobis(4-ethyl-3,5-dipropylpyrazole)copper(II) was obtained by the interaction of $\text{CuCl}_2 \cdot 2\text{H}_2\text{O}$ with pyrazole (the ratio 1:2) in cyclohexane solution with the azeotropic water distillation. After distilling off the total water and cooling the solution the crystals separated were filtered off and purified by recrystallization from cyclohexane. They were green, m.p. 74-75°.

Bis-(4-ethyl-3,5-dipropylpyrazole)dinitratocopper(II) is prepared by the above procedure. After recrystallization from

benzene light-green crystals were obtained, m.p. 126-127°.

(1,4-Di-n-butoxy-6H-indolo[2,3-b]quinoxaline)nitrate-silver(I) monohydrate. The solution of 0.22g silver nitrate in 3 ml of water was added under stirring to the solution of 0.5g X in 50ml CHCl_3 . The water formed is removed azeotropically in a Dean and Stark separator. The reaction is continued until no more water separates. Orange-red coloured solids were obtained after cooling and filtration. The yield was 0.624 (90%).

IR-Spectra

The IR-spectra were obtained on a UR-20 instrument as Nujol mulls, as hexachlorobutadiene suspensions and as well as solutions in CCl_4 .

Measurement of the distribution ratios of metals

The distribution of metals was studied by a tracer technique and by complexometric titration. ^{59}Fe (III), ^{60}Co (II), ^{64}Cu (II) and $^{115\text{m}}\text{Cd}$ (II) were used as radioactive indicators. Complexometric titration was carried out in the presence of Sulfarsazene, Xylenol Orange and Tetra as indicators.

The extraction was carried out in glass separatory funnels by mixing phases on a mechanical shaker during time required for establishing chemical equilibrium at a temperature of $20 \pm 1^\circ$. Reagents were added in the following order: to 5 ml of a metal salt solution of the known concentration an equal volume of the extractant solution in the organic diluent was added. In the case of radiochemical control the aqueous phase contained a tracer of the corresponding metal. After mixing and separating the layers (15 min) equal parts of aqueous and organic phases were taken. Radioactivity measurements were carried out with the

aid of an endwindow counter Type MST-17 in conjunction with a scintillation counting assembly PP-8 (β activity) and with a LAS-type instrument using a scintillation counter with a single crystal NaI(Tl) (γ activity). In the case of a complexometric technique the metal concentration in the organic phase was determined by titration after back extraction with 1-6N NH_4OH or 1-2N H_2SO_4 .

Results and Discussion

Effect of the structure of extractant molecule

Typical curves for the extraction with 3,4,5-trialkylpyrazoles containing alkyls of different length are presented in Fig.1. The maximum extractability is shown by the extractant (VI) containing a long chain alkyl in 4 position and two short chain alkyls in the 3 and 5 positions. For the other pyrazoles the maximum extraction is observed not at the highest resulting value of carbon atoms in alkyls but at intermediate magnitudes of that value. Thus, the increased length of 3,5-substituents offers considerable steric hindrances for complex formation resulting in decreasing extraction. The factor of steric hindrances should be most pronounced in the case of cations with a small ionic radius as well as in the case of strained geometry of coordination. In the cases studied the greatest effect was shown by copper(II) having a square-planar coordination. At the same time similar in size zinc(II) ion showing tetrahedral coordination has a less pronounced steric effect.

As it can be seen from Fig.4a the greatest selectivity for copper chloride with respect to zinc chloride is observed for extractants I and II having short chain alkyls in the 3- and 5-

positions. Further increasing chain length of alkyls in these positions reduces the selectivity (extractant II), then the selectivity towards zinc chloride (extractant III) appears which is found to decrease again following a further increase of alkyl-chain length (extractants IV and V). In the latter case the tetrahedral coordination seems to get hindered as well. In the extraction of zinc and cadmium chlorides (Fig.4b) the greatest selectivity for zinc having a smaller ionic radius is observed in the case of extractant VI, having the shortest alkyls in the 3- and 5- positions.

Effect of the acidity of the medium and anions on the distribution of metals

The most general picture is revealed in the case of extraction from chloride systems (Fig.2). Here it is possible to observe curves with two maxima for some metals. Within the range of the pH 1-4 the extraction of chlorides with neutral ligands takes place accompanied by the formation of intramolecular hydrogen bonding with chloride ions. The increased acidity gives rise to ligand protonation. An increase in the anion concentration is accompanied by the formation of complex anion particles. The retardation of one of these processes from another reduces the extraction. If these processes are simultaneous (in the region of some acid and anion concentrations) then the extraction is enhanced (the case of zinc and cadmium chlorides). The extraction of copper(II) and iron(III) chlorides represents extreme cases when the extraction of a complex chloride and neutral salt appears unfavourable respectively.

The range of 0.5-1.5 M HCl is appropriate for back extraction.

Effect of the nature of the anion on the extraction of some transition metal salts is illustrated in Fig.3 and Table 1.

Table 1

Effect of anions on the extraction

Extractant: 1M solution of II in chloroform. $C_M = 5 \times 10^{-2} M$.

Elements	R, %								
	pH 1,0			pH 2,0			pH 3,0		
	SO_4^{2-}	Cl^-	NO_3^-	SO_4^{2-}	Cl^-	NO_3^-	SO_3^{2-}	Cl^-	NO_3^-
Cu(II)	85.8	79.5	84.4	86.6	82.9	86.1	85.3	80.1	78.9
Cd(II)	4.8	66.7	17.6	1.1	68.1	19.2	2.4	63.6	17.5
Co(II)	0.3	22.1	9.1	2.1	23.6	11.4	1.1	10.0	5.4
Ni(II)	1.3	18.6	5.0	1.2	18.2	6.1	1.0	10.0	5.0
Zn(II)	2.2	80.6	20.0	2.7	82.0	22.3	2.1	80.0	15.0
Fe(III)	1.8	4.2	5.0	1.5	4.2	4.7	-	3.4	3.8
Hg(II)	-	99.8 [ⓧ]	98.2	-	99.7 [ⓧ]	98.6	-	99.8 [ⓧ]	96.8
Ag(I)	-	99.8 [ⓧ]	96.9	-	99.6 [ⓧ]	99.6	-	99.9 [ⓧ]	99.6

ⓧ - For the extraction of Hg(II) and Ag(I) from the hydrochloric acid media $C_M = 1 \times 10^{-6} M$.

For the most metal salts the maximum extraction is observed in the case of chloride systems. In the extraction of copper the maximum selectivity is found in the sulphate media which are of considerable interest for hydrometallurgy.

It was established by the method of the equilibrium shift that in the extraction of copper(II) from the chloride and nitrate systems the ratio II:Cu in the complexes extracted with the excess of II is 2:1. In the IR-spectra of dichloro-

bis(4-ethyl-3,5-dipropylpyrazole)copper(II) and bis(4-ethyl-3,5-dipropylpyrazole)dinitratocopper(II) as compared to the IR-spectrum of ligand II in CCl_4 a strong shift of an NH stretching frequency is revealed: $\nu_{\text{NH}}=3290 \text{ cm}^{-1}$; $\nu_{\text{NH}}=195 \text{ cm}^{-1}$ for CuL_2Cl_2 and $\nu_{\text{NH}}=3260 \text{ cm}^{-1}$; $\nu_{\text{NH}}=225 \text{ cm}^{-1}$ for $\text{CuL}_2(\text{NO}_3)_2$ giving evidence for the presence of intramolecular hydrogen bonding in complexes formed by the hydrogen of the ligand NH group and the anion.

The study of the IR-spectra of the organic phase after the extraction of copper(II) chloride and nitrate with the solution of II in CCl_4 showed the presence of the absorption bands corresponding to the stretching frequencies of NH involved in the hydrogen bonding to anions. The position of these absorption bands in the spectrum corresponds to the bands for complexes of the composition CuL_2X_2 , where $\text{X}=\text{Cl}^-$; NO_3^- . This confirms the fact that the extraction of the metal salts is accompanied by both the metal - nitrogen coordination and by the formation of the hydrogen bond between the ligand NH group and the anion.

Effect of diluent

In the extraction of copper(II), cadmium(II) and zinc(II) from the sulfate, chloride and nitrate solutions an increase in the diluent efficiency is observed in the order octane < carbon tetrachloride < benzene < chloroform < kerosene < 1,1,2,2-tetrachloroethane. In the case of silver(I) and mercury(II) extraction the influence of the nature of a diluent is negligible.

Separation of metals

In the extraction of 0.05 M copper sulphate solution at pH 1 with 1M solution of II in kerosene in the presence of

accompanying sulphates (0.05 M of each) the following integral factors of separation were obtained: $S_{\text{Cu}/\text{Fe(III)}}=7.2 \times 10^2$; $S_{\text{Cu}/\text{Co}}=2.9 \times 10^3$; $S_{\text{Cu}/\text{Ni}}=3.4 \times 10^2$; $S_{\text{Cu}/\text{Zn}}=4.4 \times 10^2$; $S_{\text{Cu}/\text{Cd}}=6.7 \times 10^1$.

The back extraction of copper(II) was carried by the 1.0M sulphuric acid solution as well as by the aqueous solutions of ammonia, ethanolamine or other complexing agents.

Bicyclic amidine extractants

Among bicyclic amidines studied the highest extractability from chloride and bromide solutions showed VII and VIII. However they are inferior to pyrazoles in their extractability. Indoloquinoxaline(X) shows an increased selectivity with respect to the extraction of silver(I) nitrate. The data on the factors of separation of silver(I) and copper(II) nitrates each present in wide ranges of concentrations are given in Table 2. It was established by the method of the equilibrium shift that the ratio X:silver(I) in the complex extracted is 1:1.

In the IR-spectrum of the complex as compared to the IR-spectrum of the ligand the bands of the coordinated nitrate-ion ($\nu_1=1040 \text{ cm}^{-1}$, $\nu_2=822 \text{ cm}^{-1}$, $\nu_3=1303$; 1405 cm^{-1} , $\nu_4=754 \text{ cm}^{-1}$) and the bands near 1750 and 1820 cm^{-1} appear indicating the nitrate-ion bidentation⁷. Moreover, a large shift of the absorption band of NH stretching vibrations ($\nu_{\text{NH}}=3100 \text{ cm}^{-1}$; $\Delta \nu_{\text{NH}}=325 \text{ cm}^{-1}$) is observed giving evidence for the presence of the intramolecular hydrogen bonding in a complex formed between the hydrogen of the ligand NH group and an anionic ligand.

Basing on the IR-measurement of the complex and taking into account the absence of silver nitrate extraction with isomer XI it is possible to assume the following structure for the complex(XII).

Table 2

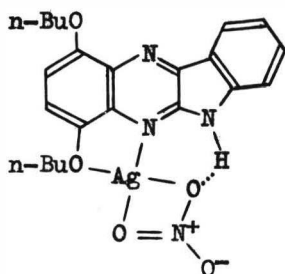
Integral factors of separation for silver(I) and copper(II) nitrates in the extraction from solution pH=2 (according to HNO_3) with $5 \times 10^{-2} \text{M}$ solution of 1,4-di-n-butoxy-6H-indolo [2.3-b] quinoxaline in chloroform

at a constant concentration
of copper(II) $1 \times 10^{-1} \text{M}$

at a constant concentration
of silver(I) $1 \times 10^{-3} \text{M}$

$[\text{AgNO}_3]_{\text{M}}$	E_{Ag}	E_{Cu}	$S_{\text{Ag/Cu}}$
1.0	31.79	1.8×10^{-2}	5.78
5×10^{-1}	23.50	1.9×10^{-3}	5.00×10^2
1×10^{-1}	22.70	2.1×10^{-3}	4.56×10^2
5×10^{-2}	21.80	2.4×10^{-3}	4.05×10^2
1×10^{-2}	17.7×10^{-1}	2.5×10^{-3}	3.96×10^2
5×10^{-3}	18.0×10^{-1}	1.0×10^{-4}	9.96×10^3
1×10^{-3}	1.90×10^2	2.7×10^{-5}	3.70×10^4
5×10^{-4}	2.39×10^2	1.7×10^{-5}	5.89×10^4
1×10^{-4}	2.49×10^2	1.5×10^{-5}	6.65×10^4
5×10^{-5}	2.67×10^2	1.4×10^{-5}	7.10×10^4
1×10^{-5}	1.90×10^2	1.4×10^{-5}	7.13×10^4

$[\text{Cu}(\text{NO}_3)_2]_{\text{M}}$	E_{Ag}	E_{Cu}	$S_{\text{Ag/Cu}}$
1.0	0.58	5.0×10^{-3}	8.50×10^1
5×10^{-1}	0.71	2.7×10^{-4}	6.74×10^2
1×10^{-1}	1.00	3.1×10^{-4}	1.60×10^3
5×10^{-2}	5.89	3.3×10^{-4}	2.49×10^3
1×10^{-2}	6.85	1.0×10^{-5}	2.84×10^3
5×10^{-3}	9.09	1.3×10^{-5}	6.90×10^4
1×10^{-3}	1.90×10^2	2.7×10^{-5}	3.70×10^4
5×10^{-4}	1.99×10^2	1.3×10^{-5}	7.69×10^4
1×10^{-4}	7.13×10^2	1.4×10^{-5}	7.13×10^4
5×10^{-5}	1.99×10^2	1.3×10^{-5}	7.65×10^4
1×10^{-5}	1.43×10^2	1.3×10^{-5}	7.70×10^4



XII

References

- ¹Dziomko, V.M., Dunaevskaya, K.A., *Acta Chimica Academiae Scientarum Hungaricae*, 1962, 32, 223
- ²Dziomko, V.M., Ivanov, O.V., Darda, L.V., *Metody Poluch. Khim. Reaktivov Prep.*, 1969, №20, 194
- ³Buděšinský, Z., Musil, V., *Collection of Czechoslovak Chemical Communications*, 1959, 24, 4022
- ⁴Dziomko, V.M., Ivashchenko, A.V., *Zh. Org. Khim.*, 1973, 10, 2191
- ⁵Dziomko, V.M., Ivashchenko, A.V., *Zh. Obshch. Khim.*, 1973, 43, 1330
- ⁶Dziomko, V.M., Ivashchenko, A.V., *Khim. Geterotsykl. Soedin.*, 1973, 340
- ⁷Lever, A.B.P., Mantovani, E., Rommaswany, B.S., *Canad. J. Chem.*, 1971, 49, 1957

Fig.1. Dependence of the extraction of Cu(II) (a), Zn(II) (b) from hydrochloric acid media, Ag(I) (c) from nitric acid media with 0.5M pyrazole solutions in chloroform on the acidity of the aqueous phase. $[M]_{\text{T}}=0.05\text{M}$. O-I, x-II, Δ -III, \square -IV, \blacktriangle -V, \bullet -VI.

Fig.2. Dependence of the extraction of Fe(III), Zn(II), Cd(II), Cu(II) from hydrochloric acid media with 0.5M solution of II in chloroform on the acidity of the aqueous phase. $[M]_{\text{T}}=0.05\text{M}$. \blacktriangle -Fe(III), \bullet -Zn(II), O-Cd(II), x-Cu(II).

Fig.3. Dependence of the Cu(II) extraction from hydrochloric acid (x), nitric acid (Δ) and sulfuric acid (\blacktriangle) media with 0.5M solution of II in chloroform on the acidity of the aqueous phase. $[Cu(II)]_{\text{T}}=0.05\text{M}$.

Fig.4. Dependence of $\log E_{\text{Cu}} - \log E_{\text{Zn}}$, $\log E_{\text{Zn}} - \log E_{\text{Cd}}$ in the extraction of Cu(II), Zn(II), Cd(II) from hydrochloric acid media with 0.5M pyrazole solutions in chloroform on the acidity of the aqueous phase. $[M]_{\text{T}}=0.05\text{M}$. O-I, x-II, Δ -III, \blacksquare -IV, \blacktriangle -V, \bullet -VI.

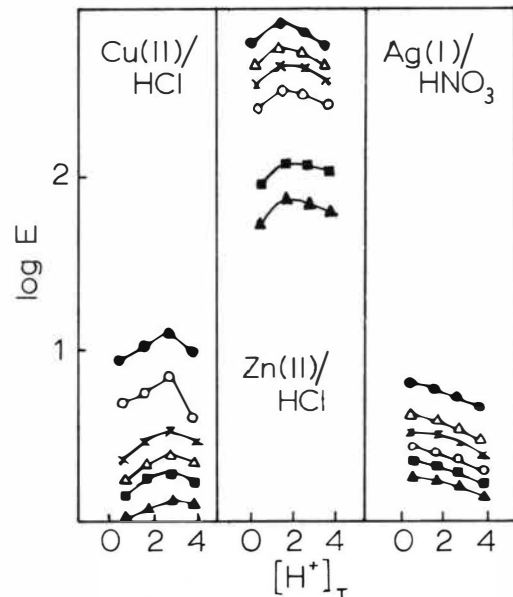


FIGURE 1 Dependence of metal extraction, $[M]_T$ 0.05M, with aqueous acidity using 0.5M pyrazole solutions in chloroform, \circ - I, \times - II, Δ - III, \blacksquare - IV, \blacktriangle - V, \bullet - VI.

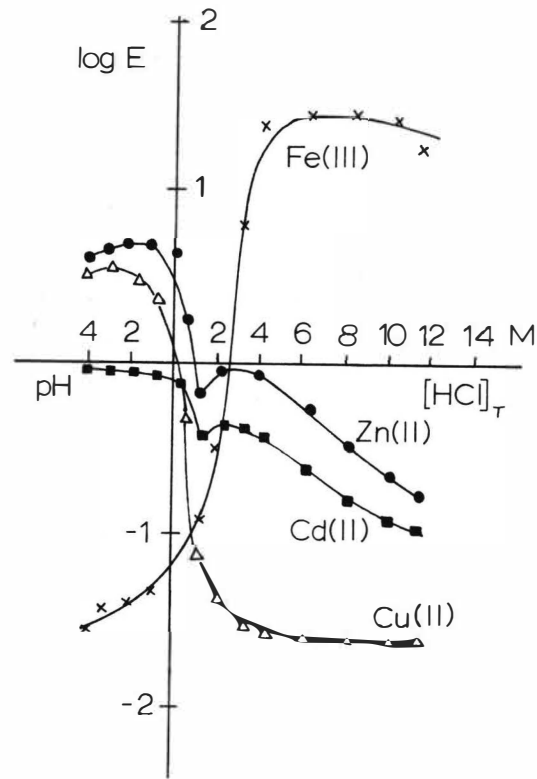


FIGURE 2 Dependence of metal extraction from HCl media with 0.5M solution of II in chloroform on the aqueous acidity. $[M]_T$ 0.05M.

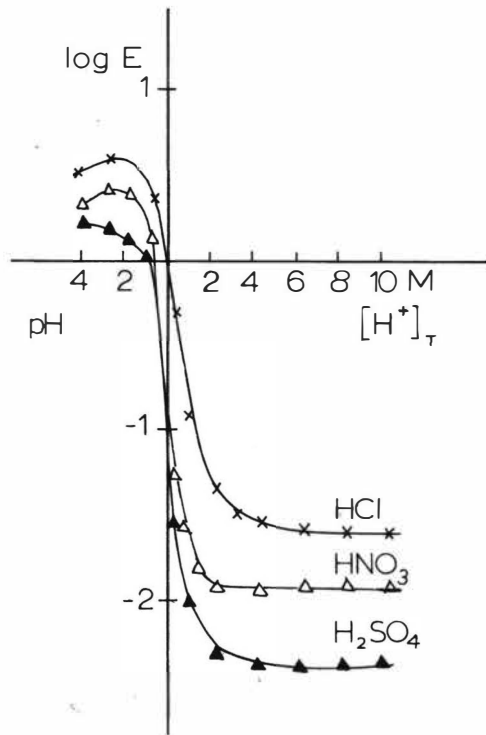


FIGURE 3 Dependence of copper extraction, $[\text{Cu(II)}]_{\text{T}} 0.05\text{M}$, on aqueous acidity using 0.5M solution of II in chloroform

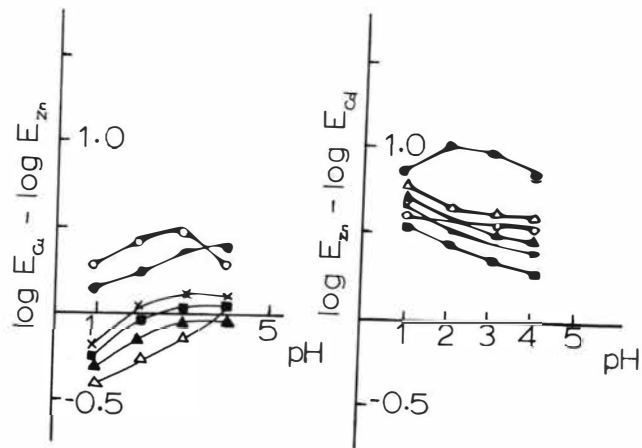


FIGURE 4 Dependence of $\log E_{\text{Cu}} - \log E_{\text{Zn}}$, $\log E_{\text{Zn}} - \log E_{\text{Cd}}$ in the extraction from HCl media with 0.5M pyrazole solutions in chloroform on the aqueous acidity. $[\text{M}]_{\text{T}} 0.05\text{M}$. \circ - I, \times - II, \triangle - III, \blacksquare - IV, \blacktriangle - V \bullet - VI.

PRINCIPLES OF SYSTEMATIC ACTIVATION AND ITS APPLICATION
FOR SYNTHESIS OF EXTRACTANTS WITH THE PREDICTED SELECTIVITY

A I Gorbanev, V B Margulis, B E Dzevitsky

Institute of Metallurgy of the Academy of Sciences of the
USSR, Moscow, USSR

V M Shalygin

All-Union Research Institute of Petrochemical Processes,
Leningrad, USSR

ABSTRACT

Application of the Langenbeck principle of systematic activation is suggested and substantiated for synthesizing extractants with the predicted selectivity towards a pair of metal ions. According to this principle, a relatively simple material with a certain value of the required property is modified by addition and substitution reactions to give a series of its derivatives; from these derivatives those are chosen that have the maximum value of the required property. These compounds yield by addition and substitution a further series of second-generation derivatives, from which those that have the maximum values of the required property are again chosen. The procedure is repeated until a certain generation of derivatives yields a compound with the predetermined value of the required property.

The principle was applied to the synthesis of an extractant for separating two pairs of metals. The most effective compounds were chosen according to the value of selectivity (separation factor) observed with a solution of given composition. The most active compounds in each of the series were the following: hexyl-bis-(1-phenyl-2,3 dimethyl-pyrazolone-5-yl)-methane and a 2-halogeno-alkyl-2,3-diglycol cyclic ester of metacarbonic acid.

The results of applying the systematic activation principle are interpreted by means of a suggested mathematical technique which could be utilized for predicting the identity of useful extractants, for planning an experimental synthesis of higher generation derivatives according to the Langenbeck method, and for studying the relation between extraction properties and the extractant structure. An actual extraction process is simulated

mathematically by means of the general systems theory and the introduction of a complex qualitative-quantitative measure of efficiency, which is used in the simplest algorithms of the mathematical theory of pattern recognition.

INTRODUCTION

It is well known that at present there is no general theory of metal extraction processes, that is, there is no way of predicting the extractive properties of a particular compound from its chemical composition and molecular structure (structural formula)⁽¹⁾. Therefore, selecting extractants in hydrometallurgy or analytical chemistry necessitates testing many substances in various media and for various metals⁽²⁾. Any prediction in the planning of such experiments assumes more or less detailed relationships between the structure and the extracting power of the compound. It is important also to solve a purely practical problem: to synthesize an extractant with a specified value of an extraction property (or properties), even with the expenditure of a considerable effort in synthesis, and without knowledge of the correlation between the extracting power of a substance and its structure.

This procedure is exemplified by the emergence of biologically active compounds as a result of evolution. The natural process of evolution is probably simulated well by the "principle of systematic activation"⁽³⁾, which Langenbeck suggested and developed for simulating natural biochemical catalysts (enzymes) by means of comparatively simple molecules. There is no doubt that the Langenbeck principle can be applied to synthesis in pursuit of any properties which are related to molecular structure. This report is concerned with the application of the Langenbeck principle to the development of extractants for metals; and with the relevant methods of predicting the extracting power of compounds and of establishing the relation of this to their molecular structures.

THEORETICAL

The "principle of systematic activation" proper was developed by Langenbeck in many of his studies⁽³⁾. According to the principle, a series of compounds is selected for their accelerating effect on a given reaction; active compounds are selected from this series and modified structurally by chemical means.

The change is effected by introducing new groups and substituting new groups for old. The most active derivatives are chosen from the products obtained and are, in their turn, subjected to transformation by addition and substitution of groups. In this way enzymic catalytic activity was successfully simulated by organic molecules with low molecular weight. Decarboxylase was the enzyme simulated: its molecular weight in the active state is about 10^6 . The first in the series of catalysts obtained by applying the principle of systematic activation was methylamine with very low activity. The enzyme was best simulated by 1-methyl-3-aminoxyindole obtained in the

fourth generation of methylamine derivatives. Its catalytic activity in decarboxylation of phenyl-glyoxylic acid was only an order of magnitude lower than that of the natural enzyme, despite a molecular weight of only 163. Table 1 presents the general scheme of the method, that is, of a limited application of the principle of systematic activation whereby only one compound out of a generation of derivatives (namely, the most active) is subjected to further transformations. Successful synthesis of a compound with high catalytic activity, naturally, suggests applying Langenbeck's approach to the synthesis of compounds with other useful properties, for instance, selective complexing and extracting agents.

TABLE 1

General scheme of the principle of systematic activation

Generation Number	Most active Substance	Groups added	Resulting compounds
0	A	-	A
1	AB	B ₁ B ₂ ... B	AB ₁ AB ₂ ... AB
2	AB C	C ₁ C ₂ ... C	AB C ₁ AB C ₂ ... ABC
3	AB C D _K	D ₁ D ₂ ... D _K	AB C D ₁ ... ABC D _K
4	AB C D _K E _e	E ₁ E _e	AB C D _K E ₁ ...

The Langenbeck principle is based, essentially, on a few assumptions which are almost self-evident to a chemist though hard to prove formally:

1^o. Any property of a compound is determined by its structure and composition.

2^o. Among all the possible molecules there are some that have a high enough value of a certain property.

3^o. Increasing molecular complexity raises the probability of a high value for a sufficiently complex property.

4^o. A relationship between a complex property and molecular structure is impossible (or difficult) to formalize.

Extraction properties or complexing with metals are phenomena almost as intricate as catalytic action. Therefore, we may apply the method in these fields since it has been proved to be applicable to the synthesis of catalysts.

The Langenbeck principle essentially simulates the processes of genetic mutations and natural selection and therefore it can also be described in mathematical terms⁽⁴⁾. We cannot dwell on this mathematical similarity here. To apply this method to the synthesis of extractants, it is not the statistical and probabilistic description of the process of emergence and intensification of a useful property in the generations of molecules obtained by utilizing the principle of systematic activation that is important, but the deterministic description of the relationship between the extraction property and the structure of the compound that is formed in this process of extractant synthesis. Let us demonstrate that from the standpoint of the general systems theory⁽⁵⁾, the Langenbeck principle, as applied to extractants, is to a considerable extent equivalent to the theory of extraction processes. Indeed, according to the general systems theory the process of extraction as a whole and individual extraction processes, too (for instance, the extractive separation of a pair of metals by a limited range of extractants) should be treated as a complex system with a certain intrinsic determinism (structure) which could be simulated by a theoretical model. This model represents the structure of the system providing its mathematical (algorithmic) description. The accuracy of this description depends on the complexity of the model, on the amount of information put into it and on the efficiency of the mathematical algorithms. The mathematical description allows the study of the properties of a system according to its structure. The solution of this problem begins in the axiomatic description of the structure. Assumptions 1⁰-4⁰ represent axioms for the structure of our system (extraction process), and for all chemical properties in general.

Let us now introduce structure into our system by defining its parameters (in the order of decreasing generality):

class of phenomena - extraction of metals by organic extractants

subclass - extractive separation of a pair of metals

variable factors - extractants (chemical compounds)

efficiency - several sublevels with qualitative and quantitative indicators:

- I - extractive power (physico-chemical property)
- II - technological parameters (costs, availability, liability to losses)
- III - sociological parameters (fire and explosion hazards, toxicity and other environmental effects).

A hierarchy of properties may be constructed for each of these sublevels (in decreasing order of generality).

For sublevel I:

qualitative indicators (features) - structural formula, i.e.:

atoms	}	the main indicators
atomic groups		
functional groups		
chemical bonds		
arrangement and amount)		

These indicators form the code of the compound.

quantitative indicators:

basic physico-chemical properties (boiling and melting points, density, thermodynamic properties)

complex properties (spectral & phase properties, reactivity, etc).

It is characteristic of parameters at the most concrete level that they are easy to determine in a rigorous manner (by measurement) but difficult to structure and arrange according to the order of their importance in our system (the process of extraction).

In other words, in terms of gnoseology all the information on an extractant is contained in its structural formula, but the derivation cannot be formulated.

Let us introduce into our model a mathematical algorithm. This is done using the complex qualitative-quantitative "efficiency measure" K_1 which is expressed as a linear combination of parameters a_i (qualitative and quantitative) and their statistical weights c_i :

$$K_1 = \sum_i a_i c_i$$

where the numerical values of the parameters and their weights may be obtained by various methods. This form expresses the measure for the l-th level in the detailed description of the system. For the (l + 1)th level the corresponding measure is obtained as the convolution of K_l expressed by a similar equation:

$$K_{(l+1)} = \sum_j K_l(j) c_l(j)$$

Rigorously treated, such problems ("organized simplicity" or "random complexity") in actual cases are represented mathematically by systems of nonlinear equations of infinite order. Such systems are insoluble even if they can be written down. Our algorithms are based on a simplified version.

Below, we discuss in detail the algorithms for our subsystem (a physico-chemical phenomenon, i.e. separation of a pair of metals) and relate the generalized measure to the selectivity parameter.

EXPERIMENTAL

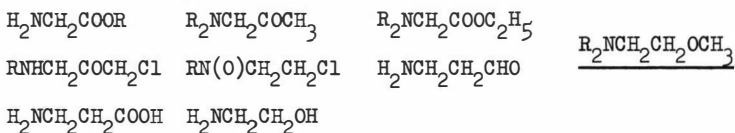
The experiment consisted of synthesizing two sets of extractants, genetically related according to the principle of systematic activation.

In each of the sets the selection was carried out on the basis of the separation factor for a given pair of metals. The separation factor was determined as the ratio of the distribution coefficients of these metals. The composition of the aqueous phase was fixed. All the reactants were synthesized from "Pure" grade compounds using standard methods of organic synthesis⁽⁶⁾. The compounds were purified only when necessary using methods described in reference⁽⁶⁾. Some syntheses involved petrochemicals.

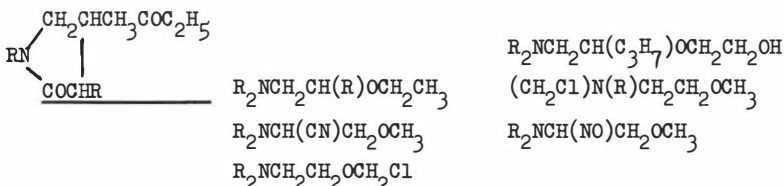
Two groups of compounds were obtained (the most active ones are underlined). Selectivity is measured by the separation factor α .

I. The initial compound was a trialkylamine R_3N ($\alpha = 3.5$).

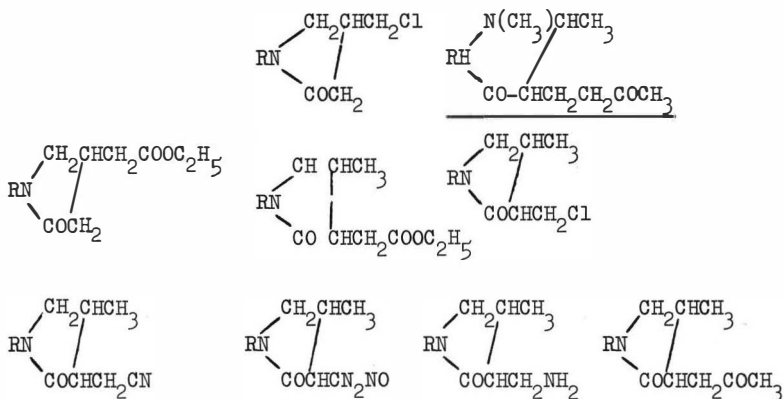
The first generation of derivatives: R_2NH RNH_2 $R - NH-NH_2$



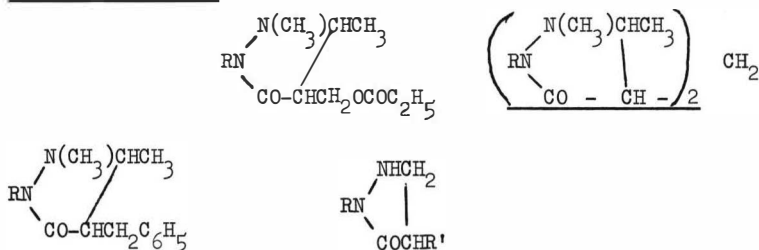
Second generation: $R(C_2H_5OCH_2)NCH(R)OCH_2CH_3$



Third generation:



Fourth generation:

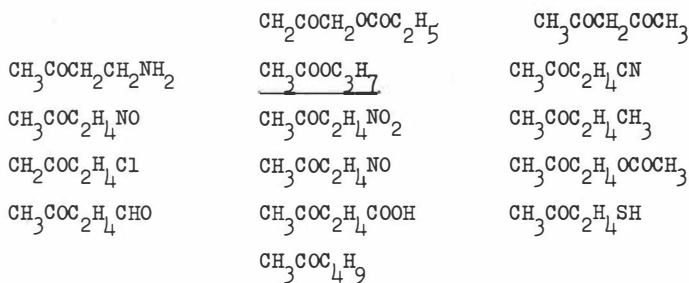


The predetermined value of the selectivity ($\alpha = 800$) was obtained in the fourth generation of derivatives of the initial tertiary amine.

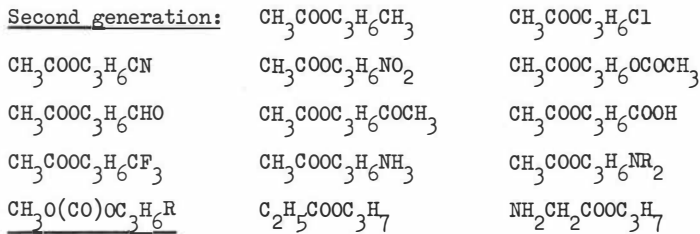
The derivatives of alkyl-bis-(1-aryl-2,3-dimethylpyrazolone-5-yl)-4-methylene proved to be fairly selective extractants in the process studied.

II. The initial compound was methyl-ethyl ketone $\text{CH}_3\text{COC}_2\text{H}_5$ ($\alpha = 1.3$).

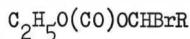
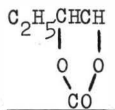
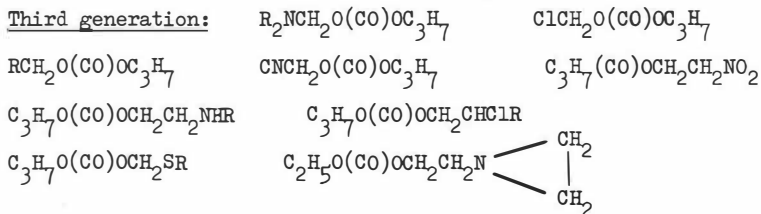
First generation:



Second generation:



Third generation:



The predetermined value of selectivity ($\alpha = 100$) was obtained in the third generation of derivatives from the initial ketone. A cyclic ester of metacarbonic acid and 1-ethyl-2-chloroalkyl-substituted ethyldiol-1,2 had the separation factor of 90.

It may be seen from the schemes above that only the simplest functional groups were used. Virtually no aromatic or heterocyclic substituents were used. An essential point is that the addition and substitution reactions used included cyclization.

DISCUSSION

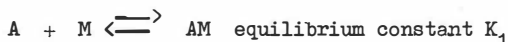
According to the general theory discussed above, the following additional simplifications are necessary in the consideration of the results of applying the systematic activation principle to the extractant syntheses.

Firstly, we shall confine ourselves to considering the phenomenon on one level only, namely on the physico-chemical level; that is, we shall isolate from the general structure the sub-system related to the selectivity ratio of our extractants.

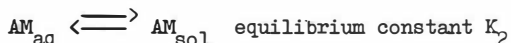
Secondly, we shall consider only those extractants which are genetically related by means of the Langenbeck principle. This makes it possible to limit the number of functional groups and bonds considered.

Thirdly, we shall assume that the following two equilibria play the determining part in the extraction process:

1. Metal - extractant complexing



2. Distribution of the complex between the phases



so that the extraction coefficient is $K_\alpha \sim K_1 \cdot K_2 \cdot [A]$.

Furthermore, we assume that the transfer of a complex from the aqueous phase to the organic phase is related to the solubility and determined by the presence of alkyl radicals. Introduction of large alkyl radicals compensates for differences in solubility between complexes of different metals, so that the selectivity of the extraction process is determined by the ratio of the constants K_1 for two metals. This has important practical consequences as we may ignore aliphatic groups, thereby reducing the dimensionality of the space of properties and simplifying the mathematical description. Then the next step may be made: retaining only the structural formula characteristic and neglecting the physico-chemical properties. We assume that complexing is determined by the structure to a greater extent than solubility. Moreover, the available information on the extractants used is virtually confined to the structural formulae.

After these assumptions, the results will be analysed using the MH-71 algorithm designed for other problems, in particular for analysing the efficiency of extractants in petrochemistry⁽⁷⁾. As discussed above, the algorithm aims at obtaining abstract indicators of efficiency for various levels and their convolutions on a higher level using similar linear formulae.

Table 2 demonstrates application of the algorithm to compare efficiencies of three extractants with four sets of parameters.

For our case (extraction of metals) we shall confine ourselves to the first group of parameters, which includes the separation factor and the structural formula of the extractant. As we can not ascribe definite statistical weights to the structural parameters at the present level of analysis, we shall reverse the problem. We assume that the selectivity is the measure of efficiency, and then determine the statistical weights in respect to the known measurements and parameters (it is more convenient to express their values in binary code). Thus, we formulate the problem of recognition⁽⁸⁾. We select from the set under consideration (set II of methyl-ethyl ketone derivatives) an arbitrary number (N) of compounds, forming a "learning" sequence. The number of parameters is taken to be equal to N (or greater than N) to reduce the problem to linear algebra. There are N extractants with the following parameters:

$$A_I \quad X_i(I) \quad i = 1, 2, \dots, N \quad \alpha_I - \text{selectivity of } A_I.$$

.....

$$A_N \quad X_i(N) \quad i = 1, 2, \dots, N \quad \alpha_N - \text{selectivity of } A_N.$$

The aggregate $\{X_i(I)\}$ forms 1 N-dimensional vectors.

Let us introduce the N-dimensional vector $\{C_i\}$ ($i = 1, 2, \dots, N$) so that the scalar product $\{C_i\} \{X_i(I)\}$ gives the "efficiency measure" (for our case α_i):

$$\alpha = (\{C_i\} \{X_i(I)\}) = \sum_i^N C_i X_i(I).$$

TABLE 2

THE COMPARISON OF EFFICIENCIES OF THREE EXTRACTANTS
(diol extraction)

Parameter group	Parameter number	Statistical weight of the parameter	Ideal case		3-methyl-3-butene-1-ol	Butanol	4,4-dimethyl-dioxane-1,3															
			4	5	6	7	8	9	10	11												
1	1.1	0.4	100	$\sqrt{40}^*$	$\frac{0.56-0.44}{0.56} \cdot 100 = 21.2$	5.3	$\frac{0.64-0.36}{0.64} \times 100 = 43.8$	$\sqrt{23.1}^*$	10.9	$\frac{0.22-0.78}{0.78} \times 100 = -66.0$	$\sqrt{-4.6}^*$	-16.5										
		0.25																				
		5																				
		Reciprocal, 100																				
		5.0																				
1.2	0.05	100	5	Reciprocal, 100	5.0	Reciprocal, 100	5.0	Reciprocal, 100	5.0	Reciprocal, 100	5.0	Reciprocal, 100										
													1.3	0.05	100	5	Reciprocal, 100	5.0	Reciprocal, 100	5.0	Reciprocal, 100	5.0
2	2.1	0.4	$\sqrt{40}^*$	30	4.5	50	$\sqrt{25.0}^*$	7.5	50	$\sqrt{19.0}^*$	7.5											
		0.15	15									Not produced, 20	3.0	Available, 90	10.5	Available, 90	10.5					
		0.15	15									0.8 vol per vol 60	6.0	0.55 vol per vol 70	7.0	3.6 vol per vol 10	1.0					
		0.10	10																			

8161

Table 2 Cont'd

1	2	3	4	5	6	7	8	9	10	11
3		0.1		[10] [*]		[6.0] [*]		[7.5] [*]		[5.0] [*]
	3.1	0.05	100	5	Possible resinification 50	2.5	80	4.0	Possible resinification and decomposition 50	2.5
	3.2	0.05	100	5	70	3.5	70	3.5	While decomposing corrosion increases 50	2.5
4		0.1		[10] [*]		[6.5] [*]		[6.5] [*]		[5.5] [*]
	4.1	0.05	100	5	60	3.0	60	3.0	60	3.0
	4.2	0.05	100	5	70	3.5	70	3.5	50	2.5
	The total efficiency coefficient			100		43.4		62.1		24.9

*The values for the group bond coefficients are given in brackets.

The system of linear equations obtained for α may be solved by methods of linear algebra which are readily computerized⁽⁹⁾. The C_i values are the statistical weights for the parameters X_i .

In set II the learning sequence was formed by 20 compounds while the remaining 23 compounds formed the control sequence. From the values obtained for C_i , the values of α were found for the control compounds and compared with the actual values. As might be expected, numerical agreement between computed and observed values is very poor. However, if the scale of α is divided into three ranges (poor, medium and good selectivity), classification of the control compounds into these ranges is 85% correct. An attempt was made to refine the algorithm by introduction of a recognition function for α , that is, $f(1) \equiv f(\alpha) \equiv \sum_i^N C_i \alpha_i(1)$,

and correlation of properties (X_i). A 7% improvement was obtained for $f = lg$. Furthermore, the simplest algorithm was used to predict extractive powers of compounds related to set II but not included in it. In this way the cyclic ester of 1-methyl-ethylidol-1:2 and metacarbonic acid, as well as the cyclic metacarbonic ester of 1-chloromethylethylidol-1:2, were found to belong to the "good" class. When tested, the first compound exhibited a high selectivity (the exact value, being so high, is not yet determined). These encouraging results obtained on the lowest theoretical level raise hopes for improvement and expansion of the method. This improvement should be in the core of the problem, as it is known that more complicated algorithms alone cannot yield better results⁽¹⁰⁾.

CONCLUSIONS

An application of the principle of systematic activation to obtain extractants with predetermined selectivity has been suggested and substantiated.

The principle was applied in practice to obtain extractants for selective separation of two pairs of metals. On the basis of the general systems theory, we proposed a formal model of an actual extraction process adequately describing the intrinsic determinism (structure) of the process. A simple algorithm for investigating the structure of the phenomenon using this model is proposed. This algorithm is shown to be related to the algorithms for pattern recognition problems and to be useful for predicting the extraction properties and for studying the relationships between these properties and the structure of an extractant.

The most selective extractants for the separation of pairs of metals considered were alkyl-bis-(1-alkyl-2,3-dimethylpyrazol-5-yl)-methylene and a cyclic ester of metacarbonic acid and 1-alkyl-ethanediol-1,2.

ACKNOWLEDGEMENTS

We are very grateful to T M Lesteva, A B Klionsky, A L Shapiro, G A Skorobogatov, Z N Tsvetkova and many other scientists who contributed to the ideas on which this work is based.

REFERENCES

1. A V Nikolaev, Dokl. Akad. Nauk USSR, 187, 817 (1969).
2. A V Nikolaev, Zhurn. VHO im. Mendeleeva, 15, No 4, 362-370 (1970).
3. "Die Organischem Katalysatoren und ihre Beziehungen zu den Fermenten". Von Wolfgang Langenbeck. Berlin u.a., Springer-Verl.
4. N P Dubinin, Evolution of a Population and Radiation, Moscow, 1966.
5. A Rappoport, Various Approaches in the General Systems Theory, in Studies of Systems, Moscow, 1969.
6. "Name reactions in organic chemistry". Alexander R Surrey. 2nd ed., rev. and enl. New York-London, Acad. Press, 1961. Chemistry of Carbon Compounds, Ed. by E H Rodd, Amsterdam, 1951.
7. T M Lesteva, V M Shalygin, Theoretical and Experimental Foundations of Separation of Complex Mixtures, Leningrad, 1971.
8. N G Zagoruiko, Recognition Methods and their Application, Moscow, 1971.
9. V I Smirnov, Textbook of Higher Mathematics, Vol. III, Part 2.



NEW SULFUR-CONTAINING EXTRACTANTS

Yu.A. Zolotov, I.V. Seryakova, G.A. Vorobyeva
VI. Vernadsky Institute of Geochemistry and Analytical
Chemistry, USSR Academy of Sciences, Moscow.

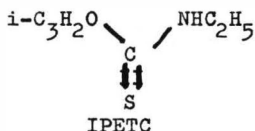
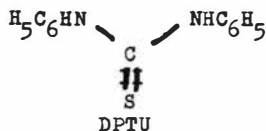
The formation of neutral mixed MX_mS_p complexes (M is the ion of metal with $m +$ charge, X is the inorganic anion, S - the neutral sulfur-containing extractant) can ensure a highly selective extraction of elements. This is connected with the low tendency of S to protonization, as a result of which anion complexes $[\text{MX}_{m+n}]^{n-}$ cannot be extracted (if an inert diluent is used). The extraction of a great number of metals from HCl, HBr, HI, H_2SO_4 , HNO_3 , HClO_4 solutions, as well as mixtures of the KI - H_2SO_4 type, by 0.05 M of solutions of diphenylthiourea (DPTU) and O-isopropyl-N-ethylthionocarbonate (IPETC), O,O'-dinonyl-N-phenyl-naphthyl-amidothiophosphate (ATP) and methoxyphenyl-N,N'-ethoxyphenyldiamidodithiophosphonate (DATP) in chloroform has been studied by experiment. The three first extractants highly selectively extract silver and mercury from nitrate and sulfate solutions. DPTU, IPETC and DATP effectively extract copper, gold and thallium in the presence of iodides.

Introduction

The selectivity of extraction by neutral oxygen-containing extractants of metal complexes with inorganic ligands is, as a rule, not very high. That is caused by the fact that oxygen-containing extractants may extract the metal both in the form of coordinatively solvated compounds and in the form of complex metal acids. Such extractants are relatively easily intruded into the inner coordination sphere of most metals and easily protonized.

The selectivity of sulfur-containing neutral extractants must be higher. They are usually difficultly protonized; therefore their solutions in inert diluents do not extract complex metal acids. On the other hand these extractants give coordinatively solvated neutral complexes only with such elements which are strongly bound up with sulfur - Ag, Au, Hg, Cu(1). When the inorganic anion-ligand and its concentration are changed as well as the extractant (changing the donor-acceptor properties of sulfur), conditions for a selective extraction also of separate chalcophilic elements may be selected. Some sulfur-containing compounds which are used for other purposes (additives to oils, flotation reagents, a.o.) are promising extractants.

We have studied extraction of a great number of elements in the presence of various anions by solutions of N,N'-diphenylthiourea (DPTU), O-isopropyl-N-ethylthionocarbamate (IPETC) and two thiophosphoramides in chloroform.



The dependences of distribution coefficients on the concentration of Cl^- , Br^- , I^- , NO_3^- , ClO_3^- , ClO_4^- anions and on the aqueous phase acidity have been obtained. For this purpose solutions of corresponding mineral acids and mixed solutions containing sulphuric acid and potassium halide were used. 0.05M solutions of extractants and solutions of metal salts labelled by radioactive isotopes with metal concentration 10^{-5} - 10^{-6} g-ion/l were utilized.

Diphenylthiourea

The extraction of Ag, Au(III), Hg(II), Cu(II), Tl(III), In, Bi, Mo(VI), W(VI), Zn, Cd, Co, Fe(III) has been studied using diphenylthiourea. The results (table 1) show that the nature and concentration of the anion in the aqueous phase exert great influence upon extraction effectivity and selectivity. From HCl solutions Ag, Au, Cu and Hg are well extracted, Ag and Hg being quantitatively extracted from 0,01-10M HCl and Au and Cu completely passing into the organic phase only at high HCl concentrations (at low HCl concentrations in case of gold a poor material balance is observed). Au and Cu extraction are almost unaltered, when concentrated HCl is used, while Ag and Hg under these conditions are already poorly extracted. Hg, Ag and Au are well extracted from solutions of hydrobromic acid and in a sufficiently wide range of acid concentration, Cu extraction increases with the increase of HBr concentration. From HI solutions copper, gold and thallium are well extracted, at low HI concentrations- bismuth.

During Tl and Bi extraction the distribution coefficients increase in the series $\text{HCl} < \text{HBr} < \text{HI}$, i.e. with stability increase of halide complexes of these metals. Silver and mercury, on the contrary are more poorly extracted from iodide solutions than from chloride and bromide ones.

This is obviously connected with the formation of stable anionic iodide complexes which are inextractable by chloroform. In this connection of interest is the behaviour of Tl(III), which is well extracted even from a solution containing 10 mol/l LiI, though the high stability of its anionic iodide complex is well known.

From perchlorate solutions Ag, Hg, Bi, Cu are extracted. Silver and mercury are completely extracted in a wide concentration of perchloric acid. The distribution coefficients of bismuth sharply increases with the increase of HClO_4 concentration, whereas copper extraction passes through the maximum (2 - 6M HClO_4).

A very high selectivity is attained during extraction from solutions of nitric and sulphuric acids. Quantitatively only Ag and Hg are extracted and in a sufficiently wide concentration range of acids, especially of sulphuric one (up to 5 - 7,5M). The distribution coefficient decreases when using nitrate solutions higher than 3M, is obviously connected with the oxidation of diphenylthiourea and this may be used for Ag and Hg stripping.

Under all investigated conditions Fe, Co and Zn cannot at all be extracted; therefore they may be easily separated from Ag, Au and a number of other metals.

O-Isopropyl-N-ethylthionocarbamate

This extractant, representing a liquid and being known as flotation reagent under the technical nomination Z-200, is in an acid medium present in the thionic form¹. Ag, Hg(II), Cd, Zn, Au(III), Cu(I,II), Tl(III), Ga, In, Bi, Mo(VI), W(VI), Se(IV,VI), Te(IV), Fe and Co extraction have been investigated in detail (table 2). From bromide and iodide solutions Cu, Au, Tl and Se are well extracted.

Copper extraction is effective in a sufficiently wide concentration range of iodide-ions, as well as at high concentrations of bromide-ions while thallium is better extracted from solutions less concentrated in bromide - and iodide-ions. The concentration of these anions especially strongly influences silver and mercury extraction. Thus these metals may be extracted from iodide solutions only at very low iodide concentrations (up to 0,1 g-ion/1) and bromides decrease the extraction already at their concentration of 1-2 g-ion/1.

In the presence of chlorides, as well as from solutions of nitric, sulphuric and perchloric acids IPETC very selectively extracts silver and mercury. Silver is quantitatively extracted in a broad concentration range of sulphuric and perchloric acids - up to 10M H_2SO_4 . When nitrate solutions are used, extraction is complete only up to 5M HNO_3 , in case of a further increase of acid concentration, the distribution coefficient of silver decreases, which apparently is connected with the extractant oxidation, Mercury like silver is well extracted from solutions of perchloric and nitric acids, but differs in its behaviour during extraction from solutions of sulphuric acid. The distribution coefficients of mercury decrease when H_2SO_4 concentration increases and mercury concentration decreases in the solution. Possibly this is connected with the formation of inextractable sulfate complexes. From 10M H_2SO_4 silver at its concentration $10^{-5} - 5 \cdot 10^{-3}$ g-ion/1 quantitatively passes to the organic phase; the mercury distribution coefficient is under these conditions equal to 0.01. we have shown the possibility of a complete silver and mercury separation at hundredfold excesses of each of these metals in the solution.

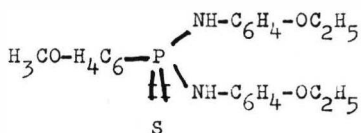
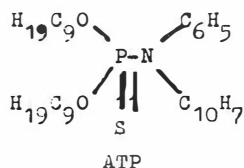
As it already has been said, in the presence of iodides IPETC well extracts Cu, Au and Tl. With the purpose of finding conditions for a selective isolation of thallium its extraction from iodide solutions has been investigated in detail; values of distribution coefficients of thallium in the presence of Ga, In, Zn, Cd, Pb and Cu have been obtained. During extraction from 2,5M H_2SO_4 in the presence of 0,01M KI by 0,05M IPETC solution hundredfold amounts of these elements do not interfere with the complete extraction of 10^{-4} g-ion/l thallium. It is of interest that copper in this case is not extracted because with a concentration increase of copper its distribution coefficient sharply decreases. Thus, during extraction from iodide solutions thallium can be separated from substantially exceeding it copper amounts.

Comparing the results for DPTU and IPETC, much common may be noted between these extractants. First of all it is the high selectivity with regard to silver and mercury during extraction from nitrate and sulfate solutions, as well as the considerable extracting ability with regard to copper, thallium and gold in the presence of iodides. However, during extraction from halide, in particular from iodide media the specificity of extractants is displayed. Copper is extracted in a wide concentration range of iodides and DPTU and IPETC ($\beta_2=8,85$) while thallium, forming one of the most stable anion-iodide complexes ($\beta_4=30,29$) is at high iodide-ion concentrations completely extracted only with DPTU. When IPETC is used, thallium is only extractable at not very high iodide-ion concentrations. When IPETC is used stronger masking influence iodide- and bromide is also observed during silver and mercury extraction. This is obviously connected with the lesser stability of the bond metal-sulfur in the complexes under extraction in consequence of the weakening of the sulfur donor capacity in IPETC at the expense of the inductive influence of the oxygen atom.

Thiophosphoramides

This is apparently a promising class of extractants².

They are nitrogen analogues of neutral ethers of phosphorus thio-acids, in particular, thiophosphates which are known as highly selective extractants. The substitution of oxygen atoms in trialkylthiophosphates for nitrogen atoms must lead to the formation of compounds with a more active thiophosphoryl group, and, hence, with a higher coordination capacity in comparison with trialkylthiophosphates. We have studied the extraction of Ag, Hg, Au, Cu, Tl, Bi, Se, Te, as well as of Zn, Fe and Co with the aid of O,O'-dinonyl-N-phenyl-naphthyl-amidothiophosphate (ATP) and methoxyphenyl-N,N'-ethoxyphenyl-diamidothiophosphate (DATP), which are recommended as inhibitors of polymer ageing.



DATP proved to be a very effective extractant almost for all investigated metals (table 3). Thus, silver and mercury are well extracted from HCl, H₂SO₄ and HNO₃ solutions. Chloride and bromide solutions are optimal for gold extraction. Copper is quantitatively extracted in a wide concentration range of various acids except hydroiodic acid. The distribution coefficients of copper during DATP extraction in contrast to DPTU and IPETC extraction sharply decrease, when the iodide-ion concentration increases. An excess of halide-ions, especially of iodide also interferes with complete bismuth extraction. Thallium is on the contrary, effectively extracted only in the presence of iodides and with high selectivity.

ATP (table 4) is a more selective extractant. Of all studied elements ATP effectively extracts only silver and mercury from nitrate and sulfate solutions in a very wide acidity range (for example, 0,01 - 10M H_2SO_4), gold from hydrochloric solutions and thallium from bromide and iodide ones. ATP strongly differs from other studied extractants with regard to copper and bismuth, the extraction maximum of which falls on solutions with low concentration of hydrogen ions, not exceeding 0,01 - 0,1 g-ion/l. The extraction strongly depends on metal concentration. For instance, when copper concentration increases from $2 \cdot 10^{-6}$ to $1 \cdot 10^{-3}$ g-ion/l., the distribution coefficient decreases from 50 to 0.1.

The rate of equilibrium attainment

The time of equilibrium reaching during copper extraction by studied sulfur-containing compounds is not very short and depends on the nature of the anion in the aqueous phase. During extraction from iodide solutions equilibrium is rapidly attained in 1-5 min, during extraction in the presence of bromide and chloride ions - slower, in 15-30 min. When copper was extracted from 0,01M HNO_3 by ATP solution, complete extraction was observed only in 2 hours. These data indirectly indicate that during the extraction process copper is reduced to monovalent one (in iodide solutions it is at once present in the form of Cu(I), the distribution coefficients of which are higher. Copper reduction by diisphenylthiourea it has been reported in literature³.

In the extraction of silver and mercury from sulfate media in a number of cases no less than 20-30 min are required for equilibrium reaching, which may be connected with the formation of inextractable sulfate complexes.

On the nature of extractable compounds

The ratios of metal-inorganic ligand in complexes of silver, mercury and thallium with DPTU, IPBTC and ATP have been determined with the aid of radioactive isotopes (^{131}I , ^{82}Br). The obtained data (table 5) witness about extraction of the corresponding neutral halides being coordinatively solvated by molecules of sulfur-containing extractants. Thallium is extracted from iodide solutions in a trivalent state which apparently is stabilized at the expense of a strong bond with iodide-ions.

References

1. Lifsnits A.K. Glembotsky A.V. Gurvich S.M. Tsvetnye metall, 1968, No2, 19.
2. Handley T.H. Analyt. Chem., 1964, 36, 2467.
3. Shylman V.M., Savelyeva Z.A., Cheremisina I.M., Vasilyev Ya.V., Anufrienko V.F. Izvestia Sibirsk Otdel. AN SSSR, 1972, No2, ser.Khim. nauk. vyp.1, 77.

Table 1
Extraction of metals by 0,05M DPTU in CHCl_3

Aqueous phase	Well extractable ($D > 10$)	Acid concentration, M	Poorly extractable ($D < 0,1$)*
HCl	Ag	0,01 - 10	Zn, Cd, In, Tl, Bi, W, Fe, Co
	Hg	0,01 - 10	
	Cu	4 - 11,6	
	Au	1 - 11,6	
HBr	Hg	0,01 - 3	Zn, Cd, In, Mo, W, Fe, Co
	Ag	0,01 - 3	
	Au	0,1 - 5,8	
	Cu	1 - 5,8	
HI	Cu	0,01 - 5,2	Zn, In, Mo, W, Fe, Co
	Ag	0,01 - 0,1	
	Hg	0,01 - 0,1	
	Au	0,01 - 3	
	Bi	0,01 - 0,5	
	Tl	0,1 - 5,2	
HClO ₄	Ag	0,1 - 10	Zn, Cd, In, Tl, Mo, W, Fe, Co
	Hg	0,1 - 10	
	Cu	2 - 6	
	Bi	2,5 - 10	
	Au	1 - 5	
HNO ₃	Ag	0,1 - 2,5	Au, Cu, Zn, Cd, In, Tl, Bi, Mo, W, Fe, Co
	Hg	0,1 - 2,5	
H ₂ SO ₄	Ag	0,1 - 5	Au, Cu, Zn, Cd, In, Tl, Bi, Mo, W, Fe, Co
	Hg	0,1 - 7,5	

Partly extractable ($D = 0,5 - 2$): Mo(5 - 11M HCl), Bi(0,01 - 0,1M HCl and HBr), Tl(2,5 - 5,8M HBr), Cd(0,01 - 0,1M HI).

Table 2

Extraction of metals by 0,05M IPETC in CHCl_3

Aqueous phase	Well extractable ($D \geq 10$)	Anion concentration, g-ion/l	Poorly extractable ($D < 0,1$)*
$\text{KCl} + 2,5\text{M H}_2\text{SO}_4$ or HCl	Ag	0,05 - 9	Cu, Au, Zn, Cd, Ga, In, Tl, Bi, Se, Te, W, Fe, Co
	Hg	0,05 - 6	
$\text{KBr} + 2,5\text{M H}_2\text{SO}_4$ or HBr	Tl	0,3 - 1	Zn, Cd, Ga, In, Bi, Te, W, Fe, Co
	Au	0,3 - 3,3	
	Se	0,3 - 3,3	
	Ag	0,01 - 2	
	Hg	0,01 - 0,5	
	Cu	3 - 6	
$\text{KI} + 2,5\text{M H}_2\text{SO}_4$ or HI	Tl	0,01 - 1	Zn, Cd, Ga, Bi, W, Fe, Co
	Au	0,3 - 3	
	Se**	0,3 - 3,3	
	Cu	0,1 - 5	
	Ag	$\leq 0,1$	
	Hg	$\leq 0,1$	
HClO_4	Ag	0,05 - 6	Cu, Au, Zn, Cd, Bi, Ga, In, Tl, Se, Te, Mo, W, Fe, Co
	Hg	0,05 - 6	
HNO_3	Ag	0,1 - 5	Cu, Au, Zn, Cd, Bi, Ga, In, Tl, Mo, Se, Te, W, Fe, Co
	Hg	0,1 - 5	
H_2SO_4	Ag	1 - 10	Cu, Au, Zn, Cd, Ga, In, Tl, Bi, Mo, W, Se, Te, Co, Fe

* Partly extractable ($D=0,5-2$) Mo(0,3M KBr; 0,3-2,5M KCl; 1-3M KI).

** Poor material balance

Table 3

Extraction of metals by 0,05M DATP in CHCl_3

Aqueous phase	Well extractable ($D > 5$)	Anion concentration, g-ion/l
KCl+2,5M H_2SO_4 or HCl	Ag	0,1 - 3
	Hg	0,1 - 3
	Cu	0,1 - 5
	Te	0,3 - 2,5
	Se	0,3 - 2,5
	Au	1 - 7
	Bi	0,01 - 0,5
KBr+2,5M H_2SO_4 or HBr	Ag	$\leq 0,3$
	Hg	$\leq 0,3$
	Cu	0,1 - 4
	Au	0,1 - 7
	Te	0,3 - 3,3
	Se	0,3 - 3,3
	Bi	0,01 - 0,2
KI+2,5M H_2SO_4	Tl	0,3 - 3,3
	Cu	$\leq 0,3$
	Bi	$\leq 0,1$
HClO_4	Ag	0,3 - 3
	Hg	0,3 - 3
	Cu	0,1 - 7
	Te	0,3 - 3
	Se	0,3 - 3
	Bi	0,1 - 3
HNO_3	Ag	0,1 - 5
	Hg	0,1 - 5
	Bi	0,1 - 2
	Cu	0,1 - 5
	Se	0,1 - 5
	Te	0,1 - 5
H_2SO_4	Cu	0,1 - 7,5
	Ag	0,1 - 5
	Hg	0,1 - 5
	Bi	0,1 - 2,5
	Te	0,1 - 5
	Se	0,1 - 5

Table 4

Extraction of metals by 0,05M ATP in CHCl_3

Aqueous phase	Well extractable (D>5)	Anion concentration, g-ion/l
HCl	Bi	$\leq 0,1$
	Cu	$\leq 0,01$
	Hg	0,1 - 1
	Ag	0,1 - 1
	Au	1 - 9
HBr	Tl	0,01 - 0,1
	Bi	$\leq 0,01$
HI	Tl	0,01 - 0,1
	Bi	$\leq 0,01$
	Se*	0,3 - 3
HNO_3	Cu	$\leq 0,01$
	Ag	0,1 - 5
	Hg	0,1 - 5
	Bi	$\leq 0,1$
H_2SO_4	Cu	$\leq 0,01$
	Hg	0,01 - 10
	Ag	0,01 - 10
	Bi	$\leq 0,1$

* $D \approx 2$

Table 5

Results of analysis of the extracts

Metal	Extraction conditions	Ratio of components
O-isopropyl-N-ethylthionocarbamate		
Tl	2N H ₂ SO ₄ + 3,8.10 ⁻¹ M KI	Tl:I = 1:3
Hg	5N H ₂ SO ₄ + 1.10 ⁻³ M KBr	Hg:Br = 1:2
N,N'-diphenylthiourea		
Ag	5N H ₂ SO ₄ + 5.10 ⁻³ M KI	Ag:I = 1:1
Hg	5N H ₂ SO ₄ + 1.10 ⁻² M KBr	Hg:Br=1:2,05
O,O'-dinonyl-N-phenylnaphtylamidothiophosphate		
Tl	5N H ₂ SO ₄ + 1.10 ⁻² M KI	Tl:I = 1:3,3
	5N H ₂ SO ₄ + 5.10 ⁻³ M KBr	Tl:Br= 1:3,3

SOLVENT EXTRACTION OF METAL CHLORIDE COMPLEX BY TRI-n-LAURILAMINE
OXIDE

Z.B.Maksimović, A.Lj.Ruvarac and R.Halaši*

Chemical Dynamics Laboratory Boris Kidrič Institute of
Nuclear Sciences, Vinča FOB 522 Beograd-Yugoslavia

Synopsis Solvent extraction of Fe(III), Ga(III), In(III) and Au(III) chloride complexes by tri-n-laurilamine oxide in n-Hexane and Xylene has been studied. Very high distribution in low acid media was observed. Two possible mechanisms of extraction of metal chloride complexes are postulated. The thermodynamic equilibrium constant of extraction for the system HAuCl_4 -TlAO-n-Hexane has also been studied.

Introduction

Recently has been studied (1,2) the solvent extraction and synergistic effect of some actinides by TlAO from different diluents and acid concentrations. From the analysis of the organic phase two mechanisms of extraction of U(VI) in low and high acid media are postulated. Also Brinkman (3) has studied the extraction of some metal chloride complexes with Alam O from different acid concentration by reverse phase chromatography. He reported in the case of Fe(III), Ga(III) and In(III) that species present in the organic extracts from different acid concentrations are found in the form of MeCl_4^- complexes.

* University Chemical Department - Novi Sad

The present work is a continuation of the study of extraction of some metal chloride complexes by TLAO and it also presents determination of the thermodynamic equilibrium constant of extraction for the HAuCl_4 -TLAO-Hexane system.

Experimental

Materials.- Tri-n-laurilamine oxide was synthesized by the modified Davis (4) method as described previously (1). The purity of TLAO was checked by thin layer chromatography (5). All other chemicals were analar grade.

Radioactive isotopes ^{59}Fe 7 Ci/gr, ^{72}Ga 3 Ci/gr, ^{114}In 0.5 Ci/gr and ^{198}Au 2 Ci/gr were obtained from Amersham-England and BKI, Vinča Radioisotope Department. Purity was checked by RCL-256 channel pulse high analyser.

Instruments - A Nuclear Chicago SD-5-D well type scintillation counter was used for γ activity measurements. The Beckman Research pH-meter with silver billet combination and glass-calomel fibre type electrodes assembly were used for chloride and acid concentration and non-aqueous measurements, respectively. Spectrophotometric measurements were carried out with a Beckman DK-1 spectrophotometer .

Methods - The equilibration of equal volumes or weights of the two phases of different metal, acid and TLAO concentrations are carried out in glass stoppered tubes in a thermostated electric shaker at desired temperatures for 10 min. This time was sufficient to reach equilibrium. Time necessary for settling was 5 min. Equal aliquot portions from each pair of phases were then withdrawn for the measurements of the distribution. The concentrations of Hydrogen (H^+) and chloride ions were determined potentiometrically with corresponding electrodes. Stability of the gold complex in

the organic and aqueous phases was checked by measuring activity for a period of 6 h. During this time the activity of gold in the solution remained constant.

Results and discussion

A. The Distribution data of metal chloride complexes

The distribution of Fe(III), Ga(III), In(III) and Au(III) between different acid concentrations and the organic phase containing $5 \cdot 10^{-2} \text{M}$ and $1 \cdot 10^{-5} \text{M}$ TLAO in Mylene or n-Hexane, respectively, are presented in Figs. 1 and 2.

The dependence of the distribution ratio D on increasing HCl concentration passes through a minimum at 0.08M for Iron, 0.1M for Galium and 0.3M for Indium. These results show high distribution values of Fe(III), Ga(III) and In(III) from low acid media. When the acid concentration increases from 0.1 to 1M HCl the distribution D also increases, as in the case of HMeCl_4 complexes extraction by amine (6,7). Contrary to these results, in the case of Au(III) (Fig. 2) a maximum exists at $1 \cdot 10^{-3} \text{M}$ of HCl and distribution decreases with increasing HCl concentration. Extraction of the gold by TLAO has very high distribution values and for this reason extraction was studied from $1 \cdot 10^{-6}$ - $5 \cdot 10^{-5} \text{M}$ of TLAO in n-Hexane as a diluent.

The distribution of Fe(III), In(III) and Au(III) between 1.0M HCl (for Au 0.02M) and organic phases containing different TLAO concentrations in n-Hexane is shown in Fig. 3. The upper scale of TLAO is for Au. The log-log dependence of D_{Me} vs. C_{TLAO} slope analysis 1.92 suggests that solvation number for all metal complexes is 2. The spectra observed in the organic phase from 0.15M TLAO 1M HCl and 0.005M FeCl_3 were in agreement with the literature data (6).

These data indicate that extractable species of HMeCl_4 exist in the organic phase and are in agreement with those obtained by other authors (7-10) for extraction of metal halides by amines.

For examination of the extraction mechanism of metal halides by TLAO in n-Hexane from low acid media we used the methods similar to those described earlier (2) in the case of uranium extraction.

Our measurements of the chloride concentrations in the organic phase, extracted from low acid media of 0.01M, correspond to three times the Iron concentrations. Spectrophotometrical measurements of the organic phase extracted from neutral or low acid media shows the existence of FeCl_3 complex. Absorption spectra having a max at 450 nm of the organic phase contains 0.15M TLAO, 0.05M FeCl_3 and 0.01M HCl from different diluents, shows the existence of FeCl_3 complex.

The experimental values indicated that the most probable species, extracted from low acid media, in the organic phase is $\text{FeCl}_3 \cdot n \text{H}_2\text{O}$ TLAO, which follows a solvation mechanism. For high acid media extraction of the anionic complex occurs rather than of the neutral complex.

B. Thermodynamics of extraction equilibria in the system:

AuCl_4^- - hydrochloric acid-TLAO-hexane

The aqueous phase was prepared as a mixture of HAuCl_4 and hydrochloric acid solutions in such a ratio that the total ionic strength of the solutions was constant, within each series of experiments ($I = 0.06\text{M}$).

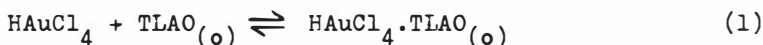
Extraction isotherms of gold ions distribution between the organic and aqueous phase, for various TLAO concentrations

in the organic phase at the temperatures of 10°C, 25°C and 40°C are shown in Figs. 4-6.

From the isotherms shown in Figs. 4-6 it is evident that the TLAO concentration in the organic phase and temperature show a big influence on extraction of gold ions. In the cases of extraction with 0.005M TLAO and 0.01M TLAO at the temperatures above 25°C, organic reagent to gold ion ratio approaches 1:1 in the high loaded organic phase. In the runs with 0.001M TLAO only at 48°C. organic reagent to gold ion ratio approaches 1:1 while at lower temperatures this ratio decrease to 1;2 at 10°C.

The temperature effect on studied extraction processes is the following: increasing temperature decreases extraction of gold ions.

Taking into account the facts mentioned above, valid for 0.005M - 0.01M TLAO and for the temperature range 25°C-50°C, and the literature data (11-14) on the extraction of HAuCl_4 species under conditions similar to those used in our experiments, we could describe the extraction process by the next reaction:



The thermodynamic equilibrium constant of reaction 1. is

$$K = \frac{[\text{HAuCl}_4 \cdot \text{TLAO}]_{(o)}}{[\text{HAuCl}_4] \cdot [\text{TLAO}]_{(o)}} \quad (2)$$

where brackets denote chemical activity of the species.

Thermodynamic equilibrium constants were calculated using the new method developed in our Laboratory (10-13). In the logarithmic form Eq. 2. can be written as:

$$\log \frac{1}{[\text{HAuCl}_4]} = \log K + \log \frac{[\text{TLAO}]_{(o)}}{[\text{HAuCl}_4 \cdot \text{TLAO}]_{(o)}} \quad (3)$$

and for calculation of thermodynamic equilibrium constant, K, it is necessary to plot Eq. 3 as a function:

$$\log \frac{1}{[\text{HAuCl}_4]} = f (C_{\text{HAuCl}_4} \cdot \text{TLOA}_{(o)}) \quad (4)$$

The function (Eq.4) has an inflexion point where

$$[\text{TLOA}]_{(o)} = [\text{HAuCl}_4 \cdot \text{TLOA}]_{(o)} \quad (5)$$

and the equilibrium constant is given by the next equation:

$$\log K = \frac{1}{[\text{HAuCl}_4]} \quad (6)$$

The location of the inflexion point was determined by the graphical differentiation analysis of the curve obtained by function (4). The determination error of the equilibrium constants did not exceed 10%.

The thermodynamic equilibrium constants and other thermodynamic values are presented in Tables. 1 and 2.

Table 1.- Thermodynamic values for the system described by Eq. (1) (organic phase is 0.01M TLOA in hexane)

t(°C)	K	$-\Delta G^\circ$ (kcal/mole)	$-\Delta H^\circ$ (kcal/mole)	$-\Delta S^\circ$ (cal/mole.deg)
25	2.19×10^4	5.86	-9.50	-19.8
40	3.81×10^3	5.11	-9.50	-16.4

Table 2.- Thermodynamic values for the system described by
Eq. (1) (organic phase is 0.005M TIAO)

t(°C)	K	$-\Delta G^{\circ}$ (kcal/mole)	$-\Delta H^{\circ}$ (kcal/mole)	$-\Delta S^{\circ}$ (cal/mole.deg)
25	3.09×10^3	4.71	-9.80	-15.9
40	5.02×10^2	3.85	-9.80	-12.4

According to the values presented in Tables 1-2, one can see that the studied extraction process (reaction (1)) is exothermic.

Acknowledgements - The authors are indebted to Mrs. D.Nemoda, Mrs.D.Dundjerski, Mrs. M.Vorkapić and Mrs. M.Katić for skilled technical assistance.

References

1. Puzić R.G. and Maksimović Z.B. Proc. Int. Solvent Extraction Conference 1971, Vol. II, p. 1180 (Soc. Chem. Ind. London).
2. Maksimović Z.B. and Puzić, R.G. J. Inorg. Nucl. Chem. 1972, 34, 1031
3. Leen, H.R., Vries G. De and Brinkman U.A. Th. J. Chromatogr. 1971, 57, 173
4. Davis M.M. and Hetzer H.B. J. Am. Chem. Soc., 1954, 76, 4247
5. Lane E.S. J. Chromatogr. 1965, 18, 426
6. Lindenbaum S. and Boyd G.E., J. Phys. Chem., 1963, 67, 1238
7. Marcus Y. and Kertes A.S., "Ion exchange and solvent extraction of metal complexes", 1969, p. 490, 634 and 787 (London: Wiley-Interscience)
8. White J.M., Kelly P., Li N.C., J. Inorg. Nucl. Chem., 1961, 16, 337
9. Kuča L. and Högfeltdt E., Acta Chem. Scand., 1968, 22, 183
10. Sherif Sh.A, Abdel-Gawad A.S. and El-Wakil, Talanta, 1970, 17, 137
11. Ruvarac A, and Vesely, V., Z. Phys. Chem (Frankfurt), 1970, 1, 73
12. Petković Dj. Kezele B. and Ruvarac A., in "Contribution to Coordination Chemistry in Solution" in memory of Lars Gunnar Sillen, ed. Erik Högfeltdt, Swedish Natural Science Research Council, Stockholm, 1972, p. 435
13. Petković Dj. Ruvarac A, Konstantinović J, and Trujić V, J.C.S. Dalton, 1973, 1649
14. Spirakov B, Petruhin, O, and Zolotov, Yu. A., Zh. Anal. Khim., 1972, 37, 1584

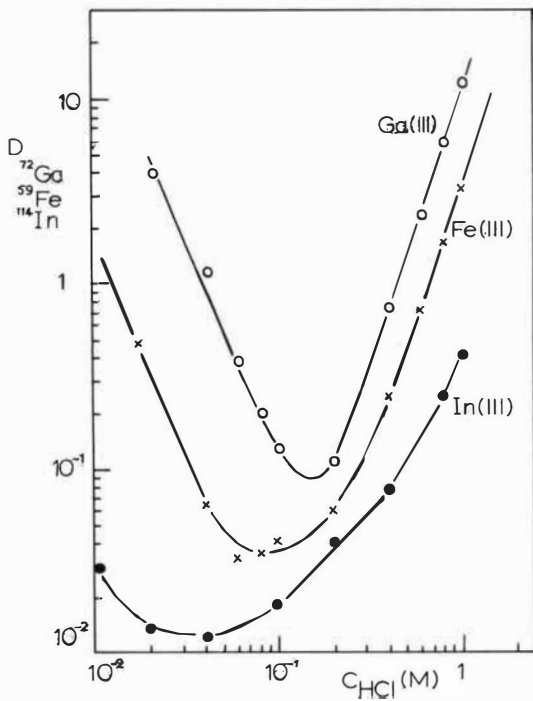


FIGURE 1 Effect of hydrochloric acid on the extraction of Ga(III) Fe(III) and In(III) by 5×10^{-2} M TLOA in xylene or n-hexane.

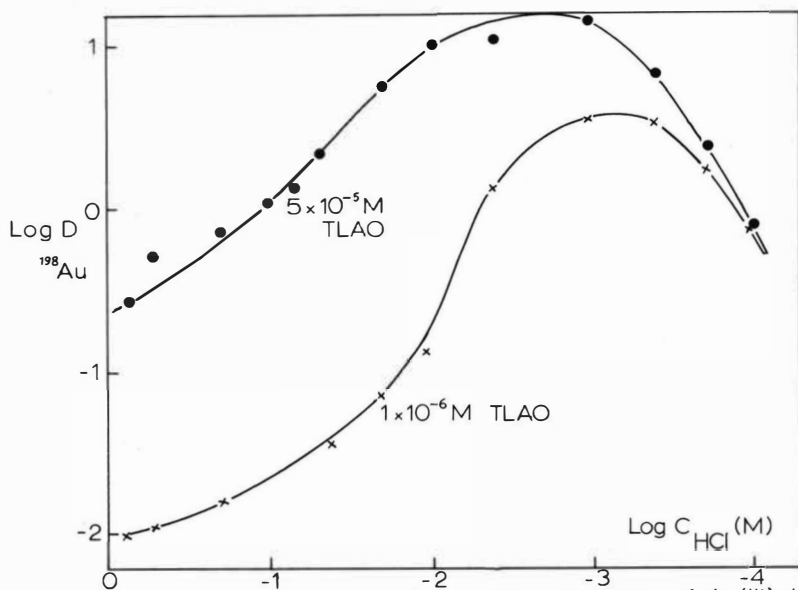


FIGURE 2 Effect of hydrochloric acid on the extraction of Au(III) by TLAO in n-hexane.

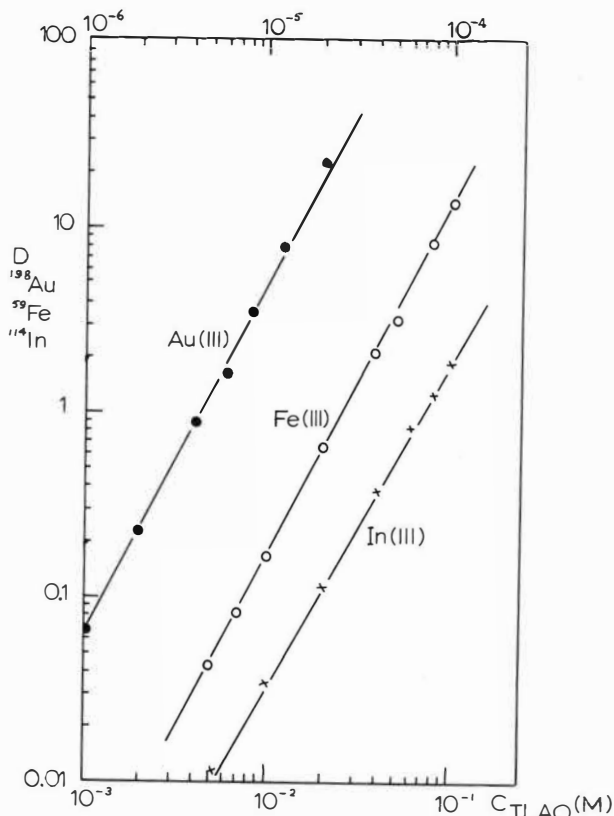


FIGURE 3 Effect of TLAO concentration on the distribution of Au(III) in 0.02M HCl, Fe(III) and In(III) in 1M HCl.

204b

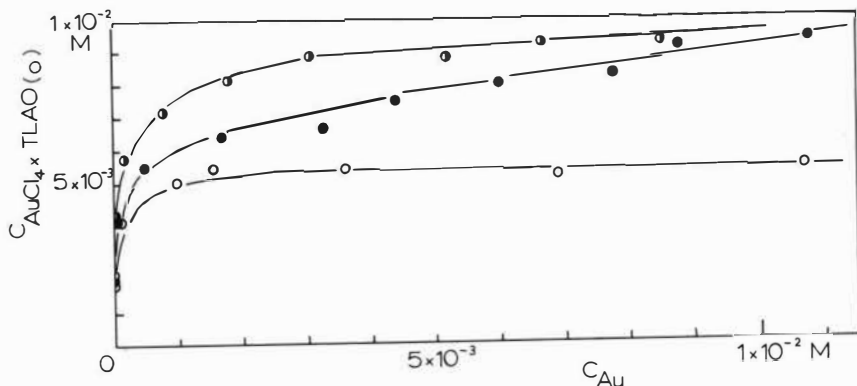


FIGURE 4 Distribution of gold ions between 0.01M TLAO in hexane and aqueous phase with total ionic strength 0.06M at 10°C (°), 25°C (•), and 40°C (•).

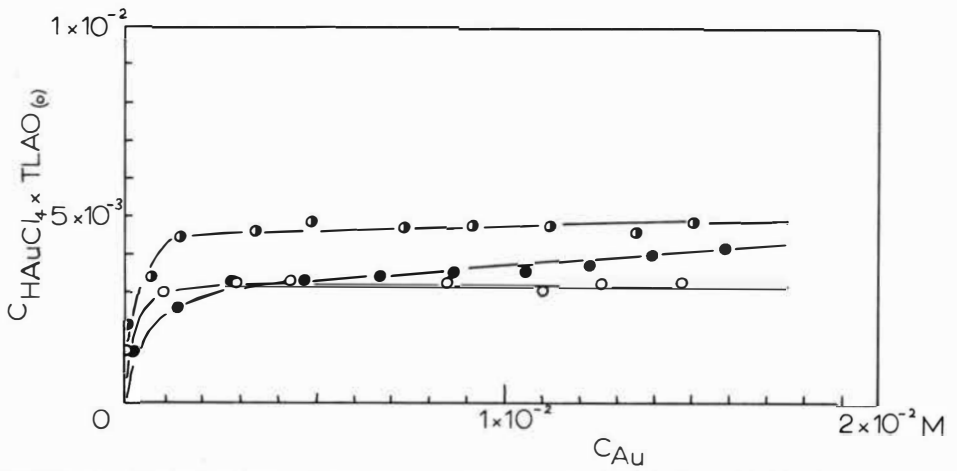


FIGURE 5 Distribution of gold ions between 0.005M TLAO in hexane and aqueous phase with total ionic strength 0.06M at 10°C (○), 25°C (◐), and 40°C (●).

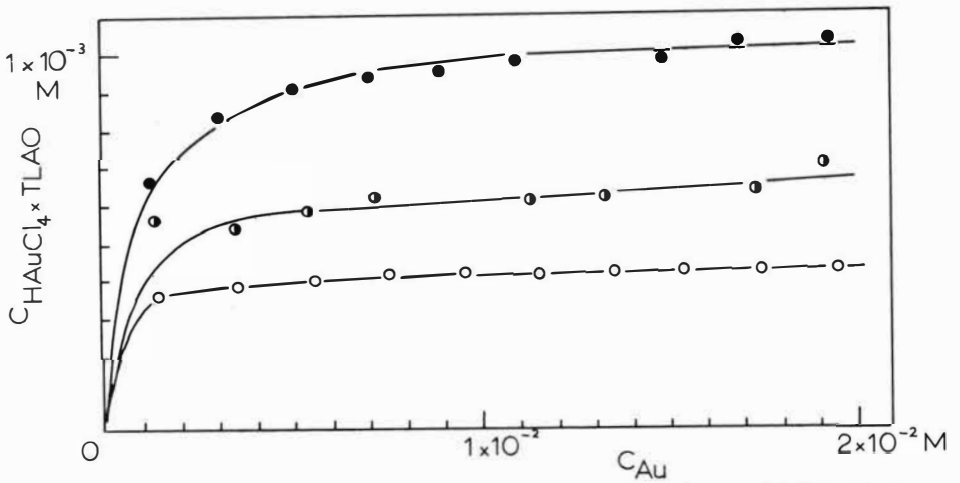


FIGURE 6 Distribution of gold ions between 0.001M TLAO in hexane and aqueous phase with total ionic strength 0.06M at 10°C (○), 25°C (◐), and 48°C (●).



Paper 154 METALS EXTRACTION BY α AND β -MONOSUBSTITUTED
TETRAHYDROFURANS IN CHLORHYDRIC MEDIUM

by G.J.Laurence , Mrs T.L.Thai (+)

J.R.Bourguignon and P.Michel (++)

The preparations, main properties and conditions of use of α and β -monosubstituted tetrahydrofurans for solvent extraction processes are given. Derivatives of tetrahydrofuran are used in their pure state, and placed in contact with aqueous chloride solutions with an acid normality less than or equal to 6.

Studies dealing with the extraction of a certain number of metal chlorides (Ga, Sn, Fe, Hg, Zn, Cd) show the influence of the structure of the organic solvents on their extractive properties.

Results of extractions of iron(III) and gallium(III) by various tetrahydrofuran derivatives are compared to those obtained using linear ethers.

(+) Laboratoire de Génie Chimique, ENSCP, 11, rue Pierre-et-Marie-Curie, 75005, Paris, France

(++) Département de Chimie, Commissariat à l'Energie Atomique, Centre d'Etudes Nucléaires, Fontenay aux Roses, France

INTRODUCTION

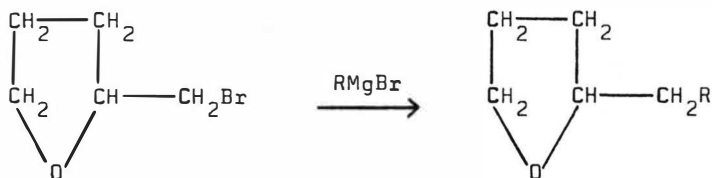
While open-chain ether extraction of mineral components has been studied, the properties of such extraction with cyclic ethers still remain not very well known. Yet, some authors^{1,2}, using spectral measurements, have demonstrated that cyclic ethers, and more particularly tetrahydrofurans (THF) are efficient donors in the hydrogen bond, better than unbranched open-chain ethers, and are therefore correlatively of much higher basicity. In any event, THF is known to form complexes with metals in a large range: rare earths and transition metal chlorides could be prepared and studied^{3,4}. However, the major difficulty arising from such molecules when using them as extractants is their miscibility with water under any proportions⁵.

The purpose of the present work is to study monosubstituted alkylated derivatives of THF as metal chloride extractants, for columns VI, VII, VIIIA, I, II, III, IV and V B of the periodic classification. In effect, the presence of an alkyl radical in either α or β position with respect to the oxygen atom of the THF molecule does not only lower the solubility property of the organic compound in aqueous solutions, but also should have a favorable influence on the donor capability of the cyclic ether molecule.

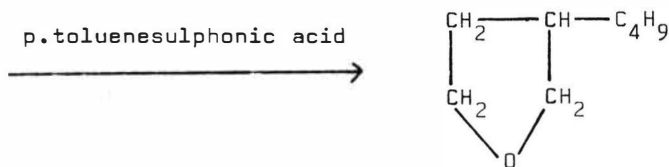
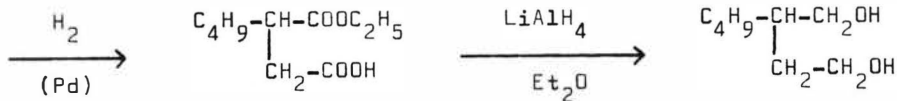
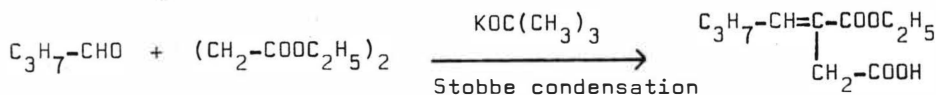
EXPERIMENTAL

The following derivatives have been prepared according to previously described synthesis methods: α -decyl-THF⁶, β -butyl and β -decyl-THF^{7,8,9}.

The synthesis of α -alkyl-THF can be reduced to a Grignard condensation:



The β -alkyl-THF are obtained through 1,4-diols cyclization:



These are colorless liquids. Their main physical properties were measured (Table 1). Solubilities were obtained using the Karl Fischer method and the infra-red absorption method, and they are perfectly satisfactory. Decyl-THF viscosities would perhaps represent a disadvantage for their use in pure state in a solvent extraction process.

Alkyl-THF stability in the presence of nitric, hydrochloric and sulphuric acids

The distribution curves of the various acids in aqueous solution with β -butyl-THF in its pure state are drawn on Fig. 1.

Acids were determined by conductimetric titration with sodium hydroxide. As far as HNO_3 is concerned, extraction is important even from low concentrations. In parallel, a deepening intense brown coloration of the organic solution and a drop in volume of the aqueous phase were noted. For HCl and H_2SO_4 , extraction becomes important only for acid molar concentration of about 6; beyond this value, the phenomenon of organic solution coloration appears again with the increased extraction of acids; with 12 molar solutions, only one phase is obtained.

These observations reveal a degradation of alkyl-THF by breaking the C-O-C bond of the ether, according to a mechanism of the following type:

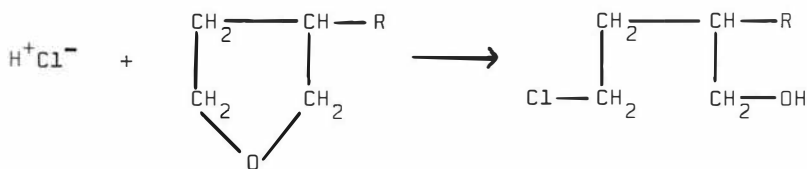


TABLE 1

Main physical properties of prepared alkyl-THF

	α -decyl-THF	β -decyl-THF	β -butyl-THF
Molar weight	212	212	128
Boiling point	67°C (2 Torr)	82°C (2 Torr)	48°C (13 Torr)
Density, g/cm ³ (22°C)	0.840	0.838	0.865
Index of refraction, n_D^{22}	1.435	1.437	1.429
Dipole moment, Debye	1.6	3.5	2.0
Viscosity, centipoises	4.50	7.70	1.06
Water solubility, g/l	7.2	26.6	7.7
Alkyl-THF solubility, g/l	0.08	0.04	1.20
Surface tension/air, dyne/cm	30.0	24.6	26.0
Surface tension/pure water, dyne/cm	15.0	9.5	2.7

The gas phase chromatography allows to check the presence of the degradation products. The stability of alkyl-THF at the contact of 6 molar hydrochloric and sulphuric solutions is confirmed through IR spectrography (1050-1075 cm^{-1}). As a result, these alkyl-THF shall only be used for extractions from hydrochloric acid solutions with concentrations between 1 and 6 molar.

Determination methods used are atomic absorption spectrophotometry (for Hg, Sn, Fe, Cr, Co, Ni, Cu), and volumetry, using EDTA (ethylenediamine tetracetic acid tetrasodium salt) (for Zn, Cd, Al, Ga, Pb), and using ceric sulphate (for Ti, Fe).

Extractions are carried out in separating funnels, at 22°C , using equal volumes of alkyl-THF in its pure state and a hydrochloric acid solution loaded with the element to be extracted, and equilibrated after a 30 minutes shaking.

RESULTS AND DISCUSSION

Metal chlorides extraction by alkyl-THF

Variations in distribution coefficients, for constant concentrations in aqueous phase equal to 0.02M, for various metals (Ga, Sn, Fe, Hg, Zn, Cd) as a function of HCl concentration in the aqueous solution have been plotted (Fig. 2, 3, 4). It appears that the extraction of these metals increases with the acidity of the aqueous solution, and that this salting out effect is particularly important for iron(III) solutions.

Gallium(III), iron(III) and tin(IV) have high distribution coefficients (between 5 and 40, with HCl 6N); cadmium(II) and zinc(II) are not well extracted (distribution coefficients less than or equal to 0.3, with HCl 6N); for mercury(II), medium values are obtained (distribution coefficients of about 1). Extraction by means of ethyl ether gives results which can be compared to those obtained for iron and gallium, but much lower for tin, mercury, zinc and cadmium¹⁰. The advantageous effect of the α and β substitution alkyl groups over the cyclic ethers donor power is so pointed out.

Fig. 5 represents the variation of the distribution coefficients, versus the nature of the extractant, for a concentration of HCl equal to 4N.

From α -decyl to β -decyl-THF, there occurs a general increase of the distribution coefficients, which is particularly important for cadmium(II) and zinc(II). Tin(IV) and iron(III) are exceptions to this rule. This can easily be explained by the more "open" structure of β -decyl-THF, for which the distance between the alkyl radical and the oxygen atom of the cycle is more remote than for α -decyl-THF. The influence of steric factors is even more evident for the extraction of gallium(III), tin(IV) and iron(III) by the β -alkyl-THF: there is a shortening of the radical chain length from decyl to butyl, and this definitely increases the value of the distribution coefficients, while still taking into account the simultaneous increase in the molarity of the pure extractant (β -decyl-THF of 3.96M, β -butyl-THF of 6.72M). This phenomenon has also been observed for phosphates and phosphonates, particularly^{11,12}.

The decrease in distribution coefficients from α -decyl to β -butyl-THF as concerning mercury(II), zinc(II) and cadmium(II) can be interpreted as a more substantial extractive process due to electronegativity rather than due to steric factors. For β -alkyl-THF, it can be thought that the inductive effect of the radical on cyclic oxygen atom is lower than for α -alkyl-THF, in accordance with the well known notion of organic chemistry¹³. The reduction of distribution coefficients for tin(IV) and iron(III) from α -decyl to β -decyl-THF can be explained by means of the same interpretation.

Extractions of other metals were tested, but these were very low (Table 2). It can be noticed in particular that iron(II) and aluminium(III) are not extracted, for all practical purposes. For analytical separations, these results allow to foresee some interesting possibilities. Iron(III), cobalt(II) and nickel(II) should

easily be separated by extraction with alkyl-THF. Gallium(III) is separated from aluminium(III) even with low hydrochloric acid content. With β -butyl-THF, at 6M HCl, a zinc-cadmium separation can be anticipated.

Most of the extraction isotherms were plotted for the elements that are more easily extracted, and for few molar concentrations. Solute distribution still follows the same laws as for low concentrations. The cases of iron(III) and gallium(III), whose behavior in the presence of linear ethers has already been studied, are specially interesting.

TABLE 2
Extraction of various metal chlorides from 4N
hydrochloric acid solutions

Metal	Extractant	Per cent. extracted
Ti (III) (0.4M)	β -decyl-THF	1
Cr (III) (0.5M)	β -decyl-THF	1
Mn (II) (0.5M)	β -decyl-THF	trace
Fe (II) (0.5M)	β -butyl-THF	4
Co (II) (0.5M)	β -butyl-THF	7
Ni (II) (0.8M)	β -decyl-THF	trace
Cu (II) (0.4M)	β -decyl-THF	5
Al (III) (2M)	β -decyl-THF	1
Pb (II) (0.01M)	β -decyl-THF	7

Iron chloride extraction in hydrochloric acid medium

Iron(III) extraction isotherms by means of the different alkyl-THF have been plotted for solutions containing up to 2 moles/l of metallic element(Fig.6,7,8).

Extraction increases quickly with a higher concentration of hydrochloric acid and with an increase in concentration of the solution in the element to extract. The distribution isotherms at low acidities(2-3N) are sigmoid, while in the higher acid media they quickly reach a saturation level; in the case of β -butyl-THF, this corresponds to a ratio of 6:1 of extractant molarity to element molarity present in the organic phase. Kato and Ishii¹⁴ have noted, for the same ratio, another value of 15:2 in the case of ethyl ether extraction.

Such extraction is not accompanied with an important variation of organic and aqueous solutions volumes, in opposition to cases involving linear ethers¹⁵; for the concentration range under study, no second organic phase was observed. Extraction of iron(III) chloride by β -butyl-THF gives figures that are near of those obtained with isopropyl ether¹⁶.

Gallium chloride extraction in hydrochloric acid medium

Fig.9 shows gallium(III) extraction isotherms with the various alkyl-THF, for a 4N hydrochloric acid content. The extraction of gallium(III) is very important, even with relatively low HCl concentrations, unlike that of iron(III). With ethyl ether, gallium(III) extraction reaches a maximum value for about 6M hydrochloric acid solutions¹⁰. The limitation in acidity imposed for alkyl-THF stabi-

-lity does not allow to observe an identical phenomenon in this case; however, the maximum performances of ethyl ether and alkyl-THF are obtained in the same range of acid concentrations, and with closely related values. Schug and Katzin¹⁷ have explained the remarkable extraction of gallium chloride even at low acidities due to the existence of the $\text{GaCl}_3 \cdot \text{H}_2\text{O}$ form, that is readily extracted: the HCl molecule is not interfering in the coordination and configuration transition as much as for the case of most other metal chlorides.

This study reveals that α and β -monosubstituted-THF are new interesting extractants, giving another opportunity of using ethers for that purpose. The light β derivatives of THF, such as β -butyl-THF, are differentiated from others due to the marked potential they offer for separating high valency metals (Sn(IV), Ga(III), Fe(III)) from other elements (Hg(II), Zn(II), Cd(II), Co(II), Ni(II), Al(III)).

REFERENCES

¹ Searles, S., & Tamres, M., J. Am. Chem. Soc., 1951, 73, 3704

² Richards, R. L., & Thompson, A., J. Chem. Soc., 1967, A, 1244

³ Fowles, G. W., Rice, D. A., & Walton, R. A., J. Inorg. Nucl. Chem., 1969, 31, 3119

⁴ Rossmannith, K., Monatsh. Chem., 1969, 100, 1484

⁵ Ferguson, L., J. Am. Chem. Soc., 1955, 77, 5288

⁶ Paul, R., Bull. Soc. Chim. Fr., 1938, 5, 1053

⁷ Wojcik, B., & Adkins, H., J. Am. Chem. Soc., 1934, 56, 2424

⁸ Marvel, B., & Myers, R. L., J. Am. Chem. Soc., 1948, 70, 1694

- ⁹Overberger, C.G., & Roberts, L.B., J. Am. Chem. Soc., 1949, 71, 3618
- ¹⁰Swift, E.H., J. Am. Chem. Soc., 1924, 46, 2375
- ¹¹Siddal, T.H., Ind. Eng. Chem., 1959, 51, 41
- ¹²Timoshev, V.G., & Petrov, K.A., Radiokhimiya, 1960, 2, 419
- ¹³Rozen, A.M., & Nikolotova, Z.I., Russian J. Inorg. Chem., 1964, 9, 933
- ¹⁴Kato, S., & Ishii, R., Papers Inst. Phys. Chem. Research Tokyo, 1939,
36, 82
- ¹⁵Dodson, R.W., Forney, G.J., & Swift, E.H., J. Am. Chem. Soc., 1936,
58, 2573
- ¹⁶Nachtrieb, N.H., & Fryxell, R.E., J. Am. Chem. Soc., 1948, 70, 3552
- ¹⁷Schug, K., & Katzin, L.I., J. Phys. Chem., 1962, 66, 907

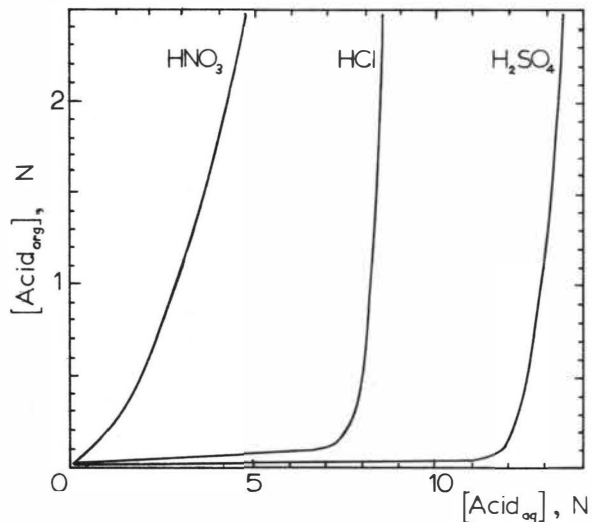


FIGURE 1 Distribution isotherms of acids in aqueous solution with β -butyl-THF

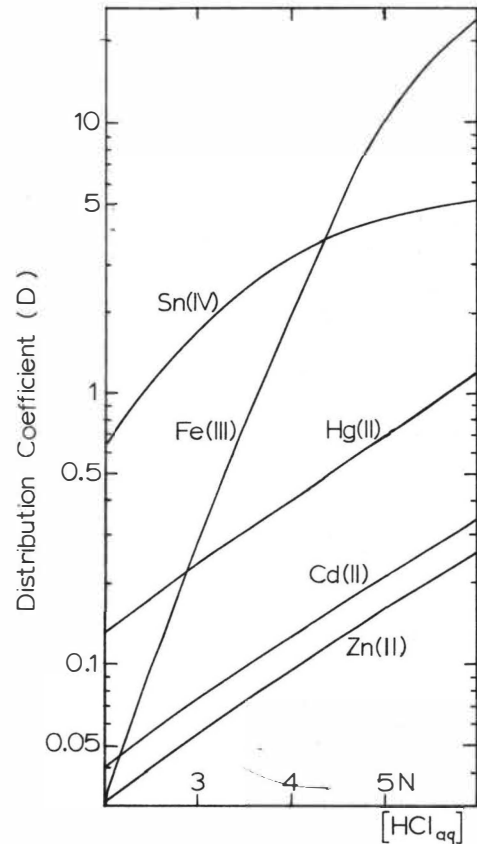


FIGURE 2 Variation of D with acidity in the extraction of metal chlorides at $[M]$ 0.02M by α -decyl-THF

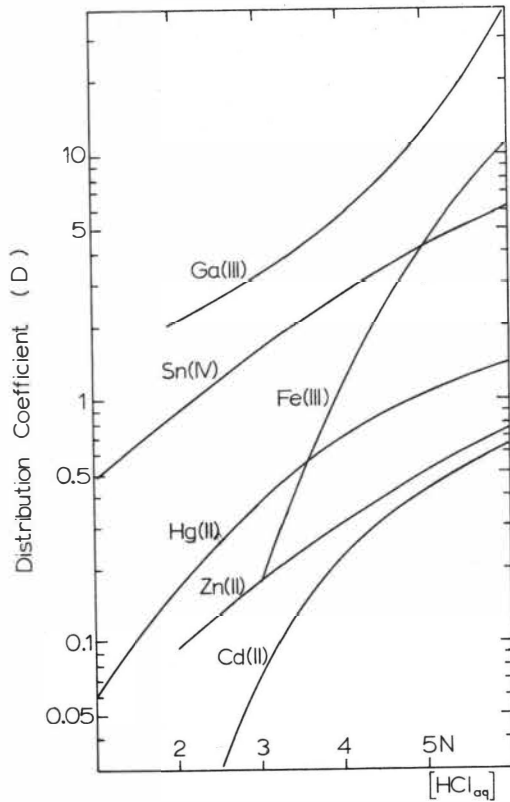


FIGURE 3 Variation of D with acidity in the extraction of metal chlorides at $[M]$ 0.02M by β -decyl-THF

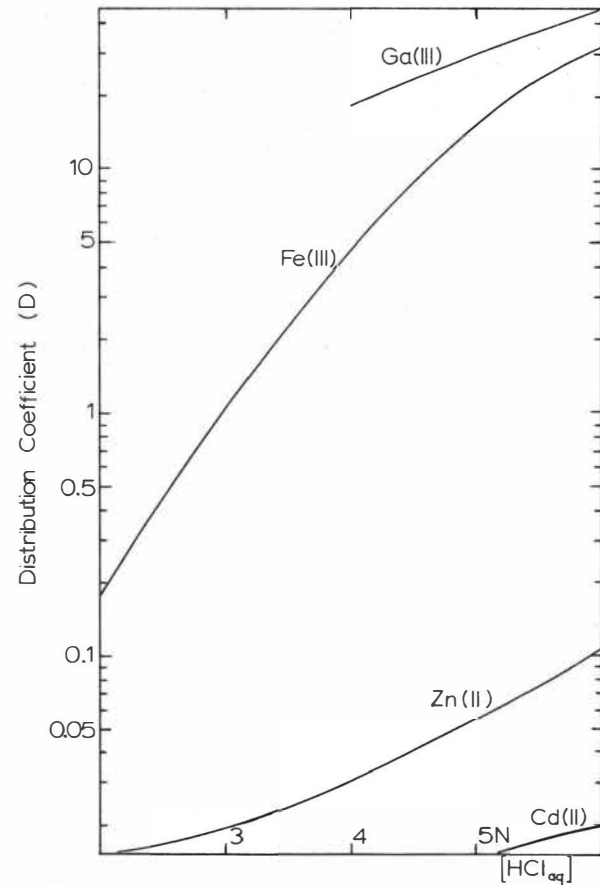


FIGURE 4 Variation of D with acidity in the extraction of metal chlorides at $[M]$ 0.02M by β -butyl-THF

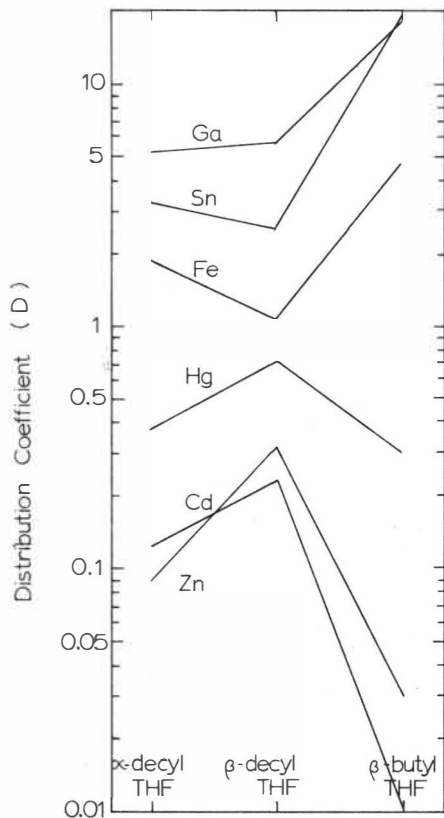


FIGURE 5 Variation of D with different alkyl-THF extractants from 4N HCl and metal concentration 0.02M

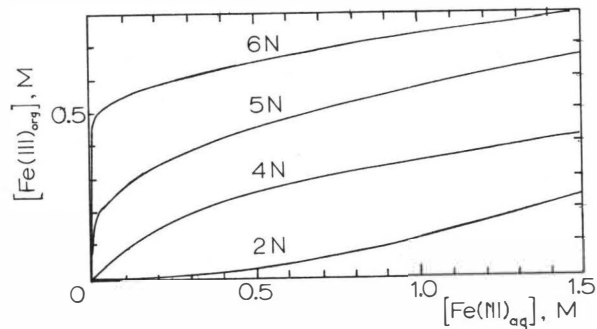


FIGURE 6 Distribution isotherms for Iron extraction by α -decyl-THF at various acidities

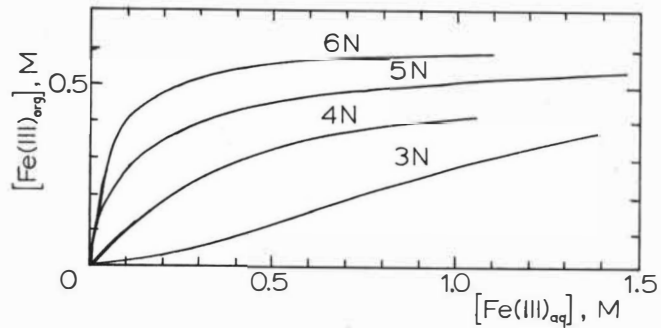


FIGURE 7 Distribution isotherms for Iron extraction by β -decyl-THF at various acidities

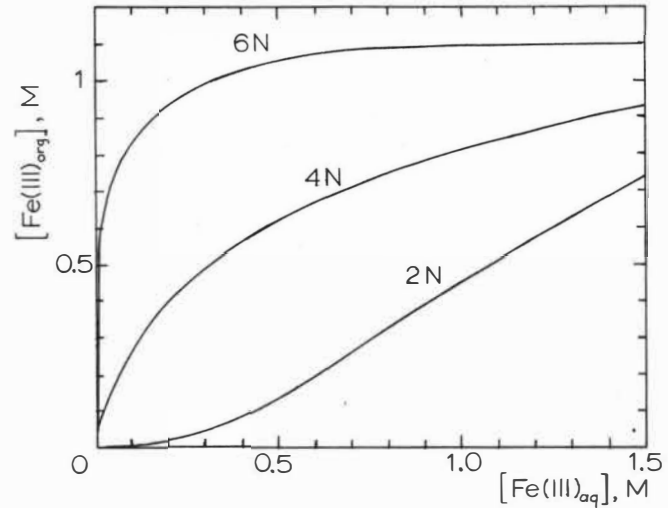


FIGURE 8 Distribution isotherms for Iron extraction by β -butyl-THF at various acidities

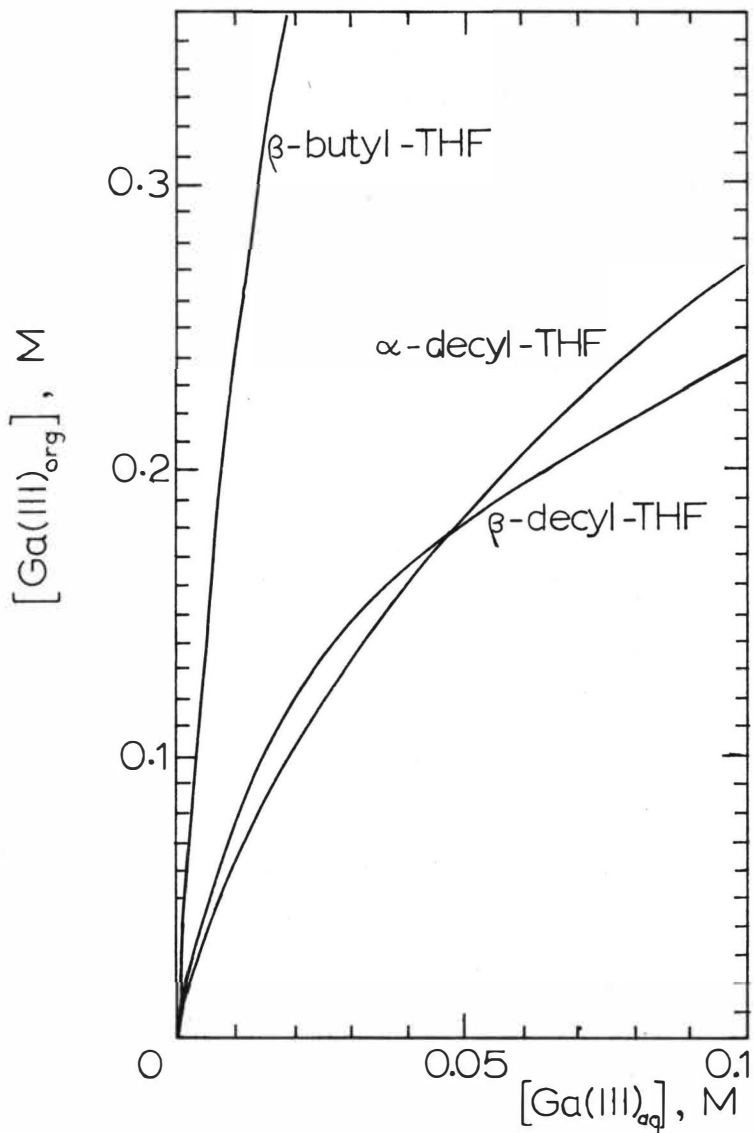


FIGURE 9 Distribution isotherms for Gallium extraction from 4N HCl by the different alkyl-THF extractants

THE EXTRACTION AND PHOTOMETRIC DETERMINATION
OF METALS BY MEANS OF THIODIBENZOYL METHANE

E. UHLEMANN

Abstract.

Thiodibenzoylmethane is reported as a new reagent for the extraction and spectrophotometric determination of traces of metals. The chelates of this ligand are well soluble in organic solvents, show a remarkable stability and are intensively coloured. Specific methods are given for copper, nickel, cobalt, cadmium, mercury and thallium.

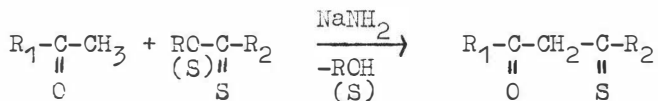
College of Education "Karl-Liebknecht"
Potsdam, DDR

Metal chelates of organic ligands are very important for the separation and determination of metals. In the extraction-photometric analysis chelates are used which combine intensive colour with good solubility in suitable solvents. Among the ligands exhibiting these properties special interest was given to the group of β -diketones. They form chelate compounds with a variety of metals. The application of β -diketones to separation procedures is possible using the pH-dependence of metal extraction and masking interfering metal ions in the aqueous phase, but generally the analytical selectivity of β -diketones is only small. It was therefore tried to obtain simultaneously higher selectivity and sensitivity introducing sulphur as donor atom in the molecule of β -diketone instead of oxygen.

Monothio derivatives of β -diketones were firstly prepared through the acid or base catalysed reaction of β -diketones respectively with hydrogen sulphide.



Another possibility for the synthesis consists in the Claisen-analogous condensation of thioesters with methylketones in the presence of alkali amide. In this way thio-β-diketones are now available in larger quantities.



The chemical behaviour of monothio-β-diketones is determined by tautomeric equilibria. The exact state of such an equilibrium depends on temperature and on the nature of substituents in the chelate system. At room temperature the concentration of the non-enolized form is normally low, and the molar ratio of enol and enthiol form is about 70 to 30.

In many cases thio-β-diketones are easily oxidised by air to give the corresponding disulphides. For this reason the stability of aliphatic thio-β-diketones and also of the interesting thiothenoyltrifluoroacetone is only limited. Monothiodibenzoylmethane apparently seems to be one of the most stable thio-β-diketones. This compound, therefore, was preferentially studied as a special reagent for the purpose of extraction and photometric determination of traces of metals.

Generally monothio-β-diketones have a greater tendency to form metal chelates with thiophilic weak cations than with hard group a) ions. By the action of the C-S-chromophore the chelates are intensively coloured, compared with compounds of β-diketones. The high molar absorption coefficients in the visible region, the excellent solubility of the chelates in organic solvents and the remarkable stability of the chelates enable us to use them in extraction photo-

metric analysis.

Acid constants and chelate stability constants for a series of different monothio- β -diketones were determined potentiometrically in dioxane-water mixture and compared with data of corresponding β -diketones. Thio- β -diketones are more acid than β -diketones, but in spite of greater acidity they form more stable chelates with class b) metals than β -diketones. From this fact it was concluded that the extraction of metals with monothio- β -diketones takes place at lower pH values than in the case of β -diketones. This was confirmed by the extraction curves determined for such metals as copper, nickel, cobalt, cadmium and zinc, but the analytical significance of the fact is only limited, because the time needed for adjusting the extraction equilibria increases with lower pH values. As an example the time dependence of copper extraction using thiodibenzoylmethane is given. Sufficient extraction rates are observed in neutral and basic solutions.

To extract metals quantitatively by means of thiodibenzoylmethane only a slight excess of ligands is needed. Free ligands, however, interfere with the photometric measurements because of its own colour, and therefore must be removed by a stripping process using alkali hydroxide. Concerning this reaction it is supposed, that the metal complexes are stable against alkali. This supposition is well fulfilled for the chelates of copper, nickel, cobalt, mercury and of the platinum group metals. A relatively high stability is also observed for the cadmium compound. Considering the remarkable thermodynamic and kinetic stability of many metal chelates thiodibenzoylmethane is a very suitable reagent for the extraction and photometric determination of copper, nickel, cobalt, zinc, cadmium, mercury and thallium in trace amounts. Some analytical data are given in the following table.

metal	working capacity (μmol)	λ (nm)	ϵ (cm^2 per μmol)	V (bo-bu) (Rel.%)
Cu	0.05 - 0.5	410	23.7	0.15 - 1.5
Ni	0.1 - 1.0	430	9.5	0.2 - 2.0
Co	0.065- 0.65	410	24.8	0.15 - 1.5
Cd	0.02 - 0.2	400	33.8	0.2 - 2.0
Hg	0.05 - 0.5	360	20.6	0.7 - 7.0
Tl	0.1 - 1.0	415	10.0	0.3 - 3.0

Analytical data for the determination of metals using thiodibenzoylmethane as an extractant

Copper is extracted with thiodibenzoylmethane readily from acid solution and the rate of extraction decreases with increasing pH values. The reverse happens, when reducing agents are present. Best results are then obtained above pH 8. It is supposed that the extraction runs via a redox mechanism. The extraction of copper in the presence of a reducing material is not influenced by usual masking reagents, hence most interfering metal ions can be masked by EDTA. The determination of copper by means of this method is highly selective and well reproduceable.

The kinetic stability of the cobalt(III) thiodibenzoylmethane chelate is used for the selective determination of traces of cobalt. Chelates of copper and nickel are extracted under similiar conditions, but they can be destroyed by cyanide solution, while the cobalt chelate remains intact in the organic phase. In a similiar way nickel is selectively extracted after having previously masked the cobalt in the aqueous phase as a kinetic stable cobalt(III) compound. The simultaneous determination of cobalt and

nickel is also possible. Both metal chelates are extracted together, then the nickel compound is redestroyed by cyanide solution. The aqueous solution now contains a certain quantity of the alkali salt of thiodibenzoylmethane, corresponding to the amount of nickel. In this way nickel is indirectly determined in the form of thiodibenzoylmethanate anion, whereas cobalt is detected as its chelate in the organic phase. The method is also applicable in the presence of many foreign metals.

The extraction of mercury does not depend on pH and is possible in the range from 2 M sulphuric acid to 2 M potassium hydroxide. The extracted species contains one mercury atom per one ligand molecule and has a mercaptide-like structure, i.e. the oxygen atom is only weakly coordinated to the mercury. This conclusion was drawn from IR and ^{13}C -NMR measurements. The extraction of mercury with thiodibenzoylmethane from strongly acid solutions is very selective, the only interference being caused by copper in a more than tenfold excess.

Thiodibenzoylmethane is also a very suitable ligand for the extraction and spectrophotometric determination of traces of thallium. The method is rapid and can be made highly selective by masking reagents such as cyanide and EDTA. Because thallium is extracted in the form of the thallium(I) complex, an oxidation to the trivalent state, necessary in many other methods can be avoided.

Useful applications of thiodibenzoylmethane also concern the metals zinc and cadmium. Both are successfully extracted from alkaline solutions. To determine cadmium interfering metal ions are masked by an excess of cyanide and cadmium is then liberated from its cyanide complex by a demasking reaction by means of chloral hydrate. Zinc which is also extracted under these conditions is stripped by means of alkali hydroxide. The method yields good results compared with other procedures for the photometric determination of

cadmium. Further work on the separation of zinc and cadmium is now in progress. A detailed report on this study will be given in the paper at the conference.

In general we conclude, that the extraction and determination of traces of metals with thiodibenzoylmethane is carried out very easily and reproduceable and in a minimum of time. This method, therefore, seems very suitable for the use in industrial laboratories.

V.A. Proskuryakov and A.A. Gaile

Lensoviet Institute of Technology, Leningrad, USSR

Effective extracting agents should combine high selectivity with fairly good solvency for the component to be extracted. In this work, like an a number of others, the relationship between activity coefficients of the hydrocarbons being separated (e.g., n-hexane and benzene) in the solvent $S = \gamma_2^H$ is used as a criterion of selectivity, and the value inverse to the activity coefficient of the hydrocarbon being extracted e.g., benzene γ_1^{-1} is a measure of solvency of the extractive agent.

The activity coefficients of hydrocarbons in solvents have been defined by the method of gas-liquid chromatography /2/.

The difficulties encountered in the selection of effective separating agents are due to the fact that highly selective solvents, as a rule, exhibit low solvency for the component to be separated, and vice versa. No theoretical explanation has been offered for this regularity noted by Gerster and co-workers /3/, for systems solvent-n-pentane-pentene-1 and confirmed by Deal and Derr for systems containing aromatic hydrocarbons /4/.

Explanation of this regularity is likely to be provided by the equation for the enthalpy part of the activity coefficient.

$$\log \gamma_1^H = K (W_{11} + W_{22} - 2W_{12}),$$

where γ_1^H is the enthalpy part of the activity coefficient of hydrocarbon in the solvent;

K is the constant;

W_{11} , W_{22} , W_{12} are energies of interaction between two hydrocarbon molecules, two solvent molecules, and the hydrocarbon molecule and the solvent, respectively.

The introduction of strong electron-accepting groups like NO_2 , CN or electron-donating substituents (OH , NH_2 etc) into the solvent molecule brings about an increase in the non-uniformity of electron density distribution and thus an enhancement of the donating-accepting interaction with hydrocarbons possessing π -electrons. The value of energy W_{12} increases by 2-3 kcal/mole on introducing these groups, which accounts for the increase in selectivity of solvents, e.g. furfuryl alcohol and furfurool on the introduction of a nitro group/Table 1/.

TABLE 1

Activity Coefficients for Hexane, Benzene and Solvent selectivity ($T = 30^\circ\text{C}$)

S o l v e n t	γ_h	γ_c	$S \cdot \frac{\gamma_h}{\gamma_c}$
Furfuryl alcohol	30.2	3,32	9,10
5-Nitrofurfuryl alcohol	118	4,76	24,9
Furfurool	20,0	2,12	9,43
5-Nitrofurfurool	121	2,99	40,6

In this case the solvent selectivity and its donating-accepting component are correlated with the Hammett-Taft constants for the substituents /5/. Simultaneously with the rise in energy W_{12} , however, there occurs, as a rule, a much greater increase in energy W_{22} which can be characterized by the heat of vaporization of the solvent molecules. The contribution of the above groups to the heat of vaporization is 5-8 kcal/mole, which accounts for the increase in activity coefficients of hydrocarbons when passing, for example, from furfurool to 5-nitrofurfurool.

The following methods are proposed for lowering the energy of interaction between solvent molecules:

1. The introduction of functional groups with low contributions to the vaporization heat into the solvent molecule.
2. Skeleton isomerization of solvent molecules known to bring about a decrease in vaporization heat.
3. The use of solvent mixtures with sufficiently high positive deviations from Raoult's law as separating agents, e.g. azeotropic mixtures of solvents with minimum boiling points.

These three methods open up possibilities for the search of new highly effective solvents to be used in the separation of hydrocarbons with various degrees of unsaturation.

Thus, low contributions to the vaporization heat and at the same time rather high values of the Hammett-Taft constants are characteristic of the following substituents: F, COOCH_3 , heteroatoms of O, N. For instance the boiling points and vaporization heats of pentafluoronitrobenzene and pentafluorobenzonitrile are lower than those of the corresponding non-fluorated analogues. Owing to the decrease in energy of interaction between molecules of fluorine-containing solvents (W_{22}) and the increase in energy of interaction between the solvent and aromatic hydrocarbons (W_{12}), the activity coefficients of benzene are appreciably lowered (Table 2). Thus, in this case fluorination of the solvents brings about a simultaneous rise both in solvency for aromatic hydrocarbons and solvent selectivity.

A number of other fluorinated compounds exhibit rather high selectivity and solvency, for example 2-4 dinitrofluorobenzene.

Fluorination of aliphatic compounds also leads to higher effectiveness in the processes of hydrocarbon separation. It is seen from Fig.1 that fluorine-containing alcohols of the general formula $\text{H}(\text{CF}_2\text{CF}_2)_n\text{CH}_2\text{OH}$, where $n = 1 - 3$, are approximately 5 times as selective for the hexane-benzene system as unfluorinated alcohols.

Cyanoethyl derivatives of fluorinated alcohols (No.6, Table 2) are also effective separating agents.

As seen from Fig.2, in which experimental data for various solvents are presented as a plot of selectivity against solvent power, heterocyclic compounds are, as a rule, more effective solvents than benzene and cyclohexane derivatives. In particular, 2-furfuryl- and 2-tetrahydrofurfuryloxypropionitrile exhibit both high selectivity and solvency (No.7 and 8, Table 2).

Compounds containing carboxymethyl groups, e.g. dimethyl esters of aliphatic dicarboxylic acids, are also effective solvents. The activity coefficients of benzene in esters are one order of magnitude lower than in diols, the selectivity of these compounds being approximately the same.

It is well known that the limitation of one of the most widely used extractive agent - sulpholane- is its comparatively low solvency for hydrocarbons. The isomeric compound - 2-methyl tri-methylenesulphone is characterized by lower energy of molecule interaction which is evidenced by a lower boiling point (251°C /7/, the boiling point of sulpholane is 286°C /1/). As a result, the activity coefficients of benzene in 2-methyltrimethylenesulphon are considerably lower than in sulpholane, i.e. 2-methyltri-methylenesulphone has higher solvency, which allows to carry out the extraction process at a lower ratio extractive agent-starting material and at decreased temperatures.

TABLE 2
Activity Coefficients of Hydrocarbons and Solvent Selectivity

S O L V E N T	T °C	γ_h	γ_c	$S = \frac{\gamma_h}{\gamma_c}$
1. Nitrobenzene	30	7.70	1.37	5.62
2. Pentafluoronitrobenzene	32	6.72	0.676	9.93
3. Benzonitrile	30	5.90	1.17	5.04
4. Pentafluorobenzonitrile	30	7.92	0.817	9.70
5. 2,4-Dinitrofluorobenzene	31.5	27.3	1.27	21.5
6. Tetrafluoropropoxypropionitrile	31.5	24.6	2.03	12.1
7. 2 - Tetrahydrofurfuryloxypropionitrile	30	12.1	1.165	10.4
8. 2 - Furfuryloxypropionitrile	30	22.8	1.70	13.4
9. Butanediol - 1,4	58	75,0	10,0	7,50
10. Dimethyl succinate	30	11,6	1,32	8,78
11. Dimethyl malonate	30	12,7	1,71	10,9
12. Sulpholane /4/	60	48,0	2,45	19,6
13. 2 - Methyltrimethylene-sulphone	30	33,3	1,90	17,5

It follows from the results of toluene extraction presented in Table 3 that the proposed solvents, viz. 2-methyltrimethylene-sulphone, tetrafluoropropoxypropionitrile and 2,4-dinitrofluorobenzene, are highly effective extractive agents allowing to obtain concentrated extracts at a high degree of extraction of aromatic hydrocarbons.

TABLE 3

Results of Single-Stage Extraction of Toluene from the Mixture with n-Heptane (toluene content in starting material 35 weight %, solvent-starting material ratio=2:1 weight)

S O L V E N T	Tempera- ture, °C	Toluene content in ex- tract, weight	Degree of toluene extracti- on, % weight	Coeffi- cient of toluene distrib- ution
1	2	3	4	5
2-methyltrimethylene - sulphone/I/	20	79,2	54,9	0,42
97 weight %/I/ + 3 weight % H ₂ O	20	86,9	52,2	0,40
Sulpholane	70	79,4	50,0	0,36
Tetrafluoropropoxypro- pionitrile	20 50	78,0 73,5	58,0 61,3	0,49 0,55
2,4-Dinitrofluoroben- zene	20	83,1	63,0	0,58
2-Tetrahydrofurfuryl- oxypropionitrile/II/	20	54,7	77,6	0,75
93,9 weight % /II/ + 6,1 weight % H ₂ O	20	71,1	62,5	0,54
84,3 weight %/II/ + 15,7 weight % ethylene glycol	20	65,8	66,0	0,57
5-Nitrofurfuryl alcohol (III)	20	92,5	26,0	0,15
50 weight %/III/ + 50 weight % N-methylpyrro- lidone	20	69,5	62,7	0,52
47 weight % /III/ + 53 weight % furfurol	20	80,3	49,0	0,36
Diethyleglycol	50	83,6	23,9	0,12

Good results are obtained with the use of mixtures of 5-nitro-furfuryl alcohol with solvents possessing increased solvency for hydrocarbons and also mixtures of 2-tetrahydrofurfuryloxy-propionitrile with water and ethylene glycol.

Dimethyl esters of aliphatic dicarboxylic acids are effective extractive agents for higher aromatic hydrocarbons (see Table 4) and can be used for refining oil and jet fuel instead of furfural and phenol.

It is seen from Figs 3 and 4 that the relationship between logarithms of specific retention volumes of hydrocarbons (V_g), e.g. n-hexane and benzene, and the composition of the mixed solvent often does not obey the additivity rule. For mixtures with positive deviations from Raoult's law, in particular for the 1,2-propyleneglycolacetophenone giving an azeotrope with a minimum boiling point /9/, one observes a positive deviation of V_g for hydrocarbons from the additive values. For the solvent mixture phenol-furfuryl alcohol which is characterized by the presence of a negative azeotrope the deviation of experimental values of V_g from those calculated according to the additivity rule is of negative nature. These results can easily be explained by the equation for the enthalpy part of activity coefficients with allowances for the inverse relationship between the values γ_i and V_g .

Thus, solvent mixtures with sufficiently high positive deviations from ideality, in particular positive azeotropic mixtures, exhibit increased solvency for hydrocarbons and can be recommended for use in separating hydrocarbons system.

TABLE 4

Results of Single-Stage Extraction of Methylnaphthalene from a Mixture with n-Tridecane (methylnaphthalene content in starting material is 35 weight %; solvent-starting material ratio=1.5 : 1 weight; temperature 30°C)

SOLVENT	Methylnaphthalene content in extract, weight %	Extraction degree, weight %	Coefficient of methylnaphthalene distribution
Dimethyl malonate	89,6	65,4	0,86
Dimethyl succinate	74,8	71,7	1,01
Furfurol	77,5	68,6	0,83

R e f e r e n c e s

1. H.Voetter, W.C.G.Kosters, Proceedings of the VI International Petroleum Congress (in Russian) M., 1965.
2. E.R.Adlard, M.A.Khan, B.T.Whitham, In "Gas chromatography", M., p.354, 1964.
3. J.A.Gerster, J.A.Gordon, R.B.Eklund, J. Chem. and Eng. Data, 5, 423 (1960).
4. C.H.Deal, E.R.Derr, Ind. Eng. Chem., Process Design Develop., 3, 394 (1964).
5. Ya.I.Leitman, A.A.Gaile. Zhurn. Fiz. Khim., 44, 1431, 1436(1970); 45, 76 (1971).
6. A.A.Abramson, Zhurn. Prikl. Khim., 40, 2598 (1967).
7. E.Grishkevich-Trakhimovsky. Zh. russ. fiz.-khim. obshch., 48, 880 (1916).
8. N.F.Grishchenko, V.N.Pokorsky, M.N.Yablochkina. In "Processes of Liquid Extraction and Chemisorption" (in Russian) M.-L., "Khimiya", 1971.
9. S.K.Ogorodnikov, T.M.Lesteva, V.B.Kogan. Azeotropic mixtures (in Russian), L., "Khimiya", 1971.

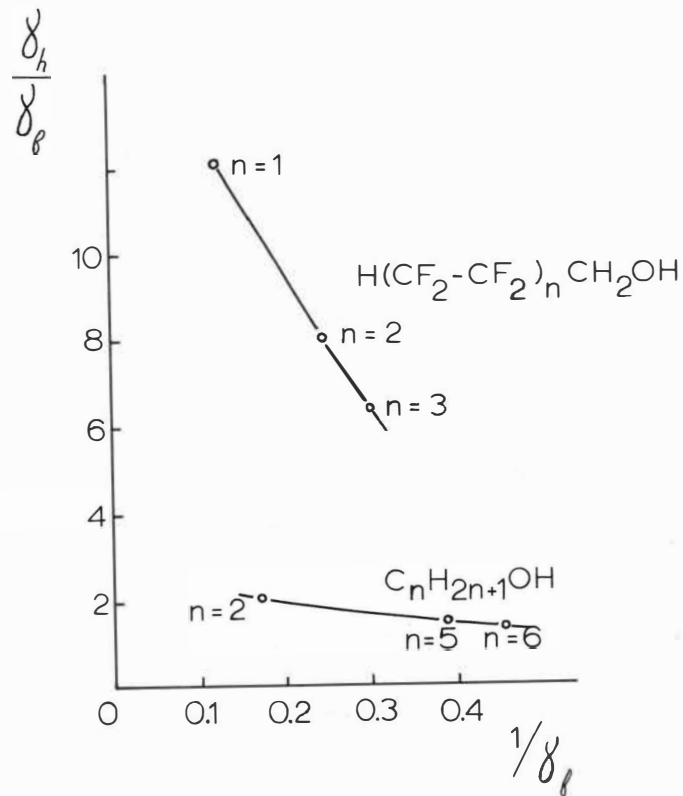


FIGURE 1 Relationship between selectivity and solvency of alcohols for benzene.

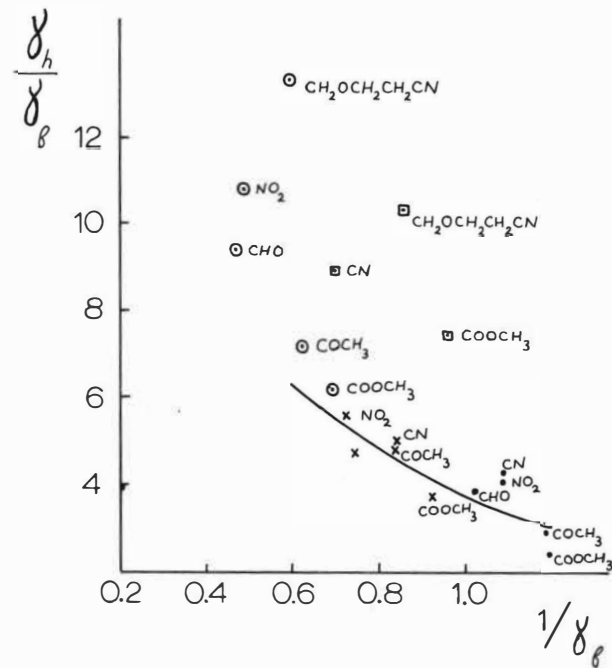


FIGURE 2 Relationship between selectivity and solvency of benzene, \times , cyclohexane, \bullet , furan, \odot , and tetrahydrofuran, \square , derivatives for benzene.

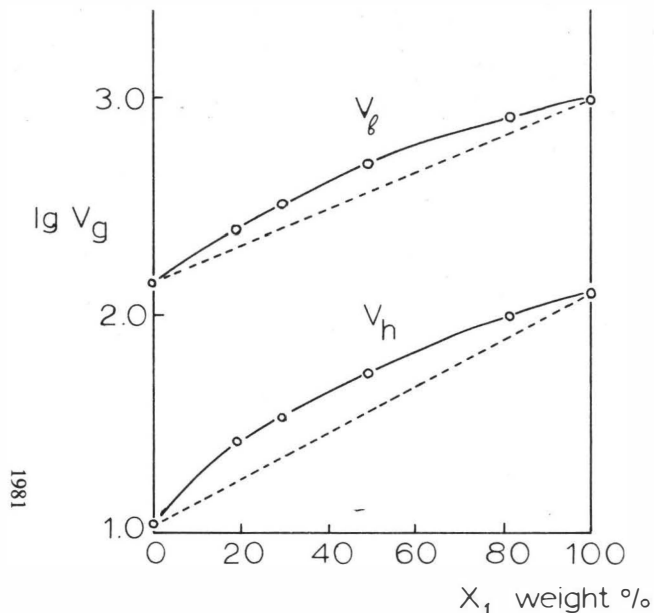


FIGURE 3. Specific retention volumes of benzene and n-hexane in the mixture 1,2-propyleneglycol - acetophenone at 30°C.

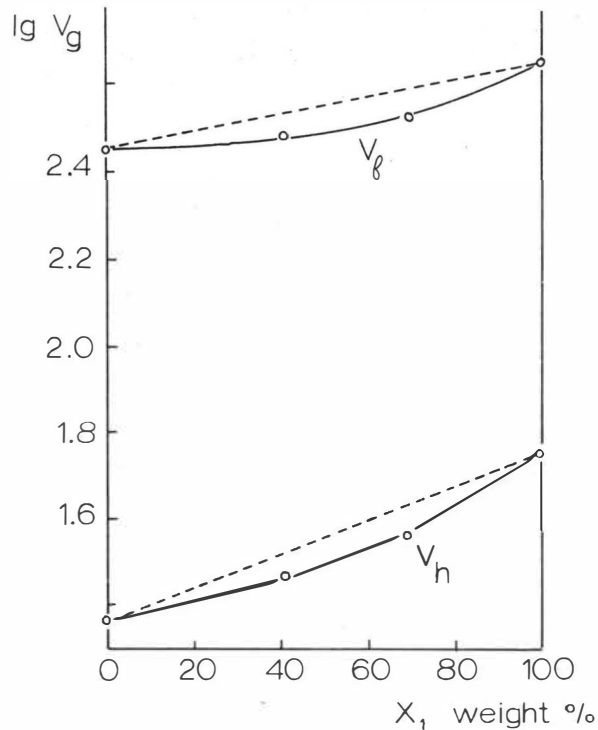


FIGURE 4. Specific retention volumes of benzene and n-hexane in the mixture furfuryl alcohol - phenol at 45°C.